Methods in Molecular Biology 1403

Springer Protocols

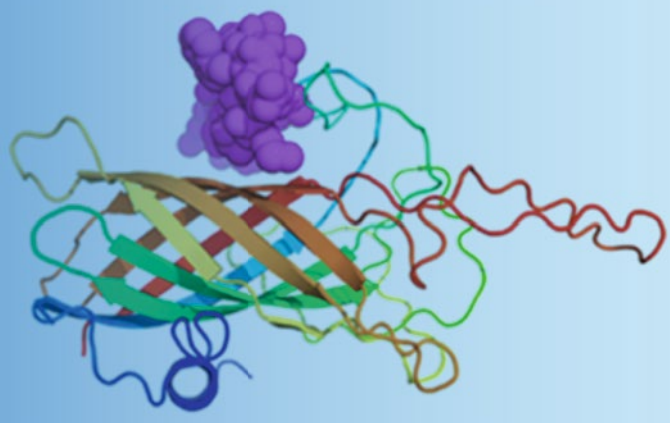

Sunil Thomas *Editor*

Vaccine Design

Methods and Protocols

Volume 1: Vaccines for Human Diseases

Humana Press

METHODS IN MOLECULAR BIOLOGY

Series Editor
John M. Walker
School of Life and Medical Sciences
University of Hertfordshire
Hatfield, Hertfordshire, AL10 9AB, UK

For further volumes:
http://www.springer.com/series/7651

Vaccine Design

Methods and Protocols:
Volume 1: Vaccines for Human Diseases

Edited by

Sunil Thomas

Lankenau Institute for Medical Research, Wynnewood, PA, USA

Humana Press

Editor
Sunil Thomas
Lankenau Institute for Medical Research
Wynnewood, PA, USA

ISSN 1064-3745 ISSN 1940-6029 (electronic)
Methods in Molecular Biology
ISBN 978-1-4939-3385-3 ISBN 978-1-4939-3387-7 (eBook)
DOI 10.1007/978-1-4939-3387-7

Library of Congress Control Number: 2016934046

Springer New York Heidelberg Dordrecht London

Printed on acid-free paper

Humana Press is a brand of Springer
Springer Science+Business Media LLC New York is part of Springer Science+Business Media (www.springer.com)

Dedication

Dedicated to
Vaccinologists (who work hard developing vaccines)
Healthcare workers in developing countries (who risk their lives vaccinating people)

Preface

> "We are protecting children from polio at the cost of our lives."
> Sabeeha Begum (a lady healthcare worker providing polio vaccines in Quetta, Pakistan)

Vaccinations have prevented several diseases; however, as yet, there are only two diseases that have been eradicated globally. Mass awareness programs and aggressive vaccination strategies in the twentieth century were able to control smallpox, and the disease was officially declared eradicated in 1980. Rinderpest, a serious disease of cattle, was officially eradicated in 2011, thereby becoming only the second disease to be completely eradicated. Recently, the Americas (North and South America) were declared free of endemic transmission of rubella, a contagious viral disease that can cause multiple birth defects as well as fetal death when contracted by women during pregnancy. The achievement was due to a 15-year effort that involved widespread administration of the vaccine against measles, mumps, and rubella (MMR) throughout the Western Hemisphere.

One of the dreaded diseases—poliomyelitis—is in the last phases of eradication, thanks to the effective vaccines against the disease. The public health effort to eliminate poliomyelitis infection around the world began in 1988, and vaccination strategies have reduced the number of annual diagnosed cases of polio from the hundreds of thousands to couple of hundreds. Nigeria was the last country in Africa to eradicate polio; as of writing this book, no polio is reported in Nigeria since last year. Currently, polio remains endemic in two countries—Afghanistan and Pakistan. Until poliovirus transmission is interrupted in these countries, all countries remain at risk of importation of polio. Illiteracy, ignorance to vaccines, death threats, as well as killing of healthcare workers providing polio vaccines have slowed immunization programs in Pakistan. This toxic scenario coupled with the migration of people has led to the persistence of polio in Pakistan and neighboring Afghanistan. With awareness on the need of vaccination, knowledge on the importance of vaccination, and new rules that may penalize resistance to vaccination, it may be possible to eliminate polio by the end of the decade.

When I was given the opportunity to author this book (*Vaccine Design*: *Methods and Protocols*), I wished to have at least one chapter on vaccine design or vaccine development from every country. Unfortunately, it dawned on me later that not every country invests in science! It was also unfortunate to realize that research and development on vaccines is not a priority even in some developed countries with resources or influence. New sustainable technologies are to be developed to create more jobs and improve the well-being of humans as well as conservation of nature; hence, it is high time countries invest at least 5 % of their GDP for science including vaccine development.

Vaccine Design: *Methods and Protocols* is a practical guide providing step-by-step protocol to design and develop vaccines. The purpose of the book is to help vaccinologists develop novel vaccines based on current strategies employed to develop vaccines against several diseases. The book provides protocols for developing novel vaccines against infectious bacteria, viruses, and parasites for humans and animals as well as vaccines for cancer, allergy, and substance abuse. The book also contains chapters on how antigenic proteins

for vaccines should be selected and designed in silico, vectors for producing recombinant antigenic proteins, and the production of antigenic proteins in plant systems. Most vaccinologists are not aware of the intellectual property (IP) of vaccines, the importance of patents before commercialization, and what components of vaccines could be patented; hence, chapters on these aspects are also included in the book. The book also contains a chapter on the regulatory evaluation and testing requirements for vaccines.

The *Methods in Molecular Biology*™ series *Vaccine Design: Methods and Protocols* contains 103 chapters in two volumes. Volume 1, *Vaccines for Human Diseases*, has an introductory section on how vaccines impact diseases, the immunological mechanism of vaccines, and future challenges for vaccinologists and current trends in vaccinology. The design of human vaccines for viral, bacterial, fungal, parasitic, and prion diseases as well as vaccines for drug abuse, allergy, and tumor are also described in this volume. Volume 2, *Vaccines for Veterinary Diseases*, includes vaccines for farm animals and fishes, vaccine vectors and production, vaccine delivery systems, vaccine bioinformatics, vaccine regulation, and intellectual property.

It has been 220 years since Edward Jenner vaccinated his first patient in 1796. This book is a tribute to the pioneering effort of his work. My sincere thanks to all the authors for contributing to *Vaccine Design*: *Methods and Protocols* Volume 1 (*Vaccines for Human Diseases*) and Volume 2 (*Vaccines for Veterinary Diseases*). The book would not have materialized without the efforts of the authors from all over the world. I would also like to thank the series editor of *Methods in Molecular Biology*™, Prof. John M. Walker, for giving me the opportunity to edit this book. My profound thanks to my wife Jyothi for the encouragement and support, and also to our twins—Teresa and Thomas—for patiently waiting for me while editing the book. Working on the book was not an excuse for missing story time, and I made sure that you were told a couple of stories every day before bedtime.

Wynnewood, PA, USA ***Sunil Thomas***

The city name for Lankenau Institute for Medical Research has been corrected. An erratum can be found at DOI 10.1007/978-1-4939-3387-7_50

Contents

Contributors

Sepideh Aboutorabian • *Bioprocess Research and Development, Sanofi Pasteur, Toronto, ON, Canada*

Gustaf Ahlén • *Division of Clinical Microbiology, Department of Laboratory Medicine, F68, Karolinska University Hospital Huddinge, Karolinska Institutet, Stockholm, Sweden*

Chunqing Ai • *School of Food Science and Technology, Jiangnan University, Wuxi, Jiangsu, People's Republic of China*

Carl R. Alving • *Laboratory of Adjuvant and Antigen Research, US Military HIV Research Program, Walter Reed Army Institute of Research, Silver Spring, MD, USA*

Karen S. Anderson • *Center for Personalized Diagnostics, The Biodesign Institute, Arizona State University, Tempe, AZ, USA*

Annaliesa S. Anderson • *Pfizer Vaccine Research and Development Unit, Pearl River, NY, USA*

Salvador F. Ausar • *Bioprocess Research and Development, Sanofi Pasteur, Toronto, ON, Canada*

Kumar Avishek • *National Institute of Pathology, Safdarjung Hospital Campus, New Delhi, India*

Dale Barnard • *Institute for Antiviral Research, Utah State University, Logan, UT, USA*

Kristen A. Batich • *Duke Brain Tumor Immunotherapy Program, Division of Neurosurgery, Department of Surgery, Duke University Medical Center, Durham, NC, USA; Department of Pathology, Duke University Medical Center, Durham, NC, USA*

Nina Bhardwaj • *Division of Hematology and Medical Oncology, Department of Medicine, Icahn School of Medicine at Mount Sinai, New York, NY, USA*

Parna Bhattacharya • *Laboratory of Emerging Pathogens, Division of Emerging and Transfusion Transmitted Diseases, Center for Biologics Evaluation and Research, Food and Drug Administration, Silver Spring, MD, USA*

Roy Bicknell • *Institute for Biomedical Research, College of Medical and Dental Sciences, University of Birmingham, Birmingham, UK*

Vesna Blazevic • *Vaccine Research Center, University of Tampere Medical School, Tampere, Finland*

Jean-Luc Bodmer • *Genocea Biosciences, Cambridge, MA, USA*

Robert C. Brunham • *Vaccine Research Laboratory, UBC Centre for Disease Control, University of British Columbia, Vancouver, BC, Canada*

Manoj K. Chakrabarti • *Division of Pathophysiology, National Institute of Cholera and Enteric Diseases, Kolkata, West Bengal, India*

Benson Yee Hin Cheng • *Department of Microbiology and Immunology, University of Rochester School of Medicine and Dentistry, Rochester, NY, USA*

Jaemi S. Chu • *Department of Pathology and Laboratory Medicine, University of Pennsylvania, Philadelphia, PA, USA*

Richard Chubet • *Protein Sciences Corporation Inc., Meriden, CT, USA*

G. Travis Clifton • *Cancer Insight, LLC, San Antonio, TX, USA; Department of Surgical Oncology, MD Anderson Cancer Center, Houston, TX, USA*

Garry T. Cole • *Department of Biology and South Texas Center for Emerging Infectious Diseases, University of Texas, San Antonio, TX, USA*
James C. Cook • *Merck Research Laboratories, West Point, PA, USA*
Manon Cox • *Protein Sciences Corporation Inc., Meriden, CT, USA*
Alejandro Delgado Daza • *Thomas Jefferson University Hospital, Philadelphia, PA, USA*
Ranadhir Dey • *Laboratory of Emerging Pathogens, Division of Emerging and Transfusion Transmitted Diseases, Center for Biologics Evaluation and Research, Food and Drug Administration, Silver Spring, MD, USA*
Rima Dilbarova • *Lankenau Institute for Medical Research, Wynnewood, PA, USA; College of Arts and Sciences, Drexel University, Philadelphia, PA, USA*
Bardya Djahanshiri • *Department of Protein Evolution, Max Planck Institute for Developmental Biology, Tübingen, Germany; Department for Applied Bioinformatics, Goethe-University, Frankfurt, Germany*
Joseph Eiden • *Pfizer Vaccine Research and Development Unit, Pearl River, NY, USA*
Diego A. Espinosa • *Department of Molecular Microbiology and Immunology and Johns Hopkins Malaria Research Institute, Bloomberg School of Public Health, Johns Hopkins University, Baltimore, MD, USA*
Maria D. Esteve-Gassent • *Department of Veterinary Pathobiology, VMA316, College of Veterinary Medicine and Biomedical Sciences, Texas A&M University, College Station, TX, USA*
Marina Etcheverrigaray • *Cell Culture Laboratory, Biochemistry and Biological Sciences School, Universidad Nacional del Litoral, Santa Fe, Argentina*
Radwa Ewaisha • *Center for Personalized Diagnostics, School of Life Sciences, The Biodesign Institute, Arizona State University, Tempe, AZ, USA*
Valentina A. Feodorova • *Department for Anthroponosis and Zoonotic Diseases, Saratov Scientific and Research Veterinary Institute of the Federal Agency for Scientific Organizations, Saratov, Russia*
James M. Fleckenstein • *Division of Infectious Diseases, Department of Medicine, Washington University School of Medicine, Saint Louis, MO, USA; Molecular Microbiology and Molecular Pathogenesis Program, Division of Biology and Biomedical Sciences, Washington University School of Medicine, Saint Louis, MO, USA; Medicine Service, Veterans Affairs Medical Center, Saint Louis, MO, USA*
Diego Fontana • *Cell Culture Laboratory, Biochemistry and Biological Sciences School, Universidad Nacional del Litoral, Santa Fe, Argentina; Biotechnological Development Laboratory, Biochemistry and Biological Sciences School, Universidad Nacional del Litoral, Santa Fe, Argentina*
Leonard J. Foster • *Centre for High-Throughput Biology, Department of Biochemistry and Molecular Biology, University of British Columbia, Vancouver, BC, Canada*
Lars Frelin • *Department of Laboratory Medicine, Division of Clinical Microbiology, F68, Karolinska University Hospital Huddinge, Karolinska Institutet, Stockholm, Sweden*
Sreenivas Gannavaram • *Laboratory of Emerging Pathogens, Division of Emerging and Transfusion Transmitted Diseases, Center for Biologics Evaluation and Research, Food and Drug Administration, Silver Spring, MD, USA*
Thomas W. Geisbert • *Galveston National Laboratory University of Texas Medical Branch, Galveston, TX, USA; Department of Microbiology and Immunology, University of Texas Medical Branch, Galveston, TX, USA*
Luke R. Green • *Pfizer Vaccine Research and Development Unit, Pearl River, NY, USA*

Abdullah A.H. Ahmad Fuaad • *School of Chemistry and Molecular Biosciences, The University of Queensland, Brisbane, QLD, Australia*
Diane F. Hale • *Cancer Insight, LLC, San Antonio, TX, USA; San Antonio Military Medical Center, San Antonio, TX, USA*
Li Hao • *Pfizer Vaccine Research and Development Unit, Pearl River, NY, USA*
Manvi Hasija • *Bioprocess Research and Development, Sanofi Pasteur, Steeles Avenue West, Toronto, ON, Canada*
Jon H. Heinrichs • *Sanofi Pasteur, Swiftwater, PA, USA*
Kirsten Heiss • *Parasitology Unit, Center for Infectious Diseases, Heidelberg University Hospital, Heidelberg, Germany; MalVa GmbH, Heidelberg, Germany*
Kathy Holtz • *Protein Sciences Corporation Inc., Meriden, CT, USA*
Yoshikazu Honda-Okubo • *Vaxine Pty Ltd., Adelaide, Australia*
Chiung-Yu Hung • *Department of Biology and South Texas Center for Emerging Infectious Diseases, University of Texas at San Antonio, San Antonio, TX, USA; Biology Department, University of Texas at San Antonio, San Antonio, TX, USA*
Tetsuro Ikegami • *Department of Pathology, The University of Texas Medical Branch at Galveston, Galveston, TX, USA*
Nevien Ismail • *Laboratory of Emerging Pathogens, Division of Emerging and Transfusion Transmitted Diseases, Center for Biologics Evaluation and Research, Food and Drug Administration, Silver Spring, MD, USA*
Kathrin U. Jansen • *Pfizer Vaccine Research and Development Unit, Pearl River, NY, USA*
Tom Jones • *Pfizer Vaccine Research and Development Unit, Pearl River, NY, USA*
Joseph G. Joyce • *Merck Research Laboratories, West Point, PA, USA*
Anna Kabanova • *Department of Life Sciences, University of Siena, Siena, Italy*
Jerzy Karczewski • *Fraunhofer USA Center for Molecular Biotechnology, Newark, DE, USA*
Karuna P. Karunakaran • *Vaccine Research Laboratory, UBC Centre for Disease Control, University of British Columbia, Vancouver, Canada*
Yuki Kinjo • *Department of Chemotherapy and Mycoses, National Institute of Infectious Diseases, Tokyo, Japan*
Ricardo Kratje • *Cell Culture Laboratory, Biochemistry and Biological Sciences School, Universidad Nacional del Litoral, Santa Fe, Argentina*
Sri Krishna • *Center for Personalized Diagnostics, The Biodesign Institute, Arizona State University, Tempe, AZ, USA; School of Biological and Health Systems Engineering, Arizona State University, Tempe, AZ, USA*
Chanoch Kronman • *The Department of Biochemistry and Molecular Genetics, Israel Institute for Biological Research, Ness-Ziona, Israel*
Jean C. Lee • *Division of Infectious Diseases, Department of Medicine Brigham and Women's Hospital and Harvard Medical School, Boston, MA, USA*
Jack C. Leo • *Department of Biosciences, University of Oslo, Oslo, Norway*
Xiao-Feng Li • *Department of Virology, Beijing Institute of Microbiology and Epidemiology, Beijing, China*
Daniele Lilleri • *Laboratori Sperimentali di Ricerca, Area Trapiantologica, Fondazione Istituto di Ricovero e Cura a Carattere Scientifico Policlinico San Matteo, Pavia, Italy*
Dirk Linke • *Department of Biosciences, University of Oslo, Oslo, Norway; Department of Protein Evolution, Max Planck Institute for Developmental Biology, Tübingen, Germany*
Lawrence L. Livornese Jr • *Drexel University School of Medicine, Philadelphia, PA, USA; Department of Medicine, Lankenau Medical Center, Wynnewood, PA, USA*

Felix F. Loeffler • *Karlsruhe Institute of Technology, Institute of Microstructure Technology, Karlsruhe, Germany*
Nandadeva Lokugamage • *Department of Pathology, The University of Texas Medical Branch at Galveston, Galveston, TX, USA*
Hoai J. Ly • *Department of Pathology, The University of Texas Medical Branch at Galveston, Galveston, TX, USA*
Marthandan Mahalingam • *Department of Biology, The Catholic University of America, Washington, DC, USA*
Shinji Makino • *Department of Microbiology and Immunology, The University of Texas Medical Branch at Galveston, Galveston, TX, USA*
Maria Malm • *Vaccine Research Center, University of Tampere Medical School, Tampere, Finland*
Kristen Marciniuk • *Department of Biochemistry, University of Saskatchewan, Saskatoon, SK, Canada; Vaccine and Infectious Disease Organization, University of Saskatchewan, Saskatoon, SK, Canada*
Luis Martínez-Sobrido • *Department of Microbiology and Immunology, University of Rochester School of Medicine and Dentistry, New York, NY, USA*
Gary R. Matyas • *Laboratory of Adjuvant and Antigen Research, US Military HIV Research Program, Walter Reed Army Institute of Research, Silver Spring, MD, USA*
Ohad Mazor • *The Department of Biochemistry and Molecular Genetics, Israel Institute for Biological Research, Ness-Ziona, Israel*
Lisa K. McNeil • *Pfizer Vaccine Research and Development Unit, Pearl River, NY, USA*
Clifton McPherson • *Protein Sciences Corporation Inc., Meriden, CT, USA*
Marcia Meseck • *Division of Hematology and Medical Oncology, Department of Medicine, Icahn School of Medicine at Mount Sinai, New York, NY, USA*
Marcin Michalik • *Department of Biosciences, University of Oslo, Oslo, Norway; Department of Protein Evolution, Max Planck Institute for Developmental Biology, Tübingen, Germany*
Chad E. Mire • *Galveston National Laboratory, University of Texas Medical Branch, Galveston, TX, USA; Department of Microbiology and Immunology, University of Texas Medical Branch, Galveston, TX, USA*
Yoshitsugu Miyazaki • *Department of Chemotherapy and Mycoses, National Institute of Infectious Diseases, Tokyo, Japan*
Mario A. Monteiro • *University of Guelph, Guelph, ON, Canada*
Vladimir L. Motin • *Department of Pathology, Department of Microbiology and Immunology, University of Texas Medical Branch, Galveston, TX, USA*
Shin Murakami • *Department of Veterinary Microbiology, Graduate School of Agricultural and Life Sciences, The University of Tokyo, Bunkyo-ku, Tokyo, Japan*
Waithaka Mwangi • *Department of Veterinary Pathobiology, VMA316, College of Veterinary Medicine and Biomedical Sciences, Texas A&M University, College Station, TX, USA*
Debbie D. Nahas • *Merck Research Laboratories, West Point, PA, USA*
Hira L. Nakhasi • *Laboratory of Emerging Pathogens, Division of Emerging and Transfusion Transmitted Diseases, Center for Biologics Evaluation and Research, Food and Drug Administration, Silver Spring, MD, USA*
Puja H. Nambiar • *Thomas Jefferson University Hospital, Philadelphia, PA, USA*

Scott Napper • *Department of Biochemistry, University of Saskatchewan, Saskatoon, SK, Canada; Vaccine and Infectious Disease Organization, University of Saskatchewan, Saskatoon, SK, Canada*
Kayo Ohkouchi • *Department of Chemotherapy and Mycoses, National Institute of Infectious Diseases, Tokyo, Japan*
George E. Peoples • *Cancer Insight, LLC, San Antonio, TX, USA*
John Perez • *Pfizer Vaccine Research and Development Unit, Pearl River, NY, USA*
Nikolai Petrovsky • *Department of Diabetes and Endocrinology, Flinders University, Adelaide, Australia; Vaxine Pty Ltd., Adelaide, Australia*
Johannes Pfeil • *Parasitology Unit, Center for Infectious Diseases, Heidelberg University Hospital, Heidelberg, Germany; General Pediatrics, Center for Pediatric and Adolescent Medicine, Heidelberg University Hospital, Heidelberg, Germany*
Debasis Pore • *Department of Immunology, Lerner Research Institute, Cleveland Clinic, Cleveland, OH, USA*
George C. Prendergast • *Lankenau Institute for Medical Research, Wynnewood, PA, USA; Department of Pathology, Anatomy and Cell Biology, Sidney Kimmel Medical School, Thomas Jefferson University, Philadelphia, PA, USA; Sidney Kimmel Cancer Center, Thomas Jefferson University, Philadelphia, PA, USA*
Claudio Prieto • *Cell Culture Laboratory, Biochemistry and Biological Sciences School, Universidad Nacional del Litoral, Santa Fe, Argentina; Biotechnological Development Laboratory, Biochemistry and Biological Sciences School, Universidad Nacional del Litoral, Santa Fe, Argentina*
Cheng-Feng Qin • *Department of Virology, Beijing Institute of Microbiology and Epidemiology, Beijing, China*
Xiangguo Qiu • *Special Pathogens Program, National Microbiology Laboratory, Public Health Agency of Canada, Winnipeg, MB, Canada; Department of Medical Microbiology, University of Manitoba, Winnipeg, MB, Canada*
Andrea J. Radtke • *Department of Molecular Microbiology and Immunology and Johns Hopkins Malaria Research Institute, Bloomberg School of Public Health, Johns Hopkins University, Baltimore, MD, USA; Lymphocyte Biology Section, Laboratory of Systems Biology, National Institute of Allergy and Infectious Diseases, National Institutes of Health, Bethesda, MD, USA*
Sima Rafati • *Department of Immunotherapy and Leishmania Vaccine Research, Pasteur Institute of Iran, Tehran, Iran*
Nausheen Rahman • *Bioprocess Research and Development, Sanofi Pasteur, Steeles Avenue West, Toronto, ON, Canada*
Venigalla B. Rao • *Department of Biology, The Catholic University of America, Washington, DC, USA*
Rino Rappuoli • *GSK Vaccines, Siena, Italy*
David A. Rasko • *Department of Microbiology and Immunology, Institute for Genome Sciences, University of Maryland School of Medicine, Baltimore, MD, USA*
Rachel Lubong Sabado • *Division of Hematology and Medical Oncology, Department of Medicine, Icahn School of Medicine at Mount Sinai, New York, NY, USA*
Tamar Sabo • *The Department of Biochemistry and Molecular Genetics, Israel Institute for Biological Research, Ness-Ziona, Israel*
Poonam Salotra • *National Institute of Pathology, Safdarjung Hospital Campus, New Delhi, India*

John H. Sampson • *Duke Brain Tumor Immunotherapy Program, Division of Neurosurgery, Department of Surgery, Duke University Medical Center, Durham, NC, USA; Department of Pathology, Duke University Medical Center, Durham, NC, USA; Department of Radiation Oncology, Duke University Medical Center, Durham, NC, USA; Department of Immunology, Duke University Medical Center, Durham, NC, USA; The Preston Robert Tisch Brain Tumor Center, Duke University Medical Center, Durham, NC, USA*
Abhay Satoskar • *Departments of Pathology and Microbiology, Wexner Medical Center, The Ohio State University, Columbus, OH, USA*
Lidiya V. Sayapina • *Department of Vaccine Control, Scientific Center for Expertise of Medical Application Products, Moscow, Russia*
Erika Schneble • *Cancer Insight, LLC, San Antonio, TX, USA*
Susan Secore • *Merck Research Laboratories, West Point, PA, USA*
Angamuthu Selvapandiyan • *Institute of Molecular Medicine, New Delhi, India*
Negar Seyed • *Department of Immunotherapy and Leishmania Vaccine Research, Pasteur Institute of Iran, Tehran, Iran*
Mariusz Skwarczynski • *School of Chemistry and Molecular Biosciences, The University of Queensland, St Lucia, QLD, Australia*
Christina M. Small • *Department of Veterinary Pathobiology, VMA316, College of Veterinary Medicine and Biomedical Sciences, Texas A&M University, College Station, TX, USA*
Johannes Sollner • *Sodatana e.U., Wien, Austria*
Adam M. Swartz • *Duke Brain Tumor Immunotherapy Program, Division of Neurosurgery, Department of Surgery, Duke University Medical Center, Durham, NC, USA; Department of Pathology, Duke University Medical Center, Durham, NC, USA*
Tahereh Taheri • *Department of Immunotherapy and Leishmania Vaccine Research, Pasteur Institute of Iran, Tehran, Iran*
Hidenori Takagi • *Functional Crop Research and Development Unit, National Institute of Agrobiological Sciences, Tsukuba, Ibaraki, Japan*
Fumio Takaiwa • *Functional Crop Research and Development Unit, National Institute of Agrobiological Sciences, Tsukuba, Ibaraki, Japan*
Kirsi Tamminen • *Vaccine Research Center, University of Tampere Medical School, Tampere, Finland*
Pan Tao • *Department of Biology, The Catholic University of America, Washington, DC, USA*
Ryan Taschuk • *Department of Biochemistry, University of Saskatchewan, Saskatoon, SK, Canada; Vaccine and Infectious Disease Organization, University of Saskatchewan, Saskatoon, SK, Canada; School of Public Health, University of Saskatchewan, Saskatoon, SK, Canada*
Kaori Terasaki • *Department of Microbiology and Immunology, The University of Texas Medical Branch at Galveston, Galveston, TX, USA*
Sunil Thomas • *Lankenau Institute for Medical Research, Wynnewood, PA, USA*
Juan Carlos de la Torre • *Department of Immunology and Microbial Science, The Scripps Research Institute, La Jolla, CA, USA*
Oscar B. Torres • *Laboratory of Adjuvant and Antigen Research, US Military HIV Research Program, Walter Reed Army Institute of Research, Silver Spring, MD, USA; U.S. Military HIV Research Program, Henry M. Jackson Foundation for the Advancement of Military Medicine, Bethesda, MD, USA*

Istvan Toth • *School of Chemistry and Molecular Biosciences, The University of Queensland, Brisbane, QLD, Australia; School of Pharmacy, The University of Queensland, Woolloongabba, QLD, Australia*
Yusuke Tsujimura • *Laboratory of Immunoregulation and Vaccine Research, Tsukuba Primate Research Center, National Institute of Biomedical Innovation, Health and Nutrition, Tsukuba, Ibaraki, Japan*
Keigo Ueno • *Department of Chemotherapy and Mycoses, National Institute of Infectious Diseases, Tokyo, Japan*
Makoto Urai • *Department of Chemotherapy and Mycoses, National Institute of Infectious Diseases, Tokyo, Japan*
Daniel O. Villarreal • *Department of Pathology and Laboratory Medicine, University of Pennsylvania, Philadelphia, PA, USA*
Hong-Jiang Wang • *Department of Virology, Beijing Institute of Microbiology and Epidemiology, Beijing, China*
Linhui Wang • *Research and Development Center, Dalian Hissen Bio-pharm. Co., Ltd., Dalian, Liaoning Province, China*
David B. Weiner • *Department of Pathology and Laboratory Medicine, University of Pennsylvania, Philadelphia, PA, USA*
Michael A. Whitt • *Department of Microbiology, Immunology, and Biochemistry, University of Tennessee Health Science Center, Memphis, TN, USA*
Gary Wong • *Special Pathogens Program, National Microbiology Laboratory, Public Health Agency of Canada, Winnipeg, MB, Canada; Department of Medical Microbiology, University of Manitoba, Winnipeg, MB, Canada*
Karen L. Wozniak • *Department of Biology and South Texas Center for Emerging Infectious Diseases, University of Texas at San Antonio, San Antonio, TX, USA*
Rachel F. Xoconostle • *Merck Research Laboratories, West Point, PA, USA*
Yasuhiro Yasutomi • *Laboratory of Immunoregulation and Vaccine Research, Tsukuba Primate Research Center, National Institute of Biomedical Innovation, Health and Nutrition, Tsukuba, Ibaraki, Japan; Department of Immunoregulation, Mie University Graduate School of Medicine, Tsu, Mie, Japan*
Hong Yu • *Vaccine Research Laboratory, UBC Centre for Disease Control, University of British Columbia, Vancouver, Canada*
Fidel Zavala • *Department of Molecular Microbiology and Immunology and Johns Hopkins Malaria Research Institute, Bloomberg School of Public Health, Johns Hopkins University, Baltimore, MD, USA*
Fred Zepp • *Department of Pediatrics, University Medicine Mainz, Mainz, Germany*
Qiuxiang Zhang • *School of Food Science and Technology, Jiangnan University, Wuxi, Jiangsu, People's Republic of China*
Xiaodong Zhuang • *Institute for Biomedical Research, College of Medical and Dental Sciences, University of Birmingham, Birmingham, UK*

Part I

Vaccines: Introduction

Chapter 1

Clinical Impact of Vaccine Development

Puja H. Nambiar, Alejandro Delgado Daza, and Lawrence L. Livornese Jr

Abstract

The discovery and development of immunization has been a singular improvement in the health of mankind. This chapter reviews currently available vaccines, their historical development, and impact on public health. Specific mention is made in regard to the challenges and pursuit of a vaccine for the human immunodeficiency virus as well as the unfounded link between autism and measles vaccination.

Key words Vaccination, Immunization, Vaccine development, Public health, History of medicine

1 Introduction

Vaccination (Latin; *vacca*: cow) and sanitation have saved more lives and improved the public's health than any other medical intervention. Even before the germ theory of disease was established artificial induction was practiced in Asia and Europe [1]. Variolation, the process of obtaining pus from a smallpox vesicle and introducing it into the skin of an uninfected patient, was performed by people in various regions of Asia in the 1500s. This practice was observed by Lady Mary Wortley Montagu in Istanbul and introduced by her to England in 1721. Variolation, while effective, was not reliable and carried the real risk of developing smallpox from the process.

In 1774 an English farmer, Benjamin Jesty, noted that he was immune to smallpox after becoming infected with cowpox; subsequently, he successfully inoculated his wife and children and they were protected from smallpox as well. In 1798, Edward Jenner proved that large-scale inoculation with cowpox was an effective means of combating smallpox. In 1880, Louis Pasteur published work demonstrating that an attenuated form of the bacteria, *Pasteurella multocida*, could be used to produce a protective vaccine in animals. The following year, Pasteur's public demonstration of the effectiveness of an anthrax vaccine in sheep marked the beginning of a new era; it was now possible that vaccines could be reliably produced in a standardized, repeatable fashion.

Sunil Thomas (ed.), *Vaccine Design: Methods and Protocols: Volume 1: Vaccines for Human Diseases*, Methods in Molecular Biology, vol. 1403, DOI 10.1007/978-1-4939-3387-7_1,

The history of vaccination, however, has not been without missteps or controversy. Early vaccines contained cells and bodily fluids and there was the legitimate concern that other infections could be transmitted through vaccination; the use of glycerin reduced this risk. The concept of introducing an infectious agent into healthy persons has been met with resistance from the start. For a time variolation was a felony crime in England. When Pasteur's rabies vaccine saved the life of Joseph Meister there was a public outcry in response to the process of purposefully injecting a lethal pathogen into a human—even one who was suffering from a uniformly fatal disease. The 1955 Cutter Incident, in which recipients of killed polio vaccine developed clinical disease due to the presence of live virus, resulted in 40,000 cases of vaccine-associated abortive polio, 164 cases of paralysis, and 10 deaths [2]. A 1998 Lancet paper by Andrew Wakefield that proposed a link between the measles-mumps-rubella vaccine and autism led to a widespread public loss of confidence in vaccines. The paper was subsequently found to be fraudulent and was withdrawn by the Lancet [3, 4]; however this, combined with the disproven theory that the thimerosal preservative in vaccines caused autism, continues to erode the public's confidence in vaccination [5].

Despite the unquestioned effectiveness and safety of vaccinations there continues to be groups of individuals who eschew vaccination for various scientific and religious beliefs. In the developing world, vaccination rates remain low for many contagious diseases. Until vaccination rates in both of these groups are increased the effectiveness of even the best designed vaccines will be limited and the public will remain at risk. In the following sections we review major vaccine-preventable diseases and the clinical impact that vaccination has had upon them.

2 Adenovirus Vaccines

Human adenoviruses are large, icosahedral, double-stranded DNA viruses belonging to family *Adenoviridae* [6]. They are further classified into seven species (A–G) and 52 serotypes. The history of *Adenoviruses* dates back to the 1950s when they were identified as a common cause for respiratory disease in children and US military trainees [7, 8]. In 1960s, the viruses caused significant morbidity and mortality among US military trainees.

Adenoviruses are spread primarily by respiratory droplets, fecooral route [9], or via direct contact. Close crowding promotes spread of virus. High-risk groups include children in day care centers and military trainees. Clinical syndromes associated with adenovirus infections in humans include respiratory adenovirus in children, acute respiratory disease (ARD) in military recruits, epidemic keratoconjunctivitis, pharyngoconjunctival fever,

hemorrhagic cystitis, infantile gastroenteritis, encephalitis, and opportunistic like infections in immunocompromised humans. Currently, there are no evidence-based guidelines supporting any specific antiviral treatment or prophylaxis for adenoviral illness. The off-label use of ribavirin and cidofovir has produced mixed results in immunocompromised patients with severe life-threatening adenoviral disease.

The first adenovirus vaccine was developed at the Walter Reed Army Institute of Research in 1956. It was an inactivated [10], injectable vaccine that protected against adenovirus infections caused by types 4 and 7. Production of this vaccine was terminated due to manufacturing issues. In 1971, Wyeth Laboratories developed live, oral enteric coated vaccines for adenovirus types 4 and 7. The rates of ARD dramatically reduced in the vaccine era. Unfortunately, the successful immunization program ended in 1999. Increasing mortality from adenovirus ARD in the postvaccination era resulted in the resumption of vaccine production for the military. Ad4 and Ad7 enteric coated live oral vaccines were reintroduced by Teva in 2011.

The CDC recommends two oral tablets to be swallowed [11], one tablet of adenovirus type 4 and one tablet of adenovirus type 7, as part of immunization schedule to military recruits, aged 17–50, who are beginning basic training. The most common side effects include nasal congestion, headache, upper respiratory infections, nausea, vomiting, and diarrhea. This vaccine is contraindicated in pregnancy and in those with anaphylaxis to vaccine components. Adenovirus vaccine in addition to secondary preventive measures including frequent hand washing, reducing crowded conditions, and cohorting has shown considerable reduction in ARD rates. A cost–benefit analysis estimated prevention of 4555 cases and $2.6 million savings with year-round vaccination [12]. Clinical trials have shown 94.5 % seroconversion, 99.3 % efficacy with Ad4 vaccine, and 93.8 % with Ad7 vaccine [13].

3 Anthrax Vaccines

Anthrax is a zoonotic disease caused by a spore-forming gram-positive bacilli *Bacillus anthracis* found in the soil. Human disease presents in three distinct clinical forms: cutaneous, inhalational, and gastrointestinal anthrax [14]. Injectional anthrax has also been described in intravenous heroin users [15]. Additionally, *Bacillus anthracis* is a Category A agent of bioterrorism.

Historically, researchers believe that anthrax originated in Egypt in 1250 BC and was responsible for the fifth and sixth biblical plagues. Clinically the disease was first described in the 1700s. In 1877, the German microbiologist, Robert Koch, studied *Bacillus anthracis* and described the causal relationship between

this specific bacterium and anthrax. In 1881, Louis Pasteur created the first vaccine using an attenuated strain of anthrax bacteria. Human anthrax was reported worldwide in the 1900s with industrial cases arising in developed countries and agricultural cases in developing Asian and African countries. With the advent of the first animal vaccine by Max Sterne in 1937 the number of human cases of anthrax dwindled. The first human vaccine against anthrax was created in the 1950s. Even though the incidence of human disease remains low, the use of *Bacillus anthracis* as a biologic weapon created the driving force for an improved human vaccine.

Anthrax is rare in the USA owing to vaccinations of livestock but remains common in developing countries that lack animal vaccination programs [16]. The bacterium produces highly resistant spores that can survive extreme environmental conditions for prolonged periods of time. The pathogenesis of disease in humans is attributed to the virulence factor of the capsule and production of two exotoxins. The anthrax toxin has three components—protective antigen (PA), lethal factor (LF), and edema factor (EF). The protective antigen with the edema factor forms the anthrax edema toxin responsible for cyclic AMP-mediated tissue swelling either in skin or mediastinum. The protective antigen with the lethal factor forms the anthrax lethal toxin responsible for cell death.

All three clinical presentations of anthrax have an incubation period of approximately 2–5 days. The cutaneous form of anthrax initially presents as a small, painless, pruritic papule that subsequently develops into a 1–2 cm large fluid-filled vesicle associated with surrounding edema, erythema, regional lymphadenopathy, and mild systemic symptoms. The vesicle ruptures in 5–7 days leaving behind an ulcer with black eschar which eventually falls off without a scar in 2–3 weeks. Antibiotics do not alter the development of cutaneous lesion. Inhalational anthrax manifests with nonspecific symptoms of myalgias, fever, and upper respiratory infection within 1–5 days of inhalation of infectious doses of *B. anthracis.* Patients then acutely develop respiratory distress syndrome from pulmonary hemorrhage and edema, and may die within 24 h. Widening of the mediastinum is a classic radiographic finding that develops secondary to lymphatic and vascular obstruction. If left untreated inhalational anthrax is 100 % fatal. Gastrointestinal anthrax develops after ingestion of anthrax-infected meat. Symptoms include abdominal pain, nausea, vomiting, diarrhea, and hematemesis with progression to septic shock and death. All three primary forms of anthrax can also manifest with bacteremia and secondary meningitis. Anthrax does not spread from person to person. Treatment involves decontamination and use of antibiotics such as ciprofloxacin, doxycycline, and penicillin. Passive immunization with human monoclonal anti-PA antibody, raxibacumab, has been approved for use in inhalational anthrax.

The human anthrax vaccine, anthrax vaccine adsorbed (AVA), is produced from a cell-free culture filtrate of attenuated,

non-encapsulated strain V770-NPI-R of *B. anthracis*. It predominantly contains the protective antigen adsorbed to aluminum hydroxide. This vaccine is mainly recommended for certain members of the US military, laboratory workers who work with anthrax [17], and individuals who work with animal and animal products. The vaccine is an intramuscular injection given as five shots at 0 and 4 weeks and 6, 12, and 18 months with annual booster [17]. For postexposure prophylaxis [17], three injections of AVA at 0, 2, and 4 weeks plus 60 days of antibiotics have been recommended. Side effects of the vaccine include mild local reaction and nonspecific systemic symptoms such as low-grade fever, headache, and myalgia. The only contraindication is hypersensitivity to the vaccine. There have been no controlled clinical trials in humans to determine either the efficacy of AVA or its use along with antibiotics for postexposure prophylaxis. However the use of AVA has reduced the incidence of anthrax among industrial and agricultural workers.

4 Cholera Vaccines

Cholera is an acute diarrheal illness caused by the bacterium *Vibrio cholerae*. It is one of the oldest infectious diseases known to mankind. In the eighteenth century the disease spread from its original reservoir, the Ganges Delta in India, causing epidemics and pandemics resulting in the death of massive numbers of people across the globe.

Cholera is an intestinal infection with toxigenic strains of *V. cholerae* serogroups O1 and O139. *V. cholerae* O1 serogroup is further classified into two serotypes—Ogawa and Inaba—and two biotypes—classical and El Tor. The mode of transmission is through ingestion of contaminated food and water [18]. The disease occurs in children and adults especially in the lower socioeconomic groups. The short incubation period of 2 h to 5 days is responsible for exponential wave of this disease. Following consumption of infected food, the bacterium uses its virulence factors—toxin-coregulated pilus (TCP) [19], hemagglutinin [20], and single flagellum to colonize the small intestine and secretes cholera enterotoxin (CT). The "-B-" subunit of CT binds to the GM1 ganglioside receptor, facilitating entry into the intestinal mucosal cells and "-A-" subunit activates adenyl cyclase leading to excess fluid and salt secretion. Clinical symptoms include acute diarrhea and vomiting rapidly leading to electrolyte imbalances, hypovolemic shock, multiorgan failure, and death. Cholera can be fatal if there is a delay in replacement of fluid and electrolytes. Diagnosis is made clinically and by identifying the bacterium in stool cultures. Serologic tests are available but are nonspecific.

The global annual incidence of cholera is uncertain but the approximate cases may be 3–5 million causing 100,000–120,000

deaths. More than half the cases occur in Africa and remainder in Asia. There have been sporadic cases along the US Gulf Coast associated with undercooked or contaminated seafood. The majority of other cases in the developed countries are secondary to travel to endemic areas.

The preparation of the earliest vaccine against cholera began in the late eighteenth century. Initial studies were made with a parenteral killed whole-cell cholera vaccine in the 1880s which had limited use owing to short-term efficacy. The currently licensed cholera vaccines contain either genetically attenuated strains, killed organisms, or antigens. Three oral vaccines—two killed and one live—have been developed and licensed in several countries. The whole-cell killed vaccine plus CTB (WC-rCTB/Dukoral) contains killed strains of *V. cholerae* O1 (classical, El Tor, Ogawa, and Inaba) with B subunit of cholera toxin. The vaccine is given as two oral doses combined with a liquid oral buffer, 7–14 days apart in adults and in three doses in children 2–6 years of age with need for further booster doses. The vaccine is WHO prequalified but remains experimental in the USA. The reformulated bivalent killed whole-cell-only vaccine (WC-only/Shancol in India/mORCVAX in Vietnam) contains killed whole cells of *V. cholerae* O1 and O139. It is given as two doses 2 weeks apart with further boosters at 3-year intervals. Since the vaccine does not contain the gastric acid-labile cholera toxin subunit, it does not have to be coadministered with a buffer. The only live oral cholera vaccine is CVD103-HgR (Orochol or Mutachol). The vaccine is a live attenuated Inaba strain, which is genetically engineered to express CTB subunit and not the active CTA subunit. The vaccine is administered as a single oral dose with a buffer and does not require booster doses. The live vaccine has not been prequalified by WHO.

The WHO recommends the use of the two killed oral vaccines in cholera endemic areas and areas at risk for outbreaks [21]. The cholera vaccine is unavailable in the USA and CDC does not recommend cholera vaccines to most travelers owing to short-term and incomplete protection. These vaccines however cannot replace the pivotal role played by hygiene and proper sanitation in the control of cholera outbreaks.

5 Diphtheria Toxoid

Diphtheria is an acute toxin-mediated disease caused by *Corynebacterium diphtheriae*, a gram-positive bacillus that is acquired via the respiratory tract. The disease has been well described throughout history with Hippocrates famously writing about it in the fifthcentury BC. Outbreaks throughout Europe occurred as early as the fifteenth century. Spain experienced a major epidemic, in 1613, known as "El Año de los garrotillos," the year of strangulation [22].

Corynebacterium diphtheriae is a toxin-producing gram-positive bacillus. It has three biotypes: gravis, intermedius, and mitis, with the most severe forms of disease being produced by the gravis serotype. Susceptible persons may acquire toxigenic bacillus in the nasopharynx. The organism produces a toxin that inhibits protein synthesis and is responsible for local tissue disease and membrane formation. The locally produced toxin is absorbed into the bloodstream and transferred to other tissues.

The clinical presentation of diphtheria can be insidious with an incubation period of 1–5 days. Usually the symptoms are nonspecific and mild in the initial stages with fever and mild pharyngeal erythema being common. Within 3–4 days patches of exudate appear that coalesce to form membranes covering the entire pharynx [22]. As the disease progresses, large adenopathies become evident and patients begin to appear toxic. Attempts to remove the membranes often result in bleeding. Patients may recover following this stage. If enough toxin has been produced, patients may develop acute disease with prostration, coma, and high fevers. Marked edema and adenopathy may result in the classic "bullneck" appearance. Although pharyngeal diphtheria is the most common form of the disease in unimmunized populations, other skin or mucosal sites may be involved. This includes the nasopharynx, cutaneous, vaginal, and conjunctival forms. Invasive disease is very rare and is due to nontoxigenic strains of *C. diphtheriae*. Most complications of diphtheria, including death, are attributable to the toxin. Myocarditis can occur early in the disease process or appear weeks later. When it does occur, it is often fatal. Neuritis often affects motor nerves and can cause pharyngeal paralysis. The overall mortality of diphtheria is 5–10 % with rates as high as 20 % in those younger than 5 years or older than 40 [22].

Diphtheria antitoxin produced from horses was first used in the USA in 1891 and it was commercially produced in Germany in 1892. Equine diphtheria antitoxin is produced by hyperimmunizing horses with diphtheria toxoid and toxin. To prevent reactivity from horse serum, current preparations are semi-purified by techniques that concentrate IgG and remove as much extraneous proteins as possible. Diphtheria antitoxin is used for the treatment of infected patients and, in the past, for persons with high-level exposures.

The development of an effective toxoid, a combination of toxin-antitoxin, was achieved in the 1920s. Beginning in the 1940s, this was combined with the pertussis vaccine and became widely used. Diphtheria toxoid is produced by growing toxigenic *C. diphtheriae* in liquid medium. The filtrate is incubated with formaldehyde to convert toxin to toxoid and is then adsorbed onto an aluminum salt. Diphtheria toxoid is available combined with tetanus toxoid as pediatric diphtheria-tetanus toxoid (DT) or adult tetanus-diphtheria (Td), and with both tetanus toxoid and acellular pertussis vaccine as DTaP and Tdap. Diphtheria toxoid is also

available as combined DTaP-HepB-IPV (Pediarix) and DTaP-IPV/Hib (Pentacel) [23].

After a primary series of three properly spaced diphtheria toxoid doses in adults or four doses in infants, a protective level of antitoxin (defined as greater than 0.1 IU of antitoxin/mL) is reached in more than 95 %. Diphtheria toxoid has been estimated to have a clinical efficacy of 97 % [2]. Revaccination is recommended every 10 years.

6 Haemophilus Influenza Vaccines

Haemophilus influenzae is an important cause of severe bacterial infections in children younger than 5 years. It was first identified by Koch in 1883 but it was not until the influenza pandemic in 1918 that *H. influenzae* was recognized as a cause for secondary infection and not the primary cause of influenza [24]. In 1931, Pittman [25] demonstrated two categories of *H. influenzae*-encapsulated and nonencapsulated forms and further designated six serotypes (a–f) [25] on the basis of capsular properties. *H. influenzae* type b (Hib) was responsible for 95 % [26] serious invasive bacterial infections in the prevaccine era.

Haemophilus influenzae is an aerobic, non-spore-forming gram-negative coccobacillus. It requires two factors "X" (hemin) and "V" (nicotinamide adenine dinucleotide) [27] for in vitro growth, a property that distinguishes it from other *Haemophilus* species. The polyribosyl-ribitol-phosphate polysaccharide capsule is responsible for virulence and immunity. Hib colonizes nasopharynx (asymptomatic carriers) and is spread through respiratory droplets. Antecedent viral infections may play a role in invasive disease. Common invasive presentations include meningitis, pneumonia, otitis media, epiglottitis, septicemia, cellulitis, and osteoarticular infections. Non-type-b-encapsulated *H. influenzae* rarely causes invasive disease. A positive culture of *H. influenzae* from infected sterile body fluid or detection of Hib polysaccharide antigen in CSF is diagnostic. Serotyping is extremely important as type b isolated in children younger than 15 years is a potentially vaccine-preventable disease.

The first-generation pure polysaccharide vaccine (HbPV) was introduced in the early 1980s in the USA but was not immunogenic in children younger than 18 months and had variable efficiency in older children (age-dependent vaccine response). It was used until 1988 and is no longer available in the USA. The conjugation of the polysaccharide to the "carrier" protein results in a T-dependent antigen and increases immunogenicity and boosts response. The annual incidence of invasive Hib disease before the use of conjugate vaccine was 20–88 cases per 100,000 cases in the USA and has dramatically reduced ever since its introduction. Four conjugate Hib vaccines have

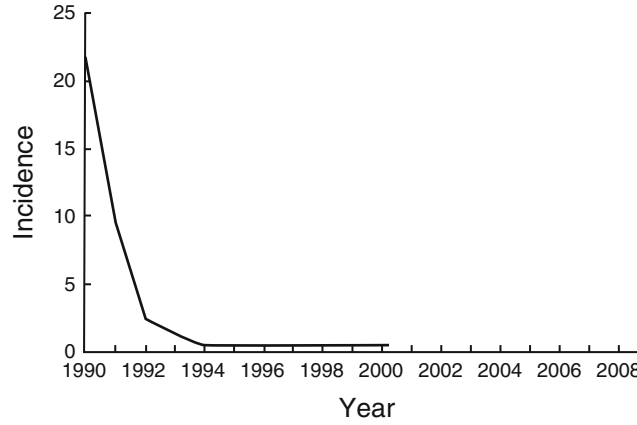

Fig. 1 Incidence of invasive Hib disease 1990–2009 (rate per 100,000 children less than 5 years of age). Graph from CDC/vaccines/pinkbook/hib

been developed [28]. The first *H. influenzae* type b polysaccharide-protein conjugate vaccine (PRP-diphtheria toxoid conjugate) was licensed in 1987 and is no longer available. The Haemophilus b oligosaccharide conjugate (HbOC) licensed in 1990 contains oligosaccharides from purified PRP from Hib Eagan strain coupled with nontoxic variant of diphtheria toxin isolated by *Corynebacterium diphtheriae*. The PRP-OMP vaccine was also licensed in 1990 and is a purified PRP from Hib Ross strain covalently bonded to an outer membrane protein complex of *Neisseria meningitides* strain B11. PRP-T is covalently bound PRP to tetanus toxoid and was licensed in 1993. The three HiB conjugate vaccines licensed for use are interchangeable. The Advisory Committee on Immunization Practices (ACIP) recommends start of immunization as early as 6 weeks of age with total of three doses of any combination HiB vaccines before the first birthday and a booster dose at 12–15 months of age. The only contraindication is hypersensitivity to vaccine components. HiB is not routinely recommended for persons 5 years and older; it can be considered in special situations such as asplenia, sickle cell anemia, or HIV infection (Fig. 1).

The routine use of HiB conjugate vaccine has dramatically decreased disease in developed countries and shown to be highly effective in reducing the incidence of disease in developing countries. Efforts are under way by the WHO to increase awareness and global availability of this effective vaccine especially in resource-limited countries.

7 Hepatitis A Vaccines

The first description of hepatitis or "episodic jaundice" dates back to the time of Hippocrates, and the earliest outbreaks were reported in Europe in the seventeenth and eighteenth centuries [29].

During World War II the scientific details regarding this disease were obtained. Hepatitis A was epidemiologically differentiated from hepatitis B in 1940s but it was only in 1970s that serological tests were developed to definitively diagnose this disease.

Hepatitis A occurs worldwide but is endemic in Central, South America, Asia, the Middle East, and Africa. It is caused by *hepatitis A virus (HAV)*, a non-enveloped RNA virus belonging to the family of *Picronaviridae*. Humans are the only natural host. HAV is resistant to most organic solvents and detergents and can survive at a pH as low as 3 but can be inactivated by high temperature (>85 °C), chlorine, and formalin [30]. *HAV* infection is acquired through fecal-oral route either by person-person contact or through ingestion of contaminated food or water. The incubation period is approximately 28 days [31]. *HAV* replicates in the liver; infected persons shed the virus for 1–3 weeks and have a very high risk of transmission 1–2 weeks prior to the onset of symptoms. Risk factors for *HAV* infection include international traveling, men who have sex with men, intravenous drug users, and persons with chronic liver disease or with clotting disorders. The clinical features are similar to other types of acute viral hepatitis. HAV infection presents as an acute febrile illness with nausea, abdominal discomfort, and jaundice. Other atypical manifestations include vasculitis, cryoglobulinemia, and neurologic, renal, and immunologic reactions. HAV is a self-limited disease that does not produce chronic infection or chronic liver disease. Fatality from acute liver failure occurs in 0.5 % of those infected. Diagnosis is made on clinical, epidemiologic, and serologic basis. The antibody test for total anti-HAV measures both IgM-HAV and IgG-HAV. IgM becomes positive in acute HAV infection within 5–10 days before the onset of symptoms and can persist up to 5–6 months. IgG appears in the convalescent phase of the disease and confers lifelong protection.

In the prevaccine era, the only methods for prevention of hepatitis A were hygienic measures and use of protective immunoglobulins. Two inactivated whole-virus hepatitis A vaccines, VAQTA and HAVRIX [32, 33], were licensed in 1995 in the USA and approved for use. The other vaccines used worldwide are AVAXIM, EPAXAL, and Heavile. All these vaccines are made from different strains of the HAV; VAQTA is based on strain CR326F, and HAVRIX is based on strain HM175 and contains a preservative unlike VAQTA. Both vaccines are highly immunogenic. ACIP recommends vaccination for all children at 12–23 months of age. Adults who are at increased risk of infection or complication from HAV infection should be routinely vaccinated. HAVRIX is administered intramuscularly as a single primary dose in children 1–18 years (0.5 ml) and adults above 19 years (1 ml) followed by a booster at 6–12 months. VAQTA is administered similarly to HAVRIX; however the booster is administered 6–18 months after primary dose. In 2001, Twinrix—a combination vaccine with adult dose of hepatitis B vaccine (Engerix-B)

and pediatric dose of HAVRIX—was approved for adults greater than 18 years of age; it is given intramuscularly at 0, 1, and 6 months. Contraindications to the vaccine include allergic reactions or moderate-to-severe illness. Adverse reactions include pain at injection site but systemic side effects are rare. The wide use of vaccines has resulted in a sustained reduction of disease in most of the developed world; however hepatitis A infection remains an ongoing issue in the developing world.

8 Hepatitis B Vaccines

Hepatitis has been recognized as a clinical entity since the times of Hippocrates when he dubbed it epidemic jaundice. However, the wide diversity of viruses that can be responsible for this entity has only recently begun to be recognized. The first case of "serum hepatitis" or what was believed to be hepatitis B was first described during an epidemic which resulted from vaccination against smallpox in shipyard workers in late nineteenth-century Germany. Jaundice developed in 15 % of the inoculated workers. The role of blood as a vehicle became clearer in 1943 when Beeson described the transmission of hepatitis to recipients of blood transfusions [34].

Hepatitis B virus is a small double-shelled DNA virus of the family *Hepadnaviridae* [34]. It has a small circular DNA genome. It contains several antigens including the hepatitis B surface antigen, hepatitis B core antigen, and the hepatitis B E antigen. Humans are the only known host to the virus.

Hepatitis B virus is primarily hepatotropic; although hepatitis B surface antigen (HbSAg) has been recovered from other organs, there is little evidence that it replicates outside of the liver. Most experimental data supports the notion that the virus is not directly cytopathic but rather the damage to tissue is mediated by an immune response to the virally infected hepatic cells. Infection can range from being asymptomatic to causing a fulminant hepatitis. Persons infected with hepatitis B can also progress to a chronic infection resulting in cirrhosis and hepatocellular carcinoma [34].

The clinical course of hepatitis B is indistinguishable from other causes of viral hepatitis. The incubation period ranges from 40 to 160 days. Definitive diagnosis requires serological assays to distinguish it from other causes of hepatitis. The preicteric phase which occurs a week before the onset of jaundice is characterized by malaise, fatigue, nausea, vomiting, and right upper quadrant pain. The icteric phase lasts from 1 to 3 weeks and is characterized by jaundice, hepatomegaly, and acholia. Approximately 40 % of people in the USA that develop acute hepatitis B are hospitalized. Fulminant hepatitis occurs in 0.5–1 % of cases and is more common in adults than children. During the convalescent phase, all symptoms resolve but fatigue may linger for weeks.

Approximately 5 % of cases will progress to chronic infection with the risk of chronic infection decreasing with age. As many as 90 % of infants who acquire the virus from their mothers progress on to chronic infection. Persistent infection is defined as having a positive HBSAg for more than 6 months. Viral replication persists throughout the course of chronic hepatitis B infection and disease progression depends on interactions between the virus and host immunity. It is a dynamic process that may span over the course of decades. Most patients can be asymptomatic but continue to spread infection. This carries a 25 % risk of developing cirrhosis and dying of liver cancer.

The incidence of hepatitis B peaked in the 1980s. Approximately 10,000 or less cases are now reported annually in the USA. Before routine childhood immunizations, most infections occurred in adults. The highest risk groups are those between 20 and 45, those who engage in high-risk sexual practices, and those who use injection drugs. Up to 16 % of patients who acquire the disease deny any risk factors [35].

Hepatitis B vaccine has been available in the USA since 1981. It consists of a 226-amino acid S gene product. This gene is injected via plasmids into *Saccharomyces cerevisiae* which produce a recombinant HbSAg protein. The final product contains 95 % purified protein surface antigen but no yeast DNA. Thus, infection cannot result from hepatitis B vaccination. The vaccine has a proven efficacy of around 90–95 % [35, 36] in normal populations with lower rates of immunogenicity in subsets of patients. A particularly challenging group has been patients with *HIV* in whom vaccine efficacy can be as low as 30 %. This is worrisome as patients with HIV are to be considered high risk for acquiring the infection [37].

9 Human Papillomavirus Vaccines

Human papillomavirus (HPV) is a DNA virus that causes epithelial lesions of mucous membranes ranging from benign papillomas to carcinoma [38–40]. The association of HPV and cancer was first described by Orth [41] in 1970s. In the 1980s, zur Hausen [42] identified HPV 16 and HPV 18 in cervical cancer cells. The introduction of screening and use of HPV vaccines have decreased the incidence of HPV-associated cervical cancers in the developed world [43]. However, the incidence of HPV-associated anal and oropharyngeal cancer is on the rise.

HPV is the most common sexually transmitted disease in the USA. It is estimated the prevalence varies from 14 to more than 90 %, the highest rate occurring in the age group 20–24. HPV is transmitted through vaginal sex, anal sex, genital-genital contact, and oral sex and rarely from pregnant women with genital HPV to their babies causing recurrent respiratory papillomatosis (RRP) in

the child. HPV replicates in the nuclei of stratified squamous epithelial cells. In majority of individuals HPV is spontaneously cleared but in small number of cases HPV persists with risk of progression to high-grade dysplasia or invasive carcinoma of the cervix, vulva, vagina, penis, anus, and oropharynx [44]. In the USA, there are approximately 17,000 women and 9000 men affected with HPV-related cancer yearly. The Pap smear used as a screening tool helps prevent HPV-associated cervical cancer in women but unfortunately the lack of screening for other HPV-related cancers results in increased morbidity and mortality.

There are two available HPV vaccines—Gardasil and Cervarix. Gardasil is a recombinant human papillomavirus quadrivalent vaccine produced in the yeast *Saccharomyces cerevisiae* [45]. It contains viruslike particles of types 6, 11, 16, and 18 which together cause around 90 % of genital warts. Cervix is a recombinant bivalent vaccine composed of viruslike particles of types 16 and 18, which causes approximately 70 % of cervical cancers worldwide. In young females, either of the vaccines may be used. The target age group is 9 through 26 years of age to prevent HPV-related genital warts, cervical intraepithelial neoplasia, and cancers. In young males, Gardasil is the only approved vaccine, with target age group being 11–12 years. HPV vaccination is also recommended for older teens who are not vaccinated when younger. Both HPV vaccines are administered intramuscularly as a three-dose schedule—with the second dose being given 1 or 2 months after the initial dose and third dose 6 months after the first dose. The vaccine series does not have to be restarted if interrupted and can be interchanged with either HPV vaccine product to complete series. The most commonly reported side effects are nausea, headache, dizziness, and local reactions at injection site. The vaccine is contraindicated in persons with history of hypersensitivity to vaccine components and in pregnancy owing to limited efficacy data. Its use is safe in immunocompromised hosts as both Gardasil and Cervarix are noninfectious vaccines.

Despite the safety and efficacy, HPV vaccines remain underutilized. It is estimated that only 57 % of adolescent girls and 35 % of adolescent boys received one or more doses of HPV vaccine. CDC data and statistics [46] illustrate that if clinicians give a stronger recommendation for adolescent HPV vaccinations before the age of 13, 91 % of adolescent girls would be protected from HPV-related cancers.

10 Influenza Vaccines

Influenza is a highly contagious viral disease caused by the single-stranded RNA *influenza virus*. Descriptions of pandemic influenza can be found in many places throughout history and its name is

derived from an epidemic in fifteenth-century Italy which was thought to have occurred under the influence of the stars [47]. At least four pandemics occurred in the nineteenth century and three occurred in the twentieth century. The infamous Spanish influenza which occurred in the early twentieth century was responsible for at least 18–19 million deaths which dwarfed World War I which was occurring at the time and may be partially responsible for ending that conflict. The virus itself was first isolated in the 1930s for the first time by Smith, Andrews, and Laidlaw. The first inactivated vaccine was first created in the 1950s and that was followed by a live attenuated vaccine in 2003.

Influenza virus is a single-stranded RNA virus of the family *orthomyxovirus* [47]. Basic antigen types A, B, and C are determined by nuclear material. Influenza A can be further characterized by two components, hemagglutinin (H1, H2, and H3) and neuraminidase (N1, N2) which play roles in viral cell penetration. Influenza A naturally infects humans, swine, and poultry among other birds and the virus can freely exchange genetic material in these hosts. The H and N antigens vary and are part of the reason why the virus is so successful at evading immunity and the reason vaccines need to be reformulated annually. The virus undergoes antigenic drift which is a minor variation of its surface antigens caused by point mutations in a gene segment. These can result in epidemics since the protection that has been conferred by prior years of infection is incomplete. Antigenic shift on the other hand is a major change in one or both H and N antigens that are likely the result of a recombinant virus exchange between those who affect birds and humans. These major changes occur at varying intervals and are responsible for worldwide pandemics.

Following respiratory transmission, the virus proceeds to invade respiratory epithelial cells in the trachea and the bronchi. This replication itself results in cellular death. Of those infected, 30–50 % will not experience symptoms and those who go on to develop them can have a wide spectrum of manifestations ranging from mild respiratory complaints to a rapidly evolving febrile illness complicated by secondary bacterial infections [48]. Primary influenza is characterized by the abrupt onset of fever, chills, myalgias, headache, sore throat, and extreme fatigue. The presence of fever and respiratory symptoms are the most sensitive indicators of illness. Fever may range from 38 to 40 °C but may vary. Symptoms usually improve within 1 week but cough and fatigue can persist for 2 weeks or more. Gastrointestinal symptoms, croup, and otitis media can occur and are more common in children. Complications from influenza tend to occur in the extremes of age and those with comorbidities. The most common complications are exacerbations of underlying conditions such as COPD, congestive heart failure, and coronary artery disease. This is coupled with the development

of bacterial pneumonia caused by usual community pathogens as well as an increased incidence of *Staphylococcus aureus* pneumonia. In the USA influenza is responsible for over 200,000 hospitalizations and 30–5000 deaths annually with the largest impact on the elderly and the very young. A greater number of hospitalizations occur in years when influenza H2N3 is the predominant strain. An increase in mortality typically accompanies influenza epidemics and a large number of these deaths are not directly related to the infection but rather to its complications such as cardiac events and exacerbation of other chronic medical conditions.

Two types of influenza vaccines are currently available: an inactivated trivalent or quadrivalent vaccine containing influenza A H3N2 and H1N1 plus influenza B-inactivated viruses, and an attenuated live virus vaccine that has the equivalent components of the inactivated trivalent vaccine. The inactivated vaccine is injected intramuscularly or intradermally. Hemagglutinin is the main component and immunogen in these vaccines. In 2003 the FDA approved a live attenuated vaccine. It contains the same components of the trivalent inactivated vaccine; they are cold adapted and reproduce effectively in the nasopharynx of the recipient. It is administered as a single dose of a spray through each nostril.

The immunity conferred by the inactivated virus vaccine is deemed to last for less than a year. On years when there is a good match between the circulating strain and the vaccine, protection can be as high as 90 % among those younger than 65 and around 40 % in older patients [49, 50]. This usually yields a vaccine efficacy close to 50–60 %. Vaccination has also been shown to be effective at preventing complications of influenza. Inactivated vaccine should be administered on a yearly basis to eligible patients which now includes all patients older than 6 months.

The live attenuated virus vaccine is 87 % effective in decreasing disease and close to 30 % effective in decreasing otitis media. The live attenuated vaccine should be administered to patients older than 2 years up to age 49 [51].

Recommendations for the antigenic composition of the vaccines are made annually to ensure that the vaccines are effective against recently circulating strains of the virus. This is subject to antigenic drift and shift which explains why certain influenza seasons feature strains not anticipated by vaccine makers. The timeline for production of the vaccine is similar each year and hinges on the activity of the WHO influenza surveillance network. Because production of the vaccine requires several months, data collection must be balanced with manufacturing times. If recommendations are made too early, then antigens could change rendering the vaccine ineffective. If recommendations are made too late, timely vaccine manufacture may be impossible.

11 Japanese Encephalitis Vaccines

Japanese encephalitis (JE) is a vaccine-preventable mosquito-borne viral infection that occurs in the developing countries of Asia. Outbreaks consistent with JE were reported as far back in 1871 in Japan and the virus was first isolated from *Culex tritaeniorhynchus* in 1938.

JE virus (JEV) is a single-stranded RNA *flavivirus* closely related to West Nile and Saint Louis encephalitis virus. JEV is transmitted through the bite of infected Culex species of mosquitoes. The natural cycle of the JEV is enzootic consisting of bird-mosquito-bird or pig-mosquito-pig circulation of the virus. Humans are incidental or dead-end hosts. Human-to-human transmission is rare but cases from vertical transmission and through organ transplant have been reported. Transmission usually occurs in rural agricultural areas, mainly associated with irrigated rice fields in the tropical and temperate regions of eastern and southern Asia. Epidemic activity is highest in summer and early fall while endemic activity is sporadic and not associated with any seasonal pattern. JE is primarily a disease of children as adults acquire immunity through natural infection. As per the CDC, the incidence of JE among travelers to Asia from non-endemic areas is less than one case per million travelers [52].

The majority of human infections with JEV are asymptomatic with less than 1 % of developing clinical symptoms. The incubation period is 5–15 days. The most common presentation is that of acute encephalitis with sudden onset of fever, headache, vomiting, and mental status changes. Other manifestations include seizures, a parkinsonian syndrome, and acute flaccid paralysis [53] resembling poliomyelitis. IgM antibody of CSF and serum samples is currently the standard test for diagnosis. Viral isolation and nucleic acid amplification tests are insensitive tools for diagnosis. There is no specific treatment and therapy consists of supportive care and managing complications.

The incidence of JE has drastically decreased over the last few decades owing to vector control programs and vaccinations. The three most important types of vaccines currently used are purified, mouse brain-derived, inactivated Nakayama or Beijing strains of JEV; cell culture-derived inactivated JE vaccine based on Beijing P3 strain; and cell culture-derived live attenuated JE vaccine from SA 14-14-2 strain. The only licensed vaccine in the USA is the inactivated vero cell culture-derived vaccine branded as Ixiaro, approved in 2009. The ACIP recommends vaccination [54] for travelers spending more than 1 month in endemic areas during the JEV transmission season or short-term travelers with high risk or uncertain activities or traveling to a region with a JE outbreak. The primary immunization schedule includes two intramuscular

injections given on days 0 and 28 to be completed at least 1 week prior to travel date. There is limited data on efficacy and use in pregnancy. The common adverse reactions include local reaction and flu-like illness.

12 Meningococcal Vaccines

Meningococcal disease is an acute, potentially life-threatening disease caused by the gram-negative, endotoxin-producing bacteria *Neisseria meningitidis* or the meningococcus. It causes meningitis, sepsis, and focal infections. Epidemics of meningococcal meningitis were first described in the early eighteenth century. Prior to the advent of antibiotics, the case fatality rate was as high as 70–85 % (Fig. 2).

Meningococcus is an aerobic, gram-negative diplococcus and is a normal commensal of the human nasopharynx. The organism has an inner cytoplasmic membrane and outer membrane separated by a cell wall. The outer membrane proteins and polysaccharide capsule serve as antigens and are responsible for the pathogenicity of the organism. Meningococci are classified on the basis of characteristics of the polysaccharide capsules—at least 13 serogroups have been described and most invasive disease is caused by serogroups A, B, C, Y, and W-135.

The meningococcus colonizes only the nasopharynx and carriage rates are highest among adolescents and young adults [55–57]. It is transmitted through aerosol droplets or direct contact with respiratory secretions. Risk factors for infection include complement deficiency [58, 59], asplenia [60], HIV, recent viral illness, and tobacco smoking. In less than 1 % of colonized humans the organism invades to cause bacteremia and around 50 % of the bacteremic patients develop meningeal involvement. The incubation period is around 2–10 days. Clinical presentations include meningitis and bloodstream infections, called meningococcemia, characterized by fever, hypotension, petechial rash, and multiorgan failure. Less common manifestations include otitis media,

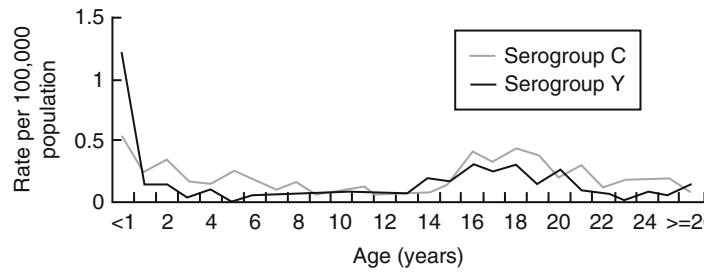

Fig. 2 Rates of meningococcal disease by age, USA, 1999–2008. Source: CDC/vaccines/meningococcal; CDC Active Bacterial Core Surveillance

pneumonia, and arthritis. Diagnosis is made by a positive gram stain and bacterial culture from a normally sterile site. Detection of polysaccharide antigen in CSF and serology may also be used in evaluation. Intravenous aqueous penicillin is considered therapy of choice.

Vaccination is the most effective method to prevent meningococcal disease. The first meningococcal polysaccharide vaccine (Menomune; MPSV4) was licensed in the USA in 1978 and is a quadrivalent A, C, Y, W-135 polysaccharide vaccine administered subcutaneously. Three meningococcal conjugate vaccines (MCV4-Menactra, Menveo, MenHibrix) are available in the USA. Menactra was licensed in 2005 [61, 62] and Menveo in 2010 [63]. Both vaccines are quadrivalent A, C, Y, W-135 conjugated to diphtheria toxoid, approved for persons 2–55 years of age. MenHibrix is a meningococcal serogroup C, Y, Haemophilus B tetanus toxoid conjugate vaccine. It is indicated to prevent meningococcal and Haemophilus disease in children 6 weeks through 18 months of age. The first meningococcal serogroup B vaccine available in the USA called Trumenba was licensed in late 2014 for individuals 10–25 years in a three-dose series at 0, 2, and 6 months. The vaccine is indicated [64] in persons aged 11–18 years, first dose at age 11–12 years and a booster at age 16 or first dose if given at 13–15 years then booster at 16–18 years. No booster is indicated if primary dose was given on or after age 16 years. Other indications [64] include persons aged 2–55 years or 9 months–2 years with functional or anatomical asplenia or complement deficiency, with increased risk for exposure or travel to hyperendemic areas. Bexsero, a second meningococcal serogroup B vaccine, was approved by the FDA in January 2015. It is administered in two doses 1 month apart. At the time of this writing, the CDC has not yet published recommendations on the use of the serogroup B vaccines; these recommendations are expected to be released in June 2015. Adverse reactions include local reactions, fever, and mild systemic symptoms. Contraindication [64] to the vaccine is moderate-severe illness or allergy to vaccine component. In most areas, invasive meningococcal disease is a reportable condition. Antimicrobial chemoprophylaxis (ciprofloxacin, rifampin, ceftriaxone) is recommended for close contacts with exposure to index patient given the high rate of secondary disease.

12.1 Measles, Mumps, and Rubella Vaccine

Measles is a ubiquitous, highly contagious disease caused by the measles virus. It was recognized as early as seventh century. Measles was described as severe disease, “more to be dreaded than smallpox”—for the first time by Persian physician Rhazes in the tenth century [65, 66]. In the pre-vaccine era, school-aged children had the highest risk of infection and more than 95 % of cases occurred by 15 years of age [67, 68] (Figs. 3, 4, and 5).

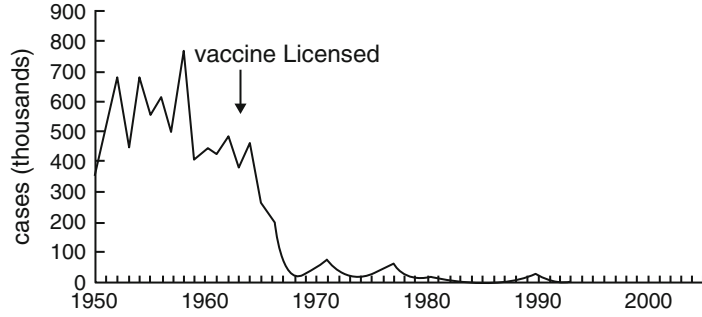

Fig. 3 Measles—USA, 1950–2009. Graph from CDC/vaccines/pinkbook/measles

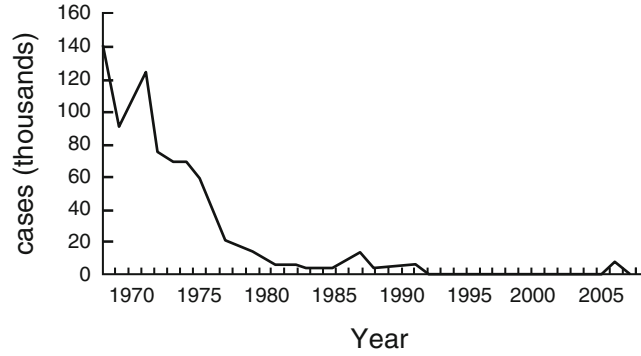

Fig. 4 Mumps—USA, 1968–2009. Graph from CDC/vaccines/pinkbook/mumps

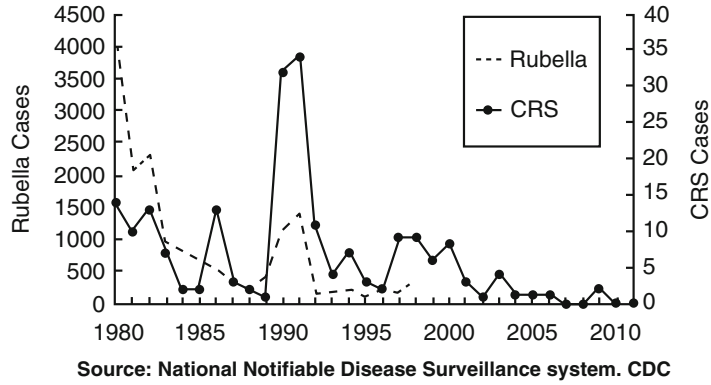

Fig. 5 Rubella cases in the USA, 1966–2009. Graph from CDC/vaccines/rubella

Measles virus is a single-stranded RNA virus member of the genus Morbilliform in the family *Paramyxoviridae*. Two membrane envelope proteins—fusion protein (F) and hemagglutinin (H)—are responsible for pathogenesis. There is only one antigenic type of measles virus. Measles is an airborne disease and is spread via respiratory transmission. The primary site of invasion and

replication is the respiratory epithelium. The incubation period is 10–12 days followed by a prodrome consisting of fever, cough, coryza, conjunctivitis, and Koplik spots—punctate bluish-white spots on red background on buccal mucosa which are pathognomonic of measles. The rash of measles is a maculopapular rash that develops 2–4 days after prodrome or 14 days after exposure and spreads from the head over the trunk to the extremities during a 3–4-day period. The rash fades over next 3–4 days in the order of its appearance. The complications of measles include diarrhea, otitis media, pneumonia, encephalitis, seizures, and rarely death. Diagnosis is clinical and is confirmed by serological testing—most commonly by ELISA.

Prior to 1963, approximately 500,000 cases and 500 deaths were reported annually in the USA [69], with epidemic cycles every 2–3 years. Following vaccine licensure in 1963, the incidence of measles decreased by more than 98 %. Between 1989 and 1991, there was a resurgence of measles with 55,622 cases in children less than 5 years of age with 123 reported deaths. Measles incidence then declined rapidly post-resurgence period owing to increased vaccination programs of preschool children, adolescents, and young adults. The Centers for Disease Control reported a total of 911 cases of measles from 2001 to 2011; however owing to vaccination delay and misguided ideas about vaccination, 159 cases have been reported in the USA in 2015, the greatest number of cases reported since measles elimination was documented since 2001.

In 1963, both a killed and a live attenuated Edmonston B strain of measles virus were licensed in the USA. The killed vaccine was withdrawn in 1967 owing to development of atypical measles. The Edmonston B strain was withdrawn in 1975 due to a high incidence of post-vaccination fever and rash. A live, further attenuated Schwarz strain was licensed in 1965, but is no longer used in the USA. The only available measles vaccine is a live, further attenuated Edmonston-Enders strain (Moraten). The vaccine is available combined with MMR, or combined with measles, mumps, rubella, and varicella as MMRV (ProQuad).

Mumps was first described by Hippocrates in the fifth century BC and scientifically detailed by Robert Hamilton, a British physician in 1790 [70]. In 1935, Johnson and Goodpasture [71] proved viral cause for this disease. Although mumps is a benign disease of childhood, it was a major cause of morbidity among soldiers during American Civil War and World Wars I and II [72–74].

Mumps virus, a *Paramyxovirus* with a single-stranded RNA genome, causes a communicable acute viral illness via airborne transmission or by direct contact with infected saliva. After acquisition, the virus replicates in the nasopharynx and regional lymph nodes. Viremia develops 12–25 days after exposure affecting the meninges and various glandular organs such as the salivary glands,

pancreas, testes, and ovaries. Prodromal symptoms include low-grade fever, myalgia, anorexia, and headache. Parotitis is the most common clinical finding occurring in 30–40 % of infected persons, although up to 20 % mumps infections are asymptomatic. Complications of mumps include aseptic meningitis, orchitis, oophoritis, pancreatitis, and rarely deafness and death. Laboratory diagnosis is made by using serology or PCR detection of the mumps virus. An estimated 212,000 cases of mumps occurred in the USA in 1964. After the licensure of the Jeryl Lynn Strain of attenuated mumps virus vaccine in 1967, the number of reported mumps cases has steadily declined except for sporadic resurgences.

The first mumps vaccine was developed in 1948 but it was withdrawn in mid-1950s owing to limited temporal immunity. All mumps vaccines currently in use contain live viruses. The various mumps vaccine strains available are Jeryl Lynn, Urabe AM9, Leningrad-Zagreb, and Leningrad-3. The currently used mumps vaccine in the USA is the Jeryl Lynn strain, a live attenuated mumps vaccine. It is available combined with measles and rubella as MMR, or combined with measles, rubella, and varicella vaccine as MMRV (ProQuad).

Rubella was initially described in the late eighteenth century and was differentiated from other exanthems by German physicians, hence the name German measles [75]. The term rubella, meaning "little red" [76], was coined by a British physician in 1841 during an outbreak in India. However it was only in 1941 that Norman McAlister Gregg [77], an Australian ophthalmologist, recognized congenital rubella syndrome (CRS). The rubella virus was first isolated by Parkman and Weller in 1962. The pandemic in Europe during 1962–1963 and in the USA in 1964–1965 spurred work on the rubella vaccine. The highest incidence of rubella in the USA was in 1969. The licensure of the vaccine that year led to a marked decrease in the incidence of rubella and CRS. A record low of seven cases was reported in 2003 and in the year 2004 rubella was no longer considered to be endemic in the USA, but it remains an ongoing problem in many parts of the developing world. On April 29, 2015, the World Health Organization declared the elimination of rubella in the Americas.

Rubella virus is an RNA virus belonging to *Togaviridae* family and genus *Rubivirus*. Rubella spreads by respiratory aerosols and primary replication occurs in the nasopharynx and regional lymph nodes. The incubation period is 14–21 days. The first week after exposure is usually symptom free followed by second week of viremia, low-grade fever, malaise, and lymphadenopathy. The characteristic maculopapular erythematous rash develops 14–17 days after exposure; it begins on the face and spreads downward. Other symptoms include arthralgia, arthritis, conjunctivitis, testalgia, or orchitis. The complications of rubella are chronic arthritis, thrombocytopenia purpura, encephalitis, orchitis, neuritis, and a rare late

syndrome of progressive panencephalitis. Congenital rubella syndrome affects 85 % of infants infected during first trimester but congenital defects are rare if infection occurs after the 20th week of gestation. The virus may affect all organs and cause congenital defects, the most common of which is deafness. Other prominent clinical findings include cataracts, glaucoma, retinopathy, patent ductus arteriosus, ventricular septal defect, pulmonic stenosis, coarctation of aorta, and neurologic and boney abnormalities. The laboratory diagnosis of rubella is made by isolation of the virus from clinical specimens or by serology using enzyme immunoassay.

In 1969, three rubella vaccines were licensed: HPV-77:DE5 (Meruva), HPV-77:DK-12 (Rubelogen), and GMK-3:RK53 (Cendevax). RA 27/3, a human diploid fibroblast strain (Meruvax-II, Merck), was licensed in 1979 and all other strains were discontinued. RA 27/3 rubella vaccine was first isolated from a rubella-infected aborted fetus in 1965. The virus was attenuated using human diploid fibroblasts. The vaccine is available combined with measles and mumps vaccines as MMR, or combined with measles, mumps, rubella, and varicella as MMRV (ProQuad).

MMR or MMRV vaccine is routinely recommended for all children 12 months of age or older [78]. The first dose of MMR should be given on or after first birthday and the second dose is given between ages 4 and 6. High schools and colleges in the USA and other countries frequently require students to have received two doses of vaccine at some point in their lives prior to matriculation. The adverse reactions include fever, rash, thrombocytopenia, arthritis/arthropathy, encephalopathy and rarely parotitis, or deafness. MMR vaccine is contraindicated in pregnancy, immunocompromised patients, during acute illness, or those with severe allergic reaction to vaccine components which include neomycin.

13 Pertussis Vaccines

Pertussis or whooping cough is an infectious disease caused by *Bordetella pertussis*, a gram-negative bacillus.

Before the introduction of the whole-cell vaccine, there were over 250,000 cases of whooping cough per year and 10,000 deaths worldwide. The incidence of pertussis declined significantly with the implementation of universal vaccination. Pertussis incidence has been gradually increasing since the early 1980s. A total of 28,000 cases were reported in 2014, the largest number since 1959. The reasons for the increase are not clear. A total of 27,550 pertussis cases and 27 pertussis-related deaths were reported in 2010. The increase in disease incidence in the USA has mostly been seen in older children and adults, likely reflecting waning

immunity conferred by the vaccine, decreasing natural immunity, as well as decreasing vaccination rates. The numbers may underestimate the reality as this disease is underdiagnosed in adults [79].

Bordetella pertussis is a small, fastidious aerobic gram-negative rod, requiring specialized medium for culture. It produces multiple antigenic and biologically active products including pertussis toxin, filamentous hemagglutinin, agglutinogens, adenylate cyclase, pertactin, and tracheal cytotoxin. These products are responsible for the clinical features of pertussis disease, and an immune response to one or more produces immunity following infection.

The clinical presentation varies slightly between children and adults. In general, whooping cough is divided into three phases: the catarrhal or prodromal stage, the paroxysmal stage, and the convalescent stage. During the catarrhal stage, children present with signs and symptoms of an upper respiratory tract infection such as rhinorrhea, conjunctivitis, occasional cough, and fever. This generally lasts from 1 to 2 weeks. The paroxysmal stage is characterized by repeated episodes of severe cough accompanied by fits of spasm and, at the end of the paroxysm, may be accompanied by the classic whooping sound produced when rapidly inspiring air against a closed glottis. With the force of the coughing, children will often cough mucous plugs and can be accompanied by post-tussive emesis. These attacks occur more frequently at night. The paroxysmal stage can last as long as 6 weeks. Lastly, symptoms begin to wane and patients move on to the convalescent phase. Pertussis in adults can have a more atypical presentation, often appearing as a chronic cough [80] with a less defined course than classically described in children.

Whole-cell pertussis vaccine is composed of a formalin-inactivated suspension of *B. pertussis* cells. It was developed in the 1930s and has been available in practice since the 1940s. Based on efficacy studies, the vaccine conferred 70–90 % efficacy in protecting from severe pertussis. Local reactions were common and occasionally would be accompanied by fever. This led to the creation of an acellular vaccine associated with less adverse effects. Whole-cell pertussis vaccine is no longer available in the USA but is still available elsewhere. Acellular vaccines are subunit vaccines that contain inactivated components of *Bordetella pertussis*. These are only available in combination with diphtheria and tetanus toxoid. Efficacy has ranged from 80 to 85 % [81]. The primary series of DTaP vaccines consists of four doses, the first three doses given at 4- to 8-week intervals (minimum of 4 weeks), and beginning at 6 weeks to 2 months of age. The fourth dose is given 6–12 months after the third to maintain adequate immunity for the ensuing preschool years [81].

14 Pneumococcal Vaccines

Pneumococcal infections which include pneumonia and invasive infections such as bacteremia and meningitis constitute a major source of morbidity and mortality both among the very young and the elderly, with a special impact in those populations unable to generate antibodies to the polysaccharide capsule of *Streptococcus pneumoniae*. The highest burden of invasive disease occurs in those with HIV, younger than 2 years and those older than 65 years, with the highest mortality occurring in those older than 65 [82].

It is estimated that before the introduction of the PCV-7 vaccine, this bacteria caused 17,000 cases of invasive disease per year including 700 cases of meningitis and 200 deaths in children younger than 5. In the USA, before the introduction of the pneumococcal conjugated vaccine there were an estimated 15 million office visits for acute otitis media resulting in 5 billion dollars annually.

Streptococcus pneumoniae causes a wide range of diseases, most commonly causing pneumonia and otitis media but also having the potential to cause invasive disease such as bacteremia and meningitis [82]. With the exception of the great apes, humans are the only organisms affected by Pneumococcus. It is carried in the nasopharynx from whence it can be readily transmitted via droplets. Carriage length varies by serotype and is usually asymptomatic but can result in acute disease such as otitis media or invasive disease. The organism's capsule is its most important virulence factor. It protects the bacteria against phagocytosis and complement activation and antibodies. It can also aid in adherence to epithelium.

Forty serogroups encompassing 93 serotypes have been described. Among these, a small proportion is responsible for the majority of invasive diseases with the ten most common ones being isolated in more than 80 % of cases in the USA. In studies done prior to the introduction of pneumococcal vaccines serotypes 14, 16b, 1, 23F, 5, and 19F in descending order were the most common. Distribution and causality have varied with the introduction of the vaccines with a trend to shift into different disease-causing strains not covered by currently available vaccines.

Currently, two types of pneumococcal vaccines are currently available. These are the 23 valent polysaccharide vaccines (PV23) and the 13 valent conjugated vaccine (PV13). They both contain purified capsular polysaccharide component of Pneumococcus. The 23 valent vaccine contains capsular materials from 23 serotypes that have historically been known to cause 85–90 % of invasive diseases. The serotypes included in this vaccine are 1, 2, 3, 4, 5, 6B, 7F, 8, 9N, 9V, 10A, 11A, 12F, 14, 15B, 17F, 18C, 19F, 19A, 20, 22F, 23F, and 33F. This vaccine has been shown to be efficacious in decreasing the incidence of invasive disease (i.e., bacteremia and meningitis) and noninvasive pneumococcal pneumonia [83, 84].

The 13 valent conjugated contains 13 capsular saccharides from the most common strains covalently linked to a nontoxic protein that is similar to diphtheria toxin. This covalent linking renders the vaccine immunogenic in infants and toddlers. It has also been shown to have increased immunogenicity in immune-compromised individuals such as asplenic patients or patients with HIV. The serotypes included by this vaccine are 1, 3, 4, 5, 6A, 6B, 7F, 9V, 14, 18C, 19A, 19F, and 23F. Several studies have demonstrated the efficacy of the conjugated pneumococcal vaccine [85, 86]. In a large clinical trial, PCV7 was shown to reduce invasive disease caused by vaccine serotypes by 97 %, and reduce invasive disease caused by all serotypes, including serotypes not in the vaccine, by 89 %. Children who received PCV7 had 7 % fewer episodes of acute otitis media and underwent 20 % fewer tympanostomy tube placements than did unvaccinated children.

The indications for both vaccines vary slightly with the conjugated vaccine being indicated in very specific groups of patients [86].

PPSV 23 alone should be given to:

- Cigarette smokers
- Alcoholics
- People with chronic heart disease excluding hypertension
- Chronic lung disease including asthmatics
- Diabetes mellitus
- Chronic liver disease

A combination of PSV 23 and the PVC13 should be given to:

- People older than 65
- Patients with cochlear implants
- Patients with CSF leak
- Functional or anatomical asplenia
- Congenital or acquired immune deficiency including HIV

The latter group of patients comprises those at greatest risk for invasive disease in whom increased immunogenicity has been demonstrated with conjugated 13 valent vaccine.

15 Rotavirus Vaccines

Rotavirus is the leading cause of acute gastroenteritis among infants and young children worldwide. *Rotavirus* is estimated to account for one-third of the estimated 1.3 million deaths yearly from diarrhea [87–89]. In the prevaccine era, rotavirus accounted for 2.7 million illness episodes and around $1 billion annually in medical costs in the USA [90, 91].

Rotaviruses are 70 nm double-stranded RNA icosahedral viruses belonging to the family *Reoviridae*. The virus is composed of an outer and inner capsid and a core. Three major structural proteins (VP 4, VP 6, VP 7) and one nonstructural protein (NSP4) are of interest in vaccine development. The exact mode of transmission of rotavirus is unknown. It is assumed to be spread from person to person contact or aerosolized respiratory droplets. Incubation period is short, usually less than 48 h. The virus replicates in the mature villous epithelial cells of the small intestine causing malabsorption. The nonstructural protein (NSP4) acts as an enterotoxin causing diarrhea [92]. Severe gastrointestinal illness by rotavirus mainly occurs in children 3–24 months [93, 94]. Infection during first month of life provides IgA-mediated protection against moderate-to-severe illness on reinfection. Rotaviral infection may be asymptomatic or cause self-limited diarrheal illness or result in severe dehydrating diarrhea complicated by electrolyte imbalances, metabolic acidosis, and multiorgan involvement. Diagnosis is made by detection of rotavirus antigen in stool by enzyme-linked immunosorbent assay.

The first rotavirus vaccine, RotaShield (RRV-TV, rhesus-based tetravalent rotavirus vaccine), was introduced in the USA in 1998 but was withdrawn from the market a year later because of its association with intussusception 3–14 days after administration of first dose of vaccine. Currently there are two rotavirus vaccines licensed in the USA—RV5 (RotaTeq) and RV1 (Rotarix). RotaTeq is a live oral vaccine licensed in 2006. It contains five reassortment rotaviruses developed from human and bovine rotavirus strains. The vaccine viruses are suspended in buffer solution. Rotarix is also a live oral vaccine, licensed in 2008. It contains one strain of live attenuated human rotavirus type G1P1A [8]. The vaccine is a lyophilized powder that is reconstituted before administration. Both these vaccines contain no preservatives or thimerosal. The vaccine effectiveness is 74–87 % against any rotavirus gastroenteritis and 85–98 % in severe rotavirus gastroenteritis. Both vaccines significantly reduce physician visits, hospitalization, and overall morbidity and mortality.

The ACIP recommends [95] routine vaccination of all infants, administered as a series of either two doses of RV1 or three doses of RV5 beginning at 2 months of age or as early as 6 weeks with subsequent doses in the series separated by 1–2 months. The maximum age for any dose is 8 months. The only contraindication to the vaccine is a severe allergic reaction to vaccine components, a history of intussusception, or severe combined immunodeficiency syndrome. The common side effects were vomiting, diarrhea, fever, and irritability and no serious reactions have been reported so far.

Rotavirus disease among infants and young children significantly decreased after the introduction of the vaccines. The vaccine prevents an estimated 50,000 hospitalizations among US infants

and indirectly protects older children and adults. The CDC uses the National Respiratory and Enteric Virus Surveillance System (NREVSS) to estimate burden of the disease and disease trend and evaluate the impact of vaccination in the USA.

16 Tetanus Toxoid

Tetanus is an acute and often fatal disease caused by an exotoxin produced by *Clostridium tetani*. It is unique among vaccine-preventable diseases in that it is not communicable. Records from antiquity contain descriptions of the disease but it was not until the late nineteenth century that the etiology of the disease was demonstrated by Carle and Rattone [96] by injecting the contents of a pustule in a human victim into the sciatic nerve of a rabbit, thus producing the symptoms of tetanus. Soil samples inoculated into rabbits would also cause disease as demonstrated by Nocolaier. In 1897, Nocard demonstrated the protective effect of passively transferred antitoxin, and passive immunization in humans was used for treatment and prophylaxis during World War I. The tetanus toxoid was first successfully synthesized in 1924.

Clostridium tetani is a slender gram-positive, anaerobic rod that can develop a distal spore giving it the semblance of a drumstick. The organism is sensitive to heat and cannot survive in the presence of oxygen. Its spores however are very resistant to heat and usual antiseptics. The spores are widely distributed in the soil and intestines of many animals. Manure-treated soils contain an abundance of spores. The organism produces two toxins, tetanolysin and tetanospasmin, of which the latter is the neurotoxin responsible for clinical disease.

Clostridium tetani usually enters the body through a wound. Although the incubation period varies, disease tends to occur within 3–21 days following spore inoculation. The site of inoculation seems to correlate with the incubation period duration. Under anaerobic conditions, the spores germinate and toxin production ensues. Toxin enters the bloodstream and lymphatics where it ultimately leads to the central nervous system and motor end plates where tetanus toxin interferes with neurotransmitter release (specifically GABA) blocking inhibitor impulses. This results in unopposed and uncontrollable muscle contraction and spasm [96].

In general, there are three forms of tetanus: localized, cephalic, and generalized. Localized tetanus is uncommon and is characterized by spastic muscle contractions at the site of initial inoculation [96]. These may persist for a week. Cephalic tetanus is a rare form of the disease usually following otitis media in which cranial nerves and facial muscles are affected. More than 80 % of cases are of generalized tetanus. This usually presents initially with trismus or lockjaw and risus sardonicus and progresses to generalized tetanus

spasm. Generalized tetanus is usually accompanied by respiratory failure caused by generalized spasticity of respiratory muscles. Before the availability of medications to counteract spams and assisted ventilation, respiratory failure was the most common cause of death with tetanus. Generalized tetanus can also result in generalized autonomic dysfunction resulting in blood pressure variations, tachycardia, bradycardia, flushing, and arrhythmias. The duration of most severe illness usually is from 1 to 4 weeks with mortality reported between 20 and 70 %.

Tetanus toxoid was first used in 1924 and was widely adopted in the armed forces during World War II. Tetanus toxoid consists of formaldehyde-treated toxin. There are two types of toxoid available, adsorbed and fluid toxoid [97]. Current preparations are available as combinations with either diphtheria and acellular pertussis or diphtheria toxoid alone. As with other inactivated vaccines and toxoids, more than one dose is required to confer immunity. After a series of three vaccines, essentially all recipients develop antitoxin levels considered protective. Effectiveness has never been objectively studied but it is inferred by antitoxin levels to be 100 % if given within the prior 10 years.

A decline in cases of tetanus was observed in the early twentieth century with a further rapid decline after tetanus toxoid was introduced. Mortality rates have also dropped significantly, demonstrated to be as low as 10 % in recent years [98]. Virtually all cases of tetanus reported have occurred in those who were never vaccinated or did not have booster vaccine in the prior 10 years.

17 Tuberculosis Vaccine

There is probably no vaccine in wide use that has been the subject of as much scrutiny and controversy as the tuberculosis vaccine commonly referred to as Bacillus Calmette-Guerin (BCG) [99]. It is one of the oldest vaccines available and has been widely adopted worldwide except for the USA and the Netherlands. The estimated efficacy rates have varied widely in different studies ranging from broad protection of more than 80 % to no efficacy at all.

Tuberculosis has caused disease in human for many millennia with cases being noted in mummies from the age of the Pharaohs in Egypt. It is likely responsible for the majority of deaths in the USA and Europe in recorded history. During the tenth century it was responsible for 400 in every 100,000 deaths. With improving living conditions, sanitation, and social advances came a decrease in the incidence and mortality in the industrialized world.

The disease is caused by the pathogen *Mycobacterium tuberculosis* first described by Koch in 1882. Tuberculosis is acquired through the respiratory tract and from there can enter a latent stage or progress to active disease. The majority of patients infected initially are asymptomatic, entering a latent stage where the

immune system keeps the disease in check. For most individuals infected with tuberculosis, the average lifetime risk of reactivation disease is roughly 10 %. Should disease become active, tuberculosis most commonly causes disease in the lungs but has the potential to disseminate to virtually any organ [99]. The time between primary infection and reactivation can span anywhere from weeks to years which is one of the more challenging aspects of conducting trials for a vaccine. It is a highly infectious disease with 25–50 % of close contacts becoming infected when exposed to an active case.

The live attenuated oral BCG vaccine was first given to infants in Paris in 1921 and has undergone substantial changes since then. The attenuated *Mycobacterium bovis* strain was first used by French scientists Calmette and Guerin where they studied a strain of *M. bovis* causing tuberculous mastitis in cows. They painstakingly cultured a strain every 3 weeks over the course of 13 years leading to a non-pathogenic and phenotypically different bacteria. BCG has been part of the expanded program for immunization of the WHO since the 1970s and has been administered some four billion times with relatively few significant side effects. Only recently has it been noted that administration of BCG can result in active infection in patients with advanced immune suppression such as those with HIV. Recommendations have changed as to not include such patients in current immunization schedules.

The extent of efficacy of this vaccine seems to depend on prior exposure to Mycobacteria which itself is a function of age. Trials on efficacy have widely varied with some trials demonstrating great protection against pulmonary tuberculosis and others showing virtually no protection at all [100]. In a meta-analysis performed in 2012, investigators found that in children who were school aged with negative prior tuberculin testing a relative risk of 0.26 was achieved and a relative risk of 0.41 was achieved in neonates. This effect seems to disappear in adolescent trials although some protection was observed in adult trials. Factors that may explain this decrease in protection during the teenage years include the fact that the immune system may not be mature enough when first administered to confer long-lasting immunity, and co-infection with certain helminthic and viral pathogens which could depress immunity (the extreme of this being HIV). The greatest efficacy of the tuberculous vaccine seems to be in decreasing disseminated disease and meningitis in children where protection can be as high as 80 % [101]. The effect of BCG on immunity seems to be greatest during the first 10–15 years after administration with no significant increased protection noted in adolescents and adults.

The BCG vaccine is currently administered to newborns in countries that have adopted the vaccine in the form of one intradermal injection. The dose of vaccine varies by age and formulation. The official WHO recommendation is to receive a single intradermal vaccine dose.

18 Yellow Fever Vaccine

Although taxonomic studies of the virus have indicated an African origin, yellow fever was first recognized during an outbreak in the Americas in 1648. The current consensus is that the virus was introduced into the new world through mosquito-infested slave trading vessels from West Africa. Epidemics affected the USA including the Philadelphia epidemic of 1793 that killed one-tenth of the city's population. Sanitary measures including the introduction of piped water inadvertently helped to diminish transmission of the disease. Advances in the early twentieth century, which included the identification of the vector, isolation of the virus, and development of a vaccine, all served to curtail the prevalence of this disease. However, more than 70 years after the development of an effective vaccine, areas of endemic transmission continue to exist with the periodic recurrence of outbreaks.

Yellow fever virus belongs to the genus *Flavivirus*. *Flaviviruses* are small spherical positive-sense single-stranded viruses with an envelope containing lipid and two envelope proteins, E and M. The genome of the prototype yellow fever virus strain 17D-204 contains 10,862 nucleotides, composed of a 5′-terminal type I cap structure, a short 5′ noncoding region, a single open reading frame of 10,233 nucleotides, and a 3′ noncoding region. The E protein exhibits important biologic properties including attachment to host cell receptors, endosomal membrane fusion, and display of sites mediating hemagglutination and viral neutralization.

Yellow fever ranges in severity from a nonspecific flu-like-type illness to a hemorrhagic fever that is fatal in 50 % of cases. A significant percentage of infections go undetected. The incubation period ranges from 3 to 6 days and is followed by the abrupt presentation of fever, headaches, and muscle aches accompanied by physical findings such as injected conjunctiva, facial flushing, and leukopenia. Most cases resolve after this phase, but some go on to develop, after being free of fever for hours or days, high fever, lumbosacral pain, headaches, abdominal pain, and somnolence. This is a severe multisystemic illness dominated by icteric hepatitis and hemorrhagic diathesis with prominent gastrointestinal bleeding, hematemesis, epistaxis, petechiae, and purpuric hemorrhages.

Yellow fever vaccine is a live-virus vaccine which has been used for several decades. A single dose protects against disease for 10 years or more. Infants, toddlers, pregnant women, and patients with HIV may not have as robust a response to the vaccine.

Adverse reactions to the yellow fever vaccine are very rare but in some instances can be severe. The more severe reactions are lumped into two syndromes known as viscerotropic adverse reactions and neurotropic adverse reactions [102]. The vaccine is contraindicated in those with allergy to the vaccine components, age less than 6 months, symptomatic HIV infection or CD4 count

less than 200, thymic disorder-associated immune dysfunction, and other immunosuppressive diseases and therapies.

Yellow fever vaccine is recommended for persons aged ≥9 months that are traveling to or living in areas at risk for yellow fever virus transmission in South America and Africa. A single dose given every 10 years is considered effective for people who are traveling to areas of high endemicity. Certain countries require record of immunization before entry is allowed including proof of vaccination by documentation on an "International Certificate of Vaccination or Prophylaxis" for yellow fever.

19 Zoster Vaccine

The *varicella zoster virus (VZV)* belongs to the family of *Alfa herpes viruses* who have the ability to maintain a latent infection in the sensory ganglia during primary infection. The virus initially presents as a diffuse vesicular eruption, varicella (chickenpox) which is a prevalent and widespread affliction worldwide. Thoracic and cervical ganglia contain VZV detectable by PCR in as many as 90 % of adults. It is from these ganglia that herpes zoster subsequently arises.

Although the mechanism by which latency is maintained is not fully understood, the evidence points at the importance of the host-specific immune response which first develops soon after the appearance of skin lesions in varicella. These responses include the development of a polyclonal anti-VZV) antibody and T-cell-mediated responses. These persist lifelong and prevent the appearance of new episodes of varicella.

With increasing age and T-cell immune suppression, the risk of developing herpes zoster increases. The CDC estimates that 1 in 3 Americans will develop herpes zoster in their lifetime. About half of the cases occur in men and women older than 60 and there are approximately 1 million new cases per year. Herpes zoster is a dermatologic vesicular disease which affects a particular dermatome in individuals as a consequence of the reactivation of the *VZV.*) The disease is characterized by a prodromal stage where pain predominates, followed by the classic appearance of a vesicular rash following the trajectory of the affected dermatome. The most severe consequence of zoster is the appearance of postherpetic neuralgia which can result in significant pain and disability in those affected by it. Zoster vaccination seeks to curtail the risk of herpes zoster and the development of postherpetic neuralgia [103].

The currently available vaccine is a live attenuated form of the virus called the Oka strain of VZV. It is essentially the same vaccine given for varicella but with 14 times the potency. It was first licensed in the USA in 2006. It is also licensed in the EU and Canada. It is currently recommended for patients 60 years of age or older

with the purpose of preventing the development of herpes zoster and postherpetic neuralgia.

Regarding efficacy, a large trial conducted between 1999 and 2004 involving thousands of patients demonstrated that the vaccine was effective in reducing the risk of disease by 51 % and the risk of postherpetic neuralgia by 67 %. Studies in younger cohorts of patients have shown similar results and this led the EU to approve the use of the zoster vaccine in patients between ages 50 and 59 [104]. In the USA the FDA has approved the vaccine beginning at age 50; however the ACIP recommends that the vaccine not be given until age 60.

Given the vaccine is an attenuated virus, it is contraindicated in those with significant immune suppression such as patients with advanced HIV, those receiving corticosteroids or other immune suppressant medication, or those with active malignancies receiving chemotherapy. Overall the safety profile for this vaccine is excellent with most patients reporting no side effects.

Current recommendation is to give one intramuscular dose in patients older than 60 years. Given this is a live vaccine, it should not be administered to patients with significant immune suppression.

20 HIV Vaccine

Since the beginning of the epidemic in the early 1980s, the natural history of HIV infection has evolved from one of certain death to a treatable chronic condition. Currently, there are about 35 million people living with HIV and the disease was responsible for 1.5 million deaths in 2013. In the USA there are approximately 1.2 million living with HIV of which 14 % are unaware of their diagnosis. Roughly 50,000 people develop new infections annually in the USA alone.

The two agents that cause AIDS are *human immunodeficiency 1 (HIV-1) and HIV-2*. These viruses are *Lentiviruses* that belong to the family *Retroviridae*. These are enveloped RNA viruses that cause slowly progressive infections which produce clinical disease after a prolonged latency. In untreated patients the subacute phase preceding clinical disease averages around 10 years. These viruses depend on, and possess, the enzyme reverse transcriptase which transforms viral RNA into proviral DNA. HIV targets CD4 cells, a central component of the immune system, and enters them by interacting with the surface coreceptors CCR5 and CXCR4. Infection leads to a steady decline of CD4 cells eventually leading to the development of AIDS in those untreated.

Current antiretroviral medications are very effective at bringing HIV under control and can result in a near-normal life-span. While public health measures have significantly decreased the incidence of new infections, it is clear that a vaccine would be the only effective

way of controlling the epidemic. There have been many obstacles to the development of an effective HIV vaccine. Chief among these is the fact that there is no documented case of a human spontaneously clearing the virus. Other important factors include the antigenic diversity and hypervariability of the virus, its ability to rapidly generate escape mutants, and the lack of an ideal animal model.

Over the last 30 years, only four vaccine concepts have been evaluated in clinical efficacy trials. These include the use of purified HIV-1 envelope proteins, recombinant adenovirus and poxvirus vectors, and plasmid DNA vaccines. While there have been several phase I and phase II trials evaluating safety and immunogenicity of proposed HIV vaccines, to date, there have only been a handful of Phase III trials that have evaluated the efficacy of HIV vaccines. Of those, only one showed a statistically significant result. Known as the "Thai trial," RV144 was a randomized placebo-controlled trial looking at the use of a *Canarypox* vector vaccine expressing gp120 clad E GAG and protease from clade B boosted by AIDSVAX (rGP protein 120 from 2 clade B). Looking at a population of around 16,000 low-risk individuals, in the modified intention-to-treat analysis, this vaccination strategy demonstrated a 31 % reduction in disease acquisition [105]. While the results are modest, it serves as a proof of concept that producing an effective vaccine against HIV is in fact possible.

An exciting field of study in which much of the current study for HIV vaccine is focused is the concept of broadly neutralizing antibodies. These are antibodies that target the conserved regions of HIV-1 Env. Although a subset of patients develop broadly neutralizing antibodies after years of infection, only a small percentage produce antibodies that are potent as well as broad. No vaccine to date has been able to elicit a broadly neutralizing antibody response. The use of passive immunization using broadly neutralizing antibodies remains an attractive but challenging proposal [106].

The landscape for the development of an effective HIV vaccine is one that should generate optimism amongst physicians and patients. The results of the RV-144 trial have generated follow-up studies that are currently under way [107]. This along with the advances in understanding of broadly neutralizing antibodies should be viewed as a great stride in the search for an effective vaccine

References

1. Leung AK (1996) Variolation and vaccination in late imperial China, CA 1570-1911. In: Plotkin SA, Fantini B (eds) Vaccina, vaccination, vaccinology: Jenner, Pasteur and their successors. Elsevier, Paris
2. Nathanson N, Langmuir AD (1963) The Cutter incident: poliomyelitis following formaldehyde-inactivated poliovirus vaccination in the United States during the spring of 1955. II. Relationship of poliomyelitis to Cutter vaccine. Am J Hyg 78: 29–60
3. Editors of the Lancet (2010) Retraction Ileal-lymphoid-nodular hyperplasia, non-specific colitis, and pervasive developmental disorder in children. Lancet 375:445

4. Godlee F, Smith J, Marcovitch H (2011) Wakefield's article linking MMR vaccine and autism was fraudulent. BMJ 342:c7452
5. Doja A, Roberts W (2006) Immunizations and autism: a review of the literature. Can J Neuro Sci 33:341–346
6. Fauquet CM, Mayo MA, Maniloff J et al (2005) International Union of Microbiological Societies, Virology Division. Virus Taxonomy: Eight report of the International Committee on Taxonomy of Viruses. Elsevier Academic Press, San Diego, CA
7. Dingle JH, Langmuir AD (1968) Epidemiology of acute respiratory disease in military recruits. Am Rev Respir Dis 97:1–65
8. Hilleman M, Gauld R, Butler R et al (1957) Appraisal of occurrence of adenovirus-caused respiratory illness in military populations. Am J Hyg 66:29–41
9. Fox JP, Brandt CD, Wassermann FE et al (1969) The virus watch program: a continuing surveillance of viral infections in metropolitan New York families VI: observations of adenovirus infections: virus excretion patterns, antibody response, efficiency of surveillance, pattern of infections, and relation to illness. Am J Epidemiol 89:25–50
10. Gaydos CA, Gaydos JC (1995) Adenovirus vaccines in the U.S. military. Mil Med 160:300–304
11. www.cdc.gov/vaccines/adenovirus
12. Hyer RN, Howell MR, Ryan MA et al (2000) Cost-effectiveness analysis of reacquiring and using adenovirus types 4 and 7 vaccines in naval recruits. Am J Trop Med Hyg 6:613–618
13. (2011) Adenovirus type 4 and adenovirus type 7 vaccine, live, oral (package insert). Teva Pharmaceuticals USA Inc, Sellersville, PA
14. Schwartz MN (2001) Recognition and management of anthrax: an update. N Engl J Med 345:1621–1626
15. Booth MG, Hood J, Brooks TJ (2010) Anthrax infection in drug users. Lancet 375:1345–1346
16. Centers for Disease Control and Prevention (2008) Summary of notifiable diseases, United States. MMWR 57:1–94
17. Centers for Disease Control and Prevention (2009) Use of anthrax vaccine in the United States. Recommendations of the Advisory Committee on Immunization of Practices (ACIP). MMWR 59(RR-6):1–30
18. Blake PA, Allegra DT, Snyder JD et al (1980) Cholera: a possible endemic focus in the United States. N Engl J Med 302:305–309
19. Tacket CO, Taylor RK, Losonsky G et al (1998) Investigation of the role of toxin coregulated pili and mannose- sensitive hemagglutinin pili in the pathogenesis of *Vibrio cholerae* 0139 infection. Infect Immun 66: 692–695
20. Silva A, Leitch G, Camilli A et al (2006) Contribution of hemagglutination/protease and motility to pathogenesis of El Tor biotype cholera. Infect Immun 74:2072–2079
21. www.who.int/cholera/vaccines
22. Epidemiology and prevention of vaccine-preventable diseases. The pink book: course textbook, 12th edn
23. (2006) Preventing tetanus, diphtheria, and pertussis among adolescents: use of tetanus toxoid, reduced diphtheria toxoid and acellular pertussis vaccines. Recommendations of the Advisory Committee on Immunization Practices. MMWR 55(RR-3):1–34
24. Tognotti E (2003) Scientific triumphalism and learning from facts: bacteriology and the "Spanish flu" challenge of 1918. Soc Hist Med 16:97–110
25. Pittman M (1931) Variation and type specificity in bacterial species Hemophilus influenzae. J Exp Med 53:471–492
26. Dajani AS, Asmar BI, Thirumoorthi MC (1979) Systemic Haemophilus influenzae disease: an overview. J Pediatr 94:355–364
27. Tebbutt GM (1983) Evaluation of some methods for the laboratory identification of Heamophilus influenzae. J Clin Pathol 36:991
28. Centers for Disease Control and Prevention. www.cdc.gov/vaccines/hib
29. Bachman L (1952) Infectious hepatitis in Europe. In: Rodenwalt E (ed) World Atlas of Epidemic Diseases. Falk-Verlag Hamburg, Germany
30. Siegl G, Weitz M, Kronauer G (1984) Stability of hepatitis A virus. Intervirology 22:218–226
31. Krugman S, Giles JP, Hammond J (1967) Infectious hepatitis: evidence of two distinctive clinical, epidemiological and immunological types of infection. JAMA 200: 365–373
32. Peetermans J (1992) Production, quality control and characterization of an inactivated hepatitis A vaccine. Vaccine 10(Suppl 1): S99–S101
33. Armstrong ME, Giesa PA, Davide JP et al (1993) Development of the formalin-inactivated hepatitis A vaccine, VAQTA from the live attenuated virus strain CR326F. J Hepatol 18(Suppl 2):S20–S26
34. Atkinson W, Wolfe S, Hamborsky J (2012) Epidemiology and prevention of vaccine-

preventable diseases, 12th edn, 2nd printing. Public Health Foundation, Centers for Disease Control and Prevention, Washington DC

35. (2006) A comprehensive immunization strategy to eliminate transmission of hepatitis B virus infection in the United States. Recommendations of the Advisory Committee on Immunization Practices (ACIP) Part II: immunization of adults. MMWR 55(RR-16): 1–33
36. Li J, Yao J, Shan H, Chen Y, Jiang ZG, Ren JJ, Xu KJ, Ruan B, Yang SG, Wang B, Xie TS, Li Q (2015) Comparison of the effect of two different doses of recombinant hepatitis B vaccine on immunogenicity in healthy adults. Hum Vaccin Immunother 11(5):1108–1113
37. Okwen MP, Reid S, Njei B, Mbuagbaw L (2014) Hepatitis B vaccination for reducing morbidity and mortality in persons with HIV infection. Cochrane Database Syst Rev 10:CD009886
38. Bernard HU, Burk RD, Chen Z et al (2010) Classification of papillomaviruses based on 189 PV types and proposal of taxonomic amendments. Virology 401:79
39. Howley PM, Lowy DR (2007) Papillomaviruses. In: Knipe DM, Howley PH (eds) Fields virology, 5th edn. Lippincott Williams and Wilkins, Philadelphia, pp 2299–2354
40. Parkin DM, Bray F (2006) Chapter 2. The burden of HPV-related cancers. Vaccine 24(suppl 3):S11–S25
41. Orth G (2008) Host defenses against human papillomaviruses: lessons from epidermodysplasia verruciformis. Curr Top Microbiol Immunol 321:59–83
42. Durst M, Gissman L, Ikenberg H et al (1983) A papillomavirus DNA from a cervical carcinoma and its prevalence I cancer biopsy samples from different geographic regions. Proc Natl Acad Sci U S A 80:3812–3815
43. Schiffman M, Castle PE, Jeronimo J et al (2007) Human papillomavirus and cervical cancer. Lancet 370:890–907
44. D'Souza G, Kreimer AR, Viscidi R et al (2007) Case–control study of human papillomavirus and oropharyngeal cancer. N Engl J Med 356:1944–1956
45. Inglis S, Shaw A, Koenig S (2006) Chapter 11: HPV vaccines: commercial research and development. Vaccine 24(suppl 3):99–105
46. Centers for Disease Control and Prevention. www.cdc.gov/vaccines/hpv
47. Atkinson W, Wolfe S, Hamborsky J (2012) Centers for Disease Control and Prevention Epidemiology and prevention of vaccine-preventable diseases, 12th edn, 2nd printing. Public Health Foundation, Washington, DC
48. Thompson WW, Shay DK, Weintraub E et al (2004) Influenza-associated hospitalizations in the United States. JAMA 292:1333–1340
49. Treanor JJ, Campbell JD, Zangwill KM et al (2006) Safety and immunogenicity of an inactivated subvirion influenza A (H5N1) vaccine. N Engl J Med 354:1343–1351
50. Osterholm MT, Kelley NS, Sommer A, Belongia EA (2012) Efficacy and effectiveness of influenza vaccines: a systematic review and meta-analysis. Lancet Infect Dis 12:36–44
51. CDC (2011) Prevention and control of influenza with vaccines: recommendations of the Advisory Committee on Immunization Practices. MMWR 60(33):1128–1132
52. Center for Disease Control and Prevention: Japanese Encephalitis vaccine. www.cdc.gov/japaneseencephalitis/vaccine
53. Solomon T, Kneen R, Dung NM et al (1998) Poliomyelitis -like illness due to Japanese encephalitis virus. Lancet 351:1094–1097
54. (2013) Center for Disease Control and Prevention: Japanese Encephalitis vaccines: ACIP recommendations. MMWR
55. Cartwright KA, Stuart JM, Jones DM, Noah ND (1987) The Stonehouse survey: nasopharyngeal carriage of meningococci and Neisseria lactamica. Epidemiol Infect 99:591–601
56. Caugant DA, Hoiby EA, Magnus P et al (1994) Asymptomatic carriage of Neisseria meningitidis in a randomly sampled population. J Clin Microbiol 32:323–330
57. Christensen H, May M, Bowen L et al (2010) Meningococcal carriage by age: a systematic review and meta-analysis. Lancet Infect Dis 10:853–861
58. Fijenn CA, Kuijper EJ, Tjia HG et al (1994) Complement deficiency predisposes for meningitis due to nongroupable meningococci and Neisseria -related bacteria. Clin Infect Dis 18:780–784
59. Linton SM, Morgan BP (1999) Properdin deficiency and meningococcal disease: identifying those most at risk. Clin Exp Immunol 118:189–191
60. Condon RJ, Riley TV, Kelly H (1994) Invasive meningococcal infection after splenectomy. BMJ 308:792–793
61. Bilukha OO, Rosenstein N (2005) Prevention and control of meningococcal disease: recommendations of the ACIP. MMWR
62. Report from the ACIP (2008) decision not to recommend routine vaccination of all children aged 2-10 years with quadrivalent meningococcal vaccine (MCV4). MMWR

63. Licensure of meningococcal conjugate vaccine (Menveo) and guidance for use (2010) ACIP MMWR
64. Center for Disease Control and Prevention (2014) ACIP recommendations for meningococcal vaccinations. MMWR
65. Abu Becr M (1748) A discourse on the smallpox and measles. J Brindley, London
66. Wilson GS (1962) Measles as a universal disease. Am J Dis Child 103:219–223
67. Black FL, Evans AS (1989) Viral infections of humans: epidemiology and control, 3rd edn. Plenum, New York, pp 451–465
68. Langmuir AD (1962) Medical importance of measles. Am J Dis Child 103:224–226
69. Centers for Disease Control and Prevention (2009) Global measles mortality. MMWR 58:1321–1326
70. Hamilton R (1790) An account of a distemper by the common people of England vulgarly called the mumps. Trans Roy Soc Edinb 2:59–72
71. Johnson CD, Goodpasture EW (1935) The etiology of mumps. Am J Hyg 21:46–57
72. Gordon JE, Heeren RH (1940) The epidemiology of mumps. Am J Med Sci 200:338–359
73. Hirsch A (1883) Handbook of Geographical and Historical Pathology. Volume I: acute infective diseases, 2nd edn. Sydenham Society London, England
74. Penttinen K, Cantell K, Somer P et al (1968) Mumps vaccination in the Finnish defense forces. Am J Epidemiol 88:234–244
75. Smith JL (1875) Rotheln (epidemic roseola-German measles-hybrid measles). Arch Dermatol 1:1–13
76. Veale H (1866) History of an epidemic of rotheln with observation on its pathology. Edinb Med J 12:404–414
77. Gregg NM (1941) Congenital cataract following German measles in the mother. Trans Ophthalmol Soc Aust 3:35–46
78. Measles, mumps, and rubella- vaccine use and strategies (1998) Recommendations of the Advisory Committee on Immunization Practices. MMWR 1–5
79. Atkinson W, Wolfe S, Hamborsky J (2012) Centers for Disease Control and Prevention. Epidemiology and prevention of vaccine, 12th edn, 2nd printing. Washington, DC: Public Health Foundation
80. Senzilet LD, Halperin SA, Spika JS et al (2001) Pertussis is a frequent cause of prolonged cough illness in adults and adolescents. Clin Infect Dis 32:1691–1697
81. CDC (2011) Updated recommendations for use of tetanus toxoid, reduced diphtheria toxoid and acellular pertussis (Tdap) Vaccine from the Advisory Committee on Immunization Practices (ACIP). MMWR 60(1):13–15
82. Centers for Disease Control and Prevention (2012) Epidemiology and prevention of vaccine-preventable diseases. Public Health Foundation, Washington, DC
83. Simonsen L, Taylor RJ, Young-Xu Y et al (2011) Impact of pneumococcal conjugate vaccination of infants on pneumonia and influenza hospitalization and mortality in all age groups in the United States. MBio 2(1):e00309–e00310
84. Robinson KA, Baughman W, Rothrock G (2001) Epidemiology of invasive *Streptococcus pneumoniae* infections in the United States 1995–1998. Opportunities for prevention in the conjugate vaccine era. JAMA 285:1729–1735
85. Simonsen L, Taylor RJ, Young-Xu Y, Haber M, May L, Klugman KP (2011) Impact of pneumococcal conjugate vaccination of infants on pneumonia and influenza hospitalization and mortality in all age groups in the United States. MBio 2(1):e00309–e00310
86. http://www.cdc.gov/vaccines/hcp/acip-recs/vacc-specific/pneumo.html
87. Bern C, Martines J, De Zoysa I (1992) The magnitude of the global problem of diarrheal disease: a ten-year update. Bull World Health Organ 70:705–714
88. Black RE, Cousens S, Johnson HL et al (2008) Global, regional, and national causes of child mortality: a systematic analysis. Lancet 375:1969–1987
89. Parashar UD, Burton A, Lanata C et al (2003) Global illness and deaths caused by rotavirus disease in children. Emerg Infect Dis 9: 565–572
90. Glass RI, Kilgore PE, Holman RC et al (1996) The epidemiology of rotavirus diarrhea in the United States: surveillance and estimated of disease burden. J Infect Dis 174(Suppl 1):S5–S11
91. Kilgore PE, Holman RC, Clarke MJ et al (1995) Trends of diarrheal disease- associated mortality in U.S. children, 1968 through 1991. JAMA 274:1143–1148
92. Ball JM, Tian P, Zeng C et al (1996) Age-dependent diarrhea induced by a rotaviral nonstructural glycoprotein. Science 272: 101–104
93. Perez-Schael I, Daoud G, White L et al (1984) Rotavirus shedding in newborn children. J Med Virol 14:127–136
94. Chrystie IL, Totterdell BM, Banatvala JE (1978) Asymptomatic endemic rotavirus

infections in the newborn. Lancet 1: 1176–1178

95. Centers for Disease Control and Prevention (2014) ACIP rotavirus vaccine recommendations. MMWR
96. Centers for Disease Control and Prevention (2012) Epidemiology and prevention of vaccine-preventable diseases
97. (2011) Updated recommendations for use of tetanus toxoid, reduced diphtheria toxoid and acellular pertussis (Tdap) vaccine from the Advisory Committee on Immunization Practices. MMWR 60(1):13–15
98. Morbidity and Mortality Weekly Report (2011) Tetanus surveillance United States, 2001–2008. MMWR 60(12):365–369
99. Plotkin SA, Orenstein WA, Offit PA (eds) Vaccines, 6th edn
100. Trunz BB, Fine PEM, Dye C (2006) Effect of BCG vaccination on childhood tuberculous meningitis and miliary tuberculosis worldwide: a meta-analysis and assessment of cost-effectiveness. Lancet 367:1173–1180
101. Rodriques LC, Diwan VK, Wheeler JG (1993) Protective effect of BCG against tuberculous meningitis and miliary tuberculosis: a meta-analysis. Int J Epidemiol 22:1154–1158
102. Rafferty E, Duclos P, Yactayo S, Schuster M (2013) Risk of yellow fever vaccine-associated viscerotropic disease among the elderly: a systematic review. Vaccine 31:5798–5805
103. Centers for Disease Control and Prevention (2012) Epidemiology and prevention of vaccine-preventable diseases
104. Levin MJ, Oxman MN, Zhang JH et al (2008) Varicella-zoster virus–specific immune responses in elderly recipients of a herpes zoster vaccine. J Infect Dis 197:825–835
105. Rerks-Ngarm S, Pitisuttithum P, Nitayaphan S, Kaewkungwal J et al (2009) Vaccination with ALVAC and AIDSVAX to prevent HIV-1 infection in Thailand. N Engl J Med 361:2209–2220
106. Chuna T-W, Murraya D, Justementa JS et al (2014) Broadly neutralizing antibodies suppress HIV in the persistent viral reservoir. Proc Natl Acad Sci U S A 111:13151–13156
107. Barouch MD (2013) The quest for an HIV-1 vaccine-moving forward. N Engl J Med 369:2073–2076

Chapter 2

Future Challenges for Vaccinologists

Sunil Thomas, Rima Dilbarova, and Rino Rappuoli

Abstract

Vaccination is one of the cheapest health-care interventions that have saved more lives than any other drugs or therapies. Due to successful immunization programs we rarely hear about some of the common diseases of the early twentieth century including small pox and polio. Vaccination programs have also helped to increase food production notably poultry, cattle, and milk production due to lower incidence of infectious diseases in farm animals. Though vaccination programs have eradicated several diseases and increased the quality of life there are several diseases that have no effective vaccines. Currently there are no vaccines for cancer, neurodegenerative diseases, autoimmune diseases, as well as infectious diseases like tuberculosis, AIDS, and parasitic diseases including malaria. Abuse of antibiotics has resulted in the generation of several antibiotic-resistant bacterial strains; hence there is a need to develop novel vaccines for antibiotic-resistant microorganisms. Changes in climate is another concern for vaccinologists. Climate change could lead to generation of new strains of infectious microorganisms that would require development of novel vaccines. Use of conventional vaccination strategies to develop vaccines has severe limitations; hence innovative strategies are essential in the development of novel and effective vaccines.

Key words Vaccine, Infectious disease, Structure-based vaccine, Antibiotic resistance, Climate change

1 Introduction

Vaccines are one of the greatest achievements of medicine providing protection against debilitating diseases and have spared millions of lives. Smallpox, polio, measles, diphtheria, pertussis, rubella, mumps, and tetanus were once common diseases of man that killed millions of people (until the first half of the twentieth century) before the advent of vaccines. Fortunately, we rarely hear about these diseases today due to the widespread introduction of immunization programs. The introduction of safe, affordable, and effective vaccines has dramatically improved public health, prevented countless hospitalizations, and substantially increased industrial output [1]. Though in the short term vaccines prevent diseases, in the long term mass vaccinations are successful in eradicating infectious diseases. Vaccinations have helped in eradicating several diseases in developed countries; however, there are only

Sunil Thomas (ed.), *Vaccine Design: Methods and Protocols: Volume 1: Vaccines for Human Diseases*, Methods in Molecular Biology, vol. 1403, DOI 10.1007/978-1-4939-3387-7_2,

two diseases that have been eradicated globally. Mass awareness programs and aggressive vaccination strategies in the twentieth century were able to control smallpox and in a landmark event the disease was officially declared eradicated in 1980. Rinderpest, a serious disease of cattle, was officially eradicated in 2011, thereby becoming only the second disease to be completely eradicated [1]. Recently the Americas (North and South America) have become the first in the world to be declared free of endemic transmission of rubella, a contagious viral disease that can cause multiple birth defects as well as fetal death when contracted by women during pregnancy. The achievement was due to a 15-year effort that involved widespread administration of the vaccine against measles, mumps, and rubella (MMR) throughout the Western Hemisphere. The declaration of elimination by Pan American Health Organization/World Health Organization (PAHO/WHO) makes rubella and congenital rubella syndrome (CRS) the third and fourth vaccine-preventable diseases to be eliminated from the Americas, following the regional eradication of smallpox in 1971 and the elimination of polio in 1994 (source: World Health Organization). This chapter reviews the future challenges of vaccinologists.

2 Antibiotic Resistance

Though vaccines prevent diseases, there are many infectious diseases without any commercial vaccines available. Hence, antibiotics are prescribed to control these diseases. Unfortunately, abuse/misuse of antibiotics has resulted in generation of antibiotic-resistant bacteria [2]. Abuse of antibiotics is the leading cause of increased morbidity and mortality from drug-resistant microorganisms [3].

Recent studies demonstrated that abuse of antibiotics could lead to several metabolic diseases including obesity, food allergy, and autoimmune diseases [3–5]. Abuse of antibiotics is not restricted to patients alone, but also occurs in the food supply chain. In veterinary medicine antibiotics are used not only in the treatment and prevention of disease but also for growth promotion in food animals [4]; though many countries have banned use of antibiotics for growth promotion there are places where banning is not enforced vigorously. One of the reasons for the incidence of antibiotic-resistant bacteria is due to the uncontrolled use of antibiotics in the food supply chain. Hence there is a need to develop new and improved vaccines for animals so that they are protected during their life-span from different pathogens. Reduced use of antibiotics for the control of diseases in animals will lead to low levels of antibiotics in the food supply chain which could lead to lowering of the incidence of antibiotic resistance.

The Centers for Disease Control and Prevention (CDC) estimates that two million patients suffer from hospital-acquired infections (HAI) (nosocomial infection) every year and nearly 100,000 of them die [5]. HAIs are infections that occur more than 48 h post-admission. HAIs are caused by viral, bacterial, and fungal pathogens. HAIs are caused by viral, bacterial, and fungal pathogens. Methicillin-resistant *Staphylococcus aureus* (MRSA), *Clostridium difficile*, *Pseudomonas aeruginosa*, and vancomycin-resistant *Enterococcus* (VRE) are the major bacteria that cause HAIs. The importance of VRE is that it is capable of genetically transferring its resistance genes to such organisms as MRSA. Vancomycin-resistant MRSA (VR-MRSA) is a major threat, because it is expected to be highly communicable and difficult to treat because of limited antibiotic therapy [5]. As yet there are no successful vaccines for the antibiotic-resistant bacterial strains. Hence there is an urgent need to develop new therapeutic strategies in the control of antibiotic-resistant bacterial infectious diseases.

3 Climate Change and Infectious Diseases

The incidence, outbreak frequency, and distribution of many infectious diseases are generally expected to change as a consequence of climate change. Climate change would affect vector-borne, food-borne, water-borne, and rodent-borne diseases [6].

Temperature and precipitation patterns influence food- and water-borne diseases [7]. Changes in seasonal precipitation and temperature influence vector-borne diseases through (1) effects on vector survival, reproduction rates, habitat suitability, distribution, and abundance; (2) the intensity and temporal pattern of vector activity (biting rates); and (3) rates of pathogen development, survival, and reproduction within vectors [8]. The projected climate changes may shift the distributional ranges of vector-borne diseases. As an example, the number of tick-borne diseases of humans has increased in incidence and geographic range over the past few decades, and there is concern that they will pose an even greater threat to public health in future. Although global warming is often cited as the underlying mechanism favoring the spread of tick-borne diseases, climate will influence which tick species are found in a given geographic region, their population density, the likelihood that they will be infected with microbes pathogenic for humans, and the frequency of tick–human contact [9]. Changes in climate will influence other insect vectors including mosquitoes, fleas, sandflies, tsetse flies, and houseflies, known to carry highly pathogenic microorganisms infecting man.

Due to changes in climate there is concern that ancient bacteria and viruses could revive as global warming melts ice at the poles. Migratory birds and insects could bring the potential

harmful microorganisms to the populated urban/suburban areas. Vaccinologists should be on the lookout for new pathogens emerging in any corner of the planet.

4 Vaccines for Diseases Associated with Urban Areas in the Developing Countries

Rabies is one of the oldest and deadliest zoonotic diseases, killing thousands of people worldwide each year. Rabies is due to viral infection typically transmitted to people via bites from infected animals, especially bats, carnivores, or domestic mammals. The disease has no cure other than vaccination. Because of aggressive vaccination programs for pets, most rabies cases in developed countries are transmitted from wildlife species. However, most rabies in developing countries is canine related, notably stray dogs. The difference between a developed nation and developing nation is how the resources (however small) are managed. Some of the offices in developing countries are occupied by people with no interest in caring the public. The characteristic feature of cities in developing nations is poor urban management. One could observe poor waste management practices—with unmoved garbage at every intersection, stray dogs and cattle sharing the road, open and overflowing drains and sewage, and stagnant water bodies which provide breeding grounds for insects. These unhygienic conditions in cities are favorable grounds for a plethora of infectious diseases. The first line of defense against rabies is controlling the stray dog population. Development of cheaper rabies vaccines for developing countries could lead to better immunization programs in humans and stray animals.

Leptospirosis, a disease caused by the bacteria *Leptospira*, is an emerging public health problem in urban centers of developing countries. The disease is transmitted through infected rodents [10]. 200 serotypes of *Leptospira* have been described [11]. Though vaccines to leptospirosis are available the efficacy is very limited because they usually only protect well against a single serovar. Hence there is a need to develop highly effective vaccines for this disease which could protect against multiple strains of this pathogen.

Other diseases of note that arise from mismanaged urban centers include mosquito-transmitted diseases including malaria, dengue fever [12], and chikungunya [13], and the rodent-transmitted plague. Crowded living conditions and refuse-contaminated flood waters around the shanty towns of Surat, India, provided a breeding ground for rats and infected fleas which were responsible for the 1994 plague caused by the bacteria *Yersinia pestis* [14]. Though targeted vector management can make a difference in terms of reducing vector abundance, once the disease is out of control vaccination is the only strategy to prevent collateral damage to a

population. Currently there are no effective vaccines for malaria, dengue, chikungunya, etc. Vaccinologists should also look out for mutant strains during an epidemic outbreak so as to develop improved and effective vaccines.

5 Vaccines for HIV and Ebola Virus

Acquired immune deficiency syndrome (AIDS) caused by HIV is a serious threat to global public health. Despite intensive research since the 1980s there are no vaccines or drugs that can successfully prevent or eradicate the disease. The major barriers to HIV vaccine development include the variability of HIV, lack of a suitable animal model, lack of correlates of protective immunity, lack of natural protective immune responses against HIV, and the reservoir of infected cells conferred by integration of HIV's genome into the host [1]. Within the main HIV-1 subgroup, Group M, there are nine clades as well as dozens of recombinant forms, and clades can vary up to 42 % at the amino acid level [15]. A vaccine immunogen derived from a particular clade may therefore be ineffective against other clades, posing a significant obstacle to the creation of a global HIV vaccine. Importantly, one of the principal barriers limiting discovery of an HIV vaccine has been that protective immune responses tend to be polyclonal and involve antibodies directed to several different epitopes; thus, antigenic variation among the different HIV-1 isolates has been the major problem in the development of an effective vaccine against AIDS [1]. Although several 3D structures of HIV-1 envelope protein fragments have been determined, this knowledge has not yet led to the design of an HIV-1 vaccine. The mechanism by which an HIV vaccine might confer protection therefore remains uncertain, and an effective vaccine may require induction of an immune response that is significantly different from that seen during natural infection [16]. Overall, current vaccination strategies have not helped in developing a vaccine for HIV; hence novel "out-of-the-box" strategies are essential in developing an HIV vaccine [17].

Ebola virus disease is a severe, often fatal, zoonotic infection caused by a virus of the Filoviridae family. The Ebola virus (EBOV) causes an acute viral syndrome that presents with fever and an ensuing bleeding diathesis that is marked by high mortality in human and nonhuman primates. Fatality rates are higher than other viral diseases with rates of up to 90 % [18]. Ebola viral disease (EVD) affects the poorest people in the African continent. Due to movement of people across borders the disease could rapidly spread and infect any people globally. EBOV spreads through human-to-human transmission via direct contact with the blood, secretions, organs, or other bodily fluids of infected people and with surfaces and materials (e.g., bedding, clothing) contaminated with these

fluids. EBOV glycoprotein (GP1,2) and matrix protein (VP40) are both major components of EBOV. The hemorrhagic disease caused by EBOV is characterized by generalized fluid distribution problems, hypotension, coagulation disorders, and a tendency to bleed, finally resulting in fulminant shock. Vascular instability and dysregulation are hallmarks of the pathogenesis in EBOV hemorrhagic fever (HF). Endothelial disturbances can be caused indirectly, by proinflammatory cytokines such as TNF-α released from EBOV-infected monocytes/macrophages, and directly, following virus infection of endothelial cells. In vitro studies demonstrated that EBOV viral proteins could activate endothelial cells and induce a decrease in blood vessel barrier function [19]. The worldwide challenge posed by the 2014 outbreak of EBOV [20] has underscored the need for effective prevention and treatment options, especially for front-line health care and emergency response workers in the field, and at hospitals and other care facilities. As yet there are no vaccines or therapeutics commercially available to protect against EVD. Hence, there is an urgent need to develop a powerful vaccine which could provide robust protection against the viral pathogen. The EBOV and its high fatality are known since the 1970s. The disease only affects a small percentage of people annually in Africa; hence government agencies as well as International Organizations were not keen to invest in vaccines. If there were vaccines available against EBOV infection, thousands of lives could have been saved in 2014.

6 Development of Powerful Influenza Vaccines

Influenza A viruses are zoonotic pathogens that continuously circulate and change in several animal hosts, including birds, pigs, horses, and humans. The viral pathogen causes infections with various consequences ranging from pandemics to seasonal flu. The emergence of novel virus strains that are capable of causing human epidemics or pandemics is a serious possibility [21]. The World Health Organization estimates that the global disease burden from influenza is around one billion infections, three million to five million cases of severe disease, and between 300,000 and 500,000 deaths annually [22].

Influenza viruses contain 8 single-stranded RNA segments encoding 11 proteins. There are three types of influenza viruses: A, B, and C, with types A and B causing annual human epidemics. A key feature of the influenza virus is its error-prone polymerase, which results in an accumulation of genetic mutations that are selected for in hemagglutinin (HA) and to a lesser extent neuraminidase (NA)—the major surface glycoproteins of the virus. This antigenic drift of the HA protein renews our susceptibility to influenza viruses and is the basis for frequent updating of the

composition of seasonal influenza vaccines. Protection after natural infection is primarily mediated by HA-specific antibodies in serum and mucosa, with the presence of antibodies against NA, conserved influenza proteins, and T-cell responses correlating with reduced disease severity [22].

A novel virus can emerge in humans either through direct interspecies transmission or as a result of molecular exchanges between influenza viruses that already infect humans. Because the influenza virus genome is segmented, coinfection of a single host cell with two or more different influenza viruses can result in a reassortment (or shuffle) of their genetic material. The antigenic shift can lead to a pandemic if the resulting progeny virus contains an HA protein to which humans have no pre-existing immunity, if it has an efficient replication-competent set of internal genes, and if it can readily spread from human to human [22].

Vaccination is the primary strategy for the prevention and control of influenza. Seasonal influenza vaccines are trivalent. Each dose is formulated to contain three viruses (or their HA proteins) representing the influenza A H3N2, influenza A H1N1, and influenza B strains considered to be the most likely to circulate in the upcoming influenza season [22]. Currently, most influenza vaccines are made from virus cultured in eggs, which is a severe production bottleneck during a serious threat of epidemic. There is an urgent need to develop a new efficacious process for influenza vaccine production which could be rapidly and cheaply manufactured [1]. The influenza virus has high mutation rate and a particular influenza vaccine usually confers protection for no more than a few years. Every year WHO predicts the strains of the virus that would be circulating in the following year and the vaccines are manufactured based on these data. The vaccine is formulated each season for a few specific flu strains but does not include all the strains active in the world during that season. A truly universal vaccine that provides lifelong protection against any strain of influenza with one or more vaccinations is certainly a goal that is worth pursuing [22].

7 Development of Vaccines for Viral Hepatitis, Coronavirus, and Norovirus

Viral hepatitis is the most common cause of liver disease and is a major global health problem all over the world. Every year millions of people are infected with the hepatitis viruses. The consequences of chronic disease include cirrhosis, liver failure, and hepatocellular carcinoma. There are six main hepatitis viruses, referred to as types A, B, C, D, E, F, and G. These six types are of greatest concern because of the burden of illness and death they cause and the potential for outbreaks and epidemic spread. In particular, types B and C lead to chronic disease in hundreds of millions of people and, together, are the most common cause of liver cirrhosis and

cancer. The hepatitis B and C are the most frequent reason for liver transplantation. Hepatocellular carcinoma which is one of the ten most common cancers is closely associated with hepatitis B, and may also be associated with hepatitis C virus [23]. As yet there are only vaccines for hepatitis A and B. Hence there is an urgent need to develop vaccines for other hepatitis viruses [24].

Coronaviruses are named for the crown-like spikes on their surface. The viruses primarily infect the upper respiratory and gastrointestinal tract. Coronaviruses probably spread through the air by coughing or sneezing, or by close personal contact. Severe acute respiratory syndrome (SARS) and Middle East respiratory syndrome (MERS) are novel coronaviruses that cause severe viral pneumonia in humans. The recent appearance of these viruses highlights the continual threat to human health posed by emerging viruses. SARS emerged in the human population in China in 2002, causing a worldwide epidemic with severe morbidity and high mortality rates, particularly in older individuals [25], whereas MERS was reported in Saudi Arabia in 2012. Bats are the natural reservoirs of SARS-like coronaviruses (CoVs) and are likely the reservoir of MERS coronavirus (MERS-CoV). Although a small number of camels have been found to have positive nasal swabs by real-time polymerase chain reaction and to carry antibody against MERS-CoV, the transmission route and the intermediary animal source remain uncertain amongst the sporadic primary cases [26]. All emerging viruses have an animal reservoir, such that the process of viral emergence can usually be categorized as cross-species transmission [27]. Vaccinologists should be aware of the viruses in the animal reservoirs as well as the mutants or recombinants in humans; proteomic and immunological data from both the animal and human mutants could be used to make effective vaccines.

The surge in economies of many developing countries since the last decades of the twentieth century coupled with low-cost airlines and cheap cruises has made air and sea travel affordable, which has led to the increased global movement of people and materials on an unprecedented scale. Outbreaks of noroviruses in cruise ships which can affect hundreds of passengers is an example of the rapid spread of an infectious pathogen; the disease is also known to spread rapidly in semi-closed populations such as hospitals and hotels [1]. These viruses cause gastrointestinal disease, resulting in recurrent bouts of vomiting and diarrhea that typically last 24–48 h. Noroviruses are transmitted via the fecal–oral route, most commonly through infected food or water or person-to-person contact, and result in 267 million infections and over 200,000 deaths each year, mostly in infants and the elderly. Vaccines and therapeutics are under development but face considerable challenges as there is no cell-culture system or small-animal model for human disease, and these viruses are highly heterogeneous and

undergo antigenic variation in response to human herd immunity, further complicating our understanding of the complex immune interactions that regulate susceptibility and disease [28, 29].

8 Development of Vaccines for Tuberculosis and Meningitis

Tuberculosis (TB) (caused by the bacteria *Mycobacterium tuberculosis*) affects the lungs and was declared a global emergency in 1993 by the WHO. More than two decades after this declaration, the disease still remains a serious and considerable threat to global health. TB is spread through air and the disease is second only to HIV/AIDS as the greatest killer worldwide due to a single infectious agent. In 2013, nine million people fell ill with TB and 1.5 million died from the disease. Standard anti-TB drugs have been used for decades, and resistance to the medicines is widespread. Disease strains that are resistant to a single anti-TB drug have been documented in every country surveyed. Multidrug-resistant tuberculosis (MDR-TB) is a form of TB caused by bacteria that do not respond to, at least, isoniazid and rifampicin, the two most powerful, first-line (or standard) anti-TB drugs (source: WHO). The only effective vaccine for TB is the BCG vaccine; however it is effective in children only, not in adults. Hence there is a need for effective vaccines for TB.

Meningococcal meningitis is a form of meningitis caused by the bacterium *Neisseria meningitidis.* Meningitis is characterized by inflammation of the membranes (meninges) around the brain or spinal cord. The bacteria are spread through the exchange of respiratory and throat secretions. For *N. meningitidis*, the amino acid sequence of the protective antigen factor H-binding protein (fHBP) has more than 300 variations. These sequence differences can be classified into three distinct groups of antigenic variants that do not induce cross-protective immunity. Scarselli et al. [30] demonstrated that the structure-based design of multiple immunodominant antigenic surfaces on a single protein scaffold is possible and represents an effective way to create broadly protective vaccines.

9 Development of Vaccines for Arthropod-Borne Bacteria and Viruses

The most important arthropods harming humans include ticks, mites, and mosquitoes. Ticks are responsible for transmission of bacteria of the order Rickettsiales, which include the genus *Ehrlichia* (causes ehrlichiosis in humans and animals and heartwater in cattle), *Rickettsia* (causes Rocky Mountain spotted fever, epidemic typhus, etc.) and *Anaplasma* (causes anaplasmosis), whereas mites are responsible for the transmission of *Orientia* (causes scrub typhus). Lyme disease is caused by the bacterium *Borrelia burgdorferi* and

is transmitted to humans through the bite of infected blacklegged ticks. Tularemia is a disease of animals and humans caused by the bacterium *Francisella tularensis*. As yet there are no commercially available vaccines against any of these pathogens.

Mosquitoes are responsible for the transmission of dengue virus, West Nile virus, chikungunya, yellow fever, Japanese encephalitis, Western equine encephalitis, Eastern equine encephalitis, etc. With the exception of yellow fever there are no vaccines for other mosquito-borne viral diseases.

10 Development of Vaccines for Water-Borne Diseases

A safe, reliable, affordable, and easily accessible water supply is essential for good health. More than a billion people lack access to safe drinking water. Shortage of water leads to people using contaminated water for drinking purposes increasing the risk of water-borne diseases. Water-borne diseases are infections that are transmitted through contact with or consumption of infected water [31]. The predominant members that cause these diseases are protozoans and bacteria. The major protozoans transmitted through contaminated water include *Entamoeba histolytica*, *Cryptosporidium parvum*, *Cyclospora cayetanensis*, and *Giardia lamblia*. The major bacteria involved in contaminated water are *E. coli*, *Vibrio cholerae*, *Clostridium botulinum*, *Salmonella*, *Shigella*, and *Campylobacter jejuni*. Vaccines against these pathogens could lead to a decrease in water-borne diseases.

Legionnaires' disease is transmitted by inhalation of aerosolized water or soil contaminated with the Gram-negative bacteria *Legionella pneumophila*. The disease is associated with the bacteria thriving in water coolers, cooling towers, etc. The bacteria cause life-threatening diseases in the urban environment. The bacterium is named after a 1976 outbreak in a Philadelphia hotel. Many American Legions attending a convention in the hotel suffered from the disease and the bacteria was tracked to the cooling tower. A milder infection, also caused by *Legionella* bacteria, is Pontiac fever. As yet there are no vaccines against *Legionella*.

11 Development of Vaccines Against Parasites

The parasites include ectoparasites like ticks, mosquitoes, fleas, and itch mite, and endoparasites including Plasmodium, Entamoeba, Leishmania, Trypanosoma, Babesia, Toxoplasma, Wuchereria, Brugia, Giardia, Ascaris, tapeworm, hookworm, pinworm, whipworm, Onchocerca, Fasciola, and Schistosoma. Most of the diseases are classified under neglected tropical diseases and are the major causes of fatality in poverty-stricken regions of the developing

world. Though the diseases caused by these parasites affect millions of people in the developing world, in the long term (due to climate change, movement of refugees, etc.) they pose a risk to people all over the world. As yet there are no vaccines against these parasites [32]. Hence there is an urgent need to develop vaccines against these parasites causing misery to millions of people.

12 Development of Vaccines for Cancer, Neurodegenerative Diseases, Substance Abuse, and Autoimmune Diseases

Cancer is the leading cause of death in the world. Though there are vaccines for some cancers induced by virus (e.g., cervical cancer) there are no vaccines against large number of cancers. Vaccines that can prevent expression of prostatic acid phosphatase in prostate prevent prostate cancer. Development of cancer vaccines should be a priority as it could reduce the incidence of the disease, thereby reducing emotional and economic hardship to millions of people.

As people live longer they are more prone to neurodegenerative diseases like Alzheimer's and Parkinson's diseases. As yet there are no cures for these diseases. A vaccine to prevent this disease will decrease the enormous burden on society.

The currently available medications for the treatment of drug abuse have had only limited success. Anti-addiction vaccines, aimed at eliciting antibodies that block the pharmacological effects of drugs, have great potential for treating drug abuse [33].

As yet there are no vaccines for arthritis, type I diabetes, allergy, multiple sclerosis, and other autoimmune diseases. A vaccine for these diseases could improve the quality of life of people suffering from these debilitating diseases.

13 Development of Vaccines for Fishes, Poultry, and Farm Animals

In intensive culture or farming, where single or multiple species are reared at high densities infectious disease agents are easily transmitted between individuals. Pathogens are easily transported through water and this helps in the quick spread of disease in fishes and other species of aquaculture. Effective vaccination strategies lead to reduced antibiotics in aquaculture [34]. Hence vaccines provide the best strategy to control infectious diseases in fishes.

The highly pathogenic avian influenza virus H5N1, which was limited to poultry, spread to migratory birds and poses a major challenge to animal and human health. Since pandemic influenza virus has its origins in avian influenza viruses, H5N1 virus has to be considered a potentially serious pandemic threat. New influenza virus pandemics in the twenty-first century are a certainty. It has

been reported that H5N1 viruses are taking a huge toll on the poultry industry in many developing countries, and this directly or indirectly impacts both economic and social well-being. While the H5N1 virus transmits zoonotically from infected poultry to humans, often with fatal consequences, such transmission remains inefficient [35]. Though there are vaccines for H5N1 in poultry, the vaccines are not commercially available for humans. It will be a challenge to vaccinologists to develop a vaccine for multiple strains of avian influenza.

As yet there are no vaccines for many infectious diseases affecting farm animals. Heartwater, a rickettsial disease of ruminants, caused by *Ehrlichia ruminantium* is one of the most important diseases of livestock in Africa. This tick-borne illness can significantly decrease productivity in regions where it is endemic. As yet there are no vaccines for this disease. Similarly, Johne's disease (JD) is a chronic disease affecting ruminants and other species caused by the pathogenic *Mycobacterium avium* subsp. paratuberculosis (MAP). This fastidious bacterium infects and survives in the intestines; MAP-infected cattle can remain asymptomatic for years while transmitting the pathogen via fecal contamination and milk. MAP is able to survive the process of pasteurization as well as chemical processes seen in irrigation purification systems. Subsequently meat, dairy products, and water serve as key vehicles in the transmission of MAP infection to humans. Recent studies demonstrate that MAP is associated with Crohn's disease (CD) in humans [36]. A novel vaccine against MAP could decrease the incidence of MAP in cows and cattle, thereby preventing its occurrence in the food supply chain.

Viruses such as coronaviruses also cause a range of diseases in farm animals and domesticated pets, some of which can be serious and are a threat to the farming industry. Economically significant coronaviruses of farm animals include porcine coronavirus and bovine coronavirus, both of which contribute to diarrhea in young animals. Development of vaccines against these viruses will be beneficial to the agriculture industry.

14 One Health Initiative and Vaccines

The number of pathogens known to infect humans is increasing with time. It is not understood whether such increase reflects improved surveillance and detection or actual emergence of novel pathogens. On average, three to four new pathogen species are detected in the human population every year. Most of these emerging pathogens originate from nonhuman animal species [37]. Zoonotic pathogens (pathogens transmissible from animals to humans) represent approximately 60 % of all known pathogens able to infect humans and 70 % of all emerging infectious diseases [38, 39].

Their occurrence in humans relies on the human-animal interface, defined as the continuum of contacts between humans and animals, their environments, or their products [37]. Certain zoonotic diseases have the potential for pandemic spread by human contagion, such as avian influenza, SARS, and the Middle East respiratory syndrome coronavirus, and others for regional cross-border epizootics, such as yellow fever, Venezuelan equine encephalitis, and Rift Valley fever [39]. Animals, including livestock and companion animals, also suffer illness and death following infection with many zoonotic infections, and livestock and poultry are subject to large-scale intentional destruction as a means of preventing human infections, resulting in huge economic losses.

A collaborative effort encompassing multiple disciplines working locally, nationally, and globally to attain optimal health for people, animals, and our environment will be beneficial and is the basis of the concept of the One Health initiative. The One Health concept is a worldwide strategy for expanding interdisciplinary collaborations and communications in all aspects of health care for humans, animals, and the environment. The synergism achieved will advance health care for the twenty-first century and beyond by accelerating biomedical research discoveries, enhancing public health efficacy, expeditiously expanding the scientific knowledge base, and improving medical education and clinical care. The complexity, timeline, and cost of development of animal vaccines and the regulatory hurdles for product approval are far less than for human vaccines. Thus interventions based on the immunization of animals could lead to rapid and relatively inexpensive advances in public health [39].

15 Future Strategies for the Development of Vaccines

Edward Jenner, Louis Pasteur, and Maurice Hilleman developed vaccines by isolating, inactivating, and injecting infectious agents. The vaccines developed by these technologies saved millions of people and many of those vaccines are still in use today. Influenza, oral and inactivated polio, measles, mumps, and rubella are good examples of the vaccines that we still use and were developed with this empirical approach. Since the 1980s new technologies started to emerge that made possible vaccines that were impossible with the empirical approach. The first technology was recombinant DNA that made vaccinologists possible to express the hepatitis B virus-like particle (VLP) in yeast and produce large amounts of vaccines. More recently recombinant DNA technologies were used to generate yeast or baculovirus strains expressing VLPs containing the L1 protein of papillomavirus. The next technology that changed the vaccine landscape was the conjugation technology. In this technology, capsular polysaccharides purified from *Haemophilus*

influenzae, 13 serogroups of pneumococcus or meningococcus A, C, Y, and W, covalently linked to carrier proteins have been licensed during the last 25 years and have completely eliminated the diseases caused by these bacteria. Finally, the advent of genomics allowed the use of the entire genome of pathogens and to search for protective antigens that were difficult or impossible to identify with conventional technologies. The prototype vaccine developed by genome-based approach, also known as reverse vaccinology, is the vaccine against Meningococcus B that was licensed in Europe in 2013 and the USA in January 2015 [40].

Many new technologies are emerging that are likely to dramatically change the world of vaccines. These include new powerful adjuvants, the ability to design immunogens using their crystal structure (structural vaccinology), and the ability to make synthetic vaccines (using different classes of RNA, peptides, carbohydrates, etc.) [41].

References

1. Thomas S, Luxon BA (2013) Vaccines based on structure-based design provide protection against infectious diseases. Expert Rev Vaccines 12:1301–1311
2. Furuya EY, Lowy FD (2006) Antimicrobial-resistant bacteria in the community setting. Nat Rev Microbiol 4:36–45
3. Porco TC, Gao D, Scott JC, Shim E, Enanoria WT et al (2012) When does overuse of antibiotics become a tragedy of the commons? PLoS One 7(12), e46505
4. Phillips I, Casewell M, Cox T et al (2004) Does the use of antibiotics in food animals pose a risk to human health? A critical review of published data. J Antimicrob Chemother 53:28–52
5. Reed D, Kemmerly SA (2009) Infection control and prevention: a review of hospital-acquired infections and the economic implications. Ochsner J 9:27–31
6. Semenza JC, Herbst S, Rechenburg A, Suk JE, Höser C et al (2012) Climate change impact assessment of food- and waterborne diseases. Crit Rev Environ Sci Technol 42:857–890
7. Semenza JC, Suk JE, Estevez V, Ebi KL, Lindgren E (2012) Mapping climate change vulnerabilities to infectious diseases in Europe. Environ Health Perspect 120:385–392
8. Semenza JC, Menne B (2009) Climate change and infectious diseases in Europe. Lancet Infect Dis 9:365–375
9. Estrada-Peña A, de la Fuente J (2014) The ecology of ticks and epidemiology of tick-borne viral diseases. Antiviral Res 108:104–128
10. Levett PN (2001) Leptospirosis. Clin Microbiol Rev 14:296–326
11. Wang Z, Jin L, Wegrzyn A (2007) Leptospirosis vaccines. Microb Cell Fact 6:39
12. Quintero J, Brochero H, Manrique-Saide P, Barrera-Pérez M et al (2014) Ecological, biological and social dimensions of dengue vector breeding in five urban settings of Latin America: a multi-country study. BMC Infect Dis 14:38
13. Nagpal BN, Saxena R, Srivastava A, Singh N, Ghosh SK et al (2012) Retrospective study of chikungunya outbreak in urban areas of India. Indian J Med Res 135:351–358
14. Clem A, Galwankar S (2005) Plague: a decade since the 1994 outbreaks in India. J Assoc Physicians India 53:457–464
15. Hemelaar J (2012) The origin and diversity of the HIV-1 pandemic. Trends Mol Med 18:182–192
16. Johnston M, Fauci A (2011) HIV vaccine development—improving on natural immunity. N Engl J Med 365:873–875
17. Cohen YZ, Dolin R (2013) Novel HIV vaccine strategies: overview and perspective. Ther Adv Vaccines 1:99–112
18. Hoenen T, Groseth A, Feldmann H (2012) Current ebola vaccines. Expert Opin Biol Ther 12:859–872
19. Wahl-Jensen VM, Afanasieva TA, Seebach J, Ströher U et al (2005) Effects of Ebola virus glycoproteins on endothelial cell activation and barrier function. J Virol 79: 10442–10450
20. Weyer J, Grobbelaar A, Blumberg L (2015) Ebola virus disease: history, epidemiology and outbreaks. Curr Infect Dis Rep 17:480

21. Medina RA, García-Sastre A (2011) Influenza A viruses: new research developments. Nat Rev Microbiol 9:590–603
22. Lambert LC, Fauci AS (2010) Influenza vaccines for the future. N Engl J Med 363: 2036–2044
23. Zukerman AJ (1996) Hepatitis viruses. In: Baron S (ed) Medical microbiology, 4th edn. Chapter 70.
24. Law LMJ, Landi A, Magee WC, Tyrrell DL, Houghton M (2013) Progress towards a hepatitis C virus vaccine. Emerg Microb Infect 2, e79
25. Weiss SR, Leibowitz JL (2011) Coronavirus pathogenesis. Adv Virus Res 81:85–164
26. Hui DS, Memish ZA, Zumla A (2014) Severe acute respiratory syndrome vs. the Middle East respiratory syndrome. Curr Opin Pulm Med 20:233–241
27. Cleaveland S, Laurenson MK, Taylor LH (2001) Diseases of humans and their domestic mammals: pathogen characteristics, host range and the risk of emergence. Philos Trans R Soc Lond B Biol Sci 356:991–999
28. Koo HL, Ajami N, Atmar RL, DuPont HL (2010) Noroviruses: the leading cause of gastroenteritis worldwide. Discov Med 10:61–70
29. Debbink K, Lindesmith LC, Donaldson EF, Baric RS (2012) Norovirus immunity and the great escape. PLoS Pathog 8(10), e1002921
30. Scarselli M, Aricò B, Brunelli B, Savino S, Di Marcello F et al (2011) Rational design of a meningococcal antigen inducing broad protective immunity. Sci Transl Med 3:91ra62
31. Hunter PR, MacDonald AM, Carter RC (2010) Water supply and health. PLoS Med 7(11), e1000361
32. Bethony JM, Cole RN, Guo X, Kamhawi S et al (2011) Vaccines to combat the neglected tropical diseases. Immunol Rev 239:237–270
33. Shen XY, Orson FM, Kosten TR (2012) Vaccines against drug abuse. Clin Pharmacol Ther 91:60–70
34. Sommerset I, Krossøy B, Biering E, Frost P (2005) Vaccines for fish in aquaculture. Expert Rev Vaccines 4:89–101
35. Peiris JS, de Jong MD, Guan Y (2007) Avian influenza virus (H5N1): a threat to human health. Clin Microbiol Rev 20:243–267
36. Ghadiali AH, Strother M, Naser SA, Manning EJ, Sreevatsan S (2004) *Mycobacterium avium* subsp. paratuberculosis strains isolated from Crohn's disease patients and animal species exhibit similar polymorphic locus patterns. J Clin Microbiol 42:5345–5348
37. Gortazar C, Reperant LA, Kuiken T, de la Fuente J, Boadella M et al (2014) Crossing the interspecies barrier: opening the door to zoonotic pathogens. PLoS Pathog 10(6), e1004129
38. Taylor LH, Latham SM, Woolhouse ME (2001) Risk factors for human disease emergence. Philos Trans R Soc Lond B Biol Sci 356:983–989
39. Monath TP (2013) Vaccines against diseases transmitted from animals to humans: a one health paradigm. Vaccine 31:5321–5338
40. Giuliani MM, Adu-Bobie J, Comanducci M, Aricò B et al (2006) A universal vaccine for serogroup B meningococcus. Proc Natl Acad Sci USA 103:10834–10839
41. Rappuoli R, Pizza M, Del Giudice G, De Gregorio E (2014) Vaccines, new opportunities for a new society. Proc Natl Acad Sci U S A 111:12288–12293

Chapter 3

Principles of Vaccination

Fred Zepp

Abstract

While many of the currently available vaccines have been developed empirically, with limited understanding on how they activate the immune system and elicit protective immunity, the recent progress in basic sciences like immunology, microbiology, genetics, and molecular biology has fostered our understanding on the interaction of microorganisms with the human immune system. In consequence, modern vaccine development strongly builds on the precise knowledge of the biology of microbial pathogens, their interaction with the human immune system, as well as their capacity to counteract and evade innate and adaptive immune mechanisms. Strategies engaged by pathogens strongly determine how a vaccine should be formulated to evoke potent and efficient protective immune responses. The improved knowledge of immune response mechanisms has facilitated the development of new vaccines with the capacity to defend against challenging pathogens and can help to protect individuals particular at risk like immunocompromised and elderly populations. Modern vaccine development technologies include the production of highly purified antigens that provide a lower reactogenicity and higher safety profile than the traditional empirically developed vaccines. Attempts to improve vaccine antigen purity, however, may result in impaired vaccine immunogenicity. Some of such disadvantages related to highly purified and/or genetically engineered vaccines yet can be overcome by innovative technologies, such as live vector vaccines, and DNA or RNA vaccines. Moreover, recent years have witnessed the development of novel adjuvant formulations that specifically focus on the augmentation and/or control of the interplay between innate and adaptive immune systems as well as the function of antigen-presenting cells. Finally, vaccine design has become more tailored, and in turn has opened up the potential of extending its application to hitherto not accessible complex microbial pathogens plus providing new immunotherapies to tackle diseases such as cancer, Alzheimer's disease, and autoimmune disease. This chapter gives an overview of the key considerations and processes involved in vaccine development. It also describes the basic principles of normal immune respoinses and its their function in defense of infectious agents by vaccination.

Key words Vaccine, Vaccination, Immunology, Pathogen, T cell, B cell, Infectious disease

1 Introduction

Vaccination is one of the most effective medical interventions to reduce morbidity and mortality of infectious diseases. The main principle of vaccination is the proactive induction of a protective immune response by mimicking the natural interaction of an infectious pathogen (bacteria, viruses, etc.) with the human immune system (Fig. 1).

Sunil Thomas (ed.), *Vaccine Design: Methods and Protocols: Volume 1: Vaccines for Human Diseases*, Methods in Molecular Biology, vol. 1403, DOI 10.1007/978-1-4939-3387-7_3,

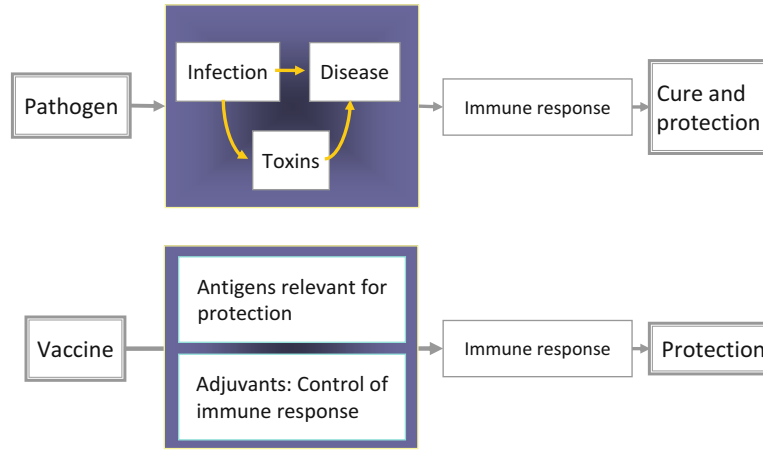

Fig. 1 Principles of vaccine development. Adapted from Moser, Leo: Key concepts in immunology. Vaccine 28S (2010) C2–C13

Table 1
Principles of vaccine design

Etiology of infectious diseases
• Biology and epidemiology of infectious agents
• Replication, polymorphism, immune evasion
• Microbial virulence factors
• Microbial sanctuary
Pathogenesis of the infectious disease
• Mode of infection
• Toxin-mediated symptoms
• Quality of naturally occurring immune response
• Capacity to evade host immune responses
Identification of protective immune responses
• Definition of relevant antigenic structures
• Evaluation of antigen processing by antigen-presenting cells
• Evaluation of (protective) B and/or T cell responses

In contrast to natural infection vaccines ideally achieve their protective effects without clinical symptoms of disease or side effects.

Vaccine design in principle builds on the structure and biological properties of an infectious agent. It is of utmost importance for vaccine developers to understand the etiology, epidemiology, pathogenesis, and immunobiology of the target infection [1] (Table 1). Moreover, an ideal vaccine should also have the capacity

to induce immune responses that provide cross-protection against variant strains of the infectious microorganism. To do so, the vaccine must elicit all the steps leading to immune activation by promoting an adequate effector mechanism, involving mediators and cellular responses, which are tailored to the specific disease.

At all times in varying degrees the development of vaccines was based on close observation of natural phenomena [2]. Early vaccinologists including Edward Jenner (*see* below) deducted their concepts from the observation that under certain conditions individuals were spared from highly contagious diseases. Over the last two centuries vaccination was strongly endorsed by the progress in biological sciences, the emergence of biochemical techniques, and the discoveries in immunology, genetics, and molecular biology. The techniques available in the late twentieth century further facilitated the development of new vaccine concepts such as subunit vaccines (purified protein or polysaccharide), DNA or mRNA vaccines, or genetically engineered antigen components based on reverse vaccinology [3]. However, the advantages of modern vaccine concepts are often associated with specific drawbacks, including the fact that highly purified vaccine antigens often provide only weak immunogens. Moreover, there are challenging diseases such as malaria, tuberculosis, or HIV/AIDS that still remain out of reach of classical vaccine design. To overcome these impediments, lately new approaches based on innovative adjuvant formulations have been established [4]. Following the recognition of the important role of the innate immunity for the induction of an adaptive immune response new adjuvants were developed that have the ability to modulate the immune response, increasing the level of immune activity to that typically seen with original live attenuated or killed vaccines. Thus, modern vaccines may have the potential to compensate even for limitations of naturally occurring immune responses.

2 A Brief History of Vaccination

Already in the ancient world it was common knowledge that an individual rarely was infested twice with the same disease. This observation led to the practice of inoculation that has been documented in China more than 1000 years before Jenner's remarkable studies [2]. Even the term "immunity" was used in reference to plague during the fourteenth century. Progress in natural sciences and the development of experimental techniques during the eighteenth century led to the systematic use of inoculation to fight smallpox, one of the most serious threats during that time. In the early eighteenth century variolation, the transmission of small, presumably sublethal volumes of liquid from smallpox pustules was introduced to England by Lady Mary Wortley Montagu. Lady Montagu survived infection with smallpox herself. Impressed

with the method of variolation she ordered the embassy surgeon, Charles Maitland, to inoculate her 5-year-old son. After her later return to London in 1721, Lady Montagu introduced the method to the physicians of the royal court. Thereafter variolation became quickly popular among physicians in Europe. However, variolation was not without risks. In average 2–3 % of variolated persons died from the disease but the mortality associated with variolation was ten times lower than that associated with naturally occurring smallpox.

Modern concepts of vaccination date back to 1796 when Edward Jenner based on empirical observation used liquid from pustules of cowpox to induce protective immunity in human individuals. Today the use of cowpox as a vaccine is considered to be the landmark of modern vaccination concepts. Edward Jenner recognized that milkmaids infected by cowpox, a generally harmless infection for humans, were rendered immune to smallpox. In 1796 Jenner deliberately inoculated people with small doses of cowpox (vaccinia) from pustules and successfully demonstrated that protection against smallpox could be achieved. Jenner termed this preventive measure "vaccination" and over the following decades inoculation against smallpox using cowpox became widely accepted in Europe. While Jenner at his time neither understood nor could explain the biological basis of "vaccination," his concept was successful and provided protection from smallpox apparently due to cross-immunity between cowpox and smallpox.

Until the end of the nineteenth century, diseases were believed to be caused by invisible microbes which were "spontaneously generated" in response to "bad air" and other environmental triggers, as well as a belief that imbalance in the body caused what were actually infectious illnesses. Progress in microbiology and virology since the late nineteenth century elucidated the modern concept of communicable diseases. Pasteur and Koch established that microorganisms were the true cause of infectious diseases. These discoveries led to the science of immunology. Hence further advances in vaccinology were gained from an increasing understanding of the etiology of infectious diseases and host-pathogen interactions. Pasteur challenged the spontaneous generation theory of microbes while Koch demonstrated that infectious agents transmit diseases. Koch defined four postulates which established an individual agent as the cause of a disease. In addition, in the late 1870s Pasteur developed the first attenuation procedure for pathogens. Pasteur's approach provided microorganisms less pathogenic but still immunogenic. Using animals as a live propagating medium, Pasteur and his team were able to produce attenuated rabies viruses of different strengths of which the weakest could be used to prepare a vaccine. In 1885, the first human individual was vaccinated with a live, attenuated rabies vaccine. However, due to technical

limitations of vaccine production at that time, fatal cases of rabies in vaccinated individuals occurred.

At the end of the nineteenth century, many of the fundamental aspects of vaccinology were established due to the pioneering work of Pasteur and Koch. Probably the most important advance was the insight that the administration of pathogens, either attenuated or killed, resulted in protection against the disease caused by the respective non-treated pathogen. The first inactivated vaccines, developed in the 1890s, were directed against the typhoid and cholera bacilli [5]. Other vaccines consisting of killed whole pathogens, produced in the early twentieth century, were directed against pertussis [6], influenza [7], and typhus. These were followed by inactivated vaccines directed against polio (IPV) [8], rabies, Japanese encephalitis, tick-borne encephalitis [9], and hepatitis A [10].

Although inactivated vaccines exhibit a lower risk of vaccine-associated disease than live vaccines, their efficacy can be reduced by the same factors, i.e., circulating antibodies (maternal antibodies) or concomitant infection. Moreover, multiple doses of inactivated vaccines are generally needed to provide sufficient stimulation of the immune system to induce durable immune responses. This observation led to the introduction of aluminum compounds as vaccine adjuvants (from the Latin word adiuvare, meaning "to help or aid"). Still today aluminum salts represent the most frequently used adjuvant system (*see* below). Further progress in biochemistry facilitated the development of inactivated vaccines based on purified toxins. The first subcellular vaccines made available in the 1920s used diphtheria and tetanus toxoids [2]. As technology improved, it became possible to purify protein or polysaccharide subunits from infectious organisms to develop increasingly specific vaccines.

Another important milestone was the development of sophisticated ways to culture and propagate infectious pathogens, like viruses, ex vivo. Based on these new techniques the development and production of purified attenuated viral pathogens as live vaccines became possible. Typical examples of vaccines that use passage in artificial media or cell culture as means of attenuation include the oral polio virus (OPV) [11] or measles, mumps, rubella, and varicella vaccines [12] as well as the Bacille Calmette-Guérin (BCG) tuberculosis vaccine [13].

Recent years have been characterized by impressive progress in the fields of immunology and molecular biology as well as important technical improvements concerning fermentation and purification. Building on the improved knowledge of the principles of host-pathogen interactions, the host's immune response today can be dissected in order to identify the individual antigenic structures that are most relevant to initiate protective immunity. The appropriate antigens are isolated as subcomponents of pathogens and subsequently produced in large quantities either by purification or

by in vitro construction using molecular genetic technologies. Moreover, innovative adjuvants have been introduced that specifically modify and augment those aspects of the immune response that are most appropriate for protection. These adjuvants also have the potential to generate long-lasting immunological memory to maintain protection.

During the last 100 years vaccine development has evolved from an empirical approach to one of more rational vaccine design where careful selection of antigens and adjuvants is key to the desired efficacy for challenging pathogens and/or challenging populations. Modern vaccine design needs to consider factors beyond target antigen selection to improve immunogenicity while conserving a favorable reactogenicity and safety profile [1]. With new vaccine technologies currently emerging, it will be possible to custom-design many vaccines for optimal efficacy, low reactogenicity, and excellent safety profiles in the near future.

3 Basic Concepts of Vaccine Immunology

The primary goal of vaccination is the induction of protective immunity against disease-causing infectious pathogens, i.e., microorganisms like bacteria, viruses, or fungi. To achieve this objective vaccines mostly are designed to address natural defense mechanisms and activate the immune system in a manner similar to natural infections. Vaccine development, therefore, strongly depends on our understanding of the human immune system [14].

The human immune system comprises two major compartments: the innate and the adaptive immune system (Fig. 2). Innate and adaptive immunity work sequentially to identify invading

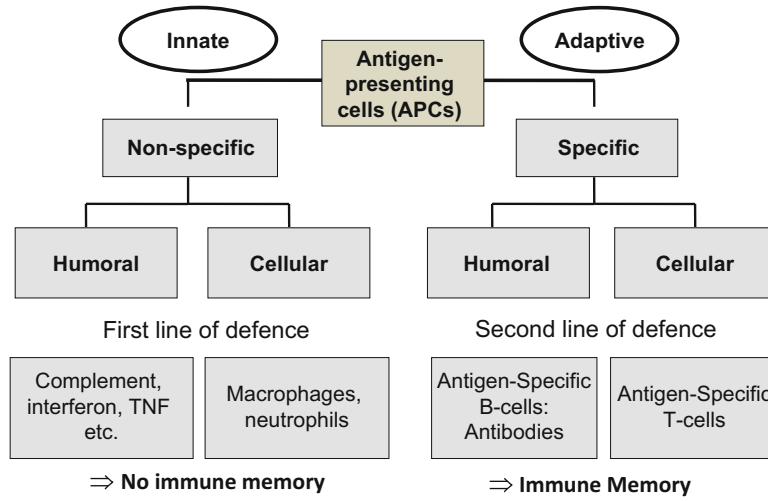

Fig. 2 Innate and adaptive immunity—overview

pathogens and initiate the most effective defense response. The interaction of innate and adaptive immunity is crucial to generate and maintain a protective immune response. Especially specialized antigen-presenting cells (APCs) are important to bridge the two compartments of the immune system [15].

4 Innate Immunity

The innate immune system represents a first line of host defense against pathogens that surmount the body's physical and chemical barriers (e.g., skin, ciliated epithelia, mucous membranes, stomach acids, and destructive enzymes in secretions). Innate defense mechanisms are mediated by cellular effector cells and noncellular effector molecules such as complement or lysozyme. Cellular elements of the innate immune system are generated in the bone marrow and migrate into blood and different tissues of the body. Tissue-residing (e.g., macrophages and dendritic cells) and "mobile" phagocytic cells (e.g., neutrophils, eosinophils, and monocytes) as well as natural killer cells represent major cellular elements of the innate immunity [16].

After invasion of a pathogen the innate immune system is responsible to detect, contain, and ideally eliminate the thread immediately. Innate immunity has only a limited number of receptor molecules available to fulfill this task. Pathogens are detected through molecular-sensing surveillance mechanisms via pattern recognition receptors (PRRs), expressed by cells of the innate immune system either on the cell surface or in intracellular compartments (i.e., DNA/RNA sensors). Typical examples of PRRs are the transmembrane Toll-like receptors (TLRs) which recognize pathogen-associated molecular patterns [PAMPs] that are shared by several pathogens (for example lipopolysaccharide expressed by all Gram-negative bacteria), thereby enabling the innate immune system to sense the occurrence of an infectious event [17]. For instance, TLR4 at the cell surface recognizes bacterial, whereas TLR9 is located intracellular and recognizes viral single-stranded RNA. PPRs sense danger signals and activate and augment proinflammatory gene expression in order to facilitate host defense capacity. Epithelial cells, fibroblasts, and vascular endothelial cells can also recognize PAMPs and activate innate immune cells when infected, stressed, or damaged. This is mediated by chemical messengers like cytokines and chemokines that are secreted by infected cells and/or innate immune cells to attract other resident and circulating innate cells to the site of infection.

Under some circumstances, pathogen elimination may be achieved by innate immune effectors alone without recruitment of a subsequent adaptive immune response. This can be accomplished by phagocytosis of pathogens and subsequent intracellular

destruction within intracellular vesicles containing oxygen radicals and digestive enzymes. Additionally, pathogens can be destroyed by soluble chemical factors secreted by innate immune cells or generated in the liver. Complement represents the most important and effective soluble effector system of innate immunity [18]. Complement proteins circulate in the blood in an inactive form. Comparable to the coagulation system the 25 complement proteins are activated in cascades. When activated, complement components fulfill several effector functions including the recruitment of phagocytes, the opsonization of pathogens to facilitate phagocytosis, and the removal of antibody-antigen complexes. The complement system also strongly promotes the effector function of the adaptive immune response by mediating lysis of antibody-coated pathogens. The innate immune response is enforced by chemotactic stimuli, released by infected epithelial and endothelial cells or other innate immune cells to recruit additional circulating cells from the bloodstream to the site of inflammation. While the defense provided by innate immune mechanisms in principle is sufficient to resolve an infection, during evolution many microorganisms have developed escape mechanisms to overcome the effectors of innate immunity. In most cases innate immunity will delay the invasion of pathogens, but intervention of the adaptive immune response is indispensable to overcome and finally clear an infection.

Although innate defense mechanisms are prearranged and fast reacting, they lack specificity and are not equipped to provide an immunological memory response. In consequence innate immunity alone is not sufficient for vaccine-related protective immune responses that depend strongly on the induction of immune memory responses [19]. Nevertheless, innate immunity fulfills an important role in the early detection of invading pathogens and subsequent activation of the adaptive immune response. The detection of pathogens and the phagocytosis of antigens by immature dendritic cells (DC) are important prerequisites to initiate adaptive immune responses. After ingestion of antigens immature DCs transform into antigen-presenting cells (APC) that migrate to the draining lymph node. The APC acts as a messenger to precisely define the nature of the perceived danger and convey this information to secondary lymphoid organs, where they activate the relevant adaptive immune response. Although vaccines in the end target the adaptive immune system, vaccine antigens must be recognizable by innate immune cells.

5 Adaptive Immunity

Adaptive immunity represents the second line of immunological defense. Antigen recognition by the adaptive immune system initiates a focused, highly specific immune response that results in

elimination of the pathogen and termination of the infectious disease. Moreover, in the course of an adaptive immune response antigen-specific memory cells are generated that will provide a faster and stronger immune response whenever the body is challenged by the same pathogen again in the future [19]. The cellular elements of the adaptive immune response are lymphocytes that are able to specifically recognize antigens, i.e., the components of an infectious pathogen "foreign" to the body and potentially dangerous. There are two main subsets of lymphocytes: B cells which initially develop in the bone marrow and T cells which are generated in the thymus. Activated B cells can produce and secret antigen-specific antibodies, i.e., proteins that will bind to antigens. T cells comprise of different types of lymphocytes that confer either regulatory or effector functions. T cells with regulatory function preferentially express the cluster of differentiation (CD) 4 cell-surface protein, and are referred to as CD4-positive T cells. Effector-T cells are characterized by the expression of the CD8 cell surface molecule.

In contrast to innate immune cells lymphocytes can express a huge diversity of antigen-specific receptor molecules (around several thousand billion) [20–22]. Antigen receptors are encoded by a set of genes that undergo multiple recombination events, eliciting the random generation of an extensive number of diverse receptor structures. The diversity of the receptor repertoire is further increased by individual changes and random gene insertions. The huge T and B cell repertoires of the human immune system provide the potential to recognize almost every naturally occurring antigenic structure. Initially the repertoire is maintained with single or very few cells expressing receptors that will recognize any given antigen, until individual clones are selectively expanded in response to a specific challenge. During the development of the adaptive immune system lymphocytes expressing receptors that potentially could recognize self-antigens are eliminated by a process named negative selection, while simultaneously cells that recognize non-self-antigens are positively selected.

6 T Cells

Each T cell expresses a unique antigen-specific receptor molecule (TCR). TCRs, however, cannot directly recognize complete pathogenic structures. Instead the TCR recognizes molecular fragments (small peptides derived from processing of larger protein antigens) that have to be presented in association with major histocompatibility complex (MHC) molecules at the cell surface of antigen-presenting cells (APC). In consequence, activation of T-lymphocytes strongly depends on the interaction with APCs. Professional APCs, derived from specialized phagocytes termed dendritic cells (DCs),

ingest pathogen-derived proteins. After phagocytosis the antigens are broken down and processed and the resulting peptide fragments are transported to the cell surface where they are embedded into MHC molecules. An individual T cell can only be activated by a peptide antigen for which it expresses the specific receptor. Moreover, besides its antigen specificity the TCR additionally can only interact with MHC molecules of its own tissue type. This quality is described as self-restriction and ensures that only cells of the same organisms will interact to mount an adaptive immune response.

T cells activated by antigen-bearing DCs express the CD4 cell surface protein and are restricted to recognize antigen in the context of MHC class II molecules. CD4+ T cells fulfill modulatory and effector functions by secreting soluble factors (cytokines) that exert direct antimicrobial properties or affect the activities of other immune cells. In most cases CD4+ cells will help other immune cells to perform their task and are, therefore, referred to as helper T cells (Th). Based on the types of cytokines the Th cells secrete and their abilities to assist other subsets of immune cells, several subpopulations of Th cells have been described. Th1 cells secrete mainly interferon-gamma (IFNγ), a cytokine known to limit pathogen survival. IFNγ also promotes the differentiation of cytotoxic lymphocytes (CD8+ cells *see* below) that are able to destroy cells infected by intracellular pathogens. T helper 2 cells produce various cytokines (interleukins [IL] IL-4, IL-5, IL-13) that preferentially activate innate immune cells (eosinophils, mast cells) especially facilitating the immune response to extracellular parasites (Fig. 3). Another subset, termed follicular T helper cell (Tfh) based on its tissue localization in follicular structures of lymph nodes, is characterized by the secretion of IL-21, a cytokine thought to favor the secretion of antibodies by antigen-specific B cells [23]. Finally regulatory T cells (Treg cells) belong to the CD4+ T cell subset. They inhibit immune or inflammatory responses by blocking the activity of effector T cells, helper T cells, and APCs. Treg are crucial to downregulate immune responses after an effective protective response, to maintain immunological self-tolerance process, and for the prevention of uncontrolled or chronic inflammatory responses.

T cells expressing the CD8 surface molecule represent T effector cells that have the capacity to eliminate cells infested with intracellular pathogens. Antigen recognition by CD8+ T cells depends on the fact that virtually all nucleated cells present fragments of intracellular proteins at their Surface-MHC-molecules as part fragments of intracellular proteins present externally derived antigen fragments in association with MHC class II molecules, non-immune cells use MHC class I molecules to present peptides derived from intracellular sources. Thus, cells infected by intracellular pathogens will express antigenic fragments of the pathogen in addition to the normal set of self-antigens. CD8+ T cells continuously screen MHC class I molecules to detect non-self-antigens indicative for an intracellular infection. Cells displaying high levels of

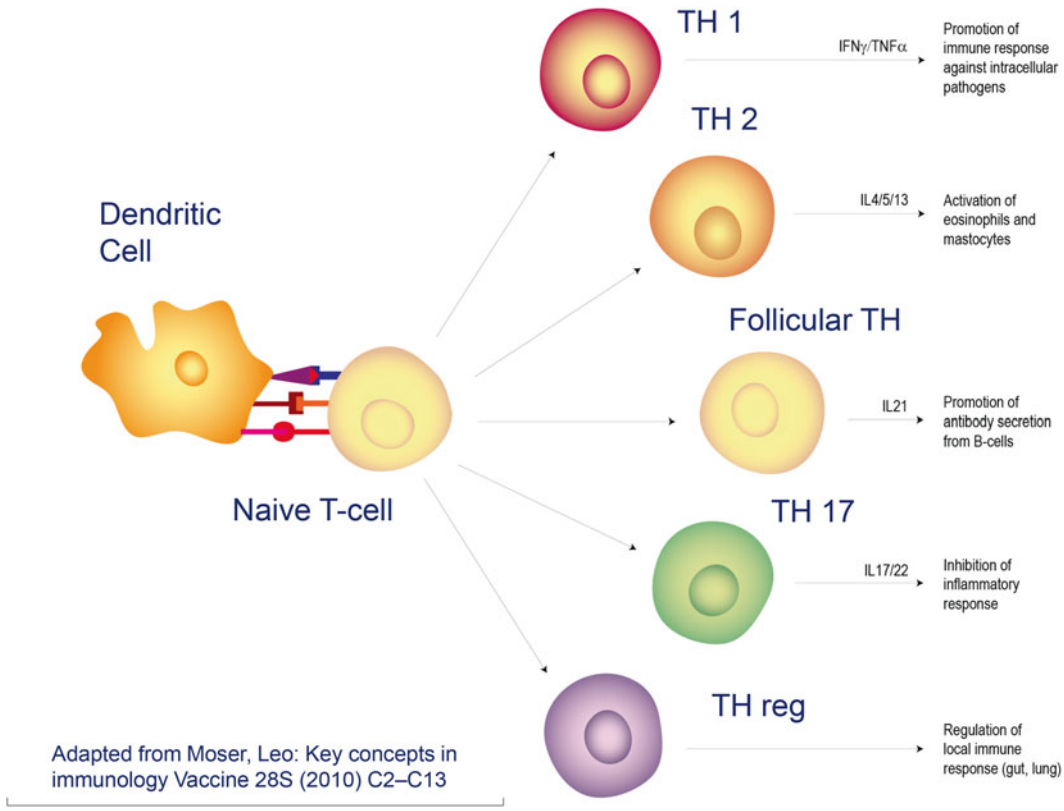

Fig. 3 Specialized T-helper cells

pathogen-derived peptides, e.g., in the case of a virus infection, subsequently will be killed by CD8+ T cells by secretion of cytotoxic factors. In addition, CD8+ T cells can inhibit viral replication without destroying the infected cells by producing cytokines that are able to interfere (interferon) with pathogen replication. CD8+ cytotoxic cells also can eliminate cells exhibiting abnormal host peptides, such as those presented by tumor cells, and therefore play an important role in the immune control of aberrant cell growth. Although CD8+ T cells can react directly to cells expressing non-self-antigen/MHC class I complexes, their optimal cytotoxic potential is achieved in the presence of cytokines produced by regulatory CD4+ T helper cells.

7 B Cells

B cells represent the second effector compartment of the adaptive immune response. Like T cells, each B cell expresses a unique antigen receptor (B cell receptor: BCR), which consists of a membrane-bound copy of the antibody molecule that can be secreted by the B cell after activation [24]. In contrast to T cell receptors the BCR

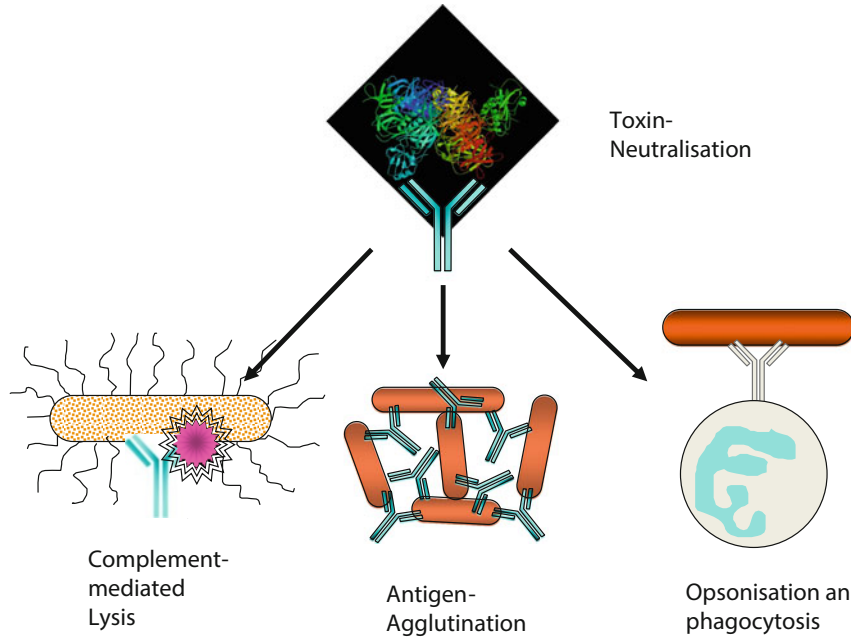

Fig. 4 Antibody-mediated protection

binds directly to molecular structures of pathogens with no need for previous antigen processing. Antigen binding by the appropriate BCR activates the B cell and induces proliferation and differentiation into plasma cells [25]. Plasma cells produce and secret large amounts of antibodies that are released in the blood and other body fluids. Antigen-specific antibodies are an important effector concept of additive immunity. Antibodies can facilitate phagocytosis or complement-mediated killing of pathogens or neutralize toxins by binding to their appropriate antigens (Fig. 4).

Antibody molecules consist of a "constant" fragment (Fc fragment), a structural feature common to all antibodies of a given isotype, and a "variable" region, which includes the region that defines the antigen specificity (Fab fragment). The constant part of the molecule exists in five different classes (isotypes) termed immunoglobulin [Ig] A, IgD, IgE, IgG, and IgM. The Ig isotype determines the ability of an antibody class to localize to particular body sites and to recruit the optimal effector cells. The variable region of the antibody exists in a huge number of randomly generated different molecular configurations. This BCR repertoire guarantees maximal capability to recognize diverse pathogenic antigen. Activation of B cells after the first encounter with an antigen and subsequent differentiation into plasma cells usually needs 10–14 days. Initially plasma cells will typically produce IgM-type antibodies. IgM antibodies are large molecules consisting of five bivalent antibody molecules linked together to exhibit ten binding regions. In the further course of the immune response antibody production

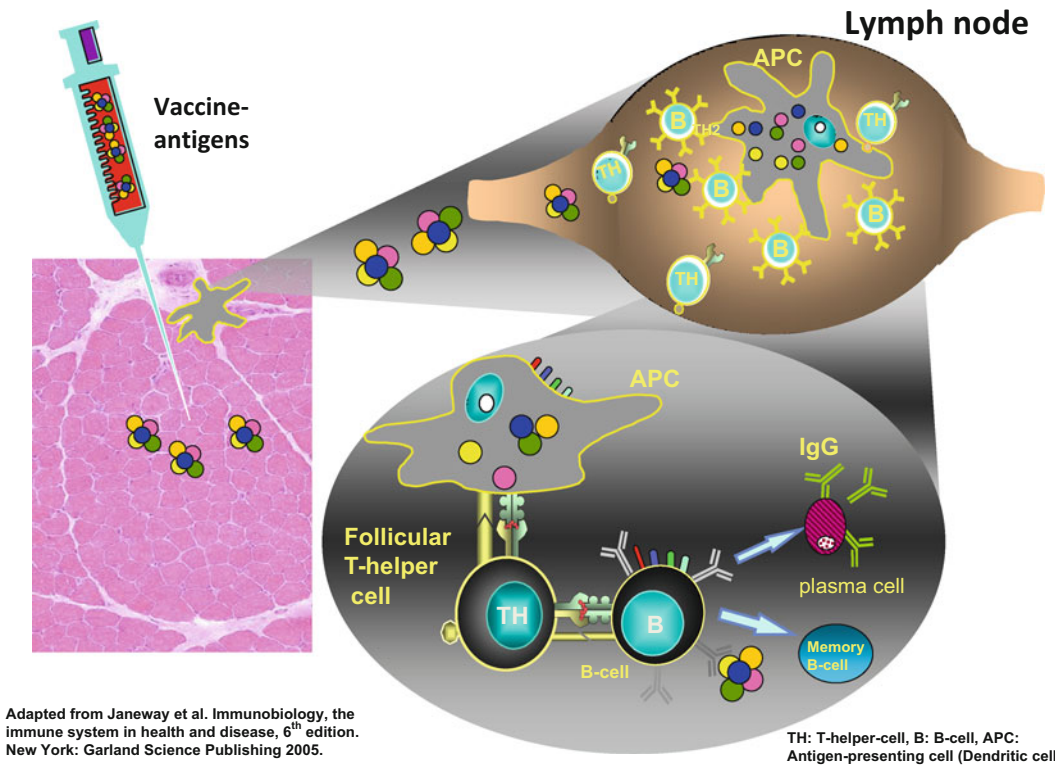

Fig. 5 Immune response after vaccination. Adapted from Janeway et al. Immunobiology, the immune system in health and disease, 6th edition. New York: Garland Science Publishing 2005

will switch to the IgG isotype, which also represents the major isotype of B cell memory responses [26]. Depending on the specific circumstances of B cell activation antibody production may switch to IgA which is secreted to mucus membranes or IgE, mainly for the defense of infections by parasites.

In most cases, optimal B cell activation and differentiation into antibody-secreting plasma cells will only be achieved when B and T cells are simultaneously activated by elements of the same pathogen (Fig. 5). T cell-independent direct activation of B cells occurs only in response to repetitive antigenic structures, such as carbohydrates found in bacterial walls. These T cell-independent immune responses are characterized by the secretion of low-affinity antibodies of the IgM type, lacking the typical memory response upon reexposure to the same antigen.

In these instances, activated B cells will recruit the help of T cells to mount an optimal response and to elicit immunological memory. After activation of the B cell by binding to a pathogen antigen the surface BCR-antigen complex will be internalized and elements of the antigen are processed and presented to an appropriate CD4+ T helper cell. The interacting CD4+ T cell will differentiate into a follicular T helper cell in order to provide helper signals

for the B cell. T cell-dependent B cell responses are characterized by the secretion of high-affinity antibodies and a large spectrum of isotypes (in particular IgG). The quality of antibody response has a bearing on protection, e.g., the antigen binding capability of antibodies (affinity, avidity) and the dynamics of the peak response (priming); long-term protection requires the persistence of antibodies and the generation of immune memory cells capable of rapid and effective reactivation [24].

8 Immune Memory

As illustrated, T-helper lymphocytes play an important role in the regulation of both T and B cell responses as well as cytotoxic T-lymphocytes. However, the most important property of adaptive immunity is its capacity to establish an immunological memory response, assuring a stronger and faster protective immune response whenever challenged again by the same pathogen. While the primary immune response on average takes 10–14 days to build up, immunological memory shortens the immunological reaction time to a couple of days, thereby effectively preventing future reinfection with the same agent (Fig. 6).

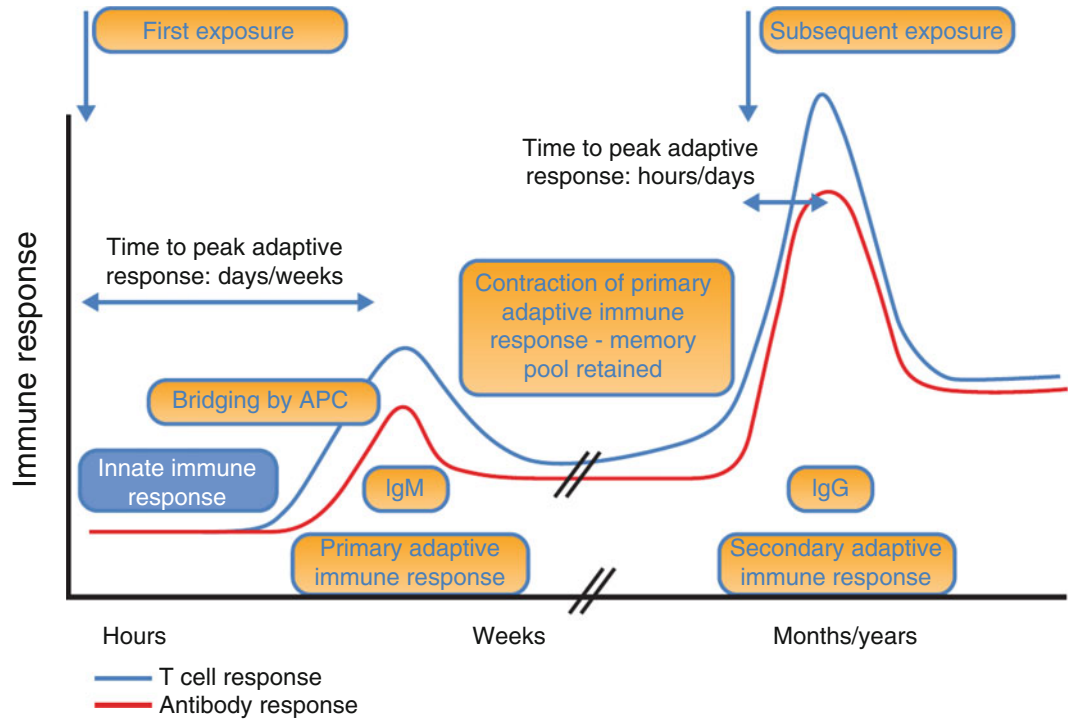

Fig. 6 Dynamics of the adaptive immune response. Adapted from "Understanding Modern Vaccines: Perspectives in Vaccinology, Volume 1", 2011 Elsevier, Oberdan, L., Cunningham, A., Stern, P.L.: Chapter2. Vaccine immunology; p. 45

At the first encounter with an antigen usually only a small number of lymphocytes expressing a given antigen specificity are available. Upon activation by antigen recognition, T and B lymphocytes will go through rapid proliferation, leading to the accumulation of an increased number of cells expressing receptors for the specific antigen. Some of these cells will differentiate into effector cells while others will become "memory cells," able to survive for longer periods of time within the host. Any exposure to an antigen (pathogen or vaccine) therefore leads to a long-term modification of the cellular repertoire, such that the relative frequency of T and B cells specific for an individual antigen is increased in antigen-exposed individuals compared with naïve individuals [27, 28]. Memory T and B cells will develop secondary (recall) responses on reencounter with their specific antigen. The adaptive response on secondary exposure leads to a rapid expansion and differentiation of memory T and B cells into effector cells, and the production of high levels of antibodies. A higher proportion of IgG and other isotypes of antibodies compared with the level of IgM characterizes memory antibody responses. During the process of reactivation the binding avidity of antibodies can be optimized by somatic hypermutation of the variable antigen-binding region.

The capacity to generate immune memory is the key feature of the adaptive immune system and is crucial for maintenance of long-term protection. This capacity to establish an immunological memory response also is the fundamental basis for the biological effects of vaccines. Initially antigen processing and presentation by dendritic cells (DCs) are key steps that define the environment and the course of efficient immune responses [6]. Therefore, innate immunity sets the scene for the subsequent adaptive response and innate and adaptive immunity have to interact vigorously in order to initiate the most effective type of protective immunity.

9 How Do Vaccines Mediate Protection?

Long-term protection is ensured by the maintenance of antigen-specific effector cells and/or by the induction of immune memory cells that can be rapidly reactivated into immune effectors whenever the organism is challenged with the same pathogen again in the future. Vaccine-induced immune effectors are essentially antigen-specific antibodies produced by plasma cells that are capable of binding specifically to a toxin or a pathogen. Other effectors are cytotoxic CD8+ T cells that can limit the spread of infectious microorganisms by killing infected cells or secreting specific antiviral cytokines. The generation and maintenance of both B and CD8+ T cell responses are supported by growth factors and signals provided by CD4+ T helper cells. Most antigens and vaccines trigger both B and T cell responses. In addition,

CD4+ T cells are required for most antibody responses, while antibodies exert significant influences on T cell responses to intracellular pathogens.

10 Immune Correlates of Protection

Ideally a successful immune response is measured by the quality of the acquired protection from infection; however, this approach usually is difficult to perform regularly on individual basis. Alternatively the emerging immune response may also be assessed by detection of antigen-specific antibodies or a particular pattern of cytokine expression by T cells. These surrogate markers or correlates of protection can only be defined based on clinical trials where protection from disease or infection is determined in cohorts of vaccinated versus unvaccinated individuals [29].

The majority of vaccines developed so far have been assessed only by their ability to elicit antigen-specific antibody responses (Table 2). However, while detection of specific antibodies in principle illustrate vaccine-related immune responses, protective antibody titers/concentrations have been defined only for a small number of vaccinations. For example in the case of rubella protective antibody titers can be reliably assessed to determine whether an individual is protected post-vaccination. However, most immune correlates of protection are not well defined. Historically, demonstration of the production of specific antibodies has been the main goal of vaccination; however, this concept appears to be insufficient or inappropriate for future vaccine development.

11 Principles of Vaccine Development

During the interaction with an infectious agent, the immune system develops and optimizes an effective defense strategy that prevents further spread of the pathogen, interrupts its life cycle, and eventually eliminates it from the body. Thereafter, the affected individual ideally acquires protective immunity that prevents the recurrence of an infection by the same agent in the future. In order to provide protection from infectious diseases vaccines have to be designed to induce immune responses comparable to the natural occurring immune response against an infectious agent. However, there is a significant difference between the expected effects of vaccines and those that are attributed to infectious agents. While it is common knowledge that infections are usually associated with clinical symptoms of disease, such a coincidence generally is not acceptable for the use of vaccines.

Table 2
Accepted immunological correlates of protection. Adapted from Plotkin SA. Correlates of protection induced by vaccination. Clinical and Vaccine Immunology; 2010; 17:1055–1065

Disease	Vaccine	Protective AB concentration/titer
Diphtheria toxoid	Toxoid	≥0.01–0.1 IU/ml
Hepatitis A	Killed	>10 IU/L
Hepatitis B (HBsAg)	Protein	>10 IU/L
Hib PS	Polysaccharide	1 μg/ml
Hib glycoconjugates	Polysaccharide-protein	>0.15 mg/L
Influenza	Killed, subunit	No correlate
Influenza intranasal	Live attenuated	No correlate
Measles	Live attenuated	≥1:2 (HHT) or ≥) 200 mIU/ml Microneutralization (EIA)
Meningococcal PS	Polysaccharide	≥1:4, Human complement bactericidy-assay
Meningococcal conjugates	Polysaccharide-protein	≥1:4, Human complement bactericidy-assay
Mumps	Live attenuated	No correlate
Papillomavirus	Viruslike particle	No correlate
Pertussis, whole cell	Killed	No correlate
Pertussis, acellular	Protein	No correlate
Pneumococcal PS	Polysaccharide	0.2 to >0.35 μg/ml depending on serotype
Pneumococcal conjugates	Polysaccharide-protein	0.2 to >0.35 μg/ml for infants depending on serotype, ELISA; Titer 1:8; opsonophagocytosis
Polio Sabin	Live attenuated	Titer≥ 1:4 to 1:8
Polio Salk	Killed	≥0.075 IU/ml Polio type 1 ≥0.18 IU/ml Polio type 2 ≥0.08 IU/ml Polio type 3
Rabies	Killed	>0.5 IE/ml or titer ≥ 1:16
Rotavirus	Live attenuated	No correlate
Rubella	Live attenuated	10–15 mIU/ml; immunoprecipitation assay
Tetanus toxoid	Toxoid	≥0.1 IU/ml
Tuberculosis (BCG)	Live mycobacterium	>0.5 IE/ml or ≥Titer 1:16
Varicella	Live attenuated	>5 gp ELISA-Units/ml
Yellow fever	Live attenuated	Titer 1:5, neutralization assay

Symptoms of an infection are either caused directly by the pathogen, or, more often, they are consequences of the emerging immune response, representing side effects of our physiological defense mechanisms. Typical complaints such as physical discomfort, malaise, fever, or organ malfunction in most cases are related to inflammatory reactions that occur in course of the immunological defense process. Since vaccines are administered to prevent infections and/or diseases, they are expected to provide protection without the risk of side effects or clinical symptoms of disease. To this end in vaccine development it is important to understand the life cycle of an infectious agent, how it multiplies and infests the human organism, and how the immune system counteracts and overcomes the microbial invasion and finally builds up a protective immunity, i.e., an effective barrier against future challenges by the same agent. Moreover, it is essential to define which elements of the natural immune response are relevant for the elimination of the pathogen and future protection, and which are responsible for symptoms of disease and discomfort. Ideally, a vaccine should induce only the elements of the natural immune response that are essential for protection, but simultaneously exclude all negative effects of natural infection. In vaccine development, therefore, not only the elements of the immune response guaranteeing best protection must be considered, but also the acceptable tolerability and safety ramifications of the induced inflammatory response. As a consequence the design of a vaccine has to be based on both structural and biological properties/qualities of an infectious agent as well as the type and quality of naturally occurring immune responses initiated by the infectious pathogen.

Initially vaccine development focused on the steps required to elicit activation of a protective immunity and generation of immunological memory by virtually mimicking the interaction of an infectious agent with the human immune system without posing any risks of the infectious disease to the vaccinee. This requires the identification of antigenic structures relevant for protection as well as definition of immune response mechanisms adequate to elicit protective immunity. The latter will vary according to specific disease (Table 3). While for many decades vaccine development concentrated primarily on targeting components of the adaptive immunity (B cells or immunoglobulins, T cells, and cytokines, such as interferon), recent research indicates that innate and adaptive immunity have to interact vigorously to initiate the most potent type of protective immune response [16]. In particular, antigen processing and presentation by DCs are key steps in the development of efficient immune responses. The recognition of the important role of innate immunity in controlling the adaptive response (Figure 7) has led to a reappraisal of the role of adjuvants in vaccinology [16].

Table 3
Quality of protective immune responses to infection differs according to type of disease

Disease	Pathogenesis	Protective immune response
Cholera	Local infection, enterotoxins	IgA (mucosa) IgG (neutralization)
Diphtheria	Local infection, exotoxins	IgG (neutralization of toxin)
Hepatitis B	Systemic infection	IgG (elimination of the virus) IFNγ, T cells (infected cells)
Human papillomavirus	Local infection	IFNγ, IgG (neutralization) T cells (lysis of infected cells)
Influenza	Local infection Systemic infection	IFNγ, IgA, IgG T cells (infected cells)
Poliomyelitis	Systemic infection	IgA (elimination of the virus) IFNγ, T cells (infected cells)
Tuberculosis	Systemic infection	T cells, IFNγ, killing of intracellular pathogen by macrophages

Ig immunoglobulin, *IFN* interferon

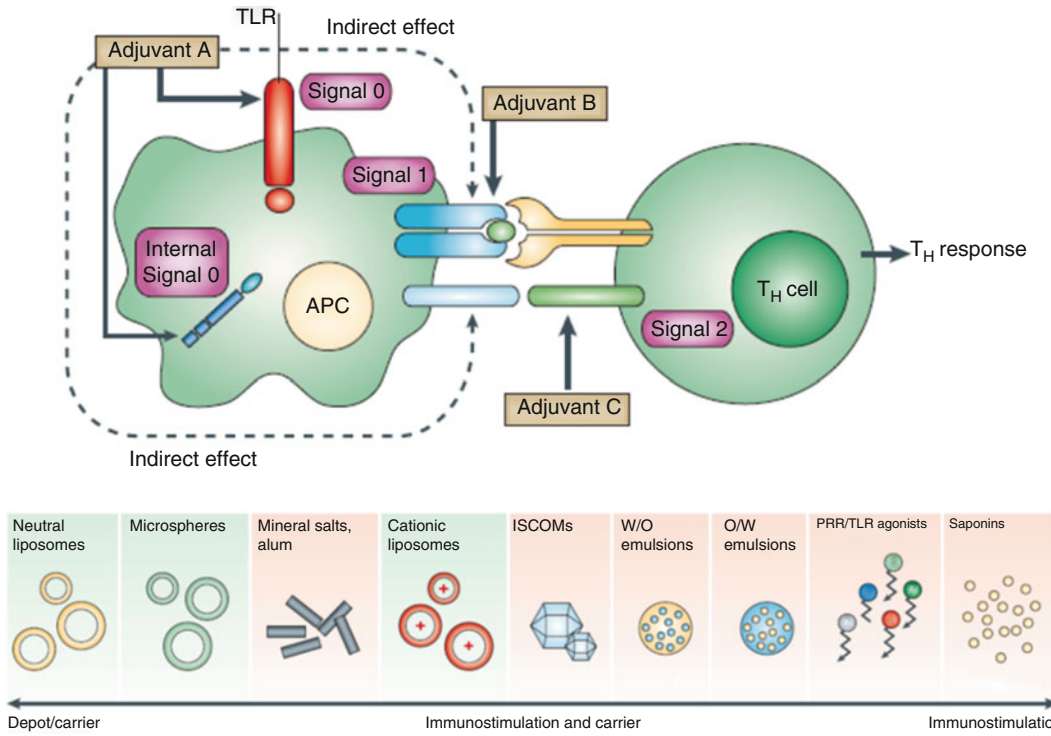

Fig. 7 Role of adjuvants in vaccinology. Adapted from Guy B: The perfect mix: recent progress in adjuvant research. Nat Rev Microbiol. 2007 Jul;5(7):505–17

In most instances, vaccines are developed to protect human beings from infectious diseases on a population-based level. This implies that vaccines should provide protection for basically every vaccinated individual within an immunogenetically heterogeneous population. Conventional vaccines formulated with whole microbial pathogens usually provide a broad range of different antigens and antigenic epitopes that in most instances guarantee sufficient immunostimulatory activity for a heterogeneous population. In contrast, highly purified antigens consisting only of a limited number of epitopes may pose the risk of insufficient interaction with individuals missing the adequate immune receptor repertoire. Moreover, genetic heterogeneity of the pathogen may counteract the expected benefit of highly purified vaccine antigens. Keeping this in mind, selection of vaccine antigens has to balance specificity and purity of antigens against sufficient antigenic variety to ensure targeting the immune system of every or at least the majority of individuals in a given population.

12 Selecting Vaccine Antigens

The identification of appropriate antigenic structures involves various considerations, based on the desired type of immune response. For example, if a neutralizing antibody response is sufficient to protect from infection, usually an antigenic structure from the bacterial/viral cell surface is selected. This has been done successfully for the *H. influenzae* type b, pneumococcal and meningococcal and hepatitis B vaccines, or from secreted toxins, like tetanus or diphtheria.

In the course of an antibody response, antigen-specific helper T cells are essential for the evolution of high-affinity antibodies and immune memory. Other antigen-specific T cells, including cytotoxic T cells, accomplish important effector functions, such as the targeted removal of host cells infected by intracellular pathogens, or support for macrophages in their removal of extracellular pathogens. In these latter cases an antigen has to be selected for the vaccine that enables these T cell effector-mediated responses. Hepatitis B vaccines, for example, induce antibodies as well as hepatitis B-specific T cell responses [30], pertussis vaccines induce antibodies and stimulate helper T cells to produce interferon [31, 32], and hepatitis A and IPV vaccines probably stimulate both T and B cells. As a matter of fact, in some instances the immune response induced by vaccination may even be stronger than the response observed after natural infection. This has been observed for human papillomavirus (HPV) vaccines that induce higher concentrations of neutralizing antibodies than in naturally occurring immune responses [33].

Purification of vaccine antigens is an important step to achieve vaccines with few unwanted side effects. Progress in biotechnology

in recent years has allowed isolating subcomponents of pathogens and producing them in large quantities. By eliminating unwanted pathogenic components, the high specificity and purity of these antigens permit the development of vaccines with reduced reactogenicity and improved safety profiles. The first attempt to select antigenic structures and to eliminate unwanted material has been made with split- or subvirion vaccines. These vaccines are prepared by using a solvent (such as ether or a detergent) to dissolve or disrupt the viral lipid envelope [7]. The technology has been applied most successfully in the development of inactivated influenza vaccines [34]. Purification steps are also engaged in the production of subunit vaccines, comprising protein or polysaccharide antigens, such as acellular pertussis proteins [6], typhoid Vi-antigen, and pneumococci polysaccharides [35, 36]. While split and subunit vaccines are less reactogenic than their conventional whole-cell counterparts, in many instances, this benefit is associated with reduced immunogenicity. For these vaccines the addition of adjuvants (*see* below) often is required to induce sufficient immunological memory and maintain protection [16].

Impaired immunogenicity may also occur with purified antigens that are unable to address sufficient elements of the immune system relevant for the protective response. Immune responses to pure polysaccharide antigens can be particularly poor in comparison with those induced by protein antigens. Polysaccharide antigens alone are not able to recruit T-helper cells in order to obtain B cell support by cell-mediated immunity. This phenomenon is especially significant in young infants and children as well as with the elderly [37]. As a result, immune responses to plain polysaccharide antigens are characterized by the secretion of low-affinity antibodies, mainly immunoglobulin M (IgM) molecules, and display a stereotyped "innate response" behavior. Repetitive encounters with the same antigen fail to induce a secondary, memory-like immune response [16]. This disadvantage was finally surmounted by the invention of the protein-conjugate technology. By covalently binding the polysaccharide antigen to a carrier protein, typically an inactivated toxoid like tetanus or diphtheria toxoid, conjugate vaccines dramatically improve immune responses to polysaccharides. With these vaccines, the polysaccharide component is recognized and bound by the B cell antigen receptor (i.e., the antibody molecule expressed on the cell surface), providing the first signal for B cell activation. Subsequently, the responding B cell serves as an antigen-presenting cell for T-helper cells that are specific for the conjugated carrier protein. The conjugated vaccine is internalized and processed and the antigen components of the conjugated protein are presented in the context of MHC molecules to be recognized by conjugate-protein/peptide-specific T-helper cells. Applying this approach, polysaccharide-specific B cells recruit help from conjugate-protein-specific T cells to

get all signals needed to promote further activation as well as isotype switching to IgG production and generation of memory B cells. Today, this elegant technique is regularly applied to vaccines containing bacterial polysaccharides for the prevention of invasive diseases caused by encapsulated bacteria. Examples include *H. influenzae* type b, pneumococcal [36] and meningococcal vaccines.

Modern molecular biology techniques allow vaccinologists today to select antigenic structures at the gene level and produce recombinant vaccines that contain only the antigen substructures relevant to elicit protective immunity [38]. The first recombinant vaccine, licensed in 1986, was achieved by cloning the gene for hepatitis B surface antigen (HBsAg) and was as effective as plasma-derived vaccines [39]. Two recombinant vaccines are also available against cervical cancer [40]. Both vaccines are based on HPV viruslike particles assembled from recombinant HPV L1 coat proteins. Quite recently research in this area has taken even a step further. By expressing multiple proteins identified in genome of meningococcus type B strains it was possible to identify new protein antigens on the surface of the microorganism that finally led to the successful development of a MenB vaccine. This technology, named reverse vaccinology, is now engaged to develop vaccines against microorganisms for which hitherto no vaccines were available, such as vaccines against *Staphylococcus aureus* or *Pseudomonas* strains.

However, as with subunit vaccines, the highly purified antigens obtained with peptide and recombinant technologies can have the disadvantage of weakened immunogenicity. The research for means to overcome this shortcoming has led to the development of innovative adjuvants to control and modify vaccine-induced immune responses, as described in the next section.

13 Improving Vaccines over Natural Immune Responses

Over the last century the approach to vaccine design has moved from vaccines (many of them still available today) that were developed empirically to the development of vaccines with higher specificity, better activation of relevant immunological mechanisms, lower reactogenicity, and better safety profiles. With these advances, a major challenge emerged; in comparison to whole inactivated microorganisms or less purified vaccines highly purified and defined antigens can have the unwanted consequence of impaired immunogenicity. While live attenuated or killed whole organisms contain a multitude of antigenic structures that can act as “intrinsic adjuvants” [4] to enhance their immunogenicity, this quality often is lost with the purification process of subunit vaccines. In order to

Table 4
Adjuvants potentiate vaccine-induced immune responses

• Prolonged antigen persistence
• Kinetics of lymphocyte trafficking
• Antigen processing and presentation
• Modulation of immune responses
– Th1–Th2 activation
– Cytokine production
– Augmentation of AB production
– Induction of "mucosa immunity"

conserve the advantages of subunit vaccines it was necessary to develop tools, i.e., adjuvants that support a sufficient activation of the immune system (Table 4).

Traditional vaccine adjuvants include aluminum salts, emulsions, and liposomes [4]. Aluminum salts have been used widely as adjuvants in human vaccines for more than 80 years [41]. It is now known that aluminum salts (and other adjuvants) are able to provide proinflammatory or immunostimulatory effects as well as prolong the persistence of vaccine antigens by slowing down antigen degradation. However, it has also been demonstrated that aluminum salts primarily promote antibody responses, with little or no effect on T-helper 1 and cytotoxic T cell immune responses, which are key for protection against many pathogens [16]. Oil-in-water (O/W) emulsions have a good safety profile and are capable of eliciting a strong humoral response. An example is MF59™, which is composed of stable droplets of the metabolizable oil squalene, and two surfactants, polyoxyethylene sorbitan monooleate (Tween 80) and sorbitan trioleate (Span-85). Enhancement of the immune response generated by MF59™ appears to be limited to antibody responses [35].

Especially for vaccines designed to induce a cytotoxic T cell-mediated immune responses, aluminum salts have been found to be inadequate to imitate the required protection. This is essentially due to a lack of "intrinsic immune defense triggers" usually provided by the pathogen, such as pathogen-associated molecular patterns (PAMPs) [16]. Naturally available PAMPs may be reduced or even become lost during the selection process for relevant vaccine antigens or in the course of the purification process. PAMPs represent conserved "danger signals" that are recognized by pattern recognition receptors (PRRs), mainly of the innate immune system and to some degree also on B and T cells, including so-called Toll-like receptors (TLRs). The targeting of PRRs by

PAMPs delivers an important early activation signal that can alert and potentiate multiple aspects of the adaptive immune responses, i.e., type, magnitude, and quality of specific B and T cell activation, and immune memory induction. Hence, it is by the recognition of particular PAMPs the innate immune system can create different immunological environments that can shape the type of protective adaptive immune responses. It was a logical step in vaccine development to target the "danger-sensing" PRRs in order to improve the quality and persistence of vaccine-related immune responses. A variety of TLR agonists have also been identified as potential vaccine immunomodulators, including deacylated monophosphoryl lipid A (MPL) [42], a purified, detoxified derivative of the lipopolysaccharide (LPS) molecule of the bacterial wall of *Salmonella minnesota* [43]. Like LPS, MPL acts through binding to TLRs, stimulating upregulation of co-stimulatory molecules and cytokine release, inducing a strong humoral and cellular response, depending on the antigen considered [55]. Most recently, the improved understanding of TLR signaling has led to the recognition of a role for immunostimulatory DNA, such as CpG [44], and other TLR agonists, such as messenger RNA molecules as vaccine adjuvants.

Other molecules besides TLR agonists have also been identified as immunomodulators and are currently investigated as vaccine adjuvants. For example, QS-21 is a highly purified immunostimulant extracted from the bark of the South American tree *Quillaja saponaria* [45]. It has the ability to optimize antigen presentation to antigen-presenting cells and stimulate both humoral and cellular responses. Importantly, the adjuvant properties of MPL and QS-21 appear synergistic. MPL and QS-21 have been studied in combination and have been shown to enhance Th1 and cytotoxic T cell responses against exogenous protein in mice.

Liposomes are synthetic nanospheres consisting of lipid layers that can encapsulate antigens and act as both a vaccine delivery vehicle and an adjuvant [46]. Liposomes promote humoral and cell-mediated immune responses to a wide range of bacterial and viral antigens as well as tumor cell antigens. Vaccines containing liposomes are available against hepatitis A and influenza [47].

Adjuvant research has demonstrated that with the right selection of antigens together with new adjuvants the immune response elicited by vaccines can be adapted to the pathogens and targeted populations. Recognizing that this cannot always be achieved with only one adjuvant type led to investigation of adjuvant systems, which combine classical adjuvants (aluminum salts, o/w emulsion, and liposomes) and immunomodulatory molecules, such as MPL and Q-S21. This concept has allowed the development of vaccines tailored to the antigen and target population, such as the HPV vaccine with adjuvant system AS04 and a malaria vaccine with adjuvant system AS02.

14 Future Prospects

Some challenges presented by infectious diseases such as malaria, tuberculosis, and HIV/AIDS so far could not be addressed successfully with classical vaccines, including those containing traditional adjuvants. This has led to new approaches including live vectors, DNA vaccines, and new adjuvant formulations as described before. Live vector technology involves the use of attenuated bacteria and viruses as vectors for the delivery of pathogen-specific DNA to enhance immunogenicity [48, 49]. The technology is of particular interest for the development of HIV vaccines and therapeutic vaccines for certain cancers. However, to date, clinical trials performed in the context of HIV have been disappointing, and the potential of such an approach is unclear.

DNA vaccines are composed of genes encoding a key antigenic determinant, often inserted into a bacterial plasmid [50]. Administration of the DNA vaccine leads to the expression of the foreign gene and synthesis of antigens derived from the infectious organism within the host cells. Presentation of the foreign proteins by the host cells can elicit an immune response similar to that induced by natural infection. Depending on the host cells targeted, DNA vaccines have the potential to stimulate a cellular immune response and, to a lesser extent, a humoral immune response. Since the foreign protein produced is expressed and processed intracellularly it can also be presented to the immune system in the context of the MHC class I system, providing the option to stimulate specific cytotoxic effector T cells. In contrast, traditional vaccines are mostly processed via the MHC class II system and therefore will preferentially stimulate T-helper lymphocytes. Clinical trials of plasmid DNA vaccines for HIV infection, Ebola hemorrhagic fever, West Nile virus infection, avian influenza, and various cancers are currently ongoing.

Many more advances can be expected in future vaccinology, not only against infectious diseases but also against other illnesses or chronic disorders not necessarily associated with an infectious pathogen. These include therapeutic cancer vaccines that have been tested with promising results with a number of spontaneous tumor animal models, including models of breast, prostate, pancreatic, and colon cancer [51]. These vaccines are designed involving antigen-specific vaccines and DC vaccines formulated with patients' DCs loaded with tumor-associated antigens. Moreover, cytokines are being evaluated as cancer vaccine adjuvants, most notably granulocyte macrophage colony-stimulating factor (GM-CSF). DC vaccines and antigen-specific cancer immunotherapeutics (ASCI) represent the most advanced approaches in cancer immunotherapy. DC vaccines work by isolating and exposing the cancer patient's DCs ex vivo to compounds that include

tumor-associated antigens. After their reintroduction to the patient, these DCs promote a cytotoxic T cell response against the tumor tissue.

Allergic diseases affect up to 25 % of the population in Western countries. Novel immunotherapies are currently under development, among them a vaccine including a TLR-9 agonist [52]. A phase 2 study with a ragweed allergen conjugated to immunostimulatory DNA (CpG) showed reduction in symptoms of allergic rhinitis during the ragweed season [53], but further studies are needed to confirm these observations. Progress is also expected from vaccines for the treatment of autoimmune diseases like type 1 diabetes, arthritis, Alzheimer's disease, or multiple sclerosis. Again encouraging results with DNA vaccines have been found in phase 1/2 studies for multiple sclerosis and type 1 diabetes [54]. The continuing progress in vaccine technologies and in the understanding of the mechanisms underlying the immune response is facilitating a more and more refined approach to vaccine design tailored to the desired effect of combating disease.

References

1. Zepp F (2010) Principles of vaccine design—lessons from nature. Vaccine 28 Suppl 3:C14–C24
2. Plotkin SL, Plotkin SA (2012) A short history of vaccination. In: Plotkin SA, Orenstein WA, Offit PA (eds) Vaccines, 6th edn. Saunders, Philadelphia, pp 1–16
3. Kelly DF, Rappuoli R (2005) Reverse vaccinology and vaccines for serogroup B Neisseria meningitidis. Adv Exp Med Biol 568:217–223
4. Leroux-Roels G (2010) Unmet needs in modern vaccinology: adjuvants to improve the immune response. Vaccine 28 Suppl 3:C25–C36
5. Girard MP, Steele D, Chaignat CL et al (2006) A review of vaccine research and development: human enteric infections. Vaccine 24:2732–2750
6. Edwards KM, Decker MD (2008) Pertussis vaccines. In: Plotkin SA, Orenstein WA, Offit PA (eds) Vaccines, 5th edn. Elsevier, New York, pp 467–518
7. Bridges CB, Katz JM, Levandowski RA et al (2008) Inactivated influenza vaccines. In: Plotkin SA, Orenstein WA, Offit PA (eds) Vaccines, 5th edn. Elsevier, New York, pp 259–290
8. World Health Organization (2003) Introduction of inactivated poliovirus vaccine into oral poliovirus vaccine-using countries. Wkly Epidemiol Rec 78:241–250
9. Demicheli V, Debalini MG, Rivetti A (2009) Vaccines for preventing tick-borne encephalitis. Cochrane Database Syst Rev (1):CD000977
10. Fiore AE, Feinstone FM, Bell BP (2008) Hepatitis A vaccines. In: Plotkin SA, Orenstein WA, Offit PA (eds) Vaccines, 5th edn. Elsevier, New York, pp 177–204
11. Sutter RW, Kew OM, Cochi SL (2008) Poliovirus vaccine—live. In: Plotkin SA, Orenstein WA, Offit PA (eds) Vaccines, 5th edn. Elsevier, New York, pp 631–686
12. Vesikari T, Sadzot-Delvaux C, Rentier B et al (2007) Increasing coverage and efficiency of measles, mumps, and rubella vaccine and introducing universal varicella vaccination in Europe: a role for the combined vaccine. Pediatr Infect Dis J 26:632–638
13. Orme IM (2015) Tuberculosis vaccine types and timings. Clin Vaccine Immunol 22:249–257
14. Siegrist CA (2012) Vaccine immunology. In: Plotkin SA, Orenstein WA, Offit PA (eds) Vaccines, 6th edn. Saunders Elsevier, Philadelphia, pp 18–36
15. Hoebe K, Janssen E, Beutler B (2004) The interface between innate and adaptive immunity. Nat Immunol 5:971–974
16. Moser M, Leo O (2010) Key concepts in immunology. Vaccine 28 Suppl 3:C2–C13
17. Barton GM, Medzhitov R (2002) Toll-like receptors and their ligands. Curr Top Microbiol Immunol 270:81–92
18. Merle NS, Noe R, Halbwachs-Mecarelli L et al (2015) Complement system part II: role in immunity. Front Immunol 6:257

19. Leo O, Cunningham A, Stern PL (2011) Vaccine immunology. Perspectives Vaccinol 1:25–59
20. Smith KA (2012) Toward a molecular understanding of adaptive immunity: a chronology, part I. Front Immunol 3:369
21. Smith KA (2012) Toward a molecular understanding of adaptive immunity: a chronology, part II. Front Immunol 3:364
22. Smith KA (2014) Toward a molecular understanding of adaptive immunity: a chronology, part III. Front Immunol 5:29
23. Vinuesa CG, Tangye SG, Moser B et al (2005) Follicular B helper T cells in antibody responses and autoimmunity. Nat Rev Immunol 5:853–865
24. Eibel H, Kraus H, Sic H et al (2014) B cell biology: an overview. Curr Allergy Asthma Rep 14:434
25. Shapiro-Shelef M, Calame K (2005) Regulation of plasma-cell development. Nat Rev Immunol 5:230–242
26. Deenick EK, Hasbold J, Hodgkin PD (2005) Decision criteria for resolving isotype switching conflicts by B cells. Eur J Immunol 35:2949–2955
27. Gasper DJ, Tejera MM, Suresh M (2014) CD4 T-cell memory generation and maintenance. Crit Rev Immunol 34:121–146
28. Takemori T, Kaji T, Takahashi Y et al (2014) Generation of memory B cells inside and outside germinal centers. Eur J Immunol 44:1258–1264
29. Plotkin SA (2010) Correlates of protection induced by vaccination. Clin Vaccine Immunol 17:1055–1065
30. Banatvala JE, Van DP (2003) Hepatitis B vaccine—do we need boosters? J Viral Hepat 10:1–6
31. Zepp F, Knuf M, Habermehl P et al (1997) Cell-mediated immunity after pertussis vaccination and after natural infection. Dev Biol Stand 89:307–314
32. Mills KH, Ryan M, Ryan E et al (1998) A murine model in which protection correlates with pertussis vaccine efficacy in children reveals complementary roles for humoral and cell-mediated immunity in protection against Bordetella pertussis. Infect Immun 66:594–602
33. Schwarz TF, Leo O (2008) Immune response to human papillomavirus after prophylactic vaccination with AS04-adjuvanted HPV-16/18 vaccine: improving upon nature. Gynecol Oncol 110(3 Suppl 1):S1–S10
34. Leroux-Roels I, Leroux-Roels G (2009) Current status and progress of prepandemic and pandemic influenza vaccine development. Expert Rev Vaccines 8:401–423
35. Fraser A, Goldberg E, Acosta CJ et al (2007) Vaccines for preventing typhoid fever. Cochrane Database Syst Rev 3, CD001261
36. Pletz MW, Maus U, Krug N et al (2008) Pneumococcal vaccines: mechanism of action, impact on epidemiology and adaption of the species. Int J Antimicrob Agents 32:199–206
37. Borrow R, Dagan R, Zepp F et al (2011) Glycoconjugate vaccines and immune interactions, and implications for vaccination schedules. Expert Rev Vaccines 10:1621–1631
38. McCullers JA (2007) Evolution, benefits, and shortcomings of vaccine management. J Manag Care Pharm 13(7 Suppl B):S2–S6
39. André FE (1990) Overview of a 5-year clinical experience with a yeast-derived hepatitis B vaccine. Vaccine 8 Suppl: S74–S78
40. Rogers LJ, Eva LJ, Luesley DM (2008) Vaccines against cervical cancer. Curr Opin Oncol 20:570–574
41. Brewer JM (2006) (How) do aluminium adjuvants work? Immunol Lett 102:10–15
42. Garçon N, Van Mechelen M, Wettendorff M (2006) Development and evaluation of AS04, a novel and improved immunological adjuvant system containing MPL and aluminium salt. In: Schijns V, O'Hagan D (eds) Immunopotentiators in modern vaccines. Elsevier Academic Press, London, pp 161–177
43. Alderson MR, McGowan P, Baldridge JR et al (2006) TLR4 agonists as immunomodulatory agents. J Endotoxin Res 12:313–319
44. Higgins D, Marshall JD, Traquina P et al (2007) Immunostimulatory DNA as a vaccine adjuvant. Expert Rev Vaccines 6:747–759
45. Garçon N, Van Mechelen M (2011) Recent clinical experience with vaccines using MPL- and QS-21-containing adjuvant systems. Expert Rev Vaccines 10:471–486
46. Aguilar JC, Rodríguez EG (2007) Vaccine adjuvants revisited. Vaccine 25:3752–3762
47. Schwendener RA (2014) Liposomes as vaccine delivery systems: a review of the recent advances. Ther Adv Vaccines 2:159–182
48. Daudel D, Weidinger G, Spreng S (2007) Use of attenuated bacteria as delivery vectors for DNA vaccines. Expert Rev Vaccines 6:97–110
49. Liniger M, Zuniga A, Naim HY (2007) Use of viral vectors for the development of vaccines. Expert Rev Vaccines 6:255–266
50. Grunwald T, Ulbert S (2015) Improvement of DNA vaccination by adjuvants and sophisticated delivery devices: vaccine-platforms for the battle against infectious diseases. Clin Exp Vaccine Res 4:1–10
51. Butterfield LH (2015) Cancer vaccines. BMJ 350:h988
52. Broide DH (2009) Immunomodulation of allergic disease. Annu Rev Med 60:279–291

53. Creticos PS, Schroeder JT, Hamilton RG et al (2006) Immunotherapy with a ragweed-toll-like receptor 9 agonist vaccine for allergic rhinitis. N Engl J Med 355: 1445–1455
54. Silva CL, Bonato VL, dos Santos-Junior RR et al (2009) Recent advances in DNA vaccines for autoimmune diseases. Expert Rev Vaccines 8:239–252
55. Evans JT, Cluff CW, Johnson DA, Lacy MJ, Persing DH, Baldridge JR. Enhancement of antigen-specific immunity via the TLR4 ligands MPL adjuvant and Ribi.529. Expert Rev Vaccines. 2003 Apr;2(2):219–29

Part II

Trends in Vaccinology

Chapter 4

Reverse Vaccinology: The Pathway from Genomes and Epitope Predictions to Tailored Recombinant Vaccines

Marcin Michalik, Bardya Djahanshiri, Jack C. Leo, and Dirk Linke

Abstract

In this chapter, we review the computational approaches that have led to a new generation of vaccines in recent years. There are many alternative routes to develop vaccines based on the technology of reverse vaccinology. We focus here on bacterial infectious diseases, describing the general workflow from bioinformatic predictions of antigens and epitopes down to examples where such predictions have been used successfully for vaccine development.

1 Introduction

The successful removal of a pathogen from the human body by the adaptive immune system requires the recognition of the pathogen's molecules as "foreign". The molecular patterns allowing the host's immune system to detect pathogens are called antigenic. Those patterns additionally capable of inducing an immune response by the host are more specifically referred to as immunogenic. Furthermore, the site of the antigen to which the antigen-binding receptors actually bind is the antigenic determinant or epitope. In most cases, antigens possess several different epitopes; however, they can vary in immunogenicity, which leads to the phenomenon of so-called immunodominant epitopes.

Any vertebrate species pursues two main strategies or systems to achieve immunity: the innate and the adaptive immune system. While the former is inherited from the parents and is genetically fixed for life, the latter is key to the recognition of new pathogenic structures. The adaptive (or specific) immune system again is composed of two arms: the humoral and the cellular immune responses. These responses are mediated by two classes of lymphocytes, called B and T cells, respectively. B cells are able to express unique immunoglobulin receptors localized on the cell surface. These immunoglobulin receptors possess a variable antigen-binding site permitting

Sunil Thomas (ed.), *Vaccine Design: Methods and Protocols: Volume 1: Vaccines for Human Diseases*, Methods in Molecular Biology, vol. 1403, DOI 10.1007/978-1-4939-3387-7_4,

vertebrates to specifically recognize and bind potentially billions of different epitopes. B cells are activated upon contact with an antigen, with or without the help of T-helper cells (see below). Protein antigens typically activate B cells directly [1]. As soon as an antigen binds to the immunoglobulin receptor of a naïve B cell, the B cell is stimulated to proliferate and differentiate into an antibody-producing plasma cell (effector cell) [2] with the sole task of amplifying a single type of specifically binding antibody that is able to bind its cognate antigen while circulating freely within the blood and lymph.

As soon as an immunoglobulin binds to a pathogen, the activity of the pathogen is reduced and it is marked (opsonized) for elimination by cells of the innate immune system, neutrophils, and macrophages, capable of phagocytosis and subsequent killing and degradation of the pathogen. Some B cells, however, differentiate into a different cell type, so-called memory B cells. In case of the same antigen entering the host again, these cells are promptly activated to accelerate a stronger, secondary immune response. Memory B cells have the ability to persist in the host for several years, thereby allowing a long-lasting protection [3]. It is this memory of the immune system that is exploited when vaccines are used.

The cellular immune response is mediated by a second type of equally important immune cells called T cells. T cells, like B cells, are stimulated to proliferate and differentiate into the mature state by specifically binding to antigens. However, antigen recognition by T cell receptors (TCRs) is only possible if the epitopes are presented as protein fragments on the surface of specialized antigen-presenting cells (APCs), which are part of the innate immune system. The presentation of protein fragments by these APCs, particularly dendritic cells and macrophages, also requires partial degradation of the proteins of the foreign matter. After several processing steps within the APCs, these fragments are displayed in the context of co-simulators on the cell surface of APCs by proteins of the major histocompatibility complex (MHC) [4]. After activation, naïve T cells can develop into two major classes of effector cells. Each of them maintains the ability to bind the same MHC peptide complexes that also led to their activation. Cytotoxic T cells (CTLs or $CD8^+$ cells[1]) destroy nearby infected or malignant/transformed cells (APCs, too). T helper cells (T_h cells, or $CD4^+$)

[1] CD8 and CD4 are transmembrane glycoproteins. They function as co-receptors of T cell receptors on the surface of T cells. "CD" is an abbreviation for cluster of differentiation; a superscripted plus or minus sign indicates whether this type of cell actually does or does not express the specific receptor. CTLs do not possess a CD4 receptor, and are therefore unable to bind to the MHC II-peptide complex. In contrast, T helper cells are unable to bind MHC I as they do not express CD8 receptors on their cell surfaces.

are a decisive factor in the activation of various immune reactions of T-dependent B cells, CTLs, macrophages, and dendritic cells. In analogy to B cells, subpopulations of both $CD4^+$ and $CD8^+$ are capable of differentiating into memory T cells similarly enabling long-term protection. MHC proteins are key to these processes. There are two classes of MHC proteins, named MHC class I and class II. Both classes have variable binding pockets which specifically bind previously processed peptides in an extended linear conformation with high affinity. In both cases, the loaded MHC receptors are subsequently translocated from the endoplasmic reticulum (where the loading takes place) to the cell surface of the APC, where these peptides are presented to bind TCRs [3]. Nevertheless, there are important differences between these two classes explained in the following paragraphs.

2 Reverse Vaccinology

Since the British physician Edward Jenner introduced his smallpox vaccine to the Western world in the late eighteenth century, classical vaccinology has become one of the most successful countermeasures in the constant battle against infectious diseases. In many cases, governmental programs for exhaustive vaccination were able to push the number of new infections per year to almost zero [5]. Prominent examples include the vaccination against smallpox that effectively eradicated the disease, and against polio, where incidence rates have dropped by more than 99 % since the late 1980s. Despite the ongoing success of classical vaccination strategies, a number of infectious diseases have remained recalcitrant to vaccine development, largely due to the inherent constraints of classical vaccine technology.

Usually the vaccine administered is a biological suspension of either inactivated or killed cells, polysaccharide capsules, or toxoids [6]. However, in many cases it is challenging to prepare a potent vaccine against a specific pathogen. Non-culturable microorganisms, antigens which are not expressed in vitro, pathogens with antigenic determinants that can trigger detrimental autoimmune reactions, as well as extremely heterogeneous strains are only a few of the severe difficulties classical vaccinologists are confronted with today.

Recently, a new impetus was given to current vaccine research thanks to the growing number of available complete microbial genomes. Based on the assumption that all (protein) antigens a pathogen can express at any time are encoded in its genome (and therefore available to the scientist without cultivation), the idea is to combine bioinformatics and biotechnology to identify protein candidates for vaccine development. As this approach begins with the genome sequence, in contrast to starting from an entire living

microorganism, it is called "reverse vaccinology" [7, 8]. The first projects based on this approach used genome information only to naïvely select surface-localized proteins as a pool of possible candidates for subsequent classical animal experiments. In their pioneering work for the development of a vaccine against *Neisseria meningitidis* B (MenB), R. Rappouli and colleagues collected 570 surface-localized proteins, of which about 350 could successfully be cloned and expressed in *Escherichia coli*. The purified proteins were then used to immunize mice, and the resulting sera were subjected to various immunoassays to test for the candidate protein's efficacy as a vaccine. The researchers found 28 proteins which showed consistently positive results in all immunoassays and were able to induce antibodies with bactericidal activity [9]. Furthermore, five of these candidates were also highly conserved in the genome of distantly related strains. A subset of these candidates became the basis for the development of a vaccine called "4CMenB," which contains three recombinant protein antigens combined with outer membrane vesicles derived from the meningococcal strain NZ98/254 and has obtained market authorization for the European Union in January 2013 (Bexsero, Novartis International AG [10]). Reverse vaccinology has since developed enormously, in particular by using increasingly sophisticated bioinformatic methods to mine the information provided by complete genomes.

In this chapter, we review the computational approaches that have led to new vaccines in recent years. We also briefly summarize the mode of action of antigens and vaccines, and how vaccines are able to provide long-term protection. There are many alternative routes for a successful reverse vaccine—here, we focus on vaccines against bacterial infectious diseases. The general workflow from bioinformatic predictions of antigens and epitopes down to examples where such predictions have been used for vaccines successfully are stated in this chapter.

3 Pan-Genomic Analysis

Apart from being a valuable approach to investigate the characteristics of a specific phylogenetic clade, pan-genomic analysis is indispensable for identifying conserved target proteins within a set of genomes of pathogenic strains within a single clade. The term "pan-genome" was first coined by Tettelin [11] and is defined as the entire genomic repertoire accessible to the clade studied. It encompasses two subsets: the "core genome" and the "dispensable" or "accessory genome." While the former describes the intersection of genes (or ORFs) shared by all strains of the clade, the latter comprises genes only found in subsets of strains. Such a classification is biologically meaningful as it allows us to

differentiate between (core) genes considered essential for growth, and (accessory) genes encoding, e.g., for supplementary pathways and functions which confer a selective advantage, such as antibiotic resistance or virulence genes that are limited to certain strains [12].

Similarity between proteins is usually determined by pairwise alignment. Particular thresholds are set for the percentage of sequence identity of the protein sequence over a percentage of pairwise-aligned sequence length. However, depending on the phylogenetic resolution and the available quality and quantity of genomes, it might be necessary to increase sensitivity. This can be done by incorporating additional methods such as orthology prediction, i.e., the prediction of genes among species or strains that originated by vertical descent from a single gene of their last common ancestor, as well as structural alignments. Relying solely on pairwise sequence alignments, Tettelin [11] chose a minimum of 50 % identity over 50 % of the sequence lengths, while Hiller [13] chose 70 % to identify similar proteins within strains of *Streptococcus agalactiae* and *S. pneumoniae*, respectively. For the purpose of identifying target proteins it is nonetheless beneficial to choose considerably higher threshold values to exclude false positives early on in the workflow. The potential loss of immunogenic sequences due to the high threshold values is relatively low. In addition, given the high specificity of the immune system receptors, this is a good trade-off for the reduction of the number of proteins to analyze in subsequent steps.

4 Surface Localization

To perform their functions at their native subcellular localization (SCL), newly synthesized proteins must be sorted and transported to their respective subcellular compartments. The subcellular localization of proteins not only provides important clues to their function in the cell, but is also important for judging the potential efficacy of vaccine targets. Surface-localized proteins are typically the first molecular patterns of pathogens that are in contact with the host immune system, and are generally considered the best candidates for recombinant vaccines.

Determining the SCL of proteins by experimental means, such as subcellular fractionation combined with mass spectrometry, is accurate but time- consuming and expensive [14]. Bioinformatics methods are an increasingly comprehensive and reliable way to determine the SCL of proteins in large datasets, as the proteins contain defined (and thus detectable) signals in their sequence.

There are two basic types of prediction tools for subcellular localization. One predicts very specific sequence features such as signal peptides for the Sec, Tat, or lipoprotein pathways using TargetP, SignalP, and related tools [15], or transmembrane segments [16].

The other type predicts the exact localization of a protein by combining various localization-specific features [17, 18] or general features like amino acid composition [19], evolutionary information [20], structure conservation information [17], or gene ontology [21]. The combination of different prediction tools in a pipeline increases the quality of the overall prediction significantly, and can reduce false-positive and false-negative results [22]. Last but not least, limiting the huge amount of protein sequence data to only the interesting, surface-localized vaccine candidates significantly reduces the workload for later immunogenicity prediction steps in the reverse vaccinology pipeline. Alternatively, experimental data such as proteomics approaches can be used to narrow down the number of candidates for further analysis [23].

5 Prediction of Epitopes

Ideal vaccine candidates are not only localized on the surface of the pathogen, but will also contain multiple epitopes that elicit strong immune responses within the host organism. However, experimental identification of epitopes within a set of proteins is a very resource- and time-intensive task making a computer-aided, complementary approach especially attractive. Numerous tools exist for such predictions, for both MHC I and MHC II, as well as B cell-mediated immunity. This chapter can only provide a crude overview of the different obstacles all prediction tools have to face and gives a brief overview of the general strategies they pursue. As for all bioinformatics tools, it is advisable to use multiple tools in parallel and to compare the results to minimize false-positive and false-negative predictions. In fact, recent publications have shown that combining prediction tools to produce a consensus-like output can achieve superior predictive performances [24, 25].

6 MHC I and MHC II Binding Predictions

Generally speaking, MHC I binds and presents epitopes which are derived from proteolytically degraded intracellular proteins (e.g., from intracellular pathogens) and are 8–11 residues long. In contrast, MHC II epitopes are derived from extracellular sources (e.g., from extracellular pathogens), and are much longer on average (up to 25 residues [26]). Originally, it was thought that these peptide epitopes would be recognized at least in part by their secondary structure, but more recent structural data suggest that they are presented mostly in an extended form. Early prediction tools working under the wrong assumption accordingly gave inconsistent results [6]. Additionally, MHC I and MHC II bind peptides very

differently: as the molecular structure of MHC II requires longer peptides, due to its "open" binding pocket, the residues extending the binding pocket on both sides contribute to the overall peptide binding affinity [26, 27]. To address this finding, modern MHC II epitope prediction tools often identify a binding core, i.e., a shorter subsequence within the longer peptide sequences of the query, which is predicted to bind to the pocket.

To use prediction tools efficiently for vaccine design, one has to consider that the human MHC molecules are encoded in a highly polymorphic locus called the human leukocyte antigen (HLA) locus on chromosome 6. There are tremendous numbers of HLA alleles with different binding affinities to the same epitope sequence: more than 10,000 different human alleles have been identified and, to complicate things even further, within different populations, different alleles (i.e., variants) of the MHC genes are present in different ratios.

Various online methods are available for the prediction of epitopes, ranging from sequence-based to structure-based (using, e.g., homology modeling or docking) methods. Table 1 shows a selection of sequence-based bioinformatics tools used for MHC I or MHC II predictions, which have the advantage of speed over structure-based methods and are therefore more favorable for large-scale analysis of peptides.

State-of-the-art sequence-based approaches attempt to predict the binding quality of a query sequence by abstracting from the sequence information of peptides with experimentally determined binding affinities. By doing so, they are able to generate models for each individual MHC variant. Matrix-based methods try to derive position-specific binding coefficients for each residue from a database of known binders of the same length. For the prediction, each position of a query sequence is evaluated individually, yielding a score of congruousness to its respective position in the abstract model of a binding sequence. To predict the binding quality of the complete query sequence, the final score is given as the sum of the scores of the individual positions. This approach can be modified by adding weights to certain positions (so-called anchor positions) to increase their impact on the final score.

A second group of prediction tools relies on machine learning approaches or stochastic models like support vector machines, artificial neural networks, or hidden Markov models to predict the binding quality of a query sequence. Generally speaking, all of these approaches attempt to refine a model by adjusting internal parameters to the sequence information provided by a collection of known binders. Therefore, a set of known binders is used to train the model, i.e., to adjust internal parameters in such a way as to

Table 1
Methods: QM: quantitative matrix-based methods (QM combine a matrix-based approach with a strategy to quantify the prediction scores), ANN: artificial neural networks

Author	Method	Publication	Output
MHC I			
Bui	QM	[28]	IC_{50} (nM)
Sidney	QM	[29]	
Nielsen	ANN	[30]	IC_{50} (nM)
Peters	QM	[31]	IC_{50} (nM)
Kim	QM	[32]	IC_{50} (nM)
Moutaftsi	QM	[33]	Percent rank
Nielsen	ANN, Pan-specific	[34]	IC_{50} (nM)
Karosiene	ANN, Pan-specific	[25]	IC_{50} (nM)
Zhang	QM	[24]	IC_{50} (nM)
MHC II			
Bui	QM	[28]	IC_{50} (nM)
Nielsen	ANN	[35]	IC_{50} (nM)
Sidney	QM	[29]	IC_{50} (nM)
Nielsen	QM	[36]	IC_{50} (nM)
Nielsen	ANN, Pan-specific	[37]	IC_{50} (nM)
Sturniolo	QM	[38]	IC_{50} (nM)
Wang	ANN, QM	[26]	Percent rank

enable accurate prediction of binding quality based on empirical data (supervised learning).

Some tools in both groups also include strategies to quantitatively predict the binding of a query sequence. By incorporating either position-specific affinity contributions (matrix-based approaches) or statistical regression analysis (machine learning approaches), the user can readily compare experimentally determined IC_{50} or K_d values with predicted ones. However, there are no predefined absolute threshold values clearly separating query sequences into either binders or non-binders. Rather, it is advisable to define cutoff values for each MHC allele individually [39].

It is important to note that all the tools, regardless of approach, heavily rely on experimental data on the measured binding affinities of peptide sequences for a specific MHC variant. Therefore, the quality of the prediction is determined by how well the binding space of a particular MHC variant is explored by the available data.

Unfortunately, for many alleles data are scarce; this has led to the development of pan-specific methods for MHC binding prediction. These use known MHC binders to known MHC alleles to infer binding for unknown pairs. Typically, such approaches are based on structural data where alleles with similar physicochemical attributes in the binding pocket are classed together using machine learning approaches [40–42].

7 B Cell Epitope Binding Predictions

B cell (or antibody) epitopes are 16 residues long on average but are not presented in the context of MHC molecules. Therefore, they are especially hard to predict as crystallographic studies have shown that BCRs are capable of binding discontinuous protein epitopes as well. Epitopes are called discontinuous if they are composed of distant sequence segments which are brought into close proximity due to the protein's tertiary structure. Contemporary tools for identifying B cell epitopes can be divided into those relying solely on primary structure information and those additionally incorporating structural data. The first group of tools calculate a prediction by considering a set of descriptors such as the propensity for a sequence segment to form a continuous, linear secondary structure, physicochemical attributes, surface accessibility, and amino acid composition [43]. In general, these tools yield reasonable accuracy for continuous (linear) epitopes, but fall short when identifying discontinuous epitopes [44]. To surmount this shortcoming, prediction calculations by the second group of tools include secondary structure information, calculated surface accessibilities, and/ or protrusion indices, in addition to information about the protein's three-dimensional structure and the structure of known antigen-BCR complexes. Popular sequence-based tools are BepiPred [45], ABCpred [46], and BEST [47]. Commonly used structure-based tools are ElliPro [48], Paratome [49], PEPOP [50], BEEPro [51], and DiscoTope [44]. The latter two tools even claim that benchmarking has shown that they are able to achieve high accuracy levels similar to MHC prediction tools [45].

Many of the tools for MHC I, II, and BCR epitope prediction offer web interfaces which allow thorough testing of their predictive powers before applying them in a larger scale. A very useful analysis resource is the immune epitope database (IEDB), funded by the National Institutes of Health [52]. In addition to providing a database of binding epitopes and their affinities, the IEDB furnishes a regularly updated compilation of self-developed and newly implemented popular prediction tools accessible via a single intuitive web interface.

8 Methods for Using Full-Length Antigens (Proteins) as Vaccines

All vaccines work in a similar way: by presenting foreign antigens to the immune system in order to activate a specific immune response. The aim of vaccination is usually to induce long-term protection through memory B cells [53]. The composition of vaccines can be diverse. Traditional formulations include live attenuated vaccines, which are composed of live viruses or bacteria that have been weakened in the laboratory to lower virulence by long-term passaging or genetic engineering (deletions in genes required for virulence) but are still able to activate the immune system. They elicit a strong response that can result in lifelong immunity with a minimum number of doses. Despite their advantages, live attenuated vaccines can have many drawbacks. Potential problems include difficulties with storage and transportation, where inappropriate handling may cause loss of vaccine efficacy. In addition, there are cases where this type of vaccine cannot be used (e.g., when patients take anti-infective drugs, or are immunocompromised for any reason). There is a risk that attenuated vaccines can revert to a fully virulent pathogen (e.g., oral poliovirus vaccine [54]). Last but not least, the attenuation process itself is lengthy and depends on random events out of the control of the researchers (examples: BCG tuberculosis vaccine, yellow fever rotavirus vaccine) [55, 56].

An alternative method is to inactivate the pathogens before use as a vaccine. This method is safer compared to the live attenuated vaccines, but is less potent in inducing immune responses. In short, such vaccines contain pathogens killed by heat or chemical treatment (i.e., formaldehyde). Risks related to such vaccines include errors in the inactivation. Because the inactivated pathogen does not reproduce in the host organism, there is a need for one or more "boosters," i.e., administration of additional doses of the vaccine after defined intervals (examples: cholera vaccine, hepatitis A vaccine, rabies vaccine) [53].

With better biochemical and immunological methods available, it has been possible to engineer vaccine formulations by only using active antigens (rather than complete pathogens). This is referred to as a subunit vaccine. It uses only specific parts of a pathogen to immunize against disease. The search for such components is typically focused on surface-bound or secreted antigens, which provide the best accessibility for antibodies and other immune mechanisms [53, 57]. Using purified proteins as a vaccine component is a widespread technique today. With bioinformatics, it is possible to select ideal antigen candidates for subunit vaccines, which have many advantages over the "whole-pathogen" approaches [58]. Subunit vaccine production is a safe process as it does not require the culturing of dangerous pathogens. The

final product is also safer to use [59, 60]: there is no infectious material, and thus no risk of the vaccine strain reverting to a harmful pathogen. In addition, it is possible to control all ingredients of the vaccine. Traditional vaccines induce very strong immunological responses with a very small dose; often this high response is not really necessary and does not always translate into later protection. In subunit vaccines, antigens are tested individually, and the kind of responses they provide are known. Thus, it is in principle possible to customize vaccines for specific patient groups (for example immunocompromised patients or patients already suffering from an infectious disease) [55].

9 Examples of Protein Subunit Vaccines

A vaccine against pertussis containing purified proteins was first created in 1981 in Japan by Sato and Sato, who purified the antigenic proteins by classical biochemical methods from cultures of the pathogen—with the obvious problems in biological safety and with upscaling of the procedure [61]. Another example is the hepatitis B vaccine which contains one of the proteins from the viral envelope—the hepatitis B surface antigen (HBsAg). This was one of the first protein-based vaccines, and while at first the protein was obtained from natural human plasma, it was later successfully expressed recombinantly in yeast cells. Today, this is the production method of choice for human vaccines [62]. Another example of a subunit vaccine on the market is the one against *Bacillus anthracis*. Although the components are still collected from pathogen cultures, which raises concerns about the safety of the procedure, the strength of the initial immune response and long-term efficacy are high [63].

Some studies have included production of plasmid-derived antigens using attenuated, avirulent *Bacillus* strains. Expressing these proteins in a *Bacillus* strain ensures properly processed and folded protein. The product is then purified from fermentation cultures and adsorbed onto an aluminum adjuvant. Preclinical studies showed that the vaccine as such is safe and well-tolerated and can induce an immune reaction with long-term immunity. Researchers are also looking for new targets using bioinformatics, now that the complete genome of the clinical strain is available [64, 65].

Two new vaccines against human papillomavirus (HPV) have been brought to the market recently—Cervarix and Gardasil (Silgard). Both contain proteins from the capsids of different virus strains—HPV16 and 18 and HPV6, 11, 16, and 18, respectively—and differ in the formulation of enhancers and adjuvants. In 2014, the US Food and Drug Administration approved another new

Table 2
Advantages of protein-based vaccines [59, 71]

• No need to culture dangerous pathogens
• Problems with toxic or oncogenic parts of the pathogen, or with antigens potentially causing allergies or autoimmune diseases, can be avoided
• Proteins can be altered by adding different chemical groups to improve immunogenicity, stability, or solubility
• Quality of the final vaccine is higher and is more reproducible
• Distribution and storage are improved (high stability, e.g., in freeze-dried form)
• No risk of reversion to a more virulent strain (as is the case for live attenuated vaccines)
• Using computational and bioinformatics methods potentially lowers the costs of initial research
• Production methods are comparatively easy to scale up

HPV vaccine from Merck, Gardasil 9, which protects against 9 subtypes of the virus (HPV6, 11, 16, 18, 31, 33, 45, 52, and 58). These vaccines are all produced recombinantly using yeast cells (or insect cells for Cervarix) [66–68].

In ongoing Phase III clinical trials, promising results have been obtained for a vaccine against *Pseudomonas aeruginosa* (IC43). This is an outer membrane protein-based vaccine containing an OprF/OprI fusion with a His tag. The product is expressed in *E. coli* from a plasmid. The vaccine gives good immune responses with and without an aluminum adjuvant [69, 70] (Table 2).

10 Methods for Using Predicted Epitopes/Peptides as Vaccines

Producing complete proteins in a stable form for vaccines or other purposes is not always straightforward. Many potential vaccine targets are membrane proteins, or are otherwise insoluble, prone to degradation, or to aggregation. Short peptide epitopes taken from vaccine target proteins are a promising alternative, as they can still be efficiently recognized and displayed by either MHC I or MHC II. In some cases, reducing a subunit vaccine to a single epitope has the additional advantage of removing deleterious further epitopes; examples include epitopes that can cause cross-reactivity leading to autoimmune responses.

In principle, an unlimited number of defined peptide epitopes can be combined to create multi-epitope vaccines. To obtain such epitopes, both reverse vaccinology approaches based on bioinformatics predictions (*see* above) and more traditional techniques based on antisera can be used to fish for epitopes [55]. One approach to using predicted peptide epitopes is to fuse them to a previously chosen protein scaffold as a carrier. This scaffold can

itself play additional important roles in enhancing the immunological response, e.g., due to the presence of T helper cell epitopes in its own sequence. A distinct advantage of this method is that multiple epitopes from different target proteins or even from diverse pathogen strains can be combined to obtain wider spectrum of protection [59]. Production and handling can also be improved in the process as the scaffold can be chosen according to desired properties (water solubility, nontoxicity, stability at room temperature, etc.).

An example for using predicted epitopes conjugated to a carrier scaffold is an ongoing study using *Aeromonas hydrophila* epitopes from outer membrane proteins (OmpF, OmpC) with the heat-labile enterotoxin B (LTB) of *Escherichia coli* as a scaffold [72]. LTB has been reported to be an efficient adjuvant capable of eliciting a strong immune response [73]. In four out of five cases (five different fusions), the authors found that the recombinant fusion proteins induce antibody production. The antisera generated this way were able to recognize the native proteins from which epitopes were taken. All epitopes in the study were predicted as B cell epitopes using bioinformatics approaches and tools as described above.

There are also potential problems with using peptide-based epitopes as vaccines: removing an epitope from its native context risks losing immunogenic efficacy and as a result general response to the vaccination [71]. Examples for such context-dependent recognition by the immune system are the loss of secondary structure, or the fact that especially B cell antigens are known to be mostly (90 %) discontinuous, nonlinear antigens—they derive from different protein regions localized closely in space due to the three-dimensional structure. Such conformation-dependent recognition cannot always be achieved using only a linear peptide/epitope [74]. Using suitable scaffold proteins for peptide epitopes can solve some of these problems, e.g., by adding sequences which will enhance binding and the stability of the peptide-MHC [75]. Another option for optimization is to modify epitopes using beta-amino acids instead of natural ones, which can increase the binding affinity to MHC dramatically. Such recombinant epitopes maintain the properties of natural epitopes because the side chains of the amino acids are identical between the alpha and beta type. However, the modification improves resistance to proteases as the epitopes do not have the same peptide backbone, so that the epitope is protected from digestion before it is loaded on the MHC. Even changing one amino acid to its beta variant has dramatic effects on the overall stability of the peptide [76–78].

Another, less well-understood disadvantages of using subunit vaccines are that they can be less efficient in inducing long-lasting immunity in some cases [79, 80]. Peptide vaccines often lack T

helper epitopes, especially when just a mix of peptides is used as a vaccine [81]. To improve the response, vaccine formulations are modified with different immunostimulants (adjuvants) and also by conjugation of the peptides to carrier proteins which will enhance immunogenicity and immune system activation [55]. The most common general adjuvant is an aluminum salt that can be found in many existing vaccines and is still used in new formulations in clinical trials and in preclinical phases [82]. Many novel adjuvants are being tested currently, with the aim of finding adjuvants that are safe to use, can enhance the immune response of even the weakly binding peptides or proteins, and can play a direct role as a delivery system at the same time. Typically, these are different types of emulsions (water-in-oil and oil-in-water), e.g., MF59 which is composed of squalene (licensed for influenza vaccines in Europe), polymeric particles like polylactic acid (PLA) or poly[lactide-co-glycolide] acid (PLGA), liposomes (which can protect peptides from enzymatic digestion, keep the folded structure of antigen, and elicit a high cellular immune response), viruslike particles (VLPs, self-assembling proteins which mimic the conformation of native viruses), inorganic nanoparticles, and carbon nanotubes [71, 83, 84]. Other adjuvants include flagellin-based adjuvants, lipopolysaccharide, and other bacterial structures that co-stimulate the immune system [58], as well as complete avirulent (and thus safe) living cells expressing the foreign antigen on the surface (for example using a type III secretion system [85]) [86, 87]. As described above, in cases where the immunological memory is not lifelong, there is a need for additional "boosting" to increase and maintain the protectivity of a vaccine [88].

The most recent developments in reverse vaccinology include personalized vaccines, which are aimed at specific patient groups or even individuals. This is particularly relevant for anticancer vaccines, where the targets (cancer cells) are highly variable from patient to patient. As an example, GAPVAC, in Phase I clinical trials, is a vaccine that uses patient-specific genes expressed in brain tumors and is based on peptides as well as cancer-specific mutations [89]. A similar study is currently being performed using HEPAVAC, a patient-specific vaccine against liver cancer [90].

Currently, no peptide-based vaccine is licensed for human use, but there are currently over 400 clinical trials of peptide vaccines in progress [59, 91]. A number of promising examples of peptide-based and other subunit vaccines are shown in Table 3.

There is an obvious need for more basic research and clinical trials and especially for long-term studies to demonstrate that reverse vaccinology approaches can yield vaccines that are potentially safer than and at least as efficient as traditional vaccines. With increasing numbers of antibiotic-resistant bacteria, and with old and new viral diseases such as Ebola, Middle East respiratory

Table 3
Selected list of ongoing clinical trials with subunit vaccines

Vaccine	Target	Notes	Stage	Active compound	References
Improvac	Boar taint	Stimulation of the (pig) immune system to produce antibodies that ultimately block and reverse the accumulation of compounds responsible for boar taint	On market (animal use)	Synthetic incomplete analogue of gonadotropin-releasing factor (GnRF) (without hormone activity) linked with carrier protein	[92]
Recombitec WNV	West Nile virus	Combination of existing canarypox vaccine (ALVAC) with genes expressing two proteins from West Nile virus	On market (animal use)	*prM/E* genes	[93]
Vacc-4x	HIV	Synthetic peptides targeting HIV protein p24	Phase III	Peptides with adjuvants	[94]
Vacc-C5	HIV	Synthetic peptides targeting HIV glycoprotein gp120 (C5)	Phase II/III	Peptides with adjuvants	[94]
RECOMBIVAX HB	Hepatitis B virus	Recombinantly produced HBsAg protein in yeast cells	On market	Protein with aluminum adjuvant	[68]
IC43	*Pseudomonas aeruginosa*	Recombinant outer membrane protein-based vaccine	Phase II/III	OprF/OprI hybrid vaccine with N-terminal His tag	[70, 91]
NDV-3	*Candida* sp.	Recombinant vaccine	Phase I/II	Agglutinin-like sequence 3 protein (Als3p) from *Candida albicans* with aluminum hydroxide adjuvant	[95, 96]

(continued)

Table 3
(continued)

Vaccine	Target	Notes	Stage	Active compound	References
SA4Ag	*Staphylococcus aureus*	Recombinant vaccine containing two different capsular polysaccharides and two surface proteins	Phase I/II	Polysaccharides CP5 and CP8; recombinant surface protein clumping factor A (rmClfA) and recombinant manganese transporter protein C (rP305A)	[91, 97]
PreviThrax	*Bacillus anthracis*	Recombinant protective antigen protein	Phase II	Purified recombinant protective antigen protein	[98]
Respiratory syncytial virus (RSV) vaccine	Respiratory syncytial virus (RSV)	F glycoprotein produced recombinantly in insect cells with a recombinant baculovirus	Phase II	Purified recombinant RSV F oligomers	[99]
Cenv3	Hepatitis C	Selected three peptides from two envelope proteins. Each was synthesized in eight multiple antigenic peptides (MAPs)	Phase II	Three envelope peptides derived from two envelope proteins E1 and E2	[91]
NeuroVax	Multiple sclerosis	Vaccine contains three peptides which correspond to potentially pathogenic TCRs on T cells (which are over-expressed in 90 % of multiple sclerosis patients)	Phase II/III	Three TCR peptides in aqueous solution and IFA	[100]
IC41	Hepatitis C	Vaccine contains five peptides derived from hepatitis C virus genotype 1 core. There are four cytotoxic T lymphocyte (CTL) epitopes and three helper epitopes	Phase I/II	Five synthetic peptides with poly-l-arginine as adjuvant	[91, 101]

syndrome (MERS), and others emerging or reemerging, tailored vaccines are promising solutions to the continuous problem of infectious diseases. The great potential of patient-specific vaccines, especially for use in cancer therapy, where traditional approaches cannot be used at all, has barely been tapped.

References

1. Janeway CAJ, Travers P, Walport M et al (2001) Immunobiology. Garland Science, New York
2. Alberts B, Johnson A, Walter P et al (2007) Molecular biology of the cell. Taylor & Francis, New York
3. Neumann J (2008) Immunbiologie. Springer-Lehrbuch, Berlin, Heidelberg
4. Saha B (2001) Encyclopedia of life sciences. Wiley, Chichester, UK
5. WHO UNICEF World Bank (2009) State of the world's vaccines and immunization. World Health Organization, Geneva
6. Flower DR (2009) Bioinformatics for vaccinology. Wiley, Chichester, UK
7. Rinaudo CD, Telford JL, Rappuoli R et al (2009) Vaccinology in the genome era. J Clin Invest 119:2515–2525
8. Seib KL, Zhao X, Rappuoli R (2012) Developing vaccines in the era of genomics: a decade of reverse vaccinology. Clin Microbiol Infect 18:109–116
9. Pizza M, Scarlato V, Masignani V et al (2000) Identification of vaccine candidates against serogroup B meningococcus by whole-genome sequencing. Science 287:1816–1820
10. Medicinal products and human use. Bexsero. Technical report, European Medicines Agency. http://www.ema.europa.eu/docs/en_GB/document_library/EPAR_
11. Tettelin H, Masignani V, Cieslewicz MJ et al (2005) Genome analysis of multiple pathogenic isolates of *Streptococcus agalactiae*: implications for the microbial pan-genome. Proc Natl Acad Sci USA 102:13950–13955
12. Vernikos G, Medini D, Riley DR et al (2014) Ten years of pan-genome analyses. Curr Opin Microbiol 23C:148–154
13. Hiller NL, Janto B, Hogg JS et al (2007) Comparative genomic analyses of seventeen *Streptococcus pneumoniae* strains: insights into the pneumococcal supragenome. J Bacteriol 189:8186–8195
14. Thein M, Sauer G, Paramasivam N et al (2010) Efficient subfractionation of Gram-negative bacteria for proteomics studies. J Proteome Res 9:6135–6147
15. Emanuelsson O, Brunak S, von Heijne G et al (2007) Locating proteins in the cell using TargetP, SignalP and related tools. Nat Protoc 2:953–971
16. Punta M, Forrest LR, Bigelow H et al (2007) Membrane protein prediction methods. Methods 41:460–474
17. Su EC-Y, Chiu H-S, Lo A et al (2007) Protein subcellular localization prediction based on compartment-specific features and structure conservation. BMC Bioinformatics 8:330
18. Yu NY, Wagner JR, Laird MR et al (2010) PSORTb 3.0: improved protein subcellular localization prediction with refined localization subcategories and predictive capabilities for all prokaryotes. Bioinformatics 26:1608–1615
19. Yu C-S, Chen Y-C, Lu C-H et al (2006) Prediction of protein subcellular localization. Proteins 64:643–651
20. Rashid M, Saha S, Raghava GP (2007) Support vector machine-based method for predicting subcellular localization of mycobacterial proteins using evolutionary information and motifs. BMC Bioinformatics 8:337
21. Chou KC, Shen HB (2006) Large-scale predictions of gram-negative bacterial protein subcellular locations. J Proteome Res 5:3420–3428
22. Paramasivam N, Linke D (2011) Clubsub-P: cluster-based subcellular localization prediction for gram-negative bacteria and archaea. Front Microbiol 2:218
23. Dunston CR, Herbert R, Griffiths HR (2015) Improving T cell-induced response to subunit vaccines: opportunities for a proteomic systems approach. J Pharm Pharmacol 67(3):290–9
24. Zhang H, Lund O, Nielsen M (2009) The PickPocket method for predicting binding specificities for receptors based on receptor pocket similarities: application to MHC-peptide binding. Bioinformatics 25:1293–1299
25. Karosiene E, Lundegaard C, Lund O et al (2012) NetMHCcons: a consensus method for the major histocompatibility complex class I predictions. Immunogenetics 64:177–186
26. Wang P, Sidney J, Dow C et al (2008) A systematic assessment of MHC class II peptide binding predictions and evaluation of a consensus approach. PLoS Comput Biol 4, e000048
27. Zhang L, Udaka K, Mamitsuka H et al (2012) Toward more accurate pan-specific MHC-peptide binding prediction: a review of current

methods and tools. Brief Bioinform 13:350–364
28. Bui H-H, Sidney J, Peters B et al (2005) Automated generation and evaluation of specific MHC binding predictive tools: ARB matrix applications. Immunogenetics 57: 304–314
29. Sidney J, Assarsson E, Moore C et al (2008) Quantitative peptide binding motifs for 19 human and mouse MHC class I molecules derived using positional scanning combinatorial peptide libraries. Immunome Res 4:2
30. Nielsen M, Lundegaard C, Worning P et al (2003) Reliable prediction of T-cell epitopes using neural networks with novel sequence representations. Protein Sci 12:1007–1017
31. Peters B, Sette A (2005) Generating quantitative models describing the sequence specificity of biological processes with the stabilized matrix method. BMC Bioinformatics 6:132
32. Kim Y, Sidney J, Pinilla C et al (2009) Derivation of an amino acid similarity matrix for peptide: MHC binding and its application as a Bayesian prior. BMC Bioinformatics 10:394
33. Moutaftsi M, Peters B, Pasquetto V et al (2006) A consensus epitope prediction approach identifies the breadth of murine T(CD8+)-cell responses to vaccinia virus. Nat Biotechnol 24:817–819
34. Nielsen M, Lundegaard C, Blicher T et al (2007) NetMHCpan, a method for quantitative predictions of peptide binding to any HLA-A and -B locus protein of known sequence. PLoS One 2, e796
35. Nielsen M, Lund O (2009) NN-align. An artificial neural network-based alignment algorithm for MHC class II peptide binding prediction. BMC Bioinformatics 10:296
36. Nielsen M, Lundegaard C, Lund O (2007) Prediction of MHC class II binding affinity using SMM-align, a novel stabilization matrix alignment method. BMC Bioinformatics 8:238
37. Nielsen M, Lundegaard C, Blicher T et al (2008) Quantitative predictions of peptide binding to any HLA-DR molecule of known sequence: NetMHCIIpan. PLoS Comp Biol 4, e1000107
38. Sturniolo T, Bono E, Ding J et al (1999) Generation of tissue-specific and promiscuous HLA ligand databases using DNA microarrays and virtual HLA class II matrices. Nat Biotechnol 17:555–561
39. Paul S, Weiskopf D, Angelo MA et al (2013) HLA class I alleles are associated with peptide-binding repertoires of different size, affinity, and immunogenicity. J Immunol 191: 5831–5839
40. Doytchinova IA, Guan P, Flower DR (2004) Identifying human MHC supertypes using bioinformatic methods. J Immunol 172:4314–4323
41. Sidney J, Peters B, Frahm N et al (2008) HLA class I supertypes: a revised and updated classification. BMC Immunol 9:1
42. Doytchinova IA, Flower DR (2005) In silico identification of supertypes for class II MHCs. J Immunol 174:7085–7095
43. Ponomarenko JV, van Regenmortel MHV (2009) B-cell epitope prediction. In: Gu J, Bourne PE (eds) Structural bioinformatics. Wiley-Blackwell, New York
44. Kringelum JV, Lundegaard C, Lund O et al (2012) Reliable B cell epitope predictions: impacts of method development and improved benchmarking. PLoS Comput Biol 8, e1002829
45. Larsen JEP, Lund O, Nielsen M (2006) Improved method for predicting linear B-cell epitopes. Immunome Res 2:2
46. Saha S, Raghava GPS (2006) Prediction of continuous B-cell epitopes in an antigen using recurrent neural network. Proteins 65:40–48
47. Gao J, Faraggi E, Zhou Y et al (2012) BEST: improved prediction of B-cell epitopes from antigen sequences. PLoS One 7, e40104
48. Ponomarenko J, Bui H-H, Li W et al (2008) ElliPro: a new structure-based tool for the prediction of antibody epitopes. BMC Bioinformatics 9:514
49. Kunik V, Ashkenazi S, Ofran Y (2012) Paratome: an online tool for systematic identification of antigen-binding regions in antibodies based on sequence or structure. Nucleic Acids Res 40:W521–W524
50. Moreau V, Fleury C, Piquer D et al (2008) PEPOP: computational design of immunogenic peptides. BMC Bioinformatics 9:71
51. Lin SY, Cheng C, Su EC (2013) Prediction of B-cell epitopes using evolutionary information and propensity scales. BMC Bioinformatics 14:S10
52. Kim Y, Ponomarenko J, Zhu Z et al (2012) Immune epitope database analysis resource. Nucleic Acid Res 40:W525–W530
53. Patronov A, Doytchinova I (2013) T-cell epitope vaccine design by immunoinformatics. Open Biol 3:120139
54. Shimizu H, Thorley B, Paladin FJ et al (2004) Circulation of type 1 vaccine-derived poliovirus in the Philippines in 2001. J Virol 78:13512–13521
55. Moyle PM (2015) Progress in vaccine development. Curr Protoc Microbiol 36:1–17
56. Centers for Disease Control and Prevention (2012) Epidemiology and prevention of vaccine-preventable diseases. Public Health Foundation, Washington DC

57. Plotkin S (2014) History of vaccination. Proc Natl Acad Sci U S A 2014:1–5
58. Moyle PM, Toth I (2013) Modern subunit vaccines: development, components, and research opportunities. ChemMedChem 8:360–376
59. Purcell AW, McCluskey J, Rossjohn J (2007) More than one reason to rethink the use of peptides in vaccine design. Nat Rev Drug Discov 6:404–414
60. Moyle PM, Toth I (2008) Self-adjuvanting lipopeptide vaccines. Curr Med Chem 15:506–516
61. Sato Y, Sato H (1999) Development of acellular pertussis vaccines. Biologicals 27:61–69
62. Michel M-L, Tiollais P (2010) Hepatitis B vaccines: protective efficacy and therapeutic potential. Pathol Biol 58:288–295
63. Cybulski RJ, Sanz P, O'Brien AD (2009) Anthrax vaccination strategies. Mol Aspects Med 30:490–502
64. Chun JH, Hong KJ, Cha SH et al (2012) Complete genome sequence of *Bacillus anthracis* H9401, an isolate from a Korean patient with anthrax. J Bacteriol 194:4116–4117
65. Keitel WA (2006) Recombinant protective antigen 102 (rPA102): profile of a second-generation anthrax vaccine. Expert Rev Vaccines 5:417–430
66. McKee SJ, Bergot A-S, Leggatt GR (2015) Recent progress in vaccination against human papillomavirus-mediated cervical cancer. Rev Med Virol 25:54–71
67. Khallouf H, Grabowska A, Riemer A (2014) Therapeutic vaccine strategies against human papillomavirus. Vaccines 2:422–462
68. Merck. http://www.merck.com
69. Vincent J-L (2014) Vaccine development and passive immunization for *Pseudomonas aeruginosa* in critically ill patients: a clinical update. Future Microbiol 9:457–463
70. Westritschnig K, Hochreiter R, Wallner G et al (2014) A randomized, placebo-controlled phase I study assessing the safety and immunogenicity of a *Pseudomonas aeruginosa* hybrid outer membrane protein OprF/I vaccine (IC43) in healthy volunteers. Hum Vaccin Immunother 10:170–183
71. Skwarczynski M, Toth I (2014) Recent advances in peptide-based subunit nanovaccines. Nanomedicine 9:2657–2669
72. Sharma M, Dixit A (2015) Identification and immunogenic potential of B cell epitopes of outer membrane protein OmpF of Aeromonas hydrophila in translational fusion with a carrier protein. Applied Microbiol Biotechnol 99(15):6277–91
73. Weltzin R, Guy B, Thomas WD et al (2000) Parenteral adjuvant activities of *Escherichia coli* heat-labile toxin and its B subunit for immunization of mice against gastric *Helicobacter pylori* infection. Infect Immun 68:2775–2782
74. Van Regenmortel MHV (1996) Mapping epitope structure and activity: from one-dimensional prediction to four-dimensional description of antigenic specificity. Methods 9:465–472
75. Sette A, Fikes J (2003) Epitope-based vaccines: an update on epitope identification, vaccine design and delivery. Curr Opin Immunol 15:461–470
76. Guichard G, Zerbib A, Gal FA et al (2000) Melanoma peptide MART-1(27-35) analogues with enhanced binding capacity to the human class I histocompatibility molecule HLA-A2 by introduction of a β-amino acid residue: implications for recognition by tumor-infiltrating lymphocytes. J Med Chem 43:3803–3808
77. Reinelt S, Marti M, Dédier S et al (2001) β-amino acid scan of a class I major histocompatibility complex-restricted alloreactive T-cell epitope. J Biol Chem 276: 24525–24530
78. Webb AI, Dunstone MA, Williamson NA et al (2005) T cell determinants incorporating β-amino acid residues are protease resistant and remain immunogenic in vivo. J Immunol 175:3810–3818
79. Brito LA, Malyala P, O'Hagan DT (2013) Vaccine adjuvant formulations: a pharmaceutical perspective. Semin Immunol 25:130–145
80. Pulendran B, Ahmed R (2011) Immunological mechanisms of vaccination. Nat Immunol 12:509–517
81. Berti F, Adamo R (2013) Recent mechanistic insights on glycoconjugate vaccines and future perspectives. ACS Chem Biol 8:1653–1663
82. Plotkin SA (2009) Vaccines: the fourth century. Clin Vaccine Immunol 16:1709–1719
83. Azmi F, Fuaad AAHA, Skwarczynski M et al (2014) Recent progress in adjuvant discovery for peptide-based subunit vaccines. Hum Vaccin Immunother 10:778–796
84. Lua LHL, Connors NK, Sainsbury F et al (2014) Bioengineering virus-like particles as vaccines. Biotechnol Bioeng 111:425–440
85. Wieser A, Magistro G, Nörenberg D et al (2012) First multi-epitope subunit vaccine against extraintestinal pathogenic *Escherichia coli* delivered by a bacterial type-3 secretion system (T3SS). Int J Med Microbiol 302:10–18

86. Bumann D, Hueck C, Aebischer T et al (2000) Recombinant live *Salmonella spp.* for human vaccination against heterologous pathogens. FEMS Immunol Med Microbiol 27:357–364
87. Garmory HS, Leary SEC, Griffin KF et al (2003) The use of live attenuated bacteria as a delivery system for heterologous antigens. J Drug Target 11:471–479
88. Demento SL, Siefert AL, Bandyopadhyay A et al (2011) Pathogen-associated molecular patterns on biomaterials: a paradigm for engineering new vaccines. Trends Biotechnol 29:294–306
89. GAPVAC. http://gapvac.eu/
90. HepaVac. http://www.hepavac.eu/
91. A service of the U.S. National Institutes of Health. https://clinicaltrials.gov/
92. Improvac. http://improvac.com
93. El Garch H, Minke JM, Rehder J et al (2008) A West Nile virus (WNV) recombinant canarypox virus vaccine elicits WNV-specific neutralizing antibodies and cell-mediated immune responses in the horse. Vet Immunol Immunopathol 123:230–239
94. Bionorpharma. http://www.bionorpharma.com
95. NovaDigm Therapeutics. http://www.novadigm.net/
96. Schmidt CS, White CJ, Ibrahim AS et al (2012) NDV-3, a recombinant alum-adjuvanted vaccine for *Candida* and *Staphylococcus aureus*, is safe and immunogenic in healthy adults. Vaccine 30: 7594–7600
97. Anderson AS, Miller A, Donald RGK et al (2012) Development of a multicomponent *Staphylococcus aureus* vaccine designed to counter multiple bacterial virulence factors. Hum Vaccin Immunother 8:1585–1594
98. Emergent Biosolutions. http://emergentbiosolutions.com/
99. Raghunandan R, Lu H, Zhou B et al (2014) An insect cell derived respiratory syncytial virus (RSV) F nanoparticle vaccine induces antigenic site II antibodies and protects against RSV challenge in cotton rats by active and passive immunization. Vaccine 32:6485–6492
100. Immune Response BioPharma, Inc. http://www.immuneresponsebiopharma.com
101. Wedemeyer H, Schuller E, Schlaphoff V et al (2009) Therapeutic vaccine IC41 as late add-on to standard treatment in patients with chronic hepatitis C. Vaccine 27:5142–5151

Chapter 5

Systems Vaccinology: Applications, Trends, and Perspectives

Johannes Sollner

Abstract

The strategies employed in vaccinology have improved since the seminal work of Edward Jenner in the eighteenth century. Stimulated by failure to develop vaccines for cancers and chronic infectious diseases as well as an emergence of a multitude of new technologies not available earlier, vaccinology has moved from a largely experimental art to a new phase of innovation. Currently, immune reactions can be predicted and modeled before they occur and formulations can be optimized in advance for genetic background, age, sex, lifestyle, environmental factors, and microbiome. A multitude of scientific insights and technological advancements have led us to this current status, yet possibly none of the recent developments is individually more promising to achieve these goals than the interdisciplinary science of systems vaccinology. This review summarizes current trends and applications of systems vaccinology, including technically tangible areas of vaccine and immunology research which allow the transformative process into a truly broad understanding of vaccines, thereby effectively modeling interaction of vaccines with health and disease. It is becoming clear that a multitude of factors have to be considered to understand inter-patient variability of vaccine responses including those characterized from the interfaces between the immune system, microbiome, metabolome, and the nervous system.

Key words Systems vaccinology, Systems biology, Vaccine, Metabolism, Prediction, Signature, Microbiome, Metabolome, Immunogenicity, Protectivity

1 Introduction

Systems vaccinology (SV) is a nascent science which has emerged as a variant of s*ystems biology* and aims to understand the effect of vaccines on the entire host system. In contrast to systems biology, SV is therefore heavily application focused, and possibly only in that respect different from the more generally used term *systems immunology*. Like all areas of systems biology, the aim of SV is to overcome reductionist thinking and generate a more comprehensive, dynamic, and in a way more realistic understanding of the interaction of components in an organism, in this specific context of reactions induced by vaccines or factors influencing efficacy of vaccines. While this is not a new concept, viewing the host as a

Sunil Thomas (ed.), *Vaccine Design: Methods and Protocols: Volume 1: Vaccines for Human Diseases*, Methods in Molecular Biology, vol. 1403, DOI 10.1007/978-1-4939-3387-7_5,

system interacting with the environment (also in many cases a set of interacting systems) allows identification of signatures and interactions critical for defining or achieving states critical for success of a therapy, drug, or vaccine. These signatures may not be evident from a reductionist point of view, at least not without complete deconvolution of all possible components. Being embedded in a complex system, understanding host components and their interaction with environment in a single picture is critical for rationally designing drugs including structure-based vaccines. This is particularly important in the case of chronic infections where the system constituting an intruding pathogen establishes a continuous but unfortunately not mutually beneficial relationship with the host system. Understanding host/pathogen interfaces will therefore be another important area within systems vaccinology and may very likely break the boundary to other areas of pharmacology to further expose and target this host/pathogen interface. Chronic infections are typically established by a pathogen by mechanisms which make host defenses at least partially ineffective by remodeling host immunity as well as by immunological stealthiness. Likewise, cancer vaccines (with few exceptions) to date have not been very successful. Understanding the complex interaction of cancers with their environment (including tumor stroma) employing the concept of SV will facilitate effective cancer vaccines. While vaccines have been tremendously successful, the modes of action of a number of commonly used vaccines are not well understood. Infectious diseases, including HIV, malaria, tuberculosis, and dengue fever, have proven to be at least partially resistant to traditional vaccination approaches. Systems vaccinology offers powerful tools to monitor a multitude of data types sampled in parallel through omics technologies to reconstruct a comprehensive picture of processes leading to success or failure of a vaccine or a vaccine prototype. As recently reviewed by Pulendran, Rappuoli, and others, SV therefore primarily offers a deeper understanding of processes leading to or prohibiting protective immunity and establishes a basis for vaccine developers to overcome old limitations [1, 2]. This approach of understanding vaccines will become even more complex as sources of variation between immune responses become more evident and tangible, specifically genetic host diversity, environmental and psychological factors, impacts of the microbiome, and socioeconomic factors including associated disorders such as obesity, diabetes, and those resulting from malnutrition. Systems vaccinology offers a way to gain deeper understanding of the ongoing pathomechanisms by comparing to successful immune responses, thereby leading to the development of new immunization strategies for diseases that do not yet have a commercially successful vaccine. Successful vaccines that induce the immune system can be modeled based on expression signatures or molecular

processes that clear pathogens during an infection. Data from entire populations as well as nonresponders could help in designing vaccines. The type and intensity of immune reactions can among other things be effectively modulated by pattern recognition receptors (PRRs) including Toll-like receptors (TLRs) and nucleotide-binding oligomerization domain (NOD) proteins, which constitute some of the most effective adjuvant targets known. Understanding the immune-evasive mechanisms as well as the latest immunological insights and mechanisms of novel adjuvants will lead to reprogram ineffective to effective immunity.

Some currently pursued and further perceivable applications of systems vaccinology are listed below:

1. Predict immunogenicity and optimal protectivity of vaccines in an individual based on host samples taken before or after vaccination. Applications include stratification of patients for clinical trials, early identification of nonresponders which may allow application of alternative medications, and risk assessment regarding adverse effects.
2. During vaccine research, taking comprehensive immunological snapshots should speed up development, reduce the risk of failures in later clinical trials, and improve understanding of immunity in risk groups including the very young and the elderly. Specific identification of novel formulations and adjuvants, ex vivo (peripheral blood mononuclear cell (PBMC)) optimization of dosage, relative and absolute adjuvant content, and better understanding of the relationship of immunity with metabolism and neuronal system are required.
3. Another goal is to understand the interface of vaccines with complex phenomena like cancer and autoimmunity, including autoantibody levels and antibody subclasses. Understanding the potential of vaccines to modify diseases with inflammatory components such as neoplastic disorders, stroke, and coronary heart diseases may have drastic beneficial effects on public health. This extends to the idea to use self-associated molecular patterns (SAMPs) to reduce inflammation, an option which seems tangible due to insights into the glycobiology of antibodies including anti-inflammatory effects of targeted Fc receptors.

2 Understanding and Prediction of Vaccine Responses

The most frequent application of systems vaccinology to date has been the definition of critical parameters associated with immunogenicity and optimal protectivity of a vaccine. The aim of a number of studies has been to define systems signatures, specifically based

on gene expression analysis, which can be used as surrogates for vaccine efficacy. Application of these signatures would allow:

1. Evaluation and optimization of vaccine candidates including choice of adjuvants or dosage based on observation of signatures in PBMCs in vitro.
2. Early identification of nonresponders after vaccination.

Meanwhile the concept has been extended to include features of the host before vaccination. A number of molecular and other properties have been identified to allow estimation of the vaccine response before treating a subject, which has so far been aimed for two related practical applications:

1. Stratification of patients for clinical trials based on likelihood to react to a vaccine.
2. Early identification of potential nonresponders before vaccination, which would allow selection of different vaccine products, dosage, or administration regimens.

Both the latter options are forms of personalized medicine. A third related option may be the early identification of candidates for adverse side effects including rare conditions such as narcolepsy.

The highly effective yellow fever vaccine, YF-17D, was the first in a study of systems vaccinology where vaccinology and immunology were combined [3–6]. The initial study by Querec et al. succeeded to define and verify early post-vaccination gene expression signatures which predicted YF-17D adaptive immune responses, specifically $CD8^+$ (cytotoxic) T-cell responses with up to 90 % accuracy and the neutralizing antibody response with up to 100 % accuracy depending on evaluation procedure. This notably only requires models involving two to three parameters each. Given the wide use of this vaccine it may also be a good candidate for better understanding and prediction of adverse side effects including rare serious adverse effects [7–9]. Technologically this initial study has been shaping the conceptual approach to systems vaccinology until now. The authors combined FACS characterization of immune cells from patients sampled after vaccination in a time series, along with a multiplex panel of cytokines and gene expression analysis of PBMCs using microarrays. Gene expression data were analyzed for statistically significant changes using analysis of variance (ANOVA) of the entire time series of fold changes. Results were corrected for multiple testing resulting in a set of 65 genes putatively differentially regulated in PBMCs upon vaccination. RT-PCR was used to validate differential expression of a subset of the indicated genes. For biological interpretation of microarray analysis results, differentially regulated genes were then subjected to gene enrichment analysis using DAVID to identify enriched pathways and modules [10]. In addition transcription factor-binding sites statistically

overrepresented in the promoters of these genes were identified using TOUCAN [11]. Obtained immune reactions were characterized by epitope-specific T-cell assays and determining neutralizing antibody titers. Interestingly the 65 differentially regulated genes were not useful (or insufficient) to predict magnitude of $CD8^+$ T-cell responses. For this purpose expression fold changes of individual genes at day 3 and separately at day 7 were individually tested for significant correlation with later $CD8^+$ T-cell response and neutralizing antibody response. In addition to PCA analysis which indicated a segregation of high and low $CD8^+$ responders, average linkage hierarchical clustering analysis was used and confirmed segregation of these two groups, followed by feature selection, model building, cross-validation, and further independent validation.

Based on samples before and after vaccination Nakaya et al. have demonstrated that signatures of protectivity between live (LAIV) and inactivated (TIV) influenza vaccines vary where the authors specifically stress IFN-related genes as differentiating signature upon LAIV administration [12]. Similar to Querec et al. this study aimed to predict vaccine efficacy based on samples taken a few days after vaccination to allow prediction of hemagglutinin-inhibiting (HAI) titers a month later and specifically to allow identification of vaccine nonresponders as early a possible. While this study technologically also focused on gene expression analysis (microarrays and RT-PCR) and FACS they individually determined gene expression for PBMC subsets separated by FACS. This approach is highly reflective of the functionally differentiated nature of PBMCs and can lead to the identification of marker signatures otherwise invisible in bulk analysis due to expression primarily in critical but low-abundance subpopulations, demonstrated here by plasmacytoid dendritic cells (pDC). More cost- and logistically affordable analysis methods also capable of differentiating cell types have been proposed, specifically a meta-analysis procedure by Nakaya et al. and also statistical deconvolution using cell type-specific significance analysis of microarrays (CSSAM) [13]. In the case of Nakaya et al. meta-analysis suggested a TIV-specific pattern of highly expressed genes in antibody-secreting cells (ASCs), whereas cell types implicated in LAIV analysis were specifically T-cells and monocytes. These results show the importance of different cell types during analysis and how they modulate protective mechanisms during vaccination. A similar study of TIV without differentiating cell types was conducted by Bucasas et al. and also indicated a distinct gene expression signature comprising 494 genes segregating high and low vaccine responders [14]. Likewise, in a study conducted by Vahey et al. for prediction of protectivity of a malaria vaccine, the immunoproteasome and apoptosis were indicated as marker processes, depending on time after vaccination [15].

Furman et al. have strived to define markers of immunological health, where their idea was to use the intensity of immune reactions against an influenza vaccine as a measure of health [16, 17]. Notably, they identified nine features available before vaccination which predicted vaccine response with 84 % accuracy, plus a number of other parameters which also were individually predictive to some degree but did not further improve the model. Overall analyzed data included patient age, whole-blood gene expression profiles, peptide-specific anti-influenza antibody titer measured by peptide microarrays, 50 cytokines and chemokines, and typing to a resolution of 15 immune cell subtypes using FACS. The authors found that taken alone, age is the most informative predictor of HAI titers, where increased age correlated to reduced titers. As previously published by others, pre-existing HAI titers (for example stemming from previous vaccination or natural infection) are negatively associated with influenza vaccine-generated HAI titers, reportedly resulting from limited dendritic cell (DC) antigen presentation caused by pre-existing memory T-cells via natural killer (NK) cells. Furman et al. were able to specify a number of peptides which are predictive of this effect before vaccination and those that provide independent information to predict vaccine efficacy. In addition, whole-blood gene expression analysis followed by analysis of gene modules proposed a number of gene sets where expression was negatively correlated with post-vaccination HAI titers, and one associated with apoptosis which was positively correlated. The identification of apoptosis as critical parameter is reminiscent of the results described by Vahey et al. in malaria. The relevant information for predicting vaccine response was also present in levels of soluble Fas ligand (sFasL) and IL-12p40, and frequency of central memory $CD4^+$ and effector memory $CD8^+$ T-cells. From a number of perspectives also the setup of this study can be seen as exemplary for the identification of predictive models of vaccine efficacy, predominantly because of the number of omics techniques applied. Furman et al. observed (epitope specific) antibody titers based on peptide arrays, gene expression analysis of blood cells, and FACS-based immune cell subtyping. Independently, Tsang et al. have compared pre- and post-vaccination PBMCs using FACS and could show that pre-vaccination cell population frequencies alone are predictive of antibody response for TIV [18]. FACS-based discrimination of immune cell types followed by microarray analysis and cytokine panels has led to identification of $PD\text{-}1^+CXCR5^+$ $CD4^+$ T-cell numbers as indicators of emergence of broadly HIV-neutralizing antibodies. This population is similar to $CD4^+$ T follicular helper (Tfh) cells critical for B-cell maturation in germinal centers (GC), indicating the potential to characterize immune systems by available cell repertoire and opening strategies to stimulate specific populations for vaccine effect [19].

At least one of the possible ways to define effective vaccines is to learn from immune responses to natural infections where the pathogens are effectively cleared. Based on the data the correlate of protection may be identified, optimally reducing the need for challenge studies. At least in a mouse model of influenza, the peptide arraybased immuno-signatures have been identified in natural infection which allows differentiation of protective and non-protective vaccine immune responses by pattern [20]. For this chip "long, pseudorandom, nonnatural" peptides are used which may, at least theoretically, also allow identification of antibodies binding posttranslational modifications (including glycosylations) through peptide molecular mimicry. This may be an interesting template in diseases where effective vaccines exist or natural immunity is protective to serve as a template. Another important factor in predicting vaccine responses accessible to systems technologies includes SNP chips and next-generation sequencing of the host genetic background. Although this factor is very difficult to differentiate from environmental factors such as the microbiome, previous studies in twins and families have suggested heritability in vaccine responses to range between 39 and 90 % depending on vaccine and degree of hereditary relationship [21–28]. Interestingly, antibody levels against a multitude of common pathogens seem to be heritable. Similarly, in autoimmune disorders genetic background along with environment plays a crucial role in establishing specific immune phenotypes [29]. It is therefore reasonable to include high-throughput screening for host genetic markers into systems vaccinology procedures for prediction of vaccine efficacy or possibly adaptation of dosage. An approach based on SNP and microarray gene expression analysis for identification of genetic markers impacting vaccine response has been implemented by Franco et al. suggesting 20 genes that show evidence of significant genotype expression association related to TIV [30].

However while proteomics, metabolomics, and glycomics might contribute beneficially to the development of more robust or less resource-intensive models, the published studies show a critical requirement of systems vaccinology (and systems biology): a large number of high-quality samples, optimally leading to significantly more samples than measured parameters (which is admittedly unlikely), or possibly integrated parameters as seen in gene sets versus individual gene expression values. In vaccines where T-cell responses play a critical role, dimensionality can be reasonably further increased by ELISPOT or comparable T-cell epitope-specific data equivalent to humoral peptide array assays. While powerful feature selection procedures exist, the factor of dimensionality needs to be considered and robustness of models can be enhanced with larger numbers of samples, specifically if biologically alternative possibilities for achieving complex immune phenotypes

such as protectivity exist. Typically numerous feature selection methods will be compared, where some like DAMIP, ClaNC, or elastic nets have proven specifically useful for high-dimensional biological data [31–34].

While the initial hope of SV has been to identify general profiles (signatures) indicative of protectivity, signatures identified so far are predictive of immune responses for a specific vaccine or vaccine type sharing a mode of action (or adjuvanting), allowing to predict success or insufficient protection in individuals [35, 36]. It can also be expected that a tighter integration of vaccinology and immunology will lead to a feedback with related disciplines, specifically research into autoimmunity where delineation of cofactors for development of immune phenotypes including gender, hormone status, or infections has a long history [37].

3 Vaccines and the Role of Pre-existing Immunity

Immune systems are typically not neutral as they have previously encountered foreign agents and have built tolerance to self-components. Furman et al. and others have shown that pre-existing titers against influenza hemagglutinin reduce effectiveness of the trivalent inactivated seasonal influenza vaccine (TIV) in terms of total HA-neutralizing (HAI) titer achieved [38, 39]. This effect does not seem to exist for an influenza live vaccine (LAIV) [40].

Current evidence suggests possible detrimental role of low-affinity antibodies stemming from previous infections with related pathogens as demonstrated in *Dengue* virus infection. Infection by a single serotype is in most cases harmless, or comparable to infection as in common cold. However, infection by three or four serotypes frequently leads to a hemorrhagic syndrome, inducing cross-reactive T-cells and (low-affinity) antibody-mediated enhancement (ADE) [41–43].

An example where pre-existing immunity against the vaccine vector increases pathogen acquisition rates is Merck's MRKAd5/HIV which is highly immunogenic but non-efficacious. This *HIV-1* vaccine uses an inactivated adenovirus serotype 5 (Ad5) vaccine vector and seems to induce high *HIV-1* infection rates in Ad5 seropositive individuals [44]. While reason behind this effect has been suggested to be at least in part antibody-mediated uptake leading to increased dendritic cell activation, recent systems analysis by Zak et al. suggests that pre-existing Ad5-neutralizing antibodies effectively reduce dose of vaccine and hence immunogenicity [45, 46].

It is also well established that stimulating the immune system in a way as to promote an immune arm unsuitable for pathogen clearance can be an immuno-evasive strategy for pathogens, exemplarily demonstrated by the Th1 versus Th2 immune signatures seen in leprosy and the role of IL-10 in *Epstein-Barr virus*

(*EBV*) infection [47, 48]. The induced state of the immune system and degree of cross-reactivity of the adaptive immune system can be expected to severely shape efficacy and precise nature the host responds to secondary natural infections and also to vaccines [49–52]. Better understanding of the precise interaction of superinfections and interaction of complex immune phenotypes with vaccines may contribute substantially to prediction of inter-patient variability in vaccine responses. This calls for advances in immunology, molecular biology, and systems vaccinology.

4 Microbiota, Chronic Infections, and Vaccines

While the extent of interaction can be expected to go substantially beyond current knowledge, analysis has shown that gut microbiota are critical for achieving potent immunity using inactivated influenza vaccines. Toll-like receptor 5 (TLR5)-mediated pathway is critical for vaccine efficacy where gut microbiota provide stimuli for development of plasma cells ultimately impacting antibody production, while live vaccines and adjuvanted vaccines may not share this dependency. Similarly, the importance of intestinal flora composition has been demonstrated for TLR7-stimulated development of inflammasomes in respiratory mucosa, where lack of TLR7 ligands leads to impaired immune responses to influenza [53, 54]. Likewise, it has recently been shown that pathogen-free mice are more sensitive to influenza challenge than other mice and that inflammation can be dampened via colonization with *Streptococcus aureus* in a TLR2-dependent way [55]. However, respiratory influenza infection can lead to gastroenteritis-like symptoms not via direct infection of gut epithelia, but rather due to a shift in gut microbiota leading to increase in Th17 cells in the small intestine and also enhanced IL15/IL17A production, an effect abolished by antibiotics [56]. Possibly adding some detail to this observation, Weber et al. conclude that IL17-producing thymocytes form a "first line of recognition" stimulated by cell wall components of diverse pathogenic and apathogenic bacteria, but that effector molecules such as IL-6 and IFN-γ determine transition to a pathological inflammation [57]. It has also been demonstrated that microbiota depletion impairs early innate immunity against the pathogen *Klebsiella pneumoniae* and that this state can be remedied by providing NOD-like (NLR) receptor ligands but not Toll-like receptor (TLR) ligands from the gastrointestinal tract, whereas NLR ligands from the upper respiratory tract were ineffective [58]. This highlights the systemic impact of local microbiota on immune responses and suggests a critical importance of microbiota derived pattern recognition receptor (PRR) ligands for establishing effective immunity. In summary it can be stated that current evidence shows heavy dependency of microbiota and

microbiota composition on activity of the immune system and efficacy of at least some of the vaccines. Bacteria are not the only microorganisms modulating the immune system; the virome can support intestinal homeostasis comparable to bacterial commensals, presumably by providing equivalent stimuli [59, 60]. Similarly, fungal diversity and species composition may prove to be a critical extension also in other areas than chronic inflammatory disorders of the gut [61]. The terrible and disfiguring childhood disease Noma (cancrum oris) is currently thought to be caused by malnutrition and microflora dysbiosis [62]. There is also clear evidence that the choice of food impacts microbiome development and ultimately immune competence [63]. The interplay of human nutrition, gut microbiome, immune system development and competence, dysfunction, and vaccine efficacy is the focus of ongoing research and is now viewed as a very likely critical dimension of immunology and hence possibly also vaccinology [63–69]. The impact of microbiota and microbial diversity on vaccine efficacy in infants has recently been investigated in a small cohort by Huda et al. where they suggest probiotics for minimizing dysbiosis [70]. Of note in this context, while microbiota have emerged as an important immunological dimension, metagenomics has emerged as a powerful tool for analysis of the microbial community in an organism. Metagenomics could be used to identify and quantitate the gut microbiota of the fecal samples. Several other body (especially mucosal) surfaces are commonly covered by microbial communities; within the gastrointestinal system several distinct regions exist which contain microbiota of typically different composition. Moreover, the gel layer and luminal communities of gut microbiota have been shown to feature different population composition [71]. Finding ways to routinely access these spatial dimensions in health and disease may open yet another possible critical aspect for integration into the growing number of systems components regarding immunity and also vaccine effects. The gut glycome is another uninvestigated area presumably providing substantial immunologically relevant mass to the human body.

The distinction between a commensal and a pathogen can be difficult to draw, depending on the potential to be involved in disease. Examples of organism with potential impact on vaccinology are immune-distorting bacteria like Mycoplasma species which can cause diverse diseases in animals and humans [72] but are also non-obvious (and often unidentified) microbes of the natural microbiome [72, 73]. As multiple roles have been suggested for the human pathogen *M. pneumoniae* this may either mean a substantial underappreciation of other causes of atypical pneumonia or otherwise of other factors contributing to the conversion from an asymptomatic infection to a severe disease. Mycoplasma species are also frequently associated with autoimmune diseases [74]. The mechanism by which Mycoplasmas modulate the immune system are not clear,

and part of the reason is that these pathogens may contribute to a pro-inflammatory or otherwise immunologically biased environment rather than being clear-cut pathogens in the sense of Koch's postulates. At least in chicken severe exacerbation of otherwise asymptomatic (avian) influenza infection with *M. gallisepticum*, a Mycoplasma phylogenetically close to *M. pneumoniae*, has been documented [75]. Several known interactions exist where these can lead to nonadditive exacerbation of other infections through intensified inflammatory responses. At least in Ureaplasma species the term pseudospecies has been used, as different isolates may vary greatly in their content of pathogenicity factors. In fact, from both a general health and a vaccine perspective it may be equally critical to consider the immuno-modulatory pathogenicity mechanisms available within a person's microbiome along with specific bacterial species, as their combined effect may be very distinct or at least nonadditively amplified from individual factor contributions [76].

Another example of frequently observed chronic pathogen includes the highly prevalent immune distorting viruses of genus lymphocryptovirus comprising *Epstein-Barr virus* (*EBV*) and *Cytomegalovirus* (*CMV*); these cause lifelong infections, and *EBV* is known for its B-cell tropism. Both viruses can establish regulatory complex periods of latency. The effect of *EBV* and *CMV* infection versus age on immunity has recently been studied by Wang et al. where they differentiated age-dependent and -independent effects [77]. Specifically, decreased diversity of antibody repertoires with accumulation of memory B-cells and lower naive B-cell populations was associated with reduced vaccine efficacy in the elderly. They report that immune-globulin heavy chain (IGHV) mutation frequency increases upon infection with *CMV*, but not *EBV*. *CMV* infection tends to increase the proportion of highly mutated IgG and IgM regions, but not IgA or IgD. The effect of *CMV* on mutation rate is stronger with age, where the effect may stem from the proportion of *CMV*-specific clones. Age and *EBV* infection correlated with persistent clonal expansion, where very few clonal lineages (possibly derived from a single ancestor) tend to be overrepresented. In the study these expanded clones may be cases of monoclonal B-cell lymphocytosis (MBL), a lymphoproliferative disorder with some characteristics of CLL typically seen in the elderly.

The inflammatory status including degree of immune system activation can have significant impact on vaccine efficacy. Recently it was shown in a YF-17D (yellow fever vaccine) trial comparing vaccination efficacy of 50 volunteers in Lausanne (Switzerland) versus the same number in Entebbe (Uganda) that the latter produced less effective humoral and $CD8^+$ responses. The authors negatively correlated the pre-existing activation level of $CD8^+$ T-cells and B-cells as well as pro-inflammatory monocytes at the time of vaccination with this reduced response [78]. Admittedly it

would also be interesting to know the cause of this inflammation, as the specific reason may affect the impact on vaccines. On the other hand the impact of pre-existing low-grade inflammatory conditions on vaccines is a recurring theme in the current review. In this context it is evident that determining protectivity profiles for vaccines is only one side of the coin. The other one is that the status of the vaccine recipient regarding inflammatory diseases, nutrition, and pre-existing immunity needs to be considered to understand inter-patient variability. Unfortunately the complex interaction of multiple clinical and subclinical infections is poorly understood. In the context of vaccines, inflammation and potential impact of chronically infecting pathogens and pathogen interactions need to be addressed.

5 Vaccines, Metabolism, Hormones, and the Nervous System

The interplay between metabolism and immune and nervous system is extensive and well beyond the scope of this review. However it is certainly beneficial to highlight some key concepts and current understanding regarding cross talk to show potential ramifications this may have on vaccine design. My aim here is to show factors similar to the preconditioning of chronically infecting pathogens impacting on the immunological environment within which a vaccine has to operate and which could be measured by a systems vaccinology approach. Indeed the relationship of inflammation and metabolic disorders has been extensively reviewed and is known to be very prominent [79]. Specifically the link and overlap between nutrient and pathogen-sensing mechanisms have been implicated in the development of inflammatory disorders. The biological rationale has been speculated to rest on the beneficial effect to coordinate short-time energy requirements during immune response with energy storage and metabolism, but the system has not evolved to deal with continuous nutrient surplus. Among others obesity, type 2 diabetes, cardiovascular disease, and certain neurologic disorders such as dementia and major depression have key low-grade (chronic) inflammatory components where this form of inflammation is distinct from acute inflammation involving swelling and pain. Low-grade inflammation is similar to classical inflammation on a molecular level, triggered by nutrients and metabolic surplus. It also turns out that immune components and metabolic organs may have evolved from the same source, as suggested by the fruit fly fat body which coordinates metabolic and pathogen-associated survival responses. Part of this link still seems to exist on pathway and physiological level. Examples are the lipopolysaccharide (LPS) receptor Toll-like receptor 4 (TLR4) which has been demonstrated to be directly activated by fatty acids and GCN2 which links dendritic cell autophagy and $CD8^+$ cell antigen

presentation (innate and adaptive immunity) to amino acid starvation [80]. TLR4 polymorphisms also have been linked to likelihood of developing type II diabetes in the Chinese population [81]. GCN2 was identified by Querec et al. within a systems vaccinology analysis as a factor frequently contained in YF-17D vaccine response efficacy determinants. Several immune receptors, including TLR4, TLR2, and NOD1, have been shown to play a role in adipocyte inflammation [82]. TNF-alpha and other pro-inflammatory cytokines are over-expressed in adipose tissue and can lead to insulin resistance [83]. In fact adipocytes share a number of similarities with lymphocytes including pathogen-sensing capabilities. Also, lipids are well known for their capacity to regulate metabolism and adaptive and innate immunity, at least partially through peroxisome-proliferator-activated receptor (PPAR) and liver X receptor (LXR) family transcription factors, repressing expression of inflammatory mediators [79]. Interestingly drugs acting through PPARγ like thiazolidinediones are potent insulin sensitizers, but inhibit TLR-mediated activation of dendritic cells [84, 85]. It has been shown that catecholamines and adipokines influence immunity, metabolism, and the central nervous system [86]. Catecholamines including dopamine, noradrenaline, and adrenaline are generated by a number of cell types and can mediate a multitude of neural, metabolic, and pro- and anti-inflammatory effects. Adipose tissues as key endocrine organs secrete adipokines and hormones which serve a number of functions, including being both pro- and anti-inflammatory immune mediators with possibly a role in neuroinflammation [87–89]. Adipocytes can be found in a number of tissues and depending on location they can have different secretory profiles of important factors including adipsin (factor D), TNF-alpha, IL-6, apelin, chemerin, resistin, MCP-1, PAI-1, RBP4, ghrelin, and visfatin. Obesity is also a well-studied factor for prediction of vaccine response. While presence of local or systemic low-grade inflammatory markers may be more informative than obesity itself it has been shown to enhance susceptibility to infections and reduce immune competence and vaccine efficacy [90–96]. Recent murine studies also suggest a specific role of B-cells and autoantibodies in obesity-related pathology [97]. Type II diabetes is now understood to contain a significant inflammatory component and has been associated with reduced efficacy of hepatitis B vaccination in China [98–101]. Another study in this context suggests that although vaccine titers are reduced this is not necessarily associated with reduced protectivity, indicating that type II diabetes alone may not significantly reduce vaccine-provided protection, at least not in children [102].

Some of the factors that may influence the immune system during vaccination include age and degree of obesity. Among the other factors known to influence the immune system and vaccine response, hormones and specifically the group of progestogens,

hormone balance, and vitamins A and D are of particular relevance [103–105]. Hormones are considered to be the driver of immune differences between males and females, typically leading to weaker infection-related immune reactions in males and higher incidence of autoimmunity in females; intrinsically these observations are age dependent [106, 107]. Given current evidence, monitoring of hormone status should be a reasonable area for observation of future systems vaccinology studies and complements current procedures of monitoring serum proteins and other metabolites. Jensen et al. reviewed correlation of administered vaccines and vitamin A supplementation (VAS) including number of administrations. The data showed a significant sex-dependent difference (positive or negative) on mortality in monitored infants and VAS effect also depended on the location where it was administered (possibly because of ethnicities and associated genetic factors). Primarily, vitamin A supplementation is actively discussed as it is a WHO recommendation, and there is a differential effect on VAS-related vaccine responses between boys and girls [108, 109]. Independently it has also been reported that malnutrition overall has little effect on vaccine responses, suggesting that VAS administration at young age should be handled with care and sex dependency has to be further considered [110]. While oral but not parenteral vaccines are observed to be less effective in the developing world, the true impact of malnutrition, environmental enteropathy (EE), breast feeding, and coinfections is currently not well defined but a matter of ongoing clinical studies [111–116]. A currently proposed model is that altered condition of gut mucosa, microbiome, and metabolome negatively affects vaccine efficacy.

Protein CAMK4 (CaMKIV) may be part of the link between adaptive immunity, vaccines, and the nervous system. Fold change at day 3 post-vaccination with TIV is negatively correlated with antibody titers at day 28 via reduction of plasmablast expansion, and it is a well-known factor in T-cells and neuronal memory consolidation [12, 117]. The autonomous nervous system and the immune system cross-talk via the neuro-immune axis, misregulation of which is implicated in hypertension and cardiovascular disease [118]. Part of this regulation is that the brain can sense inflammatory cytokines and can modulate immune responses. The neurotransmitter acetylcholine can significantly attenuate the release of pro-inflammatory cytokines [119]. The gut as an organ of both central immunological and metabolic function is also a critical link to the microbiome and the gut-brain axis is implicated in the development of autoimmune and neurodevelopmental disorders [120]. In mice it has also been shown that defects in TLR5 lead to an altered microbiome and so-called metabolic syndrome (MeS) and transplantation of this altered microbiome to wild-type mice also confer features of MeS [121]. It is also becoming clear that there is a significant feedback between the endocrine system

and the microbiome, impacting on metabolism and immunity [122]. To further stress the role of the gut and signaling molecules aside of proteins in immune homeostasis, the role of bile acids as metabolic regulators with a part in inflammatory disorders and relationship to the gut microbiome has recently been reviewed [123]. In fact there is substantial evidence that psychological distress can predict gastrointestinal disorders and vice versa; animal studies suggest the role of early life conditioning in later health and disease. In this context it is important to better understand potential effects early life vaccination plans may have on shaping microbiota and hence this may lead to improved timing of vaccination schedules [124]. Major depressive disorders have been associated with the so-called metabolic syndrome and low-grade inflammation in the central nervous system including a role of adipokines leptin and ghrelin [125, 126]. The link between immunity and the nervous system is also of relevance because of the recurring assertions of vaccines contributing to certain neurological conditions. However, recently stronger vaccine responses against meningococcal conjugate vaccine in children with symptoms of depression and anxiety have been reported [127]. At this point it may be speculated whether the reported pro-inflammatory signature of carbohydrate-containing vaccines (MedImmune, Menactra) may be enhanced by a pre-existing low-grade inflammatory condition and which effect this would have on vaccines requiring different signatures such as TIV [2]. Another recent development is the potential recognition of narcolepsy as an autoimmune disorder. Narcolepsy has recently been associated with infectious diseases and specifically the 2009 *H1N1* (swine flu) pandemic and associated vaccine. This link does not seem to be definite, however, and may depend on genetic and ethnical background including the HLA-DQB1*06:02 genotype, additional unknown cofactors, and possibly vaccine formulation [128–131].

Taken together, metabolism and nervous and immune system are tightly interacting units. In fact, differentiating them may be more the result of an artificial concept than of a biological reality. Considering the known role of some hormones and metabolic disorders on vaccine efficacy this suggests that input from beyond classical immune cells may significantly contribute to the design of future systems vaccinology studies. Sampled tissues and data types will have to reflect the system a vaccine has to operate on. Specifically metabolomics, proteomics, and lipidomics should be valuable additions to currently pursued procedures in systems vaccinology. Yet it is currently unclear whether systemic determinants such as accessible in the blood-serum metabolome and lipidome may be sufficient to predict implications on vaccine responses, or whether local distribution is critical and well predicted by systemic concentration.

6 Glycans and Immunity

Recently the role of glycans in the immune system has been reviewed by Maverakis and colleagues, pointing out the various critical implications the glycocalyx of eukaryotic cells as well as glycosylations of serum proteins including antibodies have on modulating immunity [132]. While few data are available, analyzed in relationship to vaccines the implications for immunity have become clear, signaling the need to include the glycome in future systems vaccinology analysis. Indeed the glycome is heavily underrepresented in the majority of current systems biology investigations, which is arguably caused by experimental complexity. Yet current evidence shows that it is of critical importance in modulation of immunity and may provide numerous markers of use in understanding current and future reaction of individuals to vaccines. Also it should be considered that each antigen may be target of numerous antibodies where each may potentially be differently glycosylated, potentially grossly altering the effect from pro- to anti-inflammatory or vice versa. High-dose intravenous immunoglobulin (IVIg) therapy is used to treat autoimmune disorders and transplant rejection where the effect is assumed to rest on anti-inflammatory antibodies, or specifically IgG with preference of anti-inflammatory Fc receptors [133]. The generation of anti-inflammatory glycosylation of IgG (specifically with terminal sialic acid) in tolerogenic therapies has recently been demonstrated to rest on antibody development in a non-inflammatory environment, suggesting the use of systems vaccinology for the deeper understanding of involved mechanisms and development of potentially supportive anti-inflammatory adjuvants [134]. Although the entire glycome can be analyzed using mass spectrometric approaches and great technical advances have recently been made using lectin microarrays and capillary electrophoresis, analysis of position-specific glycosylations is hindered by the non-template-based nature of glycosylations, as Maverakis et al. point out [135, 136]. Now we are in the unsatisfying situation to know there is a critical component to understanding immunity, but essentially lack tools equivalent in ease of use to other omics technologies. Optimal resolution of antibody class, isotype, and relative abundance of these should be part of any comprehensive analysis of antibody-mediated immune reactions. High titers do not necessarily mean desired effect if Fc regions of generated antibodies do not activate the intended lectins and/or Fc receptors [137, 138]. It is known that immunoglobulin Fc regions can take on hundreds of different structures with slightly or gravely different effects on targeted cell types and hence achieved effect in cancer, autoimmunity, and infectious diseases. Profiling of adjuvants should therefore consider the precise nature of produced antibodies, as biomedical effects can be

diverse and at least theoretically inverse to the intended. Changes in immunoglobulin glycosylation have been described for numerous autoimmune disorders and infectious diseases [139–141]. While there has to the author's knowledge been no definite proof that these changes are causative of disease they reflect changes in the immune system pinpointing towards biomarkers and very possibly at least contribute to development of an unbalanced immune phenotype. This assumption is based on the well-established dependence of immunoglobulin affinity to Fc receptors based on subclass and Fc glycosylation pattern as well as glycosylation of the receptor and resulting modification of antibody effect on various immune cell types [142, 143]. At least in humans pro- and anti-inflammatory effect of Fc gammaRII receptor isoforms (FcγRIIa and FcγRIIb, respectively) is well established [137]. In addition these receptors are differently responsive to single antibodies, where the majority is only responsive to immune complexes [132]. The overall effect of a particular antibody should therefore depend on affinity to Fc receptors (particularly pro- and anti-inflammatory) and relative abundance of these Fc receptors on specific target cells. Therefore unless an antibody interacts solely with FcγRIIb it may still also elicit pro-inflammatory signals.

In the case of the human pathogen dengue virus where antibody-dependent enhancement (ADE) is currently understood as a major driver of pathology, the role of FcγRIIA may primarily be enrichment of virus/antibody complexes on the cell surface [42]. However the second receptor variant FcγRIIb (that stimulates an anti-inflammatory effect) has been suggested to provide only limited ADE effect in spite of equivalent antibody Fc affinity, implicating that subtype of generated antibodies in dengue natural infection and likely also dengue vaccines may critically impact pathology and efficacy of the vaccines [144].

7 Conclusions

The last two decades have brought tremendous advancements in omics technology. Next-generation sequencing (NGS) but also microarray-based transcriptomics and peptide chips, proteomics, lipidomics, and glycomics have either been invented or significantly matured. Since the emergence of these technologies resulted in tremendous data volumes which need to be stored, analyzed, and brought into context the new science of system biology has emerged. The basic idea is to avoid reductionist approaches and view the entire investigated system and all measurable components in parallel to effectively observe system perturbations and cross talk. At the same time these advances have made immunology leap ahead, now allowing seeing many processes of health and disease in

the context of immunity. In many ways related arts and in this context especially vaccine development have sought to close the gap between basic research and application. While this is not always easy we now see the emergence of another fusion of sciences: systems vaccinology. Combining the methodologies of systems biology with the tools for interpretation stemming from modern immunology and focusing specifically at the improved understanding and development of vaccines this science has the potential to be a game changer for vaccine development. Many areas which have so far suffered from the immense complexity, interdependence and dynamic interplay of gene expression, interacting cell and tissue types, secretomes, metabolome, lipidome, genetic background, and immunological history present in immune systems are now offered an integrative approach to understand success and failure of vaccines and parameters to predict these early on. As such systems vaccinology has the intention to enhance understanding of vaccines, improve development processes of new vaccines, and possibly support clinical trials and personalized medicine. Specifically early identification of nonresponders and patient stratification in clinical trials may reduce the risk of future late-stage vaccine failures or should at least allow understanding of the reasons for failure. Also in already licensed vaccines systems vaccinology will allow deeper insights into determinants of efficacy including metabolic disorders especially those related to obesity, microbiome, and malnutrition. Ultimately it is a highly integrative development which will attempt to include as many views and technological options as possible, crossing barriers between disciplines. In fact modern immunology is already doing that, specifically when linking low-grade inflammation to metabolism and immune competence. This new understanding of disorders such as cardiovascular disease, type II diabetes and gastrointestinal dysfunction and their relationship with the microbiome is a major highlight of modern immunology. Therefore systems vaccinology only has to follow suit to bring modern vaccinology into a new era by integrating the impact of genes, environment, and the microbiome on protective immunity induced by vaccination.

References

1. Rappuoli R, Aderem A (2011) A 2020 vision for vaccines against HIV, tuberculosis and malaria. Nature 473:463–469
2. Pulendran B (2014) Systems vaccinology: probing humanity's diverse immune systems with vaccines. Proc Natl Acad Sci U S A 111:12300–12306
3. Querec TD, Akondy RS, Lee EK et al (2009) Systems biology approach predicts immunogenicity of the yellow fever vaccine in humans. Nat Immunol 10:116–125
4. Pulendran B (2009) Learning immunology from the yellow fever vaccine: innate immunity to systems vaccinology. Nat Rev Immunol 9:741–747
5. Pulendran B, Ahmed R (2011) Immunological mechanisms of vaccination. Nat Immunol 12:509–517
6. Pulendran B, Oh JZ, Nakaya HI et al (2013) Immunity to viruses: learning from successful human vaccines. Immunol Rev 255: |243–255

7. Barrett ADT, Teuwen DE (2009) Yellow fever vaccine - how does it work and why do rare cases of serious adverse events take place? Curr Opin Immunol 21:308–313
8. Biscayart C, Carrega MEP, Sagradini S et al (2014) Yellow fever vaccine-associated adverse events following extensive immunization in Argentina. Vaccine 32:1266–1272
9. Monath TP, Cetron MS, McCarthy K et al (2005) Yellow fever 17D vaccine safety and immunogenicity in the elderly. Hum Vaccin 1:207–214
10. Huang DW, Sherman BT, Tan Q et al (2007) DAVID bioinformatics resources: expanded annotation database and novel algorithms to better extract biology from large gene lists. Nucleic Acids Res 35:W169–W175
11. Aerts S, Thijs G, Coessens B et al (2003) Toucan: deciphering the cis-regulatory logic of coregulated genes. Nucleic Acids Res 31:1753–1764
12. Nakaya HI, Wrammert J, Lee EK et al (2011) Systems biology of vaccination for seasonal influenza in humans. Nat Immunol 12:786–795
13. Shen-Orr SS, Tibshirani R, Khatri P et al (2010) Cell type-specific gene expression differences in complex tissues. Nat Methods 7:287–289
14. Bucasas KL, Franco LM, Shaw CA et al (2011) Early patterns of gene expression correlate with the humoral immune response to influenza vaccination in humans. J Infect Dis 203:921–929
15. Vahey MT, Wang Z, Kester KE et al (2010) Expression of genes associated with immunoproteasome processing of major histocompatibility complex peptides is indicative of protection with adjuvanted RTS, S malaria vaccine. J Infect Dis 201:580–589
16. Furman D, Jojic V, Kidd B et al (2013) Apoptosis and other immune biomarkers predict influenza vaccine responsiveness. Mol Syst Biol 9:659
17. Furman D, Jojic V, Kidd B et al (2014) Apoptosis and other immune biomarkers predict influenza vaccine responsiveness. Mol Syst Biol 10:750
18. Tsang JS, Schwartzberg PL, Kotliarov Y et al (2014) Global analyses of human immune variation reveal baseline predictors of postvaccination responses. Cell 157:499–513
19. Locci M, Havenar-Daughton C, Landais E et al (2013) Human circulating PD-1+CXCR3-CXCR5+ memory Tfh cells are highly functional and correlate with broadly neutralizing HIV antibody responses. Immunity 39:758–769
20. Legutki JB, Johnston SA (2013) Immunosignatures can predict vaccine efficacy. Proc Natl Acad Sci USA 110:18614–18619
21. Tan PL, Jacobson RM, Poland GA et al (2001) Twin studies of immunogenicity – determining the genetic contribution to vaccine failure. Vaccine 19:2434–2439
22. Klein NP, Fireman B, Enright A et al (2007) A role for genetics in the immune response to the varicella vaccine. Pediatr Infect Dis J 26:300–305
23. Rubicz R, Leach CT, Kraig E et al (2011) Genetic factors influence serological measures of common infections. Hum Hered 72:133–141
24. Newport MJ, Goetghebuer T, Weiss HA et al (2004) Genetic regulation of immune responses to vaccines in early life. Genes Immun 5:122–129
25. Höhler T, Reuss E, Evers N et al (2002) Differential genetic determination of immune responsiveness to hepatitis B surface antigen and to hepatitis A virus: a vaccination study in twins. Lancet 360:991–995
26. Lee YC, Newport MJ, Goetghebuer T et al (2006) Influence of genetic and environmental factors on the immunogenicity of Hib vaccine in Gambian twins. Vaccine 24:5335–5340
27. Konradsen HB, Henrichsen J, Wachmann H, Holm N (1993) The influence of genetic factors on the immune response as judged by pneumococcal vaccination of mono- and dizygotic Caucasian twins. Clin Exp Immunol 92:532–536
28. O'Connor D, Pollard AJ (2013) Characterizing vaccine responses using host genomic and transcriptomic analysis. Clin Infect Dis 57:860–869
29. Ellis JA, Kemp AS, Ponsonby A-L (2014) Gene-environment interaction in autoimmune disease. Expert Rev Mol Med 16:e4
30. Franco LM, Bucasas KL, Wells JM et al (2013) Integrative genomic analysis of the human immune response to influenza vaccination. ELife 2:e00299
31. Lee EK (2007) Large-scale optimization-based classification models in medicine and biology. Ann Biomed Eng 35:1095–1109
32. Brooks JP, Lee EK (2008) Analysis of the consistency of a mixed integer programming-based multi-category constrained discriminant model. Ann Oper Res 174:147–168
33. Dabney AR (2005) Classification of microarrays to nearest centroids. Bioinformatics 21:4148–4154
34. Friedman J, Hastie T, Tibshirani R (2010) Regularization paths for generalized linear

models via coordinate descent. J Stat Softw 33:1–22
35. Li S, Rouphael N, Duraisingham S et al (2014) Molecular signatures of antibody responses derived from a systems biology study of five human vaccines. Nat Immunol 15:195–204
36. Obermoser G, Presnell S, Domico K et al (2013) Systems scale interactive exploration reveals quantitative and qualitative differences in response to influenza and pneumococcal vaccines. Immunity 38:831–844
37. Ngo ST, Steyn FJ, McCombe PA (2014) Gender differences in autoimmune disease. Front Neuroendocrinol 35:347–369
38. Beyer WE, de Bruijn IA, Palache AM et al (1999) Protection against influenza after annually repeated vaccination: a meta-analysis of serologic and field studies. Arch Intern Med 159:182–188
39. He X-S, Holmes TH, Sasaki S et al (2008) Baseline levels of influenza-specific CD4 memory T-cells affect T-cell responses to influenza vaccines. PLoS One 3:e2574
40. Sasaki S, He X-S, Holmes TH et al (2008) Influence of prior influenza vaccination on antibody and B-cell responses. PLoS One 3:e2975
41. Schmid MA, Diamond MS, Harris E (2014) Dendritic cells in dengue virus infection: targets of virus replication and mediators of immunity. Front Immunol 5:647
42. Chotiwan N, Roehrig JT, Schlesinger JJ et al (2014) Molecular determinants of dengue virus 2 envelope protein important for virus entry in FcγRIIA-mediated antibody-dependent enhancement of infection. Virology 456–457:238–246
43. Mustafa MS, Rasotgi V, Jain S, Gupta V (2015) Discovery of fifth serotype of dengue virus (DENV-5): a new public health dilemma in dengue control. Med J Armed Forces India 71:67–70
44. McElrath MJ, De Rosa SC, Moodie Z et al (2008) HIV-1 vaccine-induced immunity in the test-of-concept Step Study: a case-cohort analysis. Lancet 372:1894–1905
45. Perreau M, Pantaleo G, Kremer EJ (2008) Activation of a dendritic cell–T cell axis by Ad5 immune complexes creates an improved environment for replication of HIV in T cells. J Exp Med 205:2717–2725
46. Zak DE, Andersen-Nissen E, Peterson ER et al (2012) Merck Ad5/HIV induces broad innate immune activation that predicts CD8+ T-cell responses but is attenuated by preexisting Ad5 immunity. Proc Natl Acad Sci U S A 109:E3503–E3512
47. Nath I, Saini C, Valluri VL (2015) Immunology of leprosy and diagnostic challenges. Clin Dermatol 33:90–98
48. Lindquester GJ, Greer KA, Stewart JP, Sample JT (2014) Epstein-Barr virus IL-10 gene expression by a recombinant murine gammaherpesvirus in vivo enhances acute pathogenicity but does not affect latency or reactivation. Herpesviridae 5:1
49. Rawson TM, Anjum V, Hodgson J et al (2014) Leprosy and tuberculosis concomitant infection: a poorly understood, age-old relationship. Lepr Rev 85:288–295
50. Shankar EM, Velu V, Kamarulzaman A, Larsson M (2015) Mechanistic insights on immunosenescence and chronic immune activation in HIV-tuberculosis co-infection. World J Virol 4:17–24
51. Takem EN, Roca A, Cunnington A (2014) The association between malaria and non-typhoid Salmonella bacteraemia in children in sub-Saharan Africa: a literature review. Malar J 13:400
52. Coffey LL, Failloux A-B, Weaver SC (2014) Chikungunya virus-vector interactions. Viruses 6:4628–4663
53. Wu S, Jiang Z-Y, Sun Y-F et al (2013) Microbiota regulates the TLR7 signaling pathway against respiratory tract influenza A virus infection. Curr Microbiol 67:414–422
54. Oh JZ, Ravindran R, Chassaing B et al (2014) TLR5-mediated sensing of gut microbiota is necessary for antibody responses to seasonal influenza vaccination. Immunity 41:478–492
55. Wang J, Li F, Sun R et al (2013) Bacterial colonization dampens influenza-mediated acute lung injury via induction of M2 alveolar macrophages. Nat Commun 4:2106
56. Wang J, Li F, Wei H et al (2014) Respiratory influenza virus infection induces intestinal immune injury via microbiota-mediated Th17 cell-dependent inflammation. J Exp Med 211:2397–2410
57. Weber A, Zimmermann C, Kieseier BC et al (2014) Bacteria and their cell wall components uniformly co-activate interleukin-17-producing thymocytes. Clin Exp Immunol 178:504–515
58. Clarke TB (2014) Early innate immunity to bacterial infection in the lung is regulated systemically by the commensal microbiota via nod-like receptor ligands. Infect Immun 82:4596–4606
59. Kernbauer E, Ding Y, Cadwell K (2014) An enteric virus can replace the beneficial function of commensal bacteria. Nature 516: 94–98

60. Cadwell K (2014) Expanding the role of the virome: commensalism in the gut. J Virol 89:1951–1953
61. Li Q, Wang C, Tang C et al (2014) Dysbiosis of gut fungal microbiota is associated with mucosal inflammation in Crohn's disease. J Clin Gastroenterol 48:513–523
62. Leila Srour M, Marck KW, Baratti-Mayer D (2015) Noma: neglected, forgotten and a human rights issue. Int Health 7:149–150
63. Tilg H, Moschen AR (2015) Food, immunity, and the microbiome. Gastroenterology 148:1107–1119
64. Kamada N, Seo S-U, Chen GY, Núñez G (2013) Role of the gut microbiota in immunity and inflammatory disease. Nat Rev Immunol 13:321–335
65. Casanova J-L, Abel L (2013) The genetic theory of infectious diseases: a brief history and selected illustrations. Annu Rev Genomics Hum Genet 14:215–243
66. Le Chatelier E, Nielsen T, Qin J et al (2013) Richness of human gut microbiome correlates with metabolic markers. Nature 500:541–546
67. Ferreira RBR, Antunes LCM, Finlay BB (2010) Should the human microbiome be considered when developing vaccines? PLoS Pathog 6:e1001190
68. Kau AL, Ahern PP, Griffin NW et al (2011) Human nutrition, the gut microbiome and the immune system. Nature 474:327–336
69. Valdez Y, Brown EM, Finlay BB (2014) Influence of the microbiota on vaccine effectiveness. Trends Immunol 35:526–537
70. Huda MN, Lewis Z, Kalanetra KM et al (2014) Stool microbiota and vaccine responses of infants. Pediatrics 134:e362–e372
71. Lavelle A, Lennon G, O'Sullivan O et al (2015) Spatial variation of the colonic microbiota in patients with ulcerative colitis and control volunteers. Gut. doi:10.1136/gutjnl-2014-307873
72. Kurata S, Osaki T, Yonezawa H et al (2014) Role IL-17A and IL-10 in the antigen induced inflammation model by Mycoplasma pneumoniae. BMC Microbiol 14:156
73. Spuesens EBM, Fraaij PLA, Visser EG et al (2013) Carriage of Mycoplasma pneumoniae in the upper respiratory tract of symptomatic and asymptomatic children: an observational study. PLoS Med 10:e1001444
74. Ben Aissa-Fennira F, Sassi A, Bouguerra A, Benammar-Elgaaied A (2011) Immunoregulatory role for a public IgM idiotype in the induction of autoimmune diseases in Mycoplasma pneumoniae infection. Immunol Lett 136:130–137
75. Stipkovits L, Egyed L, Palfi V et al (2012) Effect of low-pathogenicity influenza virus H3N8 infection on Mycoplasma gallisepticum infection of chickens. Avian Pathol 41:51–57
76. Xiao L, Crabb DM, Dai Y et al (2014) Suppression of antimicrobial peptide expression by ureaplasma species. Infect Immun 82:1657–1665
77. Wang C, Liu Y, Xu LT et al (2014) Effects of aging, cytomegalovirus infection, and EBV infection on human B cell repertoires. J Immunol 192:603–611
78. Muyanja E, Ssemaganda A, Ngauv P et al (2014) Immune activation alters cellular and humoral responses to yellow fever 17D vaccine. J Clin Invest 124:3147–3158
79. Hotamisligil GS (2006) Inflammation and metabolic disorders. Nature 444:860–867
80. Ravindran R, Khan N, Nakaya HI et al (2014) Vaccine activation of the nutrient sensor GCN2 in dendritic cells enhances antigen presentation. Science 343:313–317
81. Peng D, Jiang F, Zhang R et al (2014) Association of Toll-like Receptor 4 Gene polymorphisms with susceptibility to type 2 diabetes mellitus in the Chinese population. J Diabetes 7:485–492
82. Spurohit J, Hu P, Burke SJ et al (2013) The effects of NOD activation on adipocyte differentiation. Obesity (Silver Spring) 21:737–747
83. Krogh-Madsen R, Plomgaard P, Møller K et al (2006) Influence of TNF-α and IL-6 infusions on insulin sensitivity and expression of IL-18 in humans. Am J Physiol Endocrinol Metab 291:E108–E114
84. Appel S, Mirakaj V, Bringmann A et al (2005) PPAR-gamma agonists inhibit toll-like receptor-mediated activation of dendritic cells via the MAP kinase and NF-kappaB pathways. Blood 106:3888–3894
85. Ahmadian M, Suh JM, Hah N et al (2013) PPARγ signaling and metabolism: the good, the bad and the future. Nat Med 19:557–566
86. Barnes MA, Carson MJ, Nair MG (2015) Non-traditional cytokines: how catecholamines and adipokines influence macrophages in immunity, metabolism and the central nervous system. Cytokine 72:210–219
87. Aguilar-Valles A, Inoue W, Rummel C, Luheshi GN (2015) Obesity, adipokines and neuroinflammation. Neuropharmacology 96(PtA):124–134
88. Stojsavljević S, Gomerčić Palčić M, Virović Jukić L et al (2014) Adipokines and proin-

flammatory cytokines, the key mediators in the pathogenesis of nonalcoholic fatty liver disease. World J Gastroenterol 20: 18070–18091
89. Ouchi N, Parker JL, Lugus JJ, Walsh K (2011) Adipokines in inflammation and metabolic disease. Nat Rev Immunol 11:85–97
90. Chen S, Akbar SMF, Miyake T et al (2015) Diminished immune response to vaccinations in obesity: Role of myeloid-derived suppressor and other myeloid cells. Obes Res Clin Pract 9:35–44
91. Young KM, Gray CM, Bekker L-G (2013) Is obesity a risk factor for vaccine non-responsiveness? PLoS One 8:e82779
92. Park H-L, Shim S-H, Lee E-Y et al (2014) Obesity-induced chronic inflammation is associated with the reduced efficacy of influenza vaccine. Hum Vaccin Immunother 10:1181–1186
93. Lumeng CN, Saltiel AR (2011) Inflammatory links between obesity and metabolic disease. J Clin Invest 121:2111–2117
94. Lamas O, Marti A, Martínez JA (2002) Obesity and immunocompetence. Eur J Clin Nutr 56(Suppl 3):S42–S45
95. Genoni G, Prodam F, Marolda A et al (2014) Obesity and infection: two sides of one coin. Eur J Pediatr 173:25–32
96. Prathibha Bandaru HR, Nappanveettil G (2013) The impact of obesity on immune response to infection and vaccine: an insight into plausible mechanisms. Endocrinol Metab Synd 2:113
97. Shaikh SR, Haas KM, Beck MA, Teague H (2015) The effects of diet-induced obesity on B cell function. Clin Exp Immunol 179:90–99
98. Donath MY, Shoelson SE (2011) Type 2 diabetes as an inflammatory disease. Nat Rev Immunol 11:98–107
99. Donath MY (2014) Targeting inflammation in the treatment of type 2 diabetes: time to start. Nat Rev Drug Discov 13:465–476
100. Dhillon S, Moore C, Li SD et al (2012) Efficacy of high-dose intra-dermal hepatitis B virus vaccine in previous vaccination non-responders with chronic liver disease. Dig Dis Sci 57:215–220
101. Li W, Wei Z, Cai L et al (2011) Effect of type 2 diabetes mellitus on efficacy of hepatitis B vaccine and revaccination strategy. Med J Chin Peoples Lib Army 36:1068–1070
102. Leonardi S, Vitaliti G, Garozzo MT et al (2012) Hepatitis B vaccination failure in children with diabetes mellitus? The debate continues. Hum Vaccin Immunother 8:448–452
103. Tan IJ, Peeva E, Zandman-Goddard G (2015) Hormonal modulation of the immune system - a spotlight on the role of progestogens. Autoimmun Rev. doi:10.1016/j.autrev.2015.02.004
104. Pettengill MA, van Haren SD, Levy O (2014) Soluble mediators regulating immunity in early life. Front Immunol 5:457
105. Jensen KJ, Ndure J, Plebanski M, Flanagan KL (2015) Heterologous and sex differential effects of administering vitamin A supplementation with vaccines. Trans R Soc Trop Med Hyg 109:36–45
106. Furman D (2015) Sexual dimorphism in immunity: improving our understanding of vaccine immune responses in men. Expert Rev Vaccines 14:461–471
107. Gubbels Bupp MR (2015) Sex, the aging immune system, and chronic disease. Cell Immunol 294(2):102–110
108. Ahmad SM, Raqib R, Qadri F, Stephensen CB (2014) The effect of newborn vitamin A supplementation on infant immune functions: trial design, interventions, and baseline data. Contemp Clin Trials 39:269–279
109. Fisker AB, Bale C, Rodrigues A et al (2014) High-dose vitamin A with vaccination after 6 months of age: a randomized trial. Pediatrics 134:e739–e748
110. Savy M, Edmond K, Fine PEM et al (2009) Landscape analysis of interactions between nutrition and vaccine responses in children. J Nutr 139:2154S–2218S
111. Patriarca PA, Wright PF, John TJ (1991) Factors affecting the immunogenicity of oral poliovirus vaccine in developing countries: review. Rev Infect Dis 13:926–939
112. Kirkpatrick BD, Colgate ER, Mychaleckyj JC et al (2015) The "Performance of Rotavirus and Oral Polio Vaccines in Developing Countries" (PROVIDE) study: description of methods of an interventional study designed to explore complex biologic problems. Am J Trop Med Hyg 92:744–751
113. Hoest C, Seidman JC, Pan W et al (2014) Evaluating associations between vaccine response and malnutrition, gut function, and enteric infections in the MAL-ED cohort study: methods and challenges. Clin Infect Dis 59(Suppl 4):S273–S279
114. MAL-ED Network Investigators (2014) The MAL-ED study: a multinational and multidisciplinary approach to understand the relationship between enteric pathogens, malnutrition, gut physiology, physical growth, cognitive development, and immune responses in infants and children up to 2 years of age in

resource-poor environments. Clin Infect Dis 59(Suppl 4):S193–S206
115. Haque R, Snider C, Liu Y et al (2014) Oral polio vaccine response in breast fed infants with malnutrition and diarrhea. Vaccine 32:478–482
116. Qadri F, Bhuiyan TR, Sack DA, Svennerholm A-M (2013) Immune responses and protection in children in developing countries induced by oral vaccines. Vaccine 31:452–460
117. Fukushima H, Maeda R, Suzuki R et al (2008) Upregulation of calcium/calmodulin-dependent protein kinase IV improves memory formation and rescues memory loss with aging. J Neurosci Off J Soc Neurosci 28:9910–9919
118. Abboud FM, Harwani SC, Chapleau MW (2012) Autonomic neural regulation of the immune system: implications for hypertension and cardiovascular disease. Hypertension 59:755–762
119. Borovikova LV, Ivanova S, Zhang M et al (2000) Vagus nerve stimulation attenuates the systemic inflammatory response to endotoxin. Nature 405:458–462
120. Sherman MP, Zaghouani H, Niklas V (2015) Gut microbiota, the immune system, and diet influence the neonatal gut-brain axis. Pediatr Res 77:127–135
121. Vijay-Kumar M, Aitken JD, Carvalho FA et al (2010) Metabolic syndrome and altered gut microbiota in mice lacking Toll-like receptor 5. Science 328:228–231
122. Neuman H, Debelius JW, Knight R, Koren O (2015) Microbial endocrinology: the interplay between the microbiota and the endocrine system. FEMS Microbiol Rev 39:509–521
123. Li T, Chiang JYL (2015) Bile acids as metabolic regulators. Curr Opin Gastroenterol 31:159–165
124. Keightley PC, Koloski NA, Talley NJ (2015) Pathways in gut-brain communication: Evidence for distinct gut-to-brain and brain-to-gut syndromes. Aust N Z J Psychiatry 49:207–214
125. Marazziti D, Rutigliano G, Baroni S et al (2014) Metabolic syndrome and major depression. CNS Spectr 19:293–304
126. Bakunina N, Pariante CM, Zunszain PA (2015) Immune mechanisms linked to depression via oxidative stress and neuroprogression. Immunology 144:365–373
127. O'Connor TG, Moynihan JA, Wyman PA et al (2014) Depressive symptoms and immune response to meningococcal conjugate vaccine in early adolescence. Dev Psychopathol 26:1567–1576
128. Arango M-T, Kivity S, Chapman J, Shoenfeld Y (2014) Narcolepsy – genes, infections and vaccines: the clues for a new autoimmune disease. Isr Med Assoc J 16:636–637
129. Duffy J, Weintraub E, Vellozzi C et al (2014) Narcolepsy and influenza A(H1N1) pandemic 2009 vaccination in the United States. Neurology 83:1823–1830
130. Vaarala O, Vuorela A, Partinen M et al (2014) Antigenic differences between AS03 adjuvanted influenza A (H1N1) pandemic vaccines: implications for pandemrix-associated narcolepsy risk. PLoS ONE 9, e114361
131. Partinen M, Kornum BR, Plazzi G et al (2014) Narcolepsy as an autoimmune disease: the role of H1N1 infection and vaccination. Lancet Neurol 13:600–613
132. Maverakis E, Kim K, Shimoda M et al (2015) Glycans in the immune system and The Altered Glycan Theory of Autoimmunity: a critical review. J Autoimmun. doi:10.1016/j.jaut.2014.12.002
133. Anthony RM, Nimmerjahn F (2011) The role of differential IgG glycosylation in the interaction of antibodies with FcγRs in vivo. Curr Opin Organ Transplant 16:7–14
134. Oefner CM, Winkler A, Hess C et al (2012) Tolerance induction with T cell-dependent protein antigens induces regulatory sialylated IgGs. J Allergy Clin Immunol 129:1647–1655, e13
135. Hirabayashi J, Yamada M, Kuno A, Tateno H (2013) Lectin microarrays: concept, principle and applications. Chem Soc Rev 42:4443–4458
136. Mahan AE, Tedesco J, Dionne K et al (2015) A method for high-throughput, sensitive analysis of IgG Fc and Fab glycosylation by capillary electrophoresis. J Immunol Methods 417:34–44
137. Pincetic A, Bournazos S, DiLillo DJ et al (2014) Type I and type II Fc receptors regulate innate and adaptive immunity. Nat Immunol 15:707–716
138. Collin M, Ehlers M (2013) The carbohydrate switch between pathogenic and immunosuppressive antigen-specific antibodies. Exp Dermatol 22:511–514
139. Selman MHJ, Niks EH, Titulaer MJ et al (2011) IgG fc N-glycosylation changes in Lambert-Eaton myasthenic syndrome and myasthenia gravis. J Proteome Res 10:143–152
140. Goulabchand R, Vincent T, Batteux F et al (2014) Impact of autoantibody glycosylation in autoimmune diseases. Autoimmun Rev 13:742–750

141. Gardinassi LG, Dotz V, Hipgrave Ederveen A et al. (2014) Clinical severity of visceral leishmaniasis is associated with changes in immunoglobulin g fc N-glycosylation. mBio 5:e01844.
142. Nimmerjahn F, Ravetch JV (2005) Divergent immunoglobulin g subclass activity through selective Fc receptor binding. Science 310:1510–1512
143. Hayes JM, Frostell A, Cosgrave EFJ et al (2014) Fc gamma receptor glycosylation modulates the binding of IgG glycoforms: a requirement for stable antibody interactions. J Proteome Res 13:5471–5485
144. Boonnak K, Slike BM, Donofrio GC, Marovich MA (2013) Human FcγRII cytoplasmic domains differentially influence antibody-mediated dengue virus infection. J Immunol 190:5659–5665

Chapter 6

Proteomic Monitoring of B Cell Immunity

Radwa Ewaisha and Karen S. Anderson

Abstract

Immune monitoring is critical in settings of infection, autoimmunity, and cancer, but our understanding of the diversity of the antibody immune repertoire has been limited to selected target antigens and epitopes. Development of new vaccines requires monitoring of B cell immunity and identification of candidate antigens. As vaccines become more complex, novel techniques are required for monitoring the diversity of the B cell immune response. Since antibodies recognize both linear and conformational protein and glycoprotein epitopes, recent advances in proteomic and glycomic technologies for rapid display of antigenic structures are leading to methods for proteome-wide immune monitoring. Here, we review different approaches for protein display for immune monitoring, and provide methods for in situ protein display for the rapid detection and validation of antibody repertoires.

Key words B cell, Antibody, Immunity, Epitope, Protein display, Immune monitoring, Phage display, Protein arrays

1 Introduction

Antibodies were discovered in the last decade of the nineteenth century [1]. They were the first proteins that were described to be involved in a specific immune response and they are the most critical element of adaptive immunity for the majority of current vaccines. Methods to identify the recognition of specific antigens from pathogens and other immunogens by B lymphocytes remain an active field of research, primarily limited by methods of protein and glycoprotein production and analysis.

The earliest immunization strategies were based on simulating the course of natural infection through using inactivated or live attenuated infectious agents. Despite little knowledge of the immunological pathways and targets of the immune response, highly effective vaccines were developed that stimulate the body to produce durable B cell immunity against acute infections. Examples include vaccines against smallpox, cholera, anthrax, diphtheria, pertussis, and tetanus [2]. However, live attenuated vaccines pose a risk of reversion to virulence and cause complications in

Sunil Thomas (ed.), *Vaccine Design: Methods and Protocols: Volume 1: Vaccines for Human Diseases*, Methods in Molecular Biology, vol. 1403, DOI 10.1007/978-1-4939-3387-7_6,

immunocompromised individuals. Inactivated vaccines limit this risk but are generally more expensive, not as immunogenic, and are liable to contamination [2].

A large proportion of successful vaccines in use today are pathogen subunits. These include bacterial toxoids, purified proteins, or purified polysaccharides. Of these, only a small number represent recombinant proteins such as vaccines against hepatitis B and HPV [3]. Pathogens with more complicated mechanisms of virulence require more than simple single-antigen vaccines [4]. More complex pathogens such as staphylococci, enterococci, and fungi have not yet been effectively targeted by immunization strategies [3].

In addition to vaccines against infections, cell-based vaccines [5, 6] and immune checkpoint inhibitors [7] have recently emerged as more complex immune modulation strategies for cancer. Progress of these promising novel strategies relies on deciphering immune signatures and surveillance of B cell immunity. However, identification of specific tumor-associated autoantibodies can be challenging. There are over 20,000 open reading frames in the human genome. When splice variation and polymorphism are considered, the number of potential antigens to which autoantibodies can be generated is enormous [8].

Identification of appropriate and promising target antigens for new vaccine development requires antibody-based assays [2, 9] since most current vaccines confer protection through stimulating B lymphocytes to produce neutralizing antibodies [10]. Antibodies are easily detectable, stable, and highly specific [11]. The first use of antibodies as reagents was in 1949 by Örjan Ouchterlony using the immunodiffusion assay [12]. Ten years later, the radioimmunoassay (RIA) was developed by Solomon Berson and Rosalyn Yalow for which Yalow was awarded the Nobel Prize [13]. Their invention paved the way for a variety of other immunoassays, permitting highly sensitive and specific detection of a multitude of proteins, and superseded many other bioassays including conventional pregnancy tests [14]. The main stumbling block for RIA was the need for purification of polyclonal antibodies in large quantities from animals [15], which was solved by the hybridoma method for production of monoclonal antibodies by Kohler and Milstein. To limit hazards and logistics of radiation, enzyme-linked reporters were developed [16] and the first paper on the modern ELISA was published in 1971 [17].

1.1 Proteomic Techniques for Monitoring of the Immune Response

One critical requirement for antibody-based assays is the efficient and reproducible expression, purification, and display of proteins. Sera are typically screened for antibodies to select antigens that are known to potentially be immunogenic or play a role in pathogenicity. This antigen selection does not measure the diversity of immune recognition [8]. To add complexity, proteome-wide immune monitoring requires the production of thousands of protein structures.

The need for tools to study proteins and the significant role they play in health and disease have led to the revolutionary advancements in the field of proteomics in the last 20 years. Effective targets of immunization and serological testing are best determined using a systems approach for monitoring the B cell immune response. Proteomic techniques that have been developed for epitope display are reviewed in [8, 11] and can be summarized as follows:

1.1.1 Phage Display

Phage display was first described in 1985 [18]. Candidate antigens are expressed in lambda phage from cDNA libraries constructed from a given pathogen or disease tissue. Phage-expressing proteins of interest are subsequently replicated onto nitrocellulose membranes and probed with patient sera. Phage display has been applied in antigen discovery in various pathogens such as hepatitis C virus [19], human cytomegalovirus [20], *Mycoplasma pneumoniae* [21], and *Streptococcus pneumoniae* [22]. Alternatively, solution-based phage display is used for autoantigen identification. Phage-displayed peptide libraries are subjected to affinity purification to isolate phage-carrying specific peptides. Autoantibody biomarkers of several cancers such as ovary and prostate have been identified using this technique [23–25]. However, because of the nature of cDNA cloned on the expression vectors, the major drawback of phage display is expression of proteins with truncations, frame shifts, and sometimes improper folding. In addition post-translational modifications (PTMs) are absent and abundant proteins are overrepresented.

1.1.2 Cellular Fractionation and Immunoblotting

In this strategy, candidate antigens from lysates of tissues or pathogens are separated by two-dimensional gel electrophoresis and serum reactivity is determined by immunoblotting or mass spectrometry. Next, bands are excised and proteins are identified by mass spectrometric analysis. This method has the advantage of using proteins with their relevant PTMs and it does not require cloning or expression procedures. However, proteins found in low concentrations may be masked by more abundant proteins.

1.1.3 Peptide Arrays

Peptides are displayed on a solid surface such as a glass or plastic slide. Relevant peptides that have overlapping sequences are determined bioinformatically so as to cover the whole ORFeome or a portion of the proteome. This circumvents difficulty with expression of full-length proteins, but conformational epitopes and posttranslational modifications are not detected. Recently, peptide arrays have been used to determine individual immunosignatures that can predict the protective efficacy of a given vaccine in mice [26].

1.1.4 Protein Arrays

Protein microarrays enable the display of thousands of proteins on the surface of a microscopic slide or in 96-well bead array format. A wide variety of protein expression systems are used including

E. coli, yeast, or insect cells and then antigens are purified. However, these systems can be time consuming and unsuitable for high-throughput proteomic methods. Additionally, bacteria often fail to express most proteins with intact tertiary structures or PTMs, particularly those with high molecular weights or multiple domains [27, 28]. In vitro protein expression, on the other hand, diminishes the time required to obtain protein from DNA but adds the challenges of protein purity and reproducibility of expression [8].

Protein microarrays are currently commercially available from several sources, and are provided either as purified, printed proteins or as printed cDNA that can be expressed using in vitro transcription and translation. At this time, the antigenic display on protein microarrays is primarily the protein backbone, so the diversity of displayed antigenic structures from posttranslational modifications is more limited. As the content of ORFeome collections and the cost of protein expression improve, proteome-wide screening of sera for antibody responses is becoming feasible both for human antigens and pathogens. Here, we discuss three methods and overall strategies for using in situ protein display for detection of antibody responses in human sera or plasma.

1.2 Nucleic Acid Programmable Protein Array

To improve both the cost of purification of recombinant proteins and the stability of displayed protein, the nucleic acid programmable protein array (NAPPA) technique was developed using printed expression plasmids with an anti-tag antibody on microscopic glass slides [29–31] (Fig. 1a). At the time of the assay, in vitro transcription and translation (IVTT) are used for in situ expression of tagged target proteins encoded by the arrayed plasmids. The use of a human-coupled IVTT system derived from the human cell line HeLa results in ten times higher protein yields, more robust reproducibility, and less background than the previously used rabbit reticulocyte lysate system [32]. For immune monitoring, slides are incubated with subject sera or plasma to permit binding of antibodies to their corresponding protein spot on the array. Signals are detected using either a fluorescently labeled or an HRP-labeled secondary antibody. NAPPA arrays are available from the Arizona State University protein array core, www.NAPPAproteinarray.org.

Printing DNA on the arrays has several advantages over printing proteins. Unlike protein arrays, printed plasmids retain their activity following months of storage of the arrays under arid conditions. Since the production and purification of thousands of proteins are expensive, time consuming, and liable to protein unfolding over the multistep process of protein array production, the on-demand IVTT avoids these issues [33]. However, IVTT-derived proteins are produced with limited posttranslational modifications that are a significant component of the immune response.

A key advance in the field of protein microarrays has been the steady improvement in relevant ORFeome collections. The

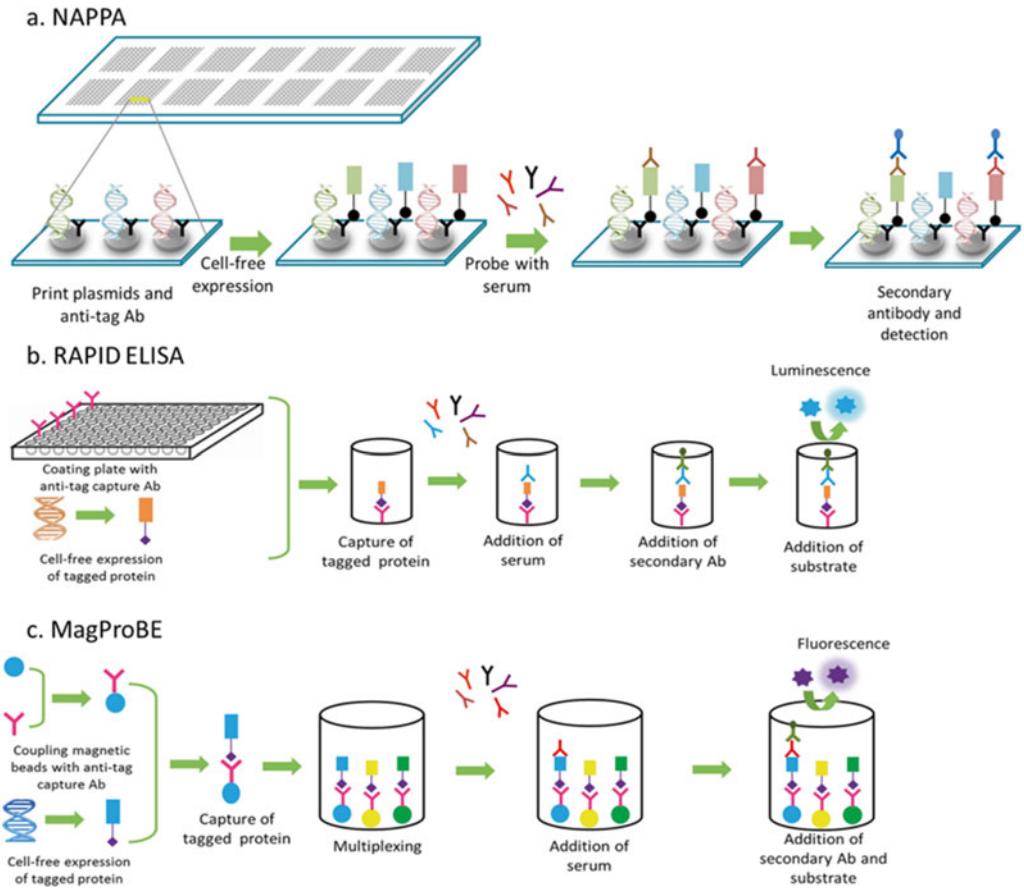

Fig. 1 Different protein array techniques that use in situ protein display for detecting antibodies in human serum or plasma. (**a**) Nucleic acid programmable protein arrays (NAPPA): cDNA-containing plasmids are printed on microscopic slides along with an anti-tag antibody. In situ cell-free expression of tagged proteins generates protein microarrays that can be used to detect antibodies in serum using an appropriate secondary antibody. (**b**) Rapid antigenic protein in situ display ELISA (RAPID ELISA): 96-well plates are coated with an anti-tag antibody to capture freshly expressed tagged proteins. Displayed proteins are probed with serum and bound antibodies are detected using a secondary antibody. (**c**) Magnetic programmable bead ELISA (MagProBE): IVTT-expressed tagged proteins are captured onto anti-tag-coupled fluorescent beads and probed with serum. Multiplexing can be achieved by capturing different antigens on different-colored beads

DNASU Plasmid Repository is the source of plasmid DNA used for NAPPA array production [34]. This plasmid collection was first started at the Harvard Institute of Proteomics in 2000 and is currently located at the Virginia G. Piper Center for Personalized Diagnostics in the Biodesign Institute (AZ, USA) [34]. The repository comprises and distributes a collection of over 200,000 plasmids containing the open reading frames (ORFs) of proteins from over 600 organisms, including 12,000 full-length human genes. The DNASU website, database, and physical repository (http://dnasu.asu.edu or http://dnasu.org) were designed to provide

annotated and sequence-verified plasmids and online resources to the research community. All ORFs are cloned onto a master plasmid (pDONR), sequence verified, and stored in the DNASU repository. ORFs in DONR plasmids can be moved to a wide array of expression vectors using Gateway recombinational cloning.

NAPPA arrays have been used for the discovery of autoantibodies in cancer patient sera, such as autoantibodies to p53 in breast and ovarian cancer, BCL2 in prostate cancer, and ML-IAP in melanoma [35–37]. As an example of screening for infectious disease antigens, *Pseudomonas aeruginosa* outer membrane proteins printed on NAPPA have been used to screen sera from *P. aeruginosa* patients to identify immunogenic proteins [38].

1.3 Rapid Antigenic Protein In Situ Display (RAPID ELISA)

NAPPA protein microarrays are excellent tools for antigen discovery. However, validation requires methods for the analysis of a few antigens, but using thousands of sera. RAPID ELISA was developed as a robust tool that can be performed in most immunology laboratories using publicly available reagents. RAPID ELISA can be used to screen hundreds of sera rapidly and cost-effectively in order to confirm antibody biomarkers and immunogenicity of antigens discovered using protein microarrays [36, 39, 40]. As with NAPPA assays, tagged proteins are expressed using an in vitro transcription and translation system, but then captured in a 96-well plate through an anti-tag antibody (Fig. 1b). Sera are then incubated with the displayed proteins, and bound immunoglobulins are detected using secondary antibodies. To overcome the background problem encountered with human sera, an optimized serum blocking buffer consisting of *E. coli* lysate diluted 1:10 in PBST and 5 % milk was developed [41]. An eightfold increase in the relative light unit (RLU) ratio of antigen-specific IgG compared with control GST protein was observed with the use of this serum blocking buffer. Additionally, human HeLa cell lysate IVTT system and automation have further enhanced the efficiency, rapidity, and reproducibility of this technique.

1.4 Magnetic Programmable Bead ELISA (MagProBE)

A similar technique as RAPID ELISA for high-throughput serum screening is the magnetic programmable bead ELISA, MagProBE [39]. As with RAPID ELISA, tagged proteins are expressed by IVTT, but then expressed proteins are captured on anti-tag-coupled fluorescent magnetic beads (such as Luminex beads) in a 96-well plate (Fig. 1c). This is followed by steps of incubation with sera and then with a secondary antibody. Beads are coupled with the anti-tag antibody in advance and they are stable for at least 1 year. Coupling efficiency is confirmed using anti-Ig secondary antibodies. Chief among the advantages of MagProBE is the high reproducibility and automated washing. Additionally, bead array ELISA can be used for multiplex assays by capturing of different antigens on beads of different colors and then pooling them.

Multiplexing saves both time and volume of serum, but the cost/antigen is higher than with RAPID ELISA. This technique has been used for multiplex detection of immunity to a panel of EBV antigens in healthy donor sera [42] and to investigate potential biomarkers of HPV-associated oropharyngeal carcinoma [43].

1.5 Recent Advances in Protein Display and Detection

Many immune-based biomarkers have clinical applications for early detection of disease. The applications require robust, reproducible, and cost-effective assays with improved limits of detection, multiplexing, and automation, all of which have substantially improved in the last decade. For example, chromogenic enzyme substrates have been the traditional reporter molecules for ELISAs. The more sensitive chemiluminescent substrates can now detect analyte concentrations in the picomolar range [15]. Ultrasensitive approaches, such as the single-molecule array technology, may allow detection of femtomolar concentrations of antibody through digital measurements of immunocomplexes. Nanoparticle-based ELISAs are reported to detect attograms of analytes [44].

Because routine laboratory diagnosis is costly and may not be accessible in resource-poor areas, point-of-care (POC) tests are emerging technologies for health screening, much of which currently depends on detection of antibodies. Affordable POC tests that give rapid and reliable results, require minimal training, and use no equipment are currently in use for HIV, syphilis, and malaria [45]. Integration of ELISA assays with microfluidics and molecular detection methods may transform vaccine monitoring and identification of at-risk individuals for clinical interventions.

2 Materials

2.1 In Vitro Protein Expression

1. DNA preparation systems (Nucleobond, Clontech, Mountain View, CA).
2. Plasmid with GST tag (DNASU, Tempe, AZ, USA).
3. 1-Step Human Coupled IVTT Kit—DNA (Life Technologies, Carlsbad, CA, USA).
4. RNaseOUT (Thermo Fisher Scientific, Waltham, MA, USA).
5. EchoTherm Chill/Heat Incubator (Thermo Fisher Scientific, Waltham, MA, USA).

2.2 Serum Sample Preparation

1. *E. coli* DH5α.
2. Luria Broth (LB) media.
3. cOmplete, Mini Protease Inhibitor Cocktail Tablets (Roche, Basel, Switzerland).
4. Bovine serum albumin: BSA (Cell Signaling, Danvers, MA, USA).

5. Sonicator.
6. Centrifuge.
7. Shaking incubator.

2.3 Nucleic Acid Programmable Protein Array

1. NAPPA microarray slides obtained from the NAPPA Protein Array Core of DNASU (DNASU, Tempe, AZ, USA).
2. HybriWell gasket adhesive (Grace Bio-Labs, Bend, OR, USA).
3. Microarray Hybridization Chamber (Corning, Corning, NY, USA).
4. Modified pipette tip box with separators to wash up to four slides.
5. SuperBlock Buffer in PBS (Pierce Biotechnology, Rockford, IL, USA).
6. Secondary fluorescence-tagged anti-human antibody (Ab) compatible with Tecan's PowerScanner excitation lasers:
   - Laser specification—red 2 635–63 nm diode laser, green 20 mW 532 nm solid-state laser.
   - Emission filter wheel: 676/37 nm filter, 579/42 nm filter, two additional free positions for customer-defined filters.
7. PowerScanner microarray scanner (Tecan, Maennedorf, Switzerland).
8. Array-Pro Analyzer software (MediaCybernetics, Rockville, MD, USA).

2.4 Rapid Antigenic Protein In Situ Display (RAPID) ELISA

1. White opaque, flat-bottom, 96-well polystyrene high-bind hydrophobic-ionic microplate (Pierce Biotechnology, Rockford, IL, USA).
2. Sodium Bicarbonate (Sigma-Aldrich, St. Louis, MO, USA).
3. RNaseOUT (Thermo Fisher Scientific, Waltham, MA, USA).
4. HRP anti-human IgG antibody (Ab) (Jackson ImmunoResearch, West Grove, PA, USA).
5. HRP anti-mouse IgG Ab (Jackson ImmunoResearch, West Grove, PA, USA).
6. Anti-GST polyclonal Ab (GE Healthcare, Little Chalfont, Buckinghamshire, UK).
7. Anti-GST mouse monoclonal antibody (mAb) (Cell Signaling, Danvers, MA, USA).
8. Supersignal ELISA Femto Chemiluminescent Substrate (Thermo Fisher Scientific, Waltham, MA, USA).
9. Nunc Immuno Washer (Thermo Fisher Scientific, Waltham, MA, USA).

10. Titer plate shaker (Thermo Fisher Scientific, Waltham, MA, USA).
11. GloMax®-96 Microplate Luminometer (Promega, Madison, WI, USA).

2.5 Magnetic Programmable Bead ELISA (MagProBE)

1. Monobasic Sodium Phosphate Anhydrous (MP Biomedicals, Santa Ana, CA, USA).
2. Sulfo-*N*-hydroxysulfosuccinimide (Sulfo-NHS) (Sigma-Aldrich, St. Louis, MO, USA).
3. 1-Ethyl-3-[3-dimethylaminopropyl]carbodiimide hydrochloride (EDC) (Thermo Fisher Scientific, Waltham, MA, USA).
4. Bio-Plex Pro Magnetic Carboxylated 6.5 μm microspheres compatible with Luminex's MAGPIX (Bio-Rad, Hercules, CA, USA) (*see* **Note 3b**).
5. 2-(*N*-Morpholino)ethanesulfonic acid (MES) (Sigma-Aldrich, St. Louis, MO, USA).
6. BSA (Cell Signaling, Danvers, MA, USA).
7. Sodium Azide (Sigma-Aldrich, St. Louis, MO, USA).
8. Goat anti-GST polyclonal Ab (GE Healthcare Life Sciences, Pittsburgh, PA, USA).
9. Donkey anti-goat IgG-PE (Jackson ImmunoResearch, West Grove, PA, USA).
10. Biotin labeled anti-human IgG (Jackson ImmunoResearch, West Grove, PA, USA).
11. Streptavidin, R-Phycoerythrin Conjugate (SAPE) (Life Technologies, Carlsbad, CA, USA).
12. Greiner Microassay 96-Well Plate (Greiner Bio-One, Monroe, NC, USA).
13. DynaMag-2 Magnet (Thermo Fisher Scientific, Waltham, MA, USA).
14. Sonicator (Cole Parmer, Vernon Hills, IL, USA).
15. Rotator (Thermo Fisher Scientific, Waltham, MA, USA).
16. TC10 Cell Counter (Bio-Rad, Hercules, CA, USA).
17. Titer plate shaker (Thermo Fisher Scientific, Waltham, MA, USA).
18. ELx405 Microplate Washer (Bio-Tek, Winooski, VT, USA).
19. MAGPIX (Luminex, Austin, TX, USA).

2.6 NAPPA, RAPID ELISA, and Magnetic Bead Array ELISA Common Materials

1. Phosphate-buffered saline (PBS) 1× Powder Concentrate (Cole Parmer, Vernon Hills, IL, USA).
2. Powdered Milk (MP Biomedicals, Santa Ana, CA, USA).
3. Tween 20 (Sigma-Aldrich, St. Louis, MO, USA).

4. Copolymer microfuge tubes (USA Scientific, Ocala, FL, USA).
5. *E. coli* lysate.
6. Serum samples.
7. cDNA—pANT7cGST (DNASU, Tempe, AZ, USA).
8. 5 % Milk PBS-Tween (PBST) 0.2 %.

3 Methods

3.1 In Vitro Transcription/ Translation of Recombinant Proteins

High-purity DNA is required for the methods described in this chapter for optimum in vitro transcription/translation (IVTT). The plasmids used in this protocol are cDNA constructs with C-terminal-tagged GST fusion protein in pANT7_cGST. The GST tag allows the protein to be readily captured and displayed in situ after IVTT.

3.1.1 DNA Preparation

1. cDNA in pANT7_cGST is publicly available and can be ordered online through the plasmid repository of DNASU (https://dnasu.org/DNASU/Home.do).
2. To achieve high-purity DNA, column-based purification methods are used such as products available from Qiagen or Nucleobond.

3.1.2 In Vitro Transcription/Translation

1. Recombinant proteins should be expressed fresh on the day of the immunoassay.
2. Thaw the components of the 1-Step Human Coupled IVTT Kit on ice.
3. For RAPID ELISA and MagProBE, add RNASE Out to the reaction mix in addition to the IVTT components.
4. Calculate the total volume needed for your assay $(n+1)$.
   (a) NAPPA: Total volume of IVTT Master Mix based on the number of microarray slides being processed. Each slide requires the injection of 150 µL IVTT mixture.
   (b) RAPID ELISA: For each antigen (Ag) per well 100 µL of diluted expressed antigen (Ag) is needed. The recombinant protein is first expressed and then after IVTT diluted 1:100 in 5 % Milk PBST-0.2 %.
   (c) MagProBE: Per Ag and reaction (reaction includes technical replicate) a total of 24.5 µL of IVTT expression mixture is combined with 2 µL of DNA at 500 ng/µL.
5. 1-Step Human Coupled IVTT components and DNA when performing RAPID ELISA and MagProBE are mixed as described below:

NAPPA	
Component	**μL per slide**
HeLa lysate	75
Accessory proteins	15
Reaction mix	30
Nuclease-free water	30
Total	150

RAPID ELISA	
Component	**μL per well**
HeLa lysate	0.57
Accessory proteins	0.11
Reaction mix	0.23
RNaseOUT	0.02
DNA (200 ng/μL)	0.24
Total	1.18

MagProBE	
Component	**μL per two wells**
HeLa lysate	5
Accessory proteins	2.5
Reaction mix	5
Nuclease-free water	3.5
PBS 1×	7.5
RNaseOUT	1
DNA (500 ng/μL)	2
Total	26.5

6. Protein expression
   (a) NAPPA: Slides are covered with HybriWell Gasket adhesive, DNA spots facing up, injected with 150 μL IVTT mixture from **step 5** and placed into a chiller/heater incubator at 30 °C for 1.5 h followed by 15 °C for 0.5 h (*see* **Note 1d**).
   (b) RAPID ELISA and MagProBE: Combine IVTT and DNA components in a polystyrene tube. Gently mix and place tubes into an incubator at 30 °C for 1.5 h.

7. Assessment of protein expression: To ensure protein abundance, protein expression levels should be determined prior to use of the plasmids in the assay. Protein expression can vary from one plasmid to another and between different extraction batches. To assess protein expression, use an anti-GST Ab and its respective secondary detection Ab. If alternative plasmids with a different tag were used, use respective anti-tag Ab and appropriate secondary detection Ab (*see* **Note 3c**).
   (a) NAPPA: Refer to the certificate of analysis provided with your order of NAPPA slides to review expression levels. All slide batches purchased will have undergone quality control to assess DNA and protein levels.
   (b) RAPID ELISA: Protein expression should be above 5.0×10^8 RLUs, while the majority of the expression should be at 1.0×10^9 RLUs.
   (c) MagProBE: Protein expression should be measured above 1000 median fluorescence intensity (MFI). The negative control wells without the expression plasmid should be well below 100 MFI.

3.2 Serum Sample Preparation

To prevent unspecific interactions from serum components to the detection Ab and maximize signal-to-noise ratios, serum samples are blocked prior to use in the assays.

3.2.1 E. coli Lysate Preparation and Utilization as a Blocking Agent

Blocking agents other than *E. coli* lysate can be used, such as 1–10 % BSA and 5 % milk in PBST-0.2 %. However, our laboratory uses *E. coli* lysate as a blocking agent which yields the lowest background and best signal-to-noise ratio.

1. Inoculate a preculture of *E. coli* DH5α into 2 mL LB liquid media and incubate at 37 °C for 7–8 h.
2. Transfer 500 μL of the preculture to 1 L of LB liquid media and grow overnight at 37 °C.
3. Pellet culture by centrifugation at 4 °C.
4. Add 20 mL of PBST to the first pellet for resuspension, then add the same 20 mL to the next pellet, and resuspend. Repeat until all pellets are resuspended.
5. Transfer suspension into a 50 mL tube, place on ice, and add three tablets of protease inhibitor. Vortex thoroughly until protease inhibitor tablets are completely dissolved.
6. Sonicate the bacteria at 500 W and 20 % amplitude for 10 min with a cycle of pulse on/off for 1 s using a microtip.
7. Aliquot lysate into tubes and boil at 99 °C for 10 min.
8. Spin down denatured precipitates at max speed for 5 min.
9. Collect supernatant and store at –20 °C for later use as a blocking agent.

3.2.2 Serum Sample Dilution

Optimal dilution in blocking reagent should be determined through optimization prior to use in the screening experiment.

NAPPA

1. For blocking serum, 50 % *E. coli* lysate in 5 % milk PBST-0.2 % is used.
2. Additionally, dilution ratios of the serum sample in blocking buffer can vary for optimal results. Typically, a sample-to-blocking buffer ratio of 1:50 is used in the assays.
3. The total volume needed to incubate the NAPPA slide with the diluted serum is 2 mL using the hybridization chambers.

RAPID ELISA

1. To make serum blocking buffer, add milk powder to 5 % into *E. coli* lysate and dilute lysate into 5 % milk PBST-0.2 % in a ratio of 1:10.
2. Serum is diluted with serum blocking buffer in a ratio of 1:100.
3. The total volume needed for serum incubation is 100 μL of diluted serum per well.

MagProBE

1. Serum blocking buffer is mixed together by adding *E. coli* lysate containing 5 % BSA to PBS 1 % BSA in a ratio of 1:10.
2. Serum is diluted 1:80 into serum blocking buffer.
3. Per reaction (including one technical replicate), 50 μL of diluted serum is needed.

3.3 Nucleic Acid Programmable Protein Array

3.3.1 Ordering NAPPA Slides

1. Go to the http://nappaproteinarray.org/ webpage. Custom arrays built for a specific project or predetermined collections are available for purchase. Pricing can be found here: http://nappaproteinarray.org/price.html.
2. Contact the NAPPA core manager to purchase arrays. All arrays are shipped along with a certificate of analysis (CofA) asserting the quality of the array. QC certificate will include quality confirmation of the DNA print by picogreen staining of the DNA spots, expression level analysis of all spots including positive and negative controls, and slide correlations within and, if applicable, between print batches (*see* **Note 1b**).

3.3.2 Assay Protocol

1. Block slides with SuperBlock for 1 h at room temperature (*see* **Note 1a**, **c**).
2. Rinse slides with ultrapure water and dry with filtered compressed air (*see* **Note 1g**).
3. With the DNA slide side facing up, apply HybriWell gasket to each slide. Seal by applying pressure with the supplied sticks on the sides of the gasket containing adhesive coating.
4. Prepare IVTT mixture as described in Subheading 3.1.2 and inject 150 μL into HybriWell Gasket injection port. To distribute the liquid throughout the entire gasket, gently massage/tap

slides to push the liquid through while injecting. Tap bubbles out through one of the injection holes and then seal with supplied seal adhesives.

5. To express the proteins, incubate the slides in heater/chiller incubator for 1.5 h at 30 °C, followed by 0.5 h at 15 °C to facilitate binding of the recombinant protein with the conjugated anti-GST (anti-tag) Ab on the slide.
6. Prepare serum samples as described in Subheading 3.2.2 and incubate on a rotator for 2 h at RT.
7. After expression, remove HybriWells from slides and rinse/wash slides with PBST in modified pipette boxes with dividers.
8. Wash slides with 5 % milk in PBST-0.2 % three times for 5 min on a rocker.
9. Block with 5 % milk in PBST-0.2 % for 30 min.
10. Take slides out of the 5 % milk in PBST-0.2 %. Gently blot off some residual milk by tapping the edge of the slide on an absorbent paper and place in the hybridization chamber with the captured protein side up, without allowing the slide to dry completely.
11. Apply 2 mL of the diluted serum preparation on top of the slide. Close the hybridization chamber gently. Secure with the supplied metal clips and place in a rotator overnight at 4 °C.
12. Disassemble hybridization chambers carefully and place slides array side up into washing containers filled with 5 % milk in PBST-0.2 %. Wash three times for 5 min on a rocking shaker.
13. Prepare secondary fluorophore-tagged detection Ab in 5 % milk PBST-0.2 % (*see* **Note 1e**, **f**).
14. Place slides array side up into new hybridization chambers and apply 2 mL directly labeled secondary detection Ab (anti-human-fluorophore tagged). Close chambers gently and secure with metal frame clips. Incubate for 1 h on rotator at RT in the dark.
15. Wash slides three times for 5 min in PBST. After last wash rinse with ultrapure water and dry with compressed air. Store in dark slide box until scanning.
16. Scan slides with previously determined scanner settings providing best signal-to-noise ratios in Tecan's PowerScanner. If best scanner settings are not determined yet, scan slides with various laser intensity and gain settings. Following are typical laser intensity and gain settings normally used and depend on variations in serum dilution and secondary detection Abs of the experiment.

Cycle number	Laser intensity	Laser gain
1	10	10
2	25	25
3	50	50
4	75	75

17. Extract data using Array Pro Analyzer program.

3.4 RAPID ELISA

3.4.1 Protocol

1. Coat 96-well plates with 100 µL/well of 10 µg/mL anti-GST Ab (polyclonal) in 0.2 M sodium bicarbonate buffer overnight (pH 9.4) at 4 °C (*see* **Note 3a**).
2. Wash 96-well plate with PBST-0.2 % three times and blot after the last wash.
3. Block GST-coated 96-well plates with 5 % milk in PBST-0.2 %, 200 µL per well, for 1.5 h at RT.
4. Block diluted serum samples from Subheading 3.2.2 for at least 2 h at room temperature on a plate shaker.
5. Prepare recombinant proteins from IVTT preparation (*see* Subheading 3.1) and incubate for 1.5 h at 30 °C. After protein expression, dilute the proteins 1:100 by adding 5 % milk PBST-0.2 %.
6. Remove blocking buffer from the anti-GST-coated plate by dumping and blotting.
7. Add 100 µL/well of diluted expressed protein to the anti-GST-coated plate and incubate for 1 h at RT on a shaker to capture the GST-tagged recombinant protein.
8. Wash assay plate with PBST-0.2 %, 200 µL/well, using the NUNC immunowash 12. Let the wash buffer sit for 1 min before repeating the wash four more times. After the last wash, blot plates to completely remove wash buffer.
9. Add 100 µL diluted sera (*see* sample preparation step in Subheading 3.2.2) and primary control antibodies to the appropriate wells (*see* **Note 2b**). Shake plate at 500 rpm for 1 h at RT.
10. Wash plates. Dump sera out and wash plates with 200 µL/well of PBST-0.2 % using the NUNC immunowash 12 as described in **step 8**.
11. Add 100 µL/well of diluted secondary Ab (HRP goat-anti-human 1:10,000 in 5 % milk PBST-0.2 %, HRP-sheep-anti-human 1:6250 in 5 % milk PBST-0.2 %) to the appropriate wells. Use anti-human Ab for the wells which contain human sera and anti-mouse Ab for the control wells. Shake plate at 600 rpm for 1 h at RT.

12. Wash plate five times as described in **step 8**.
13. Mix equal volumes of each of solutions 1 and 2 from the SuperSignal ELISA Femto kit and add 100 µL/well.
14. Immediately read plate and detect chemiluminescence in the GloMax®-96 Microplate reader per the manufacturer's instruction (*see* **Note 2c–g**).

3.5 MagProBE

To screen for antibodies using a bead array, anti-GST capture Ab is first coupled to the beads and stored. Ag proteins are produced with IVTT similar to RAPID ELISA and then captured onto the beads with the capture Ab prior to use in the MagProBE assay (*see* **Note 4.3a, d**).

3.5.1 Antibody Preparation for Bead Conjugation

The commercial anti-GST antibodies contain sodium azide, which needs to be removed first with dialysis.

1. Pre-wet dialysis cassette membrane with cold PBS.
2. Dilute Ab in 1 mL PBS.
3. Inject diluted Ab into cassette. Remove air.
4. Dialyze 3 times against 1 L cold PBS over a total of 12–24 h.
5. Remove Ab from dialysis cassette.
6. Determine concentration by absorbance (mg/mL = $UV_{280}/1.6$).
7. Aliquot and store at 20 °C.

3.5.2 Antibody Coupling to Magnetic Microspheres

The assay is optimized for the use of anti-GST Ab. For other anti-tag Abs, the Ab/bead ratios should be titered. Volumes listed are for small scale (2.5×10^6 beads) and large scale [in brackets, 12.5×10^6 beads (1 ml)].

1. Equilibrate microspheres to RT and resuspend thoroughly (*see* **Note 3g, h**).
2. Transfer 2.5×10^6 microspheres to a microcentrifuge tube.
3. Wash microspheres by placing tube on a magnet. Wait for 1 min to allow capture of the beads by the magnet. When liquid is clear, remove supernatant and add 100 µL [200 µL] sterile water. Resuspend microspheres thoroughly. Place tube back onto magnet and remove supernatant after beads are captured (*see* **Note 3f**).
4. To activate microspheres, add 80 µL 100 mM monobasic sodium phosphate (pH 6.2) and resuspend thoroughly. Then add 10 µL [50 µL] 50 mg/mL sulfo-NHS to microspheres. Mix well and add 10 µL [50 µL] of 50 mg/mL EDC. Mix well. Incubate for 20 min at RT covered in foil. Vortex for 10 s every 10 min.

5. Wash microspheres twice with 250 μL [500 μL] of 50 mM MES (pH 5.0) by placing tube in the magnetic rack, allowing spheres to be captured before removing supernatant. Resuspend thoroughly in between washes in wash buffer MES.
6. For coupling the spheres with anti-GST, resuspend microspheres in 100 μL [200 μL] 50 mM MES (pH 5.0). Add 12.5 μg [62.5 μg] anti-GST capture Ab and add 50 mM MES to a volume of 500 μL [1 mL]. Vortex for 10 s and place on a rotator for 2 h at RT. Protect reagents from light by wrapping tubes in foil or rotating in the dark.
7. Remove supernatant on the magnetic rack and wash microspheres with 500 μL [1 mL] PBS-BN (PBS, 1 % BSA, 0.05 % azide, pH 7.4). Resuspend thoroughly and incubate for 30 min on a rotator. Exchange the PBS-BN with 1 mL PBS-0.05 % Tween (pH 7.4) and resuspend spheres well. Repeat these steps one more time.
8. Resuspend in 250 μL [1 mL] PBS-BN and count cells in hemocytometer.
9. Store anti-GST-coupled microspheres at 4 °C.

3.5.3 Confirmation of Antibody Coupling to Microspheres

Prior to use in ELISA assays, the amount of anti-GST Ab that is covalently attached to the microspheres is confirmed using an independent anti-GST mAb. Beads of any fluorescent color can be used; colors in adjacent fluorescent spectra can be readily distinguished, and cross-reactivity was not observed.

1. Resuspend coupled microspheres and aliquot enough of the microspheres into a copolymer tube. Per reaction, 5000 microspheres in PBS 1 % BSA in a total volume of 50 μL/well are required.
2. Mix coupled microspheres thoroughly and add 50 μL to appropriate wells into the microassay 96-well plate.
3. Dilute donkey anti-goat IgG-PE to 4 μg/mL in enough volume for 50 μL/well.
4. Add 50 μL detection Ab per well and incubate for 30 min at RT shaking at 750 rpm.
5. Wash wells twice with 100 μL PBS-1 % BSA-0.2 % Tween using magnetic handheld washer, dump, and blot.
6. Resuspend microspheres in 100 μL/well PBS-1 % BSA. Shake for a minimum of 5 min at 750 rpm.
7. Analyze with MAGPIX per the manufacturer's instructions.

3.5.4 Capturing In Vivo-Generated Protein to Anti-GST-Coupled Microspheres: Day 1

The multiplexed bead array ELISA is a 2-day assay. Antigens are expressed with IVTT on the day of the reaction. For assay planning, sera are tested in duplicate, and protein capture onto the beads is tested in duplicate at the same time using separate wells,

using anti-GST mAbs. Controls include the vector control or any control GST fusion protein, including GST alone.

1. Express protein antigens as described in Subheading 3.1.2.
2. Prepare working stock of anti-GST-coupled microspheres. Plan for enough microspheres for 2000 magnetic beads/reaction/antigen.
3. Add expressed protein directly to diluted beads and mix protein and beads for 2 h on a rotator.

3.5.5 Detection of Autoantibodies in Human Serum: Day 1

1. While beads and antigens are mixing, block serum as described in Subheading 3.2.2 for 2 h at RT on rotator or rocker.
2. After coupling of the Ag protein to the microspheres, aliquot microspheres into a tube for 2000 magnetic beads/reaction/antigen and resuspend thoroughly. To multiplex, pipette 10 μL of each 200 beads/μL normalized Ag-bound beads together into one tube (*see* **Note 3e**).
3. Wash beads with PBS-1 % BSA-0.2 % Tween.
4. Block beads by resuspending them in 50 μL/well of 10 % *E. coli* lysate with 5 % BSA, in PBS-1 % BSA. Seal with aluminum foil and shake at 750 rpm at RT for 1 h.
5. Add 50 μL of diluted and blocked serum to the bead resuspension from the previous step. Mix well and split serum-bead mixture to two wells, each containing 50 μL. Seal plate with tape, cover with lid, and wrap in foil. Incubate overnight at 4 °C while shaking at 750 rpm on an orbital shaker.

3.5.6 Detection of Autoantibodies in Human Serum: Day 2

1. Bring plate to RT by shaking it at 750 rpm for 30 min.
2. Wash wells twice with 100 μL PBS-1 % BSA.
3. Prepare detection Ab by diluting biotin-labeled goat anti-human Ab 1:6000 in PBS-1 % BSA. Add 50 μL to each well and incubate for 30 min at RT on a shaker at 750 rpm.
4. Wash beads twice with PBS-1 % BSA-0.2 % Tween.
5. Dilute streptavidin-R-PE 1:1500 in PBS-1 % BSA. Add 50 μL to each well, seal, and incubate for 30 min at RT on a shaker at 750 rpm.
6. Wash beads twice with PBS-1 % BSA-0.2 % Tween.
7. Resuspend microspheres in 100 μL PBS-1 % BSA per well. Shake plate until ready to analyze with MAGPIX. Shake for a minimum of 5 min.
8. Analyze plate with MAGPIX per the manufacturer's instructions.

4 Notes

1. Notes on the NAPPA protocol:
   (a) NAPPA assay protocol can be fully automated using the HS 4800 Pro or 400 Pro Hybridization Station (Tecan, Maennedorf, Switzerland) for high throughput. Per our assay optimization studies, we recommend automating the steps after protein expression, beginning with the PBST wash, for best protein expression and detection results.
   (b) Always handle slides carefully without touching the array surface.
   (c) Slide blocking step with SuperBlock can be alternatively incubated overnight at 4 °C.
   (d) Avoid any air bubbles/pockets on the array for even distribution of the reagent solutions.
   (e) When handling fluorophores, keep them in the dark, wrapped in aluminum foil.
   (f) For best results in your experiment, optimize the dilution level of the secondary detection Ab to maximize signal-to-noise ratio and minimize background.
   (g) Slide drying steps can be done in a centrifuge instead by placing slides in a slide rack into a container with absorbent paper. Slides are spun at $230 \times g$ for 1 min.
2. Notes on the RAPID ELISA protocol:
   (a) All steps can be automated for high-throughput processing on liquid handlers such as the Biomek FX/NX (Beckman Coulter, Brea, CA, USA).
   (b) An expression control and a secondary Ab control should be included for each antigen.
   (c) Background ranges vary greatly between different serum samples used. The majority of the measurements between the 25–75 percentiles should be 5.0×10^7 to 8.9×10^7 RLUs. In average, the GST background is between 1.0×10^8 and 8.0×10^8 RLUs.
   (d) Secondary control measurements should be below 10^6 RLUs for anti-mouse and below 10^7 for the anti-human HRP-labeled secondary detection Ab.
   (e) Criteria for repeating samples: Samples are run in duplicates. If the duplicate samples give a signal difference greater than 50 %, this sample should be repeated.
   (f) Negative response criteria: A serum sample is considered negative in its immune response to an antigen when the ratio

of the measured RLU of the sample for that antigen to that of the same sample in the GST background well is below 2.

(g) Positive response criteria: A serum sample is positive in its immune response to an antigen if the ratio from the respective antigen to GST is above 2.

3. Notes on the MagProBE protocol:

(a) MagProBE ELISA has comparable sensitivities, specificities, and limits of detection as standard protein ELISA for the detection of antibodies in sera to the viral antigen EBNA-1 and the tumor antigen p53 [39].

(b) There are different chemical compositions of Luminex microspheres. The assay described here uses the magnetic microspheres, but also works with SeroMap microspheres, with comparable sensitivities and specificities as the magnetic microspheres.

(c) Protein expression with IVTT can vary from batch to batch. These studies have been optimized for the pANT7-c-terminal GST vector. Over 100 tumor and viral antigens have been expressed and captured using this assay on Luminex beads, with over 90 % of the antigens expressed as determined by GST detection. Both high-quality DNA and careful use of RNase-free pipettes and filter tips are needed for efficient protein expression.

(d) The cost for MagProBE is $5.00/Ag/sample.

(e) Up to ten Ags have been multiplexed at one time using MagProBE. Theoretically, this assay could be used to multiplex up to 100 Ags but is limited only by the number of spectrally distinguishable microspheres.

(f) For manual wash steps of the beads, use handheld magnetic stands. After allowing the beads to collect on the side of the magnet, remove the liquid by discarding and gentle blotting of the plate with the magnet attached. Add 100 μL/well of wash buffer PBS-1 % BSA-0.2 % Tween. Allow beads to be captured and remove the buffer by discarding and gentle blotting. Repeat wash step one more time. All washing steps can be alternatively automated using a liquid handler such as the Bio-Tek ELx 405.

(g) All bead resuspension steps should be carried out in the following manner for thorough dispersion of the beads: vortexing for 10 s, sonicating for 20 s, and vortexing again for 10 s.

(h) Luminex microspheres are light sensitive. To maintain their integrity, protect them from light exposure.

Acknowledgements

This study was supported by NCI UOI CA11734 (K.S.A.). We thank Marika Hopper for assistance in the preparation of this manuscript and Julia Cheng for techinical assistance. Dr. Anderson is a consultant and has stock options with Provista Diagnostics.

References

1. Behring K (1890) Ueber das zustandekommen der diphtherie-immunität und der tetanus-immunität bei thieren. Dtsch Med Wochenschr 16:1113–1114
2. De Veer M, Meeusen E (2011) New developments in vaccine research--unveiling the secret of vaccine adjuvants. Discov Med 12:195–204
3. Meinke A, Henics T, Nagy E (2004) Bacterial genomes pave the way to novel vaccines. Curr Opin Microbiol 7:314–320
4. Berzofsky JA, Ahlers JD, Belyakov IM (2001) Strategies for designing and optimizing new generation vaccines. Nat Rev Immunol 1: 209–219
5. FDA (2010-04-29) Approval letter – Provenge
6. Le DT, Pardoll DM, Jaffee EM (2010) Cellular vaccine approaches. Cancer J 16:304
7. Hodi FS, O' Day SJ, McDermott DF et al (2010) Improved survival with ipilimumab in patients with metastatic melanoma. N Engl J Med 363:711–723
8. Qiu J, Anderson KS (2013) Autoantibodies and biomarker discovery. In: Issaq HJ, Veenstra TD, (eds) Proteomic and metabolomic approaches to biomarker discovery. Elsevier. Massachusetts, USA
9. Silverstein AM (2009) A history of immunology. Academic, New York
10. Zinkernagel RM, Hengartner H (2006) Protective 'immunity' by pre-existent neutralizing antibody titers and preactivated T cells but not by so-called 'immunological memory'. Immunol Rev 211:310–319
11. Anderson KS, LaBaer J (2005) The sentinel within: exploiting the immune system for cancer biomarkers. J Proteome Res 4:1123–1133
12. Ouchterlony O (1949) Antigen-antibody reactions in gels. Acta Pathol Microbiol Scand A 26:507–515
13. Berson SA, Yalow RS (1959) Quantitative aspects of the reaction between insulin and insulin-binding antibody. J Clin Invest 38:1996–2016
14. Kricka LJ, Savory J (2011) International year of Chemistry 2011. A guide to the history of clinical chemistry. Clin Chem 57:1118–1126
15. Wu AH (2006) A selected history and future of immunoassay development and applications in clinical chemistry. Clin Chim Acta 369:119–124
16. Lequin RM (2005) Enzyme immunoassay (EIA)/enzyme-linked immunosorbent assay (ELISA). Clin Chem 51:2415–2418
17. Engvall E, Perlmann P (1971) Enzyme-linked immunosorbent assay (ELISA). Quantitative assay of immunoglobulin G. Immunochemistry 8:871–874
18. Smith GP (1985) Filamentous fusion phage: novel expression vectors that display cloned antigens on the virion surface. Science 228:1315–1317
19. Santini C, Brennan D, Mennuni C et al (1998) Eficient display of an HCV cDNA expression library as C-terminal fusion to the capsid protein D of bacteriophage lambda. J Mol Biol 282:125–135
20. Beghetto E, De Paolis F, Spadoni A, Del Porto P, Buffolano W, Gargano N (2008) Molecular dissection of the human B cell response against cytomegalovirus infection by lambda display. J Virol Methods 151:7–14
21. Beghetto E, De Paolis F, Montagnani F, Cellesi C, Gargano N (2009) Discovery of new Mycoplasma pneumoniae antigens by use of a whole-genome lambda display library. Microbes Infect 11:66–73
22. Beghetto E, Gargano N, Ricci S et al (2006) Discovery of novel Streptococcus pneumoniae antigens by screening a whole-genome λ-display library. FEMS Microbiol Lett 262:14–21
23. Wang X, Yu J, Sreekumar A et al (2005) Autoantibody signatures in prostate cancer. N Engl J Med 353:1224–1235
24. Chatterjee M, Mohapatra S, Ionan A et al (2006) Diagnostic markers of ovarian cancer by high-throughput antigen cloning and detection on arrays. Cancer Res 66:1181–1190

25. Chen G, Wang X, Yu J et al (2007) Autoantibody profiles reveal ubiquilin 1 as a humoral immune response target in lung adenocarcinoma. Cancer Res 67:3461–3467
26. Legutki JB, Johnston SA (2013) Immunosignatures can predict vaccine efficacy. Proc Natl Acad Sci U S A 110:18614–18619
27. Stevens RC (2000) Design of high-throughput methods of protein production for structural biology. Structure 8:R177–R185
28. Jackson AM, Boutell J, Cooley N, He M (2004) Cell-free protein synthesis for proteomics. Brief Funct Genomic Proteomic 2:308–319
29. Ramachandran N, Hainsworth E, Bhullar B et al (2004) Self-assembling protein microarrays. Science 305:86–90
30. Ramachandran N, Raphael JV, Hainsworth E et al (2008) Next-generation high-density self-assembling functional protein arrays. Nat Methods 5:535–538
31. Ramachandran N, Hainsworth E, Demirkan G, LaBaer J (2006) On-chip protein synthesis for making microarrays. New and emerging proteomic techniques. Springer, New York, NY, pp 1–14
32. Festa F, Rollins SM, Vattem K et al (2013) Robust microarray production of freshly expressed proteins in a human milieu. Proteomics-Clin Appl 7:372–377
33. Lee JR, Magee DM, Gaster RS, LaBaer J, Wang SX (2013) Emerging protein array technologies for proteomics. Expert Rev Proteomics 10(1):65–75
34. Seiler CY, Park JG, Sharma A et al (2013) DNASU plasmid and PSI: biology-materials repositories: resources to accelerate biological research. Nucleic Acids Res 42(Database issue):D1253–D260
35. Anderson KS, Ramachandran N, Wong J et al (2008) Application of protein microarrays for multiplexed detection of antibodies to tumor antigens in breast cancer. J Proteome Res 7:1490–1499
36. Ramachandran N, Anderson KS, Jv R et al (2008) Tracking humoral responses using self assembling protein microarrays. Proteomics Clin Appl 2:1518–1527
37. Anderson KS, Cramer DW, Sibani S et al (2015) Autoantibody signature for the serologic detection of ovarian cancer. J Proteome Res 14:578–586
38. Montor WR, Huang J, Hu Y et al (2009) Genome-wide study of Pseudomonas aeruginosa outer membrane protein immunogenicity using self-assembling protein microarrays. Infect Immun 77:4877–4886
39. Anderson KS (2011) 'Multiplexed Detection of Antibodies Using Programmable Bead Arrays.' In: Catherine J. Wu (ed) Protein microarray for disease analysis (Humana Press).
40. Anderson KS, Wong J, Vitonis A et al (2010) p53 autoantibodies as potential detection and prognostic biomarkers in serous ovarian cancer. Cancer Epidemiol Biomarkers Prev 19:859–868
41. Wang J, Barker K, Steel J et al (2013) A versatile protein microarray platform enabling antibody profiling against denatured proteins. Proteomics Clin Appl 7:378–383
42. Wong J, Sibani S, Lokko NN, LaBaer J, Anderson KS (2009) Rapid detection of antibodies in sera using multiplexed self-assembling bead arrays. J Immunol Methods 350:171–182
43. Anderson KS, Wong J, D'Souza G et al (2011) Serum antibodies to the HPV16 proteome as biomarkers for head and neck cancer. Br J Cancer 104:1896–1905
44. de la Rica R, Stevens MM (2012) Plasmonic ELISA for the ultrasensitive detection of disease biomarkers with the naked eye. Nat Nanotechnol 7:821–824
45. A study of a new candidate vaccine against Hepatitis C Virus (HCV). http://clinicaltrials.gov/ct2/show/NCT01070407

Part III

Vaccines for Human Viral Diseases

Chapter 7

Development of Rabies Virus-Like Particles for Vaccine Applications: Production, Characterization, and Protection Studies

Diego Fontana, Marina Etcheverrigaray, Ricardo Kratje, and Claudio Prieto

Abstract

Rabies is a viral infection of the central nervous system for which vaccination is the only treatment possible. Besides preexposure, vaccination is highly recommended for people living in endemic areas, veterinarians, and laboratory workers. Our group has developed rabies virus-like particles (RV-VLPs) with immunogenic features expressed in mammalian cells for vaccine applications. In this chapter the methods to obtain and characterize a stable HEK293 cell line expressing RV-VLPs are detailed. Further, analytical ultracentrifugation steps to purify the obtained VLPs are developed, as well as western blot, dynamic light scattering, and immunogold electron microscopy to analyze the size, distribution, shape, and antigenic conformation of the purified particles. Finally, immunization protocols are described to study the immunogenicity of RV-VLPs.

Key words Vaccine development, Virus-like particles, Rabies, Lentiviral vectors, Stable cell line, HEK293

1 Introduction

Rabies is one of the oldest and most lethal zoonotic diseases known, with a mortality approaching 100 % when clinical symptoms occur. Once the rabies virus reaches the central nervous system, death of the infected person is almost inevitable [1, 2]. The World Health Organization (WHO) recommends preexposure prophylaxis for people living in endemic zones, travellers, veterinaries, and laboratory workers. Besides, post-exposure vaccination is the only treatment available for bitten individuals. Vaccination of pets is required as infected animals (mostly dogs) are the main and most common vector of human rabies infections [3–5]. Although cell-based vaccines for rabies are available, much effort is being made to develop novel, cheaper, and safer vaccines [6, 7].

Sunil Thomas (ed.), *Vaccine Design: Methods and Protocols: Volume 1: Vaccines for Human Diseases*, Methods in Molecular Biology, vol. 1403, DOI 10.1007/978-1-4939-3387-7_7,

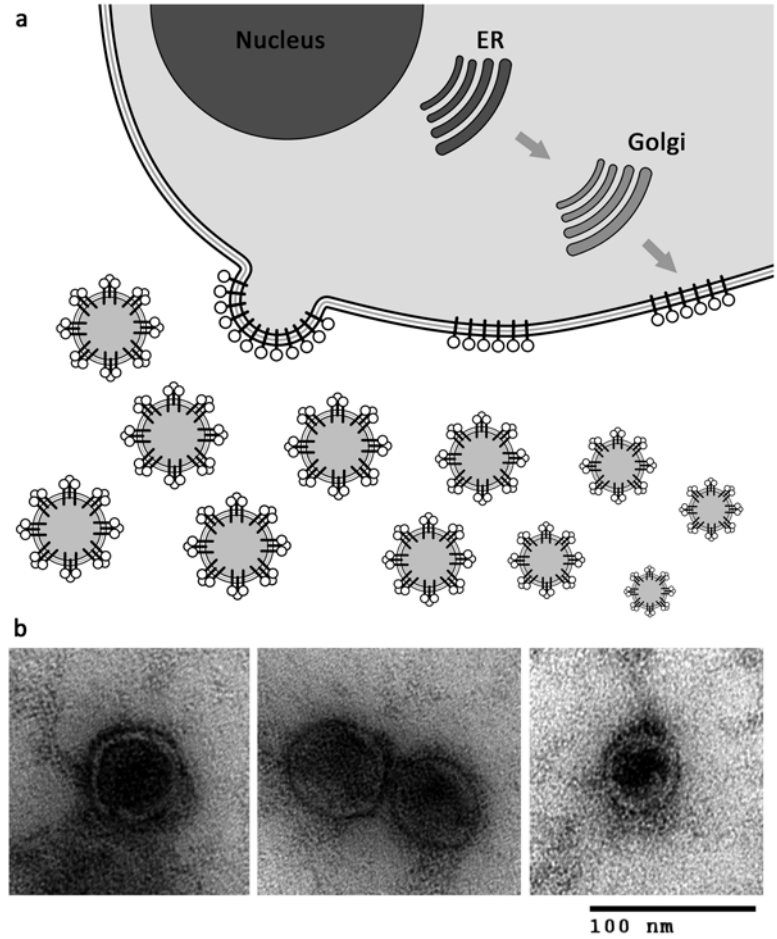

Fig. 1 (**a**) Schematic representation of enveloped VLP budding process. (**b**) Transmission electron microscopy of RV-VLPs (three different fields) found in supernatant of the stable cell line

Virus-like particles (VLPs) are great candidates for rabies vaccine development. VLPs are empty structures that mimic the native virus and are self-assembled expressing the key structural and more antigenic proteins of the virus in a chosen expression system. For enveloped viruses, the membrane glycoproteins, with or without the matrix proteins of the capsid, should be present to generate VLPs capable of inducing a protective immune response [8–10]. When these proteins are expressed adequately, they bud from the plasma membrane carrying lipids and cellular proteins present in it (Fig. 1a).

Our group has made some approaches to develop rabies virus-like particles (RV-VLPs) expressing the rabies glycoprotein (G) in mammalian cell lines [11]. When G is expressed in HEK293 cells, round-shaped VLPs have been found in the supernatant of recombinant cells (Fig. 1b). RV-VLPs proved to be immunogenic and able to induce a specific antibody response.

Here we describe the method to generate recombinant cell lines and clones that continuously express RV-VLPs. The possibility to obtain stable cell lines to produce VLPs is an interesting strategy to optimize the productivity of the production process and it has already been done [12–14]. Usually, these processes use conventional plasmids as vectors for gene transfer, the DHFR-mediated gene amplification system, or similar others. In this case, recombinant cells were constructed by lentiviral gene-mediated transfer using third-generation vectors. By using lentivirus, the introduction of genetic material to nondividing cells can be achieved and the transgene expression can be maintained stably during several passages [15–17]. The lentivirus-based gene engineering techniques have been well studied and described [18].

In this chapter, characterization of RV-VLPs is described, including density gradient analytical purification, antigenic incorporation, shape, size, and polydispersity distribution analysis. A correct particle characterization is crucial when developing novel VLPs because wrong information obtained in this stage could affect the later production process development and the downstream processing as well [10, 19]. We describe the methods to perform ultracentrifugation, western blot, dynamic light scattering (DLS), transmission electron microscopy (TEM), and immunogold electron microscopy.

Finally, the immunogenic properties of the VLPs have to be studied. As a first approach, a simple immunization protocol is recommended to analyze if the produced particles are able to trigger a specific antibody response in mice. Commercial vaccines or antigen international standards should be used to validate the experiment. In any case, in a novel vaccine candidate development, protection studies with virus challenge experiments are the proof of concept. In the case of rabies, NIH potency test is the standard method to confirm that the vaccine candidate is able to induce a protective immune response.

2 Materials

2.1 Lentivirus Production and Titration

1. Human embryonic kidney 293 cell line (HEK293T/17, ATCC® CRL-11268).
2. Dulbecco's modified Eagle's medium (DMEM) (Gibco-BRL, Bethesda, MD), supplemented with 10 % fetal calf serum (FCS, Gibco-BRL, Bethesda, MD), heat inactivated at 56 °C for 30 min.
3. Third-generation lentiviral packaging construct (pMDLg/pRRE), VSV-G expressing construct (pMD.G), the Rev-expressing construct (pRSV-Rev) (Addgene, USA; Plasmid numbers #12251, #12259, #12253, respectively) [15, 16].

4. Transfer lentiviral vector pLV-G (*see* **Note 1**).
5. Lipofectamine® 2000 reagent (Invitrogen™, USA).
6. Syringe filter units (0.45 μm).
7. HIV-1 p24 ELISA kit (QuickTiter™ Lentivirus Titer Kit, Cell Biolabs Inc., USA).

2.2 VLPs Production System

1. HEK293 cell line.
2. DMEM (Gibco-BRL, Bethesda, MD), supplemented with 10 % FCS (Gibco, Bethesda, MD), heat inactivated at 56 °C for 30 min.
3. T flasks for cell culture.
4. Trypsin for cell culture use.
5. Puromycin (Sigma-Aldrich, USA).

2.3 Cell Line Characterization

2.3.1 Flow Cytometry

1. GUAVA EasyCyte cytometer (Millipore, France) or other equivalent.
2. Primary antibody for rabies glycoprotein detection: mAb anti-glycoprotein (*see* **Note 2**).
3. AlexaFluor 488®-conjugated goat anti-mouse antibody (Invitrogen™, USA) or other equivalent for immunofluorescence analysis.

2.3.2 Fluorescence Microscopy

1. Polystyrene media chamber attached to a specially treated standard glass microscope slide (Nunc™ Lab-Tek™ II Chamber Slide™ System, Thermo Scientific, USA).
2. 4 % Paraformaldehyde solution.
3. Primary antibody for rabies glycoprotein detection: mAb anti-glycoprotein (*see* **Note 2**).
4. AlexaFluor 488®-conjugated goat anti-mouse antibody (Invitrogen™, USA) or other equivalent for immunofluorescence analysis.
5. Inverted fluorescence microscope (Eclipse Ti-S, Nikon Instruments Inc, USA, or other equivalent).

2.4 VLP Purification

1. Syringe filter units (0.45 μm).
2. RV-VLP stabilization buffer (50 mM Tris–HCl, 0.15 M NaCl, 1.0 mM EDTA, pH 7.4).
3. 30 % Sucrose in RV-VLP stabilization buffer.
4. Ultracentrifuge with a swinging bucket rotor.
5. Iodixanol density gradient (OptiPrep™ Density Gradient Medium, Axis-Shield, Scotland).
6. Amicon® Ultra centrifugal units (Millipore, USA) with a 100,000 MWCO.

2.5 VLP Characterization

2.5.1 Western Blot Analysis

1. Equipments and buffers for casting 10 % SDS-polyacrylamide gel electrophoresis (PAGE).
2. Equipments and buffers for western blot analysis.
3. Primary antibody for rabies glycoprotein detection: Anti-rabies rabbit polyclonal serum (*see* **Note 3**).
4. Secondary antibodies for western blot analysis: HRP-conjugated goat anti-rabbit immunoglobulin.
5. Chemiluminescent detection reagents.

2.5.2 Dynamic Light Scattering Analysis

1. Dynamic light scattering (DLS) equipment: Nano ZS particle-size analyzer (Malvern Zetasizer, Malvern Instruments Ltd, UK).
2. Specific DLS equipment software: Nanov510 (Malvern Ltd, UK).
3. Low-volume cuvette for aqueous samples.

2.5.3 Transmission Electron Microscopy and Immunogold Analysis

1. Formvar-coated 300-mesh copper grids for electron microscopy.
2. 2 % Uranyl acetate solution.
3. Tweezers, 0.22 μm filtered distilled water, and filter papers.
4. Primary antibody for rabies glycoprotein detection: mAb anti-glycoprotein (*see* **Note 2**).
5. Secondary antibody for immunogold detection: Anti-mouse 6 nm gold-conjugated antibody (Colloidal Gold-AffiniPure goat anti-mouse IgG, Jackson ImmunoResearch, USA).
6. Transmission electron microscope (TEM): Jeol JSM-100 CX II (Jeol, Japan) or other equivalent.

2.6 VLP Immunization

2.6.1 Humoral Immune Response Analysis

1. Female 4–5-week-old BALB/c mice.
2. Freund's incomplete adjuvant.
3. Syringes and needles for animal injection.
4. Inactivated rabies virus vaccines to be injected as a positive control: Human vaccine and veterinary vaccine.
5. Equipment and buffers for specific indirect ELISA.
6. Secondary antibodies for specific indirect ELISA analysis: HRP-conjugated goat anti-mouse immunoglobulin.

2.6.2 Protection Assays: Virus Challenge

1. CF-1 mice strain.
2. Sixth International Standard for Rabies vaccine (WHO International Standard, NIBSC code: 07/162).
3. Challenge Virus Standard (CVS, rabies virus) [20].
4. Syringes and needles for animal injection.

3 Methods

3.1 Lentivirus Production and Titration

1. The day before the assay, seed HEK293 cells at a concentration of 4×10^5 cells/ml in a 10 cm diameter plate and incubate ON at 37 °C with 5 % CO_2.
2. Transfer 2.5 ml of DMEM basal medium to a 15 ml sterile tube and add 50 μl of Lipofectamine® 2000 reagent. Incubate at RT for 5 min.
3. Transfer 2.5 ml of DMEM basal medium to another 15 ml sterile tube and add 2.5 μg of pRSV-REV, 3.6 μg of pMD.G, 6.5 μg of pMDLG/pRRE, and 10 μg of pLV-G constructs.
4. Mix the content of both tubes and vortex. Incubate at RT for 20 min to allow DNA–lipid complex formation.
5. During the incubation, wash gently the cells' monolayer with 5 ml of DMEM.
6. Discard the culture medium and add the DNA–lipid complex to the cells. Incubate for a minimum of 4 h.
7. Add medium supplemented with FCS to reach a final concentration of 10 % V/V. Incubate for 24–48 h.
8. Harvest and clarify the supernatant by centrifuging at $200 \times g$ for 10 min.
9. Filter using a 0.45 μm filter unit.
10. Aliquot the clarified supernatant containing the lentivirus and store at −80 °C.
11. Calculate the titer of the produced lentivirus with the HIV-1 p24 ELISA kit (QuickTiter™ Lentivirus Titer Kit, Cell Biolabs Inc., USA) or another analogue method (*see* **Note 4**).

3.2 Cell Line Development and Clone Selection

1. Seed HEK293 cells at a concentration of 3×10^4 cells/ml in a 6-well plate and incubate ON at 37 °C with 5 % CO_2.
2. Discard the supernatant and add the amount of lentivirus to achieve an MOI of 20 in a final volume of 1 ml. Incubate at 37 °C for 16 h.
3. Discard the supernatant with the rest of lentivirus and add 3 ml of DMEM 10 % FCS. Incubate for another 72 h.
4. Select recombinant cells with puromycin at 1 μg/ml using a not transduced well as a negative control (*see* **Note 5**).
5. Analyze the recombinant cell line to confirm the rabies glycoprotein expression by flow cytometry and fluorescent microscopy (Subheadings 3.3.1 and 3.3.2).
6. Clone the recombinant cell line by dilution method or FACS isolating single cells into 96-well plate.
7. Analyze the individual clones by flow cytometry.

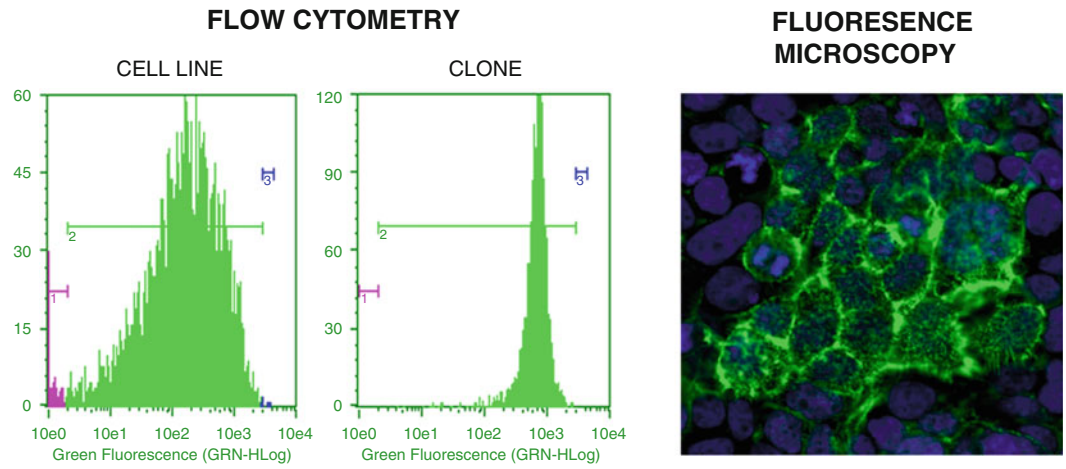

Fig. 2 Cell line and clone characterization to confirm rabies glycoprotein expression. Cells were incubated with a specific monoclonal antibody and with AlexaFluor 488®-conjugated goat anti-mouse antibody and analyzed by flow cytometry. The cell monolayer was observed by fluorescence microscopy, confirming the membrane localization of the glycoprotein

3.3 Cell Line and Clone Analysis (See Fig. 2)

3.3.1 Flow Cytometry

1. Detach the monolayer of the recombinant cell line using trypsin and count the cells. Prepare not transduced cells as a negative control for the assay.
2. Incubate a total of 1×10^5 cells in DMEM basal medium with a 1:1000 dilution of a monoclonal antibody against rabies G protein, for 30 min at RT.
3. Wash the cells with DMEM basal medium and incubate with a 1:1000 dilution of AlexaFluor 488®-conjugated goat anti-mouse antibody, for 30 min at RT.
4. Wash the cells with DMEM basal medium and analyze the cells by flow cytometry.
5. Analyze not only the percentage of fluorescent cells but also the fluorescence intensity (usually called X-*mean*) that correspond to the glycoprotein expression level.

3.3.2 Fluorescence Microscopy

1. Seed the recombinant cell line at a concentration of 1×10^5 cells/ml over a chamber slides for cell culture and incubate for 48 h.
2. Remove the supernatant and wash the monolayer gently with PBS.
3. Fix cells with a 4 % paraformaldehyde solution, during 30 min at RT.
4. Wash twice with PBS (repeat this step after each following incubation).

5. Incubate the monolayer with a G protein-specific monoclonal antibody (diluted 1:100 in PBS, 0.1 % BSA), for 30 min at RT.
6. Incubate the cells with AlexaFluor 488®-conjugated goat anti-mouse antibody for 30 min at RT (diluted 1:1000 in PBS, 0.1 % BSA).
7. Dye the nuclei with a DAPI solution (4′,6-diamidino-2-phenylindole) in a final concentration of 1 μg/ml for 5 min.
8. Analyze subcellular localization of G protein with a fluorescence microscope.

3.4 VLP Purification

1. Seed the VLPs expressing HEK293 cells in a 150 cm^2 T flask at a final concentration of 4×10^5 cells/ml with DMEM 10 % FCS and incubate ON at 37 °C with 5 % CO_2.
2. Exchange the supernatant for DMEM medium but supplemented with 1 % FCS (*see* **Note 6**). Incubate for 40–72 h at 37 °C with 5 % CO_2.
3. Harvest the medium containing the VLPs and clarify by low-speed centrifugation.
4. Centrifuge at $10{,}000 \times g$ to remove any cellular debris.
5. Filter using a 0.45 μm filter unit.
6. Layer the clarified harvest over a 30 % sucrose cushion and centrifuge for 3 h at $65{,}000 \times g$ or more.
7. Discard the supernatant and resuspend the VLP pellet with RV-VLP stabilization buffer.
8. Prepare a discontinuous iodixanol gradient (20, 30, 40, 50 %).
9. Layer the partially purified VLPs over the density gradient and centrifuge at $10{,}000 \times g$ for 6 h.
10. Analyze and aliquot the obtained band (*see* **Note 7**).
11. Exchange buffer using an Amicon® Ultra centrifugal unit with a 100,000 MWCO and RV-VLP stabilization buffer.
12. Store at 4 °C for further analysis.

3.5 VLP Characterization (See Fig. 3)

During early stages of development, VLP characterization is essential to know the main characteristics of the particles. Although there is a wide range of techniques that should be performed to fully understand the nature and structural characteristics of the particles under analysis [10, 19], simple assays, as western blot, DLS, and TEM, are recommended as the initial studies to know the size, shape, polydispersity, and antigenic content of the VLPs under development.

3.5.1 Western Blot Analysis

1. Mix 30–50 μl of the obtained band with SDS-PAGE loading buffer.
2. Load in a 10 % SDS-PAGE and run.

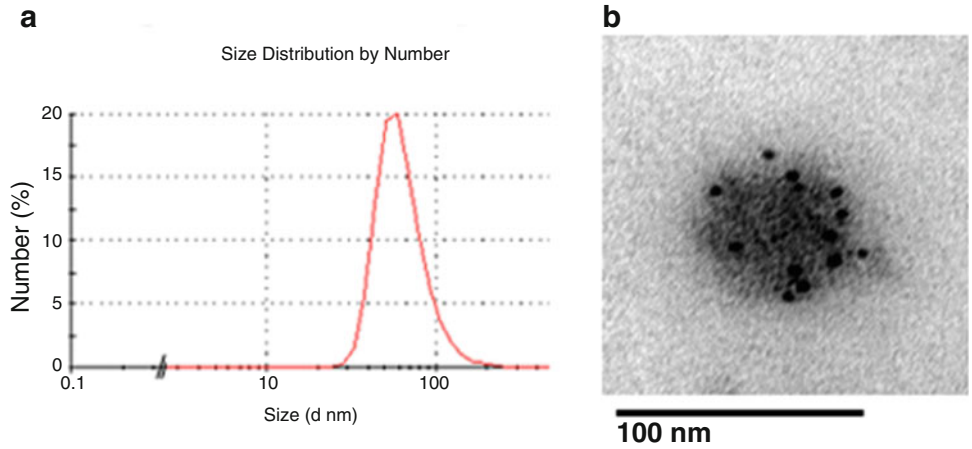

Fig. 3 Rabies virus-like particle characterization. (**a**) Dynamic light scattering analysis of purified VLPs. (**b**) Immunogold electron microscopy of purified VLPs

3. Blot gel on filter and block with 5 % skin milk in TBS buffer.
4. Incubate with a primary antibody for rabies glycoprotein detection and a secondary antibody HRP conjugated. Wash three times for 5 min with 0.05 % Tween-20/TBS buffer.
5. Reveal by chemiluminescent method.

3.5.2 Dynamic Light Scattering Analysis

1. Filter the purified VLPs through 0.45 μm and fill the cuvette for DLS.
2. Run almost ten consecutive measurement of a single sample using the specific equipment software (Nanov510, *see* **Note 8**).
3. Analyze the hydrodynamic diameter and the distribution of the purified particles (*see* **Note 9**).

3.5.3 Immunogold Electron Microscopy Analysis

1. Filter the purified VLPs, as well as all the buffers and water to be used in the assay, through 0.45 μm filter.
2. Adsorb 10 μl of purified VLPs to a formvar-coated 300-mesh copper grid for 2 min.
3. Remove the excess with filter paper and wash twice with 2 % BSA in TBS. Block with 2 % gelatine in TBS, for 30 min at RT.
4. Float the grid over a drop of monoclonal antibody anti-glycoprotein diluted in BSA/TBS and incubate for 1 h at RT (*see* **Note 10**). Wash three times with BSA/TBS.
5. Repeat the previous step but adsorbing a 1:20 dilution of secondary gold-conjugated antibody in BSA/TBS.
6. Stain the sample with 2 % uranyl acetate for 2 min.
7. Examine the grid using a transmission electron microscope.

3.6 VLP Immune Response

3.6.1 Immunization of Mice and Antibody Titration

1. Prepare the correct dilution, in RV-VLP stabilization buffer, of purified RV-VLPs containing the same glycoprotein content of a 1:20 dilution of a human rabies vaccine dose. Prepare the same dilutions of the human and veterinary rabies vaccine.
2. Mix properly the samples with Freund's incomplete adjuvant and inject 100 μl intramuscularly to five animals per group (day 0).
3. Give a booster on day 12 and collect blood samples on day 19.
4. Calculate the titer of antibodies in the obtained sera by indirect specific ELISA.

3.6.2 Protection Assays: Virus Challenge

1. Prepare 4 fivefold dilutions of the test and standard vaccine (1:5; 1:25, 1:125, 1:625) in PBS.
2. Inject intraperitoneally 16 mice per group with 0.5 ml of the dilutions of the test and reference vaccine on days 0 and 7.
3. On day 14, challenge the immunized mice injecting intracerebrally 0.03 ml of a dilution of CVS containing 25 LD_{50}. Observe mice during the following 14 days and record the number of die mice.
4. Calculate the 50 % end-point dilution ($ED_{50\%}$) of each sample and the final relative potency of the test vaccine as follows (Ref. 20):

$$RP = \frac{\text{Reciprocal of ED50 \% of TV}}{\text{Reciprocal of ED50 \% of RV}} \times \frac{\text{dose of TV}}{\text{dose of RV}}$$

where
TV = test vaccine.
RV = reference vaccine.
Dose = volume of a single vaccine dose, as stated by the producer (*see* **Note 11**).

4 Notes

1. The pLV-G [11] is a lentiviral transfer vector constructed cloning the coding sequence of the rabies glycoprotein (PV strain) into the vector pLV-PLK [21].
2. The monoclonal antibody used to analyze the rabies glycoprotein expressed by the recombinant cell lines and present in the envelope of the RV-VLPs recognizes the protein in their native form, anchored in the membrane and forming trimers. This feature is crucial when studying the antigenic properties of a protein for vaccine development, as the structural conformation is usually important to trigger the induction of neutralizing antibodies in the immune response developed.

3. For western blot analysis a polyclonal serum against rabies proteins was used. This serum was obtained by immunizing a rabbit with a commercial rabies vaccine.
4. Using this titer kit the physical titer is being calculated (the amount of p24 HIV-1 core protein associated to lentivirus particles), expressed in LP/ml. It is not the infectious titer, usually expressed as TU/ml. Generally, the infectious titer varies among different cell lines and usually 10^6 TU/ml corresponds to $10^{8–9}$ LP/ml. Other methods to quantify lentiviral particles are the reverse transcriptase (RT) activity by product-enhanced RT assay or RNA amount in viral supernatant by qPCR.
5. For recombinant cell selection a multi-step gradual selection protocol could be performed: our group has previously developed a method [21] through which cells are incubated from 1 up to 250 μg/ml of puromycin, but the selection agent is gradually changed every 7 days on the same plates. This method allows to maintain the cells in culture condition up to 200 μg/ml puromycin and achieve higher expression levels of the gen of interest.
6. It is important to reduce the total amount of FCS in the supernatant containing RV-VLPs. The FCS has a lot of bovine serum albumin (BSA) that has a similar molecular weight compared to rabies glycoprotein (62–66 kDa) and interferes in the analysis, mostly in western blot assays.
7. A simple method of determining the density of gradient fractions is to measure the absorbance (optical density) of the obtained fractions. With OptiPrep™ Density Gradient Medium it is possible to measure the absorbance at 340 nm and calculate the approximate particle density by following the manufacturer's instructions (Application Sheet C53, Axis-Shield).
8. This software could convert the intensity-based measurement to a size distribution based on the volume or number of particles. This conversion is only valid if some parameters, like particle polydispersity, are within accepted values. Besides, confirmation by other methods like TEM is recommended.
9. The hydrodynamic diameter is always higher than the diameter calculated by other methods due to the ion layer surrounding the particles in solution.
10. Several dilutions should be performed in order to achieve the best result. Try dilutions between 1:50 and 1:12,000.
11. The relative potency value obtained in the NIH test should become the minimum value recommended by WHO. The minimum potency required is 2.5 IU per human dose and 1 IU in the smallest prescribed dose for veterinary vaccine.

Acknowledgements

The authors would like to thank Juan Pablo Soto (Institutional Image, Universidad Nacional del Litoral, Argentina) for technical support.

References

1. Yousaf MZ, Qasim M, Zia S, Khan MR, Ashfaq UA, Khan S (2012) Rabies molecular virology, diagnosis, prevention and treatment. Virol J 9:50
2. Schnell MJ, McGettigan JP, Wirblich C, Papaneri A (2010) The cell biology of rabies virus: using stealth to reach the brain. Nat Rev Microbiol 8:51–61
3. Gautret P, Parola P (2012) Rabies vaccination for international travelers. Vaccine 30:126–133
4. Meslin FX, Briggs DJ (2013) Eliminating canine rabies, the principal source of human infection: what will it take? Antivir Res 98:291–296
5. World Health Organization (2013). WHO expert consultation on rabies. Second report. World Health Organ Tech Rep Ser 982
6. Ertl HC (2009) Novel vaccines to human rabies. PLoS Negl Trop Dis 3(9):e515
7. Yang DK, Kim HH, Lee KW, Song JY (2013) The present and future of rabies vaccine in animals. Clin Exp Vaccine Res 2:19–25
8. Noad R, Roy P (2003) Virus-like particles as immunogens. Trends Microbiol 11:438–444
9. Roldão A, Mellado MCM, Castilho LR, Carrondo MJT, Alves PM (2010) Virus-like particles in vaccine development. Expert Rev Vaccines 9(10):1149–1176
10. Lua LHL, Connors NK, Sainsbury F, Chuan YP, Wibowo N, Middelberg APJ (2014) Bioengineering virus-like particles as vaccines. Biotechnol Bioeng 111:425–440
11. Fontana D, Kratje R, Etcheverrigaray M, Prieto C (2014) Rabies virus-like particles expressed in HEK293 cells. Vaccine 32:2799–2804
12. Wu CY, YehYC YYC, Chou C, Liu MT, Wu HS, Chan JT, Hsiao PW (2010) Mammalian expression of virus-like particles for advanced mimicry of authentic influenza virus. Plos One 5(3):e784
13. Chuan Li C, Liu F, Liang M, Zhang Q, Wang X, Wang T, Li J, Li D (2010) Hantavirus-like particles generated in CHO cells induce specific immune responses in C57BL/6 mice. Vaccine 28:4294–4300
14. Hua RH, Li YN, Chen ZS, Liu LK et al (2014) Generation and characterization of a new mammalian cell line continuously expressing virus-like particles of Japanese encephalitis virus for a subunit vaccine candidate. BMC Biotechnol 14:62
15. Dull T, Zufferey R, Kelly M, Mandel RJ, Nguyen M, Trono D, Naldini L (1998) A third-generation lentivirus vector with a conditional packaging system. J Virol 72:8463–8471
16. Naldini L, Blomer U, Gallay P, Ory D, Mulligan R, Gage FH et al (1996) In vivo gene delivery and stable transduction of nondividing cells by a lentiviral vector. Science 272:263–267
17. Picanço-Castro V, Fontes AM, de Sousa Russo-Carbolante EM, Covas DR (2008) Lentiviral-mediated gene transfer – a patent review. Expert Opin Ther Pat 18(5):1–15
18. Federico M (ed) (2010) Lentivirus gene engineering protocols. 2nd edition. Methods in Molecular Biology, Vol. 614. Humana, UK
19. Zeltins A (2012) Construction and characterization of virus-like particles: a review. Mol Biotechnol 53:92–107
20. Wilbur LA, Aubert MFA (1996) The NIH potency test. In: Meslin FX, Kaplan MM, Koprowsky H (eds) Laboratory techniques in rabies. WHO, Geneva, Switzerland, pp 360–366
21. Prieto C, Fontana D, Etcheverrigaray M, Kratje R (2011) A strategy to obtain recombinant cell lines with high expression levels. Lentiviral vector-mediated transgenesis. BMC Proc 5(8):P7

Chapter 8

Analytic Vaccinology: Antibody-Driven Design of a Human Cytomegalovirus Subunit Vaccine

Anna Kabanova and Daniele Lilleri

Abstract

Identification of the most relevant protective antigens has represented a considerable obstacle for the development of subunit vaccines against viral infections, including human cytomegalovirus (HCMV) infection. This chapter describes the method of analytic vaccinology, centered on the clonal analysis of human B cell response to HCMV, which represents an essential tool for assessing the impact of individual viral antigens in the antiviral antibody response. By providing key information on the immunogenicity and protective properties of the antibodies elicited by viral proteins, the analytic vaccinology method guides the selection of the most appropriate vaccine candidates. Here we discuss methodologies for the generation of human monoclonal antibodies from B cells of immune donors, antibody screening in in vitro assays of antigen binding and virus neutralization, and strategies of animal immunization useful for the preclinical evaluation of selected viral antigens. The approach of analytic vaccinology could be universally applied to the characterization of B-cell immune response against any virus of interest and ultimately used for vaccine development.

Key words Virus, Subunit vaccine, Viral antigens, Human monoclonal antibodies, Screening, Neutralizing, Non-neutralizing

1 Introduction

Antibody response to viruses is typically dominated by non-neutralizing antibodies directed against internal or surface proteins in a denatured or post-fusion conformation, as it has been shown in the example of human cytomegalovirus (HCMV) and other viruses [1, 2]. Therefore, in order to design an effective vaccine, it is not enough to identify the most immunogenic antigen among whole viral proteome, but an antigen that would specifically elicit a virus-neutralizing antibody response. Among analytic methods aimed at the classification of viral antigens according to their ability to elicit neutralizing antibodies, the isolation of human monoclonal antibodies represents one of the most efficacious tools. It is useful not only for characterization of the protective properties of

Sunil Thomas (ed.), *Vaccine Design: Methods and Protocols: Volume 1: Vaccines for Human Diseases*, Methods in Molecular Biology, vol. 1403, DOI 10.1007/978-1-4939-3387-7_8,

various viral antigens and identification of the most relevant vaccine candidates, but also for their production and formulation as recombinant subunit vaccines. As a whole, such approach has been termed "analytic vaccinology," reflecting that a comprehensive analysis of the human antibody response could be efficiently translated onto the vaccine development process [3].

We have recently demonstrated the potential of analytic vaccinology in case of HCMV [1], a pathogen causing severe disease in fetuses and newborns, when acquired during pregnancy, and in immunosuppressed individuals. We analyzed the human antibody response to HCMV infection and found that only a small fraction of HCMV-specific B cells produce neutralizing antibodies, while the great majority of anti-HCMV antibodies are non-neutralizing, consistent with the notion on the low efficiency of antiviral humoral response. When we focused our attention on the antibody response to the virus surface glycoproteins that mediate virus entry into cells, we observed markedly different profiles. For instance, antibodies to glycoprotein (g)B, an abundant virion glycoprotein that has been developed as an HCMV vaccine [4], were primarily non-neutralizing, whereas most of the antibodies to the complex formed by gH, gL, pUL128, pUL130, and pUL131 (the gHgL-pUL128L pentamer complex) neutralized HCMV infection with high potency [1]. We coined a term describing this particular property of the anti-pentamer antibody response and referred to it as the antibody response of high "specific activity." Based on our analysis, we generated a recombinant soluble pentamer complex and demonstrated that, upon formulation with various adjuvants and administration to mice, it elicited a sustained potent neutralizing antibody response of a high specific activity, equal to that observed in humans after natural HCMV infection [1, 5].

Our study has highlighted the suitability of analytic vaccinology approach for characterization of the antibody response to infection and for designing novel B cell vaccine candidates for any virus of interest. Here we propose a flowchart of the analytic vaccinology method that recapitulates our research strategy for the development of a pentameric HCMV vaccine and consists of six sequential steps (Fig. 1). Initial and crucial step of the method implies an isolation of human monoclonal antibodies (Box 1 of Fig. 1), followed by their functional screenings for the ability to neutralize virus infection (Box 2 of Fig. 1) and bind to viral antigens (Box 3 of Fig. 1). Such screening process allows the identification of viral antigens targeted by neutralizing antibodies and classification of those antigens according to the specific activity of antibody response they elicit. Subsequently, viral antigens of interest could be produced in a recombinant form (Box 4 of Fig. 1) and used for ELISA binding assays (Box 5 of Fig. 1). Ultimately, the immunogenicity and protective properties of selected antigens could be assessed by animal immunization and testing of immune

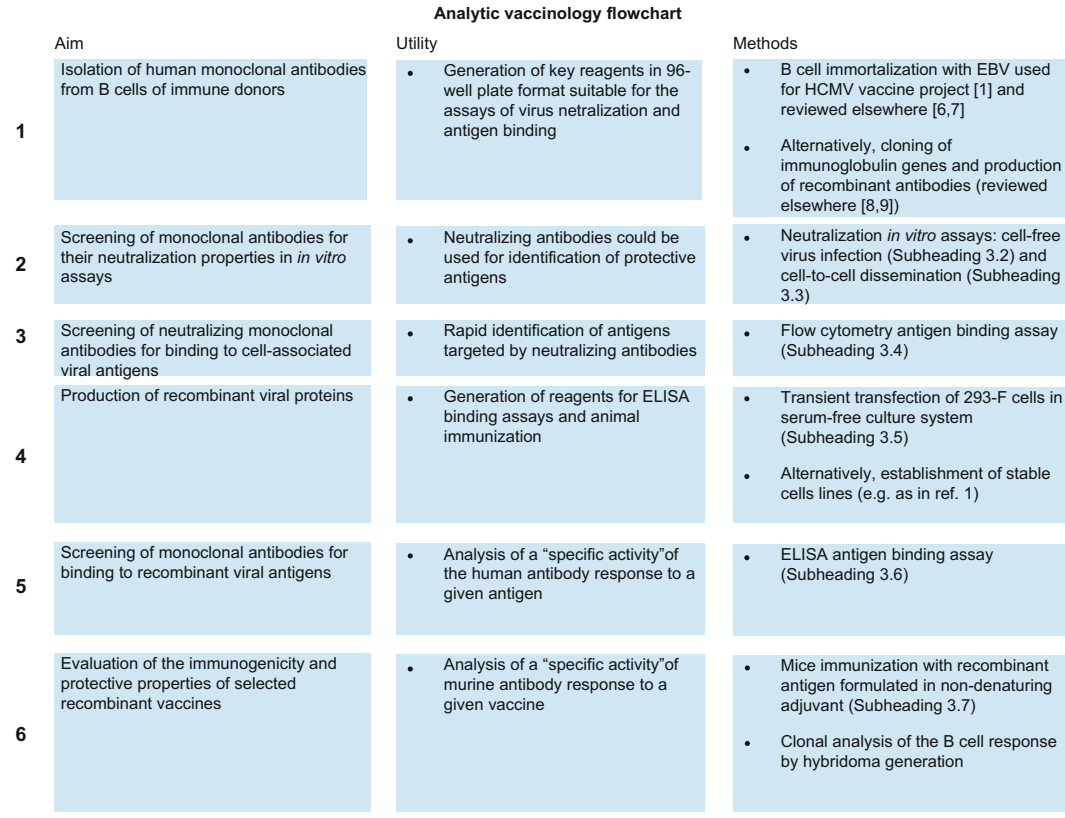

Fig. 1 Flowchart of the analytic vaccinology method

sera for virus neutralization (Box 6 of Fig. 1). B cell response to immunization could be further analyzed at the clonal level to assess the specific activity of the antibody response elicited by the vaccine.

In this chapter we do not describe protocols used for the isolation of human monoclonal antibodies, but rather share our considerations on the selection of HCMV-infected donors suitable for B cell isolation. In general, isolation of human monoclonal antibodies could be accomplished by two approaches: (1) generation of immortalized B cell clones used for the above-discussed HCMV vaccine project [1] and reviewed extensively elsewhere [6, 7], and (2) cloning of the genes for heavy and light immunoglobulin chains and their subsequent expression as recombinant antibodies, an alternative approach that has been gaining vast application in the biomedical field [8, 9]. In both cases it is essential to have an access to the peripheral blood or lymphoid tissue samples of immune donors, from which pathogen-specific immunoglobulin G-positive plasmablasts and memory B cells could be isolated and used in antibody-isolation procedures. For instance, in case of HCMV immune donors we observed that the neutralizing

antibody titers gradually rise and reach plateau at 3–6 months upon primary infection and then persist for up to 12–18 months afterwards [5]. Therefore, it is advisable to collect blood samples from HCMV donors in the range of 3–24 months after infection to obtain the highest yield of antibody-producing B cells.

1.1 Preparation of HCMV Stocks

HCMV has a broad cell tropism and exploits multiple glycoprotein complexes present on the virion envelope to gain entry into host cells. Among those, some proteins—as gB—are universally used by virus for fusion with the plasma membrane of all susceptible cells, while some surface glycoproteins are essential for infection of particular cell lineages. For instance, the pentameric gHgLpUL128L complex is essential for infection of endothelial, epithelial, and myeloid cells but not fibroblasts, while a dimeric gHgL glycoprotein complex is necessary for infection of fibroblasts [10–12].

The ability to infect endothelial, epithelial, and myeloid cells is a nonessential virus-encoded function. As a consequence, an extensive in vitro propagation of the virus in fibroblasts leads to the accumulation of mutations in pUL128L locus of the viral genome and subsequent loss of the functional pentameric gHgLpUL128L complexes in virions [10]. Accordingly, fibroblast-adapted laboratory HCMV strains (such as AD169, Towne, and Davis) have a dramatically reduced capacity to infect epithelial-like cells and are, therefore, incompatible with neutralization assays in which the activity of pentamer-specific antibodies is tested. In this section we describe a protocol for HCMV propagation in endothelial cells suitable for the preparation of viral stocks with a full spectrum of tropism.

1.2 Neutralization In Vitro Assay of Cell-Free Virus Infection

In order to assess the neutralizing potency of an HCMV-specific antibody, it is necessary to test it in neutralization assays on both epithelial and non-epithelial cell types. In this section we provide a standardized protocol of HCMV neutralization assay on epithelial cells and fibroblasts. These assays are aimed at assessing the blocking of virus entry by a purified antibody or an antibody-containing supernatant. For major convenience and an easy upscaling of the screening, we propose a 96-well plate format for both virus neutralization and antibody binding assays and suggest setting up human monoclonal antibody cultures (e.g., EBV-immortalized B cell cultures) in a similar format.

1.3 Neutralization In Vitro Assay of Virus Cell-to-Cell Dissemination

Correlation between the in vitro-neutralizing activity of an antibody and its protective function in vivo is difficult to predict, especially in case of HCMV for which no reliable animal model of the infection is available. Complications further arise from the fact that HCMV infectious pool in the body disseminates in cell-associated form rather than by cell-free viral particles [13–15]. Therefore,

virus neutralization assays should be complemented with in vitro assays of virus cell-to-cell dissemination. To measure the dissemination-inhibiting activities of the antibodies, they could be tested for their ability to block the formation of viral plaques in epithelial cells, which is a consequence of cell-to-cell virus spreading. In addition, we developed an assay to test the antibody ability to block virus transfer from infected endothelial cells to leukocytes, which are considered to be principal HCMV-spreading vehicles [16, 17]. However, due to its difficult standardization, this assay is not described in this chapter.

1.4 Flow Cytometry Antigen Binding Assay: Antibody Binding to Cell-Associated Viral Antigens

This assay allows identification of the targets for isolated monoclonal antibodies. Viral antigens of interest could be cloned and expressed in cell-associated form by transient transfection of cell lines, e.g., HEK293T or CHO cells. This experimental approach allows avoiding laborious protein purification procedures and permits to test various protein combinations, which is particularly relevant when antibody epitopes are conformational (i.e., formed by a combination of viral antigens).

1.5 Production of Recombinant Viral Antigens in Transiently Transfected 293-F Cells

Selected viral antigens could be produced in a recombinant subunit form by transient transfection of 293-F cells in serum-free FreeStyle™ 293 Expression System (Gibco®). We found this expression system suitable for (1) medium-scale production of viral proteins (0.2–1 mg of purified protein per liter of cell culture), and (2) production of viral protein-containing supernatants useful for ELISA antigen binding assays.

1.6 ELISA Antigen Binding Assay: Antibody Binding to Recombinant Viral Antigens

Since expression yields vary greatly among recombinant viral glycoproteins, the difficulties associated with their purification could pose substantial difficulties on the production of sufficient amounts of reagents for high-throughput ELISA screenings. We have therefore set up a sensitive sandwich ELISA assay using specific antibodies to capture soluble non-purified viral proteins directly from 293-F cell culture supernatants.

1.7 Mice Immunization with Recombinant Viral Antigens Formulated in Non-denaturing Adjuvant

Given the importance of preserving native conformation of soluble viral glycoproteins, it is important to use potent but non-denaturing adjuvants for vaccine formulation. A polyanionic carbomer adjuvant (carbopol C974), which was found to affect the antigenicity of the complexes only minimally [18, 19], appears to be highly suitable for this purpose. We therefore suggest to use carbopol adjuvant at the initial stages of preclinical vaccine evaluation to identify the most promising vaccine candidates, which could be subsequently tested with adjuvants approved for human use (e.g., alum, MF59, and Ribi) as exemplified in our work [1].

2 Materials

2.1 Preparation of HCMV Stocks

1. Cells: Human umbilical vein endothelial cells (HUVEC, ATCC) (*see* **Note 1**).
2. Cell culture medium: EGM-2 BulletKit medium (Lonza).
3. Cell culture flasks: 25 cm^2 sterile flasks for adherent cells.
4. Eppendorfs or cryovials for virus-containing supernatant stockage at ≤ – 80 °C.
5. Freezer or liquid nitrogen tank.
6. HCMV strain adapted to growth on endothelial cells (e.g., VR1814).

2.2 Neutralization In Vitro Assay of Cell-Free Virus Infection

1. Cells: ARPE-19 retinal pigmented epithelium cell line (ATCC), MRC-9 fibroblast cells (ATCC).
2. Cell culture medium for ARPE-19 maintenance: D-MEM/F12 (Gibco, Invitrogen) supplemented with 10 % fetal bovine serum or iron-supplemented bovine calf serum, 50 U/mL penicillin, 50 μg/mL streptomycin.
3. Cell culture medium for MRC-9 maintenance: Minimum Essential Medium Eagle (Sigma-Aldrich) supplemented with 10 % FBS, glutamine, nonessential amino acids, 50 U/mL penicillin, 50 μg/mL streptomycin, and 100 μg/mL kanamycin sulfate.
4. Cell culture flasks and plates: 75 cm^2 sterile flasks for adherent cells for routine maintenance of cell lines; sterile 96-well flat-bottom culture plates for adherent cells; sterile 96-well U-bottom plates for antibody/virus mixing.
5. Virus stocks obtained with Method 3.1 "Preparation of HCMV stocks."
6. B cell supernatants containing HCMV-specific antibodies, human/mouse immune sera, or purified HCMV-specific monoclonal antibodies.
7. Ice-cold 5 % acetic acid in methanol: Dilute 2.5 mL of acetic acid in 47.5 mL of methanol, and store at –20 °C.
8. Anti-pp72 antibody conjugated to a fluorescent dye: Prepare 1 μg/mL solution of antibody in phosphate buffer saline (PBS) (*see* **Note 2**).
9. Solution of 4′,6-diamidino-2-phenylindole dihydrochloride (DAPI): Prepare 200 ng/mL DAPI in PBS, and store at +4 °C.
10. BD Pathway Bioimaging systems or BioTek Cytation 3 cell imaging reader (*see* **Note 3**).

2.3 Neutralization In Vitro Assay of Virus Cell-to-Cell Dissemination

1. Cells: ARPE-19 retinal pigmented epithelium cell line (ATCC.
2. Cell culture medium for ARPE-19 maintenance: D-MEM/F12 (Gibco, Invitrogen) supplemented with 10 % fetal bovine serum or iron-supplemented bovine calf serum, 50 U/mL penicillin, 50 μg/mL streptomycin.
3. Cell culture flasks and plates: 75 cm^2 sterile flasks for adherent cells for routine maintenance of cell lines; sterile 96-well flat-bottom culture plates for adherent cells; sterile 96-well U-bottom plates for antibody/virus mixing.
4. Virus stocks obtained with Method 3.1 "Preparation of HCMV stocks."
5. B cell supernatants containing HCMV-specific antibodies, human/mouse immune sera, or purified HCMV-specific monoclonal antibodies.
6. Ice-cold 5 % acetic acid in methanol: Dilute 2.5 mL of acetic acid in 47.5 mL of methanol, and keep at –20 °C.
7. Anti-pp72 antibody conjugated to fluorescent dye: Prepare 1 μg/mL solution of antibody in PBS (*see* **Note 2**).
8. Solution of 4′,6-diamidino-2-phenylindole dihydrochloride (DAPI): Prepare 200 ng/mL DAPI in PBS, and store at +4 °C.

2.4 Flow Cytometry Antigen Binding Assay: Antibody Binding to Cell-Associated Viral Antigens

1. Fixed HEK293T cells ectopically expressing viral antigens and control HEK293T cells (*see* **Note 4**).
2. WASH buffer: Prepare PBS with 1 % bovine calf serum, 2 mM EDTA, 0.5 % saponin, and 0.05% NaN_3; store at +4 °C.
3. Primary HCMV-specific antibody: B cell supernatants containing HCMV-specific antibodies, purified monoclonal HCMV-specific antibodies, and human/mouse sera for positive and negative control staining.
4. Fluorescently labeled secondary antibody: Dilute at 1 μg/mL in WASH buffer.
5. Non-sterile 96-well U-bottom plate.
6. Benchtop centrifuge with the adaptors for culture plates.
7. Flow cytometer.

2.5 Production of Recombinant Viral Antigens in Transiently Transfected 293-F Cells

1. FreeStyle 293-F cells (Gibco).
2. FreeStyle 293 Expression medium (Gibco).
3. OptiPro SFM medium for transfection (Gibco).
4. Sterile vent-cap Erlenmeyer cell culture flasks (1 L capacity).
5. Orbital shaker in cell incubator.

6. Endotoxin-free water.
7. Linear polyethylenimine (PEI) solution ("Max", Mw 40,000, Polysciences): Prepare 1 mg/mL solution of PEI in endotoxin-free water, sterile filter with 0.22 μm, and store in 1.2 mL aliquots at −20 °C.
8. Purified plasmids encoding viral proteins of interest.
9. Filter flasks for large volumes, 0.22 μm.
10. Bovine serum albumin: Prepare 5 % solution in PBS, filter with 0.22 μm, and store at +4 °C.

2.6 ELISA Antigen Binding Assay: Antibody Binding to Recombinant Viral Antigens

1. Half-area polystyrene 96-well ELISA plates (flat bottom, Corning) (*see* **Note 5**).
2. Bicarbonate buffer for plate coating: Dissolve 3.03 g Na_2CO_3, 6.0 g $NaHCO_3$, 0.2 g NaN_3 in 1 L of ultrapure water, filter with 0.45 μm filter.
3. ELISA wash buffer: PBS with 0.05 % Tween-20.
4. ELISA blocking buffer: 3 % Skimmed milk in PBS.
5. Antibody dilution buffer: 10 % Bovine calf serum in PBS.
6. Primary HCMV-specific antibody: B cell supernatants containing HCMV-specific antibodies, purified monoclonal HCMV-specific antibodies, and human/mouse sera for positive and negative control staining.
7. Secondary antibody conjugated to alkaline phosphatase: Anti-human IgG in case of primary human antibody, anti-mouse IgG in case of primary mouse antibody.
8. Bicarbonate buffer for ELISA development: Dissolve 1.59 g Na_2CO_3, 2.92 g $NaHCO_3$, and 0.2 g NaN_3 in 1 L of ultrapure water, and filter with 0.45 μm filter.
9. Substrate solution: 1 mg/mL p-Nitrophenyl phosphate diluted in bicarbonate buffer for ELISA development.
10. ELISA microplate reader.

2.7 Mice Immunization with Recombinant Viral Antigens Formulated in Non-denaturing Adjuvant

1. 6–9-week-old Balb/c female mice.
2. Carbopol® 974P NF Polymer (Lubrizol Advanced Materials).
3. Endotoxin-free water.
4. 10 M NaOH solution.
5. pH paper.
6. Purified HCMV proteins.
7. Syringes with 23G needle.

3 Methods

All experimental procedures involving human biological samples, HCMV-containing supernatants, and live (non-fixed) HCMV-infected cells should be performed in laboratory with a biosafety level 2. All virus-containing liquids and materials should be trashed according to the respective guidelines.

3.1 Preparation of HCMV Stocks

1. Inoculate 1 mL of VR1814-infected HUVEC supernatant (cell-free virus, 10^7 PFU/mL) into 25 cm^2 HUVEC flask.
2. Incubate for 2 h at 37 °C to allow virus adsorption.
3. Discard inoculum and add EGM-2 BulletKit medium.
4. Refresh medium the following day.
5. When the cells are all infected (7–8 days after infection) collect and titrate the supernatant (*see* **Note 6**).
6. The supernatant can be harvested multiple times from the same flask.
7. Aliquote and store virus at –80 °C or in liquid nitrogen (*see* **Note 7**).

3.2 Neutralization In Vitro Assay of Cell-Free Virus Infection

Day 0

1. Prepare a 96-well plate layout of the neutralization assay including negative and positive controls (*see* **Note 8**).
2. Seed ARPE-19/MRC-9 at 10,000/15,000 cells per well in the final volume of 200 μL of culture medium in 96-well flat-bottom plate 18–24 h before the infection (*see* **Note 9**).

Day 1

3. Prepare antibody dilutions in ARPE-19/MRC-9 culture medium in the final volume of 50 μL per well in an empty 96-well U-bottom plate (*see* **Note 10**).
4. Prepare virus dilution in ARPE-19/MRC-9 culture medium at 6000–8000 pfu/mL considering that 50 μL of the virus should be added to each well of the neutralization assay plate (*see* **Note 11**).
5. Add 50 μL of the virus preparation to 50 μL of the antibody dilution, pipette 2–3 times, and incubate the plate in the 37 °C incubator for 1 h.
6. Aspirate cell culture medium from ARPE-19/MRC-9 plates and add virus-antibody mixture atop (*see* **Note 12**).
7. Leave cells in the 37 °C incubator for 24–40 h (*see* **Note 13**).

Day 3

8. Cell fixation: Aspirate infectious supernatants from the neutralization assay plate and add 100 μL/well of ice-cold 5 % acetic acid in methanol.

9. Leave plates on ice or at −20 °C freezer for 7 min.
10. Aspirate the fixation liquids from the neutralization assay plate and add 250 µL/well of PBS (*see* **Note 14**).
11. After 5 min of incubation, aspirate PBS and add 50 µL/well of 0.5 µg/mL anti-pp72 antibody. Incubate on ice in the dark for 1 h.
12. Aspirate anti-pp72 antibody solution and add 250 µL/well of PBS. Incubate for 5 min at RT.
13. Aspirate washing solution and add 150 µL/well of 200 ng/mL DAPI diluted in PBS.
14. Perform counting of the infected cells on automated Pathway systems or Cytation 3 and calculate the number/percentage of infected cells per each well of the neutralization assay plate (*see* **Note 15**).
15. The number of infected cells can be plotted against the serum dilution/antibody concentrations to perform a nonlinear regression analysis with a statistical software (e.g., Prism 5 GraphPad) and to calculate serum dilution factor (1/ED50 and 1/ED80) or antibody concentration (IC50 and IC80) resulting in 50 % or 80 % inhibition of infection, respectively.

3.3 Neutralization In Vitro Assay of Virus Cell-to-Cell Dissemination

Day 0

1. Seed ARPE-19 cells at 10,000 cells per well in the final volume of µL in 96-well flat-bottom plate 18–24 h before the infection (*see* **Notes 8** and **9**).

Day 1

2. Prepare antibody/serum dilutions in ARPE-19 culture medium in the final volume of 100 µL per well in an empty 96-well U-bottom plate (*see* **Note 10**).
3. Prepare virus dilution in ARPE-19 culture medium at 500 pfu/mL considering that 100 µL of the virus should be added to each well of the neutralization assay plate.
4. Aspirate cell culture medium from ARPE-19 plates and add virus atop (*see* **Note 12**).
5. After virus adsorption by centrifugation for 30 min at 700 × *g* and subsequent incubation for 1 h at 37 °C, aspirate supernatants and add antibody/serum dilutions (or control medium) to ARPE-19 plates.
6. Leave the cells in the 37 °C incubator for 96–120 h.

Days 5–6

7. Fix and stain the cells as in the Subheading 3.2 (**steps 8–13**).
8. Count the number of plaques at the epifluorescent microscope. The percentage of inhibition of plaque formation (PFI) can be

determined by dividing the difference between the number of viral plaques counted in the absence and in the presence of serum by the number of plaques in the absence of serum (×100). Subsequently, inhibition values can be plotted against the serum dilution/antibody concentrations to perform a non-linear regression analysis with a statistical software (e.g., Prism 5 GraphPad) and to calculate PFI50 resulting in 50 % inhibition of plaque formation.

3.4 Flow Cytometry Antigen Binding Assay: Antibody Binding to Cell-Associated Viral Antigens

1. Dispense 30,000 cells/well of formaldehyde-fixed HEK293T cells expressing viral antigens and control cells in a 96-well U-bottom plate.
2. Add the volume in wells up to 200 μL with WASH buffer and spin the plate in a centrifuge at 300 × *g* for 3 min. Trash supernatants by fast hand movement (cells remain in wells).
3. Add 200 μL WASH buffer per well and permeabilize cells for 15 min on ice.
4. Repeat centrifugation step and trash WASH buffer.
5. Add 30 μL/well of primary antibody diluted in WASH buffer and incubate cells for 30 min on ice (*see* **Note 16** for dilutions).
6. Add the volume in wells up to 200 μL with WASH buffer and spin the plate in a centrifuge at 300 × *g* for 3 min. Trash WASH buffer.
7. Repeat washing step.
8. Add 30 μL/well of 1 μg/mL of fluorescently labeled secondary antibody diluted in WASH buffer and incubate cells for 30 min on ice.
9. Repeat **steps 6** and **7**.
10. Resuspend cells in 100–200 μL of PBS and read the samples on flow cytometer.

3.5 Production of Recombinant Viral Antigens in Transiently Transfected 293-F Cells

1. Maintain 293-F cells in the log phase of growth in the cell incubator with orbital shaker.
2. One day before the transfection pass cells to 0.6–0.7 mln/mL. Final volume of 293-F cell culture in the 1 L culture flask should be 300 mL (*see* **Note 17**).

Day 1

3. On the day of transfection adjust cell concentration to 1 mln/mL with pre-warmed FreeStyle medium.
4. Dilute 500 μg of plasmid vector encoding viral protein in 6 mL of pre-warmed OptiPro SFM medium (*see* **Note 18**). Vortex briefly.
5. Dilute 1.2 mL of 1 mg/mL PEI solution in 6 mL of pre-warmed OptiPro SFM medium. Vortex briefly.

6. Mix DNA and PEI solution. Vortex the mixture and incubate for 10 min at room temperature.
7. Add DNA-PEI mixture dropwise into the cell culture flask.
8. Place the flask back into the incubator.

Day 8 (see **Note 19***)*

9. Dispense cells into 50 mL Falcon tubes and centrifuge at 500 × *g* for 10 min.
10. Collect cell supernatants and filter them with 0.22 μm filter flask to eliminate residual cells.
11. Add bovine serum albumin to final concentration of 0.1 % and store protein-containing supernatants in sterility at +4 °C (*see* **Note 20**). Alternatively, proceed with protein purification if the protein will be used for animal immunization (*see* **Note 21**).

3.6 ELISA Antigen Binding Assay: Antibody Binding to Recombinant Viral Antigens

1. The protocol provided is suitable for testing the reactivity of human HCMV-specific antibodies. In case of mouse HCMV-specific antibodies, the protocol should be changed accordingly (*see* **Note 22**).
2. Prepare a dilution of mouse monoclonal antibody specific for HCMV protein X in bicarbonate coating buffer at final concentration of 1 μg/mL (*see* **Note 23**).
3. ELISA plate coating: Add 25 μL/well of diluted antibody to ELISA plates and incubate for 2 h at room temperature. Alternatively, this incubation step could be performed for longer times, e.g. overnight at +4 °C. In such cases seal plates well with a special cover or parafilm.
4. Trash coating antibody and wash the plate two times with 200 μL/well of ELISA wash buffer.
5. Block plates with 100 μL/well of ELISA blocking buffer and incubate for 1 h at room temperature (*see* **Note 24**).
6. Trash and wash the plate two times with 200 μL/well of ELISA wash buffer.
7. Add 25 μL/well of 293-F cell supernatants containing HCMV protein X and incubate for 1.5 h at room temperature.
8. Wash ELISA plate two times with 200 μL/well of ELISA wash buffer.
9. Dilute primary human antibody in antibody dilution buffer: 0.001–10 μg/mL for purified antibodies, 1:100–1:10,000 dilution for HCMV-specific serum. B cell supernatants containing human monoclonal antibodies can be applied undiluted. Prepare serial dilutions, if necessary.
10. Add 25 μL/well of diluted primary antibody to ELISA plate and incubate for 1.5 h at room temperature.

11. Trash and wash the plate four times with 200 μL/well of ELISA wash buffer.
12. Dilute secondary anti-human alkaline phosphatase-conjugated antibody in antibody dilution buffer at a concentration recommended by the manufacturer.
13. Add 25 μL/well of diluted secondary antibody to ELISA plate and incubate for 45 min at room temperature.
14. Trash and wash the plate four times with 200 μL/well of ELISA wash buffer.
15. Add 80 μL/well of substrate solution to ELISA plates. Read plates at 405 nm when the signal reaches optimal values (*see* **Note 25**).

3.7 Mice Immunization with Recombinant Viral Antigens Formulated in Non-denaturing Adjuvant

Adjuvant preparation

1. Prepare 2 % weight/volume gel of carbopol in endotoxin-free H_2O: add carbopol powder slowly to endotoxin-free water (¾ of the final volume) in 50 mL Falcon tube, and mix rigorously after each addition with spatula till the gel does not appear completely transparent.
2. Equilibrate pH of the carbopol gel to 7.4 by adding 10 M NaOH dropwise. Mix rigorously with spatula after each NaOH addition. To test pH spread some carbopol on pH paper.
3. Aliquot carbopol gel in 1.5 mL Eppendorfs and store at −20 °C.

Vaccine formulation

4. On the day of the first priming immunization mix 5 μg of purified HCMV protein with 25 μL of carbopol gel (0.5 mg).
5. Formulate 2.5 μg of purified HCMV protein with 10 μL of carbopol gel (0.2 mg) for first and second boost immunizations.

Animal immunization

6. Immunize female Balb/c mice subcutaneously into flank with 100 μL of vaccine formulation on days 0 (prime), 14 (first boost), and 28 (second boost).
7. Bleed mice on days 13, 27, and 41 to evaluate serum titers of antigen-specific antibodies.
8. For hybridoma production boost mice with 10 μg of HCMV protein in PBS intravenously on day 42 (*see* **Notes 26** and **27**).

4 Notes

1. HCMV strains should be propagated in endothelial cells (HUVEC) to maintain endothelial and epithelial cell tropism, since passages in fibroblasts select virus variants unable to infect endothelial and epithelial cells [20]. Additionally, we

found that virus propagation in epithelial cells (ARPE-19) is rather inconvenient because small quantity of virus is released in culture supernatant.

2. We detect viral-infected cells at 24–48 h post-infection by immunostaining with a fluorescent dye-conjugated mouse monoclonal antibody recognizing pp72, one of the immediate early (IE) antigens of HCMV [21]. Immunostaining for IE antigens gives bright nuclear staining in alcohol-fixed HCMV-infected cells and allows easy distinction between non-infected and infected cells, especially when coupled with nuclear counterstaining (e.g., DAPI staining). To our knowledge, many commercial antibodies recognizing IE antigens are suitable for immunofluorescence staining. If an unconjugated antibody is used, the staining procedure described in Subheading 3.2 should be complemented with final incubation step with a fluorescently labeled secondary antibody specific for the primary anti-IE antibody, as in a standard immunofluorescence protocol.
3. BD Pathway Bioimaging or BioTek Cytation 3 systems are highly suitable for high-throughput automated acquisition of fluorescently stained samples in many formats, including 96-well plate format. In case of a bright nuclear staining, as observed for HCMV IE staining, it is not essential to have high image resolution for image analysis. So the neutralization assays could be performed in standard cell culture plates, without a need for costly optical imaging plates.

   High-content analysis with automated imaging systems is especially convenient in case of antibody neutralization screenings, when the number of analyzed samples (wells of a 96-well plate in our case) could easily reach a thousand. However, the use of automated cell imaging systems is not necessary per se; any wide-field epifluorescent microscope or even a simple light microscope would be sufficient for counting HCMV-infected cells. However, cell counting on light microscope implies that the staining procedure should be adapted to a standard horseradish peroxidase cytochemistry protocol.
4. Cloning and expression of HCMV genes in transiently transfected HEK293T cells were described in details in Macagno et al. [22]. Briefly, intronless full-length HCMV genes are cloned into pcDNA3 vectors (Invitrogen) by PCR with Pfu turbo on cDNA of VR1814-infected MRC-9 cells. Constructs are used to transfect HEK293T cells (ATCC) with Fugene HD (Roche) according to the manufacturer's protocol. Cells should be harvested 40–48 h after transfection, fixed with 4 % formaldehyde for 15 min at room temperature, washed, and resuspended in PBS containing 0.1 % bovine serum albumin and 0.05 % NaN_3 for storage at +4 °C. In such conditions the

cells can be stored for up to 1 year without losing antigenicity. As an alternative to HEK293T cells, other easily transfectable cell lines (e.g., CHO) could be used.

5. If you use standard ELISA plates, double all volumes indicated in the protocol.
6. We recommend titrating the virus on both ARPE-19 and MRC-9 cells, since the rate of infection varies greatly among these two cell types (cells used for the neutralization assay, Subheadings 3.2 and 3.3).
7. Aliquots should contain a number of viral pfu suitable for one neutralization assay since the aliquots can be frozen and defrozen only once. Calculate aliquote volume according to your needs considering that approximately 300–400 pfu of virus is needed per well of a neutralization assay plate.
8. A standard layout for the neutralization assay should include at least one negative control (with no antibody or with a non-neutralizing antibody) and one positive control (with a neutralizing antibody). Moreover, when neutralizing antibody titration is performed, all samples should be present in triplicates for consistent statistical analysis. This is not necessary when high-throughput antibody screenings are performed, since the antibodies are added in large excess and the assay readout is restricted to two outcomes: "infection/no neutralization" and "no infection/neutralization."
9. ARPE-19 and MRC-9 should be split twice a week by cell monolayer trypsinization (*see* ATCC instructions). These cells are non-transformed and therefore could reach confluent state without losing replication potential. Cells should be seeded at 70–80 % of confluence on day 0 of the neutralization assay protocol, so that they form a monolayer 18–24 h later. The confluence per se is not essential for HCMV infection, although we have observed that ARPE-19 infection is enhanced in monolayers.
10. As already mentioned in the Introduction of this chapter, for major convenience we recommend to set up all assays and antibody isolation procedures in a 96-well plate format, so that the antibody-virus mixtures could be transferred into neutralization assay plates by a multichannel pipette. Antibodies tested in neutralization assay could be used in non-purified form (B cell supernatants, human/mouse serum) or purified form. In the former case, you can use up to 50 μL of B cell supernatants or dilute heat-inactivated serum in cell culture medium (dilution factor of 20 and higher). When testing the immune sera, it is essential to use a non-immune serum as a negative control, since in some cases substantial levels of nonspecific neutralization can be observed. In case of a

purified antibody, good starting dilution could be 1–10 μg/mL, although the fact that IC80 for anti-HCMV antibodies could differ more than 1000 times depending on the antibody specificity should be taken into consideration [1].

11. We recommend titrating the virus on both ARPE-19 and MRC-9 cells, since the rate of infection varies greatly among these two cell types. 50 μL of the virus at 6000–8000 pfu/mL should give approximately 300–400 infectious events per well of a neutralization assay plate. For consistent statistical analysis we suggest that the acquisition parameters should be set up to acquire 150–300 infectious events in a negative control well.
12. Cell culture supernatants can be aspirated by multichannel pipette or by a vacuum aspirator with handheld eight-channel adaptor. Add antibody-virus dilutions atop quickly, not to let cells dry for too much time. All BSL2 precautions should be undertaken when aspirating supernatants from virus-infected cells.
13. IE antigens could be detected as early as 10–18 h post-HCMV infection. However, we found that optimal detection time is 40 h post-infection for ARPE-19 cells and 24 h for MRC-9 cells.
14. At this point the plate with cells could be stored at +4 °C for several days and stained subsequently. We recommend using PBS with 0.05 % NaN_3 for prolonged storages.
15. When images are acquired on BD Pathway or BioTek Cytation 3 systems, the percentage of infected cells per well can be automatically calculated by BD AttoVision or Gen5 software as $N_{\text{infected cells}}x100/N_{\text{DAPI-stained nuclei}}$. This additional step of normalization decreases the variability related to the fluctuation of cell number among wells. In case of a manual count, however, only the number of infected cells per well is counted due to time restriction. In such case we recommend including more replicates to increase the statistical significance of the assay.
16. Antibodies tested in cell binding assay could be used in non-purified form (1–10 μL of B cell supernatants) or purified form (1–5 μg/mL of purified monoclonal antibody) diluted in WASH buffer. Heat-inactivated immune serum (dilution factor of 100 and higher) can be used as a positive control to confirm HCMV antigen expression. It is essential to perform a control staining with a non-immune serum, since in some cases substantial level of nonspecific binding can be observed.
17. If necessary, the transfection can be scaled down to 30 mL of cell culture (125 mL flask) or scaled up to 1000 mL of cell culture (3 L flask). The amount of reagents for transfection should be changed proportionally.
18. Soluble HCMV glycoproteins can be obtained by cloning their extracellular domains (deprived of the transmembrane portion

and the cytoplasmic domain) into vectors compatible with mammalian cell expression systems (e.g., pcDNA3.1, Invitrogen). In case of multisubunit protein complexes, such as the gHgL-pUL128L pentamer, 293-F cells should be co-transfected with a combination of plasmids encoding individual proteins. For example, in case of the pentamer complex we co-transfected the cells with a mixture of plasmids encoding UL128, UL130, UL131, gL, and gH genes with a mass ratio of 0.6:0.6:0.6:0.8:1 (1:1:1:1:1 molar ratio, total plasmid quantity was 500 μg). All proteins but gH were cloned full length since they do not have transmembrane domains. To facilitate protein purification, protein can be cloned in fusion with tags (e.g., His-tag and Strep-tag). In case of multisubunit complexes, we reasoned that the tag should be added to the C-terminus of the biggest protein of the complex (gH), since this will likely minimize tag interference with complex folding and will promote the purification of fully folded pentamer complexes.

19. In order to increase protein yield, sometimes it helps keeping transfected cells in culture for 10 days. In such cases, 100 mL of fresh FreeStyle 293 medium should be added to the 300 mL cell culture on day 4 of the protocol.
20. Addition of bovine serum albumin to serum-free 293-F supernatants increases HCMV protein stability during long-term storage. We observed that in case of a stable protein (e.g., HCMV gB) protein-containing supernatants can be stored at +4 °C up to 1 year without losing reactivity in ELISA tests.
21. Do not add bovine serum albumin to 293-F supernatants if you are going to purify HCMV protein. Purification procedures that we carried out are standard and can be performed following instructions provided by chromatographic column providers. For example, one-step purification can be performed for His-tagged or Strep-tagged proteins on Histrap HP column (GE Healthcare) or Strep-tactin column (IBA GmbH). However, in case of His-tagged proteins we found it necessary to perform an additional step of purification with Superdex 200 gel filtration column (GE Healthcare) to collect proteins of proper molecular weight. Purified proteins should be concentrated to 0.2–1 mg/mL using ultra-filtration columns (e.g., with 30,000 dalton pores, Sartorius), dialyzed against a physiological solution (e.g., PBS) using dialysis cassettes, 0.22 μm filtered under sterile conditions, aliquoted, and stored at +4 °C (short term) or −80 °C (long term).
22. Our sensitive sandwich ELISA was set up using monoclonal antibodies to capture soluble gB, gHgL dimer, or gHgL-pUL128L pentamer to the plastic [1]. ELISA plates should be coated with mouse monoclonal antibodies to detect human primary antibody binding. And vice versa, coating should be

performed with human monoclonal antibodies to detect mouse primary antibodies. In our case [1] HCMV gB was captured by human gB-specific antibody 2B11 [22] or mouse mAb HCMV37 (Abcam). The dimer gHgL and the pentamer gHgLpUL128 were captured by human gH-specific antibodies 13H11 and 3G16 [22] or mouse gH-specific monoclonal antibody H1P73.2 isolated in-house.

Sandwich ELISA allows the coating of non-purified viral proteins directly from 293-F supernatants, which represents a great advantage in view of the typical difficulties associated with recombinant protein purification. However, one should be careful when using monoclonal antibodies for antigen capture since it may lead to the epitope masking on HCMV protein. In order to avoid such masking, a mixture of two monoclonal antibodies can be used. For example, HCMV gH has only one binding site for each gH-specific antibody that we described (A.K., D.L. unpublished data) [22]. However, capturing of the pentamer by a mixture of two monoclonal antibodies specific for two non-overlapping epitopes on gH (13H11 and 3G16) allowed us to overcome the epitope masking issue. It was likely due to the fact that the density of immobilized capturing antibody was sufficiently low and the final stoichiometry of its binding to the pentamer was 1:1; therefore, both the pentamer with "masked" 13H11 epitope and the pentamer with "masked" 3G16 were present, which finally allowed the detection of all gH epitopes in ELISA. As an alternative to protein-specific monoclonal antibodies for capture, we suggest evaluating tag-specific antibodies (e.g., Histag-specific and Streptag-specific antibodies).

23. Bicarbonate buffer (pH 9.6) works well for most of the antibodies we worked with. Alternatively, if neutral pH is preferable, antibodies can be diluted in PBS.
24. Plates can be blocked with 1 % bovine serum albumin diluted in PBS if too high background with milk blocking is observed.
25. Usually the signal develops at a slow rate; however if necessary the development reaction can be blocked by an addition of 20 μL/well of 3 M NaOH solution. Antibody titration curve usually requires at least eight points, and the best readout is achieved when the first dilution of the antibody gives OD values close to saturation (≥3.5), while the background values do not exceed OD 0.1–0.2.
26. Alternatively mice can be boosted with 5 μg protein in PBS intravenously and 2.5 μg protein + 0.2 mg carbopol intraperitoneally. In any case, no adjuvant should be used for intravenous administration. Sacrifice mice on day 46 (3 days after intravenous boost), harvest spleen, and proceed with hybridoma production according to a standard protocol.

27. We recommend implementing one additional step to the hybridoma production protocol in order to reduce background in neutralization and ELISA assays. Since splenocytes are harvested from mice at the peak of antibody production, some wells of 96-well plates, in which hybridomas are seeded, may contain non-fused cells that manage to secrete antigen-specific antibodies in culture supernatant before death. This residual antibody production may result in excessive background and "false-positive" wells (neutralizing/binding detected, but no clone is growing in the well). We therefore suggest to perform hybridoma washing 3 days before neutralization and ELISA assays are performed, as follows: spin 96-well plates containing hybridomas for 5 min at 200 × *g*; trash cell culture supernatants into a large beaker under the sterile hood by fast hand movement; add 200 μL/well of sterile PBS; repeat centrifugation step; repeat PBS washing and centrifugation step one more time; refill the plate with 200 μL/well of fresh hybridoma culture medium and let the clones produce antibodies for 3 days prior to testing.

Acknowledgements

This chapter described work conducted at the Institute for Research in Biomedicine (Bellinzona, Switzerland). The project was partially supported by Fondazione CARIPLO Grant 93043/A, Fondazione Carlo Denegri, Swiss National Science Foundation grant 141254, Ministero della Salute grant RF-2010-GR-2010-2311329, and Mäxi Foundation.

References

1. Kabanova A, Perez L, Lilleri D et al (2014) Antibody-driven design of a human cytomegalovirus gHgLpUL128L subunit vaccine that selectively elicits potent neutralizing antibodies. Proc Natl Acad Sci U S A 111:17965–17970
2. Hangartner L, Zinkernagel RM, Hengartner H (2006) Antiviral antibody responses: the two extremes of a wide spectrum. Nat Rev Immunol 6:231–243
3. Corti D, Lanzavecchia A (2013) Broadly neutralizing antiviral antibodies. Annu Rev Immunol 31:705–742
4. Griffiths PD, Stanton A, McCarrell E et al (2011) Cytomegalovirus glycoprotein-B vaccine with MF59 adjuvant in transplant recipients: A phase 2 randomised placebo-controlled trial. Lancet 377:1256–1263
5. Lilleri D, Kabanova A, Revello MG et al (2013) Fetal human cytomegalovirus transmission correlates with delayed maternal antibodies to gh/gl/pul128-130-131 complex during primary infection. PLoS One 8(3):e59863
6. Traggiai E, Becker S, Subbarao K et al (2004) An efficient method to make human monoclonal antibodies from memory B cells: potent neutralization of SARS coronavirus. Nat Med 10:871–875
7. Traggiai E (2012) Immortalization of human B Cells: analysis of B cell repertoire and production of human monoclonal antibodies. Methods Mol Biol 901:161–170
8. Tiller T, Meffre E, Yurasov S et al (2008) Efficient generation of monoclonal antibodies from single human B cells by single cell

RT-PCR and expression vector cloning. J Immunol Methods 329:112–124

9. Smith K, Garman L, Wrammert J et al (2009) Rapid generation of fully human monoclonal antibodies specific to a vaccinating antigen. Nat Protoc 4:372–384
10. Hahn G, Revello MG, Patrone M et al (2004) Human cytomegalovirus UL131-128 genes are indispensable for virus growth in endothelial cells and virus transfer to leukocytes. J Virol 78:10023–10033
11. Ryckman BJ, Rainish BL, Chase MC et al (2008) Characterization of the human cytomegalovirus gH/gL/UL128-131 complex that mediates entry into epithelial and endothelial cells. J Virol 82:60–70
12. Ciferri C, Chandramouli S, Donnarumma D et al (2015) Structural and biochemical studies of HCMV gH/gL/gO and Pentamer reveal mutually exclusive cell entry complexes. Proc Natl Acad Sci 112:1767–1772
13. Yamane Y, Furukawa T, Plotkin SA (1983) Supernatant virus release as a differentiating marker between low passage and vaccine strains of human cytomegalovirus. Vaccine 1:23–25
14. Bowden RA, Slichter SJ, Sayers M et al (1995) A comparison of filtered leukocyte-reduced and cytomegalovirus (CMV) seronegative blood products for the prevention of transfusion-associated CMV infection after marrow transplant. Blood 86:3598–3603
15. Lipson SM, Shepp DH, Match ME et al (2001) Cytomegalovirus infectivity in whole blood following leukocyte reduction by filtration. Am J Clin Pathol 116:52–55
16. Gerna G, Percivalle E, Baldanti F et al (2000) Human cytomegalovirus replicates abortively in polymorphonuclear leukocytes after transfer from infected endothelial cells via transient microfusion events. J Virol 74:5629–5638
17. Gerna G, Sarasini A, Patrone M et al (2008) Human cytomegalovirus serum neutralizing antibodies block virus infection of endothelial/epithelial cells, but not fibroblasts, early during primary infection. J Gen Virol 89:853–865
18. Krashias G, Simon AK, Wegmann F et al (2010) Potent adaptive immune responses induced against HIV-1 gp140 and influenza virus HA by a polyanionic carbomer. Vaccine 28:2482–2489
19. Lai RP, Seaman MS, Tonks P et al (2012) Mixed adjuvant formulations reveal a new combination that elicit antibody response comparable to freund's adjuvants. PLoS One 7(4):e35083
20. Grazia Revello M, Baldanti F, Percivalle E et al (2001) In vitro selection of human cytomegalovirus variants unable to transfer virus and virus products from infected cells to polymorphonuclear leukocytes and to grow in endothelial cells. J Gen Virol 82:1429–1438
21. Gerna G, Baldanti F, Percivalle E et al (2003) Early identification of human cytomegalovirus strains by the shell vial assay is prevented by a novel amino acid substitution in UL123 IE1 gene product. J Clin Microbiol 41:4494–4495
22. Macagno A, Bernasconi NL, Vanzetta F et al (2010) Isolation of human monoclonal antibodies that potently neutralize human cytomegalovirus infection by targeting different epitopes on the gH / gL / UL128-131A complex. J Virol 84:1005–1013

Chapter 9

Generation of a Single-Cycle Replicable Rift Valley Fever Vaccine

Shin Murakami, Kaori Terasaki, and Shinji Makino

Abstract

Rift Valley fever virus (RVFV) (genus *Phlebovirus*, family *Bunyaviridae*) is an arbovirus that causes severe disease in humans and livestock in sub-Saharan African countries. The virus carries a tripartite, single-stranded, and negative–sense RNA genome, designated as L, M, and S RNAs. RVFV spread can be prevented by the effective vaccination of animals and humans. Although the MP-12 strain of RVFV is a live attenuated vaccine candidate, MP-12 showed neuroinvasiveness and neurovirulence in young mice and immunodeficiency mice. Hence, there is a concern for the use of MP-12 to certain individuals, especially those that are immunocompromised. To improve MP-12 safety, we have generated a single-cycle, replicable MP-12 (scMP-12), which carries L RNA, S RNA encoding green fluorescent protein in place of a viral nonstructural protein NSs, and an M RNA encoding a mutant envelope protein lacking an endoplasmic reticulum retrieval signal and defective for membrane fusion function. The scMP-12 undergoes efficient amplification in the Vero-G cell line, which is a Vero cell line stably expressing viral envelope proteins, while it undergoes single-cycle replication in naïve cells and completely lacks neurovirulence in suckling mice after intracranial inoculation. A single-dose vaccination of mice with scMP-12 confers protective immunity. Thus, scMP-12 represents a new, promising RVF vaccine candidate. Here we describe protocols for scMP-12 generation by using a reverse genetics system, establishment of Vero-G cells, and titration of scMP-12 in Vero-G cells.

Key words Rift Valley fever virus, Vaccine, Single-cycle replicable virus, Reverse genetics, Transfection, Stable cell establishment

1 Introduction

Rift Valley fever virus (RVFV), a member of the genus Phlebovirus within the family Bunyaviridae, carries a tripartite, single-stranded, and negative-sense RNA genome [1–3]. The L RNA encodes the L protein, a viral RNA-dependent RNA polymerase. The M RNA encodes four proteins, including two accessory proteins, the NSm and 78 kDa proteins, and the two major viral envelope proteins Gn and Gc (Gn/Gc). The S RNA uses an ambisense strategy to express nucleocapsid (N) protein and an accessory protein, NSs. In infected cells, L and N proteins drive viral RNA synthesis in the cytoplasm,

Sunil Thomas (ed.), *Vaccine Design: Methods and Protocols: Volume 1: Vaccines for Human Diseases*, Methods in Molecular Biology, vol. 1403, DOI 10.1007/978-1-4939-3387-7_9,

while viral assembly and budding take place at the Golgi apparatus where Gn/Gc accumulates.

The virus is transmitted by mosquitoes and maintained by transovarial transmission in local mosquitoes in sub-Saharan Africa. The transmission of the virus among domestic ruminants has resulted in a high mortality rate and spontaneous abortions in virtually all pregnant animals [1]. Human infection occurs via RVFV-infected mosquito bites or direct transmission of the virus from infected animal tissues or blood. Human disease symptoms include febrile illness, retinitis, encephalitis, and, in about 1 % of cases, hemorrhagic fever [4–6]. Since RVFV is able to infect various species of mosquitoes [7], it has the potential to spread to other areas of the world by movement of infected vectors. Indeed, RVFV has already spread outside of the African continent, e.g., to the Arabian Peninsula. There is an increasing consensus that the spread of Rift Valley fever into North America and Europe is no longer a question of if, but when. RVFV has also been considered a potentially exploitable agent for bioterrorism [8].

RVFV spread can be prevented by the effective vaccination of animals and humans [9]. RVFV is considered to be serologically monotypic [10–12]. Also, humoral immunity, particularly neutralizing antibodies that recognize Gn/Gc, is important for protection [13–21]. Therefore, RVFV vaccines that elicit strong humoral immune responses will be able to prevent infection by any strain of RVFV. Although a good human RVFV vaccine is urgently needed, there is no approved vaccine that can be adapted to massive vaccination programs. An attenuated RVFV, MP-12, was developed by serial passage of the wild-type (wt) RVFV ZH548 strain in the presence of mutagen [2]. The MP-12 is a promising live vaccine candidate for both human and veterinary use because the virus is markedly attenuated in mice, nonhuman primates, and ruminants and retains its high immunogenicity [3, 22–27]. However, intraperitoneal (i.p.) inoculation of young mice with MP-12 can result in efficient virus replication in the central nervous system (CNS) (J. Morrill et al, unpublished data). Furthermore, i.p. inoculation of SCID mice with MP-12 results in the development of neurological signs and death of all mice [24]. These data demonstrated that MP-12 can invade and undergoes efficient replication in the CNS of young animals or immunocompromised animals, and implied that the virus potentially replicates in the CNS of humans with immature or impaired immune system. Thus, it is important to develop highly immunogenic RVFV vaccines with reduced or no neurovirulence for mass vaccination programs.

To develop a safe and immunogenic RVF vaccine, we have generated a novel, single-cycle replicable MP-12 (scMP-12), which does not cause systemic infection in immunized hosts [28]. Figure 1a shows our design of the scMP-12 system. scMP-12 carries L RNA; M RNA mutant encoding wt NSm protein, wt

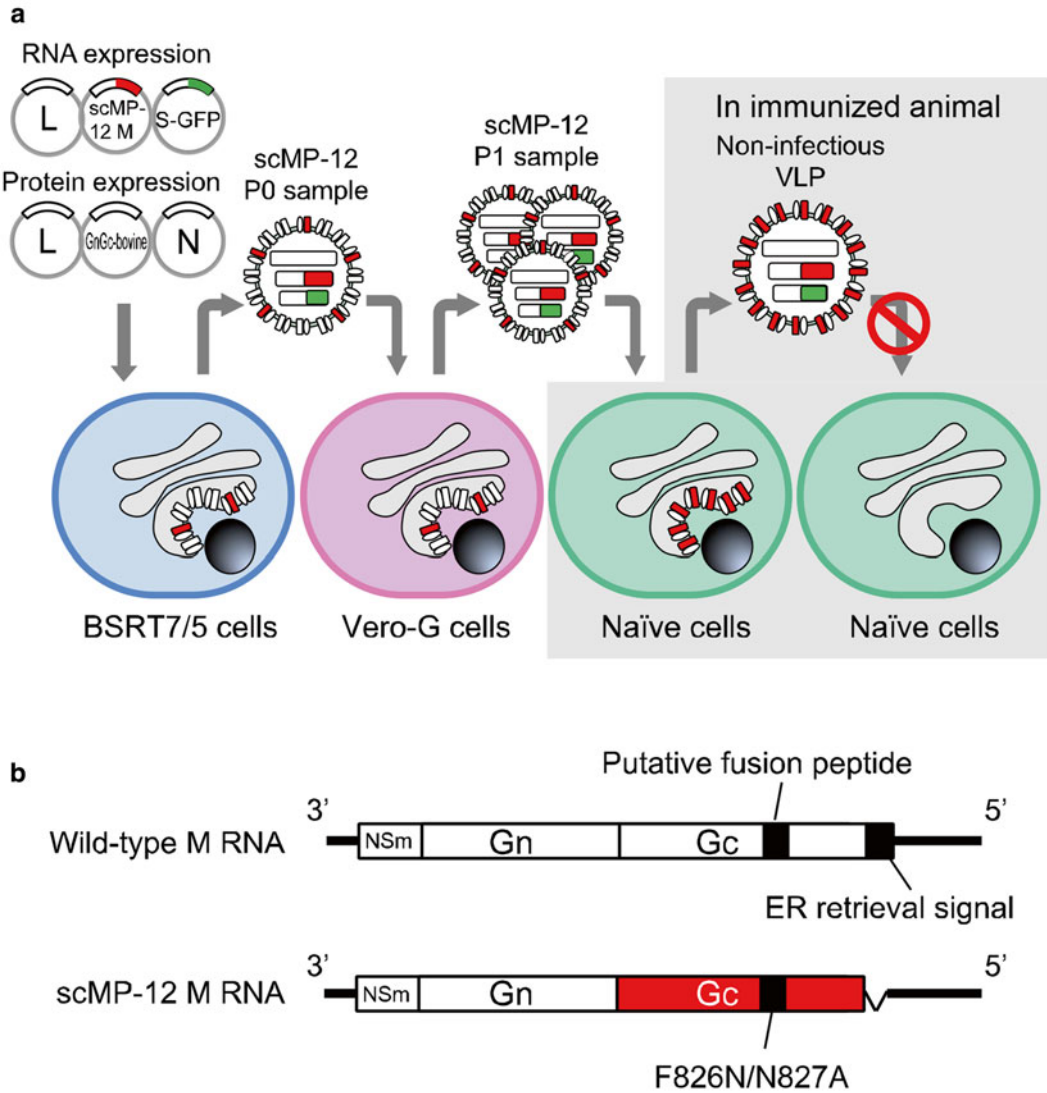

Fig. 1 Schematic diagram of the MP-12-based scMP-12 system [28]. (**a**) scMP-12 was generated in BSR-T7/5 cells stably expressing T7 polymerase by co-transfection of plasmids, which expressed the L, N, and Gn/Gc proteins, as well as the L RNA, S-GFP RNA, and scMP-12 M RNA encoding Gc mutant. Gn/Gc gene of the protein expression plasmid as bovine codon-optimized sequence. scMP-12 contains viral RNAs and is competent for initiating infection, as it carries wt Gn/Gc derived from the protein expression plasmid. scMP-12 is further propagated in Vero-G cells stably expressing wt Gn/Gc. Inoculation of scMP-12 into naïve cells results in viral RNA synthesis, expression of viral proteins, and production of noninfectious VLPs in immunized animals. (**b**) Schematic diagram of antiviral-sense M RNA and scMP-12 M RNA. The ORFs of NSm and Gn genes are shown in *white boxes*, while the Gc gene ORF appears in the *red box*. The *black bars* represent both the putative fusion peptide and the ER retrieval signal. In scMP-12 M RNA, mutations within the putative fusion peptide and deletion of the ER retrieval signal are shown

78-kDa protein, wt Gn protein, and mutant Gc protein lacking the C-terminal 5-amino-acid-long endoplasmic reticulum retrieval signal and having two amino acid substitution within a putative fusion peptide (Gn/GcΔ5); and S RNA carrying green fluorescent protein (GFP) in place of NSs protein (S-GFP RNA). Due to amino acid substitutions in the putative fusion peptide, Gc protein of scMP-12 is fusion defective. We rescued scMP-12 by using a modified MP-12 reverse genetics system [29], in which BSR-T7/5 cells stably expressing T7 polymerase [30] are co-transfected with three RNA-expression plasmids expressing the L RNA, the mutant M RNA encoding the mutant Gc protein, and S-GFP RNA, as well as three protein expression plasmids encoding the L, N, and Gn/Gc proteins. There is a possibility that the M RNA synthesized from the RNA expression plasmid acquires a wt Gc sequence from the M RNA synthesized from the Gn/Gc protein expression plasmid by homologous RNA recombination, generating infectious MP-12. To reduce a chance of homologous recombination between these two RNA transcripts, the Gn/Gc protein expression plasmid encodes a bovine codon-optimized Gn/Gc sequence. The scMP-12 that is produced from the plasmid-transfected cells is infectious due to the presence of wt Gn/Gc and undergoes amplification in Vero-G cells stably expressing Gn/Gc. In scMP-12-infected naïve cells, intracellular accumulation of all of the viral structural proteins and the production of noninfectious viruslike particles (VLPs) occur. Accordingly, in immunized hosts, scMP-12 undergoes single-cycle replication and produces noninfectious VLPs from infected cells. scMP-12 particles in the inoculum, viral proteins accumulated in scMP-12-infected cells, and released noninfectious VLPs all serve as immunogens to elicit immune responses to RVFV proteins. Due to its characteristic single-cycle replication, the scMP-12 did not cause any sign of neurovirulence after intracranial inoculation into suckling mice. scMP-12-immunized mice elicited neutralizing antibodies and efficiently protected the mice from wild-type RVFV challenge by inhibiting wild-type RVFV replication in various organs and viremia [28].

This chapter describes methods for scMP-12 generation. A flowchart presents an outline of the scMP-12 generation procedure (Fig. 2). We first describe methods for construction of the scMP-12 M RNA expression plasmid and bovine codon-optimized Gn/Gc expression plasmid. Then, procedures are given for scMP-12 generation by using a reverse genetics system. Subsequently, we describe procedures for establishment of Vero-G cells by using a plasmid encoding Gn/Gc proteins and a drug selection maker. Finally, we provide methods for propagation and titration of scMP-12 in Vero-G cells.

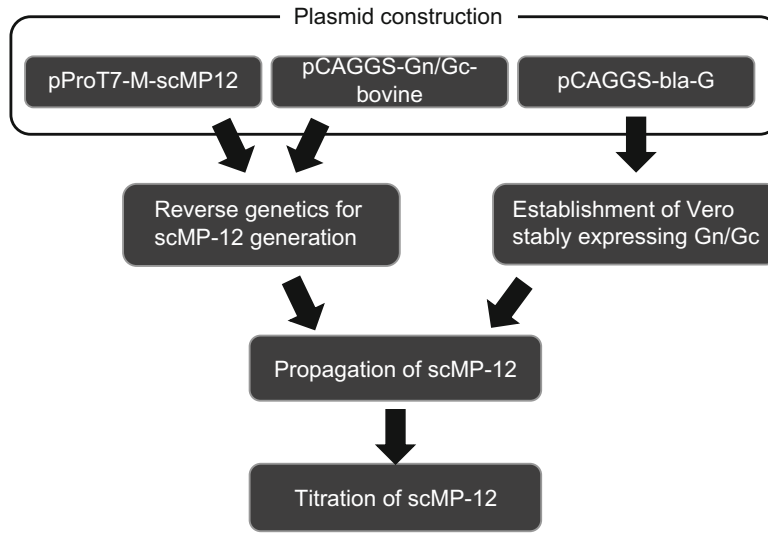

Fig. 2 A flowchart for generation of scMP-12

2 Materials

2.1 Plasmid Construction

1. Proofreading PCR enzyme: Pfu ultra DNA polymerase (Agilent), or equivalent.
2. 10 mM dNTP mix.
3. Agarose, loading dye, and nucleic acid stain suitable for gel electrophoresis.
4. Agarose gel electrophoresis system: 1.0 % agarose gel, use ultrapure agarose (electrophoresis grade) with 1× TBE. Prepare 1 L of 10× TBE stock solution in ultrapure water with 108 g of Tris base, 55 g of boric acid, 40 mL of 0.5 M EDTA (pH 8.0).
5. QIAquick Gel Extraction Kit (Qiagen).
6. QIAquick PCR Purification Kit (Qiagen).
7. 2× Rapid Ligation Buffer (Promega) and T4 DNA ligase (Promega) or equivalent.
8. Chemical-competent cells TOP10 (Invitrogen).
9. SOC medium: Add 20 g tryptone, 5 g yeast extract, 2 mL of 5 M NaCl, 2.5 mL of 1 M KCl, 10 mL of 1 M $MgCl_2$, 10 mL of 1 M $MgSO_4$, 20 mL of 1 M glucose in 1000 mL of H_2O. Sterilize by autoclaving and store at room temperature.
10. LB agar plate with ampicillin: Add 5 g tryptone, 2.5 g yeast extract, 5 g NaCl, and 15 g of Bacto Agar (BD Biosciences), in

1000 mL of H_2O. Sterilize by autoclaving. After cooling down to 55 °C in a water bath, add 1 mL of 50 mg/mL ampicillin, and mix well. Pour 15 mL of LB/agar media into 10 cm Petri dish. After solidifying the LB/agar, store at 4 °C.

11. 14 mL Round-bottomed, snap-cap tubes, sterile.
12. LB medium with ampicillin: Add 5 g tryptone, 2.5 g yeast extract, and 5 g NaCl in 1000 mL of H_2O. Sterilize by autoclaving. After cooling down to room temperature, add 1 mL of 50 mg/mL ampicillin. Store at 4 °C.
13. Qiaprep Miniprep Kit (Qiagen) or equivalent.
14. QIAGEN Plasmid Midi Kit (Qiagen) or equivalent.

2.1.1 Construction of pProT7-M-scMP12 Plasmid

1. Plasmid: pProT7-M [29].
2. Primer pair: deltaGc-tail-F, AAACGTCTCTTAGATCAGTG CGTGTAAAAGC, and deltaGc-tail-R, AAACGTCTCTTCT AGGCAGCAAGCCAC.
3. Primer pair: M F826N_N827A-F,GAATGTGGAGGATGGG GGTGTGGGTGTAACGCTGTGAACCCATCTT, and M F826N_N827A-R,AAGATGGGTTCACAGCGTTACACCC ACACCCCCATCCTCCACATTG.
4. T7 terminator primer: ATGCTAGTTATTGCTCAGCGG.
5. Restriction enzymes: *Bsm*BI, *Dpn*I (NEB).

2.1.2 Construction of pCAGGS-Gn/Gc-Bovine

1. Synthetic gene, bovine codon-optimized M RNA expression plasmid, pProT7-M-bovine.
2. BsmEco-MboGnGc-F, AAACGTCTCTAATTCACCATGGC CGGCATCGCCATG, BsmNot-MboGnGc-R, AAAACGTC TCTGGCCGCTCTAGCTAGCTTTTTTTGTAGCAGCC
3. Restriction enzymes: *Eco*RI, *Not*I, *Bsm*BI (NEB).

2.1.3 Construction of pCAGGS-bla-G

1. Plasmids: pCX4-bsr, and pCAGGS-G.
2. Restriction enzymes: *Not*I, *Stu*I, *Eco*RV (NEB).

2.2 Establishment of Vero-G Cells

1. Restriction enzyme: *Fsp*I.
2. QIAquick PCR Purification Kit (Qiagen).
3. Vero E6 cells.
4. Growth media: DMEM (HyClone) supplemented with 10 % FBS, 1× penicillin/streptomycin (100 unit/mL of penicillin, 100 μg/mL of streptomycin).
5. 6-Well plates.
6. 96-Well plates.
7. Fugene HD transfection reagent (Promega).

8. pCAGGS-Bla-G (Subheading 2.1.3).
9. Opti-MEM (Gibco).
10. Blasticidin S hydrochloride (Gibco).
11. 10 % Formalin in PBS.
12. 0.1 % TritonX-100 in PBS.
13. 2 % BSA in PBS.
14. Anti-Gn monoclonal antibody (R1-4D4) [31].
15. Alexa-594-conjugated anti-mouse IgG (Invitrogen).

2.3 scMP-12 Generation by Reverse Genetics

1. BSR T7/5 cells.
2. Glasgow's minimal essential medium supplemented with 10 % FBS, 10 % tryptose phosphate broth, 1 mg/mL G418, 1× penicillin/streptomycin (100 unit/mL of penicillin, 100 μg/mL of streptomycin).
3. 6-Well plate.
4. Plasmids: pProT7-L [29], pProT7-S-GFP [28], pProT7-M-scMP12 (Subheading 2.1.1), pT7IRES-L [29], pT7IRES-N [29], pCAGGS-Gn/Gc-bovine (Subheading 2.1.2).
5. TransIT-LT1 (Mirus).
6. Opti-MEM (Invitrogen).

2.4 Propagation of scMP-12 in Vero-G Cells

1. Vero-G cells (Subheading 2.2).
2. Growth media: DMEM 10 % FCS, 1× penicillin/streptomycin (100 unit/mL of penicillin, 100 μg/mL of streptomycin).
3. Supernatant from plasmid-transfected BSR T7/5 cells (Subheading 2.3).
4. 6-Well culture plate.

2.5 Plaque Assay for Titration of scMP-12 in Vero-G Cells

1. Vero-G cells (Subheading 2.2).
2. 6-Well culture plate.
3. scMP-12 virus stock solution (Subheading 2.4).
4. 96-Well deep-well plate.
5. Growth media: DMEM 10 % FCS, 1X penicillin/streptomycin (100 unit/mL of penicillin, 100 μg/mL of streptomycin).
6. MEM containing 0.6 % Tragacanth gum (MP Biomedicals), 5 % FBS, and 5 % tryptose phosphate broth.
7. 4 % Paraformaldehyde in PBS.
8. 0.1 % TritonX-100 in PBS.
9. Anti-N rabbit polyclonal antibody, which was generated by injecting a purified, bacterially expressed fusion protein

consisting of glutathione-S-transferase and full-length MP-12 N protein into rabbits.

10. HRP-conjugated anti-rabbit IgG antibody (Santa Cruz).
11. NovaRED peroxidase substrate (Vector Laboratories).

3 Methods

3.1 Plasmid Constructions

3.1.1 Construction of pProT7-M-scMP12 Plasmid

pProT7-M-scMP12 plasmid is produced from M RNA expression plasmid pProT7-M by deleting five amino acid residues of C-term of Gc protein and introducing F826N/N827A mutation in putative fusion peptide of Gc protein. To generate pProT7-M-scMP12, two steps are required: (1) delete five amino acid residues of C-terminal of Gc first and (2) introduce F826N/N827A mutations.

1. Prepare reaction mixture for PCR amplification,

   40 μL Nuclease-free H_2O.
   5 μL 10× reaction buffer.
   1 μL 10 mM dNTPs.
   1 μL Forward primer: deltaGc-tail-F (10 pmol/μL).
   1 μL Reverse primer: deltaGc-tail-R (10 pmol/μL).
   1 μL pProT7-M template at 10 ng/μL concentration.
   1 μL Pfu Ultra DNA Polymerase.

2. Preheat the thermal cycler to 95 °C, then heat the samples at 95 °C for 1 min, and run the thermal cycling program for 30 cycles with the following setting: 30 s at 95 °C, 30 s at 58 °C, and 6 min at 72 °C. Add one cycle at 72 °C for a final extension of 10 min.
3. Run 5 μL of the PCR product by 1 % agarose gel electrophoresis in 1× TBE buffer. Use a 1 kbp DNA ladder to control for the correct product size. Cut out the band, and the extracted PCR fragment by using QIAquick Gel Extraction Kit, eluting fragments with 30 μL of H_2O (*see* **Note 1**).
4. Digest the purified DNA fragment with 1 μL of *Bsm*BI (*see* **Note 2**) and 1 μL of *Dpn*I (*see* **Note 3**) enzymes in reaction volume 25 μL for 1 h at 37 °C and for 1 h at 55 °C. Purify the digested DNA fragments by using a QIAquick PCR purification kit, eluting fragments with 30 μL of H_2O.
5. Perform ligation using T4 DNA ligation; add 1 μL of the digested fragments and 5 μL of 2× ligation buffer, 1 μL of T4 DNA ligase, and 3 μL of H_2O into a 1.5 mL tube and incubate for 5 min at room temperature.
6. Transform 50 μL of TOP10 competent cells with the 3 μL of ligated product.

7. Add 100 μL of SOC media to the transformed cells.
8. Incubate with 180–200 rpm shaking at 37 °C for 1 h.
9. Plate onto LB agar plates supplemented with ampicillin for selection and incubate the plates at 37 °C for 16–20 h.
10. Select well-isolated colonies from the transformation plates, inoculate the colonies in 1 mL LB media for bacterial culture with ampicillin, and incubate with 180–200 rpm shaking for 10–16 h at 37 °C.
11. Make plasmid minipreps from the cultures by using the QIAprep Miniprep Kit, eluting fragments with 50 μL of H_2O.
12. Determine the DNA concentration in each preparation by measuring the absorbance at 260 nm by using a spectrophotometer.
13. Screen the clones by sequencing using T7 terminator primer.
14. Sequence entire M RNA with clones which possess Gc cytoplasmic tail deletion (*see* **Note 4**). Designate one clone possessing correct sequence as pProT7-Gn/GcΔ5.
15. Perform site-directed mutagenesis by using Quickchange II site-directed mutagenesis kit following the manufacturer's protocol with M F826N_N827A-F and M F826N_N827A-R primer.
16. Add 1 μL of *Dpn*I into PCR reaction tube in **step 15** (*see* **Note 3**).
17. Transform 50 μL of TOP10 competent cells with the 3 μL of ligated product.
18. Add 100 μL of SOC media to the transformed cells.
19. Incubate with 180–200 rpm shaking at 37 °C for 1 h.
20. Plate onto LB agar plates supplemented with ampicillin for selection and incubate the plates at 37 °C for 16–20 h.
21. Select well-isolated colonies from the transformation plates, inoculate the colonies in 1 mL LB broth for bacterial culture with ampicillin, and incubate with 180–200 rpm shaking for 10–16 h at 37 °C.
22. Make plasmid minipreps from the cultures, and using the QIAprep Miniprep Kit, elute fragments with 50 μL of H_2O.
23. Determine the DNA concentration in each preparation by measuring the absorbance at 260 nm by using a spectrophotometer.
24. Sequence entire M RNA and choose one clone possessing correct sequence (*see* **Note 4**).
25. Propagate the pProT7-M-scMP12 by midiprep.

3.1.2 Construction of pCAGGS-Gn/Gc-Bovine

1. Synthesize bovine codon-optimized MP-12 Gn/Gc gene (Gn/Gc-bovine) by commercial company.
2. PCR amplify the Gn/Gc-bovine gene to add linker sequence.

Prepare PCR reaction mix on ice:

40 μL Nuclease-free H_2O.

5 μL 10× Reaction buffer.

1 μL 10 mM dNTPs.

1 μL Forward primer: BsmEco-MboGnGc-F (10pmol/μL).

1 μL Reverse primer: BsmNot-MboGnGc-R (10pmol/μL).

1 μL Template at 10 ng/μL concentration.

1 μL Pfu Ultra DNA polymerase.

3. Preheat the thermal cycler to 95 °C, then heat the samples at 95 °C for 1 min, and then run the thermal cycling program for 30 cycles with the following setting: 30 s at 95 °C, 30 s at 58 °C, and 6 min at 72 °C. Add one cycle at 72 °C for a final extension of 10 min.
4. Analyze 5 μL of PCR product on a 1 % agarose gel with ethidium bromide in 1× TBE-buffer. Use a 1 kbp DNA ladder to control for the correct product size.
5. Purify the PCR product using QIAquick PCR purification kit, eluting fragments with 30 μL of H_2O.
6. Digest the purified DNA fragment with 1 μL of *Bsm*BI enzyme in 40 μL reaction volume for 1 h at 55 °C (*see* **Note 5**). Simultaneously, digest 1 μg of pCAGGS-G with 1 μL of *Eco*RI and 1 μL of *Not*I enzymes in 25 μL reaction volume for 1 h at 37 °C.
7. Run the digested PCR product and plasmid by 1 % agarose gel electrophoresis with ethidium bromide in 1× TBE buffer, cut out the band, and extract DNA fragment by using the QIAquick Gel Extraction Kit, eluting fragments with 30 μL of H_2O, respectively.
8. Perform ligation reaction using T4 DNA ligation; add 1 μL of the digested PCR fragment and 1 μL of the digested vector and 5 μL of 2× ligation buffer, 1 μL of T4 DNA ligase, and 2 μL of H_2O into 1.5 mL tube and incubate for 5 min at room temperature.
9. Transform 50 μL of TOP10-competent cells with the 3 μL of ligated product.
10. Add 100 μL of SOC media to the transformed cells.
11. Plate onto LB agar plates supplemented with ampicillin for selection and incubate the plates at 37 °C for 16–20 h.
12. Select well-isolated colonies from the transformation plates, inoculate the colonies in 1 mL LB media for bacterial culture with ampicillin, and incubate with 200 rpm shaking for 10–16 h at 37 °C.

13. Make plasmid minipreps from the cultures, using the QIAprep Miniprep Kit, eluting fragments with 50 μL of H_2O.
14. Determine the DNA concentration in each preparation by measuring the absorbance at 260 nm by using a spectrophotometer.
15. Sequence the either open reading frame of Gn/Gc (*see* **Note 4**).
16. Propagate pCAGGS-Gn/Gc-bovine with midiprep.

3.1.3 Construction of pCAGGS-bla-G

1. Digest pCX4-bsr with 1 μL of *Eco*RV and 1 μL of *Not*I enzymes in 25 μL reaction volume for 1 h at 37 °C. Simultaneously, digest 1 μg of pCAGGS-G with 1 μL of *Not*I and 1 μL of *Stu*I enzymes in 25 μL reaction volume for 1 h at 37 °C.
2. Run the digested pCX4-bsr and pCAGGS-G by 1 % agarose gel electrophoresis, respectively. Extract pCX4-bsr *Not*I-*Eco*RV fragment (1254 bp) and pCAGGS-G *Not*I-*Stu*I fragment (7471 bp) using the QIAquick Gel Extraction kit, eluting fragments with 30 μL of H_2O.
3. Perform ligation reaction using T4 DNA ligation; add 1 μL of the pCX4-bsr *Not*I-*Eco*RV fragment and 1 μL of the digested vector and 5 μL of 2× ligation buffer, 1 μL of T4 DNA ligase, and 2 μL of H_2O into 1.5 mL tube and incubate for 5 min at RT.
4. Transform 50 μL of TOP10-competent cells with the 3 μL of ligated product.
5. Add 100 μL of SOC media to the transformed cells.
6. Plate onto LB agar plates supplemented with ampicillin for selection and incubate the plates at 37 °C for 16–20 h.
7. Select well-isolated colonies from the transformation plates, inoculate the colonies in 1 mL LB broth for bacterial culture with ampicillin, and incubate with 200 rpm shaking for 10–16 h at 37 °C.
8. Make plasmid minipreps from the cultures, by using the QIAprep Miniprep Kit, eluting fragments with 50 μL of H_2O.
9. Identify clones with correct insert size by restriction digestion.
10. Determine the DNA concentration in each preparation by measuring the absorbance at 260 nm using a spectrophotometer.
11. Sequence the entire insertion region.
12. Propagate pCAGGS-bla-G (Fig. 3) with plasmid midiprep kit.

3.2 Generation of Vero-G Cells

To obtain a Vero cell line stably expressing Gn and Gc proteins, Vero cells were transfected with a plasmid encoding Gn/Gc and a drug selection gene. We screened individual cell clones for Gn

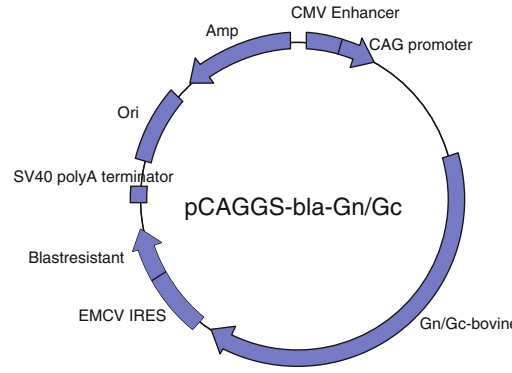

Fig. 3 Map of pCAGGS-bla-Gn/Gc. RVFV Gn/Gc and blasticidin-resistant genes were flaked with encephalomyocarditis virus internal ribosomal entry site (EMCV IRES) sequence

expression levels by using indirect immunofluorescence with an anti-Gn monoclonal antibody (R1-4D4), isolated a cell clone expressing highest levels of Gn, and designated it as Vero-G cells.

1. To linearize pCAGGS-bla-G, digest 10 μg of pCAGGS-bla-G with 2 μL of *Fsp*I enzyme in 100 μL reaction volume for 1 h at 37 °C (*see* **Note 6**).
2. Purify the digested pCAGGS-bla-G product by using QIAquick PCR purification kit, eluting fragments with 30 μL of H_2O.
3. Determine the DNA concentration in each preparation by measuring the absorbance at 260 nm using a spectrophotometer.
4. Seed 3×10^5 cells/well of Vero E6 cells at least two wells of a 6-well plate in DMEM medium supplemented with 10 % FBS and incubate the plates in a 37 °C cell incubator overnight. The cell density should be approximately 80 % confluency at the time of transfection.
5. Add 200 μL OPTI-MEM (Invitrogen) and 3 μg of pCAGGS-bla-G to a 1.5 mL tube. Add 9 μL of FuGENE HD (Promega) and mix by vortexing. Incubate for 15 min at room temperature. The entire transfection mixture was added to a well dropwise. Add 200 μL of OPTI-MEM to at least one well of the plate as mock transfection.
6. Incubate the plate overnight at 37 °C, 5 % CO_2.
7. Aspirate the media from the cells and add DMEM medium containing 10 % FCS and 20 μg/mL of blasticidin. Incubate the plate for 5–7 days at 37 °C, in a 5 % CO_2 atmosphere until all mock-transfected cells die (*see* **Note 7**).
8. Clone the cells by limiting dilution. Wash the cells once with PBS, add 0.2 mL of EDTA-trypsin, and incubate for 5 min at

37 °C. Confirm that all cells are detached. Add 2 mL of DMEM medium containing 10 % FCS and 20 μg/mL of blasticidin and suspend the cells. Adjust cell concentrations to 0.5–1 cells/well in medium containing 20 μg/mL of blasticidin, and dispense a 100 μL cell suspension to each well of 96-well culture plates.

9. Incubate these plates at 37 °C in a 5 % CO_2 atmosphere until cells are visible to the naked eye (*see* **Note 8**). Screen wells forming single colony.
10. Trypsinize the cells with 50 μL of trypsin-EDTA and resuspend in 200 μL of media. Divide into two and seed into two 48-well plate. Incubate overnight at 37 °C in a 5 % CO_2 atmosphere.
11. Wash the cells with 200 μL of PBS once.
12. Fix with 100 μL of 10 % formalin for 10 min at room temperature.
13. Remove formalin and wash the cells three times with 200 μL of PBS.
14. Add 100 μL of 0.1 % TritonX-100 in PBS and incubate for 10 min at room temperature for permeabilization.
15. Remove TritonX-100 in PBS and wash the cells three times with 200 μL of PBS.
16. Add 200 μL of blocking reagent (2 % BSA in PBS) and incubate for 60 min at room temperature.
17. Remove blocking reagent.
18. Add 100 μL of anti-Gn monoclonal antibody (R1-4D4) to the wells in PBS and incubate for 30 min at room temperature (*see* **Note 9**).
19. Remove antibody containing PBS and wash three times with 200 μL of PBS.
20. Add 100 μL of Alexa594-conjugated anti-mouse IgG to the wells in PBS and incubate for 30 min at room temperature.
21. Remove antibody containing PBS and wash three times with 200 μL of PBS.
22. Observe under fluorescent microscopy and select a cell clone expressing highest levels of Gn and designate as Vero-G cells.
23. Propagate the selected clone cells in TC75 flask and make cell stocks.

3.3 scMP-12 Generation by Reverse Genetics

1. Seed ~5×10^5 BSR T7/5 cells/well of a 6-well plate (*see* **Note 10**).
2. Incubate cells for 24 h in growth medium. Cells should be 60–80 % confluent at the time of transfection.

3. Premix DNAs for transfection:
   (a) Use 1.1 μg each of the pProT7-L, pProT7-M-scMP12, and pProT7-S-GFP RNA expression plasmids and pT7IRES-N protein expression plasmids.
   (b) Use 0.55 μg of pCAGGS-Gn/Gc-bovine and pT7IRES-L protein expression plasmids.
   (c) This gives a total of 5.5 μg of DNA to be transfected.
4. Transfection:
   (a) Add 200 μL of OPTI-MEM and premixed DNAs into a 1.5 mL tube.
   (b) Add 2 μL transfection reagent (TransIT-LT1, Mirus) per μg of DNA (*see* **Note 11**).
   (c) Incubate transfection mixture for 15 min at room temperature.
5. Aspirate media from wells and add 2 mL of growth medium, and, then, add transfection mixture dropwise to cells.
6. Incubate the plate for 10 days at 37 °C, 5 % CO_2. Check GFP-positive cell spreading under fluorescent microscopy every day (*see* **Note 12**).
7. Collect the virus-containing supernatant.
8. Remove cell debris by centrifugation (10,000 × *g*, for 5 min, at 4 °C).
9. Aliquot and store at −80 °C.

3.4 Propagation of scMP-12 in Vero-G Cells

1. Seed 5×10^5 Vero-G cells/well of a 6-well plate in growth medium (DMEM 10 % FCS, 1× penicillin/streptomycin).
2. Incubate cells for 24 h at 37 °C and 5 % CO_2; cells should be near confluent at the time of infection.
3. Remove media.
4. Add 300 μL of undiluted virus-containing supernatant to Vero-G cells (*see* **Note 13**).
5. Infect Vero-G cells for 1 h at 37 °C and 5 % CO_2.
6. Wash Vero-G cells once with growth medium to remove virus inoculum.
7. Incubate cells with growth medium for 4–5 days at 37 °C and 5 % CO_2.
8. Observe cells daily to confirm GFP signal spreading under fluorescence microscopy: GFP signal can be typically observed within 18 h of infection.
9. When ~90 % of Vero-G cells become GFP positive, harvest virus-containing supernatant.

10. Remove cell debris by centrifugation (10,000 × *g*, for 5 min, at 4 °C).
11. Transfer virus-containing supernatant to fresh tube.
12. Aliquots the virus-containing supernatant and store at −80 °C. One aliquot should be used for determination of the virus titer described below.

3.5 Plaque Assay

1. Seed 5×10^5 Vero-G cells/well of a 6-well plate in growth medium.
2. Incubate cells for 24 h at 37 °C and 5 % CO_2; cells should be near confluent at the time of infection.
3. Prepare a tenfold serial dilution of the virus stock solution (from 10^{-1} to 10^{-5} dilution): add 450 μL of media into each well of a 96-well deep-well plate. Add 50 μL of the virus stock solution to be tested into the first well and carefully pipette up and down. Then transfer 50 μL of this first dilution into the second well and continue as described for the first dilution to generate a serial dilution.
4. Remove media from 6-well-plated Vero-G cells.
5. Add 400 μL of virus dilutions prepared in Vero-G cells. Include negative control by providing cells with medium lacking virus inoculum.
6. Incubate the 6-well plates for 1 h at 37 °C and 5 % CO_2. Rock the plate gently back and forth every 15 min to keep the cells covered by virus diluent.
7. Aspirate the inoculum.
8. Wash the Vero-G cells once with media.
9. Add 2 mL of MEM containing 0.6 % Tragacanth gum (MP Biomedicals), 5 % FBS, and 5 % tryptose phosphate broth to each well and incubate the plates for 4 days at 37 °C and 5 % CO_2.
10. On day 4, remove the Tragacanth gum-containing media from 6-well plates.
11. Wash the cells with 400 μL of PBS once.
12. Fix with 400 μL of 4 % paraformaldehyde for 10 min at room temperature.
13. Remove paraformaldehyde solution and wash the cells three times with 1 mL of PBS.
14. Add 400 μL of 0.1 % TritonX-100 in PBS and incubate for 10 min at room temperature.
15. Remove TritonX-100 in PBS and wash the cells three times with 1 mL of PBS.

16. Add 400 μL of blocking reagent (2 % BSA in PBS) and incubate for 60 min at room temperature.
17. Remove blocking reagent.
18. Add 400 μL of anti-N rabbit polyclonal antibody to the wells in PBS and incubate for 30 min at room temperature (*see* **Note 14**). Remove antibody containing PBS and wash three times with 1 mL of PBS.
19. Add 400 μL of HRP-conjugated anti-rabbit IgG to the wells in PBS and incubate for 30 min at room temperature. Remove antibody containing PBS and wash three times with 1 mL of PBS.
20. The plaques were visualized with Nova RED peroxidase substrate (*see* **Note 15**) (Fig. 4).
21. Remove Nova RED peroxidase substrate solution.
22. Count plaques in wells where the plaques can clearly be distinguished and calculate the plaque-forming units (pfu). Count plaques in each well and determine the PFU per milliliter using the following formula: PFU/mL = number of plaques × dilution factor × 2.5.

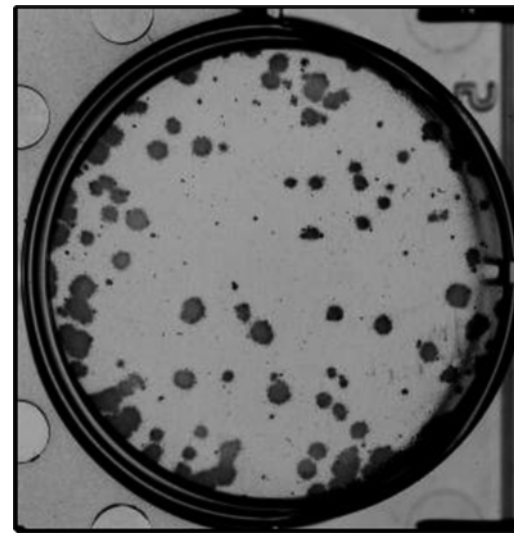

Fig. 4 Plaque formation of scMP-12 in Vero-G cells. Vero-G cells were infected with scMP-12 and overlaid with medium containing Tragacanth gum. After the cells were fixed, plaques were stained with anti-N antibody and visualized by using a Nova RED peroxidase substrate

4 Notes

1. Illumination of short-wavelength UV (254 nm) to DNA causes pyrimidine dimers, resulting in low transformation efficiency. To avoid this, long-wave UV (365 nm) or blue LED is useful.
2. Cleavage site of *Bsm*BI is downstream of the recognition site. Cleavage product does not contain the recognition site, allowing desired plasmid construction introducing insertion, deletion, and mutations (Fig. 5).
3. *Dpn*I digests only methylated plasmid produced in *E. coli* and does not digest non-methylated DNA, such as PCR products. Therefore, *Dpn*I digestion of PCR products only removes template plasmids.
4. Design sequencing primers for entire MP-12 M, which is available in Genbank (Accession number is DQ380208). Typically,

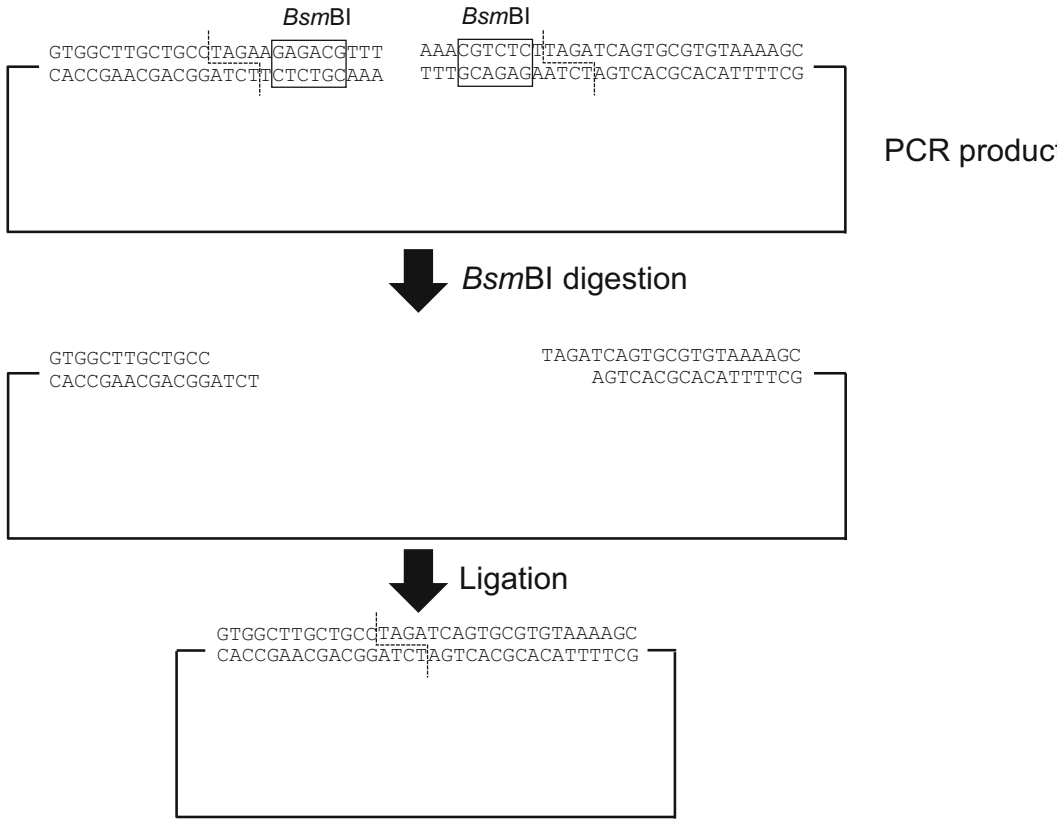

Fig. 5 Cloning strategy for the construction of pProT7-Gn/GcΔ5. (1) PCR product contains *Bsm*BI recognition sites. (2) Incubation of the PCR products with *Bsm*BI generates the same 5′- and 3′-terminal nucleotide overhangs, which can be self-ligated. (3) Cloning product deleted nucleotides encoding 5 amino acid residues from C-terminal end of Fc. *Black boxes*: *Bsm*BI recognition sites

in designing primers a 600–700 nt interval works for the regular sequencer. It depends on the performance of a sequencer.

5. Bovine codon-optimized M sequence contains *Eco*RI site. *Bsm*BI digests downstream of the recognition site with four-nucleotide overhangs. Forward and reverse primers are designed to possess four-nucleotide overhangs of *Eco*RI and *Not*I digestion by *Bsm*BI digestion, respectively.
6. Linearization of plasmid enhances the integration efficiency into cell genomes.
7. When transfected cells become confluent during drug selection, passage the cells once with 1:10 dilution.
8. Typically, 10–18 days are required for forming a visible plaque.
9. If anti-Gn antibody is not available, anti-RVFV polyclonal antibody may work for this screening.
10. If BSR T7/5 cells are not available, BHK cells stably expressing T7 RNA polymerase may work for generation of scMP-12.
11. Selection of transfection reagent is important for this experiment. TranIT-LT1 is one of the most suitable reagents for reverse genetics for RVFV production.
12. The viral titer of scMP-12 will reach its plateau when most of the cells turn to GFP positive.
13. If viral titers are too high, nearly 100 % of Vero-G cells become GFP positive at 1 day postinfection. In this case, a 10–100 times dilution is required to avoid production of defective interfering particles.
14. Anti-RVFV polyclonal antibody does not work in this experiment since anti-RVFV antibodies pick up Gn/Gc signals, causing high background.
15. If the signals are weak, an avidin-biotin complex (ABC) staining method may help to enhance the signals.

Acknowledgements

We thank Robert Tesh, C. J. Peters, and Tetsuro Ikegami for anti-MP-12 antibody, monoclonal antibodies against Gn, and bacterially expressed N protein used for anti-N protein antibody production, respectively. This work was supported by Public Health Service grant AI101772, and in part by the John Sealy Memorial Endowment Fund for Biomedical Research. S. Murakami was supported by the James W. McLaughlin Fellowship fund and by a research fellowship from the Japan Society for the Promotion of Science.

References

1. Bird BH, Nichol ST (2012) Breaking the chain: Rift Valley fever virus control via livestock vaccination. Curr Opin Virol 2:315–323
2. Caplen H, Peters CJ, Bishop DH (1985) Mutagen-directed attenuation of Rift Valley fever virus as a method for vaccine development. J Gen Virol 66(Pt 10):2271–2277
3. Morrill JC, Jennings GB, Caplen H, Turell MJ, Johnson AJ, Peters CJ (1987) Pathogenicity and immunogenicity of a mutagen-attenuated Rift Valley fever virus immunogen in pregnant ewes. Am J Vet Res 48:1042–1047
4. Balkhy HH, Memish ZA (2003) Rift Valley fever: an uninvited zoonosis in the Arabian peninsula. Int J Antimicrob Agents 21:153–157
5. Peters CJ, Meegan JM (1989) Rift Valley fever virus. CRC Press, Boca Raton, FL
6. Peters CJ, LeDuc JW (1999) Bunyaviruses, phleboviruses, and related viruses. In: Belshe RB (ed) Textbook of human Virology. Mosby Year Book, St.Louis, pp 571–614
7. Gargan TP, Clark GG, Dohm DJ, Turell MJ, Bailey CL (1988) Vector potential of selected North American mosquito species for Rift Valley fever virus. Am J Trop Med Hyg 38:440–446
8. Sidwell RW, Smee DF (2003) Viruses of the Bunya- and Togaviridae families: potential as bioterrorism agents and means of control. Antiviral Res 57:101–111
9. Ikegami T, Makino S (2009) Rift valley fever vaccines. Vaccine 27(Suppl 4):D69–D72
10. Besselaar TG, Blackburn NK, Meenehan GM (1991) Antigenic analysis of Rift Valley fever virus isolates: monoclonal antibodies distinguish between wild-type and neurotropic virus strains. Res Virol 142:469–474
11. Shope RE, Peters CJ, Walker JS (1980) Serological relation between Rift Valley fever virus and viruses of phlebotomus fever serogroup. Lancet 1:886–887
12. Tesh RB, Peters CJ, Meegan JM (1982) Studies on the antigenic relationship among phleboviruses. Am J Trop Med Hyg 31:149–155
13. Anderson GW, Smith JF (1987) Immunoelectron microscopy of Rift Valley fever viral morphogenesis in primary rat hepatocytes. Virology 161:91–100
14. Besselaar TG, Blackburn NK (1991) Topological mapping of antigenic sites on the Rift Valley fever virus envelope glycoproteins using monoclonal antibodies. Arch Virol 121:111–124
15. Harrington DG, Lupton HW, Crabbs CL, Peters CJ, Reynolds JA, Slone TW Jr (1980) Evaluation of a formalin-inactivated Rift Valley fever vaccine in sheep. Am J Vet Res 41:1559–1564
16. Niklasson BS, Meadors GF, Peters CJ (1984) Active and passive immunization against Rift Valley fever virus infection in Syrian hamsters. Acta Pathol Microbiol Immunol Scand C 92:197–200
17. Peters CJ, Reynolds JA, Slone TW, Jones DE, Stephen EL (1986) Prophylaxis of Rift Valley fever with antiviral drugs, immune serum, an interferon inducer, and a macrophage activator. Antiviral Res 6:285–297
18. Peters CJ, Jones D, Trotter R, Donaldson J, White J, Stephen E, Slone TW Jr (1988) Experimental Rift Valley fever in rhesus macaques. Arch Virol 99:31–44
19. Pittman PR, Liu CT, Cannon TL, Makuch RS, Mangiafico JA, Gibbs PH, Peters CJ (1999) Immunogenicity of an inactivated Rift Valley fever vaccine in humans: a 12-year experience. Vaccine 18:181–189
20. Schmaljohn CS, Parker MD, Ennis WH, Dalrymple JM, Collett MS, Suzich JA, Schmaljohn AL (1989) Baculovirus expression of the M genome segment of Rift Valley fever virus and examination of antigenic and immunogenic properties of the expressed proteins. Virology 170:184–192
21. Spik K, Shurtleff A, McElroy AK, Guttieri MC, Hooper JW, SchmalJohn C (2006) Immunogenicity of combination DNA vaccines for Rift Valley fever virus, tick-borne encephalitis virus, Hantaan virus, and Crimean Congo hemorrhagic fever virus. Vaccine 24:4657–4666
22. Baskerville A, Hubbard KA, Stephenson JR (1992) Comparison of the pathogenicity for pregnant sheep of Rift Valley fever virus and a live attenuated vaccine. Res Vet Sci 52:307–311
23. Hubbard KA, Baskerville A, Stephenson JR (1991) Ability of a mutagenized virus variant to protect young lambs from Rift Valley fever. Am J Vet Res 52:50–55
24. Morrill JC, Carpenter L, Taylor D, Ramsburg HH, Quance J, Peters CJ (1991) Further evaluation of a mutagen-attenuated Rift Valley fever vaccine in sheep. Vaccine 9:35–41
25. Morrill JC, Mebus CA, Peters CJ (1997) Safety of a mutagen-attenuated Rift Valley fever virus vaccine in fetal and neonatal bovids. Am J Vet Res 58:1110–1114

26. Morrill JC, Mebus CA, Peters CJ (1997) Safety and efficacy of a mutagen-attenuated Rift Valley fever virus vaccine in cattle. Am J Vet Res 58:1104–1109
27. Morrill JC, Peters CJ (2003) Pathogenicity and neurovirulence of a mutagen-attenuated Rift Valley fever vaccine in rhesus monkeys. Vaccine 21:2994–3002
28. Murakami S, Terasaki K, Ramirez SI, Morrill JC, Makino S (2014) Development of a novel, single-cycle replicable rift valley fever vaccine. PLoS Negl Trop Dis 8:e2746
29. Ikegami T, Won S, Peters CJ, Makino S (2006) Rescue of infectious rift valley fever virus entirely from cDNA, analysis of virus lacking the NSs gene, and expression of a foreign gene. J Virol 80:2933–2940
30. Buchholz UJ, Finke S, Conzelmann KK (1999) Generation of bovine respiratory syncytial virus (BRSV) from cDNA: BRSV NS2 is not essential for virus replication in tissue culture, and the human RSV leader region acts as a functional BRSV genome promoter. J Virol 73:251–259
31. Keegan K, Collett MS (1986) Use of bacterial expression cloning to define the amino acid sequences of antigenic determinants on the G2 glycoprotein of Rift Valley fever virus. J Virol 58:263–270

Chapter 10

Application of Droplet Digital PCR to Validate Rift Valley Fever Vaccines

Hoai J. Ly, Nandadeva Lokugamage, and Tetsuro Ikegami

Abstract

Droplet Digital™ polymerase chain reaction (ddPCR™) is a promising technique that quantitates the absolute concentration of nucleic acids in a given sample. This technique utilizes water-in-oil emulsion technology, a system developed by Bio-Rad Laboratories that partitions a single sample into thousands of nanoliter-sized droplets and counts nucleic acid molecules encapsulated in each individual particle as one PCR reaction. This chapter discusses the applications and methodologies of ddPCR for development of Rift Valley fever (RVF) vaccine, using an example that measures RNA copy numbers of a live-attenuated MP-12 vaccine from virus stocks, infected cells, or animal blood. We also discuss how ddPCR detects a reversion mutant of MP-12 from virus stocks accurately. The use of ddPCR improves the quality control of live-attenuated vaccines in the seed lot systems.

Key words Droplet digital PCR, Rift Valley fever, MP-12 vaccine, Copy number validation, Variant RNA detection

1 Introduction

Rift Valley fever (RVF) is a mosquito-borne zoonotic disease endemic to sub-Saharan Africa. Ruminants including sheep, cattle, or goats are highly susceptible to RVF, which cause high-rate abortion, fetal malformation, or newborn death. RVF patients generally develop self-limiting febrile illness, while some progress into a more severe form of the disease such as vision loss, encephalitis, or hemorrhagic fever, making it a public health concern. Rift Valley fever virus (RVFV) is classified as Category A Priority Pathogen by NIH, and a select agent by CDC and USDA. Though vaccination is considered to be the only way to control outbreaks and prevent disease, there are no RVF vaccines commercially available outside endemic countries. RVFV (family *Bunyaviridae*, genus *Phlebovirus*) has a tripartite negative-stranded RNA genome named S-, M-, and L-segments. The S-segment encodes for nucleocapsid (N) protein, and nonstructural S (NSs) protein. The M-segment encodes for

Sunil Thomas (ed.), *Vaccine Design: Methods and Protocols: Volume 1: Vaccines for Human Diseases*, Methods in Molecular Biology, vol. 1403, DOI 10.1007/978-1-4939-3387-7_10,

the Gn, Gc, 78-kDa, and the NSm protein. The L segment encodes for the RNA-dependent RNA polymerase (L) protein, which is necessary for viral RNA synthesis.

Currently, a live-attenuated MP-12 vaccine [1] is the only conditionally licensed RVF veterinary vaccine in the USA. MP-12 is derived from a pathogenic wild-type ZH548 strain isolated during 1977–1978 RVF outbreak in Egypt [2]. The ZH548 strain was plaque-cloned in the presence of a chemical mutagen, 5-fluorouracil, and carried out 12 passages. The resulting MP-12 strain was highly attenuated in a mouse model, and was further used for the master seed and vaccine lot production using certified human diploid lung cells (MRC-5 cells) [3]. MP-12 encodes 23 mutations in the genome, which distinguishes it from the pathogenic ZH548 strain. MP-12 vaccine is highly efficacious with a single dose, and the safety has been demonstrated in several different animals [4–10]. Accurate and reliable measurement of viral RNA copy numbers in MP-12 samples supports the quality management of the master seeds lot systems, vaccine efficacy, or safety studies using animals.

The example given in this chapter illustrates the use of ddPCR to determine the copy numbers of viral RNA from different samples, e.g., virus stock, infected cells, animal tissues, or blood. Further, the method to detect viral RNA encoding a single mutation is also described.

Bio-Rad Laboratories' QX100™ ddPCR™ system utilizes water–oil emulsion droplet technology with microfluidics to achieve partitioning of samples into roughly 20,000 droplets. Thus ddPCR is emerging as a useful tool to provide absolute quantification of target sequences in a given sample [11, 12]. This system carries out ddPCR using two instruments: the QX100 droplet generator and the QX100 droplet reader. Prepared cDNA samples are mixed with ddPCR reagents and placed onto the droplet generator to produce water–oil nanoliter-sized volume droplets. These droplets then serve as individual end-point PCR reactions on a thermal cycler, making it a key aspect for ddPCR. Following PCR amplification, each individual droplet is counted or measured in a single file on the droplet reader, which detects the fluorescent signals with two detection channels, i.e., 6-FAM (6-carboxyfluorescein: Absorbance max: 494 nm, Emission max: 518 nm) channel and hexachlorofluorescein (HEX: Absorbance max: 535 nm, Emission max: 556 nm) or VIC (Absorbance max: 538 nm, Emission max: 554 nm) channel.

1.1 Viral cDNA Samples for Droplet Digital PCR

There are at least two challenging steps for achieving ddPCR accuracy, i.e., (1) accuracy of viral RNA concentration in viral stocks, and (2) accuracy of cDNA copy numbers after reverse transcription of RNA samples. For the measurement of viral RNA copy numbers by using ddPCR, accurate measurement of sample RNA is

essential. Since the copy number of initial virus stock is unknown, and it is often below detection limits of commercially available spectrophotometers [13], we added known amounts of spike RNA into virus stock samples. This allows us to determine the amount of RNA used for cDNA synthesis. The first-stranded cDNA synthesis should occur without an increase in copy numbers due to multiple use of the same RNA template. Therefore, the use of reverse transcriptase with active RNase H is required to degrade template RNA upon cDNA synthesis. If the genomic RNA copy number is measured, contamination with viral mRNA derived from infected cells may increase the resulting RNA copy numbers. Thus, we performed nuclease digestion of virus stock samples before RNA extraction. Alternatively, proper probe and primer design may distinguish genomic RNA from mRNA.

1.2 Design of Taqman Probes and Primers

For the ddPCR using Bio-Rad QX100, a Taqman probe and a set of primers are used. An oligonucleotide (20–28 nt), which is complementary to target cDNA, and labeled with 5′ fluorescent dye: e.g., FAM, HEX, VIC, and 3′ quencher: e.g., Black Hole Quencher-1 (BHQ-1), 6-carboxytetramethylrhodamine (TAMRA), was used as the Taqman PCR probe [14, 15]. A set of primers, a forward and a reverse primer, flanking the probe-binding region, were designed to amplify a PCR product with a length of 50–200 bp. Either S-, M- or L-segment RNA can be a target for ddPCR detection; however, the ratio of S-, M-, and L-segments varies in infected cells or in virions [16]. Thus, it is recommended to pay careful attention towards analyzing viral RNA copy numbers obtained using different probes.

For the detection of a single nucleotide difference in cDNA, two Taqman probes are included in a ddPCR reaction. These probes are conjugated with different fluorescent tags at the 5′ termini, and specifically bind to either parental or mutant template cDNA [17]. For ddPCR, in optimal condition, each droplet is not saturated with multiple cDNA templates, and specific Taqman probe preferably binds to cDNA distinguishing a single nucleotide difference. If the droplet contains multiple cDNA templates, droplets will tend to express both fluorescent signals, making it difficult to differentiate between the two populations.

1.3 Droplet Digital PCR

The PCR reaction is prepared according to the manufacturer's instruction. Since ddPCR measures the cDNA copy numbers by limiting dilution of samples, and the saturation with positive droplets in a PCR reaction prevents accurate analysis due to lack of negative signals, optimization of the dilution of cDNA is required, i.e., ten-fold serial dilutions of cDNA. To avoid any contamination of DNA, control samples without reverse transcription reaction should be included. Using QX100 droplet generator (Bio-Rad), each PCR reaction mixture is converted into ~20,000 discrete

water-in-oil droplets with ~1 nl in volume in an 8-well disposable cartridge (Bio-Rad). Then, with the PCR reaction mixture encapsulated, the droplets are transferred to a 96-well plate and set in the thermal cycler, where 40-cycle end-point PCR is performed.

1.4 Analysis of ddPCR Data

After completion of PCR, the 96-well plate is set in the QX100 droplet reader (Bio-Rad) and is operated using the QuantaSoft software. The provided results include total droplet numbers, total positives and total negatives. The positive number is not a precise reflection of copy numbers, because many droplets may contain varying amount of template cDNA. Therefore, it is required to revise the positive numbers to reflect an even distribution of cDNA by applying the Poisson distribution formula, λ (average copy number per 1 nl droplet) = –ln(1–p): p = ratio of positives to total number of droplets [11]. QuantaSoft provides the copy number per μl by applying the Poisson distribution formula. To calculate the original RNA copy number in 1 ml sample or 1 g, dilution factors should be determined per sample. For example, if 250 μl of virus stock is mixed with 3 μg of spike RNA, and cDNA equivalent to 1.2 ng of RNA is used for a 25 μl ddPCR reaction, the dilution from 1 ml to 25 μl PCR reaction is as follows: (1000 μl ÷ 250 μl) × (3000 ng ÷ 1.2 ng) = 10,000. If the revised RNA copy number is 602 per μg, and total droplet count is 14,800 (each droplet = 1 nl), then the RNA copy number per 1 ml is as follows: $602 \times (25\ \mu l \div 14.8\ \mu l) \times 10{,}000 = 1.02 \times 10^7$ copy per ml. RNA copy per weight can be calculated as well, if spike RNA was not used and the initial total RNA concentration is available.

Analysis of variant populations also requires validation of two Taqman probes using *in vitro* synthesized RNA. Namely, the mixture of *in vitro* synthesized RNA (parental and mutant) at different ratios (e.g., parental only, mutant only, and the mixture of parental and mutant = 10,000:1, 1000:1, 100:1, 1:1000). The cDNA input amounts should not saturate the droplets: i.e., <10,000 positives. Resulting signals should have four clear clusters; Negatives, FAM-positives, HEX (or VIC)-positives, and double-positives. After validation of probes, sample cDNA will be analyzed and the input cDNA amounts should be optimized to avoid saturation. Copy number of parental and mutant RNA can be shown as percentage per total positives (parental and mutants).

2 Materials

2.1 Viral cDNA Samples for Droplet Digital PCR

1. Megascript T7 Transcription Kit (Life Technologies).
2. TRIzol LS Reagent (Life Technologies).
3. Direct-zol RNA MiniPrep Kit (Zymo Research).
4. RNeasy Mini Kit (Qiagen).

5. ZR Whole-Blood RNA MiniPrep kit (Zymo Research).
6. TRIzol Reagent (Life Technologies).
7. 5× iScript Reverse Transcriptase Supermix (Bio-Rad).
8. Spectrophotometer.
9. Molecular grade water (RNase and DNase free).
10. 96-well plate: V-bottom 96-well plate is recommended.
11. Adhesive seal for 96-well plates: This is used to avoid evaporation of samples.
12. Thermal cycler.

2.2 Design of Taqman Probes and Primers

1. DNA oligonucleotide design server: e.g., Primer3Plus Program (Web-interface free program for oligo design) [18].
2. Gene synthesis companies: e.g., Integrated DNA Technologies, Bio-Rad, Sigma.

2.3 Droplet Digital PCR

1. QX100 droplet generator (Bio-Rad).
2. QX100 droplet reader (Bio-Rad).
3. Droplet reader oil (Bio-Rad): This is used for QX100 droplet reader.
4. Droplet generation oil for probes (Bio-Rad): This is used to generate water-in-oil droplets using droplet generator.
5. DG8 cartridge holders (Bio-Rad): This holder is used to load disposable cartridge to droplet generator.
6. Disposable DG8 cartridge (Bio-Rad): This 8-well cartridge specifically fits into QX100 droplet generator.
7. DG8 gasket for droplet generator (Bio-Rad): This disposable gasket is used with disposable cartridge to operate droplet generator.
8. PCR plate sealer: e.g., PX1 PCR plate sealer (Bio-Rad): This is used to heat seal 96-well PCR plate for PCR reaction in a thermal cycler.
9. Foil Heat Seal: e.g., Piercesable Foil Heat Seal (Bio-Rad): This is used to heat seal 96-well PCR plate for PCR reaction in a thermal cycler.
10. 96-well plate: Eppendorf 96-well twin. Tec PCR plate: This Eppendorf 96-well plate fits into QX100 droplet reader.
11. Pipet-Lite XLS+ eight-channel 2–20 μl (Rainin): This is used to transfer 20 μl of PCR reaction to DG8 cartridge.
12. Pipet-Lite XLS+ eight-channel 20–200 μl (Rainin): This is used to transfer 70 μl of droplet generation oil to DG8 cartridge.
13. Pipet-Lite XLS+ eight-channel 5–50 μl (Rainin): This is used to transfer 40 μl of generated droplets from DG8 cartridge to 96-well PCR plate.

14. Rainin tips: e.g., Presterilized and Filtered removable-cover racked LTS tips 2–20 μl, and 200 μl (Rainin): These specific tips are recommended by Bio-Rad, and used to transfer samples for QX100 droplet generator.
15. ddPCR Supermix for Probes (Bio-Rad): This 2× PCR premix is used to prepare PCR reaction mixture with Taqman probe (250 nM), primers (each 900 nM), cDNA, and water (25 μl per reaction).
16. Taqman probe: e.g., 100× probe (25 μM) is prepared in TE, and stored at 4 °C.
17. 100× Primer: e.g., 100× primer (90 μM) is prepared in TE, and stored at −20 °C.
18. cDNA samples: cDNA samples and controls without reverse-transcriptase reaction.
19. Thermal cycler: e.g., Eppendorf Mastercycler ep Thermal Cycler.

2.4 Analysis of ddPCR Data

1. QuantaSoft (Bio-Rad): This software is used to operate QX100 droplet reader, measure the number of positives and negatives, and analyze the data.
2. MicroSoft Excel: This software is used to calculate dilution factors and RNA copy numbers.

3 Methods

3.1 Viral cDNA Samples for Droplet Digital PCR

1. Prepare *in vitro* synthesized RNA for spike RNA of ddPCR samples by using MegaScript. The RNA should be purified by using RNeasy Mini Kit (Qiagen), measured for RNA concentration, and aliquots stored at −80 °C (*see* **Note 1**).
2. Mix 250 μl of virus stock sample with 750 μl of TRIzol LS Reagent, and then add 3 μg of spike RNA.
3. Using Direct-zol RNA MiniPrep Kit, extract RNA in 10 μl of water.
4. Measure the concentration of RNA by using spectrophotometer (*see* **Note 2**).
5. Mix 2 μl of 5× iScript RT Supermix with specific amount of RNA (e.g., 100 ng) for 10 μl reaction in 0.2 ml PCR tubes or 96-well PCR plates.
6. Incubate the mixture in following temperatures: 5 min at 25 °C, 30 min at 42 °C, 5 min at 85 °C, and hold at 4 °C (optional).
7. Use the cDNA for ddPCR reaction mixture (5 μl cDNA for 25 μl mixture).

8. Alternatively, viral RNA may be analyzed in a mixture with cellular RNA (total RNA). We extract total cellular RNA by using RNeasy Mini Kit (Qiagen), and tissue RNA by using TRIzol Reagent (Life Technologies). For animal blood samples, we use ZR Whole-Blood RNA MiniPrep kit (Zymo Research) (*see* **Note 3**).

3.2 Design of Taqman Probes and Primers

1. Here, we describe an example to generate two Taqman probes that selectively detect RVFV MP-12 and reversion L-segment mutated at nt 3750 (A3750G) [3]. Using the Primer3Plus Program, input 200 nt sequence flanking the mutation site (nt 3750) in source sequence area.
2. Set the optimal length of primers as 20 nt, GC% as 50 %, and Tm as 60 °C (*see* **Note 4**).
3. Set the optimal length of probe as 23 nt, GC% as 50 %, and Tm as 65 °C (*see* **Note 5**).
4. Product size range should be less than 200: e.g., setting as 50–100, 100–150, 150–200.
5. Concentrations of each element: e.g., divalent cations: 3.0, monovalent cations: 50.0, dNTP: 0.8, oligo concentration: 50.0.
6. Pick up one set of primer and probe design, and test the specificity of primers and probe to template DNA by using software or an online program: e.g., Mac Amplify program.
7. Synthesize custom DNA oligonucleotides: e.g., primers (25 nmol scale, desalt purification), probe (5′HEX, 3′BHQ1, 100 nmol scale HPLC purification).
8. The oligoes should be dissolved in TE: e.g., 100× probe (90 μM) and 100× primer (25 μM).
9. We designed forward primer (5′- GAA GTG GAA ACA CTA GTA GC-3′: MP-12 LF), reverse primer (5′- TGT AAT GGA GAG TAC ACT GA-3′: MP-12 LR), Probe for parental MP-12 (5′-HEX- CTC CTT AGC TGC AAT **A**AT TCA G-BHQ1-3′: MP-12 L probe), Probe for L-A3750G (5′-FAM- CTC CTT AGC TGC AAT **G**AT TCA G-BHQ1-3′: L-A3750G probe). A single nucleotide difference is underlined.
10. For ddPCR to distinguish mutant population, online tool such as OligoAnalyzer (Integrated DNA Technologies) is helpful to evaluate the hydrolysis profile with a mutation in template DNA.
11. For measurement of RNA copies of MP-12 S-segment and N mRNA, we also designed the following oligoes: forward primer (5′- GGC TGG CTG GAC ATG C-3′ MP-12 NF), reverse primer (5′- AGT GAC AGG AAG CCA CTC A-3′ MP-12 NR), Probe for parental MP-12 (5′-HEX- CAG GCT TTG GTC GTC TTG AG -BHQ1-3′: MP-12 N probe).

3.3 Droplet Digital PCR

1. Prepare the PCR reaction master mix: ddPCR Supermix for Probes (12.5 μl), 100× primers (each 0.25 μl), probes (each 0.25 μl) and water (up to 20 μl per reaction total) for desired number of samples. Then, aliquot each 20 μl into V-bottom 96-well plate. Then, add 5 μl of cDNA sample to each well. Final volume of PCR reaction is 25 μl.
2. Using Rainin eight-channel pipet (2–20 μl) and Rainin filtered tip (2–20 μl), carefully, without producing any air bubbles, transfer 20 μl of the reaction onto the middle row of the disposable DG8 cartridge (*see* **Note 6**).
3. Using Rainin eight-channel pipet (20–200 μl) and Rainin filtered tip (200 μl), carefully transfer 70 μl of droplet generation oil onto the bottom row of the DG8 cartridge.
4. Attach a gasket across the top of the DG8 cartridge and set the gasket onto DG8 cartridge holder.
5. Set the cartridge into QX100 droplet generator, and close the lid. It will then automatically start generating up to 20,000 water-in-oil droplet (1 nl each) in about 2–2.5 min.
6. Once generation of droplet has completed, transfer 40 μl of droplets from the top row of the DG8 cartridge, to an Eppendorf 96-well PCR plate.
7. Seal the 96-well plate with foil using the PX1 PCR plate sealer.
8. Place the plate onto a thermal cycler and perform PCR with the following condition: initial heating at 95 °C for 10 min, 40 cycles of 30 s at 94 °C and 1 min at 60 °C, and the final step at 98 °C for 10 min (*see* **Note 7**).
9. Once PCR reaction is complete, set the PCR plate into the QX100 droplet reader.
10. Start up QuantaSoft in the PC connected to the QX100 droplet reader. Input the sample name in the 96-well table and run the reader using the software.
11. The droplet reader measures the signals from each droplet and the results are shown in QuantaSoft data output.

3.4 Analysis of ddPCR Data

1. QuantaSoft software shows two-channel graph: i.e., FAM and HEX channels. FAM signals represent the mutant (L-A3750G), while HEX signals represent parental (MP-12). With optimal dilution of cDNA, these two probes selectively detect specific templates (Fig. 1). Thus, a single cutoff value can be set for all samples, which determine the number of positive and negative droplets. We tested cDNA derived from a mixture of *in vitro* synthesized RNA encoding either full-length MP-12 L-segment or A3750G L-segment mutant at different ratio. QuantaSoft provides the copy number per μl by applying the Poisson distribution formula using the number of total droplets, positive

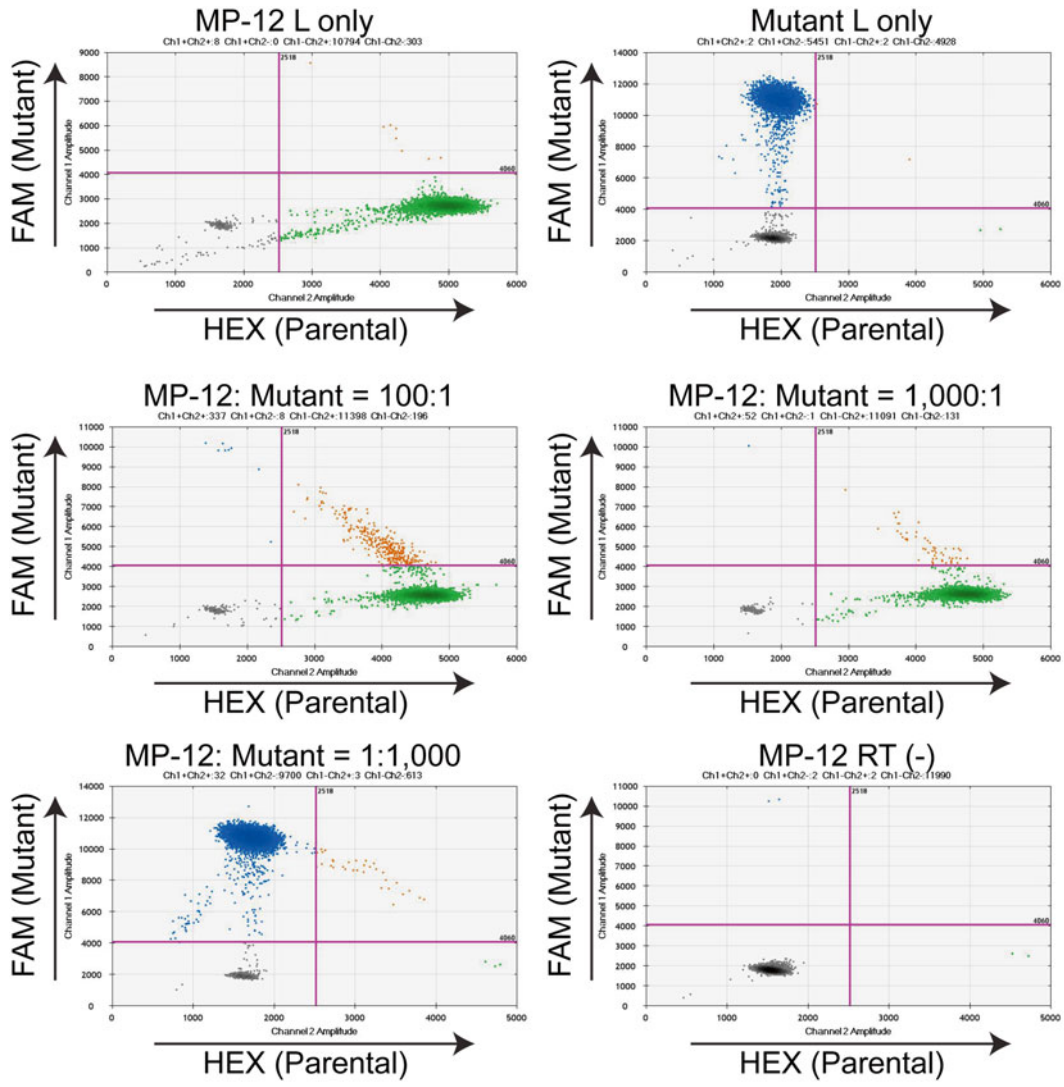

Fig. 1 2D-amplitude images of QuantaSoft data analysis. *In vitro* synthesized RNA encoding full-length MP-12 L-segment (Parental), or MP-12 L-A3750G (Mutant) was made using MegaScript Kit (Life Technologies), purified with RNeasy Mini Kit (Qiagen), mixed at indicated ratios, and reverse-transcribed to cDNA by iScript (Bio-Rad). Then, ddPCR was carried out by using a mixture of MP-12 L-probe (HEX) and L-A3750G probe (FAM). Droplets were separated into four groups: i.e., Negative (*bottom left*), FAM single-positive (*top left*), HEX single-positive (*bottom right*), Double-positive (*top right*)

and negative droplets, which assume the even distribution of template cDNA in each droplet. The results indicate that ddPCR accurately detect at least 1 % population of A3750G mutant (Fig. 2) (*see* **Note 8**).

2. MP-12 stock sample (250 μl) was mixed with *in vitro* synthesized CAT RNA as a spike (3 μg), and ddPCR was performed with MP-12 L probe (Fig. 3). To prevent saturation of drop-

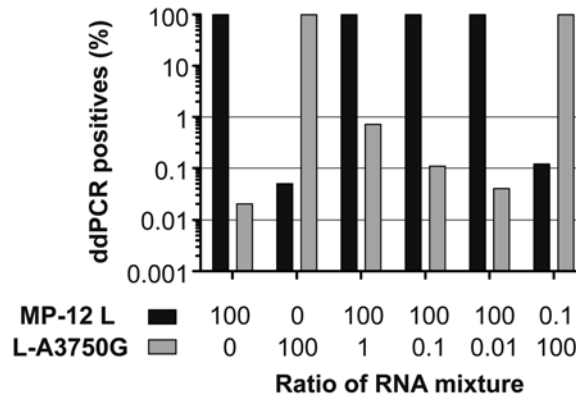

Fig. 2 Ratio of MP-12 L (Parental) and L-A3750G (Mutant) in RNA copy numbers (%). The cDNA samples were prepared from a mixture of *in vitro* synthesized RNA (*see* Fig. 1) of MP-12 L and L-A3750G. Percentage of each RNA copy number is illustrated on the graph

lets, three different dilutions of cDNA equivalent to 12, 1.2, or 0.12 ng spike RNA were tested. At 1.2 ng cDNA input, ddPCR showed optimal positive signals.

3. Outbred CD1 mice were inoculated subcutaneously with 1×10^4 PFU or 1×10^6 PFU (n = 10 per group) of an MP-12 variant (rMP12-TOSNSs). At 3 days post infection, whole blood was collected, and total RNA was extracted. For each sample, 70 ng of RNA was used for cDNA synthesis (total 10 μl), and 5 μl of cDNA (35 ng) was used for ddPCR reaction. Viral RNA copy number was measured by ddPCR using MP-12 N probe (Fig. 4). Though it is difficult to detect viremia in most mouse serum samples [19], ddPCR could detect not only rMP12-TOSNSs RNA in blood cell, but also showed the difference in RNA copy numbers among samples.

Overall, the workflow is simple: after preparation of samples, the droplet generator partitions the samples into nanoliter-sized droplets. These are then placed onto a thermal cycler to carry out amplification, and each individual droplet can be deemed as a single PCR reaction, thus magnifying the precision of the sample as well as determining the absolute quantification. Partitioning the mixture of cDNA sample into nanoliter-sized volume allows accurate quantitation of RNA copy numbers and detection of minor variant populations, unlike conventional PCR. Applying ddPCR to RVF vaccine development will allow accurate analysis of vaccine efficacy and safety.

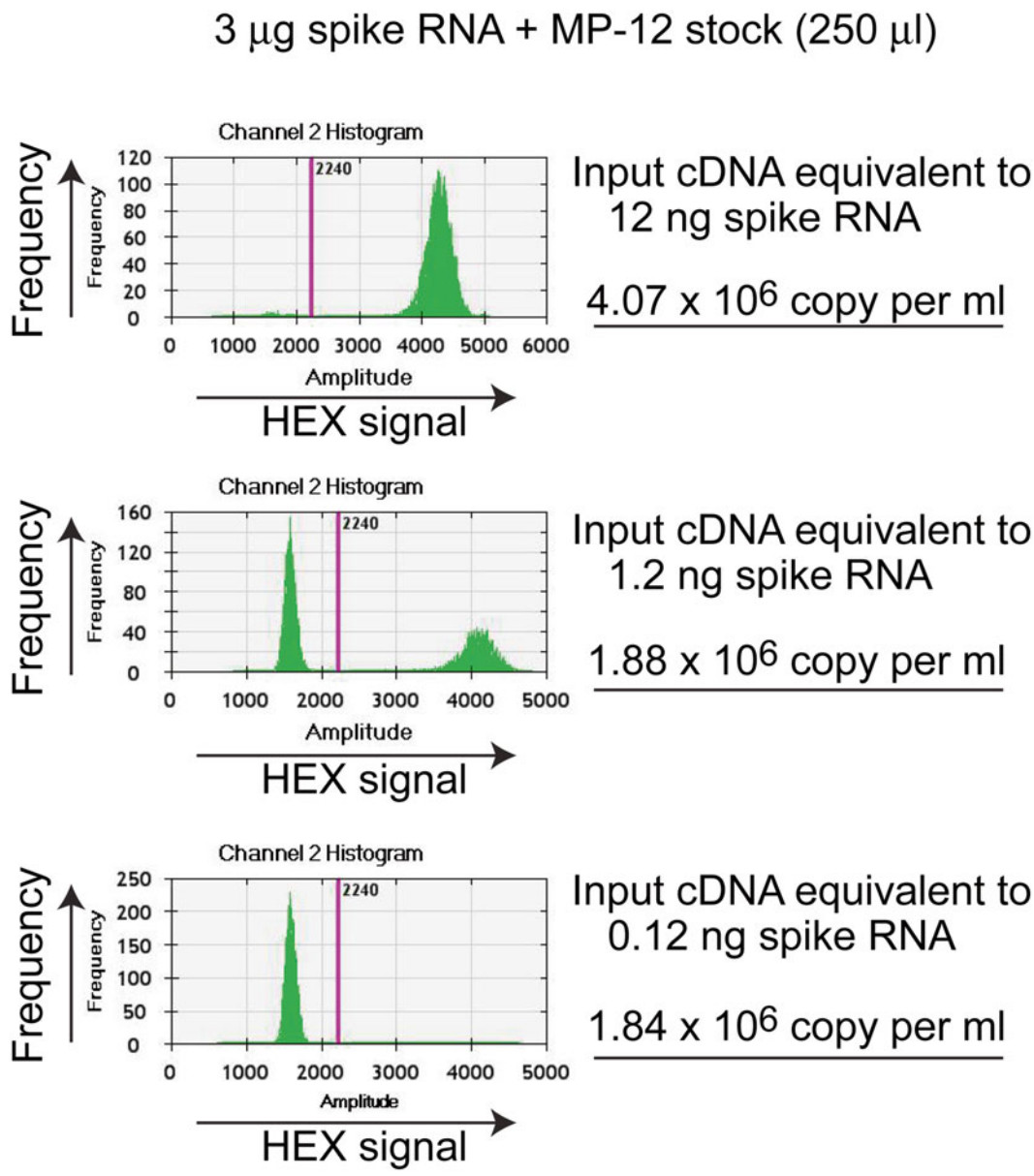

Fig. 3 Detection of Viral RNA copy numbers in MP-12 virus stock. MP-12 virus stock (250 μl) was treated with Benzonase 25 U at 37 °C for 30 min, and mixed with TRIzol LS Reagent (750 μl). *In vitro* synthesized RNA (3 μg), as a spike, was added into TRIzol mixture, and RNA was extracted using Direct-zol MiniPrep kit (Zymo research). cDNA was synthesized by iScript (Bio-Rad), and 12, 1.2, or 0.12 ng of cDNA were used for ddPCR reaction with the MP-12 L-probe (HEX). The *middle panel* (1.2 ng) shows the optimal dilution to measure cDNA copies due to a lack of droplet saturation, which can be seen in 12 ng (*top panel*), and also a more positive signal than that shown for 0.12 ng (*bottom*)

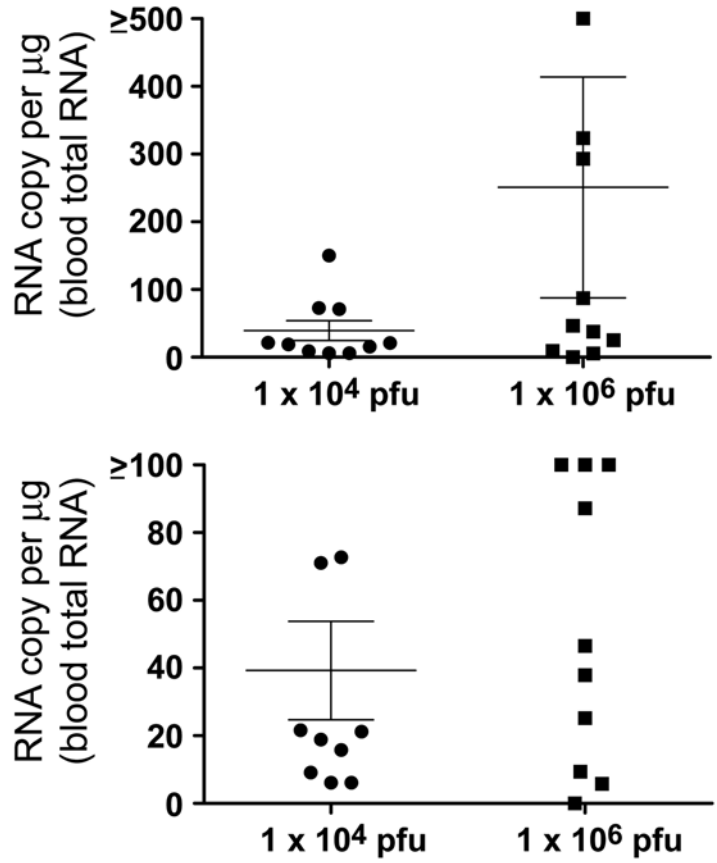

Fig. 4 Mice were inoculated subcutaneously with 1×10^4 or 1×10^6 pfu of rMP12-TOSNSs (an MP-12 variant). Blood (~100 µl) were collected at 3 days post infection, and total RNA was extracted from blood cells using ZR Whole-Blood RNA MiniPrep kit (Zymo Research). Then, 70 ng of total RNA was used for cDNA synthesis (10 µl), and 5 µl cDNA was used for ddPCR using MP-12 N probe. Viral RNA copy per 1 µg of total blood RNA was plotted onto the graph: *Bottom graph* is identical to the *top graph*, yet is shown with a measurement of up to 100 on the *Y*-axis to illustrate small differences among samples.

4 Notes

1. All work must be done on ice, since RNA is unstable at room temperature. Avoid contamination of RNase into samples: e.g., wear clean gloves.
2. Spectrophotometers have limited sensitivities [13]. Therefore, RNA measurement should be done in a reliable measurement range for the instrument. If the RNA concentrations of samples are below detection limit, use spike RNA for reliable RNA measurement of initial samples.

3. We use Qubit 2.0 Fluorometer and reagents such as Qubit RNA Assay or Qubit RNA BR Assay Kit (Life Technologies) to measure total RNA from blood cells. Fluorometer allows specific measurement of RNA concentration in the presence of DNA contamination.
4. Tm between two primers should not differ more than 2 °C.
5. Avoid G at the 5′ end of probe because it may quench fluorescence. Ideally the Tm of probe should be 3–10 °C higher than primers to allow faster annealing of probe to template than primers.
6. Rainin pipets and tips are recommended to minimize troubles: e.g., debris of tip, tight seal, and smooth pipetting operation. Carefully transfer PCR reactions into DG8 cartridge: i.e., tilting the pipet at a 15° angle before dispensing contents will prevent the formation of air bubbles on the ridge of the wells in DG8 cartridge (see Bio-Rad QX100 instruction). It is also important to fill all unused wells with control samples to avoid errors to the QX100 droplet generator.
7. After completion of PCR, samples should not be frozen. The droplets are stable at 4 °C for several days.
8. Annealing temperature should be optimized to achieve optimal separation of FAM and HEX positives. Signal changes caused by annealing temperature are published elsewhere [17]. After the droplet reader has completed, the threshold may be manually adjusted across the entire plate to ensure correct designation of the population as positives or negatives.

Acknowledgements

We thank Dr. Raymond Miller (Bio-Rad) for initial setup of ddPCR experiment. This study was supported by NIH grant R01 AI087643, and the funding from the Sealy Center for Vaccine Development at The University of Texas Medical Branch at Galveston.

References

1. Caplen H, Peters CJ, Bishop DH (1985) Mutagen-directed attenuation of Rift Valley fever virus as a method for vaccine development. J Gen Virol 66:2271–2277
2. Meegan JM (1979) The Rift Valley fever epizootic in Egypt 1977-78. 1. Description of the epizootic and virological studies. Trans R Soc Trop Med Hyg 73:618–623
3. Lokugamage N, Freiberg AN, Morrill JC, Ikegami T (2012) Genetic subpopulations of Rift Valley fever ZH548, MP-12 and recombinant MP-12 strains. J Virol 86:13566–13575
4. Morrill JC, Carpenter L, Taylor D, Ramsburg HH, Quance J et al (1991) Further evaluation of a mutagen-attenuated Rift Valley fever vaccine in sheep. Vaccine 9:35–41

5. Morrill JC, Jennings GB, Caplen H, Turell MJ, Johnson AJ et al (1987) Pathogenicity and immunogenicity of a mutagen-attenuated Rift Valley fever virus immunogen in pregnant ewes. Am J Vet Res 48:1042–1047
6. Morrill JC, Mebus CA, Peters CJ (1997) Safety of a mutagen-attenuated Rift Valley fever virus vaccine in fetal and neonatal bovids. Am J Vet Res 58:1110–1114
7. Morrill JC, Mebus CA, Peters CJ (1997) Safety and efficacy of a mutagen-attenuated Rift Valley fever virus vaccine in cattle. Am J Vet Res 58:1104–1109
8. Morrill JC, Peters CJ (2003) Pathogenicity and neurovirulence of a mutagen-attenuated Rift Valley fever vaccine in rhesus monkeys. Vaccine 21:2994–3002
9. Morrill JC, Peters CJ (2011) Mucosal immunization of rhesus macaques with Rift Valley Fever MP-12 vaccine. J Infect Dis 204:617–625
10. Morrill JC, Peters CJ (2011) Protection of MP-12-vaccinated rhesus macaques against parenteral and aerosol challenge with virulent Rift Valley fever virus. J Infect Dis 204:229–236
11. Bizouarn F (2014) Introduction to digital PCR. Methods Mol Biol 1160:27–41
12. Pinheiro LB, Coleman VA, Hindson CM, Herrmann J, Hindson BJ et al (2012) Evaluation of a droplet digital polymerase chain reaction format for DNA copy number quantification. Anal Chem 84:1003–1011
13. Aranda R, Dineen SM, Craig RL, Guerrieri RA, Robertson JM (2009) Comparison and evaluation of RNA quantification methods using viral, prokaryotic, and eukaryotic RNA over a 10(4) concentration range. Anal Biochem 387:122–127
14. Livak KJ, Flood SJ, Marmaro J, Giusti W, Deetz K (1995) Oligonucleotides with fluorescent dyes at opposite ends provide a quenched probe system useful for detecting PCR product and nucleic acid hybridization. PCR Methods Appl 4:357–362
15. Heid CA, Stevens J, Livak KJ, Williams PM (1996) Real time quantitative PCR. Genome Res 6:986–994
16. Gauliard N, Billecocq A, Flick R, Bouloy M (2006) Rift Valley fever virus noncoding regions of L, M and S segments regulate RNA synthesis. Virology 351:170–179
17. So A, Heredia N, Troupe C (2012) Detection of rare mutant alleles within a background of wild-type sequences using the QX100 droplet digital PCR system. Bio-Rad Bulletin 6260
18. Untergasser A, Cutcutache I, Koressaar T, Ye J, Faircloth BC et al (2012) Primer3--new capabilities and interfaces. Nucleic Acids Res 40:e115
19. Indran SV, Lihoradova OA, Phoenix I, Lokugamage N, Kalveram B et al (2013) Rift Valley fever virus MP-12 vaccine encoding Toscana virus NSs retains neuroinvasiveness in mice. J Gen Virol 94:1441–1450

Chapter 11

Methods to Evaluate Novel Hepatitis C Virus Vaccines

Gustaf Ahlén and Lars Frelin

Abstract

The hepatitis C virus (HCV) is a major cause of severe liver disease worldwide. It is estimated that around 130–170 million individuals are chronic carriers of the infection and they are over time at an increased risk of developing severe liver disease. HCV is often referred to as a silent epidemic because the majority of infected individuals do not develop any symptoms. Hence, many individuals are diagnosed at a late stage and thus in need of immediate treatment. Today we have very effective direct-acting antivirals (DAAs), which cure more than 90–95 % of all treated patients. However, this treatment is associated with high-costs and the use is limited to the patients with most advanced liver disease in high-income countries. Notably, a majority of the chronic HCV carriers live in resource-poor countries and do not have access to the new effective DAAs. We therefore need to develop alternative treatments for chronic HCV infection such as therapeutic vaccines. The idea with therapeutic vaccines is to reactivate the infected patient's own immune system. It is well known that patients with chronic HCV infection have dysfunctional immune responses to the virus. Hence, the vaccine should activate HCV-specific T cells that will home to the liver and eradicate the HCV infected hepatocytes. Importantly, one should also consider the combination of a therapeutic vaccine and DAAs as a treatment strategy to equip the resolving patients with post-cure HCV-specific immune responses. This would provide patients with a better protection against reinfection. Numerous genetic vaccine candidates for HCV have been developed and tested in clinical trials with limited effects on viral load and in general inefficient activation of HCV-specific immune responses. In this chapter we describe the rational of developing highly immunogenic vaccines for HCV. Different strategies to improve vaccine immunogenicity and methods to evaluate vaccine efficacy are described. Detailed description of vaccine delivery by intramuscular immunization in combination with in vivo electroporation/electrotransfer (EP/ET) is covered, as well as immunological analysis of primed immune responses by determination of interferon-γ (IFN-γ) production by ELISpot assay and direct ex vivo quantification of HCV NS3/4A-specific CD8+ T cells by pentamer staining. To analyze the in vivo functionality of primed NS3/4A-specific T cells we utilized the in vivo bioluminescence imaging technology. In conclusion, this chapter describes a method to design HCV vaccines and also a protocol to assess their efficacy.

Key words Hepatitis C virus, HCV, Vaccine, Genetic vaccination, Delivery, ELISpot, Pentamer staining, In vivo imaging

Sunil Thomas (ed.), *Vaccine Design: Methods and Protocols: Volume 1: Vaccines for Human Diseases*, Methods in Molecular Biology, vol. 1403, DOI 10.1007/978-1-4939-3387-7_11, © Springer Science+Business Media New York 2016

1 Introduction

1.1 Characteristics of the Hepatitis C Virus Infection and Treatment Options

The hepatitis C virus (HCV) is one of the major causative agents responsible for development of severe liver disease and cancer worldwide. It is estimated that 130–170 million individuals are chronically infected with HCV [1, 2]. Due to the fact that the majority of the infected individuals do not develop symptoms explains why so many are diagnosed late in their infection. Hence, patients with late stage chronic HCV infection are in need of effective treatment to avoid severe liver complications. The currently used highly efficient direct-acting antivirals (DAAs) can cure more than 90–95 % of all chronic HCV patients [3, 4]. The only limitation is the high-cost for the treatment, which only allow patients with severe liver disease to be treated. Hence, alternative treatment options are therefore needed. To understand how to develop alternative treatments for HCV a brief introduction of the virus will follow. HCV has a positive sense single stranded (ss) RNA molecule of approximately 9.6 kb that encodes for at least ten structural and nonstructural proteins. Each of these proteins may be a target for antiviral drugs and vaccines. The currently approved DAAs target the viral replication machinery by inhibiting the protease (e.g., NS3/4A), the polymerase (e.g., NS5B), and the NS5A protein, which is important for replication and assembly [5]. Notably is that the DAAs does not protect against reinfection [6], which highlights the importance of post-cure HCV-specific T cell responses. Priming of post-cure HCV-specific immune responses may preferable be achieved by vaccinating the HCV infected and/or resolving patients with a specific and potent vaccine. There are several strategies to develop HCV vaccines: such as inactivated, attenuated, subunit, and experimental (e.g., genetic) vaccines. However, the use of some of these vaccines is not possible due to safety concerns (e.g., inactivated and attenuated vaccines). In addition, inactivated, attenuated and subunit vaccines preferentially prime humoral immune responses, which is not suitable for therapeutic vaccines that require activation of T cell responses. We here focus on the development of genetic vaccines, which may be used for both prophylactic and therapeutic purposes. Numerous genetic vaccines have been developed and tested for efficacy in clinical trials [7–13], however none have so far cured HCV infection. To develop a successful vaccine for chronic HCV infection it is expected that multiple parameters need to be optimized such as the vaccine antigen, inclusion of adjuvants, dosing, tissue targeting, delivery, and possibly use of a prime-boost approach. In this chapter we describe some of these important parameters and how they affect immune priming and effector functions.

1.2 Vaccine Design

1.2.1 Antigen Optimization

Firstly, when designing a vaccine for HCV one should select the antigen or antigens carefully. The antigen/s should preferentially be highly immunogenic, advantageously be a relative large protein to maximize the number of targeted epitopes, to include epitopes that correlate with clearance or resolution of infection, and the antigen should demonstrate a low genetic variability. One such antigen is the HCV non-structural 3/4A (NS3/4A) protein, which encodes the viral protease and helicase. Herein, we show examples of strategies to improve the immunogenicity of HCV NS3/4A expressed as a DNA vaccine (e.g., naked plasmid DNA). Other genetic vaccine types include recombinant proteins, peptides, and viral vectors. Secondly, the in vivo expression level of the DNA vaccine is commonly correlated with the potency of the primed immune response. One strategy to increase the protein-expression levels of a DNA vaccine is to optimize the gene sequence based on codon usage, GC content, CpG motifs, mRNA secondary structures, RNA instability motifs, and repeat sequences. Additional sequences that preferentially should be included are Kozak sequence for efficient translation initiation and the TGA stop codon for most efficient translational termination. All mentioned parameters might affect how efficiently a gene is expressed in vivo. We have shown that antigen optimization significantly enhances the HCV NS3/4A immunogenicity [14].

1.2.2 Molecular Adjuvants

Another way to improve the immunogenicity of a selected vaccine-antigen is to add heterologous gene-sequences and/or co-expression with immune stimulatory or inhibitory molecules. When adding heterologous gene-sequences to the vaccine-antigen one should carefully consider the choice of gene-sequence/s. Ideally one should include a gene-sequence encoding a highly immunogenic antigen that will recruit healthy heterologous T cells to the site of immune priming. This is utmost important in the therapeutic vaccination setting, where the infected patient´s immune system often has encountered the viral antigen and its T cells may be dysfunctional. Here, heterologous T cells may help in reactivating the dysfunctional T cells or aid in priming new potent T cell responses targeted to HCV. We have shown that fusion constructs of HCV NS3/4A and human or stork hepatitis B core antigen (HBcAg) significantly enhance the immunogenicity of NS3/4A in a mouse model with dysfunctional T cells to HCV [15,16]. One concern with heterologous gene-sequences is whether they cause any unwanted effects when expressed in vivo. This needs to be investigated for every combination of heterologous gene-sequences and viral antigen/s.

The use of cytokine, chemokine, and co-stimulatory genes as genetic adjuvants has been tested extensively. Some of the most commonly used cytokine genes are IL-2, IL-12, and IL-15 in

respect of priming antiviral T cell responses [17, 18]. Also, TLR agonists [19] have been utilized as well as nuclear localization signals to target genetic material to the nucleus [20]. Our results show that co-expression of NS3/4A DNA and IL-12 is superior NS3/4A alone in priming potent T cell responses (Levander et al., submitted for publication). Similar beneficial effects have been shown for a DNA vaccine targeting hepatitis B virus [17].

1.2.3 *Vaccine Delivery*

It is well known that delivery of DNA vaccines to small animals and humans differs significantly in uptake and transfection efficiency [21]. Early results showed that DNA vaccines delivered with a regular needle injection primed potent immune responses in mice [22]. However, when researchers performed early DNA vaccine trials in humans the results were disappointing [23, 24]. The main reason thought to be the inefficient uptake of the injected plasmid DNA in muscle and/or skin. This was the starting point for development of delivery devices, which should facilitate the uptake of plasmid DNA in animal and human tissues. Numerous delivery devices have been developed and tested in preclinical and clinical trials. The most commonly used devices are: (1) apparatus for electroporation (EP)/electro transfer (ET), (2) biolistic delivery device (e.g., gene gun, gg), and (3) needle-free high-pressure injection device (e.g., Biojector). Early results showed that intramuscular delivery of DNA could be improved by EP/ET [25]. We have shown that intramuscular NS3/4A DNA immunization combined with in vivo EP/ET significantly improved the NS3/4A-specific T cell activation in mice [26]. The same NS3/4A DNA vaccine was later delivered as a therapeutic DNA vaccine to patients with chronic HCV infection. Results revealed that the vaccine was considered safe, induced HCV-specific T cell responses, and had a transient effect on the viral load [9] but none of the patients were cured. Hence, additional efforts are needed to improve vaccine immunogenicity. One strategy to further improve the uptake of DNA vaccines through EP/ET based delivery is to manipulate the pulse parameters and voltages [27]. Our experience is that a short high-voltage pulse followed by a longer low-voltage pulse is most efficient for in vivo transfection [21]. Herein we present results obtained using the Cliniporator^2 EP/ET device (Fig. 1, IGEA, Carpi, Italy). This EP/ET device allows customized pulse parameters, voltages, and the choice of using two to eight electrodes for intramuscular EP/ET and/or two plates for skin EP/ET. Our results show that intramuscular administration of NS3/4A DNA can be significantly improved when applying in vivo EP/ET (Fig. 2). In line with these results, frequencies of NS3-specific $CD8^+$ T cells were significantly higher in EP/ET treated mice (Fig. 3). Hence, it is evident that NS3/4A DNA immunization benefits from in vivo EP/ET. In addition, we found that NS3/4A DNA immunized mice challenged with a hydrodynamic injection [28] of NS3/4A and firefly luciferase DNA, had significantly less

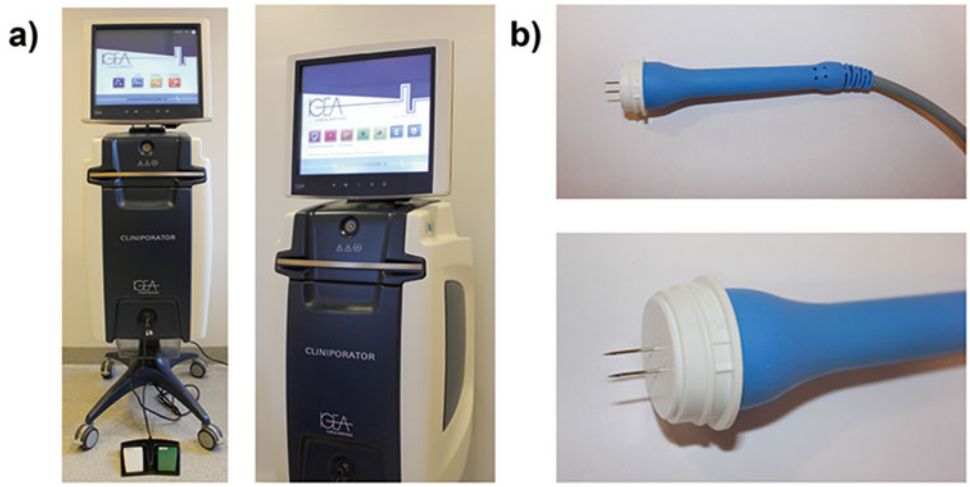

Fig. 1 Illustrative pictures of the Cliniporator[2] EP/ET device. (**a**) Picture of the complete Cliniporator[2] device. Dimensions are 43 cm × 52 cm × 147 cm (width × length × height). Weight is 49 kg. (**b**) Picture of the Cliniporator[2] handle connected with a device electrode. The two needles have a length of 10 mm and the distance between needles are 4 mm

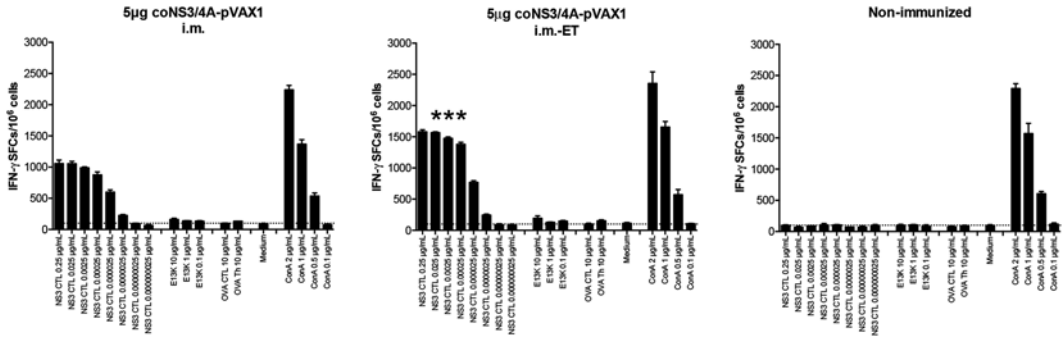

Fig. 2 In vivo EP/ET enhances the priming of HCV NS3/4A-specific T cell responses in C57BL/6 mice. Groups of five wild-type C57BL/6 mice were immunized once with 5 μg coNS3/4A-pVAX1 intramuscularly (i.m.) with or without in vivo EP/ET. One group of mice was left untreated. Two weeks after immunization the mice were sacrificed and splenocytes harvested for determination of T cell responses. A comparison of the number of IFN-γ spot forming cells (SFCs) by ELISpot assay after stimulation with indicated antigens was done in immunized and non-immunized groups of mice. Results are given as the mean SFCs/10^6 (+SD) splenocytes with a cutoff set at 50 SFCs/10^6 splenocytes. The statistical difference shown, indicate a statistical difference between groups with and without in vivo EP/ET (***$p < 0.001$, by AUC and ANOVA)

hepatic NS3/4A-firefly luciferase compared to non-immunized mice (Fig. 4a, b, $p < 0.05$). This highlights that NS3/4A DNA immunization prime T cell responses that home to the liver and eradicate NS3/4A-expressing hepatocytes. The major companies developing EP/ET devices are IGEA (Carpi, Italy), Inovio Pharmaceuticals, Inc. (Plymouth Meeting, PA), and Ichor Medical Systems Inc. (San Diego, CA).

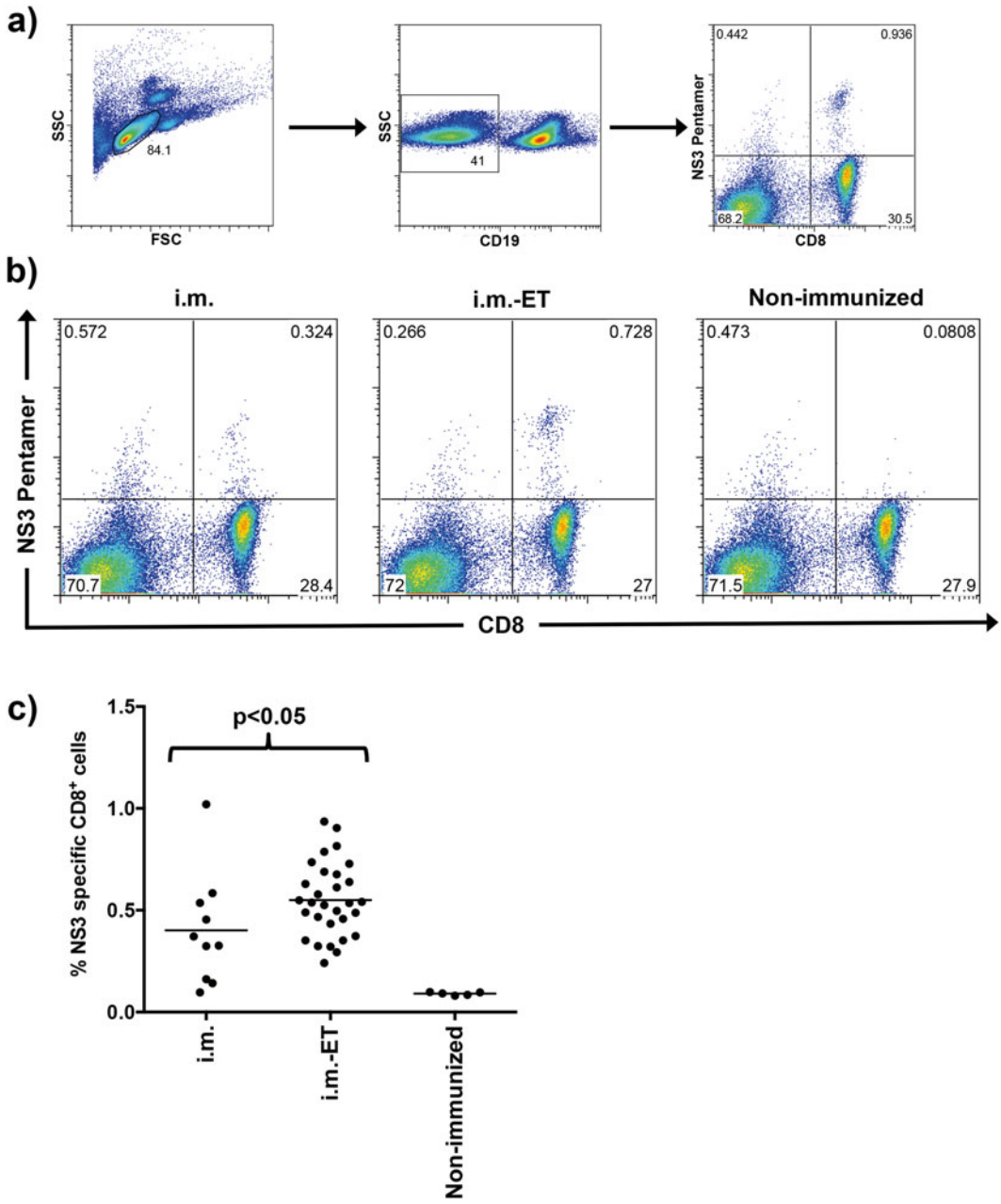

Fig. 3 In vivo EP/ET enhances the frequency of HCV NS3-specific CD8⁺ T cells after immunization. Groups of ten to thirty wild-type C57BL/6 mice were immunized once with 5 μg coNS3/4A-pVAX1 intramuscularly (i.m.) with or without in vivo EP/ET. One group of mice was left untreated (n = 5). Two weeks after immunization the mice were sacrificed and splenocytes harvested for determination of the frequency of NS3-specific CD8⁺ T cells. (**a**) Gating scheme for identification of NS3-specific CD8⁺ T cells. (**b**) Representative dot plots from each group are shown. (**c**) Expansion of NS3-specific CD8⁺ T cells was determined using direct ex vivo pentamer staining. GAVQNEVTL epitope-specific CD8⁺ T cells are shown as the percentage of NS3-pentamer positive CD8⁺ T cells where each *filled black circle* represent an individual mouse. The *black horizontal line* indicates the mean of the group. The statistical difference between the groups is indicated as $p < 0.05$ determined by the Mann–Whitney *U* test

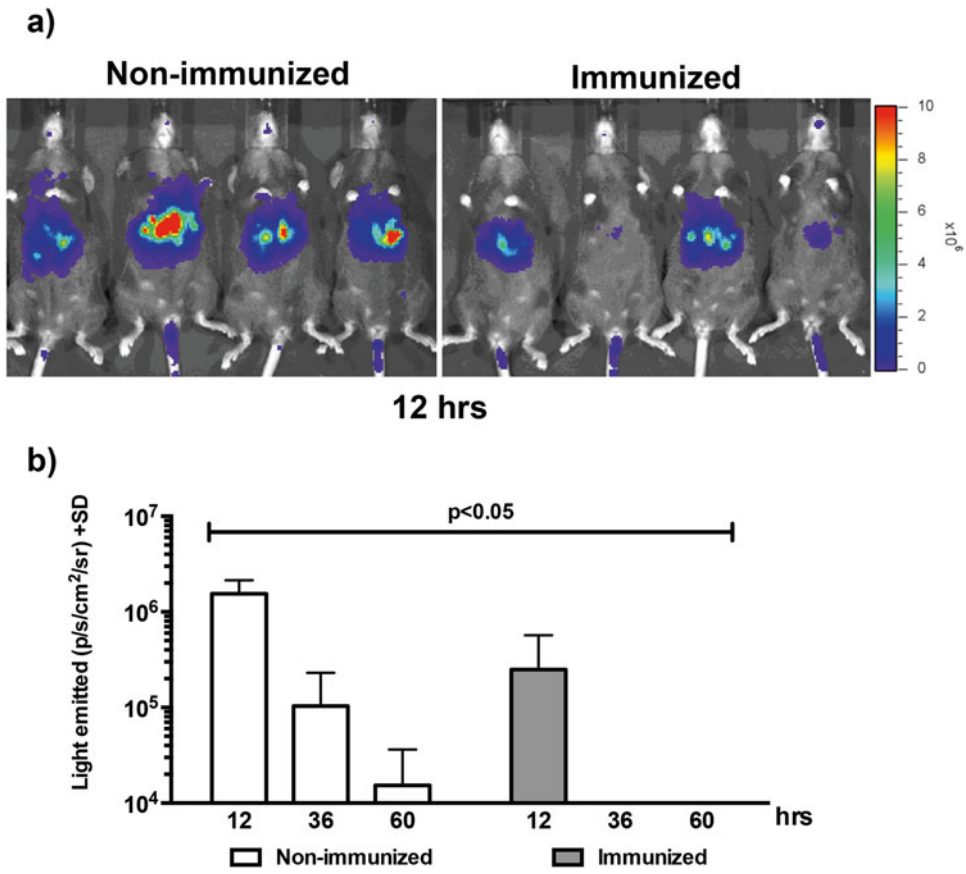

Fig. 4 In vivo clearance of HCV NS3/4A-expressing hepatocytes. (**a**) Biodistribution of NS3/4A and firefly luciferase determined by using in vivo imaging (Caliper Life Science) is shown in immunized (2 weeks post priming) and non-immunized C57BL/6 mice (four mice/group) 12 h after NS3/4A transfection of hepatocytes. (**b**) Statistical difference has been indicated ($p < 0.05$) using area under the curve (AUC) and analysis of variance (ANOVA) at 12–60 h after NS3/4A transfection of hepatocytes

Prime-Boost Approaches

One way to enhance immune activation of genetic vaccines is to employ the prime-boost approach. The idea is to utilize one antigen/vector for immune priming, followed by a booster immunization using another antigen/vector to enhance the previous immune activation. A few different prime-boost approaches have been evaluated in animal models for HCV [29–31]. So far only two HCV prime/boost studies have reached clinical trials, notably in healthy human volunteers and not in chronic HCV patients. The first study utilized human adenovirus 6 (Ad6) to prime, and chimpanzee adenovirus 3 (Ad3) to boost [7]. The second study utilized chimpanzee adenovirus 3 (Ad3) to prime, and modified vaccinia Ankara (MVA) to boost [8]. Both studies showed evidence of potent activation of HCV-specific T cell responses. However, efficacy of these vaccines to protect or clear HCV infection is so far unknown.

2 Materials

2.1 Delivery of DNA Vaccines to Mice Using Intra Muscular Immunization and In Vivo Electro Transfer

1. Ethical permission for the proposed animal experimentation.
2. Required documentation that allows you to work with laboratory mice.
3. Laboratory mice (strain of your choice, we have used H-2^b (C57BL/6)).
4. Ear puncher.
5. Hypnorm: 0.315 mg/mL fentanyl citrate, 10 mg/mL fluanisone (VetaPharma Ltd) or other neuroleptanalgesic drug.
6. Ethanol (70 %).
7. Purified plasmid DNA (1 mg/mL) resuspended in PBS. We have used a codon-optimized HCV NS3/4A gene inserted into the pVAX1 vector [14].
8. 1 mL syringe.
9. 27G, 19 mm needle.
10. Cliniporator^2 (IGEA, Carpi, Italy).
11. Cliniporator^2 handle (IGEA, Carpi, Italy).
12. Electrode tips (REF N-10-4B) using two electrodes (IGEA, Carpi, Italy).

2.2 Media Preparation and Preparation of Spleen Cells

1. Incomplete medium: RPMI 1640 plus 100 U/mL penicillin, 100 μg/mL streptomycin.
2. Complete medium: RPMI 1640 medium plus 10 % fetal bovine serum (FBS, prior to use the FBS is heat inactivated for 30 min at +56 °C), 100 U/mL penicillin, 100 μg/mL streptomycin, 10 mM HEPES buffer, 2 mM L-glutamine, 1 mM sodium pyruvate, 1 mM nonessential amino acids, 50 μM 2-mercaptoethanol.
3. Marking pen.
4. Lab timer.
5. Scissor.
6. Forceps.
7. Biological safety cabinet.
8. Cell strainer, 70 μm pore size.
9. Petri dish, 10 mm.
10. 1 mL syringe.
11. Centrifuge (+4 °C).
12. 15 mL Falcon tubes with screw-cap.
13. 50 mL Falcon tubes with screw-cap.

14. Red Blood Cell Lysing buffer (Sigma-Aldrich)
15. 1 × PBS.
16. Adjustable pipettors and tips (0.5–1000 μL) and multi-pipettors (50–200 μL).
17. Trypan blue stain 0.4 %.
18. Bürkner chamber.
19. Microscope.

2.3 ELISpot Assay

1. Marking pen.
2. Lab timer.
3. Incubator 37 °C, 5 % CO_2.
4. Adjustable pipettors and tips (0.5–1000 μL) and multi-pipettors (50–200 μL).
5. Absolute ethanol (>99.5 %). Diluted to 70 % in dH_2O.
6. 96-well PVDF plates.
7. BCIP/NBT-plus substrate (Mabtech, Nacka Strand, Sweden).
8. Primary IFNγ-antibody, AN18 (Mabtech, Nacka Strand, Sweden).
9. Secondary IFNγ-antibody, R4-6A2-biotin (Mabtech, Nacka Strand, Sweden).
10. Streptavidin-ALP (Mabtech, Nacka Strand, Sweden).
11. 10 × PBS.
12. 1 × PBS.
13. dH_2O.
14. Sterile syringe filters 0.22 μm.
15. Sterile syringe filters 0.45 μm.
16. 15 mL Falcon tubes with screw-cap.
17. 50 mL Falcon tubes with screw-cap.
18. NS3-CTL peptide, amino acid sequence: GAVQNEITL (NS3 CTL).
19. NS3-Th, peptide, amino acid sequence: EIPFYGKAIPLEAIK (E13K).
20. Ovalbumin-CTL peptide, amino acid sequence: SIINFEKL (OVA CTL).
21. Ovalbumin-Th peptide, amino acid sequence: ISQAVHAA HAEINEAGR (OVA Th).
22. Concanavalin-A (Con A).
23. Dissection microscope.
24. Automated ELISpot reader.

2.4 Quantification of CD8+ T Cell Responses

1. Marking pen.
2. Lab timer.
3. Adjustable pipettors and tips (0.5–1000 μL) and multi-pipettors (50–200 μL).
4. MHC pentamer-R-PE (stored at +4 °C in dark, ProImmune) specific for the mouse H-2D^b (GAVQNEVTL) peptide.
5. Anti-mouse CD19 (APC-label).
6. Rat anti-mouse CD8 (FITC-label, monoclonal: KT15).
7. Rat anti-mouse CD3 (PE-label).
8. Purified anti-mouse CD16/CD32 (FCγ III/II, 2.4G2) "Fc block."
9. Wash buffer/staining buffer (1 % fetal bovine serum (FBS) in PBS). Prepare fresh every time!
10. Fix solution (stock solution: 4 % paraformaldehyde (PFA) in PBS (can be stored at +4 °C for up to one month), working solution: 2 % PFA diluted in wash buffer/staining buffer).
11. V-bottom 96-well plate.
12. FACS tubes (5 mL, polystyrene round-bottom tube).
13. FACSVerse (BD Biosciences, San Jose, CA) or other brand of flow cytometer.
14. FlowJo 9.2 software (Tree Star, Ashland, OR) or other brand of analysis software.

2.5 Detection of Liver Specific Protein Expression by In Vivo Imaging

1. Transiently transgenic mice with intrahepatic expression of the gene of interest and a reporter gene (e.g., Firefly luciferase) for measurements of bioluminescence signals. The transiently transgenic mouse model has been described previously [28].
2. IVIS Spectrum in vivo imaging system (PerkinElmer, Waltham, MA) or similar system for in vivo bioluminescence detection.
3. Living Image Software version 4.2 (PerkinElmer, Waltham, MA).
4. XGI-8 Gas Anesthesia System (PerkinElmer, Waltham, MA) or similar system for anesthesia.
5. Isoflurane (IsoFlo®, Abbott Laboratories Ltd, Berkshire, UK) or similar inhalational anesthesia.
6. Oxygen supply.
7. Luciferin (15 mg/mL, D-luciferin, K$^+$ salt, PerkinElmer, Waltham, MA).
8. 1 mL syringe.
9. 27G, 19 mm needle.
10. Shaver (for laboratory mice).

3 Methods

The methodology section outlines the following procedures: (1) preparation and intramuscular delivery of DNA vaccines to laboratory mice in combination with in vivo electro transfer, (2) monitoring the primed T cell responses using (a) ELISpot assay, (b) pentamer staining, and (c) in vivo imaging.

3.1 Delivery of DNA Vaccines to Laboratory Mice Using In Vivo Electro Transfer

The following protocol describes the procedure for intramuscular immunization of laboratory mice using a regular needle and syringe in combination with in vivo electro transfer. The procedure requires laboratory work involving one person. The time needed depends on the number of laboratory mice to be immunized. Roughly, the procedure takes 1 h for immunization and in vivo electro transfer of 20 laboratory mice.

1. Prepare 5 μg DNA in 50 μL PBS (for each mouse to immunized) (*see* **Note 1**).
2. Switch on the Cliniporator[2] device (*see* Fig. 1a), connect the handle and attach the electrode tip (e.g., two electrodes, *see* Fig. 1b). Select your electro transfer program of choice (*see* **Note 2**). We used an optimized program utilizing a short high-voltage pulse followed by a long low-voltage pulse for efficient uptake of the plasmid DNA.
3. Restrain the mouse in your hand, earmark, and inject the mouse intraperitoneally with Hypnorm using a 1 mL syringe and a 27G needle 5–10 min prior to the immunization. This will anesthetize the mouse during the procedure (*see* **Note 3**).
4. Restrain the mouse in your hand with the abdominal area facing up and keep the right tibialis anterior/cranialis muscle stretched (*see* **Note 4**).
5. Wet the muscle with 70 % ethanol (*see* **Note 5**).
6. Inject the mouse with 50 μL PBS containing 5 μg DNA using a regular 1 mL syringe and a 27G needle (*see* **Notes 6** and **8**). Figure 5 visualizes a successful immunization of the tibialis anterior/cranialis muscle using a tissue marking dye instead of DNA.
7. Immediately after the DNA injection, treat the same area of the muscle with in vivo electro transfer by penetrating the muscle with the two electrodes and thereafter delivering the electrical pulses (*see* **Notes 7** and **8**).
8. Place the mouse in a cage and check the status of the mouse until fully recovered from anesthesia.

Fig. 5 Illustrative picture of a tibialis anterior/cranialis muscle injected with a tissue marking dye to visualize the injected area. The *red arrow* indicates site of injection and the direction of the needle insertion

3.2 Media Preparation

1. Prepare the media in sterile conditions working in a biological safety cabinet (BSC).
2. Discard the volume media that will be replaced by the addition of supplements (discard 70 mL for complete media and 5 mL for incomplete media).
3. Add supplements and store the media in +4 °C until use.

3.3 Preparation of Spleen Cells (for Detection of ELISpot and Quantification of CD8⁺ T Cell Responses)

The following protocol describes preparation of spleen cells to be used in ELISpot and pentamer staining/quantification of $CD8^+$ T cells. The procedure requires laboratory work involving one person. The time needed depends on the number of laboratory mice to be sacrificed and spleens to prepare. Roughly, the procedure takes 3 h for 20 laboratory mice.

1. Sacrifice the mouse through cervical dislocation and excise the spleen using scissors and forceps.
2. Immediately put the spleen in a 15 mL Falcon tube containing 2 mL of incomplete medium (*see* Subheading 2.2, **item 1**).

3. The following procedures should be performed under sterile conditions in a biological safety cabinet.
4. Make single cell suspension by teasing the spleen with the plunger of a 1 mL syringe in the cell strainer placed in a petri dish.
5. Transfer the cell suspension to a new 15 mL Falcon tube, wash the cell strainer with 5 mL of incomplete medium and collect the wash in the same tube.
6. Centrifuge for 5 min at 450 × *g*, +4 °C.
7. Discard the supernatant and resuspend the pellet in the remaining medium.
8. Add 1 mL of Red Blood Cell Lysing buffer and incubate at room temperature for 1 min (*see* **Note 9**).
9. Add 12 mL of PBS to the Falcon tube to inactivate the Red Blood Cell Lysing buffer and proceed immediately with centrifugation for 5 min at 450 × *g*, +4 °C.
10. Discard the supernatant and resuspend the cell pellet in 2 mL of complete medium (*see* Subheading 2.2, **item 2**).
11. Prepare cells for counting by mixing 10 μL cell suspension + 90 μL trypan blue stain 0.4 %.
12. Count cells in a Bürkner chamber.
13. 13a. Prepare a cell suspension (from individual or pools of spleen cells) at a concentration of 2×10^6 cells/mL for the ELISpot assay (*see* Subheading 3.4).
14. 13b. Calculate and transfer a cell suspension containing 1×10^6 cells (from individual mice) to a V-bottom plate for quantification of HCV-specific $CD8^+$ T cells (*see* Subheading 3.5).

3.4 Determination of Immune Responses after DNA Immunization by ELISpot Assay

The following section describes the procedure to determine in vitro T cell responses in spleen cells from DNA immunized mice by measuring the number of IFN-γ spot forming cells (SFCs) after stimulation with HCV-derived antigens (Fig. 2). The procedure requires laboratory work involving one person for approximately 1 h day 1, 5 h day 2, and 6 h day 4.

Day 1. Preparation of ELISpot plates (under sterile conditions). Coating of plates:

1. Dilute the coating antibody (IFN-γ, AN18) to 10 μg/mL in sterile PBS, pH 7.4.
2. Pre-wet each well with 50 μL of 70 % ethanol for maximum 1 min (**step 2–4**, one plate at a time) (*see* **Note 10**).
3. Wash plates 4 times with 200 μL sterile water (*see* **Note 11**). Immediately move to **step 3** without allowing the membrane to dry (*see* **Note 12**).

4. Coat ELIIP plates with 100 μL anti-IFN-γ (AN18) antibody in sterile PBS.
5. Incubate overnight at 4–8 °C (in a refrigerator).

Day 2. Incubation of cells in plate (under sterile conditions). Block membrane:

6. Decant primary antibody solution by flicking the plate over a waste bin.
7. Wash off unbound antibody with 200 μL PBS/well as described in **Note 11**, incubate for 5 min.
8. Decant washing buffer and repeat **item 7**, three times.
9. Block with 200 μL complete medium (*see* Subheading 2.2, **item 2**) for at least 2 h at 37 °C.

Preparation of spleen cells and antigens used for in vitro stimulation:

10. Prepare cells according to Subheading 3.3 and dilute cells to 2×10^6/mL.
11. Remove blocking media and gently add 100 μL/well (200,000 cells/well) of isolated spleen cells.
12. Prepare dilutions of your antigens of interest. In this chapter we have used different antigens from HCV NS3 (e.g., NS3-CTL peptide and NS3-Th peptide) and control antigens (Ovalbumin-CTL peptide and Ovalbumin-Th peptide). As positive control ConA was used and as negative control medium was used (*see* **Note 13**).
13. Sterile filter all antigen-solutions through a 0.22 μm filter before use.
14. Add 100 μL/well of antigen-solution according to protocol.
15. Incubate for 24–48 h in 37 °C, 5 % CO_2.

Day 4. Detection of spot-forming cells (SFCs). Secondary antibody:

16. Inspect all plates/wells and mark wells with leakage before decanting the cells (*see* **Note 14**).
17. Wash plate 5 times with PBS (*see* **Note 15**).
18. Dilute the biotinylated anti-IFN-γ antibody (R4-6A2-biotin) to 2 μg/mL in PBS + 0.5 % FBS.
19. Add 100 μL/well. Incubate for 2 h at room temperature.

Development of spot-forming cells (SFCs):

20. Wash wells 5 times with PBS as described in **item 16** and *see* **Note 15**.
21. Dilute the streptavidin-ALP 1:1000 in PBS containing 0.5 % FBS

22. Add 100 μL/well. Incubate for 1 h at room temperature.
23. Wash wells 5 times with PBS as described in **item 16** and *see* **Note 15**.
24. Filtrate the ready-to-use substrate solution (BCIP/NBT-plus) through a 0.45 μm sterile filter.
25. Add 100 μL/well of the substrate solution (*see* **Note 16**).
26. Develop plates for 12 min (IFNγ) or until distinct spot-forming cells emerge (*see* **Note 17**).
27. Stop color development by washing the plate extensively in tap water for 10 min. Wash both sides of the plate (*see* **Note 18**).
28. Forcefully decant the remaining water and wipe off excess of water using paper tissues.
29. Let the plates dry for at least 2 h before analysis.
30. When the plates are completely dry, inspect and count spot-forming cells in a dissection microscope (×40) or using an automated ELISpot reader. Herein we used the AID iSpot (EliSpot/FluoroSpot) reader system (Autoimmun Diagnostica GmbH, Strassberg, Germany).
31. The automated ELISpot reader will count the number of spots-forming cells (cytokine producing cells) at each concentration of the included antigens and the results given as the number of IFN-γ producing cells per 10^6 cells. A mean number of cytokine producing cells of less than 50 per 10^6 cells are considered as negative.
32. Store plates at room temperature in the dark (*see* **Note 19**).

3.5 Detection of HCV-Specific $CD8^+$ T Cells by Pentamer Staining

The following section describes the procedure to direct ex vivo quantify the number of HCV-specific $CD8^+$ T cells in spleen cells from DNA immunized mice (Fig. 3). The procedure requires laboratory work involving one person for approximately 10 h.

1. Centrifuge the pentamer to pellet any protein aggregates present in the solution (12,000 × *g*, 10 min, +4 °C). Thereafter, directly dilute pentamer using the supernatant after centrifugation (*see* **Note 20**).
2. Dilute 10 μL of pentamer in 40 μL of wash buffer/staining buffer (per sample). The total volume is 50 μL per sample to be stained. Store the diluted pentamer at room temperature in the dark until use.
3. Prepare a single spleen cell suspension according to Subheading 3.3.
4. Calculate the volume of cell suspension corresponding to 1×10^6 cells.

5. Add 1×10^6 spleen cells to the 96-well V-bottom plate. Individual samples should be added to single wells. In addition to the individual samples, the following controls should be included:
   (a) Unstained cells (from both immunized and non-immunized mice)
   (b) Single stained cells (from immunized mice).
   (c) Double stained cells (from immunized mice).
   (d) Cells stained with pentamer only (from both immunized and non-immunized mice)
6. Centrifuge for 3 min at 450 × *g*, +4 °C.
7. Forcefully discard the supernatant by hand.
8. Wash cells once with 200 μL wash buffer/staining buffer. Pipette the solution up and down thrice in the well to loosen the cell pellets.
9. Centrifuge for 3 min at 450 × *g*, +4 °C.
10. Forcefully discard the supernatant by hand.
11. Carefully resuspend the pellet in 50 μL of pre-diluted pentamer (**item 2**). Control wells without pentamer should instead be filled up with 50 μL wash buffer/staining buffer and resuspended.
12. Incubate the plate at room temperature for 15 min in the dark (*see* **Note 21**).
13. Centrifuge for 3 min at 450 × *g*, +4 °C.
14. Forcefully discard the supernatant by hand.
15. Wash cells once with 200 μL wash buffer/staining buffer. Pipette the solution up and down thrice in the well to loosen the cell pellets.
16. Centrifuge for 3 min at 450 × *g*, +4 °C.
17. Forcefully discard the supernatant by hand.
18. Carefully resuspend the pellet in 50 μL Fc block (purified anti-mouse CD16/CD32 (FCγ III/II)) diluted at 1:50 in wash buffer/staining buffer (*see* **Note 22**).
19. Incubate the plate on ice for 15 min in the dark.
20. Centrifuge for 3 min at 450 × *g*, +4 °C.
21. Forcefully discard the supernatant by hand.
22. Wash cells once with 200 μL wash buffer/staining buffer. Pipette the solution up and down thrice in the well to loosen the cell pellets.
23. Centrifuge for 3 min at 450 × *g*, +4 °C.
24. Forcefully discard the supernatant by hand.

25. Add optimal amounts of anti-CD8, anti-CD19, and anti-CD3 antibodies in a total volume of 50 μL. Dilute antibodies in wash buffer/staining buffer. Mix by pipetting the solution up and down thrice (*see* **Notes 23** and **24**).
26. Incubate the plate on ice for 20 min in the dark.
27. Centrifuge for 3 min at 450 × *g*, +4 °C.
28. Forcefully discard the supernatant by hand.
29. Wash cells once with 200 μL wash buffer/staining buffer. Pipette the solution up and down thrice in the well to loosen the cell pellets. Repeat **item 27–29** once.
30. Fix cells by adding 150 μL fixing solution to each well (*see* **Note 25**).
31. Transfer the fixed cell suspension to FACS vials. Add another 150 μL fixing solution to each well and transfer the remaining cells to the same FACS vials.
32. Store the fixed cell suspension at +4 °C in the dark. Perform data acquisition within 2 days of staining (*see* **Note 26**).

Flow cytometric analysis:

33. To view the pentamer-positive cells we used the following gating strategy (*see* Fig. 3a). Live lymphocytes were gated, and from this gate the $CD19^+$ cells were excluded, and further gating on $CD8^+$ and $Pentamer^+$ cells were performed to determine the frequency of HCV-specific $CD8^+$ T cells (*see* Fig. 3b, c).

3.6 Detection of Liver-Specific Protein Expression by In Vivo Imaging

The following section describes the procedure to determine the presence of intrahepatic HCV protein expression in DNA immunized and non-immunized mice (Fig. 4). Bioluminescent imaging allows longitudinal studies and comparison of data sets. The procedure requires laboratory work involving one person for approximately 2 h.

Pre-imaging procedure:

1. The IVIS Spectrum in vivo imaging system should be turned on at all time.
2. Log into the computer and start the Living Image Software.
3. Initiate the system (*see* **Note 27**).
4. Check the charcoal filters on top of the anesthesia station (XGI-8 Gas Anesthesia System) by weighing (*see* **Note 28**).
5. Turn on the evacuation pump.
6. Turn on the oxygen supply switch.
7. Turn on the gas switch for the imaging chamber.
8. Set the vaporizer at 0 % isoflurane position. Thereafter turn on the imaging chamber toggle valve and set at 0.25 L/min.

9. Turn on the induction chamber toggle valve and set at 1.0 L/min.
10. Confirm the flow rate, and then turn off the two toggles.
11. Set the vaporizer to 2.0 % isoflurane (for mice) (*see* **Note 29**).
12. How to generate mice with transient intrahepatic expression of HCV NS3 and firefly luciferase has been described previously [28] (*see* Subheading 2.5). Procedure for intramuscular immunization of mice using a regular needle and syringe in combination with in vivo electro transfer has been described in Subheading 3.1.
13. Prior to anesthetizing mice the area of interest for bioluminescent measurement should be shaved. We measure the bioluminescent signal in the liver and therefore carefully shave the abdominal area of the mouse (*see* **Note 30**).
14. Weigh all mice to be analyzed (*see* **Note 31**).
15. Thaw aliquots of luciferin on ice (*see* **Note 32**).
16. Inject 10 μL luciferin (0.15 mg)/g of body weight intraperitoneally (i.p.) (*see* **Notes 33** and **34**).
17. Wait 4 min and thereafter put the animals (maximum 5 mice) in the induction chamber and turn on the induction chamber toggle valve. Keep the mice in the induction chamber for 4 min.
18. Turn on the imaging chamber toggle valve.
19. When all mice are anesthetized, transfer them from the induction chamber to the imaging chamber. Put the mice on the back with the nose in the nose cone. The shaved mouse abdomens should be exposed (*see* **Note 35**).
20. Turn off the induction chamber toggle.
21. Acquire a luminescent image using predefined protocols. The protocol is set up in the Living Image software. Enable the auto-save function. You can select auto exposure, manual exposure, and sequence acquisition. We routinely perform both auto exposure and sequence acquisition. Using the auto exposure setting the software automatically determines the binning and F/Stop settings. Using the manual exposure setting you select the exposure time, binning, and F/Stop. Using the sequence acquisition you can select several segments with different exposure time (*see* **Note 36**).
22. Select the bioluminescent imaging mode, check mark photograph and chose an appropriate Field of View (FOV) (*see* **Note 37**).
23. Capture image/s by clicking the acquire button.
24. Enter relevant image label information.

Post-imaging procedure:

25. Carefully return mice to their cage. Continuously observe mice during recovery from the gas anesthesia (*see* **Note 38**).

Turn off the anesthesia station:

26. Turn off the vaporizer and keep the oxygen supply on for approximately 5 min to clear the isoflurane in the anesthesia system before switching off the oxygen tank.
27. Turn on the induction and imaging chamber toggle valves until the pressure drop to zero.
28. Turn off the toggle valves.
29. Turn off oxygen valve.
30. Turn off the evacuation pump.
31. Securely copy your imaging data.
32. Exit the imaging software and log out from the computer.
33. Leave the IVIS Spectrum in vivo imaging system on at all time.

Image analysis and data presentation:

34. Analyze your optical images using the Living Image Software. Within the software you can perform different analyses. You may organize your images, view image information, adjust image appearance, perform background subtraction to the image, view intensity data, make measurements, overlay multiple images, export and print images.
35. Your optical imaging results may be presented in various ways. We commonly show representative photographs of mice from different groups/time-points, supported with the light emitted/radiance within a *region of interest (ROI)* and statistical comparison (Fig. 4a, b). We present the results as light emitted/radiance (photons/second/cm^2/steradian, e.g., p/s/cm^2/sr) + standard deviation (SD).

4 Notes

1. Mix the DNA and PBS to a homogeneous solution. Measure the DNA concentration to ensure correct concentration. This is especially important when higher concentrations of DNA are prepared.
2. The electro transfer program need to be evaluated prior to use. In general, a short high-voltage pulse increases the permeability of the cellular membrane. The long low-voltage pulse is believed to facilitate the transport of the DNA into the cell. Thus, both the high- and low-voltage pulses enhance the uptake of DNA into the cell.

3. The volume of Hypnorm to be used has to be adjusted depending on mouse strain and weight of the animals. The Hypnorm will anesthetize the laboratory mice for approximately 30–60 min depending on the dose.
4. Stabilize your hand by placing it against the bench. It is important that the mouse is completely restrained during the immunization and in vivo electro transfer procedure. Movements may affect the efficiency of the primed immune response. Figure 5 visualizes a tibialis anterior/cranialis muscle successfully injected with a tissue marking dye.
5. Wipe the muscle with ethanol prior to immunization to make it more visible.
6. The 27G needle tip should be injected approximately 2–3 mm into the muscle for optimal delivery of the DNA. If injected to shallow the DNA solution may leak out (e.g., subcutaneous delivery) and if injected to deep you may pass through the tibialis anterior/cranialis muscle.
7. The electrode tips should be injected approximately 3–4 mm into the muscle for an optimal in vivo electro transfer.
8. Wait a few seconds and thereafter carefully withdraw the needle/electrodes from the muscle to avoid leakage of the DNA solution from the needle/electrode hole/s.
9. Shorter incubation time will result in insufficient lysis of the red blood cells. Longer incubation time will affect the condition of the splenocytes and may results in low cell yield.
10. If the well is pre-wetted with ethanol for longer time than 1 min, the well may dry out, which often causes leakage in the PVDF membrane.
11. Decant the wash solution by flicking the plate over a waste bin in the BSC. Remove excess of water on the plate using sterile paper tissue.
12. Leaving the plate for a longer time in water or if the membrane dries out may result in leaking wells.
13. All antigens should be prepared at a 2× final concentration since antigens will be diluted in an equal volume of cell suspension.
14. Wells with leakage will give a false signal and should be excluded. It is recommended to use triplicates for all samples and dilutions.
15. Decant cell suspension by emptying the plate in a waste bin for biological waste. Wash the plate by completely immersing it in 1 × PBS and thereafter decant the PBS in the sink. Repeat the procedure at least 5 times. After the last wash, forcefully decant the remaining PBS and wipe off excess of PBS using paper tissues before proceeding to next step.

16. If bubbles appear in some wells after pipetting the substrate solution, carefully remove them by using a pipette tip. If bubbles remain on the bottom of the plate it may cause an incomplete development and thus lack of detectible spot-forming cells.
17. The plate development time varies and needs to be determined for each new protocol. Commonly one is utilizing the dilutions of the positive control (ConA) to set the time for development. Too long development time will cause a high background due to dark wells.
18. When spot-forming cells are visible in the positive control, the development should be stopped by immersing the plate in water. The spot-forming cells will be clearly visible when the plates have dried completely.
19. Plates may be stored for several years without substantial loss of SFC intensity.
20. The protein aggregates in the pentamer solution may cause nonspecific staining.
21. Prolonged incubation time may increase the sensitivity but also the nonspecific staining.
22. Addition of Fc block is important to block nonspecific antibody binding to Fc receptors on immune cells.
23. We diluted the antibodies as follows: anti-CD8 (FITC-label) 1:33, anti-CD19 (APC-label) 1:40, and anti-CD3 (PE-label) 1:33.
24. We included the following staining controls: unstained cells, single stained cells (anti-CD19, anti-CD8, anti-CD3, pentamer), double stained cells (anti-CD8 + anti-CD19, anti-CD8 + pentamer, anti-CD19 + pentamer), and triple stained cells (anti-CD8 + anti-CD8 + penatmer).
25. The working solution should be prepared fresh every time for optimal fixation.
26. You should aim at performing the data acquisition as soon as possible after staining. The longer you wait for data acquisition, the weaker fluorescent signal you will detect. This is very important if you are detecting low frequencies of antigen-specific $CD8^+$ T cells.
27. Allow several minutes for controlling the system and for the camera to cool down to –90 °C.
28. A filter that is weighting >50 g than the original weight should be replaced. This is to ensure a good absorption of the gas anesthesia.
29. The % isoflurane needed may vary between mouse strains or if rats are used. Hence, the optimal % isoflurane needs to be predetermined.

30. The fur will significantly reduce the bioluminescent signal and should therefore be removed prior to imaging.
31. This is important to calculate the accurate dose of luciferin.
32. The luciferin solution should be sterile filtered through a 0.2 μm filter. Avoid freeze-thawing of luciferin aliquots.
33. Mice should be injected with 150 mg luciferin/kg body weight. A 20 g mouse should be injected with 200 μL = 3 mg of luciferin. This is of utmost importance since luciferin (the substrate) is the limiting factor for the luminescent signal. Thus, weight-based dosing of luciferin is important to be able to compare luminescent signals between animals. Otherwise, differences in the luminescent signal may depend on the amount of substrate administered to the animals.
34. Luciferin should be injected 11 min prior to luminescent imaging.
35. Check that all mice have their noses completely inside the nose cone. Check that all mice breathe rhythmically. If the mice are not completely anesthetized increase the percentage of isoflurane by 0.25–0.5 % and wait a few minutes before analysis. Caution: If the mice wake up during the imaging procedure they may move around inside the imaging chamber and cause damage to themselves and the instrument.
36. *Exposure time:* the length of the time that the shutter is open during image acquisition. *Binning:* Controls the pixel size on the CCD camera. Hence, increasing the binning will result in increased pixel size and sensitivity. This will reduce the spatial resolution. *F/Stop:* defines the size of the camera lens aperture. A small aperture size results in lower sensitivity since less light is collected for the image. Small apertures produce sharp images whereas large apertures maximize the sensitivity.
37. The choice of FOV depends on how many mice you will image. FOV is the size of the stage area to be imaged. FOV A (part of 1 mouse), B (1 mouse), C (up to 3 mice), and D (up to 5 mice).
38. Mice usually recover within 1–5 min.

Acknowledgements

The following work was supported by grants from the Swedish Research Council (K2012-99X-22017-01-3), the Swedish Society of Medicine, Goljes Memorial Fund, the Åke Wiberg Foundation, the Ruth and Richard Juhlin Foundation, and from Karolinska Institutet.

References

1. Mohd Hanafiah K, Groeger J, Flaxman AD, Wiersma ST (2013) Global epidemiology of hepatitis C virus infection: new estimates of age-specific antibody to HCV seroprevalence. Hepatology 57:1333–1342
2. Thomas DL (2013) Global control of hepatitis C: where challenge meets opportunity. Nature Med 19:850–858
3. Sulkowski MS, Gardiner DF, Rodriguez-Torres M, Reddy KR et al (2014) Daclatasvir plus sofosbuvir for previously treated or untreated chronic HCV infection. New Engl J Med 370:211–221
4. Feld JJ, Kowdley KV, Coakley E, Sigal S et al (2014) Treatment of HCV with ABT-450/r–ombitasvir and dasabuvir with ribavirin. New Engl J Med 370:1594–1603
5. Ahlen G, Frelin L, Brenndorfer ED, Brass A et al (2013) Containing "The Great Houdini" of viruses: combining direct acting antivirals with the host immune response for the treatment of chronic hepatitis C. Drug Resist Updat 16:60–67
6. Callendret B, Eccleston HB, Hall S, Satterfield W et al (2014) T-cell immunity and hepatitis C virus reinfection after cure of chronic hepatitis C with an interferon-free antiviral regimen in a chimpanzee. Hepatology 60:1531–1540
7. Barnes E, Folgori A, Capone S, Swadling L et al (2012) Novel adenovirus-based vaccines induce broad and sustained T cell responses to HCV in man. Sci Transl Med 4:115ra111
8. Swadling L, Capone S, Antrobus RD, Brown A et al (2014) A human vaccine strategy based on chimpanzee adenoviral and MVA vectors that primes, boosts, and sustains functional HCV-specific T cell memory. Sci Transl Med 6:261ra153
9. Weiland O, Ahlen G, Diepolder H, Jung MC et al (2013) Therapeutic DNA vaccination using in vivo electroporation followed by standard of care therapy in patients with genotype 1 chronic hepatitis C. Mol Therapy 21:1796–1805
10. Di Bisceglie AM, Janczweska-Kazek E, Habersetzer F et al (2014) Efficacy of immunotherapy with TG4040, peg-interferon, and ribavirin in a Phase 2 study of patients with chronic HCV infection. Gastroenterology 147:119–131
11. Habersetzer F, Honnet G, Bain C, Maynard-Muet M et al (2011) A poxvirus vaccine is safe, induces T-cell responses, and decreases viral load in patients with chronic hepatitis C. Gastroenterology 141:890–899
12. Klade CS, Schuller E, Boehm T, von Gabain A, Manns MP (2012) Sustained viral load reduction in treatment-naive HCV genotype 1 infected patients after therapeutic peptide vaccination. Vaccine 30:2943–2950
13. Wedemeyer H, Schuller E, Schlaphoff V, Stauber RE et al (2009) Therapeutic vaccine IC41 as late add-on to standard treatment in patients with chronic hepatitis C. Vaccine 27:5142–5151
14. Frelin L, Ahlen G, Alheim M, Weiland O et al (2004) Codon optimization and mRNA amplification effectively enhances the immunogenicity of the hepatitis C virus nonstructural 3/4A gene. Gene Ther 11:522–533
15. Chen A, Ahlen G, Brenndorfer ED, Brass A et al (2011) Heterologous T cells can help restore function in dysfunctional hepatitis C virus nonstructural 3/4A-specific T cells during therapeutic vaccination. J Immunol 186:5107–5118
16. Levander S, Sällberg M, Ahlén G, Frelin L. A non-human hepadnaviral adjuvant for hepatitis C virus-based DNA vaccines. Submitted for publication.
17. Brass A, Frelin L, Milich DR, Sallberg M, Ahlen G (2015) Functional aspects of intrahepatic Hepatitis B Virus-specific T cells induced by therapeutic DNA vaccination. Mol Therapy 23:578–590
18. Tovey MG, Lallemand C (2010) Adjuvant activity of cytokines. Methods Mol Biol 626:287–309
19. Applequist SE, Rollman E, Wareing MD, Liden M et al (2005) Activation of innate immunity, inflammation, and potentiation of DNA vaccination through mammalian expression of the TLR5 agonist flagellin. J Immunol 175:3882–3891
20. Branden LJ, Mohamed AJ, Smith CI (1999) A peptide nucleic acid-nuclear localization signal fusion that mediates nuclear transport of DNA. Nature Biotechnol 17:784–787
21. Sallberg M, Frelin L, Ahlen G, Sallberg-Chen M (2015) Electroporation for therapeutic DNA vaccination in patients. Medical Microbiol Immunol 204:131–135
22. Ulmer JB, Donnelly JJ, Parker SE, Rhodes GH et al (1993) Heterologous protection against influenza by injection of DNA encoding a viral protein. Science 259:1745–1749
23. MacGregor RR, Boyer JD, Ugen KE, Lacy KE et al (1998) First human trial of a DNA-based vaccine for treatment of human immunodeficiency virus type 1 infection: safety and host response. J Infect Dis 178:92–100

24. Calarota S, Bratt G, Nordlund S, Hinkula J et al (1998) Cellular cytotoxic response induced by DNA vaccination in HIV-1-infected patients. Lancet 351:1320–1325
25. Aihara H, Miyazaki J (1998) Gene transfer into muscle by electroporation in vivo. Nature Biotechnol 16:867–870
26. Ahlen G, Soderholm J, Tjelle T, Kjeken R, Frelin L et al (2007) In vivo electroporation enhances the immunogenicity of hepatitis C virus nonstructural 3/4A DNA by increased local DNA uptake, protein expression, inflammation, and infiltration of CD3+ T cells. J Immunol 179:4741–4753
27. Gothelf A, Gehl J (2012) What you always needed to know about electroporation based DNA vaccines. Human Vaccines Immunother 8:1694–1702
28. Ahlen G, Sallberg M, Frelin L (2013) Methods for monitoring gene gun-induced HBV- and HCV-specific immune responses in mouse models. Methods Mol Biol 940:239–267
29. Fournillier A, FrelinL JE, Ahlen G et al (2013) A heterologous prime/boost vaccination strategy enhances the immunogenicity of therapeutic vaccines for hepatitis C virus. J Infect Dis 208:1008–1019
30. Lin Y, Kwon T, Polo J, Zhu YF et al (2008) Induction of broad CD4+ and CD8+ T-cell responses and cross-neutralizing antibodies against hepatitis C virus by vaccination with Th1-adjuvanted polypeptides followed by defective alphaviral particles expressing envelope glycoproteins gpE1 and gpE2 and nonstructural proteins 3, 4, and 5. J Virol 82: 7492–7503
31. Pancholi P, Perkus M, Tricoche N, Liu Q, Prince AM (2003) DNA immunization with hepatitis C virus (HCV) polycistronic genes or immunization by HCV DNA priming-recombinant canarypox virus boosting induces immune responses and protection from recombinant HCV-vaccinia virus infection in HLA-A2.1-transgenic mice. J Virol 77:382–390

Chapter 12

Designing Efficacious Vesicular Stomatitis Virus-Vectored Vaccines Against Ebola Virus

Gary Wong and Xiangguo Qiu

Abstract

Infection with the Ebola virus (EBOV) causes an aggressive hemorrhagic disease in humans and nonhuman primates. Traditional approaches, such as vaccination with inactivated virion preparations, have had limited efficacy, whereas immunization with live-attenuated EBOV is not feasible due to the highly lethal nature of the pathogen. This has necessitated the development of other approaches towards an effective EBOV vaccine. Over the past decade, recombinant viruses expressing the EBOV glycoprotein (GP) have constituted the most promising platforms, as evidenced by their ability to protect naïve nonhuman primates from a lethal EBOV challenge. The vesicular stomatitis virus (VSV) is one such vector and is currently progressing through the clinical pipeline. This chapter presents methodologies for the design, cloning, rescue, and preparation of live, recombinant VSV vaccines expressing GP for research purposes.

Key words Ebola, Vaccines, Vesicular stomatitis virus, Glycoprotein, Nonhuman primates

1 Introduction

Since its emergence in 1976, Ebola virus (EBOV) has sporadically caused outbreaks mainly localized to the remote, humid rainforests of sub-Saharan Africa. Outbreaks are unpredictable, characterized by high case fatality rates of up to 90 % [1], and tend to be contained rapidly with most outbreaks ending within several months. Until early 2014, the total number of deaths from all EBOV outbreaks stood at 1093 deaths from 1393 infections, for an aggregate case fatality rate of 78 % [1]. As such, EBOV infections are traditionally considered a minor public health problem in Africa. However, the year 2014 witnessed the largest EBOV outbreak in history. Suspected to have originated from southeastern Guinea in December 2013, the outbreak has so far recorded 9342 deaths from 23,371 total infections, with the West African countries of Guinea, Sierra Leone, and Liberia recording the majority of cases [2]. EBOV has also been imported to Nigeria, Senegal, the USA, Mali, and Scotland through travel by road or air, and has resulted

Sunil Thomas (ed.), *Vaccine Design: Methods and Protocols: Volume 1: Vaccines for Human Diseases*, Methods in Molecular Biology, vol. 1403, DOI 10.1007/978-1-4939-3387-7_12,

in new clusters of infections in Nigeria and Mali [3]. In addition to hundreds of medical personnel that have already succumbed to EBOV infection in Africa, three nurses (two in the USA and one in Spain) also contracted the disease while providing primary care to imported or repatriated cases [4, 5]. This outbreak is an example that, with increased international travel due to globalization, geographical barriers, once considered an effective barrier against some pathogens, can be easily overcome. As evidenced by the West African EBOV outbreak, even minor pathogens will be able to cause significant problems in the absence of adequate control and prevention measures.

The development of the world's first vaccine by Edward Jenner in 1798, a live-attenuated virus vaccine against smallpox, launched a new research field that has played a significant role in the war against infectious diseases over the past 200 years. The traditional vaccine approach, which uses live-attenuated pathogen, inactivated whole pathogen, or immunogenic antigens and toxins from the pathogen, is in most cases able to provoke a sufficiently protective immune response against future infections by the same pathogen. Notable successes with the traditional vaccines include the eradication of smallpox, the near eradication of polio, as well as several vaccines against childhood diseases including measles/mumps/rubella and diphtheria/tetanus/pertussis, which has limited the effects of these pathogens in developed countries. In addition, annual immunizations against influenza virus is a common practice worldwide to limit the impact of seasonal and pandemic flu, and many more vaccines exist against other diseases, including but not limited to rabies, the hepatitis A and B viruses, and yellow fever.

Routine immunizations have saved billions of human lives from communicable diseases and vaccines are widely considered one of the greatest medical inventions of modern civilization. Despite this achievement, there are still several diseases for which researchers have yet to develop effective vaccines. This includes pathogens such as human immunodeficiency virus (HIV), malaria, Leishmania, and Dengue virus. In addition, traditional vaccine approaches have not been effective against EBOV in nonhuman primate (NHP) studies. Gamma-irradiated, inactivated EBOV virion preparations used to immunize NHPs 4 weeks prior to a high-dose EBOV challenge were not protective, with all three cynomolgus macaques succumbing to disease and only one out of two rhesus macaques surviving challenge [6]. Live-attenuated EBOV virions have not been tested as a vaccine candidate due to safety concerns. Consequently, novel approaches are necessary to develop a vaccine that is safe and efficacious in NHPs and eventually humans.

A particularly popular and successful approach has been to produce recombinant viruses which express the EBOV glycoprotein (EBOVGP) gene as vaccines against EBOV. These recombinant vaccines are able to elicit specific humoral and cellular immune responses, and have led to the development of several promising

candidates. So far, vaccine platforms based on human adenovirus serotype 5 (Ad5) with and without a DNA prime [7, 8], Ad26 prime with an Ad35 boost [9], chimpanzee adenovirus type 3 [10], human parainfluenza virus type 3 [11], rabies virus [12], Venezuelan equine encephalitis virus replicons [13], and vesicular stomatitis virus [14] have all conferred complete protection to NHPs when given 4–5 weeks before a lethal EBOV challenge.

Of all the vaccine candidates, only the replication-competent VSV-vectored vaccine (VSVΔG/EBOVGP) has been successful at protecting animals when given after a lethal challenge, as evidenced by the survival in four of eight EBOV-infected NHPs that were treated 30 min after a lethal EBOV challenge [15]. Therefore, VSVΔG/EBOVGP is the most promising candidate for the rapid immunization of a population during a filovirus outbreak. In this chapter, we describe our optimized methods for the design and production of laboratory-grade VSVΔG/EBOVGP vaccines for research purposes. Strategies for cloning, transfection, rescue, growth, purification, and titering of these recombinant viral vaccines will be presented.

2 Materials

In addition to the specific materials required for the procedures below, the researcher should also ensure the availability of the following general laboratory supplies as they will be often used:

1. Pipetman and Pipet aid.
2. Consumables including pipet tips, pipets, Eppendorf tubes, cryovials, T-150 tissue culture flasks, 6- and 12-well tissue culture plate, ice, 4 ml round-bottom snap-cap tubes, 50 ml Falcon tubes, and 60 × 15 mm petri dishes.
3. 37 °C Shaker/incubator for bacterial cultures and plates.
4. 37 °C Incubator for tissue culture purposes.
5. Low-melting-point (LMP) agarose, loading dye, stains for the visualization of nucleic acids.
6. Agarose gel electrophoresis system.
7. Gel documentation system.
8. 37, 42, and 56 °C water bath.
9. Tabletop centrifuge, microcentrifuge, and ultracentrifuge.
10. Thermomixer.
11. Vortex.
12. Thermocycler for PCR-based applications.
13. Optical (light) microscope.
14. Biosafety cabinet.

2.1 Cloning of EBOVGP into the VSVXN2ΔG Plasmid

1. Vector and insert: VSVXN2ΔG plasmid and TOPO-EBOVGP DNA.
2. Cloning primers:
   5′XhoI = AATACTCGAGGCCACCATGGGCGTTACAG GAATATTG
   3′NheI = AATAGCTAGCGATTTTCTGTTTAAACGTA TATGTC.
3. Restriction enzymes and buffers: *XhoI* (New England Biolabs, catalogue #R0146), *NheI* (New England Biolabs, catalogue #R0131), and 10× NEBuffer2.1 (New England Biolabs).
4. TOPO cloning kit: TOPO® TA Cloning® Kit (Life Technologies).
5. T4 DNA ligase: T4 DNA ligase (Life Technologies).
6. TOP10 cells: One Shot® TOP10 Chemically Competent *E. coli* (Life Technologies).
7. SOC media: Dissolve 20 g tryptone, 5 g yeast extract, 2 ml of 5 M NaCl, 2.5 ml of 1 M KCl, 10 ml of 1 M $MgCl_2$, 10 ml of 1 M $MgSO_4$, 20 ml of 1 M glucose in distilled water. Adjust volume to 1 L with distilled water, and sterilize by autoclaving. Store at room temperature.
8. LB/amp broth: Dissolve 10 g tryptone, 5 g yeast extract, and 10 g NaCl in distilled water. Adjust the pH to 7.0 using 1 N NaOH and bring volume up to 1 L with distilled water. Sterilize by autoclaving. Cool the solution to 50 °C. Add 100 mg of ampicillin. Store at room temperature.
9. LB/amp agarose plates: Dissolve 10 g tryptone, 5 g yeast extract, 15 g agar, and 10 g NaCl in distilled water. Adjust the pH to 7.0 using 1 N NaOH and bring volume up to 1 L with distilled water. Sterilize by autoclaving. Cool the solution to 50 °C. Add 100 mg of ampicillin. Pour into petri dishes with a liquid depth of approximately 3 mm. Remove surface bubbles and leave covered for room temperature until plates have solidified. Store at 4 °C.
10. Taq: Taq DNA Polymerase, recombinant (Life Technologies).
11. Miniprep and midiprep kits: QIAGEN Plasmid Mini Kit (Qiagen) and QIAGEN Plasmid Midi Kit (Qiagen).

2.2 Lipofectamine-Based Transfection and Rescue of Recombinant VSVΔG/EBOVGP

1. VeroE6 cells: VERO C1008 [Vero 76, clone E6, Vero E6] (ATCC® CRL-1586™).
2. 293T cells: 293T/17 [HEK 293T/17] (ATCC® CRL-11268™).
3. DMEM: Dulbecco's Modified Eagle's Medium (GE Healthcare).

4. FBS: Fetal bovine serum (GE Healthcare).
5. L-Glutamine: L-Glutamine, 200 mM solution (Life Technologies).
6. Pen/Strep: Penicillin/Streptomycin (Life Technologies).
7. OptiMEM: Opti-MEM® I Reduced Serum Medium (Life Technologies).

2.3 Determining the Infectious Titer of the VSVΔG/EBOVGP Starter Stock

1. VeroE6 cells: VERO C1008 [Vero 76, clone E6, Vero E6] (ATCC® CRL-1586™).
2. DMEM: Dulbecco's Modified Eagle's Medium (GE Healthcare).
3. FBS: Fetal bovine serum (GE Healthcare).
4. L-Glutamine: L-Glutamine, 200 mM solution (Life Technologies).
5. Pen/Strep: Penicillin/Streptomycin (Life Technologies).
6. MEM: Modified Eagle's Medium (Temin's modification) (2×), no phenol red (Life Technologies).
7. 3 % w/v CMC solution: 30 g Carboxymethylcellulose (CMC) in 1 L water, heat to a maximum of 65 °C. Sterilize by autoclaving. Note that CMC will take overnight to dissolve, so it is best to prepare this overlay ahead of time.
8. Crystal violet stock solution: 2 % w/v Crystal violet, two parts 100 % ethanol, one part 37 % formaldehyde, and seven parts deionized water. Store in the dark at room temperature.
9. Crystal violet working solution: One part crystal violet stock solution, one part 37 % formaldehyde, and eight parts deionized H_2O. Use immediately after making this from stock solution.

2.4 Growth of VSVΔG/EBOVGP to High Titers and Purification

1. VeroE6 cells: VERO C1008 [Vero 76, clone E6, Vero E6] (ATCC® CRL-1586™).
2. DMEM: Dulbecco's Modified Eagle's Medium (GE Healthcare).
3. FBS: Fetal bovine serum (GE Healthcare).
4. L-Glutamine: L-Glutamine, 200 mM solution (Life Technologies).
5. Pen/Strep: Penicillin/Streptomycin (Life Technologies).
6. Equilibration buffer: 20 mM Tris–HCl, pH 7.5, 0.1 M NaCl, 0.1 mM EDTA. Filter sterilize. Store at room temperature.
7. 20 % w/v Sucrose solution: Dissolve 20 g of sucrose per 100 ml of equilibration buffer. Filter sterilize. Store at room temperature.

3 Methods

The process for the cloning and expression of VSVΔG/EBOVGP was designed in-house by the Special Pathogens Program, at the Public Health Agency of Canada in the year 2004, and the generated viruses have already been characterized and published [16]. An outline of the entire production process is detailed (Fig. 1). We describe the full protocol below.

3.1 Cloning of EBOVGP into the VSVXN2ΔG Plasmid

The VSVXN2ΔG plasmid contains the full VSV genome except for the wild-type VSV glycoprotein (G), and is described in the following publication along with the accessory plasmids required to rescue the virus [16]. There exists a multiple cloning site between the VSV matrix and the RNA-dependent RNA polymerase genes, in which our gene of interest (EBOVGP) can be cloned in. For our experiments, we chose the *XhoI* and *NheI* restriction enzyme sites. The EBOVGP gene (Genbank nucleotide L11365.1, coding sequence from nucleotide 6041 to 8071, containing eight adenosine residues in the EBOVGP editing site) was used and the restriction enzyme sites *XhoI* and *NheI* were introduced by PCR to the 5′ and 3′ ends of the gene with 5′XhoI and 3′NheI, respectively, for cloning into VSVXN2ΔG (Fig. 2). The EBOVGP gene could

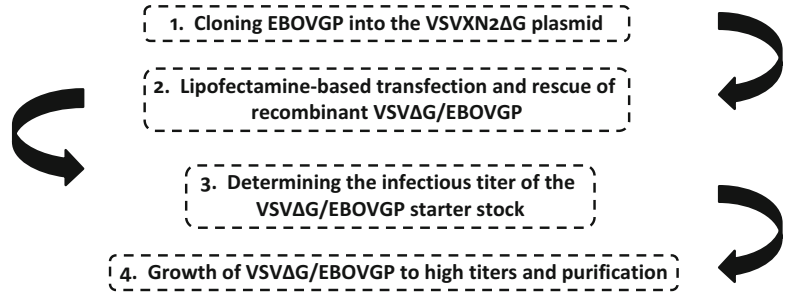

Fig. 1 Flowchart of major steps in the production of the VSVΔG/EBOVGP vaccine

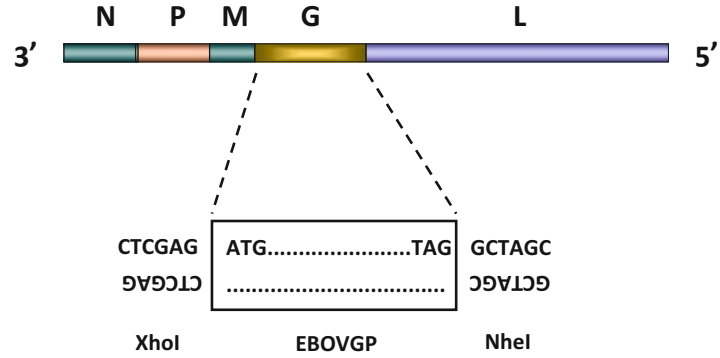

Fig. 2 Schematic of the VSV genome in pVSVXN2ΔG. The sites in which the wild-type G is replaced by EBOVGP are shown

be cloned into any vector of choice for amplification. We used the pCR™2.1-TOPO® vector, part of the TOPO® TA Cloning® Kit (Life Technologies), following the manufacturer's instructions, to create a plasmid expressing the modified EBOVGP (TOPO-EBOVGP). At least 1 μg each of the vector (VSVXN2ΔG) and insert (TOPO-EBOVGP) plasmids will be required for the following procedures.

1. Digest 1 μg of each plasmid separately with the restriction enzymes *XhoI* and *NheI* in NEBuffer2.1. Our suggested digestion conditions are as follows:

Vector or insert DNA	1 μg
Restriction enzyme buffer (10× concentration)	2 μl
XhoI/*NheI* (10 U/μl)	1 μl/enzyme
Nuclease-free water	Up to 20 μl

2. Run the samples on a 1 % w/v LMP agarose gel by electrophoresis.
3. Excise the desired vector and insert bands from the LMP gel by using a scalpel and place into separate tubes.
4. Incubate the excised gels at −80 °C for 5 min.
5. Preheat Eppendorf tubes for mixing the insert and vector on a thermomixer set at 72 °C.
6. Incubate tubes of excised gels from −80 °C at 72 °C for 10 min, and vortex every few minutes to ensure that the samples are thawed and mixed.
7. Prepare a T4 DNA ligase mixture (Life Technologies) as follows* and then incubate on ice:

T4 DNA ligase buffer (10× concentration)	4 μl
T4 DNA ligase	4 μl
Nuclease-free water	Up to 10 μl

*This reaction was made for each ligation. Multiply individual volumes accordingly if more than one ligation reaction is needed.

8. Prepare vector/insert mixtures as described below in fresh Eppendorf tubes preheated at 72 °C (10 μl total volume):
   Vector DNA = 10 μl, insert DNA = 0 μl
   Vector DNA = 3 μl, insert DNA = 7 μl
   Vector DNA = 2 μl, insert DNA = 8 μl
   Vector DNA = 1 μl, insert DNA = 9 μl
9. Centrifuge vector/insert mixtures for ~6 s at high speed, and incubate at 37 °C for 1 min.

10. Add 10 μl of T4 DNA ligase mixture to 10 μl of each vector/insert mixture; ensure thorough mixture by pipetting up and down. Vortex and spin down briefly in a tabletop centrifuge.
11. Incubate the ligation mixtures overnight at 16 °C.
12. Incubate ligation mixtures from 16 °C in a 37 °C water bath for 30 min to 1 h before transformation.
13. Thaw four tubes of chemically competent TOP10 cells (Life Technologies) at room temperature.
14. Transfer ligation mixtures to a 72 °C thermomixer. Add 100 μl of SOC media to each mixture and incubate for 5 min while vortexing intermittently to ensure that the mixture has fully melted.
15. Incubate ligation mixtures at room temperature for 5 min to bring ligation mixtures to same temperature as TOP10 cells.
16. Add the ligation mixtures to the TOP10 cells; do not pipet up and down to disrupt the cells.
17. Incubate on ice for 1 h, and mix the contents in the tubes by inverting approximately 10 min into the incubation.
18. Heat shocks the TOP10 cells in a 42 °C water bath for 1.5 min.
19. Transfer TOP10 cells onto ice immediately after the heat shock and add 700 μl of SOC media to each tube.
20. Incubate tubes for 1.5 h in a shaking 37 °C incubator.
21. Centrifuge TOP10 cells for 2 min at 4000 rpm (1500 × *g*), and decant excess supernatant to leave ~100 μl.
22. Resuspend cells in the remaining supernatant, and plate on pre-warmed LB agar plates with ampicillin (100 μg/ml).
23. Incubate plate upside-down overnight in a 37 °C incubator. The plate without any insert DNA should not have colonies, whereas the plates with vector/insert mixtures should yield colonies (*see* **Notes 1** and **2**).
24. Select four to six colonies for screening. Use a sterile pipet tip, inoculate colonies into 2 ml of LB broth, and grow in 37 °C shaking incubator overnight.
25. Extract DNA with a mini-prep kit (Qiagen) following the manufacturer's instructions, and confirm by PCR with primers 5′XhoI and 3′NheI, using the Taq DNA polymerase (Life Technologies) and following the manufacturer's instructions. The annealing temperature should be 57.5 °C if using primers 5′XhoI and 3′NheI.
26. Amplify the recombinant plasmid (pVSVXN2ΔG/EBOVGP) by standard midi-prep (Qiagen) following the manufacturer's instructions for transfection.

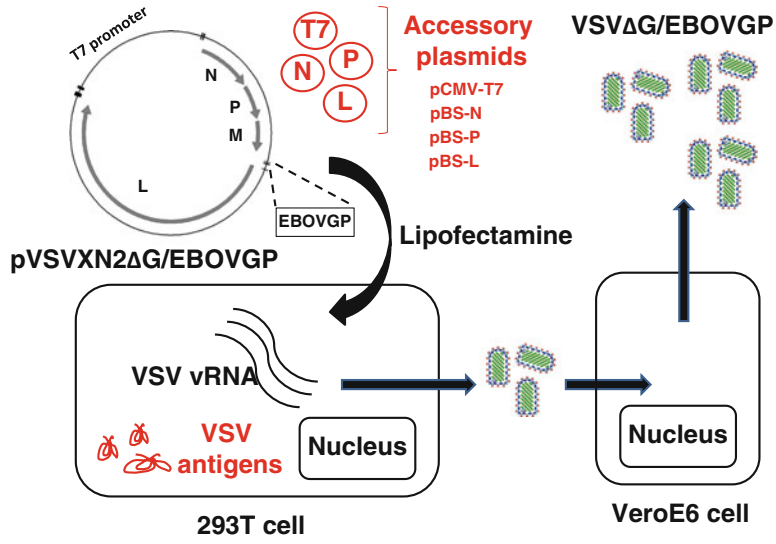

Fig. 3 Diagram of the transfection system used to rescue recombinant VSVΔG/EBOVGP

3.2 Lipofectamine-Based Transfection and Rescue of Recombinant VSVΔG/EBOVGP

While BSR-T7 cells were used initially to rescue live recombinant VSVΔG/EBOVGP vaccine [16], a 1:1 mixture of 293T:VeroE6 cells (*see* **Note 3**) are now used in place of these cells to transfect and rescue recombinant VSV (Fig. 3).

1. Plate a 1:1 mixture of 293T:VeroE6 cells in a 6-well plate. Cells should be between 70 and 80 % confluent at the time of transfection.
2. Prepare plasmids and lipofectamine in the amounts as indicated in Table 1 in separate tubes (12 tubes total). Note that each well in the 6-well plate will receive the mixed contents of 1 Tube A and 1 Tube B.
3. Allow the contents to incubate for 5 min at room temperature.
4. Combine the contents of Tube A and B by adding B to A. Incubate for 15 min at room temperature.
5. Add 720 μl of Opti-MEM media to each tube.
6. Remove media from the 6-well plates and gently wash the cells once with plain DMEM. Add the transfection mixtures to each well by slowly pipetting dropwise into the wells. Do not disturb the cell monolayer.
7. Incubate for 24 h at 37 °C, 5 % CO_2.
8. Without removing the transfection inoculum, add 1 ml of DMEM supplemented with 2 % FBS (DMEM 2 % FBS) slowly down the side of each well without disturbing the cell monolayer.

Table 1
Transfection ratios by the lipofectamine method

	Tube A: add to 90 μl Opti-MEM					Tube B: add to 90 μl Opti-MEM
Well #	pVSVXN2ΔG/EBOVGP	T7	N	L	P	Lipofectamine 2000
1	2.0 μg	2.0 μg	0.5 μg	0.25 μg	1.25 μg	14 μl
2	2.0 μg	2.5 μg	0.5 μg	0.25 μg	1.25 μg	14 μl
3	2.5 μg	2.5 μg	0.625 μg	0.75 μg	1.56 μg	14 μl
4	2.0 μg	2.5 μg	0.5 μg	0.6 μg	1.25 μg	14 μl
5	2.0 μg	2.0 μg	0.5 μg	0.25 μg	1.25 μg	0 μl
6	0 μg	0 μg	0 μg	0 μg	0 μg	14 μl

9. Incubate the plates for 48 h at 37 °C.
10. Seed fresh VeroE6 plates in 6-well plates, such that they are 90–95 % confluent by the end of the 48-h incubation.
11. Remove media from the VeroE6 plates just before infection.
12. Blind passage 500 μl of the inoculum from each well of the transfection plate onto the fresh VeroE6 cells (*see* **Note 4**).
13. Rock plates to spread inoculum evenly over the cells, and incubate for 1 h, rocking the plate every 15 min.
14. Add 2 ml of DMEM 2 % FBS to each well of the VeroE6 plate.
15. Incubate at 37 °C, 5 % CO_2, until CPE is observed. For VSVΔG/EBOVGP, this could take between 2 and 7 days depending on the amount of virus in the blind passage.
16. Collect contents from wells showing CPE, and spin at 4000 rpm ($3000 \times g$) for 5 min to separate cell lysate from the supernatant.
17. Collect and aliquot the supernatant (starter stock), and store at −80 °C until further use.
18. If desired, immunoblotting may be performed with the cell lysate to confirm for EBOVGP expression. An aliquot of starter stock may also be used to perform sequencing to confirm that VSVΔG/EBOVGP was indeed rescued.
19. Proceed with plaque assay of starter stock to determine the infectious titer of VSVΔG/EBOVGP.

3.3 Determining the Infectious Titer of the VSVΔG/EBOVGP Starter Stock

1. Seed VeroE6 cells in 12-well plates so that the cells are 100 % confluent on the day of infection.
2. Prepare the virus dilutions in plain DMEM by tenfold serial dilution from 10^{-2} to 10^{-8}.

3. Remove media from VeroE6 cells.
4. Add 250 μl of plain DMEM to the mock well.
5. Add 250 μl of the virus dilutions starting with the highest dilution to each well (in duplicate).
6. Rock plates to spread virus inoculum evenly over the cells, and incubate for 1 h at 37 °C, 5 % CO_2. Rock plates every 15 min.
7. Immediately before the 1-h incubation is complete, mix equal volumes of the 3 % w/v carboxymethylcellulose (CMC) overlay with 2× MEM supplemented with 4 % FBS.
8. Remove the virus inoculum from cells.
9. Dispense 2 ml of overlay per well. Always dispense medium or overlay gently to the side of the well to prevent the formation of holes in the monolayer. To prevent cross-contamination, start with the highest dilution (lowest amount of virus).
10. Place the plates in a 37 °C incubator, 5 % CO_2. Check plates every day until plaques can be visualized with the naked eye.
11. Add 1 ml of crystal violet working solution per well to stain the uninfected cells. Clusters of infected cells will not stain and will remain white. Leave on bench overnight.
12. Gently remove the CMC/crystal violet from each well and wash three times with PBS. Do not disturb the monolayer.
13. Count the number of white plaques (*see* **Note 5**) at an appropriate dilution (preferably 50–60 plaques per well), calculate the average, and determine the number of plaque-forming units (PFU) per ml:

$$\mathrm{PFU/ml} = \mathrm{Mean\,\#plaques} / (\mathrm{dilution} \times \mathrm{volume(inml)})$$

3.4 Growth of VSVΔG/EBOVGP to High Titers and Purification

1. Seed between 1 and 5 flasks of VeroE6 cells in T-150 tissue culture flasks, 2–3 days before infection. The cells should be 90–95 % confluent at the time of infection.
2. Infect VeroE6 cells with VSVΔG/EBOVGP diluted in DMEM 2 % FBS at an MOI of 0.001 or lower (*see* **Note 6**). For the infection, infect a T-150 culture flask with 10 ml of virus inoculum for 1 h, remove inoculum, and then add 30 ml of DMEM 2 % FBS.
3. Harvest cell lysate and supernatant between 48 and 72 h after infection, or approximately when 80 % of the cells show CPE (infected VeroE6 cells rounding and becoming non-adherent).
4. Centrifuge tubes at 4000 rpm ($3000 \times g$) for 10 min and collect the supernatant in a fresh, sterile 50 ml Falcon tube. Be sure not to disturb the pellet containing cell lysate.
5. Add 8 ml of 20 % sucrose dissolved v/v in equilibration buffer to a ultracentrifuge tube for the Beckman SW28 rotor.

6. Add plain DMEM to the harvested supernatant to bring the total volume of supernatant to 60 ml.
7. Carefully layer 30 ml of supernatant over the 20 % sucrose cushion.
8. Centrifuge the tubes in the SW28 rotor for 2 h at a speed of 27,000 rpm (1.4 x $10^5 \times g$) at a temperature of 4 °C.
9. Remove excess liquid, and resuspend the virus pellet (white-grey in color at the bottom of the tube) in 38 ml of equilibration buffer.
10. Centrifuge the tubes in the SW28 rotor for 30 min at a speed of 27,000 rpm (1.4 x $10^5 \times g$) at a temperature of 4 °C.
11. Remove excess liquid, and resuspend the pellet in 500 μl of equilibration buffer.
12. Aliquot and store the purified VSVΔG/EBOVGP vaccine in −80 °C for future use.
13. To determine the infectious titer of this new stock, perform the plaque assay as described previously in Subheading 3.3.

4 Notes

1. During the ligation process, if the vector has not been digested sufficiently there may be a significant number of colonies on the control plate without insert DNA after the transformation. In this case, only proceed with the protocol if there are significantly more colonies in the plates with insert DNA added compared to the control plate.
2. After ligation and transformation, if no colonies are present on the plates, modifying the vector/insert DNA mixtures may be considered to a ratio of 4:6 or 5:5 to increase chances of successful ligation.
3. Unless noted otherwise, VeroE6 cells and 293T cells are grown and maintained in DMEM supplemented with 10 % FBS, 1 % v/v L-glutamine, and 1 % v/v each of Pen/Strep. Infection is with DMEM supplemented with 2 % FBS, 1 % v/v L-glutamine, and 1 % v/v each of Pen/Strep. Heat inactivate FBS for 45 min in a 56 °C water bath before use.
4. During the transfection stage, a strategy to maximize the success of blind passage is to blind passage an aliquot of the transfection inoculum onto fresh VeroE6 cells every day, replacing the transfection inoculum with DMEM 2 % FBS such that there will be enough inoculum for blind passage the next day.
5. When counting plaques, the appropriate dilution should have between 30 and 300 plaques in the 12-well plate.

6. During amplification of the VSVΔG/EBOVGP vaccine, it is important to infect VeroE6 cells at a low MOI (between 0.0001 and 0.001), in order to minimize the occurrence of defective, interfering particles which may impact vaccine efficacy.

References

1. CDC.gov (2014) Outbreaks chronology: Ebola virus disease. http://www.cdc.gov/vhf/ebola/outbreaks/history/chronology.html. Accessed 15 Feb 2015
2. WHO.int (2015) Ebola response roadmap situation report update. http://apps.who.int/gho/data/view.ebola-sitrep.ebola-summary-20150220?lang=en
3. CDC.gov (2015) 2014 Ebola outbreak in West Africa—outbreak distribution map. http://www.cdc.gov/vhf/ebola/outbreaks/2014-west-africa/distribution-map.html#areas. Accessed 15 Feb 2015
4. Promedmail.org (2014) Ebola virus disease—ex Africa (27): USA (Texas) Second nurse better, test, quarantine. http://www.promedmail.org/direct.php?id=2910297. Accessed 15 Jan 2015
5. Promedmail.org (2014) Ebola virus disease—ex Africa (32): Spanish nurse recovered, USA seeks patent. http://www.promedmail.org/direct.php?id=2939861. Accessed 15 Jan 2015
6. Geisbert TW, Pushko P, Anderson K, Smith J, Davis KJ, Jahrling PB (2002) Evaluation in nonhuman primates of vaccines against Ebola virus. Emerg Infect Dis 8:503–507
7. Sullivan NJ, Sanchez A, Rollin PE, Yang ZY, Nabel GJ (2000) Development of a preventive vaccine for Ebola virus infection in primates. Nature 408:605–609
8. Sullivan NJ, Geisbert TW, Geisbert JB, Xu L et al (2003) Accelerated vaccination for Ebola virus haemorrhagic fever in non-human primates. Nature 424:681–684
9. Zahn R, Gillisen G, Roos A, Koning M et al (2012) Ad35 and ad26 vaccine vectors induce potent and cross-reactive antibody and T-cell responses to multiple filovirus species. PLoS One 7(12):e44115
10. Stanley DA, Honko AN, Asiedu C, Trefry JC et al (2014) Chimpanzee adenovirus vaccine generates acute and durable protective immunity against ebolavirus challenge. Nat Med 20:1126–1129
11. Bukreyev A, Rollin PE, Tate MK, Yang L et al (2007) Successful topical respiratory tract immunization of primates against Ebola virus. J Virol 81:6379–6388
12. Blaney JE, Marzi A, Willet M, Papaneri AB et al (2013) Antibody quality and protection from lethal Ebola virus challenge in nonhuman primates immunized with rabies virus based bivalent vaccine. PLoS Pathog 9(5):e1003389
13. Herbert AS, Kuehne AI, Barth JF, Ortiz RA et al (2013) Venezuelan equine encephalitis virus replicon particle vaccine protects nonhuman primates from intramuscular and aerosol challenge with ebolavirus. J Virol 87:4952–4964
14. Jones SM, Feldmann H, Stroher U, Geisbert JB et al (2005) Live attenuated recombinant vaccine protects nonhuman primates against Ebola and Marburg viruses. Nat Med 11:786–790
15. Feldmann H, Jones SM, Daddario-DiCaprio KM, Geisbert JB et al (2007) Effective post-exposure treatment of Ebola infection. PLoS Pathog 3(1):e2
16. Garbutt M, Liebscher R, Wahl-Jensen V, Jones S et al (2004) Properties of replication-competent vesicular stomatitis virus vectors expressing glycoproteins of filoviruses and arenaviruses. J Virol 78:5458–5465

Chapter 13

Assessment of Functional Norovirus Antibody Responses by Blocking Assay in Mice

Maria Malm, Kirsi Tamminen, and Vesna Blazevic

Abstract

Norovirus (NoV)-specific serum antibodies bind to NoV-derived virus-like particles (VLPs) and block the binding of VLPs to the host cell attachment factors/receptors, histo-blood group antigens (HBGAs). Blocking antibodies in human sera have been associated with a protection from NoV infection and disease. Studies of experimental NoV VLP-based vaccines measure blocking antibodies in animal sera instead of a traditional virus neutralization assay. This chapter describes the methodology for analyzing blocking antibodies from NoV GII.4 VLP-immunized mouse sera. Protocol for obtaining mouse NoV GII.4-specific immune sera is described, followed by the detailed protocol for blocking assay using synthetic HBGAs.

Key words Norovirus, VLPs, HBGAs, Vaccine, Antibody, Blocking assay

1 Introduction

Norovirus (NoV) is the most common cause of gastroenteritis causing >90 % of viral gastroenteritis cases and 50 % of gastroenteritis outbreaks worldwide [1]. NoV outbreaks occur usually in closed or semi-closed settings such as hospitals, cruise ships, and holiday resorts [2]. In outbreak settings NoV was associated with ~69,000 cases of acute gastroenteritis (AGE), ~1000 hospitalizations, and 125 deaths during 1 year in the USA only [3]. The economic burden is very high; NoV accounts for ~2.5 billion $ cost due to loss of productivity and hospitalizations in the USA each year [4]. NoV causes also sporadic cases of AGE being responsible for 900,000 clinic visits and 64,000 hospitalizations in developed countries, and ~200,000 deaths of children in developing countries annually [1].

Human NoVs belong to the family *Caliciviridae*, genus *Norovirus*. Positive-sense, single-stranded RNA genome is approximately 7.5 kb in length and consists of three open reading frames (ORF). ORF-1 encodes nonstructural proteins; ORF2 encodes viral protein 1 (VP1), the major capsid protein, and ORF3 encodes VP2 [5, 6]. NoVs are classified into six genogroups (GI-GVI) of

Sunil Thomas (ed.), *Vaccine Design: Methods and Protocols: Volume 1: Vaccines for Human Diseases*, Methods in Molecular Biology, vol. 1403, DOI 10.1007/978-1-4939-3387-7_13,

which GI, GII, and GIV infect human beings and contain at least 35 different genotypes [7]. Genotype GII.4 has dominated for the last two decades causing large epidemics every 2–4 years worldwide [8, 9]. The capsid protein VP1, specifically protruding (P) domain, is the most exposed, antigenic and it likely contains determinants for host cell attachment [10, 11]. Expression of NoV VP1 in vitro results in virus-like particles (VLPs) which are structurally and antigenically similar to the virus but lack genetic material [11]. VLPs based on the sequences of VP1 from GI.1 and GII.4 NoVs produced in baculovirus expression system have been used in phase I/II clinical trials as promising vaccine candidates against NoV [12–14]. Other NoV VLP-based vaccine candidates are being tested in animal (preclinical) immunogenicity studies [15–18].

Human histo-blood group antigens (HBGA), complex carbohydrates found on the surface of red blood cells and enterocytes as well as free antigens in body secretions, e.g., saliva, act as NoV host cell attachment factors/receptors [19–21]. As NoVs are uncultivable in cell cultures in vitro, NoV-specific serum antibody blocking of VLP binding to the HBGA found in human secretor-positive saliva [22–24] or to the synthetic biotinylated carbohydrates [18, 23, 25] is considered a surrogate neutralization assay for NoVs [23, 26, 27]. More recently, pig gastric mucin has also been used as a source of HBGAs [28]. Protection from NoV infection has been correlated with the blocking antibodies found in serum of infected [25, 26, 29, 30] and vaccinated individuals [14].

In this chapter, intramuscular immunization of BALB/c mice with NoV GII.4 VLPs (Subheading 3.1) produced in baculovirus expression system and purified as described in detail elsewhere [31, 32] is described. Optimized method for detection of blocking antibodies in serum (blocking assay) of immune mice using synthetic biotinylated H-type-1 HBGA is described in detail (Subheading 3.2) (Fig. 1). Although the blocking assay described here relates to detection of blocking antibodies in serum of animals following experimental immunization, similar method can be used to test blocking antibodies in human serum following vaccination in clinical trials or following infection with NoV [26].

2 Materials

Prepare all solutions using ultrapure water and analytical grade reagents. Prepare and store all regents at indicated temperatures. Follow safety regulations when working with the reagents and dispose of waste materials according to waste disposal regulations.

2.1 BALB/c Mice Immunization with NoV GII.4 VLPs and Serum Collection

1. BALB/c mice (e.g., BALB/cOlaHsd mice, Harlan, The Netherlands).
2. Commercially available sterile-grade phosphate-buffered saline (PBS) without Ca and Mg (0.0067 M PO_4) (e.g., Lonza).

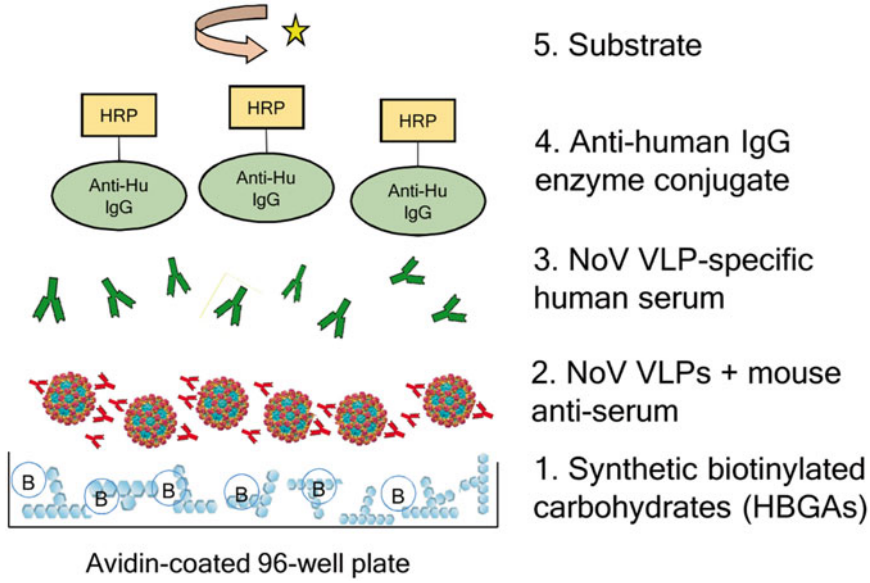

Fig. 1 Blocking assay. Avidin-coated 96-well plates are incubated with synthetic biotinylated HBGAs. Norovirus (NoV) VLPs preincubated with the serum of VLP-immunized mice are added to the plates. Binding of the VLPs to the HBGAs is detected with NoV-specific human serum. Enzyme-conjugated anti-human IgG antibodies are used for detection of bound human antibodies. Substrate reaction is measured by an ELISA plate reader

3. NoV GII.4 VLP stock solution in PBS (*see* **Notes 1** and **2**).
4. Sterile H_2O.
5. 0.3 mL Insulin syringes (29 G × 1/2″ – 0.33 × 12 mm).
6. Working solution of medetomidine (1 mg/kg) and ketamine (75 mg/kg): Prepare by mixing medetomidine (1 mg/mL), ketamine (50 mg/mL), and sterile H_2O in the ratio of 1:1.5:2.5, respectively (*see* **Note 3**).
7. Working solution of atipamezole (0.17 mg/mL): Prepare by diluting atipamezole (5 mg/mL) 1:30 with sterile H_2O (*see* **Note 3**).
8. Sterile surgical scissors.
9. Eppendorf tubes, pipette, and pipette tips for blood collection.
10. Centrifuge.

2.2 Blocking Assay

1. Phosphate-buffered saline (1 × PBS) (0.0067 M PO_4).
2. Distilled water.
3. NoV GII.4 VLP stock solution in PBS (*see* **Notes 1** and **2**).
4. Avidin precoated/preblocked 96-well plates (Thermo/Pierce).
5. 0.2 M Monobasic stock (2 L): 55.2 g $NaH_2PO_4 \times H_2O$ (MW 137.99 g/mol) in 2.0 L distilled water. Store at RT.

6. 0.2 M Dibasic stock (1 L): 28.4 g Na_2HPO_4 (MW 141.96 g/mol) in 1.0 L distilled water. Store at RT.
7. 0.1 M Sodium phosphate (pH 6.4): Mix 1102.5 mL of 0.2 M monobasic stock with 397.5 mL of 0.2 M dibasic stock and fill to 3.0 L with distilled water. Store at RT.
8. Blocking assay dilution buffer: 0.1 M Sodium phosphate (pH 6.4) supplemented with 0.25 % bovine serum albumin (BSA). Store at +4 °C.
9. Blocking assay washing buffer: 0.1 M Sodium phosphate (pH 6.4) buffer. Store at RT.
10. Synthetic H-type-1 (tri)-PAA-biotin HBGA (*see* **Note 4**) (Glycotech).
11. 1.5 mL Protein low-binding tubes with a cap (e.g., Eppendorf® Protein LoBind microcentrifuge tubes, Eppendorf).
12. Detection serum (*see* **Note 5**): Human NoV-positive serum.
13. Secondary antibody (*see* **Notes 5** and **6**): Horseradish peroxidase (HRP)-conjugated goat anti-human IgG-HRP (e.g., Life Technologies).
14. Ready-to-use o-phenylenediamine dihydrochloride (OPD) substrate: Prepare the substrate by dissolving one OPD tablet and one buffer tablet (Sigma) in 20 mL distilled water by vortexing. Use immediately after preparation. The final concentrations of the ready-to-use substrate are 0.4 mg/mL OPD, 0.4 mg/mL urea hydrogen peroxide, and 0.05 M phosphate-citrate, pH 5.0.
15. 2 M H_2SO_4: 56.1 mL 95 % H_2SO_4. Fill to 0.5 L with distilled water.
16. 37 °C Incubator.
17. ELISA plate reader (e.g., Victor2 1420, Perkin Elmer).

3 Methods

The methods describe intramuscular immunization of BALB/c mice with NoV GII.4 VLPs for the generation of GII.4-specific serum (Subheading 3.1) tested in blocking assay (Subheading 3.2), a surrogate NoV neutralization assay.

3.1 BALB/c Mice Immunization with NoV GII.4 VLPs and Serum Collection

1. Acclimatized 6–9-week-old BALB/c female mice at least 1 week prior to immunization. All procedures performed on the animals need to be authorized by the national Animal Ethical Committee approval and conducted according to the national guidelines, making all efforts to minimize animal suffering.

2. Dilute VLP stock solution in sterile-grade PBS to obtain desirable concentration (i.e., 200 μg/mL for 10 μg dose/50 μL PBS/immunization).
3. Prepare working stock dilution in sterile H_2O of medetomidine (1 mg/kg) and ketamine (75 mg/kg) and anesthetize the mice 0.05 mL/10 g subcutaneously (SC) (*see* **Note 3**). Administer 50 μL (10 μg/dose) of the NoV VLPs (at 200 μg/mL) intramuscularly (IM) (*see* **Note 7**) to cranial or caudal tight muscles with 0.3 mL insulin syringe (29G × 1/2″ – 0.33 × 12 mm). Administer 50 μL sterile-grade PBS (a carrier only) to negative control mice.
4. Reverse the sedation of medetomidine/ketamine by injecting 0.01–0.02 mL/10 g SC working stock of atipamezole (*see* **Note 3**).
5. To obtain strong immune response (especially IgG antibody response), mice should be immunized twice (i.e., at days 0 and 21) with the above protocol.
6. Two weeks after the final immunization sacrifice mice. Anesthetize mice as described above. Sacrifice mice by cutting the axillary artery and/or vein and collect the whole blood in Eppendorf tube.
7. Let the blood settle at least for 2 h at RT.
8. Centrifuge at 3500 × *g* for 20 min at RT.
9. Collect the serum into clean tube. Serum can be stored at –20 °C until the analysis or used fresh.

3.2 Detection of Blocking Antibodies in Serum (Blocking Assay)

1. Prepare solutions of 0.1 M sodium phosphate (pH 6.4) supplemented with 0.25 % BSA (dilution buffer) and 0.1 M sodium phosphate (pH 6.4) (wash buffer). Dilute all reagents and test samples in dilution buffer.
2. Wash the avidin-coated plate three times with wash buffer (200 μL/well).
3. Dilute synthetic biotinylated H-type-1 HBGA to 2.5 μg/mL (*see* **Note 8**). Add 100 μL of diluted HBGA into each well.
4. Cover the plate with plate-sealing tape and incubate for 1 h at RT.
5. Prepare serial dilutions of the mouse immune sera (*see* **Note 9**) in 1.5 mL low-binding Eppendorf tubes. Start with the serum dilution two times stronger than the final dilution in the plate as adding VLPs will dilute the samples 1:1 (*see* **Note 10** and Fig. 2).
6. Vortex the NoV GII.4 VLP stock solution very well (~5 s) and prepare 0.8 μg/mL dilution in dilution buffer. This will yield to a final concentration of 0.4 μg/mL when mixed with serum dilutions (*see* **Note 11**).

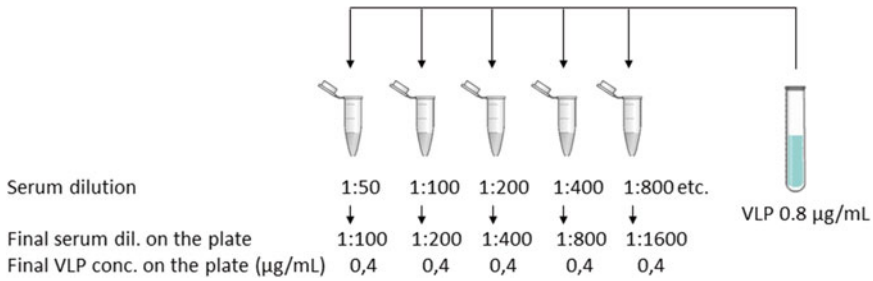

Fig. 2 Pipetting scheme for **steps 5–7** in Subheading 3.2. Serial dilutions of the sera are prepared in 1.5 mL low-binding tubes and the VLP is added to each serum tube (volume 1:1). Adding the VLP at the concentration of 0.8 μg/mL will give the final concentration of 0.4 μg/mL VLP in the analysis

7. Add equal amount of the VLP dilution made in **step 6** to each serum dilution tube (1:1) and vortex briefly (~3 s) (Fig. 2).
8. Prepare "maximum binding control" (a tube containing only the VLPs at 0.4 μg/mL final concentration and no serum) by mixing the VLPs prepared in **step 6** with dilution buffer 1:1 (Fig. 2). Vortex briefly (~3 s).
9. Incubate serum—VLP sample tubes made in **step 7** and the "maximum binding control" tube made in **step 8** for 1 h at +37 °C.
10. Wash the plate 6× with wash buffer (300 μL/well).
11. Add the serum—VLP samples and the "maximum binding control" to the plate (100 μL/well) in duplicates. Include blank wells (dilution buffer only, 100 μL/well).
12. Cover the plate with plate-sealing tape and incubate for 2 h at +4 °C.
13. Wash the plate 6× with wash buffer (300 μL/well).
14. Dilute detection serum, e.g., NoV GII.4 IgG-positive human serum using predetermined dilution factor (*see* **Note 5**). Add 100 μL per well.
15. Cover the plate with plate-sealing tape and incubate at +4 °C for 1 h.
16. Wash the plate 6× with wash buffer (300 μL/well).
17. Dilute anti-human IgG—horseradish peroxidase (HRP)—conjugate using predetermined dilution factor (*see* **Note 6**), and add 100 μL per well.
18. Cover the plate with plate-sealing tape and incubate for 1 h at +4 °C.
19. Wash the plate 6×with wash buffer (300 μL/well).
20. Add ready-to-use OPD substrate (0.4 mg/mL) to each well (100 μL/well).

21. Cover the plate with plate-sealing tape and incubate for 20 min at RT in the dark.
22. Stop the reaction with 2 M H_2SO_4 (50 μL/well).
23. Measure optical density (OD) at λ 490 nm using ELISA microplate reader.
24. Analyze the results:
    (a) Subtract the mean OD value of blank wells from all other OD values on the plate.
    (b) Calculate the mean OD value for all duplicate wells including the "maximum binding control" wells.
    (c) Calculate blocking index (% blocking) for each serum dilution using the following equation:

$$100\% - (\text{meanOD VLPwithserumdilution} / \text{meanOD Maximumbinding} \times 100\%)$$

4 Notes

1. NoV GII.4 VLP antigen has been produced using a baculovirus–insect cell expression system and purified by sucrose gradient ultracentrifugation [31, 32].
2. Instead of the GII.4 VLPs any other type of NoV VLPs may be used for immunization of mice and blocking assay. HBGA binding profile of the VLPs is dependent on the NoV genotype [33]; therefore verify the binding of the VLP to the particular HBGA with the protocol described in Subheading 3.2 but omit the use of mouse immune serum.
3. Other equivalent anesthetics can be applied. Check the need for reversing the anesthesia with atipamezole if you use other anesthetics than medetomidine/ketamine.
4. Other synthetic polyvalent biotinylated HBGAs can be used in the blocking assay but binding of the VLPs to the biotinylated HBGA should be confirmed using the protocol (Subheading 3.2) without the use of mouse immune sera.
5. Detection serum must be positive for NoV GII.4-specific IgGs or any other VLPs used. Use detection serum from other species than the serum used for blocking. If mice serum is used for blocking of GII.4 VLP binding, e.g., human, rabbit, or guinea pig, polyclonal immune serum may be used for detection. Final dilution of a given detection serum should be determined by the user to give high OD for the VLP maximum binding. An $OD \geq 0.7$ is considered appropriate [33]. We use final dilution of 1:1000 of the detection human serum. Some human sera react strongly with the avidin [34], so the reactivity should be determined prior to conducting the blocking assay and such

sera should not be used. If using detection serum originating from an animal, matching HRP-conjugate antibody should be used in **step 17**.

6. The final dilution of the secondary HRP-conjugate antibody should be determined by the user.
7. Different doses of NoV VLPs can be used for immunizations. Volume of 50 μL is the preferred volume per injection site for IM administration route. Other immunization routes such as intradermal and intranasal immunization can be applied to generate immune serum.
8. The concentration of HBGA used for coating of the wells needs to be determined for each HBGA batch separately; however, 2.5 μg/mL has worked well for several synthetic HBGAs tested with this protocol.
9. Similar method can be used to test blocking antibodies in human serum following vaccination in clinical trials or following infection with NoV [26]. In that case, the detection antibody needs to be changed accordingly.
10. Starting from final serum dilution of 1:100 and further serially diluting the serum is an optimal procedure for the blocking assay described in this chapter. If blocking of heterologous VLP (other genotype than the one used for the immunizations) binding to the HBGAs needs to be tested, it is recommended to start at a lower final serum dilution of, e.g., 1:10.
11. Final VLP concentration needs to be predetermined for each VLP to obtain high OD value ($OD \geq 0.7$) for VLP maximum binding. VLP used should be titrated first with the protocol described in Subheading 3.2 without adding mouse immune serum to determine which concentration gives an appropriate OD value.

Acknowledgements

We thank all personnel of Vaccine Research Center, University of Tampere, for their support in this work, especially Ms. Leena Huhti for the VLP production and Ms. Marianne Karlsberg for excellent technical help.

References

1. Patel MM, Widdowson MA, Glass RI, Akazawa K, Vinje J, Parashar UD (2008) Systematic literature review of role of noroviruses in sporadic gastroenteritis. Emerg Infect Dis 14:1224–1231
2. Vega E, Barclay L, Gregoricus N, Shirley SH, Lee D, Vinje J (2014) Genotypic and epidemiologic trends of norovirus outbreaks in the united states, 2009 to 2013. J Clin Microbiol 52:147–155

3. Hall AJ, Wikswo ME, Manikonda K, Roberts VA, Yoder JS, Gould LH (2013) Acute gastroenteritis surveillance through the national outbreak reporting system, United States. Emerg Infect Dis 19:1305–1309
4. Bartsch SM, Lopman BA, Hall AJ, Parashar UD, Lee BY (2012) The potential economic value of a human norovirus vaccine for the united states. Vaccine 30:7097–7104
5. Clarke IN, Lambden PR (1997) The molecular biology of caliciviruses. J Gen Virol 78(Pt 2):291–301
6. Thorne LG, Goodfellow IG (2014) Norovirus gene expression and replication. J Gen Virol 95(Pt 2):278–291
7. Kroneman A, Vega E, Vennema H, Vinje J, White PA et al (2013) Proposal for a unified norovirus nomenclature and genotyping. Arch Virol 158:2059–2068
8. Lindesmith LC, Costantini V, Swanstrom J, Debbink K et al (2013) Emergence of a norovirus GII.4 strain correlates with changes in evolving blockade epitopes. J Virol 87:2803–2813
9. Debbink K, Lindesmith LC, Donaldson EF, Costantini V et al (2013) Emergence of new pandemic GII.4 Sydney norovirus strain correlates with escape from herd immunity. J Infect Dis 208:1877–1887
10. Prasad BV, Hardy ME, Dokland T, Bella J et al (1999) X-ray crystallographic structure of the norwalk virus capsid. Science 286:287–290
11. Jiang X, Wang M, Graham DY, Estes MK (1992) Expression, self-assembly, and antigenicity of the norwalk virus capsid protein. J Virol 66(11):6527–6532
12. Atmar RL, Bernstein DI, Harro CD, Al-Ibrahim MS et al (2011) Norovirus vaccine against experimental human norwalk virus illness. N Engl J Med 365:2178–2187
13. Bernstein DI, Atmar RL, Lyon GM, Treanor JJ et al (2014) Norovirus vaccine against experimental human GII.4 virus illness: a challenge study in healthy adults. J Infect Dis 211(6):870–8
14. Treanor JJ, Atmar RL, Frey SE, Gormley R et al (2014) A novel intramuscular bivalent norovirus virus-like particle vaccine candidate-reactogenicity, safety, and immunogenicity in a phase 1 trial in healthy adults. J Infect Dis 210:1763–1771
15. Blazevic V, Lappalainen S, Nurminen K, Huhti L, Vesikari T (2011) Norovirus VLPs and rotavirus VP6 protein as combined vaccine for childhood gastroenteritis. Vaccine 29:8126–8133
16. Tamminen K, Lappalainen S, Huhti L, Vesikari T, Blazevic V (2013) Trivalent combination vaccine induces broad heterologous immune responses to norovirus and rotavirus in mice. PLoS One 8(7), e70409
17. Velasquez LS, Shira S, Berta AN, Kilbourne J et al (2011) Intranasal delivery of norwalk virus-like particles formulated in an in situ gelling, dry powder vaccine. Vaccine 29:5221–5231
18. LoBue AD, Lindesmith L, Yount B, Harrington PR et al (2006) Multivalent norovirus vaccines induce strong mucosal and systemic blocking antibodies against multiple strains. Vaccine 24:5220–5234
19. Marionneau S, Cailleau-Thomas A, Rocher J, Le Moullac-Vaidye B et al (2001) ABH and lewis histo-blood group antigens, a model for the meaning of oligosaccharide diversity in the face of a changing world. Biochimie 83:565–573
20. Hutson AM, Atmar RL, Graham DY, Estes MK (2002) Norwalk virus infection and disease is associated with ABO histo-blood group type. J Infect Dis 185:1335–1337
21. Ravn V, Dabelsteen E (2000) Tissue distribution of histo-blood group antigens. APMIS 108:1–28
22. Tan M, Jiang X (2005) Norovirus and its histo-blood group antigen receptors: an answer to a historical puzzle. Trends Microbiol 13:285–293
23. Harrington PR, Lindesmith L, Yount B, Moe CL, Baric RS (2002) Binding of norwalk virus-like particles to ABH histo-blood group antigens is blocked by antisera from infected human volunteers or experimentally vaccinated mice. J Virol 76:12335–12343
24. Huang P, Farkas T, Marionneau S, Zhong W et al (2003) Noroviruses bind to human ABO, lewis, and secretor histo-blood group antigens: identification of 4 distinct strain-specific patterns. J Infect Dis 188:19–31
25. Nurminen K, Blazevic V, Huhti L, Rasanen S et al (2011) Prevalence of norovirus GII-4 antibodies in Finnish children. J Med Virol 83:525–531
26. Reeck A, Kavanagh O, Estes MK, Opekun AR et al (2010) Serological correlate of protection against norovirus-induced gastroenteritis. J Infect Dis 202:1212–1218
27. Atmar RL, Estes MK (2012) Norovirus vaccine development: next steps. Expert Rev Vaccines 11:1023–1025
28. Lindesmith LC, Debbink K, Swanstrom J, Vinje J et al (2012) Monoclonal antibody-based antigenic mapping of norovirus GII.4-2002. J Virol 86:873–883
29. Malm M, Uusi-Kerttula H, Vesikari T, Blazevic V (2014) High serum levels of norovirus

genotype-specific blocking antibodies correlate with protection from infection in children. J Infect Dis 210:1755–1762

30. Cannon JL, Lindesmith LC, Donaldson EF, Saxe L et al (2009) Herd immunity to GII.4 noroviruses is supported by outbreak patient sera. J Virol 83:5363–5374
31. Huhti L, Tamminen K, Vesikari T, Blazevic V (2013) Characterization and immunogenicity of norovirus capsid-derived virus-like particles purified by anion exchange chromatography. Arch Virol 158:933–942
32. Koho T, Mantyla T, Laurinmaki P, Huhti L et al (2012) Purification of norovirus-like particles (VLPs) by ion exchange chromatography. J Virol Methods 181:6–11
33. Uusi-Kerttula H, Tamminen K, Malm M, Vesikari T, Blazevic V (2014) Comparison of human saliva and synthetic histo-blood group antigens usage as ligands in norovirus-like particle binding and blocking assays. Microbes Infect 16:472–480
34. Bubb MO, Green F, Conradie JD, Tchernyshev B et al (1993) Natural antibodies to avidin in human serum. Immunol Lett 35:277–280

Chapter 14

Development of a SARS Coronavirus Vaccine from Recombinant Spike Protein Plus Delta Inulin Adjuvant

Clifton McPherson, Richard Chubet, Kathy Holtz, Yoshikazu Honda-Okubo, Dale Barnard, Manon Cox, and Nikolai Petrovsky

Abstract

Given periodic outbreaks of fatal human infections caused by coronaviruses, development of an optimal coronavirus vaccine platform capable of rapid production is an ongoing priority. This chapter describes the use of an insect cell expression system for rapid production of a recombinant vaccine against severe acute respiratory syndrome coronavirus (SARS). Detailed methods are presented for expression, purification, and release testing of SARS recombinant spike protein antigen, followed by adjuvant formulation and animal testing. The methods herein described for rapid development of a highly protective SARS vaccine are equally suited to rapid development of vaccines against other fatal human coronavirus infections, e.g., the MERS coronavirus.

Key words Coronavirus, SARS, MERS, Vaccine, Adjuvant, Delta inulin, Advax adjuvant, Baculovirus, Manufacture, cGMP

1 Introduction

The severe acute respiratory syndrome coronavirus (SARS) was first identified in 2003 after a series of fatal pneumonia cases characterized by an inflammatory cell infiltrate with diffuse alveolar damage [1] started in Hong Kong before spreading to other countries [2]. Before being controlled by quarantine measures, ~8000 humans were infected, with fatality as high as 50 % in the elderly and an overall case fatality rate of ~10 % [2]. More recently, the Middle East respiratory syndrome coronavirus (MERS) has caused a series of serious and, in some cases, fatal human infections [3]. Given the risk of future serious human coronavirus outbreaks, development of a suitable vaccine platform to protect against such viruses is a major priority. These vaccines present several challenges including the rapidity with which these outbreaks develop and hence the need for rapid vaccine manufacture. Hence, a successful coronavirus vaccine platform must overcome multiple challenges.

Sunil Thomas (ed.), *Vaccine Design: Methods and Protocols: Volume 1: Vaccines for Human Diseases*, Methods in Molecular Biology, vol. 1403, DOI 10.1007/978-1-4939-3387-7_14,

SARS CoV is a positive-stranded RNA virus 29.7 kb in length with 14 open reading frames [4]. Initial SARS vaccine candidates were produced from inactivated virus. Inactivated whole-virus vaccines provided only modest protection, inducing low-neutralizing antibody titers that did not protect against infection but were associated with faster lung clearance of virus [5]. However, immunization of mice with inactivated vaccines either alone or formulated with alum adjuvant resulted in severe lung eosinophilic pathology in response to virus challenge [6–9], similar to enhanced lung pathology seen with SARS virus reexposure after primary infection [10]. Hence a major challenge when developing a SARS vaccine is to identify strategies to avoid lung eosinophilic pathology.

A further challenge when developing vaccines based on inactivated SARS virus is the need for high-containment biosafety level 3 cGMP manufacturing facilities [11]. This makes vaccine manufacture more complex and expensive and restricts the number of vaccine doses that can be rapidly manufactured. To counter these challenges, it would be preferable to produce a subunit vaccine that just like inactivated virus was able to induce neutralizing antibodies against SARS-CoV, but rather than requiring BSL3 manufacture was able to be produced in a regular recombinant protein manufacturing environment.

The potential solution to this problem lies in the coronavirus spike protein (S protein), which in the case of SARS virus binds to angiotensin-converting enzyme 2 and CD209L and induces receptor-mediated virus endocytosis, thereby being critical to virus entry into target cells [12, 13]. S protein could thereby provide an ideal antigen with which to induce neutralizing antibodies against SARS virus [14, 15]. However, while immunization with S protein in animal models provided some protection against SARS virus [16, 17], S protein-immunized animals when subsequently challenged with live virus developed severe lung eosinophilic immunopathology, with this problem exacerbated even further when S protein vaccine was formulated with alum adjuvant [6, 9]. A similar problem of lung eosinophilic immunopathology has been seen with other viruses including respiratory syncytial virus (RSV) vaccines, which prime for an excessive and harmful Th2-dominated lung immune response upon subsequent virus exposure [18]. Lung eosinophilic immunopathology is exacerbated by formulation of such vaccines with any adjuvant that induces excess Th2 immune polarization, e.g., aluminum salt adjuvants [6, 9]. Hence, while S protein would appear to be an ideal SARS vaccine antigen, there is first the need to reduce the risk of lung eosinophilic immunopathology being induced by the vaccine.

Described below are methods used for the development and manufacture of a recombinant subunit vaccine based on an S protein antigen lacking transmembrane and cytoplasmic domains (S ΔTM) that was expressed using a baculovirus insect cell expression

platform. As the S ΔTM protein antigen itself has low immunogenicity [16, 17], steps are also described for formulation with a safe and effective adjuvant [19]. As aluminum adjuvants are contraindicated for SARS vaccines given they may exacerbate lung eosinophilic pathology; instead methods are described for formulation of the S ΔTM protein with Advax™, a safe and effective adjuvant based on delta inulin [20, 21] that has been previously shown in animal models to enhance the immunogenicity of a broad range of viral and bacterial antigens [22–30] and has also been shown safe and effective in preliminary human clinical trials [31, 32]. Notably, Advax adjuvant was recently shown to enhance the immunogenicity and protection conferred by both inactivated and recombinant SARS vaccines, without the excess Th2 bias of alum adjuvants and hence without the risk of inducing lung eosinophilic immunopathology [33].

For this project a recombinant baculovirus was designed to express the ectodomain of the SARS S protein, lacking the transmembrane and cytoplasmic domains [17]. The recombinant protein expressed by this vector was termed SARS S ΔTM. This truncated version of the S protein was selected as it contains the receptor-binding domain (RBD) and was able to be expressed in insect cells at a higher level than the full-length membrane-bound version. The SARS S RBD has been shown to induce neutralizing antibodies against the SARS CoV [14, 15]. After infection of *expres*SF+® insect cells with the recombinant baculovirus, the S ΔTM protein is expressed and secreted into the cell culture medium [17]. The procedure detailed below for purifying the SARS S ΔTM protein can be followed after production of the protein in a baculovirus/insect cell system. The process is designed for a 45 L fermentation in a 60 L bioreactor but may be adjusted to other scales as necessary. Following harvest, the SARS S ΔTM protein is purified by column chromatography; a schematic is provided in Fig. 1. In the first step, the supernatant is flowed through linked UNOsphere S (UNO S) and DEAE sepharose columns. DNA and protein impurities are removed, and the SARS S ΔTM protein remains in the flow through. The flow through from the UNO S/DEAE step is applied to lentil lectin sepharose, SARS S ΔTM binds, and impurities are removed. Following elution from the lentil lectin sepharose column, the protein is concentrated, and buffer is exchanged by ultrafiltration. The retentate from the ultrafiltration step is processed through a 0.22 μm filter, and the purified protein is stored at −20 °C. Prior to intended use, the purified SARS S ΔTM protein is mixed under conditions with a suspension of Advax™ delta inulin adjuvant particles and either aseptically filled into single-dose vials or loaded directly into syringes ready for vaccination. Lastly, the adjuvanted SARS vaccine is tested for efficacy and safety in animal immunogenicity and SARS challenge models.

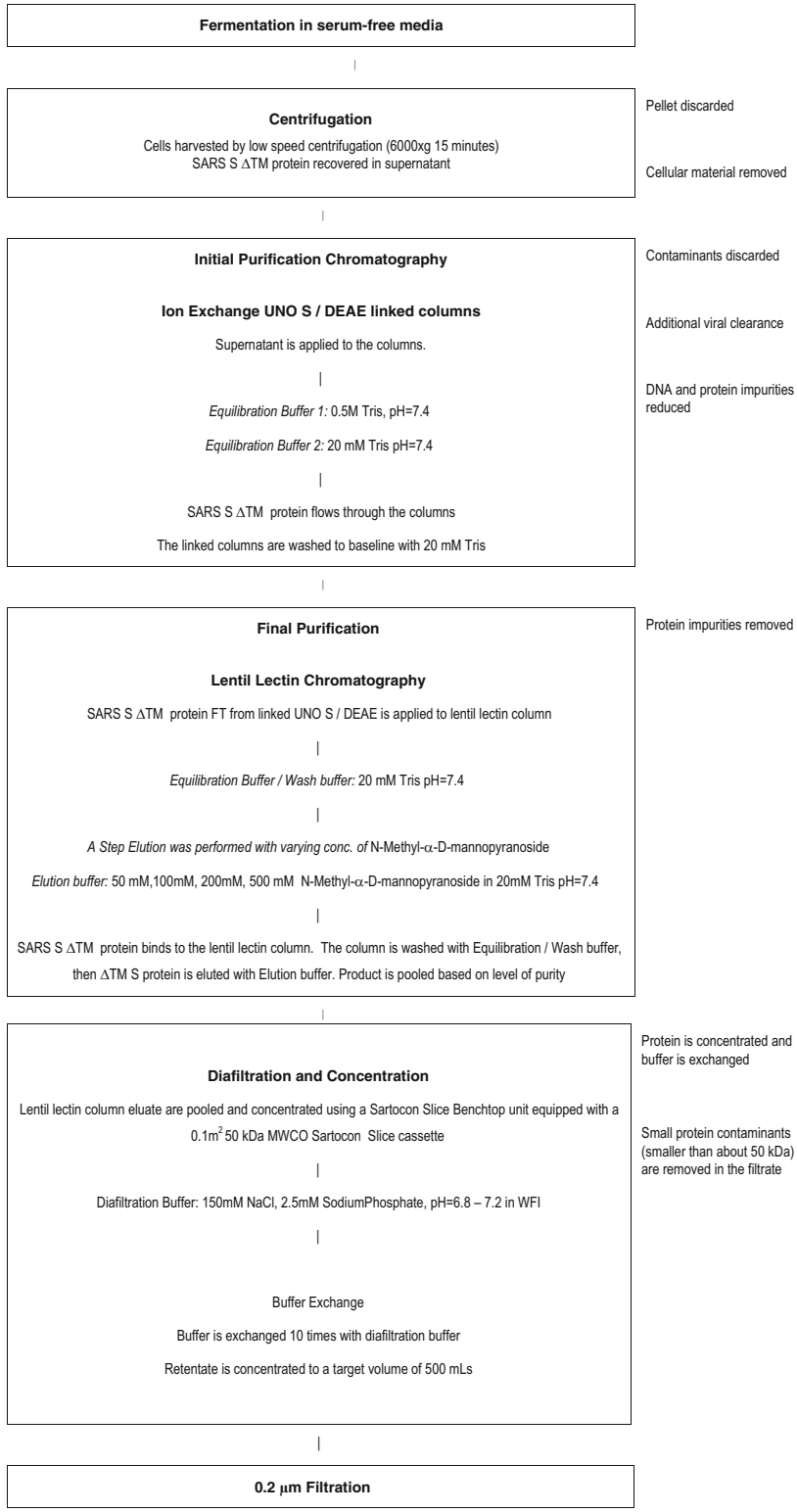

Fig. 1 Process flow diagram of SARS S ΔTM protein

2 Materials

2.1 Fermentation Harvest

1. 1 L Nalgene centrifuge bottles (Thermo Scientific).
2. High-speed centrifuge.
3. Centrifuge rotor to accommodate 1 L bottles.
4. Sterile 50 L Nalgene carboy (Thermo Scientific).
5. 0.22 μm filter (EMD Millipore).

2.2 UNO S/DEAE Column Chromatography

1. Two BPG columns (GE Healthcare).
2. UNOsphere S chromatography resin (Bio-Rad).
3. DEAE Sepharose Fast Flow chromatography resin (GE Healthcare).
4. Chromatography system equipped with UV and conductivity monitors.
5. Tris(hydroxymethyl)aminomethane (Trizma; Sigma-Aldrich).
6. Concentrated HCl.
7. Purified water.
8. Sterile 50 L Nalgene carboy (Thermo Scientific).

2.3 Lentil Lectin Capture Chromatography

1. XK 50 column (GE Healthcare).
2. Lentil lectin Sepharose 4B (GE Healthcare).
3. Chromatography system equipped with UV and conductivity monitors.
4. Tris(hydroxymethyl)aminomethane (Sigma-Aldrich).
5. Concentrated HCl.
6. Purified water.
7. N-methyl-α-D-mannopyranoside (Sigma-Aldrich).
8. Sterile Nalgene square 250 mL polycarbonate bottles (Thermo Scientific).

2.4 Concentration, Ultrafiltration, and 0.22 μm Filtration

1. Sartocon Slice 200 bench top system (Sartorius).
2. Sartocon Slice 200 PESU cassette (Sartorius).
3. Pump.
4. Sodium phosphate monobasic monohydrate (Sigma-Aldrich).
5. Sodium phosphate dibasic 12-hydrate (Sigma-Aldrich).
6. Sodium chloride (Sigma-Aldrich).
7. Purified water.
8. Pipettes.
9. Microcentrifuge tubes.
10. Sterile Nalgene square 500 mL polycarbonate bottle (Thermo Scientific).

2.5 Adjuvant Formulation

1. Delta inulin adjuvant suspended in bicarbonate buffer (Vaxine Pty Ltd).
2. CpG oligonucleotide powder (Oligo Factory, USA).
3. Water for injection (Baxter).

2.6 Mouse Immunogenicity Testing

1. Female 6–8-week-old BALB/c mice weighing 18–20 g.
2. 0.5 mL Insulin syringes (BD).
3. 5 mL Syringes.
4. 25G 5/8 needles.
5. Animal lancet, 4 mm (Medipoint Inc., USA).
6. 96-Well ELISA plates (Greiner Bio-One).
7. 24-Well culture plates (Greiner Bio-One).
8. 0.1 M Sodium carbonate buffer, pH 9.6.
9. 1 % BSA/PBS.
10. Biotinylated anti-mouse IgG, IgG1, IgG2a, IgG2b, IgG3, or IgM antibodies (Abcam).
11. Streptavidin-HRP (BD Biosciences).
12. TMB substrate (KPL, USA).
13. 1 M Phosphoric Acid.
14. Cell strainers, 70 μm Nylon (Falcon).
15. RPMI complete medium with 10 % heat-inactivated FBS (Invitrogen Life Technologies).
16. Red blood cell (RBC) lysis buffer (155 mM NH_4Cl; 10 mM $KHCO_3$; 0.1 mM EDTA, pH 7.3).
17. Carboxy-fluorescein diacetate succinimidyl ester (CFSE) (Invitrogen Life Technologies).
18. MultiScreen HTS, 96-well filtration plate (Merck Millipore).
19. Anti-mouse CD16/CD32 (BD Biosciences).
20. Anti-mouse CD4-APC (BD Biosciences).
21. Anti-mouse CD8a-PE-Cy7 (BD Biosciences).
22. Anti-mouse IFN-γ, IL-2, IL-4 antibody pairs (BD Biosciences).
23. LEAF anti-mouse IL-17A and biotin-anti-mouse IL-17A antibody (BioLegend, USA).

2.7 Animal Challenge Studies

1. Female 4–8-week-old BALB/c mice weighing 18–20 g.
2. SARS-CoV virus strain Urbani (200300592), Centers for Disease Control and Prevention, Atlanta, GA, USA.
3. Vero 76 cell line (American Type Culture Collection, Manassas, VA, USA).
4. Hematoxylin and eosin stain.

5. Rat monoclonal antibody (Clone MT-14.7) to eosinophil major basic protein MBP (Lee Laboratory, Mayo Clinic, Arizona).
6. DAB chromogen.

3 Methods

3.1 Fermentation Harvest

1. Separate cells and culture supernatant by centrifugation at 5900 × *g* at 2–8 °C for 15 min.
2. Transfer culture supernatant to a sterile 50 L carboy.
3. After all culture supernatant is collected, filter through 0.22 μm filter into a second sterile 50 L carboy (*see* **Note 1**).
4. Store at 2–8 °C.

3.2 UNO S/DEAE Column Chromatography

1. Pack a BPG column with 1.9 L of UNO S resin (*see* **Note 2**).
2. Pack a BPG column with 1.5 L of DEAE Sepharose Fast Flow resin.
3. pH equilibrate the UNO S column with 0.5 M Tris pH 7.4 at a flow rate of 200–400 mL/min until outflow pH is 7.0–7.7. This step typically requires 3 column volumes of buffer (*see* **Note 3**).
4. Continue equilibration of the UNO S column with 20 mM Tris pH 7.4 at a flow rate of 200–400 mL/min until outflow is pH 7.2–7.5 and conductivity is ≤500 mS. This step typically requires 5 column volumes.
5. pH equilibrate the DEAE column with 0.5 M Tris pH 7.4 at a flow rate of 200–400 mL/min until outflow pH is 6.9–7.6. This step typically requires 3 column volumes of buffer.
6. Continue equilibration of the DEAE column with 20 mM Tris pH 7.4 at a flow rate of 200–400 mL/min until outflow is pH 7.0–7.5 and conductivity is ≤500 mS. This step typically requires 5 column volumes.
7. Connect the DEAE column to the outflow of the UNO S column.
8. Equilibrate the linked UNO S and DEAE columns with 20 mM Tris pH 74 at a flow rate of 200–400 mL/min until outflow is pH 6.9–7.6 and conductivity is ≤500 mS.
9. Apply the culture supernatant from Subheading 2.1 to the linked UNO S/DEAE columns at a flow rate of not more than 300 mL/min (*see* **Note 4**).
10. Begin collecting the flow through from the linked columns into a 50 L carboy when the UV trace begins to rise.
11. Wash the linked columns with 20 mM Tris pH 7.4 and collect the wash in the carboy with the column flow through.

12. Collect ≤10 L of wash, and stop collection of the wash when the UV trace returns to baseline.
13. Proceed to lentil lectin capture chromatography.

3.3 Lentil Lectin Capture Chromatography

1. Pack XK-50 column with 250 mL of lentil lectin sepharose (*see* **Note 2**).
2. Equilibrate lentil lectin column with 20 mM Tris pH 7.4 at a flow rate of 50–100 mL/min using 10 column volumes of buffer. pH should be 7.2–7.5.
3. Load UNO S/DEAE flow through to the lentil lectin column at a flow rate of 50–100 mL/min (*see* **Note 5**).
4. Wash column with 20 mM Tris pH 7.4 at a flow rate of 50–100 mL/min for 5 column volumes or until UV trace returns to baseline.
5. Collect fractions in sterile Nalgene square 250 mL polycarbonate bottles.
6. Elute with 2 column volumes of 50 mM N-methyl-α-D-mannopyranoside and 20 mM Tris pH 7.4 at a flow rate of 50–100 mL/min. Collect two 250 mL fractions.
7. Elute with 2 column volumes of 100 mM N-methyl-α-D-mannopyranoside and 20 mM Tris pH 7.4 at a flow rate of 50–100 mL/min. Collect two 250 mL fractions.
8. Elute with 2 column volumes of 200 mM N-methyl-α-D-mannopyranoside and 20 mM Tris pH 7.4 at a flow rate of 50–100 mL/min. Collect two 250 mL fractions.
9. Elute with 5 column volumes of 500 mM N-methyl-α-D-mannopyranoside and 20 mM Tris pH 7.4 at a flow rate of 50–100 mL/min. Collect 250 mL fractions until UV trace is flat and stable.
10. Store fractions at 2–8 °C.
11. Analyze all fractions by SDS-PAGE and Western blot to determine which fractions contain SARS S ΔTM protein.
12. Pool fractions containing detectable SARS S ΔTM protein.

3.4 Concentration, Ultrafiltration, and 0.22 μm Filtration

1. Assemble Sartocon Slice 200 bench top ultrafiltration system with a 0.1 m^2 50 kDa molecular weight cutoff Sartocon Slice cassette according to the manufacturer's instructions.
2. Attach a process tank according to the manufacturer's instructions.
3. Fill process tank with water for injection (WFI).
4. Close permeate valve and circulate WFI through the system at 200 mL/min for 3–4 min.
5. Open permeate valve.
6. Increase circulation rate to 600–800 mL/min.

7. Adjust retentate valve to obtain a transmembrane pressure (TMP) of 8.0–17.0 psi.
8. Continue rinsing for 5–10 min.
9. Repeat **steps 3–8** using diafiltration buffer (150 mM NaCl, 2.5 mM $NaPO_4$ pH 6.8–7.2 in WFI).
10. Fill process tank with pooled SARS S ΔTM protein.
11. Retentate line should be connected to process tank, and valve should be open.
12. Allow S ΔTM to recirculate through the system at a flow rate of ≤200 mL/min for 3–4 min.
13. Increase recirculation flow rate to 600–800 mL/min.
14. Ensure a TMP of 13.0–17.0 psi.
15. Monitor volume in process tank.
16. Stop concentration when volume in process tank is approximately 400 mL. This is the initial concentration retentate.
17. Set up a 2 L vessel to siphon into process tank.
18. Fill container with 2 L of diafiltration buffer (150 mM NaCl, 2.5 mM $NaPO_4$ pH 6.8–7.2 in WFI).
19. Retentate valve should be open.
20. Start pump and circulate at a flow rate of ≤200 mL/min for 3–4 min.
21. Increase flow rate to 600–800 mL/min.
22. Adjust retentate valve to maintain a TMP of 13.0–17.0 psi.
23. Monitor volume of diafiltration buffer in vessel.
24. Continue until a total volume of diafiltration buffer equal to 10 times the volume of initial concentration retentate has been used.
25. Volume in process tank should be approximately equal to initial concentration retentate volume. This is the diafiltration retentate.
26. Process the diafiltration retentate through a 0.22 μm filter into a sterile Nalgene polycarbonate bottle. This is the S ΔTM bulk drug substance.
27. Remove aliquots for testing.
28. Store bulk drug substance at −20 °C.

3.5 Antigen Release Testing

1. Testing and acceptance criteria for SARS S ΔTM are listed in Table 1.

3.6 Vaccine Adjuvant Formulation

1. Advax™ is a preservative-free sterile suspension of delta inulin microparticles at 50 mg/mL in a bicarbonate buffer, which when combined with vaccine antigen enhances both Th1 and Th2 immunity in a balanced fashion.

Table 1
SARS S ΔTM analytical tests and acceptance criteria

Parameter	Method	Acceptance criterion
Identity	SDS-PAGE/Western blot	Detection of approx. 150 kDa protein with SARS S antiserum
DNA content	PicoGreen	≤15 ng/dose
pH	USP <791>	7.0 ± 0.4
Osmolality	USP <785>	≤330 mOsm/hg
Bacterial endotoxin	USP <85>	<10 EU/dose
Purity	SDS-PAGE/Western blot	≥90 %
Lentil lectin content	SDS-PAGE/Western blot	<10 ng lentil lectin/μg SARS S ΔTM
Microbial limits	USP <61>	<10 CFU/mL
Total protein	Bicinchoninic acid assay	Perform and report
Potency	ELISA	≥60 % of total protein content

2. To further enhance Th1 and reduce Th2 immune bias, 10 μg CpG oligonucleotide per 1 mg delta inulin is added to the Advax™ adjuvant, as a simple admixture.
3. Advax™ adjuvant formulations are administered to mice at a standardized dose of 1 mg delta inulin per mouse, irrespective of the antigen dose.
4. Advax™ adjuvant is formulated with S ΔTM bulk drug substance in a laminar flow hood by aseptic simple admixture of the Advax™ suspension with the S ΔTM bulk drug substance and drawing up the combined milky white suspension into a 0.5 mL insulin syringe immediately prior to immunization.

3.7 Animal Immunogenicity Testing

1. Vaccine immunogenicity studies can be conveniently performed on adult female BALB/c mice at 6–8 weeks of age but can also be performed on other strains such as C57BL/6 (*see* **Note 6**).
2. Mice are immunized twice 3 weeks apart by an intramuscular injection into the thigh, in order to mimic the most common route of human vaccine administration. The maximum volume that can be injected into an adult mouse thigh muscle is 50 μl. If the vaccine cannot be reduced to this volume, then providing the vaccine is not reactogenic and then larger vaccine volumes can be administered by injection of 50 μl amounts into multiple legs.
3. Starting at 1 week post-immunization, at intervals of 1–4 weeks mice are bled using cheek vein bleeding using a lancet in order to obtain ~25–50 μl of blood from which serum is

obtained by centrifugation and then stored at −20 °C for later use in antibody assays.

4. SARS-specific antibodies are conveniently determined in mouse serum by ELISA. S ΔTM protein is absorbed to ELISA plates in 0.1 M sodium carbonate buffer, pH 9.6 and incubated overnight at 4 °C. After blocking with 1 % BSA/PBS for 1 h, serum samples diluted in 1 % BSA/PBS are incubated for 2 h at room temperature (RT) and then washed. Subsequently, 100 μl biotinylated anti-mouse IgG, IgG1, IgG2a, IgG2b, IgG3, or IgM antibodies (Abcam) plus streptavidin-HRP (BD Biosciences) are added and incubated for 1 h at RT. After washing, wells are incubated with 100 μl of TMB substrate for 10 min and then stopped by 1 M phosphoric acid. The optical density is measured at 450 nm (OD450 nm) with a VersaMax ELISA microplate reader (Molecular Devices, CA, USA) and analyzed using SoftMax Pro Software.
5. At the termination of immunogenicity studies, mice are killed by cervical dislocation and bones and spleens are collected to enable measurement of SARS-specific memory T and B cells. Bone marrow is isolated from femurs by flushing with 3 % FBS/PBS. Splenocytes are released by pressing against a cell strainer with a rubber syringe plunger and RBCs are removed by osmotic shock. Cells are washed with 3 % FBS/PBS and then resuspended in RPMI complete medium with 10 % heat-inactivated FBS.
6. For T cell proliferation assays, splenocytes are labeled with 5 μM CFSE (Invitrogen Life Technologies) for 8 min at RT. CFSE starts to react when exposed to aqueous solutions. It is, therefore, important to avoid dilution of CFSE until immediately before cell labeling.
7. Labeled cells are cultured in 24-well plates at 10^6 cells/mL/well with or without S ΔTM protein 1 μg/mL. After 5-day incubation at 37 °C and 5 % CO_2, cells are washed with 0.1 % BSA/PBS, treated with anti-mouse CD16/CD32 (BD Biosciences) for 5 min at 4 °C and then stained with anti-mouse CD4-APC and anti-mouse CD8a-PE-Cy7 (BD) for 30 min at 4 °C. Cells are washed with 0.1 % BSA/PBS and then analyzed by FACS (FACSCanto II, BD Biosciences) with FACSDiva software. For each lymphocyte subset, proliferation is expressed as the percentage of divided cells (CFSE low) compared to undivided cells (CFSE high). Dot plots representing analysis of 10^5 cells are generated by FlowJo software. It is important to have CFSE-labeled, unstimulated cells as a nondividing cell control.
8. The frequency of antigen-specific antibody- or cytokine-secreting cells is analyzed using biotinylated anti-mouse IgG,

IgG1, IgG2a, or IgM antibodies (Abcam) or anti-mouse IFN-γ, IL-2, and IL-4 antibody pairs (BD) or LEAF anti-mouse IL-17A and biotin-anti-mouse IL-17A antibody (BioLegend, USA) with streptavidin-HRP (BD Biosciences), according to the manufacturer's instruction. Briefly, single-cell suspensions are prepared from bone marrow and spleens of mice at indicated time points, plated at 2×10^5 cells/well in 96-well filtration plates pre-coated with S ΔTM protein (for antibody detection) or anti-mouse cytokine mAb (for cytokine detection) overnight at 4 °C, and then blocked with RPMI/10 % FBS. For cytokine assays, the cells are incubated with S ΔTM protein (10 μg/mL) at 37 °C and 5 % CO_2 for 2 days. Wells are washed and incubated with biotinylated anti-mouse Ig or anti-mouse cytokine mAb at RT for 2 h, and washed, and then streptavidin-HRP is added for 1 h before washing and addition of AEC substrate solutions (BD Biosciences). Spots are counted by ImmunoSpot S6 ELISPOT analyzer (CTL, USA) and analyzed using ImmunoSpot Software. Spots in negative control wells are subtracted from the number of spots in S protein wells and the results are expressed as antibody-secreting cells (ASC) per 10^6 BM cells or spots per 10^6 splenocytes.

9. For statistical analysis, group comparisons for antibody and ELISPOT tests are done by Mann–Whitney test.

3.8 SARS CoV Mouse Challenge Studies

1. Female 4–6-week-old BALB/c mice weighing 18–20 g are obtained from Charles River Laboratories (Wilmington, MA), maintained on Wayne Lab Blox, and fed with standard mouse chow and tap water ad libitum (*see* **Note 6**).
2. To generate a mouse-adapted SARS-CoV, the SARS-CoV strain Urbani (200300592) was obtained from Centers for Disease Control and Prevention (CDC, Atlanta, GA, USA). This strain was propagated and titrated in Vero 76 cells obtained from American Type Culture Collection (ATCC, Manassas, VA), and grown in minimal essential medium (MEM) supplemented with 10 % heat-inactivated fetal bovine serum (FBS, Thermo Fisher Scientific Co., Logan, UT). For in vitro antiviral assays, the serum was reduced to 2 % FBS and gentamicin was added to the medium up to a final concentration of 50 μg/mL. BALB/c mice were infected with the Urbani strain. Three or five days after infection, the lungs were removed and homogenized and then used to reinfect a subsequent group of mice. This infection step was continued 25 times through BALB/c mice lungs. The virus was then plaque-purified three times and yielded a virus causing severe lung disease and mortality in infected mice. The virus was verified as SARS-CoV by enzyme-linked immunosorbent assay (ELISA) and polymerase chain reaction (PCR). All experiments involving

infectious SARS-CoV viruses need to be conducted in an approved biosafety level 3+ laboratory.

3. At days 3 and 6 post-virus challenge, five mice from each immunized and control group are sacrificed and the lungs harvested for gross pathology (lung score), lung weights, lung virus titers, and measurement of anti-SARS IgG in lung homogenate.
4. For lung scoring, samples from each mouse lung lobe are weighed and placed in a petri dish. Lungs are scored based on surface appearance of lungs. Lungs are then assigned a score ranging from 0 to 4, with 0 indicating that the lungs looked normal and 4 denoting that the entire surface area of the lungs was inflamed and exhibited plum-colored lung discoloration. Significant differences in lung scores are determined by Kruskal-Wallis test followed by Dunn's pairwise comparison post tests. Analysis of variance (ANOVA) is used to determine significant differences in lung weights. Pairwise comparisons are made by Newman-Keuls posttests.
5. Lung virus titers are analyzed from mice sacrificed on days 3 and 6 post-virus exposure. A lobe from each mouse lung is homogenized in MEM supplemented with 10 % FBS and the tissue fragments are allowed to settle. The varying dilutions of the supernatant fluids are assayed in triplicate for infectious virus in Vero 76 cells by cytopathic effect (CPE) assay. The titers (50 % tissue culture infectious dose, CCID50 values) are calculated using the Reed-Muench method. Significant differences are detected by ANOVA. Pairwise comparisons are made by Newman-Keuls posttests.
6. For SARS-CoV neutralizing antibody assay sera are harvested by submandibular bleeding from surviving mice at days 7 and 14 after virus challenge. 7 μl aliquot of each serum sample is added to approximately 63 μl of MEM, mixed, and then serially diluted by ½ to achieve 1/40 to 1/8192 dilutions in 96-well plates. Virus stock is diluted in MEM to approximately 200 CCID50 per 60 μl. Next 60 μl of virus is added to each well, and the plates are vibrated for approximately 1 min, and then incubated for 1 h at 37 °C for neutralization. 100 μl of the liquid from each well is then transferred to 96-well plates containing sub-confluent monolayers of Vero 76 cells, and 100 μl of MEM + 4 % FBS added to each well. Plates are sealed with tape, incubated for 5 days at 37 °C with 5 % CO_2, and scored for the presence or absence of virus CPE. Uninfected wells serve as a negative cell control, and a serum sample with known anti-SARS antibody as a positive control. Results are reported as the inverse of the greatest dilution where virus CPE is not detected.
7. To assess for effects of vaccines on lung eosinophilic immunopathology, immunized and vehicle-treated mice are sacrificed at days 3 and 6 post-virus challenge, and lungs removed.

Formalin-fixed lungs are mounted in paraffin blocks. Paraffin-embedded lung sections are stained with hematoxylin and eosin (H&E) and a rat monoclonal antibody (Clone MT-14.7) to eosinophil major basic protein MBP (Lee Laboratory, Mayo Clinic, Arizona) following a standard IHC procedure. DAB chromogen identifies eosinophils as brown-stained cells. Eosinophil infiltration is scored without knowing animal identity using H&E-stained slides. An overall infiltration score, 0–3, is assigned to each section according to the amounts of eosinophils in the parenchyma and their distributions through the lung. Score 0 = no to a few eosinophils; score 1 = mild eosinophil infiltration; score 2 = moderate infiltration; score 3 = severe infiltration. For confirmation, immunohistochemistry to the eosinophil major basic protein is performed in sections with the highest score of each treatment group.

8. The remainder of the mice are followed for 2 weeks post-challenge to assess survival. Survival analysis is done using the Kaplan-Meier method and a Logrank test. If that analysis reveals statistically significant differences among the treatment groups, pairwise comparison of survivor curves is analyzed by the Mantel-Cox Logrank test, and the relative significance adjusted to a Bonferroni-corrected significance threshold for the number of treatment comparisons done. All group comparisons of virus titers are done using analysis of variance to determine experimental significance followed by Newman-Keuls pairwise comparison tests.

4 Notes

1. Because the S ΔTM protein the culture supernatant is in a rich culture medium, all practical precautions should be taken to prevent microbial growth. All containers should be sterile, buffers should be 0.22 μm filtered, columns and chromatography systems should be thoroughly sanitized after use, and process intermediates should be processed immediately or stored at 2–8 °C.
2. Columns should be packed ahead of time and stored according to the resin manufacturer's recommendations.
3. Columns may be equilibrated during harvest of the culture.
4. Culture supernatant containing S ΔTM may be loaded onto the linked UNO S/DEAE columns immediately after harvest.
5. The lentil lectin sepharose column may be loaded immediately after completion of the UNO S/DEAE step, and the load may be run overnight.
6. BALB/c mice are typically used for vaccine studies as they have a Th2 immune bias and hence are good at making antibody responses, whereas C57BL/6 mice have a Th1 bias.

References

1. Nicholls J, Dong XP, Jiang G et al (2003) SARS: clinical virology and pathogenesis. Respirology 8 Suppl:S6–S8
2. Berger A, Drosten C, Doerr HW et al (2004) Severe acute respiratory syndrome (SARS)—paradigm of an emerging viral infection. J Clin Virol 29:13–22
3. Assiri A, McGeer A, Perl TM et al (2013) Hospital outbreak of Middle East respiratory syndrome coronavirus. N Engl J Med 369:407–416
4. Marra MA, Jones SJ, Astell CR et al (2003) The Genome sequence of the SARS-associated coronavirus. Science 300:1399–1404
5. Darnell ME, Plant EP, Watanabe H et al (2007) Severe acute respiratory syndrome coronavirus infection in vaccinated ferrets. J Infect Dis 196:1329–1338
6. Bolles M, Deming D, Long K et al (2011) A double-inactivated severe acute respiratory syndrome coronavirus vaccine provides incomplete protection in mice and induces increased eosinophilic proinflammatory pulmonary response upon challenge. J Virol 85: 12201–12215
7. See RH, Zakhartchouk AN, Petric M et al (2006) Comparative evaluation of two severe acute respiratory syndrome (SARS) vaccine candidates in mice challenged with SARS coronavirus. J Gen Virol 87:641–650
8. Yasui F, Kai C, Kitabatake M et al (2008) Prior immunization with severe acute respiratory syndrome (SARS)-associated coronavirus (SARS-CoV) nucleocapsid protein causes severe pneumonia in mice infected with SARS-CoV. J Immunol 181:6337–6348
9. Tseng CT, Sbrana E, Iwata-Yoshikawa N et al (2012) Immunization with SARS coronavirus vaccines leads to pulmonary immunopathology on challenge with the SARS virus. PLoS One 7, e35421
10. Clay C, Donart N, Fomukong N et al (2012) Primary severe acute respiratory syndrome coronavirus infection limits replication but not lung inflammation upon homologous rechallenge. J Virol 86:4234–4244
11. Roper RL, Rehm KE (2009) SARS vaccines: where are we? Expert Rev Vaccines 8:887–898
12. Li W, Moore MJ, Vasilieva N et al (2003) Angiotensin-converting enzyme 2 is a functional receptor for the SARS coronavirus. Nature 426:450–454
13. Jeffers SA, Tusell SM, Gillim-Ross L et al (2004) CD209L (L-SIGN) is a receptor for severe acute respiratory syndrome coronavirus. Proc Natl Acad Sci U S A 101:15748–15753
14. He Y, Zhou Y, Wu H et al (2004) Identification of immunodominant sites on the spike protein of severe acute respiratory syndrome (SARS) coronavirus: implication for developing SARS diagnostics and vaccines. J Immunol 173: 4050–4057
15. He Y, Lu H, Siddiqui P et al (2005) Receptor-binding domain of severe acute respiratory syndrome coronavirus spike protein contains multiple conformation-dependent epitopes that induce highly potent neutralizing antibodies. J Immunol 174:4908–4915
16. Huang J, Cao Y, Du J et al (2007) Priming with SARS CoV S DNA and boosting with SARS CoV S epitopes specific for CD4+ and CD8+ T cells promote cellular immune responses. Vaccine 25:6981–6991
17. Zhou Z, Post P, Chubet R et al (2006) A recombinant baculovirus-expressed S glycoprotein vaccine elicits high titers of SARS-associated coronavirus (SARS-CoV) neutralizing antibodies in mice. Vaccine 24: 3624–3631
18. Openshaw PJ, Culley FJ, Olszewska W (2001) Immunopathogenesis of vaccine-enhanced RSV disease. Vaccine 20 Suppl 1:S27–S31
19. Petrovsky N, Aguilar JC (2004) Vaccine adjuvants: current state and future trends. Immunol Cell Biol 82:488–496
20. Cooper PD, Barclay TG, Ginic-Markovic M et al (2013) The polysaccharide inulin is characterized by an extensive series of periodic isoforms with varying biological actions. Glycobiology 23:1164–1174
21. Cooper PD, Petrovsky N (2011) Delta inulin: a novel, immunologically active, stable packing structure comprising beta-D-[2 -> 1] poly(fructo-furanosyl) alpha-D-glucose polymers. Glycobiology 21:595–606
22. Honda-Okubo Y, Saade F, Petrovsky N (2012) Advax, a polysaccharide adjuvant derived from delta inulin, provides improved influenza vaccine protection through broad-based enhancement of adaptive immune responses. Vaccine 30:5373–5381
23. Lobigs M, Pavy M, Hall RA et al (2010) An inactivated Vero cell-grown Japanese encephalitis vaccine formulated with Advax, a novel inulin-based adjuvant, induces protective neutralizing antibody against homologous and heterologous flaviviruses. J Gen Virol 91: 1407–1417
24. Feinen B, Petrovsky N, Verma A et al (2014) Advax-adjuvanted recombinant protective antigen provides protection against inhalational anthrax that is further enhanced by addi-

tion of murabutide adjuvant. Clin Vaccine Immunol 21:580–586

25. Honda-Okubo Y, Kolpe A, Li L et al (2014) A single immunization with inactivated H1N1 influenza vaccine formulated with delta inulin adjuvant (Advax) overcomes pregnancy-associated immune suppression and enhances passive neonatal protection. Vaccine 32:4651–4659
26. Larena M, Prow NA, Hall RA et al (2013) JE-ADVAX vaccine protection against Japanese encephalitis virus mediated by memory B cells in the absence of CD8+ T cells and pre-exposure neutralizing antibody. J Virol 87:4395–4402
27. Layton RC, Petrovsky N, Gigliotti AP et al (2011) Delta inulin polysaccharide adjuvant enhances the ability of split-virion H5N1 vaccine to protect against lethal challenge in ferrets. Vaccine 29:6242–6251
28. Petrovsky N, Larena M, Siddharthan V et al (2013) An inactivated cell culture Japanese encephalitis vaccine (JE-ADVAX) formulated with delta inulin adjuvant provides robust heterologous protection against West Nile encephalitis via cross-protective memory B cells and neutralizing antibody. J Virol 87:10324–10333
29. Saade F, Honda-Okubo Y, Trec S et al (2013) A novel hepatitis B vaccine containing Advax, a polysaccharide adjuvant derived from delta inulin, induces robust humoral and cellular immunity with minimal reactogenicity in preclinical testing. Vaccine 31:1999–2007
30. Cristillo AD, Ferrari MG, Hudacik L et al (2011) Induction of mucosal and systemic antibody and T-cell responses following prime-boost immunization with novel adjuvanted human immunodeficiency virus-1-vaccine formulations. J Gen Virol 92:128–140
31. Gordon D, Kelley P, Heinzel S et al (2014) Immunogenicity and safety of Advax, a novel polysaccharide adjuvant based on delta inulin, when formulated with hepatitis B surface antigen: a randomized controlled Phase 1 study. Vaccine 32(48):6469–6477
32. Gordon DL, Sajkov D, Woodman RJ et al (2012) Randomized clinical trial of immunogenicity and safety of a recombinant H1N1/2009 pandemic influenza vaccine containing Advax polysaccharide adjuvant. Vaccine 30:5407–5416
33. Honda-Okubo Y, Barnard D, Ong CH et al (2015) Severe acute respiratory syndrome-associated coronavirus vaccines formulated with delta inulin adjuvants provide enhanced protection while ameliorating lung eosinophilic immunopathology. J Virol 89:2995–3007

Chapter 15

Generation and Characterization of a Chimeric Tick-Borne Encephalitis Virus Attenuated Strain ChinTBEV

Hong-Jiang Wang, Xiao-Feng Li, and Cheng-Feng Qin

Abstract

Tick-borne encephalitis (TBE), caused by TBE virus (TBEV), is one of the most serious human viral diseases endemic in Europe and East Asia. No effective treatment for TBEV infection exists and the primary preventive measure is vaccination. Although several inactivated vaccines have been licensed, the development of novel and more effective vaccines remains a high priority especially in disease-endemic countries. Here we describe a universal vaccine design approach to construct a live chimeric recombinant TBEV attenuated strain ChinTBEV based on the infectious full-length cDNA clone of Japanese encephalitis virus using standard reverse genetic technology. The *in vitro* and *in vivo* characterization of the ChinTBEV is also presented here.

Key words Tick-borne encephalitis virus, Vaccine, Chimeric flavivirus

1 Introduction

Tick-borne encephalitis virus (TBEV) is a member of flavivirus genus together with other important human pathogens including dengue virus (DENV), West Nile virus (WNV), Japanese encephalitis virus (JEV), and yellow fever virus (YFV). TBEV infection in human causes severe disease termed tick-borne encephalitis (TBE) that is characterized by typical neurological complications including meningitis, meningoencephalitis, and encephalomyelitis, even death in both children and adults [1]. In Europe and Asia, there are approximately 8500 human cases reported annually, with a mortality rate ranging from 0.5 to 30 % [2–4]. During the past decades, a great increase in morbidity and new endemic foci have been reported in many European and Asian countries [5, 6].

At present, no effective treatments are available for TBEV infection and only vaccination can offer the protection against TBE. Four inactivated, cell culture-derived vaccines, Encepur®, TBE-Immun®, TBE-Moscow vaccine®, and EnceVir®, are available currently [7]. Although the use of these vaccines has led to a

Sunil Thomas (ed.), *Vaccine Design: Methods and Protocols: Volume 1: Vaccines for Human Diseases*, Methods in Molecular Biology, vol. 1403, DOI 10.1007/978-1-4939-3387-7_15,

dramatic decline in the annual incidence of TBE [8], some adverse factors have limited their clinical use. Inactivated vaccines need multiple doses of immunizations, and the production cost is very high. Even side effects particularly in children have aroused special attention and vaccination failures have been documented [9, 10].

Alternatively, live attenuated TBE vaccines generated by advanced reverse genetic technology represent a promising vaccine design approach. A well-known strategy for generating attenuated flavivirus strains is to construct a chimeric flavivirus by replacing its structural proteins with the corresponding regions of another attenuated flavivirus strain. A panel of attenuated flavivirus strains including yellow fever 17D and DENV-4 strain 814669 have been well used as backbone to construct novel chimeric flaviviruses [11–17].

The JE live vaccine strain SA14-14-2 has been widely used in more than four billion children with ideal safety and efficacy profile [18, 19]. In this chapter, we explain a method for generating a chimeric TBEV-attenuated strain using JEV SA14-14-2 as backbone through standard reverse genetic technology. This novel flavivirus chimera, ChinTBEV, represents a potential vaccine candidate against TBEV infection that deserves further development [20].

2 Materials

2.1 Cell Lines and Viruses

1. Baby hamster kidney (BHK-21) (ATCC Number: CCL-10) and Vero cell lines (ATCC Number: CCL-81) are maintained in Dulbecco's minimal essential medium (DMEM; Life Technologies) supplemented with 10 % fetal bovine serum (FBS), 100 U/ml penicillin, and 100 μg/ml streptomycin and cultured at 37 °C with 5 % CO_2.
2. *Aedes albopictus* C6/36 cell line (ATCC Number: CRL-1660) is grown in RPMI 1640 supplemented with nonessential amino acids (Life Technologies), and 10 % FBS, and cultured at 28 °C with 5 % CO_2.
3. TBEV strain Senzhang (GenBank no. JQ650523.1) was generated in our laboratory. It was isolated from a patient brain and had been passaged 37 times in the mouse brain (*see* **Note 1**).
4. JEV live attenuated vaccine strain SA14-14-2 (GenBank no. D90195) was from Chengdu Institute of Biological Products (*see* **Note 2**).

2.2 Plasmid Construction and Virus Rescue

1. Infectious full-length cDNA clone of JEV [21].
2. *E. coli* strain MC1061 cells (*see* **Note 3**).
3. QIAGEN Plasmid Midi Kit (QIAGEN).
4. RiboMAX Large Scale RNA Production System-Sp6 (Promega).

Table 1
Primers for chimeric plasmid construction

Primer	Sequence	Note
prME-F	AGCTTGTGCAGGCGCCGTGACACTTGCAGCCACAGT	Kas I cutting site
prME-R	GCACATCCAGTGTCAGCATGCACTCCGAGTGTCATG GCCAGAACCAGT	Complementary sequences
ENS1-F	CATGACACTCGGAGTGCATGCTGACACTGGATGTGC CATTGACATC	Complementary sequences
ENS1-R	CCGTACCAGCAGCCATTTTCTGTCCGGAATCGTAGG	BspE I cutting site

5. m7GpppA cap analogue (Promega).
6. Lipofectamine 2000 (Life Technologies).
7. PureLink™ RNA mini kit (Life Technologies).
8. PrimeScript™ II Reverse Transcriptase (TaKaRa).
9. OL-PCR: TBEV or JEV-specific oligonucleotide primers (*see* Table 1).

2.3 Antibodies

1. Primary monoclonal antibodies against the JEV E protein (4AD5F5D5D6), the TBEV E protein (4A4), and the JEV NS1 protein (JN1, Abcam).
2. Alexa fluor 488-conjugated goat anti-mouse IgG antibody.
3. HRP-conjugated house anti-mouse IgG antibody.

2.4 Animals

BALB/c mice maintained under specific pathogen-free (SPF) conditions.

3 Methods

3.1 Construction of Full-Length cDNA Clone of ChinTBEV

All plasmids were constructed using standard molecular cloning protocols. Cloning sites were engineered to permit replacement of the entire prM and E coding sequences of JEV with the corresponding sequences of TBEV. Sites for posttranslational cleavage of the capsid and prM proteins and the E and NS1 proteins were preserved (Figs. 1 and 2).

1. Extract the TBEV and JEV genomic RNAs using a PureLink™ RNA mini kit following the manufacturer's protocol.
2. Using reverse oligonucleotide primers specific to TBEV or JEV, obtain the TBEV and JEV cDNAs using PrimeScript™ II Reverse Transcriptase according to the manufacturer's protocol.

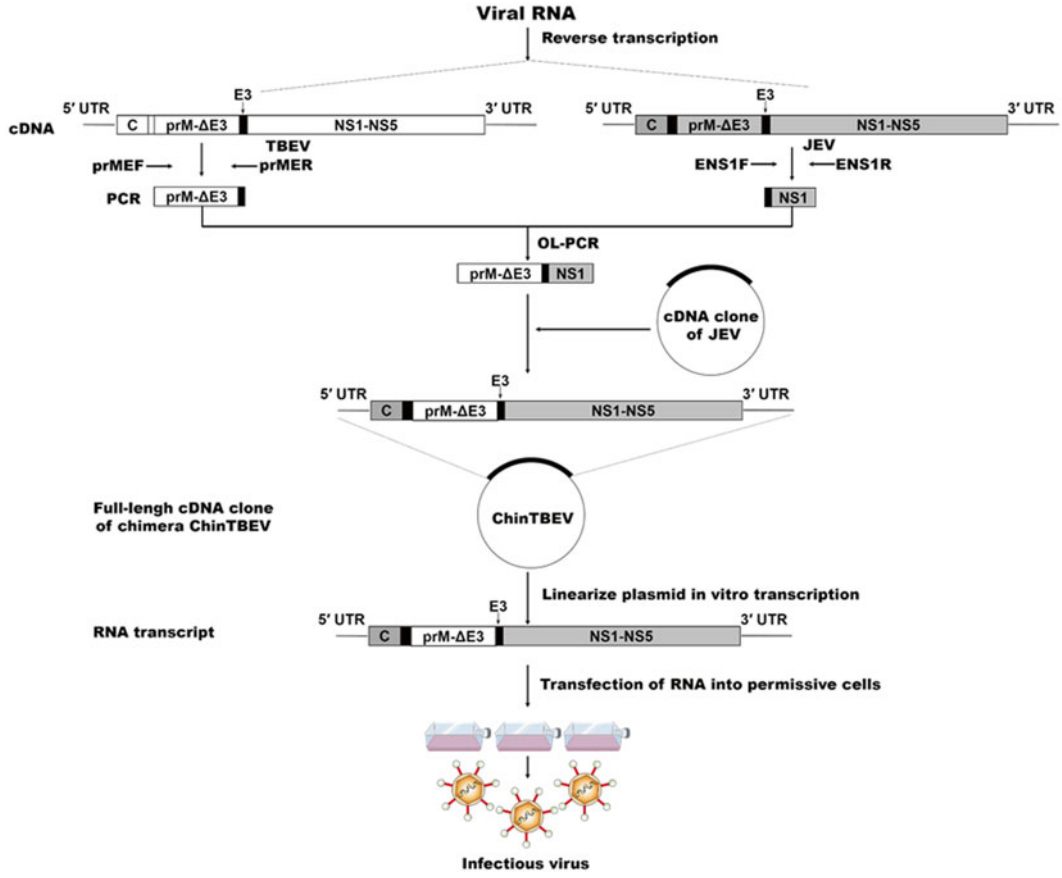

Fig. 1 Construction of the cDNA clone of chimera ChinTBEV. Viral cDNAs are obtained using reverse oligonucleotide primers specific to TBEV or JEV. cDNA fragments encoding prM and E region of TBEV (TBEV-prME) or NS1 region of JEV (JEV-ENS1) are generated using primers prME-F and prME-R or ENS1-F and ENS1-R, respectively. TBEV-prME and JEV-NS1 are fused using OL-PCR to construct the chimeric fragment named prME-NS1. Replace the prME region of full-length cDNA clone of JEV with the digested fragment prME-NS1 to generate a plasmid containing the full-length cDNA of JEV/TBEV chimera (pChinTBEV). The plasmid pChinTBEV is linearized and transcribed in vitro using an Sp6 RNA polymerase promoter to produce RNA transcripts. The RNA transcripts are transfected into permissive cells to recover recombinant virus that can then be characterized

3. cDNA clone encoding prM and E region of TBEV is generated using oligonucleotide primers prME-F and prME-R, named TBEV-prME; cDNA fragment encoding NS1 region of JEV is obtained using oligonucleotide primers ENS1-F and ENS1-R, named JEV-ENS1.
4. Fuse the TBEV-prME and JEV-NS1 using OL-PCR to construct the chimeric fragment named prME-NS1, which contains prM and E region of TBEV and NS1 of JEV.
5. Digest prME-NS1 with Kas I and BspE I. Replace the prME region of full-length cDNA clone of JEV (ref) with the digested fragment prME-NS1 to generate a plasmid containing the full-length cDNA of JEV/TBEV chimera, named pChinTBEV.

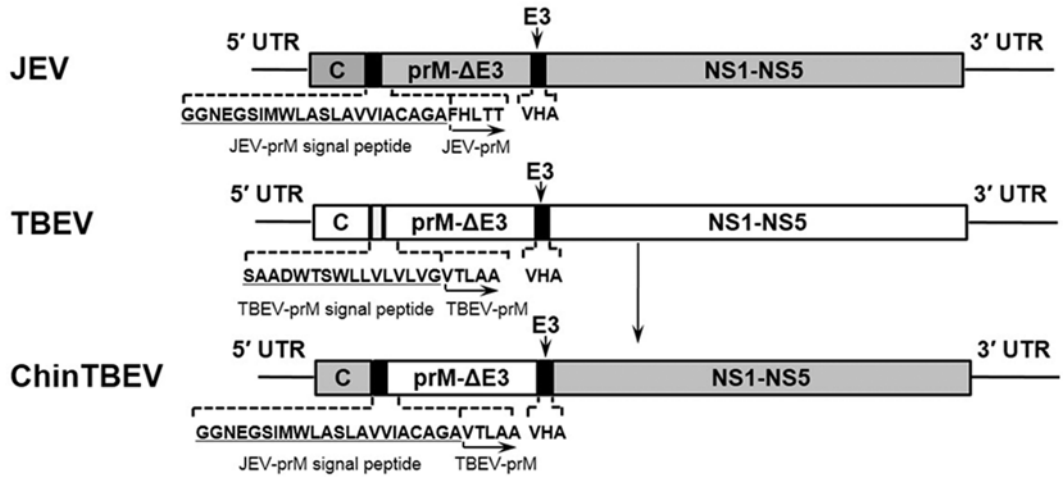

Fig. 2 Graphic representation of the genomic constructs of ChinTBEV and its parental viruses. The JEV and TBEV prM signal peptides are *underlined*. The C-terminal 3 amino acids of JEV or TBEV E proteins (E3) are indicated. The prM-E protein lacking the C-terminal 3 amino acids of the E protein is indicated as prM-ΔE3

6. Transform pChinTBEV into *E. coli* strain MC1061 cells for storage and amplification (*see* **Note 4**). Sequence the cDNA clones to ensure that no mutations have been introduced into the cDNA fragments during the cloning process.
7. The correct plasmid is then propagated using QIAGEN Plasmid Midi Kit according to the manufacturer's protocol (*see* **Notes 5** and **6**).

3.2 Recovery of the Chimeric ChinTBEV Virus

1. Linearize 5 μg of pChinTBEV plasmid with Xho I.
2. Purify the linearized plasmid by phenol:chloroform:isoamyl alcohol (25:24:1) extraction followed by extraction with chloroform:isoamyl alcohol (24:1).
3. Precipitate the DNA by the addition of 0.1 volumes of 3 M sodium acetate (pH 5.2) and 2.5 volumes of 100 % ethanol. Incubate at −70 °C for at least 30 min.
4. Collect the precipitate by centrifugation at (13,400×*g*) for 20 min at 4 °C. Wash the pellet with 70 % ethanol and collect the DNA by centrifugation.
5. Air-dry the DNA pellet and resuspend in sterile, nuclease-free H_2O at an approximate concentration of 0.5 μg/μl (*see* **Note 7**).
6. Transcribe the Xho I linearized pChinTBEV plasmid in vitro using RiboMAX Large Scale RNA Production System-Sp6. The following mix is used in a 30 μl reaction: 2–3 μg DNA template in 14 μl of nuclease-free H_2O, 6 μl 5× transcription buffer, 6 μl 25 mM rNTP mix (7.5 mM each of rATP, rCTP, and UTP and 2.5 mM rGTP), 2 μl 10 mM m7GpppA cap

analogue, and 2 μl of Sp6 enzyme mix. The transcription reaction is incubated at 37 °C for 2–3 h. The DNA template is then removed by the addition of 2 U of RNase-free DNase I followed by incubation at 37 °C for 20 min.

7. The in vitro RNA transcripts are then purified from the reaction mix using a PureLink™ RNA mini kit following the manufacturer's protocol. The RNA is stored at −70 °C until required for transfection.
8. Seed BHK-21 cells in a 6-well plate. Incubate the cells for about 24 h until they achieve 80 % confluency at the time of transfection.
9. Transfect the BHK-21 cells with about 2 μg of the RNA transcript using Lipofectamine 2000 according to the manufacturer's protocol (*see* **Note 8**). Incubate the transfected BHK-21 cells at 37 °C with 5 % CO_2.
10. After 72–96 h, the culture supernatant from the transfected cells is transferred to 90 % confluent BHK-21 cells in a 25 cm^2 T flask. Incubate at 37 °C for 60 min. Add 5 ml of maintenance media to the cells and incubate at 37 °C with 5 % CO_2 for 4 days.
11. The aliquoted culture supernatant samples are then used as working stocks for determining the virus titer and further virus characterization.

3.3 In Vitro and In Vivo Characterization of ChinTBEV

Perform the comparison of the plaque morphology of ChinTBEV with its parental viruses using the standard plaque-forming assay method [22]. The plaque formed by ChinTBEV is much smaller than its parent viruses (Fig. 3).

3.3.1 Plaque Morphology

3.3.2 Growth Curves in Multiple Cell Lines

1. Seed BHK-21, Vero, or C6/36 cells in a 12-well plate.
2. Infect the cells with the ChinTBEV, JEV, or TBEV at an MOI of 0.01.
3. Collect the culture supernatants at successive 24-h intervals.
4. Quantitate the virus titers by plaque assay on BHK-21 cells.

3.3.3 Indirect Immunofluorescence Assay (IFA)

1. Seed BHK-21 cells in a 6-well plate, each containing sterile glass cover slips (10 mm × 10 mm).
2. Infect the BHK-21 cells with ChinTBEV, JEV, or TBEV at an MOI of 0.01, and incubate the infected cells at 37 °C for 48 h.
3. Fix the cells on the cover slips by incubation in ice-cold acetone at −20 °C for at least 30 min and wash them with PBS (*see* **Note 9**).
4. Incubate the cover slips with the primary antibodies at 37 °C for 1 h and wash them with PBS three times (*see* **Note 10**).

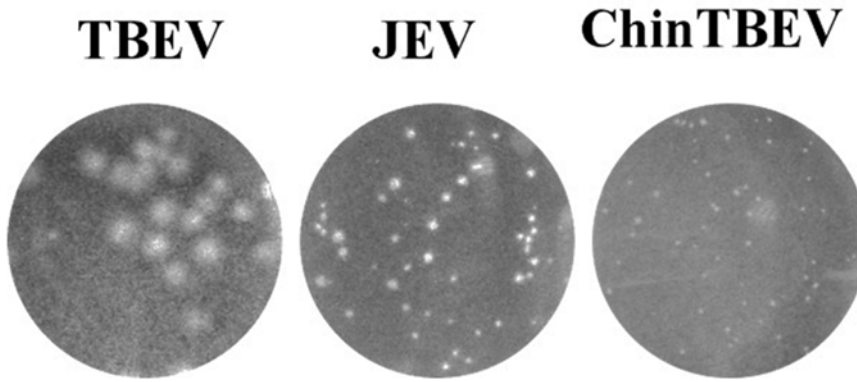

Fig. 3 Plaque morphologies of ChinTBEV and its parental viruses. BHK-21 cells grown in 6-well plates were infected with a tenfold serial dilution of viruses. The plates were incubated at 37 °C for 1 h. Supernatant was removed and cells were overlaid with 1 % low-melting-point agarose in DMEM containing 2 % FBS. After further incubation at 37 °C for 3–4 days, the cells were fixed with 4 % formaldehyde and stained with 0.2 % crystal violet to visualize the plaques

5. Incubate the cover slips with secondary antibody (Alexa fluor 488-conjugated goat anti-mouse IgG antibody) at 37 °C for 45 min and wash them three times with PBS.
6. Examine the positive cells using a fluorescent microscope (Olympus).

3.3.4 Genetic Stability Assay

1. Serially passage the ChinTEBV virus on Vero cells (*see* **Note 11**) at an MOI of 0.01.
2. Extract the viral RNA from each passage and sequence the full-length genome.
3. At the same time, compare the plaque phenotypes of virus at each passage.

3.3.5 Mouse Experiments

Virulence Test

1. Inoculate groups of 4-week-old mice (*see* **Note 12**) by the intraperitoneal (i.p.), subcutaneous (s.c.), or intracerebral (i.c.) route with ChinTBEV, TBEV, or JEV at varying doses.
2. Observe and record the clinical symptom and mortality. Calculate the 50 % lethal dose (LD_{50}) according to the method of Reed and Muench [23].

Immunogenicity Assay

1. Inoculate 4-week-old mice by the i.p. or s.c. route with varying dose of ChinTBEV (*see* **Note 13**), and the PBS group is set as a control.
2. Collect the blood by tail vein puncture 4 weeks post-immunization and obtain the serum (*see* **Note 14**).
3. Measure the TBEV-special IgG titer and neutralizing antibodies of the serum by ELISA and $PRNT_{50}$, respectively.

Protection Assay

1. Challenge the ChinTBEV-immunized or PBS-immunized mice with 500 PFU of TBEV at 4 weeks after the immunization by the i.p. route.
2. Monitor for the signs of illness and death for at least 21 days.
3. Analyze Kaplan–Meier survival curves by a log-rank test (GraphPad Prism software 5.0, San Diego, CA).

4 Notes

1. The virus stock is prepared in BHK-21 cells and titrated by standard plaque-forming assay. After 48 h, the peak titer can reach 10^8 PFU/ml at an M.O.I of 0.01.
2. The virus stock is prepared in BHK-21 cells as TBEV, and the peak titer can reach 10^7 PFU/ml.
3. This bacteria strain is most suitable for stable amplification of the plasmid. Some other widely used cells, such as DH5α, and TOP10, are also acceptable.
4. Here we use the heat shock method to transform the plasmid.
5. The plasmid is of low-copy-number DNA.
6. Culture at 30 °C contributes to plasmid stabilization.
7. Store at –20 °C for later use.
8. Because of the cell toxicity of the Lipofectamine 2000, there is sometimes no difference between the experiment group and the control group on cell condition. Then passage the virus one or more times and observe the CPE.
9. Store at –20 °C for later use.
10. The glasses can be placed into 24-well plate, one glass per well to facilitate operation.
11. The Vero cell lines are widely accepted in the preparation of human use vaccines. The stability of the virus on this cell lines is an important feature in virus safety evaluation.
12. Five to nine mice per group.
13. Usually the immunizing dose we recommend is above 10^4 PFU per mouse.
14. It is easier to obtain the serum form the blood that was standing at 4 °C for 30 min.

Acknowledgement

We thank Chengdu Institute of Biological Products for providing the JE vaccine strain. Research in Dr. Qin's lab is supported by State Key Laboratory of Pathogen and Biosecurity.

References

1. Lindquist L, Vapalahti O (2008) Tick-borne encephalitis. Lancet 371:1861–1871
2. Gritsun TS, Lashkevich VA, Gould EA (2003) Tick-borne encephalitis. Antiviral Res 57: 129–146
3. Poponnikova TV (2006) Specific clinical and epidemiological features of tick-borne encephalitis in Western Siberia. Int J Med Microbiol 296(Suppl 40):59–62
4. Weber E, Finsterbusch K, Lindquist R et al (2014) Type I interferon protects mice from fatal neurotropic infection with langat virus by systemic and local antiviral responses. J Virol 88:12202–12212
5. Mansfield KL, Johnson N, Phipps LP et al (2009) Tick-borne encephalitis virus—a review of an emerging zoonosis. J Gen Virol 90: 1781–1794
6. Suss J (2011) Tick-borne encephalitis 2010: epidemiology, risk areas, and virus strains in Europe and Asia—an overview. Ticks Tick Borne Dis 2:2–15
7. Zent O, Broker M (2005) Tick-borne encephalitis vaccines: past and present. Expert Rev Vaccines 4:747–755
8. Heinz FX, Holzmann H, Essl A et al (2007) Field effectiveness of vaccination against tick-borne encephalitis. Vaccine 25:7559–7567
9. Andersson CR, Vene S, Insulander M et al (2010) Vaccine failures after active immunisation against tick-borne encephalitis. Vaccine 28:2827–2831
10. Grgic-Vitek M, Avsic-Zupanc T, Klavs I (2010) Tick-borne encephalitis after vaccination: vaccine failure or misdiagnosis. Vaccine 28:7396–7400
11. Wright PF, Ankrah S, Henderson SE et al (2008) Evaluation of the Langat/dengue 4 chimeric virus as a live attenuated tick-borne encephalitis vaccine for safety and immunogenicity in healthy adult volunteers. Vaccine 26:882–890
12. Rumyantsev AA, Chanock RM, Murphy BR et al (2006) Comparison of live and inactivated tick-borne encephalitis virus vaccines for safety, immunogenicity and efficacy in rhesus monkeys. Vaccine 24:133–143
13. Pletnev AG, Men R (1998) Attenuation of the Langat tick-borne flavivirus by chimerization with mosquito-borne flavivirus dengue type 4. Proc Natl Acad Sci U S A 95:1746–1751
14. Kofler RM, Heinz FX, Mandl CW (2002) Capsid protein C of tick-borne encephalitis virus tolerates large internal deletions and is a favorable target for attenuation of virulence. J Virol 76:3534–3543
15. Heiss BL, Maximova OA, Thach DC et al (2012) MicroRNA targeting of neurotropic flavivirus: effective control of virus escape and reversion to neurovirulent phenotype. J Virol 86:5647–5659
16. Heiss BL, Maximova OA, Pletnev AG (2011) Insertion of microRNA targets into the flavivirus genome alters its highly neurovirulent phenotype. J Virol 85:1464–1472
17. Lai CJ, Zhao BT, Hori H et al (1991) Infectious RNA transcribed from stably cloned full-length cDNA of dengue type 4 virus. Proc Natl Acad Sci U S A 88:5139–5143
18. Kumar R, Tripathi P, Rizvi A (2009) Effectiveness of one dose of SA 14-14-2 vaccine against Japanese encephalitis. New Engl J Med 360:1465–1466
19. Hennessy S, Liu Z, Tsai TF et al (1996) Effectiveness of live-attenuated Japanese encephalitis vaccine (SA14-14-2): a case–control study. Lancet 347:1583–1586
20. Wang HJ, Li XF, Ye Q et al (2014) Recombinant chimeric Japanese encephalitis virus/tick-borne encephalitis virus is attenuated and protective in mice. Vaccine 32:949–956
21. Ye Q, Li XF, Zhao H et al (2012) A single nucleotide mutation in NS2A of Japanese encephalitis-live vaccine virus (SA14-14-2) ablates NS1' formation and contributes to attenuation. J Gen Virol 93(9):1959–1964
22. Li SH, Dong H, Li XF et al (2013) Rational design of a flavivirus vaccine by abolishing viral RNA 2′-O methylation. J Virol 87: 5812–5819
23. Reed LJ, Muench H (1938) A simple method of estimating fifty percent endpoints. Am J Hyg 27:493–497

Chapter 16

Single-Vector, Single-Injection Recombinant Vesicular Stomatitis Virus Vaccines Against High-Containment Viruses

Michael A. Whitt, Thomas W. Geisbert, and Chad E. Mire

Abstract

There are many avenues for making an effective vaccine against viruses. Depending on the virus these can include one of the following: inactivation of whole virions; attenuation of viruses; recombinant viral proteins; non-replication-competent virus particles; or surrogate virus vector systems such as vesicular stomatitis virus (VSV). VSV is a prototypic enveloped animal virus that has been used for over four decades to study virus replication, entry, and assembly due to its ability to replicate to high titers in a wide variety of mammalian and insect cells. The use of reverse genetics to recover infectious and single-cycle replicating VSV from plasmid DNA transfected in cell culture began a revolution in the study of recombinant VSV (rVSV). This platform can be manipulated to study the viral genetic sequences and proteins important in the virus life cycle. Additionally, foreign genes can be inserted between naturally occurring or generated start/stop signals and polyadenylation sites within the VSV genome. VSV has a tolerance for foreign gene expression which has led to numerous rVSVs reported in the literature. Of particular interest are the very effective single-dose rVSV vaccine vectors against high-containment viruses such as filoviruses, henipaviruses, and arenaviruses. Herein we describe the methods for selecting foreign antigenic genes, selecting the location within the VSV genome for insertion, generation of rVSV using reverse genetics, and proper vaccine study designs.

Key words Vaccine, Single-injection, Immunity, Vesicular stomatitis virus, Ebola virus, Marburg virus, Filovirus, Nipah virus, Henipavirus, Lassa virus, Arenavirus, Glycoprotein, Fusion protein, Attachment protein, Guinea pig, Ferret, Nonhuman primate

1 Introduction

Vesicular stomatitis virus (VSV) is a non-segmented, negative-strand RNA virus in the family *Rhabdoviridae*. VSV has been a platform of study for viral entry, transcription, replication, and assembly for many years. This is a direct result of its simple genome, broad cell tropism, and ability to grow to high titers in cell culture. There are two main serotypes of VSV found in the Western Hemisphere: the Indiana and New Jersey serotypes. Outside of the laboratory, mammals, mosquitoes, mites, and sand flies are among the hosts

Sunil Thomas (ed.), *Vaccine Design: Methods and Protocols: Volume 1: Vaccines for Human Diseases*, Methods in Molecular Biology, vol. 1403, DOI 10.1007/978-1-4939-3387-7_16,

that can be infected by both serotypes. Of particular importance is the economic impact of the disease it causes, vesiculo stomatitis, in cattle, swine, and horses [1]. This disease is characterized by vesicular lesions on the hooves, teats, and gums of infected animals, which are similar characteristics to foot and mouth disease. Though rare, VSV infections of humans can occur by accidental exposure in the laboratory or contact with infected animals in rural areas [2]. Infection can result in flu-like symptoms for a few days, with vesicular lesions of the mouth, or no symptoms at all.

Laboratory strains of VSV, such as VSV-Indiana, have been used as models to study many aspects of negative-strand RNA virus entry and replication. The assembly of VSV occurs at the plasma membrane and results in the budding of virions from the cell surface. As VSV buds from the host cell an envelope, derived from the plasma membrane, is acquired which consists of a lipid bilayer containing the trimeric spike glycoprotein (G protein) of VSV. The successful recovery of VSV virions from plasmid DNA containing the positive-sense VSV anti-genome (reverse genetics), when transfected in cell culture [3, 4], began a revolution in the study of recombinant VSV (rVSV). This platform has been used to study viral genetic sequences [5–9] and proteins important in the virus life cycle [10–18]. As predicted from the modular organization of the genome, VSV can accommodate the insertion and expression of foreign genes that are introduced between naturally occurring or newly created start/stop signals and polyadenylation sites within the genome. This tolerance results in foreign gene expression from the rVSV genome in infected cells, which has led to numerous rVSVs being used as vaccine vectors. Additionally, VSV has the remarkable property in which VSV virions are not particularly selective in regard to the type of membrane protein that can be incorporated into the viral envelope. Initial coinfection studies with VSV and other enveloped viruses demonstrated that VSV can readily form pseudotypes [19–22]. A pseudotype is defined as a virion that has the envelope protein of a heterologous virus incorporated into the VSV membrane. The VSV pseudotype formation mechanism is likely due to the nature of VSV budding [23], which has been reported not to require the VSV G protein [24, 25]. Interestingly, noninfectious, spikeless or "bald" particles are produced in the absence of G protein [26]. The fact that VSV particles can bud in the absence of G protein, along with the promiscuous nature with which heterologous glycoproteins can be incorporated into VSV, led to the development of recombinant viruses in which the VSV glycoprotein gene was deleted and replaced with genes encoding foreign glycoproteins of biosafety level 4 (BSL-4) high-containment viruses with the intent to use the resulting rVSVs as vaccine vectors [27]. Additionally if a high-containment virus glycoprotein cannot function in entry and/or assembly as the sole provided spike protein to produce a replication-competent rVSV,

there are two strategies to produce single-round replication, semi-replication, or replication-competent vaccine vectors which require the use of VSV G in some capacity [28–30]. Finally, additional high-containment virus antigenic, non-glycoprotein foreign proteins have been inserted and successfully expressed from rVSV vaccine vectors [31, 32] showing the breadth of the rVSV vaccine vector system.

This manuscript provides a detailed description of the methods used to recover, produce, and quantify replication-competent rVSV vaccine vectors and single-round and semi-competent replication VSV G-complemented rVSV-ΔG vaccine vectors. This information should allow any laboratory skilled in virological methods and cell culture technology to recover and maintain working stocks of infectious rVSV vaccine vectors for high-containment viruses. Additionally, this manuscript provides the proper implementation of vaccine studies for the development and advancement of rVSV vaccines against high-containment viruses.

1.1 Design of High-Containment rVSV Vaccine Vectors

As discussed above, the rVSV platform is very accommodating to foreign gene insertion and expression. In fact, the limitation of type and size of foreign antigen that can be inserted into rVSV vaccine vector genomes has yet to be reached for biosafety level 4 (BSL-4) viruses such as the filoviruses, henipaviruses, and arenaviruses. While the platform is accommodating, thought must be given to the placement of the foreign gene(s) within the rVSV genome. For instance, the location of a gene within the VSV genome determines the transcription level of mRNA as the genes are transcribed in a gradient from 3′–5′ (Fig. 1a): the gene in the first position having the highest level of transcripts and the last gene having the lowest level of transcripts. Theoretically, insertion of a foreign gene closer to the 3′ end of the genome should lead to higher expression of the antigen versus, the gene being located closer to the 5′ end of the genome. This is typically the case; however, when designing multivalent rVSV vaccines with multiple foreign gene insertions there sometimes can be a preference for actual protein expression of one antigen over the others (Geisbert and Mire unpublished observation) leading to a disconnect of mRNA level to protein expression and the need for further refinement of the vectors to find the right balance of foreign antigen expression. Another consideration is that the insertion of any foreign gene will most likely affect the typical transcriptional gradient of wild-type rVSV possibly attenuating the replication of the vector. Indeed this has been reported on for the rVSV N4CT1 *Zaire ebolavirus* (ZEBOV) glycoprotein (GP) vaccine vector (Fig. 1b) where placing the foreign antigen at the most 3′ end leads to high expression of antigen but movement of the VSV nucleoprotein (N) gene to the fourth gene position leads to attenuation in replication of the vector [29]. The rVSV vaccine platform can overcome many gene

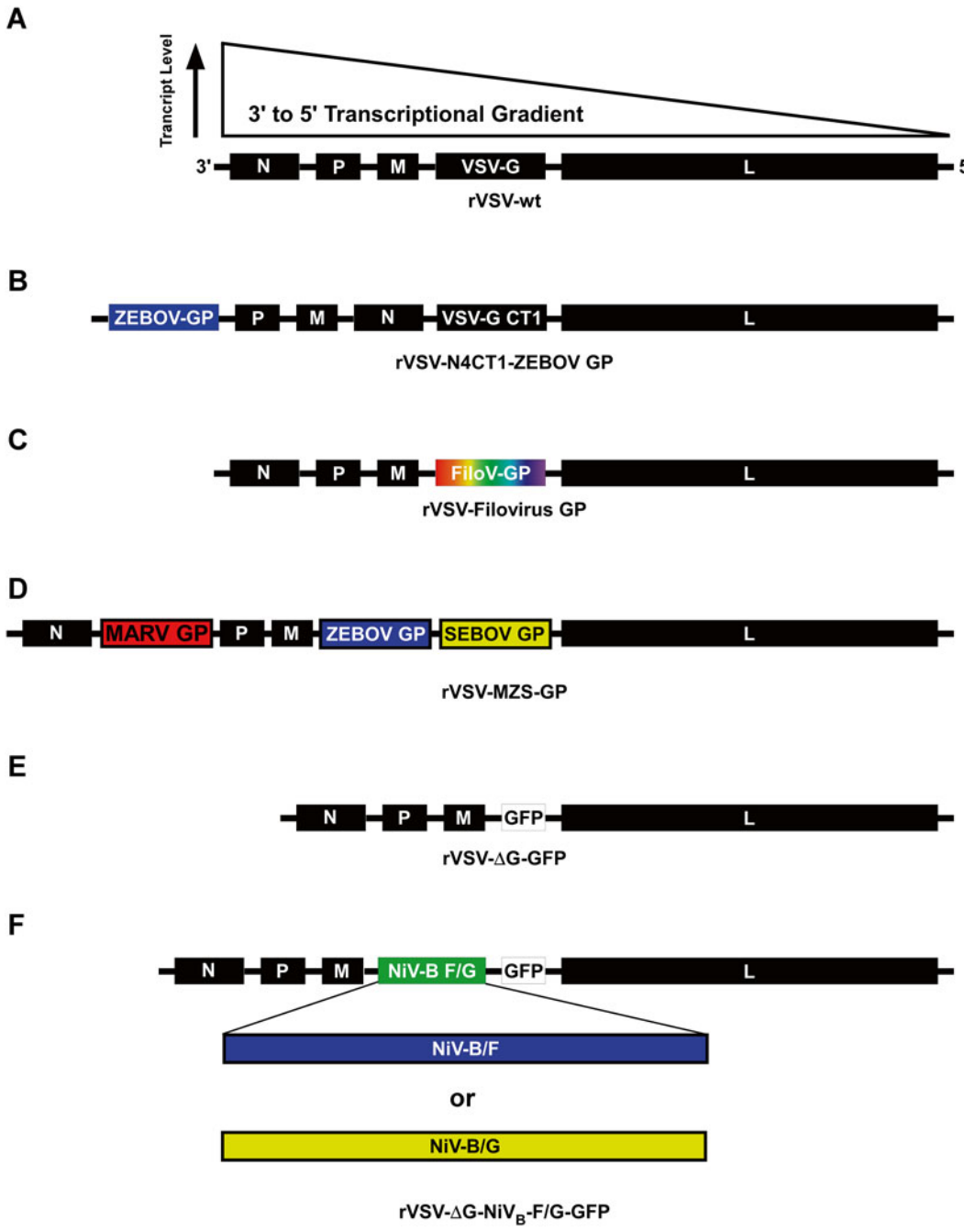

Fig. 1 rVSV genomes. Wild-type version of the rVSV-wt genome depicting the 3′–5′ transcriptional gradient of VSV (**a**). rVSV vaccine vector named rVSV-N4CT1-ZEBOV-GP that uses VSV G as the main entry and attachment glycoprotein expressing the ZEBOV GP (*blue*) as the dominant transcript as described [29] (**b**). Example of rVSV filovirus (FiloV) GP (multi-colored) vector as described [27, 46] (**c**). The LASV GPC is placed in the same position as described [46]. Tri-valent rVSV FiloV GP vector as described [34] where the MARV GP (*red*), ZEBOV GP (*blue*), and SEBOV GP (*yellow*) antigens are expressed from the rVSV-MZS-GP vaccine vector (**d**). Typical rVSV-ΔG-GFP vector used to test the recovery efficiency of VSV G complementation of single-round rVSV vaccine vectors (**e**) [37]. Illustration of the rVSV vaccine vector(s) against NiV as described [30] where one vector expresses the NiV F protein (*blue*) and the other expresses the NiV G protein (*yellow*) (**f**)

insertions and gene rearrangements; however, it is important to note that a careful characterization of the expression levels of foreign antigens and vaccine vector replication kinetics should be undertaken.

1.1.1 Replication-Competent rVSV Vaccine Vectors

Replication-competent rVSV vaccine vectors are defined as having the ability to infect and replicate in host cells culminating in the production of infectious virus. In some cases the foreign glycoproteins can participate in the productive infection of rVSV vaccine vectors and therefore can be generated through the "standard" recovery protocol as described in **Note 1**. The single foreign antigen and multivalent platforms both have the ability to use the "standard" recovery method to produce rVSV vaccine vectors.

Single Foreign Antigen Platform

The location of multiple cloning sites (MCSs) flanked by VSV start/stop and poly-adenylation signal sequences varies between the Bluescript plasmid vectors that contain the anti-genome (commonly referred to as a full-length plasmid) of the desired rVSV at the end of the recovery process. There are two rVSV vaccine vector approaches described in this section which require a "standard" rVSV recovery protocol as described below in **Note 1**. One approach for the single foreign antigen rVSV vaccine vectors uses the MCS located between the M and L genes as depicted in Fig. 1c where the filovirus (FiloV) GP gene is inserted to replace the VSV G gene. The rVSV vaccine vector against Lassa virus (LASV) also has the LASV GPC gene inserted in place of the VSV G gene.

Another approach to the single foreign antigen rVSV vaccine vector consists of a foreign antigen gene being expressed solely for its antigenic properties but not necessarily for its contribution toward entry and assembly. An example of this type of rVSV vaccine vector as depicted in Fig. 1b uses VSV G as the main driver of entry and assembly. To date there appears to be no interference with the antigenicity of the foreign antigen as this type of rVSV vaccine vector was able to protect mice and nonhuman primates (NHPs) from lethal ZEBOV-induced disease [29, 33].

Multivalent Foreign Antigen Platforms

To date, there are two rVSV vaccine vector platforms published in the literature where multiple filovirus antigens can be expressed from a single vector. The first vector reported was based on a dual-filovirus antigen-expressing platform where the GP and either NP, VP40, or VP24 were expressed [31]. The other vector was a trivalent platform expressing the MARV, ZEBOV, and SEBOV GPs from three separate open reading frames [34] as depicted in Fig. 1d. Both of these platforms were able to support productive rVSV infection and exhibited varying degrees of cross protection against heterologous filovirus challenge. The implications these vectors have on the ability to make a single-vaccine formulation to protect against multiple viruses will be beneficial to the manufacturing and safety testing of vaccine preparations.

1.1.2 Single-Round and Semi-replication-Competent rVSV Vaccine Vectors

Single-round rVSV vaccine vectors are defined as virions which can enter a cell and release the viral genome into the cytoplasm to undergo transcription (leading to foreign antigen mRNA) and replication but because the genome does not encode a glycoprotein capable of mediating virus entry (Fig. 1e, f), no infectious virions are produced, such as the "bald" particles referred to in Subheading 1. Semi-replication-competent rVSV vaccine vectors are defined as virions which can support at least two rounds of replication where there is a more finite restriction on replication when compared to a replication-competent vector. Regardless of which technique is chosen for a replication-limited rVSV vaccine vector the initial recovery and propagation of the virions require complementation with a functional glycoprotein. The recovery protocol for these rVSVs is covered in **Note 2**.

Single-Round rVSV Vaccine Vectors

Examples of single-round rVSV vaccine vectors are the NiV vaccine vectors that express either the NiV fusion (F) or G proteins as illustrated in Fig. 1f. NiV entry requires both the F and G proteins where G functions as the attachment protein bringing the virus in close proximity to the cell surface and F fuses the viral membrane with the host cell plasma membrane releasing the viral genome into the cytoplasm. Using the VSV G complementation technique described in **Note 2** an rVSV expressing either the F or the G protein can be propagated. During the single round of infection, either protein is expressed on the cell surface and subsequently incorporated into virions. After vaccination with a VSV-G-complemented NiV G- or F-expressing virus, cells proximal to the vaccination site become infected and express antigen on the surface for detection by the immune system. These infected cells also produce particles containing the antigen similar to a particle-based vaccine, but because they lack the attachment or fusion function, the particles are noninfectious, thereby limiting spread, but potentially increasing safety.

Semi-replication-Competent rVSV Vaccine Vectors

The vectors described in Subheading 2.2, **item 1**, comprise an example of single-round replicating rVSVs, but in the case of rVSVs expressing either NiV F or G, coinfection of a single cell with both vectors results in virions that will contain both the NiV F and G proteins on the surface. Coinfection at a multiplicity of infection (MOI) of 5 for both genome types results in expression of both the F and G proteins within a single host cell resulting in infectious virions containing either the F or the G gene in the viral genome [30]. If one of these virions singly infects a cell it will express either the F or the G gene resulting in the noninfectious virions described in Subheading 2.2, **item 1**. However, the potential for another round of coinfection exists though this most likely has a limit.

2 Materials

2.1 Cells, Viruses, Transfection Reagents, and Media

1. Baby hamster kidney (BHK-21) cells (clone WI-2) [35]. The WI-2 clone of BHK cells (available through KeraFAST; www.kerafast.com) has a higher transfection efficiency compared to that available through ATCC (*see* **Note 1**). A high transfection efficiency is critical for the successful recovery of rVSV from plasmids.
2. Dulbecco's modified Eagle's medium with L-glutamine (DMEM; Life Technologies, CA) supplemented with 5 % fetal bovine serum (FBS) (Life Technologies; *see* **Note 2**). This is called D-5.
3. Serum-free DMEM (SF-DMEM).
4. Minimum Essential Medium (MEM; Life Technologies) supplemented with Glutamax (Life Technologies) and 10 % FBS. This is called E-10.
5. 2× MEM (Life Technologies).
6. Trypsin-EDTA in phosphate-buffered saline minus calcium and magnesium (0. 25 % trypsin + 0.1 % EDTA in PBS minus).
7. 1.8 % Bacto-agar in water: Sterilized and melted by autoclaving. For use, heat in microwave oven until agar is molten.
8. 20× $NaHCO_3$: Dissolve 5.92 g $NaHCO_3$ in a total volume of 80 ml Milli-Q-dH_2O. Sterilize through a 0.2 μm bottle-top filter and store at 4 °C.
9. 2× DMEM stock solution: Dissolve a 1 L packet of powdered DMEM (Invitrogen/Gibco) in 450 ml Milli-Q-dH_2O. Filter sterilize using 0.2 μ bottle-top filter and store at 4 °C.
10. 2× DMEM working solution: To prepare a 200 ml 2× DMEM working solution add 10 ml 20× $NaHCO_3$ to 170 ml 2× DMEM stock and then add 20 ml FBS (final FBS = 10 %).
11. Agar overlay: Melt 1.8 % Bacto-agar in a microwave oven. Add the volume needed for titering to a sterile tube or bottle and cool to 45 °C. Mix equal volumes of pre-warmed (to 37 °C) 2× DMEM (BHK-21) or 2× MEM (Vero E6) working solution containing 10 % FBS with the molten 1.8 % agar. Add 2 ml directly to infected cells and let solidify.
12. TransfectACE reagent: Dissolve 0.1 g DDAB (dimethyldioctadecyl ammonium bromide; Sigma-Aldrich) in 1 ml 100 % ethanol by placing in a 37 °C water bath with occasional vortex mixing. The DDAB stock must be made fresh each time. Dissolve L-α-phosphatidyl ethanolamine-dioleoyl (Sigma-Aldrich) in 100 % ethanol to 10 mg/ml. Add 40 μl DDAB stock to 1 ml 10 mg/ml L-α-phosphatidyl ethanolamine-dioleoyl, mix by vortexing, and then inject, just below the

meniscus, the ~1 ml lipid/EtOH mix into 9 ml sterile deionized water at room temperature using a micropipette while vortexing. Store the liposome suspension at 4 °C. The reagent will be good for at least 9 months after preparation.

13. Opti-MEM Reduced Serum Medium (Life Technologies).
14. Lipofectamine (Life Technologies).
15. Sterile, 15 ml or 50 ml polystyrene centrifuge tubes.
16. Sterile 5 ml snap-cap polypropylene and polystyrene tubes.
17. African green kidney cells; Vero E6 (C1008) cells (ATCC #CRL-1586).

2.2 Plasmids

1. pVSV-9.1(+), a.k.a. pVSV-FL; wild-type recombinant vector.
2. pVSV-ΔG-GFP, a.k.a. pVSV-ΔG* (Fig. 1a; [25]).
3. pVSV-ΔG-DsRed, a.k.a. pVSV-ΔG-RFP [36].
4. pVSV-ΔL-GFP [37].
5. pBS-N-TΦ [38].
6. pBS-P-TΦ [38].
7. pBS-L-TΦ [38].
8. pBS-G [11].
9. pC-T7 [39].
10. pC-VSVG [25], a.k.a. pCAGGS-G_{Ind} [40].

3 Methods

The success of VSV-based vaccines against viruses that require high-level biosafety level-4 BSL-4 containment requires that protective antigens from these viruses are cloned into the VSV genome at the appropriate position relative to the 3′ end of the genome. Generally, the goal is to have the vaccine elicit neutralizing antibody so that individuals immunized with the vaccine are afforded protection against infection. Because BSL-4 viruses typically cause acute, life-threatening infections, antigens that induce primarily cytotoxic T cell responses are less effective. Using this premise, the design of VSV-based vaccines typically involves replacement of the VSV glycoprotein (G) with the glycoprotein of the BSL-4 agent.

The methods described below include those for the recovery of replication-competent rVSV and are followed by the methods used to generate rVSV-ΔG vectors expressing foreign antigens that are pseudotyped with VSV G. Important controls used to evaluate the efficiency of virus recovery, and methods used to troubleshoot the basis for poor recovery efficiencies, are included. Finally, methods used to quantify infectivity and to analyze glycoprotein incorporation into rVSV-ΔG particles are described.

3.1 Recovery of Replication-Competent rVSVs from Plasmids

The standard protocol for recovery of replication-competent rVSVs from plasmids involves the transfection of cells with a plasmid that expresses the positive-sense, anti-genomic RNA of VSV from a bacteriophage T7 RNA polymerase promoter together with plasmids encoding the VSV nucleocapsid (N), phosphoprotein (P), and large VSV RNA polymerase subunit (L). VSV RNA by itself is not infectious. Instead it must be encapsidated by the N protein to form an N-RNA complex, which serves as the template for recognition, transcription, and replication by the VSV P/L polymerase (Fig. 2).

Expression of the VSV anti-genome by T7 polymerase must occur in the cytoplasm and can be achieved by either infecting cells with a recombinant vaccinia expressing bacteriophage T7 RNA polymerase [41, 42], by using cells stably expressing T7 polymerase (BSR-T7 [43, 44]), or transfection of a plasmid that expresses T7 polymerase (pC-T7 [39]). If BSR-T7 cells or transfection with pC-T7 is used, the plasmids expressing N, P, and L must contain an IRES since the T7 transcripts expressed in the cytoplasm will not have a 5′ cap and therefore will not be translated. When the rVSV anti-genomic RNA and the N, P, and L proteins are expressed in the proper ratios the anti-genomic RNA will be encapsidated by the VSV N protein which will serve as the template for synthesis of genomic RNA by the VSV polymerase. The genomic RNA, which is also encapsidated by N protein, serves as the template for synthesis of capped and polyadenylated mRNAs encoded by the rVSV genome, completing the replication cycle and resulting in the release of infectious virus. The protocol to recover replication-competent rVSV using the recombinant vaccinia-T7 system is outlined below.

3.1.1 Primary Recovery

The VSV reverse genetic systems developed to date have all used BHK-21 or Vero cells for the initial recovery. We prefer using the WI-2 clone of BHK-21 cells because of their rapid division time, high transfection efficiency, and support of robust VSV replication. For successful recoveries it is critical that the cells be maintained at a low passage number and that they have never been allowed to reach 100 % confluence. This ensures that the cells retain optimal transfectability. Approximately 16–24 h before starting the primary recovery, seed BHK cells into 6-well plates at a density of 5×10^5 to 9×10^5 cells/well. When plating, ensure that the cells are evenly disbursed in the well. To evenly distribute the cells slide the plate back and forth and side to side multiple times to achieve a very even monolayer. Do not swirl the plate since this causes the cells to accumulate in the middle of the well or dish and this will adversely affect transfection efficiency (*see* **Note 3**). Several different seeding densities can be used depending on the time of day the cells will be plated and the time interval between seeding the 6-well plates and the time cells are transfected to start the recovery. After plating,

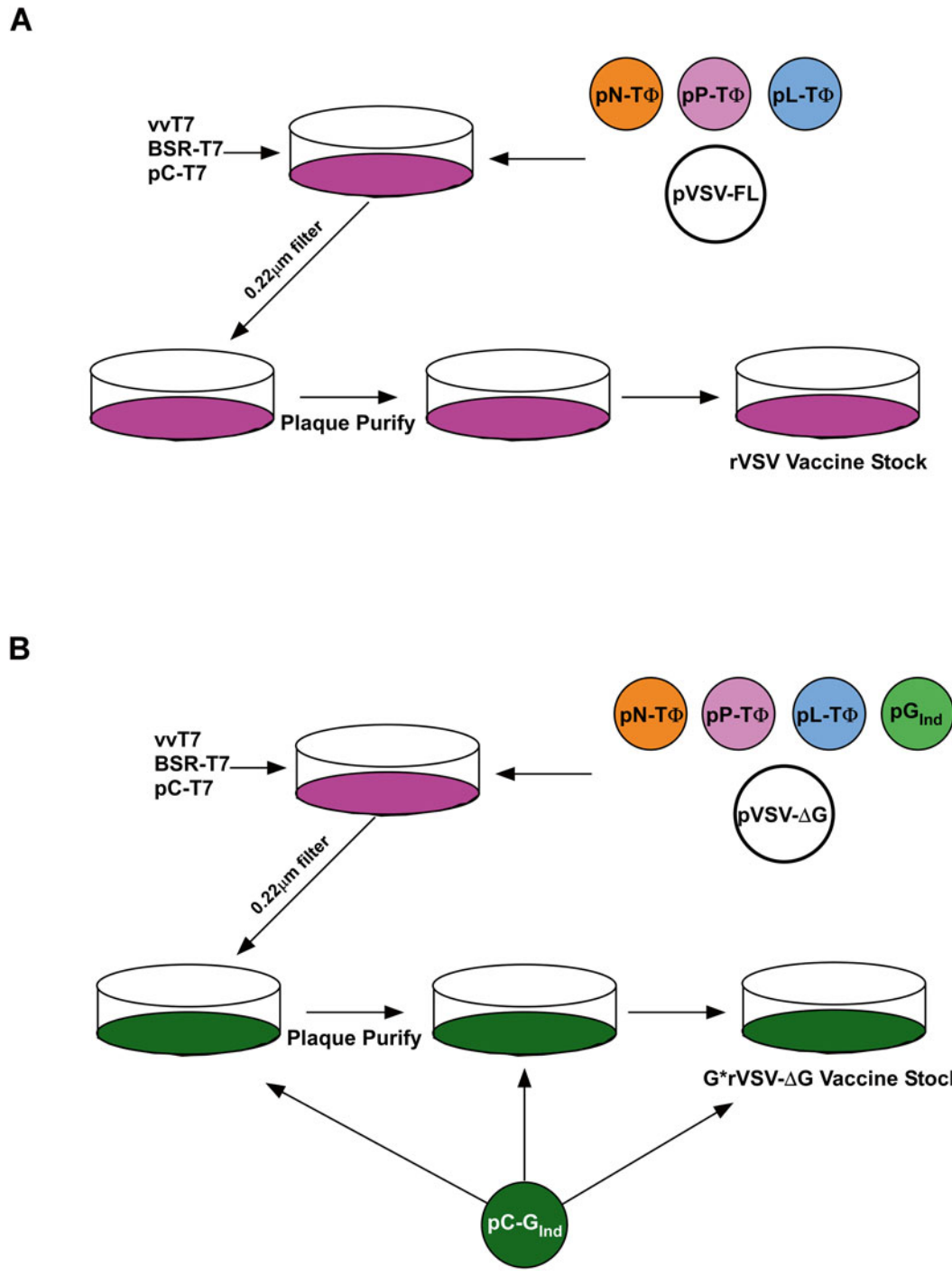

Fig. 2 Recovery diagram for rVSV recoveries. An illustration of the key points involved in generating and characterizing replication-competent (**a**) and single-round (semi-replication) (**b**) rVSV vectors. Initially cells are cotransfected with the plasmid pVSV-FL (**a**) or pVSV-ΔG (**b**) plasmids and the four (**a**) support plasmids encoding the VSV N, P, G, and L proteins; additional VSV G for pVSV-ΔG (**b**). This is followed by virus propagation after 0.22 μm filtration, with subsequent plaque purification. rVSV single-round (*semi-replication*) vectors require growth on cells transfected with pC-G_{Ind} (*dark green*) for transient expression of VSV G to G-complement these working stocks (**b**)

incubate the cells at 37 °C in a humidified incubator containing 6–8 % CO_2 for 14–16 h. The cells should be ~90–95 % confluent for virus recovery using the vaccinia-T7 expression system (Fig. 2). Infect with either vvT7 or MVA-T7 (*see* **Note 4**) at a multiplicity of 5–10. Adsorb by occasional rocking or by placing the plate on the platform rocker in a 37 °C, 6–8 % CO_2, incubator (*see* **Note 5**) for ~45–60 min. During adsorption, prepare the transfection mix containing the pVSV-FL plasmid and the N, P, and L support plasmids. The amount of transfection mix to be prepared will depend on the number of recoveries being done. Each well will receive an N, P, and L plasmid mixture that has a ratio of 3:5:1 μg of each plasmid, respectively, plus 5 μg of the rVSV plasmid (*see* **Note 6**) to be recovered (Fig. 2a). For each virus that will be recovered, it is recommended that the transfection be done in duplicate. In addition, 2 wells should be used for a "positive control" transfection using a plasmid called pVSV-ΔL-GFP. This plasmid has the polymerase (L) gene replaced with GFP. If the N, P, and L support plasmids are provided in the proper ratios and the transfection efficiency is sufficiently high, there should be at least 30–60 % of the cells that are GFP positive using the pVSV-ΔL-GFP plasmid. For transfection, either a commercially available transfection reagent can be used or a reagent (TransfectACE) that can be prepared in the lab can be used as described [37, 45]. It may be necessary to determine the optimal transfection reagent:DNA ratio for "in-house"-prepared TransfectACE. Typically, between 3 and 5 μl of TransfectACE per μg of plasmid DNA results in high transfection efficiencies (*see* **Note 6**). Following transfection, incubate at 37 °C for 40–48 h. Typically, virus recovery supernatants will be harvested between 42 and 46 h post-transfection.

3.1.2 *Virus Amplification*

The day before harvesting the supernatant from the primary recovery wells, plate cells that have the receptor for the virus to which you are generating the vaccine. For example, Vero E6 cells have been used for rVSV-EBOV recovery [46]. Approximately 40–48 h post-transfection, collect the medium from each well of the primary recovery and pass it through a 0.22 μm filter. VSV is sufficiently small to pass through a 0.22 μm filter; however, the vaccinia virus will be retained by the filter. This step should remove the entire vaccinia virus, but caution should be used because occasionally some vaccinia will pass through the membrane, possibly due to membrane rupture (*see* **Note 7**). Filter ~1/2 of the supernatant directly onto the appropriate well of the new 6-well plate and store the other filtered half at −80 °C. Note that the ΔL-GFP supernatant does not need to be harvested and filtered since this is used only to determine the efficiency of the recovery transfection by the expression of GFP. Place the plate(s) with the filtered recovery supernatants in a 37 °C, 6–8 % CO_2, incubator for 24–72 h.

To determine the efficiency of the primary transfection, aspirate the supernatant from the ΔL-GFP control wells and rinse the wells

with 2 ml PBS. Remove the PBS, add ~2 ml fix solution, and incubate for ~20 min to inactive the vaccinia virus. Remove the fix solution and rinse with PBS-glycine, and then examine the cells for GFP expression using a fluorescence microscope. If between 30 and 60 % of the cells are GFP positive then the chances that the primary recovery will be successful are good. If there are fewer than 20 % GFP-positive cells in the ΔL-GFP recovery wells, then the transfection and/or ratios of the support plasmids may need to be optimized.

The new plate(s) containing the filtered recovery supernatants should be monitored daily for the development of VSV-induced cytopathic effects (CPE), which are seen as areas (or foci) of rounded, refractile cells. Generally cell rounding will be obvious by 48 h, but may be observed as early as 12 h if the recovery is very efficient for rVSV-wt. When 40–100 % of the cells show signs of VSV-induced CPE, the supernatants can be harvested. Ideally it is best to wait until most of the cells show signs of VSV CPE; however, if the recovery is inefficient (for example only one infectious particle is generated in the recovery) then the percentage of cells showing signs of CPE after 72 h may be low (e.g., ~40 %). If VSV-G is being replaced with another glycoprotein that induces cell-cell fusion at neutral pH, then cell rounding may be less obvious and instead syncytium formation may occur [30]. To confirm that an rVSV has been successfully recovered, the medium from the amplification wells is collected and the cells can be stained for VSV M, or for expression of the heterologous glycoprotein. The use of VSV M for staining ensures that the CPE observed is not due to vaccinia-T7 and supports plasmid carryover since M is not included in the primary recovery transfection mix.

After collecting the media from the amplification wells, transfer the media to a sterile conical centrifuge tube and remove cells and cell debris by centrifugation for 10 min at ~450×*g*. Aliquot the cleared supernatants into appropriately labeled sterile freezer vials/tubes and store frozen at −80 °C. This is referred to as the first passage (P1) supernatant. The P1 can be stored frozen at −80 °C indefinitely.

3.2 Recovery of Single-Round rVSVs from Plasmids

Single-round vectors are defined as being able to infect cells, and replicate and express proteins encoded by the vector genome, but because they lack a functional glycoprotein or glycoprotein complex that can mediate binding of virus to cell surface receptors and initiate membrane fusion, the virus does not spread beyond the initial site of infection. These types of vectors are generically called rVSV-ΔG because they lack an envelope glycoprotein. The initial recovery steps for single-round vectors are similar to those of the replication-competent viruses, except that VSV-G is provided in trans via expression from a plasmid. A detailed protocol for recovery and characterization of rVSV-ΔG vectors has been published [37], so it will be briefly described here.

3.2.1 Primary Recovery and Amplification of rVSV-ΔG Vectors

Cells that express T7 polymerase (either stably or transiently from vaccinia or plasmids) are transfected with a plasmid encoding the rVSV-ΔG single-round replication vector and support plasmids expressing the VSV N, P, G, and L proteins in a ratio of 3:5:8:1 (Fig. 2b). Inclusion of a ΔL-GFP control is critical since inclusion of the additional VSV-G plasmid can significantly reduce the transfection efficiency. Here, at least 30 % of the cells should be GFP positive to ensure that the support proteins are being expressed in the proper amounts. Culture medium is collected exactly as for the replication-competent virus and filtered; however, to amplify the virus VSV-G must be provided in trans during each round of amplification (Fig. 2b).

To amplify rVSV-ΔG vectors, cells (either BHK or Vero) are transfected with a plasmid (pC-G) that expresses VSV G protein from a strong pol-II promoter the day before the media from primary recoveries are harvested. For optimal transfection the cells should be evenly distributed as described above and should be ~85 % confluent the next morning. Although VSV-G is a pH-dependent fusion protein, meaning that low pH (~ pH 6.3–6.1) induces a conformational change in G protein which results in activation of its membrane fusion activity, when G protein is expressed at sufficiently high levels on the cell surface of certain cell types (BHK-21 and HEK 293) a fraction of the G protein trimers convert to the low-pH conformation and induce cell-cell fusion in the absence of a low-pH trigger. To evaluate the efficiency of the transfection, cells should be assessed for syncytia formation starting at 24 h post-transfection. Small (three to four cell) syncytia should be distributed throughout the monolayer by 20–24 h. This indicates that sufficient G protein has been expressed on the cell surface to be incorporated into the rVSV-ΔG vectors to produce a high-titer P1 virus stock during the amplification step.

After confirming that the pCAGGS-G transfection was successful as indicated by syncytia formation, pass the media from primary recovery through a 0.22 μm filter if using the vaccinia virus-T7 system onto the pCAGGS-G-transfected cells. If using BSR-T7 cells or if cells were transfected with pC-T7, then filtering is not necessary. Monitor the cells for the development of VSV-induced cytopathic effects (CPE). Generally cell rounding will be obvious by 48 h, but may be observed by 24 h if the recovery is very efficient. When 40–100 % of the cells show signs of VSV-induced CPE, the supernatants can be harvested. Ideally it is best to wait until most of the cells are showing signs of VSV CPE; however, do not incubate more than 72 h as G-complemented rVSV-ΔG virus will lose infectivity. Generally, CPE is evident after 24–36 h. Harvest the media, clarify by centrifugation, and then store aliquots frozen at −80 °C. Determine the titer, plaque-purify, and generate a large working stock as described below.

3.3 Plaque Purification and Titering of VSV Vectors

Although the recovered viruses should be genetically homogenous, for RNA viruses with a high mutational frequency it is recommended that the viruses be plaque-purified. This ensures that no sub-genomic, replicating RNAs, also known as defective interfering (DI) particles, are present. The following procedure describes a general method for titering rVSV vectors by plaque assay and recovering plaque isolates. Plaque purification also ensures that there is no residual vaccinia virus that may have carried over during the initial amplification after filtering.

Cells with an appropriate receptor for the vector are plated into 6- or 12-well plates and the next day serial dilutions of the P1 supernatant are added. Virus is adsorbed for 1–3 h and then a molten agar-overlay (D-5 containing 0.9 % agar) is added. After solidifying, the plates are incubated until plaques are visible (typically 24 h, but may be longer depending on envelope glycoprotein expressed from the vector, the cell type used, and the cell density at the time of infection). To pick plaque isolates, choose plaques that are well separated. Use a sterile Pasteur pipette and insert into the agar to the bottom of the plate to remove the plaque and agar plug by gentle aspiration. Elute virus from the agar plug by placing in 0.5 ml of D-5 growth medium for 1–2 h at 4 °C. Store the eluted plaque isolate at −80 °C, or use an aliquot directly to amplify the virus to make a plaque-purified P1 stock.

For titering and plaque purification of single-cycle rVSV-ΔG vectors, transfect a 10 cm dish of BHK cells with pCAGGS-G (Fig. 2b). Approximately 30 h post-transfection, trypsinize the cells and divide into two 6-well plates. Let the cells attach for at least 6 h, but not more than 18 h since the cell density will get too high. Prepare tenfold serial dilutions of the virus stock, adsorb virus, and add an agar-overlay as described above. Plaque isolates can be obtained in the same way as for replication-competent virus by picking a well-isolated plaque and eluting in growth medium.

3.4 Vaccine Development and Study Design

Evaluation of vaccines for high-containment viruses generally requires at least a two-step approach influenced by the FDA animal rule of 2002 [47] which established requirements for evidence needed to demonstrate effectiveness of new drugs and biological products when human efficacy studies are not ethical or feasible. To effectively evaluate a designed and recovered rVSV vaccine vector against high-containment viruses, a thorough understanding of the pathogenesis of the viruses in relevant animal models is essential. This rule, which states that a product can be licensed based on evidence of effectiveness derived from studies in well-characterized animal models and the usual demonstration of biological activity and safety in humans, would most likely be enacted for high-containment virus vaccines. Thus, the validation of rodents and NHPs as accurate and reliable models of human disease has been and will be critical to the final evaluation and testing of candidate

vaccines. Vaccine efficacy should first be proven in rodent models and then in NHPs as ultimately no vaccine or treatment should be approved for human use until it can protect NHPs from viremia and clinical illness.

4 Notes

1. The BHK-21 cells that are used are not those available from the ATCC. The cells from ATCC are very fibroblast-like. Instead the BHK-21 clone WI-2 cells are more epithelial-like. These cells have much higher transfection efficiencies which appear to be one of the critical factors that influence the efficiency of virus recovery from plasmids.
2. The FBS used for cell culture for vaccine vector prep should be heat inactivated.
3. Use cells that have not been allowed to overgrow at any time, not even once. If they overgrow thaw a new vial. Generally, cells used for pseudotyping should be passaged every day to ensure that overgrowth does not occur; additionally this will produce a homogeneous cell suspension after trypsinizing. To evenly distribute the cells move the plate back and forth and side to side multiple times. Re-plate cells if the plate is swirled as this causes the cells to accumulate in the middle of the well or dish and overgrow in that section which will adversely affect cell transfection and pseudotype production.
4. The vv-T7 or MVA-T7 stocks can be frozen and thawed approximately three times without significant loss of infectivity.
5. The BHK-21 clone WI-2 cells grow best in a 6–8 % CO_2 environment. All cell culture work used for rVSV vaccine vector recovery should be performed in 6–8 % CO_2 incubator.
6. After making a stock of TransfectACE or new plasmids it is highly recommended to determine the optimal TransfectACE:DNA ratio for "in-house"-prepared TransfectACE. Typically, between 3 and 5 μl of TransfectACE per μg of plasmid DNA results in high-efficiency transfections.
7. Pass the supernatant through the filter very slowly (~1 drop per second) since the high hydrostatic pressure obtained using a 3 ml syringe can rupture the filter.

Acknowledgements

Funding to T.W.G. for rVSV vaccine vectors presented was as follows: DHHS/NIH U01 AI082197; U01 AI082121; and R01 AI09881701.

References

1. Letchworth GJ, Rodriguez LL, Del Cbarrera J (1999) Vesicular stomatitis. Vet J 157:239–260
2. Fields BN, Hawkins K (1967) Human infection with the virus of vesicular stomatitis during an epizootic. N Engl J Med 277:989–994
3. Lawson ND, Stillman EA, Whitt MA, Rose JK (1995) Recombinant vesicular stomatitis viruses from DNA. Proc Natl Acad Sci U S A 92:4477–4481
4. Whelan SP, Ball LA, Barr JN, Wertz GT (1995) Efficient recovery of infectious vesicular stomatitis virus entirely from cDNA clones. Proc Natl Acad Sci U S A 92:8388–8392
5. Barr JN, Whelan SP, Wertz GW (1997) Role of the intergenic dinucleotide in vesicular stomatitis virus RNA transcription. J Virol 71:1794–1801
6. Stillman EA, Whitt MA (1997) Mutational analyses of the intergenic dinucleotide and the transcriptional start sequence of vesicular stomatitis virus (VSV) define sequences required for efficient termination and initiation of VSV transcripts. J Virol 71:2127–2137
7. Stillman EA, Whitt MA (1998) The length and sequence composition of vesicular stomatitis virus intergenic regions affect mRNA levels and the site of transcript initiation. J Virol 72:5565–5572
8. Whelan SP, Barr JN, Wertz GW (2000) Identification of a minimal size requirement for termination of vesicular stomatitis virus mRNA: implications for the mechanism of transcription. J Virol 74:8268–8276
9. Li T, Pattnaik AK (1999) Overlapping signals for transcription and replication at the 3′ terminus of the vesicular stomatitis virus genome. J Virol 73:444–452
10. Das SC, Nayak D, Zhou Y, Pattnaik AK (2006) Visualization of intracellular transport of vesicular stomatitis virus nucleocapsids in living cells. J Virol 80:6368–6377
11. Fredericksen BL, Whitt MA (1995) Vesicular stomatitis virus glycoprotein mutations that affect membrane fusion activity and abolish virus infectivity. J Virol 69:1435–1443
12. Fredericksen BL, Whitt MA (1996) Mutations at two conserved acidic amino acids in the glycoprotein of vesicular stomatitis virus affect pH-dependent conformational changes and reduce the pH threshold for membrane fusion. Virology 217:49–57
13. Harty RN, Brown ME, McGettigan JP, Wang G, Jayakar HR, Huibregtse JM, Whitt MA, Schnell MJ (2001) Rhabdoviruses and the cellular ubiquitin-proteasome system: a budding interaction. J Virol 75:10623–10629
14. Jayakar HR, Murti KG, Whitt MA (2000) Mutations in the PPPY motif of vesicular stomatitis virus matrix protein reduce virus budding by inhibiting a late step in virion release. J Virol 74:9818–9827
15. Jayakar HR, Whitt MA (2002) Identification of two additional translation products from the matrix (M) gene that contribute to vesicular stomatitis virus cytopathology. J Virol 76:8011–8018
16. Jeetendra E, Ghosh K, Odell D, Li J, Ghosh HP, Whitt MA (2003) The membrane-proximal region of vesicular stomatitis virus glycoprotein G ectodomain is critical for fusion and virus infectivity. J Virol 77:12807–12818
17. Mire CE, White JM, Whitt MA (2010) A spatiotemporal analysis of matrix protein and nucleocapsid trafficking during vesicular stomatitis virus uncoating. PLoS Pathog 6, e1000994
18. Mire CE, Whitt MA (2011) The protease-sensitive loop of the vesicular stomatitis virus matrix protein is involved in virus assembly and protein translation. Virology 416:16–25
19. Huang JW, Davey MW, Hejna CJ, Von Muenchhausen W, Sulkowski E, Carter WA (1974) Selective binding of human interferon to albumin immoblized on agarose. J Biol Chem 249:4665–4667
20. Weiss RA, Boettiger D, Murphy HM (1977) Pseudotypes of avian sarcoma viruses with the envelope properties of vesicular stomatitis virus. Virology 76:808–825
21. Witte ON, Baltimore D (1977) Mechanism of formation of pseudotypes between vesicular stomatitis virus and murine leukemia virus. Cell 11:505–511
22. Zavada J, Rosenbergova M (1972) Phenotypic mixing of vesicular stomatitis virus with fowl plague virus. Acta Virol 16:103–114
23. Jayakar HR, Jeetendra E, Whitt MA (2004) Rhabdovirus assembly and budding. Virus Res 106:117–132
24. Schnell MJ, Johnson JE, Buonocore L, Rose JK (1997) Construction of a novel virus that targets HIV-1-infected cells and controls HIV-1 infection. Cell 90:849–857
25. Takada A, Robison C, Goto H, Sanchez A, Murti KG, Whitt MA, Kawaoka Y (1997) A system for functional analysis of Ebola virus glycoprotein. Proc Natl Acad Sci U S A 94:14764–14769
26. Robison CS, Whitt MA (2000) The membrane-proximal stem region of vesicular stomatitis

virus G protein confers efficient virus assembly. J Virol 74:2239–2246

27. Jones SM, Feldmann H, Stroher U, Geisbert JB, Fernando L et al (2005) Live attenuated recombinant vaccine protects nonhuman primates against Ebola and Marburg viruses. Nat Med 11:786–790
28. Lo MK, Bird BH, Chattopadhyay A, Drew CP, Martin BE et al (2013) Single-dose replication-defective VSV-based Nipah virus vaccines provide protection from lethal challenge in Syrian hamsters. Antiviral Res 101:26–29
29. Mire CE, Matassov D, Geisbert JB, Latham TE, Agans KN et al (2015) Single-dose attenuated Vesiculovax vaccines protect primates against Ebola Makona virus. Nature 520:688–691
30. Mire CE, Versteeg KM, Cross RW, Agans KN, Fenton KA, Whitt MA, Geisbert TW (2013) Single injection recombinant vesicular stomatitis virus vaccines protect ferrets against lethal Nipah virus disease. Virol J 10:353
31. Marzi A, Ebihara H, Callison J, Groseth A, Williams KJ, Geisbert TW, Feldmann H (2011) Vesicular stomatitis virus-based Ebola vaccines with improved cross-protective efficacy. J Infect Dis 204(Suppl 3):S1066–S1074
32. Safronetz D, Mire C, Rosenke K, Feldmann F, Haddock E, Geisbert T, Feldmann H (2015) A recombinant vesicular stomatitis virus-based Lassa fever vaccine protects guinea pigs and macaques against challenge with geographically and genetically distinct Lassa viruses. PLoS Negl Trop Dis 9, e0003736
33. Matassov D, Marzi A, Latham T, Xu R, Ota-Setlik A et al (2015) Vaccination with a highly attenuated recombinant vesicular stomatitis virus vector protects against challenge with a lethal dose of ebola virus. J Infect Dis pii: jiv316. [Epub ahead of print] PubMed PMID: 26109675.
34. Mire CE, Geisbert JB, Versteeg KM, Mamaeva N, Agans KN, Geisbert TW, Connor JH (2015) A single-vector, single-injection trivalent filovirus vaccine: proof of concept study in outbred guinea pigs. J Infect Dis pii: jiv126. [Epub ahead of print] PubMed PMID: 25957964.
35. Kaariainen L, Gomatos PJ (1969) A kinetic analysis of the synthesis in BHK 21 cells of RNAs specific for Semliki Forest virus. J Gen Virol 5:251–265
36. Porotto M, Carta P, Deng Y, Kellogg GE, Whitt M, Lu M, Mungall BA, Moscona A (2007) Molecular determinants of antiviral potency of paramyxovirus entry inhibitors. J Virol 81:10567–10574
37. Whitt MA (2010) Generation of VSV pseudotypes using recombinant DeltaG-VSV for studies on virus entry, identification of entry inhibitors, and immune responses to vaccines. J Virol Methods 169:365–374
38. Stillman EA, Rose JK, Whitt MA (1995) Replication and amplification of novel vesicular stomatitis virus minigenomes encoding viral structural proteins. J Virol 69:2946–2953
39. Neumann G, Feldmann H, Watanabe S, Lukashevich I, Kawaoka Y (2002) Reverse genetics demonstrates that proteolytic processing of the Ebola virus glycoprotein is not essential for replication in cell culture. J Virol 76:406–410
40. Jeetendra E, Robison CS, Albritton LM, Whitt MA (2002) The membrane-proximal domain of vesicular stomatitis virus G protein functions as a membrane fusion potentiator and can induce hemifusion. J Virol 76:12300–12311
41. Fuerst TR, Niles EG, Studier FW, Moss B (1986) Eukaryotic transient-expression system based on recombinant vaccinia virus that synthesizes bacteriophage T7 RNA polymerase. Proc Natl Acad Sci U S A 83:8122–8126
42. Wyatt LS, Moss B, Rozenblatt S (1995) Replication-deficient vaccinia virus encoding bacteriophage T7 RNA polymerase for transient gene expression in mammalian cells. Virology 210:202–205
43. Buchholz UJ, Finke S, Conzelmann KK (1999) Generation of bovine respiratory syncytial virus (BRSV) from cDNA: BRSV NS2 is not essential for virus replication in tissue culture, and the human RSV leader region acts as a functional BRSV genome promoter. J Virol 73:251–259
44. Harty RN, Brown ME, Hayes FP, Wright NT, Schnell MJ (2001) Vaccinia virus-free recovery of vesicular stomatitis virus. J Mol Microbiol Biotechnol 3:513–517
45. Rose JK, Buonocore L, Whitt MA (1991) A new cationic liposome reagent mediating nearly quantitative transfection of animal cells. Biotechniques 10:520–525
46. Garbutt M, Liebscher R, Wahl-Jensen V, Jones S et al (2004) Properties of replication-competent vesicular stomatitis virus vectors expressing glycoproteins of filoviruses and arenaviruses. J Virol 78:5458–5465
47. Roberts R, McCune SK (2008) Animal studies in the development of medical countermeasures. Clin Pharmacol Ther 83:918–920

Chapter 17

Reverse Genetics Approaches to Control Arenavirus

Luis Martínez-Sobrido, Benson Yee Hin Cheng, and Juan Carlos de la Torre

Abstract

Several arenavirus cause hemorrhagic fever disease in humans and pose a significant public health problem in their endemic regions. To date, no licensed vaccines are available to combat human arenavirus infections, and anti-arenaviral drug therapy is limited to an off-label use of ribavirin that is only partially effective. The development of arenavirus reverse genetics approaches provides investigators with a novel and powerful approach for the investigation of the arenavirus molecular and cell biology. The use of cell-based minigenome systems has allowed examining the *cis*- and *trans*-acting factors involved in arenavirus replication and transcription and the identification of novel anti-arenaviral drug targets without requiring the use of live forms of arenaviruses. Likewise, it is now feasible to rescue infectious arenaviruses entirely from cloned cDNAs containing predetermined mutations in their genomes to investigate virus-host interactions and mechanisms of pathogenesis, as well as to facilitate screens to identify anti-arenaviral drugs and development of novel live-attenuated arenavirus vaccines. Recently, reverse genetics have also allowed the generation of tri-segmented arenaviruses expressing foreign genes, facilitating virus detection and opening the possibility of implementing live-attenuated arenavirus-based vaccine vector approaches. Likewise, the development of single-cycle infectious, reporter-expressing, arenaviruses has provided a new experimental method to study some aspects of the biology of highly pathogenic arenaviruses without the requirement of high-security biocontainment required to study HF-causing arenaviruses. In this chapter we summarize the current knowledge on arenavirus reverse genetics and the implementation of plasmid-based reverse genetics techniques for the development of arenavirus vaccines and vaccine vectors.

Key words Recombinant arenavirus, Arenavirus rescue systems, Arenavirus reverse genetics, Arenavirus GP-expressing cells, Reporter genes, Minigenome assays, Tris-segmented arenavirus, Single-cycle infectious arenavirus, Virus vectors, Reporter virus, Vaccines, Antiviral drugs

Abbreviations

αDG	Alpha-dystroglycan
AHF	Argentine hemorrhagic fever
ATCC	American Type Culture Collection
BHK-21	Baby hamster kidney cells
BSA	Albumin bovine serum
BSL	Biosafety level
CAT	Chloramphenicol acetyltransferase

Sunil Thomas (ed.), *Vaccine Design: Methods and Protocols: Volume 1: Vaccines for Human Diseases*, Methods in Molecular Biology, vol. 1403, DOI 10.1007/978-1-4939-3387-7_17,

CD	Codon optimization
CHPV	Chapare virus
Cluc	Cypridina luciferase
CPE	Cytopathic effect
cRNA	Complementary RNA
DMEM	Dulbecco's modified Eagle's medium
DN	Dominant negative
FBS	Fetal bovine serum
FDA	Food and Drug Administration
FFU	Fluorescence forming units
Gluc	Gaussia luciferase
GFP	Green fluorescent protein
GOI	Gene of interest
GP	Glycoprotein
GTOV	Guanarito virus
HF	Hemorrhagic fever
HTS	High-throughput screening
IGR	Intergenic region
ING	Investigational new drug
JUNV	Junin virus
IMP	Inosine-5′-monophosphate
L	Large RNA segment
LASV	Lassa virus
LCMV	Lymphocytic choriomeningitis virus
LF	Lassa fever
LUJV	Lujo virus
LPF2000	Lipofectamine 2000
MACV	Machupo virus
MG	Minigenome
MHC	Major histocompatibility complex
MOI	Multiplicity of infection
MOPV	Mopeia virus
mRNA	Messenger RNA
MVB	Multivesicular endosomes
NHP	Nonhuman primates
NW	New World
NP	Nucleoprotein
NS	Negative-stranded
OCEV	Ocozocoautla de Espinosa virus
ON	Overnight
ORF	Open reading frame
OW	Old World
PBS	Phosphate-buffered saline
pA	Polyadenylation signal
PICV	Pichinde virus
Pol-I	Polymerase I
Pol-II	Polymerase II
PS	Penicillin/streptomycin

RdRp	RNA-dependent RNA polymerase
Rib	Ribavirin
RT	Room temperature
r3	Recombinant tri-segmented
S	Small RNA segment
SABV	Sabia virus
S1P	Site-1 protease
SAH	S-adenosylhomocysteine
siRNA	Small interfering RNA
TCRV	Tacaribe virus
TCS	Tissue culture supernatants
TNF	Tumor necrosis factor
UTR	Untranslated regions
vRNA	Viral RNA
VSV	Vesicular stomatitis virus
vRNPs	Viral ribonucleoproteins
WWAV	Whitewater Arroyo virus
WT	Wild-type
Z	Matrix-like small RING finger protein

1 Introduction

1.1 Arenaviruses and Their Impact on Human Health

Arenaviruses cause chronic infections in rodents with a worldwide distribution [1]. Asymptomatically infected animals move freely in their natural habitat and may invade human dwellings. Humans are infected most likely through mucosal exposure to aerosols, or by direct contact between infectious materials and abrade skin. These infections are common and in some cases severe [1].

The family *Arenaviridae* consists currently of two genera: (1) Mammarenavirus with 25 recognized virus species that are classified into two distinct groups, Old World (OW) and New World (NW) arenaviruses [1], and (2) Reptarenavirus, a new genus that has been established to accommodate the recently discovered snake arenaviruses [2–5]. Classification of members of the genus Mammarenavirus was originally established based on serological cross-reactivity, but it is well supported by recent sequence-based phylogenetic studies [1]. Genetically, OW arenaviruses constitute a single lineage, while NW arenaviruses segregate into clades A, B, A/B, and C [1]. The OW arenavirus, Lassa virus (LASV), causes hemorrhagic fever (HF) disease in humans, which represents a serious public health problem in its endemic areas of West Africa [1, 6–10]. LASV is estimated to infect several hundred thousand individuals yearly in its endemic regions of West Africa resulting in a high number of Lassa fever (LF) cases associated with high morbidity and significant mortality. Moreover, increased travel has led to the importation of cases of Lassa fever into the USA, Europe, Japan, and Canada [11–13]. Moreover, recent studies indicate that

LASV endemic regions are expanding [14] and the association of Lujo virus (LUJV) [15], a newly identified OW arenavirus associated with an outbreak of HF in Southern Africa in 2008, has raised concerns about the emergence of novel HF OW arenaviruses outside their current known endemic regions. On the other hand the NW arenavirus Junin virus (JUNV), endemic to the pampas of Argentine, causes Argentine HF (AHF) with a high (15–30 %) case fatality rate [6]. Likewise, NW arenavirus Machupo virus (MACV) [16, 17] and Chapare virus (CHPV) [18], Sabia virus (SABV) [19, 20], Guanarito virus (GTOV) [21–23], Whitewater Arroyo virus (WWAV) [24, 25], and Ocozocoautla de Espinosa virus (OCEV) [26] are responsible for causing HF in Bolivia, Brazil, Venezuela, the USA, and Mexico, respectively. Moreover, mounting evidence indicates that the worldwide-distributed prototypic arenavirus lymphocytic choriomeningitis virus (LCMV) is a neglected human pathogen of clinical significance, especially in cases of congenital infection [27–31]. In addition, LCMV poses a special threat to immunocompromised individuals, which has been illustrated by fatal cases of transplant-associated infections by LCMV [32–34]. OW arenaviruses LASV and LUJV and NW arenavirus JUNV, MACV, GTOV, and CHPV have features that make them credible biodefense threats and have been included by the National Institute of Allergy and Infectious Diseases (NIAID) as Category A biological agents that pose a significant biodefense concern [35]. Concerns about human pathogenic arenavirus infections are aggravated by the lack of Food and Drug Administration (FDA)-licensed vaccines and antiviral drug treatment being limited to the use of ribavirin (Rib) [36] that is only partially effective [37–39]. Evidence indicates that morbidity and mortality of LASV infections, and likely other HF arenavirus infection, are associated with, at least partly, the failure of the host's innate immune response to restrict virus replication and to facilitate the initiation of an effective adaptive immune response [9]. Accordingly, viremia is a highly predictive factor for the outcome of LF patients [9]. Therefore, therapeutic interventions resulting in reduced virus load, despite lack of virus clearance, are expected to promote the recovery of appropriate host defense responses to control arenavirus multiplication and associated disease.

1.2 Current Strategies to Combat Human Arenavirus Infections

1.2.1 Arenavirus Vaccines

The live-attenuated Candid#1 strain of JUNV induces a strong neutralizing antibody response in several animal model systems, and it has been shown to be an effective vaccine to combat AHF in humans without causing serious adverse effects [6, 40, 41]. However, the Candid#1 vaccine is licensed only as an investigational new drug (IND) in the USA and studies addressing the stability of its attenuation, long-term immunity, and safety have not been conducted. Moreover, Candid#1 does not protect against LASV (Dr. Paessler and colleagues, personal communication), the

HF arenavirus with the highest impact in public health [1, 6–10]. Despite significant efforts dedicated to the development of LASV vaccines, not a single LASV vaccine candidate has entered a clinical trial but the MOPV/LASV reassortant ML29 as well as recombinant vesicular stomatitis virus (VSV) and vaccinia virus expressing LASV antigens have shown promising results in animal models, including nonhuman primates (NHP), of LASV infection [42]. However, the high prevalence of HIV within LASV-endemic regions in West Africa raises safety concerns about the use of VSV- or vaccinia-based platforms. Likewise, the mechanisms of ML29 attenuation remain poorly understood and additional mutations in ML29 or reassortants between ML29 and circulating virulent LASV strains could result in viruses with enhanced virulence.

The recent development of reverse genetics systems for JUNV [43, 44] and LASV [45, 46] would facilitate the elucidation of the genetic determinants of JUNV and LASV virulence. This, in turn, should help with the design of safer live-attenuated arenavirus vaccines by minimizing concerns related to reversion of virulence, establishment of persistent infection, and in general conditions associated with high risk for replicating viruses including immunocompromised individuals.

1.2.2 *Arenavirus Antiviral Drugs*

In vitro and in vivo studies have documented the prophylactic and therapeutic value of the nucleoside analogue Rib (1-b-D-ribofuranosyl-1,2,4-triazole-3-carboxamide) against several arenaviruses [36]. Moreover, Rib has been shown to reduce significantly both morbidity and mortality associated with LASV infection in humans [36, 47], and experimentally in MACV [48] and JUNV [49] infections, if given early in the course of clinical disease. The mechanisms by which Rib exerts its anti-arenaviral action remain poorly understood, but likely involve targeting different steps of the virus life cycle [50, 51]. Recent evidence indicates that Rib can be used as substrate by the RNA-dependent RNA polymerase (RdRp) of some riboviruses leading to C to U and G to A transitions [52, 53], and this mutagenic activity of Rib has been linked to its antiviral activity via lethal mutagenesis. However, Rib was also shown to strongly inhibit LCMV replication without exerting any noticeable mutagenic effect on the viral genome RNA [54]. Anemia and congenital disorders are two significant side effects associated with the use of Rib. In addition, oral Rib is significantly less effective than the one administered intravenously, which poses logistic complications in regions with limited clinical infrastructure [37–39].

Several inhibitors of inosine-5′-monophosphate (IMP) dehydrogenase, as well as acyclic and carbocyclic adenosine analogue inhibitors of the S-adenosylhomocysteine (SAH) hydrolase, have been shown to have also anti-arenavirus activity [36]. Likewise, the pyrimidine biosynthesis inhibitor A3, that exhibits broad-spectrum antiviral activity against negative- and positive-sense RNA viruses,

retroviruses, and DNA viruses [55], has been shown to be more efficient than Rib in controlling arenavirus multiplication and this inhibitory effect is due, at least in part, to its ability to interfere with viral RNA replication and transcription [56]. Moreover, since Rib and A3 target different metabolic pathways within the cell, they are excellent candidates for combination anti-arenaviral therapy to circumvent some limitations of Rib monotherapy [56]. A variety of sulfated polysaccharides, phenothiazines, and myristic acid have been reported to have activity against several arenaviruses [36]. However, in general these compounds displayed only modest and rather nonspecific effects often associated with significant toxicity. Nevertheless, favipiravir, a broad-spectrum RdRp inhibitor, has shown promising results including some protection (20 % survival) in a guinea pig model of fatal AHF [57, 58]. Recently a high-throughput screening (HTS) based on a virus-induced cytopathic effect (CPE) assay successfully identified a potent small-molecule inhibitor of HF NW arenaviruses that acts by targeting the viral GP [59]. Likewise, cell-based HTS based on the use of pseudotyped virion particles bearing the GP of highly pathogenic arenaviruses identified several small-molecule inhibitors of virus cell entry mediated by LASV GP [60]. These findings illustrate how complex chemical libraries used in the context of appropriate screening assays can be harnessed into a powerful tool to identify candidate antiviral drugs with highly specific activities. To achieve this goal, recent progress in the molecular and cell biology of arenaviruses including the development of reverse genetics systems has opened new avenues for the identification of steps in the arenavirus life cycle that are amenable to drug targeting, and the development of appropriate screening strategies to identify such drugs.

1.3 Arenavirus Virion Structure and Genome Organization

Arenavirus are bi-segmented negative-sense, single-stranded, RNA viruses that belong to the *Arenaviridae* family [1]. Each arenaviral segment encodes, using an ambisense coding strategy, two viral proteins in opposite orientation separated by a noncoding intergenic region (IGR) between the two viral genes (Fig. 1a) [1]. The large (L) segment encodes the viral RdRp or L polymerase protein (Fig. 1a, blue) involved in viral replication and gene transcription [61], and, in opposite direction, the small really interesting new gene (RING) finger protein Z (Fig. 1a, orange) that is the counterpart of the matrix (M) protein present in other negative-stranded (NS) RNA viruses and the major driving force of arenavirus budding and assembly [62–64]. The small (S) segment encodes for the viral glycoprotein precursor (GP) (Fig. 1a, green) that is posttranslationally cleaved to form the two mature virion glycoproteins (GP1 and GP2) involved in receptor binding, cell entry, and fusion [65–67], and the viral nucleoprotein (NP) (Fig. 1a, red), which encapsidates the viral RNA and, together with the polymerase L and the viral RNA, constitutes the viral ribonucleoproteins (vRNPs) that are the minimal

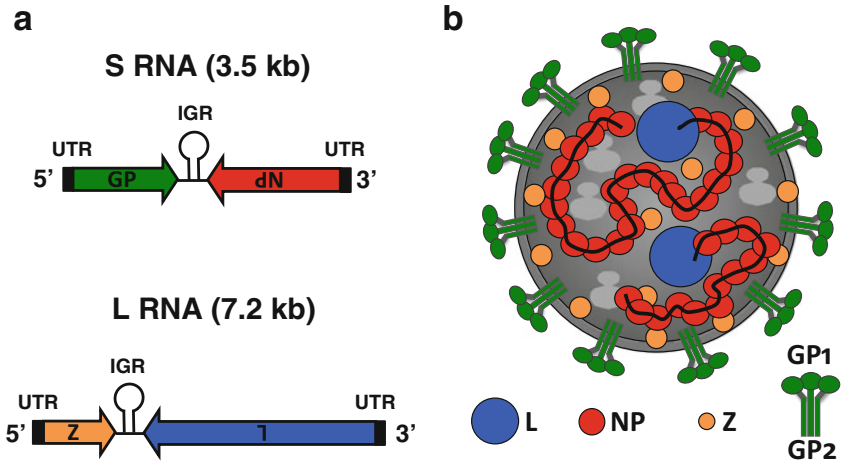

Fig. 1 Arenavirus genome organization and virion structure. (**a**) Genome organization: Arenaviruses are enveloped viruses with a single-stranded, bi-segmented RNA genome of negative polarity. Each of the two viral RNA genome segments uses an ambisense coding strategy to direct the synthesis of two viral polypeptides in opposite orientation. The small (S) RNA segment (3.5 kb, *top*) encodes the viral glycoprotein precursor (GP, *green*) and nucleoprotein (NP, *red*). The large (L) RNA segment (7.2 kb, *bottom*) encodes the RNA-dependent RNA polymerase (L, *blue*) and the small RING finger protein (Z, *orange*). (**b**) Virion structure: Arenaviruses are surrounded by a lipid bilayer containing the posttranslationally processed viral glycoprotein involved in receptor binding (GP1) and viral cell entry (GP2). Underneath the lipid bilayer is a protein layer composed of the Z protein (*orange*), which plays a major role in viral assembly and budding, and is the arenavirus counterpart of the matrix protein present in other enveloped NS RNA viruses. The core of the virus is made of a viral ribonucleoprotein (vRNP) complex, composed of the viral genome segments encapsidated by the viral NP (*red*). Incorporation of the vRNPs into newly nascent virions is mediated by NP-Z interaction. Associated with the vRNPs is the L polymerase protein (*blue*) that, together with NP, are the minimal components for viral genome replication and gene transcription. *Indicated* are also host cell ribosomes incorporated into the virus particle

factors involved in arenavirus genome replication and gene transcription [1, 68, 69]. In addition, arenavirus NP mediates the incorporation of the vRNPs into mature infectious virions by interacting with Z [70]. Furthermore, NP has also been shown to counteract the cellular host type-I interferon (IFN-I) [71–76] and inflammatory [75, 77] responses during viral infection.

1.4 Arenavirus Life Cycle

Arenavirus replication cycle takes place entirely in the cytoplasm of infected cells [1]. Homo-trimer complexes, consisting of the GP1 globular head and GP2 stalk region, form the spikes that decorate the surface of the arenavirus envelope [1, 78] (Fig. 1b). GP1, located at the top of the spike, mediates attachment of the virus particle to receptors located in the surface of the cell [79]. Alpha-dystroglycan (αDG) has been described as the main receptor for OW and NW clade C arenaviruses [80–82]. However, clade A, B, and A/B NW arenaviruses appear to use the human transferrin receptor I as the cellular receptor for viral entry [83]. Upon viral attachment, arenavirus virions enter the cell via receptor-mediated

endocytosis [79, 84]. Fusion of the virion and the endosome membranes is triggered by acidification of the endosome, which induces a conformational change in the viral GP1/GP2 complex [84]. Fusion of the viral and cellular membranes releases the vRNPs into the cytoplasm of infected cells, where viral RNA replication and gene transcription occur [1].

Arenavirus gene transcription is mediated by the viral promoters located within the untranslated regions (UTRs) at the 3′ termini of viral (v)RNA and complementary (c)RNA species [1] (Fig. 2). NP and L proteins, located at the 3′ end of the S and L viral segments, respectively, are translated from mRNAs with antigenomic sense polarity transcribed directly from the vRNAs and, therefore, are the first arenaviral proteins encoded upon infection [1] (Fig. 2). Transcription termination is mediated by a secondary stem-loop structure formed by the IGR found in both vRNA segments, between each of the two viral genes [1], that function as a bona fide transcription termination signal for the virus polymerase complex (Fig. 2). GP and Z proteins, on the other hand, are located, respectively, at the 5′ end of the S and L viral segments

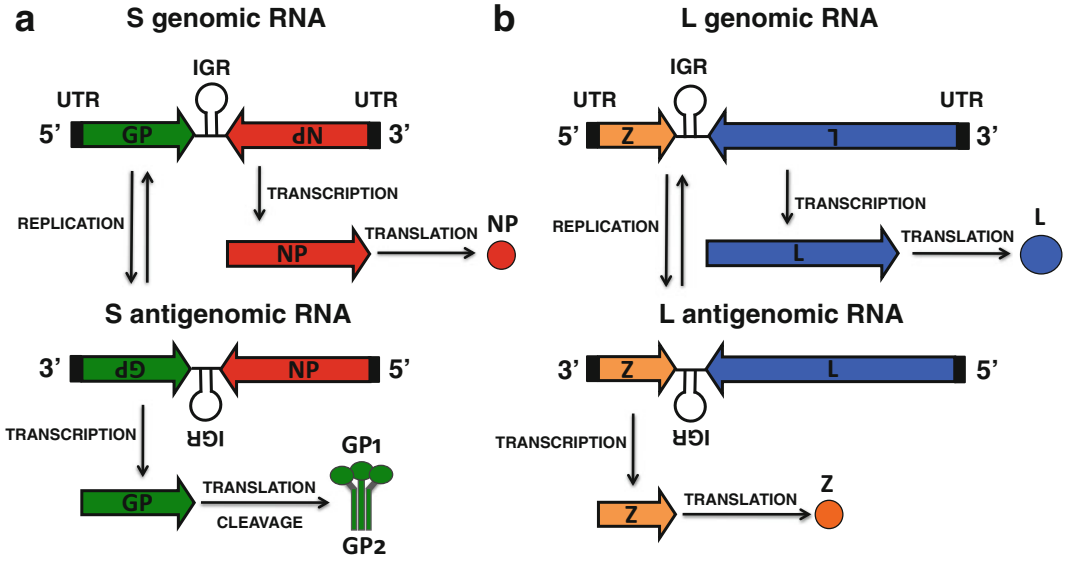

Fig. 2 Arenavirus genome replication and gene transcription: Arenavirus replication cycle takes place entirely in the cytoplasm of infected cells. The L polymerase associated with the vRNPs initiates transcription from the viral promoter located within the untranslated region (UTR, *black boxes*) at the 3′ termini of the vRNAs. Primary transcription results in the synthesis of NP (**a**) and L (**b**) mRNAs from the S and L segments, respectively, Transcription termination is mediated by a secondary stem-loop structure formed by the intergenic region (IGR) found in both vRNA segments between each of the two viral genes. Subsequently, the virus polymerase L adopts a replicase mode and moves across the IGR to generate a copy of the full-length antigenome S and L vRNAs. The antigenomic RNA S and L segments serve as templates for the synthesis of GP (**a**, S segment) and Z (**b**, L segment) mRNAs. The antigenomic RNA S and L segments also serve as templates for the amplification of the corresponding viral RNA genome species. For more details *see* text

and are not translated directly from mRNA derived from the vRNAs but from antigenome complementary RNA species after replication of the vRNAs [1] (Fig. 2). Complementary RNA segments also serve as templates for the synthesis of nascent vRNAs [1]. Newly synthesized vRNAs are encapsidated by the viral NP to form the vRNP complexes and are packaged into progeny infectious virions by interaction of the viral Z [70]. Arenavirus assembly involves the interaction of the new vRNP complexes with the GP1/GP2 complexes present in the membrane of infected cells, a process mediated by interaction with the Z protein [85]. Newly synthesized and assembled virions bud from infected cells, a process mediated by the Z protein, and are released from infected cells to infect new cells [62, 63, 86, 87].

1.5 Reverse Genetics Approaches for the Investigation of the Molecular and Cellular Biology of Arenavirus

The introduction of reverse genetic approaches to rescue infectious recombinant arenaviruses from plasmid DNA had significantly advanced the arenavirus field and had led to many important discoveries surrounding arenavirus biology [1, 61]. Reverse genetics systems had facilitated the investigation of the *cis*-acting and the *trans*-acting factors that control the replication cycle of arenaviruses, including viral cell entry, genome viral replication, and gene transcription, assembly, and budding [88–91]. Reverse techniques have also allowed the generation of recombinant arenaviruses with mutations in their genomes to examine their contribution in viral replication using cell cultures as well as in viral pathogenesis and associated disease using validated animal models of infection [72, 92–95]. Likewise, implementation of arenavirus reverse genetics has allowed researchers to study arenavirus-host interactions [90, 96, 97], and potentiated the generation of novel candidate live-attenuated arenavirus vaccines [91, 96–100] as well as the development of screening methods to identify and evaluate novel anti-arenavirus drugs targeting specific steps of the virus life cycle [96, 99]. Reverse genetics of arenaviruses have also been used for the generation of recombinant tri-segmented (r3) arenavirus expressing additional genes of interest (GOI) [91, 96, 97, 100, 101] to facilitate the study of several members in the family, including the identification of antivirals inhibiting the replication cycle of arenaviruses [56] as well as their possible implementation as vaccine vector candidates [91, 96, 97, 101]. Finally, arenavirus reverse genetics have been used for the generation of a single-cycle infectious, reporter-expressing, recombinant arenaviruses that are limited to replicate in GP-expressing complementing cell lines [99, 102], allowing the study of some aspects of the biology of highly pathogenic arenaviruses (e.g., neutralizing antiviral responses and identification of inhibitors of GP-mediated cell entry) without the use of special biosafety conditions [99]. In this chapter we focus on arenavirus reverse genetics techniques, based on human cells, for the prototype member in the family, LCMV [70, 91, 96, 97, 103].

Generation of recombinant LCM viruses can be performed under biosafety level (BSL)-2 conditions. Rescue of other arenaviruses may require higher BSL facilities and appropriate safety and security measures may be adopted [104].

2 Materials

2.1 Plasmids for the Generation of Recombinant Arenaviruses

The plasmids used for the generation of recombinant arenaviruses can be transformed and amplified in DH5α competent cells and grown in LB media at 37 °C for 16–18 h, with the exception of the pPol-I L plasmid (*see* **Note 1**). Plasmids can be prepared using commercially available maxiprep kits following the manufacturer's recommendations. Plasmids can be stored at −20 °C until use (*see* **Notes 2** and **3**).

2.1.1 pCAGGS Protein Expression Plasmids

The pCAGGS protein expression plasmid uses the chicken β-actin promoter and the rabbit β-globin polyadenylation (pA) signal sequence [105] to direct the synthesis of arenavirus NP and L polymerase, which are the minimal components for viral gene transcription and genome replication [56, 61, 69, 70, 91, 92, 96–98] (Fig. 3a).

The pCAGGS plasmid expressing LCMV GP is required to initiate the first round of virus production for the rescue of single-cycle LCMV [99, 102].

A pCAGGS plasmid expressing the secreted luciferase from the ostracod *Cypridina noctiluca* (Cluc) is used in the minigenome (MG) experiments (Fig. 4) to normalize transfection efficiencies [56, 91, 96, 98] (*see* **Notes 4** and **5**).

2.1.2 pPol-I vRNA Expression Plasmids

Arenavirus reverse genetic approaches were originally developed with the use of the mouse RNA polymerase I (Pol-I) promoter to direct intracellular synthesis of S and L genome, or antigenome, RNA species [106]. However, unlike the Pol-II promoter, the transcriptional activity of the Pol-I promoter exhibits stringent species specificity [96, 107] (*see* **Note 6**).

To evaluate viral genome replication and gene transcription, a vRNA-like MG plasmid is used (pPol-I MG) (Fig. 4) [56, 69, 70, 91, 92, 96–98]. In this plasmid, the viral GP and NP open reading frames (ORFs) are replaced by reporter genes. In our case, we replaced GP for Gluc and NP for the green fluorescent protein (GFP) (Fig. 4) (*see* **Notes 7** and **8**).

For the generation of recombinant wild-type (WT) bi-segmented arenaviruses (Fig. 5), two pPol-I plasmids expressing the S (pPol-I S) and L (pPol-I L) viral genomic or antigenomic RNAs are used (Fig. 3b) [56, 69, 70, 91, 92, 96–98].

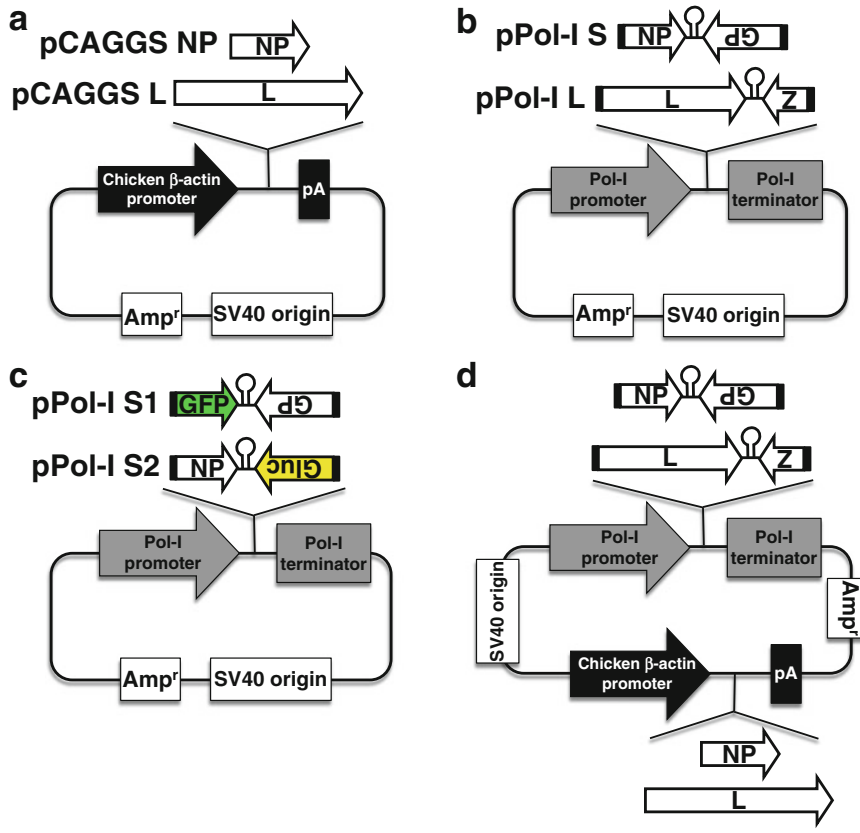

Fig. 3 Arenavirus reverse genetics plasmids: Schematic representation of the plasmids used for the arenavirus minigenome (MG) assays, and for the generation of recombinant WT and r3 arenaviruses. (**a**) Schematic representation of the mammalian protein pCAGGS expression plasmid: Protein expression pCAGGS plasmids use the chicken β-actin promoter (*black arrow*) and the rabbit β-globin polyadenylation (pA) signal (*black box*) sequences to direct the synthesis of the viral NP (*top*) and L (*bottom*) arenavirus proteins. These plasmids are required to provide the arenavirus minimal proteins required to initiate viral gene transcription and genome replication. (**b**) Schematic representation of the polymerase I-driven vRNA expression plasmid: vRNA expression plasmid under the control of the polymerase I (Pol-I) promoter (*gray arrow*) and terminator (*gray box*) sequences directs the synthesis of the arenavirus vRNA S (*top*) and L (*bottom*) segments. For generation of recombinant arenavirus from murine or human cells, these plasmids contain the murine or human Pol-I promoters, respectively. (**c**) Schematic representation of the r3 polymerase I expression plasmids encoding the split S segment: For generation of r3 arenaviruses, the pPol-I plasmid expressing the S vRNA segment is separated into two plasmids. In the pPol-I S1 plasmid, the viral NP is replaced by GFP (*top*) and in the pPol-I S2 plasmid, the viral GP is replaced by Gluc (*bottom*). Alternatively, GFP can be expressed instead of the viral GP in the pPol-I S2 plasmid and Gluc from the pPol-I S1 plasmid. *Gray arrow* and *boxes* indicate the positions the Pol-I promoter and terminator sequences, respectively. (**d**) Schematic representation of the plasmids used for the two-plasmid arenavirus rescue system: Plasmids encoding either NP under the chicken β-actin promoter (*black arrow*) and the rabbit β-globin polyadenylation (pA) signal (*black box*) sequences, and the vRNA L segment under the Pol-I promoter (*gray arrow*) and terminator (*gray box*) sequences (pC-NP/pPol-I L), or the plasmid encoding the L protein and the vRNA S segment (pC-L/pPol-I S) are indicated. All plasmids are ampicillin resistant (Amp^r) and contain the simian virus 40 (SV40) origin of replication. Untranslated regions (UTR, *black boxes*) and intergenic regions (IGR) in each of the vRNA segments are indicated

To generate r3 arenavirus (Fig. 6), the pPol-I plasmid expressing the S vRNA segment is separated into two (S1 and S2) plasmids (Fig. 3c) [91, 96, 97, 100]. In the pPol-I S1 plasmid, the viral NP is replaced by GFP (or an alternative reporter or foreign GOI) and in the pPol-I S2 plasmid, the viral GP is replaced by Gluc (or an alternative reporter or foreign gene) (Fig. 3c) [91, 96, 97] (*see* **Note 9**).

For the generation of a single-cycle infectious arenavirus (Fig. 7), the viral GP is substituted with GFP (or an alternative reporter or foreign GOI) within the pPol-I S vRNA (pPol-I S ΔGP/GFP) (Fig. 7a) [99, 102].

To generate recombinant arenaviruses use the two-plasmid-based approach (Fig. 8) [96], plasmids containing both the RNA Pol-II and -I promoters, to allow for Pol-II-mediated expression of the minimal viral *trans*-acting factors NP and L required for viral genome replication and gene transcription, and Pol-I to mediate initial intracellular synthesis of the S and L vRNA genomic or antigenomic segments (Fig. 3d) [96] (*see* **Note 10**).

2.2 Cell Lines for the Generation of Recombinant Arenaviruses

As discussed above, the gold standard to assess virus replication and transcription using the MG approach or to rescue recombinant arenaviruses relies on the mouse Pol-I promoter and rodent BHK-21 cells, as these cell lines are easy to maintain, have high transfection efficiencies, and are able to produce high viral titers [91, 96, 97, 100]. However, BHK-21 cells do not meet guidelines set forth by the FDA for human vaccine generation due to the presence of tumorigenic agents that may affect the purity of the vaccine seed [96]. Vero cells, on the other hand, have received approval from the FDA for the generation of vaccine seeds [96, 97, 108]. While Vero cells are easy to maintain and produce high viral titers, the transfection efficiencies in Vero cells are generally lower and thus may lead to difficulties in rescuing recombinant arenaviruses [96]. Alternatively, human 293 T cells can be used to evaluate MG activities or to generate recombinant arenaviruses [96] (*see* **Note 11**). All cells are grown at 37 °C in a 5 % CO_2 atmosphere.

Vero cells: African green monkey kidney epithelial cells available from the American Type Culture Collection (ATCC).

Human 293 T cells: Human embryonic kidney cells available from the ATCC.

BHK-21 cells: Baby hamster kidney cells available from the ATCC.

GP-expressing BHK-21 or Vero cells: To generate GP-deficient, reporter-expressing, recombinant LCMV (rLCMVΔGP/GFP), BHK-21 or Vero cell lines constitutively expressing LCMV GP are generated by co-transfection of the LCMV GP-expressing pCAGGS protein expression plasmid, together with a hygromycin (or other drug) resistance pCB7 plasmid, using Lipofectamine 2000 (LPF2000) [99, 102]. After transfection, cells are plated

into 10 cm dishes at low density and incubated in the presence of normal media supplemented with hygromycin B (250–500 μg/ml) [92, 99, 109, 110]. Individual cell clones are isolated using cloning rings or any other selection method (e.g., fluorescence-activated cell sorting, FACS) and evaluated for LCMV GP expression using immunofluorescence, flow cytometry, or western blot approaches with appropriate antibodies [92, 99, 109, 110] (*see* **Note 12**). Uniformly (~85–95 %) LCMV GP-expressing cell clones are then evaluated for complementation of the rLCMVΔGP/GFP, using parental cells as negative controls [99, 102]. Transiently transfected GP-expressing cells should be used as internal positive controls. Constitutively LCMV GP-expressing, rLCMVΔGP/GFP-complementing, cell clones should be maintained in normal media supplemented with hygromycin B [99, 102] (*see* **Note 13**).

2.3 Tissue Culture Media and Reagents

DMEM 10 % FBS, 1 % PS: This media is used for maintenance of BHK-21, 293 T, and Vero cells [97]. To prepare this media, mix 445 ml Dulbecco's modified Eagle's medium (DMEM), 50 ml of fetal bovine serum (FBS), and 5 ml of 100× penicillin/streptomycin (PS) [56, 69, 70, 91, 92, 96–98]. DMEM 10 % FBS 1 % PS supplemented with 250–500 mg/ml of hygromycin B is used for maintenance of GP-expressing stable cell lines [92, 99, 109, 110]. Store at 4 °C.

OptiMEM: OptiMEM media is used in the transfection protocol for MG assays and for the rescue of recombinant arenaviruses [56, 69, 70, 91, 92, 96–98].

Infectious media: This media is used during and after viral infections [97]. To prepare this media, mix (2:1) OptiMEM and DMEM 10 % FBS 1 % PS. Store at 4 °C [56, 69, 70, 91, 92, 96–98].

10× Phosphate-buffered saline (PBS): 80 g of NaCl, 2 g of KCl, 11.5 g of $Na_2HPO_4{\cdot}7H_2O$, 2 g of KH_2PO_4. Add ddH_2O up to 1 L. Adjust pH to 7.3. Sterilize by autoclaving. Store at room temperature (RT). Working concentration should be prepared by diluting 10× PBS 1:10 with ddH_2O (1× PBS). Autoclave to sterilize and store at RT [56, 69, 70, 91, 92, 96–98].

2.5 % Bovine serum albumin (BSA): This is used as a blocking solution for immunofluorescence assays: 2.5 g of BSA in 97.5 ml of 1× PBS. Store at 4 °C [56, 69, 70, 91, 92, 96–98].

Lipofectamine 2000 (LPF2000): LPF2000 is used for plasmid DNA transfection in BHK-21, 293 T, or Vero cells. We recommend an LPF2000:DNA ratio of 2.5:1 for both MG and arenavirus rescue approaches (*see* Tables 1, 2, 3, and 4) [56, 69, 70, 91, 92, 96–98].

Trypsin-EDTA: Trypsin-EDTA is used to detach cell monolayer from the tissue culture plate, prior to DNA transfection or for the passaging of transfected cells [56, 69, 70, 91, 92, 96–98].

Biolux Gaussia Luciferase Assay kit: To measure Gluc activities from TCS in the MG assays or from r3 arenavirus-infected cells, we use the Biolux Gaussia Luciferase Assay kit [56, 69, 70, 91, 92, 96–98].

Biolux Cypridinia Luciferase Assay kit: To assess Cluc activities from TCS in the MG assay or from cells infected with r3 arenaviruses expressing Cluc, we used the Biolux *Cypridinia* Luciferase Assay kit [56, 69, 70, 91, 92, 96–98].

3 Methods

3.1 Arenavirus Minigenome (MG) Assays to Evaluate Viral Genome Replication and Gene Transcription

Arenavirus MG approaches have been developed to investigate the *trans*-acting factors and *cis*-acting sequences that control arenavirus genome replication and gene transcription [56, 61, 69, 70, 91, 92, 96–98]. Arenavirus MG systems have also allowed the identification of arenavirus L and NP as the minimal *trans*-acting factors required for arenavirus genome replication and gene transcription [61]. Likewise, MG approaches can be used to evaluate amino acid residues in NP and L critical for viral genome replication and gene transcription [69, 70, 92, 96–98]. Moreover, MG approaches have been used for the identification of the genomic promoter recognized by the virus polymerase to initiate viral replication and gene transcription [111]. Implementation of MG approaches has also allowed the identification of arenavirus IGR as a bona fide transcription termination signal [112]. Furthermore, results from MG assays demonstrated that arenavirus Z has a dose-dependent inhibitory effect on both viral replication and gene transcription [113]. In addition, MG approaches were used to confirm the importance of both GP and Z for arenaviral genome packaging [68].

Other than understanding arenavirus biology, MG assay approaches have been instrumental in demonstrating the specificity and efficacy of siRNAs targeting viral mRNAs encoding NP and/or L [114]. In accordance, MG assays have also been used for the identification of anti-arenavirals targeting viral replication and transcription, as evidenced with the ribonucleoside analog Rib [58] and the pyrimidine biosynthesis inhibitor A3 [56]. A major advantage in using MG assays to identify effective therapeutics is that such approaches can be performed without the need of BSL-4 containment, an issue that bottlenecks most researchers from screening effective anti-arenavirals and specific siRNAs to target the human pathogenic arenaviruses of highest public health concern [104]. MG reverse genetics approaches have been developed, to date, for the OW LCMV [61, 91, 96–98], LASV [45, 46], and Lujo, LUJV [115] arenaviruses; and for the NW Tacaribe, TCRV [116], Junin, JUNV [43, 44, 96, 98], Pichinde, PICV [117], and Machupo, MACV [118] arenaviruses.

For arenavirus MG assays, susceptible cells are co-transfected with a Pol-I-driven plasmid regulating expression of a reporter-expressing vRNA-like segment (e.g., Gluc and GFP) together with the Pol-II-driven pCAGGS protein expression plasmids encoding the minimal *trans*-acting elements for replication and transcription (NP and L) [61], and a Pol-II-dependent Cluc to normalize transfection efficiencies (Fig. 4) [91, 96–98] (*see* **Note 14**). The pPol-I plasmid encodes the reporter genes in the place of the viral ORFs; thereby replication and transcription can be easily measured by reporter gene activity [91, 96–98]. To easily evaluate MG activities under a fluorescence microscope, we used a fluorescent protein (e.g., GFP). To quantify MG activities using luminometer, we used secreted forms of luciferase proteins (e.g., Gluc) [91, 96–98]. Since NP expression levels during viral infection are higher than those of GP, it is important to determine what reporter gene should substitute the viral ORFs [91]. In our case NP is substituted by GFP and GP is substituted by Gluc (Fig. 4) [97]. The other RNA sequences required for viral genome replication and gene transcription (e.g., UTRs and IGRs) are identical to those found in the viral S segment (Fig. 4). Efficient recognition of the viral-like reporter RNA by the viral NP and L requires precise vRNA 3′ and 5′ ends [44, 46, 106, 115, 119, 120]. Efficient vRNA 5′ ends are obtained with the use of the Pol-I promoter [44, 106]. To obtain authentic vRNA 3′ ends, both the self-cleaving hepatitis delta virus ribozyme (HDVR) and the Pol-I terminator (T) sequences can be used [96, 119, 120] (*see* **Note 15**).

3.1.1 Arenavirus MG Experimental Approach (Fig. 4)

1. *OptiMEM-Lipofectamine 2000 (LPF2000)*: The MG assay can be performed in either 12- or 6-well plate, although the amount of DNA and the number of cells transfected should be adjusted accordingly (Table 1). Prepare 250 μl of OptiMEM media with 3.75 or 7.5 μg of LPF2000 (2.5 μg LPF2000/μg plasmid DNA) per transfection in 12- or 6-well plates, respectively (Table 1) (*see* **Notes 16** and **17**). Incubate the OptiMEM-LPF2000 mixture for 5–10 min at RT. During this incubation time, prepare the OptiMEM-DNA plasmid mixture.
2. *OptiMEM-DNA plasmid*: In a separate tube, prepare the DNA plasmid mixture using the recommended amounts provided in Table 1 in a total volume of 50 μl of OptiMEM media.
3. *Combine OptiMEM-LPF2000 and OptiMEM-DNA plasmid*: Pipette 250 μl of OptiMEM-LPF2000 (**step 1**) into the OptiMEM-DNA (**step 2**) and incubate this mixture for 20–30 min at RT. During this incubation period, prepare the cells for transient transfection in suspension.
4. *Preparation of cells*: MG assays can be conducted in either human 293 T or rodent BHK-21 cells, depending on whether the MG reporter plasmid is regulated by the human or murine

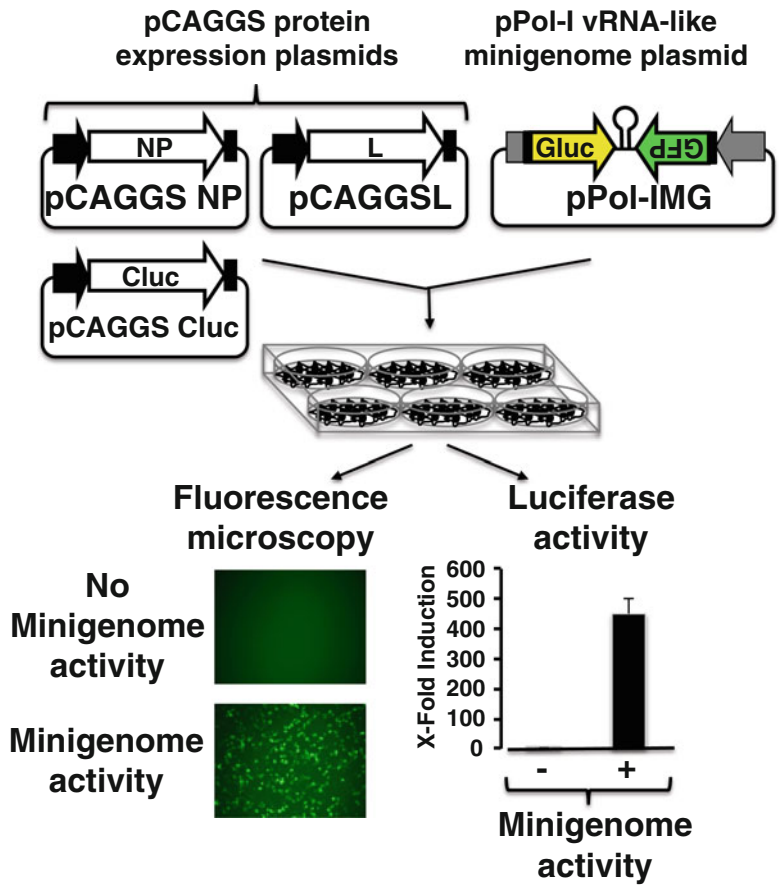

Fig. 4 Arenavirus minigenome (MG) assays: To evaluate arenavirus genome replication and gene transcription using an MG, susceptible cells (6- or 12-well plate, triplicates) are transiently co-transfected, using LPF2000, with the pCAGGS protein expression plasmids driving the expression of the viral polymerases L and NP, and the pPol-I vRNA expression plasmid S where reporter genes substitute for the viral NP (GFP) and GP (Gluc), together with a pCAGGS plasmid expressing Cluc to normalize transfection efficiencies. Recommended amounts of plasmids, LPF2000, and cells for MG assays using 12- or 6-well plates are indicated in Table 1. Reporter gene expression is then evaluated by fluorescence microscopy (GFP) using a fluorescent microscope (*bottom left*) and by Gluc activity using a luminometer (*bottom right*). Reporter gene activation (Gluc) is expressed as fold induction over cells transfected with an empty pCAGGS plasmid instead of the viral NP (negative control, –). The chicken β-actin promoter (*black arrow*) and the rabbit β-globin polyadenylation (pA) signal are indicated in the pCAGGS protein expression plasmids. Viral untranslated regions (UTR, *black boxes*) and intergenic region (IGR) in the pPol-I vRNA-like MG plasmid are indicated. The Pol-I promoter and terminator sequences in the pPol-I vRNA-like MG plasmid are indicated by a *gray arrow* and a *gray box*, respectively. For more details *see* text

pPol-I promoters, respectively [96] (*see* **Note 18**). Prior to manipulating the cells, bring the 1× PBS, DMEM 10 % FBS, 1 % PS media, and trypsin-EDTA mixture to 37 °C for ~10 min.

(a) Wash the cells, twice, with 5 ml 1× PBS.

(b) Trypsinize cells using 1 ml trypsin-EDTA. Cell detachment is usually accomplished by incubating the cells in a

Table 1
Plasmid DNA and LPF2000 concentrations for arenavirus minigenome (MG) assays: recommended amounts of pCAGGS and pPol-I plasmids and LPF2000 required to assess viral gene replication and genome transcription using an arenavirus MG assay in 12-well (*left*, 5.0–6.0 × 10^5 cells/well) or 6-well (*right*, 1.0–1.2 × 10^6 cells/well) plates are indicated

Plasmid	12-Well plates (μg)	6-Well plates (μg)
pCAGGS NP	0.3	0.6
pCAGGS L	0.6	1.2
pPol-I S MG	0.5	1.0
pCAGGS Cluc	0.1	0.2
Total DNA	1.5	3.0
LPF2000	3.75	7.5
Cells	~5.0–6.0 × 10^5/well	~1.0–1.2 × 10^6/well

humidified 37 °C, 5 % CO_2, chamber, for ~5 min. Gently tapping the tissue culture plate will expedite this process.

(c) Carefully resuspend the cells in 9 ml of DMEM 10 % FBS, 1 % PS, once the cells have been fully detached. Place the cells in a 15 ml tube and centrifuge for 5 min at 1000 × *g*.

(d) Remove the media and resuspend the cell pellet in 10 ml of fresh DMEM 10 % FBS, 1 % PS, and count the cells using a hemocytometer. Adjust the cell concentration to 10^6 cells/ml. Successful MG assay is typically achieved by transfecting ~5–6 × 10^5 (12-well plates) or ~1–2 × 10^6 (6-well plates) cells per transfection (Table 1).

5. *Mix LPF2000/DNA with cells*: After 20–30-min LPF2000/DNA incubation, pipette into each LPF2000/DNA tube (**step 3**) the appropriate concentration of cells (**step 4**). Let the LPF2000/DNA/cell mixture incubate for ~5 min at RT.
6. *LPF2000/DNA/cell plating*: Transfer the LPF2000/DNA/cell mixture into individual 12- or 6-well tissue culture plate. Gently tap the plate to distribute the cells uniformly and incubate the cells in a 5 % CO_2 humidified 37 °C incubator for ~6–12 h, after which the TCS is removed and replaced with 1 ml of fresh DMEM 10 % FBS, 1 % PS.
7. *Measure MG reporter gene activity*: After incubating the cells for a total of ~48 h, measure the MG reporter gene activity. Depending on the genes encoded by the MG plasmid, the assay can be determined qualitatively by fluorescence microscopy (e.g., GFP expression) or quantitatively using a luminometer (e.g., Gluc) (*see* **Note 19**).

3.2 Generation of Recombinant Arenaviruses

The ability to generate recombinant arenaviruses with specific mutations and study their phenotype in vitro and in vivo in their natural hosts has allowed researches to evaluate the contribution of viral determinants to the virus life cycle [89], virus-host interactions [90], mechanisms of pathogenesis [121], role of NP in the inhibition of the IFN-I response [72, 94], and potential development of live-attenuated arenavirus vaccines [69, 70, 92, 96–98]. Moreover, these reverse genetics techniques have allowed the generation of r3 arenaviruses expressing foreign GOI, opening the possibility of implementing live-attenuated arenavirus as vaccine vectors [91, 96, 97, 101]. Moreover, the recent development of single-cycle infectious, reporter-expressing, arenaviruses has provided a new experimental method to study some aspects of the biology of highly pathogenic members in the arenavirus family without the requirement of special biosafety conditions [104], currently required to study HF-causing members in the family [99].

Originally established for the prototyped member in the family, LCMV [106, 122], plasmid-based arenavirus reverse genetics techniques have expanded, to date, for the generation of OW LASV [45, 46] and LUJV [115] arenaviruses, and for the NW JUNV [43, 44], PICV [117], and MACV [118] arenaviruses. Initially, arenavirus reverse genetics approaches were developed based on the use of the bacteriophage T7 promoter [122]. However, current approaches for the generation of recombinant arenaviruses rely on the use of RNA Pol-I promoters to launch the intracellular synthesis of the S and L RNA genome or antigenome species, which are subsequently replicated and transcribed by the virus L and NP, the minimal viral *trans*-acting factors required for viral genome replication and gene transcription, encoded by RNA Pol-II-dependent promoter protein plasmids [106]. Although these techniques were established with the use of murine Pol-I promoters [106], the transcriptional activity of the RNA Pol-I exhibits species specificity preventing the development of vaccine candidates that can be administered to humans [96, 107]. This barrier was recently solved by the implementation of human Pol-I promoters to drive vRNA expression, which allowed for the generation of recombinant OW (LCMV) and NW (Candid#1) arenaviruses from human 293 T and FDA-approved Vero cell lines [96, 97].

Originally established with the co-transfection of the two pCAGGS protein expression plasmid driven by the expression of the viral RdRp L and NP, together with the Pol-I-driven plasmids expressing the viral S and L segments, the ability to successfully generate recombinant arenaviruses has been reduced to two plasmids by combining within the same plasmid Pol-I-driven vRNA with Pol-II-driven protein constructs (Fig. 6) [96] (*see* **Note 20**).

3.2.1 Arenavirus Four-Plasmid Rescue System Experimental Approach (Fig. 5)

1. *OptiMEM-LPF2000*: Prepare 250 µl of OptiMEM media with 10 µg of LPF2000 (2.5 µg LPF2000/µg plasmid DNA) per transfection (Table 2a). Virus rescues are performed in 6-well plates (*see* **Note 21**). Incubate the OptiMEM-LPF2000 mixture for 5–10 min at RT. During this incubation time, prepare the OptiMEM-DNA plasmid mixture.

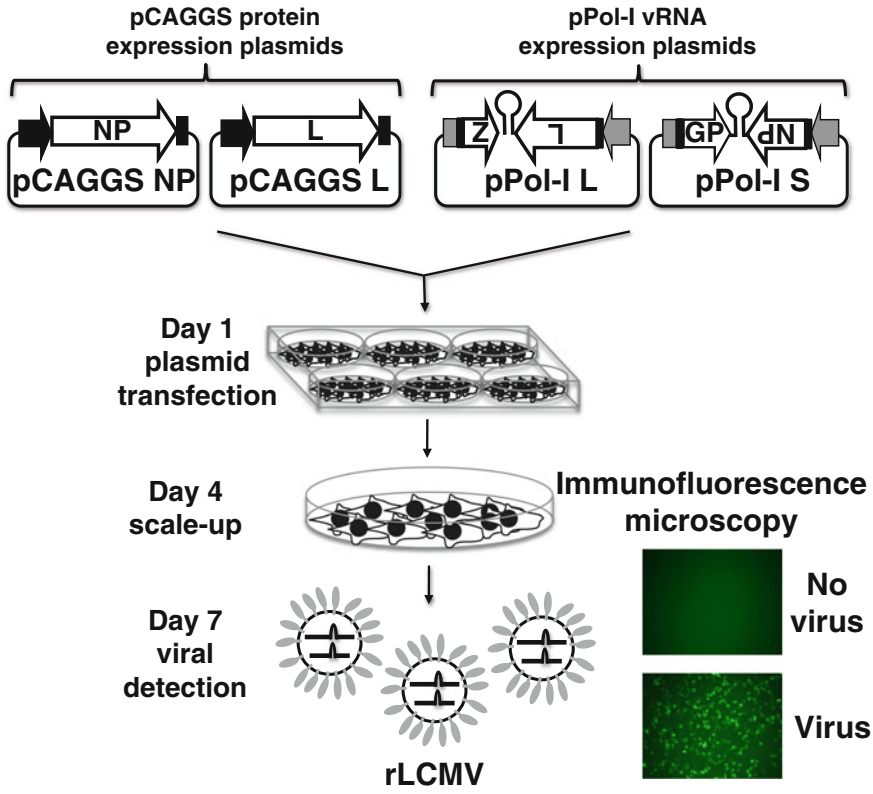

Fig. 5 Generation of recombinant wild-type (WT) arenaviruses: Arenavirus rescues are performed in rodent BHK-21 (using the mouse Pol-I promoter) or in human (using the human Pol-I promoter) cells in 6-well plate format (triplicates). Cells are transiently co-transfected, using LPF2000, with the pCAGGS protein expression plasmids encoding the viral NP and polymerase L (required to initiate viral gene transcription and genome replication) together with the pPol-I vRNA expression plasmids for the viral S and L segments (required to provide the arenavirus vRNAs to initiate viral gene transcription and genome replication). Recommended amounts of plasmids, LPF2000, and cells for LCMV WT virus rescues are indicated in Table 2a. At 72 h post-transfection, cells are trypsinized and scaled up into 10 cm dishes. After an additional 72-h incubation period, TCS are collected and presence of virus is determined by plaque assay or immunofluorescence using arenavirus-specific antibodies. The chicken β-actin promoter (*black arrow*) and the rabbit β-globin polyadenylation (pA) signal are indicated in the pCAGGS protein expression plasmids. Viral untranslated regions (UTR, *black boxes*) and intergenic region (IGR) in the pPol-I vRNA expression plasmid are indicated. The Pol-I promoter and terminator sequences in the pPol-I plasmids are indicated by *gray arrows* and *boxes*, respectively. For more details *see* text

Table 2
LPF2000/plasmid DNA concentrations for arenavirus rescues: recommended amounts of pCAGGS and pPol-I plasmids and LPF2000 to generate recombinant WT arenaviruses using the 4 (A) and the 2 (B) plasmid approaches in 6-well (1.0–1.2 × 10^6 cells/well) plates are indicated

Plasmid	6-Well plates (μg)
(A)	
pCAGGS NP	0.8
pCAGGS L	1.0
pPol-I S	0.8
pPol-I L	1.4
Total DNA	4.0
LPF2000	10
Cells	~1.0–1.2 × 10^6/well
(B)	
pCAGGS NP/pPol-I L	2.0
pCAGGS L/pPol-I S	1.0
Total DNA	3.0
LPF2000	7.5
Cells	~1.0–1.2 × 10^6/well

2. *OptiMEM-DNA plasmid*: In a separate tube, prepare the DNA plasmid mix using the recommended amounts provided in Table 2a in a total volume of 50 μl of OptiMEM media.
3. *Combined OptiMEM-LPF2000 and OptiMEM-DNA plasmid*: Pipette 250 μl of OptiMEM-LPF2000 (**step 1**) into the OptiMEM-DNA (**step 2**) and incubate this mixture for 20–30 min at RT. During this incubation period, prepare the cells for transient transfection in suspension.
4. *Preparation of cells*: Arenavirus rescues can be performed in either rodent (BHK-21), human (293T), or African green monkey kidney (Vero) cells, depending on the source of the Pol-I promoter in the vRNA expression plasmids. Before manipulating the cells, bring the 1× PBS, DMEM 10 % FBS, 1 % PS media, and trypsin-EDTA mixture to 37 °C for ~10 min.
   (a) Wash the cells, twice, with 5 ml 1× PBS.
   (b) Trypsinize cells using 1 ml trypsin-EDTA. Cell detachment is usually accomplished by incubating the cells in a humidified 37 °C, 5 % CO_2, chamber, for ~5 min. Gently tapping the tissue culture plate will uniformly detach the cells.
   (c) After cells are completely detached from the plate, carefully resuspend the cells with 9 ml of DMEM 10 % FBS, 1 % PS. Place the total media/cell mixture in a 15 ml centrifuge tube and centrifuge the cells for 5 min at 1000 × *g*.

(d) Remove the media and resuspend the cells in 10 ml of fresh DMEM 10 % FBS, 1 % PS, and count the cells using a hemocytometer. Adjust the cell concentration to ~1.0–1.2×10^6 cells/ml (Table 2a).

5. *Mix LPF2000/DNA with cells*: After 20–30-min incubation, pipette into each LPF2000/DNA mixture tube (**step 3**) ~1.0–1.2×10^6 cells/well (**step 4**). Let the LPF2000/DNA and cell mixture incubate for ~5 min at RT.
6. *LPF2000/DNA/cell plating*: Transfer the LPF2000/DNA/cell mixture into individual wells of a 6-well tissue culture plate. Gently tap the plate to distribute the cells uniformly and incubate the cells in a 5 % CO_2 humidified 37 °C incubator for ~6–12 h.
7. *Transfection media change*: After ~6–12-h incubation, replace the TCS from the transfection with 2 ml of infectious media and return the cells to the incubator and incubate for 48 h.
8. *Cell passage*: After 2-day incubation, transfected cells should reach ~100 % confluence.
   (a) Remove TCS and gently wash the cells, twice, with 1× PBS.
   (b) Trypsinize cells by adding 500 μl of trypsin-EDTA/well. Return the cells to the incubator and let them incubate for ~5 min. Gently tap the cells to completely detach them from the plate.
   (c) Carefully resuspend the cells with 1 ml of DMEM 10 % FBS, 1 % PS, and transfer to a 1.5 ml microcentrifuge tube.
   (d) Centrifuge the cells for 5 min at 5000×*g*, 4 °C, in a microcentrifuge.
   (e) Remove the TCS and resuspend the cells in 1 ml of infectious media and transfer to a 10 cm tissue culture dish. Bring up the volume in the plate to 10 ml with infectious media. Gently shake the 10 cm tissue culture dish to allow uniform distribution of the cells and incubate the cells at 37 °C, 5 % CO_2, for 72 h.
9. *Virus recovery from TCS*: After 3 days of incubation, collect the TCS from the 10 cm tissue culture plates (**step 8**) into a 15 ml centrifuge tube and centrifuge at 2500×*g*, 4 °C, for 5 min. Collect the TCS containing the virus and discard the cell pellet.
10. *Storage of virus*: Aliquot the virus in cryotubes and store them at −80 °C (*see* **Note 22**). Virus can be stored at −80 °C until confirmation of the presence of virus.

3.2.2 Two-Plasmid Arenavirus Rescue System Experimental Approach (Fig. 6)

To generate recombinant arenavirus using the two-plasmid approach (Figs. 4d and 6), follow steps described above but using the proper DNA plasmid concentrations indicated in Table 2b [96, 97].

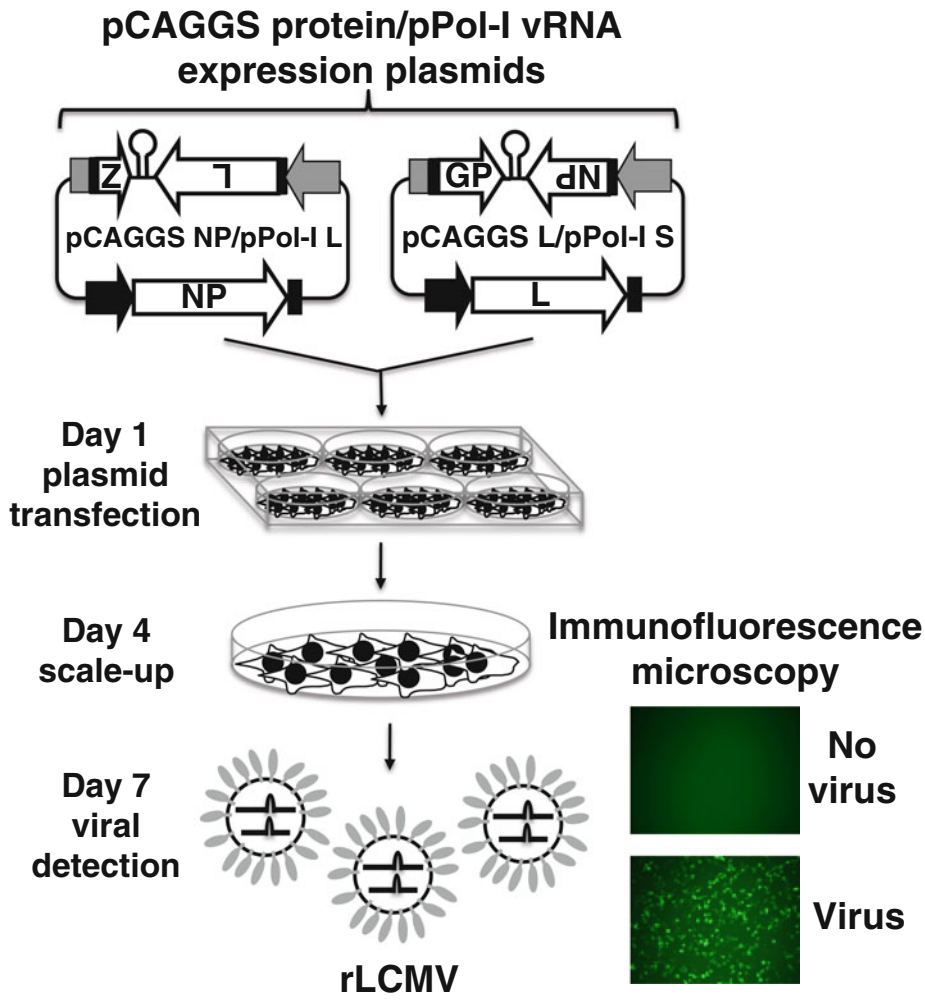

Fig. 6 Generation of recombinant WT arenaviruses using a two-plasmid-based system: A plasmid encoding NP and the vRNA L segment (pCAGGS NP/pPol-I L, *left*), along with the L polymerase protein and the vRNA S segment (pCAGGS L/pPol-I S, *right*) plasmid, is transiently co-transfected, using LPF2000, in 6-well plates (triplicates). Recommended amounts of plasmids, LPF2000, and cells for LCMV WT virus rescues using the two-plasmid-based approach are described in Table 2b. At 72 h post-transfection, cells are trypsinized and re-seeded into 10 cm dishes. After 72-h incubation, TCS are collected and presence of virus is determined by plaque assay or immunofluorescence using arenavirus-specific antibodies. The chicken β-actin promoter (*black arrow*) and the rabbit β-globin polyadenylation (pA) signal are indicated in the pCAGGS protein expression plasmids. Viral untranslated regions (UTR, *black boxes*) and intergenic region (IGR) in the pPol-I vRNA expression plasmid are indicated. The Pol-I promoter and terminator sequences in the pPol-I vRNA plasmids are indicated by *gray arrows* and *boxes*, respectively. For more details *see* text

3.3 Generation of Recombinant Tri-Segmented (r3) Arenaviruses

Several approaches have been used to successfully generate recombinant NS RNA viruses expressing foreign genes. These include the use of the self-cleavage 2A protease of picornaviruses [123], the use of dicistronic genome segments containing internal promoters [124, 125], the use of internal ribosome entry sites (IRES)

[126, 127], and the use of virus-specific packaging signals within vRNA segments [128, 129]. Although a viable strategy in other NS-segmented RNA viruses, these approaches were unsuccessful in yielding recombinant arenaviruses encoding foreign genes [100]. Successful rescue of r3 arenavirus packaging two S segments into mature, infectious virions has been described for the OW arenavirus LCMV [91, 96, 97, 100, 101] and the NW arenavirus JUNV [96, 97, 100]. Within this approach, the S segment is altered to replace one of the viral-encoded proteins (e.g., GP and NP) by a foreign GOI [91, 96, 97, 100, 101]. The physical separation of the GP and NP proteins into two different S segments (S1 and S2) represents a strong selective pressure to maintain a virus capable of packaging 1 L segment and 2 S segments. The ability of arenavirus to package 2 S segments has been previously suggested based on genetics [130] and structural [131, 132] analysis. Moreover, because of the stability of the r3LCM viruses, these findings suggest that production of infectious arenavirus particles containing two S and one L segments is a common event [1, 100]. Importantly, each of the S segments can direct expression of a GOI and therefore two foreign proteins can be expressed within the same virus, contrary to the situation observed with other NS-segmented RNA viruses. Notably, regulation of foreign protein expression depended on the location in the S segment [91]. Expression of a GOI in the NP locus is higher than that observed when the GOI was located in the GP locus, similar to the situation observed during viral infection [91]. Moreover, results obtained with the generation of r3 arenaviruses suggest that, unlike the situation observed with other NS-segmented RNA viruses [133] but similar to members in the bunyamwera family [134], the arenavirus NP- and GP-coding regions do not appear to play a critical role in the packaging of the viral S segment [100]. Several r3 arenaviruses have been generated that express one or two additional GOI [91, 96, 97, 100, 101]. Depending on the GOI expressed (protein function, size, etc.), these r3 arenaviruses showed little or no attenuation in cultured cells and they exhibited long-term genetic stability as reflected by unaltered expression levels during serial virus passages of the GOI incorporated into the S segments [100]. Although the r3 arenavirus rescue approach is as efficient as the WT bi-segmented and arenaviruses containing 2 S segments exhibit WT growth properties in vitro, including genetic and phenotypic stability, r3 arenaviruses exhibit, as compared to WT arenaviruses, attenuation in vivo [100]. Since r3 arenaviruses are not attenuated in vitro (ideal for vaccine production) but are attenuated in vivo, these r3 arenaviruses represent a great approach for their implementation not only as arenavirus vaccines but also as vaccine vectors [91, 96, 97, 101]. Importantly, the use of r3 arenaviruses expressing appropriate GOI (e.g., reporter genes) could be used to facilitate the identification of antiviral compounds or

drugs amenable to HTS approaches or siRNA-based screening of libraries to identify host cell genes involved in the arenavirus life cycle [135].

To generate r3 arenaviruses, susceptible cells (e.g., murine or human cells) are co-transfected with the pCAGGS protein expression plasmids encoding NP and L together with the pPol-I L segment, and two pPol-I S segments, where the GP ORF is replaced with a foreign gene (pPol-I S1 NP/GOI1) and the NP ORF is replaced by another foreign gene in the second S segment (pPol-I S2 GOI2/GP) (Fig. 3c). So far, several r3 arenaviruses expressing CAT, fluorescent, and luciferase genes have been described [91, 96, 97, 100, 101].

3.3.1 R3 Arenavirus Rescue System Experimental Approach (Fig. 7)

R3 arenavirus rescue protocol is similar to the steps outlined above for WT bi-segmented arenaviruses. However, follow the proper plasmid DNA preparations and concentrations recommended in Table 3 [91, 96, 97, 100, 101].

3.4 Generation of Single-Cycle Infectious Recombinant Arenaviruses

Although replication-competent arenaviruses are the most biologically relevant systems for studying arenavirus biology, research with highly pathogenic HF-causing arenaviruses requires the use of BSL-4 containments [1]. Two OW arenaviruses (LASV and LUJV) and seven NW arenaviruses (JUNV [6], MACV [16, 17], CHPV [18], SABV [19, 20], GTOV [21–23], WWAV [24, 25], and OCEV [26]) are known to cause HF disease in humans. Accordingly, they are classified as NIAID Category A priority pathogens. HF-causing arenavirus research has been hampered by the requirement of BSL-4 facilities to handle live forms of these viruses [104]. Research with HF-causing arenaviruses could be facilitated by the development and implementation of valid surrogate systems that could be used under less strict biosafety conditions to circumvent the intrinsic complications associated with the use of BSL-4 facilities. These include, among others, disposal of biological waste, costs associated with BSL-4 facilities, safety, and expression of reporter genes as a valid surrogate to detect and quantify arenavirus infections [104]. Arenavirus GP-pseudotyped retroviruses or lentivirus approaches have been used instead to evaluate arenavirus cell entry [136, 137]. However, these approaches are limited to the investigation of arenavirus cell entry without addressing the contribution of other viral proteins (L, NP, and Z) to viral fitness, including the identification of antivirals targeting multiple steps in the replication cycle of arenaviruses. Generation of single-cycle infectious arenavirus offers the advantage of using a bona fide arenavirus and therefore would recreate all the steps of the arenavirus life cycle in GP-complementing cells, making this system more suitable for the screening of inhibitors targeting other steps than arenavirus cell entry [99]. Moreover,

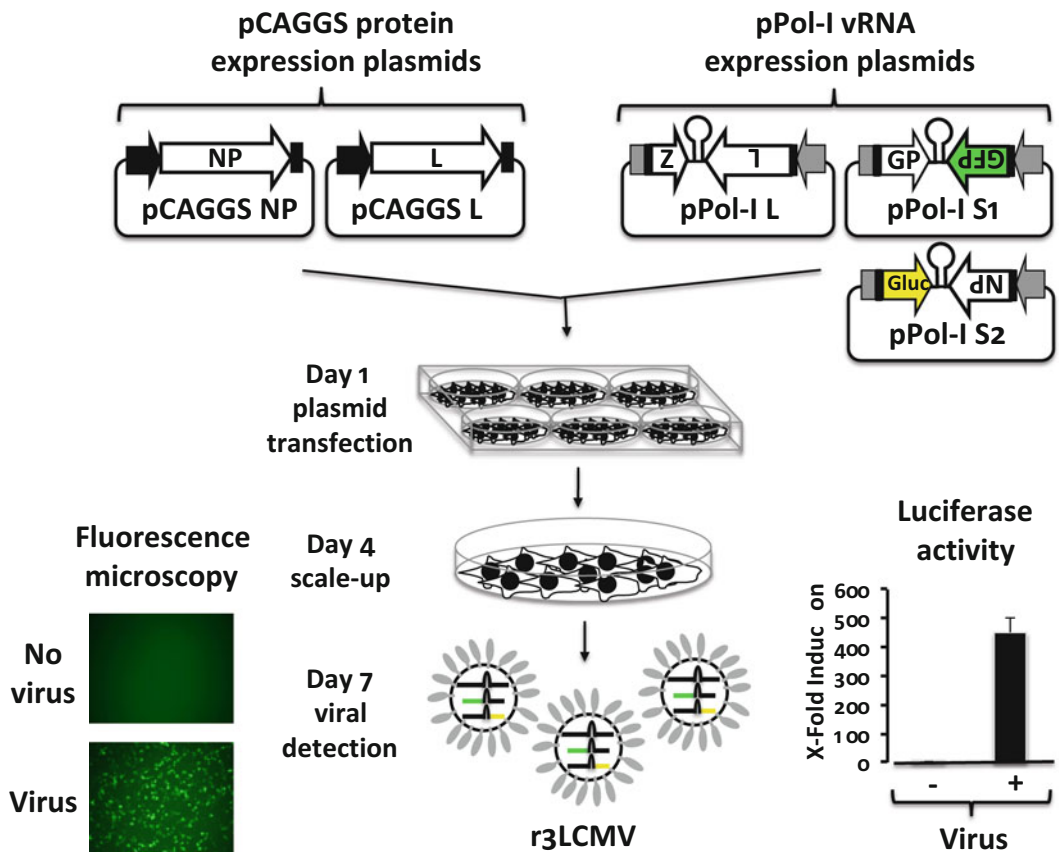

Fig. 7 Generation of recombinant tri-segmented (r3) arenavirus: Generation of r3 arenavirus is performed similarly to the rescue of recombinant WT arenavirus (Fig. 5) with the exception that the vRNA expression plasmid for the S segment (pPol-I S) is separated into two (pPol-I S1 and pPol-I S2) plasmids. In the pPol-I S1 plasmid the viral NP is replaced by GFP, and in the pPol-I S2 plasmid Gluc replaces the viral GP. Alternatively, the viral NP can be replaced by Gluc and the viral GP by GFP. Recommended amounts of plasmids, LPF2000, and cells for r3 arenavirus rescues are shown in Table 3. The chicken β-actin promoter (*black arrow*) and the rabbit β-globin polyadenylation (pA) signal are indicated in the pCAGGS protein expression plasmids. Viral untranslated regions (UTR, *black boxes*) and intergenic region (IGR) in the pPol-I vRNA expression plasmid are indicated. The Pol-I promoter and terminator sequences in the pPol-I vRNA plasmids are indicated by *gray arrows* and *boxes*, respectively. For more details *see* text

expression of the reporter gene facilitates its implementation to the HTS of libraries of compounds where expression of the reporter gene can be used as a valid surrogate for efficient viral replication [99]. Several single-cycle infectious viruses have been documented, including BSL-2 (rabies virus, influenza viruses, herpes simplex virus, and simian immunodeficiency virus) [109, 138–140], BSL-3 (influenza viruses, West Nile virus, and Kunjin virus) [110, 141, 142], and BSL-4 (Ebola virus) [143] viral pathogens. These single-cycle infectious viruses have been shown to be safe candidates for the identification of neutralizing antibodies and antivirals, and for

Table 3
Plasmid DNA and LPF2000 conditions to generate recombinant tri-segmented (r3) arenaviruses: Amounts of plasmid DNA and LPF2000 recommended to generate r3 arenaviruses using 6-well (1.0–1.2 × 10^6 cells/well) plates are indicated

Plasmid	6-Well plates (μg)
pCAGGS NP	0.8
pCAGGS L	1.0
pPol-I S1	0.8
pPol-I S2	0.8
pPol-I L	1.4
Total DNA	4.8
LPF2000	12
Cells	~1.0–1.2 × 10^6/well

studying other aspects of viral replication cycle. Because of the advantages associated with this approach, a replicating-competent, single-cycle infectious, recombinant LCMV where GFP substitutes for the viral GP gene (rLCMVΔGP/GFP) was generated [99, 102]. Replication of the rLCMVΔGP/GFP was restricted to cells expressing LCMV GP. Moreover, by generating constitutively expressing OW or NW arenavirus GP-expressing stable cell lines, rLCMVΔGP/GFP can be used to generate rLCMVΔGP/GFP pseudotyped with GPs from other members in the *Arenaviridae* family for the safe identification of neutralizing antibodies and inhibitors of arenavirus GP-mediated cell entry without the need for BSL-4 facilities [99].

Generation of single-cycle arenaviruses requires the co-transfection of susceptible cells with pPol-I L, pPol-I SΔGP/GFP (where the GP ORF is replaced by GFP) (Fig. 8a), and pCAGGS protein expression plasmids NP and L for replication and transcription, together with the pCAGGS protein expression plasmid encoding GP to initiate the first round of virion production (Fig. 8b) [99]. While infectious virions can be recovered from these transfected cells, these viruses will be able to infect cells but not produce infectious particles, unless they are complemented *in trans* by constitutively GP-expressing cells [99, 102]. Using similar stable or transient transfection strategies, the single-cycle infectious rLCMVΔGP/GFP can also be used to infect cells expressing the surface GP from other OW or NW arenaviruses to generate GP-pseudotyped rLCMVΔGP/GFP viruses (Fig. 7c) [99] (*see* **Note 23**).

3.4.1 Single-Cycle Infectious Recombinant Arenavirus Experimental Approach (Fig. 8)

Generation of single-cycle infectious rLCMVΔGP/GFP is similar to the steps outlined above for LCMV WT, following the DNA plasmid and LPF2000 concentrations included in Table 4 [99]. Once generated, the growth properties of rLCMVΔGP/GFP should be evaluated in both parental and GP-expressing cells to confirm the single-cycle nature of the virus [99, 102]. To generate GP-pseudotyped rLCMVΔGP/GFP with arenavirus GPs of interest, constitutively expressing or transient transfected GP cells are infected with the rLCMVΔGP/GFP at low multiplicity of infection,

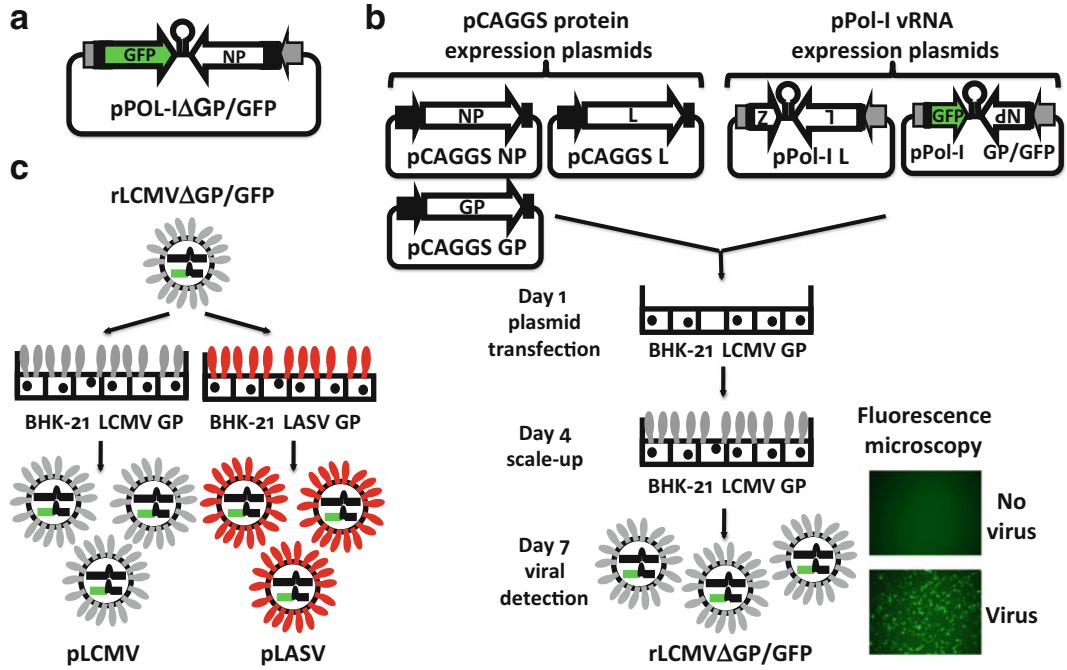

Fig. 8 Generation of single-cycle infectious recombinant arenavirus (rLCMVΔGP/GFP). (**a**) Schematic representation of the pPol-IΔGP/GFP plasmid: LCMV GP is substituted with GFP within the pPol-I S vRNA plasmid (pPol-IΔGP/GFP). The Pol-I promoter (*gray arrow*) and terminator (*gray box*) sequences are indicated. Viral untranslated regions (UTR, *black boxes*) and intergenic region (IGR) in the pPol-IΔGP/GFP plasmid are indicated. (**b**) Schematic representation of the single-cycle infectious rLCMVΔGP/GFP rescue: BHK-21 cells (6-well plates, triplicates) are transiently co-transfected, using LPF2000, with the pCAGGS protein expression plasmids encoding NP, L, and GP (to facilitate initial viral rescue) together with the pPol-I vRNA-expressing plasmids encoding for the L and modified S (ΔGP/GFP) segments. Recommended amounts of plasmids, LPF2000, and cells for single-cycle arenavirus rescues are indicated in Table 4. At 72 h post-transfection, TCS are scaled up. After additional 72-h incubation, TCS are collected and used to infect BHK-21 cells constitutively expressing LCMV GP and virus rescue is confirmed by the appearance of GFP loci. The chicken β-actin promoter (*black arrow*) and the rabbit β-globin polyadenylation (pA) signal are indicated in the pCAGGS protein expression plasmids. Viral untranslated regions (UTR, *black boxes*) and intergenic region (IGR) in the pPol-I vRNA expression plasmid are indicated. The Pol-I promoter and terminator sequences in the pPol-I vRNA plasmids are indicated by *gray arrows* and *boxes*, respectively. (**c**) Generation of GP-pseudotyped single-cycle infectious rLCMVΔGP/GFP: Single-cycle infectious rLCMVΔGP/GFP is used to infect BHK-21 cells constitutively expressing LCMV (*left, gray*) or LASV (*right, red*) GP to produce GP-pseudotyped LCMV (pLCMV) and LASV (pLASV). For more details *see* text

Table 4
Amount of plasmid DNA and LPF2000 to generate recombinant single-cycle infectious LCMV: Plasmid DNA and LPF2000 concentrations are indicated to generate a recombinant single-cycle infectious LCMV using 6-well (1.0–1.2 × 10^6 cells/well) plates

Plasmid	6-Well plates (μg)
pCAGGS NP	0.8
pCAGGS L	1.0
pCAGGS GP	0.8
pPol-IΔGP/GFP	1.0
pPol-I L	1.4
Total DNA	5
LPF2000	12.5
Cells	~1.0–1.2 × 10^6/well

MOI (0.01), and incubated for 48–72 h [99]. Viral titers in TCS can be assessed by infecting GP-expressing cell lines and observe for fluorescent (GFP) loci at ~18–24 h post-infection [99].

3.5 Confirmation of Successful Recombinant Arenavirus Rescue

Arenaviruses do not display classic cytopathic effect (CPE) observed with other NS RNA viruses [1]. Thus, successful rescue of WT arenaviruses must be evaluated by performing classical plaque assays [144] or by immunofluorescence using arenavirus-specific antibodies [56, 69, 70, 91, 92, 96–98] (*see* **Notes 24** and **25**).

3.5.1 Wild-Type (WT) Arenavirus

Experimental Approach

1. A day before confirming viral rescue or titration, trypsinize Vero cells from 10 cm dishes as above. In this case, adjust the cell density to 2 × 10^5 cells/ml. Seed the cells in 96-well plates (100 μl/well) and gently tap the plate so that a uniform cell monolayer of 80–90 % confluence (~4 × 10^4 cells/well) is reached the next day upon culturing the cells at 37 °C, 5 % CO_2.
2. On the day of virus titration, serially dilute (tenfold dilutions) viral TCS recovered from transfected cells in OptiMEM.
3. Remove the media and wash Vero cells twice with 50 μl of 1× PBS. Infect the cells with 50 μl of the serially diluted virus. Allow virus adsorption at 37 °C, 5 % CO_2, for 90 min, rocking the plates every 15 min to allow uniform virus infection of the cell monolayer.
4. After 90-min infection, remove the viral inoculum and add 100 μl of infectious media. Allow the cells to incubate for 16–18 h (*see* **Note 26**).

5. Remove the TCS, and fix and permeabilize the cells with 4 % formaldehyde and 0.1 % triton X-100 diluted in 1× PBS for 15 min at RT (*see* **Note 27**).
6. Remove the fixation/permeabilization solution and wash the cells, three times, with 1× PBS.
7. Block the cells with 2.5 % BSA in 1× PBS for 1 h at RT (*see* **Note 28**).
8. During cell blocking, prepare the primary antibody. Antibodies specific to viral antigen should be diluted in blocking solution (2.5 % BSA), and centrifuge for 15 min at 3500 × *g* before use (*see* **Note 29**).
9. After blocking the cells, remove the blocking solution and incubate the cells with 50 μl of the primary antibody at 37 °C, 5 % CO_2, for 1 h.
10. After 1-h incubation with the primary antibody, wash the cells three times with 1× PBS, and incubate with 50 μl of the fluorescein-conjugated secondary antibody diluted (following manufacturer recommendations) in blocking solution (2.5 % BSA) at 37 °C, 5 % CO_2, for 30 min (*see* **Note 30**).
11. Following the 30-min incubation, remove the secondary antibody and wash the cells three times with 1× PBS.
12. At this moment, arenavirus rescue or titers can be determined under a fluorescent microscope. Viral titration is calculated by counting the fluorescent focus-forming units (FFU) and the respective dilutions.

3.5.2 Tri-Segmented (r3) Arenavirus

R3 arenaviruses typically encode for two foreign genes, such as fluorescent or luminescent reporter genes [91, 96, 97, 100, 101]. In such case, successful viral rescue and viral titers can be evaluated following the previously described protocol, without the need of primary or secondary antibodies, under a fluorescent microscope (GFP expression) [91, 96, 97, 100, 101]. Alternatively, a luciferase assay can be used to evaluate the presence of virus from TCS [91, 96, 97, 100, 101]. If the r3 arenavirus does not encode for a reporter gene, presence and quantification of the rescued r3 arenavirus should be evaluated similar to that previously described for WT arenaviruses.

3.5.3 Single-Cycle Arenavirus

As with r3 arenavirus expressing reporter genes, single-cycle infectious recombinant arenavirus expressing GFP or luciferase can be evaluated and titrated under a fluorescent microscope or using a luciferase assay, respectively [99, 102]. If the single-cycle arenavirus expresses a foreign gene that does not encode for a reporter gene, presence and titration of the virus should be evaluated by immunofluorescence, as previously described for WT arenaviruses.

3.6 Amplification of Viral Rescue

Successful arenavirus rescue depends on multiple factors, including the proper maintenance of cells used for generation of recombinant viruses, the quality of the plasmid preparations to generate recombinant arenaviruses, and the transfection efficiency of the cell line used for generation of recombinant viruses, among others. Thus, we recommend performing the arenavirus rescues in triplicate in order to increase the likelihood of a successful rescue. It is possible that arenavirus titers in TCS from initial virus rescue are low and, therefore, the viruses need to be amplified to generate a stock. To that end, we recommend infecting fresh Vero or BHK-21 cells at low MOI (0.01) and allow virus amplification for 48–72 h before collecting the new TCS for viral titration, as described above.

4 Notes

The development of arenavirus reverse genetics systems has provided investigators with a novel and powerful experimental approach to study basic aspects of arenavirus biology including the identification of viral determinants, and their mechanisms of action, which contribute to arenaviral human diseases. Moreover, the ability to manipulate the genome of the prototypic arenavirus LCMV, which has proven to be a superb model system to study virus-host interactions and associated disease, and generate rLCMV with predetermined mutations, is allowing investigators to gain a detailed understanding of virus-host interactions that can lead to a large array of phenotypic outcomes of virus infection ranging from an acute and fatal meningitis to immunosuppression and chronic infections that although clinically silent can be associated with neurobehavioral abnormalities. Likewise, the generation of recombinant arenaviruses expressing appropriate reporter genes together with the development of specific cell-based assays for each of the different steps of the arenavirus life cycle will facilitate novel approaches to discover and characterize antiviral drugs against these important human pathogens. Moreover, as some of these assays do not involve the use of live forms of the virus, they overcome the difficulties posed by the need of BSL-4 facilities to handle live HF arenaviruses like LASV and JUNV.

1. We recommend growing the pPol-I L plasmid at 30 °C for 24 h.
2. Plasmid concentrations can be determined using spectrophotometry at 260 nm, with DNA purity being estimated using the 260:280 nm ratio (it is optimal to reach a 1.8–2.0 ratio for optimal arenavirus rescue).
3. All plasmids can be generated using standard cloning techniques and sequenced using standard protocols.

4. We use a secreted luciferase, so both the MG *Gaussia* luciferase (Gluc) and Cluc can be measured directly from tissue culture supernatants (TCS) [56, 91, 96, 98, 145] (Fig. 4).
5. Other polymerase II (Pol-II)-driven expression plasmids can be used instead of pCAGGS for arenavirus MG and rescue approaches. Likewise, other alternative reporter luciferase genes can be used for MG assays to normalize transfection efficiencies.
6. If arenavirus MG or rescue attempts are going to be performed in murine cells, the pPol-I vRNA expression plasmids should contain the murine Pol-I promoter [96, 106]. Alternatively, if human 293 T or monkey Vero cells are used to assess viral replication and gene transcription (MG assay) or generation of recombinant viruses, the pPol-I plasmids should be used to drive the expression of the arenavirus vRNAs under the human Pol-I promoter [56, 91, 96–98].
7. Alternative reporter genes can be used to evaluate viral replication and gene transcription using these MG approaches.
8. The viral GP can be replaced by GFP and NP by Gluc [91]. It is important to state that reporter gene expression will depend on their location in the vRNA-like MG plasmid since it has been shown higher expression levels of arenavirus NP than GP during viral infection and MG transfections [91].
9. As indicated above, arenavirus NP expression levels are higher than those of the viral GP [91] during viral infection and therefore reporter or foreign GOI expression will depend on their location in the viral S segment [91].
10. To avoid possible recombination that could occur by including the sequence of the same viral protein twice in the same plasmid, we introduced the NP ORF within the plasmid containing the L vRNA segment (pCAGGS NP/pPol-I L) and the L polymerase ORF within the plasmid containing the S segment (pCAGGS L/pPol-I S) (Figs. 3d and 6) [96].
11. It is important to choose the proper cell line to successfully evaluate viral MG activities and to generate recombinant arenaviruses using plasmid-based reverse genetics techniques [96]. One of the advantages of using human 293 T in MG approaches is the identification of anti-arenavirals for their potential use in humans [96].
12. We recommended the use of immunofluorescence or flow cytometry approaches to evaluate the percentage of LCMV GP-expressing cells.
13. Alternatively to the generation of stable LCMV GP-expressing cells, rLCMVΔGP/GFP complementation can be achieved by transiently transfecting the pCAGGS LCMV GP expression plasmid 24 h prior to infection [110].

14. As indicated above, because of the species specificity of Pol-I promoters [96, 107], MG assays in murine and human cells should use murine and human Pol-I promoters, respectively [96, 107].
15. We have found that the Pol-I T sequence is more efficient than HDVR sequences in producing arenavirus-like RNAs with the precise 3′ ends in both MG and virus rescue approaches [96].
16. We typically perform the MG assay in triplicate to get a good representation of the experiment and for statistical analysis.
17. Transfection in the absence of the protein expression plasmid encoding for NP (pCAGGS NP) should be included as a negative control.
18. We recommend transfecting cells that are more susceptible to LPF2000/DNA transfection, such as 293 T or BHK-21 cells, to improve the quality and reproducibility of the MG experiments.
19. The use of GFP and Gluc as reporter genes allows the measurement of MG activities at different times post-transfection using the same transfected cells [69, 70, 92, 96–98].
20. The benefit of performing arenavirus rescues using a two-plasmid approach is to increase successful co-transfection of cells that are poorly transfected, such as Vero cells, with the goal of vaccine implementation [96, 97].
21. To increase the likelihood of successful virus rescue, virus rescues are attempted in triplicate. Therefore, prepare enough OptiMEM-LPF2000 based on the number of virus rescues planned.
22. Make small-volume aliquots to prevent multiple thaw cycles, which may reduce virus titers.
23. Transient transfection with GP is likely to vary in efficiencies and GP expression levels and, therefore, rLCMVΔGP/GFP stocks. Thus, we recommend the use of GP-stable expressing cells for both the generation of rLCMVΔGP/GFP and GP-pseudotyped rLCMVΔGP/GFP [99, 102].
24. Because of the long incubation period (5–6 days) and the need of immunostaining arenavirus plaques in Vero cells, we recommend the use of immunofluorescence assays (~16–18 h) for confirmation of recombinant arenavirus rescues and for viral titrations [56, 69, 70, 91, 92, 96–98].
25. We usually evaluate viral titers in triplicates, using 96-well plates.
26. Viral infection lasting over 18 h post-infection may lead to secondary infections and, therefore, result in over-estimation of viral titers.

27. Alternatively you can fix the cells with 4 % formaldehyde diluted in 1× PBS for 15 min at RT, before permeabilizing the cells with 0.1 % triton X-100 for 15 min at RT.
28. Alternatively cells can be blocked ON at 4 °C.
29. An antibody specific to arenavirus NP is recommended, as NP is the most abundantly produced viral protein in infected cells and will assist in easy detection of the virus [1]. The species (e.g., mouse, rabbit, etc.), nature (e.g., monoclonal or polyclonal), and proper dilution of the antibody used for viral detection and/or titration should be determined previously. For LCMV, we use the mouse monoclonal antibody 1.1.3 from hybridoma TCS diluted in 2.5 % BSA.
30. For LCMV, we use a secondary FITC-conjugated α-mouse antibody from Dako at 1:100 dilution [56, 69, 70, 91, 92, 96–98].

Acknowledgements

Arenavirus research in LM-S laboratory was partially funded by the NIH grants RO1 AI077719 and RO3AI099681-01A1, and by the University of Rochester Drug Discovery Pilot Award Program. Research in J.C.T. laboratory is supported by grants RO1 AI047140, RO1 AI077719, and RO1 AI079665.

References

1. Buchmeier MJ, de la Torre, J. C., Peters, C. J. (2007) Arenaviridae: The Viruses and Their Replication. In: David Knipe P, Peter Howley, MD, Diane Griffin, MD, PhD, Robert Lamb, PhD, ScD, Malcolm Martin, MD, Bernard Roizman, ScD, Stephen Straus, MD, editor. Fields Virology. 5th ed. Philadelphia, PA, 19106, USA: Lippincott Williams & Wilkins. pp. 1791–1827
2. Radoshitzky SR, Bao Y, Buchmeier MJ, Charrel RN, Clawson AN et al (2015) Past, present, and future of arenavirus taxonomy. Arch Virol 160:1851–1874
3. Stenglein MD, Jacobson ER, Chang LW, Sanders C, Hawkins MG et al (2015) Widespread recombination, reassortment, and transmission of unbalanced compound viral genotypes in natural arenavirus infections. PLoS Pathog 11:e1004900
4. Stenglein MD, Leavitt EB, Abramovitch MA, McGuire JA, DeRisi JL (2014) Genome sequence of a Bornavirus recovered from an African Garter snake (Elapsoidea loveridgei). Genome Announc 2:e00779–e00814
5. Stenglein MD, Sanders C, Kistler AL, Ruby JG, Franco JY et al (2012) Identification, characterization, and in vitro culture of highly divergent arenaviruses from boa constrictors and annulated tree boas: candidate etiological agents for snake inclusion body disease. MBio 3:e00180-00112
6. Enria DA, Briggiler AM, Sanchez Z (2008) Treatment of Argentine hemorrhagic fever. Antiviral Res 78:132–139
7. Geisbert TW, Jahrling PB (2004) Exotic emerging viral diseases: progress and challenges. Nat Med 10:S110–S121
8. Khan SH, Goba A, Chu M, Roth C, Healing T et al (2008) New opportunities for field research on the pathogenesis and treatment of Lassa fever. Antiviral Res 78:103–115
9. McCormick JB, Fisher-Hoch SP (2002) Lassa Fever. In: Oldstone MB (ed) Arenaviruses I. Springer, Berlin, Heidelberg, New York, pp 75–110
10. Peters CJ (2002) Human Infection with Arenaviruses in the Americas. In: Oldstone

MB (ed) Arenaviruses I. Springer, Berlin, Heidelberg, New York, pp 65–74

11. Freedman DO, Woodall J (1999) Emerging infectious diseases and risk to the traveler. Med Clin North Am 83:865–883, v
12. Holmes GP, McCormick JB, Trock SC, Chase RA, Lewis SM et al (1990) Lassa fever in the United States. Investigation of a case and new guidelines for management. N Engl J Med 323:1120–1123
13. Isaacson M (2001) Viral hemorrhagic fever hazards for travelers in Africa. Clin Infect Dis 33:1707–1712
14. Richmond JK, Baglole DJ (2003) Lassa fever: epidemiology, clinical features, and social consequences. BMJ 327:1271–1275
15. Briese T, Paweska JT, McMullan LK, Hutchison SK, Street C et al (2009) Genetic detection and characterization of Lujo virus, a new hemorrhagic fever-associated arenavirus from southern Africa. PLoS Pathog 5:e1000455
16. Kuns ML (1965) Epidemiology of Machupo virus infection. II. Ecological and control studies of hemorrhagic fever. Am J Trop Med Hyg 14:813–816
17. Webb PA, Johnson KM, Mackenzie RB, Kuns ML (1967) Some characteristics of Machupo virus, causative agent of Bolivian hemorrhagic fever. Am J Trop Med Hyg 16:531–538
18. Delgado S, Erickson BR, Agudo R, Blair PJ, Vallejo E et al (2008) Chapare virus, a newly discovered arenavirus isolated from a fatal hemorrhagic fever case in Bolivia. PLoS Pathog 4:e1000047
19. Gonzalez JP, Bowen MD, Nichol ST, Rico-Hesse R (1996) Genetic characterization and phylogeny of Sabia virus, an emergent pathogen in Brazil. Virology 221:318–324
20. Armstrong LR, Dembry LM, Rainey PM, Russi MB, Khan AS et al (1999) Management of a Sabia virus-infected patients in a US hospital. Infect Control Hosp Epidemiol 20:176–182
21. Tesh RB, Jahrling PB, Salas R, Shope RE (1994) Description of Guanarito virus (Arenaviridae: Arenavirus), the etiologic agent of Venezuelan hemorrhagic fever. Am J Trop Med Hyg 50:452–459
22. Weaver SC, Salas RA, de Manzione N, Fulhorst CF, Duno G et al (2000) Guanarito virus (Arenaviridae) isolates from endemic and outlying localities in Venezuela: sequence comparisons among and within strains isolated from Venezuelan hemorrhagic fever patients and rodents. Virology 266:189–195
23. Gonzalez JP, Sanchez A, Rico-Hesse R (1995) Molecular phylogeny of Guanarito virus, an emerging arenavirus affecting humans. Am J Trop Med Hyg 53:1–6
24. Fulhorst CF, Bowen MD, Ksiazek TG, Rollin PE, Nichol ST et al (1996) Isolation and characterization of Whitewater Arroyo virus, a novel North American arenavirus. Virology 224:114–120
25. Charrel RN, de Lamballerie X, Fulhorst CF (2001) The Whitewater Arroyo virus: natural evidence for genetic recombination among Tacaribe serocomplex viruses (family Arenaviridae). Virology 283:161–166
26. Cajimat MN, Milazzo ML, Bradley RD, Fulhorst CF (2012) Ocozocoautla de espinosa virus and hemorrhagic fever, Mexico. Emerg Infect Dis 18:401–405
27. Barton LL, Mets MB (1999) Lymphocytic choriomeningitis virus: pediatric pathogen and fetal teratogen. Pediatr Infect Dis J 18:540–541
28. Barton LL, Mets MB (2001) Congenital lymphocytic choriomeningitis virus infection: decade of rediscovery. Clin Infect Dis 33:370–374
29. Barton LL, Mets MB, Beauchamp CL (2002) Lymphocytic choriomeningitis virus: emerging fetal teratogen. Am J Obstet Gynecol 187:1715–1716
30. Jahrling PB, Peters CJ (1992) Lymphocytic choriomeningitis virus. A neglected pathogen of man. Arch Pathol Lab Med 116:486–488
31. Mets MB, Barton LL, Khan AS, Ksiazek TG (2000) Lymphocytic choriomeningitis virus: an underdiagnosed cause of congenital chorioretinitis. Am J Ophthalmol 130:209–215
32. Fischer SA, Graham MB, Kuehnert MJ, Kotton CN, Srinivasan A et al (2006) Transmission of lymphocytic choriomeningitis virus by organ transplantation. N Engl J Med 354:2235–2249
33. Palacios G, Druce J, Du L, Tran T, Birch C et al (2008) A new arenavirus in a cluster of fatal transplant-associated diseases. N Engl J Med 358:991–998
34. Peters CJ (2006) Lymphocytic choriomeningitis virus-an old enemy up to new tricks. N Engl J Med 354:2208–2211
35. Borio L, Inglesby T, Peters CJ, Schmaljohn AL, Hughes JM et al (2002) Hemorrhagic fever viruses as biological weapons: medical and public health management. JAMA 287:2391–2405
36. Damonte EB, Coto CE (2002) Treatment of arenavirus infections: from basic studies to the challenge of antiviral therapy. Adv Virus Res 58:125–155

37. Harvie P, Omar RF, Dusserre N, Desormeaux A, Gourde P et al (1996) Antiviral efficacy and toxicity of ribavirin in murine acquired immunodeficiency syndrome model. J Acquir Immune Defic Syndr Hum Retrovirol 12:451–461
38. Omar RF, Harvie P, Gourde P, Desormeaux A, Tremblay M et al (1997) Antiviral efficacy and toxicity of ribavirin and foscarnet each given alone or in combination in the murine AIDS model. Toxicol Appl Pharmacol 143:140–151
39. Snell NJ (2001) Ribavirin—current status of a broad spectrum antiviral agent. Expert Opin Pharmacother 2:1317–1324
40. Enria DA, Barrera Oro JG (2002) Junin virus vaccines. Curr Top Microbiol Immunol 263:239–261
41. Maiztegui JI, McKee KT Jr, Barrera Oro JG, Harrison LH, Gibbs PH et al (1998) Protective efficacy of a live attenuated vaccine against Argentine hemorrhagic fever. AHF Study Group. J Infect Dis 177:277–283
42. Falzarano D, Feldmann H (2013) Vaccines for viral hemorrhagic fevers—progress and shortcomings. Curr Opin Virol 3:343–351
43. Albarino CG, Bergeron E, Erickson BR, Khristova ML, Rollin PE et al (2009) Efficient reverse genetics generation of infectious Junin viruses differing in glycoprotein processing. J Virol 83:5606–5614
44. Emonet SF, Seregin AV, Yun NE, Poussard AL, Walker AG et al (2011) Rescue from cloned cDNAs and in vivo characterization of recombinant pathogenic Romero and live-attenuated Candid #1 strains of Junin virus, the causative agent of Argentine hemorrhagic fever disease. J Virol 85:1473–1483
45. Hass M, Golnitz U, Muller S, Becker-Ziaja B, Gunther S (2004) Replicon system for Lassa virus. J Virol 78:13793–13803
46. Albarino CG, Bird BH, Chakrabarti AK, Dodd KA, Erickson BR et al (2011) Efficient rescue of recombinant Lassa virus reveals the influence of S segment noncoding regions on virus replication and virulence. J Virol 85: 4020–4024
47. McCormick JB, King IJ, Webb PA, Scribner CL, Craven RB et al (1986) Lassa fever. Effective therapy with ribavirin. N Engl J Med 314:20–26
48. Kilgore PE, Ksiazek TG, Rollin PE, Mills JN, Villagra MR et al (1997) Treatment of Bolivian hemorrhagic fever with intravenous ribavirin. Clin Infect Dis 24:718–722
49. McKee KT Jr, Huggins JW, Trahan CJ, Mahlandt BG (1988) Ribavirin prophylaxis and therapy for experimental argentine hemorrhagic fever. Antimicrob Agents Chemother 32:1304–1309
50. Leyssen P, De Clercq E, Neyts J (2008) Molecular strategies to inhibit the replication of RNA viruses. Antiviral Res 78:9–25
51. Parker WB (2005) Metabolism and antiviral activity of ribavirin. Virus Res 107:165–171
52. Cameron CE, Castro C (2001) The mechanism of action of ribavirin: lethal mutagenesis of RNA virus genomes mediated by the viral RNA-dependent RNA polymerase. Curr Opin Infect Dis 14:757–764
53. Crotty S, Maag D, Arnold JJ, Zhong W, Lau JYN et al (2000) The broad-spectrum antiviral ribonucleotide, ribavirin, is an RNA virus mutagen. Nat Med 6:1375–1379
54. Ruiz-Jarabo CM, Ly C, Domingo E, de la Torre JC (2003) Lethal mutagenesis of the prototypic arenavirus lymphocytic choriomeningitis virus (LCMV). Virology 308:37–47
55. Hoffmann HH, Kunz A, Simon VA, Palese P, Shaw ML (2011) Broad-spectrum antiviral that interferes with de novo pyrimidine biosynthesis. Proc Natl Acad Sci U S A 108: 5777–5782
56. Ortiz-Riano E, Ngo N, Devito S, Eggink D, Munger J et al (2014) Inhibition of arenavirus by A3, a pyrimidine biosynthesis inhibitor. J Virol 88:878–889
57. Gowen BB, Juelich TL, Sefing EJ, Brasel T, Smith JK et al (2013) Favipiravir (T-705) inhibits Junin virus infection and reduces mortality in a guinea pig model of Argentine hemorrhagic fever. PLoS Negl Trop Dis 7:e2614
58. Mendenhall M, Russell A, Juelich T, Messina EL, Smee DF et al (2011) T-705 (favipiravir) inhibition of arenavirus replication in cell culture. Antimicrob Agents Chemother 55: 782–787
59. Bolken TC, Laquerre S, Zhang Y, Bailey TR, Pevear DC et al (2005) Identification and characterization of potent small molecule inhibitor of hemorrhagic fever New World arenaviruses. Antiviral Res 69:86–97
60. Lee AM, Rojek JM, Spiropoulou CF, Gundersen AT, Jin W et al (2008) Unique small molecule entry inhibitors of hemorrhagic fever arena viruses. J Biol Chem 283:18734–18742
61. Lee KJ, Novella IS, Teng MN, Oldstone MB, de La Torre JC (2000) NP and L proteins of lymphocytic choriomeningitis virus (LCMV) are sufficient for efficient transcription and replication of LCMV genomic RNA analogs. J Virol 74:3470–3477

62. Strecker T, Eichler R, Meulen J, Weissenhorn W, Dieter Klenk H et al (2003) Lassa virus Z protein is a matrix protein and sufficient for the release of virus-like particles [corrected]. J Virol 77:10700–10705
63. Perez M, Craven RC, de la Torre JC (2003) The small RING finger protein Z drives arenavirus budding: implications for antiviral strategies. Proc Natl Acad Sci U S A 100:12978–12983
64. Urata S, Noda T, Kawaoka Y, Yokosawa H, Yasuda J (2006) Cellular factors required for Lassa virus budding. J Virol 80:4191–4195
65. Pinschewer DD, Perez M, Sanchez AB, de la Torre JC (2003) Recombinant lymphocytic choriomeningitis virus expressing vesicular stomatitis virus glycoprotein. Proc Natl Acad Sci U S A 100:7895–7900
66. Beyer WR, Popplau D, Garten W, von Laer D, Lenz O (2003) Endoproteolytic processing of the lymphocytic choriomeningitis virus glycoprotein by the subtilase SKI-1/S1P. J Virol 77:2866–2872
67. Rojek JM, Sanchez AB, Nguyen NT, de la Torre JC, Kunz S (2008) Different mechanisms of cell entry by human-pathogenic Old World and New World arenaviruses. J Virol 82:7677–7687
68. Lee KJ, Perez M, Pinschewer DD, de la Torre JC (2002) Identification of the lymphocytic choriomeningitis virus (LCMV) proteins required to rescue LCMV RNA analogs into LCMV-like particles. J Virol 76:6393–6397
69. Ortiz-Riano E, Cheng BY, de la Torre JC, Martinez-Sobrido L (2012) Self-association of lymphocytic choriomeningitis virus nucleoprotein is mediated by its N-terminal region and is not required for its anti-interferon function. J Virol 86:3307–3317
70. Ortiz-Riano E, Cheng BY, de la Torre JC, Martinez-Sobrido L (2011) The C-terminal region of lymphocytic choriomeningitis virus nucleoprotein contains distinct and segregable functional domains involved in NP-Z interaction and counteraction of the type I interferon response. J Virol 85:13038–13048
71. Pythoud C, Rodrigo WW, Pasqual G, Rothenberger S, Martinez-Sobrido L et al (2012) Arenavirus nucleoprotein targets interferon regulatory factor-activating kinase IKKepsilon. J Virol 86:7728–7738
72. Martinez-Sobrido L, Emonet S, Giannakas P, Cubitt B, Garcia-Sastre A et al (2009) Identification of amino acid residues critical for the anti-interferon activity of the nucleoprotein of the prototypic arenavirus lymphocytic choriomeningitis virus. J Virol 83: 11330–11340
73. Martinez-Sobrido L, Giannakas P, Cubitt B, Garcia-Sastre A, de la Torre JC (2007) Differential inhibition of type I interferon induction by arenavirus nucleoproteins. J Virol 81:12696–12703
74. Martinez-Sobrido L, Zuniga EI, Rosario D, Garcia-Sastre A, de la Torre JC (2006) Inhibition of the type I interferon response by the nucleoprotein of the prototypic arenavirus lymphocytic choriomeningitis virus. J Virol 80:9192–9199
75. Borrow P, Martinez-Sobrido L, de la Torre JC (2010) Inhibition of the type I interferon antiviral response during arenavirus infection. Viruses 2:2443–2480
76. Pythoud C, Rothenberger S, Martinez-Sobrido L, de la Torre JC, Kunz S (2015) Lymphocytic choriomeningitis virus differentially affects the virus-induced type I interferon response and mitochondrial apoptosis mediated by RIG-I/MAVS. J Virol 89: 6240–6250
77. Rodrigo WW, Ortiz-Riano E, Pythoud C, Kunz S, de la Torre JC et al (2012) Arenavirus nucleoproteins prevent activation of nuclear factor kappa B. J Virol 86:8185–8197
78. Igonet S, Vaney MC, Vonrhein C, Bricogne G, Stura EA et al (2011) X-ray structure of the arenavirus glycoprotein GP2 in its postfusion hairpin conformation. Proc Natl Acad Sci U S A 108:19967–19972
79. Burri DJ, da Palma JR, Kunz S, Pasquato A (2012) Envelope glycoprotein of arenaviruses. Viruses 4:2162–2181
80. Cao W, Henry MD, Borrow P, Yamada H, Elder JH et al (1998) Identification of alpha-dystroglycan as a receptor for lymphocytic choriomeningitis virus and Lassa fever virus. Science 282:2079–2081
81. Kunz S, Borrow P, Oldstone MB (2002) Receptor structure, binding, and cell entry of arenaviruses. Curr Top Microbiol Immunol 262:111–137
82. Kunz S, Sevilla N, McGavern DB, Campbell KP, Oldstone MB (2001) Molecular analysis of the interaction of LCMV with its cellular receptor [alpha]-dystroglycan. J Cell Biol 155:301–310
83. Radoshitzky SR, Abraham J, Spiropoulou CF, Kuhn JH, Nguyen D et al (2007) Transferrin receptor 1 is a cellular receptor for New World haemorrhagic fever arenaviruses. Nature 446:92–96
84. Pasqual G, Rojek JM, Masin M, Chatton JY, Kunz S (2011) Old world arenaviruses enter the host cell via the multivesicular body and depend on the endosomal sorting complex

required for transport. PLoS Pathog 7: e1002232

85. Capul AA, Perez M, Burke E, Kunz S, Buchmeier MJ et al (2007) Arenavirus Z-glycoprotein association requires Z myristoylation but not functional RING or late domains. J Virol 81:9451–9460
86. Perez M, Greenwald DL, de la Torre JC (2004) Myristoylation of the RING finger Z protein is essential for arenavirus budding. J Virol 78:11443–11448
87. Strecker T, Maisa A, Daffis S, Eichler R, Lenz O et al (2006) The role of myristoylation in the membrane association of the Lassa virus matrix protein Z. Virol J 3:93
88. Loureiro ME, D'Antuono A, Levingston Macleod JM, Lopez N (2012) Uncovering viral protein-protein interactions and their role in arenavirus life cycle. Viruses 4:1651–1667
89. de la Torre JC (2008) Reverse genetics approaches to combat pathogenic arenaviruses. Antiviral Res 80:239–250
90. Emonet SE, Urata S, de la Torre JC (2011) Arenavirus reverse genetics: new approaches for the investigation of arenavirus biology and development of antiviral strategies. Virology 411:416–425
91. Cheng, B. Y., Ortiz-Riano, E., de la Torre, J. C. & Martinez-Sobrido, L. Arenavirus Genome Rearrangement for the Development of Live Attenuated Vaccines. Journal of virology 89, 7373–7384, doi:10.1128/JVI.00307-15 (2015).
92. Ortiz-Riano E, Cheng BY, de la Torre JC, Martinez-Sobrido L (2012) D471G mutation in LCMV-NP affects its ability to self-associate and results in a dominant negative effect in viral RNA synthesis. Viruses 4:2137–2161
93. Russier M, Reynard S, Carnec X, Baize S (2014) The exonuclease domain of Lassa virus nucleoprotein is involved in antigen-presenting-cell-mediated NK cell responses. J Virol 88:13811–13820
94. Reynard S, Russier M, Fizet A, Carnec X, Baize S (2014) Exonuclease domain of the Lassa virus nucleoprotein is critical to avoid RIG-I signaling and to inhibit the innate immune response. J Virol 88:13923–13927
95. Seregin AV, Yun NE, Miller M, Aronson J, Smith JK et al (2015) The glycoprotein precursor gene of Junin virus determines the virulence of Romero strain and attenuation of Candid #1 strain in a representative animal model of Argentine Hemorrhagic Fever. J Virol 89:5949–5956
96. Ortiz-Riano E, Cheng BY, Carlos de la Torre J, Martinez-Sobrido L (2013) Arenavirus reverse genetics for vaccine development. J Gen Virol 94:1175–1188
97. Cheng BY, Ortiz-Riano E, de la Torre JC, Martinez-Sobrido L (2013) Generation of recombinant arenavirus for vaccine development in FDA-approved Vero cells. J Vis Exp 78:e50662
98. Cheng, B. Y., Ortiz-Riano, E., Nogales, A., de la Torre, J. C. & Martinez-Sobrido, L. Development of liveattenuated arenavirus vaccines based on codon deoptimization. Journal of virology, doi:10.1128/JVI.03401-14 (2015).
99. Rodrigo WW, de la Torre JC, Martinez-Sobrido L (2011) Use of single-cycle infectious lymphocytic choriomeningitis virus to study hemorrhagic fever arenaviruses. J Virol 85:1684–1695
100. Emonet SF, Garidou L, McGavern DB, de la Torre JC (2009) Generation of recombinant lymphocytic choriomeningitis viruses with trisegmented genomes stably expressing two additional genes of interest. Proc Natl Acad Sci U S A 106:3473–3478
101. Popkin DL, Teijaro JR, Lee AM, Lewicki H, Emonet S et al (2011) Expanded potential for recombinant trisegmented lymphocytic choriomeningitis viruses: protein production, antibody production, and in vivo assessment of biological function of genes of interest. J Virol 85:7928–7932
102. Flatz L, Hegazy AN, Bergthaler A, Verschoor A, Claus C et al (2010) Development of replication-defective lymphocytic choriomeningitis virus vectors for the induction of potent CD8+ T cell immunity. Nat Med 16:339–345
103. Salvato M, Borrow P, Shimomaye E, Oldstone MB (1991) Molecular basis of viral persistence: a single amino acid change in the glycoprotein of lymphocytic choriomeningitis virus is associated with suppression of the antiviral cytotoxic T-lymphocyte response and establishment of persistence. J Virol 65:1863–1869
104. Nisii C, Castilletti C, Raoul H, Hewson R, Brown D et al (2013) Biosafety Level-4 laboratories in Europe: opportunities for public health, diagnostics, and research. PLoS Pathog 9:e1003105
105. Niwa H, Yamamura K, Miyazaki J (1991) Efficient selection for high-expression transfectants with a novel eukaryotic vector. Gene 108:193–199
106. Flatz L, Bergthaler A, de la Torre JC, Pinschewer DD (2006) Recovery of an arenavirus entirely from RNA polymerase I/

II-driven cDNA. Proc Natl Acad Sci U S A 103:4663–4668

107. Heix J, Grummt I (1995) Species specificity of transcription by RNA polymerase I. Curr Opin Genet Dev 5:652–656
108. Hess RD, Weber F, Watson K, Schmitt S (2012) Regulatory, biosafety and safety challenges for novel cells as substrates for human vaccines. Vaccine 30:2715–2727
109. Martinez-Sobrido L, Cadagan R, Steel J, Basler CF, Palese P et al (2010) Hemagglutinin-pseudotyped green fluorescent protein-expressing influenza viruses for the detection of influenza virus neutralizing antibodies. J Virol 84:2157–2163
110. Baker SF, Guo H, Albrecht RA, Garcia-Sastre A, Topham DJ et al (2013) Protection against lethal influenza with a viral mimic. J Virol 87:8591–8605
111. Perez M, de la Torre JC (2003) Characterization of the genomic promoter of the prototypic arenavirus lymphocytic choriomeningitis virus. J Virol 77:1184–1194
112. Pinschewer DD, Perez M, de la Torre JC (2005) Dual role of the lymphocytic choriomeningitis virus intergenic region in transcription termination and virus propagation. J Virol 79:4519–4526
113. Kranzusch PJ, Whelan SP (2011) Arenavirus Z protein controls viral RNA synthesis by locking a polymerase-promoter complex. Proc Natl Acad Sci U S A 108:19743–19748
114. Sanchez AB, Perez M, Cornu T, de la Torre JC (2005) RNA interference-mediated virus clearance from cells both acutely and chronically infected with the prototypic arenavirus lymphocytic choriomeningitis virus. J Virol 79:11071–11081
115. Bergeron E, Chakrabarti AK, Bird BH, Dodd KA, McMullan LK et al (2012) Reverse genetics recovery of Lujo virus and role of virus RNA secondary structures in efficient virus growth. J Virol 86:10759–10765
116. Lopez N, Jacamo R, Franze-Fernandez MT (2001) Transcription and RNA replication of tacaribe virus genome and antigenome analogs require N and L proteins: Z protein is an inhibitor of these processes. J Virol 75:12241–12251
117. Lan S, McLay Schelde L, Wang J, Kumar N, Ly H et al (2009) Development of infectious clones for virulent and avirulent pichinde viruses: a model virus to study arenavirus-induced hemorrhagic fevers. J Virol 83: 6357–6362
118. Patterson M, Seregin A, Huang C, Kolokoltsova O, Smith J et al (2014) Rescue of a recombinant Machupo virus from cloned cDNAs and in vivo characterization in interferon (alphabeta/gamma) receptor double knockout mice. J Virol 88:1914–1923
119. Neumann G, Watanabe T, Ito H, Watanabe S, Goto H et al (1999) Generation of influenza A viruses entirely from cloned cDNAs. Proc Natl Acad Sci U S A 96:9345–9350
120. Fodor E, Devenish L, Engelhardt OG, Palese P, Brownlee GG et al (1999) Rescue of influenza A virus from recombinant DNA. J Virol 73:9679–9682
121. McLay L, Ansari A, Liang Y, Ly H (2013) Targeting virulence mechanisms for the prevention and therapy of arenaviral hemorrhagic fever. Antiviral Res 97:81–92
122. Sanchez AB, de la Torre JC (2006) Rescue of the prototypic Arenavirus LCMV entirely from plasmid. Virology 350:370–380
123. Nogales A, Baker SF, Martinez-Sobrido L (2015) Replication-competent influenza A viruses expressing a red fluorescent protein. Virology 476:206–216
124. Flick R, Hobom G (1999) Transient bicistronic vRNA segments for indirect selection of recombinant influenza viruses. Virology 262:93–103
125. Vieira Machado A, Naffakh N, Gerbaud S, van der Werf S, Escriou N (2006) Recombinant influenza A viruses harboring optimized dicistronic NA segment with an extended native 5′ terminal sequence: induction of heterospecific B and T cell responses in mice. Virology 345:73–87
126. Marschalek A, Finke S, Schwemmle M, Mayer D, Heimrich B et al (2009) Attenuation of rabies virus replication and virulence by picornavirus internal ribosome entry site elements. J Virol 83:1911–1919
127. Garcia-Sastre A, Muster T, Barclay WS, Percy N, Palese P (1994) Use of a mammalian internal ribosomal entry site element for expression of a foreign protein by a transfectant influenza virus. J Virol 68:6254–6261
128. Goto H, Muramoto Y, Noda T, Kawaoka Y (2013) The genome-packaging signal of the influenza A virus genome comprises a genome incorporation signal and a genome-bundling signal. J Virol 87:11316–11322
129. Liang Y, Hong Y, Parslow TG (2005) cis-Acting packaging signals in the influenza virus PB1, PB2, and PA genomic RNA segments. J Virol 79:10348–10355
130. Meyer BJ, de la Torre JC, Southern PJ (2002) Arenaviruses: genomic RNAs, transcription, and replication. Curr Top Microbiol Immunol 262:139–157

131. Buchmeier MJ (2002) Arenaviruses: protein structure and function. Curr Top Microbiol Immunol 262:159–173
132. Young PR, Howard CR (1983) Fine structure analysis of Pichinde virus nucleocapsids. J Gen Virol 64(Pt 4):833–842
133. Marsh GA, Rabadan R, Levine AJ, Palese P (2008) Highly conserved regions of influenza a virus polymerase gene segments are critical for efficient viral RNA packaging. J Virol 82:2295–2304
134. Kohl A, Lowen AC, Leonard VH, Elliott RM (2006) Genetic elements regulating packaging of the Bunyamwera orthobunyavirus genome. J Gen Virol 87:177–187
135. Lavanya M, Cuevas CD, Thomas M, Cherry S, Ross SR (2013) siRNA screen for genes that affect Junin virus entry uncovers voltage-gated calcium channels as a therapeutic target. Sci Transl Med 5:204ra131
136. Beyer WR, Westphal M, Ostertag W, von Laer D (2002) Oncoretrovirus and lentivirus vectors pseudotyped with lymphocytic choriomeningitis virus glycoprotein: generation, concentration, and broad host range. J Virol 76:1488–1495
137. Miletic H, Fischer YH, Neumann H, Hans V, Stenzel W et al (2004) Selective transduction of malignant glioma by lentiviral vectors pseudotyped with lymphocytic choriomeningitis virus glycoproteins. Hum Gene Ther 15: 1091–1100
138. Gomme EA, Faul EJ, Flomenberg P, McGettigan JP, Schnell MJ (2010) Characterization of a single-cycle rabies virus-based vaccine vector. J Virol 84:2820–2831
139. Bozac A, Berto E, Vasquez F, Grandi P, Caputo A et al (2006) Expression of human immunodeficiency virus type 1 tat from a replication-deficient herpes simplex type 1 vector induces antigen-specific T cell responses. Vaccine 24:7148–7158
140. Tang Y, Swanstrom R (2008) Development and characterization of a new single cycle vaccine vector in the simian immunodeficiency virus model system. Virology 372:72–84
141. Mason PW, Shustov AV, Frolov I (2006) Production and characterization of vaccines based on flaviviruses defective in replication. Virology 351:432–443
142. Chang DC, Liu WJ, Anraku I, Clark DC, Pollitt CC et al (2008) Single-round infectious particles enhance immunogenicity of a DNA vaccine against West Nile virus. Nat Biotechnol 26:571–577
143. Halfmann P, Ebihara H, Marzi A, Hatta Y, Watanabe S et al (2009) Replication-deficient ebolavirus as a vaccine candidate. J Virol 83:3810–3815
144. Wainwright S, Mims CA (1967) Plaque assay for lymphocytic choriomeningitis virus based on hemadsorption interference. J Virol 1:1091–1092
145. Nakajima Y, Kobayashi K, Yamagishi K, Enomoto T, Ohmiya Y (2004) cDNA cloning and characterization of a secreted luciferase from the luminous Japanese ostracod, Cypridina noctiluca. Biosci Biotechnol Biochem 68:565–570

Part IV

Vaccines for Human Bacterial Diseases

Chapter 18

DNA Vaccines: A Strategy for Developing Novel Multivalent TB Vaccines

Jaemi S. Chu, Daniel O. Villarreal, and David B. Weiner

Abstract

Multivalent DNA vaccines that are delivered by electroporation (EP) through muscle tissue provide a novel method for eliciting immunity against tuberculosis (TB) as well as a broad range of diseases including HIV and cancers. Proper plasmid construction containing suitable protective TB antigens capable of evoking desired vaccine-induced responses would lead to the appropriate induction of both humoral and cellular immunity. DNA vaccines are safe and of low cost in comparison to traditional vaccines while also providing potentially effective prophylactic or therapeutic modalities against currently untreatable diseases. Here, we describe the steps for developing a rational multivalent TB DNA vaccine delivered with intramuscular EP in mice.

Key words DNA vaccines, Tuberculosis, TB, Electroporation, *Mycobacteria tuberculosis*, Intramuscular, Multivalent vaccines, Antigens

1 Introduction

Advances in biotechnology provide massive potential in disease treatment using synthetic vectors to deliver genes of interest, but oftentimes there are more than a single protein involved [1]. Thus, there is a need to efficiently deliver multiple genes while taking into consideration the target cell type, activity of the protein of interest, and subcellular protein localization. DNA vaccines allow expression of foreign genes in a host and their presentation of the specific encoded proteins to the immune system resulting in the induction of broad, antigen-specific humoral and cellular immunity. Some advantages of using DNA vaccines over traditional vaccines (whole killed or live attenuated) include the following: stability; simple production; favorable safety profile of plasmid integration in humans; ability to administer repeatedly since plasmid vector efficiencies are not influenced by preexisting neutralizing antibodies; ability to target multiple antigens; low production cost [2, 3]. Moreover, DNA immunization may induce robust humoral

Sunil Thomas (ed.), *Vaccine Design: Methods and Protocols: Volume 1: Vaccines for Human Diseases*, Methods in Molecular Biology, vol. 1403, DOI 10.1007/978-1-4939-3387-7_18,

responses and strong cellular responses, especially with the aid of adjuvants or specific delivery techniques [4].

Before developing a vaccine for any particular target pathogen, one must first have an extensive understanding of the desired vaccine-induced immune responses required for establishing appropriate vaccine efficacy. Therefore, given that CD4 T_H1 responses have been strongly implicated in protective immunity in addition to the essential nature of CD8 T_c cells [5], effector immune responses should be aimed for tuberculosis (TB) vaccine efficacy. The second step in vaccine design involves identifying one or multiple TB antigens that can induce specificity of the desired immune response. Current results of the MVA85A trial did not statistically improve the protective efficacy against TB in infants [6] which raises questions regarding the ultimate benefit of targeting a single antigen and if this approach will actually confer protection in a heterogeneous human population [5]. In fact, several studies have shown that combining several TB-associated antigens could enhance levels of protective cellular immunity [5, 7–10]. Therefore, vaccination with multiple multistage potent T cell-based antigens from TB may be important for driving broad repertoire coverage to improve the protective effect of any new TB vaccination [5]. As a result, the combination of suitable novel prominent TB antigens could be incorporated into DNA vaccines in order to drive both a CD4 and CD8 T cell-mediated immune response, which has emerged as a promising approach [2, 5].

There are multiple strategies when developing novel DNA vaccines to target specific infectious pathogens, and they often involve multiple genes that are not always expressed at the same level. It is now possible to express multiple protein targets within a single open reading frame, and small sequences cloned between genes produce discrete protein products efficiently (Fig. 1) [11–14]. Current strategies for creating multivalent vectors include use of internal ribosome entry sites (IRES), multiple promoters, and fusion proteins [15]. The foot-and-mouth disease virus 2A or 2A-like *cis*-acting hydrolase elements have been used to create multiple proteins from one transcript, and picornavirus has been utilized for their self-cleaving properties (Fig. 1a, c) [11–14]. These 2A-like sequences mediate cotranslational cleavage to release individual protein products; thus they have been commonly used to allow efficient cleavage and functional protein expression [11–14]. In addition, DNA vaccines may be constructed to contain multiple immunogens by inserting them separately via incorporation of an endoproteolytic furin cleavage site (e.g., RGRKRSS) to facilitate proper protein folding and better CD8 T cell processing (Fig. 1b, c) [16]. Moreover, dual promoters within the same plasmid could express multiple genes, which may prevent imbalanced protein expression or homologous recombination when using a long, continuous transgene (Fig. 1g) [17]. Furthermore,

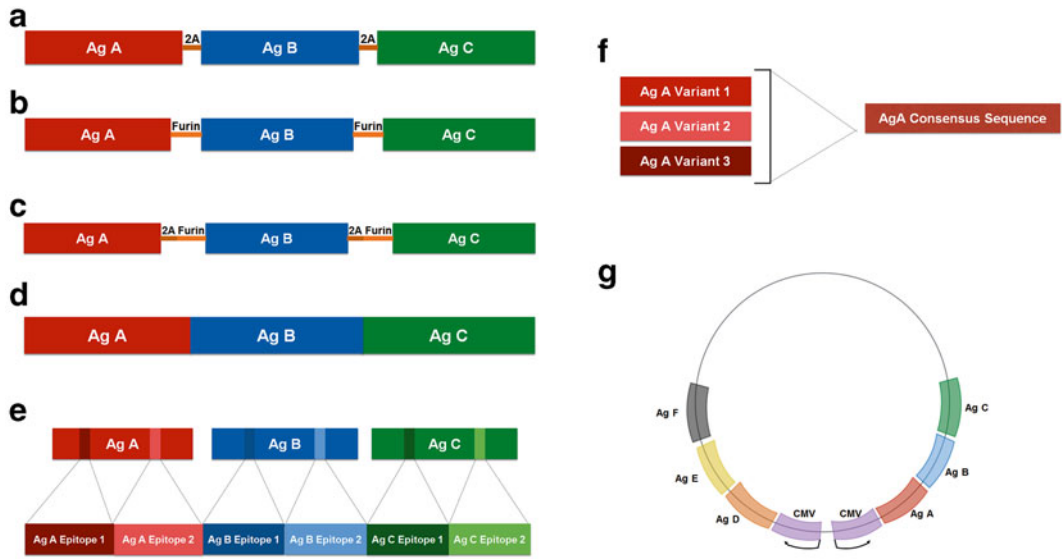

Fig. 1 Multivalent TB antigen design for DNA vaccines. (**a**) Multivalent transgene with 2A cleavage sites between each selected expressing antigen. (**b**) Furin cleavage site between each selected expressing antigen. (**c**) 2A and furin-linked cleavage site between each selected expressing target antigen. (**d**) Transgene of all antigen-expressing transgenes without any cleavage sites. (**e**) Selective CD4 and CD8 epitopes from selected prominent protective antigens. (**f**) Optimized consensus sequence by aligning variable target antigens between similar or different species and selecting for most conserved codons to create an optimized DNA construct. (**g**) Dual-promoter expressing DNA plasmid (e.g., pVAX1). The inserts in the plasmids could be designed similarly as in part figures (**a**)–(**f**)

alternative approaches are (1) fusing all selected TB antigens without any cleavage sites (Fig. 1d) or (2) fusing together selected known CD4 and CD8 immunogenic epitopes (Fig. 1e). Finally, besides identifying hyperconserved protective TB antigens capable of inducing protection, successfully targeting highly variable TB antigens is essential to maximizing protection against any variable antigens expressed by TB. DNA vaccine technology offers the strategy of using consensus sequences to overcome challenges from genetic variation of highly variable pathogens (Fig. 1f) [16, 18]. Consensus antigens are usually designed to encode the most commonly occurring amino acids at each position in a sequence from a collection of target antigens, thus providing a more effective response to highly divergent pathogens [18]. Overall, using all of these different sequence design approaches as transgenes for immunization may maximize protection against TB (Fig. 1).

The third step in improving or evoking the desired immune responses in DNA vaccination is delivery method via electroporation or in combination with a genetically engineered cytokine adjuvant [2]. Electroporation (EP) allows for more efficient DNA transfer and expression by temporarily generating an electrical field to increase the cell membrane permeability for plasmid entry

through temporary pores [17]. EP of muscle or skin has proven to be efficient in enhancing gene delivery, transgene expression, and the immunogenicity of DNA vaccines encoding antigens in both small and large animals [18]. In fact, antigen expression in muscle is improved 100- to 1000-fold in comparison with antigen expression from intracellular uptake of plasmids by naked injection [2]. Moreover, the addition of genetic molecular adjuvants may be a key method for enhancing the potency of protective immunity generated by current vaccination. Indeed, the addition of immune modulatory adjuvants as part of a vaccine cocktail has been demonstrated to boost the quantity and quality of the vaccine-induced adaptive immune responses [2]. Collectively, all these promising approaches highlight DNA vaccines as an advantageous platform to develop novel effective multivalent TB vaccines.

2 Materials

Prepare all solutions using ultrapure water and analytical grade reagents. Prepare and store all reagents at room temperature (unless indicated otherwise).

2.1 Plasmid DNA Constructs

1. Identify and select protective antigens capable of inducing protection in the heterogeneous population.
2. Design a plasmid vaccine construct encoding the desired multivalent transgene sequence for the protein antigen target(s) as mentioned in Subheading 1 and shown in Fig. 1.
3. After generating the desired multivalent sequence, several modifications must be performed to increase expression of the selected antigens: (1) RNA optimization (regions of very high (>80 %) or very low (<30 %) GC content and cis-acting sequence motifs such as internal TATA boxes, χ-sites, and ribosomal entry sites were avoided); (2) codon optimization (addition of Kozak and IgE leader sequence upstream of transgene) to facilitate proper expression and secretion of antigen; and if required (3) proper addition of any endoproteolytic cleavage sites between conjugated antigens.
4. After codon/RNA optimization the transgene is subcloned into the backbone of the clinically relevant or approved gene-expression DNA vector (e.g., pVAX1).
5. Store commercially synthesized DNA vaccine at 4 °C.

2.2 Preparation of DNA

1. Place concentrated stock of DNA at room temperature.
2. Add the appropriate amount of DNA to water or 1×PBS (total volume 30–50 μL per mouse) (*see* **Note 1**).

3. Vortex diluted DNA and quick spin in table centrifuge (*see* **Note 2**).

2.3 Electroporation Device

1. Charge the CELLECTRA electroporation (EP) device (Inovio Pharmaceuticals) before use.

3 Methods

Carry out all procedures at room temperature.

3.1 Setup

1. Connect the electroporation applicator to the EP device and turn on.
2. Set device to short firing delay parameters for small animals: 0.1 A, 4 s, DIS, 2×2 pulse pattern.
3. Place a triangular three-electrode array consisting of 26-gauge solid stainless steel electrodes at the tip of the applicator.
4. Anesthetize each mouse with 300-400 μL 1× Avertin (tribromoethanol) or via isoflurane before immunizing the mice.

3.2 Immunization

1. Inject the tibialis anterior muscle with 30–50 μL of DNA vaccine using a 3/10 cc U-100 29G1/2 syringe (*see* **Notes 3** and **4**).
2. Immediately after injection, EP the same site (*see* **Notes 5**–7).

4 Notes

1. Recommended or desired DNA volume and concentration: 30 μL is the commonly used volume; 5-50 μg of DNA has been commonly used in dosing studies.
2. TB DNA vectors may be co-delivered as a cocktail with the appropriate vector-encoded cytokine adjuvant(s) to further augment desired immune responses [2, 17, 19]. Plasmid-encoded adjuvant should be RNA/codon optimized as mentioned in Subheading 2.1, **item 3**.
3. Shave around the injection site prior to immunization with EP.
4. If only one injection site, always administer to right side for consistency.
5. Apply EP applicator needle probes to area right above the site of needle entry, where DNA is expected to be located.
6. Replace the electrode array probes for each mouse.
7. Using a current of 0.1 A reduces inflammation and improves antigen expression compared to a 0.2 A current.

Disclosure

D.B.W. discloses grant funding, industry collaborations, speaking honoraria, and fees for consulting. His service includes serving on scientific review committees and advisory boards. Remuneration includes direct payments, stock, or stock options. In the interest of disclosure, he therefore notes potential conflicts associated with his work with Pfizer, Bristol Myers Squibb, Inovio, Touchlight, Oncosec, Merck, VGXI, and others. Licensing of technology from his laboratory has created over 100 jobs in the private sector of the biotech/pharma industry. The other authors declare no competing financial interests. No writing assistance was utilized in the production of this manuscript.

References

1. Szymczak AL, Vignali DA (2005) Development of 2A peptide-based strategies in the design of multicistronic vectors. Expert Opin Biol Ther 5:627–638
2. Villarreal DO, Talbott KT, Choo DK, Shedlock DJ, Weiner DB (2013) Synthetic DNA vaccine strategies against persistent viral infections. Expert Rev Vaccines 12:537–554
3. Bagarazzi ML, Yan J, Morrow MP, Shen X et al (2012) Immunotherapy against HPV16/18 generates potent TH1 and cytotoxic cellular immune responses. Sci Transl Med 4:1–14
4. Baliban SM, Michael A, Shammassian B, Mudakha S, Khan AS et al (2014) An optimized, synthetic DNA vaccine encoding the toxin A and toxin B receptor binding domains of Clostridium difficile induces protective antibody responses in vivo. Infect Immun 82: 4080–4091
5. Villarreal DO, Walters J, Laddy DJ, Yan J, Weiner DB (2014) Multivalent TB vaccines targeting the esx gene family generate potent and broad cell-mediated immune responses superior to BCG. Hum Vaccin Immunother 10:2188–2198
6. Tameris MD, Hatherill M, Landry BS, Scriba TJ et al (2013) MVA85A 020 Trial Study Team. Safety and efficacy of MVA85A, a new tuberculosis vaccine, in infants previously vaccinated with BCG: a randomised, placebo-controlled phase 2b trial. Lancet 381: 1021–1028
7. Aagaard C, Hoang T, Dietrich J, Cardona PJ, Izzo A et al (2011) A multistage tuberculosis vaccine that confers efficient protection before and after exposure. Nat Med 17:189–194
8. Khera A, Singh R, Shakila H, Rao V, Dhar N et al (2005) Elicitation of efficient, protective immune responses by using DNA vaccines against tuberculosis. Vaccine 23:5655–5665
9. Grover A, Ahmed MF, Singh B, Verma I, Sharma P, Khuller GK (2006) A multivalent combination of experimental antituberculosis DNA vaccines based on Ag85B and regions of difference antigens. Microbes Infect 8: 2390–2399
10. Derrick SC, Yang AL, Morris SL (2004) A polyvalent DNA vaccine expressing an ESAT6-Ag85B fusion protein protects mice against a primary infection with Mycobacterium tuberculosis and boosts BCG-induced protective immunity. Vaccine 23:780–788
11. Szymczak AL, Workman CJ, Wang Y, Vignali KM, Dilioglou S, Vanin EF, Vignali DA (2004) Correction of multi-gene deficiency in vivo using a single 'self-cleaving' peptide-based retroviral vector. Nat Biotechnol 22:589–594
12. Szymczak-Workman AL, Vignali KM, Vignali DA (2012) Design and construction of 2A peptide-linked multicistronic vectors. Cold Spring Harb Protoc 2:199–204
13. Szymczak-Workman AL, Vignali KM, Vignali DA (2012) Generation of 2A-linked multicistronic cassettes by recombinant PCR. Cold Spring Harb Protoc 2:351–354
14. Szymczak-Workman AL, Vignali KM, Vignali DA (2012) Verification of 2A peptide cleavage. Cold Spring Harb Protoc 2:255–257
15. Osborn MJ, Panoskaltsis-Mortari A, McElmurry RT, Bell SK et al (2005) A picornaviral 2A-like sequence-based tricistronic vector allowing for high-level therapeutic gene

expression coupled to a dual-reporter system. Mol Ther 12:569–574

16. Yan J, Reichenbach DK, Corbitt N, Hokey DA et al (2009) Induction of antitumor immunity in vivo following delivery of a novel HPV-16 DNA vaccine encoding E6/E7 fusion antigen. Vaccine 27:431–440
17. Kalams SA, Parker SD, Elizaga M, Metch B et al (2013) Safety and comparative immunogenicity of an HIV-1 DNA vaccine in combination with plasmid interleukin 12 and impact of intramuscular electroporation for delivery. J Infect Dis 208:818–829
18. Lin F, Shen X, McCoy JR, Mendoza JM et al (2011) A novel prototype device for electroporation-enhanced DNA vaccine delivery simultaneously to both skin and muscle. Vaccine 29:6771–6780
19. Villarreal DO, Wise MC, Walters JN, Reuschel EL et al (2014) Alarmin IL-33 acts as an immunoadjuvant to enhance antigen-specific tumor immunity. Cancer Res 74:1789–1800

Chapter 19

Overcoming Enterotoxigenic *Escherichia coli* Pathogen Diversity: Translational Molecular Approaches to Inform Vaccine Design

James M. Fleckenstein and David A. Rasko

Abstract

Enterotoxigenic *Escherichia coli* (ETEC) are a genetically diverse *E. coli* pathovar that share in the ability to produce heat-labile toxin and/or heat-stable toxins. While these pathogens contribute substantially to the burden of diarrheal illness in developing countries, at present, there is no suitable broadly protective vaccine to prevent these common infections. Most vaccine development attempts to date have followed a classical approach involving a relatively small group of antigens. The extraordinary underlying genetic plasticity of *E. coli* has confounded the antigen valency requirements based on this approach. The recent discovery of additional virulence proteins within this group of pathogens, as well as the availability of whole-genome sequences from hundreds of ETEC strains to facilitate identification of conserved molecules, now permits a reconsideration of the classical approaches, and the exploration of novel antigenic targets to complement existing strategies overcoming antigenic diversity that has impeded progress toward a broadly protective vaccine. Progress to date in antigen discovery and methods currently available to explore novel immunogens are outlined here.

Key words *Escherichia coli*, Enterotoxigenic, Subunit vaccines, Bacterial genome, Antigenic diversity

1 Introduction

1.1 Global Importance of Enterotoxigenic Escherichia coli

Enterotoxigenic *E. coli* (ETEC) are among the leading causes of diarrheal illness worldwide. These organisms are particularly prevalent in developing countries where basic sanitation and clean water are often limited. Here, these pathogens preferentially affect young children, many of whom continue to succumb to rapid dehydration resulting from severe diarrheal illness [1]. ETEC infections occur following ingestion of contaminated food or water, and these infections have emerged in recent years in the form of large-scale food-borne outbreaks in the industrialized countries including the USA, presumably due to importation of imported food.

Sunil Thomas (ed.), *Vaccine Design: Methods and Protocols: Volume 1: Vaccines for Human Diseases*, Methods in Molecular Biology, vol. 1403, DOI 10.1007/978-1-4939-3387-7_19,

1.2 Toxins Define the Enterotoxigenic E. coli Pathovar

The enterotoxigenic *E. coli* are a diverse collection of pathogens that are defined by the production of at least one of the three diarrheagenic toxins known as heat-labile toxin (LT), or the heat-stable toxins (STh, and STp) [2]. Heat-labile toxin shares approximately 80 % molecular identity with cholera toxin and both toxins activate production of the second messenger cAMP in target intestinal epithelial cells. Both heat-stable toxins, like the native human intestinal peptide guanylin, bind to the extracellular portion of guanylate cyclase C to stimulate the production of cGMP. Both cAMP [3] and cGMP [4–6] stimulate protein kinases that phosphorylate the cystic fibrosis transmembrane regulatory channel (CFTR), thereby enhancing export of chloride ions into the intestinal lumen. Concurrent inhibition of sodium hydrogen ion exchange results in a net loss of NaCl and water into the intestinal lumen with ensuing watery diarrhea.

All three toxin genes are usually encoded on extrachromosomal plasmids and are frequently flanked by insertion sequences (IS), implicating mobile genetic elements in evolution of these genetically diverse pathogens. Indeed, it has been suggested that the diversity of the ETEC pathotype of diarrheagenic *E. coli* is driven largely by widespread dissemination of toxin gene encoding plasmids among a diverse collection of *E. coli* host strains [7].

1.3 The Challenge Posed by Pathogen Diversity

In essence, it appears that a diverse population of *E. coli* can potentially serve as effective hosts for production of these plasmid-encoded toxins. This is perhaps best exemplified by the diversity of serotypes that are represented among the ETEC pathovar [8]. While some specific O and H serotypes are more common, more than 75 O-antigen serogroups and more than 50 different H serogroups are represented in ETEC. A single study of 100 ETEC strains in Egypt identified 59 different O:H combinations [9]. Large-scale whole-genome sequencing of ETEC and other pathogenic *E. coli*, as well as some commensal strains, has provided some additional insight into the nature of this diversity [10, 11]. When considered in general, the *E. coli* pangenome, or collection of all genes present in those genomes sequenced to date, is quite large [12]. Remarkably, as each new genome sequence is analyzed, an estimated 300 unique genes will be added to this "open" pangenome [10, 12]. The appreciable underlying genetic plasticity of *E. coli* coupled with horizontal transfer of essential virulence genes on mobile elements may suggest that the ETEC pathovar will constantly evolve as toxin genes and other essential features are transferred into new host backgrounds.

1.4 Limits on ETEC Diversity Imposed by Key Virulence Requirements

Despite the underlying plasticity of *E. coli* genomes, there are two constraints imposed on ETEC genome content. First, all *E. coli* have at their core a collection of approximately 2200 genes that are mostly involved in essential metabolic functions of these organisms

[10, 12]. This core subset of genes, common to all *E. coli*, are at least theoretically devoid of viable vaccine targets since they are largely shared with commensal strains that are present in and a component of the natural human gastrointestinal microbiota.

The requirement for other virulence traits in addition to the toxins themselves imposes another potential constraint on pathogen evolution that is more relevant to antigen discovery, and vaccine target selection. While the genes encoding the known enterotoxins define the ETEC pathovar, genes that encode additional features required for effective delivery of toxin payloads to cognate receptors on the epithelial surface can essentially serve as diversity checkpoint. ETEC must survive ingestion, navigate to lumen of the small intestine, and ultimately interact directly with intestinal enterocytes [13] bringing the pathogen in close proximity to epithelial cell surface receptors for the delivery of LT and ST. The relatively small number of pathovar-specific features in addition to the known toxins suggests that there are only a limited number of ways in which this can be accomplished [10]. Within this context, it should be possible then to discover relatively conserved virulence molecules that are either exclusive to ETEC or shared with other diarrheagenic pathovars, but not commensal strains.

1.5 Immunologic and Structural Diversity of Major Vaccine Targets

The best-studied antigens of ETEC to date are the colonization factors (CFs), plasmid-encoded structures that have been a major focus of vaccine development. Perhaps the best published data in support of CFs as vaccine targets come from passive [14, 15] immunization studies demonstrating anti-CF antibodies administered orally to afford significant protection against experimental challenge with homologous strains of ETEC. A number of active vaccination studies with different vaccine ETEC constructs have yielded significant increases in anti-CF antibodies; however overall protection afforded by these vaccines has varied [16–18]. Nevertheless, emerging data suggest that protection can be improved by targeting individual CF fimbrial subunits particularly tip adhesin structures [19, 20].

A variety of different fimbrial, fibrillar, long pilus [21] and small linear fiber [22] colonization factor structures have been described thus far. A formidable challenge to vaccine development based exclusively on colonization factors has been the significant antigenic heterogeneity exhibited by the CFs. Although more than 25 different antigenically distinct CFs have been described to date [23, 24], it has been estimated that approximately 40–50 % of ETEC strains do not make one of these established CFs [25, 26].

1.6 Identification of Novel Vaccine Antigens in ETEC

There is no single method for identification of putative vaccine antigens in ETEC, and the technology for antigen identification is evolving rapidly. The approach outlined here encompasses a variety of complementary methods that are currently being used to

	advantages	limitations
classical genetics	once completed the targets are well identified and characterized	time consuming and labor intensive - requires specialized knowledge
comparative genomics	easy to generate large amounts of data from clinically relevant samples	gene presence and absence provides no information about expression
transcriptomics	global and unbiased methods have been developed that are easy to employ	cost to generate data and use of relevant conditions for virulence not always clear
proteomics	protein data demonstrates that the gene is active and produced	global, high-througput tools are still developing
immunoproteomics	direct evidence for immune reactivity	global, high-througput tools are still developing

Fig. 1 Methodologies employed to identify and characterize potential vaccine antigens for enterotoxigenic *Escherichia coli*

identify and validate candidate vaccine targets for ETEC. As shown in Fig. 1, these include classical genetic approaches, genomics, and whole-genome sequencing, transcriptomics, proteomics, and immunoproteomics using protein microarray technology. Each of these methodologies has specific merits as well as disadvantages to consider in developing antigen discovery platforms.

1.7 Classical Genetic Approaches

Transposon mutagenesis has been widely used in bacterial pathogenesis studies to identify virulence genes involved in pathogen-host interactions. Tn*phoA*, originally introduced by Manoil and Beckwith [27] 30 years ago, has been extensively used for identification of surface antigens in Gram-negative pathogens, including the EatA autotransporter which is secreted by ETEC [28]. Briefly, Tn*phoA* incorporates a truncated version of the gene for alkaline phosphatase (lacking a signal peptide-encoding region) within the Tn5 transposable element. Transposon "hops" which result in gene fusions of *phoA* with those encoding surface antigens can be detected by colony screening on agar containing the antibiotic in the transposon and an alkaline phosphatase indicator. Original versions of Tn*phoA* included the transposase within the transposable element. This occasionally created problems in attempting to clone and sequence the insertions due to subsequent rearrangements or continued transposition. To avoid these problems and to establish a system where insertions could be easily cloned and sequenced, pTnphoA.ts was developed by placing the transposase gene on a temperature-sensitive suicide plasmid outside of the inverted repeats of the Tn5 transposable element [29] (Fig. 2). This temperature-sensitive "plasposon" has been used to identify a number of candidate antigens in ETEC including EtpA [29]. Because the temperature-sensitive origin of replication is contained within the transposed element, the region of insertion can easily be identified by restriction endonuclease digestion and re-ligation of the target DNA into a recombinant temperature-sensitive plasmid for isolation and subsequent sequencing as outlined in the protocol below.

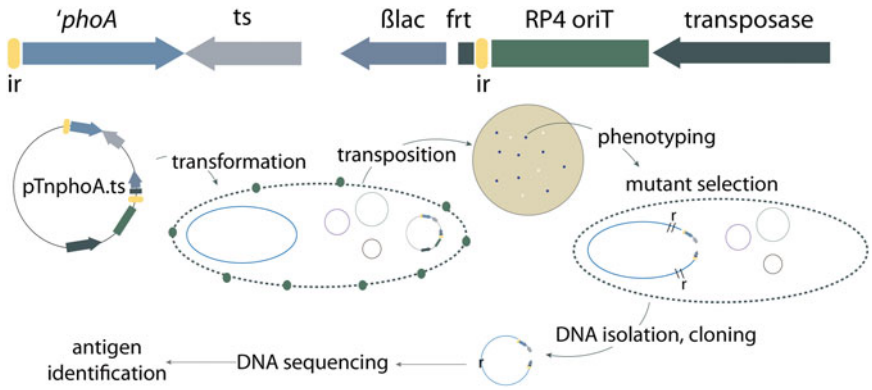

Fig. 2 TnphoA.ts mutagenesis strategy: (*top*) linear plasmid map of pTnphoA.ts. The transposon is shown between the two inverted repeat elements (ir, *yellow*). Within the transposon are a truncated version of the alkaline phosphatase gene (*'phoA*), a temperature-sensitive origin of replication (ts), beta lactamase gene encoding ampicillin resistance (ßlac), and a flp recombinase recognition site (frt). Encoded on the plasmid backbone outside the repeat element are the RP4 transfer locus (RP4 oriT), and the Tn5 transposase gene. Shown below the map are major steps in transposon mutant generation starting with transformation of the recipient strain at permissive temperature (30 °C). Selection for transposition events with productive fusions then takes place at higher temperature under antibiotic and XP (*blue colony*) selection. Resulting colonies can then be tested to identify mutants phenotypically different than the parental ETEC strain. Total genomic DNA (plasmid and chromosome) is then digested with a restriction enzyme that cuts outside of the transposon, re-ligated, and used to transform a laboratory cloning strain to ampicillin resistance at 30 °C. The resulting plasmid can be sequenced from to identify the gene interrupted by transposition, and the corresponding protein can be identified in GenBank

2 Materials

2.1 TnphoA.ts Mutagenesis Materials

1. DH10BT1 (pTnphoA.ts) available from Fleckenstein laboratory.
2. Target ETEC strain.
3. Electroporation apparatus, cuvettes.
4. Ampicillin.
5. Luria agar base: Tryptone (1 %), yeast extract (0.5 %), agar (1.5 %).
6. Luria agar plates containing ampicillin at final concentration of 100 μg/ml.
7. 5-Bromo-4-chloro-3-indolyl-phosphate (*p*-toluidine salt) (XP) prepared as a 20 mg/ml stock solution in N,N-dimethyl-formamide.
8. Gene fusion indicator plates: XP final concentration 40 μg/ml, ampicillin 100 μg/ml (protect from light).
9. Sterile wooden toothpicks.
10. Restriction endonuclease(s), buffer.
11. Genomic DNA preparation kits (e.g., MasterPure DNA Purification Kit, Epicentre).

2.2 In Vitro Analysis Materials

1. Gastrointestinal cell line(s) which support bacterial adhesion and/or toxin delivery assays (*see* Table 3) seeded into 96-well tissue culture plates.
2. Luria broth (LB).
3. Sterile culture tubes (Falcon 2059 or equivalent).
4. Sterile Hanks' Balanced Salt Solution (HBSS) (e.g., Life Technologies or equivalent containing Ca^{2+}, Mg^{2+}).
5. Triton-X-100 [0.1 %] sterile solution in PBS.
6. Luria agar plates.
7. Cyclic nucleotide assay kits.
   (a) cAMP (e.g., Arbor Assays K019).
   (b) cGMP (e.g., Arbor Assays K020).

2.3 In Vivo Intestinal Colonization and Vaccine Testing Materials

1. Strain with antibiotic resistance marker in a permissive location in the genome to facilitate counter selection.
   (jf876 which contains a kanamycin resistance cassette in the *lacZYA* locus that does not contribute to colonization) [13].
2. Mice (adult 5–8-week-old females, e.g., CD-1, Charles River), $n = 20–30$ (at a minimum ten mice will be needed for adjuvant-only controls and ten for adjuvant + vaccine antigen group comparisons).
3. Purified antigen (amount will depend on the route of vaccination).
4. Adjuvant appropriate for route of immunization.
5. Autoclaved food and bedding material.
6. Luria agar culture plates containing antibiotic (e.g., kanamycin (25 μg/ml)).
7. Water containing streptomycin 5 g/L.
8. Famotidine (sterile) for I.P. injection of mice.
9. Saponin 5 % sterile solution in PBS.

3 Methods

3.1 pTnphoA.ts Plasposon Transformation Steps

1. Grow DH10BT1 (pTnphoA.ts) overnight at 30 °C in Luria broth containing ampicillin, 100 μg/ml.
2. Isolate plasmid DNA.
3. Transform target strain by electroporation.
4. Select transformants overnight at 30 °C, on plates containing ampicillin 100 μg/ml.
5. Pool multiple transformants into single tube (e.g., Falcon 2059) containing 2 ml of Luria broth with ampicillin 100 μg/ml.

6. Grow overnight at 30 °C, and dilute 1:2 in glycerol freezing media.
7. Transformant mix can be preserved at –80 °C for future use.

3.2 Generation of TnphoA.ts Mutants

1. Grow transformant mixture or glycerol stock from above at 30 °C overnight in Luria broth containing ampicillin 100 μg/ml.
2. The following morning dilute 1:100 in fresh media (ampicillin 100 μg/ml) and grow with shaking (250 rpm) for 90 min at 30 °C.
3. Plate 100 μl of dilutions (~1:100) onto fresh gene fusion indicator plates and grow at 37 °C overnight.
4. Isolate individual blue colonies from indicator plates with sterile toothpicks and streak-purify onto fresh indicator agar.
5. Incubate at 37 °C overnight.
6. Select isolated, blue colonies for growth overnight in 2 ml of Luria broth containing ampicillin 100 μg/ml.
7. Use 1 ml of overnight culture for isolation of genomic DNA (follow the manufacturer's protocol).
8. Preserve the remaining 1 ml of overnight culture as a frozen glycerol stock.

3.3 TnphoA.ts Mutant Screening

Because the Tn5-based transposition occurs largely at random resulting in the production of (at least) thousands of independent mutants, mutagenesis ideally can be coupled with a relatively high-throughput in vitro phenotypic assay. The results of these phenotypic screening assays can then be used to direct cloning and identification of insertion sites.

3.4 Identification of Transposon Insertion Sites

Because the transposition element contains a temperature-sensitive origin of replication in addition to the beta lactamase gene between the inverted repeats, recovery of DNA regions flanking the insertion is relatively straightforward.

1. Isolate total genomic DNA (plasmid and chromosomal DNA). (Most commercial genomic DNA preparation kits, e.g., Wizard® Genomic DNA Purification, Promega work well with ETEC strains.)
2. Digest an aliquot of genomic DNA with a restriction endonuclease that does not cut between the inverted repeats of the transposon (for instance, *MluI*).
3. Ligate the DNA with T4 DNA ligase.
4. Transform ligation mixture into commercially available ampicillin-sensitive *E. coli cloning strain* (e.g., DH10BT1, DH5α, Top10), selecting on Luria agar containing ampicillin, 100 μg/ml, at 30 °C.

5. Grow isolated ampicillin-resistant colonies in Luria broth overnight at 30 °C.
6. Isolate plasmid DNA using commercially available plasmid preparation kit that yields DNA of sufficient quality for sequencing.
7. Set up separate sequencing reactions with the primers TnphoA.179 (5′-CC ATCCCATCGCCAATCA-3′) and TnphoA.ts1 (5′-CGAAATTAATACGACTCA-3′).
8. Resulting DNA sequence information can then be used in BLASTN or BLASTX program searches of NCBI databases (http://blast.ncbi.nlm.nih.gov/Blast.cgi) to identify potential homologues.

3.5 De Novo Identification of Vaccine Antigens from Whole-Genome Sequences

The cost and time required for sequencing and assembling entire bacterial genomes have declined dramatically since the genome of *Haemophilus influenza* was first assembled now over 20 years ago [30]. This has permitted both the de novo identification of candidate antigens and a recent assessment of the conservation of known antigens and putative vaccine targets in multiple ETEC strains from different geographic regions isolated over time [31].

One approach to the identification of candidate vaccine antigens is the "*in silico*" interrogation of genome sequence data using algorithms or programs that select molecules which have at least a theoretical likelihood of being exposed on the surface of the organism or secreted. These exposed or surface-expressed molecules are at least in principle amenable to neutralization by vaccination. Complex multifactorial investigations involving multiple genomes require training and experience in bioinformatics; however individual genomes can be interrogated using fairly simple Web-based interfaces.

In addition to identification of surface molecules, the approach to characterization of potential novel ETEC vaccine antigens involves an assessment of the degree to which these antigens are unique to ETEC genomes and to which they are shared with commensal strains. By definition, all ETEC strains make at least one of the known toxins (LT, STh, and/or STp). However, there is no other universally shared antigen that is common to all ETEC that is not also represented in the rest of *E. coli* including the nonpathogenic commensal strains that make up a small portion of the microbiome of most humans [32]. The challenge therefore lies in defining appropriate vaccine targets among the population of antigens that are uniquely pathovar/ETEC associated.

1. General approaches to defining potential vaccine antigens from genome data.

   Traditional identification of candidate antigens has relied on empirical microbial pathogenesis studies or genetic techniques

outlined above to define surface features that could be exploited in vaccines. However, with the advent of high-throughput whole-genome sequencing, it is now possible to use "reverse vaccinology" [33, 34] to identify candidate antigens by in silico interrogation of data from multiple ETEC genomes. To some extent, draft or complete genomes can be interrogated by those without specific training in informatics to identify putative vaccine antigens with publicly available Web-based platforms (Table 1). However, application of these and other algorithms on a broader scale, that potentially involves hundreds of genomes, will certainly require more extensive bioinformatic capabilities. Both approaches follow the same general scheme outlined in Fig. 3.

2. Identification of pathovar-specific features.

   The scheme for *in silico* identification of potential candidates essentially involves two main tasks. The first is to identify features of ETEC genomes that are relatively pathovar specific, but which are not shared with commensal *E. coli* strains. A potential pitfall of this analysis is that there are at present a very limited number of true commensal isolates from healthy humans for which DNA sequence data are available (Table 2). Nevertheless, the many *E. coli* genes that provide for essential metabolic functions and core structural elements of these organisms can be digitally subtracted from pathogen genomes. Ideally, candidates would be shared broadly among a diverse population of ETEC. To this end, genome data from several hundred ETEC strains are presently available [11, 31, 35] permitting pan-ETEC genome comparative analyses to identify features that are relatively conserved in this pathovar.

3. Identification of putative vaccine antigens from genome-subtracted data.

   Following the identification of conserved, pathovar-specific features, the next major task is to identify those antigens that are potentially surface expressed, and/or which share features in common with known vaccine antigens using the algorithms outlined in Table 1 and Fig. 3. These approaches are complementary. The inclusion of molecules with motifs or domains conserved in other vaccine antigens permits the investigator to capture putative antigens where surface expression may not be obvious, or alternatively to prioritize antigens that share features with effective vaccine targets.

3.6 Preclinical Antigen Validation In Vivo

3.6.1 General Approach to In Vivo Studies

One of the problems facing investigators hoping to develop effective enteric vaccines is the lack of a small animal model that faithfully recapitulates the nature of the illness in humans. Mice do not develop diarrhea with any of the common enteric pathogens that infect humans, including enterotoxigenic *E. coli*, even at high doses

Table 1

Bioinformatic links applicable to ETEC reverse vaccinology

Name	Predictions	Site URL	Reference(s)
PredictProtein	Subcellular location, protein structure, functional regions	http://ppopen.informatik.tu-muenchen.de/	[59]
SignalP	Signal peptide cleavage sites	http://www.cbs.dtu.dk/services/SignalP/	[60]
SecretomeP	Nonclassical secretion	http://www.cbs.dtu.dk/services/SecretomeP/	[61, 62]
TMHMM	Transmembrane helices	http://www.cbs.dtu.dk/services/TMHMM/	
Tmpred	Transmembrane spanning	http://www.ch.embnet.org/software/TMPRED_form.html	
PSORT	Subcellular localization	http://www.psort.org/psortb/	[63]
CELLO	Subcellular localization	http://cello.life.nctu.edu.tw	[64]
VAXIGN	Multiple target	http://www.violinet.org/vaxign/docs/index.php	[65]
RAST	Genome annotation and comparisons	http://rast.nmpdr.org	[66, 67]
EDGAR	Comparative genomics	https://www.uni-giessen.de/fbz/fb08/bioinformatik/software/EDGAR	[68]
C-Sibelia	Comparative genomics	http://etool.me/software/csibelia	[69]
Pfam	Protein family homology	http://pfam.sanger.ac.uk	[70]
CDD	Conserved domains	http://www.ncbi.nlm.nih.gov/cdd/	[71]
Motif	Functional domains, motifs	http://www.genome.jp/tools/motif/	

that typically cause serious illness in volunteers. Nevertheless, mice do become colonized with ETEC following oral (gavage) challenge with inocula as small as 10^3–10^4 colony-forming units, permitting a straightforward assessment of the impact of vaccination with candidate antigens on intestinal colonization, a critical step in pathogenesis [36]. Studies to date in this model have revealed that colonization of the small intestine is really a very complex phenotype involving a variety of different virulence factors in addition to the fimbrial structures that have been the traditional targets for ETEC vaccines [37–40], thereby affording additional approaches to vaccine development to overcome the limitations of CF-based vaccines. The basic protocol for mouse vaccination studies follows:

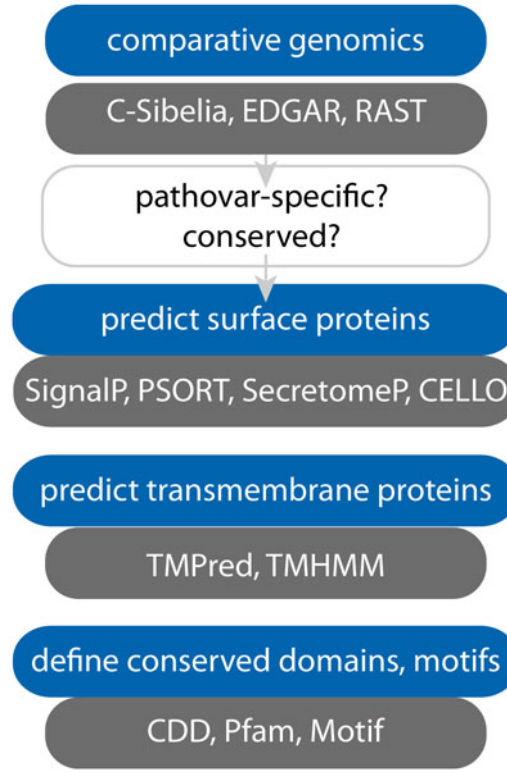

Fig. 3 Algorithms useful in identification and in silico characterization of candidate vaccine antigens

1. (~Day 7) Acquire and acclimate mice (at least 1 week prior to experimentation).
2. (Day 0) Vaccinate mice ($n \geq 10$) with adjuvant and antigen (dose will depend on adjuvant, and route of administration). Vaccinate an equal number with adjuvant-only as control group.
3. (Day 14) Administer first booster vaccination.
4. (Day 28) Administer second booster vaccination.
5. (Day 40) Add streptomycin (5 g/L) to drinking water.
6. (Day 41) Remove streptomycin, and return to regular drinking water. Grow challenge strain overnight.
7. (Day 42) Challenge with ~10^4–10^5 colony-forming units of ETEC by gavage. Plate dilutions of inoculum onto selective media.
8. (Day 43) Sacrifice mice, harvest segments of small intestine in saponin, and plate undiluted, 10^{-1}, 10^{-2}, dilutions onto selective media.
9. Determine cfu/mouse in vaccinated and control groups.

Table 2
Commensal *E. coli* strains with sequenced genomes

Strain designation	NCBI/EMBL accession number(s)	Origin	Reference
HS	NC_009800.1	Healthy adult, USA	[10]
Nissle 1917	CP007799.1	Healthy adult, Germany	[72]
SE11	AP009240.1 (chromosome) AP009241.1 (pSE11-1) AP009242.1 (pSE11-2) AP009243.1 (pSE11-3) AP009244.1 (pSE11-4) AP009245.1 (pSE11-5) AP009246.1 (pSE11-6)	Healthy adult, Japan	[73]
SE15	NC_013654.1(chromosome) NC_013655.1 (plasmid)	Healthy adult, Japan	[74]
EDM1c[a]	ERS155053	Healthy child, Norway	[75]
EDM3c[a]	ERS155049	Healthy child, Norway	
EDM16c[a]	ERS155051	Healthy child, Norway	
EDM70c[a]	ERS155055	Healthy child, Norway	
EDM49c[a]	ERS155056	Healthy child, Norway	
EDM101c[a]	ERS155057	Healthy child, Norway	
EDM106c[a]	ERS155058	Healthy child, Norway	
EDM116c[a]	ERS155052	Healthy child, Norway	
EDM123c[a]	ERS155054	Healthy child, Norway	
EDM530c[a]	ERS155050	Healthy child, Norway	

[a]Draft genomes

3.7 Preclinical Antigen Studies In Vitro

3.7.1 Bacterial Adhesion Assays

Effective interaction with intestinal epithelial cells is a key event in ETEC pathogenesis. Bacterial adhesion assays in which bacteria are added to intestinal epithelial cells cultured in vitro have become a mainstay of ETEC molecular pathogenesis investigations [29, 37, 41–44]. Despite the simplicity of these assays, in which bacteria remaining attached to epithelial cells are quantitated after a finite period of incubation, they have been instrumental in characterizing the role of a number of essential virulence factors, including several different adhesins. Likewise, they have been used in a number of preclinical vaccinology studies, where antibodies raised against specific surface antigens are tested for their ability to mitigate bacterial-host interactions [39, 45, 46]. The basic ETEC adhesion assay follows:

1. Plate target epithelial cell line (e.g., Caco-2) into 96-well tissue culture-treated plates.
2. Incubate at 37 °C, 5 % CO_2 to establish confluent monolayers.
3. Inoculate 2 ml of LB media in 15 ml round-bottom tube with frozen glycerol stock of the ETEC testing strain (e.g., H10407).

4. Incubate overnight at 37 °C, 200 rpm.
5. Dilute 1:100 into 2 ml of fresh LB; grow for ~90′ to mid-logarithmic phase growth.
6. Immediately prior to addition of bacteria, add antibody against target antigen(s).
7. Inoculate tissue culture wells with 1–2 μl of bacteria per well.
8. Return plate to tissue culture incubator for 1 h.
9. During incubation, plate dilutions of inoculum onto Luria agar.
10. After 1 h, remove plate from tissue culture incubator and wash 4–5× with HBSS, 100 μl/well.
11. Lyse epithelial cells with 0.1 % Triton-x-100 for 5 min.
12. Plate dilutions of lysate in PBS onto Luria agar.
13. The following day count inoculum and output colonies.
14. Express results as % cell-associated bacteria (recovered cfu/input cfu × 100).

3.7.2 Toxin Delivery Assays

ETEC delivery of heat-labile and/or heat-stable enterotoxins, which, respectively, activate cAMP and cGMP production in target intestinal epithelial cells, is the *sine qua* nonvirulence feature that defines this pathovar. Therefore, much can be learned in detailed investigation of the molecular events that culminate in bacterial activation of these cyclic nucleotides. In vitro studies using intestinal epithelial cell lines (Table 3) can be used to investigate the efficiency with which mutant strains lacking candidate virulence features deliver LT and/or ST enterotoxin payloads. Consequently, cAMP and cGMP assays also provide a convenient surrogate marker to gauge the effectiveness of antibodies to individual candidate antigens or to a combination of targets [46] in abrogating

Table 3
Gastrointestinal cell lines used to examine ETEC pathogen-host interactions

Cell line	Distinguishing characteristics	ATCC	Toxin response		Reference(s)
			LT	ST	
Caco-2	Polarize	HTB-37	+	+/−	
C2BBe1	Form brush borders	CRL-2102	+	+/−	[76]
LS-174 T	Goblet cell like; abundant MUC2 production	CL-188	−	−	[77]
T84	Polarity	CCL-248	+	+	[78]
HT-29	Blood group A, MUC2	HTB-38	+	−	

ATCC American Type Culture Collection

toxin delivery. A basic protocol for assessing delivery of the respective toxins follows:

1. Plate target epithelial cell line (e.g., Caco-2) into 96-well tissue culture-treated plates.
2. Incubate at 37 °C, 5 % CO_2, to establish confluent monolayers.
3. Inoculate 2 ml of LB media in 15 ml round-bottom tube with frozen glycerol stock of the ETEC testing strain (e.g., H10407).
4. Incubate overnight at 37 °C, 200 rpm.
5. Dilute 1:100 into 2 ml of fresh LB; grow for ~90′ to mid-logarithmic phase growth.
6. Immediately prior to addition of bacteria, add antibody against target antigen(s).
7. Inoculate tissue culture wells with 1–2 μl of bacteria per well.
8. Return plate to tissue culture incubator for ~3 h.
9. Wash three times with pre-warmed tissue culture media.
10. Return to incubator for an additional 2 h.
11. Wash gently with HBSS.
12. Process cells for cyclic nucleotide quantitation following instructions provided in assay.

4 Notes

1. TnphoA.ts mutagenesis notes
   (a) While resident plasmids of ETEC will co-purify with chromosomal DNA in commercial genomic DNA isolation kits, this is not true of commercial plasmid preparation kits. ETEC plasmids are often quite large and do not purify easily with most commercial plasmid kits.
   (b) Re-ligation will generally favor intramolecular ligation; therefore the resulting plasmid should have a single unique restriction site joining the flanking regions. This can be confirmed by restriction endonuclease digestion.
2. Sample strategy: Identification of EtpA as a vaccine antigen.
   The investigation of EtpA as a candidate vaccine antigen to date has involved many of the strategies outlined above. Therefore, in the following section, we use EtpA to illustrate the application of the different bioinformatic algorithms to vaccine candidate selection.
   (a) Identification of conserved, pathovar-specific antigens
      - Comparison of sequence of the large plasmid of ETEC H10407 (p948) (http://www.ncbi.nlm.nih.gov/

nuccore/FN649418.1) with the sequenced genomes of HS, SE11, SE15, and *E. coli* K-12 (MG1655) (e.g., using the singleton method in EDGAR) yields a list of only 33 candidate genes that are not found in any of the commensals or *E. coli* K-12. Included in this list are genes involved in synthesis of the colonization factor antigen CFA/I, the *EtpBAC* operon, and the EatA serine protease autotransporter.

- BLAST-P (http://blast.ncbi.nlm.nih.gov) analysis of EtpA peptide sequence (GenBank accession number AAX13509) identifies many close homologues of EtpA. However, these are strictly confined to ETEC strains that have been sequenced to date. In fact, recent studies suggest that this antigen is relatively conserved in the ETEC pathovar [31]. Conversely, BLAST-P against commensals HS, SE11, SE15, Nissle 1917, or the laboratory isolate MG1655 fails to reveal any significant homology, further suggesting that this particular protein is "pathovar specific."

(b) Examination of potential surface expression: Analysis of the EtpA peptide sequence with each of the cell localization and domain characterization algorithms outlined in Table 1 yields results provided in Table 4. Without prior knowledge of EtpA function, these algorithms would have (correctly) predicted that this protein shares a number of features with filamentous hemagglutinin (FHA), a component of the acellular pertussis vaccine and that similar to FHA it belongs to the two-partner family of secretion

Table 4
EtpA as a prototype molecule in reverse vaccinology algorithms

Program	Result/prediction	Notes/score
Signal-P	No signal peptide identified	–
PredictProtein	Predicted location: secreted	–
Secretome	Secreted	(SecP) 0.939918
Psortb	Extracellular	10.00
CELLO	Extracellular	2.777
Vaxign	Adhesin	via SPAAN [47]
Motif[a]	Multiple domains identified: CDD130956, adhes_NPXG CDD214908, haemagg_act CDD257462, ESPR	Domain description Filamentous hemagglutinin family N-terminal domain Hemagglutination activity domain Extended signal peptide of type V secretion system

[a]Motif searches both CDD and Pfam databases

molecules, which feature atypical extended signal peptides. Like FHA, EtpA is correctly predicted to function as an extracellular adhesin [47] molecule. Collectively, these results suggest that when applied to ETEC, reverse vaccinology approaches have the potential to select novel candidate antigens for downstream validation in vitro and ultimately for vaccine testing in vivo.

3. Refining antigen selection.
   (a) Using immunoproteomics to narrow antigen selection: While the bioinformatics approaches above can offer a list of candidates, the list may be extensive, and additional criteria will likely be needed to refine selection of molecules for further testing as vaccine candidates. Therefore a number of additional modalities have recently been used to highlight key antigens that can be exploited in a vaccine. Previous efforts have combined an examination of the proteome of ETEC with immune responses generated during experimental infection of animals or natural infections in humans to identify novel antigens [48]. A number of antigens that are not currently targeted in ETEC vaccine approaches were identified including the secreted proteins EtpA, EatA, and YghJ, and antigen 43, an autotransporter protein. To date, three of these proteins EtpA, EatA, and antigen 43 have been shown to offer protection against ETEC infection in an animal model [40, 49, 50]. Nevertheless, this approach has a number of very important limitations: (1) it requires fractionation of bacterial samples to separate proteins which are secreted or which localized to the outer membrane; (2) only one strain can be examined at a time; (3) laboratory culture conditions may not reflect those in vivo, impeding identification of proteins which are not optimally expressed or present in low abundance; (4) it is laborious requiring 2D separation of proteins, subsequent identification of immunoreactive spots by immunoblotting, and extraction of the corresponding protein from a parallel sample which is then identified using mass spectrometry.
   (b) Protein microarrays: It is now possible to overcome many of the limitations inherent in the approach outlined above through the use of protein microarrays [51]. These arrays, which have been applied in the investigation of immune responses to diverse pathogens [52–55], offer a number of theoretical advantages. (1) First, they can incorporate features from a number of isolates, thereby coupling bioinformatic analysis of many strains to the printing of key conserved antigens onto the array. (2) It is now possible to synthesize sufficient protein by in vitro transcription-

translation to accomplish high-throughput antigen synthesis needed to construct hundreds of arrays. (3) The relatively small format of these arrays greatly reduces the sample volumes required for analysis of thousands of candidate antigens simultaneously. Several unpublished projects using ETEC-specific protein microarrays show significant promise in profiling protective immune responses to candidate ETEC vaccines, and in assessing responses that follow natural infections. While experimental and natural ETEC infections offer protection against subsequent disease, the mechanistic correlates of protection have not been established. Protein microarrays potentially afford an unbiased approach to finding immunologic signatures associated with protection that can then be mined to prioritize antigens for subsequent vaccine testing.

4. Summary.

Since the discovery of ETEC now more than 40 years ago in individuals with severe cholera-like diarrheal illness [56, 57], vaccine development efforts have largely focused on a small group of plasmid-encoded antigens, namely the colonization factors (CFs). With time, investigators have gained an increased appreciation for the complex valency requirements for vaccines based exclusively on CFs [9, 23] and/or heat-labile toxin [58], stimulating the discovery of additional antigens that could complement existing approaches. A compilation of more than 100 sequenced ETEC genomes provides a very rich dataset to interrogate in pursuit of additional vaccine targets.

Acknowledgements

The work described was supported by Grant Number 2R01AI089894 from the National Institute of Allergy and Infectious Diseases (NIAID), the PATH Enteric Vaccine Initiative (EVI), the Bill and Melinda Gates Foundation (OPP1099494), and the Department of Veterans Affairs. Its contents are solely the responsibility of the authors and do not necessarily represent the official views of the funding agencies.

References

1. Kotloff KL, Nataro JP, Blackwelder WC, Nasrin D et al (2013) Burden and aetiology of diarrhoeal disease in infants and young children in developing countries (the Global Enteric Multicenter Study, GEMS): a prospective, case–control study. Lancet 382:209–222
2. Fleckenstein JM, Hardwidge PR, Munson GP, Rasko DA, Sommerfelt H, Steinsland H (2010) Molecular mechanisms of enterotoxigenic *Escherichia coli* infection. Microbes Infect 12:89–98
3. Cheng SH, Rich DP, Marshall J, Gregory RJ, Welsh MJ, Smith AE (1991) Phosphorylation of the R domain by cAMP-dependent protein kinase regulates the CFTR chloride channel. Cell 66:1027–1036

4. Vaandrager AB, Smolenski A, Tilly BC, Houtsmuller AB et al (1998) Membrane targeting of cGMP-dependent protein kinase is required for cystic fibrosis transmembrane conductance regulator Cl- channel activation. Proc Natl Acad Sci U S A 95:1466–1471
5. Golin-Bisello F, Bradbury N, Ameen N (2005) STa and cGMP stimulate CFTR translocation to the surface of villus enterocytes in rat jejunum and is regulated by protein kinase G. Am J Physiol Cell Physiol 289:C708–C716
6. Chao AC, de Sauvage FJ, Dong YJ, Wagner JA, Goeddel DV, Gardner P (1994) Activation of intestinal CFTR Cl- channel by heat-stable enterotoxin and guanylin via cAMP-dependent protein kinase. EMBO J 13(5):1065–1072
7. Crossman LC, Chaudhuri RR, Beatson SA, Wells TJ, Desvaux M et al (2010) A commensal gone bad: complete genome sequence of the prototypical enterotoxigenic *Escherichia coli* strain H10407. J Bacteriol 192:5822–5831
8. Wolf MK (1997) Occurrence, distribution, and associations of O and H serogroups, colonization factor antigens, and toxins of enterotoxigenic *Escherichia coli*. Clin Microbiol Rev 10:569–584
9. Peruski LF Jr, Kay BA, El-Yazeed RA, El-Etr SH et al (1999) Phenotypic diversity of enterotoxigenic *Escherichia coli* strains from a community-based study of pediatric diarrhea in periurban Egypt. J Clin Microbiol 37:2974–2978
10. Rasko DA, Rosovitz MJ, Myers GS, Mongodin EF, Fricke WF et al (2008) The pangenome structure of *Escherichia coli*: comparative genomic analysis of *E. coli* commensal and pathogenic isolates. J Bacteriol 190:6881–6893
11. von Mentzer A, Connor TR, Wieler LH, Semmler T et al (2014) Identification of enterotoxigenic *Escherichia coli* (ETEC) clades with long-term global distribution. Nat Genet 46:1321–1326
12. Touchon M, Hoede C, Tenaillon O, Barbe V et al (2009) Organised genome dynamics in the *Escherichia coli* species results in highly diverse adaptive paths. PLoS Genet 5(1), e1000344
13. Dorsey FC, Fischer JF, Fleckenstein JM (2006) Directed delivery of heat-labile enterotoxin by enterotoxigenic *Escherichia coli*. Cell Microbiol 8:1516–1527
14. Tacket CO, Losonsky G, Link H, Hoang Y, Guesry P, Hilpert H, Levine MM (1988) Protection by milk immunoglobulin concentrate against oral challenge with enterotoxigenic *Escherichia coli*. N Engl J Med 318:1240–1243
15. Freedman DJ, Tacket CO, Delehanty A, Maneval DR, Nataro J, Crabb JH (1998) Milk immunoglobulin with specific activity against purified colonization factor antigens can protect against oral challenge with enterotoxigenic *Escherichia coli*. J Infect Dis 177:662–667
16. McKenzie R, Darsley M, Thomas N, Randall R et al (2008) A double-blind, placebo-controlled trial to evaluate the efficacy of PTL-003, an attenuated enterotoxigenic *E. coli* (ETEC) vaccine strain, in protecting against challenge with virulent ETEC. Vaccine 26:4731–4739
17. Darsley MJ, Chakraborty S, Denearing B, Sack DA et al (2012) ACE527 oral, live attenuated ETEC vaccine reduces the incidence and severity of diarrhea in a human challenge model of diarrheal disease. Clin Vaccine Immunol 19:1921–1931
18. Sack DA, Shimko J, Torres O, Bourgeois AL et al (2007) Randomised, double-blind, safety and efficacy of a killed oral vaccine for enterotoxigenic *E. coli* diarrhoea of travellers to Guatemala and Mexico. Vaccine 25: 4392–4400
19. Li YF, Poole S, Rasulova F, McVeigh AL, Savarino SJ, Xia D (2007) A receptor-binding site as revealed by the crystal structure of CfaE, the colonization factor antigen I fimbrial adhesin of enterotoxigenic *Escherichia coli*. J Biol Chem 282:23970–23980
20. Li YF, Poole S, Nishio K, Jang K et al (2009) Structure of CFA/I fimbriae from enterotoxigenic *Escherichia coli*. Proc Natl Acad Sci U S A 106:10793–10798
21. Giron JA, Levine MM, Kaper JB (1994) Longus: a long pilus ultrastructure produced by human enterotoxigenic *Escherichia coli*. Mol Microbiol 12:71–82
22. Roy SP, Rahman MM, Yu XD, Tuittila M, Knight SD, Zavialov AV (2012) Crystal structure of enterotoxigenic *Escherichia coli* colonization factor CS6 reveals a novel type of functional assembly. Mol Microbiol 86:1100–1115
23. Isidean SD, Riddle MS, Savarino SJ, Porter CK (2011) A systematic review of ETEC epidemiology focusing on colonization factor and toxin expression. Vaccine 29:6167–6178
24. Del Canto F, Botkin DJ, Valenzuela P, Popov V et al (2012) Identification of the Coli Surface Antigen 23 (CS23), a novel adhesin of enterotoxigenic *Escherichia coli*. Infect Immun 80:2791–2801
25. Rockabrand DM, Shaheen HI, Khalil SB, Peruski LF Jr, Rozmajzl PJ et al (2006) Enterotoxigenic *Escherichia coli* colonization factor types collected from 1997 to 2001 in US military personnel during operation Bright Star in northern Egypt. Diagn Microbiol Infect Dis 55:9–12

26. Peruski LF Jr, Kay BA, El-Yazeed RA, El-Etr SH, Cravioto A et al (1999) Phenotypic diversity of enterotoxigenic *Escherichia coli* strains from a community-based study of pediatric diarrhea in periurban Egypt. J Clin Microbiol 37:2974–2978
27. Manoil C, Beckwith J (1985) TnphoA: a transposon probe for protein export signals. Proc Natl Acad Sci U S A 82:8129–8133
28. Patel SK, Dotson J, Allen KP, Fleckenstein JM (2004) Identification and molecular characterization of EatA, an autotransporter protein of enterotoxigenic *Escherichia coli*. Infect Immun 72:1786–1794
29. Fleckenstein JM, Roy K, Fischer JF, Burkitt M (2006) Identification of a two-partner secretion locus of enterotoxigenic *Escherichia coli*. Infect Immun 74:2245–2258
30. Fleischmann RD, Adams MD, White O, Clayton RA, Kirkness EF et al (1995) Whole-genome random sequencing and assembly of *Haemophilus influenzae* Rd. Science 269:496–512
31. Luo Q, Qadri F, Kansal R, Rasko DA, Sheikh A, Fleckenstein JM (2015) Conservation and immunogenicity of novel antigens in diverse isolates of enterotoxigenic *Escherichia coli*. PLoS Negl Trop Dis 9(1), e0003446
32. Human Microbiome Project C (2012) Structure, function and diversity of the healthy human microbiome. Nature 486:207–214
33. De Gregorio E, Rappuoli R (2014) From empiricism to rational design: a personal perspective of the evolution of vaccine development. Nat Rev Immunol 14:505–514
34. Rinaudo CD, Telford JL, Rappuoli R, Seib KL (2009) Vaccinology in the genome era. J Clin Invest 119:2515–2525
35. Sahl JW, Steinsland H, Redman JC, Angiuoli SV, Nataro JP, Sommerfelt H, Rasko DA (2011) A comparative genomic analysis of diverse clonal types of enterotoxigenic *Escherichia coli* reveals pathovar-specific conservation. Infect Immun 79:950–960
36. Allen KP, Randolph MM, Fleckenstein JM (2006) Importance of heat-labile enterotoxin in colonization of the adult mouse small intestine by human enterotoxigenic *Escherichia coli* strains. Infect Immun 74:869–875
37. Sheikh A, Luo Q, Roy K, Shabaan S, Kumar P, Qadri F, Fleckenstein JM (2014) Contribution of the highly conserved EaeH surface protein to enterotoxigenic *Escherichia coli* pathogenesis. Infect Immun 82:3657–3666
38. Roy K, Hamilton D, Allen KP, Randolph MP, Fleckenstein JM (2008) The EtpA exoprotein of enterotoxigenic *Escherichia coli* promotes intestinal colonization and is a protective antigen in an experimental model of murine infection. Infect Immun 76:2106–2112
39. Luo Q, Kumar P, Vickers TJ, Sheikh A, Lewis WG, Rasko DA, Sistrunk J, Fleckenstein JM (2014) Enterotoxigenic *Escherichia coli* secretes a highly conserved mucin-degrading metalloprotease to effectively engage intestinal epithelial cells. Infect Immun 82:509–521
40. Kumar P, Luo Q, Vickers TJ, Sheikh A, Lewis WG, Fleckenstein JM (2014) EatA, an immunogenic protective antigen of enterotoxigenic *Escherichia coli*, degrades intestinal mucin. Infect Immun 82:500–508
41. Fleckenstein JM, Holland JT, Hasty DL (2002) Interaction of an outer membrane protein of enterotoxigenic *Escherichia coli* with cell surface heparan sulfate proteoglycans. Infect Immun 70:1530–1537
42. Roy K, Kansal R, Bartels SR, Hamilton DJ, Shaaban S, Fleckenstein JM (2011) Adhesin degradation accelerates delivery of heat-labile toxin by enterotoxigenic *Escherichia coli*. J Biol Chem 286:29771–29779
43. Fleckenstein JM, Kopecko DJ, Warren RL, Elsinghorst EA (1996) Molecular characterization of the tia invasion locus from enterotoxigenic *Escherichia coli*. Infect Immun 64:2256–2265
44. Roy K, Hilliard GM, Hamilton DJ, Luo J, Ostmann MM, Fleckenstein JM (2009) Enterotoxigenic *Escherichia coli* EtpA mediates adhesion between flagella and host cells. Nature 457:594–598
45. Sheikh A, Luo Q, Roy K, Shaaban S, Kumar P, Fleckenstein JM (2014) Contribution of the highly conserved EaeH surface protein to enterotoxigenic *Escherichia coli* pathogenesis. Infect Immun 82:3657–3666
46. Roy K, Hamilton DJ, Fleckenstein JM (2012) Cooperative role of antibodies against heat-labile toxin and the EtpA Adhesin in preventing toxin delivery and intestinal colonization by enterotoxigenic *Escherichia coli*. Clin Vaccine Immunol 19:1603–1608
47. Sachdeva G, Kumar K, Jain P, Ramachandran S (2005) SPAAN: a software program for prediction of adhesins and adhesin-like proteins using neural networks. Bioinformatics 21:483–491
48. Roy K, Bartels S, Qadri F, Fleckenstein JM (2010) Enterotoxigenic *Escherichia coli* elicits immune responses to multiple surface proteins. Infect Immun 78:3027–3035
49. Roy K, Hamilton D, Ostmann MM, Fleckenstein JM (2009) Vaccination with EtpA glycoprotein or flagellin protects against colonization with enterotoxigenic *Escherichia coli* in a murine model. Vaccine 27:4601–4608

50. Harris JA, Roy K, Woo-Rasberry V, Hamilton DJ, Kansal R, Qadri F, Fleckenstein JM (2011) Directed evaluation of enterotoxigenic *Escherichia coli* autotransporter proteins as putative vaccine candidates. PLoS Negl Trop Dis 5(12), e1428
51. Davies DH, Liang X, Hernandez JE, Randall A et al (2005) Profiling the humoral immune response to infection by using proteome microarrays: high-throughput vaccine and diagnostic antigen discovery. Proc Natl Acad Sci U S A 102:547–552
52. Crompton PD, Kayala MA, Traore B, Kayentao K et al (2010) A prospective analysis of the Ab response to *Plasmodium falciparum* before and after a malaria season by protein microarray. Proc Natl Acad Sci U S A 107:6958–6963
53. Liang L, Juarez S, Nga TV, Dunstan S et al (2013) Immune profiling with a *Salmonella Typhi* antigen microarray identifies new diagnostic biomarkers of human typhoid. Sci Rep 3:1043
54. Lee SJ, Liang L, Juarez S, Nanton MR et al (2012) Identification of a common immune signature in murine and human systemic Salmonellosis. Proc Natl Acad Sci U S A 109:4998–5003
55. Felgner PL, Kayala MA, Vigil A, Burk C, Nakajima-Sasaki R et al (2009) A *Burkholderia pseudomallei* protein microarray reveals serodiagnostic and cross-reactive antigens. Proc Natl Acad Sci U S A 106:13499–13504
56. Sack RB (2011) The discovery of cholera-like enterotoxins produced by *Escherichia coli* causing secretory diarrhoea in humans. Indian J Med Res 133:171–180
57. Sack RB, Gorbach SL, Banwell JG, Jacobs B, Chatterjee BD, Mitra RC (1971) Enterotoxigenic *Escherichia coli* isolated from patients with severe cholera-like disease. J Infect Dis 123:378–385
58. Riddle MS, Savarino SJ (2013) Moving beyond a heat-labile enterotoxin-based vaccine against enterotoxigenic *Escherichia coli*. Lancet Infect Dis 14:174–175
59. Yachdav G, Kloppmann E, Kajan L, Hecht M, Goldberg T et al (2014) PredictProtein—an open resource for online prediction of protein structural and functional features. Nucleic Acids Res 42(Web Server issue):W337–W343
60. Petersen TN, Brunak S, von Heijne G, Nielsen H (2011) SignalP 4.0: discriminating signal peptides from transmembrane regions. Nat Methods 8:785–786
61. Bendtsen JD, Jensen LJ, Blom N, Von Heijne G, Brunak S (2004) Feature-based prediction of non-classical and leaderless protein secretion. Protein Eng Des Sel 17:349–356
62. Bendtsen JD, Kiemer L, Fausboll A, Brunak S (2005) Non-classical protein secretion in bacteria. BMC Microbiol 5:58
63. Yu NY, Wagner JR, Laird MR, Melli G, Rey S et al (2010) PSORTb 3.0: improved protein subcellular localization prediction with refined localization subcategories and predictive capabilities for all prokaryotes. Bioinformatics 26:1608–1615
64. Yu CS, Lin CJ, Hwang JK (2004) Predicting subcellular localization of proteins for Gram-negative bacteria by support vector machines based on n-peptide compositions. Protein Sci 13:1402–1406
65. He Y, Xiang Z, Mobley HL (2010) Vaxign: the first web-based vaccine design program for reverse vaccinology and applications for vaccine development. J Biomed Biotechnol 2010:297505
66. Aziz RK, Bartels D, Best AA, DeJongh M, Disz T, Edwards RA et al (2008) The RAST Server: rapid annotations using subsystems technology. BMC Genomics 9:75
67. Brettin T, Davis JJ, Disz T, Edwards RA, Gerdes S et al (2015) RASTtk: a modular and extensible implementation of the RAST algorithm for building custom annotation pipelines and annotating batches of genomes. Sci Rep 5:8365
68. Blom J, Albaum SP, Doppmeier D, Puhler A, Vorholter FJ, Zakrzewski M, Goesmann A (2009) EDGAR: a software framework for the comparative analysis of prokaryotic genomes. BMC Bioinformatics 10:154
69. Minkin I, Pham H, Starostina E, Vyahhi N, Pham S (2013) C-Sibelia: an easy-to-use and highly accurate tool for bacterial genome comparison. F1000Res 2:258
70. Finn RD, Bateman A, Clements J, Coggill P et al (2014) Pfam: the protein families database. Nucleic Acids Res 42(Database issue): D222–D230
71. Marchler-Bauer A, Zheng C, Chitsaz F, Derbyshire MK et al (2013) CDD: conserved domains and protein three-dimensional structure. Nucleic Acids Res 41(Database issue): D348–D352
72. Grozdanov L, Raasch C, Schulze J, Sonnenborn U et al (2004) Analysis of the genome structure of the nonpathogenic probiotic *Escherichia coli* strain Nissle 1917. J Bacteriol 186: 5432–5441
73. Oshima K, Toh H, Ogura Y, Sasamoto H, Morita H et al (2008) Complete genome sequence and comparative analysis of the wild-type commensal *Escherichia coli* strain SE11 isolated from a healthy adult. DNA Res 15:375–386

74. Toh H, Oshima K, Toyoda A, Ogura Y, Ooka T et al (2010) Complete genome sequence of the wild-type commensal *Escherichia coli* strain SE15, belonging to phylogenetic group B2. J Bacteriol 192:1165–1166
75. de Muinck EJ, Lagesen K, Afset JE, Didelot X et al (2013) Comparisons of infant *Escherichia coli* isolates link genomic profiles with adaptation to the ecological niche. BMC Genomics 14:81
76. Peterson MD, Mooseker MS (1992) Characterization of the enterocyte-like brush border cytoskeleton of the C2BBe clones of the human intestinal cell line, Caco-2. J Cell Sci 102(Pt 3):581–600
77. Tom BH, Rutzky LP, Jakstys MM, Oyasu R, Kaye CI, Kahan BD (1976) Human colonic adenocarcinoma cells. I. Establishment and description of a new line. In Vitro 12:180–191
78. Dharmsathaphorn K, McRoberts JA, Mandel KG, Tisdale LD, Masui H (1984) A human colonic tumor cell line that maintains vectorial electrolyte transport. Am J Physiol 246(2 Pt 1):G204–G208

Chapter 20

Design and Purification of Subunit Vaccines for Prevention of *Clostridium difficile* Infection

Jerzy Karczewski, Jean-Luc Bodmer, James C. Cook, Rachel F. Xoconostle, Debbie D. Nahas, Joseph G. Joyce, Jon H. Heinrichs, and Susan Secore

Abstract

Clostridium difficile is a gram-positive bacterium responsible for a large proportion of nosocomial infections in the developed world. *C. difficile* secretes toxins A and B (TcdA and TcdB) and both toxins act synergistically to induce a spectrum of pathological responses in infected individuals ranging from pseudomembranous colitis to *C. difficile*-associated diarrhea. Toxins A and B have been actively investigated as components of prophylactic vaccine as well as targets for therapeutic intervention with antibodies. Expression of such toxins by recombinant technology is often difficult and may require special handling and adherence to strict safety regulations during the manufacturing process due to the inherent toxicity of the proteins. Both toxins are large proteins (308 kDa and 270 kDa, respectively) and contain distinct domains mediating cell attachment, cellular translocation, and enzymatic (glucosidase) activity. Here we describe methods to produce fragments of Toxin B for their subsequent evaluation as components of experimental *C. difficile* vaccines. Methods presented include selection of fragments encompassing distinct functional regions of Toxin B, purification methods to yield high quality proteins, and analytical evaluation techniques. The approach presented focuses on Toxin B but could be applied to the other component, Toxin A, and/or to any difficult to express or toxic protein.

Key words *E. coli*, Recombinant subunit vaccine, *Clostridium difficile*, Protein purification, Immobilized metal affinity chromatography (IMAC), His-tag, Anion exchange chromatography, Clostridial toxin

1 Introduction

Recombinant protein expression systems offer a very powerful method to produce novel vaccines. Several recombinant vaccines are currently marketed, including Recombivax®-(Hepatitis B vaccine), Gardasil®, Cervarix® (HPV vaccines), Trumenba®, Bexsero® (meningococcal group B vaccines), FluBlock® (Influenza vaccine), and other candidate subunit vaccines which are in various stages of clinical and preclinical evaluation [1–4]. The major advantage of

Sunil Thomas (ed.), *Vaccine Design: Methods and Protocols: Volume 1: Vaccines for Human Diseases*, Methods in Molecular Biology, vol. 1403, DOI 10.1007/978-1-4939-3387-7_20, © Springer Science+Business Media New York 2016

the use of recombinant technology during the vaccine discovery phase is an ability to express multiple antigens or their fragments in parallel and produce these antigens in a quantity and quality adequate for in vivo evaluation. In this chapter we describe methods for the design and production of recombinant antigen fragments of a bacterial toxin allowing their evaluation as components of an experimental vaccine [5]. Toxin B was chosen in part because a substantial knowledge existed about the role of this protein in *C. difficile* infection which supports its selection as a candidate for vaccine development, but also because of the structural complexity and distinct functional domains within the molecule [6, 7]. Toxin B is a large, multi-domain protein composed of an N-terminal enzymatic domain (GTD) which contains the toxin's glucosidase activity, a cysteine protease domain (CPD), a translocation domain (TD), and a repetitive binding region referred to as the combined repetitive oligopeptide (CROPs) domain at the C terminal end (Fig. 1). To examine the contribution of each domain in the induction of a desired immune response, we expressed several fragments representing each domain (Fig. 1), including the N terminal enzymatic domain (GTD), several fragments encompassing the C terminal CROPs (B0, B1, B2, B3, B4) [8] as well as a near-full length molecule encompassing the complete sequence except for the deletion of the enzymatic domain (TC). All fragments except ED were expressed as wild type sequences. To reduce the enzymatic

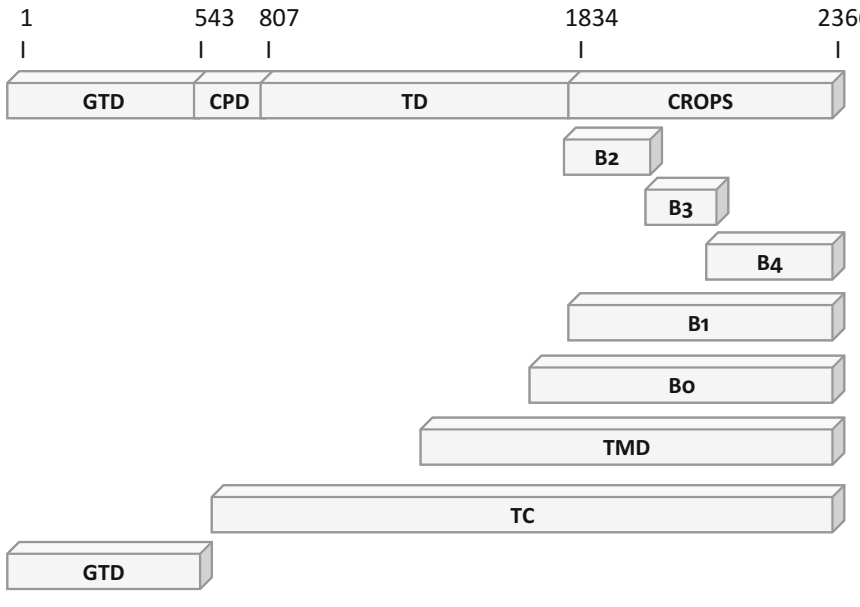

Fig. 1 Schematic diagram of Toxin B domains and fragments selected for expression and purification. A series of peptides representative of each functional domain of Toxin B were selected. TC-complete sequence except for the deletion of the enzymatic domain, GTD-enzymatic domain, CPD-cysteine protease domain, TD-translocation domain, CROPS-combined repetitive oligopeptide

activity of GTD and its associated cytotoxicity, four residues in this fragment were mutated: W102A, D288A, E515Q, and S518A [6, 9, 10].

Synthetic genes encoding each fragment were synthesized (DNA2.0, Menlo Park, CA) (*see* **Note 1**). Flanking *Nde*I and *Xho*I restriction sites were added to the sequences to facilitate cloning into the *E. coli* expression vector pET-30a (Novagen). All sequences were evaluated for the presence of additional *Nde*I or *Xho*I sites and any unwanted sites were excluded from the final sequence through alteration of the DNA sequence prior to synthesis, while ensuring these changes did not alter the encoded protein sequence. A C-terminal hexahistidine (6-His) tag to facilitate downstream purification was encoded by the expression vector and therefore a stop codon was not incorporated into the optimized sequences. All DNA sequences were optimized for expression in *E. coli* [11].

The advantages of bacterial expression include rapid growth, scalability, and availability of a broad array of tools and strategies for cloning and expression of heterologous proteins [12]. Disadvantages include absence of mechanisms for posttranslational modification, occasional erroneous disulfide bond pairing leading to formation of inclusion bodies containing mis-folded product and in some cases expression of proteins prone to precipitation during the purification process. Expression of large and complex proteins may be challenging, as we observed during our initial attempts to produce full length native Toxin B and its larger fragments [5].

Expression of each protein fragment was first evaluated in small scale fermentation and selected clones were expanded to 1 L cultures. Cells were collected by centrifugation, lysed, and the soluble fraction was fractionated by a two-step purification process, using immobilized metal affinity chromatography (IMAC) followed by anion exchange chromatography. Biochemical and biophysical assessment of purified proteins included SDS/PAGE, western blot analysis and analytical size exclusion chromatography. Purity of the final products, DNA contamination and purification step yields were calculated from SDS/PAGE and UV spectral data. The in vivo evaluation of purified antigens as candidate vaccines in the golden Syrian hamster model of *C. difficile* disease was published in Ref. [5].

2 Materials

2.1 Molecular Biology Reagents

1. Expression plasmid pET30a vector (EMD Millipore, Billerica, MA).
2. Calf intestinal alkaline phosphatase (New England Biolabs).
3. 1 % agarose gels containing TAE plus ethidium bromide (EmbiTec, San Diego, CA).

4. QIAquick Gel Extraction Kit (Qiagen, Hilden, Germany).
5. Quick Ligase (New England Biolabs).
6. DH10B competent cells (Invitrogen, Grand Island, NY).
7. Luria Broth (LB) containing kanamycin (30 μg/ml) agar plates (Teknova, Hollister, CA).
8. TAE (100 ml 10× TAE (Invitrogen) diluted in 900 ml distilled water).
9. Luria broth (LB) (Teknova).
10. 50 mg/ml kanamycin (Teknova, Hollister, CA).
11. QIAprep Spin Miniprep Kit (Qiagen, Hilden, Germany).
12. BLR(DE3) competent *E. coli* (EMD Millipore, Billerica, MA).
13. 100 mM isopropyl β-D-1-thiogalactopyranoside (IPTG) (Teknova, Hollister, CA) in distilled water.

2.2 Bacterial Growth Media and Buffers

1. Luria Broth (LB), Sigma-Aldrich, St. Louis, MO.
2. LB-kanamycin, 30 μg/ml kanamycin in LB.
3. Extraction buffer, 50 mM Tris, pH 8.0, 300 mM NaCl, 20 mM imidazole plus one tablet of protease inhibitor cocktail Complete® (Roche Diagnostics, Mannheim, Germany) per 50 ml of extract and 2500 units of nuclease (Benzonase®, EMD Chemicals, Gibbstown, NJ).
4. IMAC buffer A, 50 mM Tris-HCl, pH 8.0, 300 mM NaCl, 20 mM imidazole.
5. IMAC wash buffer, 50 mM Tris, pH 8.0, 300 mM NaCl, 60 mM imidazole.
6. IMAC Buffer B, 50 mM Tris, pH 8.0, 300 mM NaCl, 500 mM imidazole.
7. AEX Buffer A, 20 mM Tris, pH 7.4.
8. AEX Buffer B, 20 mM Tris, pH 7.4, 1 M NaCl.

2.3 Protein Purification

1. IMAC HiTrap™ HP column (GE Healthcare Biosciences Corp. Piscataway, NJ).
2. 6 ml Resource Q anion exchange column (GE Healthcare Biosciences Corp. Piscataway, NJ).
3. NuPAGE® Novex® 4–12 % Bis-Tris Gels (Life Technologies, Grand Island, NY).
4. NuPAGE SDS MES running buffer (Life Technologies).
5. NuPAGE® LDS 4× Sample Buffer (Life Technologies).
6. Coomassie SimplyBlue SafeStain (Life Technologies).
7. iBlot® Transfer Stack (Nitrocellulose, Life Technologies).
8. Blocking solution, PBS, 0.1 % Tween 20, 5 % skim milk.

9. Primary antibody (anti 6×HIS or Toxin B monoclonal antibody (Clone 5A8-E11, Novus)).
10. TBS-T, TBS, 0.1 % Tween 20.
11. 2nd antibody (Goat Anti-Mouse IgG, whole molecule–Alkaline Phosphatase, Sigma-Aldrich).
12. 1-Step NBT/BCIP Solution (Thermo Fisher Scientific Inc., Rockford, IL).

2.4 Equipment

1. Akta Purifier (GE Healthcare Biosciences Corp. Piscataway, NJ).
2. NanoDrop™ ND-2000c Spectrophotometer (Cole Palmer).
3. NuPAGE® Novex® Gel Electrophoresis system (Life Technologies, Grand Island, NY).
4. iBlot® Dry Blotting System (Life Technologies, Grand Island, NY).
5. SNAP i.d.® Protein Detection System (EMD Millipore, Billerica, MA).
6. Microfluidizer (Model 110Y, Microfluidics Corp. Newton, MA).

3 Methods

3.1 DNA Cloning

1. Digest 0.5 μg each of the codon optimized gene and pET30a vector separately with 10 units *Xho*I and *Nde*I for 3 h at 37 °C. Next add 1 μl calf intestinal alkaline phosphatase to the pET30a digest and incubate at 37 °C for 30 min.
2. Isolate restriction digest products by gel electrophoresis using 1 % agarose gels in TAE containing ethidium bromide. Divide each sample evenly between two wells. Perform electrophoresis at 200 V for 45 min. Visualize DNA using a long wave UV light box. Extract desired bands from the gel using no.11 disposable scalpels. Transfer isolated fragments to a Falcon 5 ml polypropylene tube and store at −20 °C.
3. Perform DNA purification from agarose using Qiagen's QIAquick Gel Extraction Kit according to the manufacturer's instructions.
4. Perform ligations using New England Biolabs quick ligase. Add 200 ng of pET30a to a threefold molar excess of insert in a 1.5 ml microtube. Add 5 μl 2× Quick Ligation reaction mix and 1 μl Quick T4 ligase to the 10 μl reactions. Continue reaction at room temperature for 1–2 h. Store reaction products at 4 °C.
5. Transform ligations into DH10B competent cells. Thaw competent cells on ice. Add 50 μl DH10B cells and 2 μl of the ligation reaction to a pre-chilled 15 ml Falcon polypropylene tube. Incubate on ice for 30 min. Heat shock cells at 42 °C for

30 s. Incubate cells on ice 2 min and then add 450 μl of SOC and incubate at 37 °C shaking at 250 rpm for 1 h. Streak 20 μl and 100 μl of transformation mix on LB Agar Kan-30 plates and incubate overnight at 37 °C.

6. Plasmid screening: Pick 12 individual colonies using a 200 μl pipettor and 200 μl filter tips and add to 4 ml LB broth containing 30 μg/ml kanamycin in 15 ml polypropylene tubes. Incubate cultures overnight at 37 °C with shaking at 250 rpm.
7. Isolate plasmid DNA from 4 ml minipreps using Qiagen Qiaprep spin minipreps kit. Screen purified plasmids by restriction digest with *Nde*I and *Xho*I following the procedure in **steps 1** and **2**.
8. Select plasmids showing the correct restriction pattern and confirm by sequencing.
9. Upon sequence verification, transform 1 μl of plasmid into the BLR(DE3) competent *E. coli* as in 5 (20 μl BLR(DE3) and 100 μl SOC media). Spread 20 μl of the transformation mix on an LB-kanamycin plate, incubate at 37 °C overnight.

3.2 Protein Expression

1. Seed cultures: Inoculate 50 ml LB containing 30 μg/ml kanamycin with a single colony and place in 250 ml baffled flasks. Incubate cultures overnight at 37 °C, with shaking at 250 rpm (*see* **Note 2**).
2. Production cultures: The next day, add 600 ml LB containing 30 μg/ml kanamycin to 2 L baffled flasks. Inoculate flasks with 6 ml of the seed culture.
3. Incubate cultures at 37 °C, 250 rpm until an OD600 reaches 0.8, about 3 h. Add 6 ml of 100 mM IPTG to induce expression. Incubate cultures for 3 h at 37 °C, 250 rpm shaking (*see* **Note 3**).
4. Harvest cell paste by centrifugation at 10,000 × *g* for 10 min and store at −70 °C.

3.3 Extraction and Purification of Recombinant Antigens

1. Weigh out 100 g of cell paste.
2. Thaw on ice, add 500 ml (five volumes to generate a 20 % slurry) of extraction buffer.
3. Homogenize using a Polytron (or equivalent blender).
4. Pass three times through a Microfluidizer, after each pass cool extract on ice.
5. Clarify by centrifugation at 10,000 × *g* for 30 min, 4 °C, and collect supernatant (*see* **Note 4**).
6. Filter supernatant through a 0.22 μm filter unit, collect the filtrate.
7. Prepare the IMAC column (such as a HiTrap HP), selecting appropriate size for expected amount of target protein. Typical

binding capacity of this column is ~40 mg histidine-tagged protein/ml medium when charged with Ni^{2+}. In most cases, one 5 ml HiTrap IMAC column will be sufficient. The capacity of the IMAC capture step can be increased by connecting additional HiTrap columns in series (up to three columns). During equilibration, loading, and elution, maintain a flow rate of 5 ml/min (flow velocity = 170 cm/h, residence time = 0.88 min). Monitor backpressure and do not exceed 0.5 MPa (70 psi). Charge the column with 100 mM $NiSO_4$, then wash with distilled H_2O and equilibrate in IMAC Buffer A.

8. Load the sample at 5 ml/min and wash with IMAC Buffer A for 10 column volumes.
9. Remove weakly bound impurities by washing with IMAC Wash Buffer, collect eluted material (fraction X1) and then elute product using a linear gradient of 60–500 mM imidazole (IMAC Buffer B) in 20 min (20 column volumes), collect fractions. In most cases, His-tagged protein will elute around 250–350 mM imidazole and will be relatively homogenous (Fig. 2a) (*see* **Note 5**).
10. Analyze chromatographic fractions by SDS/PAGE and pool fractions containing the majority of target protein (Fig. 2b).

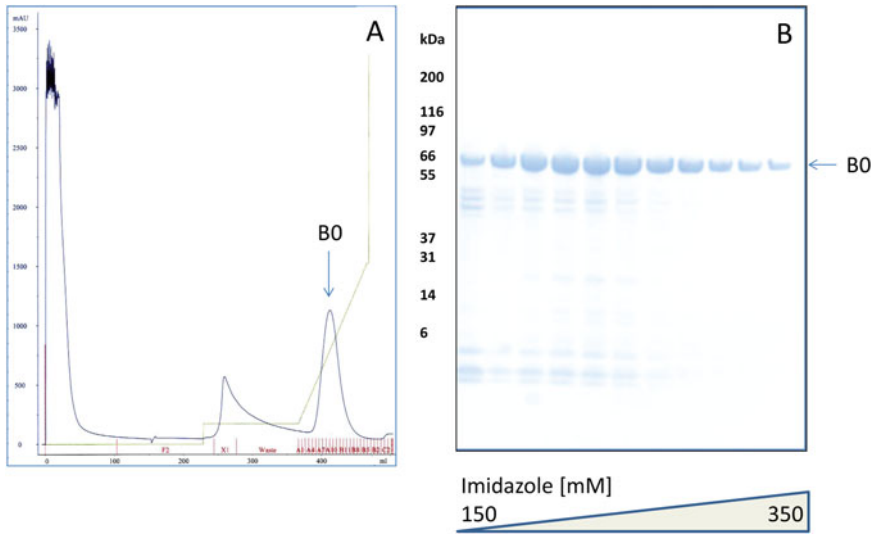

Fig. 2 Chromatographic purification of fragment B0 on immobilized metal affinity chromatography (IMAC). (**a**) Chromatogram obtained during purification of fragment B0 on 5 ml HiTrap IMAC column. Weakly bound host cell proteins were eluted using 60 mM imidazole. Fragment B0 was recovered in fractions collected during gradient elution (60–500 mM imidazole). (**b**) SDS/PAGE (5–12 %) analysis of fractions collected during gradient elution. Note that fractions eluting earlier in the gradient (~150 mM imidazole) contain substantially more contaminating (host cell) proteins than those eluted with a higher concentration of imidazole. The gel was stained with Coomassie SimplyBlue SafeStain

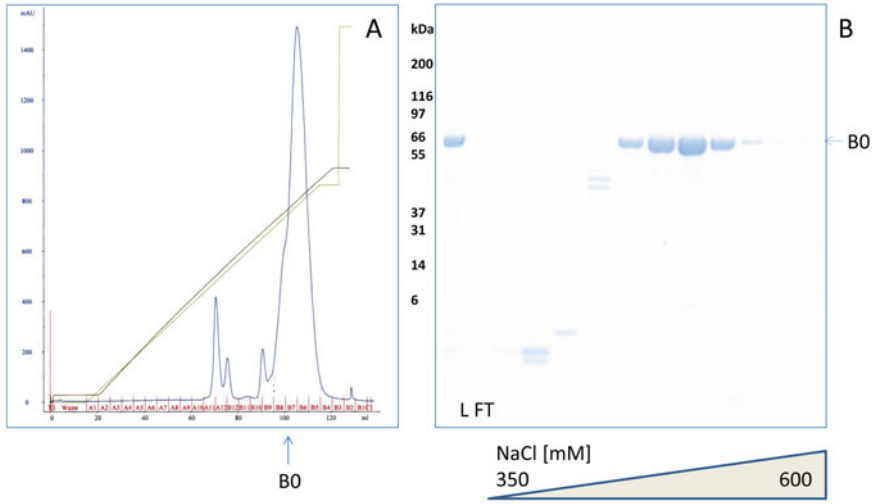

Fig. 3 Separation of IMAC purified B0 by anion exchange chromatography. (**a**) Pooled samples from IMAC were diluted and applied onto 6 ml Resource Q (Sample L). Unbound material was collected (FT) and proteins were eluted with a linear gradient of 0–0.6 M NaCl. The baseline separation was achieved between the target protein and impurities. (**b**) SDS/PAGE analysis of fractions collected during gradient elution. The gel was stained with Coomassie SimplyBlue SafeStain

11. Anion exchange chromatography (AEX). Prepare 6 ml Resource Q column and equilibrate in 10 % AEX Buffer B (0.1 M NaCl). Reduce salt content of the IMAC product to 100 mM NaCl by dilution in AEX Buffer A. Filter diluted sample through a 0.22 μm filter unit, load the sample onto the Resource Q column at 10 ml/min (flow velocity = 340 cm/h, residence time = 0.28 min). Wash the column for 10 column volumes (CV), reduce flow rate to 5 ml/min, and then elute with a gradient of 0–60 % AEX Buffer B (0.1–0.6 M NaCl) for 25 CV. Elute remaining proteins with a step to 100 % AEX Buffer B (1 M NaCl). Collect fractions, analyze on SDS/PAGE, and pool fractions containing the highest purity target protein with <5 % host cell proteins (HCP) (Fig. 3a, b) (*see* **Note 6**).
12. Concentrate sample to the desired concentration using Centricon centrifugal filter device (YM-30) according to the manufacturer's instructions.
13. Dialyze pooled fractions into a desired buffer (such as PBS or HBS), filter-sterilize sample and aliquot under aseptic conditions, store frozen at −70 °C.
14. Measure absorbance of the product at 280 nm (A_{280}, using a NanoDrop spectrophotometer). Calculate theoretical absorbance of 0.1 % solution of the product from its amino acid composition (A_{280} 0.1 %), divide measured A_{280} by (A_{280} 0.1 %) to calculate protein concentration (in mg/ml). Calculate process yields by dividing the final amount of product (in mg) by the original volume of the bacterial culture (Table 1).

Table 1
Summary of purification yields for all fragments purified using two-step purification method

Fragment	Amino acids	Mw (kDa)	Yield (mg/L)
GTD	1–543	62.2	505
TC	544–2367	207	39
B0	1786–2367	68	822
B1	1834–2366	62.4	582
B2	1834–2101	31.6	1836
B3	1949–2275	39.1	686
B4	2102–2366	32	800

3.4 Purity Analysis by SDS/PAGE

1. Load an SDS/PAGE gel (NuPAGE® Novex® 4–12 % Bis-Tris) with MES running buffer with 8 µl sample containing 2 µl NuPAGE® LDS 4× Sample Buffer (containing 50 mM dithiothreitol), undiluted sample (typically 2–10 mg/ml) and several serial dilutions of the tested sample (incubating all samples at 95 °C for 5 min prior to electrophoresis).
2. Stain the gel following electrophoresis with Coomassie SimplyBlue SafeStain, and wash in water until the background is clear.
3. Quantitate the proteins by densitometry of all protein bands, using a GelDoc or similar imaging program.
4. To calculate sample purity, measure densitometric intensity of all impurities in the undiluted sample = IM (Fig. 4b) and intensity of the product in the most diluted sample (Fig. 4c), multiplied by its dilution factor = PR.
5. Calculate protein purity (in %) as $100 \times PR/(IM + PR)$. Prepare an identical gel for western blot analysis (Fig. 4d) (*see* **Notes 7**, **8, 9**, **10**).

3.5 Western Blot Analysis

1. Immediately after electrophoresis, briefly immerse the SDS/PAGE gel in distilled water.
2. Transfer proteins to nitrocellulose using an iBlot® Dry Blotting System (Life Technologies Corporation) and iBlot® Transfer Stack (Nitrocellulose) using a 7 min protocol.
3. For probing with antibodies, use the SNAP i.d.® Protein Detection System. Remove membrane from iBlot® Transfer Stack, pre-wet in distilled water and place in the blot holder, protein side down. Remove air bubbles using a roller, place the spacer, close the cassette, and place in system chamber.

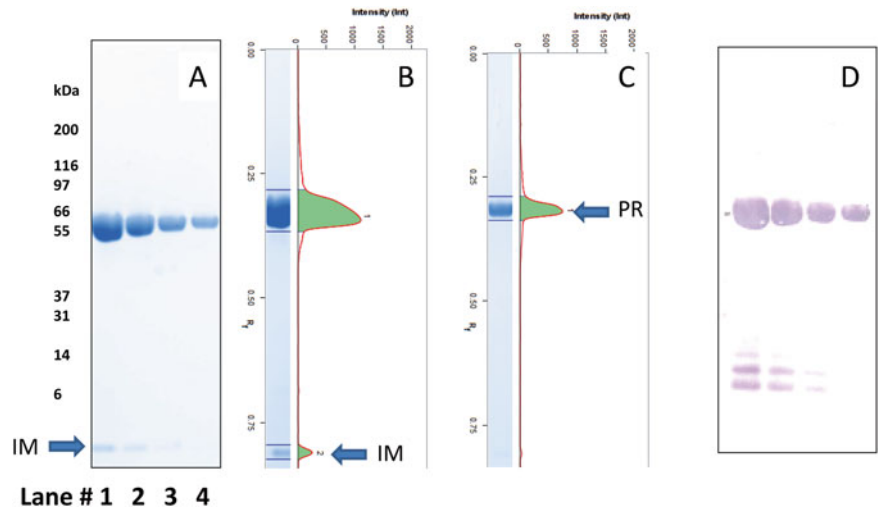

Fig. 4 The analysis of the final product from two-step purification. (**a**) Coomassie stained SDS/PAGE analysis of the serial dilutions of the final product (ED). (**b**) Densitometric analysis of Lane 1 (undiluted sample). (**c**) Densitometric analysis of lane 4 (eightfold dilution of the sample). To calculate sample purity, measure densitometric intensity of the impurity in the undiluted sample (IM) and intensity of the product in the most diluted sample (PR). Calculate protein purity (in %) as 100 × [Dilution factor] × PR/(IM + [Dilution factor] × PR). (**d**) Western blot analysis using anti-HIS monoclonal antibody conjugated to alkaline phosphatase. Immunoreactive bands were visualized using 1-Step NBT/BCIP solution

4. Block membrane using blocking solution for 30 min. Remove blocking solution by applying vacuum.
5. Incubate with 10 ml of a dilution of primary antibody in blocking solution for 1 h.
6. Wash membrane in 20 ml TBST three times for 5 min each.
7. If Monoclonal Anti-poly-Histidine-Alkaline Phosphatase (Clone HIS-1) is used, there is no need for secondary antibody, so proceed to chromogenic detection
8. In case of unconjugated primary antibody, incubate with 2nd antibody for 1 h and wash membrane as above.
9. Remove membrane from blot holder, rinse in water and immerse in 10 ml 1-Step NBT/BCIP Solution.
10. Incubate membrane for 5–15 min or until the color reaches the desired intensity. Rinse the membrane with water.
11. Visualize using an available imaging system (Fig. 4b).

4 Notes

1. The codon bias in *C. difficile* is very different from that of highly expressed genes in *E. coli* resulting in poor expression and necessitating codon optimization [13].

2. Initial screening of small scale expression cultures to test solubility allows rapid selection of the most promising variants. We have observed that most proteins containing only the translocation domain were completely insoluble and therefore were not considered for scale-up.
3. The typical time of induction (with IPTG) was ~3 h at 37 °C. We have also tested longer induction (5 h) at 37 °C and overnight induction at 16 °C. Similar expression levels and stability of final product were seen under all conditions.
4. Extraction of recombinant proteins from the cell paste was greatly improved by addition of a nuclease and processing of the extract through a Microfluidizer® [14]. Both treatments resulted in an increased quantity of target protein in the soluble fraction following clarification and facilitated filtration in preparation for chromatographic purification. In certain cases, supplementing the extraction buffer with surfactants (detergents) or glycerol could also be advantageous [15].
5. The elution of His-tagged proteins from the IMAC resin by gradually increasing the concentration of imidazole (rather than step elution) is a preferred method, in particular if there is no previous experience with the protein.
6. Anion exchange chromatography. This step was very useful for realizing improved purity and could also be considered when it is necessary to concentrate samples, exchange buffers or remove detergents.
7. Samples of varying molecular weights are usually well separated on gradient (4–12 %) SDS/PAGE under reducing conditions. When testing samples eluted from IMAC, dilute samples prior to electrophoresis to avoid aberrant mobility due to the presence of imidazole.
8. The western blot process is facilitated if the iBlot® semi-dry transfer system and SNAP i.d.® Protein Detection System are available. His-tagged proteins could be rapidly detected using monoclonal anti-His antibody conjugated to alkaline phosphatase (or horseradish peroxidase). The sensitivity observed using a primary antibody alone is comparable to the primary-secondary antibody method. It is important to confirm the identity of the final product using antigen specific antibodies or other means of positive identification (like proteomic analysis or N-terminal sequencing).
9. Analytical SEC. Molecular size of the final purified product can be estimated using an analytical SEC column, such as the Superdex 200 GL. Molecular weight markers such as Bio-Rad Gel Filtration Standards are used to generate a standard curve, and the retention time of the protein in the final product can then be used to calculate the approximate molecular weight.

10. The final protein concentration is calculated based on UV adsorption at 280 nm utilizing the adsorption coefficient. The concentration calculated by this method should be confirmed in an independent assay such as quantitative amino acid composition analysis. The final process yields are expressed in mg/L (as in Table 1) or in mg/kg and refer to the milligrams of final product divided by initial volume of culture (in liters) or mass of cell paste (in kilograms), respectively.

References

1. McVoy MA (2013) Cytomegalovirus vaccines. Clin Infect Dis 57 Suppl 4:S196–S199
2. Morrison TG, Walsh EE (2013) Subunit and virus-like particle vaccine approaches for respiratory syncytial virus. Curr Top Microbiol Immunol 372:285–306
3. O'Connell RJ, Kim JH, Corey L, Michael NL (2012) Human immunodeficiency virus vaccine trials. Cold Spring Harb Perspect Med 2:a007351
4. Coller BA, Clements DE, Bett AJ, Sagar SL, Ter Meulen JH (2011) The development of recombinant subunit envelope-based vaccines to protect against dengue virus induced disease. Vaccine 29:7267–7275
5. Karczewski J, Zorman J, Wang S, Miezeiewski M, Xie J et al (2014) Development of a recombinant toxin fragment vaccine for Clostridium difficile infection. Vaccine 32:2812–2818
6. Reinert DJ, Jank T, Aktories K, Schulz GE (2005) Structural basis for the function of Clostridium difficile toxin B. J Mol Biol 351:973–981
7. Pruitt RN, Lacy DB (2012) Toward a structural understanding of Clostridium difficile toxins A and B. Front Cell Infect Microbiol 2:28
8. Orth P, Xiao L, Hernandez LD, Reichert P, Sheth PR et al (2014) Mechanism of action and epitopes of Clostridium difficile toxin B-neutralizing antibody bezlotoxumab revealed by X-ray crystallography. J Biol Chem 289:18008–18021
9. Jank T, Giesemann T, Aktories K (2007) Clostridium difficile glucosyltransferase toxin B-essential amino acids for substrate binding. J Biol Chem 282:35222–35231
10. Busch C, Hofmann F, Gerhard R, Aktories K (2000) Involvement of a conserved tryptophan residue in the UDP-glucose binding of large clostridial cytotoxin glycosyltransferases. J Biol Chem 275:13228–13234
11. Gustafsson C, Govindarajan S, Minshull J (2004) Codon bias and heterologous protein expression. Trends Biotechnol 22:346–353
12. Rosano GL, Ceccarelli EA (2014) Recombinant protein expression in Escherichia coli: advances and challenges. Front Microbiol 5:172
13. Yang G, Zhou B, Wang J, He X, Sun X et al (2008) Expression of recombinant Clostridium difficile toxin A and B in Bacillus megaterium. BMC Microbiol 8:192
14. Cook JC, Joyce JG, George HA, Schultz LD, Hurni WM et al (1999) Purification of virus-like particles of recombinant human papillomavirus type 11 major capsid protein L1 from Saccharomyces cerevisiae. Protein Expr Purif 17:477–484
15. Bass RB, Spencer RH (2006) Approaches for ion channel structural studies. In: Clare JJ, Trezise DJ (eds) Approaches for ion channel structural studies, in expression and analysis of recombinant ion channels: from structural studies to pharmacological screening. Wiley-VCH Verlag, Weinheim, FRG

Chapter 21

The Design of a *Clostridium difficile* Carbohydrate-Based Vaccine

Mario A. Monteiro

Abstract

Clostridium difficile vaccines composed of surface polysaccharides (PSs) have the potential to simultaneously control infection and colonization levels in humans. Hot water–phenol treatment of *C. difficile* biomass can extricate water-soluble PS-I and PS-II; and water- and phenol-soluble PS-III. *C. difficile* vaccines based on PS-II have attracted the most attention due its facile purification and ubiquitous expression by *C. difficile* ribotypes. Anti PS-II antibodies recognize both *C. difficile* vegetative cell and sporulating preparations and confer protection against *C. difficile* infection in a mouse model. The design of such an efficacious *C. difficile* PS-II conjugate vaccine is described here.

Key words *Clostridium difficile*, Vaccine, Polysaccharide, *C. difficile* PS-II, Conjugate, TEMPO-mediated conjugation

1 Introduction

Clostridium difficile surface polysaccharides (Table 1) are attractive vaccine candidates to control *C. difficile* disease and reduce colonization levels in the population. In previous reports [1, 2], we described the fine structures of two water-soluble *C. difficile* polysaccharides obtained from hot water–phenol extraction; polysaccharide I (PS-I), composed of a pentasaccharide phosphate repeat of rhamnose (Rha), glucose (Glc), and phosphate (P): [→4)-α-L-Rha*p*-(1-3)-β-D-Glc*p*-(1-4)-[α-L-Rha*p*-(1-3]-α-D-Glc*p*-(1-2)-α-D-Glc*p*-(1-P→]; and polysaccharide II (PS-II), made up of a hexasaccharide phosphate repeat with Glc, mannose (Man), *N*-acetyl-galactosamine (GalNAc), and P: [→6)-β-D-Glc*p*-(1-3)-β-D-Gal*p*NAc-(1-4)-α-D-Glc*p*-(1-4)-[β-D-Glc*p*-(1-3)]-β-D-Gal*p*NAc-(1-3)-α-D-Man*p*-(1-P→]. Water-soluble PS-I and PS-II attracted immediate attention as potential *C. difficile* vaccines and the corresponding oligosaccharide repeating blocks were promptly synthesized by several groups [3–7].

Sunil Thomas (ed.), *Vaccine Design: Methods and Protocols: Volume 1: Vaccines for Human Diseases*, Methods in Molecular Biology, vol. 1403, DOI 10.1007/978-1-4939-3387-7_21,

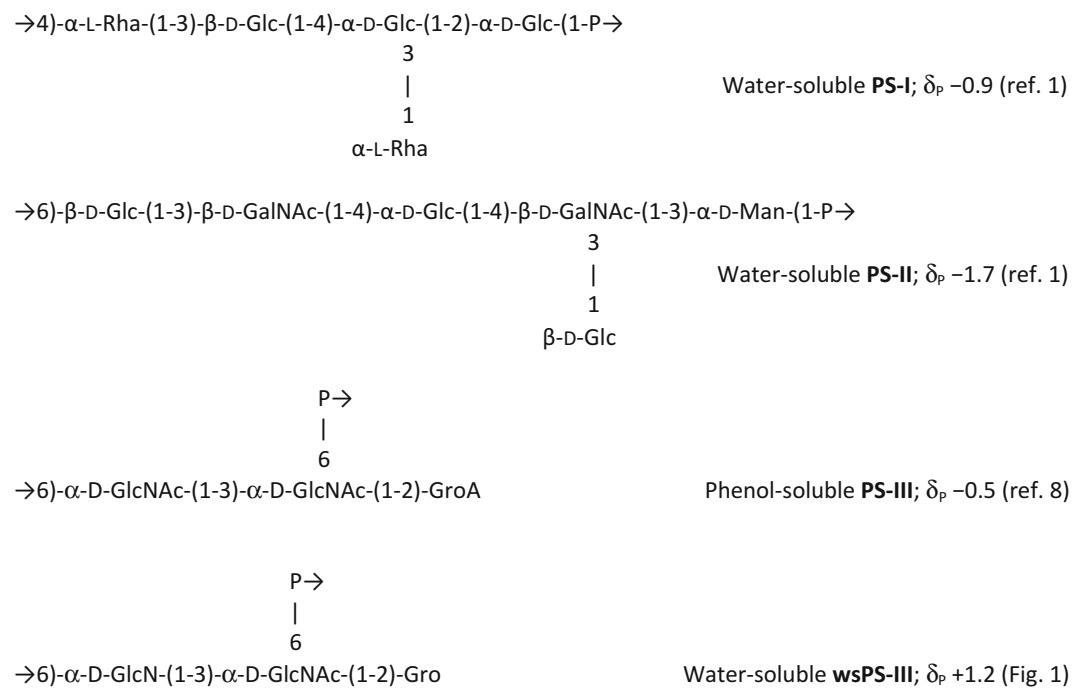

Table 1 The oligosaccharide phosphate repeating blocks of *C. difficile* polysaccharides and their characteristic ^{31}P NMR spectroscopy resonances

Along with the description of water-soluble PS-I and PS-II polysaccharides, early evidence was also obtained for another phosphorylated *C. difficile* glycan, a phenol-soluble polysaccharide, named PS-III, composed of P, Glc, *N*-acetyl-glucosamine (GlcNAc), and glycerol (Gro) [2]. This phenol-soluble PS has now also been fully analyzed and its repeating oligosaccharide synthesized [8–10]. The majority of the repeating units of the phenol-soluble PS-III were found to be composed of P, GlcNAc, and glyceric acid (GroA): →6)-α-GlcNAc-(1-3)-α-GlcNAc-[-6-P→]-(1-2)-GroA, with minor repeats of Glc and Gro moieties at the reducing-end regions. Akin to lipoteichoic-acids, fatty-acids capped the reducing-terminus of this phenol-soluble polysaccharide. A structural variant of the phenol-soluble PS-III has also been isolated from *C. difficile*, but in the aqueous phase, and with an alternate major repeating structure having glycerol (in place of glyceric acid) and 6-substituted glucosamine (in place of 6-substituted *N*-acetyl-glucosamine): →6)-α-D-GlcN-(1-3)-α-D-GlcNAc-[-6-P→]-(1-2)-Gro (submitted for publication). In the water-soluble PS-III, the combination of the negatively charged phosphate entity (PO_3^-) with the high content of positively charged glucosamine ($GlcNH_3^+$) affords this water-soluble PS-III a zwitterionic character, which may contribute in part for its solubilization in water.

A (1→4)-glucan has also been observed in *C. difficile* [11] and in two other Clostridia species, *C. butyricum* [12] and *C. botulinum* [13] and although in minor quantities, some sporulating preparations have been observed to contain Man units in the form of end-groups [α-Man-(1→], 2-linked linear units [→2)-α-Man-(1→] and 2,6-linked branch-points [→2,6)-α-Man-(1→] (Monteiro, unpublished results).

Fine structural validation of *C. difficile* polysaccharides is beyond the reach of non-carbohydrate vaccine scientists. Therefore, a rapid detection protocol for the characterization of *C. difficile* polysaccharides based on one-dimensional phosphorous (^{31}P) Nuclear Magnetic Resonance (NMR) spectroscopy is revealed here. This NMR-based evaluation of *C. difficile* PSs can be performed by any NMR center. Each *C. difficile* polysaccharide listed in Table 1 furnishes a distinctive ^{31}P NMR resonance, which can be used after size-exclusion chromatography for polysaccharide scrutiny. *C. difficile* water-soluble PS-I yields a ^{31}P NMR resonance at δ_P −0.9 [1], water-soluble PS-II at δ_P −1.7 [1], phenol-soluble PS-III at δ_P −0.5 [8], and water-soluble PS-III (called wsPS-III) at δ_P +1.2 (submitted for publication). Shown below in the Methods section, is an easy to follow collection of ^{31}P NMR spectra identifying water-soluble PS-II and water-soluble PS-III materials obtained from size-exclusion chromatography.

Several studies have shown that *C. difficile* polysaccharides and their synthetic oligosaccharide repeating blocks are antigenic and immunogenic [2, 4, 5, 7, 9, 11, 14]. However, in terms of an attractive vaccine candidate, only the native water-soluble PS-II absorbed instant interest, mainly due to the fact that PS-II is a conserved antigen ubiquitously expressed by *C. difficile* ribotypes [1, 2, 8, 15]. Other advantages of PS-II include its constant good yield and solubility in water, which facilitates purification protocols, and its low endotoxicity level of 3.77 EU/μg, well below that required for cGMP production (100 EU/μg). On the other hand, water-soluble PS-I and phenol-soluble PS-III carry some limitations; PS-I is not regularly produced by *C. difficile* and thus only the synthetic route can be reliably used in vaccine development; and phenol-soluble PS-III requires many manipulations to attain a cGMP acceptable product, because of the need for extensive phenol removal and high endotoxicity levels due to its fatty-acid content. The water-soluble PS-III overcame the purification obstacles of phenol-soluble PS-III, but no significant immunogenic studies have yet been carried out with this PS. For these reasons, the most advanced *C. difficile* carbohydrate-based vaccine data has been afforded by PS-II, and these pages describe such progress.

The most encouraging set of results have been yielded by a recent preclinical protection study, which showed that a parenteral vaccine, composed of PS-II adjoined to the immunostimulatory protein keyhole limpet hemocyanin (KLH), protected 90 % of

mice when challenged with an LD_{50} dose of *C. difficile* spores [15]. In this piece, the detailed instructions are given for: (1) hot water–phenol extraction of PS-II; (2) purification of PS-II by size-exclusion chromatography; (3) quick characterization of PS-II by ^{31}P NMR; (4) selective and stoichiometric activation of primary hydroxyls of PS-II by (2,2,6,6-Tetramethylpiperidin-1-yl)oxy (TEMPO); and (5) carbodiimide-dependent conjugation of PS-II to a protein carrier. The design of a *C. difficile* challenge study in an established mouse model to test the aforementioned PS-II conjugate vaccine is also explained.

2 Materials

2.1 Extraction of PS-II from C. difficile Biomass

1. High vacuum lyophilizer (220 V).
2. 99 % liquefied phenol (if crystallized, heat to liquefied form in microwave).
3. Dialyzed water.
4. Heating plate with magnetic stirring capability.
5. Water bath (or heating blanket).
6. Thermometer.
7. Round-bottom flask with stopper.
8. Magnetic stirrer.
9. Dialysis bag 1000 MWCO.

2.2 Purification and Rapid Characterization of C. difficile PS-II

1. Sephadex G-50.
2. Glass column (1 m × 1 cm).
3. Fraction collector.
4. Lyophilizer.
5. Deuterium oxide (D_2O).
6. NMR instrument with a ^{31}P NMR probe.
7. NMR spectroscopy tubes.
8. Ortho-phosphoric acid.

2.3 Stoichiometric Activation of C. difficile PS-II by TEMPO-Mediated Oxidation

1. Ingredients for oxidation of PS-II: TEMPO (0.6 mg), 1 M NaOAc, NaBr (9.0 mg), NaClO (4 %, 0.375 mL), deionized water (15 mL).
2. 4 dram vial.
3. *C. difficile* PS-II (60.0 mg).
4. Stir bar.
5. Ice bath.
6. Ethanol (0.5 mL).
7. 1000 MWCO dialysis bag.

2.4 Conjugation of the Partially Oxidized *C. difficile* PS-II to an Immunostimulatory Protein Carrier

1. Components for conjugation: 1-Ethyl-3-(3-dimethylaminopropyl) carbodiimide (EDC) (200 μL), 10 ml of 0.5 M of 2-(*N*-morpholino)ethanesulfonic acid (MES) buffer (pH 5.5); 5.0 M HCl (220 μL).
2. TEMPO oxidized PS-II (30.0 mg).
3. Protein carrier (15.0 mg).
4. Reaction vial.
5. Stir plate and stirrer.
6. 25,000 MWCO dialysis bag.

2.5 Evaluation of *C. difficile* PS-II Conjugate in a *C. difficile* Infection Mouse Model

1. C57BL6 mice.
2. *C. difficile* PS-II conjugate vaccine.
3. Adjuvant (Alum or KLH).
4. Antibiotic cocktail (Vancomycin and Clindamycin).
5. *C. difficile* spores.

3 Methods

3.1 Extraction of PS-II from *C. difficile* Biomass

1. In a 1 L round-bottom flask, *C. difficile* wet cell paste (2.5 g) is dissolved in 250 ml of deionized water and stirred at 70 °C for 30 min (a water bath or heating blanket may be used).
2. Following this, 200 ml of 99 % liquefied phenol is added and the hot water–phenol solution is stirred for 3 h. If water bath is used, use thermometer to control temperature.
3. Then, the round-bottom flask with the hot preparation is placed in an ice-bath and allowed to stay overnight.
4. On the following morning, the top distinguishable aqueous layer is collected and dialyzed against water for 2 days in a dialysis bag (1000 MWCO) mainly for phenol removal.
5. The dialyzed solution is then lyophilized and purified by size-exclusion chromatography (Subheading 3.2).

The water layer of all *C. difficile* ribotypes will afford PS-II and wsPS-III, but seldom will PS-I be detected (*see* **Note 1**). Extended dialysis of the phenol layer will yield phenol-soluble PS-III and protein- and ribonucleotide-rich material, and thus extended treatment with proteinase and ribonuclease is necessary obtain a purified phenol-soluble PS-III preparation.

3.2 Purification and Rapid Characterization of *C. difficile* PS-II

1. The lyophilized water layer (50 mg from 2.5 g wet paste) is dissolved in 5 ml of distilled water and placed at the top of a Sephadex G-50 column (3 cm × 1 m) with water as eluent.
2. A fraction collector, without a physical pump, accumulates 1 ml fractions.

3. The first ten tubes (fractions) consist of the void volume with the PS material eluting after fraction 10.
4. The fractions containing material may be detected by a UV (210 nm) or refractive index detector, or simply by freeze-drying the independent fractions.
5. The fractions containing PS-II can be easily identified by ^{31}P NMR spectroscopy (Fig. 1) due to the fact that PS-II and wsPS-III exhibit distinct ^{31}P NMR resonances, PS-II at δ_P −1.7 and wsPS-III at δ_P +1.2. Ortho-phosphoric acid is used as the external reference (δ_P 0.0). Figure 1 shows the typical elution profile of PS-II, which is usually accompanied by wsPS-III.
6. The material is dissolved once in 99 % D_2O and lyophilized and then it is dissolved again in 0.5 ml 99 % and placed in a 5 mm NMR tube.
7. At least 256 scans per each NMR experiment should be acquired. Here (Fig. 1), the first two fractions contained PS-II, but also small amounts of wsPS-III. Fractions 13–17 afforded pure PS-II, and pure wsPS-III was collected during the later fractions, fraction 22 and 23. Physicochemical analyses have shown that the average length of PS-II is seven repeating blocks. Fractions containing pure PS-II may now be pooled to yield on average 25–30 mg of bulk PS-II.

3.3 Stoichiometric Activation of *C. difficile* PS-II by TEMPO-Mediated Oxidation

1. TEMPO (0.6 mg) and NaBr (9.0 mg) are dissolved in deionized water (15 mL) by vigorous vortexing in a 4 dram vial. Then, NaOAc (1.23 g) is added (*see* **Note 2**).
2. PS-II (30.0 mg) and a stir bar are added to the buffer solution described above.
3. The reaction vial is kept in an ice bath and stirred for 10 min.
4. NaClO (4 %, 0.375 mL) is added drop wise at 0 °C.
5. The solution was kept at 0 °C for 24 h (stirred for 8 h and then kept in a fridge in an ice bath for 16 h).
6. For work up, ethanol (0.5 mL) is added and the reaction mixture dialyzed in a 1000 MWCO dialysis bag against water overnight.
7. The retentate is lyophilized to yield the partially (10 %) oxidized PS-II.

Monosaccharide analysis of the partially TEMPO-oxidized PS-II has revealed that the 3-substituted GalNAc is the unit that more prominently undergoes oxidation at its C-6 position (Fig. 2).

3.4 Conjugation of the Partially Oxidized *C. difficile* PS-II to an Immunostimulatory Protein Carrier

1. EDC (200 μL) is added to 10 mL of 0.5 M MES buffer (pH 5.5) and then neutralized with 5.0 M HCl (220 μL).
2. TEMPO oxidized PS-II (20.0 mg) is added and the mixture stirred for 15 min at room temperature.

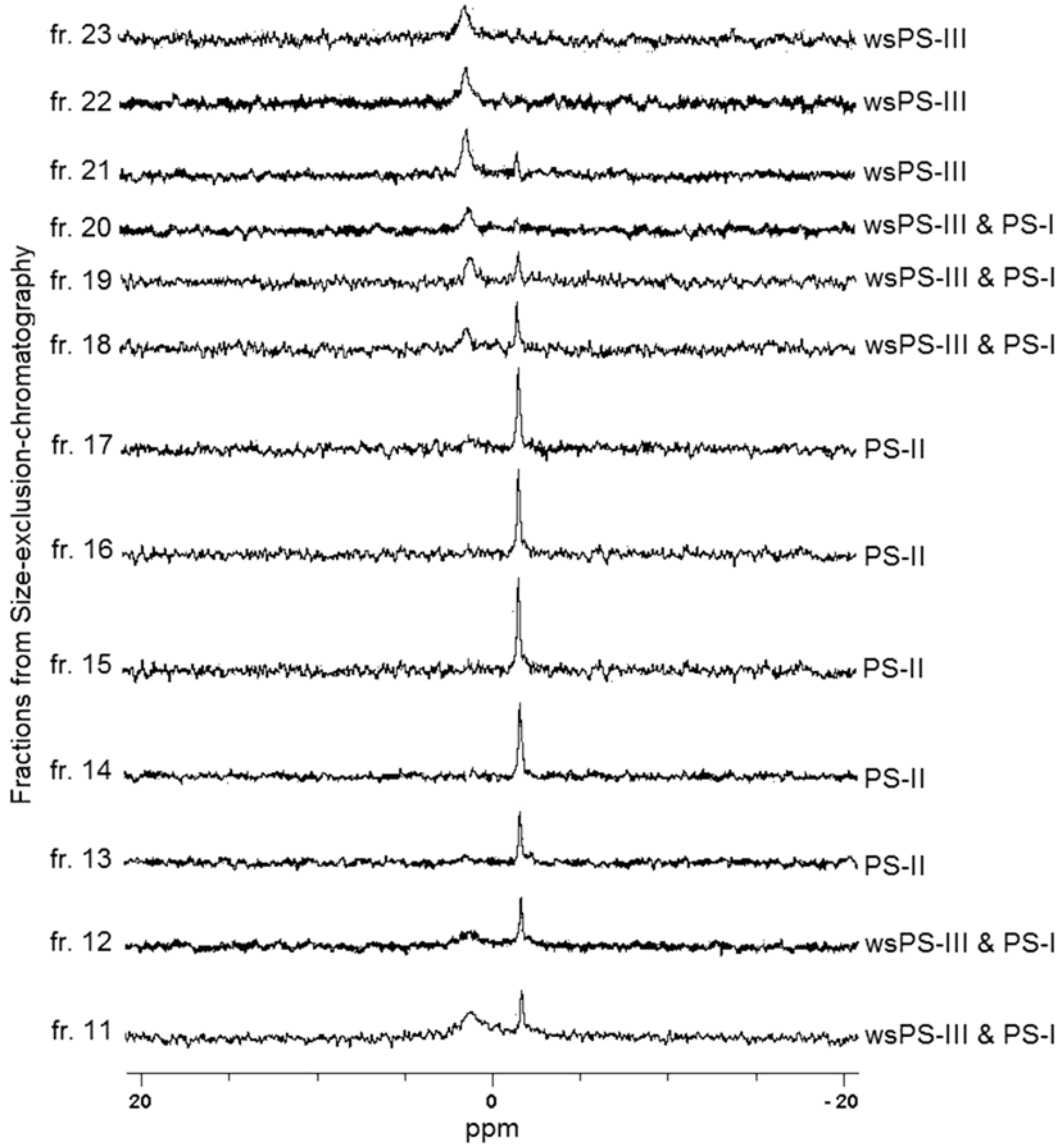

Fig. 1 ^{31}P NMR spectra of the fractions obtained by fractionation of the water layer through a Sephadex G-50 column. ^{31}P NMR can be used to identify the location of ***C. difficile*** PS-II through the detection of its distinctive resonance at –1.7 ppm

3. Following this, a carrier protein such as BSA, LTB, CRM_{197}, toxin [11] or KLH (10.0 mg) is transferred into the reaction vial with 10 mL of 0.5 M MES buffer (pH 5.5).
4. The reaction is stirred at room temperature for 1 day and then stirred at 37 °C for 2 days.
5. The reaction mixture is subsequently dialyzed in a 25,000 MWCO bag against water for 3 days (*see* **Note 3**).

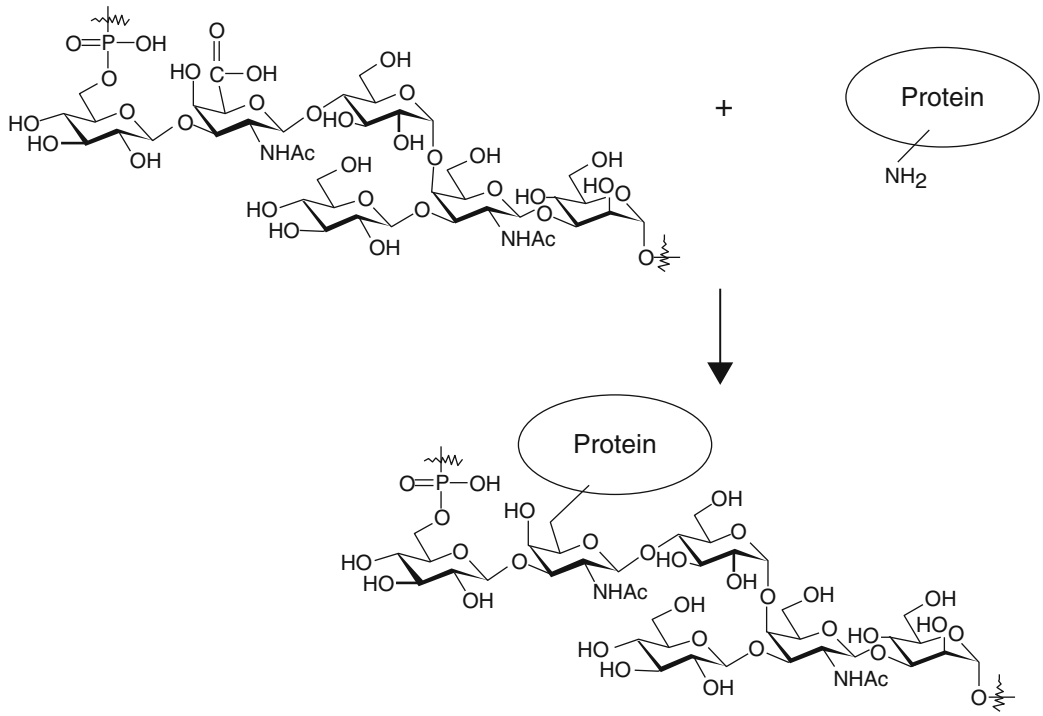

Fig. 2 The primary position of the three-substituted GalNAc is the site of preferential oxidation when ***C. difficile*** PS-II is subjected to stoichiometric TEMPO-mediated oxidation

6. The retentate is lyophilized to yield the PS-II conjugate.

Since the primary position of the 3-substituted GalNAc is the PS-II site most readily oxidized under the aforementioned conditions, the majority of protein ligation occurs at this point (Fig. 2).

3.5 Guidance for the Analysis of PS-II Conjugates

The resulting PS-II conjugates may be analyzed by matrix assisted laser desorption/ionization (MALDI) mass-spectrometry or by standard gel electrophoresis. However, due to the unreliable behavior of large molecular weight conjugates in MALDI mass-spectrometry, the widely used gel electrophoresis (Coomassie stain procedure that detect proteins) and Western blot analysis have became our methods of choice for rapid confirmation of conjugation between activated PS-II and protein carrier.

Gel electrophoresis [16] confirms that conjugation has occurred through the observation of a shift towards a higher molecular weight (Fig. 3a, b), and the reactivity of the PS-II conjugate with PS-II antisera in a Western Blot [17] confirms that the PS-II structure in the conjugate format retains and exposes the important immunogenic epitopes (Fig. 3c). The Western blot analysis of the PS-II conjugate must be performed with antisera raised previously by native PS-II. Also, if accessible, immunofluorescence [5] studies can also confirm that the antibodies raised by the PS-II conjugate recognize the native PS-II on the surface of *C. difficile*.

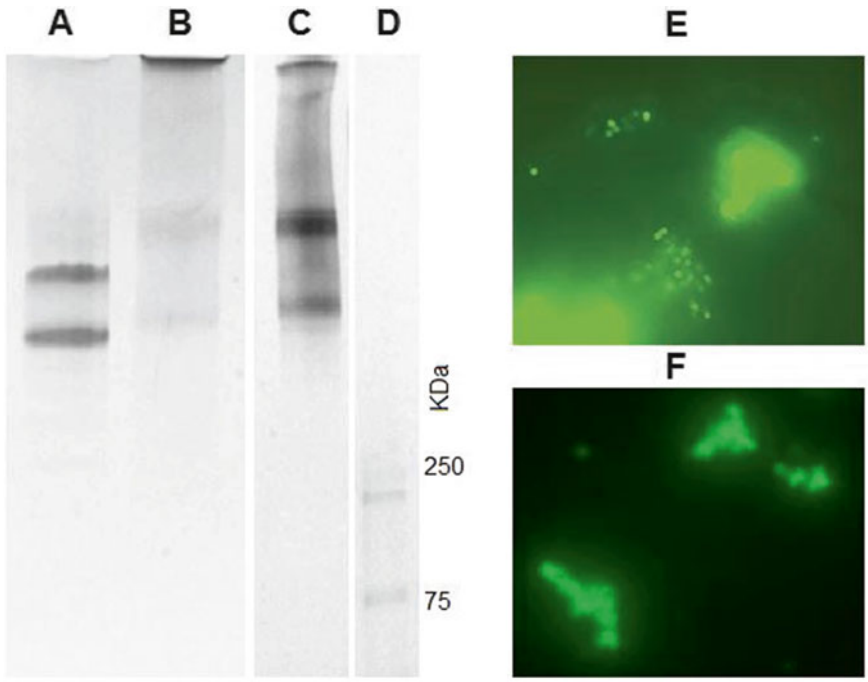

Fig. 3 (**a**) Gel electrophoresis (Coomassie stain) of KLH and (**b**) PS-II/KLH conjugate. The shift towards high molecular weight observed in (**b**) attests to the fact that conjugation between PS-II and KLH took place; (**c**) A Western Blot showing the recognition of PS-II in a conjugate format (PS-II/KLH) with PS-II antisera; (**d**) Standard molecular weigh marker; and immunofluorescence images illustrating that ***C. difficile*** vegetative cells (**e**) and sporulating preparations (**f**) are recognized by PS-II antibodies (performed by Dr. Martin Sagermann). These data were presented at the 7th Vaccine and ISV Annual Global Congress and at the International Conference on the Molecular Biology and Pathogenesis of the Clostridia [15]

The aforementioned procedures have been previously described in detail elsewhere [5, 16, 17], but as an illustration, Fig. 3 displays examples of these verifications of PS-II conjugates: (A) and (B) are gel electrophoreses of the carrier protein, KLH, and (B) is a gel electrophoresis of the PS-II/KLH conjugate; (C) is a Western Blot showing that anti PS-II antibodies (raised in rabbits against native PS-II beforehand) can detect PS-II in a PS-II/KLH conjugate produced by TEMPO-mediated activation; and (E) and (F) are immunofluorescence analyses showing that antibodies raised by a PS-II conjugate recognize the PS-II on *C. difficile* surface.

3.6 Guidance for the Evaluation of a C. difficile PS-II Conjugate in a C. difficile Infection Mouse Model

Animal vaccine models of *C. difficile* infection are still limited in scope and in the number of institutions that can perform such trials. In most cases, academic scientists have to work in partnership with industrial contract research organization to have their vaccines evaluated. For such purposes, a mouse model now exists, the C57BL6 *C. difficile* model [18], which can be used as a primary

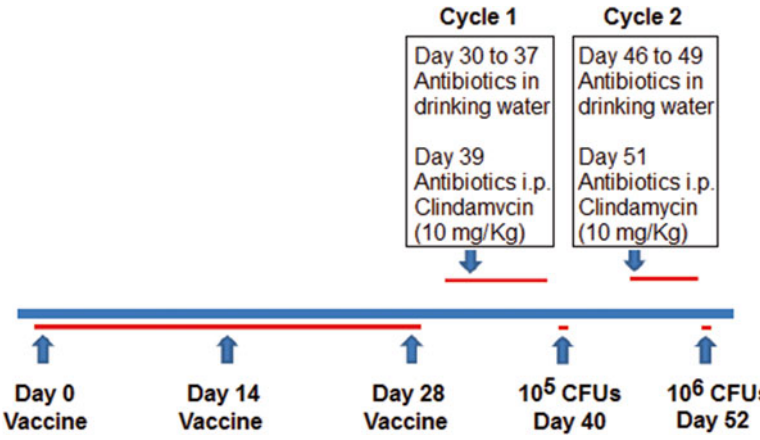

Fig. 4 Schematic representation of a C. difficile infection mouse model (C57BL6) challenge study that may be used to evaluate PS-II conjugate vaccines

test for a *C. difficile* vaccine candidate. Here, the approach taken to evaluate the efficacy of the *C. difficile* PS-II/KLH conjugate vaccine is described (Fig. 4) [15].

C57BL6 mice are vaccinated with three intramuscular and subcutaneous injections of 100 μg PS-II conjugate (in this case a PS-II/KLH vaccine produced via TEMPO-mediated activation) (*see* **Note 4**) admixed with an adjuvant (100 μg of KLH here) on Day 1, 14, and 28. Sera samples may be collected on Day 35 to analyze titers of anti PS-II IgG. Following vaccination, the mice were rendered susceptible to *C. difficile* with multiple antibiotics and were then challenged with an LD_{50} dose of *C. difficile* spores orally at Day 40 (Fig. 4). The animals that survive the *C. difficile* spore challenge are allowed to rest for 7 days. Then, the mice are exposed to another 3 day course of antibiotic pretreatment and challenged with a 10× LD_{50} dose of *C. difficile* spores to mimic a recurrent *C. difficile* infection in humans. In this case [15] 90 % (38 of 42) of the vaccinated mice survived the first *C. difficile* challenge (40 % of the unvaccinated mice survived), and all vaccinated animals survived the second challenge.

4 Notes

1. The water layer has been found not to contain oligonucleotide- or protein-related contents (these are found in the phenol layer). However, it is advisable that the fresh experimentalist have the aqueous content analyzed for RNA and protein contamination.
2. TEMPO does not dissolve well in 1 M NaOAc buffer; therefore do not reverse the two aforementioned steps [19].

3. Depending on the carrier protein being used, conjugation reactions between activated PS-II and protein carrier may yield very high molecular weight lattice-type conjugates. In these cases, one may observe particulates in the solution after dialysis. Even though these preparations may have low solubility, they may be also be used in vaccine studies.
4. Prior to challenge studies in animal models, the PS-II conjugate vaccine to be employed must be analyzed by Western Blot to confirm that it is recognized by anti PS-II antibodies (raised by previously performed immunogenicity studies).

Acknowledgements

This work was supported in part by a Discovery grant from the Natural Sciences and Engineering Research Council (Canada) to M.A.M. The KLH conjugation immunogenic analysis and mouse model studies were funded and carried out by Stellar Biotechnologies, Inc. (Herbert Chow, Martin Sagermann).

References

1. Ganeshapillai J, Vinogradov E, Rousseau J, Weese JS, Monteiro MA (2008) *Clostridium difficile* cell-surface polysaccharides composed of pentaglycosyl and hexaglycosyl phosphate repeating units. Carbohydr Res 343:703–710
2. Monteiro MA, Ganeshapillai J (2013) Polysaccharide immunogens from *Clostridium difficile*. US Patent 8597663 B2, 3 Dec 2013
3. Danieli E et al (2011) First synthesis of *C. difficile* PS-II cell wall polysaccharide repeating unit. Org Lett 13:378–381
4. Oberli MA et al (2011) A possible oligosaccharide-conjugate vaccine candidate for *Clostridium difficile* is antigenic and immunogenic. Chem Biol 18:580–588
5. Adamo R et al (2012) Phosphorylation of the synthetic hexasaccharide repeating unit is essential for the induction of antibodies to *Clostridium difficile* PSII cell wall polysaccharide. ACS Chem Biol 7:1420–1428
6. Martin CE, Weishaupt MW, Seeberger PH (2011) Progress toward developing a carbohydrate-conjugate vaccine against *Clostridium difficile* ribotype 027: synthesis of the cell-surface polysaccharide PS-I repeating unit. Chem Commun (Camb) 47:10260–10262
7. Jiao Y et al (2013) *Clostridium difficile* PSI polysaccharide: synthesis of pentasaccharide repeating block, conjugation to exotoxin B subunit, and detection of natural anti-PSI IgG antibodies in horse serum. Carbohydr Res 378:15–25
8. Reid CW et al (2012) Structural characterization of surface glycans from *Clostridium difficile*. Carbohydr Res 354:65–73
9. Martin CE et al (2013) Glycan arrays containing synthetic *Clostridium difficile* lipoteichoic acid oligomers as tools toward a carbohydrate vaccine. Chem Commun (Camb) 49: 7159–7161
10. Wouter FJ et al (2014) Total synthesis of five lipoteichoic acids of *Clostridium difficile*. Chemistry 20:13511–13516
11. Bertolo L et al (2012) *Clostridium difficile* carbohydrates: glucan in spores, PSII common antigen in cells, immunogenicity of PSII in swine and synthesis of a dual *C. difficile*-ETEC conjugate vaccine. Carbohydr Res 354:79–86
12. Hobson PN, Nasr H (1951) An amylopectin-type polysaccharide synthesised from sucrose by *Cl. butyricum*. J Chem Soc 1855–1857
13. Whyte JNC, Strasdine GA (1972) An intracellular alpha-D-glucan from *Clostridium botulinum*, type E. Carbohydr Res 25:435–441
14. Monteiro MA et al (2013) Carbohydrate-based *Clostridium difficile* vaccines. Expert Rev Vaccines 12:421–431

15. Chow H, Sagermann M, Ma Z, Vandentam G, Monteiro MA (2013) Vaccination with *Clostridium difficile* PSII polysaccharide antigen adjuvanted with KLH induced broad-based enhancement of adaptive immune responses and protection in mice. Paper presented at the 7th Vaccine and ISV Congress Sitges, Spain, 27–29 Oct 2013; and Pequegnat B, Sagermann M, Arroyo L, Chow H, Monteiro MA (2013) An anti-*C. difficile* PSII polysaccharide-KLH conjugate vaccine is efficacious in mice. Paper presented at the international conference on the molecular biology and pathogenesis of the Clostridia (ClostPath 8), Queensland, Australia, 22–26 Oct 2013
16. Laemmli UK (1970) Cleavage of structural proteins during the assembly of the head of bacteriophage T4. Nature 227:680–685
17. Towbin H, Staehelin T, Gordon J (1979) Electrophoretic transfer of proteins from polyacrylamide gels to nitrocellulose sheets: procedure and some applications. Proc Natl Acad Sci U S A 76:4350–4354
18. Chen X, Katchar K, Goldsmith JD et al (2008) A mouse model of *Clostridium difficile*-associated disease. Gastroenterology 135:1984–1992
19. Ma Z, Bertolo L, Arar A, Monteiro MA (2011) TEMPO-mediated glycoconjugation: a scheme for the controlled synthesis of polysaccharide conjugates. Carbohydr Res 346:343–347

Chapter 22

Murine Models of Bacteremia and Surgical Wound Infection for the Evaluation of *Staphylococcus aureus* Vaccine Candidates

Linhui Wang and Jean C. Lee

Abstract

There is an unmet need for an effective vaccine to prevent infections caused by *Staphylococcus aureus*. Murine models of staphylococcal infections are useful tools for evaluation of experimental vaccines and adjuvants in preclinical studies. Mice can be actively immunized with vaccines or passively immunized with antibodies prior to bacterial challenge. We described two infection models, bacteremia and surgical wound infection, that are relevant to human disease. To achieve a persistent bacteremia, mice are challenged with a sublethal inoculum of *S. aureus* by the intraperitoneal route. Bacteremia is assessed 2 h after challenge, and weight loss and renal infection are quantified after 4 days. Surgical wound infection can be achieved by inoculation of *S. aureus* directly into the sutured incision of a thigh muscle. After 3 days the tissue bacterial burden and weight loss are evaluated in this localized infection. Protective efficacy of experimental vaccines is analyzed by comparison with mice immunized with appropriate control vaccines.

Key words *Staphylococcus aureus*, Vaccine, Animal model, Bacteremia, Surgical wound infection, Immunization, Mouse

1 Introduction

Staphylococcus aureus is a leading cause of superficial and invasive human infections that are often refractory to antimicrobial therapy. Vaccines have the potential to reduce the morbidity, mortality, and economic impact associated with these infections. However, no experimental vaccine has yet achieved its clinical endpoint in human clinical trials [1]. To evaluate the efficacy of vaccine candidates in preclinical studies, rodent models of staphylococcal infection are most commonly utilized. These include models of bacteremia [2], pneumonia [3], renal abscess formation [4], lethality [5], endocarditis [6–8], surgical wound infection [9], osteomyelitis [10, 11], skin and soft tissue infections [12, 13], and arthritis [14, 15]. Most of these models have been well

Sunil Thomas (ed.), *Vaccine Design: Methods and Protocols: Volume 1: Vaccines for Human Diseases*, Methods in Molecular Biology, vol. 1403, DOI 10.1007/978-1-4939-3387-7_22,

characterized. Here we describe experimental protocols for performance of two particularly relevant *S. aureus* disease models—bacteremia and surgical wound infection.

2 Materials

2.1 Experimental Animals

Species: inbred or outbred mice may be used. Sex: female. Age: 4 weeks for active immunization; 6–8 weeks for passive immunization. Housing: 4–5 mice per cage in a specific pathogen-free facility. Food and water: ad libitum. Animal studies are conducted according to Institutional Animal Care and Use Committee guidelines.

2.2 Immunization and Tail Vein Bleeding

1. Tris-buffered saline (TBS), pH 6.5.
2. 1-cc syringes with 27-g × ½ in. needles.
3. A scalpel blade #19 (RS-9861-19, Roboz Surgical Instrument) suitable for bleeding the mice by tail vein nick.
4. Mouse restrainer.
5. 2-in. × 2-in. gauze sponges.
6. Heat lamp.
7. 70 % ethanol.
8. 1.5 ml microcentrifuge tubes.
9. Microfuge.

2.3 Bacteremia Model with Renal Infection

1. Bacterial strain: encapsulated *S. aureus* strains, such as Reynolds (CP5) or Reynolds (CP8) [2] marked with antibiotic resistance (*see* **Note 1**).
2. Columbia salt agar (CSA): Columbia medium supplemented with 2 % NaCl and 1.5 % agar (*see* **Note 2**).
3. Tryptic soy broth (TSB).
4. Tryptic soy agar (TSA): tryptic soy medium supplemented with 1.5 % agar.
5. Blood agar plates (BAP): TSA with 5 % sheep blood.
6. TSA + streptomycin (Sm): TSA supplemented with 500 μg/ml Sm.
7. Disposable sterile 12 × 75 mm 5-ml snap-cap polypropylene tubes.
8. Balance for weighing mice and tissue samples.
9. Mouse restrainer.
10. Vortex for mixing of the inoculum.
11. Heat lamp.

2.4 Surgical Wound Infection Model

1. *S. aureus* strain: marked with antibiotic resistance (*see* **Note 1**).
2. TSB for tissue homogenization and sample dilutions.
3. Solid media: TSA plates, BAP, and TSA + Sm.
4. Disposable sterile 12 × 75 mm 5-ml snap-cap polypropylene tubes.
5. Mini cordless small animal trimmer (Harvard Apparatus).
6. Sutures: 4–0 silk and 5–0 Prolene sutures (Ethicon, Somerville, NJ).
7. Alternative to Prolene sutures: Autoclip wound closure system (Harvard Apparatus).
8. Surgical instruments: Scalpel blade #15 with curved edge (catalogue #: RS-9801-15, Roboz Surgical Instrument, Gaithersburg, MD), surgical scissors, forceps.
9. Ultramicropipet and tips.
10. Vortex.
11. Analgesic: Buprenorphine.
12. Ketamine hydrochloride for injection (Ketaset®, Fort Dodge Animal Health, Fort Dodge, IA).
13. Xylazine (AnaSed®, Lloyd Inc., Shenandoah, IA).
14. Betadine.
15. 70 % ethanol.
16. Tissue homogenizer.
17. Surgical drapes.
18. Phosphate buffered saline (PBS): 0.01 M phosphate, 0.15 M NaCl, pH 7.2–7.4.
19. Balance for weighing mice and tissue samples.

3 Methods

3.1 Formulation of Vaccines

Prepare the vaccine in TBS at its target concentration. The optimal vaccine antigen and adjuvant dose must be determined empirically. A common adjuvant is aluminum phosphate or aluminum hydroxide at a dose of 100 μg/0.1 ml. Mix the vaccine antigen with the alum for 1 h at room temperature to allow adsorption of the protein component of the vaccine to alum (*see* **Note 3**).

3.2 Active Immunization of Mice

1. A common vaccination regimen is to administer the vaccine on days 0, 14, and 28. Deliver a 0.1 ml dose to each mouse by the subcutaneous route into the loose skin over the interscapular or inguinal area.
2. Mice should be bled prior to each immunization, i.e., on days 1, 13, 27, and 41. Restrain the mouse and notch the ear to

identify the animal. Disinfect the tail with 70 % ethanol and warm the tail under a heat lamp. Nick the distal portion of the tail with a clean sharp scalpel blade, and collect blood into a 1.5 ml microcentrifuge tube. Apply pressure to the nicked tail with gauze to stop the bleeding. Allow the collected blood to clot for 1 h at room temperature. Centrifuge (20,800 × *g*, 4 °C, 10 min) the samples in a microfuge and transfer the bloody serum to a fresh 1.5 ml microcentrifuge tube. Centrifuge as above, and carefully transfer the clarified serum to a fresh 0.6 ml microcentrifuge tube. Store sera at –20 °C. Sera can be tested by ELISA starting at a 1:100 dilution. Functional serum antibody assays, such as opsonophagocytic killing assays, cytolytic neutralization assays, or binding inhibition assays, may also be performed with immunized mouse sera.

3.3 Passive Immunization of Mice

1. Serum, protein A purified serum IgG, or affinity purified IgG can be administered intravenously (IV) in the tail vein one day prior to bacterial challenge by the IP route (*see* **Note 4**). Doses of 100 μg to 1 mg IgG can be administered in a 0.2 ml volume.

3.4 Preparation of the S. aureus Inoculum for Challenge

1. Streak the *S. aureus* strain on a CSA plate and incubate at 37 °C for 24 h.
2. Transfer *S. aureus* single colonies from the CSA plate to 1 ml of PBS with an inoculating loop and vortex to achieve a homogenous turbid suspension.
3. Transfer a portion of the bacterial suspension to 5 ml of PBS in a 16 × 150 mm glass tube until the $OD_{650\,nm}$ is 0.431 (~4×10^8 CFU/ml).
4. Dilute the bacterial suspension to the desired concentration for mouse inoculation (0.5 ml/mouse in the bacteremia model and 3 μl/mouse in the surgical wound infection model) (*see* **Note 5**).
5. Serially dilute the bacterial suspension and plate in triplicate on TSA plates to determine the bacterial concentration.

3.5 Bacteremia Model

1. For active immunization experiments, the mice should be challenged no sooner than 14 days after the last immunization. For passive immunization studies, the mice can be challenged 1 day after administration of the IgG preparation.
2. Weigh each mouse prior to bacterial challenge. Inject each animal by the IP route with 0.5 ml of a bacterial suspension containing 1×10^7 to 1×10^8 CFU *S. aureus*, depending on the bacterial strain (*see* **Note 5**).
3. Quantitative blood cultures can be performed 1–4 h after bacterial challenge. The mouse is placed into a restrainer, and

the tail is disinfected with betadine followed by 70 % ethanol. After warming the tail under a heat lamp, a small nick in the distal portion of the tail is made with a sterile scalpel. Blood is aseptically collected (*see* **Note 6**) into a microcentrifuge tube containing the desired anticoagulant. We use heparin at a final concentration in the blood of 20 U/ml. Store the blood on ice until it is plated for culture.

4. Measure the volume of blood sample for each mouse. Because the mice are bacteremic, the blood volume recovered can be quite variable, ranging from 50 µl to 200 µl. Perform quantitative cultures of neat and diluted blood samples in duplicate on BAP (*see* **Note 7**). After 24–48 h, the colonies are enumerated, and the results are expressed as CFU/ml blood.
5. The mice are checked daily (*see* **Note 8**). On day 4 after bacterial challenge, the mice are euthanized by CO_2 asphyxiation, followed by cervical dislocation, and weighed. Weight loss between days 0 and 4 is calculated for each mouse.
6. Both kidneys are excised aseptically, and their weight is recorded. The kidneys are transferred to a 12 × 75 mm sterile tube containing 1 ml TSB. The samples are homogenized on ice for 30 s before they are serially diluted tenfold in TSB in microcentrifuge tubes. Each dilution is plated in duplicate on TSA plates that are incubated for 24–48 h. Colonies are enumerated, and the CFU/ml of the tissue homogenate is calculated (*see* **Note 9**). This CFU/ml is divided by the weight of the sample in grams/ml, so that the bacterial burden data can be expressed as CFU/g kidney.
7. Vaccine-mediated protection against infection is analyzed by the Student *t* test for parametric data or by the Mann–Whitney test for nonparametric data.
8. Representative results for capsule vaccine-mediated protection against bacteremia, bacterial burden in the kidneys, and weight loss are depicted in Fig. 1.

3.6 Surgical Wound Infection Model

1. For active immunization experiments, the mice should be challenged no sooner than 14 days after the last immunization. For passive immunization studies, the mice can be challenged 1 day after administration of the IgG preparation.
2. Prepare a turbid bacterial suspension containing *S. aureus* in 5 ml of PBS according the method described in Subheading 3.4. Dilute the inoculum to achieve between 10^2 and 10^7 CFU/3 µl in PBS for bacterial challenge [9]. To confirm the inoculum dose, dilute the sample and plate in triplicate on TSA plates (*see* **Note 5**).
3. Weigh the mice and anesthetize groups of four to five animals by IP injection of 0.1 ml of a freshly made mixture of ketamine (120 mg/kg) and xylazine (12 mg/kg) (*see* **Note 10**).

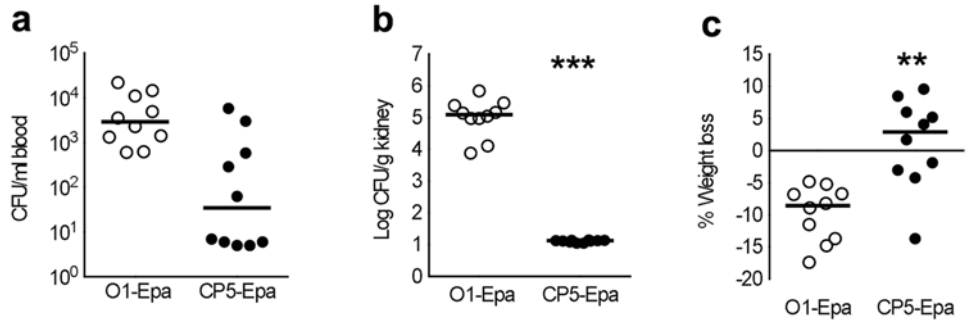

Fig. 1 Active immunization with *Staphylococcus aureus* glycoconjugate vaccines protects mice against bacteremia, renal abscesses, and weight loss. Mice were immunized on days 0, 14, and 28 with *S. aureus* type 5 capsular polysaccharide conjugated to *Pseudomonas aeruginosa* exoprotein A (CP5-Epa). Control animals received an irrelevant *Shigella* O-antigen bioconjugate vaccine (O1-Epa). Mice were challenged by the IP route with 10^7 colony-forming units (CFU) of *S. aureus* Reynolds (CP5). (**a**) Mice given CP5-Epa had fewer bacteria recovered from the blood ($P = 0.0029$) and (**b**) kidneys ($P < 0.0001$) and (**c**) showed reduced weight loss ($P = 0.005$), compared with mice given *Shigella* O1-Epa. (Adapted from Ref. [16] by permission of Oxford University Press)

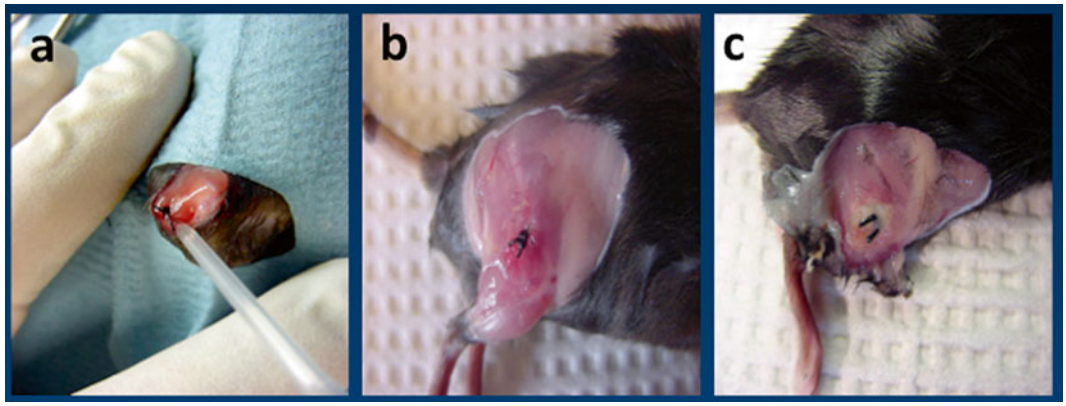

Fig 2 *S. aureus* surgical wound infection. (**a**) The surgical wound is inoculated with 3 μl of PBS or an *S. aureus* suspension. After 3 days, the wound inoculated with (**b**) PBS shows normal gross pathology, whereas the wound inoculated with (**c**) 10^6 *S. aureus* shows inflammation and accumulation of pus around the silk suture

4. Shave the skin over the right thigh muscle of the mouse. Disinfect the surgical area overlaying the thigh muscle with iodine and 70 % ethanol.
5. Put a sterile surgical drape on the disinfected area. Make an incision in the skin overlaying the thigh to expose the muscle. Make a 1-cm incision with a scalpel directly into the thigh muscle to the depth of the bone.
6. Put one suture (4–0 silk) in the middle of the 1-cm incision. Introduce 3 μl of the *S. aureus* suspension into the incision under the suture (Fig. 2a).
7. Resect the skin and close with four 5–0 prolene sutures. Alternatively, close the wound with three wound clips (*see* **Note 11**).

8. Treat mice subcutaneously with the analgesic buprenorphine (0.05–1 mg/kg) every 12 h for 48 h. Alternatively, buprenorphine sustained-release polymer injection (Animalgesic Lab, Inc., Millersville, MD) can be delivered only once by the subcutaneous route (3.25 mg/kg), since it provides analgesia for 72 h.
9. Return the mice to their cage to recover from the anesthesia.
10. After 3 days, the mice are euthanized by CO_2 asphyxiation, followed by cervical dislocation, and weighed. Weight loss between days 0 and 3 is calculated for each mouse.
11. The skin overlaying the wound is clipped off and discarded, exposing the wound (Fig. 2b, c). The wounded muscle is excised and weighed. The tissue is transferred to a 12 × 75 mm polypropylene tube containing 1 ml of TSB.
12. Homogenize the muscle on ice for 30 s.
13. Plate tenfold dilutions of the tissue homogenates in duplicate on TSA. Incubate plates at 37 °C for 24–48 h. The CFU/ml of the tissue homogenate is calculated (*see* **Note 9**). This CFU/ml is divided by the tissue weight in grams/ml, so that the bacterial burden data are expressed as CFU/g tissue.

4 Notes

1. It is helpful to infect animals with *S. aureus* strains carrying an antibiotic resistance marker for positive identification. If the plated specimen (blood or wound tissue) is contaminated with mouse hair or skin flora, the BAP or TSA plates may yield a mixed population of colonies. To definitively distinguish the challenge strain from the bacterial contaminants, one can replica plate samples yielding 30–300 colonies to an antibiotic-containing medium. As a control, one should also replica plate the sample to a nonselective medium such as TSA and BAP to insure adequate replica plating and to evaluate *S. aureus* colony morphology and hemolysis. Useful antibiotic markers include resistance to streptomycin (Sm), erythromycin, tetracycline, and chloramphenicol. It is relatively easy to isolate spontaneous Sm-resistant mutants from most staphylococcal strains, and this provides a useful antibiotic marker. To insure that we have not altered the metabolic profile or growth characteristics of the Sm-resistant isolate compared to the wild-type strain, we verify the identity of the strain by API (bioMérieux, Durham, NC) and growth curves.
2. Capsule is an important virulence factor in *S. aureus* bacteremia as it renders the bacterium resistant to uptake and killing by polymorphonuclear leukocytes. Capsule is not expressed by *S. aureus* in the exponential growth phase. Capsule is produced

by *S. aureus* grown overnight with aeration in media such as TSB or Columbia broth + 2 % NaCl, but not in brain heart infusion medium [17]. Optimal capsule production is achieved on solid medium [18] such as Columbia medium + 2 % NaCl.

3. Aluminum adjuvant is approved for use in humans, whereas many other more potent adjuvants (e.g., Freund's adjuvant) are too reactogenic for human use. The alkaline isoelectric point for aluminum hydroxide makes it suitable for adsorption of proteins with an acidic isoelectric point (e.g., *Pseudomonas aeruginosa* exoprotein A). In contrast, the acidic isoelectric point of aluminum phosphate makes it suitable for adsorption of proteins with an alkaline isoelectric point such as *S. aureus* alpha-toxin. The use of phosphate buffers with alum adjuvants should be avoided. Experimental vaccines should be tested empirically for alum adsorption prior to use. This can be accomplished by mixing the vaccine with the appropriate dose of alum (hydroxide or phosphate) for 1 h at room temperature. Controls include vaccine samples with no alum or alum alone. After adsorption is complete, the samples are centrifuged to pellet the insoluble alum and adsorbed vaccine components. The supernatants are then assessed for unadsorbed vaccine components by an appropriate test, e.g., protein assay. Adsorption of the vaccine to alum results in little to no detectable vaccine antigen in the supernatant compared to control samples incubated without alum.
4. In passive bacteremia experiments, the IgG is given IV 24 h prior to IP challenge. Bacterial challenge by the IP route allows for a persistent seeding of the bloodstream and a prolonged bacteremia. In contrast, the bacteria are more rapidly cleared from the blood following IV challenge [19]. The IgG and bacterial inoculum are delivered to different routes (IV and IP) to avoid IgG-mediated bacterial clearance within the peritoneum, resulting in lower bacteremia levels.
5. For both the bacteremia and surgical wound infection models, preliminary experiments may be needed to determine the optimal challenge inoculum for a particular *S. aureus* strain. In order to demonstrate significant differences between immunized groups, we seek an inoculum dose that will yield ~1000 CFU/ml blood 2 h after challenge in control animals. For surgical wound infection model, the inoculum should be high enough to obtain a tissue bacterial burden of 5- to 6-log CFU/g tissue in control animals. These values allow one to easily evaluate vaccine-mediated protection by a >1 log decrease in the tissue bacterial burden.
6. To avoid contamination of quantitative blood cultures, avoid touching the microcentrifuge tube to the disinfected mouse

tail when collecting heparinized blood from bacteremic mice. Blood cultures are plated onto BAPs to make it easy to distinguish the challenge *S. aureus* strain from the normal flora that sometimes contaminates the blood sample. *S. aureus* strains are generally hemolytic but the contaminating flora, such as *Staphylococcus epidermidis*, gram-negative bacteria, or enterococci show different colony morphologies and are rarely hemolytic. If necessary, replica plating to identify antibiotic marked *S. aureus* strains can be performed, as described above.

7. For quantitative blood cultures, attempt to obtain ~200 μl of blood from each mouse by tail vein nick. Sometimes only ~50 μl can be obtained from bacteremic animals. In that case, one should plate 20 μl of blood in duplicate (plus 80 μl of TSB to make spreading of the inoculum more consistent) to BAPs. Always save at least 10 μl of blood for replating the next day if the colony count is problematic or too numerous to count. Blood samples can be replated with accuracy after storage at 4 °C for ≤24 h.
8. For both models, the bacterial inoculum is intended to be sublethal. Nonetheless, the animals are checked daily, and those found in a moribund condition are euthanized.
9. Culture plates with 30–300 colonies should be counted and used for CFU/ml determinations. Plates with fewer than 30 colonies give statistically unreliable results, while plates with more than 300 colonies are difficult to count accurately. Usually, more than one dilution in a series is plated to be sure that results in a countable range will be obtained. Ignore colony counts from dilutions giving results outside of the countable range.
10. The mice should be fully anesthetized with ketamine/xylazine before the surgical procedure is initiated. The depth of anesthesia can be assessed by pinching their footpad.
11. Skin sutures used to close the surgical wound infection are sometimes removed by the mice during the 3-day infection period, resulting in exposure of the wound and contamination. Use of surgical wound clips is faster, and the clips are difficult for the mouse to remove.

Acknowledgements

This work was supported by National Institutes of Health (grant number R01 AI088754 to J.C.L.). All authors report no potential conflicts.

References

1. Wang L, Lee JC (2015) *Staphylococcus aureus*. In: Bagnoli F, Rappuoli R (eds) Advanced vaccine research methods for the decade of vaccines. Caister Academic Press, Portland, OR, pp 423–445
2. Watts A, Ke D, Wang Q, Pillay A, Nicholson-Weller A, Lee JC (2005) *Staphylococcus aureus* strains that express serotype 5 or serotype 8 capsular polysaccharides differ in virulence. Infect Immun 73:3502–3511
3. Wardenburg JB, Schneewind O (2008) Vaccine protection against *Staphylococcus aureus* pneumonia. J Exp Med 205:287–294
4. Lee JC, Betley MJ, Hopkins CA, Perez NE, Pier GB (1987) Virulence studies, in mice, of transposon-induced mutants of *Staphylococcus aureus* differing in capsule size. J Infect Dis 156:741–750
5. Kuklin NA, Clark DJ, Secore S, Cook J et al (2006) A novel *Staphylococcus aureus* vaccine: iron surface determinant B induces rapid antibody responses in rhesus macaques and specific increased survival in a murine *S. aureus* sepsis model. Infect Immun 74:2215–2223
6. Heraief E, Glauser MP, Freedman LR (1982) Natural history of aortic valve endocarditis in rats. Infect Immun 37:127–131
7. Nemeth J, Lee JC (1995) Antibodies to capsular polysaccharides are not protective against experimental *Staphylococcus aureus* endocarditis. Infect Immun 63:375–380
8. Lee JC, Park JS, Shepherd SE, Carey V, Fattom A (1997) Protective efficacy of antibodies to the *Staphylococcus aureus* type 5 capsular polysaccharide in a modified model of endocarditis in rats. Infect Immun 65:4146–4151
9. McLoughlin RM, Solinga RM, Rich J, Zaleski KJ et al (2006) CD4+ T cells and CXC chemokines modulate the pathogenesis of *Staphylococcus aureus* wound infections. Proc Natl Acad Sci U S A 103:10408–10413
10. Li D, Gromov K, Soballe K, Puzas JE, O'Keefe RJ, Awad H, Drissi H, Schwarz EM (2008) Quantitative mouse model of implant-associated osteomyelitis and the kinetics of microbial growth, osteolysis, and humoral immunity. J Orthop Res 26:96–105
11. Lattar SM, Noto Llana M, Denoel P, Germain S, Buzzola FR, Lee JC, Sordelli DO (2014) Protein antigens increase the protective efficacy of a capsule-based vaccine against *Staphylococcus aureus* in a rat model of osteomyelitis. Infect Immun 82:83–91
12. Malachowa N, Kobayashi SD, Braughton KR, DeLeo FR (2013) Mouse model of *Staphylococcus aureus* skin infection. Methods Mol Biol 1031:109–116
13. Portoles M, Kiser KB, Bhasin N, Chan KHN, Lee JC (2001) *Staphylococcus aureus* Cap5O has UDP-ManNAc dehydrogenase activity and is essential for capsule expression. Infect Immun 69:917–923
14. Bremell T, Lange S, Yacoub A, Ryden C, Tarkowski A (1991) Experimental *Staphylococcus aureus* arthritis in mice. Infect Immun 59:2615–2623
15. Nilsson I-M, Lee JC, Bremell T, Ryden C, Tarkowski A (1997) The role of staphylococcal polysaccharide microcapsule expression in septicemia and septic arthritis. Infect Immun 65:4216–4221
16. Wacker M, Wang L, Kowarik M, Dowd M et al (2014) Prevention of *Staphylococcus aureus* infections by glycoprotein vaccines synthesized in *Escherichia coli*. J Infect Dis 209:1551–1561
17. Risley AL, Loughman A, Cywes-Bentley C, Foster TJ, Lee JC (2007) Capsular polysaccharide masks clumping factor A-mediated adherence of *Staphylococcus aureus* to fibrinogen and platelets. J Infect Dis 196:919–927
18. Lee JC, Takeda S, Livolsi PJ, Paoletti LC (1993) Effects of in vitro and in vivo growth conditions on expression of type-8 capsular polysaccharide by *Staphylococcus aureus*. Infect Immun 61:1853–1858
19. Thakker M, Park J-S, Carey V, Lee JC (1998) *Staphylococcus aureus* serotype 5 capsular polysaccharide is antiphagocytic and enhances bacterial virulence in a murine bacteremia model. Infect Immun 66:5183–5189

Chapter 23

Using MHC Molecules to Define a *Chlamydia* T Cell Vaccine

Karuna P. Karunakaran, Hong Yu, Leonard J. Foster, and Robert C. Brunham

Abstract

Vaccines based on humoral immunity alone are unlikely to protect against infections caused by intracellular pathogens and today's most pressing infectious diseases of public health importance are caused by intracellular infections that include tuberculosis, malaria, HIV/AIDS, and others such as *Chlamydia trachomatis*. For these infections, vaccines that induce cellular immune responses are essential. Major impediments in developing such vaccines include difficulty in identifying relevant T cell antigens and delivering them in ways that elicit protective cellular immunity. Genomics and proteomics now provide tools to allow unbiased empirical identification of candidate T cell antigens. This approach represents an advance on bioinformatic searches for candidate T cell antigens. This chapter discusses an immunoproteomic approach we have used to identify *Chlamydia* T cell antigens. We further discuss how these T cell antigens can be developed into a human vaccine.

Key words Vaccine, Antigen, MHC, T cell, Chlamydia, Dendritic cells, Immunoproteomics

1 Introduction

CD4 T cell-mediated immunity is the major component of host defense against *Chlamydia* infection [1] and the identification of epitopes presented by major histocompatibility complex (MHC) class II molecules should enable the development of a *Chlamydia* T cell vaccine [2]. Dendritic cells (DCs) are at the center of initiation of T cell mediated immune responses [3]. DCs capture antigen in the periphery and migrate to regional lymph nodes where they present processed antigen on MHC molecules to naïve T cells to induce T cell mediated immune responses. Since T cells mainly recognize protein antigens, protective vaccine candidates are to be found within the proteome of an organism.

An approach called immunoproteomics (sometimes immunopeptidomics), in which peptides presented by MHC molecules are identified by tandem mass spectrometry (MS/MS) [4, 5], allows genomic information to guide the delineation of the complete T

Sunil Thomas (ed.), *Vaccine Design: Methods and Protocols: Volume 1: Vaccines for Human Diseases*, Methods in Molecular Biology, vol. 1403, DOI 10.1007/978-1-4939-3387-7_23,

cell immunoproteome of the organism. These methods have been applied to several immunological problems [6] but instrument sensitivity has prevented its applicability to pathogens. Recent advancements in MS/MS technology now provide sensitivity limits at or below one femtomole and are able to measure peptide masses to within one part-per-million accuracy [7]. This brings the detection technology into a range compatible with the levels of microbial peptides that can reasonably be purified from MHC molecules presented on the surface of antigen presenting cells such as DCs. The immunoproteomic approach directly identifies T cell epitopes presented by antigen presenting cells resulting in a vast improvement in the positive validation rate. Another advantage in using immunoproteomics versus reverse vaccinology is that the peptides identified are the result of physiological processing and presentation pathways and are based on both the affinity for the MHC molecules as well as the frequency of their presentation.

We tested this approach in our laboratory to identify T cell antigens for *Chlamydia* and these antigens have been shown to protect mice from *Chlamydia* infection [2, 8]. We have also shown that MHC binding peptides "tag" proteins that are preferentially presented to T cells in other genetic variations of the MHC molecule. Thus this method reliably identifies T cell antigenic proteins that can be used as vaccines in genetically outbred populations. It appears likely that the immunoproteomic approach we have successfully used in *Chlamydia* vaccine research may be useful for other problematic intracellular pathogens such as *Salmonella* and *Mycobacterium tuberculosis* for which vaccine solutions are desperately sought.

2 Materials

2.1 DC Generation

1. Mice: Female C57BL/6 (H2-IA^b) mice at 6–8 weeks of age (Charles River Canada, Saint Constant, Canada). The mice were maintained and used in strict accordance with University of British Columbia guidelines for animal care.
2. DC medium: IMDM supplemented with 10 % FCS, 0.5 mM 2-ME, 4 mM L-glutamine, 50 μg/ml gentamicin, and 5 % of culture supernatant of murine GM-CSF-transfected plasmacytoma X63-Ag8 and 5 % of culture supernatant of murine IL-4 transfected plasmacytoma X63-Ag8 which contained 10 ng/ml GM-CSF and 10 ng/ml IL-4, respectively.

2.2 Immunoaffinity Chromatography

1. Lysis buffer (freshly made): 1 % 3-[(3-Cholamidopropyl) dimethylammonio]-1-propanesulfonate (Sigma-Aldrich), 150 mM NaCl, 20 mM Tris–HCl, pH 8, 0.04 % sodium azide, protease inhibitors (5 μg/ml Aprotinin, 10 μg/ml Leupeptin, 10 μg/ml Pepstatin A, 0.04 % Na Azide, and 1 mM PMSF).

2. 20 mM Tris–HCl, pH 8.0, 150 mM NaCl.
3. 20 mM Tris–HCl, pH 8.0, 1 M NaCl.
4. 20 mM Tris–HCl, pH 8.0.
5. Monoclonal antibody (mAb): Y-3P (specific to H2-IA MHC class II allele).
6. rProtein A Sepharose Fast Flow (rPAS; GE Healthcare).
7. Poly-prep chromatography columns (Bio Rad).
8. Amicon Ultra 10,000 Da cutoff filter units (Millipore).
9. HPLC grade glacial acetic acid.

2.3 Mass Spectrometry

1. Q-Exactive mass spectrometer on-line coupled to a EasyLC 1000 ultra-high performance liquid chromatography system (Thermo Fisher).
2. 2.1 μm ReproSil Pur C18 AQ beads (Dr. Maisch, www.Dr-Maisch.com).
3. 5 μm-diameter Aqua C-18 beads (Phenomenex, www.phenomenex.com).

2.4 ELISPOT

1. 96-well MultiScreen-HA filtration plates (Millipore).
2. Complete RPMI medium: RPMI 1640 supplemented with 10 % FCS, 0,5 mM 2-ME, 4 mM L-glutamine and 50 μg/ml gentamicin.
3. Heat-killed *C. muridarum* elementary bodies (HK-EB) (56 °C 30 min).
4. *Chlamydia* T cell antigens (peptides or proteins).
5. PBST (PBS containing 0.05 % Tween 20).
6. IFN-γ specific monoclonal antibody (BD PharMingen, Clone R4-6A2).
7. Biotinylated murine IFN-γ specific monoclonal antibodies (BD PharMingen, Clone XMG1.2).
8. Streptavidin–alkaline phosphatase (BD PharMingen).
9. 5-bromo-4-chloro-3-indolyl phosphate and nitro blue tetrazolium tablet (Sigma-Aldrich).

2.5 Molecular Cloning, Expression and Purification of Recombinant Proteins

1. Herculase Enhanced DNA polymerase (Agilent Technologies).
2. QIAquick PCR purification kit (Qiagen).
3. pET32a expression vector (Novagen).
4. Restriction endonucleases and T4 DNA ligase (NEB).
5. *Escherichia coli* BL21(DE3) chemically competent cells (Stratagene).
6. Luria broth (Sigma).
7. Isopropyl-β-D-thiogalactoside pyranoside (Invitrogen).
8. Nickel column using the His bind purification system (Qiagen).

2.6 Immunization

1. T cell antigens (recombinant chlamydial proteins).
2. Dimethyldioctadecylammonium (DDA; Avanti Polar Lipids).
3. Monophosphoryl lipid A (MPL; Avanti Polar Lipids).

2.7 Murine Genital Tract Infection Challenge Model

1. Female C57BL/6 ($H2^b$) mice, 6–8 week of age (Charles River, Canada).
2. Medroxyprogesterone acetate (Depo-Provera; Pharmacia and Upjohn).
3. Non-Surgical Embryo Transfer Device for Mice (ParaTechs, Product # 60010).
4. Cell Homogenizer (MP Biomedicals).
5. Cycloheximide (Sigma-Aldrich).
6. Anti-EB mouse polyclonal antibody (Home-made).
7. Peroxidase-conjugated donkey anti-mouse IgG (Jackson ImmunoResearch Code: 715-035-150).
8. 3,3′-diaminobenzidine (DAB) substrate (Vector Laboratories).

2.8 Multiparameter Flow Cytometry

1. Complete RPMI medium.
2. Heat killed-*Chlamydia* elementary bodies and T cell antigens.
3. Antibodies: PerCP/Cy5.5 anti-mouse CD3ε (Clone: 145-2C11), Pacific Blue anti-mouse CD4 (Clone: RM4.5), APC/Cy7 anti-mouse CD8 (Clone: 53-6.7), APC anti-mouse IFN-γ (Clone: XMG1.2), PE-Cy7 anti-mouse TNF-α (Clone: MP6-XT22), and anti-mouse CD28 (Clone: 37.51).
4. Cell viability dye, red fluorescent reactive dye (L23102; Molecular Probes).
5. BD Cytoperm Plus Fixation/Permeabilization kit (BD Pharmingen).
6. 4 % formaldehyde solution.
7. FlowJo software program (Tree Star).

3 Methods (see Fig. 1)

3.1 Generation of BMDCs and Chlamydia Infection

1. Bone marrow cells flushed from the femurs of C57BL/6 mice are cultured in Falcon petri dishes at 4×10^7 cells in 50 ml DC medium.
2. On day 3, half of culture supernatants are removed and fresh DC medium is added.
3. On day 5, nonadherent cells (purity of >50 % CD11c+) are harvested and cultured in fresh DC medium for *Chlamydia* infection.

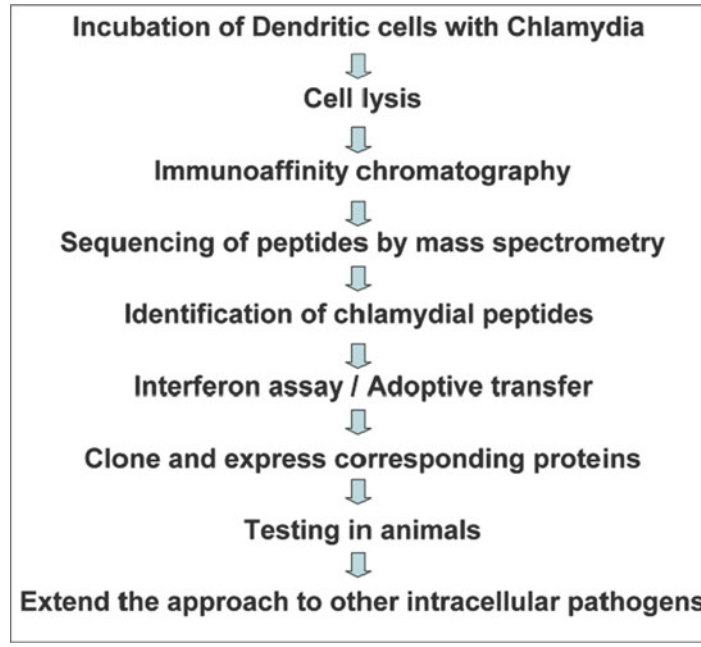

Fig. 1 Schematic depiction of the sequence of steps involved in the immunoproteomic approach for *Chlamydia* T cell vaccine development

4. Immature BMDCs are infected at a 1:1 multiplicity of infection with *Chlamydia* for 12 h.
5. Infected matured BMDCs are harvested, washed twice with PBS and the pellets are stored at −80 °C.
6. **Steps 1–5** are repeated until four to six billion infected BMDCs are collected and stored.

3.2 Purification of MHC Class II-Bound Peptides

1. Different batches of BMDCs infected with *Chlamydia* are pooled and solubilized in cold lysis buffer (10^8 BMDCs/ml buffer) by rocking at 4 °C for 2–3 h (all tubes kept in ice).
2. Lysates are centrifuged at 110,000 × *g* for 1 h at 4 °C.
3. Pellets are discarded and the supernatant centrifuged again at 110,000 × *g* for 30 min at 4 °C.
4. Supernatant containing MHC molecules bound to peptides is transferred to a 50 cc tube that has pre-washed rPAS beads (no mAb bound for pre-clear) and pellets are discarded. Usually ~0.8–1.0 ml of rPAS beads is used for the pre-clear step.
5. Rotate at 4 °C for 2–3 h.
6. rPAS beads are spinned down (1 min spin at 160 × *g*) and supernatant collected into a 50 cc tube containing mAb-bound rPAS.
7. Rotate at 4 °C overnight.
8. mAb-bound rPAS beads are spinned down (1 min at 160 × *g*) and supernatant removed.

9. Beads are transferred to a 15 cc tube and the beads are washed twice with 10 ml lysis buffer by centrifuging at 160 × *g* for 1 min.
10. Beads are transferred to a Bio-Rad Poly-prep chromatography column by washing with 5 ml 20 mM Tris–HCl, pH 8.0, 150 mM NaCl.
11. Beads are washed with 5 ml of following buffers (all kept on ice).
    (a) 1 time 20 mM Tris–HCl, pH 8.0, 150 mM NaCl
    (b) 2 times 20 mM Tris–HCl, pH 8.0, 1 M NaCl
    (c) 3 times 20 mM Tris–HCl, pH 8.0
12. Peptide-bound MHC molecules are eluted from rPAS by adding 4 bed volumes of 0.2 N acetic acid (bed volume of Ab bound rPAS is usually around 1 ml) and 380 µl acetic acid is then added to the 4 ml elute to further separate the peptides from MHC molecules.
13. For isolation of class II associated peptides, 4 ml elute is transferred to a filter unit with 10,000 DA cutoff and centrifuged at 1000 × *g* (prior to use, the filter units are pre-wet with 20 mM Tris–HCl, pH 8.0, and spun for 30 min at 1000 × *g*).

3.3 Identification of MHC Class II-Bound Peptides

1. Isolated MHC class II-bound peptides are purified, concentrated, filtered, and desalted using STop And Go Extraction tips [9].
2. Peptides are analyzed by LC-MS/MS using a Q-Exactive mass spectrometer on-line coupled to a EasyLC 1000 UPLC.
3. Analytical columns are packed into 30 cm long, 75 µm inner diameter fused silica columns packed with 2.1 µm diameter ReproSil Pur C18 AQ beads, joint with 2-cm-long, 100-µm-inner diameter fused silica trap column packed with 5 µm-diameter Aqua C-18 beads and a 20-µm-inner diameter fused silica gold coated spray tip with 6-µm-diameter opening.
4. LC buffer A consists of 0.5 % acetic acid and buffer B consists of 0.5 % acetic acid and 80 % acetonitrile. Gradients are run from 10 % B to 32 % B over 51 min, then from 32 % B to 40 % B in the next 5 min, then increased to 100 % B over 2 min period, held at 100 % B for 2.5 min, and then dropped to 0 % B for another 20 min to recondition the column.
5. The Q-Exactive is set to acquire a full range scan at 60,000 resolution, from which the ten most intense multiply charged ions per cycle are isolated for fragmentation.
6. The search is performed with MaxQuant (v1.5.1.12) against a database comprising the protein sequences from the mouse and *Chlamydia* proteome. The estimated false discovery rate is below 2 % (*see* **Note 1**) (Tables 1 and 2).

Table 1
Summary of chlamydial and murine derived unique MHC class II-bound peptides, epitopes, and source proteins identified in one sample study

	Peptides	Epitopes	Proteins
Mouse	331	159	145
Chlamydia	13	8	8
Total	344	166	153

Table 2
MHC class II-bound *C. muridarum* peptides identified using immunoproteomics [2]

Peptide sequence	Source protein	Abbreviation[a]	Entrez Gene ID
GNEV**FVSPAAHII**D GNEV**FVSPAAHII**DRPG KGNEV**FVSPAAHII**DRPG EV**FVSPAAHII**DRPG	Ribosomal protein L6	$RplF_{51–59}$	1246168
SPGQTN**YAAAKAGII**GFS SPGQTN**YAAAKAGII**G	3-oxoacyl-(acyl carrier protein) reductase	$FabG_{157–165}$	1245868
KLDG**VSSPAVQES**ISE	Anti-anti-sigma factor	$Aasf_{24–32}$	1246070
ASPI**YVDPAAAGG**QPPA SPI**YVDPAAAGG**QPPA	Polymorphic membrane protein G	$PmpG_{303–311}$	1246433
DLN**VTGPKIQTD**VD	Hypothetical protein TC0420	$TC0420_{54–62}$	1245773
IGQE**ITEPLANTV**IA	ATP-dependent Clp protease, proteolytic subunit	$Clp\text{-}1_{36–44}$	1245608
AFHL**FASPAANYI**HTG	Polymorphic membrane protein F	$PmpE/F\text{-}2_{351–359}$	1246432
MTT**VHAATATQS**VVD	Glyceraldehyde 3-phosphate dehydrogenase	Gap_{148156}	1246159

[a]The range of numbers next to the protein abbreviation represent the nine core amino acid residues (in *bold*) for MHC class II peptides

3.4 Screening of Immunodominant Antigens (Peptides and Proteins) Using IFN-γ ELISPOT Assay (See Fig. 2)

1. 96-well MultiScreen-HA filtration plates are coated overnight at 4 °C with 2 μg/ml of murine IFN-γ specific monoclonal antibody.
2. The plates are washed with sterile PBS and blocked with complete RPMI medium at 37 °C for 2 h.
3. Splenocytes from mice who have been previously infected with live *Chlamydia* are harvested and resuspended in complete RPMI medium at 1×10^7/ml.
4. Splenocytes are added to the plates (1×10^6/well) and stimulated in vitro with 1 μg/ml individual *Chlamydia* antigens or 5×10^5 IFU/ml heat killed-EBs (a positive control) for 20 h at 37 °C and 5 % CO_2.

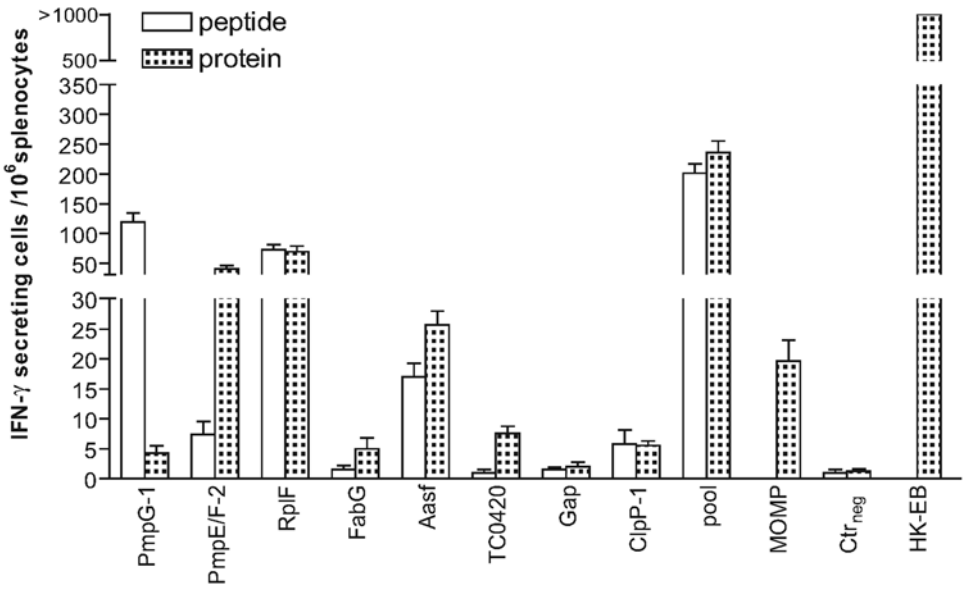

Fig. 2 Recognition of individual *Chlamydia* peptides eluted from DCs and their source proteins in C57BL/6 mice recovered from live *C. muridarum* infection identified by IFN-γ ELISPOT assay. Mice are infected intranasally with 1000 IFU live *C. muridarum*. One month later, the splenocytes from recovered mice are harvested and stimulated in vitro for 20 h with 2 μg/ml individual peptide, 1 μg/ml individual protein, pooled peptides, or pooled proteins. One irrelevant OVA peptide and GST are used as peptide and protein negative controls (Ctr_{neg}), respectively, and HK-EB as positive control. Chlamydial major outer membrane protein (MOMP, a leading vaccine candidate previously studied by many investigators) stimulation was also set up as a reference. The results represent the average of duplicate wells and are expressed as the means ± SEM of *Chlamydia* Ag-induced IFN-γ-secreting cells per 10^6 splenocytes for groups of six mice. These data are representative of three similar experiments [8]

5. The cells are dumped and the plates are flooded with cold distilled water for 5 min to lyse the cells. Then the plates are washed with distilled cold water and PBST to completely remove the cells.
6. The plates are incubated with biotinylated murine IFN-γ specific monoclonal antibodies at 2 μg/ml for 2 h at room temperature.
7. The plates are washed with PBST and then incubated with streptavidin–alkaline phosphatase at a 1:1000 dilution for 1 h at room temperature.
8. The plates are washed with PBST followed by water and 50 μl of BCIP/NBT solution (1 tablet in 10 ml H_2O) is added to each well to develop spots in about 30 min.
9. The plate are washed with water and dried by air.

3.5 Molecular Cloning, Expression, and Purification of Recombinant Proteins

1. DNA fragments encoding the recombinant proteins are generated by PCR using genomic DNA isolated from *Chlamydia*. PCR reactions are carried out using Herculase Enhanced DNA polymerase.
2. The PCR product is purified with the QIAquick PCR purification kit and the purified DNA fragments are cloned into pET32a expression vector after restriction enzyme digestion with BamHI / NotI using standard molecular biology techniques.
3. The accuracy of the subcloned genes is confirmed by sequencing.
4. Plasmids containing the genes encoding recombinant proteins are transformed into the *E. coli* strain BL21(DE3).
5. Protein expression is carried out by inducing the lac promoter for expression of T7 RNA polymerase using isopropyl-β-D-thiogalactoside pyranoside.
6. The expressed recombinant proteins with N-terminal His-tag are purified by nickel column using the His bind purification system.
7. LPS removal of these proteins is carried out by adding 0.1 % Triton-114 in one of the wash buffers during purification.

3.6 Adjuvant (DDA/MPL) Formulation

1. DDA is mixed into 10 mM Tris-HCl buffer at pH 7.4 to a concentration of 3.3 mg/ml and heated to 80 °C while being stirred continuously on a magnetic hot plate for 20 min and then cooled to room temperature.
2. MPL was suspended in distilled water containing 0.2 % triethylamine to a concentration of 1 mg/ml. The MPL solution was heated in a 70 °C water bath for 30 s and then vortexed for 60 s. The heating and vortexing procedure was repeated three times.
3. The MPL was mixed with DDA at 1:3 volume ratio immediately before use. The emulsion consisted of 250 μg DDA and 25 μg MPL per 100 μl (*see* **Note 2**).

3.7 Immunization

1. Five micrograms of recombinant protein is diluted in 100 μl of 10 mM Tris buffer (pH 7.4) and mixed by briefly vortexing with 100 μl DDA-MPL adjuvant for each dose of immunization.
2. Mice are immunized three times subcutaneously at the base of the tail at 2-week intervals.
3. A group of mice immunized with phosphate-buffered saline (PBS) is used as a negative control. A prior *Chlamydia* infection group is used as a positive control in which mice have been previously intravaginally or transcervically infected with live *Chlamydia*.

3.8 Intravaginal Infection Challenge Model (for *C. muridarum*) (See Figs. 3 and 4)

1. Mice are injected subcutaneously with 2.5 mg of medroxyprogesterone acetate.
2. One week after Depo-Provera treatment, mice are challenged intravaginally with 1500 IFU of *C. muridarum*.
3. Cervicovaginal washes are taken at selected dates after infection.
4. Samples are vortexed in 0.5 ml of SPG buffer and stored at −80 °C until analysis.

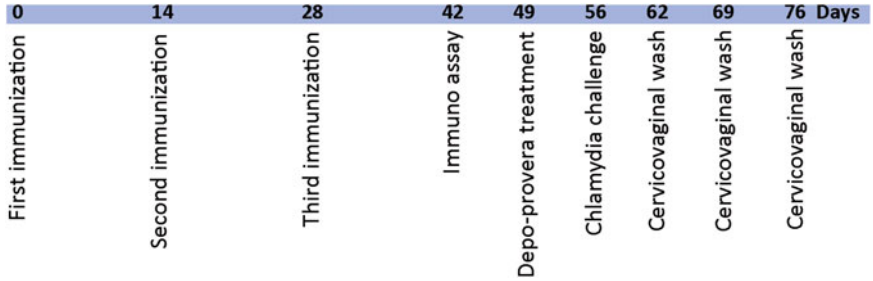

Fig. 3 Timeline for the evaluation of protection, pathology, and immune response in mice

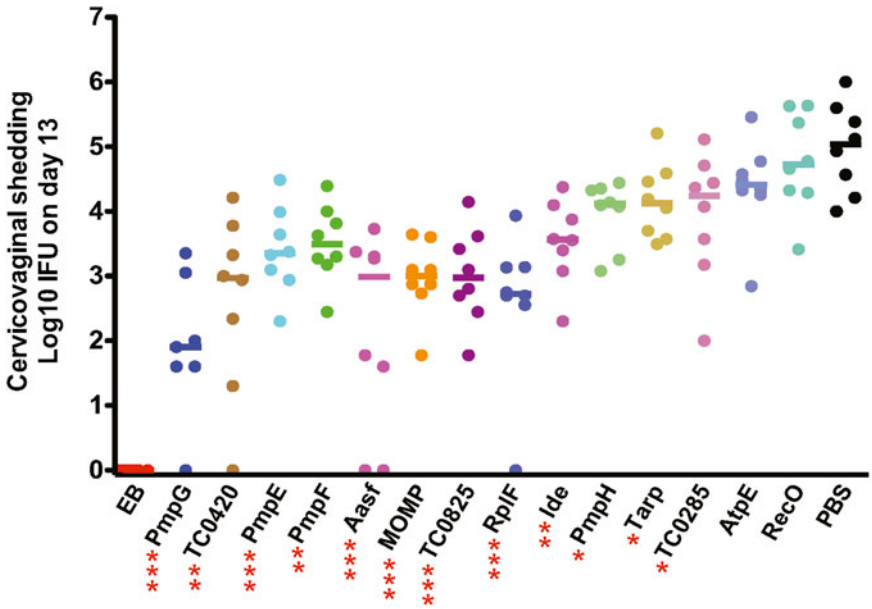

Fig. 4 Protective efficacy against *C. muridarum* genital tract infection in C57BL/6 mice vaccinated with different *C. muridarum* proteins formulated with DDA-MPL adjuvant. Four weeks after the final immunization, mice are challenged intravaginally with 1500 IFU of *C. muridarum*. Cervicovaginal washes are taken at day 13 after challenge, and bacterial shedding was measured on HeLa 229 cells. Mice immunized with PBS serve as a negative control, and mice intranasally infected once with 1500 IFU of *C. muridarum* are used as a positive control. A group of mice immunized with MOMP was set up as a reference. *, **, and ***, *P* values of <0.05, <0.01, and <0.001, respectively, in comparison to results for the PBS group [12]

5. Quantitative shedding of *Chlamydia* is measured by infection of Hela 229 cell monolayers with a titrated volume of the sample suspension. The plates are centrifuged at $1600 \times g$ for 30 min at room temperature followed by incubation at 37 °C for 30 min.
6. Infection medium is replaced with fresh medium containing 1 μg/ml cycloheximide, and the cells are incubated at 37 °C for 24 h.
7. Hela cells are fixed in methanol containing 0.3 % H_2O_2 for 30 min and inclusions are visualized by staining with anti-EB mouse polyclonal antibody, followed by peroxidase-conjugated donkey anti-mouse IgG and a 3,3′-diaminobenzidine (DAB) substrate as described previously [10].

3.9 Transcervical Infection Challenge Model (for C. trachomatis) [11] (See Note 3)

1. Mice are infected with *C. trachomatis* serovar D transcervically after two s.c. injections with 2.5 mg of medroxyprogesterone acetate at day 3 and day 10 prior to infection.
2. Transcervical inoculation of *C. trachomatis* is performed using NSET—a speculum is inserted into the mouse vaginal tract and the NSET tip directly inserted into the upper genital tract.
3. *C. trachomatis* inoculum (2×10^7 IFU in 10 μl) is pipetted into the upper genital tract and the NSET device and speculum are removed.
4. At day 6 post infection, vaginal swabs and whole genital tracts are collected. Whole genital tracts in 1 ml SPG are homogenized using FastPrep-24 Tissue and Cell Homogenizer. The samples are stored at −80 °C for titration. *Chlamydia* titers in homogenates of genital tract tissue and in vaginal swabs are measured by inclusion counts on Hela cells.

3.10 Multiparameter Flow Cytometry (See Fig. 5)

1. Splenocytes from mice who have been previously infected with live *Chlamydia* EBs or vaccinated with *Chlamydia* antigens are harvested and resuspended in complete RPMI medium at 1×10^7/ml.
2. Splenocytes are added to 96 well round bottom plates (1×10^6 cells/well) and incubated with anti-mouse CD28 (2 μg/ml) and heat killed-EBs (5×10^5 IFU/ml) or individual *Chlamydia* antigens (1 μg/ml) for 4 h at 37 °C and 5 % CO_2.
3. Brefeldin A is added at a final concentration of 1 μg/ml, and cells are incubated for an additional 12 h before intracellular cytokine staining.
4. Cells are surface stained for CD3, CD4, and CD8 as well as the viability dye, red-fluorescent reactive dye followed by staining for IFN-γ, TNF-α using BD Cytoperm Plus Fixation/Permeabilization kit according to the manufacturer's instruction.

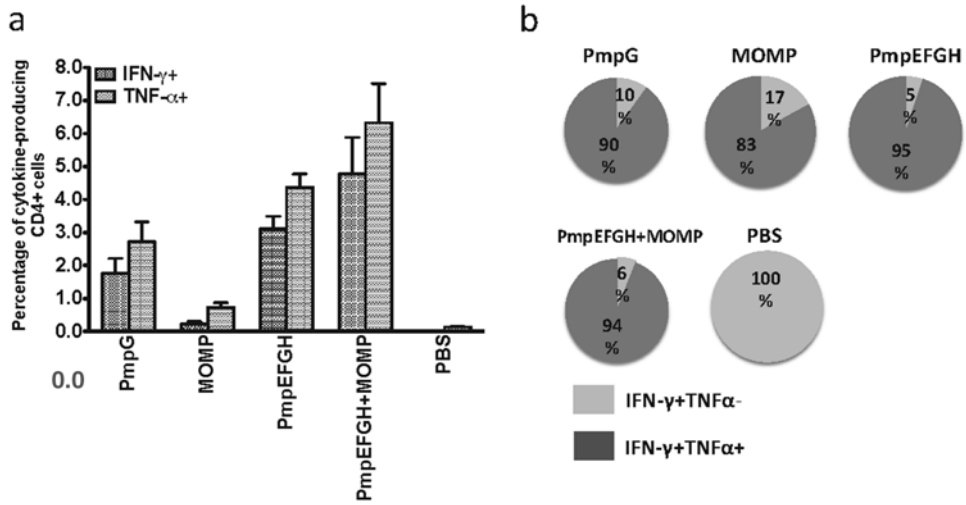

Fig. 5 *C. muridarum*-specific cytokine responses after immunization with different vaccine formulations in C57BL/6 mice. Two weeks after the final immunization, splenocytes from different vaccine groups are harvested and stimulated with HK-EB (5×10^5 IFU/ml). IFN-γ- or TNF-α-producing CD4 T cells are analyzed by multiparameter flow cytometry. (**a**) Percentage of IFN-γ- or TNF-α-producing CD4 T cells from each vaccine group. The results are expressed as means ± SEM for groups of six mice. (**b**) Fraction of IFN-γ single- and IFN-γ/TNF-α double-positive cells in total IFN-γ-producing CD4 T cells. All vaccine formulations most commonly elicited double positive cytokine producing CD4 T cells [13]

5. Cells are finally resuspended in 4 % formaldehyde solution.
6. Generally 200,000 live lymphocytes per sample are acquired on the flow cytometer and data are analyzed using the FlowJo software program.

4 Notes

1. The false dsiscovery rate was calculated using a reversed database search where hits against the reversed database at a given threshold were considered false discoveries and expressed as a fraction of total discoveries from both forward and reversed databases.
2. We did a systematic evaluation of different adjuvants that elicits potent protective immunity exhibiting a strong Th1 bias. We evaluated lipid nanoparticles as delivery vehicles with CpG as immunomodulator to deliver our protein antigens. The results were negative in terms of generating protective immunity. When using ISCOMs marginally better results were observed. We also tried to deliver the immunogen to the mucosal immune system, using plasmid DNA encoding protein antigens delivered via hepatitis E virus like particles; the results were again negative. We next evaluated five other adjuvants, three of which

used cationic liposomes as delivery system (DDA-MPL, DDA-Trehalose dibehenate [DDA-TDB], DDA-monomycolyl glycerol [DDA-MMG], Montarnide ISA720/CpG-ODN1826, and alum). The results showed that DDA/MPL and DDA/TDB are the most promising adjuvants at inducing protective immunity against *Chlamydia* genital tract infection in mouse models, characterized by the generating high frequency of multifunctional CD4+ T cells that coexpress IFN-γ and TNF-α cytokines. We found that the frequency of multifunctional T cells coexpressing IFN-γ, TNF-α with or without IL-2 induced by live *C. muridarum* and immunization with DDA/MPL most accurately correlated with the pattern of protection against *Chlamydia* genital tract infection, suggesting that IFN-γ+ producing CD4+ T cells that highly coexpress TNF-α are the optimal effector cells for protective immunity.

3. Since *C. trachomatis* does not infect the murine genital tract as efficiently as does *C. muridarum*, the standard vaginal inoculation method used for *C. muridarum* does not work equally well to immunologically evaluate *C. trachomatis* antigens. We therefore utilized the transcervical infection model established by Gondek et al. [11] using *C. trachomatis* serovar D instead of serovar L2.

Acknowledgement

This work was supported by a grant from the National Institutes of Health (grant no. R01AI076483).

References

1. Brunham RC, Rey-Ladino J (2005) Immunology of Chlamydia infection: implications for a Chlamydia trachomatis vaccine. Nat Rev Immunol 5:149–161
2. Karunakaran KP, Rey-Ladino J, Stoynov N, Berg K et al (2008) Immunoproteomic discovery of novel T cell antigens from the obligate intracellular pathogen Chlamydia. J Immunol 180:2459–2465
3. Steinman RM, Pope M (2002) Exploiting dendritic cells to improve vaccine efficacy. J Clin Invest 109:1519–1526
4. Hunt DF, Michel H, Dickinson TA, Shabanowitz J et al (1992) Peptides presented to the immune system by the murine class II major histocompatibility complex molecule I-Ad. Science 256:1817–1820
5. Hunt DF, Henderson RA, Shabanowitz J, Sakaguchi K et al (1992) Characterization of peptides bound to the class I MHC molecule HLA-A2.1 by mass spectrometry. Science 255:1261–1263
6. de Jong A (1998) Contribution of mass spectrometry to contemporary immunology. Mass Spectrom Rev 17:311–335
7. Olsen JV, de Godoy LM, Li G, Macek B, Mortensen P et al (2005) Parts per million mass accuracy on an Orbitrap mass spectrometer via lock mass injection into a C-trap. Mol Cell Proteomics 4:2010–2021
8. Yu H, Jiang X, Shen C, Karunakaran KP, Brunham RC (2009) Novel Chlamydia muridarum T cell antigens induce protective immunity against lung and genital tract infection in murine models. J Immunol 182:1602–1608
9. Ishihama Y, Rappsilber J, Mann M (2006) Modular stop and go extraction tips with stacked disks for parallel and multidimensional

Peptide fractionation in proteomics. J Proteome Res 5:988–994
10. Bilenki L, Wang S, Yang J, Fan Y et al (2005) NK T cell activation promotes Chlamydia trachomatis infection in vivo. J Immunol 175: 3197–3206
11. Gondek DC, Olive AJ, Stary G, Starnbach MN (2012) CD4+ T cells are necessary and sufficient to confer protection against Chlamydia trachomatis infection in the murine upper genital tract. J Immunol 189:2441–2449
12. Yu H, Karunakaran KP, Jiang X, Shen C, Andersen P, Brunham RC (2012) Chlamydia muridarum T cell antigens and adjuvants that induce protective immunity in mice. Infect Immun 80:1510–1518
13. Yu H, Karunakaran KP, Jiang X, Brunham RC (2014) Evaluation of a multisubunit recombinant polymorphic membrane protein and major outer membrane protein T cell vaccine against Chlamydia muridarum genital infection in three strains of mice. Vaccine 32:4672–4680

Chapter 24

An Approach to Identify and Characterize a Subunit Candidate *Shigella* Vaccine Antigen

Debasis Pore and Manoj K. Chakrabarti

Abstract

Shigellosis remains a serious issue throughout the developing countries, particularly in children under the age of 5. Numerous strategies have been tested to develop vaccines targeting shigellosis; unfortunately despite several years of extensive research, no safe, effective, and inexpensive vaccine against shigellosis is available so far. Here, we illustrate in detail an approach to identify and establish immunogenic outer membrane proteins from *Shigella flexneri* 2a as subunit vaccine candidates.

Key words *Shigella flexneri* 2a, Outer membrane proteins, Protective immune response, Macrophages, T cell, B cell

1 Introduction

Shigellosis or bacillary dysentery, an acute intestinal infection caused by bacteria of genus *Shigella*, is a leading cause of childhood morbidity and mortality particularly in developing countries where it is estimated that over 163 million cases occur annually, leading to possibly one million deaths per year worldwide [1]. While control and treatment of shigellosis outbreaks with antibiotics is feasible, the high cost of antibiotics and the constant emergence of antibiotic resistant *Shigella* species, even to the newest antibiotics, stress the prerequisite for an effective vaccine to combat against shigellosis in the developing regions of the world [2].

Numerous strategies to develop vaccines targeting *Shigella* have been explored over several decades; nevertheless, a licensed vaccine is not accessible so far. Some of the important approaches of *Shigella* vaccines include live attenuated vaccines [3, 4], delivery of *Shigella* LPS or O polysaccharides with carriers such as proteosomes [5], tetanus toxoid [6], or ribosomes [7], conjugate vaccines, in which *Shigella* O-specific polysaccharide (O-Ag) is conjugated with protein from other strains [8], a hybrid vaccine, in which attenuated *Shigella* bacteria are used as vectors for expressing

Sunil Thomas (ed.), *Vaccine Design: Methods and Protocols: Volume 1: Vaccines for Human Diseases*, Methods in Molecular Biology, vol. 1403, DOI 10.1007/978-1-4939-3387-7_24,

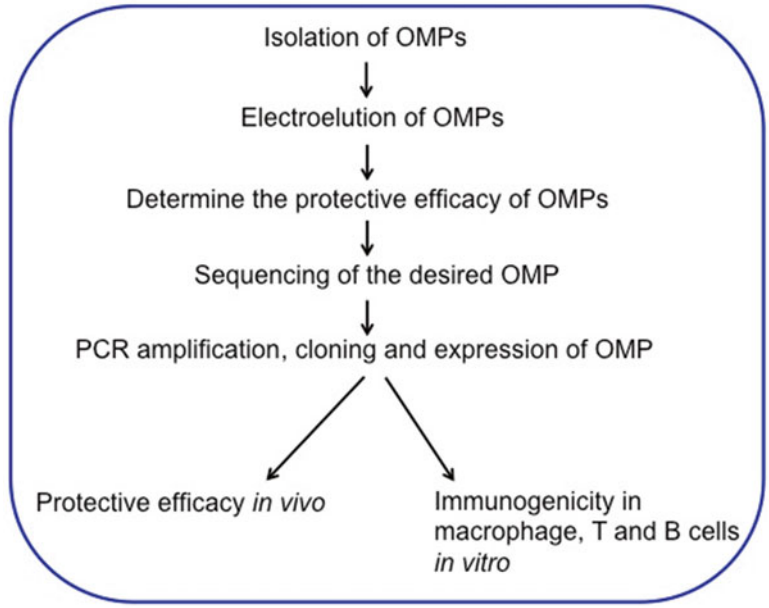

Fig. 1 Flowchart for identification of an effective vaccine antigen

enterotoxigenic *Escherichia coli* (ETEC) antigen [9], invasion proteins [10], etc. However, it has been observed that the current vaccine candidates are not immunogenic enough [11, 12], implying the identification of novel protective antigens capable of triggering robust immune response.

Recent studies have shown that bacterial outer membrane proteins (OMP) are attractive vaccine antigens [13, 14] and we have established outer membrane protein A (OmpA) of *S. flexneri* 2a as an immunogenic and efficacious protective subunit vaccine candidate against shigellosis [15–20]. Here we describe in detail of how OMPs of *S. flexneri* 2a can be identified and characterized as fruitful protective subunit vaccine antigens against shigellosis (Fig. 1).

2 Materials

Prepare all reagents and solutions using ultrapure water and store at room temperature unless stated otherwise. Please note we do not employ sodium azide to the reagents.

2.1 Components for Isolation of Outer Membrane Proteins

2.1.1 Bacterium

Shigella flexneri 2a (N.Y-962/92).

2.1.2 Culture Medium

Tryptic soy broth; Suspend 30 g of dehydrated media in 1 L of ultrapure water. Sterilize at 121 °C for 15 min. Cool to 45–50 °C. Mix gently and dispense into sterile culture tubes and store the tubes at 4 °C.

2.1.3 Buffer and Detergent

HEPES (N-2 hydroxyethyl piperazine N′-ethanesulfonic acid); 1 M HEPES, pH 7.0. Weigh 238.30 g HEPES and transfer to a glass beaker. Add ultrapure water to a volume of 900 ml. Mix and adjust pH with sodium hydroxide. Finally, bring the final volume to 1 L with ultrapure water. Use filtration for sterilization.

10 % N-lauroylsarcosine sodium salt; Dissolve 10 g of N-lauroylsarcosine sodium salt in 100 ml of 100 mM HEPES, pH 7.

2.2 Components for Evaluating Immune Response in Rabbit and Electroelution of Proteins

2.2.1 Animal

For immunization experiments use outbred New Zealand white rabbits of either sex weighing between 1.7 and 2.5 kg. Acclimatize all the animals in laboratory for a week before performing the experiments.

2.2.2 Preparation of Heat-Killed Bacteria

Grow *S. flexneri* 2a in TSB with 0.6 % yeast extract overnight at 37 °C with shaking (200 rpm). Harvest bacteria by centrifugation at 10,000 × *g* for 10 min, wash the bacterial pellet twice with phosphate buffer saline (PBS) and adjust to a concentration of 10^{10} bacteria per ml. Expose the bacterial cells under steaming condition for 1 h at 100 °C in an autoclave under normal atmospheric pressure.

2.2.3 Preparation of Working Solutions for SDS-PAGE

Solution A: 30 % acrylamide stock solution [29.2 % (w/v) acrylamide and 0.8 % N,N′-methylene bis-acrylamide]; Solution B: 1.5 M Tris–HCl, pH 8.8; Solution C: 0.5 M Tris–HCl, pH 6.8; Solution D: 10 % (w/v) ammonium persulfate (prepare just prior to use); 10 % sodium dodecyl sulfate solution.

2.2.4 Preparation of Electrophoresis Buffer (pH 8.3)

Glycine—14.4 g; Tris–HCl—3.0 g; 0.1 % SDS—1.0 g; distilled water—1000 ml.

2.2.5 Preparation of 5× Sample Buffer (10 ml)

0.6 ml 1 M Tris–HCl, pH 6.8; 5 ml 50 % glycerol; 2 ml 10 % SDS; 0.5 ml 2-mercaptoethanol; 1 ml 1 % bromophenol blue; 0.9 ml distilled water.

Stable for weeks in the refrigerator or for months at –20 °C.

2.2.6 Solutions for Preparing SDS-PAGE Resolving Gels

↓Components/Gel %→	5 %	7.5 %	10 %	12.5 %	15 %	20 %
Water	10.5	9.00	7.50	6.00	4.50	1.50
Solution A (ml)	3.00	4.50	6.00	7.50	9.00	12.00
Solution B (ml)	4.50	4.50	4.50	4.50	4.50	4.50
Solution D (ml)	0.08	0.08	0.08	0.08	0.08	0.08
10 % SDS (ml)	0.10	0.10	0.10	0.10	0.10	0.10
TEMED (ml)	0.01	0.01	0.01	0.01	0.01	0.01

2.2.7 Solutions for Preparing 5 % SDS-PAGE Stacking Gel

Water—3.60 ml; Solution A—0.90 ml; Solution C—1.50 ml; Solution D—0.20 ml; 10 % SDS—0.10 ml; TEMED—0.01 ml.

3 Methods

3.1 Preparation of Outer Membrane Proteins

Prepare outer membrane proteins according to the method of Fillip et al. [21].

1. Grow *S. flexneri* 2a (N.Y-962/92) in tryptic soy broth at 37 °C for 18 h under shaking condition.
2. Harvest the cells by centrifugation at 10,000 × *g* (Beckman) for 10 min and then wash twice in 100 mM HEPES (N-2 hydroxyethyl piperazine N′-ethanesulfonic acid, pH 7.0) buffer.
3. Suspend the harvested cells in 50 ml of HEPES buffer, pH 7.0 and disrupt the cells with an ultrasonic disintegrator (MICROSON) at 4 °C with intermittent bursts of 1 min.
4. Remove the unbroken cells by centrifugation at (10,000 × *g*) for 10 min at 4 °C.
5. Treat the envelope fraction with 0.5 % (w/v) N-lauroylsarcosine sodium salt for 20 min at room temperature to selectively solubilize the inner membrane part. Recover the insoluble outer membrane protein (OMP) fraction by centrifugation at 100,000 × *g* for 1 h at 4 °C.
6. Wash the OMP fraction twice with HEPES buffer, pH 7.0 and use this fraction immediately or preserve at −20 °C for further processing.

3.2 Identification and Electroelution of Major Outer Membrane Protein

In order to identify the immunogenic major outer membrane proteins, rabbits were immunized with heat-killed *S. flexneri* 2a and the serum was collected to measure OMP-specific antibodies. Additionally, the OMP fraction was immunoblotted with the raised

serum to profile the major outer membrane proteins (MOMP). The individual MOMP was electroeluted and protective efficacy of each MOMP was assessed in rabbit model of shigellosis.

3.2.1 Identification of Outer Membrane Proteins as Immunogens

1. Prepare heat-killed *S. flexneri* 2a as described in Subheading 2.
2. Immunize adult male/female white New Zealand rabbits (2–2.5 kg) on days 0, 7, 14, and 21 with heat-killed bacteria or PBS.
3. Orally administer 10 ml of heat-killed bacteria (containing 10^{11} bacteria) through orogastric tube following a dose of 5 % sodium bicarbonate to neutralize the gastric acidity.
4. Collect non-immunized and immunized serum 6 days after each dose of immunization.
5. Perform ELISA to determine the antibody level (IgG and IgA) against the OMP fraction.
6. Carry out immunoblotting with the serum to identify the MOMP using OMP as antigen.

3.2.2 Electroelution of MOMPs

1. Mix the OMP fraction with equal volume of sample buffer, boil for 5–7 min at 100 °C, cool on ice, gently vortex, and centrifuge the sample.
2. Resolve the sample on 12.5 % SDS-PAGE at a constant voltage of 150.
3. Visualize the protein bands by placing the gel in chilled 1 M KCl.
4. Excise each band corresponding to MOMP using clean surgical blade.
5. Electroelute each MOMP via electroelution (Bio-Rad).
6. Dialyze each protein fraction against 1× PBS at 4 °C, change the buffer at least three times each with 6 h interval.

3.2.3 Protective Efficacy of the Gel Cut MOMPs

1. Homogenize individual electroeluted MOMP in PBS, pH 7.2.
2. Immunize rabbits with each of the MOMP or PBS with five intramuscular injections at 15 days intervals.
3. Anesthetize the animals with intravenous injection of pentothal sodium (at a dose of 30 mg/kg of body weight), open the abdomen and make a tie at 3–5 cm proximal to the ceco-colic junction to completely obstruct the cecum while maintaining continuity between ileum and colon.
4. Flush the colon with NaCl (0.9 %) warmed at 37 °C, then inject 10 ml of virulent *S. flexneri* 2a culture into the colon, at about 10 cm distal to the ceco-colic junction and close the abdomen.
5. Observe the rabbits for development of diarrhea (bloody mucoid stools characteristics of shigellosis) or protection from the disease (normal pellet stool) up to 96 h.

3.3 Sequencing, Cloning, and Expression the OMP

Among the different MOMP, which showed discernible protective activity in rabbit model of shigellosis was sequenced, identified from database, amplified, cloned in expression vector and finally expressed in *Escherichia coli*.

3.3.1 Sequencing of the OMP

1. Perform electrophoresis of the OMP fraction harvested from *S. flexneri 2a*, visualize protein bands by Coomassie brilliant blue staining, destain, excise the concerned MOMP from gel, and send it for full-length sequencing (MALDI-TOF MS).
2. Carry out in-gel protein digestion, concentrate the resulting peptides on a ZipTip micropurification column and elute onto an anchorchip target for analysis on MALDI-TOF MS instrument.
3. Analyze the peptide mixture in positive reflector mode for accurate peptide mass determination and select five to ten of the peptides for analysis by MS/MS fragmentation for partial peptide sequencing.
4. Combine the MS and MS/MS spectra and use for a database search in an in-house protein database by the Mascot software.

3.3.2 Cloning and Expression of the OMP

1. Retrieve the sequence of the concerned OMP from the GenBank and design a set of primer using the sequence to amplify the respective coding sequence from *S. flexneri* 2a genome using PCR.
2. Resolve the PCR amplified product in 1 % agarose gel by electrophoresis and analyzed using Gel-Doc and ligate the PCR amplified product of OMP gene to commercial pET100/D-TOPO® linearized vector (Invitrogen).
3. Transform the ligated product into One Shot® TOP10 chemically competent *E. coli* cells by heat shock, select the recombinant transformants using ampicillin (100 mg/ml) on LB agar plates and perform DNA sequencing using the resulting colonies to confirm the sequence identity and proper cloning orientation of the amplified product (OMP gene).
4. Isolate the plasmid from the correct transformant from an overnight culture of recombinant *E. coli* Top 10 cell using alkaline lysis protocol, transform the plasmid into BL21 Star™ (DE3) One Shot® Chemically Competent *E. coli* cells by heat shock and use the transformed *E. coli* BL21 (DE3) cells harboring the recombinant plasmid in the expression study.
5. Inoculate the entire transformation reaction into 10 ml of LB broth containing 100 mg/ml ampicillin and incubate at 37 °C with shaking (200 rpm) until the OD at 600 nm is 0.5–1.2.
6. Prepare the big batch of bacteria culture for protein expression. Add an aliquot of the starter culture into 1.5 L of sterile LB

medium (containing 100 mg/ml ampicillin) and incubate at 37 °C with shaking (200 rpm).

7. Once an optical density at 600 nm of the cultures reach 0.5–0.8 (mid log), induce the cells to express protein by adding appropriate amount of isopropyl thiogalactoside (IPTG). Caution: IPTG is light sensitive and also cannot be freeze-thawed too often. Typically prepare about 0.5 ml aliquots of 0.5 M each and freeze at –20 °C, freeze thaw aliquots only 2–3 times.
8. After adding IPTG, incubate the cultures at 37 °C with shaking (200 rpm) for appropriate time. After induction, centrifuge the bacterial culture at 4000 × *g* for 15 min in 4 °C. Freeze the cell pellet at –80 °C if necessary.

3.4 Purification of Recombinant OMP and Removal of Endotoxin

The recombinant outer membrane protein expressed in *E. coli* was purified from the cells using Ni-NTA (nickel-nitrilotriacetic acid) affinity chromatography and any lipopolysaccharide present in the expressed protein was removed in order to eliminate the possibility that the immunogenicity of the protein is due to LPS contamination as LPS can evoke protective immunity in shigellosis.

3.4.1 Purification of the Recombinant OMP

1. After induction, lyse the recombinant cells (0.5 g) by gentle stirring in lysis buffer (8 M urea; 0.1 M NaH_2PO_4; 0.01 M Tris–HCl; pH 8.0) for 30 min at room temperature and then centrifuge at 10,000 × *g* for 30 min at 4 °C.
2. Mix the lysate with 50 % Ni-NTA slurry (4:1) and kept at 4 °C for 1 h. Load the Ni-NTA slurry on the column and finally elute the protein using elution buffer (8 M urea; 0.1 M NaH_2PO_4; 0.01 M Tris–HCl; pH 4.5) after washing with wash buffers (8 M urea; 0.1 M NaH_2PO_4; 0.01 M Tris–HCl; pH 6.3 and 5.9).

3.4.2 Endotoxin Removal

The lipopolysaccharide present in the recombinant protein was removed by passing the protein through Detoxi-Gel endotoxin-removing resin and S3Δ peptide affinity gel columns, respectively.

1. Pass the purified recombinant protein through 1 ml of Detoxi-Gel endotoxin-removing resin, prepacked in a 5 ml disposable column by gravity.
2. Wash the column once with 5 ml of 1 % sodium deoxycholic acid, followed by 5 ml of 2 M NaCl and thrice with 5 ml each of pyrogen-free water before and after each lipopolysaccharide removal.
3. Under pyrogen-free conditions, pass the purified protein further through a column of 1 ml S3Δ peptide affinity gel to further remove traces of endotoxin, follow the same steps as for the Detoxi-Gel endotoxin-removing resin column.

4. Confirm the absence of traces of LPS in the purified protein by the *Limulus* amoebocyte lysate chromogenic assay with Kinetic-QCL® (Lonza) (*see* **Note 1**).

3.5 Determining the Immunogenicity of the Recombinant OMP In Vitro

Effective response to and control of microbial infection seems to require several levels of interactions between the innate and adaptive immune systems and hence an ideal subunit vaccine antigen should has the capacity to stimulate both innate and adaptive arms of the host immune system. The macrophage is a pivotal mediator of innate immunity and a precursor of the host response to tissue invasion. Once activated, macrophages produce an enormous diversity of microbicidal effectors, immunoregulatory cytokines as well as express major histocompatibility complex and co-stimulatory molecules on their surface that are require for innate immunity and priming of the acquired immune response, namely activation of T and B cells [22].

3.5.1 Isolation of Murine Peritoneal Macrophages

1. Euthanize the mice with CO_2 inhalation followed by cervical dislocation and clean thoroughly with 70 % ethyl alcohol (*see* **Note 2**).
2. Inject 2 ml of the sterile DPBS in the peritoneal cavity to each mouse. Make an incision into the abdomen and then rise the peritoneal cavity 3–4 times through the opening with cold sterile DPBS.
3. Collect the peritoneal washing containing the macrophages on sterile petri dishes and incubate at 37 °C in 5 % CO_2 for 2 h. The cells of the monocyte macrophage lineage will adhere on the surface of the petri dishes to form a confluent cell monolayer during the incubation period.
4. Remove the non-adherent peritoneal cells by repeated washing of the plates with cold DPBS and harvest the adherent peritoneal cells from the surface with a rubber scraper.
5. Wash the cells by suspending in DPBS and subsequent centrifugation at 300 × *g* for 5 min in 4 °C. Resuspend the cell pellet in RPMI 1640 medium containing 10 % FBS and determine the viability and count of macrophages by trypan blue exclusion. (Macrophages should be 90–95 % viable).

3.5.2 Determining Activation of Macrophages by the Recombinant Protein

1. Culture macrophages (0.5×10^6 cells) in a final volume of 200 μl in round-bottomed 96-well plates in presence of the recombinant OMP or media alone for appropriate duration of time at 37 °C.
2. Harvest the cells and cell culture supernatants by centrifugation at 300 × *g* for 5 min at 4 °C (*see* **Note 3**).
3. Determine the level of antibacterial cytokines (IL1β, IL-6, TNF-α, IFN-γ, and IL-12p70) by ELISA in the culture supernatants.

4. Use the cells to check surface expression of TLR2, MHC-II, CD80, and CD86 (activation markers) by labeling with fluorochrome-conjugated anti-mouse TLR2, MHC-II, CD80, and CD86 antibodies for 30 min on ice and then examine the stained cells by flow cytometry.

3.5.3 Activation of T and B Cells

T and B cells are crucial players of adaptive immune response, T cells are involved in cell-mediated immune response while B cells regulate humoral immunity.

T Cell Activation

Activated Th1 cells secrete IL-2 and IFN-γ, which have been shown to regulate cellular immune responses by inducing Th1 differentiation [23].

1. Immunize mice (BALB/c or C57BL/6) with the recombinant protein by intranasal route on days 0, 14, and 28.
2. Anesthetize the mice by intramuscular injection of a mixture of 0.3 mg of xylazine hydrochloride and 1.0 mg of ketamine hydrochloride in 50 μl of saline before each immunization.
3. Immunize each mouse intranasally with 3–5 μg of the recombinant protein. Deliver a total antigen volume of 25 μl in five to six small drops to the external nares with a micropipette. Immunize the control animals with 0.9 % saline.
4. One week after the final immunization, excise spleens from both immunized and nonimmunized mice and isolate $CD4^+$ T cells using $CD4^+$ T Cell Isolation Kit (Miltenyi Biotec).
5. Stimulate the purified $CD4^+$ T cells in vitro with 2 μg/ml of plate-bound (96-well plate) anti-mouse CD3ε and 1 μg/ml of soluble anti-CD28 for 48 h.
6. Harvest the cell culture supernatants after 48 h of incubation by centrifuging the plate at 300 × *g* for 5 min at 4 °C. Measure secretion of IFN-γ and IL-2 in the culture supernatants by ELISA.

Activation of B Cells

Activated B cells upregulate the expression of MHC-II, CD80, or CD86 on the surface as well as proliferate and differentiate into antibody secreting cells [24].

1. Excise spleen from mice and isolate B cells from spleen by negative selection using mouse B cell isolation kit (Miltenyi Biotec). Resuspend the cells in DMEM medium containing 10 % FBS, count and assess the cell viability by trypan blue exclusion.
2. Stimulate B cells with 5 μg/ml of the recombinant OMP for 24 h. After stimulation stain the cells for surface expression of MHC-II, CD80, and CD86 and then analyze by flow cytometry.
3. For determining B cell proliferation, label the cells (1×10^6 cells) with 1 μM CFSE in prewarmed PBS at 37 °C for 15 min in dark.

4. Quench the staining by the addition of ice-cold complete medium, wash twice and then stimulate with the recombinant OMP for 96 h.
5. Analyze the cells every 24 h by flow cytometry.
6. To assess differentiation of B cells into antibody secreting cells (ASCs), culture B cells in presence of the recombinant protein into flat-bottom 96-well tissue culture plates for 72 h.
7. Transfer the cells to ELISPOT plates precoated with unlabeled anti-mouse Ig for 16–18 h at 37 °C, wash, incubate the plates with HRP-conjugated anti-IgM and anti-IgG Abs for 2 h at room temperature, developed with AEC Chromogen (BD Biosciences) and finally image and analyze the plates using Immunospot plate reader.

3.5.4 In Vivo Protective Immune Response by the Recombinant OMP

1. Prepare a frozen lot of *S. flexneri* 2a from the log phase of growth, which is the time of optimal invasiveness for *Shigellae* and then store in liquid nitrogen for the challenge experiment.
2. Immunize mice with the recombinant OMP intranasally as described above. Three weeks (day 49) after the final immunization, challenge all mice intranasally with a lethal dose of *S. flexneri* 2a (1×10^7 CFU/30 μl) as describe for the mouse lung model [25].
3. Bleed all mice on days 0, 28, 42, and 63, harvest the serum and store them in −80 °C for antibody ELISA.
4. Harvest pulmonary lavage by inflating the lungs with cold RPMI 1640 and by withdrawing the fluid through trachea. Remove the cellular debris from the lavage by centrifugation at $300 \times g$ for 5 min in 4 °C and then store the lavage fluids for antibody and cytokine ELISA at −80 °C.
5. Monitor all mice for weight loss, lethargy, fur ruffling, and death for 14 days after challenge.

4 Notes

1. After the final level of purification keep the recombinant protein in PBS and store at 4 °C (for short term storage) or −20 °C (for long term storage). For each lot of purification we usually perform CD spectroscopy in order to confirm that the secondary structure of the protein remains unaltered.
2. All the procedures should be performed under aseptic condition to avoid bacteria contamination, which can give false positive data.
3. The culture supernatants can be kept at −20 °C for short-term storage (2–3 months) or −80 °C for years.

References

1. Kotloff KL, Winickoff JP, Ivanoff B, Clemens JD et al (1999) Global burden of *Shigella* infections: implications for vaccine development and implementation of control strategies. Bull World Health Organ 77:651–666
2. Ashkenazi S, Levy I, Kazaronovsky V, Samra Z (2003) Growing antimicrobial resistance of *Shigella* isolates. J Antimicrob Chemother 51:427–429
3. Noriega FR, Wang JY, Losonsky G, Maneval DR et al (1994) Construction and characterization of attenuated (delta)aroA (delta)virG *Shigella flexneri* 2a strain CVD 1203, a prototype live oral vaccine. Infect Immun 62: 5168–5172
4. Sansonetti PJ (1991) Genetic and molecular basis of epithelial cell invasion by *Shigella* species. Rev Infect Dis 13:S285–S292
5. Orr N, Robin G, Cohen D, Arnon R, Lowell GH (1993) Immunogenicity and efficacy of oral or intranasal *Shigella flexneri* 2a and *Shigella sonnei* proteosome-lipopolysaccharide vaccines in animal models. Infect Immun 61:2390–2395
6. Cohen D, Ashkenazi S, Green MS, Gdalevich M, Robin G, Slepon R et al (1997) Double-blind vaccine-controlled randomised efficacy trial of an investigational *Shigella sonnei* conjugate vaccine in young adults. Lancet 349:155–159
7. Levenson VI, Egorova TP, Belkin ZP, Fedosova VG, Subbotina JL, Rukhadze EZ et al (1991) Protective ribosomal preparation from *Shigella sonnei* as a parenteral candidate vaccine. Infect Immun 59:3610–3618
8. Passwell JH, Harlev E, Ashkenazi S, Chu C, Miron D, Ramon R et al (2001) Safety and immunogenicity of improved *Shigella* O-specific polysaccharide-protein conjugate vaccines in adults in Israel. Infect Immun 69:1351–1357
9. Berry EM, Wang J, Wu T, Davis T, Levine MM (2006) Immunogenicity of multivalent Shigella-ETEC candidate vaccine strains in a guinea pig model. Vaccine 24:3728–3734
10. Turbyfill KR, Kaminski RW, Oaks EV (2008) Immunogenicity and efficacy of highly purified invasin complex vaccine from *Shigella flexneri* 2a. Vaccine 26:1353–1364
11. Coster TS, Charles HW, Lillian L, VanDeVerg A, Hartman AB et al (1999) Vaccination against shigellosis with attenuated *Shigella flexneri* 2a strain SC602. Infect Immun 67:3437–3443
12. Kotloff KL, Noriega FR, Samandari T, Sztein MB, Losonsky GA et al (2000) *Shigella flexneri* 2a strain CVD 1207, with specific deletions in virG, sen, set, and guaBA, is highly attenuated in humans. Infect Immun 68:1034–1039
13. Peng X, Ye X, Wang S (2004) Identification of novel immunogenic proteins of *Shigella flexneri* 2a by proteomic methodologies. Vaccine 22:2750–2756
14. Dumetz F, LaPatra SE, Duchaud E, Claverol S, Henaff ML (2007) The *Flavobacterium psychrophilum* OmpA, an outer membrane glycoprotein, induces a humoral response in rainbow trout. J Appl Microbiol 103:1461–1470
15. Pore D, Chowdhury P, Mahata N, Pal A, Yamasaki S, Mahalanabis D, Chakrabarti MK (2009) Purification and characterization of an immunogenic outer membrane protein of *Shigella flexneri* 2a. Vaccine 27:5855–5864
16. Pore D, Mahata N, Pal A, Chakrabarti MK (2010) 34 kDa MOMP of *Shigella flexneri* promotes TLR2 mediated macrophage activation with the engagement of NF-κB and p38 MAP kinase signaling. Mol Immunol 47:1739–1746
17. Pore D, Mahata N, Pal A, Chakrabarti MK (2011) Outer membrane protein A (OmpA) of *Shigella flexneri* 2a, induces protective immune response in a mouse model. PLoS One 6(7), e22663
18. Pore D, Mahata N, Chakrabarti MK (2012) Outer membrane protein A (OmpA) of *Shigella flexneri* 2a links innate and adaptive immunity in a TLR2 dependent manner and with the involvement of IL-12 and nitric oxide (NO). J Biol Chem 287:12589–12601
19. Pore D, Chakrabarti MK (2013) Outer membrane protein A (OmpA) from *Shigella flexneri* 2a: a promising subunit vaccine candidate. Vaccine 31:3644–3650
20. Bhowmick R, Pore D, Chakrabarti MK (2014) Outer membrane protein A (OmpA) of *Shigella flexneri* 2a induces TLR2-mediated activation of B cells: involvement of protein tyrosine kinase, ERK and NF-κB. PLoS One 9(10), e109107
21. Filip C, Fletcher G, Wullf JL, Earhart CF (1973) Solubilization of the cytoplasmic membrane *Escherichia coli* by the ionic detergent sodium lauryl sarcosinate. J Bacteriol 115: 717–722
22. Hoffmann JA, Kafatos FC, Janeway CA, Ezekowitz RA (1999) Phylogenetic perspectives in innate immunity. Science 284:1313–1318
23. Mosmann TR, Coffman RL (1989) TH1 and TH2 cells. Different patterns of lymphokine secretion lead to different functional properties. Annu Rev Immunol 7:145–173

24. Lanzavecchia A, Sallusto F (2007) Toll-like receptors and innate immunity in B cell activation and antibody responses. Curr Opin Immunol 19:268–274

25. Mallett CP, VanDeVerg L, Collins HH, Hale TL (1993) Evaluation of *Shigella* vaccine safety and efficacy in an intranasally challenged mouse model. Vaccine 11:190–196

Chapter 25

Approach to the Discovery, Development, and Evaluation of a Novel *Neisseria meningitidis* Serogroup B Vaccine

Luke R. Green, Joseph Eiden, Li Hao, Tom Jones, John Perez, Lisa K. McNeil, Kathrin U. Jansen, and Annaliesa S. Anderson

Abstract

In this chapter, we describe a research and development pathway to identify and demonstrate the efficacy of a *Neisseria meningitidis* non-capsular vaccine, the recently licensed *N. meningitidis* serogroup B (MnB) vaccine, Trumenba®. While other approaches have been followed in the identification of a MnB vaccine (Pizza et al. Science 287:1816–1820, 2000), the methods described here reflect the distinctive approach and experiences in discovering and developing Trumenba®. In contrast to the development and licensure of polysaccharide-conjugate vaccines against meningococcal serotypes A, C, W, and Y, the development of a vaccine to produce broadly protective antibodies against meningococcal serogroup B has proved difficult, due to the antigenic mimicry of the serogroup B polysaccharide capsule, which is composed of polysialic acid structures similar to those expressed on human neuronal cells. Early development efforts for these vaccines failed because the MnB polysaccharide structures resemble autoantigens and thus were poorly immunogenic. The development of an MnB vaccine has therefore focused on non-polysaccharide approaches. It was critical to identify MnB cell surface-exposed antigens capable of inducing a protective response against diverse, circulating strains of invasive MnB to ensure global coverage. Once candidate antigens were identified, it was important to characterize antigenic variation and expression levels, and subsequently to assure that antigens were expressed broadly among diverse clinical isolates. Prior to the initiation of clinical trials in humans, candidate vaccine antigens were tested in functional immunogenicity assays and yielded responses that were correlated with protection from meningococcal disease. These functional immunogenicity assays (serum bactericidal assays using human complement, hSBAs) measure the titer of complement-dependent bactericidal antibodies in serum from immunized test animals using diverse clinical MnB isolates as targets. Following optimization of vaccine antigenic components based on hSBA responses in preclinical models, animal toxicology tests were performed. Initial clinical studies (Phase 1 and 2) subsequently provided data to support (1) safety and immunogenicity of the vaccine formulation, and (2) the dose and schedule. Phase 3 clinical trials were carried out in the target populations to provide the clinical confirmation of safety and efficacy required for vaccine licensure.

Key words *Neisseria meningitidis* serogroup B, Vaccine, Factor H-binding protein (fHBP), Serum bactericidal assay (SBA), Surveillance, Genetic conservation, Clinical development

Sunil Thomas (ed.), *Vaccine Design: Methods and Protocols: Volume 1: Vaccines for Human Diseases*, Methods in Molecular Biology, vol. 1403, DOI 10.1007/978-1-4939-3387-7_25,

1 Introduction

1.1 Neisseria meningitidis Disease and Prevention by Vaccination

The gram-negative bacteria, *N. meningitidis,* is the causative agent of meningococcal disease. Invasive disease caused by *N. meningitidis* is devastating and results in high levels of morbidity and mortality [2]. *N. meningitidis* strains can be grouped by their capsular polysaccharide structures. Though 12 capsular polysaccharide serogroups have been identified, 5 (A, B, C, Y, and W) cause most of the disease cases [3]. *N. meningitidis* serogroup B (MnB) is responsible for approximately 33 % and 74 % of meningococcal cases in the USA and Europe, respectively [4, 5]. Peak incidence of MnB disease occurs among young infants, with more than 50 % of meningococcal disease cases within US children aged 0–6 months caused by serogroup B [6]. A second peak is observed in adolescents and young adults aged 11–24 years, driven by endemic disease but also by unexpected sporadic outbreaks in settings such as universities, army barracks, and prisons [7].

MnB causes both endemic and epidemic disease worldwide. To date, epidemic disease has been controlled using vaccines composed of outer membrane vesicles (OMVs) derived from the epidemic strain [8–13], where protection is mediated by the specific and immunodominant Porin A (PorA) [14]. However, OMV vaccines provide protection only against the outbreak strain and strains expressing the same PorA variant and do not provide the breadth of coverage required for a global vaccine [15]. These limitations of OMV vaccines and the inability to employ capsular polysaccharide antigens for development of MnB vaccines highlight the importance of a protein-based approach to develop a vaccine capable of providing protection against diverse MnB strains.

Vaccines that target bacterial capsular polysaccharide have been effective at controlling capsule type-specific meningitis and septicemia caused by *Streptococcus pneumoniae*, *Haemophilus influenzae*, and *Neisseria meningitidis* [4, 16, 17]. In the case of *N. meningitidis* serogroup A and C polysaccharide vaccines, efficacy for prevention of clinical disease was demonstrated in large-scale clinical trials before licensure [18–21]. Subsequent licensures of quadrivalent meningococcal polysaccharide vaccines (e.g., MPSV4 (Menomune)) and meningococcal serogroup C conjugate vaccines were based on surrogate endpoints that employed serum bactericidal assays (SBA), the correlate of protection [22–27]. Clinical efficacy of these polysaccharide vaccines was confirmed in post-marketing studies. These efficacy data, and others (reviewed in [28, 29]), provided additional evidence that hSBA responses may be used as a surrogate of efficacy in clinical trials. SBA has therefore been critical in antigen identification for, and the development and licensure of, meningococcal vaccines.

As noted previously, the development of polysaccharide conjugate vaccines for serogroup B has not been feasible due to

the structural homology of the MnB capsular polysaccharide with human autoantigens [30]. While an investigational MnB polysaccharide-conjugate vaccine did induce immune responses, the antibodies generated did not have functional activity [31]. Alternative approaches were thus required to provide safe and effective vaccines for prevention of invasive disease due to MnB. The identification of alternative approaches for the development of a non-capsular global MnB vaccine is challenging due to the multiple mechanisms *N. meningitidis* uses to evade immune-mediated killing. The capsular polysaccharide protects the bacterium from nonspecific killing by the innate immune system [32]. Surface protein antigens may be differentially expressed and the organism is genetically competent to acquire or lose DNA from other organisms, allowing for more genetic variation [33]. Many immunodominant antigens are hypervariable, such as PorA [34]. Other surface-exposed antigens, such as Neisserial adhesin A (NadA), are not universally expressed on disease isolates and, therefore, are not required for bacterial survival in the host [35]. Thus, the challenge for MnB vaccine development was to identify antigenic components that would be genetically conserved among disease-causing isolates and provide broad protection across the spectrum of MnB disease-causing strains.

The significant unmet medical need for an MnB vaccine has recently been addressed using two approaches; the antigenic composition for 4CMenB (Bexsero®) was identified by scanning the genome of an MnB strain to identify vaccine candidates using cell surface pattern recognition software [1]. Bivalent rLP2086 (Trumenba®) was discovered by isolating and identifying proteins from the cell surface of MnB that could induce functional bactericidal antibodies capable of in vitro killing of a diverse panel of MnB strains [15].

In this chapter, we describe the methodology to produce an MnB vaccine, based upon experience with Trumenba®, recognizing that similar approaches might be considered for other pathogens for which in vitro correlates of protection are available. Although critical for the effective development of a meningococcal vaccine, formulation development, toxicology studies, and manufacturing of vaccine components are not addressed in this chapter.

1.2 Identification of Candidate Vaccine Antigens That Induce a Functional Response (Preclinical Phase)

To identify antigen vaccine candidates for MnB, a biochemical and immunological approach (differential detergent extraction of outer membrane proteins and multidimensional separation by isoelectric focusing and ion-exchange chromatography) was used to identify native outer membrane proteins that elicit broadly cross-reactive antibodies against a number of diverse meningococcal isolates [15].

1.2.1 An Immunological Approach to Identify Native Outer Membrane Protein Vaccine Candidate(s)

In this section, we describe how biochemical preparations of cell membrane extracts can be used to immunize mice and to identify fractions capable of generating serum bactericidal antibodies that kill diverse meningococcal strains (Subheading 1.2.4).

Strain diversity can be measured using common *N. meningitidis* molecular epidemiological markers. Candidate proteins can be identified from the fractions using mass spectrometry followed by amino acid sequencing of protein antigens. To test whether these candidate antigens induce the desired functional immune responses, i.e., serum bactericidal antibody activity, the candidate antigens were recombinantly expressed. In vivo immunity studies were conducted with different antigen constructs and formulations to identify the appropriate antigen configuration that generated the desired immune response. For example, the meningococcal protein, factor H-binding protein (fHBP), one of the protective antigens identified during antigen discovery, is a lipoprotein in its native form. To determine whether the lipidated or non-lipidated antigen would induce the broadest functional immune response, both antigen forms were produced and formulated. It was found that the lipidated form was markedly better suited to induce a functional immune response against a broad spectrum of diverse MnB clinical strains than the non-lipidated form [15].

1.2.2 A Method to Determine the Number of Antigens Required to Provide Broad Coverage against Invasive MnB Disease

Surveillance of both disease-causing and carriage isolates is important to understand the genetic diversity of bacterial populations and to guide vaccine antigen selection and help forecast vaccine coverage. Such studies, best conducted with input from meningococcal reference laboratories, are important to establish if the antigen is expressed by most strains and is sufficiently conserved across diverse disease isolates. For example, analysis of fHBP sequences from a variety of *N. meningitidis* clinical strains identified multiple unique fHBP variants that could be classified into two subfamilies, designated subfamily A and subfamily B based on their sequence homology. Protein sequence analyses showed a high degree of sequence identity (>83 %) within the subfamily, but limited sequence identity (60–75 %) across subfamilies of fHBPs [36]. Preclinical studies demonstrated that bivalent vaccines composed of one fHBP variant from subfamily A (variant A05) and a second from subfamily B (variant B01) elicited broadly protective bactericidal antibodies against strains harboring fHBP variants from either subfamily, while monovalent vaccines elicited predominantly subfamily-specific bactericidal responses [37].

To assess the potential for a protein antigen to confer broad protection against MnB invasive disease isolates requires a comprehensive understanding of the prevalence and diversity of the protein variants in invasive strains that are representative of those currently causing disease globally. In addition, continued surveillance of disease-causing isolates is recommended to monitor the effectiveness of vaccine-elicited bactericidal responses against strains expressing these new variants. With the advancement of next-generation sequencing (NGS) technology and the development of sequence assembly algorithms, a whole-genome

sequencing (WGS) approach can now be routinely used to quickly extract critical genotype data and perform detailed molecular surveillance analyses, to aid in assessment of conservation of candidate vaccine antigens in diverse disease-causing strains [38].

1.2.3 A Method to Determine That the Vaccine Candidate(s) Are Surface Accessible to Antibody Binding

Antigen-specific monoclonal antibodies are useful to (1) confirm that the antigen can be detected on the surface of the bacterium, (2) that the recombinant protein has the correct native configuration and (3) identify functional epitopes using hSBA. Monoclonal antibodies against the candidate proteins can be obtained by a variety of means, including immunizing mice with recombinant proteins or evaluating the natural human antibody repertoire to the antigens [15, 39, 40]. Once obtained, the antibodies can be used to screen for surface expression on diverse *N. meningitidis* strains. To determine if potential vaccine candidate antigen(s) are expressed on the surface of bacteria, flow cytometry is a convenient way to not only detect expression, but also quantify surface expression and accessibility of the candidate protein on *N. meningitidis* strains. Ideally, a broadly cross-reactive monoclonal antibody that can detect essentially all variants of the protein of interest should be used to identify and accurately measure expression.

1.2.4 A Method to Evaluate the Ability of the Vaccine Candidate(s) to Induce Antibodies That Kill Diverse MnB Strains

In the case of *N. meningitidis*, sero-epidemiological studies determined that serum bactericidal antibodies to the bacteria measured in hSBA (titers $\geq$ 1:4) correlated with protection from meningococcal disease [28, 29, 41, 42]. The protective immunological correlate enabled the preclinical evaluation of potential vaccine antigens to determine whether protective responses would be elicited by the candidate antigen(s), which candidate antigen form or formulation would be optimal, and how many candidate antigens would be required to provide broad protection. Taken together, these comprise the rational design of a vaccine candidate.

Prior to identifying a candidate antigen, hSBAs used in the preclinical research phase should be sufficiently robust and optimized to carefully guide vaccine design. Biological and complex assays such as the hSBA must be rigorously controlled and the critical biological reagents used in the assays, i.e., complement and bacterial strains, should be carefully selected and evaluated for adequate performance, as they have a profound effect on the assay results. In addition, evaluation of assay specificity, precision, and dilutional linearity/relative accuracy, as well as limits of detection and quantification, is critical to be able to properly interpret hSBA results. To establish a robustly qualified hSBA, assay performance has to be evaluated over a period of time to assess temporal differences, using different operators with human or animal control sera. The qualification results are used to determine the assay range, which is the titer range within the lower and upper limits of quantitation (LLOQ and ULOQ, respectively), across which there is both reasonable precision and accuracy.

1.3 Clinical Development of the Investigational Vaccine

Early during the vaccine research and development process, a project team, including individuals with expertise in the preclinical research, epidemiology, toxicology, process development, clinical research, and vaccine regulations, should define a target product profile (TPP) that will guide the overall vaccine design and development process, including clinical development. The availability of licensed meningococcal vaccines and recommendations for their use for specific age or risk groups in the countries or regions of interest were important in guiding the clinical and regulatory plans for a new investigational vaccine directed at prevention of invasive disease due to MnB. The overall clinical development program should incorporate appropriate consideration of the anticipated requirements of vaccine licensure, including (1) the total number of study subjects of each relevant age group who receive the investigational vaccine, (2) comparator vaccines or controls if it is anticipated that the MnB vaccine would be given concomitantly with other licensed vaccines, and (3) specific endpoints and measures of interest for proof of vaccine safety and efficacy. Identification of these factors and the definition of the required success criteria for each clinical trial will help guide the specific trial design at each stage of development, from the first Phase 1 clinical trial through Phase 2 and Phase 3 stages. Since hSBA titers correlate with protection against invasive disease, the rigorous development and validation of appropriate hSBAs, using well-controlled reagents, were paramount also in the clinical evaluation of an MnB vaccine (Subheading 3.3.3).

2 Materials

2.1 Identification of Candidate Vaccine Antigens That Induce a Functional Response

2.1.1 Materials Required for the Immunological Approach to Identify Native Outer Membrane Protein Vaccine Candidate(s)

1. Bacterial wash buffer: 10 mM HEPES-NaOH, pH 7.4, 1 mM Na_2EDTA.
2. 110Y microfluidizer equipped with a ceramic microfluidizing chamber.
3. Tissuemizer Homogenizer.
4. Cell envelope extraction buffer: 1 % (w/v) Triton X-100 in 10 mM HEPES-NaOH, pH 7.4, 1 mM $MgCl_2$.
5. Rotophor unit (Bio-Rad Laboratories, USA).
6. Trimethylaminoethyl (TMAE).
7. Cyanogen bromide.
8. Endoproteinases (V8, Lys-C, or Arg-C).
9. LASERGENE software (DNASTAR, Inc., USA).

2.1.2 Materials Required to Confirm That the Vaccine Candidate(s) Are Surface Accessible to Antibody Binding

1. GC agar.
2. Kellogg's supplement.
3. GCK medium: Add 1 mL Kellogg's supplement to 100 mL GC medium with 0.42 % $NaHCO_3$.
4. Phosphate-buffered saline (PBS): 150 mM NaCl, 1 mM KH_2PO_4, 5.6 mM Na_2HPO_4 pH 7.2 (Corning, Inc., USA).
5. 1 % Paraformaldehyde in PBS.
6. Flow wash buffer: 1 % BSA diluted in PBS.
7. Primary antibody(s) at appropriate dilution in flow wash buffer: The "appropriate dilution" must be empirically defined. Primary antibody concentrations typically range from 1 to 50 μg/mL. Include an appropriate species-specific negative control antibody.
8. Biotinylated secondary antibody diluted in flow wash buffer (e.g., biotinylated mouse anti-IgG). As with the primary antibody, appropriate dilutions must be empirically defined. Typical dilutions of secondary antibody range from 1:50 to 1:200. Use secondary antibody against the same species as the primary antibody.
9. Streptavidin-PE (SA-PE) at 1:100 in flow wash buffer.
10. BD Accuri C6 flow cytometer with CSampler (Becton, Dickinson and Company).
11. Flowjo v10.06 or current version (Treestar, USA).

2.1.3 Materials Required to Determine the Number of Antigens Required to Provide Broad Coverage against Invasive MnB Disease

1. Primers specific for candidate protein-encoding gene.
2. Chocolate agar.
3. Premix Taq™ DNA Polymerase (Takara Bio, Inc., USA).
4. Agencourt® AMPure XP PCR Purification Kit (Beckman Coulter, Inc., USA).
5. Sequencing primers for candidate protein-encoding gene.
6. BigDye® Terminator v3.1 Cycle Sequencing Kit (Thermo Fisher Scientific, Inc., USA).
7. BioRobot Universal System (QIAGEN, USA).
8. 3730 DNA Analyzer (Thermo Fisher Scientific, Inc.).
9. Sequencher v4.0 (Gene Codes Corp., USA).
10. Molecular Evolutionary Genetic Analysis (MEGA) software v4.0.

2.1.4 Materials for Whole-Genome Sequencing

1. Chocolate agar.
2. GC media.
3. Agencourt® Genfind™ v2 (Beckman Coulter, Inc.).

4. RNase A (QIAGEN).
5. Tris-EDTA (TE) buffer: 6.2 mM Tris–HCl, 3.8 mM Tris, 1 mM EDTA (Corning, Inc.).
6. Qubit® dsDNA HS Assay Kit (Thermo Fisher Scientific, Inc.).
7. Nextera® XT DNA Sample Preparation Kit (Illumina, Inc., USA).
8. Agencourt® AMPure XP PCR Purification Kit (Beckman Coulter, Inc.).
9. Agilent High Sensitivity DNA Kit (Agilent Technologies, Inc., USA).
10. Agilent 2100 Bioanalyzer (Agilent Technologies, Inc.).
11. Power SYBR® Green PCR Mastermix (Thermo Fisher Scientific, Inc.).
12. 7500 Real Time PCR System (Thermo Fisher Scientific, Inc.).
13. 7500 System SDS software (Thermo Fisher Scientific, Inc.).
14. MiSeq Desktop Sequencer (Illumina, Inc.).
15. MiSeq Reporter Software v2.3.32 (Illumina, Inc.).
16. CLC Genomic Workbench v6.5.1 (QIAGEN).

2.2 Clinical Development of the Investigational Vaccine

2.2.1 Materials for Immunological Evaluation of the Efficacy Potential of Vaccine Antigen Candidates

1. GC agar.
2. GCK media: As above.
3. 80 % Glycerol.
4. Dulbecco's phosphate-buffered saline with Ca^{2+}/Mg^{2+} (DPBS): 0.9 mM $CaCl_2$, 2.7 mM KCl, 1.5 mM KH_2PO4, 1.1 mM $MgCl_2$, 136.9 mM NaCl, and 15.3 mM Na_2HPO_4 (Corning, Inc.).
5. Quality control sera (QCS).
6. Active human complement.
7. Multiscreen 96-well plate with MCE membrane (Merck KGaA, Germany).
8. QC Calloidal Coomassie solution (Bio-Rad Laboratories, Inc., USA).
9. Coomassie Brilliant Blue R-250 Destaining solution (Bio-Rad Laboratories, Inc.).
10. CTL-Immunospot® S6 Macro Analyzer (Cellular Technology Ltd., USA).

3 Methods

3.1 Identification of Candidate Vaccine Antigens That Induce Bactericidal Antibodies

3.1.1 A Method for the Immunological Approach to Identify Native Outer Membrane Protein Vaccine Candidate(s)

1. Suspend bacterial cells (100 g wet weight) in bacterial wash buffer (five times wet weight) and lyse by passage through a 110Y microfluidizer equipped with a ceramic microfluidizing chamber at ~18,000 psi.
2. Clarify cell lysate and isolate the cell envelope by centrifugation at 300,000 × *g* for 1 h at 10 °C.
3. Wash twice with bacterial wash buffer by suspension with a tissuemizer followed by centrifugation at 300,000 × *g* for 1 h at 10 °C.
4. Extract the cell envelopes with 320 mL of cell envelope extraction buffer.
5. Fractionate cell envelope extracts and purify by preparative isoelectric focusing (IEF) in a BioRad Rotophor unit. Ampholyte concentrations are 1 % 3–10 mixed with 1 % 4–6 to maximize the separation in the pH 4–6 range.
6. Concentrate pooled IEF fractions and remove ampholytes by ethanol precipitation prior to chromatographic separation.
7. Further purification is achieved with the anion-exchange resin TMAE to adsorb many of the minor components.
8. Candidate proteins are identified from the fractions using mass spectrometry amino acid sequencing and are confirmed by cloning before vaccination of mice with the recombinantly expressed protein. Sera from the vaccinated mice are used in hSBA to verify the presence of bactericidal antibodies.

3.1.2 A Method for Vaccine Antigen Candidate Sequencing

1. Generate peptide maps from the proteins of interest by either chemical cleavage with cyanogen bromide or proteolytic cleavage with the endoproteinases, V8, Lys-C, or Arg-C followed by peptide separation by reverse-phase HPLC.
2. Peptide sequences obtained as described can be translated to nucleotide sequences to enable the cloning of genes of interest.
3. Translate the DNA sequences of potential candidate antigens from several different MnB strains into amino acid sequences using the LASERGENE software.
4. Align deduced amino acid sequences using ClustalW.
5. Construct initial phylogenetic trees using the neighbor joining, unweighted pair group method with arithmetic means analysis (UPGMA), and ClustalW24 to identify if the target falls into defined groups that may have antigenic differences.
6. The phylogenetic tree can be used to select several different variants of the potential vaccine candidate to further assess their ability to elicit broadly cross-functional antibody responses.

3.1.3 A Method to Confirm That the Vaccine Candidate(s) Are Surface Accessible to Antibody Binding

Bacterial Growth Conditions

1. Grow *N. meningitidis* bacteria from frozen stock on GC agar plates and incubate overnight in a 37 °C 5 % CO_2 incubator (*see* **Notes 1–4**).
2. Inoculate GCK media with isolated colonies from overnight culture using a sterile polyester swab to a starting OD_{650} of 0.15–0.20. Incubate in a 37 °C shaker incubator (150 rpm) until the OD_{650} reaches 0.50–0.60.
3. Centrifuge bacterial cells for 4 min at 1825 × *g*, and resuspend the pellet with an equal volume of 1 % paraformaldehyde (*see* **Note 5**).

Bacterial Staining Conditions

1. Add 50 μL of cultured bacteria to each well of a round-bottom 96-well plate. Centrifuge the 96-well plate for 4 min at 1825 × *g* (*see* **Note 6**).
2. Add 50 μL of the primary antibody to each well. Each bacterial strain can be stained with multiple primary antibodies, each in a separate well (*see* **Notes 7** and **8**). Stain bacterial strains in duplicate with primary antibody(s) or a negative control antibody.
3. Incubate the plate on ice for 30 min.
4. Wash twice with flow wash buffer and centrifuge for 4 min at 1825 × *g*.
5. Add 50 μL of the biotinylated secondary antibody to all wells. Incubate the plate on ice for 30 min (*see* **Note 9**).
6. Wash twice with flow wash buffer and centrifuge for 4 min at 1825 × *g*.
7. Add 50 μL of the diluted SA-PE to all wells. Incubate the plate on ice in the dark for 30 min (SA-PE is light sensitive).
8. Wash twice with flow wash buffer and centrifuge for 4 min at 1825 × *g*.
9. Resuspend bacterial pellet in 200 μL of 1 % paraformaldehyde. Store plates in the dark at 4 °C.

Data Acquisition and Analysis

1. Resuspend the bacterial pellet in all wells before running on the flow cytometer. Gate bacteria using the logarithmic FSC/SSC dot plot and calculate mean fluorescence intensity (MFI) from the PE channel histogram (*see* **Note 10**).
2. Collect a minimum of 20,000 events per well using a slow fluidics rate. Run blank wells for 5 s to minimize carryover between wells.
3. Adjust the voltages and threshold so that all the bacteria are on scale and fall within the bacterial gate (P2 in Fig. 1). If necessary, adjust the PE voltage on a setup control (unstained sample) so that it is within the first decade.

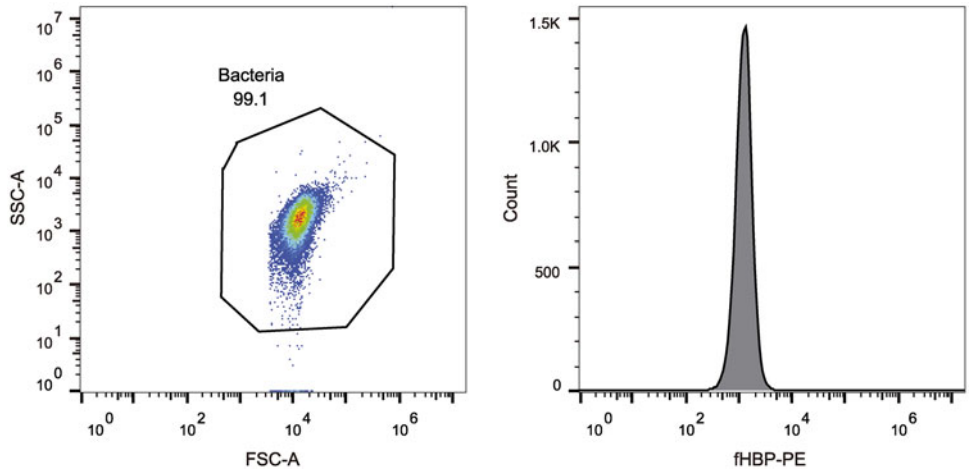

Fig. 1 Gating of bacteria to determine PE MFI

4. After the run is completed, check PE MFI for all wells. Re-collect wells with <20,000 events and with disparate MFIs between replicates.
5. An MFI is considered positive if it is >100 MFI and at least three times the negative control for that strain.

3.1.4 A Method to Evaluate the Ability of the Vaccine Candidate(s) to Induce Antibodies That Kill Diverse MnB Strains (Preclinical)

Preclinical and exploratory hSBAs should be developed to a point where it is reasonably certain that highly reliable results will be obtained. Depending on the intended use, preclinical and exploratory hSBAs may be qualified to demonstrate adequate specificity, and to define precision and dilutional linearity/relative accuracy in order to determine the assay range (i.e., LLOQ and ULOQ). For full assay methodology see clinical SBA (Subheading "A Method to Evaluate the Ability of the Vaccine Candidate(s) to Induce Antibodies That Kill Diverse MnB Strains (Clinical)").

3.2 Methods to Determine the Number of Antigens Required to Provide Broad Coverage against Invasive MnB Disease

1. Conduct active surveillance for meningococcal disease in collaboration with national meningococcal reference laboratories at various sites.
2. Collect strains in a systematic way, for example, all strains from a defined period of time or in cases where the numbers are high every *n*th isolate is selected and included in a global MnB strain pool to allow for strain variation.

3.2.1 A Method for the Surveillance of Circulating MnB Strains

Strain Collections

3.2.2 Methods to Identify Variation in a Vaccine Candidate

PCR Amplification and Sequencing Vaccine Candidates

1. Grow *N. meningitidis* strain from frozen stock on chocolate agar plates. Incubate bacteria at 37 °C, 5 % CO_2, overnight (*see* **Notes 1** and **2**).
2. Boil *N. meningitidis* colonies from chocolate agar plates in 100 μL of distilled H_2O for 5 min before a 1:4 dilution in distilled H_2O.
3. Amplify candidate gene using Taq DNA polymerase and candidate-specific primers.
4. Purify amplified DNA using AMPure magnetic beads and resuspend in 80 μL 10 nmol/L Tris-acetate buffers (pH 8.0).
5. Using a Rapid Plate 96 channel Qiagen BioRobot with a Multi-probe II 4 tip system, amplify DNA using the AmpliTaq® DNA polymerase with specific candidate primers. Ensure that sequencing primers hybridize to conserved regions and to subfamily-specific regions allowing capture of heterologous family members.
6. Fractionate DNA by electrophoresis on an ABI3730 DNA sequencer.
7. Examine sequence traces to verify quality and double-stranded coverage with Sequencher v4.0, trim sequences to match the length of mature protein.

Variants Assignment and Phylogenetic Analysis

1. Compare candidate sequences from different MnB strains to the existing collection of alleles through BLAST (Basic Local Alignment Search Tool).
2. Confirm new heterologous candidate sequences by repeat PCR and sequencing.
3. Assign new validated candidate sequences to new variants sequentially using a nomenclature that includes subfamily, protein, and nucleotide variant (e.g., A22_003 indicates the third nucleotide sequence variant of subfamily A protein variant number 22).
4. Align candidate protein sequences with ClustalW. Phylogenetic distances were calculated by the neighbor-joining method in ClustalW, with correction for multiple substitutions. Phylogenetic trees were displayed using MEGA software, v.4.0.

3.2.3 Methods for Whole-Genome Sequencing

Genomic DNA Extraction

1. Grow *N. meningitidis* strain from frozen stock on chocolate agar plates. Incubate bacteria at 37 °C, 5 % CO_2, overnight (*see* **Notes 1** and **2**).
2. Resuspend bacterial growth from a quarter of the plate into 100 μL of GC media and boil at 95 °C for 5 min.
3. Add an additional 100 μL GC media to resulting boilate and transfer into a 96 deep-well plate containing lysis buffer, Proteinase K, and RNase. Incubate bacterial lysates at RT overnight. Lysates are stable at −20 °C.

4. Follow the Agencourt® Genfind™ v2 protocol from the addition of binding buffer to the lysates. Elute DNA from beads with 100 μL of TE buffer. Determine DNA concentrations with the Qubit dsDNA HS Assay Kit and adjust to a final concentration of 0.2 ng/μL.

Genome Sequencing Using MiSeq Desktop Sequencer with 2X250bp Paired-End Sequencing Chemistry

1. Prepare a DNA library according to the NexteraXT DNA sample preparation kit protocol.
2. Fragment 1 ng of genomic DNA and add DNA linkers and indexes using abbreviated PCR amplification (limited to 12 cycles).
3. Purify DNA using Agencourt® AMPure XP beads. Evaluate the quality and fragment size distribution of the DNA library using the Agilent High Sensitivity DNA Kit and the Agilent 2100 Bioanalyzer.
4. Following normalization of the library, dilute 1:10 in TE buffer and evaluate 5 μL of product with Power SYBR® Green PCR Mastermix using the Applied Biosystems 7500 Real Time PCR System and the 7500 System SDS software.
5. Pool the DNA libraries generated from multiple bacterial strains, each identified by the unique index incorporated during the PCR step, and load onto the MiSeq Desktop Sequencer.

WGS Data Analysis

1. Analyze base calls and produce sequence read files (FASTQ format) using the MiSeq Reporter Software for each bacterial strain after demultiplexing steps.
2. Import FASTQ sequence files into the CLC Genomic Workbench for contig assembly (*see* **Note 11**).
3. Generate the coverage depth in CLC; this should range from approximately 50× to 100×. Export assembled sequence contigs to BIGSdb for detailed genetic characterization [38] (*see* **Note 12**).

3.3 Clinical Development of the Investigational Vaccine

3.3.1 Designing the Overall Clinical Development Program for a Vaccine to Prevent Invasive Meningococcal Disease (IMD) due to N. meningitidis Serogroup B

Target Product Profile

1. Build target product profile (TPP) including consideration of the following:
   (a) Indication for use of the licensed vaccine.
   (b) Age group(s) for product license indication.
   (c) Special populations, for example, high-risk groups.
   (d) Countries for vaccine licensure.
   (e) Vaccine efficacy against epidemiologically relevant and antigenically diverse, disease-causing MnB strains.
   (f) Vaccine safety and reactogenicity profile.
   (g) Dosing regimen(s).
   (h) Concomitant vaccination characterization.
   (i) Reduction in throat carriage of *N. meningitidis*.

(j) Protection against invasive disease due to other serogroups.

(k) Duration of protection measured in years.

Clinical Development Plan

1. Prepare a clinical development plan (CDP) which ensures the following:
   (a) Scope is aligned with the TPP.
   (b) Supports program goals and timelines.
   (c) Fully consistent with vaccine licensure requirements for proof of safety and efficacy. Anticipate communications and meetings with regulatory authorities.
   (d) Allows integration of safety and efficacy data across the various stages of the clinical program.
   (e) Includes overall size and scope of clinical trials, including age group(s) and geographical considerations.
   (f) Appropriate comparator vaccines or control groups are available.
      - Choose control vaccines whose safety profile is well characterized, and licensed for use in the intended population, and which could be employed in the investigational vaccine clinical trials for comparison.
   (g) Select appropriate clinical trial subjects, and ensure that subject populations are evaluable and recruitment is feasible.
      - Epidemiology trials or evaluation of similar vaccines used in the intended population would be valuable to review.
   (h) Include estimates for subject retention and dropout rate for subject population of interest (*see* **Note 13**).

3.3.2 Planning, Conduct, and Reporting of Clinical Trials

1. Design the initial clinical trials with the following considerations:
   (a) Collect safety and reactogenicity data through characterization of local and systemic reaction profiles and collection of adverse events [46]. Consider the required duration for data storage.
   (b) Measurement of immune response characterization through hSBA (*see* Subheading "A Method to Evaluate the Ability of the Vaccine Candidate(s) to Induce Antibodies That Kill Diverse MnB Strains (Clinical)").
   (c) Determine sample sizes, and ensure that the number of study subjects is appropriate to assess safety and efficacy and to support advancement of the clinical development program.

- Safety considerations will often drive sample size rather than immunogenicity.

(d) Identification of formulation, route of administration, dose and schedule of vaccination.

(e) Assess age groups and potential populations at high risk for development of meningococcal disease.

(f) Define the criteria for safety and efficacy results required for each clinical trial to support program advancement at each stage, from Phase 1 through Phase 3 clinical trials.

- Specify safety and immunogenicity measures that would be incompatible with moving forward with further studies in the clinical development program.

2. Confirmatory (Phase 2)/proof-of-concept clinical trials should provide data needed for:

(a) Confirmation of formulation, route of administration, dose, schedule, duration of protection/immune response.

(b) Design of Phase 2 studies.

- The data generated should be adequate to determine the sample size and power statements for Phase 3.
- Ideally all measures intended for use in Phase 3 will be tested and evaluated in earlier phase studies.

(c) Evaluation of results relative to TPP.

(d) Agreement with regulatory authorities on strategy to license the vaccine.

3. Design Phase 3 studies to:

(a) Support the intended product licensure. Ensure that attributes of TPP have been addressed.

(b) Demonstrate proof of safety using control or vaccine comparison groups. Define the measures of interest to include reactogenicity, serious adverse events, and adverse events of special interest. Sample size may be driven by overall safety considerations if there are no specific safety concerns of interest.

(c) Demonstrate proof of efficacy using endpoint measures agreed upon with regulatory authorities. Statistical analysis plans should ensure appropriate hypothesis testing for primary study endpoints.

3.3.3 Target Meningococcal Strains and hSBA

Target meningococcal strains used in the hSBA should be selected from a large pool of disease-causing isolates obtained from the intended target population(s) of the candidate vaccine, from both an age and geographical perspective. The target strains should be selected in a largely unbiased fashion, and represent the observed

prevalence of the vaccine antigen variants (i.e., based on amino acid sequence and surface expression level) and other common epidemiological markers, such as MLST clonal complex. In regard to surface expression level, strains with unusually high levels of expression that are not representative of the vaccine antigen variant group should be avoided (*see* **Notes 14** and **15**).

After selection of target MnB test strains for the hSBAs, bacterial bank lots and human complement must be prepared for use in the hSBA. These methods, including the hSBA method, are described below.

Preparation of Bacterial Lots

1. Grow *N. meningitidis* bacteria on GC agar plates and incubate overnight in a 37 °C, 5 % CO_2, incubator.
2. Inoculate GCK media with isolated colonies from the GC agar plate and incubate in a 37 °C shaker incubator (150 rpm) until the OD_{600} reaches 1.2–1.4.
3. Mix 20 mL of the bacteria culture with 5 mL of 80 % glycerol.
4. Aliquot 100 μL portions into cryovials, place at −70 to −80 °C, and slowly freeze (*see* **Notes 16**–**18**).

Human Serum Complement and Preparation of Large-Volume Pooled Lots of Human Serum Complement

The accepted complement source for MnB serum bactericidal assays is human complement [29]. While human plasma complement is used in some laboratories, human serum complement is typically used. Either complement source must be rigorously screened and evaluated for suitable performance in each hSBA for which it may be used. The requirements for complement used in preclinical and clinical studies may be different in terms of volume required and the degree of evaluation required prior to its use in an hSBA. Human serum complement is obtained from normal healthy adults. Each human serum complement lot used in an hSBA should minimally meet the following criteria: (1) lacks substantial intrinsic bactericidal activity against the target MnB strain when exposure times of 0 and 30 min are compared; (2) lacks demonstrable anti-meningococcal antibodies by SBA; (3) has complement protein levels within the normal range (i.e., CH50 assay); and (4) yields appropriate hSBA titers when known positive and negative control sera are used. The final concentration of human serum complement in an hSBA is usually 20–25 %.

Collection and Storage of Human Serum Complement

1. Collect venous blood in a blood collection tube or bag that lacks anticoagulants. Allow blood to clot for 2–4 h at room temperature.
2. Centrifuge at 2200 × *g* for 20 min at 4 °C to separate serum from cellular and fibrin clot components, retain the serum, snap freeze in a dry ice/ethanol bath, and store at −70 to −80 °C (*see* **Notes 19** and **20**).

Pooling of Human Serum Complement

1. Screen individual human complement lots for a lack of substantial intrinsic nonspecific bactericidal activity; the passing criterion was a T_{30}/T_0 CFU ratio ≥75 %.
2. Evaluate passing complement lots in hSBA with a small panel of immune indicator sera with known titers, based on hSBA titer data obtained using complement lots from at least 30 subjects. Individual complement lots with an hSBA titer within a predefined limit of the geometric mean titer (GMT) may be candidates for pooling.
3. Select five to seven individual complement lots to create one pooled complement lot for an hSBA. Initial small test pools are created and tested to confirm the lack of substantial intrinsic nonspecific bactericidal activity (i.e., T_{30}/T_0 CFU ratio ≥75 %) and expected titers with the indicator panel sera.
4. Prepare large-volume pooled complement lots from sera of individuals found acceptable within small test pools.
   (a) Thaw and gently mix sera from each individual. Aliquot on ice in single-use volumes at 4 °C and snap freeze in dry ice/ethanol. Lots can be stored at −70 to −80 °C (*see* **Notes 21** and **22**).

3.3.4 A Method to Evaluate the Ability of the Vaccine Candidate(s) to Induce Antibodies That Kill Diverse MnB Strains (Clinical)

The method utilized for hSBAs described in this chapter was based on the assay described previously [43, 44], as reported previously [45]. Briefly, test serum is serially diluted in twofold steps and added to 96-well assay plates. MnB SBA test strains and human serum complement are added, initiating the bactericidal reaction. After incubation of the assay plates at 37 °C for 30–60 min (depending on SBA test strain; called T_{30}), the reaction mixture (containing bacteria surviving this incubation) is diluted and transferred to microfilter plates. Following overnight incubation, surviving bacteria expressed as colony-forming units (CFU) are enumerated using an ImmunoSpot Analyzer. A typical hSBA run consists of one T_0 plate, 4–12 test serum-containing titer-determining plates, and one antibiotic control plate (*see* **Note 34**).

1. Grow bacteria as described in Subheading "Bacterial Growth Conditions."
2. Dilute the bacteria about 1:2500 to 1:5000 with DPBS containing Ca^{2+}/Mg^{2+} to reach ~100–300 CFU/μL.
3. Add twofold serially diluted test sera to rows A–G (i.e., 1:4 to 1:4096 dilutions in DPBS) across the 96-well assay plate from column 1 to column 11 such that the volume is 25 μL. Add serially diluted QCS to row H and DPBS to column 12. T_{30} CFU is determined from column 12 of each assay plate (*see* **Notes 22–28**).
4. Add 15 μL of diluted bacteria and 10 μL of active human complement to all wells.

5. Incubate assay plate on an orbital shaker in a 37 °C incubator with 5 % CO_2 and humidity at 700 RPM for 30–60 min.
6. Dilute reaction mixture in each well with 140 μL DPBS containing Ca^{2+}/Mg^{2+}; transfer 15 μL from each well to the corresponding well in 96-well microfilter plates containing 200 μL of GCK medium.
7. Generate T_0 plate using one column of the plate, identical to column 12 of assay plate, containing 25 μL of DPBS, 15 μL bacteria, and 10 μL human complement. Do not incubate the T_0 plate; instead dilute the reaction and transfer to a microfilter plate (T_0 microfilter plate), as described above.
8. Generate an antibiotic control plate to test sera for intrinsic, non-antibody-mediated bactericidal activity. Add 1:4 diluted test sera and heat-inactivated human complement, incubate, and handle as any of the test plates described above.
9. Vacuum-filter the microfilter plates just long enough to drain visible medium from each well.
10. Place microfilter plates in a small biohazard bag with zip closure and incubate the plates overnight at 37 °C in 5 % CO_2 with a humidified atmosphere.
11. Fix and stain the microcolonies with 0.04 % Coomassie Blue Working Solution and destain solution.
12. Use a qualified ImmunoSpot Analyzer to scan and count bacterial microcolonies (i.e., CFU). The hSBA step titer is the reciprocal of the highest twofold dilution of a test serum that results in at least a 50 % reduction of MnB bacteria (50 % bacterial survival) compared to the T_{30} colony-forming units value (i.e., the number of bacteria surviving after incubation in assay wells containing all assay components except test serum; 100 % bacterial survival) (*see* **Notes 29–34**).

4 Summary and Conclusion

This guide offers a step-by-step insight into a pathway for production of a global MnB vaccine. We describe methods to identify a vaccine candidate antigen, defining both its variation and expression throughout invasive MnB populations. We characterize methodology for the hSBA which provides a demonstration of efficacy in both preclinical and clinical studies. Finally, we provide a clinical overview for the planning and execution of vaccine efficacy trials. The above methodologies describe our experience during development of Trumenba®, and while other approaches are available, this technique has proved successful. The methods described here demonstrate an important breakthrough in vaccinology with the production of a global MnB protein conjugate vaccine, necessary in the prevention of a life-threatening disease.

5 Notes

1. Expression of surface-expressed proteins varies due to growth phase, temperature, cell density, and nutrient availability. Carefully select the culture and agar plate media and growth conditions when looking at antigens of interest.
2. The growth conditions for the flow cytometry assay should be identical to the growth of the bacteria for the human SBA.
3. *N. meningitidis* does not grow well immediately upon thawing from a frozen glycerol stock. Grow bacteria overnight on agar, before inoculation of a liquid culture.
4. Diverse heterologous strains should be tested for surface expression including strains of different ST clonal complexes, PorA subtypes, serogroups, and fHBP variants.
5. Fixation with 1 % paraformaldehyde preserves the candidate antigen and leaves the bacteria intact while allowing for synchronization of bacterial growth between all strains. In addition, fixing the bacterial strains after growth minimizes the safety risk due to potential exposure to live *N. meningitidis*.
6. Include a blank well, filled with flow wash buffer, immediately below each experimental well. Acquire this blank immediately after an experimental well to prevent bacterial cell spillover which could lead to false positives.
7. It is important to use the appropriate negative control antibody. For example, for mouse monoclonal primary antibodies, a mouse IgG antibody should be used or for rabbit polyclonal sera, unimmunized rabbit sera (pre-sera) should be used. This negative control antibody shows how much nonspecific antibody is binding to each particular strain.
8. Include a capsular polysaccharide-specific antibody if desired in order to differentiate between different serogroups.
9. It is important to match the species and isotype of the primary antibody to the secondary antibody, i.e., mouse or rabbit or IgG or IgM.
10. Any flow cytometer capable of detecting PE (excitation-max 496 nm/emission-max 578 nm) can be used to acquire the stained bacteria. A flow cytometer with a plate-based automated acquisition would be easiest, such as the Accuri C6 cytometer with the C-Sampler. In order to determine that the lasers are functioning optimally, the flow cytometer should be calibrated daily before use with fluorescent beads.
11. The CLC Genomic Workbench provides a customized automated assembly workflow, including the merge of overlapping pairs and de novo assembly. This tool permits the assembly of

thousands of short sequence reads into contigs. The assembled MnB genome size is roughly ~2 Mbp and using these methods is typically assembled in 200–300 contigs.

12. The BIGSdb (Bacterial Isolate Genome Sequence Database) [38] was implemented to allow for efficient high-throughput analysis of WGS data. Assembled contigs from each isolate were uploaded into BIGSdb and scanned to extract genetic information for gene targets of interest. These include the MLST housekeeping genes (*abcZ*, *adk*, *aroE*, *fumC*, *gdh*, *pdhC*, and *pgm*), *porA*, diagnostic genes in the capsular polysaccharide biosynthetic operon for serogroup assignment, and fHBP.
13. Healthy adolescent and young adult populations may have substantial rates of early withdrawal from investigational clinical trials (e.g., 10–30 %). For studies that are not appropriate for inclusion of pregnant individuals, the study protocol and procedures should include appropriate specifications.
14. Confirmation of the candidate antigen expression threshold is important as low expression levels, under in vitro growth conditions, hinder the development of robust hSBAs needed to support high-throughput clinical sample testing. Thus, exclude strains with expression levels below the threshold from the selection process.
15. Ensure that selection of representative strains will address epidemiological markers such as clonal complexes, candidate antigen sequence diversity (including prevalent variants and subgroups), and in vitro expression levels.
16. In order to maintain control of the bacterial strains used in the hSBA, well-characterized, colony-purified master bank lots are created for each SBA test strain, preferably in sufficient quantity to last the lifetime of the project.
17. The identity and purity of bacterial banks used in assays to support clinical testing need to be thoroughly studied and documented. A meningococcal strain that is gram stain negative and oxidase positive and had a biochemical utilization profile that is characteristic of *N. meningitidis* is >99 % certain to be *N. meningitidis*. Microbiological tests can be determined using commercially available kits, for example the API NH system. The serogroup of a bacterial bank can be determined using commercially available agglutination tests or via flow cytometric analysis. Whole-genome sequence analysis (WGS) is used to provide genotypic information (Subheading 3.2.3).
18. The performance of bacterial banks used in the clinical hSBA should be qualified. The performance of bacterial banks in the hSBA is confirmed using a panel of immune sera (whose titers cover the assay range). At least three hSBA runs are performed over at least 3 days. The primary evaluation to assess perfor-

mance of a test bank in hSBA, compared to a qualified reference bank, is hSBA titer bias analysis. The bias is calculated as the difference in log-titers for each panel serum sample, as follows:

Log 10Bias = log 10(titerTest) − log 10(titerReference) = log 10(titerTest/titerReference).

The mean titer bias is the average of bias determinations for all panel members. The 90 % confidence interval for the mean titer bias of serum panel hSBA titers must be within 67–150 % of the reference lot for the test lot to qualify for use in clinical testing.

19. Due to the lability of complement, repeated thawing and refreezing of serum complement should be avoided or limited. Accordingly, serum complement is usually aliquoted in volumes designed for single use.
20. Often preclinical testing and exploratory hSBAs are performed with relatively small numbers of samples (<50) in assays that were not qualified or validated in order to get an early indication of an outcome to facilitate at-risk strategic decision making. In this case, human serum complement from a single individual may be used (Subheading "Collection and Storage of Human Serum Complement"). It should be recognized that there is some variability of hSBA titers obtained between human serum complement lots obtained from different individuals.
21. Large-volume pooled complement lots are qualified for use in the hSBAs by comparability testing to a reference complement lot using a panel of ~20 immune sera, in multiple independent hSBAs. System suitability criteria, as well as titer bias relative to the reference complement lot, are examined in these hSBAs. System suitability criteria, including T_{30} CFU within 50–300 and acceptable T_{30}/T_0 ratios, should be obtained regularly. Titer bias using the pooled test complement lot relative to the reference complement lot is determined. The bias method is identical to that described above for evaluating bacteria banks (*see* **Note 18**).
22. The hSBA utilizes two QCS that contain bactericidal antibodies at either a low or a medium/high hSBA titer. Each clinical assay plate will have a single sample position occupied with one of the QCS. The two QCS will alternate from plate to plate. The data derived from the QCS are used to evaluate the system suitability of each assay run, and each assay plate within a run. Specification limits for QCS are required for evaluating hSBA plate and run suitability, as well as monitoring consistency of hSBA performance. The specification range defines the limits of acceptance; if the range is exceeded, the assay plate fails and the test sera on that plate are repeated.

23. QCS sera should have a substantial volume available in order to provide information on assay performance over time, throughout a study and across studies. Ideally, the QCS sera should be from vaccinated individuals so that it contains antibodies directed against the antigen of interest. The initial performance of the candidate QCS is monitored to determine if the variability of its performance is within acceptable limits. Initial performance should be examined in several assays performed by several operators over several days.
24. A database of control values is generated that will be used to determine the QCS performance and specification limits. The database should contain at a minimum 40 data points for each QCS collected from a minimum of 6 assays performed over 2 weeks. QCS are selected for routine use based upon the volume available, geometric mean, and observed variability (i.e., %RSD). The two QCS selected for use in an assay should have different geometric means (e.g., a low or medium/high hSBA titer). QCS with %RSD of ~≤50 % is typically used to monitor assay performance effectively.
25. Robotic automation may be considered for hSBAs. Automation facilitates higher sample throughput and reduces the opportunity for human error. In the hSBA method described in this chapter, automation can be used to (1) generate serially diluted test samples and introduce those samples to assay plate wells; (2) add target bacteria and/or complement to assay plate wells; (3) transfer reaction mixes from assay plates to microfilter plates; and (4) add fixative and/or Coomassie Blue stain to microfilter plate wells. When automation is utilized in a test method such as hSBA, the robot must be validated for use in the assay and regular fluid delivery verification assessments must be performed.
26. To provide the highest level of confidence in the titer outcome obtained for a test sample, samples may be run in replicate (i.e., two individual titer determinations) within an assay and the consensus result reported. When serum samples are tested in replicate within an assay, the individual titers for each test serum must pass a pre-specified extravariability criterion, which puts limits on the acceptable fold difference of these titers. The extravariability limit may be set based on convention or based on repeatability data obtained during qualification or validation. Often, the extravariability limit is approximately twofold.
27. Interpolated or step titers (i.e., 1:2, 1:4, 1:8) may be reported, depending on need. Traditionally, hSBA titers obtained from clinical sera from vaccine trials were reported using step titers.
28. System suitability criteria are assessed at the run and plate levels in the hSBA. For a microfilter plate to pass plate suitability

criteria, (1) the average number of CFU in the microfilter plate column 12 T_{30} wells (i.e., wells that received reaction mixtures containing all assay components except test serum) must be within 50–300 CFU; (2) the T_{30}/T_0 ratio must be greater than a pre-specified limit (≥50 %); and (3) the QCS on the plate must be within the specification limits.

29. To facilitate hSBA runs containing large numbers of test samples (i.e., runs testing clinical samples), barcoding of test samples and electronic tracking of samples are preferred and reduce the possibility of error.
30. Test serum samples must be screened for intrinsic bactericidal activity (i.e., antibiotic-like activity or direct killing of bacteria in the absence of active complement) in order to assure that hSBA titers are only reported for antibody-mediated, complement-dependent bactericidal activity. A test serum sample fails this test when there is >50 % killing of bacteria in the absence of active complement.
31. A consistent and objective method for interpretation of hSBA kill curves should be utilized, preferably one that is standardized by automation. One method that is objective and amenable to automation is the conversion of the kill curve CFU count data to a binary code (i.e., a string of 0 or 1 s), based on whether the well CFU count is greater than 50 % of the T_{30} value (1), or less than or equal to 50 % of the T_{30} value (0). Theoretically, there are $2x$ possible kill curves, where x is the number of wells in the test serum twofold dilution series. Thus, when there are 11 serum dilution wells, there are 2048 possible binary codes. Each code must have an outcome: numerical hSBA titer or a sample repeat test code.
32. There should be criteria for defining and handling prozone kill curves, when little or no bactericidal activity is observed at the highest antibody concentration(s) compared to lower concentrations. In such cases, the kill curve crosses the 50 % survival threshold twice. hSBA titers may be reported for samples when prozone curves achieve certain minimum standards, such as when two consecutive points are less than 40 % survival. If such minimum standards are not achieved, the outcome of the sample is indeterminate and the sample may be repeat tested.
33. Poor titration kill curves are defined as the kill curve crossing the 50 % survival threshold two or more times, and are not prozone or prozone-like kill curves. Such curves are uninterpretable and the sample may be repeat tested.
34. Clinical hSBAs may be utilized over extended periods of time, so assay performance over the long term should be monitored for shifts and trends. Tracking titers from the routine QCS and/or from periodic testing of proficiency panels of sera may be used for such purposes.

References

1. Pizza M, Scarlato V, Masignani V et al (2000) Identification of vaccine candidates against serogroup B meningococcus by whole-genome sequencing. Science 287:1816–1820
2. Girard MP, Preziosi MP, Aguado MT et al (2006) A review of vaccine research and development: meningococcal disease. Vaccine 24(22):4692–4700
3. Gasparini R, Panatto D (2011) Meningococcal glycoconjugate vaccines. Hum Vaccin 7:170–182
4. Cohn AC, MacNeil JR, Clark TA et al (2013) Prevention and control of meningococcal disease: recommendations of the Advisory Committee on Immunization Practices (ACIP). MMWR Recommendations and reports : Morbidity and mortality weekly report Recommendations and reports/Centers for Disease Control 62 (Rr-2):1–28
5. Whittaker R (2013) Invasive meningococcal disease (IMD). In: Whittaker R, Bacci S (eds) Surveillance of invasive bacterial diseases in Europe, 2011. ECDC, Stockholm, pp 38–52
6. MacNeil J, Cohn A (2011) Meningococcal disease. In: Roush SW, Baldy LM (eds) Manual for the surveillance of vaccine-preventable diseases, 5th edn. Centers for Disease Control and Prevention (CDC), Atlanta, GA, USA, p. 1–11
7. Centers for Disease Control and Prevention (CDC) (1998) Outbreaks of group B meningococcal disease—Florida, 1995 and 1997. MMWR Morb Mortal Wkly Rep 47(39): 833–837
8. Jafri RZ, Ali A, Messonnier NE et al (2013) Global epidemiology of invasive meningococcal disease. Popul Health Metr 11(1):17
9. Boslego J, Garcia J, Cruz C et al (1995) Efficacy, safety, and immunogenicity of a meningococcal group B (15:P1.3) outer membrane protein vaccine in Iquique, Chile. Chilean National Committee for Meningococcal Disease. Vaccine 13:821–829
10. O'Hallahan J, Lennon D, Oster P (2004) The strategy to control New Zealand's epidemic of group B meningococcal disease. Pediatr Infect Dis J 23(12 Suppl):S293–S298
11. Bjune G, Hoiby EA, Gronnesby JK et al (1991) Effect of outer membrane vesicle vaccine against group B meningococcal disease in Norway. Lancet 338:1093–1096
12. de Moraes JC, Perkins BA, Camargo MC et al (1992) Protective efficacy of a serogroup B meningococcal vaccine in Sao Paulo, Brazil. Lancet 340:1074–1078
13. Milagres LG, Ramos SR, Sacchi CT et al (1994) Immune response of Brazilian children to a Neisseria meningitidis serogroup B outer membrane protein vaccine: comparison with efficacy. Infect Immun 62:4419–4424
14. Tappero JW, Lagos R, Ballesteros AM et al (1999) Immunogenicity of 2 serogroup B outer-membrane protein meningococcal vaccines: a randomized controlled trial in Chile. JAMA 281:1520–1527
15. Fletcher LD, Bernfield L, Barniak V et al (2004) Vaccine potential of the Neisseria meningitidis 2086 lipoprotein. Infect Immun 72:2088–2100
16. Tomczyk S, Bennett NM, Stoecker C et al (2014) Use of 13-valent pneumococcal conjugate vaccine and 23-valent pneumococcal polysaccharide vaccine among adults aged >/=65 years: recommendations of the Advisory Committee on Immunization Practices (ACIP). MMWR Morb Mortal Wkly Rep 63(37):822–825
17. Briere EC, Rubin L, Moro PL et al (2014) Prevention and control of haemophilus influenzae type b disease: recommendations of the advisory committee on immunization practices (ACIP). MMWR Recommendations and reports : Morbidity and mortality weekly report Recommendations and reports/Centers for Disease Control 63(Rr-01):1–14
18. Gotschlich EC, Goldschneider I, Artenstein MS (1969) Human immunity to the meningococcus. V. The effect of immunization with meningococcal group C polysaccharide on the carrier state. J Exp Med 129:1385–1395
19. Artenstein MS, Gold R, Zimmerly JG et al (1970) Prevention of meningococcal disease by group C polysaccharide vaccine. NEJM 282:417–420
20. Miller E, Salisbury D, Ramsay M (2001) Planning, registration, and implementation of an immunisation campaign against meningococcal serogroup C disease in the UK: a success story. Vaccine 20(Suppl 1):S58–S67
21. Wahdan MH, Sallam SA, Hassan MN et al (1977) A second controlled field trial of a serogroup A meningococcal polysaccharide vaccine in Alexandria. Bull World Health Organ 55(6):645–651
22. Jackson LA, Jacobson RM, Reisinger KS et al (2009) A randomized trial to determine the tolerability and immunogenicity of a quadrivalent meningococcal glycoconjugate vaccine in healthy adolescents. Pediatr Infect Dis J 28:86–91
23. Stamboulian D, Lopardo G, Lopez P et al (2010) Safety and immunogenicity of an investigational quadrivalent meningococcal CRM(197)

conjugate vaccine, MenACWY-CRM, compared with licensed vaccines in adults in Latin America. Int J Infect Dis 14:e868–e875

24. Richmond P, Borrow R, Goldblatt D et al (2001) Ability of 3 different meningococcal C conjugate vaccines to induce immunologic memory after a single dose in UK toddlers. J Infect Dis 183:160–163
25. Gold R, Artenstein MS (1971) Meningococcal infections. 2. Field trial of group C meningococcal polysaccharide vaccine in 1969-70. Bull World Health Organ 45:279–282
26. Pasteur S (2013) Menactra® (Meningococcal (Groups A, C, Y and W-135) Polysaccharide Diphtheria Toxoid Conjugate Vaccine) Package Insert (v03)
27. Daugla DM, Gami JP, Gamougam K et al (2014) Effect of a serogroup A meningococcal conjugate vaccine (PsA-TT) on serogroup A meningococcal meningitis and carriage in Chad: a community study [corrected]. Lancet 383:40–47
28. Borrow R, Balmer P, Miller E (2005) Meningococcal surrogates of protection--serum bactericidal antibody activity. Vaccine 23:2222–2227
29. Frasch CE, Borrow R, Donnelly J (2009) Bactericidal antibody is the immunologic surrogate of protection against meningococcal disease. Vaccine 27(Suppl 2):B112–B116
30. Finne J, Leinonen M, Makela PH (1983) Antigenic similarities between brain components and bacteria causing meningitis. Implications for vaccine development and pathogenesis. Lancet 2:355–357
31. Bruge J, Bouveret-Le Cam N, Danve B et al (2004) Clinical evaluation of a group B meningococcal N-propionylated polysaccharide conjugate vaccine in adult, male volunteers. Vaccine 22:1087–1096
32. Lo H, Tang CM, Exley RM (2009) Mechanisms of avoidance of host immunity by Neisseria meningitidis and its effect on vaccine development. Lancet Infect Dis 9:418–427
33. Sun YH, Exley R, Li Y et al (2005) Identification and characterization of genes required for competence in Neisseria meningitidis. J Bacteriol 187:3273–3276
34. van der Ley P, Heckels JE, Virji M et al (1991) Topology of outer membrane porins in pathogenic Neisseria spp. Infect Immun 59:2963–2971
35. Wang X, Cohn A, Comanducci M et al (2011) Prevalence and genetic diversity of candidate vaccine antigens among invasive Neisseria meningitidis isolates in the United States. Vaccine 29:4739–4744
36. Murphy E, Andrew L, Lee KL et al (2009) Sequence diversity of the factor H binding protein vaccine candidate in epidemiologically relevant strains of serogroup B Neisseria meningitidis. J Infect Dis 200:379–389
37. Jiang HQ, Hoiseth SK, Harris SL et al (2010) Broad vaccine coverage predicted for a bivalent recombinant factor H binding protein based vaccine to prevent serogroup B meningococcal disease. Vaccine 28:6086–6093
38. Jolley KA, Maiden MC (2010) BIGSdb: scalable analysis of bacterial genome variation at the population level. BMC Bioinformatics 11:595
39. Litt DJ, Savino S, Beddek A et al (2004) Putative vaccine antigens from Neisseria meningitidis recognized by serum antibodies of young children convalescing after meningococcal disease. J Infect Dis 190:1488–1497
40. Norheim G, Aseffa A, Yassin MA et al (2008) Specificity of subcapsular antibody responses in Ethiopian patients following disease caused by serogroup A meningococci. Clin Vaccine Immunol 15:863–871
41. Borrow R, Carlone GM, Rosenstein N et al (2006) Neisseria meningitidis group B correlates of protection and assay standardization--international meeting report Emory University, Atlanta, Georgia, United States, 16-17 March 2005. Vaccine 24:5093–5107
42. Goldschneider I, Gotschlich EC, Artenstein MS (1969) Human immunity to the meningococcus. I The role of humoral antibodies. J Exp Med 129:1307–1326
43. Jodar L, Cartwright K, Feavers IM (2000) Standardisation and validation of serological assays for the evaluation of immune responses to Neisseria meningitidis serogroup A and C vaccines. Biologicals 28:193–197
44. Borrow R, Carlone GM (2001) Serogroup B and C serum bactericidal assays. Methods Mol Med 66:289–304
45. Richmond PC, Marshall HS, Nissen MD et al (2012) Safety, immunogenicity, and tolerability of meningococcal serogroup B bivalent recombinant lipoprotein 2086 vaccine in healthy adolescents: a randomised, single-blind, placebo-controlled, phase 2 trial. Lancet Infect Dis 12:597–607
46. Food and Drug Administration (FDA) (2014) Guidance for industry: toxicity grading scale for healthy adult and adolescent volunteers enrolled in preventive vaccine clinical trials. Available http://www.fda.gov/downloads/BiologicsBloodVaccines/GuidanceComplianceRegulatoryInformation/Guidances/Vaccines/ucm091977.pdf. Accessed 23 Mar 2015

Chapter 26

Anti-Lyme Subunit Vaccines: Design and Development of Peptide-Based Vaccine Candidates

Christina M. Small, Waithaka Mwangi, and Maria D. Esteve-Gassent

Abstract

Vaccinology today has been presented with several avenues to improve protection against infectious disease. The recent employment of the reverse vaccinology technique has changed the face of vaccine development against many pathogens, including *Borrelia burgdorferi*, the causative agent of Lyme disease. Using this technique, genomics and *in silico* analyses come together to identify potentially antigenic epitopes in a high-throughput fashion. The forward methodology of vaccine development was used previously to generate the only licensed human vaccine for Lyme disease, which is no longer on the market. Using reverse vaccinology to identify new antigens and isolate specific epitopes to protect against *B. burgdorferi*, subunit vaccines will be generated that lack reactogenic and nonspecific epitopes, yielding more effective vaccine candidates. Additionally, novel epitopes are being utilized and are presently in the commercialization pipeline both for *B. burgdorferi* and other spirochaetal pathogens. The versatility and methodology of the subunit protein vaccine are described as it pertains to Lyme disease from conception to performance evaluation.

Key words *Borrelia burgdorferi*, Vaccine, Reverse vaccinology, *In silico*, Epitope, Multimeric, Immunization, Challenge, Lyme disease

1 Introduction

Vaccinology began via the exposure of a patient to whole microorganisms with the goal of utilizing the resultant immunological response to protect from infection in subsequent exposures to the infectious agent. With the development of the first protein subunit vaccines, a breakthrough in vaccine design was born, due to both the increased plasticity and practicality of the subunit vaccine design. A fully functional immune response to *Borrelia burgdorferi*, consisting of both cellular and humoral immunity (*see* **Note 1**), is necessary [1–6]. However, immunization using whole-cell *B. burgdorferi* is not generally used. This is due both to the presence of a highly variant and immunogenic protein, VlsE, on the cell surface, and the propensity of the bacterium to lose virulence plasmids

Sunil Thomas (ed.), *Vaccine Design: Methods and Protocols: Volume 1: Vaccines for Human Diseases*, Methods in Molecular Biology, vol. 1403, DOI 10.1007/978-1-4939-3387-7_26,

and exhibit markedly decreased survivability in the host [7, 8]. As such, the generation of subunit-based peptide vaccines for Lyme disease (LD) may be ideal due to the ability to incorporate several subunits to stimulate different types of immune response while excluding potentially detrimental epitopes of the same proteins.

Through the incorporation of several epitopes conferring desired characteristics, designer constructs may be generated. Both the human and canine LD vaccines are based on the antigen outer surface protein A (OspA). Within a few years of licensure, the human vaccine was withdrawn from the market, citing low sales following concerns about safety due to potential cross-reactivity and unintended inflammatory side effects [9–11]. Veterinary vaccines for canids are still available and are presently in use. There are, however, modified vaccine candidates based on the OspA antigen lacking the potentially autoreactive OspA epitopes [12]. Comstedt and collaborators have formulated one such vaccine candidate, using an updated multimeric OspA vaccine lacking the region of the OspA potentially responsible for the problematic side effects. They have taken the idea one step further, incorporating protective regions of OspA from various isolates found throughout the world and combined to generate a broadly protective hexavalent anti-Lyme vaccine [1]. Due to the increased control of subunit vaccine design on epitope use, this method may prove extremely effective for the generation of new LD vaccines.

2 Materials

2.1 Rehydration of Peptide Vaccine Constructs

1. Solvents that may be used include double-distilled water, phosphate-buffered saline (PBS, recipe below), polyethylene glycol (PEG-400), dimethyl sulfoxide (DMSO), or absolute ethanol.

2.2 Immunization

1. Adjuvant, commercially purchased.
2. 1 mL SubQ syringes with twenty-six 5/8-gauge needle.
3. 70 % Ethanol.
4. Cotton balls.

2.3 Growth and Infection with Borrelia

1. *Borrelia burgdorferi sensu stricto.*
2. Heat-inactivated normal rabbit serum (iNRS): Thaw from −80 °C on ice until completely thawed. Heat inactivate serum in 60 °C water bath for 30 min.
3. BSK II Media [13]: Note that for our studies, iNRS is used.
4. Incubator with temperature and carbon dioxide level regulation: Adjust to 32 °C and 1 % CO_2.

5. Hanks' Balance Salt Solution without phenol red (HBSS, Hyclone, Thermo Scientific, Inc.)

2.4 ELISA

1. PBS, 10× [14].
   (a) 1370 mM NaCl.
   (b) 27 mM KCl.
   (c) 81 mM Na_2HPO_4.
   (d) 14.7 mM KH_2PO_4.
   (e) Make in dH_2O, autoclave, and dilute to 1:10 with dH_2O prior to use.
2. Washing buffer/PBS-T: Add 0.1 % Tween-20 to necessary volume of 1× PBS.
3. Blocking buffer: PBS-T with 3 % bovine serum albumin (BSA).
4. Diluting buffer: PBS-T with 1 % BSA.
5. Coating buffer/carbonate buffer.
   (a) 15 mM Na_2CO_3.
   (b) 35 mM $NaHCO_3$.
   (c) Make in dH_2O. Adjust pH to 9.1 and autoclave.
6. Citrate buffer, for *o*-phenylenediamine dihydrochloride (OPD) substrate.
   (a) 25 mM Citric acid.
   (b) 50 mM Na_2PO_4.
   (c) Make in dH_2O, and adjust pH to 5.0.
   (d) Add 40 μL 30 % H_2O_2 to 100 mL citrate buffer immediately prior to use. Add OPD at 0.4 mg/mL. Dissolve fully.
7. Antibodies: Horseradish peroxidase (HRP)-conjugated anti-mouse IgM- and IgG-specific antibodies are required.
8. 96-Well microtiter plates: Nunc™ MaxiSorp® are recommended (Thermo Scientific, Inc.).

2.5 Sample Collection

1. Goldenrod Animal Lancets with 3–4 mm point, one per mouse.
2. Sterile dissection tools for final sampling (scissors, pins, needles, tweezers).
3. Dissection trays.
4. Formalin, to fix tissue for histopathology.
5. Sterile pestles, for crushing tissues during culture.
6. Sterile collection tubes, one per sample per mouse.

2.6 Dark-Field Microscopy

1. Microscope slides.
2. Cover slips.

3 Methods

3.1 Choosing a Target Protein

1. Selection of protein targets is the primary step in designing a potential subunit vaccine. For LD, it is necessary to stimulate both innate and adaptive immunity (*see* **Note 1**). A protein epitope selected to contribute to a subunit vaccine against LD must have a few key attributes. A summary of methods of enhancing subunit vaccine immune response is noted in Table 1.
   (a) The protein selected should not be reactogenic, causing either excessive fever or inflammation. Taking into consideration previous work, homology studies of other known inflammatory proteins, and in vivo experiments, the immunoreactivity potential of a given protein can be evaluated. For the design of a vaccine against LD specifically, using proteins that will not cause excessive immune-mediated side effects is a necessity as these reactions are similar to

Table 1
Methods of enhancing the immune response

Identity	Type	Function	Reference
VQGEESNDK from human IL 1	Stimulatory	Stimulates T cell proliferation/activation	[15]
WKYMVm	Stimulatory	Neutrophil activation	[56]
GGSG	Linker region	Separation of subunits, flexible	[57]
Loop region of *B. burgdorferi*	Linker region	Separation of subunits without inclusion of potentially cross-reactive epitopes	[3]
Keyhole limpet hemocyanin	Carrier protein	Increases visibility of small antigen to the immune system	[58]
Bovine serum albumin	Carrier protein	Increases visibility of small antigen to the immune system	[59]
Lipid A tag	Adjuvant (self)	Lipidation added by expression host	[21]
OspA, *Borrelia burgdorferi*	Adjuvant (self)	Activation of monocytes, stimulation of innate and adaptive immunity. Lipidation occurs through expression host	[22, 23]
Emulsions	Adjuvant	Depot function, stimulation of antibody production. Some formulations licensed for human use	[60, 61]
Aluminum salts	Adjuvant	Enhancement of immune system via depot function and inflammation. Stimulates antibody production and thymocytes. Some formulations licensed for human use	[62]

those found in the course of infection with LD. One such application of this concept is human interleukin 1, which incites a strong inflammatory response when introduced into patients as a whole protein. The extensive inflammatory side effects may be eliminated when only the immunostimulatory domain of interleukin 1 is used as a subunit of a larger construct [15].

(b) Another consideration is the ability of the selected protein to confer broad protection. In the USA, LD is thought to be caused mainly by *B. burgdorferi sensu stricto*, while in Europe and Asia, other genospecies such as *B. garinii* and *B. afzelii* are known to cause disease, with several other species suspected to have pathogenic potential [16]. It is, therefore, important to ensure protection across a range of organisms by using an antigen that is highly conserved within the *B. burgdorferi* genospecies complex [1]. Along these same lines, it is important that the antigen is not present on microbes of other genera that the vaccine-induced immune response could react with, which could generate undesirable side effects [17].

(c) The antigen should be exposed to the extracellular milieu. Extracellular exposure of the antigen highly improves odds of recognition by the immune system by being persistently available to immune cells. This exposure allows for the generation of antibodies, which play a role in the neutralization and blocking of pathogen targets, as well as the elimination of pathogen through complement-mediated killing and enhanced phagocytosis via opsonization [18–20].

(d) Lipidation tags may be included in order to generate a self-adjuvating vaccine construct, which is capable of attracting and stimulating an immune response independently of an additional adjuvant [21–23]. Difficulties in purification may be noted with the inclusion of lipidation tags.

3.2 In Silico Evaluation of Epitopes

Once proteins are selected, it is necessary to identify the regions of these proteins that can generate a strong, protective immune response. There are several *in silico*-predictive platforms available to identify potentially protective epitopes (Table 2). The localization of a protein on the surface of the cell can imply exposure to the immune system, although it is not a guarantee of recognition. This can be particularly important when using uncharacterized or hypothetical proteins, as is often the case when using reverse vaccine development methods. Additionally, the inclusion of signal sequences, glycosylation sites, or known B cell and T cell epitopes can enhance subunit construct. A few of these platforms may be employed to predict potentially useful epitopes of a protein.

Table 2
Protein feature prediction programs

Program name	Prediction	Website	Citation
DAS-TM filter	Topology	http://mendel.imp.univie.ac.at/sat/DAS/DAS.html	[49]
ΔG prediction	Topology	http://dgpred.cbr.su.se/	[50]
MEMSAT3	Topology	http://bioinf.cs.ucl.ac.uk/psipred/ Use MEMSAT3 & MEMSAT-SVM selection	[51]
TMHMM	Topology	http://www.cbs.dtu.dk/services/TMHMM/	[52]
GlycoPP	Glycosylation	http://www.imtech.res.in/raghava/glycopp/index.html	[53]
SignalP 4.1 Server	Signal sequence	http://www.cbs.dtu.dk/services/SignalP/ Select "Gram-negative bacteria"	[54]
Protscale	Hydrophobicity	http://web.expasy.org/protscale/ Use Kyte and Doolittle selection	[55]
Antibody epitope prediction	Antigenicity	http://tools.immuneepitope.org/tools/bcell/iedb_input/ Use selections for: Chou and Fasman Beta-Turn Prediction, Emini Surface Accessibility, Kolaskar and Tongaonkar Antigenicity, Parker Hydrophilicity, or Bepipred Linear Epitope Prediction, respectively	[24–28]

All user-adjustable parameters were left at their default values unless otherwise specified. The protein analysis tools in MacVector® 13.5.5 (MacVector Inc.) were also used

1. To check for potential transmembrane domains and thereby predict potential regions of surface exposure, transmembrane prediction and hydropathy plots can be utilized to identify putative membrane-spanning regions. Programs found in Table 2 (*see* Prediction: Topology) will assist in determining the predicted topology of a given protein. Additionally, transmembrane domains can be toxic to expression hosts by causing lysis of membranes, so the elimination of a few or all transmembrane domains serves to simplify protein expression and purification. It is also possible to evaluate the protein of interest for the presence of signal sequences or glycosylation sites in order to gain more information about surface-targeting tendencies and orientation of hydrophilic regions of the protein. Glycosylated proteins may have additional protection from immune recognition through the presence of sugars, which could obscure an otherwise antigenic epitope. Online programs for signal sequence (*see* Prediction: Signal Sequence) and glycosylation site evaluation (*see* Prediction: Glycosylation) are also found in Table 2. Signal sequences may be used in conjunction with topology to further confirm orientation of proteins.

2. With the information regarding regions of potential surface exposure, it is beneficial to evaluate the entire protein for antigenic regions, as determined by the Antibody Epitope Prediction program, found in Table 2 (*see* Prediction: Antigenicity). Various selections will allow the user to identify regions with greater antigenicity based on the presence of beta turns, accessibility, flexibility, hydrophilicity, and amino acid composition [24–28]. Similarly, linear epitopes that are potentially recognized by B cells can be predicted using the Bepipred Linear Epitope Prediction method of the Antibody Epitope Prediction [27]. Often, these epitopes will encompass turns which lack secondary structure, as determined using the Chou and Fasman Secondary Structure Prediction via the Antibody Epitope Prediction selection [24]. Although surface exposure and thereby hydrophilicity are among the primary considerations, Kolaskar and Tongaonkar determined that surface-exposed hydrophobic residues are likely to be present in antigenic regions of the protein. As such, the Kolaskar and Tongaonkar prediction of antigenicity may be used to predict useful epitopes [26].
3. Alignment of the information gathered using the programs above will reveal regions of the protein with overlapping characteristics. Potentially surface-exposed regions demonstrating predicted antigenicity and agreeable secondary structure could prove to be a highly protective antigen and thereby be useful in the production of quality subunit candidates for evaluation. Ideally, an epitope used in the subunit vaccine will span regions of antigenicity and hydrophilicity and include either 8–11 amino acids or 12–25, depending on if MHC I or MCH II receptors are targeted, respectively [29]. Normally a number of these antigenic peptides can be generated from each protein tested. In order to further pinpoint effective peptide regions, confirmation of protection may be completed in vitro or in vivo.

3.3 Production of the Subunit Vaccine Constructs

1. Cloning and expression from the genomic DNA of *B. burgdorferi* (*see* **Note 2**).
2. Commercial synthesis of vaccine constructs.
   (a) Orders may be placed via a company capable of solid-phase synthesis, or, if equipment is in place, may be done in the lab. The order of subunits within the polypeptide being generated can make a difference in protective response due to differing visibility and accessibility of the protein epitopes with varied secondary and tertiary structures between constructs. As such, it may be valuable to order and test different combinations of subunits to determine which will generate the best immune response.

(b) Additionally, any required amino acids must be present in order to facilitate conjugation to carrier molecules. For example, in order to conjugate either keyhole limpet hemocyanin (KLH) or BSA to the vaccine construct, an N- or C-terminal cysteine must be present with an available amine group to perform chemistry, which may be either naturally occurring or synthetically added [30].

(c) Purity is a particular concern in in vivo experiments, and 95–98 % purity is recommended for such experiments. This purity can be specified during ordering or must be evaluated in products generated in the lab.

3. Once received, peptides will most likely be lyophilized and must be resuspended in a solvent appropriate for downstream applications. However, there is no perfect fit concerning solvents due to the various biochemical properties even between similar constructs. Commonly used solvents include water, PBS, DMSO, PEG-400, and ethanol, among others [31, 32]. There have been studies evaluating the dose response of animals to varying levels of these solvents. For a given construct study, the appropriate solvent type and amount must be chosen based on route of administration, volume, and frequency of administration, in addition to the solubility requirements of the protein constructs. A more effective solvent, such as DMSO, with the potential to cause more side effects than other solvents, may be utilized in the case of a single-injection study. However, in a study requiring multiple boosts this solvent may not be appropriate and a more mild solvent like PBS is a better choice [31, 33]. Finally, in order to determine an acceptable immunization volume, the maximum volume for the animal model using a specified mode of vaccination must be considered [32] (Fig. 1).

3.4 Vaccination and Challenge Protocols

1. Before beginning an animal-based experiment, the determination of how many animals to use per test group in order to yield statistically significant results must be performed using a power analysis [34]. Working through the analysis with a statistician prior to ordering animals may improve experimental data strength and simplify the workflow through immunization.

2. To test a subunit vaccine construct against LD, the mouse model should be considered. C3H/HeN mice are the strain of choice to evaluate protection induced by a vaccine candidate against LD, due to their ability to demonstrate cardiac- and arthritis-related symptoms that are similar to human disease. In contrast, C57BL/6 and BALB/c mice show decreased LD symptoms and IgG titers after infection with *B. burgdorferi*, and thus are not as valuable for vaccination studies [35]. Age also plays a role in the severity of resultant

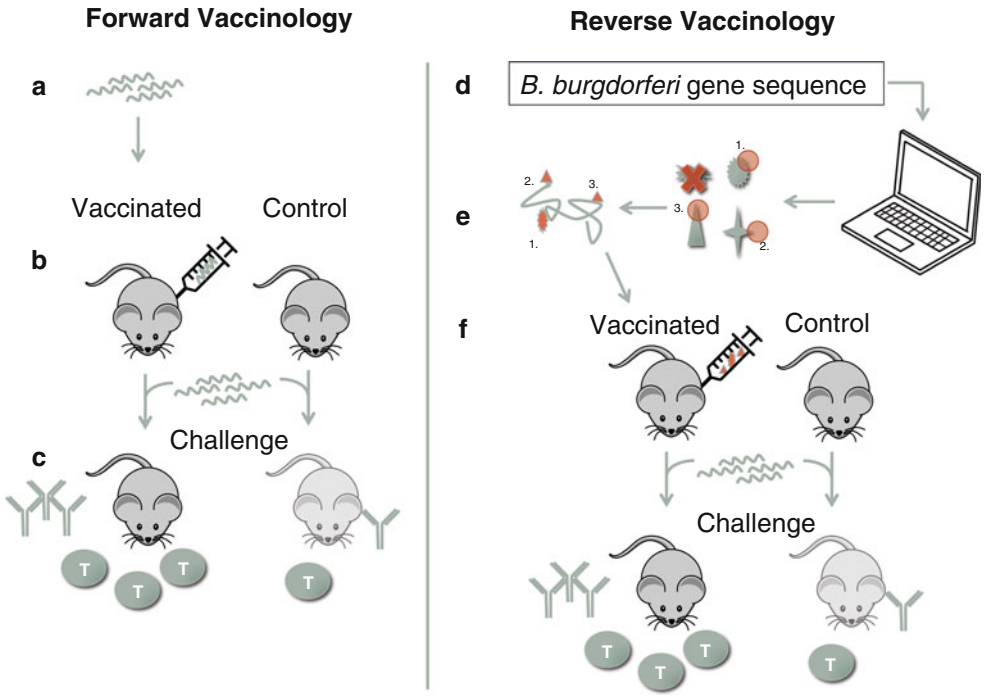

Fig. 1 Forward and reverse vaccinology for the identification of novel vaccine candidates. In the forward vaccinology technique, live, attenuated, or killed *B. burgdorferi* are used to vaccinate naïve animals (**a**). Both vaccinated and unvaccinated animals are then challenged with live, virulent *B. burgdorferi* (**b**). Upon challenge, vaccinated animals may demonstrate improved immune response and ability to survive challenge with fewer side effects than control animals (**c**). Reverse vaccinology makes use of the known sequence of genes of *B. burgdorferi* to determine vaccine candidate targets using various *in silico* analyses (**d**). Selected vaccine candidate(s) are formulated to generate prototype immunogen (**e**) which is then used to immunize naïve mice prior to challenge with live, infectious *B. burgdorferi* (**f**)

symptoms and as such 6–8-week-old female mice are normally used in these type of studies, as severity of disease decreases as age increases [35, 36].

3. Once the construct has been generated, standardization of the immunization protocol and evaluation of protection specific to the vaccine construct, model organism, and mode of immunization may take place. One protocol that has been successful for LD vaccine candidates is the following. Female C3H/HeN mice between 6 and 8 weeks of age are bled to evaluate antibody titers prior to the first immunization. The mice are then immunized subcutaneously by mixing 50 μg protein construct per mouse *v:v* with a water-in-oil adjuvant, for a final volume of 100 μL/mouse. Prior to immunizing, a cotton ball with 70 % ethanol is used to wipe the area of immunization. Negative control mice receive buffer without peptide and adjuvant or an irrelevant peptide and adjuvant. At week 2 and potentially

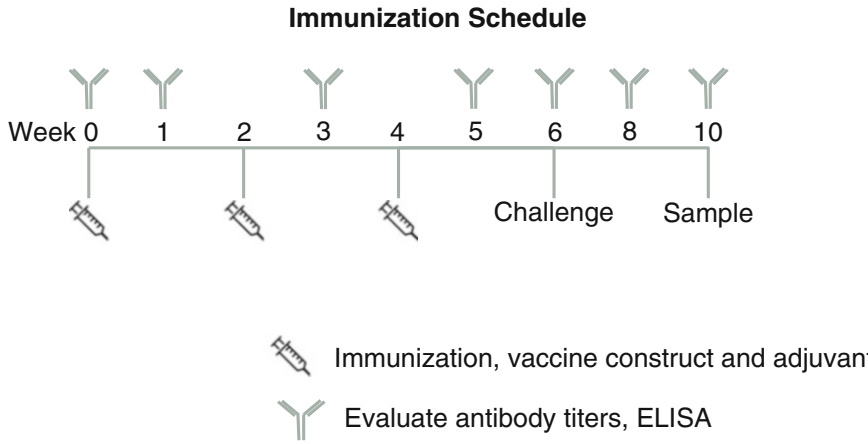

Fig. 2 Example of immunization schedule for evaluating a potential antigen of *B. burgdorferi* for protection via vaccination. At week 0, blood is taken to evaluate baseline titers. At this time, the priming immunization is administered. Titers may be evaluated at weeks 0, 1, 3, 5, 6, 8, and 10. Mice are boosted at weeks 2 and 4, and then challenged with *B. burgdorferi* at week 6 post-priming. Sampling is performed at 4 weeks post-challenge

week 4 post-priming, the mice are boosted with the same formulation as used previously. Titers may then be monitored at weeks 1, 3, and 5 post-priming to track antibody response throughout the course of immunization. Once titers have returned to nearly baseline levels, mice are challenged as detailed below. For this protocol, the challenge is at week 6, 2 weeks after the final boost; however, it is important to standardize the immunization schedule to determine optimal conditions for a given antigen, as detailed in **Note 3**. Final sampling takes place at week 10, 4 weeks post-challenge (Fig. 2).

4. To determine antibody titers, blood can be drawn using the submandibular facial puncture technique. The blood is then kept at 4 °C, and after clotting serum can be separated by centrifuging samples at 9,400 × *g* for 20 min at room temperature. The sera can then be evaluated by ELISA to determine antibody titers or stored at −80 °C. To measure antibody titers, 96-well microtiter plates are coated overnight at 4 °C in carbonate buffer with 500 ng/well of vaccine construct protein or with *B. burgdorferi* whole-cell lysate (10^7 *B. burgdorferi*/well). After washing three times with washing buffer, plates are blocked with blocking buffer for 2 h at room temperature. Plates are washed three times using washing buffer before application of the serum. Each serum sample may be serially diluted in diluting buffer and run in either duplicate or triplicate. After 1-h incubation at room temperature, plates are washed three times with washing buffer prior to application of the secondary antibody. The horseradish peroxidase-conju-

gated secondary antibody for detection of mouse antibodies, either IgM or IgG specifically, is applied at an appropriate dilution as detailed by the manufacturer in diluting buffer and incubated for 1 h before being washed three times in washing buffer. The reaction is then visualized using 100 μL per well of OPD (*o*-phenylenediamine dihydrochloride) color substrate, and plates are incubated in the dark for 20 min prior to detection at a wavelength of 450 nm.

5. After mice complete the immunization course, they are challenged using either the needle or the tick methods of infection. For the needle method, low (10^3 spirochaetes/mL) and high (10^5 spirochaetes/mL) doses may be utilized. *Borrelia* is typically grown in BSK-II media complemented with 6 % iNRS at 32 °C and 1 % CO_2 until the appropriate cell density is achieved. At this point, cells will be harvested via centrifugation and washed three times using Hanks' Balanced Salt Solution (HBSS) containing inactivated normal rabbit serum (iNRS, *v:v*). Cultures are then quantified and cells are diluted to the appropriate cell density using HBSS/iNRS [4]. For the tick method of infection, pathogen-free *Ixodes scapularis* ticks are required and can be purchased from the Oklahoma State University Tick Laboratory in the nymphal stage and infected artificially with *B. burgdorferi* B31 A3 strain by immersion. After desiccation for 4 days at 79 % relative humidity, nymphs are infected by immersion in a suspension of 10^8 spirochetes/mL for 45 min. After the 45-min infection, the ticks are washed and returned to the 79 % RH chamber for 3 more days to facilitate attachment of the nymphs to mice. The mice are briefly housed individually in wire-bottom cages prior to infestation with 8–10 *B. burgdorferi*-infected *I. scapularis* nymphs, which are allowed to feed to repletion [4, 37]. Tick infection rate is measured using quantitative PCR (qPCR) on a subset of infected ticks compared to non-infected ticks. Engorged ticks are collected and stored in 80 % ethanol for further analysis. Four weeks post-infection, mice are euthanized and protection is evaluated as described below [4].

3.5 Evaluation and Quantification of Protection In Vivo

1. Protection is evaluated and quantified using a few methods. At 28 days post-challenge, mice are euthanized and blood is collected as previously discussed in order to determine final antibody titers against both the specific vaccine candidate and *B. burgdorferi*.
2. For the final sample collection, several tissues are collected from each mouse, including skin, spleen, heart, bladder, inguinal lymph nodes, and a tibiotarsal joint. These tissues are used to quantify bacterial load. The tissues are incubated, crushed in collection tubes with pestles, then added to 5.0 mL BSK-II

media with 6 % iNRS at 32 °C with 1 % CO_2 5 days prior to blind passage to fresh media, and incubated under the same conditions for 15 days before evaluation for bacterial recovery using dark-field microscopy [4, 38].

3. Histopathology of heart and joint tissues can also be blindly evaluated by a board-certified pathologist to evaluate inflammation [4].
4. qPCR of the skin, spleen, joint, and an inguinal lymph node can be performed to further characterize the effect of the immunization protocol on the bacterial burden present in each tissue [4].
5. A passive/adoptive transfer experiment may be performed to further characterize protection after challenge (Fig. 3). After the full immunization schedule (Fig. 2), antibodies and splenocytes (SPC) are collected and are transferred to naïve mice. These mice are then challenged after 1–3 days with *B. burgdorferi* infection. Protection is evaluated as detailed above,

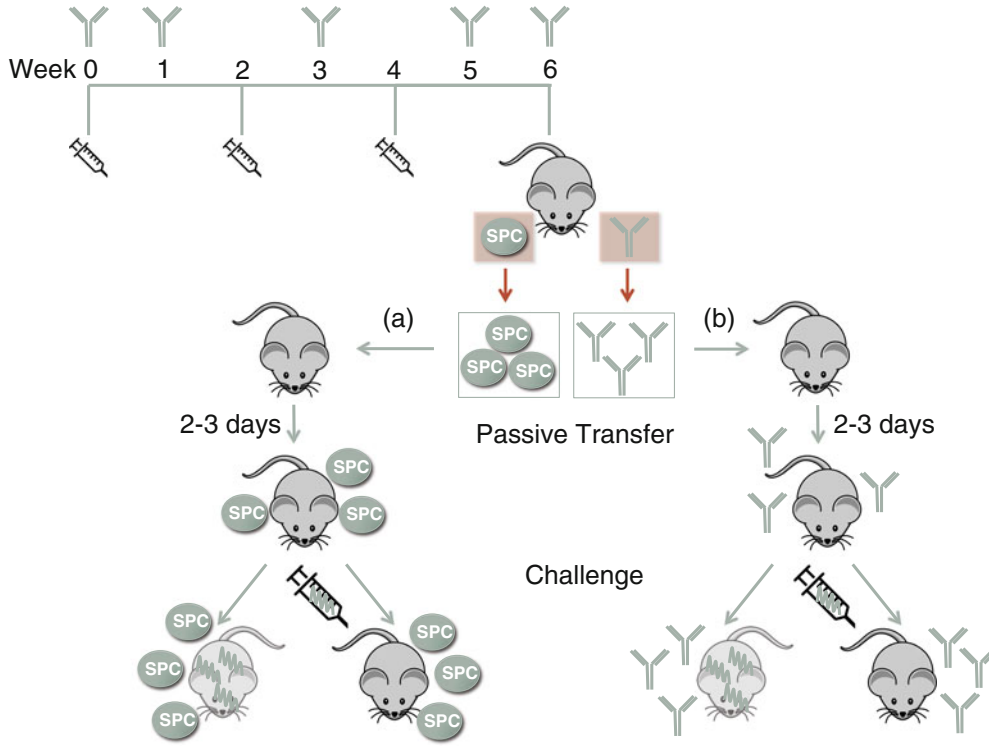

Fig. 3 Experimental schematic for passive/adoptive transfer. For passive transfer experiments, mice are immunized according to immunization schedule (Fig. 2) and allowed to generate full immune response. At week 6, splenocytes, denoted SPC, (**a**) or antibodies (**b**) may be harvested for the passive/adoptive transfer. The antibodies or splenocytes are introduced into naïve mice and then the mice are challenged with *B. burgdorferi* in order to determine whether protection is due to antibody response, T cell response, or a combination of both

and protection can be attributed to one or both branches of immunity. This information can enhance future constructs by allowing for the ability to use additional subunits to supplement the missing or lacking immune response, either antibody or T cell mediated.

4 Notes

1. Particularly in the case of LD, it is necessary to have both cellular and humoral immune responses [39–41]. Cellular immunity plays an important role in targeting the pathogen entering the host via the dermis as well as in upregulating adaptive immunity. However, cellular responses can be fruitless if inflammation and tissue damage are generated without noticeably enhancing protection from infection, as inflammation-mediated symptoms are a primary concern in LD infection. Additionally, antibody responses are necessary to generate a strong, protective memory response, particularly due to their role in opsonization and phagocytosis of the pathogen [18–20, 42–44]. During natural infection, the immunodominance of certain epitopes of the surface lipoprotein VlsE coupled with the high level of variation in other variable regions of VlsE can make targeting *B. burgdorferi* using antibodies difficult [7]. Additionally, *Borrelia* is seen to differentially regulate gene expression depending on the environment [45]. Particularly using reverse vaccinology, it is important to ensure that the protein selected is expressed during infection or colonization and dissemination to be actively targeted [2, 45]. In total, stimulation of a well-rounded immune response is absolutely necessary for control and clearance of LD and will be most directly achieved using a subunit vaccine composed of epitopes designed to enhance both cellular and humoral immunity.
2. Cloning and expression will be highly variable depending on genes, restriction enzymes, and expression systems utilized. To clone and express subunits, the genomic DNA of *B. burgdorferi* must be extracted utilizing conventional methods of phenol/chloroform extraction [46–48]. After standard cloning protocols, purification of the protein post-expression will also greatly depend on the biochemical properties of the protein produced. Dialysis, centrifugal filters, chromatography, SDS-PAGE, and MALDI among other methods may be required to achieve desired purity. Required purity depends on application; for example, for in vitro applications, 80 % or higher purity may be acceptable; however, for *in vivo* applications, 95 % or higher may be required to avoid side effects in the immunized animals.

3. For each antigen and combination of antigens, an ideal schedule of immunization may be standardized to yield the strongest immune response. Figure 2 is an example of a timeline appropriate for work with LD vaccines. Included are the suggested times needed between primary and boosting immunizations as well as time points to monitor antibody titers. It is important to closely monitor antibody titers and allow titers to return to near baseline before boosting or proceeding to challenge animals with *B. burgdorferi*. Typically, preliminary study on protection from the epitope and identification of the ideal time line will be performed before evaluating more variables, such as additional construct subunits or adjuvant choice.

References

1. Comstedt P, Hanner M, Schuler W, Meinke A, Lundberg U (2014) Design and development of a novel vaccine for protection against Lyme borreliosis. PLoS One 9(11):e113294
2. Rappuoli R (2000) Reverse vaccinology. Curr Opin Microbiol 3:445–450
3. Wressnigg N, Barrett PN, Pollabauer EM, O'Rourke M, Portsmouth D et al (2014) A Novel multivalent OspA vaccine against Lyme borreliosis is safe and immunogenic in an adult population previously infected with *Borrelia burgdorferi* sensu lato. Clin Vaccine Immunol 21:1490–1499
4. Small CM, Ajithdoss DK, Rodrigues Hoffmann A, Mwangi W, Esteve-Gassent MD (2014) Immunization with a *Borrelia burgdorferi* BB0172-derived peptide protects mice against Lyme disease. PLoS One 9(2):e88245
5. Palaniappan RU, McDonough SP, Divers TJ, Chen CS, Pan MJ, Matsumoto M, Chang YF (2006) Immunoprotection of recombinant leptospiral immunoglobulin-like protein A against *Leptospira interrogans* serovar Pomona infection. Infect Immun 74:1745–1750
6. Downie AW (1951) Jenner's cowpox inoculation. Br Med J 2:251–256
7. Zhang JR, Hardham JM, Barbour AG, Norris SJ (1997) Antigenic variation in Lyme disease borreliae by promiscuous recombination of VMP-like sequence cassettes. Cell 89:275–285
8. Labandeira-Rey M, Skare JT (2001) Decreased infectivity in *Borrelia burgdorferi* strain B31 is associated with loss of linear plasmid 25 or 28-1. Infect Immun 69:446–455
9. de Silva AM, Telford SR 3rd, Brunet LR, Barthold SW, Fikrig E (1996) *Borrelia burgdorferi* OspA is an arthropod-specific transmission-blocking Lyme disease vaccine. J Exp Med 183:271–275
10. Nigrovic LE, Thompson KM (2007) The Lyme vaccine: a cautionary tale. Epidemiol Infect 135:1–8
11. Steere AC, Sikand VK, Meurice F, Parenti DL, Fikrig E, Schoen RT, Nowakowski J, Schmid CH, Laukamp S, Buscarino C, Krause DS (1998) Vaccination against Lyme disease with recombinant *Borrelia burgdorferi* outer-surface lipoprotein A with adjuvant. Lyme Disease Vaccine Study Group. N Engl J Med 339:209–215
12. Willett TA, Meyer AL, Brown EL, Huber BT (2004) An effective second-generation outer surface protein A-derived Lyme vaccine that eliminates a potentially autoreactive T cell epitope. Proc Natl Acad Sci U S A 101:1303–1308
13. Barbour AG (1984) Isolation and cultivation of Lyme disease spirochetes. Yale J Biol Med 57:521–525
14. Dulbecco R, Vogt M (1954) Plaque formation and isolation of pure lines with poliomyelitis viruses. J Exp Med 99:167–182
15. Antoni G, Presentini R, Perin F, Tagliabue A, Ghiara P, Censini S, Volpini G, Villa L, Boraschi D (1986) A short synthetic peptide fragment of human interleukin 1 with immunostimulatory but not inflammatory activity. J Immunol 137:3201–3204
16. Rudenko N, Golovchenko M, Grubhoffer L, Oliver JH Jr (2011) Updates on *Borrelia burgdorferi* sensu lato complex with respect to public health. Ticks Tick-Borne Dis 2:123–128
17. Lovrich SD, Callister SM, Lim LC, DuChateau BK, Schell RF (1994) Seroprotective groups of Lyme borreliosis spirochetes from North America and Europe. J Infect Dis 170:115–121
18. Kochi SK, Johnson RC, Dalmasso AP (1993) Facilitation of complement-dependent killing of the Lyme disease spirochete, *Borrelia burgdorferi*, by specific immunoglobulin G Fab antibody fragments. Infect Immun 61:2532–2536

19. Lawrenz MB, Wooten RM, Zachary JF, Drouin SM, Weis JJ, Wetsel RA, Norris SJ (2003) Effect of complement component C3 deficiency on experimental Lyme borreliosis in mice. Infect Immun 71:4432–4440
20. Szczepanski A, Benach JL (1991) Lyme borreliosis: host responses to *Borrelia burgdorferi*. Microbiol Rev 55:21–34
21. Johnson AG, Gaines S, Landy M (1956) Studies on the O antigen of *Salmonella typhosa*. V Enhancement of antibody response to protein antigens by the purified lipopolysaccharide. J Exp Med 103:225–246
22. Vaz A, Glickstein L, Field JA, McHugh G, Sikand VK, Damle N, Steere AC (2001) Cellular and humoral immune responses to *Borrelia burgdorferi* antigens in patients with culture-positive early Lyme disease. Infect Immun 69:7437–7444
23. Haupl T, Landgraf S, Netusil P, Biller N, Capiau C, Desmons P, Hauser P, Burmester GR (1997) Activation of monocytes by three OspA vaccine candidates: lipoprotein OspA is a potent stimulator of monokines. FEMS Immunol Med Microbiol 19:15–23
24. Chou PY, Fasman GD (1978) Prediction of the secondary structure of proteins from their amino acid sequence. Adv Enzymol Relat Areas Mol Biol 47:45–148
25. Emini EA, Hughes JV, Perlow DS, Boger J (1985) Induction of hepatitis A virus-neutralizing antibody by a virus-specific synthetic peptide. J Virol 55:836–839
26. Kolaskar AS, Tongaonkar PC (1990) A semi-empirical method for prediction of antigenic determinants on protein antigens. FEBS Lett 276:172–174
27. Larsen JE, Lund O, Nielsen M (2006) Improved method for predicting linear B-cell epitopes. Immunome Res 2:2
28. Parker JM, Guo D, Hodges RS (1986) New hydrophilicity scale derived from high-performance liquid chromatography peptide retention data: correlation of predicted surface residues with antigenicity and X-ray-derived accessible sites. Biochemistry 25:5425–5432
29. Appella E, Padlan EA, Hunt DF (1995) Analysis of the structure of naturally processed peptides bound by class I and class II major histocompatibility complex molecules. EXS 73:105–119
30. Jones DS, Coutts SM, Gamino CA, Iverson GM, Linnik MD, Randow ME, Ton-Nu HT, Victoria EJ (1999) Multivalent thioether-peptide conjugates: B cell tolerance of an anti-peptide immune response. Bioconjug Chem 10:480–488
31. Montaguti P, Melloni E, Cavalletti E (1994) Acute intravenous toxicity of dimethyl sulfoxide, polyethylene glycol 400, dimethylformamide, absolute ethanol, and benzyl alcohol in inbred mouse strains. Arzneimittelforschung 44:566–570
32. Turner PV, Pekow C, Vasbinder MA, Brabb T (2011) Administration of substances to laboratory animals: equipment considerations, vehicle selection, and solute preparation. J Am Assoc Lab Anim Sci 50:614–627
33. Thackaberry EA, Wang X, Schweiger M, Messick K, Valle N, Dean B, Sambrone A, Bowman T, Xie M (2014) Solvent-based formulations for intravenous mouse pharmacokinetic studies: tolerability and recommended solvent dose limits. Xenobiotica 44:235–241
34. Dell RB, Holleran S, Ramakrishnan R (2002) Sample size determination. ILAR J 43:207–213
35. Barthold SW, Beck DS, Hansen GM, Terwilliger GA, Moody KD (1990) Lyme borreliosis in selected strains and ages of laboratory mice. J Infect Dis 162:133–138
36. Radolf JD, Caimano MJ, Stevenson B, Hu LT (2012) Of ticks, mice and men: understanding the dual-host lifestyle of Lyme disease spirochaetes. Nat Rev Microbiol 10:87–99
37. Bouchard KR, Wikel SK (2004) Care, maintenance and experimental infestation of ticks in the laboratory setting. In: Marquart WC (ed) Biology of disease vectors, 2nd edn. Elsevier, New York, pp 705–711
38. Maruskova M, Esteve-Gassent MD, Sexton VL, Seshu J (2008) Role of the BBA64 locus of *Borrelia burgdorferi* in early stages of infectivity in a murine model of Lyme disease. Infect Immun 76:391–402
39. Fikrig E, Barthold SW, Sun W, Feng W, Telford SR 3rd, Flavell RA (1997) *Borrelia burgdorferi* P35 and P37 proteins, expressed in vivo, elicit protective immunity. Immunity 6:531–539
40. Keane-Myers A, Nickell SP (1995) T cell subset-dependent modulation of immunity to Borrelia burgdorferi in mice. J Immunol 154:1770–1776
41. Montgomery RR, Lusitani D, de Boisfleury CA, Malawista SE (2002) Human phagocytic cells in the early innate immune response to *Borrelia burgdorferi*. J Infect Dis 185:1773–1779
42. Fikrig E, Kantor FS, Barthold SW, Flavell RA (1993) Protective immunity in Lyme borreliosis. Parasitol Today 9:129–131
43. McKisic MD, Barthold SW (2000) T-cell-independent responses to *Borrelia burgdorferi* are critical for protective immunity and resolution of lyme disease. Infect Immun 68:5190–5197

44. Simon MM, Schaible UE, Kramer MD, Eckerskorn C, Museteanu C, Muller-Hermelink HK, Wallich R (1991) Recombinant outer surface protein a from *Borrelia burgdorferi* induces antibodies protective against spirochetal infection in mice. J Infect Dis 164:123–132
45. Revel AT, Talaat AM, Norgard MV (2002) DNA microarray analysis of differential gene expression in *Borrelia burgdorferi*, the Lyme disease spirochete. Proc Natl Acad Sci U S A 99:1562–1567
46. Chomczynski P, Sacchi N (1987) Single-step method of RNA isolation by acid guanidinium thiocyanate-phenol-chloroform extraction. Anal Biochem 162:156–159
47. Chomczynski P, Sacchi N (2006) The single-step method of RNA isolation by acid guanidinium thiocyanate-phenol-chloroform extraction: twenty-something years on. Nat Protoc 1:581–585
48. Kirby KS (1956) A new method for the isolation of ribonucleic acids from mammalian tissues. Biochem J 64:405–408
49. Cserzo M, Eisenhaber F, Eisenhaber B, Simon I (2002) On filtering false positive transmembrane protein predictions. Protein Eng 15:745–752
50. Hessa T, Meindl-Beinker NM, Bernsel A, Kim H et al (2007) Molecular code for transmembrane-helix recognition by the Sec61 translocon. Nature 450:1026–1030
51. Nugent T, Jones DT (2009) Transmembrane protein topology prediction using support vector machines. BMC Bioinformatics 10:159
52. Krogh A, Larsson B, von Heijne G, Sonnhammer EL (2001) Predicting transmembrane protein topology with a hidden Markov model: application to complete genomes. J Mol Biol 305:567–580
53. Chauhan JS, Bhat AH, Raghava GP, Rao A (2012) GlycoPP: a webserver for prediction of N- and O-glycosites in prokaryotic protein sequences. PLoS One 7(7):e40155
54. Petersen TN, Brunak S, von Heijne G, Nielsen H (2011) SignalP 4.0: discriminating signal peptides from transmembrane regions. Nat Methods 8:785–786
55. Kyte J, Doolittle RF (1982) A simple method for displaying the hydropathic character of a protein. J Mol Biol 157:105–132
56. Boxio R, Bossenmeyer-Pourie C, Vanderesse R, Dournon C, Nusse O (2005) The immunostimulatory peptide WKYMVm-NH activates bone marrow mouse neutrophils via multiple signal transduction pathways. Scand J Immunol 62:140–147
57. Arai R, Ueda H, Kitayama A, Kamiya N, Nagamune T (2001) Design of the linkers which effectively separate domains of a bifunctional fusion protein. Protein Eng 14:529–532
58. Harris JR, Markl J (1999) Keyhole limpet hemocyanin (KLH): a biomedical review. Micron 30:597–623
59. Chu FS, Lau HP, Fan TS, Zhang GS (1982) Ethylenediamine modified bovine serum albumin as protein carrier in the production of antibody against mycotoxins. J Immunol Methods 55:73–78
60. Freund J, Casals J, Hosmer EP (1937) Sensitization and antibody formation after injection of tubercle bacilli and paraffin oil. Proc Soc Exp Biol Med 37:509–513
61. O'Hagan DT, Ott GS, De Gregorio E, Seubert A (2012) The mechanism of action of MF59 - an innately attractive adjuvant formulation. Vaccine 30:4341–4348
62. Edelman R (1980) Vaccine adjuvants. Rev Infect Dis 2:370–383

Chapter 27

Assessment of Live Plague Vaccine Candidates

Valentina A. Feodorova, Lidiya V. Sayapina, and Vladimir L. Motin

Abstract

Since its creation in the early twentieth century, live plague vaccine EV has been successfully applied to millions of people without severe complications. This vaccine has been proven to elicit protection against both bubonic and pneumonic plague, and it is still in use in populations at risk mainly in the countries of the former Soviet Union. Despite extensive efforts in developing subunit vaccines, there is a reviving interest in creation of a precisely attenuated strain of *Yersinia pestis* superior to the EV that can serve as a live plague vaccine with improved characteristics. Here we summarize decades of experience of the Russian anti-plague research in developing a standard protocol for early-stage evaluation of safety and immunogenicity of live plague vaccines. This protocol allows step-by-step comparison of the novel test candidates with the EV vaccine by using subcutaneous immunization and bubonic plague infection models in two animal species, e.g., guinea pigs and mice.

Key words *Yersinia pestis*, Plague, Live vaccine, Animal model, Protection, Virulence, Attenuation, Infectious disease, Vaccine candidate, Mutant

1 Introduction

Yersinia pestis, the causative agent of plague, has been identified as one of the most devastating human pathogens to have had a severe impact on human history resulting in epidemics that have taken the lives of more than 200 million people [1]. Despite the urgency of finding a means of preventing plague, the Western world is currently left without a prophylactic option against this dangerous disease, since the production of previously used killed plague vaccines has been discontinued, and the plague vaccines under development are not quite ready for human use [2, 3]. The subunit plague vaccine that is currently undergoing clinical trials consists of two protective antigens, the capsular subunit F1 and major virulence protein LcrV (V antigen) [4]. Taking into account an existing polymorphism of LcrV antigen [5, 6], and the fact that a capsule is dispensable for *Y. pestis* virulence [7, 8], it is clear that the subunit vaccine will need further improvement. The F1/LcrV-based vaccines protect rodents and nonhuman primates from both bubonic

Sunil Thomas (ed.), *Vaccine Design: Methods and Protocols: Volume 1: Vaccines for Human Diseases*, Methods in Molecular Biology, vol. 1403, DOI 10.1007/978-1-4939-3387-7_27,

and pneumonic plague [2–4]; however, there is concern about the ability of these vaccines to provide robust protection in humans, particularly with respect to eliciting an appropriate level of cellular immunity [9, 10]. Moreover, correlates of protection for the F1/V vaccines are not well defined at the moment [11]. On the other hand, for the past 70 years, countries of the former Soviet Union have accumulated tremendous experience in using live plague vaccine for immunizing populations at risk, as well as plague workers [12, 13]. The vaccine EV, created by French scientists G. Girard and J. Robic [14], has been distributed to different laboratories around the world, including the former Soviet Union where it was named EV line NIIEG [4, 13]. The Western lineages generally designated as EV 76 were widely tested in different animal models, and were found to be not safe enough for human use [15]. Recently, different lineages of EV 76 were sequenced and compared to each other in an effort to define the base of attenuation in the EV vaccine [16].

Currently, there is a reviving interest in creation of live plague vaccines by using modern methods of recombinant technology to precisely attenuate the virulent *Y. pestis* organism. The major advantage of such vaccines will be eliciting robust humoral and cellular immunity to multiple *Y. pestis* antigens, as well as knowledge of the exact mechanism underlying attenuation of virulence. Several laboratories have begun testing attenuated *Y. pestis* mutants as potential live plague vaccines [2–4, 17, 18]. However, we found that there is no standard and unified protocol, which can be used across the labs in evaluation of protective properties of such strains, especially in comparison with the EV vaccine. The examples of head-to-head comparison between the EV vaccine and novel live plague vaccine candidates were limited to the studies of the LpxM [19, 20] and NlpD [21, 22] mutants in mice and guinea pigs, and to recent investigation of the vaccine properties of Microtus 201 in rhesus macaques [23].

Here, we would like to share the experience that Russian anti-plague researchers have accumulated in decades of efforts in improving a live plague vaccine. The described protocol is the first step in evaluating live plague vaccine candidates, and many strains that successfully passed this stage have been further evaluated in studies of nonhuman primates, aerosol challenge, and human volunteers. This protocol employs guinea pigs as a major model, an animal species that is rarely used these days in Western laboratories to evaluate protection against plague. Nevertheless, guinea pigs were commonly used to investigate plague infection in the past. This model is well developed and can serve particularly well for testing live vaccine strains of *Y. pestis*. One of the major differences with the mouse model is that guinea pigs are relatively unresponsive to capsule antigen of *Y. pestis*. In contrast to mice that develop fast and excessive response to the capsular antigen F1 upon immu-

nization with live plague vaccine EV, protection of immunized guinea pigs relies on antigens other than F1. As a result, mice vaccinated with EV NIIEG are not protected against challenge with capsule-negative virulent *Y. pestis*, while guinea pigs in the equivalent situation are immune [4, 13]. The recent testing of *Y. pestis* NlpD live vaccine candidate in mice and guinea pigs revealed a striking difference in protective properties between two animal species [22]. The protocol described here is mainly adapted from the guidelines for testing vaccine strains of *Y. pestis* [24] with inclusion of the personal research experience of the authors. The key point of this protocol is a direct comparison of novel live plague vaccine candidates with EV NIIEG vaccine in two animal models, such as guinea pigs and mice. The EV NIIEG vaccine has been used on millions of humans without severe complications and has an established feature of providing protection against both bubonic and pneumonic plague.

2 Materials

2.1 Bacteriological Media

1. We refer here to Hottinger agar as a major medium to grow *Y. pestis* as described in the Guidance [23]. Additionally, other rich media, such as heart infusion broth or Luria-Bertani medium, can be used instead. For bacteriological studies of the organs of animals inoculated with *Y. pestis*, it is recommended to supplement Hottinger agar with 0.025 % sodium sulfite (Na_2SO_3).
2. To prepare blood agar plates, we suggest using 5 % defibrinated sheep blood supplement to the Hottinger agar or tryptic soy blood agar base.
3. Endo agar is also used for bacteriological studies of the organs of experimental animals.

2.2 Yersinia pestis Strains

The inoculation doses of *Y. pestis* are calculated in colony-forming unit (CFU) obtained after actual plating of the cultures in dilution.

1. We refer here to a standard control live plague vaccine as *Y. pestis* EV NIIEG [23]. It remains to be determined whether the lineages of EV76 available in different countries [16] match closely with the NIIEG line.
2. The *Y. pestis* strain used for challenge to evaluate protective properties of live vaccine candidates should be highly virulent for both mice and guinea pigs. Typically, the virulence potential of the pathogen is expressed in the dose likely to cause death in a certain percentage of test animals, such as LD_{50}

(median lethal dose), or absolute lethal dose LD_{100}. The latter is often referred to as Dosis Certa Letalis (DCL). For vaccine testing, 1 DCL of the challenge strain of *Y. pestis* should not exceed 100 CFU.

2.3 Reagents

The fixation of the tissue is conducted in commercial 10 % neutral-buffered formalin (NBF).

2.4 Animals

1. Outbred strain of guinea pigs of both genders, such as Dunkin-Hartley guinea pigs (250–350 g).
2. Outbred strain of mice of both genders, such as Swiss Webster mice (18–20 g).

3 Methods

3.1 Evaluation of Vaccine Candidate in Guinea Pigs

Determination of residual virulence, dissemination, and ability to colonize organs of immunized animals, as well as reactogenicity of the tested strains, can be done in one experiment by using the same group of guinea pigs by the following procedure:

1. Weigh guinea pigs supplied by the vendor and measure rectal temperature (should not exceed 38.5 °C). Keep animals in observation for at least 10 days. Weigh and measure temperature again on the day of administration of *Y. pestis*. For each strain and each dose, divide animals into similar groups based on their body weight.

   Evaluation of each vaccine candidate requires 150 guinea pigs. Make five similar groups (by weight) with 30 animals per group. The test will compare vaccine candidate(s) with the reference vaccine strain *Y. pestis* EV NIIEG. Bacteria grown on agar plates at 26–28 °C for 48 h will be administered subcutaneously (s.c.) into the inner side of the right thigh at a volume of 0.5 ml at the dose of 10^2, 5×10^2, 10^7, 2×10^9, and 1.5×10^{10} CFU. Each dose will be administered to 30 animals (day 0).
2. To determine dissemination, colonization of organs, and characterization of pathological changes, three animals should be euthanized from each group for corresponding doses on days 1, 3, 5, 7, 10, 14, 30, and 45. Consequently, animals should be necropsied within 20–30 min after death. Record visible pathological changes, and internal organs should be collected for bacteriological and histological investigation.
3. Fix the pieces of organs, tissue, and lymphatic nodes in 10 % NBF. During dissection observe the condition of the skin, subcutaneous tissue, and underlying muscles at the place of inoculation of bacterial culture. Pay attention on the presence and

intensity of vasodilatation, edema, hemorrhage, pus fluid, and necrosis in subcutaneous tissue surrounding the injection site. Measure size (in mm) of regional inguinal lymph nodes, their color, density, and cohesion with the surrounding tissues, and note the condition of the axillary lymph nodes. Take tissue pieces from the injection site and touch the surface of the agar plate multiple times (touch smear technique) to assess the presence of *Y. pestis* there. Then tissue should be fixed in NBF. After opening a peritoneal cavity, record the condition of hyperemia of internal organs, state of pleural cavities, omentum, visceral peritoneum, and intestines. Use the touch smear method to bacteriologically evaluate the internal organs, such as the liver, spleen, lungs, and heart. Pay attention to the development of interstitial inflammatory reaction in lungs, as well as the presence of necrotic lesions in liver and spleen, and record their number, size, and appearance. Measure the size of the spleen. Fix the pieces of organs containing abnormalities in NBF. Then collect kidney, make incision, and fix in NBF. In addition, collect the adrenal gland, and the iliac and mesenteric lymph nodes for visual evaluation, and fix in NBF. Finally, obtain bone marrow together with the piece of shaft of femur. Fix all material in NBF for 14 days at 18–25 °C and examine histologically.

4. For bacteriological investigation, plate the following samples by the touch smear method. Plate on Hottinger agar the samples obtained from the injection site, right iliac lymph node, bone marrow (first plate), right and left inguinal and axillary lymph nodes (second plate), liver and spleen (third plate), and lungs and heart (fourth plate). Also, plate samples from the lungs, heart, liver, and spleen on blood agar and Endo agar, respectively. Incubate Hottinger agar plates at 26–28 °C and blood and Endo agar plates at 37 °C for 5 days. Evaluate the plates after 2 days of incubation and then finally on day 5. Animals deceased during the experiment should be investigated as described for those euthanized. In addition, samples from deceased guinea pigs taken from small and large intestines, as well as mesenteric lymph nodes, should be plated on Endo agar (*see* **Note 1**).

Interpretation of the results and safety criteria:

- Tested and reference vaccine strain EV NIIEG should not cause death of animals inoculated with all five doses used (10^2 to 1.5×10^{10} CFU).
- Bacteria of highly immunogenic vaccine strains should multiply in guinea pigs during the first 3–15 days to elicit a robust immune response. 30 days post-inoculation (pi), the animals should be free of the vaccine strain. Bacteria can be detected

from the inoculation site and regional lymph nodes during 20–30 days pi. When high doses, such as 2×10^9 and 1.5×10^{10} CFU, are used, bacteria can be found in spleen and liver up to 15 days pi.

- The results of plating of samples obtained from lungs, heart, and bone marrow should be negative, although in some animals (less than 1 %) bacteria can be detected during the first 3–5 days pi after injection of high doses (2×10^9 and 1.5×10^{10} CFU).
- Vaccine strain at doses 1×10^7 and 1×10^9 CFU causes inflammation peaking at about 7 days pi followed by reduction by 10–12 days and complete healing without rough scarring by the end of the experiment (30–45 days).
- Light microscopy detection of typical *Y. pestis* clusters in the inflammation foci; *Y. pestis* vaccine cells should not be present within and outside of the capillaries.
- Accepted changes at *injection site* include the following: at dose 10^2 and 5×10^2 CFU, insignificant edema and small lesions resolved by day 30; at dose 10^7 CFU, in some animals appearance of the sites of inflammatory infiltration with the size not exceeding 0.5–0.7 cm and foci of purulent infiltration without tissue melting and hemorrhage up to 0.5 cm; at dose 2×10^9 CFU, during the initial period of 7–10 days pi appearance in some animals of the sites of inflammatory infiltration with the size not exceeding 1–1.5 cm, edema in an inguinal region without further spread, and foci of purulent infiltration without tissue melting and hemorrhage up to 0.5 cm, as well as, in rare cases, necrotic lesions up to 0.5–0.7 cm, ulcers, and abscesses.
- Accepted changes at *regional lymph nodes* (inguinal and iliac): at all doses, slight enlargement of the nodes (up to 0.5 cm) with hyperemia and infiltration without hemorrhage and necrosis but with formation of a granuloma.
- Accepted changes at *distant lymph nodes*: at all doses, slight enlargement of the nodes without acute infiltration.
- Accepted changes in *spleen*: at all doses, moderate increase of the size of the organ (1.5- to 2-fold); at dose of 2×10^9 CFU, in some animals the development of a limited number (up to 10) of separated miliary nodules without necrosis or abscesses that are completely resolved by day 30, as well as formation of a granuloma; similarly, at lower doses, the miliary nodules should be resolved by day 3 pi.
- Accepted changes in *liver*: at doses 10^7 and 2×10^9 CFU, in some animals slight increase in size and grayish color of the organ, development of a limited number (up to 10) of sepa-

rated miliary nodules without necrosis or abscesses, granulomas without foci of necrosis, abscesses or incapsulation; at low doses, rare granuloma formation.

- Accepted changes in *lungs*: at all doses, sites of local hypoxia and cyanosis; at dose 2×10^9 CFU formation of miliary and submiliary nodules (up to ten in both lungs) without positive bacteriological finding of *Y. pestis* in lungs.

3.2 Reactogenicity of the Vaccine Strain in Guinea Pigs

Reactogenicity of the vaccine candidate is determined by characterizing the changes after administration of five immunization doses (10^2 to 1.5×10^{10} CFU) described above at the inoculation site, regional lymph nodes, as well as changes in temperature and body weight of the animals. Vaccinated guinea pigs should be evaluated on days 1–2, 3–4, 7–8, and 10–11 pi. The reaction at the injection site should be revealed by palpation and measurement of the regions of induration, infiltration, size of the lymph nodes, their mobility, and consistency. Measurement of the body temperature should be conducted via rectal or oral routes. The body weight of the animals should be determined with a precision 1 g scale.

Interpretation of the results:

- Small inoculation dose of 10^2 CFU results in an insignificant increase of body temperature and reduction in body weight; during the first 7–10 days pi, the palpation reveals the foci of induration of the soft tissue and swelling of regional lymph nodes, which stay mobile without any cohesion with the surrounding tissues.
- Massive doses, such as 2×10^9 and 1.5×10^{10} CFU, can cause, in some animals, a temperature increase by 1.5–2 °C; however, the mean increase of body temperature in a group ($n = 30$–40) should not exceed 1 °C in each of the five doses used; the temperature should be back to normal by days 7–12 pi.
- Administration of large doses, 2×10^9 and 1.5×10^{10} CFU, typically causes weight loss during the first 5 days pi; nevertheless, by days 6–7 pi weight reduction should not exceed 1/5 of the original weight.
- Large doses, 2×10^9 and 1.5×10^{10} CFU, can cause extensive edema at the site of inoculation, increase in size of the regional lymph nodes, and their cohesion with the surrounding tissues in half of the animals.

3.3 Stability of the Loss of Virulence of the Vaccine Strain in Guinea Pigs

The stability of attenuation of the vaccine candidate should be determined by serial passages via s.c. administration of the tested strains.

1. For the first passage, inject two guinea pigs via the s.c. route with 1×10^9 CFU in 0.5 ml of bacteria grown for 2 days on the agar plates at 26–28 °C.
2. Euthanize both animals on day 4 pi, collect inguinal lymph nodes and spleens, and homogenize the organs. Add 5 ml of sodium chloride physiological solution, mix well, and let the tube with the homogenate stand allowing precipitation of the large tissue sections. Then collect the supernatant.
3. For the second passage, inoculate two animals with 0.5 ml of the supernatant. Repeat **step 2** to complete the passage. Also, plate several tenfold dilutions of the supernatant to determine the actual concentration of bacteria in the inoculum.
4. Make ten passages overall. All subcultures obtained from different passages should be tested for the morphological and biochemical properties characteristic of *Y. pestis*.
5. Determine the residual virulence of the stains after ten passages by using a shorter version of the protocols described in Subheadings 3.1 and 3.4. Use doses of 10^2, 10^7, and 2×10^9 CFU for guinea pigs and 10^2, 10^5, and 10^7 CFU for mice. Animals should be necropsided on days 7, 14, and 21 pi.

Interpretation of the results:

The virulence of the vaccine candidate obtained after the 10th passage should stay same as that of the parent strain. No changes should be seen in cultural, morphological, and biochemical properties, as well as in a plasmid profile. Nevertheless, the ability to colonize organs of the immunized animals may increase; however, the vaccine strain after the passages should not revert back to the virulent form, which causes the changes characteristic of the plague infection.

3.4 Residual Virulence of the Tested Vaccine Candidate in Mice

Testing the live vaccine candidates in mice is performed in comparison with the standard *Y. pestis* EV NIIEG strain in doses of 10^2, 10^3, 10^5, and 10^7 CFU by s.c. challenge into the inner side of the right thigh at a volume of 0.2 ml ($n = 10$). The administration of the indicated doses should not cause any death in immunized animals. The observation period is 20 days. In case some mice succumbed to the vaccination, their organs should be investigated for histopathological changes, as well as bacteriologically, as described for guinea pigs in Subheading 3.1. The organs of surviving mice are evaluated bacteriologically to exclude the possibility of a hidden chronic infection (*see* **Note 1**).

3.5 Immunogenicity of the Vaccine Candidate

Protective properties of the vaccine candidates should be tested in comparison with the standard strain EV NIIEG in both animal models, such as guinea pigs and outbred albino mice. *Y. pestis*

strains grown on agar for 48 h at 26–28 °C are used in both immunization and challenge experiments. All vaccinated animals that died after the challenge with virulent *Y. pestis* are dissected and investigated bacteriologically (*see* **Notes 2** and **3**).

1. To determine minimal immunization dose and calculation of 50 % effective dose (ED_{50}): Immunize guinea pigs s.c. into the inner side of the right thigh at a volume of 0.5 ml at the dose of 4×10^1, 2×10^2, 1×10^3, and 5×10^3 CFU. Similarly, immunize mice at a volume of 0.2 ml at the dose of 2×10^2, 1×10^3, 5×10^3, and 2.5×10^4 CFU. The sample size is ten animals per dose group.

   Challenge animals on day 21 pi by the s.c. route into the inner side of the left thigh at the same volume as that for immunization at the dose of 200 DCL of the virulent *Y. pestis*, followed by 20 days of observation, and calculate the ED_{50}.
2. To estimate time of formation of specific immunity in guinea pigs: Immunize animals ($n = 30$ per vaccine) s.c. in a dose of 5×10^3 CFU in 0.5 ml. Challenge guinea pigs with 200 DCL of virulent *Y. pestis* on days 3, 5, and 7 pi (ten animals per group). Challenge simultaneously control naïve animals ($n = 5$) on those days with 1 DCL and 200 DCL of the virulent strain. Observe animals for 20 days and calculate the day on which the vaccine candidate protects 50 % of animals.
3. To evaluate the potency of immunity in mice and guinea pigs: Immunize by s.c. route guinea pigs and mice with 5×10^3 CFU and 1×10^4 CFU, respectively ($n = 40$ per vaccine). Challenge animals on day 21 pi with four doses of virulent *Y. pestis*, such as 10^2, 10^4, 10^6, and 10^8 CFU (ten animals per dose group). Challenge simultaneously control naïve animals ($n = 5$) with doses 1, 5, 25, and 125 CFU, and observe animals for 20 days. Calculate the LD_{50} and LD_{100} of the virulent strain obtained on immunized and intact animals.
4. To determine the duration of immunity in guinea pigs: Immunize animals ($n = 30$ per vaccine) s.c. in a dose of 5×10^3 CFU in 0.5 ml. Challenge guinea pigs with 200 DCL of virulent *Y. pestis* after 3, 6, and 9 months pi (10 animals per group). Challenge simultaneously control group of naïve animals of the same age with 1 DCL and 200 DCL (5 animals per dose group). Assess the duration of immunity by the number of surviving animals.

Interpretation of the results:

- The ED_{50} calculated for the tested and reference EV NIIEG vaccine strains should not exceed 1×10^3 CFU and 1×10^4 CFU for guinea pigs and mice, respectively. The tested vaccine can

be considered to be more immunogenic versus control if its ED_{50} is less than that of the EV NIIEG strain.

- The minimal immunization dose corresponds to the minimal amount of bacterial cells capable of eliciting the specific immunity that provides protection to at least 80 % of animals after the challenge with 200 DCL of virulent *Y. pestis*. Nevertheless, the minimal immunization dose of both tested and reference EV NIIEG strains should not exceed 5×10^3 CFU for guinea pigs.
- The vaccine strains used at a dose of 5×10^3 CFU should provide protection of at least 50 % of the immunized animals on day 7 pi against 200 DCL of virulent *Y. pestis*.
- The potency of immunity is determined by the ability of the vaccine to provide protection against massive doses of virulent *Y. pestis*. This can be assessed by the LD_{50} value calculated on animals immunized with 5×10^3 CFU (guinea pigs) and 1×10^4 CFU (mice). In addition, the potency of immunity can be compared by calculating the Immunity Index, which is the ratio of LD_{50} values of the vaccinated versus intact animals. The potency of immunity elicited by the tested strain cannot be less than that of EV NIIEG.
- The duration of immunity after immunization of guinea pigs with 5×10^3 CFU cannot be less in a tested strain in comparison with the EV NIIEG vaccine.

4 Notes

1. We limited this protocol to investigation of the efficacy and safety of live plague vaccines in a bubonic plague infection model. In case of successful selection of the novel vaccine candidate with improved characteristics over the EV NIIEG strain, the next step should be a comparative study of the test candidate versus the EV NIIEG vaccine in a pneumonic plague model, preferably with aerosol challenge of the virulent *Y. pestis*, by using the same guinea pig and mouse models. In addition, since EV NIIEG showed excellent safety and immunogenicity in immunizing humans by the aerosol route [13], the test vaccine should be compared with the EV NIIEG by pulmonary vaccine delivery, followed by evaluation of protective properties in bubonic and pneumonic models of plague in guinea pigs and mice. The additional use of the capsule-negative strain of virulent *Y. pestis* in challenge experiments should be beneficial to further clarify the potential differences in protection observed in two animal models.
2. Also, we avoided in the protocol a detailed evaluation of the parameters of humoral and cellular immunity, since this is an

entirely separate task. In general, total IgG and immunoglobulin subclass titers to at least two protective antigens, such as F1 and LcrV, should be determined first. An ideal situation would be screening the antibody response to a complete proteome representing *Y. pestis* antigens. The T cell recall analysis and cytokine profiling in response to stimulating antigens can be used to evaluate cellular immunity [25]. One of the major disadvantages of the EV NIIEG vaccine is a short-lived state of protection against plague. Therefore, humans at risk are vaccinated annually [13]. Thus, creation of the improved plague vaccine with the extended duration of protection is an immediate priority.

3. Other important concerns that are not addressed in the current protocol are the following: evaluation of the phenotypical features characteristic to *Y. pestis* together with the genome rearrangement in the novel vaccine candidate; possible immunosuppressive effect after immunization with live plague vaccine with respect to the general state of the immune system, as well as in response to heterologous antigens; testing stability, growth, and survival characteristics of the candidate during production of lyophilized dry formulation of the vaccine; and then study of the protective properties of the dry formulation.

Acknowledgements

This work was supported by a grant from the Defense Threat Reduction Agency (HDTRA1-11-1-0032) to V.L.M. and by a subaward with the University of Texas Medical Branch at Galveston (No. 13-091) to V.A.F.

References

1. Perry RD, Fetherston JD (1997) *Yersinia pestis*—etiologic agent of plague. Clin Microbiol Rev 10:35–66
2. Feodorova VA, Corbel MJ (2009) Prospects for new plague vaccines. Expert Rev Vaccines 8:1721–1738
3. Feodorova VA, Motin VL (2012) Plague vaccines: current developments and future perspectives. Emerg Microb Infect 1, e36
4. Feodorova VA, Motin VL (2011) Plague vaccines. In: Feodorova VA, Motin VL (eds) Vaccines against bacterial biothreat pathogens. Research Signpost, Kerala, pp 176–233
5. Motin VL, Pokrovskaya MS, Telepnev MV et al (1992) The difference in the *lcrV* sequences between *Yersinia pestis* and *Yersinia pseudotuberculosis* and its application for characterization of *Y. pseudotuberculosis* strains. Microb Pathog 12:165–175
6. Anisimov AP, Dentovskaya SV, Panfertsev EA et al (2010) Amino acid and structural variability of *Yersinia pestis* LcrV protein. Infect Genet Evol 10:137–145
7. Anderson GW, Leary SEC, Williamson ED et al (1996) Recombinant V antigen protects mice against pneumonic and bubonic plague caused by F1-capsule-positive and -negative strains of *Yersinia pestis*. Infect Immun 64:4580–4585
8. Davis KJ, Fritz DL, Pitt ML et al (1996) Pathology of experimental pneumonic plague

produced by fraction 1-positive and fraction 1-negative *Yersinia pestis* in African green monkeys (*Cercopithecus aethiops*). Arch Pathol Lab Med 120:156–163

9. Smiley ST (2008) Current challenges in the development of vaccines for pneumonic plague. Expert Rev Vaccines 7:209–221
10. Smiley ST (2008) Immune defense against pneumonic plague. Immunol Rev 225:256–271
11. Williamson ED (2012) The role of immune correlates and surrogate markers in the development of vaccines and immunotherapies for plague. Adv Prev Med 2012:365980
12. Saltykova RA, Faibich MM (1975) Experience from a 30-year study of the stability of the properties of the plague vaccine strain EV in the USSR. Zh Mikrobiol Epidemiol Immunobiol 6:3–8
13. Feodorova VA, Sayapina LV, Corbel MJ, Motin VL (2014) Russian vaccines against especially dangerous bacterial pathogens. Emerg Microb Infect 3, e86
14. Girard G (1963) Immunity in plague infection. Results of 30 years of work with the *Pasteurella pestis* EV strain (Girard and Robic). Biol Med 52:631–731
15. Meyer KF, Smith G, Foster L et al (1974) Live, attenuated *Yersinia pestis* vaccine: virulent in nonhuman primates, harmless to guinea pigs. J Infect Dis 129(Suppl):S85–S112
16. Cui Y, Yang X, Xiao X et al (2014) Genetic variations of live attenuated plague vaccine strains (*Yersinia pestis* EV76 lineage) during laboratory passages in different countries. Infect Genet Evol 26:172–179
17. Sun W, Curtiss R (2013) Rational considerations about development of live attenuated *Yersinia pestis* vaccines. Curr Pharm Biotechnol 14:878–886
18. Wang X, Zhang X, Zhou D, Yang R (2013) Live-attenuated *Yersinia pestis* vaccines. Expert Rev Vaccines 12:677–686
19. Feodorova VA, Pan'kina LN, Savostina EP et al (2007) A *Yersinia pestis lpxM*-mutant live vaccine induces enhanced immunity against bubonic plague in mice and guinea pigs. Vaccine 25:7620–7628
20. Feodorova VA, Pan'kina LN, Savostina EP et al (2009) Pleiotropic effects of the *lpxM* mutation in *Yersinia pestis* resulting in modification of the biosynthesis of major immunoreactive antigens. Vaccine 27:2240–2250
21. Tidhar A, Flashner Y, Cohen S et al (2009) The NlpD lipoprotein is a novel *Yersinia pestis* virulence factor essential for the development of plague. PLoS One 4, e7023
22. Dentovskaya SV, Ivanov SA, Kopylov PK et al (2015) Selective protective potency of *Yersinia pestis* Delta*nlpD* mutants. Acta Naturae 7:102–108
23. Tian G, Qi Z, Qiu Y et al (2014) Comparison of virulence between the *Yersinia pestis* Microtus 201, an avirulent strain to humans, and the vaccine strain EV in rhesus macaques, *Macaca mulatta*. Hum Vaccin Immunother 10:3552–3560
24. Vaccine prophylaxis. Basic requirements for the vaccine strains of plague microbe (2002) Testing guidelines. MU 3.3.1.1113-02, Moscow (in Russian)
25. Braciale VL, Nash M, Sinha N et al (2008) Correlates of immunity elicited by live *Yersinia pestis* vaccine. In: Georgiev VS, Western K, McGowan JJ (eds) Infectious disease. Springer, Totowa, NJ, pp 473–480

Chapter 28

Highly Effective Soluble and Bacteriophage T4 Nanoparticle Plague Vaccines Against *Yersinia pestis*

Pan Tao, Marthandan Mahalingam, and Venigalla B. Rao

Abstract

Plague caused by *Yersinia pestis* is an ancient disease, responsible for millions of deaths in human history. Unfortunately, there is no FDA-approved vaccine available. Recombinant subunit vaccines based on two major antigens, Caf 1 (F1) and LcrV (V), have been under investigation and showed promise. However, there are two main problems associated with these vaccines. First, the *Yersinia* capsular protein F1 has high propensity to aggregate, particularly when expressed in heterologous systems such as *Escherichia coli*, thus affecting vaccine quality and efficacy. Second, the subunit vaccines do not induce adequate cell-mediated immune responses that also appear to be essential for optimal protection against plague. We have developed two basic approaches, structure-based immunogen design and phage T4 nanoparticle delivery, to construct new plague vaccines that may overcome these problems. First, by engineering F1 protein, we generated a monomeric and soluble F1V mutant (F1mutV) which has similar immunogenicity as wild-type F1V. The NH_2-terminal β-strand of F1 was transplanted to the COOH-terminus and the sequence flanking the β-strand was duplicated to retain a key $CD4^+$ T cell epitope. Second, we generated a nanoparticle plague vaccine that can induce balanced antibody- and cell-mediated immune responses. This was done by arraying the F1mutV on phage T4 via the small outer capsid (Soc) protein which binds to T4 capsid at nanomolar affinity. Preparation of these vaccines is described in detail and we hope that these would be considered as candidates for licensing a next-generation plague vaccine.

Key words *Yersinia pestis*, F1V, Bacteriophage T4, Nanoparticle vaccine

1 Introduction

Plague caused by *Yersinia pestis* (*Y. pestis*) is a deadly disease that wiped out one-third of Europe's population in the 14th century and it still exists in parts of the world today [1, 2]. Due to its exceptional virulence, the organism is listed by the CDC as Tier-1 biothreat agent. Although it has been a national priority to stockpile an efficacious plague vaccine, no FDA-approved plague vaccine is yet available. Previously, a killed whole-cell (KWC) vaccine was in use in the USA. But this vaccine was discontinued because it requires multiple immunizations, exhibits high reactogenicity, and does not provide complete protection [3]. Although a

Sunil Thomas (ed.), *Vaccine Design: Methods and Protocols: Volume 1: Vaccines for Human Diseases*, Methods in Molecular Biology, vol. 1403, DOI 10.1007/978-1-4939-3387-7_28,

live-attenuated plague vaccine (strain EV76) is still in use in the states of former Soviet Union [4], it may not meet FDA approval because of the highly infectious nature of the *Y. pestis* and the virulence mechanisms of vaccine strains have not been fully understood [3, 5].

Efforts in the past two decades led to recombinant vaccine candidates containing two *Y. pestis* virulence factors, the capsular protein Caf1 (F1) and the low calcium response protein LcrV (V) [3, 6]. F1 assembles into flexible linear fibers via a chaperone/*usher* mechanism [7]http://www.plospathogens.org/article/info%3Adoi/10.1371/journal.ppat.1003495-ppat.1003495-Zavialov1, forming a capsular layer that is pivotal for bacteria to escape phagocytosis [8] (Fig. 1). The V forms a "pore" at the tip of the "injectisome" structure of the type 3 secretion system (T3SS), regulating delivery of bacterial virulence factors into the host cytosol [9]. Two types of F1/V recombinant vaccines have been under investigation, one containing a mixture of F1 and V antigens (F1 + V) [10], and another, a single F1 – V fusion protein (F1V) [11, 12]. The problem, however, is that F1 naturally assembles into a fiber on the surface of the bacterium, and when expressed in heterologous systems such as *Escherichia coli* (*E. coli*), it forms

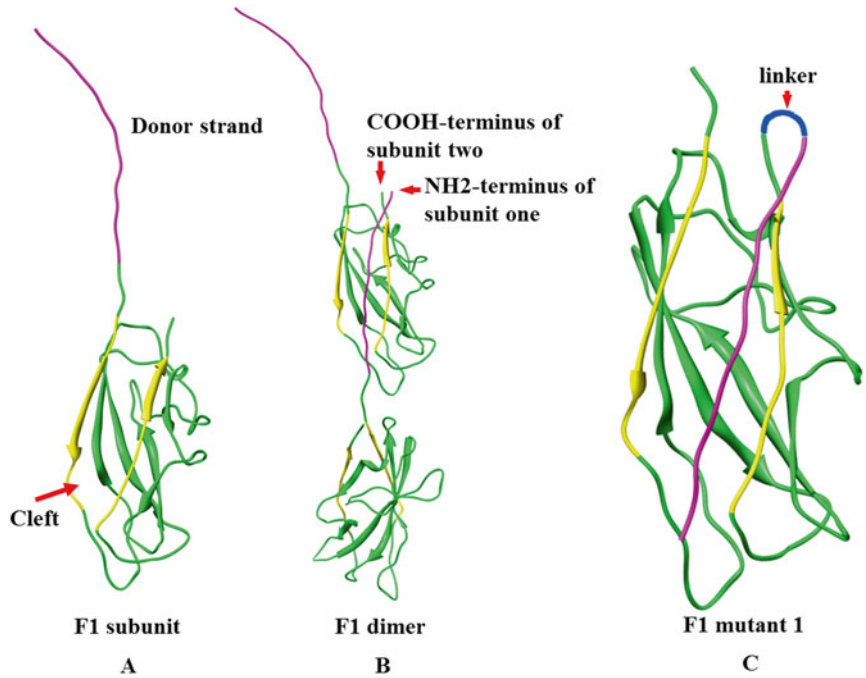

Fig. 1 Reorientation of the NH_2-terminal β-strand of F1 protein to generate monomeric F1. (**a**) Structure of F1 subunit, *purple strand* indicates donor β-strand, *yellow strands* indicate the strands that form groove. (**b**) F1 dimer showing how F1 monomers oligomerize to generate a linear fiber. (**c**) Schematic of F1 mutant 1 in which the NH_2-terminal β-strand is reoriented

insoluble and heterodisperse aggregates. These properties cause variability in the structure of the vaccine components and might compromise the efficacy [11, 13–16]. Second, the subunit vaccines do not induce adequate cell-mediated immune responses that also appear to be essential for optimal protection against plague [17].

In this chapter, we first describe methods to engineer a soluble F1V mutant, which we call F1mutV [18]. We then describe the preparation of nanoparticle F1mutV vaccine in which the F1mutV antigen is arrayed on bacteriophage T4 capsid using our recently developed phage T4 vaccine delivery system [18–20].

1.1 Construction of a Soluble F1mutV Vaccine

Previous structural studies have demonstrated that F1 polymerizes into a linear fiber by head-to-tail interlocking of F1 subunits through a donor strand complementation mechanism [7] (Fig. 1a, b). Each subunit consists of a seven-stranded antiparallel β-barrel with immunoglobulin-like fold. Six of the β-strands form an incomplete sandwich with a hydrophobic cleft that exposes the hydrophobic core. The cleft is then filled with the NH_2-terminal β-strand of the adjacent subunit, thereby connecting the two subunits. By repeating this process, referred to as intermolecular complementation, a linear F1 fiber is assembled (Fig. 1a, b). Prior to filling with the β-strand of adjacent subunit, the cleft is occupied by a "spare" β-strand of Caf1M, a chaperone for F1 fiber assembly, with the assistance of an outer membrane *usher* protein, Caf1A. Overexpression of F1 protein in *E. coli* exposes the unfilled hydrophobic cleft causing aggregation and formation of insoluble inclusion bodies [21, 22]. We have constructed an F1 mutant by shifting the NH_2-terminal β-strand of F1 to the COOH-terminus and reorienting the β-strand such that it could fill its own cleft (intramolecular complementation) (Fig. 1c). Furthermore, it no longer requires the assistance of chaperone and *usher* proteins. Consequently, a soluble F1 monomer was produced.

In order to construct this F1 mutant, we first deleted the NH_2-terminal donor strand [amino acid (aa) residues 1–14] and fused it to the COOH-terminus with a short two aa serine-alanine linker in between (Fig. 1c and 2). This was named pET-F1mut1 (Fig. 2) and over-expressed the F1mut1 protein in *E. coli* and confirmed that it is soluble and monomeric [18]. The aa residues 7–20 are reported to contain a mouse H-2-IA*d*-restricted $CD4^+$ T cell epitope [23], which was disrupted in pET-F1mut1. To restore this epitope, we added these residues to the switched β-strand, which resulted in the duplication of the residues 15–21 at the COOH-terminus (Fig. 2). We then fused the mutated F1 to the NH_2-terminus of V with a two aa linker in between to generate the F1mutV fusion protein (Fig. 2). F1mutV was over-expressed in *E. coli* and also shown to be soluble and monomeric. Importantly, F1mutV retained full immunogenicity of wild-type F1V and conferred complete protection against challenge with *Y. pestis* CO92 [18].

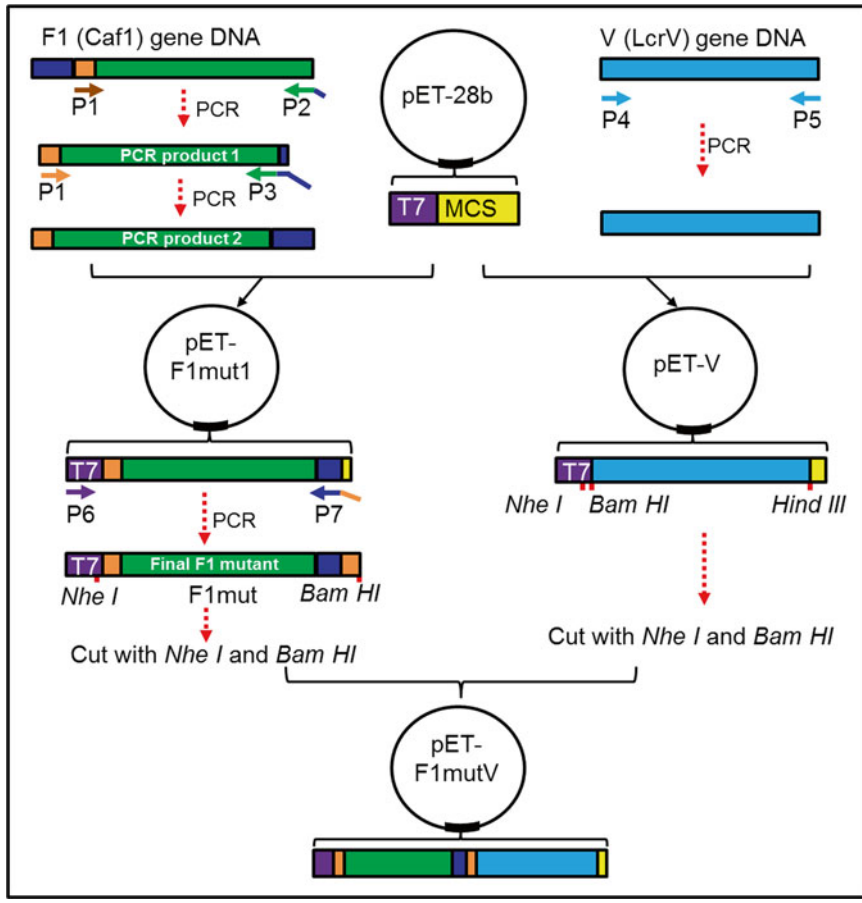

Fig. 2 Cloning strategy to generate pET-F1mutV plasmid. *T7* indicates T7 promoter sequence, *MCS* indicates multiple cloning site, *P1–P7* indicate primers 1–7, *blue* indicates the first 14-aa residues of F1, and *orange* indicates aa residues 15–21 of F1. The remaining region of F1 is shown in *green*. V gene is shown in *cyan*. The linkers in F1mut or between F1mut and V are not shown

1.2 Generate a T4 Bacteriophage Nanoparticle-Displayed F1mutV Vaccine

Recently, we have developed a novel bacteriophage T4 platform to deliver vaccine antigens [18, 20, 24, 25]. Pathogen antigens are displayed on the 120 nm × 86 nm phage T4 capsid at high density. The T4 capsid (head) is composed of three essential capsid proteins: 930 copies of major capsid protein, gp23* ("*" refers to cleaved and matured form); 55 copies of vertex protein, gp24*; and 12 copies of portal protein, gp20 (Fig. 3a) [26, 27]. A unique feature of T4 head is that it is decorated with two nonessential proteins, the *s*mall *o*uter *c*apsid protein (Soc) and the *h*ighly antigenic *o*uter *c*apsid protein (Hoc) (Fig. 3a) [28].

Approximately 870 molecules of Soc protein (9 kDa) assemble into trimers at the quasi threefold axes of the head. The binding sites appear after the head undergoes maturation cleavages and expansion [29]. Each Soc molecule clamps two adjacent gp23 capsomers, forming a reinforced cage around the shell (Fig. 3a) [29].

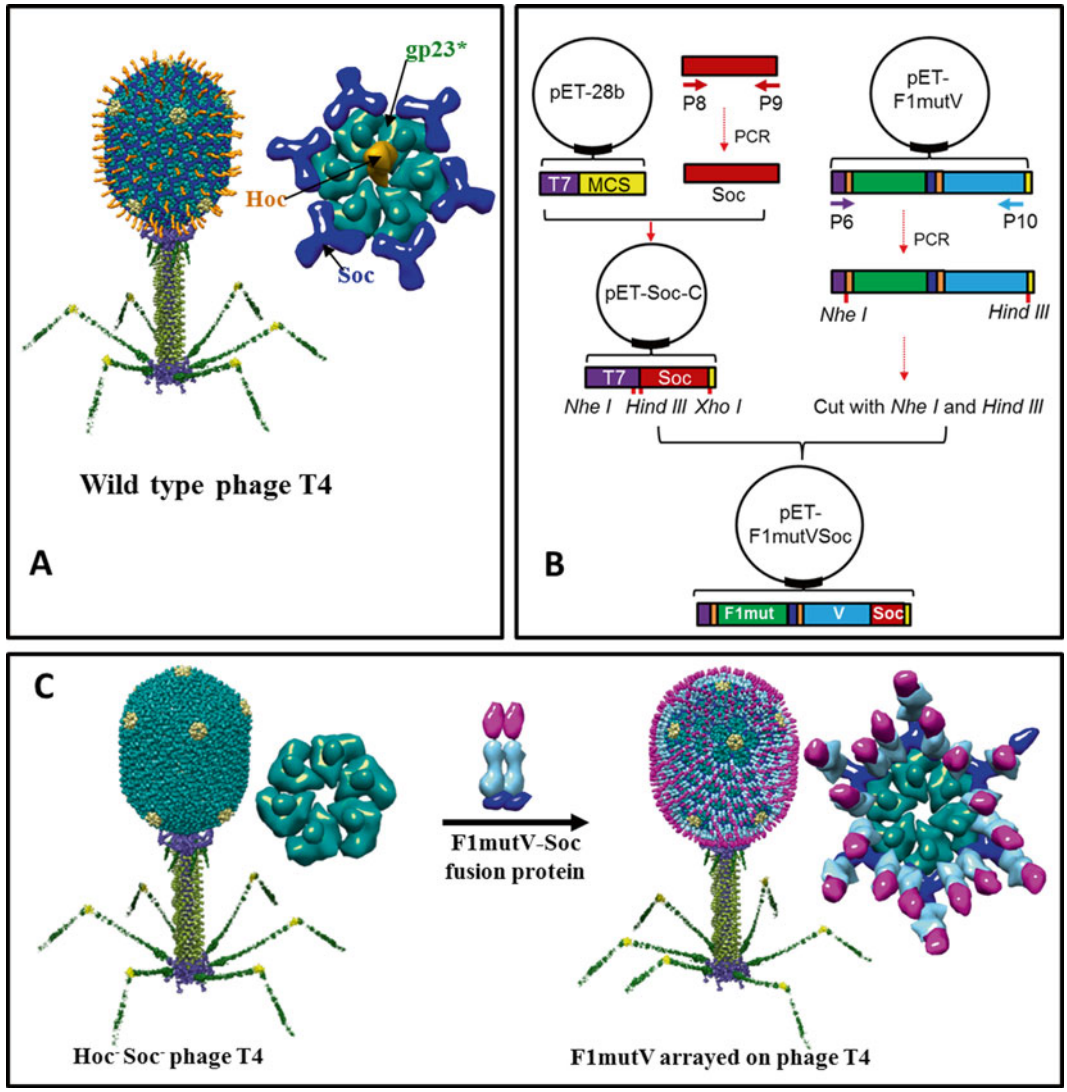

Fig. 3 Preparation of T4 nanoparticle-arrayed plague vaccine. (**a**) Structural model of bacteriophage T4. The enlarged capsomer on *right* shows the major capsid protein gp23* (*green*; "*" represents the cleaved mature form) (930 copies), Soc (*blue*; 870 copies), and Hoc (*orange*; 155 copies). *Yellow* subunits at the fivefold vertices correspond to gp24*. The portal vertex (not visible in the picture) connects the head to the tail. (**b**) Cloning strategy to generate pET-F1mutVSoc. *Red* indicates Soc. The other components are shown as in Fig. 2. *P6–P10* indicate primers 6–10. (**c**) Display of F1mutV-Soc fusion protein on the Hoc⁻Soc⁻ phage particle. Shown on the *right* are models of the enlarged capsomers before and after F1mutV-Soc display

Hoc consists of a string of four domains of which three are Ig-like. One hundred and fifty-five copies of these fiber-like Hoc molecules assemble on the capsid, one each at the center of the capsomer (Fig. 3a) [30]. The COOH-terminal domain contains the capsid-binding site; hence it is attached to the capsid surface whereas the NH_2-terminal domain is projected out to ~160 Å

distance from the capsid wall. Soc and Hoc are completely dispensable under laboratory conditions showing no significant effect on phage productivity or infectivity when deleted from the genome [28]. Purified Soc and Hoc proteins bind to Hoc⁻ Soc⁻ capsid in vitro with high specificity and nanomolar affinity. Pathogen antigens as large as 116 kDa can be fused to Soc without compromising its ability to bind to the capsid (Fig. 3c) [18–20, 25]. Alternatively, multilayered oligomeric complexes of >500 kDa can be assembled through Hoc or Soc. Essentially all the Soc and Hoc molecules can be occupied by pathogen antigens [19, 31]. Importantly, these T4 nanoparticle-displayed antigens induce strong humoral and cellular immune responses [18, 20], making it a robust antigen display and delivery system.

In order to array F1mutV on T4 capsid we first constructed a "universal" Soc vector, pET-Soc-C, which contains multiple cloning sites upstream of NH_2-terminus of Soc, by inserting Soc into expression vector pET28b (Fig. 3b). Any foreign protein can be inserted upstream of NH_2-terminus of Soc, generating an in-frame fusion protein (Fig. 3b, c). F1mutV was amplified by PCR from pET-F1mutV and inserted into pET-Soc-C. The F1mutV-Soc was over-expressed in *E. coli* in soluble form and purified by nickel affinity chromatography and gel filtration chromatography. The purified F1mutV-Soc was then arrayed on T4 capsid by incubation with Hoc⁻ Soc⁻ T4 phage (Fig. 3c).

2 Materials

Prepare all solutions using autoclaved Milli-Q water (Millipore) and analytical grade reagents. Prepare and store all reagents at room temperature (unless indicated otherwise).

2.1 Construction of Plasmids

1. *E. coli* expression vector pET28b (Novagen, MA).
2. Competent *E. coli* DH5α cells (NEB, MA).
3. Luria–Bertani (LB) medium (Quality Biological, MD).
4. SOC medium (Quality Biologicals, MD).
5. 1000× Kanamycin (50 mg/ml): Add 0.5 g kanamycin (Gold Biotechnology, MD) to 10 ml Milli-Q water.
6. Kanamycin LB plates: Add 2 g LB powder (Affymetrix, OH) and 1.5 g agar to 100 ml Milli-Q water, and sterilize by autoclaving. When cooled to about 50 °C, add 0.1 ml 1000× kanamycin. Mix and pour into sterile petri plates.
7. PCR kit: 2× Phusion High-Fidelity PCR Master Mix (Thermo Scientific).
8. Restriction enzymes: FastDigest NheI, FastDigest HindIII, FastDigest BamHI, FastDigest XhoI (all were purchased from Thermo Scientific).

9. FastAP Thermosensitive Alkaline Phosphatase (Thermo Scientific).
10. T4 DNA Ligase (Thermo Scientific).
11. Agarose gel running buffer: Add 100 ml 10× AccuGENE™ Tris-borate-EDTA (TBE) agarose gel running buffer (Lonza Chemicals Company, Switzerland) to 900 ml Milli-Q water to make 1× agarose gel running buffer.
12. GeneJET Gel Extraction kit (Thermo Scientific).
13. GeneJET Plasmid Miniprep Kit (Thermo Scientific).

2.2 Protein Purification

1. Competent *E. coli* BL21-CodonPlus (DE3)-RIPL cells (Agilent Technologies, CA).
2. SOC medium (Quality Biologicals, MD).
3. 1000× Kanamycin (50 mg/ml): Add 0.5 g kanamycin (Gold Biotechnology, MD) to 10 ml Milli-Q water.
4. 1000× Chloramphenicol (50 g/ml): Add 0.5 g chloramphenicol (Amresco) to 10 ml ethanol.
5. Kanamycin/chloramphenicol LB plates: Add 2 g LB powder (Affymetrix, OH) and 1.5 g agar to 100 ml Milli-Q water, and sterilize by autoclaving. When cooled to about 50 °C, add 0.1 ml 1000× kanamycin and 0.1 ml 1000× chloramphenicol. Mix and pour into sterile petri plates.
6. Moore's medium: To 800 ml Milli-Q water, add 20 g tryptone, 15 g yeast extract, 8 g NaCl, 2 g dextrose, 2 g Na_2HPO_4, and 1 g KH_2PO_4, adjust to 1 L with Milli-Q water, and sterilize by autoclaving. Add 1 ml 1000× kanamycin and 1 ml 1000× chloramphenicol before use.
7. Isopropyl β-D-1-thiogalactopyranoside (IPTG) (Gold Biotechnology, MO).
8. Complete proteinase inhibitor cocktail (Roche).
9. HisTrap binding buffer: 50 mM Tris–HCl pH 8.0, 300 mM NaCl, and 20 mM imidazole.
10. HisTrap washing buffer: 50 mM Tris–HCl pH 8.0, 300 mM NaCl, and 50 mM imidazole.
11. HisTrap elution buffer: 50 mM Tris–HCl pH 8.0, 300 mM NaCl, and 400 mM imidazole.
12. Gel filtration buffer: 20 mM Tris–HCl, pH 8.0 and 100 mM NaCl. All protein purification buffers have to go through 0.22 μm filter and be made the day before use and kept at 4 °C.
13. Nickel affinity chromatography column: 1 ml HisTrap HP column (GE Healthcare).
14. Amicon Ultra-4 centrifugal filter units (Millipore, MA).

15. Gel filtration chromatography column: Hi-load 16/60 Superdex 200 column (GE Healthcare).
16. 4–20 % (w/v) polyacrylamide gel (Life Technologies).
17. Acetylated bovine serum albumin (BSA) standard (Affymetrix, OH).
18. SDS-loading buffer: 20 mM Tris–HCl pH 6.8, 100 mM dithiothreitol, 2.5 % β-mercaptoethanol, 1 % SDS (w/v), 0.1 % bromophenol blue, and 10 % glycerol.
19. Tris–glycine running buffer: Add 100 ml 10× Tris–glycine running buffer (Bio-Rad) to 900 ml Milli-Q water to make 1× Tris–glycine running buffer.
20. Coomassie blue R-250 staining solution (Teknova, CA).
21. Destaining solution: Add 100 ml methanol and 100 ml acetic acid to 800 ml Milli-Q water.

2.3 T4 Phage Purification

1. *E. coli* P301 (stored in our lab).
2. $Hoc^{-}Soc^{-}$ phage T4 mutant.
3. LB medium (Quality Biological, MD).
4. M9CA medium broth: To 800 ml Milli-Q water, add 12.5 g M9CA medium broth powder (Amresco, OH), adjust to 1 L with Milli-Q water, and sterilize by autoclaving.
5. Top-agar: Add 2 g LB powder (Affymetrix, OH) and 0.75 g agar to 100 ml Milli-Q water, sterilize, and keep it at 42 °C.
6. LB plates: Add 2 g LB powder (Affymetrix, OH) and 1.5 g agar to 100 ml Milli-Q water, and sterilize by autoclaving. Mix and pour into sterile petri plates.
7. Pi-Mg buffer: 26 mM Na_2HPO_4, 22 mM KH_2PO_4, 70 mM NaCl, 1 mM $MgSO_4$.
8. Deoxyribonuclease I (DNase I) (Sigma-Aldrich).
9. HPLC-grade chloroform (Fisher Scientific).
10. Cesium chloride (CsCl) stock solution: 8 M CsCl, 100 mM Tris–HCl pH7.5, 85 mM NaCl, 20 mM NH_4Cl.
11. Slide-A-lyzer dialysis cassette (0.5–3 ml capacity; Pierce).
12. Dialysis buffer I: 10 mM Tris–HCl pH 7.5, 200 mM NaCl, 5 mM $MgCl_2$.
13. Dialysis buffer II: 10 mM Tris–HCl pH 7.5, 50 mM NaCl, 5 mM $MgCl_2$.

2.4 Antigen Preparation

1. Alhydrogel (Al^{3+} concentration: 10 mg/ml) (Brenntag Biosector, Denmark).
2. PBS pH 7.4 (Quality Biological, MD).
3. 5 M NaCl (Quality Biological, MD).

3 Methods

Here, we first provide a procedure to construct and test the immunogenicity of our recently developed monomeric F1mutV. Then, we provide a step-by-step protocol for how to prepare our bacteriophage T4 nanoparticle vaccine to deliver monomeric F1mutV.

3.1 F1mutV Immunogens as Next-Generation Plague Vaccines

3.1.1 Construction of F1mutV

In order to generate pET-F1mutV, we first constructed two intermediate plasmids (pET-F1mut1 and pET-V) as depicted in Fig. 2. Plasmid pET-F1mut1 was constructed by two rounds of PCR. The first round of PCR was performed to amplify F1 fragment in which the NH_2-terminal 14 aa residues were deleted and at the same time the NH_2-terminal 7 amino acids were fused to the COOH-terminus of F1. This PCR product was used as a template for the second round of PCR using a forward primer containing *NheI* restriction site and a reverse primer containing the NH_2-terminal 14 aa residues and *XhoI* restriction site. The PCR fragment was then inserted into *Nhe*I and *Xho*I linearized pET28b vector to generate pET-F1mut1. The final F1 mutant, in which the NH_2-terminal 14 aa residues were deleted but the NH_2-terminal 21 aa residues were added to the COOH-terminus, was amplified from pET-F1mut1. Finally, the PCR product was inserted into the upstream of V in pET-V plasmid to generate pET-F1mutV.

3.1.1.1 Construct pET-F1mut1

1. Amplify F1 mutant intermediate 1, in which NH_2-terminal 14 aa residues (*see* **Note 1**) were removed and at the same time NH_2-terminal 7 amino acids were added to the C-terminus of F1, with primers 1 and 2 using Thermo 2× Phusion High-Fidelity PCR Master Mix. *Y. pestis* CO92 plasmid pMT1 was used as a template.

   Primer 1: Forward primer binding to nt 43–61 of 5′-end of F1, including the *Nhe I* restriction site (highlighted in bold) at the 5′-end (*see* **Note 2**).

   5′-CCATCT **GCTAGC** GAACCAGCCCGCATCACTC-3′

   Primer 2: Reverse primer binding to the 3′-end nucleotide sequence of F1, including the first 21 nt of the F1 (underline) at the 5′-end.

   5′-GGTGCTTGCAGTTAAATCTGC *TGCAGA* TTGGTTAGATACGGTTACGGTTACAGC-3′ (Italics indicates the sequence for the two aa (Ser-Ala) linker).
2. Purify PCR product by agarose gel electrophoresis and gel extraction using Thermo GeneJET gel extraction kit, according to the manufacturer's instructions (*see* **Note 3**).
3. Use F1 mutant intermediate 1 as template to amplify F1 mutant intermediate 2 with primers 1 and 3 using Thermo 2× Phusion High-Fidelity PCR Master Mix.

Primer 3: Reverse primer binding to the 3′-end of F1 mutant intermediate 1, including the first 42 nt of F1 (underline) and the *Xho I* restriction site (bold) at the 5′-end.

5′-CGT **CTCGAG** TTAAACAAGAGTTGCCGT TGCAGTGGTGCTTGCAGTTAAATCTGC-3′

4. Purify PCR product by gel electrophoresis and gel extraction using Thermo GeneJET gel extraction kit, according to the manufacturer's instructions.
5. Cut the insert (PCR product) with restriction enzymes, *Nhe I* and *Xho I*, and at the same time cut the pET28b vector plasmid DNA using the same restriction enzymes.
6. Purify insert and vector using gel electrophoresis and Thermo GeneJET gel extraction kit, following the manufacturer's instructions.
7. Ligate insert and vector using T4 DNA ligase for 1 h at 22 °C.
8. Transform *E. coli* DH5α with the ligation product according to the manufacturer's instructions and incubate LB plate overnight at 37 °C.
9. Pick a single colony, and inoculate into a 125 ml flask containing 10 ml LB medium with 50 μg/ml kanamycin. Incubate the flask in shaking incubator at 220 rpm, 37 °C overnight.
10. Isolate plasmid DNA using Thermo GeneJET plasmid miniprep kit, following the manufacturer's instructions. The generated plasmid was named pET-F1mut1.

3.1.1.2 Construct pET-V

1. Amplify V with primers 4 and 5 using Thermo 2× Phusion High-Fidelity PCR Master Mix, according to the manufacturer's instructions. *Y. pestis* CO92 plasmid pCD1 was used as a template.

   Primer 4: Forward primer binding to the 5′-end nucleotide sequence of V, including the *BamH* I restriction site (highlighted in bold) at the 5′-end.

   5′-CA **GGATCC** ATGATTAGAGCCTACGAACA AAACC-3′

   Primer 5: Reverse primer binding to the 3′-end nucleotide sequence of the V, including the *Hind* III restriction site (highlighted in bold) at the 5′-end (*see* **Note 4**).

   5′-CCT **AAGCTT** TTTACCAGACGTGTCATCTAG CAGAC-3′
2. Purify PCR product by gel electrophoresis and gel extraction using Thermo gel extraction kit, according to the manufacturer's instructions.
3. Digest the insert (PCR product) with restriction enzymes, *BamH* I and *Hind* III, and at the same time cut the pET28b vector plasmid DNA using the same restriction enzymes.

4. Repeat **steps 6–9** of Subheading "Construct pET-F1mut1."
5. Isolate plasmid DNA using Thermo GeneJET plasmid miniprep kit, following the manufacturer's instructions. The generated plasmid was named pET-V.

3.1.1.3 Construct pET-F1mutV

1. Amplify final F1 mutant from pET-F1mut1 with primers 6 and 7 using Thermo 2× Phusion High-Fidelity PCR Master Mix.

   Primer 6: Forward primer binding to the T7 promoter of pET28b vector.

   5′-TAATACGACTCACTATAGGGGA-3′

   Primer 7: Backward primer binding to the 3′-end of the F1 mutant intermediate 2, including the first 21 nt of the F1 mutant intermediate 2 (predicted $CD4^+$ T cell epitope, underlined) and the *BamH* I restriction site (highlighted in bold) at the 5′-end.

   5′-CTG **GGATCC** AAGAGTGATGCGGGCTGGTTC AACAAGAGTTGCCGTTGCAGTG-3′
2. Purify PCR product by gel electrophoresis and gel extraction using Thermo gel extraction kit, according to the manufacturer's instructions.
3. Cut the insert (PCR product) with restriction enzymes, *Nhe I* and *BamH* I, and at the same time cut the pET-V vector DNA using the same restriction enzymes.
4. Repeat **steps 6–9** of Subheading "Construct pET-F1mut1."
5. Isolate plasmid DNA using Thermo GeneJET plasmid miniprep kit, following the manufacturer's instructions. The resulting pET-F1mutV plasmid contained F1mut in-frame fusion with V, a 23-aa vector sequence containing the hexa-histidine sequence at the NH_2-terminus of F1, and also a 13-aa vector sequence containing the hexa-histidine sequence at the COOH-terminus of V.

3.1.2 Purification of Recombinant F1mutV from E. coli

1. Transform 10 ng of pET-F1mutV into 25 μl BL21-CodonPlus (DE3)-RIPL competent cells, according to the manufacturer's instructions (*see* **Note 5**). Incubate plate overnight at 37 °C.
2. Pick a single colony, and inoculate into a 125 ml flask containing 30 ml Moore's medium with 50 μg/ml kanamycin and 50 μg/ml chloramphenicol. Incubate the flask in shaking incubator at 220 rpm, 37 °C overnight.
3. Inoculate 20 ml of overnight cultures into a 2 L flask containing 1 L of Moore's medium with 50 μg/ml kanamycin and 50 μg/ml chloramphenicol. Incubate the flask in a shaking incubator at 220 rpm, 37 °C, until the cell density raises to 3.0×10^8 cells/ml.
4. Transfer the flask to 30 °C shaking incubator and shake for 30 min at 220 rpm (*see* **Note 6**).

5. Add IPTG to the culture to a final concentration of 1 mM, and induce protein expression for 2 h at 30 °C.
6. Harvest the cells by centrifugation at 7000 rpm (8,288 g) for 10 min at 4 °C with GS3 rotor in Sorvall RC-5C plus centrifuge. Discard the supernatant, and store the pellet at −80 °C for further purification.
7. Resuspend the pellet with 40 ml HisTrap binding buffer supplemented with one pill of complete proteinase inhibitor cocktail (*see* **Note 7**).
8. Lyse the cells by French press at 12,000 psi twice.
9. Centrifuge the cell lysate at 17,000 rpm (34,572 g) for 20 min at 4 °C with SS34 rotor in Sorvall RC-5C plus centrifuge.
10. Collect the supernatant which contains soluble F1mutV protein, and filter it through 0.22 μm filters (*see* **Note 8**).
11. Set up 1 ml HisTrap HP column on AKTA-prime system. First, wash column with 20 ml of water, and then equilibrate the column with 20 ml of HisTrap binding buffer.
12. Load the supernatant collected in **step 10** onto HisTrap HP column and wash the column with 20 ml HisTrap washing buffer (*see* **Note 9**).
13. Elute protein with 20–400 mM linear imidazole gradient with HisTrap binding buffer as buffer A and HisTrap elution buffer as buffer B. AKTA-prime was set as follows:

    Concentration (% buffer B): 0; gradient length: 40; target (% buffer B): 100; flow rate: 1 ml/min; fraction base: ml; fraction size: 1; pressure limit: 0.3.
14. Collect and pool the peak fractions, and concentrate using Amicon Ultra-4 centrifugal filtration (10 kDa cutoff) according to the manufacturer's instructions.
15. Wash Hi-load 16/60 Superdex 200 column with 150 ml gel filtration buffer, and then load the concentrated peak fractions onto Hi-load 16/60 Superdex 200 column with flow rate of 1.0 mg/ml.
16. Collect and pool the peak fractions from gel filtration elution and concentrate using Amicon Ultra-4 centrifugal filtration (10 kDa cutoff).
17. Aliquot the concentrated F1mutV protein and store at −80 °C for future use. Following steps are intended to determine the concentration of F1mutV protein by SDS-PAGE with BSA (1 mg/ml) as standard.
18. Mix equal volume of F1mutV or BSA with 2× SDS loading buffer, boiled for 5 min.
19. Load 1 μl, 2 μl, 3 μl, and 4 μl of F1mutV protein, and 1 μg, 2 μg, 4 μg, and 8 μg of BSA to each well, and run SDS-PAGE

using 4–20 % Tris–glycine gel, according to the manufacturer's instructions.

20. Disassemble the gels, transfer gel into a clean tray, and rinse with water.
21. Add Coomassie blue R-250 staining solution to the tray, microwave for 1 min, and keep shaking gently at room temperature for 15 min.
22. Discard Coomassie blue R-250 staining solution, add destain solution to the tray, and keep shaking gently at room temperature overnight (*see* **Note 10**).
23. Scan gel with laser densitometry (PDSI, GE Healthcare), and quantify protein bands with ImageQuant 5.2 software (GE Healthcare), according to the manufacturer's instructions.
24. Generate BSA standard curve using Microsoft Excel with the number calculated in **step 23**, and calculate the concentration of F1mutV protein based on BSA standard curve.

3.1.3 Preparation of Vaccine Formulations for Animal Immunization

The exact amount of protein depends on the number of animals per group. Here, we describe the dose for one animal (10 μg antigen/animal).

1. Prepare 2× aluminum hydrogel solution. The final dose of aluminum for each mouse is 100 μg in 50 μl buffer (2.0 mg/ml); hence concentration of aluminum in 2× aluminum hydrogel solution should be 4.0 mg/ml. Add 1.0 ml aluminum hydrogel solution (10 mg/ml), 72.6 μl 5 M NaCl, and 1427.4 μl H_2O to make 2.5 ml of 2× aluminum hydrogel solution (Al^{3+} concentration: 4 mg/ml, NaCl: 0.145 mol/L = 0.85 %) (*see* **Note 11**).
2. Mix antigen with 2× aluminum hydrogel solution. For naïve group: take 25 μl 2× aluminum hydrogel solution, add 25 μl PBS (pH 7.4) to make the total volume to 50 μl, and vortex. This is for one mouse (50 μl/mouse). For F1mutV group: take 25 μl 2× aluminum hydrogel solution, and mix with 23.5 μl PBS (pH 7.4) and 1.5 μl F1mutV (6.5 mg/ml). The total volume is 50 μl. Vortex the mixture. This is for one mouse (50 μl/mouse).

3.1.4 Immunization

Immunizations of mice and immunological analyses and challenges with *Y. pestis* CO92 were performed using methods as described elsewhere [18, 31].

3.2 Preparation of Bacteriophage T4 Nanoparticles Arrayed with Mutated F1mutV Plague Antigen

Two nonessential proteins of T4, Hoc and Soc, can bind to $Hoc^{-}Soc^{-}$ T4 capsid with nanomolar affinity in vitro. In order to display plague antigens, we first have to fuse F1mutV to Soc protein. The reason we chose Soc is because it has 5.6 times higher binding sites (870 per capsid) when compared to Hoc (155 per capsid). Thus, Soc fusion can display more antigen molecules per capsid.

3.2.1 Construction of pET-F1mutVSoc

We first constructed a "universal" vector, pET-Soc-C, which contains multiple cloning sites upstream of NH_2-terminus of Soc, by inserting Soc into expression vector pET28b. Any foreign protein can be inserted into upstream of NH_2-terminus of Soc and generate an in-frame fusion with the NH_2-terminal end of SOC. F1mutV was amplified by PCR from pET-F1mutV and inserted into pET-Soc-C to generate pET-F1mutVSoc.

1. Use Thermo 2× Phusion High-Fidelity PCR Master Mix to amplify RB69 Soc gene DNA from RB69 phage genome DNA, using the end primers 8 and 9 containing *Hind III* and *Xho I* restriction sites (highlighted in bold), respectively (*see* **Note 12**).

   Primer 8: 5′-TCGAC **AAGCTT** CT GCT GGTGGTT ATGTAAACATCAAA-3′

   Primer 9: 5′-TGGTG **CTCGAG** ACCACTTAC TGGTGTAGGGGT-3′
2. Purify PCR product by gel electrophoresis and gel extraction using Thermo gel extraction kit.
3. Cut the insert (PCR product) with restriction enzymes, *Hind III* and *Xho I*, and at the same time cut the pET28b vector plasmid DNA using the same restriction enzymes.
4. Repeat **steps 6–9** of Subheading "Construct pET-F1mut1."
5. Isolate plasmid DNA using Thermo GeneJET plasmid miniprep kit, following the manufacturer's instructions. The generated plasmid was named pET-Soc-C.
6. Amplify F1mutV DNA from template, pET-F1mutV, using the primer 6 and primer 10 which contains *HindIII* restriction sites using Thermo 2× Phusion High-Fidelity PCR Master Mix.

   Primer 6: 5′-TAATACGACTCACTATAGGGGA-3′

   Primer 10: 5′-CCT **AAGCTT** CTTTACCAGACGT GTCATCTAGCAGAC-3′
7. Cut the insert (PCR product) with restriction enzymes, *NheI* and *Hind III*, and at the same time cut the pET-Soc-C vector DNA (described in **step 5**) using the same restriction enzymes.
8. Repeat **steps 6–9** of Subheading "Construct pET-F1mut1."
9. Isolate plasmid DNA using Thermo GeneJET plasmid miniprep kit, following the manufacturer's instructions. The resulting clone, pET-F1mutVSoc, contained F1mutV fused in-frame to the NH_2-terminus of RB69 Soc and also the flanking vector sequences containing two hexa-histidine tags at both NH_2- and COOH-termini.

3.2.2 Purification of Recombinant F1mutV-Soc from E. coli

1. Transform 10 ng of pET-F1mutVSoc into 25 μl BL21-CodonPlus (DE3)-RIPL competent cells, according to the manufacturer's instructions. Incubate plate overnight at 37 °C.
2. Repeat all procedures from **steps 2** to **24** of Subheading 3.1.2.

3.2.3 Purification of Hoc⁻Soc⁻ Phage T4

1. Use pipette tip to streak the glycerol stock of *E. coli* P301 cells on an LB plate. Incubate at 37 °C overnight.
2. Pick a single colony, inoculate into a 125 ml flask containing 20 ml LB medium, and incubate the flask in shaking incubator at 220 rpm, 37 °C, for 8 h.
3. Inoculate 10 ml of cultures in **step 2** into a 2 L flask containing 500 ml of LB and M9CA medium (250 ml LB + 250 ml M9CA). Incubate the flask in a shaking incubator at 220 rpm and 37 °C until the cell density raises to 2.0×10^8 cells/ml.
4. Infect the culture with Hoc⁻Soc⁻ phage T4 at multiplicity of infection (MOI) of 0.2 by adding 2×10^{10} plaque-forming units (PFU) Hoc-Soc- phage T4 (*see* **Note 13**).
5. Incubate the flask in shaking incubator at 200 rpm, 37 °C, for 30 min, allow the culture to grow for 2–3 h, and observe for phage growth (*see* **Note 14**).
6. After confirmation of phage growth, add 10 ml chloroform into the flask and keep it shaking at 200 rpm for 10 min at 37 °C.
7. Distribute the culture into 250 ml centrifugation tubes, and centrifuge for 45 min at 12,000 rpm (23,440 g) with GSA rotor in Sorvall RC-5C plus centrifuge.
8. Discard the supernatant and resuspend the pellet by adding 15 ml Pi-Mg buffer.
9. Add DNase I to a final concentration of 10 μg/ml and 500 μl chloroform, and keep shaking at 220 rpm in 37 °C for 30 min.
10. Centrifuge at 6000 rpm (4,300 g) for 10 min with SS34 rotor in Sorvall RC-5C plus centrifuge, discard the pellet, and collect the supernatant which contains phage.
11. Centrifuge at 16,000 rpm (30,624 g) for 45 min with SS34 rotor in Sorvall RC-5C plus centrifuge, discard the supernatant, and resuspend the pellet in 2 ml Pi-Mg buffer.
12. Make CsCl gradient solution. First, prepare layer buffer as in the table below; then from the bottom to the top, sequentially add 750 μl of layer buffer No. 6, No. 5, No. 4, No. 3, No. 2, and No. 1 to 5 ml Beckman centrifuge tube.

Layer no.	Stock CsCl (ml)	H_2O (ml)	Total volume (ml)
1	1	4	5
2	1.5	3.5	5
3	2	3	5
4	2.5	2.5	5
5	3	2	5
6	3.5	1.5	5

13. Add 0.5 ml resuspended phage sample from **step 11** to the top of the CsCl gradient solution, and centrifuge at 35,000 rpm (148,596 g) for 1 h at 4 °C using SW55 Ti rotor in Beckman L-60 Ultracentrifuge.
14. Following centrifugation, observe for the visible turbid phage bands. Fasten the tube to a vertical holder and using syringe needle, pierce the wall of centrifugation tube at the bottom of the phage band. Aspirate the phage band into 5 ml syringe.
15. Injection of phage sample into Slide-A-lyzer dialysis cassette and dialyze first against dialysis buffer I for 5 h at 4 °C and then against dialysis buffer II overnight at 4 °C.
16. Collect the phage sample and store at 4 °C for future use. The following steps will determine the titer of the phage using standard method.
17. Take seven clean glass tubes labeled 1–7, and add 990 μl Pi-Mg buffer into each tube.
18. Add 10 μl phage sample into the tube 1 and vortex to mix. Transfer 10 μl sample from tube 1 into tube 2 and vortex to mix. Continue to dilute the phage sample till tube 6. Add 10 μl Pi-Mg buffer into tube 7 which services as a control (*see* **Note 15**).
19. Transfer 100 μl of diluted phage samples or control from tubes 1 to 7 separately into 7 new clean glass tubes.
20. Add 400 μl of freshly grown *E. coli* P301 into each tube and keep tubes at 37 °C for 7–8 min.
21. Add 2.5 ml of top-agar to each tube and mix; immediately pour onto LB plates, shake the plates for uniform distribution, and keep the plates at room temperature for 10 min to solidify the top-agar (*see* **Note 16**).
22. Incubate the plates at 37 °C overnight.
23. Count the number of plaques in each plate and calculate the titer of phage sample.

3.2.4 Preparation of Antigen and Animal Immunizations

The exact amount of Hoc$^-$Soc$^-$ T4 phages and protein depends on how many animals will be used. Here the dose we will describe is for one animal (10 μg antigen/animal).

1. Take about 1.5×10^{11} phage particles and centrifuge at 15,000 rpm (21,130 g) in 1.5 ml LoBind Eppendorf tubes for 45 min at 4 °C using AM 2.18 rotor in Jouan MR-23i centrifuge (*see* **Note 17**).
2. Wash the pellet by adding 1.0 ml PBS and another round of centrifugation as in **step 1**.
3. Discard the supernatant, add 400 μl PBS to the tube, and resuspend the phage pellet overnight.

4. Add 290 μg F1mutV-Soc to the tube that contains phage, adjust the volume to 800 μl with PBS, gently vortex to mix, and incubate at 4 °C for 45 min.
5. Sediment the phage particles at 15,000 rpm (21,130 g) for 45 min at 4 °C using AM 2.18 rotor in Jouan MR-23i centrifuge, and the supernatant containing the unbound protein was discarded.
6. Wash the phage pellet containing the bound plague antigen (F1mutV) twice by adding 1.0 ml PBS and centrifugation as in **step 1**.
7. Add 50 μl PBS to the pellet, resuspend at 4 °C overnight, and analyze by SDS-PAGE as described in procedures from **steps 18** to **24** of Subheading 3.1.2. Determine the copy numbers of F1mutV per capsid.
8. Immunize the animals by i.m. injection.

4 Notes

1. F1 protein has a 21-aa signaling peptide, which was not included in the numbering of nucleotides (nt) or amino acids (aa). Thus F1 starts with *GCAGATTTAACTGCAA*…(nt) or *ADLTASTTATATL*…(aa).
2. To ensure restriction enzyme digestion after PCR amplification, an additional 2–6 bp (depends on the enzyme) should be included at the 5′-end of the primers.
3. Purification is necessary in order to remove resident primer 2 as well as F1 gene template. Both of these should be avoided in order to get a pure F1 mutant intermediate 2.
4. There is no stop codon before restriction site in reverse primer. So, the resultant plasmid contains V gene fused in-frame with a 13-aa vector sequence that includes the hexa-histidine sequence at the C-terminus.
5. RIPL cells produce higher yields when compared to any other BL21 host cells available in the Novagen.
6. The flask should be kept shaking at 30 °C for at least 30 min to cool down the *E coli*. The higher temperature may increase the chance of partitioning the over-expressed protein into the inclusion bodies, thus reducing the yield of soluble protein.
7. Proteinase inhibitors are necessary during purification. **Steps 7–17** have to be carried out at 4 °C.
8. All the solutions and samples that go to column have to go through 0.22 μm filter; otherwise the viscous sample will clog the column.

9. Keep the flow rate at 1 ml/min for 1 ml HisTrap column or max 5 ml/min for 5 ml HisTrap column. Increased flow rate will decrease protein binding to column.
10. BIORAD Bio-Safe™ Coomassie stain is used, which does not need special handing. If regular Coomassie stain is used, follow procedures on use and disposal of the stain.
11. Alhydrogel is thick and settles down. Shake vigorously to get a uniform suspension before using.
12. Since recombinant phage T4 Soc protein is not soluble, it is strongly recommended to use the T4-related phage RB69 Soc to construct fusion protein. Previous studies showed that the recombinant RB69 Soc is soluble and binds to T4 capsid at nearly the same affinity as T4 Soc.
13. Mix it immediately after adding the phage so that phage will be distributed uniformly.
14. The growth of phage can be assessed either by looking for turbidity and floating cell debris in the culture flask or after chloroform treatment, and by observation under light microscope.

    Chloroform treatment: Take 1 ml of culture in a test tube and add four drops of chloroform. If the cells are infected well, they lyse instantly clearing the cell suspension and cellular debris can be seen floating in the sample.

    Observation under light microscope: Put a drop of culture on the chamber of cell counter and cover it with a cover slip. Focus at individual *E. coli* cells by fine adjustment. The appearance of clear center and black/dark spots at the poles (ends) of the cells indicates good phage infection.
15. To get accurate titer, keep changing the pipette tip during the dilution of the phage sample.
16. The plates have to be kept at room temperature for at least 10 min to make sure that the top-agar solidifies.
17. Protein and DNA may nonspecifically bind to Eppendorf tube. Thus it is recommended to use low-binding tubes such as LoBind Eppendorf tube.

Acknowledgements

This work was supported by grants from the National Institutes of Health (NIAID U01-AI082086 and R01-AI111538). The authors thank Dr. Ashok Chopra, Department of Microbiology and Immunology, University of Texas Medical Branch, Galveston, TX, for his collaboration in testing the immunogenicity and protective efficacy of the vaccine formulations described in this chapter.

References

1. Wagner DM et al (2014) *Yersinia pestis* and the plague of Justinian 541–543 AD: a genomic analysis. Lancet Infect Dis 14:319–326
2. Guernier V et al (2014) Fleas of small mammals on Reunion Island: diversity, distribution and epidemiological consequences. PLoS Negl Trop Dis 8(9), e3129
3. Smiley ST (2008) Current challenges in the development of vaccines for pneumonic plague. Expert Rev Vaccines 7:209–221
4. Zilinskas RA (2006) The anti-plague system and the Soviet biological warfare program. Crit Rev Microbiol 32:47–64
5. Sha J et al (2013) Deletion of Braun lipoprotein encoding gene and altering the function of lipopolysaccharide attenuate plague bacterium. Infect Immun 81:815–828
6. Rosenzweig JA et al (2011) Progress on plague vaccine development. Appl Microbiol Biotechnol 91:265–286
7. Zavialov AV et al (2003) Structure and biogenesis of the capsular F1 antigen from *Yersinia pestis*: preserved folding energy drives fiber formation. Cell 113:587–596
8. Stenseth NC et al (2008) Plague: past, present, and future. PLoS Med 5(1), e3
9. Derewenda U et al (2004) The structure of *Yersinia pestis* V-antigen, an essential virulence factor and mediator of immunity against plague. Structure 12:301–306
10. Williamson ED et al (1995) A new improved sub-unit vaccine for plague: the basis of protection. FEMS Immunol Med Microbiol 12: 223–230
11. Anderson GW Jr, Heath DG, Bolt CR, Welkos SL, Friedlander AM (1998) Short- and long-term efficacy of single-dose subunit vaccines against *Yersinia pestis* in mice. Am J Trop Med Hyg 58:793–799
12. Heath DG et al (1998) Protection against experimental bubonic and pneumonic plague by a recombinant capsular F1-V antigen fusion protein vaccine. Vaccine 16:1131–1137
13. Goodin JL et al (2007) Purification and protective efficacy of monomeric and modified *Yersinia pestis* capsular F1-V antigen fusion proteins for vaccination against plague. Protein Expr Purif 53:63–79
14. Goodin JL et al (2011) Purification and characterization of a recombinant *Yersinia pestis* V-F1 "Reversed" fusion protein for use as a new subunit vaccine against plague. Protein Expr Purif 76:136–144
15. Mizel SB et al (2009) Flagellin-F1-V fusion protein is an effective plague vaccine in mice and two species of nonhuman primates. Clin Vaccine Immunol 16:21–28
16. Powell BS et al (2005) Design and testing for a nontagged F1-V fusion protein as vaccine antigen against bubonic and pneumonic plague. Biotechnol Prog 21:1490–1510
17. Parent MA et al (2005) Cell-mediated protection against pulmonary *Yersinia pestis* infection. Infect Immun 73:7304–7310
18. Tao P et al (2013) Mutated and bacteriophage T4 nanoparticle arrayed F1-V immunogens from *Yersinia pestis* as next generation plague vaccines. PLoS Pathog 9(7), e1003495
19. Li Q, Shivachandra SB, Leppla SH, Rao VB (2006) Bacteriophage T4 capsid: a unique platform for efficient surface assembly of macromolecular complexes. J Mol Biol 363: 577–588
20. Sathaliyawala T et al (2006) Assembly of human immunodeficiency virus (HIV) antigens on bacteriophage T4: a novel in vitro approach to construct multicomponent HIV vaccines. J Virol 80:7688–7698
21. Andrews GP, Heath DG, Anderson GW Jr, Welkos SL, Friedlander AM (1996) Fraction 1 capsular antigen (F1) purification from *Yersinia pestis* CO92 and from an *Escherichia coli* recombinant strain and efficacy against lethal plague challenge. Infect Immun 64:2180–2187
22. Miller J et al (1998) Macromolecular organisation of recombinant *Yersinia pestis* F1 antigen and the effect of structure on immunogenicity. FEMS Immunol Med Microbiol 21:213–221
23. Musson JA et al (2006) Sequential proteolytic processing of the capsular Caf1 antigen of *Yersinia pestis* for major histocompatibility complex class II-restricted presentation to T lymphocytes. J Biol Chem 281:26129–26135
24. Li Q, Shivachandra SB, Zhang Z, Rao VB (2007) Assembly of the small outer capsid protein, Soc, on bacteriophage T4: a novel system for high density display of multiple large anthrax toxins and foreign proteins on phage capsid. J Mol Biol 370:1006–1019
25. Shivachandra SB et al (2007) Multicomponent anthrax toxin display and delivery using bacteriophage T4. Vaccine 25:1225–1235
26. Black LW, Rao VB (2012) Structure, assembly, and DNA packaging of the bacteriophage T4 head. Adv Virus Res 82:119–153
27. Fokine A et al (2004) Molecular architecture of the prolate head of bacteriophage T4. Proc Natl Acad Sci U S A 101:6003–6008
28. Ishii T, Yanagida M (1977) The two dispensable structural proteins (soc and hoc) of the T4

phage capsid; their purification and properties, isolation and characterization of the defective mutants, and their binding with the defective heads in vitro. J Mol Biol 109:487–514

29. Qin L, Fokine A, O'Donnell E, Rao VB, Rossmann MG (2009) Structure of the small outer capsid protein, Soc: a clamp for stabilizing capsids of T4-like phages. J Mol Biol 395:728–741
30. Sathaliyawala T et al (2010) Functional analysis of the highly antigenic outer capsid protein, Hoc, a virus decoration protein from T4-like bacteriophages. Mol Microbiol 77:444–455
31. Tao P et al (2013) In vitro and in vivo delivery of genes and proteins using the bacteriophage T4 DNA packaging machine. Proc Natl Acad Sci U S A 110:5846–5851

Chapter 29

Development of Structure-Based Vaccines for Ehrlichiosis

Sunil Thomas

Abstract

The obligate intracellular bacterium *Ehrlichia chaffeensis* that resides in mononuclear phagocytes is the etiologic agent of human monocytotropic ehrlichiosis (HME). HME is an emerging and often life-threatening zoonotic, tick-transmitted infectious disease in the USA. Lack of early diagnosis and treatment of HME are the main factors that lead to severe and fatal disease. *Ehrlichia* also causes diseases in companion animals and domesticated ruminants. *E. chaffeensis* and *E. canis* cause canine ehrlichioses in dogs, whereas *E. ruminantium* causes heartwater in cattle, sheep, and goats. As yet there are no commercially available vaccines to protect against these pathogens. This chapter describes a protocol to develop a structure-based vaccine for *Ehrlichia* based on the antigenic proteins P28-19 and *Ehrlichia* Hsp60.

Key words Vaccine, *Ehrlichia*, Ehrlichiosis, Rickettsiales, Structure-based vaccines, Diagnostics, Eastern blotting

1 Introduction

The genera *Anaplasma*, *Ehrlichia*, *Neorickettsia*, *Orientia*, and *Wolbachia* of the order Rickettsiales encompass a group of obligate intracellular bacteria that reside in the vacuoles of eukaryotic cells [1]. Members of the genus *Ehrlichia* are tick-borne obligately intracellular bacteria that cause persistent infection of natural animal hosts, but are also associated with emerging human zoonoses of public health importance. *E. chaffeensis* is the etiologic agent of human monocytotropic ehrlichiosis (HME) [2], the most severe of the human ehrlichioses. In humans, many (40–60 %) *E. chaffeensis* infections require hospitalization and the case fatality rate is 3 % owing to the difficulty in making an accurate diagnosis and delays in treatment. White-tailed deer are the primary reservoir for *E. chaffeensis*, but dogs and coyotes may also be significant natural reservoirs [3]. *E. chaffeensis* is transmitted primarily by the lone star tick, *Amblyomma americanum* [3]. The emergence of *E. chaffeensis* is attributed to demographic and ecologic factors including increased human contact with natural foci, immunocompromised

Sunil Thomas (ed.), *Vaccine Design: Methods and Protocols: Volume 1: Vaccines for Human Diseases*, Methods in Molecular Biology, vol. 1403, DOI 10.1007/978-1-4939-3387-7_29,

and aging human populations, increases in vector and mammalian host populations, and availability of improved diagnostic methods and mandated reporting [3]. Heartwater, one of the most economically important ehrlichioses, is a devastating endemic disease of livestock in sub-Saharan regions of Africa and a few eastern Caribbean islands [4]. As yet there are no commercially available vaccines to protect against ehrlichiosis.

1.1 Murine Models for Ehrlichia Vaccine Development

Murine models of persistent and lethal ehrlichiosis have greatly facilitated understanding of the pathogenesis and mechanisms of host defenses against ehrlichial infections. Mildly virulent *Ehrlichia muris* infection in immunocompetent C57BL/6 mice results in persistent infection and mimics *E. chaffeensis* infection in its natural host, white-tailed deer [5], whereas infection with the highly virulent *Ehrlichia* species isolated from *Ixodes ovatus* ticks (*Ixodes ovatus* ehrlichia-IOE) mimics severe *E. chaffeensis* infection in humans [6]. *E. muris* is antigenically and genetically closely related to *E. chaffeensis* [7]. A recent study reported a new *Ehrlichia* species in Minnesota and Wisconsin infecting humans [8] and deer [9] which are closely related to *E. muris*.

1.2 Immunity to Ehrlichia

Studies of the immune response to *E. chaffeensis*, *E. ruminantium*, and *E. canis* have all contributed to the overall understanding of the cell-mediated and humoral host responses to *Ehrlichia* spp. Generally, strong evidence exists to support antibody- and cell-mediated involvement in protective immunity. MyD88-dependent signaling is required for controlling ehrlichial infection by playing an essential role in the immediate activation of the innate immune system and inflammatory cytokine production, as well as in the activation of the adaptive immune system at a later stage by providing for optimal Th1 immune responses [10]. Numerous studies with multiple *Ehrlichia* spp. indicate that IFN-γ is an essential mediator of protection [11, 12]. Moreover, $CD4^+$ and $CD8^+$ T cells both contribute to IFN-γ production [13]. Notably, similar conclusions regarding the importance of MHC class I, $CD4^+$, and $CD8^+$ T cells, and the synergistic roles of IFN-γ and TNF-α have been reported in mice infected with *E. muris* [14]. An important role for $CD4^+$ T cells in immunity to *E. ruminantium* and IOE has been suggested [15, 16]. Similarly, mice lacking functional MHC class II genes are unable to clear *E. chaffeensis* infection, suggesting that $CD4^+$ T cells are essential for ehrlichial clearance [17]. The intradermal environment (natural route of inoculation) appears to promote the induction of protective type-1 responses characterized by increased $CD4^+$ and $CD8^+$ T cells and IFN-γ-producing $CD4^+$ T cells [18]. Overall, these studies demonstrate that innate and adaptive immunity is essential in the control of *Ehrlichia* bacteria.

1.3 Ehrlichia Hsp60 and OMP-1 (P28-19) Are Vaccine Candidates for Ehrlichiosis

The OMP-1/P28 is the major antigen of *Ehrlichia* and they are the most studied *E. chaffeensis* outer membrane proteins (OMPs) with multiple predicted transmembrane β strands. Analysis of *E. muris* splenocyte lysate by polyclonal antibodies from *E. muris*-infected mice demonstrated *Ehrlichia* Hsp60 (GroEL) and OMP-1 (P28) as the major antigenic protein of *E. muris* [19] and these proteins are also posttranslationally modified as detected by eastern blotting [19]. As both P28-19 and *Ehrlichia* Hsp60 are found to be the major antigenic proteins we generated peptides based on the principles of structure-based design for diagnosis and vaccine application. Initial studies demonstrated that the antibodies generated against P28-19 and *Ehrlichia* Hsp60 could be used in the diagnostics of different strains of *Ehrlichia* [20]. As both P28-19 and *Ehrlichia* Hsp60 could generate polyclonal antibody we reasoned that the peptides could also function as vaccines. We observed a significant reduction in bacterial load in spleen and liver of *Ehrlichia* Hsp60-vaccinated mice ($p < 0.005$) after challenge with *E. muris*. Our studies also demonstrated that *Ehrlichia* Hsp60 as well as P28-19 could induce IFN-gamma in *E. muris*-specific CD4 T cells, but not in naïve T cells [21]. As both the antigens *Ehrlichia* Hsp60 and P28-19 could induce B cells and T cells, based on our studies we conclude that both the antigenic proteins are highly efficient vaccine candidates to protect against *Ehrlichia* infection.

1.4 Structure-Based Vaccines

The genetic diversity of microorganisms, coupled with the high degree of sequence variability in antigenic proteins, presents a challenge to developing broadly effective conventional vaccines. The observation that whole-protein antigens are not necessarily essential for inducing immunity has led to the emergence of a new branch of vaccine design termed "structural vaccinology." Structural vaccinology combines elements of structural biology and bioinformatics into a promising new method for the identification of antigenic protein elements of interest based on the protein amino acid sequence and the resulting secondary and tertiary structure. The enabling principle is that the entire antigenic protein is not essential for inducing an immune response as only the epitope sequence per se actually induces the immune response and provides protection against pathogens. Recent studies demonstrated that designing structure-based vaccine candidates with multiple epitopes induces a higher immune response. As yet there are no commercial vaccines available for any diseases based on structure-based design, most of the structure-based vaccine candidates are in the preclinical stages of development (reviewed in Thomas and Luxon, 2013) [22]. The methods and protocols followed to generate structure-based vaccines (based on *Ehrlichia* Hsp60 and P28-19) to protect against *Ehrlichia* are described in this chapter.

2 Materials

Prepare all solutions using double-distilled water and analytical grade reagents. Wear clean laboratory coat and gloves in all the experiments.

2.1 Cell Culture

1. Bacterial strains: *Ehrlichia muris*, *Ehrlichia chaffeensis*, and *Ixodes ovatus* Ehrlichia (IOE).
2. Cell lines: DH82.
3. Dulbecco's modified Eagle medium (DMEM).
4. Bovine calf serum.
5. Cell culture Petri dish.
6. Bicinchoninic acid protein assay kit (Pierce, Rockford, IL).

2.2 Animals

1. C57BL/6 (Jackson Laboratories, ME, USA).

2.3 Electrophoresis and Western Blotting

1. Gels: NuPAGE Novex 4–12 % Bis-Tris protein gels (1-well PAGE gel for 2D electrophoresis, 12-well PAGE gel for 1D electrophoresis) (Life Technologies, CA).
2. IEF strip gels (pH 4–7) (NuPage, Life Technologies, CA).
3. Electrophoresis tanks (1D: X cell SureLock Mini-Cell, Life Technologies, and 2D electrophoresis: ZOOM IPG Runner System, Life Technologies, CA).
4. Trans-Blot Semi Dry Transfer Cell (Bio-Rad, CA).
5. Electrophoresis power pack (ZOOM Dual Power Supply, Life Technologies).
6. Filter paper.
7. Nitrocellulose membrane (Millipore, MA).
8. Nonfat milk powder.
9. Tween 20.
10. Cholera Toxin B subunit (Sigma, MO) (*see* **Note 1**).
11. Rabbit anti-cholera toxin B subunit (CTB).
12. Goat anti-rabbit AP.
13. Goat anti-mouse alkaline phosphatase (AP).
14. AP chemiluminescence substrate (KPL, MD).
15. Biotinylated Con-A (Vector Laboratories, CA).
16. Streptavidin-HRP.
17. Gelcode phosphoprotein detection kit (Pierce-Thermofisher, IL).
18. Phosphate-buffered saline (PBS): 10× PBS (Sigma, USA) diluted in double-distilled water to make 1× PBS.
19. Lysis buffer: RIPA (radioimmunoprecipitation assay buffer) lysis buffer (1×; 100 ml solution), 50 mM Tris–HCl, pH 7.4;

150 mM NaCl; 0.1 % SDS; 0.5 % sodium deoxycholate; 1 % Triton X 100 or NP-40 (*see* **Note 2**). Alternately, RIPA buffer from commercial vendors (Life Technologies, CA) can be used. Add protease and phosphatase inhibitors before use.

20. Sample buffer: 1.0 ml 0.5 M Tris, pH 6.8; 0.8 ml glycerol; 1.6 ml 10 % SDS; 0.4 ml 2-mercaptoethanol; 0.4 ml 1 % bromophenol blue; 3.9 ml deionized water (5× buffer). Alternately, NuPAGE LDS sample buffer; 4× (Life Technologies, CA) (*see* **Note 3**).
21. SDS PAGE buffer (running buffer): Dissolve 30.0 g of Tris base, 144.0 g of glycine, and 10.0 g of SDS in 1000 ml of H_2O. The pH of the buffer should be 8.3 and no pH adjustment is required (10× buffer). Store the running buffer at room temperature and dilute to 1× before use. Alternately, NuPAGE MES-SDS running buffer, 20× (Life Technologies, CA) could be used. Dilute to 1× before use.
22. Towbin buffer (transfer buffer; for transfer of proteins from PAGE gel to nitrocellulose [NC] membrane): For 10× buffer in 1 L double-distilled water: 25 mM Tris base (30.0 g); 192 mM glycine (144 g); pH 8.3. Dilute to 1× with 10 % methanol before use (*see* **Note 4**). Close the container after the addition of methanol. Alternately, NuPAGE transfer buffer (20×) (Life Technologies, CA) could be used.
23. Coomassie stain for PAGE gel: 400 ml Methanol, 100 ml acetic acid (glacial), 500 ml H_2O, 1 g Coomassie blue R-250. Keep the container closed during staining (*see* **Note 5**).
24. Blocking and dilution buffer (A): PBS-0.05 % Tween20-5 % nonfat milk.
25. Dilution buffer (B): PBS-0.05 %Tween 20-3 % bovine serum albumin (BSA).
26. Destain: 400 ml Methanol, 100 ml acetic acid (glacial), 500 ml H_2O. Keep the container closed during de-staining.
27. Wash buffer: PBS-0.05 %Tween 20.
28. Tabletop shaker/rocker.
29. Sterile knife/blade.
30. ChemiDoc (Bio-Rad, CA) (gel and blot documentation system).

2.4 Enzyme-Linked Immunosorbent Assay

1. Enzyme-linked immunosorbent assay (ELISA) 96-well plate (MaxiSorp; Nunc, Thermo Fisher, NY).
2. Coating buffer (bicarbonate/carbonate coating buffer (100 mM)): Antigen or antibody should be diluted in coating buffer to immobilize them to the wells. 3.03 g Na_2CO_3; 6.0 g $NaHCO_3$; 1000 ml distilled water; pH 9.6.

3. Phosphate-buffered saline (PBS): 10× PBS (Sigma, USA) diluted in double-distilled water to make 1× PBS.
4. Washing buffer: PBS-Tween 20 (0.05 %) or alternately double-distilled water (in a wash bottle) can be used for washing.
5. Substrate solution (for HRP): 2,2′-Azino-di-(3 ethylbenzthiazoline sulfonic acid) (ABTS). 1 mM ABTS in 70 mM citrate-phosphate buffer, pH 4.2.
6. Substrate solution (for AP): p-Nitrophenyl phosphate.
7. Stop solution: 0.2 M H_2SO_4.
8. Anti-mouse horseradish peroxidase (HRP) or anti-mouse alkaline phosphatase (AP).
9. ELISA reader.

2.5 Microscopy

1. PBS: 10× PBS (Sigma, USA) diluted in double-distilled water to make 1× PBS.
2. Tween-20.
3. BSA.
4. Anti-mouse Alexa 488 (Life Technologies, CA).
5. Mounting medium with DAPI (Vectashield, Vector Laboratories, CA).
6. Modified Geimsa stain (Diff-Quik stain).
7. Culture slide (Corning, NY).
8. Epifluorescence microscope.

2.6 Quantitative PCR (qPCR)

1. Real-time PCR detection system (Bio-Rad, CA).
2. Real-time PCR reagents (Bio-Rad, CA).

2.7 Software

1. Adobe Photoshop (Adobe Systems, CA).
2. GraphPad Prism (GraphPad Software, CA).
3. Lasergene (DNAStar, WI).
4. I-Tasser (http://zhanglab.ccmb.med.umich.edu/I-TASSER/).
5. Phyre (http://www.sbg.bio.ic.ac.uk/phyre2/html/page.cgi?id=index).
6. Pubmed (http://www.ncbi.nlm.nih.gov/pubmed).

3 Methods

3.1 Determination of Ehrlichial Antigenic Proteins

Two monocytotropic ehrlichial strains were used in the study—highly virulent *Ehrlichia* spp. (designated IOE) isolated from *Ixodes ovatus* ticks and the mildly virulent *E. muris*.

3.1.1 Bacterial Culture

1. *Ehrlichia muris* is cultured in DH82 cells at 37 °C in DMEM supplemented with 5 % heat-inactivated bovine calf serum.

2. Ehrlichiae are harvested when approximately 90–100 % of the cells are infected (*see* **Note 6**). To view infectivity, a loop of DH82 cells infected with *E. muris* is streaked onto a clean glass slide and stained with modified Geimsa stain (Diff-Quik stain). *Ehrlichia* morulae stain purple.
3. To produce infectious stocks for reproducible studies, C57BL/6 mice are inoculated i.p. with 1 mL of a 10^{-1} dilution (5×10^8 *E. muris*) of the frozen stock.
4. For western blotting to detect antigenic proteins of *E. muris* on day 7 after inoculation, the mice are sacrificed, the spleens harvested, and splenic homogenate prepared and suspended in DMEM medium. After centrifugation at $5000 \times g$, the supernatant is discarded and the cells washed twice with PBS at $5000 \times g$ (5 min each wash).
5. After discarding the supernatant the cells are suspended in 0.5 ml RIPA buffer. The cells are vortexed and left on ice for 15 min with multiple vortexing every 5 min.
6. The lysate is sonicated for 1 min on ice (30 s × 2 times) and after centrifugation at $5000 \times g$ the supernatant is collected and total protein concentrations of the resulting bacterial preparations are determined using a bicinchoninic acid protein assay kit (Pierce, Rockford, IL). DH82 cells or uninfected mouse spleen is used as the negative control. The samples are stored at –20 °C.

3.1.2 Generation of Polyclonal Antibodies

1. For polyclonal antibody production *E. muris* (from infected mouse spleen) is inoculated intraperitoneally into mice and the blood collected on day 45 after the first injection.
2. To generate IOE-specific antibodies sublethal doses of IOE are inoculated at 2-week intervals, and serum collected after 30 days.
3. For *E. muris/IOE* antibody, mice primed with *E. muris* are infected with IOE on day 30 and the blood collected on day 50 after primary infection.

3.1.3 SDS-PAGE and Western Blotting

1. Total cell lysate (25 μg/lane) from uninfected spleen, spleen infected with *E. muris*, and IOE are added to sample buffer and heated at 70 °C for 10 min (or boiling water for 5 min). The samples are cooled to room temperature for 5 min.
2. The samples are loaded onto 4–12 % Bis-Tris gel. SDS-PAGE buffer/running buffer is used in the electrophoresis tank. The samples are run at low voltage (100 V for 10 min) which is increased to 160–180 V after 10 min.
3. After electrophoresis is completed the PAGE gel cassette is open and the gel is transferred to a semidry transfer system for blotting. The filter paper and nitrocellulose membrane are

immersed in the Towbin buffer. Make sure that no air bubbles are trapped between the gel and membrane using a roller. Proteins are transferred to the nitrocellulose membrane at 200 mA (45 min).

4. After the protein transfer is complete, transfer the blot to PBS-Tween-5 % milk for 40 min (with shaking).
5. The membranes are probed with polyclonal sera against *E. muris*, IOE, and *E. muris*/IOE (1:100 dilution in dilution buffer (A)) (room temperature, 1 h). Wash the blot with wash buffer, three washes, 10 min each wash.
6. Incubate the blot in goat anti-mouse alkaline phosphatase (AP) (1:1000) (room temperature, 1 h). Wash the blot with wash buffer, three washes, 10 min each wash.
7. The protein bands are detected by a chemiluminescence substrate (KPL, MD) and the image documented by ChemiDoc.
8. Simultaneously, a protein gel is run with the same samples as in western blot and the gel stained with Coomassie blue for 15 min.
9. The gel is destained until the background is clear.
10. The protein profiles are matched and common bands corresponding to western blot and Coomassie stain are analyzed. Using a sterile sharp knife the bands of interest are excised and placed in a sterile microcentrifuge tube containing 0.5 ml sterile double-distilled water. The bands are immediately sent for mass spectrophotometry analysis (*see* **Note 7**).

3.1.4 2D Electrophoresis and Western Blotting

Hundreds of polypeptides can be analyzed in a single run using 2D electrophoresis. The proteins can be separated in pure form from the resultant spots.

1. The IEF strip is used to separate proteins in the first dimension. Use IEF strip (pH 4–7) (NuPage, Invitrogen, CA) to separate the proteins based on pI. Multiple samples are run on the IEF apparatus and the strips can be stored at –80 °C.
2. The second dimension is run as a regular electrophoresis. The IEF strip is placed in 4–12 % Bis-Tris gel followed by separation of proteins according to the protocol of the manufacturers.
3. The proteins are transferred from the gel to a nitrocellulose membrane using Towbin buffer in a semidry transfer system (as in Subheading 3.1.3).
4. The nitrocellulose membrane is blocked in blocking buffer (A).
5. The membranes are probed with polyclonal sera against *E. muris*, IOE, and *E. muris*/IOE (1:100 dilution). Wash the blot with wash buffer, three washes, 10 min each wash.

6. Incubate with goat anti-mouse alkaline phosphatase (AP) (1:1000) (incubate for 1 h at room temperature, on a shaker). Wash the blot with wash buffer, three washes, 10 min each wash.
7. The protein spots are detected by a chemiluminescence substrate (KPL, MD) and the image documented by ChemiDoc.
8. Simultaneously, a protein gel is run with the same samples and the gel stained with Coomassie blue.
9. After destaining, the protein profiles are matched and common spots corresponding to western blot and Coomassie stain are analyzed. Using a sterile sharp knife the spots of interest are excised and placed in a sterile microcentrifuge tube containing 0.5 ml sterile double-distilled water. The spots of interest are immediately sent for mass spectrophotometry analysis.
10. The major antigenic proteins, *Ehrlichia* Hsp60 (GroEL) and P28-19, described in this chapter were determined by mass spectrophotometry analysis.

3.1.5 Probes for Detecting Antigenic Protein Modification (Eastern Blotting)

As the protein profiles of *E. muris* and IOE were observed to be identical, we determined whether there was a change in posttranslational protein modifications.

3.1.5.1 Detection of Lipo-proteins

1. Samples are run as in Subheading 3.1.4 and the 2D blots are probed with cholera toxin B subunit (10 μg/mL) (use dilution buffer B).
2. Wash with wash buffer, three washes, 10 min each wash.
3. Probe the blot with rabbit anti-CTB (1:5000) (1 h at room temperature). Wash with wash buffer, three washes, 10 min each wash.
4. Probe the blot with goat anti-rabbit AP (1:1000). Wash with wash buffer, three washes, 10 min each wash.
5. The protein bands are detected by a chemiluminescence substrate and the image documented by ChemiDoc.

3.1.5.2 Detection of Glyco-proteins

1. Glucosyl residues are detected using concanavalin-A (Con-A). Con-A binds glucosyl and mannosyl residues. Con-A (0.005 μg/mL) (Vector Laboratories, CA) is diluted in PBS-BSA 3 %-Tween 20 (0.05 %) and the nitrocellulose membrane probed for 1 h at room temperature.
2. Wash with wash buffer, three washes, 10 min each wash. This is followed by incubating the blot with streptavidin-HRP (1:15,000). Wash with wash buffer, three washes, 10 min each wash.
3. The protein bands are detected by a chemiluminescence substrate and the image documented by ChemiDoc.

3.1.5.3 Detection of Phosphoproteins

Phosphoproteins can be detected directly on the gel using the gelcode phosphoprotein detection kit (Pierce-Thermofisher, IL).

1. After the second-dimension gel is run, wash with water for 1 min and stain the gel with gelcode phosphoprotein detection kit (Pierce-Thermofisher, IL) following the instruction of the manufacturer (*see* **Note 8**).

Detection of posttranslational protein modification is Eastern blotting. We observed that the *Ehrlichia* Hsp60 (GroEL) and P28-19 of *E. muris* were more posttranslationally modified than those of IOE [19]. Hence these two antigenic proteins were selected as vaccine candidates.

3.2 Structure-Based Design

To determine a protein sequence for potential antigenic epitopes, sequences that are hydrophilic, surface oriented, and flexible are selected. Most naturally occurring proteins in aqueous solutions have their hydrophilic residues on the protein surface and hydrophobic residues buried in the interior.

3.2.1 Design of P28-19 and Ehrlichia Hsp60 Peptides

1. Download the protein sequence from Pubmed (insert in the database search box: Protein) (P28-19) (Search). Using Lasergene software (DNAStar, WI, USA) to analyze and select the protein sequences with good hydrophilicity. Three regions of the *E.* muris P28-19 (Fig. 1) and Hsp60 protein sequence (Fig. 2) had good hydrophilicity. Usually the C- or N-terminal of the protein is used, as those parts of protein are exposed.
2. Select hydrophilic sequences of both the *Ehrlichia* P28-19 and Hsp60 proteins with no hydrophobic residues. The hydrophilic regions of P28-19 correspond to amino acids 55–75, 91–103, and 124–145 (Fig. 1). The hydrophilic regions of *Ehrlichia* Hsp60 correspond to amino acids 43–63, 179–199, and 387–406 (Fig. 2). The sequences showed homology to other *Ehrlichia* species. In our study the peptides (underlined) were synthesized and conjugated to keyhole limpet hemocyanin (KLH) (Biosynthesis, Lewisville, TX) and used as probes to detect antibodies to *E. canis* and *E. chaffeensis* or to raise antibodies.

3.2.2 3D Structure Prediction

1. The 3D structure of P28-19 in Fig. 1 is modeled using the online I-TASSER (iterative threading assembly refinement) server [23, 24]. I-TASSER builds 3D models from an amino acid sequence using fold recognition and multiple-threading alignments by LOMETS, a meta-threading server in the Zhang lab at the Univ. of Michigan which combines seven state-of-the-art threading programs (FUGUE, HHsearch, MUSTER, PROSPECT, PPA, SP3, and SPARK), and then performs iterative structural assembly simulations.
2. The function of the predicted models is inferred by structurally matching the 3D models with known proteins using protein

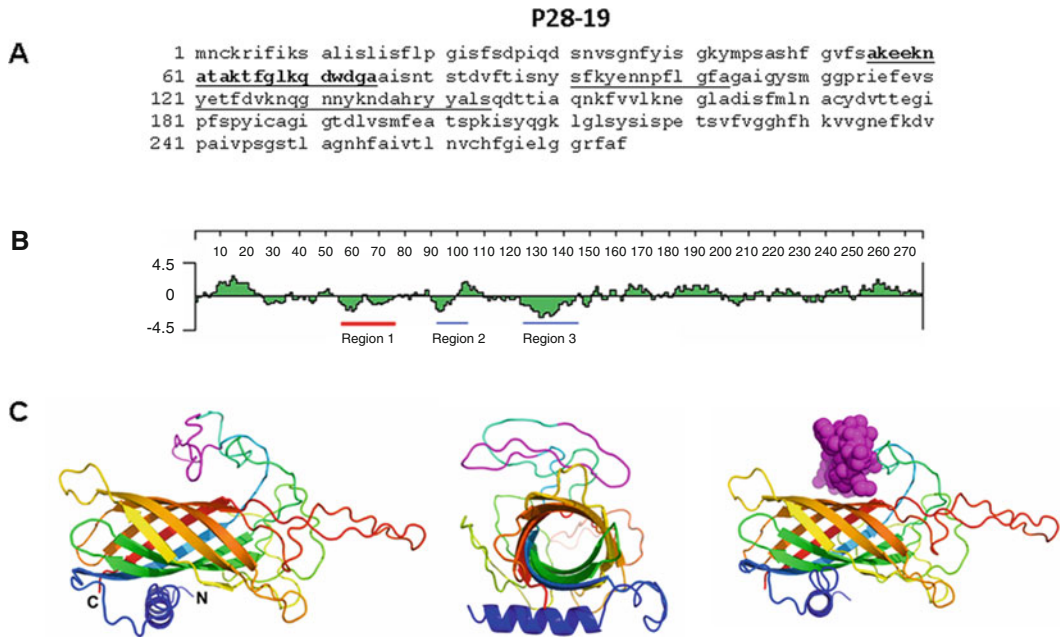

Fig. 1 Amino acid sequence of P28-19. (**a**) P28-19 peptides corresponding to the underlined predicted hydrophilic sequence were synthesized. The peptide corresponding to the bold underlined (55–75) sequence was found to react with antibodies to *Ehrlichia* as well as to induce antibody production. (**b**) Hydrophobicity plot of P28-19. The sequences underlined (*in red and blue*) were used for synthesizing peptides; however the best peptide sequence selected is underlined in *red*. (**c**) (*Left*) Predicted 3D structure of P28-19 (side view), (*middle*) predicted 3D structure of P28-19 (basal view), (*right*) predicted 3D structure of P28-19 with the van der Waals radii of the heavy atoms highlighting the region of interest (P28-19 $_{55–75}$)

function databases. The best predicted model from I-TASSER (Fig. 1) gave a C-score of −3.338, a TM-score of 0.34 ± 0.12, and an Exp. RMSD of 14.1 ± 3.8. The C-score is a confidence value for estimating the quality of the model and generally ranges from [−5, 2] with a higher score being better; TM-scores measure structural similarity and are used to measure the accuracy of structural modeling with a TM-score >0.5 indicating a model having the correct topology and a TM-score <0.17 showing random similarity. RMSD is simply the average distance of all amino acid pairs between two structures. Protein segments that are relatively unstructured such as loops and coils can result in high RMSD scores. Based on these results the beta-barrel portion of the model in Fig. 1 is likely to be a reasonable representation of the 3D structure of body of the protein. The model is double-checked against the best model produced by Phyre2 [25].

3. The 3D structure of *Ehrlichia* Hsp60 in Fig. 2 is modeled using the online Phyre2 server [25]. Phyre2 aligns hidden Markov models via HHsearch to improve alignment accuracy and detection rate. In "intensive" mode, which is used here, Phyre2 also incorporates Poing [26], a new ab initio folding

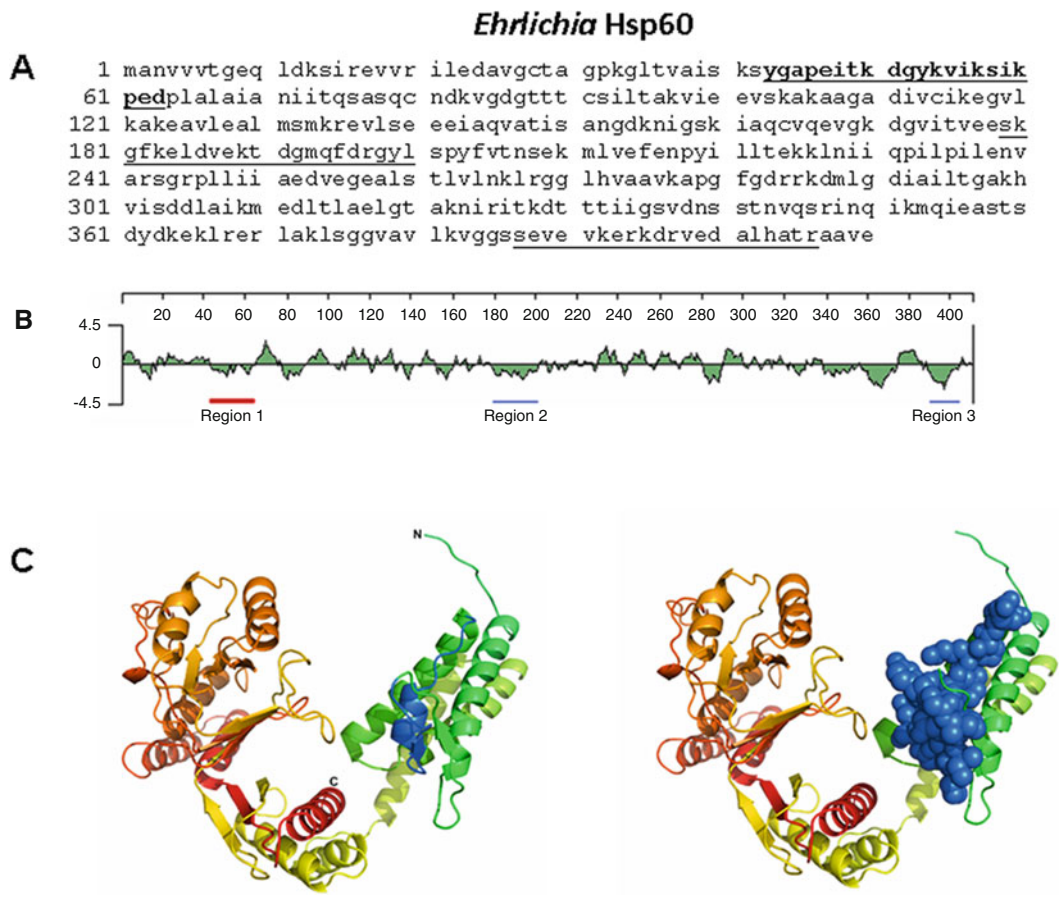

Fig. 2 Amino acid sequence of *Ehrlichia* Hsp60. (**a**) Hsp60 peptides corresponding to the underlined predicted hydrophilic sequence were synthesized. The peptide corresponding to the bold underlined (43–63) sequence was found to react with antibodies to *Ehrlichia* as well as to induce antibody production. (**b**) Hydrophobicity plot of *Ehrlichia* Hsp60. The sequences underlined (in *red* and *blue*) were used for synthesizing peptides; however, the best peptide sequence selected is underlined in *red*. (**c**) (*Left*) Predicted 3D structure of *Ehrlichia* Hsp60, (*right*) predicted 3D structure of *Ehrlichia* Hsp60 with the van der Waals radii of the heavy atoms highlighting the region of interest (Hsp60 $_{43–63}$).

simulation based on Langevin dynamics, to model regions of the protein that have no detectable homology with known structures. For the Hsp60 sequence, 100 % of the residues are modeled at >90 % confidence level. The top three PDB models, all GroEL chaperone proteins, had 100 % confidence levels and sequence ids of 51–56 %.

3.3 Generation of P28-19 and Ehrlichia Hsp60 Antibodies and Detection of Specific Antibodies by ELISA

1. *Ehrlichia* Hsp60 (GroEL) or P28-19 peptides conjugated to KLH were synthesized by Biosynthesis, Inc. (Lewisville, TX) and injected (50 μg per mouse) (i.p.—three times) into C57BL/6 mice.
2. Blood is collected 40 days after the first injection from the tail vein or retro-orbital collection.

3. Antibody is purified from the blood [27] and its specificity determined by ELISA.
4. For determining specificity of the antibody by ELISA, coat 1.0 μg/mL of the *Ehrlichia* Hsp60 or P28-19 peptide (volume = 100 μl per well) in ELISA plate. The peptides are dissolved in ELISA coat buffer. Incubate at room temperature for 1 h or overnight at 4 °C. Make sure to cover the ELISA plate with a clean aluminum foil in all incubation steps.
5. After the coating step, wash the ELISA plate with PBS-Tween (*see* **Note 9**).
6. Block with PBS-Tween-5 % BSA for 40 min at room temperature (volume = 110 μl per well).
7. Flick the plate and add the diluted antibodies (in PBS) (1 h at room temperature).
8. Wash the plate three times with PBS-Tween, and remove any traces of buffer by tapping the plate on a stack of paper towels.
9. Incubate with anti-mouse HRP (diluted in PBS-Tween) for 1 h at room temperature (volume = 110 μl per well). Repeat **step 8**.
10. Add substrate ABTS in the dark. Immediately prior to adding ABTS to assay plates, add 1 μl 30 % H_2O_2 solution/ml ABTS. The assay will not work if H_2O_2 is not added (*see* **Note 10**).
11. Add stop solution after 15-min substrate incubation and read the plate at 450 nm in an ELISA reader.

The protocol can also be useful for diagnosis application. The test could be used in the detection of *Ehrlichia* antibodies in infected animals. Presence of *Ehrlichia* antibodies correlates to infection with *Ehrlichia*.

3.4 Detection of Ehrlichia by Microscopy

E. muris and *E. chaffeensis* are grown in DH82 cells and the efficacy of the *Ehrlichia* Hsp60 or P28-19 antibodies was determined by immunofluorescence microscopy.

1. The *E. muris* and *E. chaffeensis* are grown in DH82 cells for 2 days on culture slides (*see* **Note 11**).
2. Cells are fixed in 50 % methanol-acetone for 5 min.
3. After washing three times with PBS, cells are blocked with 5 % normal goat serum in PBS-Tween (30 min).
4. Incubate with *Ehrlichia* Hsp60 or P28-19 antibodies (1:125) (45 min) (in PBS-Tween-3 % BSA).
5. After three washes with PBS-0.05 %Tween 20 (5 min per wash), they were reacted with anti-mouse immunoglobulin G conjugated to Alexa 488 (in PBS-Tween-3 %BSA) (45 min).

6. After several washes with PBS-0.05 %Tween 20 (5 min per wash), they were mounted in mounting medium containing DAPI (Vectashield, Vector Labs, Burlingame, CA).
7. Specimens are visualized under an epifluorescence microscope with appropriate filters.

3.5 Immunization and *Ehrlichia muris* Challenge

1. Mice are immunized i.p., with two doses of 50 μg (0.02 μM) of each P28-19 $_{55–75}$ peptide or *Ehrlichia* Hsp60 $_{43–63}$ peptide conjugated to KLH 15 days apart (the first immunization with complete Freund's adjuvant and the second immunization with incomplete Freund's adjuvant).
2. Thirty days after the first immunization mice are challenged intraperitoneally (i.p.) with a high dose of *E. muris* ($\sim 1 \times 10^4$ bacterial genomes) and observed daily. Controls included unchallenged naïve mice as well as unvaccinated mice injected with *E. muris* alone.
3. Mice are sacrificed on days 7, 14, and 21 after ehrlichial challenge, and spleen and liver are harvested and sera collected.
4. The ehrlichial load in spleen and liver is determined by quantitative RT-PCR [28]. Sera are assayed for determination of antibody titers (follow protocol 3.3). The vaccinated mice will have low copy numbers of ehrlichial DNA and low titers of antibodies in the blood.

4 Notes

1. Cholera toxin B subunit conjugated to HRP/or AP can reduce the time of eastern blotting.
2. RIPA buffer effectively extracts cytoplasmic, nuclear, and membrane proteins.
3. 2-Mercaptoethanol has an unpleasant smell and could be substituted with 3 mL of 1 M dithiothreitol (DTT).
4. Use high-quality analytical grade methanol. Impure methanol yields poor transfer. Methanol is neurotoxic, hence handle carefully.
5. For quick and easy detection of proteins on gels Coomassie G250 can be used (Coomassie G250: 70 mg; HCl: 35 mM; make up to 1 L with double-distilled water). After treating the SDS-PAGE gel with the Coomassie G250 stain for 15 min, water is used for destaining.
6. As antibiotics are not used during culture of *E. muris* the work should be performed in sterile conditions.
7. It is preferable to acquire images of the gel before excising bands of interest. When images are taken make sure not to

allow your gel to contact any contaminated surfaces during the process of acquiring an image of your gel. To excise the bands be sure to use extremely clean surfaces and new razor blades or scalpels if possible. Ideally this should be done in a laminar flow hood to minimize the possibility of any dust, hair, flakes of skin, or other forms of dirt. Even trace amounts of such contaminants usually contain keratins. Once cut, gel bands can be stored frozen in water in clean, sealed sample tubes. Wear clean gloves and laboratory coat at all times.

8. There are 30 posttranslational protein modifications. As yet there are no substrates to detect all the posttranslational protein modifications; hence use of antibodies or mass spectrometry may be the alternate choice to detect posttranslational protein modifications.
9. Double-distilled water can also be used to wash ELISA plates.
10. If secondary antibody conjugated to alkaline phosphatase is employed in ELISA, the substrate p-nitrophenyl phosphate is used.
11. Culture approximately 500 DH82 cells per slide. If cells are left for longer than 3 days it forms a confluence and individual cells are hard to detect. *Ehrlichia* induce filopodium formation which is visible within 2 days of culture. No filopodium is visible when the host cells cover the entire slide [20].

Acknowledgements

My sincere thanks to Dr. Bruce A. Luxon Department of Biochemistry and Molecular Biology, University of Texas Medical Branch, Galveston, TX, for helping with bioinformatics and 3D modeling.

References

1. Dumler JS, Barbet AF, Bekker CP, Dasch GA, Palmer GH, Ray SC, Rikihisa Y, Rurangirwa FR (2001) Reorganization of genera in the families Rickettsiaceae and Anaplasmataceae in the order Rickettsiales: unification of some species of *Ehrlichia* with *Anaplasma*, Cowdria with *Ehrlichia* and *Ehrlichia* with *Neorickettsia*, descriptions of six new species combinations and designation of *Ehrlichia equi* and 'HGE agent' as subjective synonyms of *Ehrlichia phagocytophila*. Int J Syst Evol Microbiol 51(Pt 6):2145–2165
2. Anderson B (1992) Etiologic agent of human ehrlichiosis. Pediatr Infect Dis J 11:597–598
3. Paddock CD, Childs JE (2003) Ehrlichia chaffeensis: a prototypical emerging pathogen. Clin Microbiol Rev 16:37–64
4. Provost A, Bezuidenhout JD (1987) The historical background and global importance of heartwater. Onderstepoort J Vet Res 54:165–169
5. Olano JP, Wen G, Feng HM, McBride JW, Walker DH (2004) Histologic, serologic, and molecular analysis of persistent ehrlichiosis in a murine model. Am J Pathol 165:997–1006
6. Sotomayor EA, Popov VL, Feng HM, Walker DH, Olano JP (2001) Animal model of fatal

human monocytotropic ehrlichiosis. Am J Pathol 158:757–769

7. Yu X-J, Zhang XF, McBride JW, Zhang Y, Walker DH (2001) Phylogenetic relationships of *Anaplasma marginale* and '*Ehrlichia platys*' to other *Ehrlichia* species determined by GroEL amino acid sequences. Int J Syst Evol Microbiol 51:1143–1146
8. Pritt BS, Sloan LM, Johnson DK, Munderloh UG, Paskewitz SM et al (2011) Emergence of a new pathogenic *Ehrlichia* species, Wisconsin and Minnesota, 2009. N Engl J Med 365:422–429
9. Telford SR, Goethert HK, Cunningham JA (2011) Prevalence of *Ehrlichia muris* in Wisconsin deer ticks collected curing the mid 1990s. Open Microbiol J 5:18–20
10. Koh YS, Koo JE, Biswas A, Kobayashi KS (2010) MyD88-dependent signaling contributes to host defense against ehrlichial infection. PLoS One 5(7), e11758
11. Totté P, Blankaert D, Zilimwabagabo P, Wérenne J (1993) Inhibition of Cowdria ruminantium infectious yield by interferons alpha and gamma in endothelial cells. Rev Elev Med Vet Pays Trop 46:189–194
12. Totté P, McKeever D, Jongejan F, Barbet A, Mahan SM, Mwangi D, Bensaid A (1998) Analysis of cellular responses to native and recombinant proteins of Cowdria ruminantium. Ann N Y Acad Sci 849:155–160
13. Esteves I, Walravens K, Vachiéry N, Martinez D, Letesson JJ, Totté P (2004) Protective killed Ehrlichia ruminantium vaccine elicits IFN-gamma responses by CD4+ and CD8+ T lymphocytes in goats. Vet Immunol Immunopathol 98:49–57
14. Feng HM, Walker DH (2004) Mechanisms of immunity to *Ehrlichia muris*: a model of monocytotropic ehrlichiosis. Infect Immun 72:966–971
15. Totté P, McKeever D, Martinez D, Bensaid A (1997) Analysis of T-cell responses in cattle immunized against heartwater by vaccination with killed elementary bodies of Cowdria ruminantium. Infect Immun 65:236–241
16. Bitsaktsis C, Huntington J, Winslow G (2004) Production of IFN-gamma by CD4 T cells is essential for resolving ehrlichia infection. J Immunol 172:6894–6901
17. Ganta RR, Wilkerson MJ, Cheng C, Rokey AM, Chapes SK (2002) Persistent Ehrlichia chaffeensis infection occurs in the absence of functional major histocompatibility complex class II genes. Infect Immun 70:380–388
18. Stevenson HL, Jordan JM, Peerwani Z, Wang HQ, Walker DH, Ismail N (2006) An intradermal environment promotes a protective type-1 response against lethal systemic monocytotropic ehrlichial infection. Infect Immun 74:4856–4864
19. Thomas S, Thirumalapura N, Crossley E, Ismail N, Walker DH (2009) Antigenic protein modifications in *Ehrlichia*. Parasite Immunol 31:296–303
20. Thomas S, Popov VL, Walker DH (2010) Exit mechanisms of the intracellular bacterium *Ehrlichia*. PLoS One 5(12), e15775
21. Thomas S, Thirumalapura N, Crocquet-Valdes PA, Luxon BA, Walker DH (2011) Structure based vaccines provides protection in a mouse model of ehrlichiosis. PLoS One 6(11), e27981
22. Thomas S, Luxon BA (2013) Structure-based vaccines provides protection against infectious diseases. Expert Rev Vaccines 12:1301–1311
23. Zhang Y (2007) Template-based modeling and free modeling by I-TASSER in CASP7. Proteins 69 Suppl 8:108–117
24. Roy A, Kucukural A, Zhang Y (2010) I-TASSER: a unified platform for automated protein structure and function prediction. Nat Protoc 5:725–738
25. Kelley LA, Sternberg MJE (2009) Protein structure prediction on the web: a case study a case study using the Phyre study using the Phyre server. Nat Protoc 4:363–371
26. Jefferys BR, Kelley LA, Sternberg MJE (2010) Protein folding requires crowd control in a simulated cell. J Mol Biol 397:1329–1338
27. Greenfield EA (2014) Antibodies: a laboratory manual. Cold Spring Harbor Laboratory Press, Cold Spring Harbor, NY
28. Doyle CK, Labruna MB, Breitschwerdt EB, Tang YW et al (2005) Detection of medically important Ehrlichia by quantitative multicolor TaqMan real-time polymerase chain reaction of the dsb gene. J Mol Diagn 7:504–510

Part V

Vaccines for Human Fungal Diseases

Chapter 30

Dendritic Cell-Based Vaccine Against Fungal Infection

Keigo Ueno, Makoto Urai, Kayo Ohkouchi, Yoshitsugu Miyazaki, and Yuki Kinjo

Abstract

Several pathogenic fungi, including *Cryptococcus gattii*, *Histoplasma capsulatum*, *Coccidioides immitis*, and *Penicillium marneffei*, cause serious infectious diseases in immunocompetent humans. However, currently, prophylactic and therapeutic vaccines are not clinically used. In particular, *C. gattii* is an emerging pathogen and thus far protective immunity against this pathogen has not been well characterized. Experimental vaccines such as component and attenuated live vaccines have been used as tools to study protective immunity against fungal infection. Recently, we developed a dendritic cell (DC)-based vaccine to study protective immunity against pulmonary infection by highly virulent *C. gattii* strain R265 that was clinically isolated from bronchial washings of infected patients during the Vancouver Island outbreak. In this approach, bone marrow-derived DCs (BMDCs) are pulsed with heat-killed *C. gattii* and then transferred into mice prior to intratracheal infection. This DC vaccine significantly increases interleukin 17A (IL-17A)-, interferon gamma (IFN-γ)-, and tumor necrosis factor alpha (TNF-α)-producing T cells in the lungs and spleen and ameliorates the pathology, fungal burden, and mortality following *C. gattii* infection. This approach may result in the development of a new means of controlling lethal fungal infections. In this chapter, we describe the procedures of DC vaccine preparation and murine pulmonary infection model for analysis of immune response against *C. gattii*.

Key words Cryptococcosis, *Cryptococcus gattii*, Acapsular mutant, Glucuronoxylomannan, Fungal vaccine, Bone marrow-derived dendritic cells, DC vaccine, T-cell-inducing vaccine, Pulmonary infection

1 Introduction

Cryptococcus gattii is an emerging fungal pathogen that infects immunocompetent humans via the respiratory tract. This pathogen can colonize the lungs and often disseminates to the brain, causing cryptococcosis, a life-threatening infectious disease with a mortality rate of 8–20 %. Although *C. gattii* infection is typically endemic in tropical areas such as Australia and Papua New Guinea, outbreaks have recently been reported on Vancouver Island and in surrounding areas [1–4]. To promote awareness of this outbreak,

Sunil Thomas (ed.), *Vaccine Design: Methods and Protocols: Volume 1: Vaccines for Human Diseases*, Methods in Molecular Biology, vol. 1403, DOI 10.1007/978-1-4939-3387-7_30,

public health working groups have been organized in the Centers for Disease Control and Prevention of the United States and British Columbia [5, 6].

It is a key feature of highly virulent strains of *C. gattii* that they do not induce a strong inflammatory response after infection. Previous studies showed less migration of leukocytes and lower amounts of inflammatory cytokines in the lungs of mice experimentally infected with the *C. gattii* R265 strain that was clinically isolated during the Canadian outbreak than in those infected with *Cryptococcus neoformans* standard strain H99 [7–9]. A smaller amount of inflammatory cytokines was also observed in the cerebrospinal fluid of humans infected with *C. gattii* [10, 11]. A recent study induced a mixed infection of *C. neoformans* strain H99 and highly virulent *C. gattii* strain R265. Consequently, R265 infection inhibited chemokine expression and the infiltration of Th1 and Th17 cells in the lungs of mice infected with H99 [12]. These data suggest that the highly virulent *C. gattii* strain can suppress the inflammatory response rather than evade it.

This immunosuppressive response might be explained by the characteristics of cell components of *C. gattii*. It is known that *C. gattii* as well as *C. neoformans* cells are enveloped with capsular polysaccharides consisting of glucuronoxylomannan (GXM) and galactoxylomannan (GalXM) [13]. These polysaccharides not only protect yeast cells from environmental stress but can also be released in culture supernatant, where they are known as exopolysaccharides [13]. GXM and GalXM account for approximately 90 % and 10 %, respectively, of the total exopolysaccharides of *C. neoformans* [14, 15]. These polysaccharides can play an inhibitory role in numerous immune responses including cytokine production and leukocyte migration in vitro and in vivo [16]. Administration of purified GXM can inhibit inflammatory responses and improve symptoms in experimental endotoxin shock and rheumatoid arthritis [17, 18]. The results of these reports suggest that capsular polysaccharides play a role in the virulence of *C. gattii*.

The high virulence and immunosuppressive behavior of *C. gattii* often interfere with the analysis of protective immunity against *C. gattii* infection. In other words, the experimental "loss-of-function" approach using gene knockout mice may interfere with the study of protective immunity, owing to the immunosuppressive effect. A few studies have demonstrated protective immunity against highly virulent *C. gattii* using gene knockout mice, and this immunity remains to be elucidated [19, 20].

Recently, we demonstrated protective immunity against *C. gattii* infection by a gain-of-function approach using a dendritic cell (DC)-based vaccine [21]. DCs play a central role in T-cell activation [22] and can also be used as antigen delivery systems for vaccines against cancers or infections [23, 24]. Adoptive transfer of DCs pulsed with fungal cells or with fungal RNA has also been

used as a means of assessing T-cell-mediated immunity against pathogenic fungi [25–27]. In our study, mouse bone marrow-derived DCs (BMDCs) were pulsed with heat-killed *C. gattii* and were then adoptively transferred into mice prior to intratracheal *C. gattii* infection. This DC vaccine markedly increased interleukin 17A (IL-17A)-, interferon gamma (IFN-γ)-, and tumor necrosis factor alpha (TNF-α)-producing T cells in the lungs and spleen and ameliorated pathology, fungal burden, and mortality following *C. gattii* infection [21].

In this chapter, we describe an experimental DC vaccine used to study protective immunity against the fungal pathogen *C. gattii*. As described above, capsular components are known to suppress several immune responses by DCs [28, 29]. Accordingly, we used a capsule-deficient mutant of *C. gattii* (*cap60* deletion mutant, Δ*cap60* strain) as a vaccine antigen. To evaluate the vaccine's efficacy, serum antibody titer, T-cell response to antigen restimulation, and protective effect against infection are generally measured. We also describe the pulmonary infection model used to evaluate the efficacy of the DC vaccine.

2 Materials

2.1 Preparation of Heat-Killed C. gattii for Vaccine Antigen

1. *C. gattii* Δ*cap60* or other acapsular strains.
2. Yeast extract peptone dextrose (YPD) medium: 1 % [weight/volume (w/v)] yeast extract, 2 % (w/v) Bacto-Peptone, and 2 % (w/v) dextrose, sterilized by autoclaving. Add 2 % (w/v) agar to prepare YPD agar plate.
3. 50-mL Conical tubes with screw cap with 0.2-μm filter membrane (Greiner Bio-One).
4. Sterile and endotoxin-free Dulbecco's phosphate-buffered saline (DPBS; Invitrogen).
5. Disposable hemocytometer.

2.2 Preparation of BMDCs

1. C57BL/6J mice (Japan SLC).
2. RPMI 1640 complete medium: RPMI 1640 medium (Sigma) supplemented with 10 % fetal bovine serum (FBS), 1 % streptomycin–penicillin solution (Sigma; 10,000 units of penicillin and 10 mg/mL of streptomycin), 44 μM 2-mercaptoethanol.
3. Murine granulocyte–macrophage colony-stimulating factor (mGM-CSF; PeproTech).
4. 10-cm-diameter Petri dishes: Untreated for cell culture.
5. 26 G × 1/2 needle (TERUMO).
6. 2.5-mL syringe (TERUMO).
7. 70-μm Cell strainer (Corning).

8. Red blood cell (RBC) lysis buffer: Mix 9 volumes of 0.83 % (w/v) NH_4Cl and 1 volume of 200 mM Tris–HCl pH 7.6, prior to use. Sterilize each stock solution by filtering through a sterile 0.2-μm membrane and store at 4 °C.
9. Hemocytometer.
10. Trypan blue solution, 0.4 % (w/v), sterile-filtered (Sigma).

2.3 Vaccination with DC Vaccine

1. Heat-killed Δ*cap60* strain (1×10^9 cells/mL).
2. RPMI 1640 complete medium: RPMI 1640 medium (Sigma) supplemented with 10 % FBS, 1 % streptomycin–penicillin solution (Sigma; 10,000 U of penicillin and 10 mg/mL of streptomycin), 44 μM 2-mercaptoethanol.
3. Mouse granulocyte–macrophage colony-stimulating factor (mGM-CSF; PeproTech).
4. 10-cm-diameter Petri dishes, untreated for cell culture.
5. Sterile and endotoxin-free DPBS.
6. Hemocytometer.
7. Trypan blue solution, 0.4 % (w/v), sterile-filtered (Sigma).
8. C57BL/6J mice (Japan SLC).
9. 30 G × 1/2 needle (BD) and 1-mL syringe (TERUMO).

2.4 Evaluation of DC Vaccine Efficacy (Murine Pulmonary Infection Model)

1. Vaccinated and non-vaccinated C57BL/6J mice.
2. *C. gattii* clinical isolate R265, highly virulent strain.
3. YPD medium: 1 % (w/v) yeast extract, 2 % (w/v) Bacto-Peptone, and 2 % (w/v) dextrose, sterilized by autoclaving. Add 2 % (w/v) agar to prepare YPD agar plate.
4. 50-mL Conical tubes with screw cap with 0.2-μm filter membrane (Greiner Bio-One).
5. Sterile and endotoxin-free DPBS (Invitrogen).
6. Disposable hemocytometer.
7. Vaporizer and isoflurane.
8. 24 G × 3/4 indwelling needle (TOP Corporation).
9. Sterile stainless steel mesh (portable tea strainer with handle).
10. 2.5-mL Syringe (TERUMO).

3 Methods

The procedural scheme and representative results are shown in Figs. 1 and 2, respectively.

3.1 Preparation of Heat-Killed *C. gattii* for Vaccine Antigen

1. Fungal strains are generally maintained at −80 °C in glycerol stocks. To revive *C. gattii* cells, scrape off splinters of solid ice from glycerol stock using a sterile toothpick or disposable

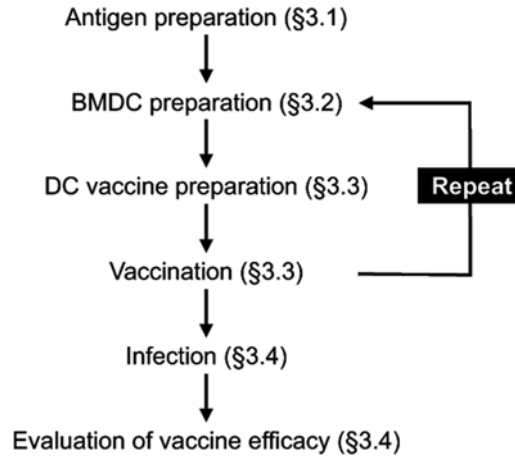

Fig. 1 Procedure scheme in this chapter. Each section number corresponds to the main text. In this chapter, we describe an experimental DC vaccine for studying protective immunity against the fungal pathogen *C. gattii* using a murine pulmonary infection model

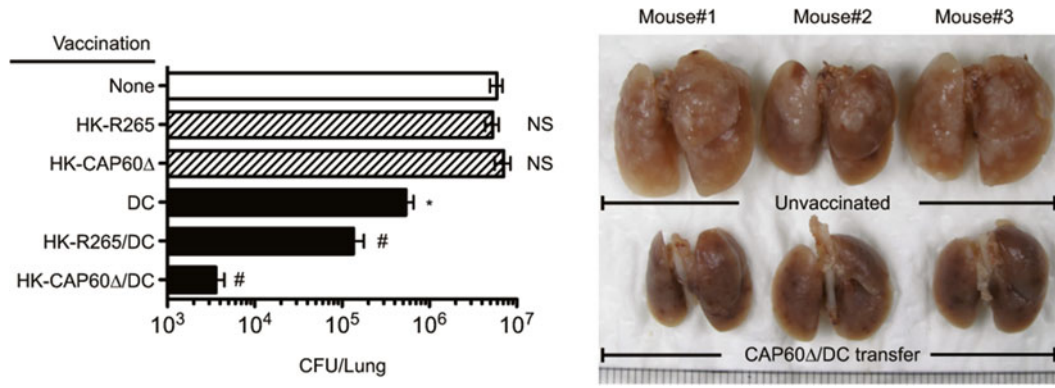

Fig. 2 Representative results of *C. gattii* murine pulmonary infection model. (**a**) Fungal burden in lungs. Heat-killed fungi (HK-R265 or HK-CAP60Δ: 5×10^6 CFUs/mouse), bone marrow-derived dendritic cell (DC: 5×10^5 cells/mouse), and DC pulsed with heat-killed fungi (HK-R265/DC or HK-CAP60Δ/DC: 5×10^5 cells/mouse) were administered intravenously twice 14 days and 1 day before the intratracheal infection of R265 (3×10^3 CFUs/mouse). Fungal burden in lungs was evaluated on day 14 postinfection. NS: nonsignificant difference vs. unvaccinated mice (None), * *t*-test $p < 0.05$ vs. None, # *t*-test $p < 0.05$ vs. DC. (**b**) Gross pathology of lungs. Lungs dissected from three mice at day 13 postinfection were fixed in 10 % formalin. The lungs of unvaccinated mice were swollen and showed awkward shapes and bumps. Lung homogenates of unvaccinated mice are usually very sticky and may contain higher amounts of the capsular component glucuronoxylomannan (GXM) produced by *C. gattii* cells

inoculation loop and streak onto a YPD plate. Incubate the plate at 30 °C for 2 days.

2. Pick five to ten colonies and inoculate into 10 mL of YPD liquid medium. Because *C. gattii* and other fungal cells strongly require oxygen for their propagation, aeration of culture containers should be ensured. It is recommended to use 50-mL

conical tubes that have a screw cap with a 0.2-μm filter membrane.

3. Shake YPD culture medium (170–200 rpm) overnight at 30 °C.
4. Harvest yeast cells (5000 × *g*, 5–20 min) and wash twice with sterile DPBS.
5. Resuspend yeast cells in a 1/10 volume ratio of DPBS. If cells are harvested from 10-mL cultures, cells are resuspended in 1 mL DPBS. At this point, approximately 2×10^9 cells/mL *C. gattii* suspension can be obtained. Using a hemocytometer, count cells, and adjust cell density to 1×10^9 cells/mL.
6. Transfer cell suspension to a new thermal-tolerant conical tube and boil for 1 h to kill fungal cells. Vortex the suspension every 15 min (*see* **Note 1**). Do not further wash heat-treated cells.
7. Spread the suspension onto YPD agar and incubate the plate at 30 °C for 7 days to verify that all *C. gattii* cells are dead.
8. Dispense the heat-killed cells in a small quantity (500–1000 μL), and store at −20 °C.

3.2 Preparation of BMDCs

1. Prepare two sterile 50-mL conical tubes and add 10 mL of RPMI 1640 complete medium to one and 40 mL of 70 % ethanol to the other. Place the tube containing medium in crushed ice until use (*see* **Note 2**).
2. Euthanize one to three mice with carbon dioxide and harvest femurs and tibias from both legs using forceps and scissors. Using paper towels, remove surrounding muscles and tissues manually and carefully. Soak bones in 70 % ethanol (50-mL conical tube) for 10 s to sterilize them, and then transfer bones into the complete medium (50-mL conical tube) with forceps. Keep the conical tube containing the bones in crushed ice until the next step (*see* **Note 3**).
3. Prepare three sterile 10-cm-diameter Petri dishes. Transfer medium and bones into the first Petri dish from the 50-mL conical tube. Because this medium contains a small amount of ethanol used for the sterilization described above, transfer bones to the second Petri dish and add 10–30 mL of fresh complete medium to the dish (*see* **Note 4**).
4. Hold the bone with forceps above the second dish and cut off both ends (epiphyses) of each bone using scissors. Mince the epiphyses in the second dish. To obtain the marrow, repeatedly flush out each of the shafts with the complete medium in the second dish using a 26 G × 1/2 needle and 2.5-mL syringe. Collect the marrow clumps in the third dish (*see* **Note 5**).
5. Prepare a sterile 50-mL conical tube and a 70-μm cell strainer, and set the strainer on the conical tube. Suspend the marrow

clumps in the second and third dishes, and pass the suspension through the cell strainer. The marrow clumps will be trapped on the cell strainer and a single-cell suspension will be collected in the conical tube.

6. Mash the marrow clumps on the cell strainer using the piston of a 2.5-mL syringe. Using 10 mL of fresh complete medium, rinse the second and third dishes. Pass the rinse fluid through the cell strainer. Verify that the membrane has been washed out completely.
7. Centrifuge (300 × *g*, 5 min, 4 °C) the cell suspension and harvest all cells including RBCs. To lyse erythrocytes, resuspend the harvested cells in 2–4 mL of RBC lysis buffer. Incubate for 5 min at room temperature and then add 9 volumes of complete medium (18–36 mL) to stop the lysis reaction.
8. Centrifuge (300 × *g*, 5 min, 4 °C) the cell suspension and resuspend in 10 mL of the complete medium. To remove debris, pass the suspension through a 70-μm cell strainer set on a 50-mL conical tube. Rinse the conical tube with 10 mL of the complete medium, and then pass the rinse fluid through the cell strainer. Finally, 20 mL of cell suspension will be obtained.
9. Centrifuge (300 × *g*, 5 min, 4 °C) the cell suspension to remove supernatant, and resuspend in 10 mL of the complete medium.
10. Count the viable cells using trypan blue dye. From one mouse, approximately 4×10^7 bone marrow cells can be obtained.
11. Adjust the cell concentration to 3×10^6 cells/mL with the complete medium, and then add recombinant mGM-CSF at 10 ng/mL. Transfer 10 mL of suspension (3×10^7 cells) to a sterile 10-cm-diameter Petri dish (untreated for cell culture). Ten dishes can be prepared from the bone marrow suspension derived from one mouse.
12. Incubate dishes for 3 days at 37 °C under 5 % CO_2.
13. On day 3, remove 6 mL of the medium in the culture and add 7 mL of fresh complete medium to the dish.
14. On day 5, add 5 mL of fresh complete medium. On day 6, collect nonadherent cells in the 15-mL culture by flushing the medium against the dish with a pipette, and pool the cell suspension of each dish. Rinse each dish with 5 mL of complete medium, and pool the rinse fluid together with the initially collected suspension (*see* **Note 6**).
15. Centrifuge (300 × *g*, 5 min, 4 °C) the cell suspension and resuspend in 10 mL of complete medium.
16. The viable cells can then be counted as BMDCs. From one mouse, approximately 1×10^8 BMDCs can be obtained (*see* **Note 7**).

3.3 Vaccination with DC Vaccine

1. Adjust the density of BMDCs to 1×10^6 cells/mL with complete medium and then add murine recombinant GM-CSF at 10 ng/mL and 5×10^6 cells/mL (MOI = 5) of heat-killed *C. gattii* (Δ*cap60* strain) to pulse BMDCs. Transfer 10 mL of suspension to a sterile 10-cm-diameter Petri dish (untreated for cell culture). Incubate dish for 24 h at 37 °C, under 5 % CO_2 (*see* **Notes 8–10**).
2. After incubation, BMDCs engulfing several acapsular *C. gattii* cells can be observed by microscopy. Collect nonadherent cells by flushing the medium against the dish with a pipette and pool the cell suspension of each dish. Rinse each dish with 10 mL of DPBS and pool the rinse fluid with the initially collected suspension.
3. Centrifuge ($300 \times g$, 5 min, 4 °C) the cell suspension, and wash harvested cells twice with sterile DPBS to remove residual mGM-CSF (*see* **Note 11**).
4. Count the viable cells. BMDCs and *C. gattii* cells can be distinguished by differing cellular sizes. From 12 dishes, approximately 3×10^7 cells (60 injections) can be harvested. Adjust the density of BMDCs pulsed with the heat-killed Δ*cap60* strain to 2.5×10^6 cells/mL with sterile DPBS, and keep the tube containing the suspension in crushed ice until next step (*see* **Note 12**).
5. Inject 200 μL of suspension (5×10^5 cells) via the tail vein as DC vaccine using a 30 G × 1/2 needle and 1-mL syringe. DC vaccines are administered twice every 2 weeks.

3.4 Evaluation of Vaccine Efficacy (Murine Pulmonary Infection Model)

1. Cultivate highly virulent *C. gattii* strain R265 in YPD liquid medium as described in Subheading 3.1.
2. After cultivation, dispense 1 mL culture suspension into a 1.5-mL microcentrifuge tube. Harvest yeast cells ($16{,}000 \times g$, 2 min) and wash twice with sterile DPBS (*see* **Note 13**).
3. Resuspend yeast cells in 1 mL of DPBS. Using a hemocytometer, count viable cells and adjust cell density to 6×10^4 cells/mL. Dilute this suspension serially and spread onto YPD medium to determine the colony-forming units (CFUs) in this suspension. Keep the tube containing the suspension in crushed ice until use.
4. Anesthetize mice using a vaporizer and isoflurane and intratracheally inject 50 μL of R265 suspension (3×10^3 CFUs/mouse) using a 24 G × 3/4 indwelling needle (*see* **Note 14**).
5. On the day before mouse dissection, prepare 15-mL conical tubes to include 2-mL sterile DPBS, and then weigh the tubes.
6. On day 14 post-infection, euthanize the mice by carbon dioxide inhalation and carefully and aseptically harvest their left and right lung lobes with forceps and scissors. Transfer dissected

lungs into the 15-mL conical tubes containing 2-mL sterile DPBS described above. Before dissecting the next mouse, soak the forceps and scissors in 70 % ethanol to sterilize them. Keep the tubes containing lungs in crushed ice until next step.

7. Weigh the tubes containing DPBS and harvested lungs. To calculate the lung weight, subtract the weight measured at **step 5** from the weight measured at this step. The infected lungs of nonvaccinated mice weigh approximately 500–600 mg.
8. Set the stainless steel mesh (autoclavable portable tea strainer with handle) on a sterile 10-cm-diameter Petri dish. Transfer the lungs and DPBS onto the steel mesh and manually homogenize using the piston of a 2.5-mL syringe. Collect the homogenates using a pipette and place back into the 15-mL conical tube (*see* **Note 15**).
9. Add 3–4 mL of sterile DPBS onto the steel mesh to rinse the mesh, dish, and pipette, and pool the rinse fluid together with the initial collecting suspension. Add sterile DPBS to the suspension to a final volume of 5–6 mL. Keep the tube containing the suspension in crushed ice until next step.
10. Serially dilute homogenates and spread 100 μL of the suspension onto YPD plates to determine the CFUs in this suspension. Incubate the plates at 30 °C for 24 h, after which the colonies can be counted. At day 14 postinfection, approximately 5×10^6 CFUs are detected in the lungs of nonvaccinated C57BL6 mice, in which sex, age, and individual differences are generally minor in this test. Thus, 30–200 colonies are detected on a YPD plate spread with 100 μL suspension of 10^3 diluting solution. Representative data of the fungal burden are shown in Fig. 2.

4 Notes

1. Although several protocols recommend a 1-h incubation period at 60 °C, this often results in incomplete killing of fungal cells.
2. For the preparation of BMDCs, ensure sterile practice. The protocol for BMDC preparation has also been described elsewhere [30].
3. Select mouse sex depending on experiment design. Male mice have bigger bones and larger numbers of progenitor cells for BMDCs [30]. If DCs are transferred to female mice, female mice are preferably chosen to prepare BMDCs.
4. It is recommended to use untreated Petri dishes for cell culture, which are generally used to prepare agar plates for microbial cultivation. If the cell-culture-grade dishes are used, BMDCs

will adhere strongly to the dishes and the yield of BMDCs will be decreased.

5. After the epiphyses are cut off, the bone shaft looks like a tube filled with red marrow. Marrow suspension, once flushed out, should not be aspirated again with the needle and syringe. Repeated flushing through the thin needle might damage the cells. The first dish should receive the uncut bone, the second dish is a reservoir of fresh medium and cut bone, and the third dish receives the marrow suspension flushed with fresh medium from the second dish.
6. If the cells are harvested on day 7, add 10 mL of fresh complete medium at this point. One dish will contain 20 mL of culture medium.
7. Harvested cells consist of $CD11c^+$ and $CD11c^-$ cells. Depending on the experiment design, $CD11c^+$ cells should be enriched using CD11c-MicroBeads and a MACS® Cell Separator (Miltenyi Biotec).
8. To boost the immunological function of BMDCs, it is not always necessary to add toll-like receptor ligands or vaccine adjuvant such as lipopolysaccharide. Interestingly, when BMDCs were pulsed with Δ*cap60* and α-galactosylceramide that is displayed on CD1d molecule-expressing BMDCs to stimulate natural killer T cells, the efficacy of DC-based vaccination against *C. gattii* infection was significantly decreased (unpublished data).
9. Protein antigens of *C. gattii* stimulating T-cell responses have not yet been identified. A recent immune-blotting analysis has indicated that protein antigens are recognized by serum antibodies harvested from mice infected with *C. gattii* [31]. Two protein antigens, MP98 (synonym for Cda2: chitin deacetylase) and d25 (polysaccharide deacetylase) of *C. neoformans*, have been reported to induce T-cell responses [32–35]. Immunization using recombinant d25 protein induces a Th1 response and decreases fungal burden in organs and mortality after *C. neoformans* infection in an IFN-γ-dependent manner [34, 35]. In contrast, a recent report suggested that MP98-specific T cells in the lungs on day 14 postinfection predominantly expressed the Th2 cytokines IL-5 and IL-13 when restimulated for 6 h with phorbol myristate acetate and ionomycin. Induction of MP98-specific T cells required priming with interferon regulatory factor 4-expressing conventional DC in the lungs and also required the digested cell wall produced by chitotriosidase, a host intrinsic factor encoded by the *Chit1* gene. This study also suggested that the digested fungal chitin stimulates pulmonary epithelial cells to release several Th2-inducing alarmins such as thymic-stromal lymphopoietin

(TSLP), and results in Th2 polarization during *C. neoformans* infection. Indeed, conventional DC accumulated in lungs highly expressing TSLP receptors after *C. neoformans* infection. Furthermore, survival rate was improved in *Chit1*-deficient mice after *C. neoformans* infection, correlated with the decrease of MP98-specific Th2 cells in lungs [32]. The amino acid sequences of MP98 and d25 are also highly conserved in *C. gattii*. Depending on the experiment design, appropriate antigen proteins should be used.

10. Capsular components are known to suppress several DC immune responses [28, 29]. We usually use heat-killed *C. gattii* capsule-deficient mutant (Δ*cap60*) as vaccine antigen.
11. Because *C. gattii* cells can also be precipitated with BMDCs by the centrifugation, they cannot be removed from the suspension.
12. Because some cells pulsed with heat-killed Δ*cap60* strain tend to adhere to the dish, cell yield tends to be greatly reduced. It was not tested in our study whether the adherent cells can be used for the vaccination; if they are, they should be gently collected by scraping the plates with a soft rubber spatula.
13. It is difficult to precipitate yeast cells enveloped with capsular polysaccharide. Culture supernatant should be removed as carefully as possible.
14. We usually use five mice per group for the fungal burden evaluation and eight mice per group for the mortality evaluation. Median survival time of nonvaccinated C57BL/6 mice infected with *C. gattii* R265 strain (3×10^3 CFUs) is 23–35 days, and mice begin to die on days 16–20 after infection. Thus, the fungal burden in lungs should be evaluated on days 3–15 after infection.
15. Because the lung homogenates of unvaccinated mice are generally very sticky at day 14 postinfection, the homogenates including the residual solution in the pipette should be carefully collected. An automatic homogenizing mixer (cf. ULTRA-TURRAX® Tube Drive Control and DT-20-M tube, IKA) can also be used to prepare lung homogenate.

Acknowledgements

This chapter described work supported by Health Science Research Grants for Research on Emerging and Re-emerging Infectious Diseases (H25-Shinkou-Shitei-001, H25-Shinkou-Shitei-002, H25-Shinkou-Wakate-005, H25-Shinkou-Ippan-006, and H26-Shinkoujitsuyouka-Ippan-010) from the Ministry of Health, Labor and Welfare of Japan, by the Research program on Emerging and

Re-emerging Infectious Diseases from Japan Agency for Medical Research and development, AMED, by KAKENHI (15K21644) from the Ministry of Education, Culture, Sports, Science, and Technology of Japan, and by a grant from the NOVARTIS Foundation (Japan) for the Promotion of Science.

References

1. Chen S, Sorrell T, Nimmo G et al (2000) Epidemiology and host- and variety-dependent characteristics of infection due to *Cryptococcus neoformans* in Australia and New Zealand. Australasian Cryptococcal Study Group. Clin Infect Dis 31:499–508
2. Galanis E, MacDougall L, Kidd S et al (2010) Epidemiology of *Cryptococcus gattii*, British Columbia, Canada, 1999–2007. Emerg Infect Dis 16:251–257
3. Smith RM, Mba-Jonas A, Tourdjman M et al (2014) Treatment and outcomes among patients with *Cryptococcus gattii* infections in the United States Pacific Northwest. PLoS One 9, e88875
4. Lizarazo J, Escandón P, Agudelo CI et al (2014) Retrospective study of the epidemiology and clinical manifestations of *Cryptococcus gattii* infections in Colombia from 1997–2011. PLoS Negl Trop Dis 8, e3272
5. BCCDC (2011) Environmental pathogens, *Cryptococcus gattii*. British Columbia annual summary of reportable diseases 2011, pp 112–113
6. CDC (2010) Emergence of *Cryptococcus gattii*, Pacific Northwest, 2004–2010. Morb Mortal Wkly Rep 59:865–868
7. Ngamskulrungroj P, Chang Y, Sionov E, Kwon-Chung KJ (2012) The primary target organ of *Cryptococcus gattii* is different from that of *Cryptococcus neoformans* in a murine model. mBio 3:e00103–e00112
8. Okubo Y, Wakayama M, Ohno H et al (2013) Histopathological study of murine pulmonary cryptococcosis induced by *Cryptococcus gattii* and *Cryptococcus neoformans*. Jpn J Infect Dis 66:216–221
9. Cheng P-Y, Sham A, Kronstad JW (2009) *Cryptococcus gattii* isolates from the British Columbia cryptococcosis outbreak induce less protective inflammation in a murine model of infection than *Cryptococcus neoformans*. Infect Immun 77:4284–4294
10. Einsiedel L, Gordon DL, Dyer JR (2004) Paradoxical inflammatory reaction during treatment of *Cryptococcus neoformans* var. *gattii* meningitis in an HIV-seronegative woman. Clin Infect Dis 39:e78–e82
11. Brouwer AE, Siddiqui AA, Kester MI et al (2007) Immune dysfunction in HIV-seronegative, *Cryptococcus gattii* meningitis. J Infect 54:e165–e168
12. Angkasekwinai P, Sringkarin N, Supasorn O et al (2014) *Cryptococcus gattii* infection dampens Th1 and Th17 responses by attenuating dendritic cell function and pulmonary chemokine expression in the immunocompetent hosts. Infect Immun 82:3880–3890
13. O'Meara TR, Alspaugh JA (2012) The *Cryptococcus neoformans* capsule: a sword and a shield. Clin Microbiol Rev 25:387–408
14. Frases S, Nimrichter L, Viana NB et al (2008) *Cryptococcus neoformans* capsular polysaccharide and exopolysaccharide fractions manifest physical, chemical, and antigenic differences. Eukaryot Cell 7:319–327
15. Cherniak R, Reiss E, Turner SH (1982) A galactoxylomannan antigen of *Cryptococcus neoformans* serotype A. Carbohydr Res 103: 239–250
16. Vecchiarelli A, Pericolini E, Gabrielli E et al (2013) Elucidating the immunological function of the *Cryptococcus neoformans* capsule. Future Microbiol 8:1107–1116
17. Monari C, Bevilacqua S, Piccioni M et al (2009) A microbial polysaccharide reduces the severity of rheumatoid arthritis by influencing Th17 differentiation and proinflammatory cytokines production. J Immunol 183: 191–200
18. Piccioni M, Monari C, Kenno S et al (2013) A purified capsular polysaccharide markedly inhibits inflammatory response during endotoxic shock. Infect Immun 81:90–98
19. Gibson JF, Johnston SA (2014) Immunity to *Cryptococcus neoformans* and *C. gattii* during cryptococcosis. Fungal Genet Biol 78:76–86
20. Mershon KL, Vasuthasawat A, Lawson GW et al (2009) Role of complement in protection against *Cryptococcus gattii* infection. Infect Immun 77:1061–1070
21. Ueno K, Kinjo Y, Okubo Y et al (2015) Dendritic cell-based immunization ameliorates pulmonary infection with highly virulent *Cryptococcus gattii*. Infect Immun 83: 1577–1586

22. Steinman RM, Witmer MD (1978) Lymphoid dendritic cells are potent stimulators of the primary mixed leukocyte reaction in mice. Proc Natl Acad Sci U S A 75:5132–5136
23. Palucka K, Banchereau J (2013) Dendritic-cell-based therapeutic cancer vaccines. Immunity 39:38–48
24. García F, Climent N, Assoumou L et al (2011) A therapeutic dendritic cell-based vaccine for HIV-1 infection. J Infect Dis 203:473–478
25. d'Ostiani CF, Del Sero G, Bacci A et al (2000) Dendritic cells discriminate between yeasts and hyphae of the fungus *Candida albicans*. Implications for initiation of T helper cell immunity in vitro and in vivo. J Exp Med 191:1661–1674
26. Bozza S, Perruccio K, Montagnoli C et al (2003) A dendritic cell vaccine against invasive aspergillosis in allogeneic hematopoietic transplantation. Blood 102:3807–3814
27. Roy RM, Klein BS (2012) Dendritic cells in antifungal immunity and vaccine design. Cell Host Microbe 11:436–446
28. Siegemund S, Alber G (2008) *Cryptococcus neoformans* activates bone marrow-derived conventional dendritic cells rather than plasmacytoid dendritic cells and down-regulates macrophages. FEMS Immunol Med Microbiol 52:417–427
29. Vecchiarelli A, Pietrella D, Lupo P et al (2003) The polysaccharide capsule of *Cryptococcus neoformans* interferes with human dendritic cell maturation and activation. J Leukoc Biol 74:370–378
30. Inaba K, Swiggard WJ, Steinman RM et al (2009) Isolation of dendritic cells. Curr Protoc Immunol 3.7.1–3.7.19
31. Chaturvedi AK, Hameed RS, Wozniak KL et al (2014) Vaccine-mediated immune responses to experimental pulmonary *Cryptococcus gattii* infection in mice. PLoS One 9, e104316
32. Wiesner DL, Specht CA, Lee CK et al (2015) Chitin recognition via chitotriosidase promotes pathologic type-2 helper T cell responses to cryptococcal infection. PLoS Pathog 11, e1004701
33. Levitz SM, Nong S, Mansour MK et al (2001) Molecular characterization of a mannoprotein with homology to chitin deacetylases that stimulates T cell responses to *Cryptococcus neoformans*. Proc Natl Acad Sci U S A 98: 10422–10427
34. Biondo C, Beninati C, Delfino D et al (2002) Identification and cloning of a cryptococcal deacetylase that produces protective immune responses. Infect Immun 70:2383–2391
35. Biondo C, Beninati C, Bombaci M et al (2003) Induction of T helper type 1 responses by a polysaccharide deacetylase from *Cryptococcus neoformans*. Infect Immun 71:5412–5417

Chapter 31

Flow Cytometric Analysis of Protective T-Cell Response Against Pulmonary *Coccidioides* Infection

Chiung-Yu Hung, Karen L. Wozniak, and Garry T. Cole

Abstract

The incidence of systemic fungal infections has increased throughout the world, spurring much interest in developing effective vaccines. Coccidioidomycosis, also known as San Joaquin Valley fever, is a potentially life-threatening respiratory mycosis. A vaccine against *Coccidioides* infection would contribute significantly to the well-being of the approx. 30 million residents in the Southwestern USA as well as the multitude of travelers who annually visit the endemic regions. We have applied a live, attenuated vaccine (ΔT) to explore the nature of vaccine immunity in mice after intranasal challenge with a potentially lethal dose of *Coccidioides* spores. *Coccidioides* spores are airborne and highly infectious for mammalian hosts and classified as a biosafety level 3 agent. T cells are critical in the development of protective immunity against a variety of microorganisms as well as the development of autoimmune disease and allergic responses. Profiles of cytokines detected in lung homogenates of ΔT-vaccinated mice were indicative of a mixed Th1, Th2, and Th17 immune response. We have developed an intracellular cytokine staining and flow cytometric (ICS) technique to measure activated $CD4^+$ and $CD8^+$ T cells and IFN-γ-, IL-4-, IL-5-, and IL-17A-producing T cells in the lungs of mice that are challenged with a potentially lethal dose of *Coccidioides* spores. The numbers of pulmonary Th1 and Th17 cells during the first 2 weeks post-challenge showed a progressive increase in vaccinated mice and corresponded with reduction of fungal burden. In this protocol, we describe the methodology for culture and isolation of the live, attenuated ΔT spores of *Coccidioides* used to vaccinate mice, preparation of pulmonary cells, and staining protocol for cell surface markers and intracellular cytokines. This is the most reliable and robust procedure to measure frequencies and numbers of each selected T-cell subsets in lungs of vaccinated versus control mice and can be readily applied to evaluate T-cell response against other microbial infections.

Key words Coccidioidomycosis, Antifungal immunity, IFN-γ, Th1 cells, IL-17A, Th17 cells

1 Introduction

A key challenge in the field of vaccine research has been the identification of correlates for vaccine efficacy [1–3]. Four methods have been commonly used for evaluation of cytokine expression of a particular population of immune cells: quantitative real-time PCR (RT-PCR), enzyme-linked immunosorbent assays (ELISA), enzyme-linked immunospot (ELISPOT), and immunohistochemistry (IHC)

Sunil Thomas (ed.), *Vaccine Design: Methods and Protocols: Volume 1: Vaccines for Human Diseases*, Methods in Molecular Biology, vol. 1403, DOI 10.1007/978-1-4939-3387-7_31,

and intracellular cytokine staining (ICS) followed by flow cytometric analysis. All have advantages and drawbacks: RT-PCR only measures mRNA levels of targeted cytokine genes, ELISA quantitates integrated amounts of secreted cytokines, IHC is useful for localization of cytokine-producing cells in tissues, while ELISPOT and ICS are the most appropriate ways to measure the frequency and numbers of cytokine-producing cells in blood samples or infected tissue. ICS flow cytometry is used to characterize the vaccine-induced response and evaluate phenotype and activation status of immune cells. In addition, this analytical method has also been employed to measure the proliferative capacity and polyfunctionality of T cells. The methodology and application of flow cytometry to measure intracellular cytokines have been well reviewed elsewhere [4–6]. The detection of intracellular cytokines by flow cytometry can be technically demanding, and often requires optimization by individual laboratories. In this chapter, we describe an optimized method to enumerate cytokine-producing $CD4^+$ and $CD8^+$ T cells in lungs of mice that are vaccinated with a candidate vaccine against respiratory *Coccidioides* infection, compared to non-vaccinated mice.

1.1 *Coccidioides* spp. are Formidable Fungal Pathogens of Mammalian Hosts

Coccidioides spp. are soilborne, etiological agents of coccidioidomycosis, also known as San Joaquin Valley fever, a potentially life-threatening mycosis endemic to the southwestern USA and arid regions of Mexico and Central and South America [7]. Two species of *Coccidioides* have been reported on the basis of molecular and biogeographical differences: *Coccidioides immitis* is found primarily in the San Joaquin Valley of California, while *Coccidioides posadasii* is widespread through other endemic regions [8]. In spite of the genetic diversity revealed by comparative genomic sequence analysis of these two species [9, 10], laboratory animal studies have shown no significant difference in either the virulence or the growth and development of the organism. The pathogen is a diphasic fungus that produces mycelia and air-dispersed spores when grown on a simple glucose-yeast extract (GYE) agar medium and a complex spherule-endospore cycle when cultured in a defined glucose/salt medium [11]. Inhalation of airborne spores by a mammalian host is followed by development of an elaborate parasitic cycle in lung tissue, which is unique amongst the medically important fungi. The parasitic cycle is initiated by conversion of the tiny barrel-shaped arthroconidia (spores; ca. 2×6 μm) into multinucleate round cells that grow isotropically to produce large spherules (60 to >100 μm in diameter). The content of a mature spherule undergoes a complex process of differentiation to yield an average of 200–300 endospores in vivo, each with an initial diameter of approximately 4–6 μm. Endospores that are released from the maternal spherule and survive within the host undergo isotropic growth and give rise to a second generation of endosporulating spherules [12]. Plate cultures of the saprobic phase of *Coccidioides*

grown in laboratory incubators produce large numbers of dry spores which can easily contaminate the environment if not handled properly. All mammals that reside in the endemic regions are at risk of contracting coccidioidal infection. The C57BL/6, BALB/c, and HLA-DRB1*0401 (HLA-DR4) transgenic mouse strains are highly susceptible to intranasal infection with *Coccidioides* spores ($LD_{100} < 50$ spores; [13, 14]). Handling of live cultures of *Coccidioides* spp. and infected animals must be maintained in a facility with biological safety level 3 (BSL3) containment because of the highly infectious nature of *Coccidioides* arthroconidia.

Every year, an estimated 150,000 people in the USA become infected with *Coccidioides*. Approximately 60 % of these human exposures are asymptomatic infections, while 40 % present with symptoms that range from a self-limited pulmonary, influenza-like illness to a life-threatening, disseminated disease [15]. Progressive pulmonary coccidioidomycosis, resembling other examples of community-acquired pneumonia, is responsible for nearly one-third of patients presenting with lower respiratory tract symptoms in endemic areas [16, 17]. Given that there are no good measures to avoid exposure to this typically airborne fungal pathogen, development of a vaccine and effective adjuvant platform for enhancement of host responses are badly needed. A compelling argument for the feasibility of such a vaccine is based on retrospective clinical evidence that individuals who recover from symptomatic coccidioidal infection remain skin test positive and likely acquire lifelong immunity to this disease. Vaccination against *Coccidioides* infection has been argued to be a cost-effective intervention [18].

1.2 Whole-Cell Vaccines against Coccidioides Infection

The development of safe and efficacious vaccines has been a major hurdle for prevention and treatment of fungal infections. The use of a formalin-killed spherule (FKS) vaccine in murine models of coccidioidomycosis has been shown to be effective [19]. Mice were immunized by the intramuscular route with approximately 3.2 mg of a formalin-fixed mixture of immature and mature spherules and endospores. Vaccinated C57BL/6 and BALB/c mice were fully protected against a potentially lethal respiratory challenge with the pathogen. However, in spite of its success as a protective reagent in mice and nonhuman primates, FKS failed as a candidate human vaccine in a phase 3 clinical trial [20]. The killed spherule vaccine did not demonstrate significant reduction of the incidence or severity of coccidioidomycosis in humans. The FKS vaccine elicits an intense inflammatory reaction at sites of vaccination [21]. The lack of efficacy in humans may have been due, at least in part, to severe inflammatory response at the sites of injection which necessitated adoption of a suboptimal dose of FKS.

Live vaccines typically elicit a broad spectrum of antigen-specific antibody responses by plasma cells as well as development of long-term T and B cell memory, thereby inducing optimal

immunity by activation of many effectors targeted by a multitude of antigenic molecules of the pathogen [22]. The essential factor shared by live vaccine strains which have been promoted to clinical trials is that their disease-causing capacity is eliminated by genetic or technical manipulations, thus prohibiting reversion to the virulent state. A genetically defined, live-attenuated strain of *C. posadasii* (ΔT) was generated which lost its ability to endosporulate in vivo but is able to elicit protective immunity to coccidioidomycosis (100 % survival) in disease-susceptible mice [23]. Loss of reproductive capacity of the *Coccidioides* mutant was attributed to targeted disruption of two chitinase genes (*CTS2* and *CTS3*). The combined expression of these genes in the parental strain was shown to be essential for endospore differentiation and reproduction of the pathogen both in vitro and in infected lung tissue [23]. The vaccine strain grows normally in GYE agar and produces spores that are isolated and used to vaccinate mice. The spores convert to sterile parasitic cells (Fig. 1) and remain localized at sites of immunization for 6–8 weeks after completion of the vaccination protocol. Immunological studies of C57BL/6 and BALB/c mice immunized with the live ΔT vaccine against a potentially lethal *Coccidioides* lung infection have yielded new insights into the nature of vaccine immunity to coccidioidomycosis [24–28]. These information can be harvested for developing a safe and effective subunit vaccine that is under way [29].

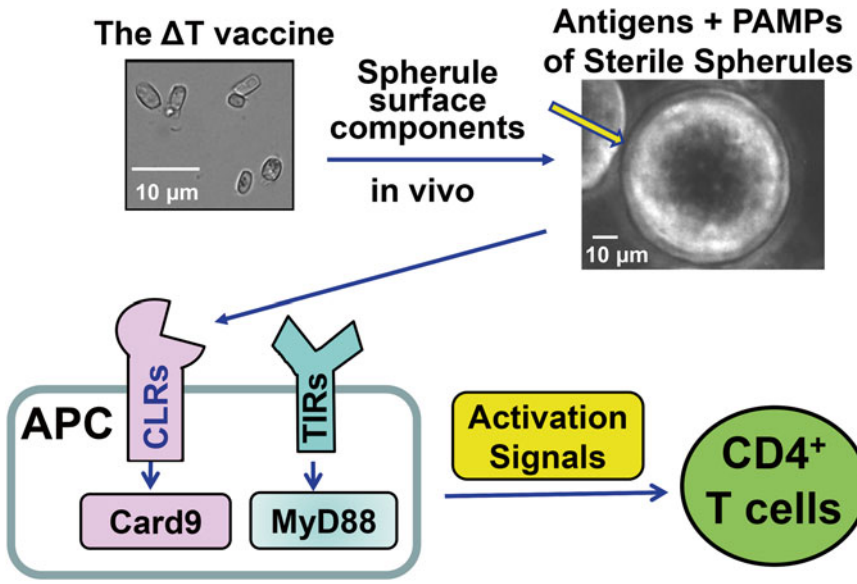

Fig. 1 The live, attenuated ΔT vaccine elicits protective T-cell-mediated immunity against lung infection with *Coccidioides*. The live ΔT spores convert into sterile spherules that provide antigens and pathogen-associated molecular patterns (PAMPs) to interplay with the innate immune receptors including C-type lectin receptors (CLRs) and Toll-like/IL-1 receptors (TIRs). Immune adaptors Card9 and MyD88 transduce the signals to prime and activate $CD4^+$ T cells

1.3 Protective Vaccine Immunity against the Respiratory Disease

T cells are essential for protective cell-mediated immune responses against fungal infections. Studies of the signal pathways required for T-cell immunity have revealed that induction of MyD88- and Card9-mediated Th17 responses is essential for vaccine immunity to *Coccidioides* infection [26, 27] (Fig. 1). The ability of T cells to differentiate into different types of memory and effector cell populations is a critical determinant of host protection against microbial pathogens (Fig. 2). Different subsets of T cells play specific roles in an immune response induced by different antigens and pathogens [30]. They are highly adaptive cells that initiate as naive cells and gradually mature through different antigen-specific stages until they become exhausted, senescent T cells [31, 32]. Host defenses mounted in response to invasion by dimorphic fungi are largely Th1 driven and disease exacerbation is a consequence of an imbalance between type 2 immunity and/or IL-10 and Th1 responses [33–38]. Many studies of coccidioidomycosis conducted before Th17 was discovered have reported IFN-γ production as a correlate of vaccine-induced protection in mice [21, 37–40]. Our data support the concept that activation of $CD4^+$ effector T cells including Th17 and Th1 cells can enhance recruitment of phagocytes to alveoli and promote early reduction of fungal burden while dampening inflammatory pathology at infection sites [25, 41, 42].

1.4 Application of ICS to Evaluate T-Cell Activity in Coccidioides-Infected Lungs

Multicolor flow cytometry allows single-cell analysis of markers and cytokines that are differentially expressed during T-cell activation and differentiation, shedding light on their distinct functional properties and relative contribution to vaccine immunity [43, 44]. The successful application of this technique is generally composed of (1) in vitro activation and inhibition of cytokine secretion to accumulate cytokines intracellularly, (2) immobilization of cytokines within the cells by fixation, (3) permeabilization, followed by (4) immune staining with specific fluorochrome-conjugated antibodies that bind cytokines in their fixed form. Flow cytometers are complex instruments that require a well-trained and in most instances a full-time operator. However, a cytometer is sometimes not available when samples cannot be brought out of a high-contaminant laboratory, which is the case for *Coccidioides*-infected tissues. We have developed an optimized ICS analysis using a four-color cytometer housed inside a biosafety level 3 laboratory used to measure the vaccine-induced T-cell responses.

2 Materials

Prepare all media and buffers using ultrapure water with resistivity of 18 MΩ·cm at 25 °C. Use only tissue-culture-grade reagents. Store all reagents at 4 °C unless otherwise indicated.

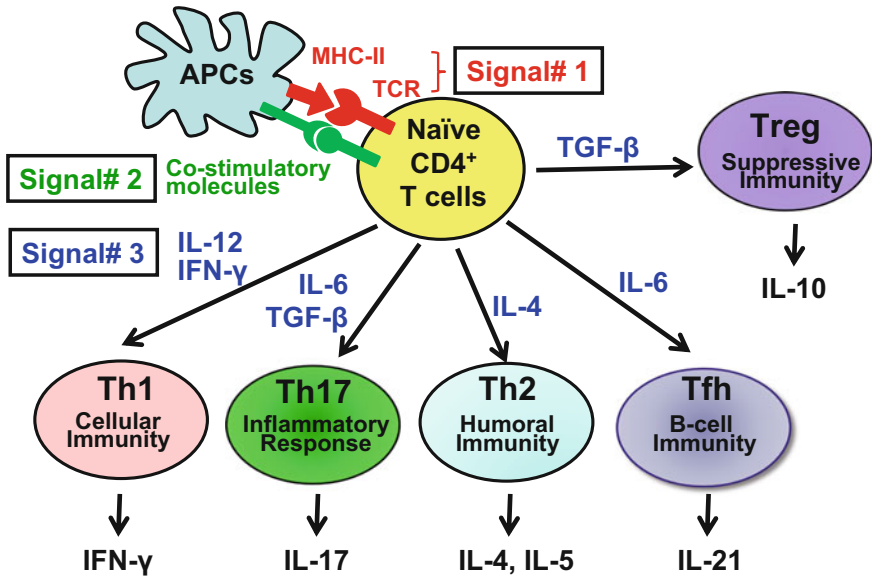

Fig. 2 Subsets of polarized CD4+ T helper (Th) cells produce restricted patterns of cytokines. Three vaccine-induced signals are required for the development and differentiation of T cells. Their selective cytokine production is important for the proper elimination of microbial pathogens; intracellular microbes for Th1 cells, and helminths for Th2 cells. However, recent studies of Th cells have revealed more flexibility in cytokine production than predicted by earlier work [30]

2.1 Preparation of the Live-Attenuated Δ T Vaccine and Vaccination Protocol

1. GYE agar plates: 1 % glucose, 0.5 % yeast extract, 2 % Bacto-agar. Add 5 g glucose plus 2.5 g yeast extract to 400 ml water in a 1 L flask and stir the solution until both ingredients are dissolved. Add water to a final volume of 500 ml and then add 10 g of Bacto-agar to the flask. Cover the flask with a piece of aluminum foil and autoclave for 20 min at 121 °C and 18 psi. Cool the autoclaved medium to 55–60 °C and pour 25 ml into each Petri dish (100 × 15 mm) (*see* **Note 1**).
2. Autoclaved 5 mm diameter glass beads (Kimble-Chase; *see* **Note 2**).
3. 50 ml polycarbonate Oak Ridge tubes with silicon gasket and screw cap.
4. Cell lifters (Corning).
5. T-shaped spreader.
6. 1 ml syringes (27 G) for vaccination.
7. A centrifuge with covered rotors for 50 ml conical tubes and 96-well tissue culture plates.

2.2 Harvesting Lungs and Preparing Pulmonary Cells

1. Sterile dissecting equipment.
2. Sterile droppers and 10 ml pipettes.

3. 200 µl pipette tips with large orifice (USA Scientific Inc.).
4. 50 ml conical tubes.
5. Petri dishes (60 mm × 15 mm diameter).
6. 3 ml Syringes.
7. 70 µm Cell strainers (Fisher scientific).
8. 40 µm Cell strainers (Fisher scientific).
9. 6-Well flat-bottom tissue culture plates.
10. Tissue disruption (TD) buffer: RPMI 1640 + 1 % (v/v) heat-inactivated fetal bovine serum (FBS).
11. cRPMI 1640: RPMI 1640 + 10 % (v/v) heat-inactivated FBS + 100 IU/ml penicillin + 100 µg/ml streptomycin.
12. ACK lysing buffer (Lonza) used to lyse red blood cells.
13. 0.4 % Trypan blue.
14. Hemocytometer, cover glasses, and a microscope.

2.3 Staining Cell Surface Markers

1. FACS buffer: 1 × PBS + 0.5 % (v/v) heat-inactivated FBS.
2. Fc block reagent (anti-mouse CD16/CD32): 2.5 µl in 1 ml FACS buffer; 100 µl per staining sample.
3. 96-Well round (U)-bottom plates.
4. Fluorochrome-conjugated monoclonal antibodies (*see* Table 1 and **Note 3**).
5. Splenocytes used for staining compensation tubes and isotype control tubes.
6. 2 % (w/v) paraformaldehyde in 1× PBS without Ca^{2+} and Mg^{2+}.
7. Sheath solution.

Table 1
Fluorochrome-conjugated monoclonal antibodies

Name of antigen	Fluorochrome conjugate	Antibody clone no.	Working concentration (µg/50 µl)	Isotype control
Cell surface markers				
CD45	APC, PerCP	1730-F11	0.20	Rat IgG2b
CD4	FITC	RM4-5	0.25	Rat IgG2a
CD8	PerCP	53-6.7	0.25	Rat IgG2a
CD44	PE	IM7	0.20	Rat IgG2b
Intracellular cytokine markers				
IL-4	APC	11B11	0.25	Rat IgG1
IL-5	PE	TRFK-5	0.25	Rat IgG1
IL-17A	PE	TC11-18H10	0.25	Rat IgG1
IFN-γ	APC	XMG1.2	0.25	Rat IgG1

8. 5 ml FACS tubes (12 × 75 mm).
9. FACSCalibur or any four-color cytometer that can detect FITC, PE, PerCP, and APC.
10. FLOWJo software for data analysis (FLOWJO, LLC).

2.4 Intracellular Cytokine Staining

1. Cell stimulation buffer: cRPMI1640 containing 0.1 μg/ml anti-CD3e (BD Biosciences) and 1 μg/ml anti-CD28 (BD Biosciences) antibodies, 4 ml per mouse.
2. GolgiStop (BD Biosciences), an inhibitor for cytokine secretion.
3. Fixative: Cytofix/Cytoperm (BD Biosciences), 100 μl per staining sample.
4. 1× Permeabilization buffer: Add 1 part of 10× Perm/Wash buffer (BD Biosciences) with 9 parts of FACS buffer, 400 μl per staining sample.

3 Methods

3.1 Preparation of the Live-Attenuated Δ T Vaccine, Immunization, and Challenge

1. All culturing and preparatory procedures which involved live cells of *Coccidioides* are conducted in an annually certified biosafety cabinet located inside a biosafety level 3 laboratory. Prepare 1 L of freshly made 20 % bleach in a 2 L beaker and an autoclaveable red bag inside the biosafety cabinet as a disinfectant station and a waste collection container, respectively. Discard all solution and used consumable supplies into the disinfectant tank immediately after usage.
2. Collect spores (arthroconidia) from 4 to 8 GYE agar plate cultures of *Coccidioides* (2–4 weeks old) by scraping the plates with a sterile cell lifter (Corning Inc.). Transfer the spore mat into an autoclaved Oak Ridge tube provided with a silicone gasket and screw cap. Add 10 ml 1× PBS and 15 autoclaved glass beads (5 mm diameter, Kimble Chase), screw the cap tightly, and shake vigorously by hand for 30 s.
3. Filter the suspension through a 40 μm sterile cell strainer to remove hyphal fragments. Collect the spores in a sterile Oak Ridge centrifuge tube.
4. Pellet the spores by centrifugation at 1200 × *g* for 10 min at room temperature, discard the supernatant into the disinfectant tank, and resuspend the spores in 5 ml 1× PBS.
5. Determine the concentration of spores using a hemocytometer.
6. Dilute the spores to 10^7 spores/ml with 1× PBS for long-term storage in a 4 °C refrigerator (*see* **Note 4**).
7. Prepare an aliquot of diluted spores (10^3 spores/ml) with 1× PBS. Plate five GYE plates each with 100 μl of the diluted spores for testing viability (*see* **Note 5**).

8. Incubate the plates upside down in a 30 °C steady incubator for 3 days.
9. Count colony-forming units (CFUs) at the end of the 3-day incubation (*see* **Note 6**).
10. Prepare an aliquot of the ΔT spores at a concentration of 2.5×10^5 CFUs/ml.
11. Vaccinate C57BL/6 mice with 200 μl (5×10^5 CFU) of the spore solution via the subcutaneous route on the abdominal site. The mice are boosted once with 100 μl (2.5×10^5 CFU) of the spore solution at 2 weeks after the first immunization (*see* **Note 7**).
12. Control mice are injected with 200 μl of 1× PBS.
13. The vaccinated and control mice are housed for 4 weeks before challenge inside an animal biosafety level 3 laboratory.
14. Prepare the wild-type inoculum using *Coccidioides posadasii* C735 isolate, a highly virulent strain as described in **steps 2–9**.
15. Prepare an aliquot of C735 spores at a concentration of 2.5×10^3 CFU.
16. Both the vaccinated and control mice are anesthetized with isoflurane using an isoflurane vaporizer and challenge with potentially lethal dose of spores (75–90 spores in 35 μl) via an intranasal instillation method.
17. Plate five GYE plates, each with 35 μl of the spore solution to confirm the challenge dose.

3.2 Preparation of Pulmonary Cell Suspension and Activation of T Cells

1. Dissect lungs from euthanized mice at 7, 9, 11, and 14 days postchallenge into 5 ml RPMI + 1 % FBS medium (*see* **Note 8**).
2. Place lungs from individual mice in a 70 μl cell strainer that is placed in a Petri dish. Mash lungs with the back of a 3 ml syringe plunger. Filter the cells through a 70 μm cell strainer into a 50 ml conical tube (*see* **Note 9**).
3. Mash the tissue with an additional 3 ml of RPMI + 1 % FBS medium. Combine the total of 8 ml cell solution from each mouse in a 50 ml conical tube.
4. Centrifuge for 10 min at 300 × *g*, 4 °C.
5. Aspirate and discard the supernatant, resuspend the cells in 2 ml of ACK lysing buffer, and then wait for 5 min at room temperature.
6. Stop the reaction by adding 6 ml of RPMI + 1 % FBS medium.
7. Filter the sample through a 40 μm cell strainer into a 50 ml conical tube to remove membrane debris.
8. Centrifuge for 10 min at 300 × *g*, 4 °C.
9. Aspirate and discard the supernatant. Resuspend the cells in 1 ml cRPMI.

10. Determine the concentration of cells using a hemocytometer (*see* **Note 10**). *The total cell number per lung organ is determined to contain N cells.*
11. Aliquot 50–100 μl of cell suspension (~10^6 cells) into a well of a 96-well round-bottom plate for cell surface marker staining to detect percentages of $CD45^+$, $CD4^+$, $CD8^+$, and $CD44^+$ cells (*see* Table 1).
12. The remaining cells are pelleted down and resuspended in 4 ml cell stimulation buffer (*see* **Note 11**).
13. Transfer the cells into a well of a 6-well tissue culture.
14. Add 2 μl GolgiStop immediately into each well. Incubate the cells in a CO_2 incubator (5 %) at 37 °C for 4 h.

3.3 Staining Cell Surface Markers

1. Add 100 μl of Fc block solution to each sample well. Pipet up and down 2–3 times using a large-orifice 200 μl tip to break up cell clumps. Incubate at 4 °C for 15 min.
2. While cells are incubating, prepare the required amount of fluorochrome-conjugated anti-CD45, CD4, CD8, and CD44 antibody working solution for all the samples (*see* Table 1 and **Note 12**). The required volume is calculated as follows: (sample number + 1) × 50 μl.
3. Aliquot 2×10^6 splenocytes into each well of total of 5 wells that are separately stained with isotype antibodies, anti-CD45-APC, anti-CD4-FITC, anti-CD8-PerCP, and anti-CD44-PE, respectively. These samples incubated with isotype antibodies are used as a negative control while the other four tubes are used to create the compensation matrix and cytometer settings.
4. Centrifuge the plate for 10 min at 300 × *g*, 4 °C.
5. Aspirate the supernatant and resuspend the cells in 50 μl of the antibody cocktail. Pipette cells up and down to break cell clumps. Incubate at 4 °C for 30 min in the dark.
6. At the end of incubation, add 200 μl of ice-cold FACS buffer to each well.
7. Centrifuge for 10 min at 300 × *g*, 4 °C. Aspirate and discard the supernatant.
8. Wash one more time with 200 μl ice-cold FACS buffer.
9. Add 200 μl 2 % paraformaldehyde in PBS
10. Transfer each sample to a labeled FACS tube. Add 200–300 μl sheath solution.
11. Perform flow cytometry analysis on the surface-stained cells.

3.4 Intracellular Cytokine Staining

1. At the end of 4 h of incubation, the cell culture is filtered through a 40 μm cell strainer into a 50 ml conical tube.
2. Centrifuge for 10 min at 300 × *g*, 10 °C. Aspirate and discard the supernatant.

3. Resuspend all samples in 200 μl of Fc block solution. Pipette up and down to break cell clumps.
4. Aliquot entire sample equally into two wells of a 96-well round-bottom plate. Incubate for 15 min at 4 °C
5. Centrifuge for 10 min at 300 × *g*, 10 °C. Aspirate and discard the supernatant.
6. Resuspend in 100 μl Cytofix/Cytoperm (BD Biosciences).
7. Incubate at 4 °C for 20 min in the dark.
8. While the sample incubates, prepare 1× Perm/Wash buffer (BD Biosciences).
9. Pellet the cells down and resuspend in 200 μl 1× Perm/Wash buffer.
10. Pellet the cells down and wash one more time.
11. Stain the cells with 50 μl of fluorochrome-conjugated staining cocktail containing antibodies to CD4, CD8, IL-17A, and IFN-γ or antibodies to CD4, CD8, IL-4, and IL-5.
12. The stained cells are washed and cytometrically analyzed as described in **steps 5–10** of the cell surface staining protocol.

3.5 Gating Strategy and Data Analysis

1. The stained cells are analyzed using a four-color DB FACSCalibur cytometer. The instrument settings and compensation matrix are determined using splenocytes separately stained with isotype control antibodies, anti-CD4-FITC, anti-CD44-PE, anti-CD8-PerCP, and anti-CD45-APC. The positive signal for each fluorochrome-labeled sample is used to determine the positive gates. The data are exported using the FSC3.0 format type.
2. The data is first displayed in an FSC vs. SSC dot plot to gate out debris at the left lower corner and aggregates on the right and top borders (Fig. 3a).
3. The percentages of $CD45^+$ cells within the gated pulmonary cells are determined. The gated $CD45^+$ cells are displayed on a CD4 vs. CD8 plot to determine $CD4^+CD8^-$ and $CD4^-CD8^+$ cell populations. The percentages for $CD45^+$, $CD4^+CD8^-$, and $CD4^-CD8^+$ cells are delegated as P_{CD45}, P_{CD4}, and P_{CD8} %, respectively (Fig. 3b, c).
4. The percentages of $CD44^+$ cells within the gated $CD4^+CD8^-$ and $CD4^-CD8^+$ cell population are also determined (Fig. 3d, e).
5. The numbers of $CD4^+CD8^-$ and $CD4^-CD8^+$ T cells in lungs of each individual mouse are determined by $N \times P_{CD45}\ \% \times P_{CD4}\ \%$ (N_{CD4}) and $N \times P_{CD45}\ \% \times P_{CD8}\ \%$ (N_{CD8}), respectively.
6. The numbers of activated $CD4^+$ and $CD8^+$ T cells are calculated by $N_{CD4} \times P_{CD4+CD44+}\ \%$ and $N_{CD8} \times P_{CD8+CD44+}\ \%$, respectively.
7. The numbers of Th1, Th17, and double-positive cells for IFN-γ and IL-17A are calculated by $N_{CD4} \times$ Th1 %, $N_{CD4} \times$ Th17

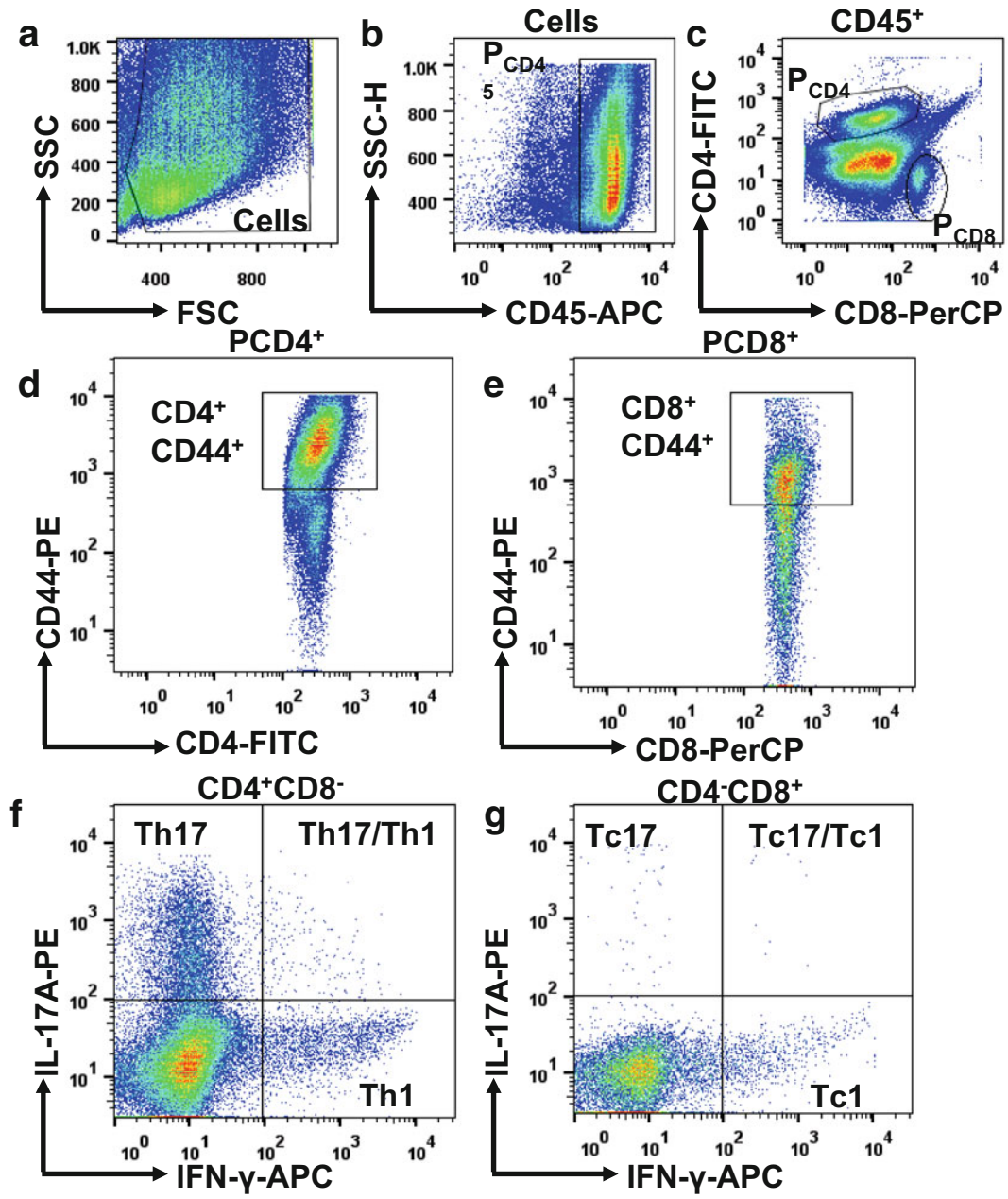

Fig. 3 Gating strategy for determination of percentages and numbers of activated $CD4^+$ and $CD8^+$ T cells as well as IFN-γ- and IL-17A-producing $CD4^+$ and $CD8^+$ T cells. Data are compensated and gated using FLOWJo software to define $CD4^+$ and $CD8^+$ T-cell subsets. (**a**) Total events are displayed in an FSC versus SSC plot. (**b**) Gated pulmonary cells are analyzed in a CD45-APC versus SSC plot. $CD45^+$ cells are gated and displayed in (**c**) in a CD4 versus CD8 plot. (**d**, **e**) $CD44^+$ cells are shown in gated $CD4^+CD8^-$ and $CD4^-CD8^+$ populations. (**f**, **g**) The gated $CD4^+CD8^-$ and $CD4^-CD8^+$ cells are analyzed in an IFN-γ versus IL-17A plot to determine percentages of Th1, Th17 Th17/Th1, Tc1, Tc17, and Tc17/Tc1 populations

% and $N_{CD4} \times$ Th17/Th1%, respectively (Fig. 3f). Similarly, subsets of $CD8^+$ T cells (Tc 1, Tc17, Tc17/Tc1) can also be calculated (Fig. 3g).

8. At least four mice per group at selected time points after *Coccidioides* infection are required for calculation of statistical significance using Mann–Whitney ranking test.

4 Notes

1. These plates are used to culture the saprobic phase of *Coccidioides* and to produce spores (arthroconidia). *Coccidioides* will produce spores on GYE plates after incubation for 2–4 weeks at 30 °C.
2. Add 10–15 beads in 50 ml Oak Ridge tubes with 10 ml 1× PBS for gently breaking *Coccidioides* hyphae and harvest spores (arthroconidia). Check the presence of an O-ring before capping the tube to avoid leakage.
3. All fluorochrome-conjugated antibodies are purchased from BD Pharmingen. The use of antibodies purchased from other commercial sources may require optimization of titers.
4. *Coccidioides* spores are very hardy. We observe that a low density ($<10^6$ spores/ml) of spores tend to adhere to the wall of the 50 ml conical tube and cause loss of spore density over time. Storing the spores at 10^7 spores/ml can last for a period of 6 months in a 4 °C refrigerator.
5. Only the spore preparation with cell viability over 90 % can be used for vaccination and challenge.
6. *Coccidioides* spp. form a white to milky color, spider web-like colonies about 1–2 mm in diameter at the end of the 3-day incubation. Presence of smooth and big colonies on GYE plates is an indication of contamination.
7. Redness of injection sites with the ΔT vaccine begins after 24 h and it disappears within 5 days after the immunization.
8. Take care to exclude the thymus, a white tissue located above the heart. Otherwise, the total number of lung cells will appear to be greatly increased.
9. Mash lung tissue quickly until the majority of red color disappears.
10. We routinely obtain $5–15 \times 10^6$ pulmonary cells from each mouse weighted 20–23 g.
11. Cell pellets are lost in the bottom of centrifugation tubes. Carefully aspirate and discard the supernatant to avoid cell loss.

12. Examples of staining antibody cocktails for cell surface markers:

    Cell surface marker antibody cocktail: ___10___ samples

    FACS buffer: ___463___ μl

    CD4-FITC (BD Cat. #553047; 0.5 μg/μl; 0.50 μl/sample): ___5___ μl

    CD44-PE (BD Cat. #563134; 0.2 μg/μl; 1 μl/sample): ___10___ μl

    CD8a-PerCP (BD Cat. #551162; 0.2 μg/μl; 1.25 μl/sample): ___12___ μl

    CD45-APC (BD Cat. #559864; 0.2 μg/μl; 1 μl/sample): ___10___ μl

    ICS antibody cocktail: ___10___ samples

    FACS buffer: ___461___ μl

    CD4-FITC (BD Cat. # 553047; 0.5 μg/μl; 0.50 μl/sample): ___5___ μl

    IL-17A-PE (BD559502; 0.2 μg/μl; 1 μl/sample): ___10___ μl

    CD8a-PerCP (BD551162; 0.2 μg/μl; 1.25 μl/sample): ___12___ μl

    IFN-γ-APC (BD554413; 0.2 μg/μl; 1.25 μl/sample): ___12___ μl

Acknowledgements

This work was supported by research grants from the National Institutes of Health, NIAID (R01 AI-071118 and R21 AI-114762) awarded to G.T.C.and C.Y.H., respectively. Additional support was provided by the Margaret Batts Tobin Foundation, San Antonio, TX, and *Coccidioides* research funds donated by the Valley Fever of the Americas Foundation and community supporters. We would like to acknowledge the assistance of the Immune Defense Core Facility at UTSA supported by a grant from the National Institute on Minority Health and Health Disparities from the National Institutes of Health (G12MD007591).

References

1. Bhatt K, Verma S, Ellner JJ et al (2015) Quest for correlates of protection against tuberculosis. Clin Vaccine Immunol 22:258–266
2. De Pascalis R, Chou AY, Ryden P et al (2014) Models derived from in vitro analyses of spleen, liver, and lung leukocyte functions predict vaccine efficacy against the Francisella tularensis Live Vaccine Strain (LVS). MBio 5, e00936
3. Matsumiya M, Satti I, Chomka A et al (2015) Gene expression and cytokine profile correlate with mycobacterial growth in a human BCG challenge model. J Infect Dis 211:1499–1509

4. De Rosa SC (2012) Vaccine applications of flow cytometry. Methods 57:383–391
5. Pala P, Hussell T, Openshaw PJM (2000) Flow cytometric measurement of intracellular cytokines. J Immunol Methods 243:107–124
6. Prussin C, Metcalfe DD (1995) Detection of intracytoplasmic cytokine using flow cytometry and directly conjugated anti-cytokine antibodies. J Immunol Methods 188:117–128
7. Brown J, Benedict K, Park BJ et al (2013) Coccidioidomycosis: epidemiology. Clin Epidemiol 5:185–197
8. Fisher MC, Koenig GL, White TJ et al (2002) Molecular and phenotypic description of *Coccidioides posadasii* sp. nov., previously recognized as the non-California population of *Coccidioides immitis*. Mycologia 94:73–84
9. Sharpton TJ, Stajich JE, Rounsley SD et al (2009) Comparative genomic analyses of the human fungal pathogens *Coccidioides* and their relatives. Genome Res 19:1722–1731
10. Neafsey DE, Barker BM, Sharpton TJ et al (2010) Population genomic sequencing of *Coccidioides* fungi reveals recent hybridization and transposon control. Genome Res 20:938–946
11. Levine HB (1961) Purification of the spherule-endospore phase of *Coccidioides immitis*. Sabouraudia 1:112–115
12. Cole G, Xue J, K S et al (2006) Virulence mechanisms of *Coccidioides*. In: Heitman J, Filler S, Edwards J et al (eds) Molecular principles of fungal pathogenesis. Am Soc Microbiol Press, Washington, DC, pp 363–391
13. Tarcha EJ, Basrur V, Hung CY et al (2006) Multivalent recombinant protein vaccine against coccidioidomycosis. Infect Immun 74:5802–5813
14. Tarcha EJ, Basrur V, Hung CY et al (2006) A recombinant aspartyl protease of *Coccidioides posadasii* induces protection against pulmonary coccidioidomycosis in mice. Infect Immun 74:516–527
15. Galgiani JN, Ampel NM, Blair JE et al (2005) Coccidioidomycosis. Clin Infect Dis 41:1217–1223
16. Hage CA, Knox KS, Wheat LJ (2012) Endemic mycoses: overlooked causes of community acquired pneumonia. Respir Med 106:769–776
17. Thompson GR 3rd (2011) Pulmonary coccidioidomycosis. Semin Respir Crit Care Med 32:754–763
18. Barnato AE, Sanders GD, Owens DK (2001) Cost-effectiveness of a potential vaccine for *Coccidioides immitis*. Emerg Infect Dis 7:797–806
19. Levine HB, Pappagianis D, Cobb JM (1970) Development of vaccines for coccidioidomycosis. Mycopathol Mycol Appl 41:177–185
20. Pappagianis D (1993) Evaluation of the protective efficacy of the killed Coccidioides immitis spherule vaccine in humans. The Valley Fever Vaccine Study Group. Am Rev Respir Dis 148:656–660
21. Xue J, Hung CY, Yu JJ et al (2005) Immune response of vaccinated and non-vaccinated mice to *Coccidioides posadasii* infection. Vaccine 23:3535–3544
22. Kamei A, Coutinho-Sledge YS, Goldberg JB et al (2011) Mucosal vaccination with a multivalent, live-attenuated vaccine induces multifactorial immunity against Pseudomonas aeruginosa acute lung infection. Infect Immun 79:1289–1299
23. Xue J, Chen X, Selby D et al (2009) A genetically engineered live attenuated vaccine of *Coccidioides posadasii* protects BALB/c mice against coccidioidomycosis. Infect Immun 77:3196–3208
24. Hung CY, Castro-Lopez N, Cole GT (2014) Vaccinated C57BL/6 mice develop protective and memory T cell responses to Coccidioides posadasii infection in the absence of interleukin-10. Infect Immun 82:903–913
25. Hung CY, Gonzalez A, Wuthrich M et al (2011) Vaccine immunity to coccidioidomycosis occurs by early activation of three signal pathways of T helper cell response (Th1, Th2, and Th17). Infect Immun 79:4511–4522
26. Hung CY, Jimenez-Alzate Mdel P, Gonzalez A et al (2014) Interleukin-1 receptor but not toll-like receptor 2 is essential for MyD88-dependent Th17 immunity to Coccidioides infection. Infect Immun 82:2106–2114
27. Wang H, LeBert V, Hung CY et al (2014) C-type lectin receptors differentially induce th17 cells and vaccine immunity to the endemic mycosis of North America. J Immunol 192:1107–1119
28. Wüthrich M, Gern B, Hung C-Y et al (2011) Vaccine-induced protection against 3 systemic mycoses endemic to North America requires Th17 cells in mice. J Clin Invest 121:554–568
29. Cole GT, Hung CY, Sanderson SD et al (2013) Novel strategies to enhance vaccine immunity against coccidioidomycosis. PLoS Pathog 9, e1003768
30. O'Shea JJ, Paul WE (2010) Mechanisms underlying lineage commitment and plasticity of helper CD4+ T cells. Science 327:1098–1102
31. Larbi A, Fulop T (2014) From "truly naive" to "exhausted senescent" T cells: when markers predict functionality. Cytometry A 85:25–35

32. Cosmi L, Maggi L, Santarlasci V et al (2014) T helper cells plasticity in inflammation. Cytometry A 85:36–42
33. Allendorfer R, Brunner GD, Deepe GS Jr (1999) Complex requirements for nascent and memory immunity in pulmonary histoplasmosis. J Immunol 162:7389–7396
34. Wüthrich M, Warner T, Klein BS (2005) IL-12 is required for induction but not maintenance of protective, memory responses to *Blastomyces dermatitidis*: implications for vaccine development in immune-deficient hosts. J Immunol 175:5288–5297
35. Wüthrich M, Filutowicz HI, Warner T et al (2002) Requisite elements in vaccine immunity to *Blastomyces dermatitidis*: plasticity uncovers vaccine potential in immune-deficient hosts. J Immunol 169:6969–6976
36. Cox RA, Magee DM (1998) Protective immunity in coccidioidomycosis. Res Immunol 149: 417–428
37. Cox RA, Magee DM (2004) Coccidioidomycosis: host response and vaccine development. Clin Microbiol Rev 17:804–839
38. Cole GT, Xue JM, Okeke CN et al (2004) A vaccine against coccidioidomycosis is justified and attainable. Med Mycol 42:189–216
39. Li K, Yu JJ, Hung CY et al (2001) Recombinant urease and urease DNA of *Coccidioides immitis* elicit an immunoprotective response against coccidioidomycosis in mice. Infect Immun 69:2878–2887
40. Shubitz LF, Dial SM, Perrill R et al (2008) Vaccine-induced cellular immune responses differ from innate responses in susceptible and resistant strains of mice infected with *Coccidioides posadasii*. Infect Immun 76:5553–5564
41. Hung CY, Hurtgen BJ, Bellecourt M et al (2012) An agonist of human complement fragment C5a enhances vaccine immunity against *Coccidioides* infection. Vaccine 30:4681–4690
42. Wuthrich M, Hung CY, Gern BH et al (2011) A TCR transgenic mouse reactive with multiple systemic dimorphic fungi. J Immunol 187:1421–1431
43. Beliakova-Bethell N, Jain S, Woelk CH et al (2014) Maraviroc intensification in patients with suppressed HIV viremia has limited effects on CD4+ T cell recovery and gene expression. Antiviral Res 107:42–49
44. Mahnke YD, Brodie TM, Sallusto F et al (2013) The who's who of T-cell differentiation: human memory T-cell subsets. Eur J Immunol 43:2797–2809

Part VI

Vaccines for Human Parasitic Diseases

Chapter 32

High-Density Peptide Arrays for Malaria Vaccine Development

Felix F. Loeffler, Johannes Pfeil, and Kirsten Heiss

Abstract

The development of an efficacious and practicable vaccine conferring sterile immunity towards a *Plasmodium* infection represents a not yet achieved goal. A crucial factor for the impact of a given anti-plasmodial subunit vaccine is the identification of the most potent parasitic components required to induce protection from both infection and disease. Here, we present a method based on a novel high-density peptide array technology that allows for a flexible readout of malaria antibodies. Peptide arrays applied as a screening method can be used to identify novel immunogenic antibody epitopes under a large number of potential antigens/peptides. Ultimately, discovered antigen candidates and/or epitope sequences can be translated into vaccine prototype design. The technology can be further utilized to unravel antibody-mediated immune responses (e.g., involved in the establishment of semi-immunity) and moreover to confirm vaccine potency during the process of clinical development by verifying the induced antibody responses following vaccination.

Key words Immunogenic malarial antigens, Antibody readout, Peptide binding, Malarial subunit vaccine, Antibody epitope mapping, Antigen screening

1 Introduction

Malaria remains a major cause of global morbidity and mortality. By current estimates, approximately 200 million cases occurred globally in 2013, and severe malaria induced by the protozoan parasite *Plasmodium falciparum* kills roughly 1600 persons per day, mostly young children living in malaria endemic settings in sub-Saharan Africa [1].

A safe and effective malaria vaccine is an urgently needed tool for sustainable malaria control. Since the 1970s, it was shown that sterile protection against malaria can be induced via immunization with attenuated whole organisms [2–8], but practical challenges still hamper the use of whole-parasite vaccines for wide-scale human use. In contrast, current subunit malaria vaccine developments, with RTS,S as the leading candidate [9–11], only generate modest protection against malaria infection.

Sunil Thomas (ed.), *Vaccine Design: Methods and Protocols: Volume 1: Vaccines for Human Diseases*, Methods in Molecular Biology, vol. 1403, DOI 10.1007/978-1-4939-3387-7_32,

Protective immunity following immunization with attenuated parasites is directed against plasmodia-infected hepatocytes. Several studies demonstrated that T cell-mediated immune responses are required to achieve protection against *Plasmodium* infection at the clinically silent liver stage (reviewed in refs. 12, 13). In addition, it appears that not only cellular but also antibody-derived mechanisms play a considerable role in decreasing parasite infection of the liver and hence contribute to protective immune responses (reviewed in ref. 14). Following the completion of intrahepatic development, *Plasmodium* parasites continue to replicate within erythrocytes and thereby cause the clinical symptoms of malaria. At the pathogenic blood stage phase, humoral responses are the central immune effector mechanisms (reviewed in refs. 13, 15). To date, the entire picture of antigens crucial for inducing potent (protective) anti-plasmodial immune responses remains incomplete. Hence, the identification of novel antigens involved in the establishment of protective immune responses represents a field of intensive research. Revealing new vaccine candidates will open up new perspectives for rational malaria vaccine development and the combination of multiple antigens, including antigens from different stages of the parasite's life cycle, may ultimately result in the development of highly protective subunit malaria vaccines.

High-density peptide arrays presented in this chapter allow for the identification of antigens/antigenic peptides recognized by antibodies and at the same time for the mapping of respective epitope sequence(s) within an entire antigen. Current data on malarial antibody profiling by high-throughput array methodologies are based on protein microarrays [16–20], a technology accompanied with the labor-intensive prerequisite of recombinant expression of the antigens in soluble form. In contrast, the chemical synthesis of peptides in the form of an array is a standardized and straightforward process. Peptide arrays offer a wide range of applications, such as (1) to pinpoint biomarkers for diagnostics (e.g., a peptide that binds a disease-specific antibody), (2) to develop rationally designed vaccines (by identifying antibodies and their protein targets in immune individuals), or (3) to find therapeutic targets (e.g., by identifying peptides that can block a specific pathway). Peptides with their 20 different amino acid building blocks are a major class of antibody binders, which qualifies them for the readout of antibody responses. However, high costs have hampered the large-scale application of peptide arrays until recently, when technological advances opened up new avenues for the methodology. With a coverage of up to 30,000 individual peptide sequences per array [21], high-density peptide arrays now represent an emerging high-throughput tool, which can be used to screen a large diversity of linear antibody epitopes. The technology thereby permits a highly cost-efficient identification and down-selection of (linear) immunogenic sequence stretches within an entire antigen, which offers a straightforward approach for the translation into vaccine design.

In a recent study on HIV [22], peptide arrays were used to characterize the individual diversity of antibody epitope binding (e.g., from infected versus vaccinated individuals).

A pivotal tool to use the array technology for the identification of novel malarial antigens and thus for malaria vaccine development is the appropriate sera. Data on antibodies induced during a natural *Plasmodium* infection can be drawn utilizing sera from individuals exposed to malaria in endemic areas [16, 17, 20, 23–25]. In-depth analysis of sera collected from individuals differing in age and immune status enables the identification of antigens/antigenic motifs crucial for the establishment of naturally acquired immunity, which mediate protection from severe disease (reviewed in ref. 26). In addition, sera from immunized and protected individuals collected in the course of a clinical study evaluating whole-parasite approaches [7, 8] could ultimately result in the description of novel antigens involved in sterilizing immunity [18, 19, 27]. A prerequisite for verifying the specificity of newly identified malarial antigenic epitopes for vaccine design is the use of sera from malaria-naïve individuals. A clear and accurate clinical definition of the sera is of utmost importance to exclude non-*Plasmodium*-specific cross-reactive antigen-antibody interactions.

Peptide arrays are offered by various providers, such as PEPperPRINT [28], JPT [29], Intavis [30], and others (*see* also ref. 21). Here, we describe a detailed protocol for the PEPperPRINT peptide array technology [31], which we successfully applied for the detection of novel malaria antigens (own unpublished data). Briefly, the peptide array synthesis principle is based on printing different amino acids in a spot pattern with a laser printer onto glass surfaces. Together with intermittent wet chemistry steps, the amino acids are printed and thereby coupled to the previous ones. Thus, similar to assembling pearls to a string, all peptides on the array are simultaneously elongated in a layer-by-layer manner, finally resulting in the desired peptide array.

By utilizing different secondary antibodies recognizing IgG, IgM, or IgA (each conjugated with different fluorescent dyes) the technology permits the detection of different antibody classes within the same array. Hence, it is feasible to simultaneously investigate the prevalence of the respective antibody classes in a specific patient serum and, moreover, to differentiate the reactivity to all epitopes recognized by IgG, IgM, and/or IgA.

A clear limitation of the methodology is its restriction to linear peptides, whereas confirmation-dependent antibody recognition motifs cannot be identified with conventional peptide microarrays. Advanced techniques, e.g., developed by PEPSCAN [32], exploit novel synthesis strategies to circumvent these limitations (inducing peptide folding by introducing backbone structures). Together with novel very-high-density strategies [33, 34], peptide arrays have the potential to evolve into rapid and versatile tools for rational vaccine development.

1.1 Array Design

The assembly of the peptide selection on an array depends on the application and can be chosen in a peptidome-like manner with peptides derived from a broad range of antigens (e.g., in order to screen for novel immunogenic peptide sequences) or a tailor-made design with peptides derived from a limited number of antigens (e.g., in order to verify the efficacy of a certain subunit vaccine to trigger antibody responses or to investigate a certain set of antigens in the establishment of semi-immunity and hence protection from disease). In order to arrange the information of the antigens of choice on an array, the respective antigen sequences have to be divided into peptides with a length of usually 15 (up to 20) amino acids with an overlap of 7–14 amino acids. Figure 1 illustrates the principle of generating and designing the peptide array content.

The larger the overlap, the more precise is the epitope mapping. Individual peptides are generated in duplicates on the array, to increase the reliability of the experiments by reducing the impact of artifacts. Since the genome of *Plasmodium falciparum* consists of about 5400 protein-coding genes [37], comprising over four million amino acids, it is not yet possible to cover the entire proteome of *Plasmodium falciparum* on one array. By employing arrays with 30,000 different peptides, it is possible to cover up to 6 % of the proteome, depending on the selected amino acid overlap. Because of this limitation, a preselection of potential candidate antigens (especially for the peptidome-like approach) is required, e.g., based on bioinformatical prediction algorithms.

PEPperPRINT currently offers six different standard designs with 1 (4488 peptide double spots), 2 (2040 peptide double spots), 3 (1156 peptide double spots), 4 (816 peptide double spots), 5 (680 peptide double spots), and 16 (110 peptide double spots) replicas per slide. For each design, an individual incubation tray is available (*see* Subheading 2) and should be used to minimize incubation volume. Preferably, the envisaged peptide selection should

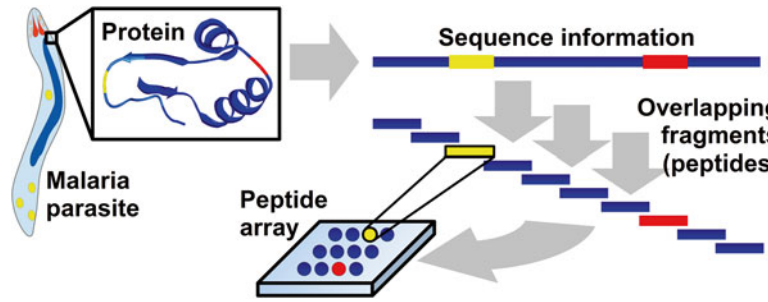

Fig. 1 Design of the peptide array content. The primary structure (amino acid sequence) of a malaria antigen is divided into overlapping fragments of 15–20 amino acids in length. Subsequently, the peptide array is produced according to the sequence of the fragments (example protein structure from [35], modeled with Swiss-PdbViewer [36] and POV-Ray software).

closely match one of the latter numbers of peptide spots. For example, if arrays with exactly 1960 peptide spots are designed, it is possible to acquire two replicas per slide. Furthermore, it is important to reserve some peptide spots on the array for internal peptide controls. In this example, 80 peptide double spots are left for controls, which is the minimum amount of controls for this array size. For control spots, PEPperPRINT offers the hemagglutinin (HA) peptide sequence from *Influenza* spp. and/or the FLAG peptide, which are currently the standard controls on PEPperPRINT arrays. These internal array controls are not only necessary for verifying the array quality, but also for inter-array normalization. To account for serum and array variation, the raw fluorescence intensity of each peptide spot on one array is adjusted by a factor derived from the HA control spot staining (*see* Subheading 3.3).

1.2 Detection of Malarial Epitopes Involved in Immunity

For the identification of malarial epitopes involved in immunity, peptide arrays are incubated with sera and stained with a fluorescent secondary antibody (exemplified in Fig. 2). The image acquisition is performed with a LI-COR infrared fluorescence scanner. Subsequently, the control peptides (HA epitopes and/or FLAG epitope) on the arrays are stained using peptide-specific fluorescently conjugated antibodies.

1.3 Analysis

The raw fluorescence images obtained after scanning are quantitatively analyzed using a suitable software program (*see* Subheadings 2 and 3), resulting in a fluorescence intensity value for each peptide spot on the array (including background subtraction and allocation of the duplicates per individual peptide). For further analysis, data are normalized and transformed accordingly (*see* Subheading 3).

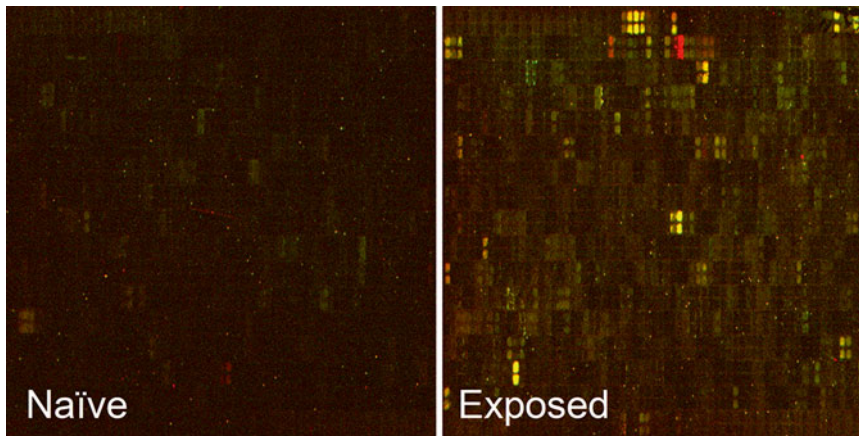

Fig. 2 Example staining of two peptide arrays with the same content (1104 peptide double spots), incubated with the serum of a malaria-naïve (*left*) and an exposed (*right*) individual. The IgG reactivity is depicted in *red*, and the IgM reactivity is shown in *green*. *Yellow* staining is the result of both IgG and IgM binding.

2 Materials

2.1 Arrays

The peptide arrays—PEPperCHIP Custom Peptide Microarrays—were supplied by PEPperPRINT, Germany. The arrays are provided on a standard glass slide (format: 3″ × 1″, 75.4 mm × 25.0 mm × 1 mm). Depending on the amount of peptides per array, up to 16 array replicates can be printed onto one slide, whereas each array replicate can be incubated with an individual sample. The array slides are stable for several months, when stored at 4 °C and sealed from the surrounding gas atmosphere.

2.2 Equipment

1. PEPperCHIP Incubation Tray (PEPperPRINT, Germany): The specific type of the incubation tray depends on the number of array replicates per glass slide (between 1 and 16). The total number of peptides per array will result in different possible numbers of array copies on one particular slide.
2. Odyssey Imaging System (LI-COR) for infrared wavelengths (700 nm and 800 nm channel, 21 μm scanning resolution): Fluorescent dyes of the antibodies have to be chosen according to the detection wavelengths available in the scanning system.
3. Orbital shaking device (circular shaking motion).

2.3 Antibodies

1. Primary samples: Sera of malaria-exposed and/or vaccinated individuals and control samples from non-malaria-exposed individuals.
2. Labeled secondary antibodies: Goat anti-human IgG DyLight™680 secondary antibody (Rockland Immunochemicals Inc., USA), goat anti-human IgM DyLight™800 secondary antibody (Rockland Immunochemicals Inc., USA).
3. Labeled control antibodies: PEPperCHIP Staining Kit (PEPperPRINT, Germany) for the detection of the control peptides HA and FLAG (labeled with DyLight™680 or DyLight™800).

2.4 Buffers

1. Buffer: PBS-T (PBS + 0.05 % Tween 20).
2. Blocking buffer: Rockland Blocking Buffer (RBB) for IR Western Blotting MB-070 (Rockland Immunochemicals Inc., USA).
   Or
   Blocking buffer: PBS-T (PBS + 0.05 % Tween 20) with 1 % bovine serum albumin (BSA).

According to our experience, the blocking buffer from Rockland is more efficient in blocking the peptide array surface, and thus prevents unspecific background staining. Therefore, we recommend using the RBB instead of the blocking buffer of 1 % BSA in PBS-T.

2.5 Software

For the quantitative fluorescent analysis of the raw fluorescent images, we used the PepSlide Analyzer Software (Sicasys, Germany). This software is easy to use and specifically designed for the analysis of PEPperPRINT arrays. An alternative to this can be the GenePix Pro Software.

3 Methods

The assembly of peptide sequences on the array is designed (Subheading 3.1), plasmodial-driven humoral immune responses are discovered and visualized (Subheading 3.2), and finally immunogenic antigens and, moreover, B cell epitope sequences are identified and mapped (Subheading 3.3).

3.1 Array Design

The array design for the tailor-made approach does not necessarily require a preselection process since only a defined number of antigens are in focus for this application. However, in order to screen for potential novel antigens/antigenic motifs, a broad range of candidates is often desired (peptidome-like approach). Bioinformatical analysis as a possible approach to perform a preselection of antigens is facilitated by constantly advancing transcriptomic and proteomic data available for different *Plasmodium* life cycle stages [38–44]. Based on these data, potential candidates for peptide array assembly can be selected depending on their expression profile, e.g., screening of stage-specific candidates being expressed during pre-erythrocytic and/or erythrocytic development [16, 18]. Further criteria for candidate selection may include predictions on antigen localization or homologies to (already) known antigens [24]. This approach has been pursued in order to identify target antigens of protective humoral responses of merozoites [24, 25]. Thereby, the authors focused on proteins presumably expressed on the surface of merozoites and, moreover, candidates being located in secretory organelles essentially involved in invasion.

In addition, a prioritization of candidate antigens can also be based on data derived from previous studies, as performed by Felgner and colleagues [19], or on differential screenings using a cDNA-derived library [45, 46].

3.2 Detection of Malarial Epitopes Involved in Immunity

First, we have to prepare the PEPperCHIP incubation tray. The incubation tray consists of four parts: the base plate, the silicone seal, the upper part (containing the screws and the openings for the incubation liquid), and a lid (shielding from dust). For detailed information and a training video, *see* also [28]. Assembled, its dimensions are very similar to a 96-well plate. Before initial use, rinse all parts (especially the seal) thoroughly with water and detergent (*see* **Note 1**). Now, to find the correct surface of the peptide

array on the glass slide, you need to have a closer look at the slide: The back side of the slide is marked with an individual number. If you turn the slide so that the number appears in the top right (in a mirror view manner), you are directly looking at the peptide array surface (*see* **Note 1**).

The base plate of the PEPperCHIP incubation tray can hold up to three slides simultaneously. The peptide array slide is placed correctly into the base plate, if the numbers on the slide are in the upper right corner (in a mirror view manner). Then, place the seal (glossy side facing downwards) onto the base plate and the array. Afterwards, place the upper part on top of the seal and tighten all screws equally (do not fasten too tight or you might break the array).

Always place the incubation tray onto the orbital shaker at a rotation speed of 200 rpm, to achieve optimal array wetting conditions. The liquid should always cover the array completely. All incubation steps are performed on the shaker at room temperature, except for the serum incubation, where the shaker is placed into the cold room or a refrigerator.

Use a pipette to deposit and remove the solutions (buffers, diluted serum, antibodies) in/from the edge of the well. Never directly put the solution onto the array surface. Be careful not to scratch the surface of the slide with the pipette.

Depending on the amount of replicas (arrays) per slide, use the following incubation volumes for each well (i.e., each array): 1000 μL for 1 or 2 replicas, 500 μL for 3 or 4 replicas, 400 μL for 5 replicas, or 100 μL for 16 replicas.

3.2.1 Preincubation with Secondary Antibodies

It is possible that the secondary antibodies interact with the peptides on the array. To distinguish these signals from specific signals, always preincubate your array with the secondary antibodies. It is sufficient to perform this only once with one type of peptide array content and check whether the interaction is negligible. Otherwise, these signals have to be subtracted from the sample-specific interaction signals.

1. Incubate the array with PBS-T for 10 min.
2. Incubate with pure RBB for 30 min to reduce nonspecific interactions with the surface.
3. Wash shortly with PBS-T.
4. Incubate with secondary antibodies diluted 1:5000 in PBS-T with 1:10 RBB for 30 min (you can add the anti-IgG and anti-IgM antibodies to the same solution).
5. Wash twice with PBS-T (~10 s, ~30 s), disassemble the incubation tray, and carefully remove the peptide array slides.
6. Dip the slides shortly into Milli-Q water to remove salt remnants and dry the slides carefully in an airstream.
7. Scan (intensity for each channel 7.0, if overexposed, use intensity 5.0).

3.2.2 Scanning

1. Start the Odyssey imaging software (e.g., Odyssey V3.0 software).
2. Place the slide(s) onto the scanner with the number in the lower left corner (*see* **Note 1**).
3. Create a new project (and project folder) and click on the image acquisition button (make sure that you have the appropriate access rights).
4. Select the respective scanning area (standard for one slide: height 8, width 3).
5. Set the scanning resolution to 21 μm, set the scan intensity for the 700 and 800 nm channels to 7.0 (if white areas in the image indicate overexposure, rescan with intensity 5.0), set the scanning quality to medium, and select the check-box to automatically flip the image after scanning (if you carefully follow these instructions, the acquired image should be already flipped correctly for subsequent image analysis).
6. Set the offset to 0.8 (this value is assigned in millimeter and should be more or less equal to the thickness of the slide; we obtained best results with 0.8, but you can try to adjust it to 0.7 or 0.9, if the 700 and 800 nm channels are misaligned).
7. Start the acquisition of the fluorescence image (do not forget to save the images and the project).
8. Export the acquired image as a colorized 16-bit "tif" file.
9. Copy the "700.tif" and "800.tif" (which are the raw image files for subsequent analysis), and the "COLORIZED.tif" for visualization purposes.

3.2.3 Main Staining with Serum and Secondary Antibodies

1. Incubate the array with PBS-T for 10 min.
2. Incubate with pure RBB for 30 min to reduce nonspecific interactions with the surface.
3. Wash shortly with PBS-T.
4. Incubate with serum diluted 1:1000 in PBS-T with 1:10 RBB overnight in the cold room (about 12–16 h) at 4 °C.
5. Wash three times with PBS-T (~10 s, ~30 s, 1 min; the actual time is not so critical).
6. Incubate with secondary antibodies diluted 1:5000 in PBS-T with 1:10 RBB for 30 min (you can add the anti-IgG and anti-IgM antibodies to the same solution).
7. Wash twice with PBS-T (~10 s, ~30 s), disassemble the incubation tray, and carefully remove the peptide array slides.
8. Dip the slides shortly into Milli-Q water to remove salt remnants and dry the slides carefully in an airstream.
9. Scan (*see* Subheading 3.2.2).

3.2.4 Staining of FLAG/HA Control Peptides

It is important to stain all arrays with the same batch of diluted control antibodies. This will assure the same dilution of antibodies and improves the comparability of the control staining.

1. Incubate with PBS-T with 1:10 RBB for 10 min.
2. Incubate with control antibodies diluted 1:1000 in PBS-T with 1:10 RBB for 1 h (you can add the anti-HA and anti-FLAG antibodies to the same solution).
3. Wash twice with PBS-T (~10 s, ~30 s), disassemble the incubation tray, and carefully remove the peptide array slides.
4. Dip the slides shortly into Milli-Q water to remove salt remnants and dry the slides carefully in an airstream.
5. Scan (*see* Subheading 3.2.2).

3.3 Peptide Array Fluorescence Intensity and Data Analysis

3.3.1 Pepslide Analyzer

Peptide arrays by PEPperPRINT are always provided with an Excel spreadsheet with the microarray layout and peptide sequences. In addition, a ".psf" file is provided, which includes the array layout (grid) for the Pepslide Analyzer software. It is possible to start with a 30-day free trial version before buying the software. The raw fluorescence images are acquired with the Odyssey software during the scanning process. Now, the raw 16-bit images will be analyzed with PepSlide Analyzer software. Raw spot intensities are detected and measured in an arbitrary fluorescence intensity unit (AU) and range from 0 to 65,535 AU. The raw spot intensity is determined as the median brightness of the measured pixels in the image corresponding to the peptide spot.

1. After starting the software, in the top bar, select "Images" and open the raw image (e.g., 700.TIF) from the Odyssey scanner.
2. In the left bar, select the tab "Images" and turn on the "Enhance contrast automatically"; use manual.
3. Now, check if the slide number (written in a mirror view manner) is in the top right corner; otherwise rotate and flip the image, using the "Image Rotation" options.
4. In the top bar select "Arrays" and open the .psf file, which was provided with the array(s) by PEPperPRINT. This opens the array grid, which has to be aligned to the image.
5. In the left bar, select the tab "Arrays." Click anywhere in the "Imaging" window, showing the image, and press "Ctrl + a" to select the array grid.
6. Align the array grid according to the fluorescent image with the mouse and using the "Array Rotation" options.
7. Right click outside of the array grid in the "Imaging" window, select "Create Background Control," and create a horizontal area where number of spots is 10 (*see* **Note 2**). Select and drag this background control bar outside of the incubation area, but

still on the glass slide. This will subtract the autofluorescence of the glass from your measured interactions.

8. Again, left click somewhere in the "Imaging" window and press "Ctrl + a" to select the array grid and the background control bar.
9. Now, right click on the array grid and select "Quantify Selection." The data can now be exported to a CSV file; the columns with the title "Red Foreground Median" and "Aggregate R. F. Median" represent the median fluorescence intensity of the corresponding peptide spot and the mean (aggregate) of the two median spot values with the same sequence.

3.3.2 Data Analysis

For subsequent data analysis (*see* also ref. 47), the two main computational tasks are (1) to identify positive antigens within one array experiment and (2) to identify positive antigens within one group of arrays, i.e., one group of individuals with protected/susceptible or semi-immune immune status.

To account for serum and inter-array variations, we adjust (i.e., normalize) the raw fluorescence intensity of each peptide spot on one array by a factor derived from the HA control spot staining: First, we calculate the median of all HA control spots on each array. Then, we calculate the mean of all these (median) values. Thus, the normalization factor for one array is the ratio of the array-specific median HA intensity to the mean of all (median) HA intensities from all arrays.

Subsequently, we performed the asinh transformation (as in ref. 47) to account for the inherent variance-mean dependence in low and high signal intensities. Then, we grouped samples into two groups, protected (experimental) and susceptible (control), and performed a Bayes regularized *t*-test. Therefore, we used the online available algorithm Cyber-T (http://molgen51.biol.rug.nl/cgi-bin/cybert/CyberT-8.0.form.pl?DATATYPE=CE), based on the publication of Baldi and Long [48]. This renders Bayes-corrected *p*-values for the prediction of immunogenic peptides.

Finally, to translate identified immunogenic epitope sequences into vaccine design, the functionality of the respective antibodies (e.g., inhibition of parasite motility and/or invasion, parasite neutralization and/or opsonization) has to be validated in subsequent assays.

4 Notes

1. *Slide handling and artifacts*: Always handle the arrays with appropriate gloves and only touch the edges of the slide. Try to prevent dust particles and other contaminations on the array and on the scanner. These may cause artifacts that

influence the results. Thoroughly clean the scanner before image acquisition.

2. *Definition of background control spots*: For fluorescent image analysis, we defined the background spots (i.e., the background noise intensity) as the autofluorescence of the glass surface, which was not in contact with serum or secondary antibodies. It would be also possible to define the background within the area, where the array surface was exposed to serum and secondary antibodies, but features no peptide spots (which we call the "serum background"). However, some human serum samples (in contrast to serum acquired from laboratory animals) exhibit a very high background staining. In this case the fluorescence obtained by peptide spots may be lower than this background (due to hydrophobic/hydrophilic interactions). This would result in negative fluorescence intensity values for many peptide spots, which is why we defined the background as the lowest possible background.

Acknowledgements

We thank Ann-Kristin Mueller for critical discussions and helpful comments on the manuscript. This work was supported by the University Heidelberg Frontier Innovation Fund of the Excellence Cluster (0077.3.5.2.86) to K.H., the Carl-Zeiss-Foundation, the Gips-Schuele-Foundation, and the Karlsruhe House of Young Scientists to F.L. J.P. is the recipient of an HRCMM (Heidelberg Research Center for Molecular Medicine) Career Development Fellowship.

References

1. WHO (2013) World malaria report: 2013
2. Nussenzweig RS, Vanderberg J, Most H, Orton C (1967) Protective immunity produced by the injection of x-irradiated sporozoites of plasmodium berghei. Nature 216:160–162
3. Hoffman SL, Goh LM, Luke TC et al (2002) Protection of humans against malaria by immunization with radiation-attenuated Plasmodium falciparum sporozoites. J Infect Dis 185: 1155–1164
4. Mueller AK, Labaied M, Kappe SH, Matuschewski K (2005) Genetically modified Plasmodium parasites as a protective experimental malaria vaccine. Nature 433:164–167
5. VanBuskirk KM, O'Neill MT, De La Vega P et al (2009) Preerythrocytic, live-attenuated Plasmodium falciparum vaccine candidates by design. Proc Natl Acad Sci U S A 106: 13004–13009
6. Belnoue E, Costa FT, Frankenberg T et al (2004) Protective T cell immunity against malaria liver stage after vaccination with live sporozoites under chloroquine treatment. J Immunol 172:2487–2495
7. Roestenberg M, McCall M, Hopman J et al (2009) Protection against a malaria challenge by sporozoite inoculation. N Engl J Med 361: 468–477
8. Seder RA, Chang LJ, Enama ME et al (2013) Protection against malaria by intravenous immunization with a nonreplicating sporozoite vaccine. Science 341:1359–1365
9. Agnandji ST, Lell B, Soulanoudjingar SS et al (2011) First results of phase 3 trial of RTS, S/AS01 malaria vaccine in African children. N Engl J Med 365:1863–1875
10. Agnandji ST, Lell B, Fernandes JF et al (2012) A phase 3 trial of RTS, S/AS01 malaria vaccine

in African infants. N Engl J Med 367: 2284–2295
11. RTS, S Clinical Trials Partnership (2014) Efficacy and safety of the RTS, S/AS01 malaria vaccine during 18 months after vaccination: a phase 3 randomized, controlled trial in children and young infants at 11 African sites. PLoS Med 11(7), e1001685
12. Hafalla JC, Silvie O, Matuschewski K (2011) Cell biology and immunology of malaria. Immunol Rev 240:297–316
13. Vaughan AM, Kappe SH (2012) Malaria vaccine development: persistent challenges. Curr Opin Immunol 24:324–331
14. Dups JN, Pepper M, Cockburn IA (2014) Antibody and B cell responses to Plasmodium sporozoites. Front Microbiol 5:625
15. Beeson JG, Osier FH, Engwerda CR (2008) Recent insights into humoral and cellular immune responses against malaria. Trends Parasitol 24:578–584
16. Doolan DL, Mu Y, Unal B et al (2008) Profiling humoral immune responses to P. falciparum infection with protein microarrays. Proteomics 8:4680–4694
17. Crompton PD, Kayala MA, Traore B et al (2010) A prospective analysis of the Ab response to Plasmodium falciparum before and after a malaria season by protein microarray. Proc Natl Acad Sci U S A 107:6958–6963
18. Trieu A, Kayala MA, Burk C et al (2011) Sterile protective immunity to malaria is associated with a panel of novel P. falciparum antigens. Mol Cell Proteomics 10(9):M111.007948
19. Felgner PL, Roestenberg M, Liang L et al (2013) Pre-erythrocytic antibody profiles induced by controlled human malaria infections in healthy volunteers under chloroquine prophylaxis. Sci Rep 3:3549
20. Baum E, Badu K, Molina DM et al (2013) Protein microarray analysis of antibody responses to Plasmodium falciparum in western Kenyan highland sites with differing transmission levels. PLoS One 8(12), e82246
21. Katz C, Levy-Beladev L, Rotem-Bamberger S et al (2011) Studying protein-protein interactions using peptide arrays. Chem Soc Rev 40:2131–2145
22. Stephenson KE, Neubauer GH, Reimer U et al (2014) Quantification of the epitope diversity of HIV-1-specific binding antibodies by peptide microarrays for global HIV-1 vaccine development. J Immunol Methods 416: 105–123
23. Dodoo D, Hollingdale MR, Anum D et al (2011) Measuring naturally acquired immune responses to candidate malaria vaccine antigens in Ghanaian adults. Malar J 10:168
24. Richards JS, Arumugam TU, Reiling L et al (2013) Identification and prioritization of merozoite antigens as targets of protective human immunity to Plasmodium falciparum malaria for vaccine and biomarker development. J Immunol 191:795–809
25. Osier FH, Mackinnon MJ, Crosnier C et al (2014) New antigens for a multicomponent blood-stage malaria vaccine. Sci Transl Med 6(247):247ra102
26. Langhorne J, Ndungu FM, Sponaas AM, Marsh K (2008) Immunity to malaria: more questions than answers. Nat Immunol 9:725–732
27. Nahrendorf W, Scholzen A, Bijker EM et al (2014) Memory B-cell and antibody responses induced by Plasmodium falciparum sporozoite immunization. J Infect Dis 210:1981–1990
28. PEPperPRINT GmbH, Germany. http://www.pepperprint.com/
29. JPT Peptide Technologies, Germany. http://www.jpt.com/
30. INTAVIS Bioanalytical Instruments AG, Germany. http://www.intavis.com/
31. Stadler V, Felgenhauer T, Beyer M et al (2008) Combinatorial synthesis of peptide arrays with a laser printer. Angew Chem Int Ed Engl 47:7132–7135
32. PEPSCAN, Netherlands. http://www.pepscan.com/
33. Maerkle F, Loeffler FF, Schillo S et al (2014) High-density peptide arrays with combinatorial laser fusing. Adv Mater 26:3730–3734
34. Buus S, Rockberg J, Forsstrom B et al (2012) High-resolution mapping of linear antibody epitopes using ultrahigh-density peptide microarrays. Mol Cell Proteomics 11:1790–1800
35. Teeter MM (1984) Water structure of a hydrophobic protein at atomic resolution: pentagon rings of water molecules in crystals of crambin. Proc Natl Acad Sci U S A 81:6014–6018
36. Guex N, Peitsch MC (1997) SWISS-MODEL and the Swiss-PdbViewer: an environment for comparative protein modeling. Electrophoresis 18:2714–2723
37. Gardner MJ, Hall N, Fung E et al (2002) Genome sequence of the human malaria parasite Plasmodium falciparum. Nature 419:498–511
38. Florens L, Washburn MP, Raine JD et al (2002) A proteomic view of the Plasmodium falciparum life cycle. Nature 419:520–526
39. Wang Q, Brown S, Roos DS et al (2004) Transcriptome of axenic liver stages of Plasmodium yoelii. Mol Biochem Parasitol 137:161–168
40. Kaiser K, Matuschewski K, Camargo N, Ross J, Kappe SH (2004) Differential transcriptome

profiling identifies Plasmodium genes encoding pre-erythrocytic stage-specific proteins. Mol Microbiol 51:1221–1232

41. Gruner AC, Hez-Deroubaix S, Snounou G et al (2005) Insights into the P. y. yoelii hepatic stage transcriptome reveal complex transcriptional patterns. Mol Biochem Parasitol 142:184–192
42. Sacci JB Jr, Ribeiro JM, Huang F et al (2005) Transcriptional analysis of in vivo Plasmodium yoelii liver stage gene expression. Mol Biochem Parasitol 142:177–183
43. Daily JP, Le Roch KG, Sarr O et al (2005) In vivo transcriptome of Plasmodium falciparum reveals overexpression of transcripts that encode surface proteins. J Infect Dis 191: 1196–1203
44. Tarun AS, Peng X, Dumpit RF et al (2008) A combined transcriptome and proteome survey of malaria parasite liver stages. Proc Natl Acad Sci U S A 105(1):305–310
45. Nixon CP, Friedman J, Treanor K et al (2005) Antibodies to rhoptry-associated membrane antigen predict resistance to Plasmodium falciparum. J Infect Dis 192:861–869
46. Raj DK, Nixon CP, Nixon CE et al (2014) Antibodies to PfSEA-1 block parasite egress from RBCs and protect against malaria infection. Science 344:871–877
47. Sundaresh S, Doolan DL, Hirst S et al (2006) Identification of humoral immune responses in protein microarrays using DNA microarray data analysis techniques. Bioinformatics 22: 1760–1766
48. Baldi P, Long AD (2001) A Bayesian framework for the analysis of microarray expression data: regularized t-test and statistical inferences of gene changes. Bioinformatics 17:509–519

Chapter 33

Development and Assessment of Transgenic Rodent Parasites for the Preclinical Evaluation of Malaria Vaccines

Diego A. Espinosa, Andrea J. Radtke, and Fidel Zavala

Abstract

Rodent transgenic parasites are useful tools for the preclinical evaluation of malaria vaccines. Over the last decade, several studies have reported the development of transgenic rodent parasites expressing *P. falciparum* antigens for the assessment of vaccine-induced immune responses, which traditionally have been limited to in vitro assays. However, the genetic manipulation of rodent *Plasmodium* species can have detrimental effects on the parasite's infectivity and development. In this chapter, we present a few guidelines for designing transfection plasmids, which should improve transfection efficiency and facilitate the generation of functional transgenic parasite strains. In addition, we provide a transfection protocol for the development of transgenic *P. berghei* parasites as well as practical methods to assess the viability and infectivity of these newly generated strains throughout different stages of their life cycle. These techniques should allow researchers to develop novel rodent malaria parasites expressing antigens from human malaria species and to determine whether these transgenic strains are fully infectious and thus represent stringent platforms for the in vivo evaluation of malaria vaccine candidates.

Key words Malaria, Vaccines, *Plasmodium*, Pre-erythrocytic stages, Transfection, Transgenic parasites, Sporozoites

1 Introduction

Despite significant advances in our understanding of the biology and immunogenicity of *Plasmodium* parasites, a safe and fully effective vaccine against malaria has not been developed.

Research on malaria vaccine development has traditionally targeted one of the three stages of the *Plasmodium* parasite life cycle: (1) pre-erythrocytic stages, from sporozoite inoculation through mosquito bites to hepatocyte infection; (2) asexual blood stages, from the release of merozoites within an infected hepatocyte to their continuous infection of red blood cells; and (3) sexual stages, from the development of blood-stage gametocytes in the mammalian host to the development of sporozoites in the mosquito.

Sunil Thomas (ed.), *Vaccine Design: Methods and Protocols: Volume 1: Vaccines for Human Diseases*, Methods in Molecular Biology, vol. 1403, DOI 10.1007/978-1-4939-3387-7_33,

Among these strategies, pre-erythrocytic vaccines are appealing as they have the potential to prevent infection and clinical disease, as well as block transmission.

The circumsporozoite protein (CSP), the most abundant protein on the surface of *Plasmodium* sporozoites, is one of the best studied malaria antigens and a leading vaccine candidate. Studies in animal models and human volunteers have shown that antibodies and T-cell responses against CSP can inhibit sporozoite infection in mammalian hosts and provide protective immunity [1, 2]. Human vaccine trials using the CSP-based malaria vaccine candidate RTS,S—currently the most successful subunit malaria vaccine formulation—have shown that RTS,S is capable of preventing the development of clinical malaria in 30–50 % of vaccinees. In addition, the RTS,S vaccine was found to reduce the incidence of severe disease in children living in malaria endemic areas [3, 4]. In spite of these encouraging advances, it is apparent that RTS,S does not confer protection to a large proportion of vaccinees and its protective efficacy seems to wane after 1–2 years [3–5]. These results may, in part, be explained by the over-reliance of RTS,S on a single antigen, CSP. And while CSP remains the most studied target of pre-erythrocytic malaria vaccines, additional antigens capable of eliciting a protective immune response have been identified [6]. It is hoped that more complex subunit vaccines with multiple antigens, including CSP, may greatly improve protective efficacy [7].

Rodent and nonhuman primate malaria parasites have been helpful for addressing basic questions in malaria biology and are valuable models for the preclinical evaluation of vaccine candidates. However, a fundamental limitation of murine malaria species is that rodent orthologues (i.e., functionally similar genes) are antigenically distinct from human-infecting *Plasmodium* species. This is a critical shortcoming of rodent models as conclusions based on rodent malaria antigens, while valuable from a conceptual view point, are limited as they cannot account for significant differences in the antigenic structure of murine and human parasite antigens. The development of transgenic rodent parasites expressing human malaria antigens has emerged as a practical solution to this problem [8]. Over the last few years newly developed transgenic parasite strains have been used for the preclinical evaluation of vaccine candidates against malaria pre-erythrocytic stages [9–12]. Importantly, these parasite strains have facilitated the systematic evaluation of different immunizing routes, antigen constructs, adjuvant formulations, and immunization regimens. And while the optimization of transfection protocols for rodent *Plasmodium* species has significantly simplified genetic manipulation [13, 14], the substitution and/or deletion of essential genes or regulatory sequences can negatively impact the parasite's infectivity and life cycle [10, 15, 16]. This is a major obstacle because transgenic parasite strains with decreased viability and virulence are not adequate tools to evaluate vaccine candidates.

In this chapter, we describe useful guidelines for the design of transfection plasmids, provide a standardized *P. berghei* transfection protocol, and present practical methodology to assess the viability and infectivity of transgenic *P. berghei* parasites throughout their life cycle. Importantly, these methods have been applied to transgenic strains developed by our group and others, in which different endogenous genes of *P. berghei* have been replaced by orthologues found in human malaria *Plasmodium* species [9, 11, 12]. Ultimately, the careful selection of highly infectious strains is critical for the stringent evaluation of malaria vaccine candidates in vivo.

2 Materials

2.1 Transfection of Rodent Malaria Parasites

2.1.1 Establishment of Infection and Subpassage to Schizont Donor Mice

1. Frozen blood aliquot of wild-type *P. berghei* parasites.
2. Three Swiss Webster mice (5–8 weeks old; ~25 g) (*see* **Note 1**).
3. Hanks' Balanced Salt Solution (HBSS) (Gibco) supplemented with 1 % (v/v) heat-inactivated mouse serum (Sigma).
4. Scissors.
5. Glass slides (25 × 75 mm).
6. Methanol.
7. Giemsa stain (Sigma).
8. 100× Giemsa buffer: 59.24 g Na_2HPO_4, 36.38 g $NaH_2PO_4H_2O$, 1000 ml deionized water.
9. 1 cc Insulin syringe (28G ½).
10. 1.5 ml microcentrifuge tubes.
11. 1000 µl and 20 µl micropipettes with corresponding plastic tips.

2.1.2 Schizont In Vitro Culture

1. Glass slides (25 × 75 mm).
2. Methanol.
3. Giemsa stain (Sigma).
4. 100× Giemsa buffer: 59.24 g Na_2HPO_4, 36.38 g $NaH_2PO_4H_2O$, 1000 ml deionized water.
5. Heparin solution (200 U/ml in 1× PBS).
6. Complete culture medium (200 ml per culture): RPMI 1640 medium with L-glutamine (Gibco), 25 mM Hepes buffer, 5 U/ml penicillin, 5 mg/ml streptomycin, adjust pH to 7.3 and filter (0.22 µm pore). Supplement with 25 % (v/v) of heat-inactivated fetal bovine serum (Hyclone).
7. 2 % Avertin anesthetizing solution: 2.4 g 2,2,2-Tribromoethanol (99 %) (Alfa Aesar), 1.488 ml Tert-amyl alcohol (Sigma), 118.5 ml 1× PBS.

8. 1 cc Insulin syringe (28G ½).
9. Gas mixture: 5 % CO_2, 5 % O_2, and 90 % N_2.
10. Cell culture flask (150 cm^2 with plug seal).
11. Biosafety laminar flow hood.
12. Incubator.
13. Orbital shaker.
14. Phase-contrast microscope.
15. Immersion oil.
16. Forceps.
17. Scissors.
18. 70 % Ethanol.
19. 7 in. glass Pasteur pipette.
20. Pipette bulb.
21. 50 ml Polypropylene tubes.
22. 1.5 ml Microcentrifuge tubes.
23. 200 µl and 20 µl micropipettes with corresponding plastic tips.
24. 10 ml Serological pipettes (sterile).
25. Pipette aid.
26. Water bath set at 37 °C.
27. Swing bucket table-top centrifuge with no-brake capacity.

2.1.3 Schizont Purification

1. Histodenz stock solution: 138 g of Histodenz (Sigma) in 500 ml of stock buffer. Autoclave immediately at 120 °C for 20 min and store at 4 °C.
2. Stock buffer medium: 5 mM Tris/HCl, 3 mM KCl, 0.3 mM $CaNa_2EDTA$; pH 7.5.
3. 1× PBS.
4. Swing bucket table-top centrifuge with no-brake capacity.
5. 7 in. glass Pasteur pipette.
6. Pipette bulb.

2.1.4 Schizont Electroporation and Injection

1. Basic Parasite Nucleofector Kit 2: Basic Parasite Nucleofector Solution 2, Supplement P2, cuvettes, pipettes (Lonza).
2. Nucleofector II Electroporator (Amaxa).
3. Purified schizonts as described in Subheading 2.1.3.
4. Linearized transfection vector (5–10 µg in 10 µl of PCR-grade water for each transfection).
5. 1.5 ml Microcentrifuge tubes.
6. 200 µl Micropipette with corresponding plastic tips.

7. 1 cc Insulin syringe (28G ½).
8. Infrared heating lamp.
9. Swiss Webster mice (5–8 weeks old; ~25 g; considering one mouse per each transfection, usually five mice are needed for a transfection experiment).

2.1.5 Selection of Transfected Parasites by Treatment with Pyrimethamine in Drinking Water

1. Pyrimethamine solution: Pyrimethamine powder (Sigma) dissolved in DMSO (Sigma) to a final concentration of 7 mg/ml and diluted 100× with tap water. pH must be adjusted to 3.5–5 using 1 M HCl. Protect from light.
2. Opaque drinking bottles (if opaque drinking bottles are not available, cover the bottles in foil to protect the pyrimethamine from light).
3. Glass slides (25 × 75 mm).
4. Methanol.
5. Giemsa stain (Sigma).

2.1.6 Cryopreservation of Drug-Resistant Parasites

1. Cryovials.
2. Scissors.
3. Forceps.
4. 7 in. glass Pasteur pipette.
5. Pipette bulb.
6. 2 % Avertin anesthetizing solution: 2.4 g 2,2,2-Tribromoethanol (99 %) (Alfa Aesar), 1.488 ml Tert-amyl alcohol (Sigma), 118.5 ml 1× PBS.
7. 1 cc Insulin syringe (28G ½).
8. Heparin solution (200 U/ml in 1× PBS).
9. Parasite freezing solution: 10 % (v/v) Glycerol/Alsever's Solution (Sigma).
10. 200 µl Micropipette with corresponding plastic tips.
11. 1.5 ml Microcentrifuge tubes.

2.2 Evaluation of the Biological Characteristics of Transgenic Parasites

2.2.1 Exflagellation of Male Gametocytes

1. Mouse infected with *P. berghei* strain under evaluation (*see* **Note 2**).
2. Heparin solution (40 U/ml).
3. Complete ookinete medium: RPMI 1640 medium with L-glutamine (Gibco), 20 % (v/v) heat-inactivated fetal bovine serum (FBS) (Hyclone), 25 mM Hepes buffer, 2 mM glutamine, 367 µM hypoxanthine, 23.8 mM sodium bicarbonate, 5 U/ml penicillin, 5 mg/ml streptomycin, 100 µM xanthurenic acid. Adjust pH to 7.4.
4. 1.5 ml Microcentrifuge tubes.

5. Scissors.
6. Methanol.
7. Giemsa stain (Sigma).
8. 100× Giemsa buffer: 59.24 g Na_2HPO_4, 36.38 g $NaH_2PO_4H_2O$, 1000 ml deionized water.
9. 10 μl Micropipette with corresponding plastic tips.
10. Glass slides (25 × 75 mm).
11. Microscope cover slip (18 × 18 mm).
12. Mineral oil.
13. Phase-contrast microscope.

2.2.2 Assessment of Midgut Oocyst Development

1. Female *Anopheles stephensi* mosquitoes: 10–14 days after infectious blood meal (*see* **Note 3**).
2. Aspirator for collecting mosquitoes.
3. Ice bucket/ice.
4. 70 % Ethanol.
5. 1× PBS.
6. Mercury dibromofluorescein solution: 0.1 % (w/v) Mercury dibromofluorescein disodium salt (Sigma) in 1× PBS.
7. Two plastic Petri dishes.
8. Two pairs of fine-point forceps.
9. One-side concavity glass slide (Thomas Scientific).
10. Glass slides (25 × 75 mm).
11. Microscope cover slip (22 × 60 mm).
12. Dissecting stereoscopic microscope.
13. Phase-contrast microscope.
14. Laboratory counter.

2.2.3 Salivary Gland Infection Rate and Mosquito Sporozoite Yield

1. Female *A. stephensi* mosquitoes: 18–22 days after infectious blood meal (*see* **Note 3**).
2. Aspirator for collecting mosquitoes.
3. Ice bucket/ice.
4. 70 % Ethanol.
5. 1× PBS.
6. 1× PBS with 1 % (w/v) bovine serum albumin (BSA) (Sigma).
7. Hanks' Balanced Salt Solution (HBSS) (Gibco) supplemented with 1 % heat-inactivated mouse serum (Sigma).
8. 200 μl Micropipette with corresponding plastic tips.

9. 10 μl Micropipette with corresponding plastic tips.
10. Two plastic Petri dishes.
11. One pair of fine-point forceps.
12. 1 cc Insulin syringe (28G ½)
13. Glass slides (25 × 75 mm).
14. Microscope cover slip (22 × 60 mm).
15. 7 in. glass pipette.
16. Pipette bulb.
17. Benchtop microcentrifuge (set at 4 °C).
18. Cell strainer (70 μm—nylon).
19. 1.5 ml Microcentrifuge tubes.
20. Pestle to fit microcentrifuge tubes.
21. Hemocytometer.
22. Dissecting stereoscopic microscope.
23. Phase-contrast microscope.
24. Laboratory counter.
25. Paper towels.

2.2.4 Development of Blood-Stage Forms upon Infectious Mosquito Bites

1. Female *A. stephensi* mosquitoes: 18–22 days after infectious blood meal (*see* **Note 3**).
2. Mice ($n = 5–10$): 5–8-week-old C57BL/6 mice.
3. 2 % Avertin anesthetizing solution: 2.4 g 2,2,2-Tribromoethanol (99 %) (Alfa Aesar), 1.488 ml Tert-amyl alcohol (Sigma), 118.5 ml 1× PBS.
4. Same materials as for salivary gland infection rate and mosquito sporozoite yield.
5. 12 oz. paper cups individually capped with mosquito netting (polyester mesh).
6. Methanol.
7. Giemsa stain (Sigma).
8. 100× Giemsa buffer: 59.24 g Na_2HPO_4, 36.38 g $NaH_2PO_4H_2O$, 1000 ml deionized water.
9. Timer/stop watch.
10. Scissors.
11. Mineral oil.
12. CO_2 chamber for euthanizing mice.
13. Mouse ear tags with corresponding applicator.

3 Methods

3.1 Transfection Plasmid Design

The careful design of transfection plasmids is critical for the development of transgenic rodent malaria parasites. We describe a few factors that should be considered when designing a transfection vector:

- *Length of the homology arms flanking a replacement construct*—Longer homology arms increase the frequency and efficiency of double-homologous recombination events [15]. Based on our experience, we recommend homology arms 800–1000 base pairs in length.
- *Position of the drug-selectable markers*—When using a drug-selectable marker it is necessary to account for its position (upstream/downstream) in relation to the gene or target of interest. This is because, in some cases, the location of the drug-selectable marker in the replacement construct can interfere with regulatory sequences of genes that are in close proximity to the gene of interest and are critical for parasite development.
- *Length of the untranslated regions (UTRs)*—We recommend that transfection constructs should incorporate a minimum of 500 base pairs of UTRs upstream and downstream of the gene(s) of interest and the drug-selectable marker. UTRs encode regulatory sequences recognized by proteins needed for gene transcription.
- *Codon harmonization*—It is advisable to codon harmonize the replacement construct in order to optimize protein synthesis and folding in the transgene host [17]. In addition, significant differences in codon usage between different *Plasmodium* species have been reported [18].

3.2 Transfection of Rodent Malaria Parasites

The guidelines and methodology provided below have been previously described by Philip et al. [15] and Janse et al. [13]. We encourage readers to review the original methodology for additional details.

3.2.1 Establishment of Infection and Subpassage to Schizont Donor Mice

1. On day 0, infect a mouse with a wild-type *P. berghei* blood aliquot by intraperitoneal (I.P.) injection
2. 2–3 days later, perform a blood smear on a glass slide.
3. Fix the smear with methanol for 30 s.
4. Without rinsing the slide, stain the smear for 15 min using a 10 % solution of Giemsa stain diluted in 1× Giemsa buffer.
5. Observe the slide under the phase-contrast microscope (100×, using immersion oil).

6. If parasitemia has reached 1–3 %, draw a blood sample by snipping the tip of the tail—no more than 3 mm from the end and pipette 10–15 μl of blood into a microcentrifuge tube containing 500 μl of HBSS-1 % mouse serum. Mix the sample thoroughly.
7. Inject (I.P.) 200 μl of the blood sample prepared in **step 6** into two mice.

3.2.2 Schizont In Vitro Culture

1. 3–4 days after infection, check the blood-stage parasitemia of the schizont donor mice by performing a thin blood smear. If parasitemia is 1–3 % proceed to next step; otherwise, wait another day and check again at the same time of day (*see* **Note 4**).
2. If proceeding with the experiment, gather all needed materials inside a biosafety laminar flood hood; make sure to set up the orbital shaker inside the incubator; place ~50 μl of heparin solution in a 50 ml polypropylene tube; and warm up the complete culture medium by placing the container in a water bath set at 37 °C.
3. Anesthetize mice using 400–500 μl of 2 % Avertin, delivered by I.P. injection (*see* **Note 1**).
4. Carefully, working one mouse at a time, moisten the torso and abdomen with 70 % ethanol and place the mouse inside of the hood.
5. Collect 1–1.5 ml of blood in the polypropylene tube with heparin. With a mouse firmly restrained, perform a small incision on the right side of the torso. Collect the blood flowing through the right axillary vein using the 7 in. Pasteur pipette attached to the bulb. Efforts should be made to work swiftly and to minimize discomfort to animals; after blood collection euthanize animal according to your institute's protocol (*see* **Note 1**).
6. Once blood collection is completed (estimate ~2 ml from two mice), add 20 ml of pre-warmed culture medium using the serological pipette and homogenize with the blood by gentle inversion.
7. Centrifuge the sample at 200 × *g* for 8 min at *room temperature* in a swing bucket table-top centrifuge *without brake*. In the meantime, place 50 ml of warm culture medium in the cell culture flask.
8. Using a serological pipette, gently remove the supernatant trying not to disturb the red blood cell pellet.
9. Add 30 ml to the red blood cells and mix by gentle inversion.
10. Carefully decant the contents of the tube into the cell culture flask previously filled with culture medium warmed to 37 °C.

11. Wash the 50 ml tube by adding 20 ml of culture medium and mixing by inversion. Then, add this to the culture flask.
12. Gas the culture with the 5 % CO_2, 5 % O_2, and 90 % N_2 gas mixture (this usually takes 1 min). Cap the culture flask and adjust the plug seal cap tightly.
13. Place the flask in the incubator set at 37 °C and rest it for 5 min.
14. Start the orbital shaker at minimum speed (20–30 rpm), enough to keep the cells in suspension.
15. Incubate the parasite culture overnight (~18 h).
16. Take a 200–500 μl aliquot from the culture and place it in a microcentrifuge tube.
17. Pellet the red blood cells by spinning the sample at maximum speed (16,000 × *g*) for 5–10 s and gently aspirate the supernatant.
18. Take 10–20 μl of the red blood cell pellet and make a thin blood smear. Giemsa stain the slide and examine under the phase-contrast microscope. If 70–80 % of parasites are healthy looking, proceed to the next step (*see* **Note 5**).

3.2.3 Schizont Purification

1. Bring the Histodenz solution to room temperature. Then, prepare 50 ml of a 55 % Histodenz/PBS solution (v/v).
2. Transfer the schizont culture to three 50 ml polypropylene tubes (~30 ml per tube).
3. Using a serological pipette attached to a pipette aid, gently add 15 ml of the Histodenz solution to each tube. Make sure to take the pipette to the bottom of the tube, under the culture suspension, before gradually releasing the Histodenz solution in order to prevent disruption of the gradient. If performed correctly, a contrasting division is seen between the two suspensions.
4. Centrifuge for 20 min at 450 × *g* in a swing bucket table-top centrifuge, without brake and gentle acceleration (as an example, set acceleration to "3" in Eppendorf centrifuge model 5810R).
5. Using a 7 in. Pasteur pipette attached to a bulb, gently collect the brown-colored layer at the interface between the two suspensions, and place this material in a clean 50 ml polypropylene tube. Typically, ~30 ml is collected from three tubes.
6. Keep the gradient tubes as the culture medium from the top layers is needed for subsequent steps.
7. To wash and concentrate the parasites, add 20 ml of culture medium from the previous step to the tube containing the schizonts and centrifuge at 200 × *g* for 8 min.
8. Discard the supernatant and resuspend the pellet in 5 ml of culture medium from **step 6**.

3.2.4 Schizont Electroporation and Injection

1. Start warming up mice by placing them at a safe distance under the infrared heating lamp. Monitor animals regularly for any signs of discomfort.
2. Distribute the schizont-containing suspension in five microcentrifuge tubes (1 ml in each tube). One tube is used for each transfection.
3. Prepare Nucleofector solutions and DNA material. For each transfection mix 90 μl of Basic Parasite Nucleofector Solution 2, 20 μl of Supplement P2, and 5–10 μl of linearized plasmid DNA (1 μg/μl).
4. Working one tube at a time, pellet the cells by centrifugation (5 s at maximum speed, 16,000 × *g*) and discard the supernatant.
5. Resuspend the schizonts in 100 μl of the previously made transfection mix.
6. Using a micropipette, transfer the parasite-containing mixture to a cuvette. Avoid introducing bubbles when dispensing the solution.
7. Transfect using the Amaxa Nucleofector set to protocol U-033 to electroporate.
8. Immediately after transfection, add 50 μl of culture medium (from **step 6** of Subheading 3.2.3) to the cuvette.
9. Transfer the contents of the cuvette to a microcentrifuge tube using one of the plastic pipettes provided by the transfection kit.
10. Quickly inject the transfected parasites into the tail vein of a mouse.
11. Repeat **steps 4–10** until all parasite material is used.
12. 24 h after injection of transfected parasites, perform a thin blood smear to determine if parasites survived the transfection procedures.

3.2.5 Selection of Transfected Parasites by Treatment with Pyrimethamine in Drinking Water

Currently, the most commonly used drug-selectable marker for transfection of *P. berghei* parasites is the dihydrofolate reductase-thymidylate synthase (DHFR-TS), an enzyme involved in folate metabolism. The DHFR-TS genes of *P. berghei* and *Toxoplasma gondii,* as well as the human DHFR gene, are capable of conferring resistance to pyrimethamine when administered in drinking water [19, 20].

1. Upon confirmation of blood-stage parasitemia, provide mice pyrimethamine in drinking water.
2. Drug treatment takes place for 4–7 days.
3. 7 days after transfection, determine the presence of blood-stage parasites by Giemsa-stained blood smears.

4. Once parasitemia has reached 1–5 %, cryopreserve two to three blood aliquots from each mouse and use the remaining material for DNA analysis.

3.2.6 Cryopreservation of Drug-Resistant Parasites

1. Anesthetize mice using 400–500 μl of 2 % Avertin, delivered by I.P. injection.
2. Collect blood from each mouse as described in Subheading 3.2.2 (**step 5**).
3. Place the collected blood (~1 ml/mouse) in a microcentrifuge tube containing 50 μl of heparin (200 U/ml) and mix thoroughly.
4. Distribute 100 μl of blood in each cryovial and mix it with 200 μl of parasite-freezing solution.
5. Place the cryovials in an isopropanol cryobox and store them at −80 °C. Samples can be then frozen directly in liquid nitrogen.
6. Use the remaining blood for DNA extraction and molecular analysis.

3.3 Evaluation of the Biological Characteristics of Transgenic Parasites

It is critical to ensure that transgenic parasites remain as infectious as their unmodified counterparts, i.e., the parental strain. The assays described below should allow a thorough assessment of their developmental characteristics.

3.3.1 Exflagellation of Male Gametocytes

1. To determine the presence of blood-stage gametocytes, perform a blood smear from the infected mouse by snipping the tip of the tail, no more than 3 mm from the end, and place a drop of blood on a glass slide.
2. Using another glass slide, make a thin smear of the blood drop.
3. Fix the smear with methanol for 30 s.
4. Without rinsing the slide, stain the smear for 15 min using a 10 % solution of Giemsa stain diluted in 1× Giemsa buffer.
5. Determine the presence of gametocytes. Visualize several fields using the 100× objective of the phase-contrast microscope with mineral oil.
6. If gametocytes are observed (ideally, one gametocyte per field), combine in a 1.5 ml microcentrifuge tube 7 μl of complete ookinete medium, 1.5 μl of heparin, and 1.5 μl of mouse blood.
7. Mix well and incubate for 15–20 min at room temperature.
8. Place 10 μl of this mix on top of a glass slide. Then, place a glass cover slip on top of the drop, making sure that the blood distributes evenly under the cover slip.

9. Observe the slide with a phase-contrast microscope, first using the 40× objective and then switching to the 100× (using mineral oil). Look for exflagellating male gametocytes, characterized by highly motile forms erupting from the infected red blood cells.

3.3.2 Assessment of Midgut Oocyst Development

1. Aspirate 15–25 mosquitoes and place them in a Petri dish containing 10 ml of 70 % ethanol (mosquitoes will die upon contact with the ethanol).
2. Using fine-point forceps, transfer the mosquitoes to a Petri dish with 5 ml of 1× PBS.
3. Working under the stereoscopic microscope, gently hold the mosquitoes by the thorax and carefully pull out the midguts through the rear end of the abdomen (*see* **Note 6**).
4. Using fine-point forceps, collect the midguts in a one-side concavity containing 200 µl of 1× PBS.
5. Transfer the midguts to a one-side concavity slide containing 200 µl of mercury dibromofluorescein solution and incubate at room temperature for 20 min.
6. Rinse the midguts by transferring them to a one-side concavity slide containing 200 µl of 1× PBS; incubate at room temperature for 10 min.
7. Using the fine-point forceps, transfer the midguts to a glass slide and arrange them in a way that facilitates microscope observation. Use a few microliters of 1× PBS to keep them wet and place a cover slip on top of the slide.
8. Observe the slide with a phase-contrast microscope, first using the 10× objective and then switching to the 40×.
9. Count the number of oocysts in each mosquito midgut. *P. berghei*-infected midguts in our laboratory-adapted wild-type strain tend to harbor 50–100 oocysts each. However, some mosquitoes might develop significantly milder infections.

3.3.3 Salivary Gland Infection Rate and Mosquito Sporozoite Yield

The efficient migration of sporozoites to mosquito salivary glands is critical for evaluating the biology and immunogenicity of transgenic parasites in the mammalian host.

3.3.3.1 Salivary Gland Isolation and Infection Assessment

1. Aspirate 15–25 mosquitoes and place them in a Petri dish containing 10 ml of 70 % ethanol (mosquitoes will die upon contact with the ethanol).
2. Using fine-point forceps, rinse the mosquitoes by placing them in a Petri dish with 5 ml of 1× PBS.
3. Place the mosquitoes on a paper towel on ice during the isolation of the salivary glands.

4. Place a glass slide under the stereoscopic microscope and wet the slide's surface with 100–150 μl of cold 1× PBS-1 % BSA.
5. Working in groups of five to ten mosquitoes, isolate the salivary glands on the glass slide. Use the fine-point forceps to gently hold each mosquito by its thorax and carefully pull the head away from the rest of the body using the needle of a 1 cc insulin syringe. If performed correctly, the trilobed salivary glands should remain attached to the mosquito's head.
6. Manipulate the mosquito's head to remove the salivary glands using the needle of a 1 cc insulin syringe. Always keep the glands wet and separated from the mosquito debris.
7. Using a paper towel, carefully clean the glass slide to remove all the mosquito material. Avoid disturbing the salivary glands.
8. Add a drop of 1× PBS-1 % BSA to wet the surface of the glass slide. Use the 1 cc insulin syringe to evenly distribute the salivary glands, and try to keep them 0.5–1 cm away from each other.
9. Place a cover slip on top of the salivary glands and focus on them using a phase-contrast microscope with a 40× objective. With the tip of a pencil, gently squeeze the gland under the objective. Infected glands usually harbor hundreds of sporozoites that can be identified by their crescent shape.
10. Determine the proportion of infected salivary glands to calculate the mosquito infection rate.

3.3.3.2 Sporozoite Purification and Mosquito Sporozoite Yield

1. Isolate the mosquito salivary glands as described in Subheading "Salivary Gland Isolation and Infection Assessment" (**steps 1–6**) (*see* **Note 7**).
2. Count the number of dissected mosquitoes before disposing of the carcasses. It may be helpful to collect the carcasses in groups of three to five mosquitoes using fine-point forceps, place them over a damp paper towel, and then count. Write down the number of dissected mosquitoes.
3. Carefully aspirate the salivary glands using the 7 in. glass pipette attached to the bulb and place them in a previously chilled microcentrifuge tube containing 50 μl of HBSS-1 % mouse sera. Keep the glands wet at all times and try to keep the overall collection volume under 500 μl.
4. Spin the glands for 3 min at 3300 × *g* in a microcentrifuge to facilitate homogenization.
5. Disrupt the glands to release the sporozoites by squeezing and turning the pestle against the bottom of the tube. Repeat this process until no large pieces of mosquito debris can be seen.
6. Spin the microcentrifuge tube at 600 × *g* for 3 min. Aspirate all the supernatant and pass it through a cell strainer into a clean microcentrifuge tube sitting on ice. This removes any large

pieces of mosquito debris that could still be present in the salivary gland homogenate.

7. Repeat **steps 5** and **6** using 150 μl of HBSS-1 % mouse sera and combine with the previously collected material. At the end of this process, determine the total volume of the sporozoite suspension.
8. Thoroughly mix the sporozoite suspension and place 10 μl on the hemocytometer. Let the sporozoites settle for 5–10 min at room temperature before counting. Allowing the parasites to get to the bottom of the hemocytometer significantly facilitates counting.
9. Use a phase-contrast microscope (40× objective) to determine the number of sporozoites by counting the four corner sections of the hemocytometer (each subdivided in 16 squares in a 4×4 arrangement). The parasites look like black eye lashes and are approximately 10 μm in length.
10. Determine the mosquito sporozoite yield by performing the following calculations: [(number of counted sporozoites in the four corner sections)/4]×10=number of sporozoites/μl. Then, multiply this number by the total volume of the sporozoite suspension to obtain the total amount of sporozoites. Finally, the number of sporozoites per mosquito is total amount of sporozoites/number of mosquitoes dissected.

3.3.4 Development of Blood-Stage Forms upon Infectious Mosquito Bites

This is an assessment of the overall infective capacity of a parasite strain. We evaluate the parasite's capacity to infect and develop within hepatocytes as well as the subsequent initiation of blood infection. Most important, exposure to infectious mosquito bites is the preferred method to evaluate the efficacy of different vaccine formulations as this is the natural route of infection.

1. Determine the salivary gland infection rate as detailed in Subheading "Salivary Gland Isolation and Infection Assessment."
2. Based on the previous estimate, sort the needed mosquitoes in each of the paper cups (*see* **Note 8**). Label each cup to match the ear tag numbers of the mice meant for this experiment and starve the mosquitoes for 12–24 h.
3. Tag mice.
4. The day of the experiment, anesthetize mice using 2 % Avertin (200–250 μl for a ~20 g mouse).
5. Place each mouse on top of its corresponding paper cup containing the starved mosquitoes. Cover the cups using a piece of cloth or towel.
6. Allow the mosquitoes to feed on the mice for 5–10 min. Then, return mice to their cages and monitor their recovery.
7. Working one cup at a time, aspirate the mosquitoes, place them on a Petri dish with 5 ml of 70 % ethanol, and determine

how many fed on each mouse. This can be easily done by looking at their abdomens for the presence of blood (it may be helpful to perform observations using the stereoscopic microscope).

8. Using a Petri dish with 5 ml of 1× PBS, rinse the mosquitoes that blood-fed in each cup and determine the salivary gland infection rate of the blood-fed mosquitoes (Subheading "Salivary Gland Isolation and Infection Assessment"). At this stage, score the dissected salivary glands of the blood-fed mosquitoes as "uninfected" or "infected" and do not focus on the absolute number of sporozoites obtained from each mosquito. These values can be used to determine how many infectious blood meals each mouse received.
9. To determine the onset of patency, start performing daily thin blood smears 4 days after the mosquito feeding assay. For accuracy, perform blood smears at the same time each day (i.e., exactly at 96, 120, and 144 hours after the assay).
10. Giemsa-stain the blood smears by fixing them with methanol for 30 s and then staining for 15 min with Giemsa working solution (10 % Giemsa stain in 1× Giemsa buffer). Rinse the slides with tap water and dry at room temperature.
11. Read the slides using the phase-contrast microscope (100× objective) with mineral oil.
12. Once the presence of blood-stage parasites becomes evident, euthanize mice immediately in a CO_2 chamber or according to your animal study protocol. In our experience, a naïve mouse that received three infectious mosquito bites will become patent for blood-stage parasites 4–6 days post-infection.
13. Continue performing daily blood smears on mice that do not develop blood-stage parasitemia for up to 14 days after the mosquito biting assay. After this time period, it is very unlikely that they will develop blood stages.
14. With the collected data, estimate the percentage of mice that developed blood-stage parasitemia upon infected mosquito bites and the pre-patent period for the tested parasite line. Pre-patent period = (1st day of positive blood smear for mouse 1 + 1st day of positive blood smear for mouse 2 + 1st day of positive blood smear for mouse 3, etc.)/(total number of mice positive for blood stage parasitemia).

4 Notes

1. All experiments involving the use of mice should be approved by the relevant ethics committees and strictly adhere to local and international regulations. Appropriate training is necessary for all personnel handling animals.

2. To procure optimal blood-stage gametocytemia when starting from a frozen blood sample, infection must be first established in a starter mouse and then subpassaged to additional naïve mice. Infect a mouse with a frozen blood aliquot and allow parasitemia to reach 3 %. Draw a blood sample from this mouse (~50–100 μl), dilute it to 1 % in 1× PBS, and infect a mouse I.P. with 200 μl. 2–3 days later, proceed to the exflagellation assay.
3. Infection of 3–7-day-old female *A. stephensi* mosquitoes is performed with *P. berghei*-infected mice in which the presence of exflagellating gametocytes has been verified. Mosquitoes are allowed to feed on anesthetized mice for 30 min (use 200–250 μl of 2 % Avertin for an ~20 g mouse). Knock down the mosquitos by placing them at 4 °C for 5–10 min. Then, working in a cold room, dispose of the mosquitoes that did not take a blood meal (i.e., do not have blood in their abdomens) and keep those ones that did. Mosquitoes are kept at 19 °C until *P. berghei* sporozoites develop and reach the salivary glands (18–22 days after the infectious blood meal).
4. Parasitemia above 3 % is not recommended and could impair the development of schizonts in culture. Higher parasitemia will result in multiply infected erythrocytes or in parasites residing in normocytes (older erythrocytes) and not in reticulocytes [13].
5. Healthy, viable schizonts are characterized by having 12–16 merozoites within one erythrocyte and a cluster of hemozoin. However, the red cell membrane is occasionally broken when blood is thinly smeared, resulting in merozoite release. Deteriorated schizonts tend to display a compact morphology, making it difficult to distinguish individual merozoites. If at this stage schizonts look underdeveloped, then gas the culture again and incubate for an additional 2–3 h before starting the purification procedure.
6. When isolating midguts, it is important to properly distinguish them from other structures of the mosquito anatomy. It is not unusual for inexperienced researchers to confuse the midguts with structures belonging to the hindgut or even the reproductive system. A practical way to distinguish the midguts is by looking for the Malpighian tubes, slender threadlike structures attached to the base of the midgut.
7. In our experience, it is preferable to use HBSS-1 % mouse serum instead of 1× PBS-1 % BSA if the isolated sporozoites are going to be injected into mice.
8. When testing a newly developed transgenic line, it is useful to determine the minimum number of infected mosquitoes that must take a blood meal for mice to develop blood-stage parasitemia. Sporozoites from both our wild-type and transgenic parasite lines can infect mice and result in blood-stage parasitemia 4–5 days after feeding of one to three infected mosquitoes.

Acknowledgements

Research in Dr. Fidel Zavala's laboratory is supported by PATH Malaria Vaccine Initiative (MVI) and the National Institutes of Health (NIH) (grant number AI44375). D.A.E. received a predoctoral fellowship from the Johns Hopkins Malaria Research Institute. The authors thank the Bloomberg Family Foundation for continued support. This research was supported in part by the Intramural Research Program of NIAID, NIH; A.J.R. is supported by the Intramural Research Program of NIAID, NIH.

References

1. Zavala F, Tam JP, Barr PJ et al (1987) Synthetic peptide vaccine confers protection against murine malaria. J Exp Med 166:1591–1596
2. Kester KE, Cummings JF, Ofori-Anyinam O et al (2009) Randomized, double-blind, phase 2a trial of falciparum malaria vaccines RTS, S/AS01B and RTS, S/AS02A in malaria-naive adults: safety, efficacy, and immunologic associates of protection. J Infect Dis 200:337–346
3. Agnandji ST, Lell B, Soulanoudjingar SS et al (2011) First results of phase 3 trial of RTS, S/AS01 malaria vaccine in African children. N Engl J Med 365:1863–1875
4. Agnandji ST, Lell B, Fernandes JF et al (2012) A phase 3 trial of RTS, S/AS01 malaria vaccine in African infants. N Engl J Med 367: 2284–2295
5. The RTS SCTP (2014) Efficacy and safety of the RTS, S/AS01 malaria vaccine during 18 months after vaccination: a phase 3 randomized, controlled trial in children and young infants at 11 African sites. PLoS Med 11(7), e1001685
6. Doolan DL, Southwood S, Freilich DA et al (2003) Identification of Plasmodium falciparum antigens by antigenic analysis of genomic and proteomic data. Proc Natl Acad Sci U S A 100:9952–9957
7. Heppner DG Jr, Kester KE, Ockenhouse CF et al (2005) Towards an RTS, S-based, multistage, multi-antigen vaccine against falciparum malaria: progress at the Walter Reed Army Institute of Research. Vaccine 23:2243–2250
8. Cockburn I (2013) Chimeric parasites as tools to study Plasmodium immunology and assess malaria vaccines. Methods Mol Biol 923: 465–479
9. Persson C, Oliveira GA, Sultan AA et al (2002) Cutting edge: a new tool to evaluate human pre-erythrocytic malaria vaccines: rodent parasites bearing a hybrid Plasmodium falciparum circumsporozoite protein. J Immunol 169(12): 6681–6685
10. Tewari R, Spaccapelo R, Bistoni F et al (2002) Function of region I and II adhesive motifs of Plasmodium falciparum circumsporozoite protein in sporozoite motility and infectivity. J Biol Chem 277(49):47613–47618
11. Espinosa DA, Yadava A, Angov E et al (2013) Development of a chimeric Plasmodium berghei strain expressing the repeat region of the P. vivax circumsporozoite protein for in vivo evaluation of vaccine efficacy. Infect Immun 81:2882–2887
12. Bauza K, Malinauskas T, Pfander C et al (2014) Efficacy of a Plasmodium vivax malaria vaccine using ChAd63 and modified vaccinia Ankara expressing thrombospondin-related anonymous protein as assessed with transgenic Plasmodium berghei parasites. Infect Immun 82:1277–1286
13. Janse CJ, Ramesar J, Waters AP (2006) High-efficiency transfection and drug selection of genetically transformed blood stages of the rodent malaria parasite Plasmodium berghei. Nat Protoc 1(1):346–356
14. Janse CJ, Franke-Fayard B, Mair GR et al (2006) High efficiency transfection of Plasmodium berghei facilitates novel selection procedures. Mol Biochem Parasitol 145:60–70
15. Philip N, Orr R, Waters AP (2013) Transfection of rodent malaria parasites. Methods Mol Biol 923:99–125
16. Wengelnik K, Spaccapelo R, Naitza S et al (1999) The A-domain and the thrombospondin-related motif of Plasmodium falciparum TRAP are implicated in the invasion process of mosquito salivary glands. EMBO J 18:5195–5204
17. Angov E, Hillier CJ, Kincaid RL et al (2008) Heterologous protein expression is enhanced by harmonizing the codon usage frequencies of

the target gene with those of the expression host. PLoS One 3(5)

18. Yadav MK, Swati D (2012) Comparative genome analysis of six malarial parasites using codon usage bias based tools. Bioinformation 8:1230–1239
19. van Dijk MR, McConkey GA, Vinkenoog R et al (1994) Mechanisms of pyrimethamine resistance in two different strains of Plasmodium berghei. Mol Biochem Parasitol 68:167–171
20. Fidock DA, Wellems TE (1997) Transformation with human dihydrofolate reductase renders malaria parasites insensitive to WR99210 but does not affect the intrinsic activity of proguanil. Proc Natl Acad Sci U S A 94:10931–10936

Chapter 34

DNA Integration in *Leishmania* Genome: An Application for Vaccine Development and Drug Screening

Tahereh Taheri, Negar Seyed, and Sima Rafati

Abstract

Transfection technology is an important tool in the investigation of gene function and the modulation of gene expression, thereby contributing to the advancement of basic cellular research, drug discovery, and target validation. Creation of the mutant cells through gene disruption and exogenous protein expression with noticeable phenotype like reporter genes are among other key applications. In this chapter, protocols for generating recombinant *Leishmania* expressing EGFP or EGFP-Luciferase and their applications are given in detail.

Key words *Leishmania* transfection, Reporter genes, In vivo imaging, Bioluminescence, Vaccine, Drug screening

1 Introduction

Gene replacement technology has two main applications in *Leishmania* studies: first, targeting and manipulating genes involved in pathogenicity making genetically attenuated live or nonpathogenic strains as live vaccine [1, 2] and second, generation of reporter parasites that have several biological applications from basic research to evaluation of vaccine and drug efficacy [1, 3]. Early-stage detection of *Leishmania* infection in experimental animal models is so critical and is routinely achieved by means of conventional methods including footpad swelling measurements, microscopic observations, parasite burden evaluation by limiting dilution, and cell culture. The major drawback intrinsically associated with these methods is to sacrifice a large number of animals during the course of the study.

Recently, optical reporter genes such as enhanced green fluorescent protein (EGFP) and luciferase (LUC) have emerged as invaluable recognition tools to help better detect and quantify microbial agents in situ. The major application of EGFP or LUC genes expressed in *Leishmania* is to track the infection in different

Sunil Thomas (ed.), *Vaccine Design: Methods and Protocols: Volume 1: Vaccines for Human Diseases*, Methods in Molecular Biology, vol. 1403, DOI 10.1007/978-1-4939-3387-7_34,

organs or tissues and to estimate in vivo parasite burden by imaging and ex vivo/in vitro evaluation by fluorescence microscopy or flow cytometry. EGFP and LUC individually or fused with other peptides or reporter genes are used for in vivo studies and live-cell imaging. Reporter genes could be expressed transiently or permanently based on specific experimental conditions.

Leishmania is a very-well-known eukaryotic parasite with promoter-less genes (except rRNA genes). In this parasite, posttranscriptional modifications through trans-splicing by intergenic regions (IR), 5′ splice leader and 3′ poly-adenylation, are responsible for gene regulation. Therefore it is highly substantial to take into consideration the regulatory elements for expression of exogenous genes in *Leishmania* system. Usually, two main strategies, episomal (out of genome) and stable (genome integrated), are used to express endogenous or exogenous genes in *Leishmania* [4]. Transfection protocol is the same for both approaches although vectors could be different. Episomal transfection or directly introducing an intact plasmid into parasite without any genomic manipulation is suitable for transient expression of a gene/s for a few generations. Successful expression in episomal system requires a simple backbone prokaryotic plasmid consisting of leishmanial specific IRs (such as DST [5], 1.7 K [6] or CPB 2.8 K [7]) flanking multiple cloning site (MCS). Besides, an eukaryotic selection marker (such as neomycin, hygromycin B, or streptothricinacetyltransferase resistance genes) is also required to select for recombinant parasites.

Stable integration of a foreign DNA into the genome through homologous recombination enables long-term gene expression. To integrate gene into a target locus (knock in), replacement vectors should carry the same mentioned elements of episomal vectors plus two additional flanking regions of target locus (like small subunit (SSU) of ribosomal RNA gene). At other locus, transcription is dependent on adjacent IRs to integration site. Stable transfection is more time consuming compared to episomal transfection due to additional experimental steps.

There are several specific vectors to express a gene in *Leishmania* such as pXG [8, 9], p6.5 [10], and pLEXSY vectors [11, 12]. Here we describe pLEXSY-*neo*-2 vector (EGE-233, Jena Bioscience, Germany) as a suitable example that promotes gene expression in both episomal and stable transfection in 18srRNA locus. This vector bears some IR regions in different locations to provide required signals to add splice acceptor and poly A sites for the target and the marker (*neo*^{r}) genes. Flanking homologous sequences are responsible for accurate incorporation of the target gene into 18srRNA locus of *Leishmania* genome. This vector provides both cytoplasmic and secretory systems for expression of target. Figure 1 schematically illustrates pLEXSY-*neo*-2 backbone, secretory and cytoplasmic enzymatic options, and flanking homologous sequences as 5'SSU and 3′SSU.

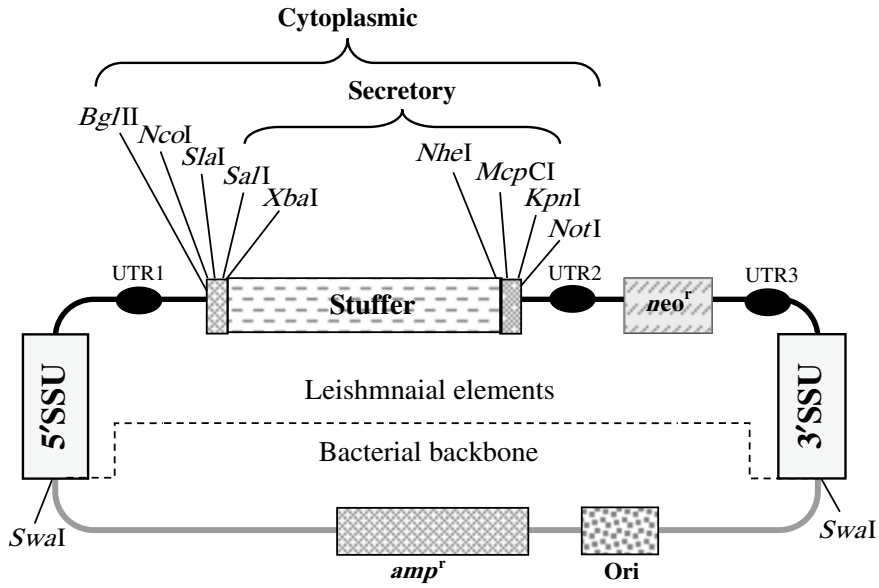

Fig. 1 Schematic diagram of pLEXSY-*neo* expression vector. This plasmid bears three specific IRs of *Leishmania* to provide splice acceptor and poly A signals (UTR 1; 5′UTR of *aprt* gene of *Leishmania* for splicing of target gene, UTR 2; 1.4 k IR from *cam* operon providing poly A site for target gene and splice acceptor site for marker gene, UTR 3; 5′UTR of *dhfr-ts* gene adding poly A sequence to marker gene). *Black line* shows leishmanial region and *gray line* presents bacterial region of plasmid. Both 5′SSU and 3′SSU are required for successful incorporation of expression cassette into 18srRNA locus by homologous recombination. *Swa*I restriction enzyme is used to release a linear fragment by deletion of bacterial backbone of plasmid. Stuffer fragment will be replaced with desired gene of interest

2 Materials

2.1 Media and Reagents

1. *Complete parasite media:* 100 ml M199 media (Sigma) supplemented with 5 % heat-inactivated fetal calf serum (hiFCS-Gibco), 40 mM HEPES (Sigma), 2 mM L-glutamine (Sigma), 0.1 mM adenosine (Sigma), 0.5 μg/ml hemin (Sigma), and 50 μg/ml gentamicin (Sigma). Adjust pH at 7.2 and sterile through a 0.22 μm filter.
2. *Hyman's solution:* $HgCl_2$ (2.5 g), NaCl (5 g), and $Na_2SO_4 \cdot 10H_2O$ (57.5 g) dissolved in dH_2O at a final volume of 1 l.
3. *Electroporation buffer (EPB):* Dissolve 21 mM HEPES (Sigma), 137 mM NaCl, 5 mM KCl, 0.7 mM Na_2HPO_4, and 6 mM glucose in dH_2O. Adjust to pH 7.5 [13] and pass through 0.22 μm filter.
4. *Geneticin (G418) stock solution (10 mg/ml):* Dissolve 100 mg of Geneticin (G418, Gibco) in 10 ml dH_2O and sterile through 0.22 μm syringe filter.

5. *M199 2× media:* Mix 20 ml M199 5× (7.35 g M199 powder and 0.175 g $NaHCO_3$), hi-FCS (20 %), HEPES (1 M), adenosine (10 mM), hemin (0.5 μg/ml), 0.1 ml biotin, 0.025 ml biopterin, L-glutamine (2 mM), and gentamicin (50 mg/ml) in 50 ml dH_2O (adjust pH at 6.85 and sterile using 0.22 μm filter). Warm up in a 56 °C water bath before use [13].
6. *Noble agar 2 %:* Freshly dissolve 2 g of Noble agar (Difco) in 100 ml H_2O. Boil and immediately autoclave; then incubate in a 56 °C water bath until use [13].
7. *Anesthetic solution:* Mix 10 % ketamine (100 mg/ml) with 2 % xylazine (20 mg/ml) in 0.22 μm filtered sterile normal saline (0.9 %).
8. *Luciferin substrate solution:* Dissolve D-luciferin potassium salt (Caliper Life Science) in calcium and magnesium-free PBS (Dulbecco's PBS, PAA) to obtain 15 mg/ml concentration. Pass through a 0.22 μm filter and divide into small aliquots. Store at −70 °C until use and keep from direct light.

2.2 Equipment

1. *Electroporation cuvettes* (0.2 cm; Bio-Rad, sterile).
2. *Electroporation instrument* (Bio-Rad Gene Pulser with capacitance extender).
3. *Epi-fluorescence microscope* (with blue filter set).
4. *Imaging instrument:* Kodak imaging system (system F Pro or imaging station 4000 MM Pro) and software V.5.0.1.27 for data analysis.

3 Methods

3.1 Target Gene Cloning

1. Make pLEXSY-*egfp* or pLEXSY-*egfp-luc* constructs.
   (a) Amplify the DNA fragment containing the ORF of *egfp* (~750 bp) by PCR from pEGFP-N1 plasmid (Clontech Laboratories) as DNA template (10 ng/reaction) with the following primers (0.6 pmol/reaction) [11]:

   EGFP-F: 5′-ATGATATCAAGATCTATGGTGAGCAAGGGC-3′.

   EGFP-R: 5′-GCTCTAGATTAGGTACCCTTGTACAGCTCGTC-3′.

   (Underlined nucleotides are representatives of *Bgl*II and *Kpn*I restriction sites on forward and reverse primers, respectively.) The PCR reaction consists of one denaturation step at 95 °C for 5 min, followed by 30 cycles of denaturation at 94 °C for 1 min, annealing at 62 °C for 2 min, and extension at 72 °C for 3 min and one step of final extension at 72 °C for 20 min. PCR product should be digested by *Bgl*II/*Kpn*I and be purified for further steps (gel and PCR cleanup system).

(b) To build a pLEXSY-*egfp-luc* construct, use the plasmid expression vectors pEGFP-LUC (Clontech Laboratories) encoding EGFP and LUC (from firefly photinu spyralis, ~1650 bp). The two ORFs are separated by an ~40 bp polylinker [12].

2. Insert and clone the gel-purified target gene (*egfp* or *egfp-luc*) into predetermined insertion site dictated by flanking enzymes upstream of *neo*^{r} gene in pLEXSY-*neo* (Fig. 1) following standard cloning steps [14].
3. Transform the recombinant plasmids into bacterial hosts such as DH5α and screen by conventional selection approaches (alkaline lysis methods or Mini-preparation kits).
4. For transient transfection (Fig. 2b), concentrate the purified plasmids by Midi-preparation DNA plasmid kit or any available high-quality kit (*see* **Notes 1** and **2**) and precisely calculate the concentration (*see* **Note 3**). For stable transfection, follow the steps in Subheading 3.2. Figure 2 schematically illustrates stable (A) and transient (B) transfection procedure.

3.2 Construct Preparation for Stable Transfection

First step for stable transfection is to carefully choose for size and location of recombination locus on the genome in order to design a replacement vector as in the previous step. The second step is to digest out the piece of vector that consists of two flanking regions, the insert and the selection marker. The final step is genome integration by homologous recombination. Quality of transcription is fully dependent on the integration locus. At rRNA locus, transcription is under the control of Pol I promoter.

1. Linearize the recombinant pLEXSY-*egfp-neo* or pLEXSY-*egfp-luc-neo* construct with *Swa*I restriction enzyme (Fig. 1) to obtain one small fragment (about 2.8 kbp containing prokaryotic elements) and a larger fragment encoding reporter gene of interest, flanking SSU segments and neomycin resistance gene (~7 or >7 kbp).
2. Purify the fragment by gel cleanup system (or any other available high-quality kits) and resuspend in distilled water.
3. Determine the concentration of DNA by any available spectrophotometer using the following formula:

$$\text{DNA concentration} = \text{OD}_{260}\text{nm} \times \text{dilution factor} \times 50$$

3.3 Transfection

1. Culture *Leishmania* promastigotes in 5 % hi-FCS-supplemented M199 medium and sub-culture every 2 or 3 days by diluting and pipetting to dissociate cells' clumps. Cultures of parasites should be incubated at 26 °C in a dark place (*see* **Notes 4–6**).

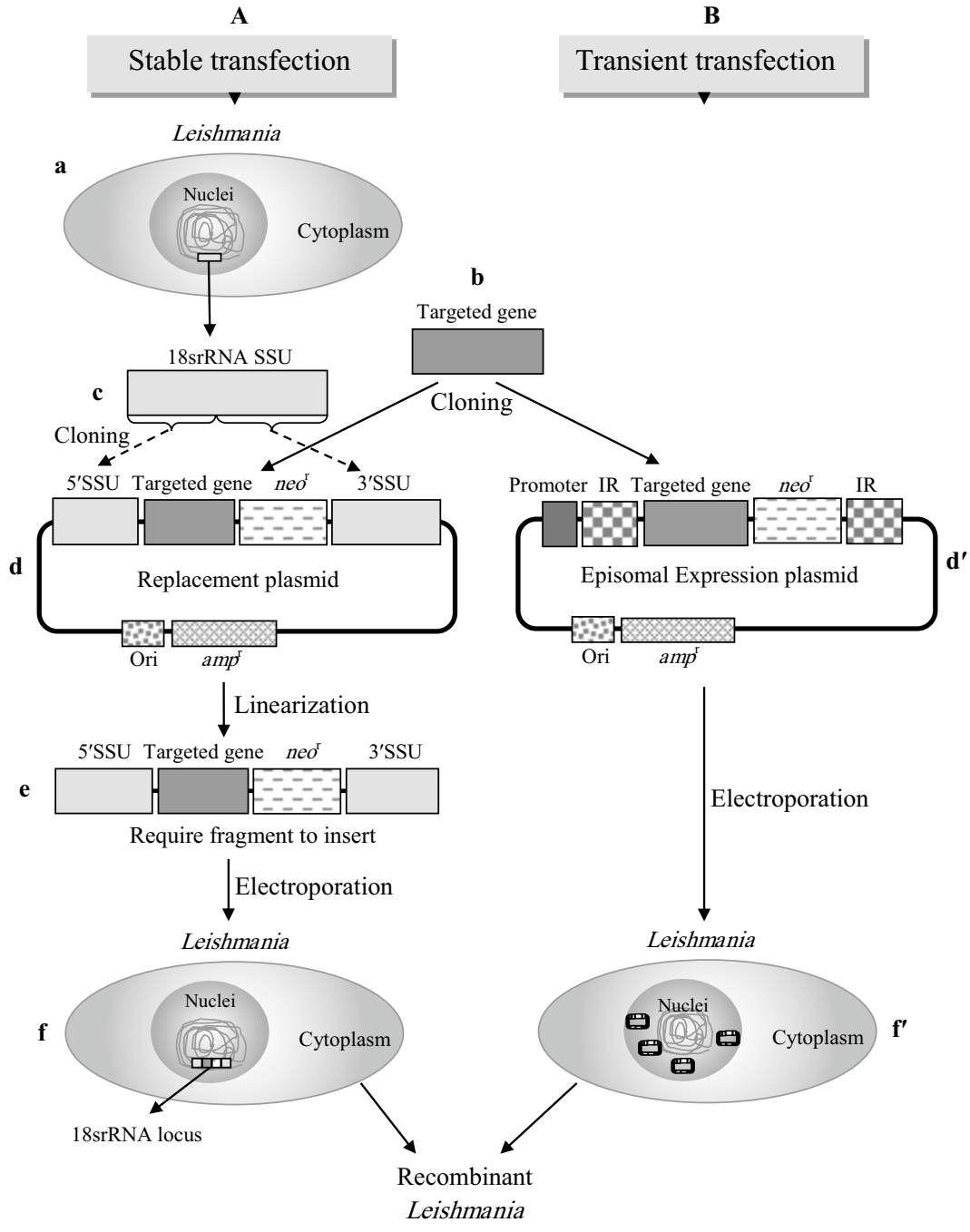

Fig. 2 Schematic illustration of target gene expression in *Leishmania* by stable transfection into 18srRNA locus (**A**) and episomal transient transfection (**B**). (**a**) Wild-type *Leishmania*, (**b**) target gene, (**c**) 18srRNA locus of *Leishmania* genome, (**d**) plasmid constructs (containing target gene, antibiotic resistance gene (*neo*^{r}), and IR) for stable and (**d′**) for transient transfection, (**e**) linearized plasmid containing target gene, *neo*^{r}, and IR (not shown in figure) and homologous sequences, (**f**, **f′**) *Leishmania* transfectants expressing target gene in stable and episomal forms

2. Centrifuge promastigotes at mid-log phase of growth curve (1–2 days after last passage) at $100 \times g$ for 7 min to precipitate dead cells and recentrifuge the supernatant at $1100 \times g$ for 10 min to harvest live parasites.
3. Resuspend parasite pellet in 10 ml of ice-cold EPB, centrifuge at $1100 \times g$ for 10 min, resuspend in 1 ml of EPB, and then count by Hyman's solution (*see* **Notes 7** and **8**).
4. Prepare a suspension of parasite in EPB at a concentration of $\sim 1 \times 10^8$/ml (*see* **Note 9**).
5. Mix 50 μl of purified DNA (5–10 μg linearized DNA for stable transfection or 20 μg of plasmid DNA for transient transfection) with 300 μl of parasite in EBP very gently.
6. Gently transfer the mixture into a sterile electroporation cuvette (2 mm cuvettes, Bio-Rad, USA) between two electrodes without any bubbles and cap it.
7. Store the cuvettes on ice for 10 min.
8. Turn on the Gene pulser and adjust the voltage at 450 V and capacitance at 500 μF.
9. Insert the cuvette into the electroporator (Bio-Rad Gene Pulser with capacitance extender) between two electrodes. Press the "Pulse button" to deliver the pulse to the sample chamber within seconds. After 30–45 s press the "Pulse button" again for a second pulse with the same conditions. The actual voltage delivered to the cuvette and the time constant are measured and displayed digitally.
10. Transfer cuvettes on ice immediately after electroporation and incubate for 5 min.
11. Add the electroporated parasites to 3 ml of G418-free M199 medium supplemented with 10 % hi-FCS (*see* **Note 10**).
12. Incubate for at least 24 h in 26 °C to enhance expression of the target gene/s (about 2–3 generations) (*see* **Note 11**).

3.4 Plating and selection

1. Estimate the number of required plates and amount of Noble agar and M199 2× to make semisolid plates.
2. Gently mix one volume of Noble agar (2 %) and one volume of supplemented M199 2× and pour into plates (up to a medium thickness) without bubbles. Do not forget to add selection antibiotic (*see* **Notes 12** and **13**). For each electroporated cell you need two plates (one plate without and one plate with proper concentration of selection antibiotic). In each experiment electroporate parasite without DNA as control. Always prepare selection plates freshly
3. Air-dry for 20–30 min in a sterile hood in semi-capped position.

4. Leave the capped plates overnight in the dark (cover with foil and avoid cooling).
5. Centrifuge cell suspension, after at least 24 h culture, at 100 × *g* for 1 min to remove cell debris (clumps of dead cells).
6. Transfer supernatant containing live parasites into new sterile tube and recentrifuge at 1100 × *g* for 10 min to pellet live cells. Resuspend the pellets in 200 μl complete M199 medium supplemented with 10 % hi-FCS.
7. Spread a determined volume of resuspended pellet on different semisolid plates (with or without 50 μg/ml G418 as selection antibiotic). Using a scraper (make a scraper by heating Pasteur pipettes at two distinct points), drag back and forth the droplets at all directions until the plate is fully covered by the cells.
8. Air-dry the plates in a sterile hood for 10–15 min. Wrap the plates in parafilm and incubate at 26 °C in the dark with the agar side on top.
9. Monitor the plates daily for clones to appear. Successful transfection occurs when clones grow on both plates (with and without selection antibiotic). Observation of some clones on plates without any selective drug but not on the drug containing plates indicates an unsuccessful transfection.
10. Selection of transient recombinant parasites could be done in liquid media supplemented with the least concentration of the selective drug. Increase the concentration of the selection antibiotic daily. This is an important factor enhancing the desired gene expression for episomal transfection (*see* **Notes 14–16**).

Figure 3 schematically summarizes the plating and screening procedure in both stable and transient transfection.

3.5 Genotype Confirmation of Stable Transfectants

Positive clone selection includes insertion confirmation of target gene and recombination event. To reach this, both PCR and Southern blot techniques could be used. Insertion of target gene is easily confirmed by PCR and specific primers. Recombination confirmation using PCR is faster and easier. Usually the PCR strategy is designed for shorter arm while Southern blot is designed for longer arm where PCR is problematic. These primers should be highly specific with no homology to unrelated homologous sequences.

DNA integration is confirmed by PCR using two specific primers for 5′SSU region (outside homologue sequence). Forward primer matches to upstream sequence of 5′SSU (from genomic DNA) and reverse primer matches to downstream sequence (from plasmid DNA). Figure 4 illustrates the annealing site for pairs of primers used in homologous recombination confirmation.

1. Extract genomic DNA from transfected parasites (using high-quality commercial genomic DNA extraction kits).

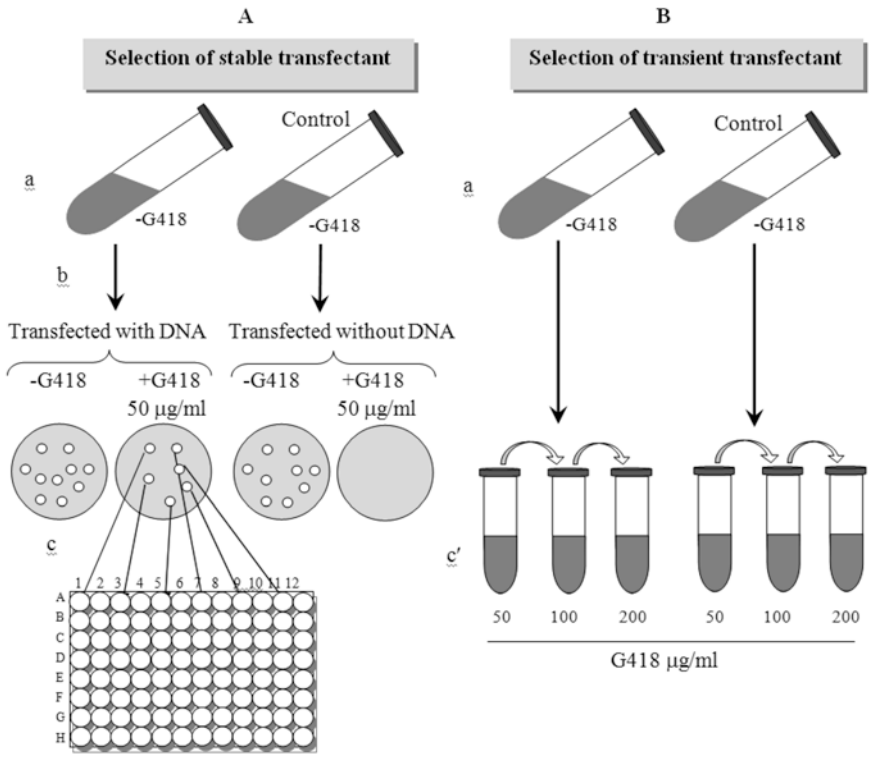

Fig. 3 Plating and screening of positive parasites bearing target gene based on G418 in both stable (**A**) and transient (**B**) transfection. (**a**) Electroporated parasites transferred to fresh media culture without adding any drug for 24 h. (**b**) For stable transfectants, selection of positive cells should be done on semisolid agar plate containing G418 (50 μg/ml). (**c**) Transfer individual clones to distinct wells of 96- or 24-well plate. (**c′**) For transient transfection strategy, concentration of G418 increases gradually during daily passage

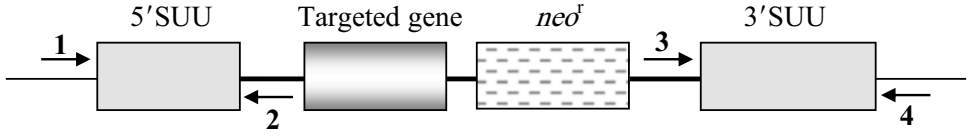

Fig. 4 Annealing site of pairs of primers for PCR screening. Thin line represents genomic DNA and thick line represents plasmid DNA. (1, 2) Show annealing site of primers to confirm homologous recombination and genome integration in 5′SSU side (~1 kbp). (3, 4) Present annealing site for pairs of primers that validate homologous recombination and genome integration in 3′SSU direction

2. Use a standard PCR protocol to amplify target gene (*egfp* and *luc*) by specific primers. Figure 5 shows *egfp* (lane 2) and *luc* (lane 3) confirmation by specific PCR reactions.

3.6 Expression Confirmation

To confirm reporter protein expression both western blot and RT-PCR techniques can be used. Figure 6 represents western blot analysis of the stable integration and expression of EGFP and

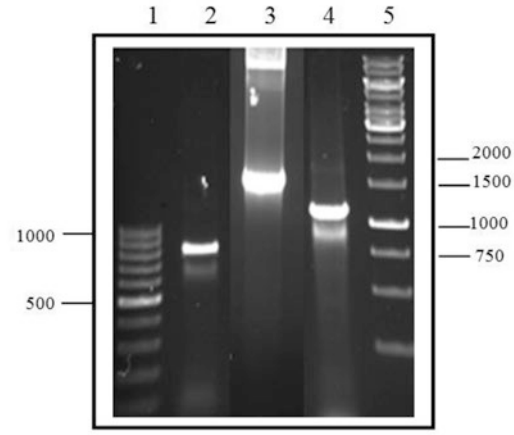

Fig. 5 Confirmation of stable *L. major*$^{EGFP\text{-}LUC}$ transfectants by diagnostic PCR. *Lanes 1* and *5*: DNA ladder (100 bp and 1 kbp, Fermentase), *lane 2: egfp* (~720 bp), *lane 3*: *luc* (~1700 bp), *lane 4*, product of integration of pLEXSY-*egfp-neo* expression cassette into the *ssu* locus of *L. major* by primers F3001 and A1715

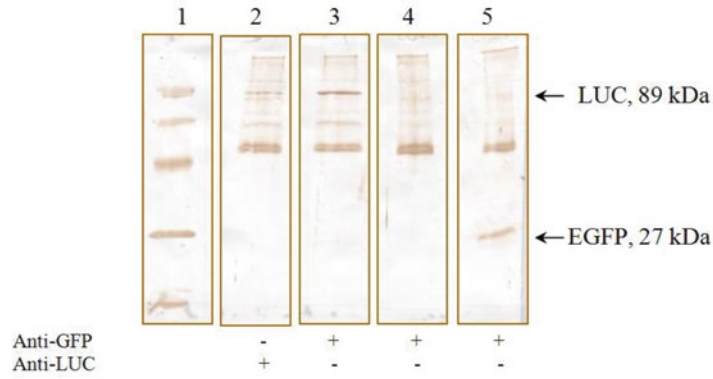

Fig. 6 Western blot using specific antibodies. Monoclonal anti-GFP antibody detected an 89 kDa band in *L. major* $^{EGFP\text{-}LUC}$ (*lane 3*) and a 27 kDa band in *L. major* ^{EGFP} (*lane 5*). Monoclonal anti-LUC showed an 89 kDa in *L. major* $^{EGFP\text{-}LUC}$ (*lane 2*). No reaction was detected in wild-type *L. major* as negative control (*lane 4*). The *arrows* indicate the expected bands. *Lane 1* shows MW marker

EGFP-LUC in recombinant *L. major* using anti-GFP- and anti-LUC-specific antibodies (*see* **Note 17**).

1. Mix the pellet from 10^5 parasite with sample buffer, boil in water bath, and load on 12.5 % SDS-PAGE.
2. Transfer the separated proteins onto nitrocellulose (Protean, Schleicher & Schuell) and block in 2.5 % BSA/0.1 % Tween20 in TBS overnight at 4 °C.

3. Incubate the blots with a diluted horseradish peroxidase (HRP)-conjugated anti-GFP monoclonal antibody 1:6000 or anti-LUC (both from Acris antibodies GmbH) in blocking solution.
4. Remove the extra antibody; wash the blot 3 × 10 min in wash buffer.
5. Incubate in 0.05 % w/v 3,3′-Diaminobenzidine tetrahydrochloride (DAB, Sigma) solubilized in 50 mM Tris–HCl (pH 7.4) and 0.01 % v/v in H_2O_2 (Sigma) as substrate to develop the bands.
6. Immediately stop the reaction by immersing in water to obtain highest resolution.

3.7 Evaluation of EGFP Activity in EGFP-Expressing Transfectants

Expression of integrated *egfp* gene can be confirmed qualitatively and quantitatively through microscopic observation (Epifluorescence microscope with blue filter set, Nikon) and flow cytometric analysis (480 nm argon ion laser-equipped instrument), respectively. Validation of EGFP expression in both forms of parasite, promastigote and amastigote, is very important. Figure 7A shows qualitative evaluation of positive clones by microscopic observation of both promastigotes (a and b) and amastigotes (c and d). GFP expression makes the transfectants shine green under UV illumination. Figure 7B shows quantitative evaluation of positive clones by flow cytometric analysis of promastigotes expressing EGFP in logarithmic (a) and stationary (b) phase. The EGFP intensity decreases at stationary phase of recombinant parasites.

3.8 Evaluation of Luciferase Activity in Luciferase-Expressing Transfectants

1. Seed the live promastigotes of recombinant *L. major*$^{\text{EGFP-LUC}}$ (or homogenized infected organ of mice if working ex vivo) in a 96-well white plate (BRAND) to avoid any background luminescence from neighboring wells.
2. Incubate the cells with lysis buffer (Glo lysis buffer, Promega) at room temperature for 5 min.
3. Add the same volume of defreezed D-luciferin (Promega) to each well at room temperature. Since luciferase activity is temperature sensitive, all reagents should be pre-warmed to ambient temperature before use.
4. Immediately read the luminescence signal adjusted on 1 s/well, sensitivity of 100 and top reading mode using a microtiter plate luminometer (luminometer/fluorometer reader, Multimode Microplate Reader, Synergy, BioTech). Figure 8 represents the graphical results of scanning by Kodak imaging system and measurement of relative luciferase unit (RLU) versus promastigote number.

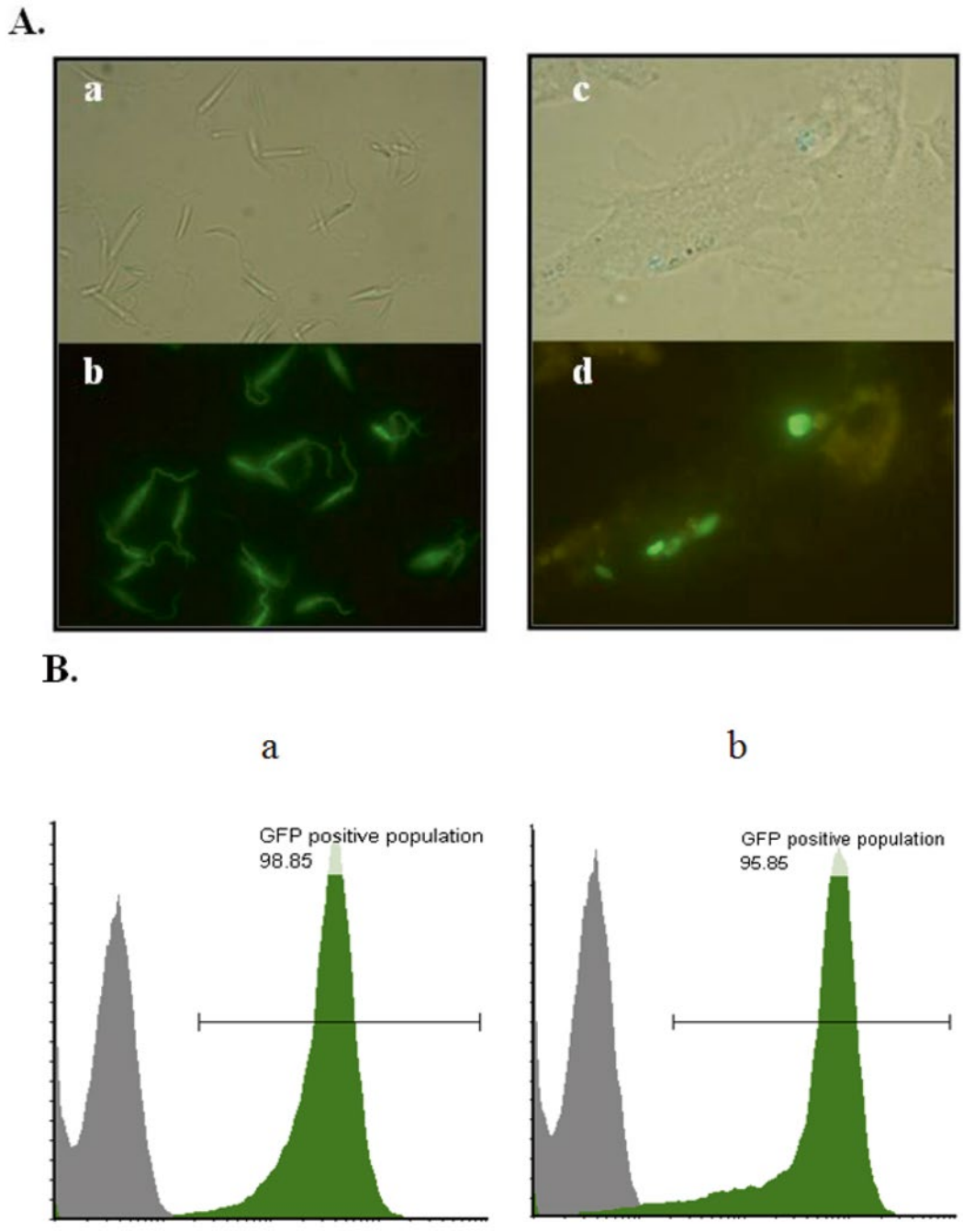

Fig. 7 (**A**) EGFP detection by epi-fluorescence microscopy; fluorescence microscopic images show expression of EGFP in transfected *L. major* promastigotes (before and after emission of fluorescence: **a** and **b**; *left*) and intracellular amastigotes expressing EGFP (before and after emission of fluorescence: **c** and **d**, *right*) in bone marrow-derived macrophages 48 h post-infection with recombinant *L. major*. High amounts of EGFP were observed in both life cycle stages. (**B**) Quantitative evaluation of positive clones by flow cytometric analysis of promastigotes expressing EGFP in logarithmic (**a**) and stationary (**b**) phase

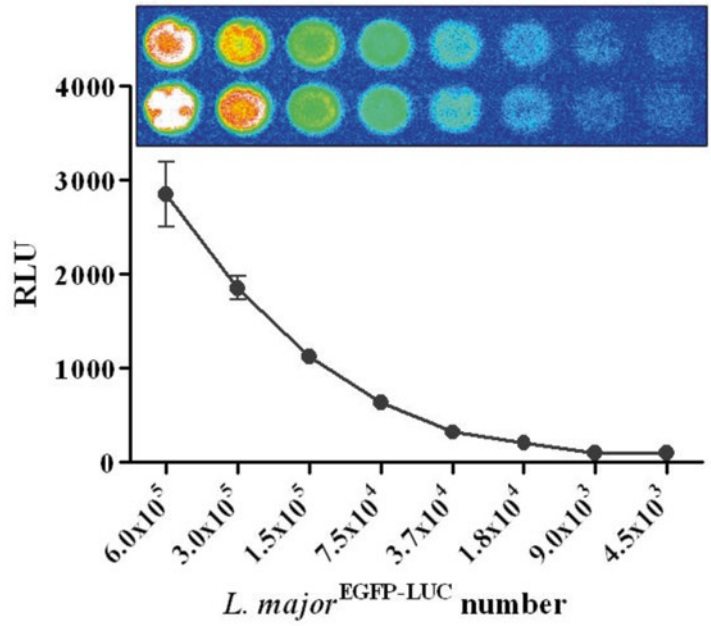

Fig. 8 Measurement of luciferase activity in promastigote stage. A range of *L. major*$^{EGFP\text{-}LUC}$ promastigote (6.0×10^5 to 4.5×10^3) was serially diluted twofold in lysis buffer (Glo lysis buffer, Promega) in a white 96-well microplate. After 5 min, luciferase substrate was added on lysed cells and derived light was measured by a luminometer. The same plates were qualitatively analyzed by Kodak imaging system. RLU: relative luminescence units

3.9 Evaluation of Reporter Signal (Parasite Load) in Live BALB/c Mice

Optical reporter proteins, EGFP and LUC, enable us to monitor infection level in internal organs of live small animals. Since mammalians lack GFP or luciferase, recombinant parasites could be easily tracked in different organs of small animals such as mice. Based on reporter protein's origin, different imaging modalities are used. The BALB/c mice infected with recombinant *L. major*^{EGFP} or *L. major*$^{EGFP\text{-}LUC}$ are monitored by EGFP or LUC signals in situ. The crucial point is that monitoring proceeds without scarification and each animal is used as its own control at any time point during study. EGFP is a natural autofluorescent protein that has an excitation wavelength of 470 nm and emission wavelength of 535 nm. This background emission generates some limitations in imaging. Unlike EGFP, luciferase background is very low resulting in increased sensitivity. Oxidized luciferin by luciferase emits a light that is monitored by bioluminescence detection systems. Both fluorescence and bioluminescence imaging (BLI) need a sensitive detector such as charge-coupled device (CCD).

3.9.1 In Vivo Imaging by Fluorescence

1. Epilate the region of interest to reduce the fluorescence background level (*see* **Note 18**).

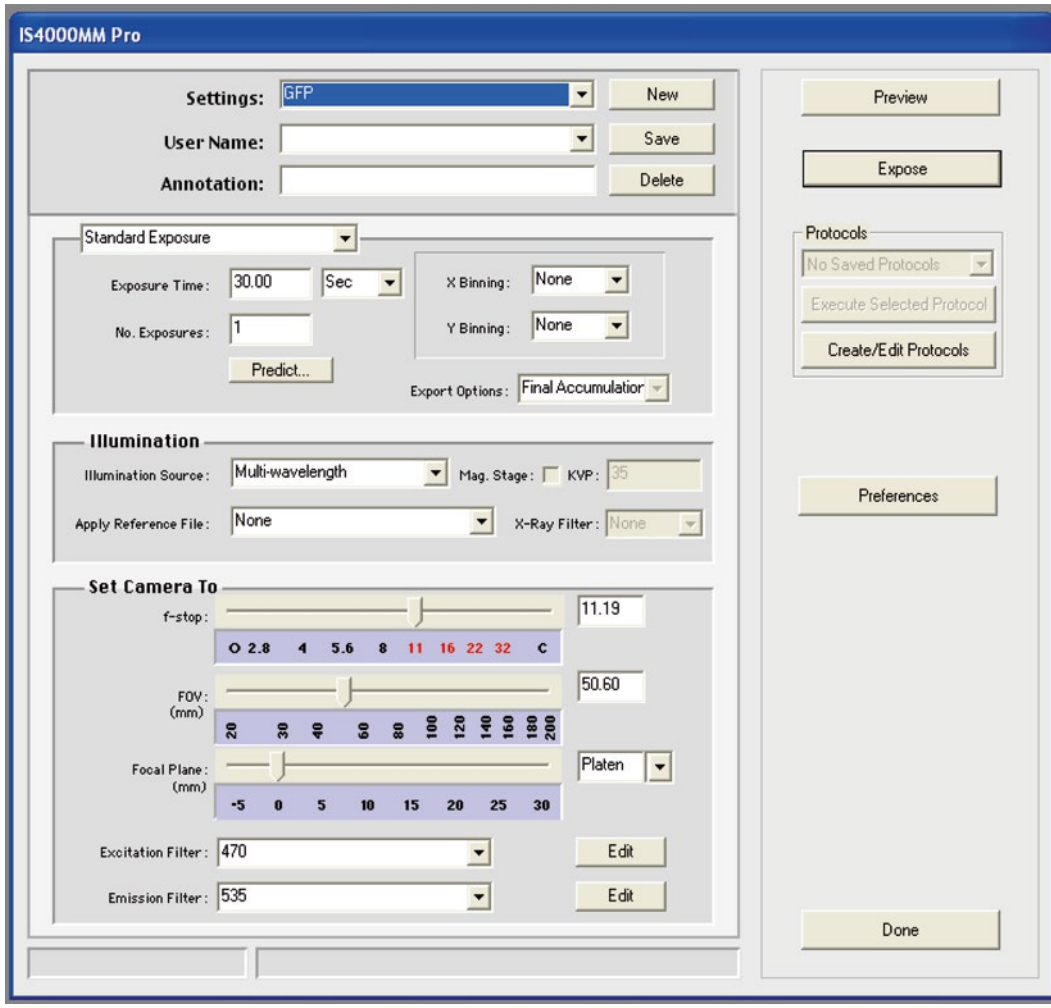

Fig. 9 GFP mode adjustments on the capture window for fluorescence imaging

2. Anesthetize and fix the mouse/mice (individually or in group) on imaging stage of Kodak imaging system.
3. Adjust animal position with door open. You can image whole body or zoom in on a part. For capture, adjust position of animal with f-stop set on 11, preview the image, press "Done" tab, and then decrease the f-stop value to lowest level (about 2.5). For GFP mode adjust exposure time on 30 s, and check filter wavelength (excitation/emission filters 470/535 nm) on capture window (Fig. 9).
4. Close the door, select the exposure tab, and wait for image to be captured. This approach takes less than a minute and is repeatable. If you find no signals *see* **Notes 19–24**.

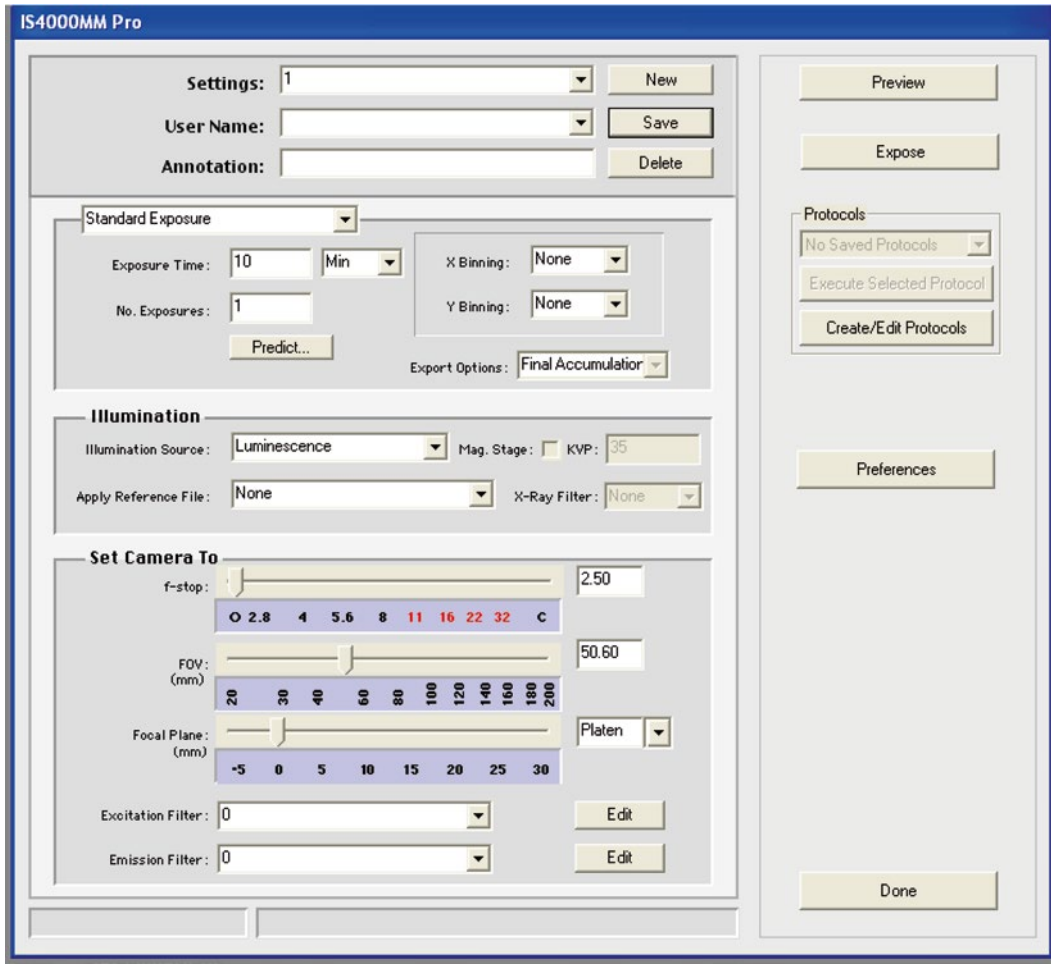

Fig. 10 BLI mode adjustments on the capture window for luminescence imaging

3.9.2 In Vivo Imaging by Bioluminescence (BLI)

1. Inject 200 μl D-luciferin potassium salt as substrate (15 mg/ml) intraperitoneally to infected mice (20–22 g) with *L. major*$^{\text{EGFP-LUC}}$, 5 min before anesthetization.
2. Anesthetize and fix the mouse/mice (individually or in group) on imaging stage of Kodak imaging system.
3. Adjust animal position with door open. You can image whole body or zoom in on a part. Adjust position of animal with f-stop set on 11, preview the image, press "Done" tab, and then decrease the f-stop value to lowest (about 2.5) level (Fig. 10).
4. Capture the BLI images in the following order: first take a photo from the mouse with white light for 1 s while chamber door is open. Then close the door and adjust for luciferase for 10 min. Eventually capture the image for GFP in 30 s. Record GFP signaling on black-white and BLI on rainbow color over-

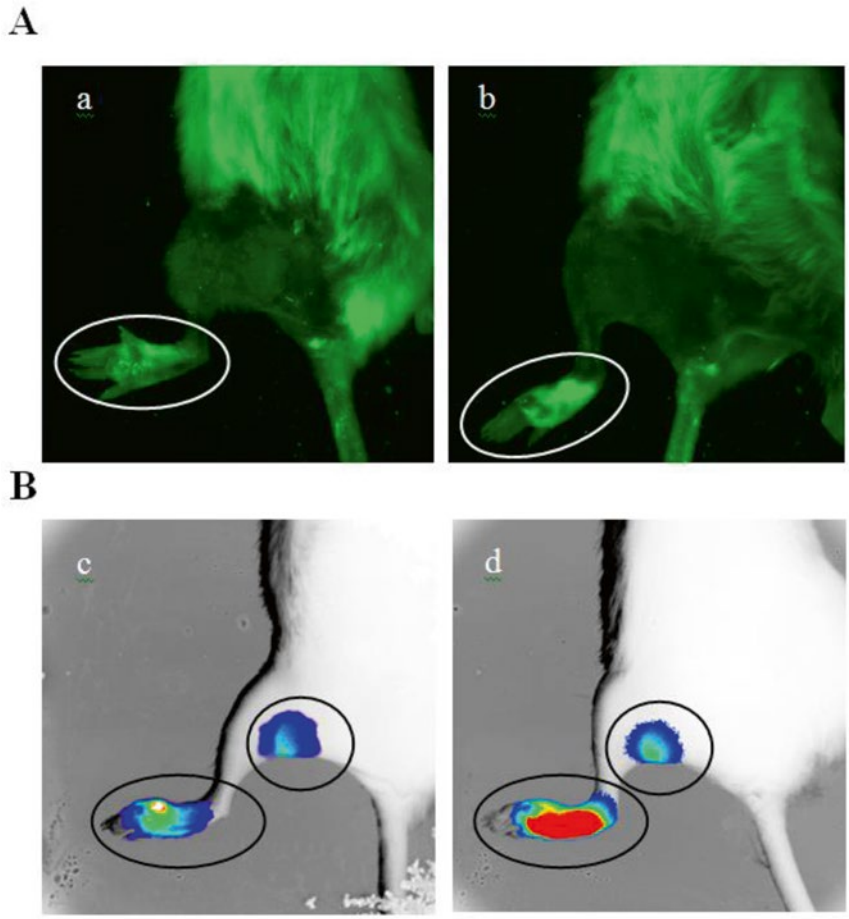

Fig. 11 In vivo imaging of reporter parasite in infected mice. Mice were infected with 5×10^6 parasites in left footpad subcutaneously and were anesthetized before imaging. (**A**) Fluorescence imaging of *L. major*^{EGFP}-infected BALB/c mice at 50 days post-infection (**a**, mouse 1 and **b**, mouse 2). GFP fluorescence shows infection in left footpad of mice. *White ellipses* show ROIs in footpad. (**B**) BLI imaging of *L. major*$^{EGFP\text{-}LUC}$-infected BALB/c mice at 50 days post-infection (**c**, mouse 1 and **d**, mouse 2). Luciferase signaling is visualized in left footpad and lymph node. *Black ellipses* and *circles* illustrate the ROIs in footpad and LNs, respectively

laid on light normal image. This approach takes 20–25 min and imaging in this mode is repeatable in less than an hour, due to short half-life of enzyme. Figure 11b depicts images of two *L. major*$^{EGFP\text{-}LUC}$-infected BALB/c mice by BLI system. As shown parasite infection is accurately detectable in lymph node 50 days post-infection. If you find no signals see **Notes 19–24**

3.10 Image and Data Processing

1. Save the images as *.bip file types for analyzing by Molecular Imaging V.5.0.1.27 software and *.tif for demonstrating images by any specific software such as Adobe Image ready software.

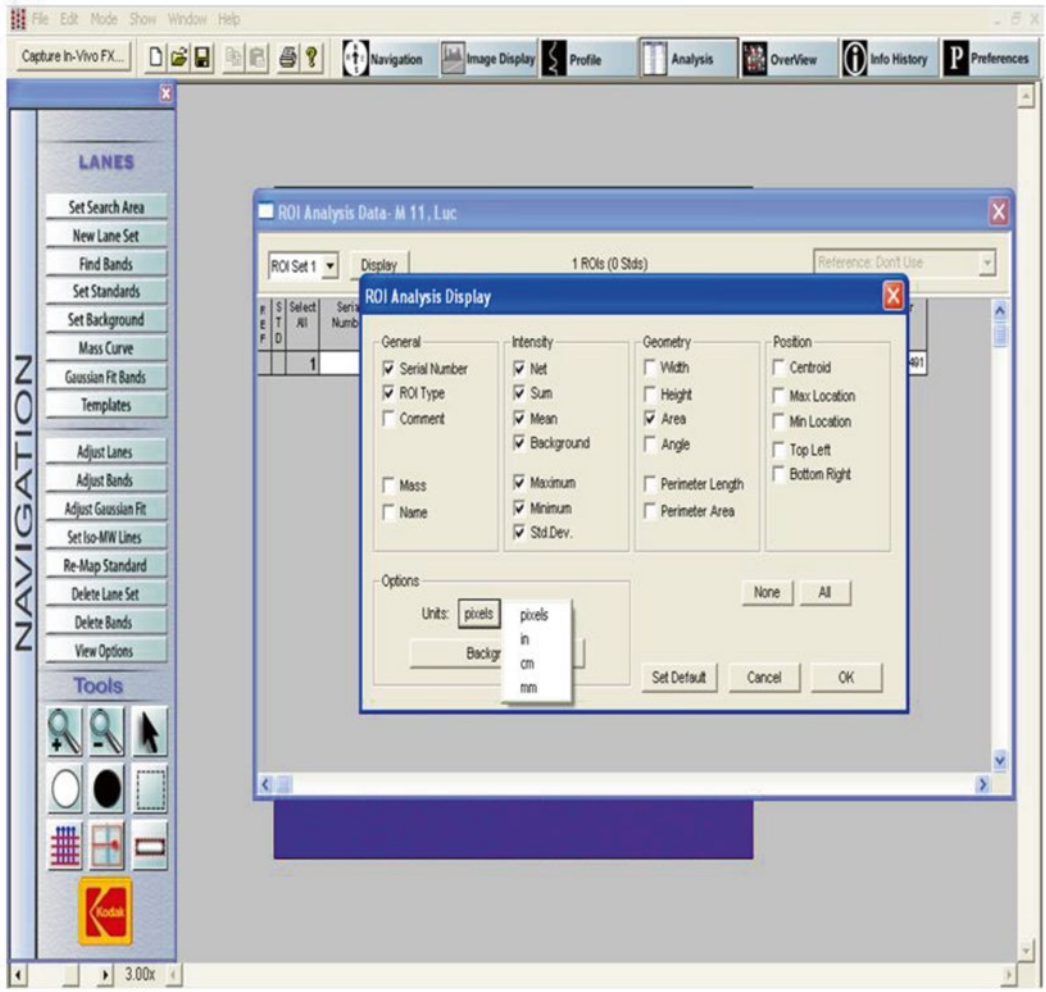

Fig. 12 Calculation of number of pixels in ROI by Molecular Imaging V.5.0.1.27 software

2. To display BLI images, overlay captured rainbow color regions on black and white images using Adobe Imageready software.
3. Open "ROI analysis data" window, click "ROI analysis display", and mark all options of "intensity" box and "pixel" as unit for each image individually (Fig. 12).
4. Present the results as a graphical presentation and compare between mice in different time points.

4 Notes

To increase the efficiency rate of transfection, factors like DNA concentration, buffer quality, time of incubation, and electric pulses should be optimized. If no clones were observed on plates

after 2 weeks, recheck the parasite number, quality and quantity of DNA, quality of EPB, electric pulses, and screening condition. It is quite important to note that different species of *Leishmania* are transfected by variable efficiencies and some species resist manipulation very hard [15].

1. The quality and quantity of DNA are very important. DNA should be highly pure (no nonspecific band) and salt-free. Qualify the integrity of DNA by agarose gel electrophoresis before use.
2. DNA integrity is highly important for efficient transfection. Avoid DNA fragmentation by repeated freezing and thawing.
3. The concentration of DNA is too critical. If not sufficient, concentrate by ETOH/sodium acetate precipitation or concentrator.
4. Always use promastigotes at early or mid-logarithmic phase. At this stage, protein degradation is extremely low due to inactivation of lysosomal enzymes.
5. Monitor the quality and viability of parasites by microscope and vital staining before transfection.
6. Avoid too many passages before and after transfection in order to maintain virulence potency.
7. Always use freshly prepared sterile buffers.
8. Check the quality and pH of electroporation buffer before use.
9. Avoid too low or too high number of parasite for transfection.
10. Always use fresh liquid or semisolid media (noble agar plate) for parasite culture before and after transfection.
11. Stably transfected parasites are usually ready to be plated at least 24 h after the transfection. You can extend the culture to 48 h when efficiency rate is low. This allows sufficient expression of antibiotic resistance protein to resist hostile environment with antibiotic.
12. Culture electroporated parasites in the presence of minimum concentration of appropriate selective antibiotic. Usually this is determined based on the concentration that is toxic for wild-type or un-transfected cells.
13. Optimum concentration of G418 is variable for different species of *Leishmania* and should be predetermined for each species individually. It is recommended to use a concentration about two to three times the IC50 value (concentration needed to kill 50 % of parasites) of the selected antibiotic. This concentration eliminates un-transfected parasites. If you find no clones, reduce the amount of used drug.
14. Always include appropriate controls. For example, in a separate cuvette electroporate same number of parasites in EPB without

any DNA that is called mock transfection. This way you can check the process of normal transfection and can determine any nonspecific effects or unusual phenotypes that may be generated by transfection reagents or electric pulses.

15. Be sure that all inserts match together. If inserted gene has cross resistance with used antibiotic resistance gene, use alternative drug or antibiotic resistance gene. Antibiotic resistance gene is removable using hit-and-run approach.
16. Do not forget to use bacterial antibiotics like gentamycin or penicillin/streptomycin in liquid and semisolid culture media. After transfection and during screening, you should add two types of antibiotics in media culture (eukaryotic antibiotic like G418 and prokaryotic antibiotic like gentamycin). All culture media and buffers should be used in sterile condition. All experiment should be performed in sterile conditions and under biological hoods.
17. Confirm expression of integrated gene/s using RT-PCR and western blot or any other way to detect the given phenotypes (for example check the fluorescence of EGFP in live parasites using fluorescence microscope at least 48–72 h post-transfection). If there is no expression, confirm the correct location of gene in the genome after integration (not ectopic or unusual integration) by PCR or Southern blot for stable transfection.
18. To reduce high background or noise of EGFP, epilate mice body before imaging. Even unclean skin could create nonspecific intensity.
19. Be sure to have precisely adjusted instrument settings since the adjustments differ according to each reporter protein (EGFP or LUC). Preview the images before capturing the final picture.
20. Always include positive controls and focus on the correct infected tissue. For example, if you have infected the footpad, signals are detected in early days after infection in footpad and then later in lymph node.
21. Check the correct recombination and expression of reporter gene in recombinant parasite before inoculating the animal.
22. Increase the number of parasite for mice infection, because there is a direct relation between the level of infection and the reporter protein activity. On the other hand, sensitivity of reporter proteins in different tissues is dissimilar.
23. Switch to the right filter according to required application and turn on fluorescent lamp for fluorescence imaging
24. Optimize the total settings when *Leishmania* species other than *Leishmania major* are used. Use different concentrations of parasite and suitable time after injection for imaging.

References

1. Zahedifard F, Gholami E, Taheri T, Taslimi Y, Doustdari F et al (2014) Enhanced protective efficacy of nonpathogenic recombinant Leishmania tarentolae expressing cysteine proteinases combined with a sand fly salivary antigen. PLoS Negl Tropical Dis 8:e2751
2. Saljoughian N, Taheri T, Zahedifard F, Taslimi Y, Doustdari F et al (2013) Development of novel prime-boost strategies based on a trigene fusion recombinant L. tarentolae vaccine against experimental murine visceral leishmaniasis. PLoS Negl Trop Dis 7:e2174
3. Doroud D, Zahedifard F, Vatanara A, Najafabadi AR, Taslimi Y et al (2011) Delivery of a cocktail DNA vaccine encoding cysteine proteinases type I, II and III with solid lipid nanoparticles potentiate protective immunity against Leishmania major infection. J Control Release 153:154–162
4. Roy G, Dumas C, Sereno D, Wu Y, Singh AK et al (2000) Episomal and stable expression of the luciferase reporter gene for quantifying Leishmania spp. infections in macrophages and in animal models. Mol Biochem Parasitol 110:195–206
5. LeBowitz JH, Coburn CM, McMahon-Pratt D, Beverley SM (1990) Development of a stable Leishmania expression vector and application to the study of parasite surface antigen genes. Proc Natl Acad Sci U S A 87: 9736–9740
6. Ha DS, Schwarz JK, Turco SJ, Beverley S (1996) Use of the green fluorescent protein as a marker in transfected *Leishmania*. Mol Biochem Parasitol 77:57–64
7. Misslitz A, Mottram JC, Overath P, Aebischer T (2000) Targeted integration into a rRNA locus results in uniform and high level expression of transgenes in Leishmania amastigotes. Mol Biochem Parasitol 107:251–261
8. Lye LF, Kang SO, Nosanchuk JD, Casadevall A, Beverley SM (2011) Phenylalanine hydroxylase (PAH) from the lower eukaryote Leishmania major. Mol Biochem Parasitol 175:58–67
9. Robinson KA, Beverley SM (2003) Improvements in transfection efficiency and tests of RNA interference (RNAi) approaches in the protozoan parasite Leishmania. Mol Biochem Parasitol 128:217–228
10. Varela MRE, Lorena Muñoz D, Robledo SM, Kolli BK, Dutta S et al (2009) Leishmania (Viannia) panamensis: an in vitro assay using the expression of GFP for screening of antileishmanial drug. Exp Parasitol 122:134–139
11. Bolhassani A, Taheri T, Taslimi Y, Zamanilui S, Zahedifard F et al (2011) Fluorescent Leishmania species: development of stable GFP expression and its application for in vitro and in vivo studies. Exp Parasitol 127:637–645
12. Taheri T, Saberi Nik H, Seyed N, Doustdari F, Etemadzadeh M-H et al (2015) Generation of stable *L. major*$^{+EGFP\text{-}LUC}$ and simultaneous comparison between EGFP and luciferase sensitivity. Exp Parasitol 150:44–55
13. Beverley SM, Clayton CE (1993) Transfection of Leishmania and Trypanosoma brucei by electroporation. Methods Mol Biol 21:333–348
14. Sambrook J, Russel DW (2001) Molecular cloning: a laboratory manual. Cold Spring Laboratory Press, Cold Spring Harbor, NY
15. Myler PJ, Fasel N (2007) Leishmania after the genome. Caister Academic Press, Norfolk, UK, p 306

Chapter 35

Methods to Evaluate the Preclinical Safety and Immunogenicity of Genetically Modified Live-Attenuated *Leishmania* Parasite Vaccines

Sreenivas Gannavaram, Parna Bhattacharya, Ranadhir Dey, Nevien Ismail, Kumar Avishek, Poonam Salotra, Angamuthu Selvapandiyan, Abhay Satoskar, and Hira L. Nakhasi

Abstract

Live-attenuated parasite vaccines are being explored as potential vaccine candidates since other approaches of vaccination have not produced an effective vaccine so far. In order for live-attenuated parasite vaccines to be tested in preclinical studies and possibly in clinical studies, the safety and immunogenicity of these organisms must be rigorously evaluated. Here we describe methods to test persistence in the immunized host and immunogenicity, and to identify biomarkers of vaccine safety and efficacy with particular reference to genetically attenuated *Leishmania* parasites.

Key words Safety, Persistence, Non-pathogenicity, Innate immunity, Immunogenicity, Protective antigens, Immune suppression, Biomarkers

1 Introduction

The protozoan parasite *Leishmania donovani (L. donovani)* is one of the major causative agents of visceral leishmaniasis (VL) and represents the second most challenging infectious disease worldwide leading to nearly 500,000 new cases and 60,000 deaths annually [1]. Over the past decades, chemotherapy of VL has shown only moderate success owing to serious side effects and the widespread emergence of drug-resistant strains [2]. Due to the limitations associated with current treatments, vaccination seems to be the most feasible alternative for eradication of the disease [3]. Previous attempts at vaccination based on killed *Leishmania* parasites or defined parasite antigens resulted in a limited protection. The limited efficacy of vaccines based on DNA, subunit, heat-killed parasites suggests that acquisition of durable immunity against the protozoan parasites requires a controlled infection with a

Sunil Thomas (ed.), *Vaccine Design: Methods and Protocols: Volume 1: Vaccines for Human Diseases*, Methods in Molecular Biology, vol. 1403, DOI 10.1007/978-1-4939-3387-7_35,

live-attenuated organism [4]. Based on this reasoning, several *Leishmania* gene deletion mutants have been developed and tested as vaccines first against cutaneous and subsequently against visceral leishmaniasis in various experimental animal models [4, 5]. Recent success of irradiated malaria sporozoites as a vaccine candidate in human trials further strengthens this approach to vaccination [6]. We developed several gene deletion mutants in *L. donovani* as potential live-attenuated vaccines [7, 8] and reported extensively on the immunogenicity of *LdCentrin*1 deleted mutant in mice, hamsters, and dogs [9–11]. The major concerns with the use of live-attenuated parasites as vaccines include safety/lack of virulence and immunogenicity [8]. For the live-attenuated parasite vaccines, optimized methods to evaluate persistence of the attenuated parasites in the host are necessary to assess the safety of these vaccines. Safety of the attenuated parasites in terms of non-pathogenicity, limited survival in the host, and non-reversion to virulence are important aspects of the safety profile of these vaccines. In addition, there is a need to identify immune correlates of protection that can be readily extrapolated to humans using systems vaccinology.

In the following sections, we describe methods to evaluate safety of live-attenuated vaccines in terms of non-pathogenicity and absence of persistence in the infected host. Even though many of the methods described here are tested against *Leishmania donovani* mutants (*LdCen−/−* and *Ldp27−/−*), they are nonetheless pertinent to the evaluation of live-attenuated parasites against cutaneous and other forms of Leishmaniasis.

1.1 Methods to Evaluate Safety

Since limited replication of the live-attenuated parasites is a characteristic feature of the live-attenuated parasites, evaluating the complete clearance of the mutant parasites from the immunized host is critical for the safety. While the luminescence-based assays might allow detection of *Leishmania* parasites using in vivo imaging protocols, these methods have not advanced to a point where very low numbers of parasites can be detected in potentially cryptic sites. The current sensitivity of in vivo imaging ($2–4 \times 10^4$ parasites/mg tissue) [12] does not allow it to be a reliable substitute for methods using immunosuppression to detect parasites in the immunized host. Immunosuppression-based methods allow for emergence of parasites from nonimmune surveillance sites and therefore are preferable method for assessing the safety.

1.2 Methods to Evaluate of Immunogenicity

It is well established that the protective immunity in parasitic vaccines is primarily T cell based; therefore it is the current standard practice to demonstrate an induction of robust and specific T cell immunity after immunization. Previous studies have typically showed a Th1 skewed immune response as evidence for establishment of protective immunity. More recent studies have identified

the presence of multifunctional T cells that can produce multiple cytokines (IFN-γ, TNF-α, and IL-2) in response to *Leishmania* antigens as a strong predictor of protective immunity in *Leishmania* [13]. Since most immunological reagents to phenotype the T cell immunity are not available for hamsters and dogs, the methods described here to detect multifunctional CD4+ and CD8+ T cells in mice immunized with live-attenuated parasites pertain to mice.

1.3 Methods to Evaluate Innate Immunity

Leishmania parasites reside predominantly in the host macrophages which they enter by phagocytosis and consequently establish within parasitophorous vacuole. Since macrophages are specialized for the destruction of invading pathogens and priming the innate immune response [14], *Leishmania* has evolved mechanisms to overcome macrophage microbicidal activities through depletion of antimicrobial agents such as reactive oxygen species and nitric oxide (NO) [15]. *L. donovani* infection of macrophages also prevents the activation of an effective immune response by impairing the production of pro-inflammatory cytokines such as tumor necrosis factor (TNF-α, IL-12), and IFN-γ [15]. We describe here tests to evaluate the innate immune response in macrophages upon infection with live-attenuated *Leishmania* parasites. Bone marrow-derived macrophages (BMDM) have been used for these experiments.

1.4 Evaluating the Physiology of Macrophage Membrane Followed by Infection with Either LdWT or Live-Attenuated Parasites to Measure the Antigen-Presenting Capability

Leishmania infection displaces the cholesterol from the macrophage membrane, leading to enhanced membrane fluidity and inhibiting its ability to display parasite antigens to other components of the immune system [16, 17]. Hence, we analyzed whether live-attenuated parasite infection affected the a) membrane cholesterol and b) membrane fluidity in BMDM using the following method. To identify *Leishmania* parasites within the parasitophorous vacuoles, recombinant parasites that express fluorescent proteins (red fluorescent protein or mCherry) were used. Specifically, red fluorescent protein (RFP)-expressing *LdWT* and *Ldp27–/–* parasites were developed using the pA2RFPhyg plasmid for the integration of a RFP/hygromycin B resistance gene expression cassette into the parasite 18S rRNA gene locus as described previously [18]. mCherry-expressing *LdCen–/–* parasites were generated using the pLEXSY-cherry-sat2 plasmid and following the company's protocols (Jena Bioscience, USA).

1.5 Discovery of Biomarkers of Vaccine Safety and Efficacy

A major shortcoming in the vaccine development against bloodborne parasitic agents such as *Leishmania* is the inadequate predictive power of the early immune responses mounted in the host against the experimental vaccines. Often immune correlates derived from in-bred animal models do not yield immune markers of protection that can be readily extrapolated to humans. Recently, several recombinant *Leishmania* antigens were evaluated in

peripheral blood obtained from a limited number of cases of healed VL and previously unexposed controls to test if the cytokines released in response to *Leishmania* antigen can reveal markers that could predict efficacy of these antigens [19]. Of the cytokines tested IFN-γ, IL-2, IL-4, IL-5, IL-10, and TNF-α, only soluble *Leishmania* antigen-specific IFN-γ in healed VL cases showed significantly higher secretion compared to controls [19]. While informative, such studies cannot reveal immune markers of protection and safety other than the previously known correlates assayed. Recent progress in understanding how the innate immune system recognizes microbial stimuli and regulates adaptive immunity is being applied to vaccine discovery in what is termed "systems vaccinology" [20]. This line of analysis using the following tools enables system-wide unbiased molecular measurements, which could be used to reconstruct the immune pathways that could correlate with vaccine-mediated protection. While a number of high-throughput technologies including DNA microarrays, RNA-seq, protein arrays, deep sequencing, and mass spectrometry have been used to identify novel biomarkers of protection using yellow fever and influenza vaccine models [20], we focus on genomic microarray hybridization-based methods for the discovery of biomarkers associated with protection and safety of *Leishmania* genetically modified live-attenuated vaccine candidates.

2 Materials

2.1 Methods to Evaluate Safety

1. Female Balb/C mice (5–8 weeks); Golden Syrian hamsters.
2. Metacyclic *Leishmania* parasites.
3. 26-Gauge syringes.
4. Dexamethasone.
5. PBS.
6. 96-Well plates.
7. Parasite growth medium.

2.2 Methods to Evaluate Immunogenicity

1. Mice.
2. CD16/32 (BD Bioscience, USA).
3. Protein Transport Inhibitor (BD Bioscience, USA).
4. LIVE/DEAD Fixable Aqua (Invitrogen, USA).
5. CD3 APC-eFluor@780 (eBioscience, USA).
6. CD4 eFluor@450 (eBioscience, USA).
7. CD8a eFluor@605NC (eBioscience, USA).
8. CD44 FITC (eBioscience, USA).

9. CCR7 PE-Cy5 (Biolegend, USA).
10. IFN-γ PE-Cy7 (eBioscience, USA).
11. TNF-α PerCp-eFluor@710 (eBioscience, USA).
12. IL-2 APC (eBioscience, USA).
13. IL-10 PE (eBioscience, USA).
14. 96-Well plates.
15. Surgical instruments for spleen recovery.
16. 96-Well ELISA plates.
17. Plate Reader (Luminex-100™ or equivalent).
18. Multiplex mouse cytokine/chemokine magnetic panel from Millipore.

2.3 Methods to Evaluate Innate Immunity

1. RPMI media.
2. ACK lysis buffer (Lonza, USA).
3. 10 % BALB/c serum (Bioreclamation IVT).
4. Macrophage colony-stimulating factor (M-CSF) (eBioscience, USA).
5. Granulocye macrophage colony-stimulating factor (GM-CSF) (eBioscience, USA).
6. LPS (Sigma Cat# L3024).
7. Lab-Tek culture chamber incubation slides (Thermo Scientific, USA).
8. Diff-Quick Stain set (Baxter Healthcare Corporation, Miami, FL, USA).
9. 2′, 7′-Dichlorofluorescin diacetate (H2DCFDA) (Sigma, USA).
10. Griess Reagent (Sigma, USA).
11. Arginase assay kit (Abnova).

2.4 Evaluating the Physiology of Macrophage Membrane Followed by Infection with Either LdWT or Live-Attenuated Parasites to Measure the Antigen-Presenting Capability

1. Filipin III from Streptomyces filipinensis (Sigma, USA).
2. DPH (Sigma, USA).
3. Tetrahydrofuran (Sigma, USA).
4. Fluorescent-labeled parasites.
5. Formaldehyde (Polysciences).
6. Spectrofluorometer (Spectramax M5 or equivalent).
7. CD16/32 (BD Bioscience, USA).
8. CD40 Fluorescein isothiocyanate (FITC) (eBioscience, USA).
9. CD80 Phycoerythrin (PE) (BD Bioscience, USA).
10. CD86 APC (eBioscience, USA).

11. MHC-II Alexa Fluor 700 (eBioscience, USA).
12. $OVA^{329-337}$-peptide (Ana-Spec, USA).
13. Cell Trace TM CFSE Cell proliferation kit (Invitrogen Cat#C34554).
14. $CD4^{+}$T cell isolation kit (Miltenyi Biotec, USA).

2.5 Discovery of Biomarkers of Vaccine Safety and Efficacy

1. Human elutriated monocytes.
2. Human macrophage colony-stimulating factor (Cell Sciences).
3. Human genomic microarray (Affymetrix Array, HUGENE 2.0 ST Array).
4. Affymetrix GeneChip.
5. Human CD11c antibodies for flow cytometry.
6. Hemocytometer.
7. RNA isolation kit.
8. 8-Well chamber slides (Permanox Plastic Chamber Slide System, Thermo Fisher, USA).

3 Methods

3.1 Methods to Evaluate Safety

1. *Intravenous injection*: 5–8-week-old female BALB/c mice were immunized intravenously in the tail vein with 3×10^6 stationary-phase live-attenuated promastigote parasites in a volume of 50 μl.
2. *Intradermal injection*: 5–8-week-old female BALB/c mice were immunized intradermally in the ear with 3×10^6 stationary-phase live-attenuated promastigote parasites in a volume of 10–20 μl.
3. *Intracardiac injection:* 8-week-old Syrian golden hamsters were immunized with 1×10^7 stationary-phase live-attenuated parasites and were given intracardiac injection in a volume of 50 μl.
4. *Immunosuppression:* Mice immunized with live-attenuated parasites for 20–25 weeks were administered 2 mg/kg dexamethasone sodium phosphate (Sigma Aldrich) in PBS subcutaneously three times per week for a period of 4–8 weeks.
5. At several time points during the immunosuppression and the end of the treatment mice were sacrificed and evaluated for parasite burden from spleen and liver by limiting dilution assays.
6. As an additional confirmation of the presence of parasites in tissues, total DNA obtained from spleens of mice was also used as template in real-time PCR [21]. The real-time PCR was based on the target from kinetoplast minicircle DNA using

primers (5′-CCTATTTTACACCAACCCCCAGT-3′; primer 2, 5′-GGGTAGGGGCGTTCTGCGAAA-3′; the probe sequence 5′-RAAARKKVRTRCA GAAAYCCCGT-3′; a black hole quencher moiety is coupled to the 3-end and Calfluor Red coupled to a C6 linker at the 5′end).

3.2 Methods to Evaluate of Immunogenicity

1. Spleens recovered from mice under aseptic conditions were macerated and single-cell suspensions were prepared by filtering through 70 μm nylon mesh filters. Removal of erythrocytes was accomplished by lysis in ACK lysis buffer.
2. Splenocytes were plated in 24-well plates in complete RPMI medium at 37 °C and stimulated with or without FTAg (80 μg/ml).
3. After 48 h at 37 °C Protein Transport Inhibitor (Golgi Stop) was added to the wells.
4. After incubation in Golgi stop (BD Biosciences) for 6 h cells were blocked at 4 °C with rat anti-mouse CD16/32 (5 μg/ml) for 20 min.
5. Cells were surface stained with anti-mouse CD3, anti-mouse CD4, anti-mouse CD8a, anti-mouse CD44, and anti-mouse CCR7 antibodies for 30 min (each with 1:200 dilution; 4 °C).
6. The cells were stained with Live/Dead Fixable Aqua to stain dead cells. Cells were washed with wash buffer and fixed with the Cytofix/Cytoperm kit (BD Bioscience) for 20 min (room temperature).
7. Intracellular staining was done with anti-mouse IFNγ, anti-mouse TNFα, anti-mouse IL-2, and anti-mouse IL-10 for 30 min (each with 1:300 dilution; 4 °C).
8. Cells were acquired on LSRII (BD Biosciences, USA) equipped with 405, 488, 532, and 638 laser lines using DIVA 6.1.2 software. Data were analyzed with the FlowJo software version 9.1.5 (Treestar, San Carlos, CA).
9. For the analysis, doublets were removed using width parameter and dead cells were excluded based on staining with the Live/Dead Aqua dye. Lymphocytes were identified according to their light-scattering properties (Fig. 1).
10. CD4 and CD8 T cells were identified as CD3+ lymphocytes uniquely expressing either CD4 or CD8. Upon further gating intracellular cytokines were measured in $CD44^{Hi}$ $CCR7^{Low}$ cells. FMO controls were used for proper gating of positive events for designated cytokines.
11. Multifunctional T cells are identified as those T cells that produce multiple cytokines (IFN-γ, TNF-α, and IL-2) in response to *Leishmania* FTAg suggesting an effector response. The effector cells that are multifunctionally associated with protec-

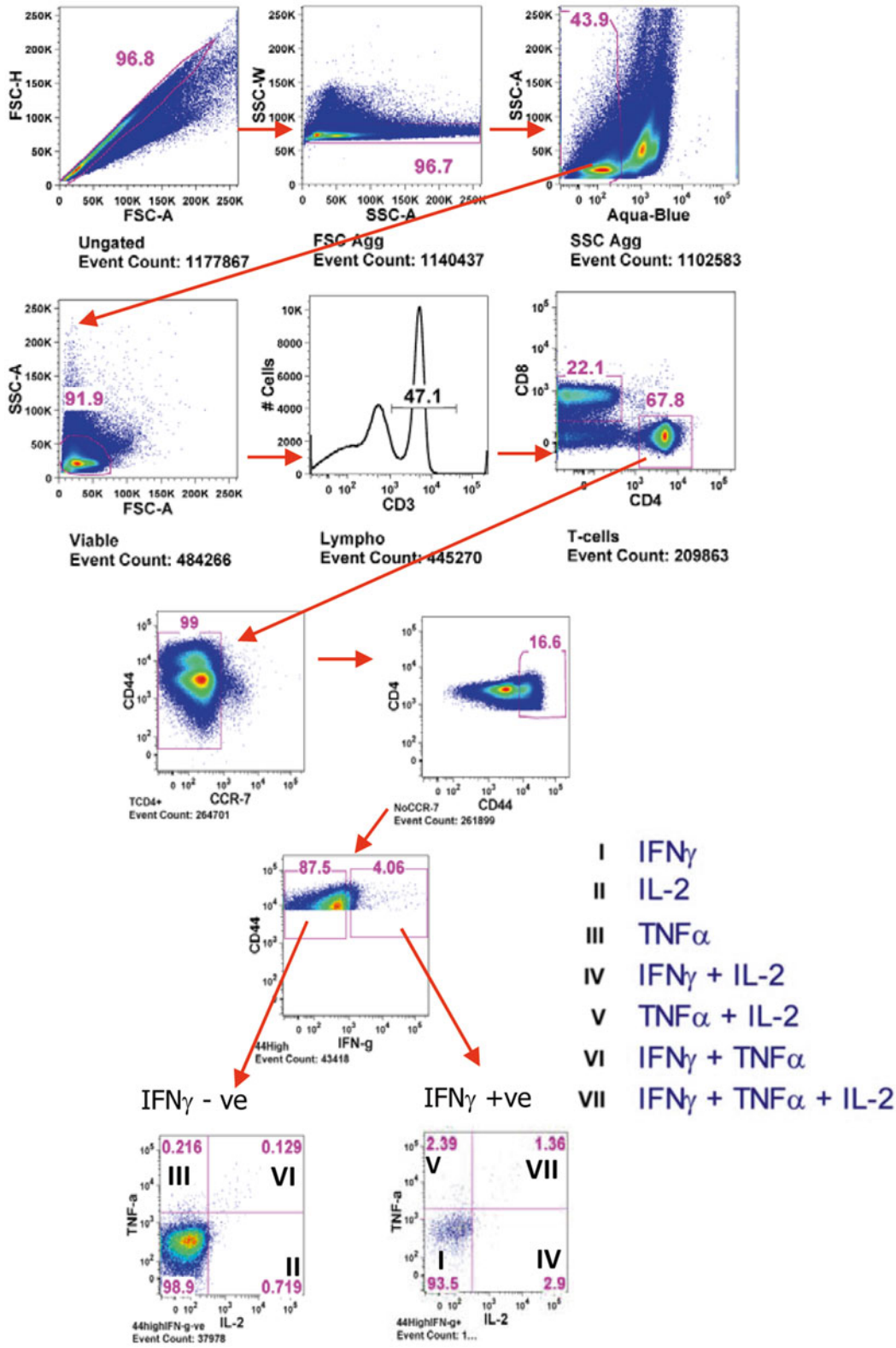
96.8
FSC-H
FSC-A
Ungated
Event Count: 1177867
96.7
SSC-W
SSC-A
FSC Agg
Event Count: 1140437
43.9
SSC-A
Aqua-Blue
SSC Agg
Event Count: 1102583
91.9
SSC-A
FSC-A
Viable
Event Count: 484266
47.1
Cells
CD3
Lympho
Event Count: 445270
22.1
67.8
CD8
CD4
T-cells
Event Count: 209863
99
CD44
CCR-7
TCD4+
Event Count: 264701
16.6
CD4
CD44
NoCCR-7
Event Count: 261899
87.5
4.06
CD44
IFN-g
44High
Event Count: 43418
I IFNγ
II IL-2
III TNFα
IV IFNγ + IL-2
V TNFα + IL-2
VI IFNγ + TNFα
VII IFNγ + TNFα + IL-2
IFNγ - ve
IFNγ +ve
0.216
0.129
III
VI
II
98.9
0.719
TNF-a
IL-2
44highIFN-g-ve
Event Count: 37978
2.39
1.36
V
VII
I
IV
93.5
2.9
TNF-a
IL-2
44HighIFN-g+
Event Count: 1...

tion against *Leishmania* have been described by many in rodents vaccinated with either Leish-111f recombinant polyproteins plus adjuvant [22], with *Leishmania* MML protein expressed in a replication-defective adenovirus [13], in *Ld centrin* or *Ld p27* gene-deleted live-attenuated *Leishmania* parasites [7, 9]. Thus to measure the cell-mediated responses induced by the attenuated parasites/vaccines and find a correlate of protective immunity of Th1 cytokines IFN-γ, TNFα, and IL-2 produced by CD4+ and CD8+ T cells from the animals, multiparameter flow cytometry was followed. Spleen cells grown in vitro with or without freeze-thaw antigens followed by multicolor/parameter staining were gated based on forward and side scatter initially in FlowJo to select only the lymphocyte population devoid of dead cells and other larger leukocytes and further gating of the lymphocytes for the CD3+ followed by gating of CD3+ into CD44+, CCR7-, CD4+, and CD8+ T cells (Fig. 1). Seven distinct populations of cytokine-producing cells were defined from the CD4+ and CD8+ T cells based on different combinations of IFN-γ, TNFα, and IL-2 (a representative analysis is shown in Fig. 1).

To Measure Extracellular Cytokines by Multiplex ELISA

1. Single-cell suspensions were prepared from the spleens recovered from the immunized mice after lysis of red blood cells by using ACK lysing buffer.
2. Cells were washed with complete RPMI medium, plated in 24-well plates, and stimulated with or without freeze-thaw *L. donovani* antigen (FTAg) at 37 °C in 5 % CO_2 with 95 % humidity incubator.
3. After 72 h of culture, cell supernatants were collected and stored in −80 °C until analyzed using multiplex kits, Milliplex Mouse Cytokine/Chemokine Magnetic Panel from Millipore, USA, and the plate was read in a Luminex-100™ (Luminex, Austin, USA) system using Bioplex manager software 5.0.
4. The cytokine analysis procedure has been performed according to the manufacturer's instructions and the level of cytokine concentration determined by using standard curve of each specific analyte.

Fig. 1 The common gating steps to identify cells of interest. Splenocytes from mice were stimulated with FTAg for 48 h and stained with various cell surface markers and antibodies against intracellular cytokines. The single cells are identified using area and width parameters on side scatter. Aqua Blue-negative cells are selected as live cells. T cells are selected based on CD3 positivity. CD4 and CD8 cells were separated based on the surface antibody staining. CD44hi cells are identified as activated CD4 or CD8 T cells. IFN-γ-positive cells among the activated CD4 T cells were identified based on the staining and IFN-γ-positive cells were further gated to identify TNF-α- and IL-2-expressing triple-positive cells (multifunctional T cells)

3.3 Methods to Evaluate Innate Immunity

Preparation of Bone Marrow-Derived Macrophages, Bone Marrow-Derived Dendritic Cells, In Vitro Infection, and Stimulation

1. Macrophages were cultured in vitro from bone marrow progenitors. BALB/c mice were sacrificed and their femurs and tibias were excised, cleaned of tissue, and flushed with 2–5 ml of the RPMI wash medium, until bone cavity appears white and were collected in a sterile 50 ml conical centrifuge tube on ice.
2. The collected cells were centrifuged at 500 × *g* for 10 min at room temperature and then the pellet was suspended in ACK lysis buffer for the depletion of erythrocytes for 5 min at room temperature.
3. The cells were then washed (500 × *g* for 10 min) and cultured with complete RPMI medium supplemented with 10 % (v/v) fetal bovine serum, 1 % penicillin, 20 units/ml streptomycin, and 20 ng/ml M-CSF and incubated for 7 days at 37 °C incubator under 5 % CO_2 to differentiate into macrophages.
4. After 7 days of culture, the adherent cells were harvested and based on the specific expression of a number of macrophage-specific surface markers including CD11b and CD14, >90 % pure macrophages were obtained as evaluated by flow cytometry.
5. On day 7 of the culture, the differentiated macrophages are infected in vitro with stationary-phase promastigote parasites (LdWT and live-attenuated parasites).
6. Bone marrow-derived dendritic cells (BMDCs) also play critical role during *Leishmania* infection. Hence, in some experiments BMDCs also were obtained by isolating the bone marrow from the mice following the abovementioned protocol and subsequently cultured with complete RPMI medium supplemented with 10 % (v/v) FBS and 1 % penicillin (20 units/ml)/streptomycin (20 mg/ml) and GM-CSF for 7 days at 37 °C incubator under 5 % CO_2 to obtain 85 % purity of CD11c+DCs. BMDCs were harvested and plated on 24-well tissue culture plates and infected with various groups of parasites.
7. For in vitro infection, stationary-phase cultures of Leishmania promastigotes were incubated in 10 % mouse (BALB/c) serum for 15 min at 37 °C for complement opsonization followed by washing with PBS three times. The infection was done at a ratio of 5 parasites to 1 macrophage.
8. The infection was done in triplicate chamber slides along with uninfected controls. The infection was allowed to continue for 6 h at 37 °C incubator under 5 % CO_2 environment. After 6 h, the cells were washed with culture medium to remove the extracellular parasites and incubated for different time periods.

9. At 6, 24, 48, and 72 h post-infection, the culture medium was removed from a sample of the culture slides, and the slides were air-dried, fixed by immersion in absolute methanol for 5 min at room temperature, and stained using Diff-Quick Stain set and intracellular parasite numbers were evaluated microscopically.
10. To measure parasite load in these cultures, a minimum of 300 macrophages were counted. The results are expressed either as percentages of macrophages that were infected by parasites or as the mean number of parasites/infected macrophage.
11. In order to stimulate the BMDM, the infected BMDMs were treated with lipopolysaccharide (LPS) for 24 h.

Measurement of Innate Response

12. Macrophage activation for enhanced microbial activity is a critical requirement leading to the successful elimination of Leishmania parasites. The ability of macrophages to secrete reactive oxygen intermediates (ROS), as well as reactive nitrogen intermediates (RNI), correlates closely with their capacity to kill Leishmania parasites whereas Leishmania infection-induced arginase-1 activity in host macrophages leads to parasite survival [15,23]. Hence, we have studied the generation of these molecules in response to live-attenuated parasite infection and compared it with LdWT infection using the methods described below:

Measurement of Reactive Oxygen Species

13. For monitoring the level of reactive oxygen species (ROS) (including superoxide, hydrogen peroxide, and other reactive oxygen intermediates) produced within the cell, the cell-permeable, nonpolar, H_2O_2-sensitive probe DCFDA was used. Mice-derived BMDM from different infection time points were incubated with H2DCFDA (2 μg/ml) at room temperature for 20 min in the dark. Extent of H_2O_2 generation was defined as ROS generation for our convenience. Relative fluorescence was measured in a SpectramaxTM Molecular Diagnostics at an excitation wavelength of 510 nm and an emission wavelength of 525 nm. For each experiment, fluorometric measurements were performed in triplicate and data are expressed as mean fluorescence intensity units.

Quantification of Nitric Oxide

14. Nitrite accumulation in culture was measured colorimetrically by the Griess assay. For each assay, freshly generated BMDM were cultured in 96-well tissue culture plates at a concentration of 105 cells/ml followed by infection with different groups of opsonized parasites and then stimulated with LPS (1 μg/ml) for 24 h.

15. Cell-free supernatants were collected at 24 h post-infection, and the mixture of culture supernatant and Griess Reagent at 1:1 ratio was incubated for 15 min at room temperature in the dark, and the OD was determined at 550 nm by spectrophotometer (Spectramax). Data are expressed in terms of μM nitrite.

Arginase Activity Assay

16. Arginase activity, measuring the conversion of arginine to ornithine and urea, was determined using a quantitative colorimetric assay at 430 nm, employing an arginase assay kit.
17. An aliquot (40 μl) of protein extract (40 μg) from BMDM infected with various groups of opsonized parasites in 0 × 1 % Triton X-114 was combined with 10 μl of the substrate buffer and incubated at 37 °C for 2 h.
18. Samples were added to a 96-well flat-bottomed plate (Corning, Inc.) with the appropriate blank controls. Urea reagent (supplied with kit) was then added to the individual wells to stop the arginase reaction and incubated at room temperature for 60 min. The absorbance was then measured at 430 nm and enzyme activity (in IU) calculated according to the kit instructions.

3.4 Evaluating the Physiology of Macrophage Membrane Followed by Infection with Either LdWT or Live-Attenuated Parasites to Measure the Antigen-Presenting Capability

Membrane Cholesterol Profile Estimation

1. For analyzing the cholesterol content in the macrophage membrane we have stained the cells with the cholesterol-binding probe Filipin III from Streptomyces filipinensis followed by fluorescence confocal microscopy as follows:
2. BMDM were grown on cover slip chambered slides, infected with various groups of opsonized fluorescent parasites (red fluorescent LdWT RFP, Ldp27−/− RFP, or LdCen−/− m-cherry) for 24 h.
3. Cells were then washed in PBS and fixed for 30 min with 3 % (vol/vol) paraformaldehyde in PBS at room temperature and the paraformaldehyde-fixed cells were incubated for 30 min with filipin (0.5 mg/ml in PBS) and then were washed with PBS.
4. Cells stained with filipin were imaged using the 364 nm UV laser on the Zeiss LSM510 Meta microscope, with fluorescence emission collected using a 435–485 nm band-pass emission filter.

Measurement of Fluorescence Anisotropy (FA)

1. The fluorescent probe DPH was dissolved in tetrahydrofuran at 2 mM concentration and then added to 10 ml of rapidly stirring PBS (pH 7.2).

2. The BMDM (infected with either LdWT or live-attenuated parasites) were labeled by mixing 106 cells with an equal volume of DPH in PBS (Cf 1 μM) and incubated for 2 h at 37 °C. The cells were then washed thrice and resuspended in PBS.
3. The DPH probe bound to the membrane of the cell was excited at 365 nm and the intensity of emission was recorded at 430 nm in a spectrofluorometer. The FA value was calculated using the equation $FA = [(I\| - I\perp)/(I\| + 2I\perp)]$, where $I\|$ and $I\perp$ are the fluorescent intensities oriented, respectively, parallel and perpendicular to the direction of polarization of the excited light [17].

Antigen-Presenting Assay

Since live-attenuated parasite infection did not lead to any change in membrane architecture, i.e., membrane fluidity in BMDM, we therefore analyzed the antigen-presenting function of the BMDM upon infection with live-attenuated parasites. The expression of co-stimulatory molecules after infection with LdWT and live-attenuated parasites was first analyzed and subsequently functional antigen presentation assay was performed as described below:

Co-stimulatory Molecule Expression Studies

1. BMDM were blocked at 4 °C with rat anti-mouse CD16/32 for 20 min.
2. Cells were then stained with anti-mouse CD40 (FITC), anti-mouse CD80 (PE), anti-mouse CD86 APC, and anti-mouse MHC-II Alexa Fluor 700 for 30 min (each with 1:200 dilution; at 4 °C). The cells were then stained with Live/Dead Fixable Aqua to stain dead cells.
3. Cells were washed twice with PBS and were finally suspended in PBS having 1 % PFA and were kept at 4 °C in the dark till acquired on flow cytometer. Cells were acquired on Fortessa (BD Biosciences, USA) equipped with 355, 405, 488, 532, and 638 laser lines using FACSDIVA 8.0 software (BD). Data were analyzed with the FlowJo software version 9.7.5.

Functional Antigen Presentation Assay

1. BMDM were pulsed with OVA peptide (2 μg/ml) (323–339) for 2 h at 37 °C in 5 % CO_2-humidified chamber and infected with LdWT or live-attenuated parasites for 24 h.
2. CD4 + T cells were purified from spleens of DO11.10 transgenic mice (mice carrying this MHC class II-restricted rearranged T cell receptor transgene on an H2d background react to ovalbumin peptide antigen) using CD4 + T cell isolation kit

stained with 5 μM CFSE for 10 min in RPMI 1640 without fetal calf serum (FCS) at 37 °C in 5 % CO_2-humidified chamber.

3. Cells were incubated for 5 min with ice-cold RPMI1640 plus 10 % FCS for quenching the CFSE and subsequently washed thoroughly before plating in 96-well tissue culture plates along with OVA-pulsed BMDM.
4. Cells were cultured for 5 days at 37 °C with 5 % CO_2 and T cell proliferation was then estimated by flow cytometry by gating on CD4+ cells. For each sample 10,000 CD4 positive cells were measured.
5. Cells were acquired on Fortessa (BD Biosciences, USA) equipped with 355, 405, 488, 532, and 638 laser lines using FACSDIVA 8.0 software (BD). Data were analyzed with the FlowJo software version 9.7.5.

3.5 Discovery of Biomarkers of Vaccine Safety and Efficacy

1. Human elutriated monocytes were suspended in RPMI medium containing 10 % FCS and 20 ng/ml human MCSF pre-warmed to 37 °C. The cell suspension was plated in 8-well chamber slides at a concentration of 125,000 monocytes per well in a volume of 0.5 ml. The plates were incubated in 37 °C incubator with 5 % CO_2 for differentiating the monocytes into macrophages.
2. The growth medium is changed once every 3 days by gently aspirating the medium from the wells and replacing with a fresh medium containing human MCSF. To confirm the differentiation of the macrophages, a flow cytometric analysis using CD11c antibody staining was performed.
3. On day 9 of the culture, the differentiated macrophages are infected with stationary-phase promastigote parasites (wild-type and live-attenuated parasites). Stationary-phase Leishmania cultures were pelleted, washed in cold PBS three times, and suspended in RPMI medium containing 10 % FCS. The infection was done at a ratio of 10 parasites to 1 macrophage. The infection was done in triplicate chamber slides along with uninfected controls.
4. The infection was allowed to continue for 6 h by incubation in the 37 °C incubator. The medium containing the parasites was aspirated and macrophages were extensively washed with fresh RPMI medium to remove the extracellular parasites. Absence of uninfected parasites is confirmed using microscopic examination of the chamber slides.
5. The infection was allowed to continue for an additional 18 h. At the end of infection, the medium was aspirated out and the infected macrophages were recovered in RNA lysis solution.

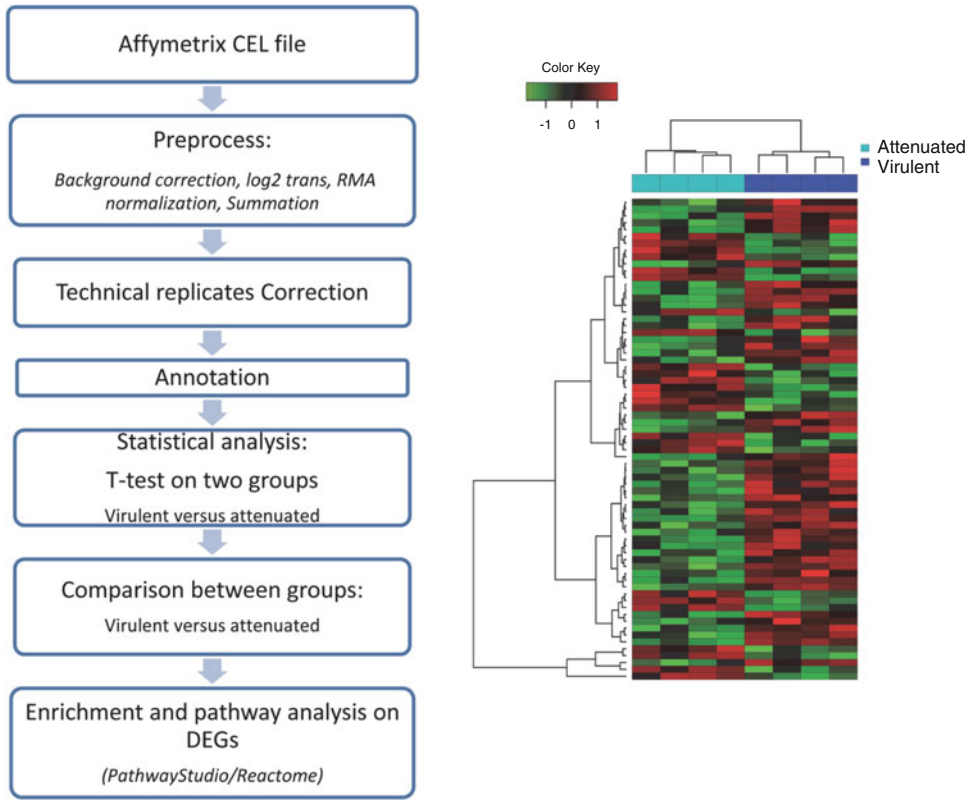

Fig. 2 (**a**) Common elements of work flow after hybridization of human genomic microarray are shown. These steps may vary slightly depending on the platform used. (**b**) A typical output file is shown as heat map. The four columns in each group in the heat map represent four individual biological samples (attenuated and virulent)

Fluorescently labeled cDNA prepared from the RNA isolated above is hybridized to human genomic microarray. The hybridization reaction is performed at least in duplicate per each group tested. Uninfected control is also tested on the human genomic microarray to establish the baseline expression patterns.

6. Post-hybridization analysis of the gene expression typically follows the following steps (Fig. 2). The post-hybridization files are processed for background correction followed by logarithmic transformation of the raw data and robust microarray average normalization. Discrepancies in the technical replicates of each sample are corrected manually. The resulting expression patterns are used for gene annotation. Comparison between the different groups (virulent vs. live attenuated) followed by pathway analysis yields differentially expressed genes in the target group.

References

1. Das A, Ali N (2012) Vaccine development against Leishmania donovani. Front Immunol 3:99
2. Murray HW (2000) Treatment of visceral leishmaniasis (kala-azar): a decade of progress and future approaches. Int J Infect Dis 4:158–177
3. Mutiso JM, Macharia JC, Kiio MN, Ichagichu JM, Rikoi H et al (2013) Development of Leishmania vaccines: predicting the future from past and present experience. J Biomed Res 27:85–102
4. Selvapandiyan A, Dey R, Gannavaram S, Lakhal-Naouar I, Duncan R et al (2012) Immunity to visceral leishmaniasis using genetically defined live-attenuated parasites. J Trop Med 2012:631460
5. Selvapandiyan A, Duncan R, Debrabant A, Lee N, Sreenivas G et al (2006) Genetically modified live attenuated parasites as vaccines for leishmaniasis. Indian J Med Res 123:455–466
6. Seder RA, Chang LJ, Enama ME, Zephir KL, Sarwar UN et al (2013) Protection against malaria by intravenous immunization with a nonreplicating sporozoite vaccine. Science 341:1359–1365
7. Dey R, Dagur PK, Selvapandiyan A, McCoy JP, Salotra P et al (2013) Live attenuated Leishmania donovani p27 gene knockout parasites are nonpathogenic and elicit long-term protective immunity in BALB/c mice. J Immunol 190:2138–2149
8. Gannavaram S, Dey R, Avishek K, Selvapandiyan A, Salotra P et al (2014) Biomarkers of safety and immune protection for genetically modified live attenuated leishmania vaccines against visceral leishmaniasis – discovery and implications. Front Immunol 5:241
9. Selvapandiyan A, Dey R, Nylen S, Duncan R, Sacks D et al (2009) Intracellular replication-deficient Leishmania donovani induces long lasting protective immunity against visceral leishmaniasis. J Immunol 183:1813–1820
10. Fiuza JA, Santiago Hda C, Selvapandiyan A, Gannavaram S, Ricci ND et al (2013) Induction of immunogenicity by live attenuated Leishmania donovani centrin deleted parasites in dogs. Vaccine 31:1785–1792
11. Fiuza JA, Gannavaram S, Santiago Hda C, Selvapandiyan A, Souza DM et al (2015) Vaccination using live attenuated Leishmania donovani centrin deleted parasites induces protection in dogs against Leishmania infantum. Vaccine 33:280–288
12. Michel G, Ferrua B, Lang T, Maddugoda MP, Munro P et al (2011) Luciferase-expressing Leishmania infantum allows the monitoring of amastigote population size, in vivo, ex vivo and in vitro. PLoS Negl Trop Dis 5:e1323
13. Darrah PA, Patel DT, De Luca PM, Lindsay RW, Davey DF et al (2007) Multifunctional TH1 cells define a correlate of vaccine-mediated protection against Leishmania major. Nat Med 13:843–850
14. Meier CL, Svensson M, Kaye PM (2003) Leishmania-induced inhibition of macrophage antigen presentation analyzed at the single-cell level. J Immunol 171:6706–6713
15. Olivier M, Gregory DJ, Forget G (2005) Subversion mechanisms by which Leishmania parasites can escape the host immune response: a signaling point of view. Clin Microbiol Rev 18:293–305
16. Banerjee S, Ghosh J, Sen S, Guha R, Dhar R et al (2009) Designing therapies against experimental visceral leishmaniasis by modulating the membrane fluidity of antigen-presenting cells. Infect Immun 77:2330–2342
17. Chakraborty D, Banerjee S, Sen A, Banerjee KK, Das P et al (2005) Leishmania donovani affects antigen presentation of macrophage by disrupting lipid rafts. J Immunol 175: 3214–3224
18. Chagas AC, Oliveira F, Debrabant A, Valenzuela JG, Ribeiro JM et al (2014) Lundep, a sand fly salivary endonuclease increases Leishmania parasite survival in neutrophils and inhibits XIIa contact activation in human plasma. PLoS Pathog 10:e1003923
19. Kumar R, Goto Y, Gidwani K, Cowgill KD, Sundar S et al (2010) Evaluation of ex vivo human immune response against candidate antigens for a visceral leishmaniasis vaccine. Am J Trop Med Hyg 82:808–813
20. Pulendran B, Li S, Nakaya HI (2010) Systems vaccinology. Immunity 33:516–529
21. Selvapandiyan A, Duncan R, Mendez J, Kumar R, Salotra P et al (2008) A Leishmania minicircle DNA footprint assay for sensitive detection and rapid speciation of clinical isolates. Transfusion 48:1787–1798
22. Coler RN, Goto Y, Bogatzki L, Raman V, Reed SG (2007) Leish-111f, a recombinant polyprotein vaccine that protects against visceral Leishmaniasis by elicitation of CD4+ T cells. Infect Immun 75:4648–4654

Chapter 36

The Use of Microwave-Assisted Solid-Phase Peptide Synthesis and Click Chemistry for the Synthesis of Vaccine Candidates Against Hookworm Infection

Abdullah A.H. Ahmad Fuaad, Mariusz Skwarczynski, and Istvan Toth

Abstract

A protein-based vaccine approach against hookworm infection has failed to deliver the expected outcome, due to a problem with an allergic response in the patient or difficulties in the proteins' production. This implication could be overcome by using a chemically synthesized peptide-based vaccine approach. This approach utilizes minimal pathogenic components that are necessary for the stimulation of the immune response without triggering adverse side effects. To boost the peptide's immunogenicity, a lipid core peptide (LCP) system can be utilized as a carrier molecule/immunostimulant. This chapter describes in detail the synthesizing of protected lipoamino acid, the self-adjuvanting moiety (LCP core), the peptide epitope, and the final vaccine candidate. The subunit peptide and the LCP core were synthesized using microwave-assisted solid-phase peptide synthesis (SPPS). Then the final hookworm vaccine construct was assembled using the copper-catalyzed azide-alkyne cycloaddition, or "click," reaction.

Key words Synthetic vaccine, Peptide-based vaccine, Fmoc-solid-phase peptide synthesis, Microwave-assisted solid-phase peptide synthesis, Copper-catalyzed azide-alkyne cycloaddition, Click chemistry, Hookworm

1 Introduction

Necator americanus (hookworm) infects over half a billion people worldwide [1]. Commonly, anthelminthic drugs are used to treat the infection; however, the reinfection rate is high in endemic areas. Consequently, vaccination is considered a viable disease control strategy [2, 3]. The blood-feeding parasite feeds on host protein (hemoglobin) for survival. As such, depriving the parasite of digesting hemoglobin should starve the parasite to death [4, 5]. Consequently, we have designed a vaccine based on a peptide epitope derived from an aspartic protease from *N. americanus* (*Na*-APR-1) [6]. It was previously demonstrated that LCP can be recognized by Toll-like receptor 2 on the surface of the dendritic cell and therefore stimulate immune responses against attached

Sunil Thomas (ed.), *Vaccine Design: Methods and Protocols: Volume 1: Vaccines for Human Diseases*, Methods in Molecular Biology, vol. 1403, DOI 10.1007/978-1-4939-3387-7_36, © Springer Science+Business Media New York 2016

antigens [7, 8]. Thus, *Na*-APR-1-derived peptides were conjugated to self-adjuvanting lipid core peptide (LCP) systems via stepwise solid-phase peptide synthesis (SPPS) and copper catalyst azide-alkyne cycloaddition (click) reactions. The LCP vaccine candidates self-assembled into nanoparticles, were administered to mice without the use of additional adjuvant, and generated antibodies that recognized not only the parent epitope, but also the *Na*-APR-1 protein. This chapter focuses on the synthetic techniques used to develop such vaccines.

In this protocol, the synthesis of one of the LCP vaccine candidates against hookworm infection is presented (Scheme 1). The procedure includes five subparts: (1) synthesis of 2-(*R/S*)-hexadecanoic acid (C16-OH) protecting group, *N*-(4,4-dimethyl-2,6-dioxycyclohexylidene)ethyl alcohol (Dde-OH), (2) synthesis of Dde-protected lipoamino acid (Dde-C16-OH), (3) synthesis of *Na*-APR-1-derived peptide epitope (A_{291}YG) peptides via microwave-assisted solid-phase peptide synthesis (MW-SPPS), (4) synthesis of LCP core via MW-SPPS, and (5) synthesis of the final LCP-based vaccine using click reaction. Synthesis of analogous lipoamino acid itself was presented in the previous protocol in this book series [9].

2 Materials

2.1 Synthesis of N-[1-(4,4-Dimethyl-2,6-dioxocyclohexylidene)ethyl Alcohol (Dde-OH)

1. 5,5-Dimethyl-1,3-cyclohexanedione (dimedone).
2. Acetic acid.
3. *N,N′*-Dicyclohexylcarbodiimide (DCC).
4. 4-Dimethylaminopyridine (DMAP).
5. Silica-coated thin-layer chromatography (TLC) plate.
6. Hydrochloric acid (5 % v/v).
7. Saturated aqueous sodium chloride solution (brine).
8. Silica powder (230–400 mesh).
9. Anhydrous magnesium sulfate.
10. Solvents: Dichloromethane (DCM), ethyl acetate, acetic acid, methanol, chloroform, and hexane.

2.2 Synthesis of Dde-protected 2-(R/S)-hexadecanoic Acid (Dde-C16-OH)

1. Dde-OH.
2. 2-(R/S)-hexadecanoic acid (C16-OH).
3. Triethylamine (TEA).
4. Hydrochloric acid (5 % v/v HCl).
5. Saturated sodium chloride solution (brine).
6. Solvents: Ethanol, ethyl acetate, acetonitrile.

2.3 Synthesis of Azido Acetic Acid (AAA)-Modified Peptide via Microwave-SPPS

1. Rink-amide methylbenzhydrylamine (rink amide-MBHA) resin (substitution 0.45 meq/g; 100–200 mesh).
2. 9-Fluorenylmethyloxycarbonyl (Fmoc)-protected amino acids.
3. Azido acetic acid.
4. *N,N*-diisopropylethylamine (DIPEA).
5. Piperidine/*N,N*-dimethylformamide (DMF) (20 % v/v).
6. 1-[Bis(dimethylamino)methylene]-1H-1,2,3-triazolo[4,5-b] pyridinium 3-oxid hexafluorophosphate (HATU) solution: 0.5 M HATU in DMF. Store solution at 0 °C, no longer than 1 week after preparation.
7. Capping solution: Acetic anhydride/DIPEA/DMF (5/5/90 % v/v/v).
8. Cleaving cocktail: TFA/TIS/water (95/2.5/2.5 % v/v/v).
9. Solvents: DMF, DCM, and methanol.
10. Solvent A: Trifluoroacetic acid/triisopropylsaline/water (TFA/TIS/H_2O 95/2.5/2.5 % v/v/v).
11. Solvent B: Acetonitrile/H_2O/TFA (50/50/0.1 % v/v/v).

2.4 Synthesis of LCP Core via Microwave-Assisted SPPS

1. All materials listed in Subheading 2.3 above.
2. Dde-C16-OH.
3. Propiolic acid.
4. *N*-Ethoxycarbonyl-2-ethoxy-1,2-dihydroquinoline (EEDQ).
5. Hydrazine hydride/DMF (2 % v/v).

2.5 Synthesis of LCP System via Click Chemistry

1. LCP core and AAA-modified peptide.
2. Copper wire.
3. Balloon.
4. Syringe needle.
5. Nitrogen gas.
6. Solvent: DMF.

2.6 Equipment

1. Laboratory glassware and apparatus.
2. Magnetic stirrer with hot plate, magnetic bar, silicon oil bath.
3. Rotary evaporator.
4. Desiccator.
5. Nuclear magnetic resonance (NMR) spectrometer (Bruker Avance™ 300 MHz).
6. CEM microwave-SPPS (with Discovery software).
7. Lyophilizer.

8. Reverse-phase high-performance liquid chromatography (RP-HPLC) system with preparative and analytical C4 and C18 columns.
9. Mass spectrometer (Perkin-Elmer-Sciex API3000).
10. Thermometer.

3 Methods

In this book series, we have demonstrated previously the synthesis of an LCP system for vaccine development against group A streptococcus, utilizing manual, stepwise Boc-SPPS [8]. Herein, alternative methods in constructing LCP-based vaccine via microwave-assisted Fmoc-SPPS and copper-catalyzed azide-alkyne cycloaddition reaction, or "click," are detailed (Scheme 1).

The LCP system comprises of lipoamino acids (LAAs) with serine spacer as the core, attached to a branching unit (i.e., lysine) to which peptide antigens are conjugated. LAAs are α-amino acids bearing a distinctive (long) alkyl side chain. As SPPS was used to synthesize the LPC core, at first, C16-OH was protected with the Dde group. The use of the Dde-protecting group allows peptide synthesis on a rink amide resin using Fmoc strategy. Similarly Fmoc-SPPS was used for peptide epitope synthesis. This method allowed modification of the LCP core and epitope (A_{291}YG) N-termini with alkyne and azide groups, respectively, without the risk of the products' instability during their cleavage from the resin. These two

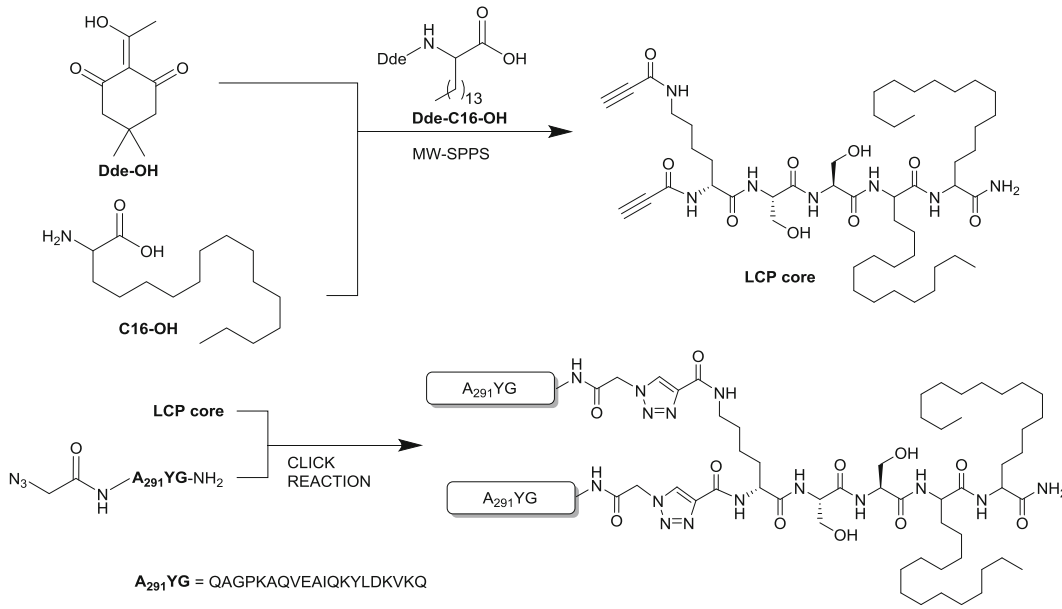

Scheme 1 Synthesis of an LCP-based vaccine candidate against hookworm infection

functional groups were incorporated into the above structures to allow their conjugation via the click reaction. Thus, the final vaccine candidate was synthesized by the conjugation of two purified smaller units, LCP core and peptide epitopes (Scheme 1).

In the procedures 3.3 and 3.4, microwave-assisted reactions can be replaced by room-temperature coupling/deprotection cycles; however the duration of each reaction needs to be increased by fivefold and the reaction vessel needs to be shaken during the processes.

3.1 Synthesis of N-[1-(4,4-Dimethyl-2,6-dioxocyclohexylidene)ethyl (Dde-OH)

1. To a 500 mL round-bottom flask containing 100 mL DCM, add dimedone (28.8 g, 200 mmol) and gently stir the mixture until fully dissolved (*see* **Note 1**).
2. To a beaker containing 100 mL DCM, add DCC (42.3 g, 204 mmol) and DMAP (25.0 g, 205 mmol) with stirring until the solution becomes clear.
3. Then, add the above solution to the 500 mL flask containing dimedone/DCM.
4. After 5 min, add acetic acid (12 mL, 210 mmol) to the reaction mixture and stir at room temperature for 24 h.
5. Periodic TLC analysis should be performed using chloroform/methanol/acetic acid (90/8/2 % v/v/v) mixture with dimedone (dissolved in DCM), as a reference compound. Product $R_f = 0.14$; dimedone $R_f = 0.42$ (*see* **Note 2**).
6. After reaction completion, pour the black reaction mixture through a sintered glass funnel under gravity. Rinse the white solid using DCM (3 × 5 mL).
7. Evaporate the eluate under reduced pressure to obtain an (oily) yellow crude product.
8. Dissolve the crude product using ethyl acetate (300 mL). White precipitation should be observed (dicyclohexyl urea—by-product produced from DCC).
9. Wash organic phase with 5 M HCl (3 × 100 mL) in a separation funnel. Occasionally, open the knob to release pressure. Discard the aqueous fractions.
10. Repeat **step 10** using brine (2 × 50 mL). Collect the organic layer into a 500 mL conical flask.
11. Add anhydrous magnesium sulfate to dry the solution and filter off through a cotton/celite funnel into a 500 mL round-bottom flask by vacuum filtration (Fig. 1).
12. Then, evaporate the ethyl acetate under reduced pressure.
13. Add a small amount of hexane (20–40 mL) to the oil, mix thoroughly, and evaporate again to ensure the absence of ethyl acetate, to produce a dark orange viscous liquid.

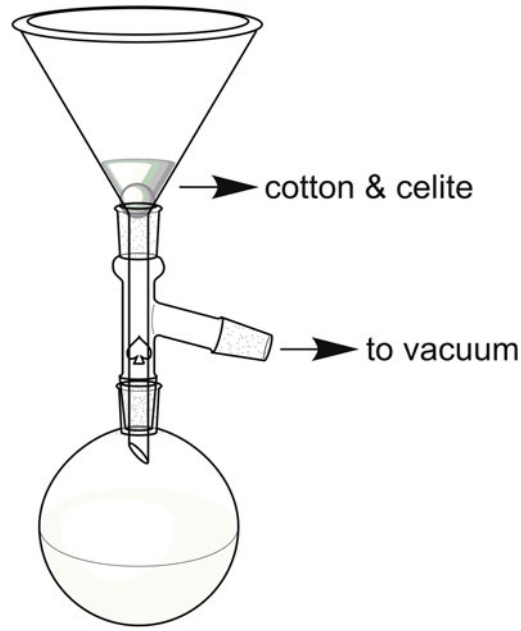

Fig. 1 Filtration setup using cotton and celite

14. Dissolve the product using a small amount of hexane (~30 mL).
15. Perform flash chromatography using a fritted glass funnel. To prepare a silica gel, dissolve 50 g of silica powder (230–400 mesh) into a 250 mL beaker containing 100 mL hexane (*see* **Note 3**).
16. Carefully transfer the gel into the glass funnel; equally distribute it to form a leveled gel layer.
17. Place a filter paper on the surface of the layer (*see* **Note 4**).
18. Drain the hexane until just above the filter paper (or gel layer).
19. Carefully transfer the solution (from **step 15**) onto the surface of the gel/paper.
20. Run the chromatography. Occasionally, add additional hexane (*see* **Note 5**).
21. Follow the movement of the product (yellow) and collect the yellow elute (product) in small vials.
22. Upon completion, perform TLC for each vial. A single spot should be observed from the pure fractions.
23. Combine pure fractions and evaporate the solvent under reduced pressure. Leave the concentrated product under vacuum overnight.
24. Perform ^{1}H-NMR to verify product purity (^{1}H-NMR (300 MHz, $CDCl_3$) δ 2.55 (s, 3H, C$\underline{H_3}$-CH(OH)-cyclohexanedione),

2.31 and 2.49 (s, 4H, methylene protons of cyclohexanedione ring), 1.03 (s, 6H, ring-($C\underline{H}_3$)$_2$). Repeat **steps 15–25** if impurity is detected on NMR spectrum (*see* **Note 6**).

25. Store the product (Dde-OH) in −20 °C freezer.

3.2 Synthesis of Dde-C16-OH

1. 2-Aminohexadecanoic acid (C16-OH) was synthesized as previously reported [9].
2. Prepare a reflux setup using a 500 mL round-bottom flask.
3. Transfer purified Dde-OH (23.5 g, 128 mmol) into the flask using 200 mL of ethanol.
4. Then, transfer C16-OH (26.9 g, 125 mmol) into the flask. Use an additional 100 mL of ethanol to wash and transfer all reagents.
5. Stir the reaction mixture at room temperature until uniform suspension is formed (*see* **Note 7**).
6. Add TEA (55 mL, 387 mmol).
7. Reflux the mixtures for 2 days with stirring.
8. After 2 days, cool the suspension to room temperature.
9. The color of the reaction mixture should change into a dark orange. Perform TLC—spot corresponding to C16-OH should be diminished (*see* **Note 8**).
10. Evaporate the solvent under reduced pressure.
11. Add minimal ethyl acetate (20–40 mL) to the oil, mix thoroughly, and evaporate again to ensure the absence of ethanol.
12. Then, extract the product using ethyl acetate (3 × 100 mL) using a separation funnel. Discard the aqueous layer.
13. Wash the organic layer with 5 % HCl (2 × 100 mL) and then brine (100 mL). Add anhydrous magnesium sulfate to dry the solution and filter off through a celite/cotton funnel into a 500 mL round-bottom flask by vacuum filtration.
14. Evaporate the solvent under reduced pressure till completely removed (*see* **Note 9**).
15. Add cold acetonitrile to the round-bottom flask and crush (powderize) the solids with a glass rod (*see* **Note 10**).
16. Filter the mixtures using a Bühner's funnel under vacuum.
17. Keep the product (Dde-C16-OH) in a desiccator for drying.
18. Perform NMR on dry product (^{1}H-NMR (300 MHz, $CDCl_3$): δ 4.39 (m, 1H, N$\underline{H}$), 2.53 (s, 3H, $C\underline{H}_3$-CH(OH)-cyclohexanedione), 2.40 (s, 4H, methylene groups on Dde), 1.93 (m, 1H, methine group), 1.42 (m, 2H, first methene groups on alkyl chain), 1.24 (mbs, 24H, methylene groups on alkyl chain), 0.87 (t, 3H, -CH_3), 1.04 (s, 6H, Dde-($C\underline{H}_3$)$_2$).

3.3 Synthesis of Azido Acetic Acid-Modified $A_{291}Y$ Peptide

($N_3CH_2C(O)$-QAGPKAQVEAIQKYLDKVKQ-NH_2) via microwave-SPPS.

1. Resin swelling: Transfer the rink amide-MBHA resin (222 mg, 0.100 mmol) to the microwave peptide reaction vessel. Add DMF (~3 mL) and stir gently using a glass rod, insert the temperature probe, and irradiate at 70 °C for 10 min (*see* **Note 11**).
2. Remove the solvent by vacuum filtration using a complementary vacuum system. Wash the resin using DMF (3 × 5 mL) (*see* **Note 12**).
3. Fmoc deprotection: Remove the temperature probe and the solution under vacuum filtration and wash the probe and the vessel thoroughly using DMF (5 × 5 mL). Add 20 % piperidine/DMF solution (5 mL), insert the probe, and irradiate vessel for 2 min at 70 °C. Drain the solution under vacuum filtration, add another portion of the piperidine/DMF, and irradiate for 5 min at 70 °C.
4. Preactivation of amino acids: Add 148 mg (0.420 mmol) of Fmoc-Leu-OH amino acids into a scintillation vial. Then add 0.5 M HATU solution in DMF (0.8 mL, 0.40 mmol), DIPEA (0.11 mL, 0.62 mmol), and DMF (~2 mL). Swirl the vial gently to promote dissolution or alternatively use an ultrasonicator to speed up the process. Each amino acid should be preactivated 2–5 min before reaction.
5. Add the preactivated amino acid to the reaction vessel and stir gently.
6. Insert vessel into microwave and irradiate for 10 min at 70 °C (*see* **Note 13**).
7. Repeat **steps 2** and **4–6** for double coupling.
8. Remove the reaction mixture via filtration under vacuum. Wash the reaction vessel thoroughly by adding DMF (5 × 5 mL), followed by draining under vacuum, between washes.
9. After the first amino acid coupling, add freshly prepared capping solution (~3 mL) and irradiate for 10 min at 70 °C.
10. Drain the solution under vacuum filtration.
11. Add additional freshly prepared capping solution (~3 mL) and irradiate for 10 min at 70 °C for double coupling.
12. Repeat **step 8**.
13. Repeat **steps 3–8** and **10** twenty-one more times using the following amino acids in sequence: Fmoc-Glu(OtBu)-OH, Fmoc-Ala-OH, Fmoc-Gly-OH, Fmoc-Ile-OH, Fmoc-Tyr(tBu)-OH, Fmoc-Lys(Boc)-OH, Fmoc-Gln(Trt)-OH, Fmoc-Ile-OH, Fmoc-Ala-OH, Fmoc-Glu(OtBu)-OH, Fmoc-Val-OH, Fmoc-Gln(Trt)-OH, Fmoc-Ala-OH, Fmoc-Lys(Boc)-OH,Fmoc-Pro-OH,Fmoc-Gly-OH,Fmoc-Ala-OH,

Fmoc-Ile-OH, Fmoc-Leu-OH, Fmoc-Ser(tBu)-OH, and Fmoc-Thr(tBu)-OH.

14. Then, transfer the resin to a glass peptide synthesis vessel (separation funnel with a fritted disk). Use a minimal amount of DMF to help the transfer process.
15. Repeat **step 4** using azido acetic acid (42.5 mg, 0.420 mmol) as a substitution for the amino acid (*see* important hazard-related **Note 14**).
16. Add the preactivated acid to the resin and shake the mixture for 60 min in the vessel. Cover with aluminum foil to protect from light.
17. Repeat **step 2**, and then **step 15**, for double coupling.
18. Remove the reaction mixture by filtration under vacuum and wash the resin thoroughly using DMF (5 × 5 mL), followed by dichloromethane (5 × 5 mL) and methanol (2 × 5 mL).
19. Place the resin in the desiccator under reduced pressure overnight.
20. Measure the weight of the obtained resin-peptide.
21. Peptide cleavage: Transfer a known amount of the resin-peptide to a 50 mL Falcon tube. Add 10 mL/g of the cleaving cocktail and shake at room temperature for 2–3 h.
22. Evaporate cleaving cocktail under reduced pressure, wash resin twice with 30 mL of cold diethyl ether, and remove and dispose of the solvent by filtration through a sintered glass funnel (*see* **Note 15**).
23. Dissolve the white precipitate using minimal Solvent B and filter off the resin into a round-bottom flask. Use additional Solvent B to wash the resin. Lyophilize the filtrate to obtain a yellow-white solid product.
24. Purify the product by preparative reverse-phase HPLC using C18 column. The final product (peptide $A_{291}YG$) is a white solid. The product was analyzed by ESI-MS and HPLC. Molecular weight: 2325.7. ESI-MS: $[M+1H^+]^{1+}$ m/z 2326 (calc. 2326.7), $[M+2H^+]^{2+}$ m/z 1163.5 (calc. 1163.9), $[M+3H^+]^{3+}$ m/z 775.9 (calc. 776.0). t_R = 19.1 min (0–100 % Solvent B, 40 min; C18 column), purity ≥98 %.
25. Store the final compound at −20 °C (or below) to prolong its shelf life.

3.4 Synthesis of LCP Core via Microwave-Assisted SPPS

1. Resin swelling: Transfer the rink amide-MHBA resin (111 mg, 0.05 mmol) to the microwave peptide reaction vessel. Add DMF (~3 mL) and stir gently using a glass rod, add the temperature probe, and irradiate at 70 °C for 10 min.
2. Remove the solvent. Wash the resin using DMF (3 × 5 mL) by filling with DMF, stirring, and draining under vacuum.

3. Fmoc deprotection: Remove the temperature probe and the solution under vacuum filtration. Wash the probe and the vessel thoroughly using DMF (5 × 5 mL). Add 20 % piperidine/DMF solution (5 mL), insert the probe, and irradiate for 2 min at 70 °C. Remove the solvent, add another portion of the piperidine/DMF, and irradiate for 5 min at 70 °C.
4. Remove the reaction mixture via filtration under vacuum. Wash the reaction vessel thoroughly by adding DMF (5 × 5 mL), followed by filtering under vacuum, between washes.
5. Preactivation of amino acids: To a scintillation vial, weight 94.8 mg (0.210 mmol) of Dde-C16-OH. Then add 0.5 M HATU solution (0.40 mL, 0.20 mmol), DIPEA (0.05 mL, 0.31 mmol), and DMF (~3 mL). Swirl the vial gently to promote dissolution or alternatively use an ultrasonicator to speed up the process. Preactivation should take between 5 and 10 min.
6. Add the preactivated Dde-C16-OH to the reaction vessel and stir gently.
7. Insert the probe and perform microwave irradiation for 10 min at 70 °C.
8. Repeat **steps 2** and **5**–7 for double coupling.
9. Repeat **step 4**.
10. After the first amino acid coupling, add freshly prepared capping solution (~3 mL), insert the temperature probe, and irradiate for 10 min at 70 °C.
11. Drain the solution under vacuum filtration and add additional freshly prepared capping solution (~3 mL); insert the temperature probe and irradiate for 10 min at 70 °C.
12. Repeat **step 4**.
13. Dde deprotection: Remove the probe and solution by vacuum filtration and wash thoroughly using DMF (5 × 5 mL). Add 2 % hydrazine/DMF solution (5 mL), stir the mixture, and leave for 5 min at room temperature.
14. Remove the solution by filtration under vacuum and add an additional 5 mL of the 2 % hydrazine/DMF solution; stir and leave the mixture for another 5 min.
15. Repeat **step 14** ten times (*see* **Note 16**).
16. Repeat **step 4**.
17. Repeat **steps 5–9** and **13–16** for the second Dde-C16-OH coupling.
18. Then, repeat **steps 5–9**, **3**, and **4** with the following changes: instead of Dde-C16-OH, use 0.31 mmol of the following amino acids (written in order): Fmoc-Ser-OH, Fmoc-Ser-OH, and Fmoc-Lys(Fmoc)-OH. For the Fmoc-Lys(Fmoc)-OH amino acid, repeat only **steps 5–9**.

19. Add freshly prepared capping solution (~3 mL), insert the temperature probe, and irradiate for 10 min at 70 °C.
20. Repeat **step 4**, add additional capping solution (~3 mL), insert the temperature probe, and irradiate for 10 min at 70 °C.
21. Repeat **steps 3** and **4**.
22. To a scintillation vial, add 85.8 mg (0.420 mmol) of propiolic acid and 98.8 mg (0.400 mmol) of EEDQ. Add DMF (~3 mL) and swirl the vial gently to promote dissolution or use an ultrasonicator to speed up the process. Preactivation should take between 1 and 2 min.
23. Transfer the preactivated propiolic acid to the reaction vessel and shake the vessel for 2 h at room temperature.
24. Repeat **step 4** and then **steps 22** and **23** for double coupling.
26. Remove the reaction mixture by filtration under vacuum and wash the resin thoroughly using DMF (5 × 5 mL), followed by DCM (5 × 5 mL) and methanol (2 × 5 mL).
27. Put the resin in the desiccator under reduced pressure, overnight.
28. Measure the weight of the obtained resin-peptide.
29. Peptide cleavage: Transfer a known amount of the resin-peptide to a 50 mL Falcon tube. Add 10 mL/g of the cleaving cocktail and shake at room temperature for 2–3 h.
30. Evaporate cleaving cocktail under reduced pressure; wash resin twice with 30 mL of cold diethyl ether/hexane 50/50 % v/v; remove and dispose the solvent by filtration through a sintered glass funnel (*see* **Note 17**).
31. Dissolve the precipitate using a small amount of Solvent B (20–30 mL) and filter off the resin. Collect solution into a 50 mL round-bottom flask. Use additional Solvent B for washing and then lyophilize solution.
32. Purify the solid by preparative reverse-phase HPLC using C4 column. The final product (LCP core) is a light yellowish solid. The product was analyzed by ESI-MS and HPLC. Molecular weight: 931.2. ESI-MS: $[M+2H^+]^{2+}$ m/z 465.2 (calcd. 466.6). $t_R = 29.1$ min (20–60 % Solvent B; 40 min, C4 column), purity ≥96 %.
33. Store the final compound at −20 °C (or below) to prolong its shelf life.

3.5 Synthesis of LCP System via Click Chemistry

1. Using a microbalance, weigh the A_{291}YG peptide (10.9 mg, 4.00 μmol) and LCP core (1.04 mg, 1.00 μmol). Then, transfer the starting materials to a 5 mL round-bottom flask.
2. Add 2 mL of DMF to the flask, 30 mg (0.47 mmol) of 99.9 % copper pallet or wires, and a micro stirrer bar.

3. Superseal the flask using a rubber stopper.
4. Prepare a balloon with nitrogen gas and insert it into the rubber stopper using a needle. Insert a second needle (for approximately 15 s) to replace most of the air inside the flask with nitrogen gas.
5. Stir the reaction mixture for 9 h at 50 °C in a temperature-controlled oil bath (*see* **Note 18**).
6. Next, cool the reaction to room temperature.
7. Filter off the copper pallet and dilute the reaction mixture using Solvent A (2 mL).
8. Purify the product by preparative reverse-phase HPLC on C4 column. The final product (LCP-A_{291}YG) is a white solid. The product was analyzed by ESI-MS and HPLC. Molecular weight: 5579.6. ESI-MS: $[M+3H^+]^{3+}$ m/z 1861.4 (calcd 1860.9), $[M+4H^+]^{4+}$ m/z 1395.8 (calcd 1395.9), $[M+5H^+]^{5+}$ m/z 1116.9 (calcd 1116.9), $[M+6H^+]^{6+}$ m/z 931.4 (calcd 930.9), $[M+7H^+]^{7+}$ m/z 798.5 (calcd 798.1), $[M+8H^+]^{8+}$ m/z 698.7 (calcd 698.5). $t_R = 18.4$ min (0–100 % Solvent B, 40 min; C4 column), purity ≥95 %.

4 Notes

1. DCC usually forms a rock-solid clump. When trying to break the DCC clump, extra force is required. Breaking the DCC under a fully operative fume hood is highly recommended (DCC is a strong allergen). Also, cover the flask with aluminum foil, as dimedone is sensitive to light.
2. To perform TLC analysis, first, cut the TLC plate into a smaller sheet (2.5 × 5 cm). Using capillary tubes, transfer a small amount of the reaction mixtures (sample) and dimedone/DCM (reference) onto the TLC sheet, making two separate spots on the same level close to the bottom of the sheet. Then, transfer the 90/8/2 % v/v/v solution mixture to a TLC beaker to about 0.5 mm from the base of the beaker. Dip the TLC sheet into the TLC chamber (be sure that the solution does not touch the spots). Close the TLC chamber using watch glass or cover with foil. Remove the TLC sheet when the 90/8/2 % v/v/v solvent reaches ~0.5 mm from the top. Mark the solvent front using a pencil. Dip (quickly) the TLC sheet into an anisaldehyde solution and wipe the aluminum side to dry, and then heat with a heating gun until dark spots are clearly visible. Similarly, mark the spots using a pencil and calculate the R_f values. Ensure that the dimedone is fully consumed during reaction and thus its spot from the reaction

mixture is not visible before proceeding to the next step. We recommend performing the TLC analysis at least three times, at 0, 12, and 24 h.

3. Silica powder is very light and is considered a health hazard when inhaled. For safety reasons, perform tasks in a fume cupboard.
4. This is an optional step to ensure an undisturbed gel layer during product transfer. If you choose to perform this step, ensure that filter paper lies flat on the layer.
5. Ensure that silica gel is always covered by solvent. When adding the hexane, be sure to add slowly and gently to prevent the silica layer from moving. A dried or relocated gel layer disturbs the separation process.
6. Purity of the product depends on the scale of the reaction. For this 0.2 mol reaction scale, the use of 50 g of silica gel was sufficient to ensure high product purity (>99 %).
7. The C16-OH will not fully dissolve under this condition; however, as long as reactants are well suspended in the ethanol, the reaction will proceed.
8. In our experience, the reaction can take up to 5 days to complete. However, after 2 days, we observed almost 100 % yield from TLC analysis.
9. Yellow solid is formed upon drying.
10. The product (Dde-C16-OH) does not dissolve in cold acetonitrile but the reactants/by-products do. For maximum yield, always keep the flask cool (e.g., by performing this step in an ice bucket).
11. Each microwave irradiation system usually has its own complementary peptide reaction vessels and vacuum filtration apparatus. Consult with your microwave provider for further information.
12. Each washing must be performed carefully to ensure removal of all reagents and by-product unbound to the resin. Improper washing could result in the formation of side products during synthesis.
13. Fmoc-amino acids are commonly irradiated at 70 °C for 10 min during peptide synthesis. The first coupling can be reduced to 5 min with the second coupling maintaining 10 min. Cysteine, histidine, and arginine are exceptions that should be coupled at room temperature for 5 min, followed by microwave irradiation at 50 °C for 15 min.
14. *Important.* Azido acetic acid has explosive properties under certain conditions. Thus, it should not be exposed to UV light and microwave irradiation (or other heating) [10].

15. Evaporation to dryness is not required; however, ensure that less than 1–2 mL of cleaving solution is remaining. Alternatively, when cleavage is performed in small scale in Falcon tube (maximum 1–2 mL of cleavage solution is used), add 30 mL of cold diethyl ether to the Falcon tube, shake vigorously for ~30 s (or ultrasonicate), and then centrifuge the mixture in the Falcon tube at 900g for 10 min. Remove the solvent carefully (decantate) and repeat the step above twice.
16. Repeat Dde deprotection for a minimum of ten times. An additional method can be utilized to qualitatively determine the end point of the deprotection reaction. Add 1 mL of 2 % hydrazine hydride/DMF into a quartz cuvette. Insert the cuvette into a UV/Vis spectrometer and run a background scan at $\lambda = 460$ nm. Then, replace the solution with ~1 mL of hydrazine filtrate (after cleavage) and measure the absorbance. An absorbance value of >0 indicates the presence of Dde-hydrazine adducts and therefore the deprotection step should be repeated.
17. The LCP peptide could be precipitated more easily using a 50/50 % v/v mixture of cold diethyl ether/hexane. This solvent is commonly used for peptides with high hydrophobic content (e.g., LCPs).
18. Upon reaction completion, color change was observed. We have experienced light green and light blue color for different click products. If color change was not observed, the reaction did not proceed. Thus the reaction should not be stopped before the blue/green color appears.

References

1. Hotez PJ, Brooker S, Bethony JM et al (2004) Hookworm infection. N Engl J Med 351:799–807
2. Loukas A, Bethony J, Brooker S, Hotez P (2006) Hookworm vaccines: past, present, and future. Lancet Infect Dis 6:733–741
3. Loukas A, Bethony JM, Mendez S, Fujiwara RT et al (2005) Vaccination with recombinant aspartic hemoglobinase reduces parasite load and blood loss after hookworm infection in dogs. PLoS Med 2:1008–1017
4. Hotez PJ, Bethony JM, Diemert DJ, Pearson M, Loukas A (2010) Developing vaccines to combat hookworm infection and intestinal schistosomiasis. Nat Rev Microbiol 8:814–826
5. Pearson MS, Bethony JM, Pickering DA, de Oliveira LM et al (2009) An enzymatically inactivated hemoglobinase from Nector americanus induces neutralizing antibodies against multiple hookworm species and protects dogs against heterologous hookworm infection. FASEB J 23:3007–3019
6. Skwarczynski M, Dougall AM, Khoshnejad M, Chandrudu S, Pearson MS, Loukas A, Toth I (2012) Peptide-based subunit vaccine against hookworm infection. PLoS One 7:e46870
7. Dougall AM, Skwarczynski M, Khoshnejad M, Chandrudu S et al (2014) Lipid core peptide targeting the cathepsin D hemoglobinase of Schistosoma mansoni as a component of a schistosomiasis vaccine. Hum Vaccin Immunother 10:399–409
8. Skwarczynski M, Zaman M, Toth I (2013) Lipo-peptides/saccharides in peptide vaccine delivery. In: Kastin A (ed) Handbook of the biologically active peptides, 2nd edn. Elsevier Inc, Burlington, pp 571–579

9. Skwarczynski M, Toth I (2011) Lipid-core-peptide system for self-adjuvanting synthetic vaccine delivery. In: Mark SS (ed) Bioconjugation protocols: strategies and methods, 2nd edn. pp 297–308

10. Dyke JM, Groves AP, Morris A, Ogden JS, Dias AA et al (1997) Study of the thermal decomposition of 2-azidoacetic acid by photoelectron and matrix isolation infrared spectroscopy. J Am Chem Soc 119:6883–6887

Part VII

Vaccines for Prion Diseases

Chapter 37

Methods and Protocols for Developing Prion Vaccines

Kristen Marciniuk, Ryan Taschuk, and Scott Napper

Abstract

Prion diseases denote a distinct form of infectivity that is based in the misfolding of a self-protein (PrP^{C}) into a pathological, infectious conformation (PrP^{Sc}). Efforts to develop vaccines for prion diseases have been complicated by the potential dangers that are associated with induction of immune responses against a self-protein. As a consequence, there is considerable appeal for vaccines that specifically target the misfolded prion conformation. Such conformation-specific immunotherapy is made possible through the identification of vaccine targets (epitopes) that are exclusively presented as a consequence of misfolding. An immune response directed against these targets, termed disease-specific epitopes (DSEs), has the potential to spare the function of the native form of the protein while clearing, or neutralizing, the infectious isomer.

Although identification of DSEs represents a critical first step in the induction of conformation-specific immune responses, substantial efforts are required to translate these targets into functional vaccines. Due to the poor immunogenicity that is inherent to self-proteins, and that is often associated with short peptides, substantial efforts are required to overcome tolerance-to-self and maximize the resultant immune response following DSE-based immunization. This often includes optimization of target sequences in terms of immunogenicity and development of effective formulation and delivery strategies for the associated peptides. Further, these vaccines must satisfy additional criteria from perspectives of specificity (PrP^{C} vs. PrP^{Sc}) and safety (antibody-induced template-driven misfolding of PrP^{C}). The emphasis of this report is on the steps required to translate DSEs into prion vaccines and subsequent evaluation of the resulting immune responses.

Key words Prion disease, Vaccine, Disease-specific epitopes, Proteinopathies, Conformation-specific vaccines, Immunotherapy

1 Introduction

1.1 Prion Diseases

Transmissible spongiform encephalopathies (TSEs), or prion diseases, are fatal neurodegenerative disorders afflicting humans as well as a number of animal species. Despite sharing a conserved molecular mechanism, these diseases display considerable inter- and intra-species variability in their symptoms, pathologies, and patterns of onset and

Author contributed equally with all other contributors.

Sunil Thomas (ed.), *Vaccine Design: Methods and Protocols: Volume 1: Vaccines for Human Diseases*, Methods in Molecular Biology, vol. 1403, DOI 10.1007/978-1-4939-3387-7_37,

progression [1]. For example, a number of human prion diseases of distinct origins and pathologies have been characterized, including iatrogenic, familial, and spontaneous forms of the disease as well as forms of the disease that result as a consequence of the consumption of prion-infected materials, as is the case with kuru (consumption of infected human flesh) and variant Creutzfeldt-Jakob disease (vCJD) (consumption of prion infected beef) [2]. At the present time, prion diseases have a fatal outcome in all species with no effective treatment options [3].

Prion diseases within domesticated animals include scrapie of sheep, bovine spongiform encephalopathy (BSE) of cattle, and chronic wasting disease (CWD) of cervids (elk and deer). These diseases are of priority because of their economic importance for their ability to spread within and between agricultural species, and are of further importance for their potential zoonotic potential. For example, the UK BSE outbreak in the 1980s led to the consumption of tainted beef and subsequent transference of a fatal neurodegenerative disorder (vCJD) to over 200 people and had devastating economic impacts on the cattle livestock industry within the UK and abroad [4–6]. At the present time, as a consequence of its wide and ongoing spread in both wild and farmed cervids, CWD is the greatest priority animal prion disease [7]. While there are no documented cases of transmission to humans, circumstantial evidence raises concern of both the zoonotic potential of CWD and its potential to spread into cattle [8–13]. Efforts to manage CWD, in particular within wild cervids utilizing population control measures, have been unsuccessful, highlighting the need for novel disease management tools, such as vaccines [14–16].

1.2 A New Paradigm of Infectivity

Prion diseases revolutionized the field of infectious diseases by demonstrating infectivity that is exclusive of a nucleic acid agent. The "protein-only" hypothesis stipulates that PrP^{Sc} functions as a template to promote the conversion of PrP^{C} into the infectious conformation in an autocatalytic, self-propagating manner (Fig. 1a) [17, 18]. This characteristic of self-promoted protein misfolding was generally viewed as a unique and defining feature of the prion diseases; however, in recent years there is increasing evidence that mechanisms associated with prion self-propagation are conserved, to varying extents, in other neurodegenerative diseases such as Alzheimer's disease, Parkinson's disease, amyotrophic lateral sclerosis, and Huntington's disease [19–23]. Most notably, these diseases all represent proteinopathies, defined by the propagated misfolding of a self-protein into an aggregate structure. From this perspective the protein aggregates represent not only pathological hallmarks of diseases but also critical factors in the initiation and progression of disease, making them attractive vaccine targets [24].

1.3 Vaccine Development for Prion Diseases

Despite representing a novel paradigm of infectivity, there is nevertheless proof-of-principle evidence that traditional approaches of medicine, including vaccines, may have utility in the treatment and

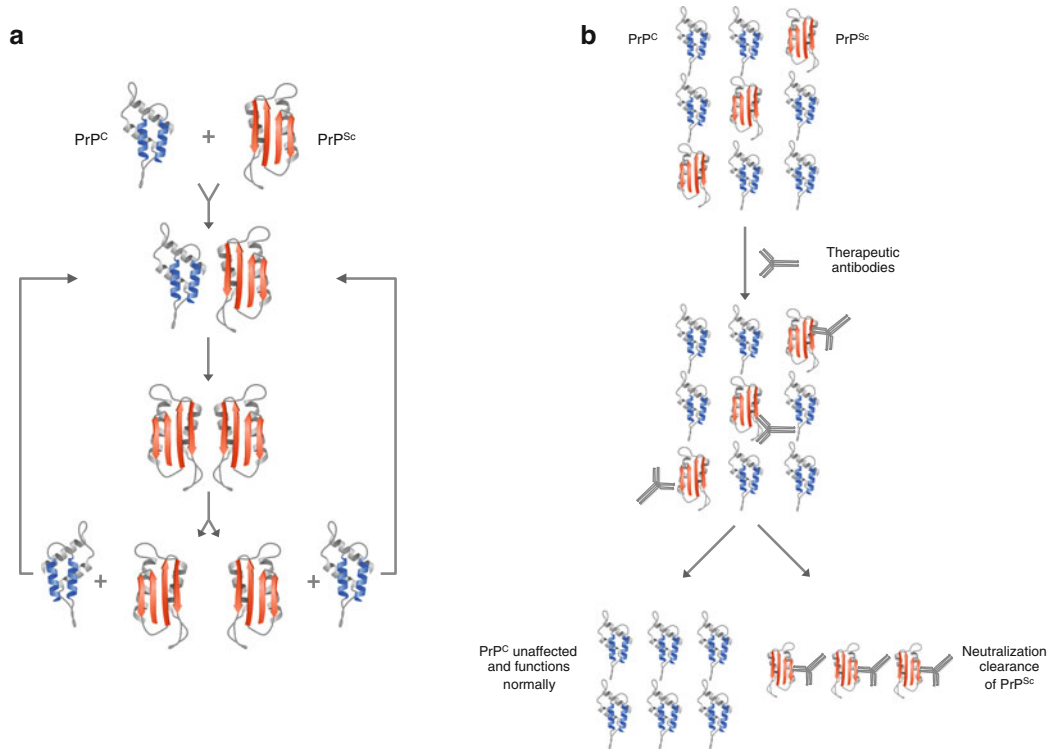

Fig. 1 Proposed mechanism of infectivity and immunotherapeutic treatment of prion diseases. (**a**) The prion protein preferentially adopts an alpha-helical structure under homeostatic cellular conditions (PrPC) but can also exist as mainly a betasheet structure with infectious and pathogenic biophysical properties (PrPSc). Interaction of PrPC with an infectious molecule or oligomer promotes the misfolding of the PrPC (purple structure) into the transmissible disease-causing PrPSc conformation. (**b**) Potential mechanism of action for immune responses raised against disease-specific prion epitopes

prevention of prion diseases. Specifically, antibodies to PrP^C have been shown to offer degrees of protection in both in vitro and in vivo models [25–31]. While encouraging, there are both technical challenges and safety concerns to the development of a prion vaccine. From a technical perspective, the induction of protective immune responses depends on overcoming immunological tolerance to the self-protein PrP^C. While numerous investigations, utilizing a variety of carrier systems and adjuvants, have achieved induction of immune responses to PrP^C, most of the approaches are impractical for either humans or livestock [26–31]. From a perspective of safety, there is concern that the generation of circulating antibodies to PrP^C, a ubiquitously expressed cell surface protein, could have adverse consequences. These concerns are supported by the observation that PrP^C-reactive antibodies induce apoptosis of neurons in the brain and instigate inappropriate cell signaling and cellular function of immune cells [32–34].

1.4 Disease-Specific Immunotherapy

A potential way to circumvent the potential safety issues associated with the induction of immune responses that include reactivity

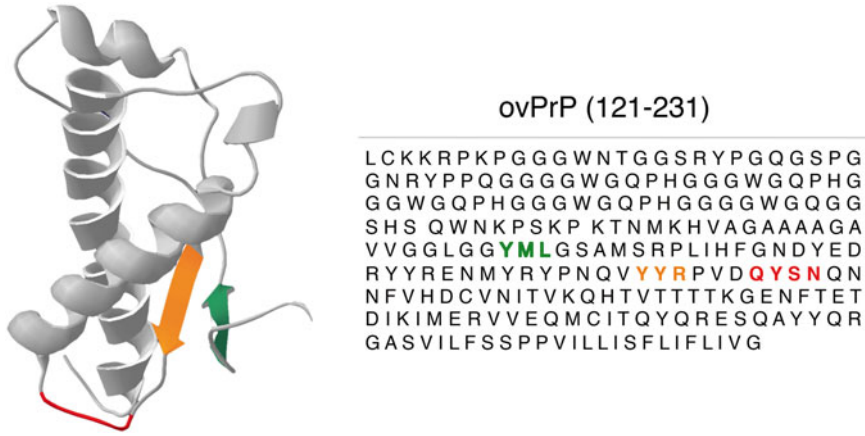

Fig. 2 Location of PrP DSEs previously translated into PrPSc vaccines. Sequence of core YML (*green*), YYR (*orange*), and RL (*red*) sequence within tertiary and primary structure of PrP

with natively folded PrP^{C} is to strive for immune responses that are specific to the misfolded isomer. Such conformation-specific immunotherapy is made theoretically possible by the unique molecular mechanism of prion diseases in which the misfolding of PrP^{C} to PrP^{Sc} surface exposes regions of the protein that are normally buried within the native structure. These disease-specific epitopes (DSEs) represent highly attractive targets for vaccine development as the associated immune responses have the potential to spare the function of the native protein while prioritizing the misfolded, problematic species (Fig. 1b). To date, three DSEs of PrP^{C} have been translated into PrP^{Sc} vaccines [24] (Fig. 2).

The tendency of the misfolded forms to generate insoluble aggregates that are not amenable to structural determination has prevented identification of DSEs based on comparative structural analysis. As such, the identification of DSEs is done through experimental approaches to mimic the pathological misfolding events or through predictive programs.

1.5 Translation of DSEs into Vaccines

The first DSE proposed for PrP was a YYR motif that was found to be selectively exposed on experimental misfolding of PrP^{C} [35]. The initial efforts to develop a vaccine based on this epitope highlighted the challenges separating DSE identification from the generation of a functional vaccine. Specifically, even with an aggressive vaccination regime involving harsh adjuvants, the immune responses to the YYR epitope were limited to IgM antibodies [35]. Further, presentation of this peptide epitope in the context of an effective, established delivery system for self-peptides failed to induce an epitope-specific antibody response [36].

The inability of conventional strategies of vaccine formulation and delivery to generate a PrP^{Sc}-specific vaccine based on the YYR epitope prompted consideration of the necessity to incorporate additional strategies for optimizing epitope immunogenicity.

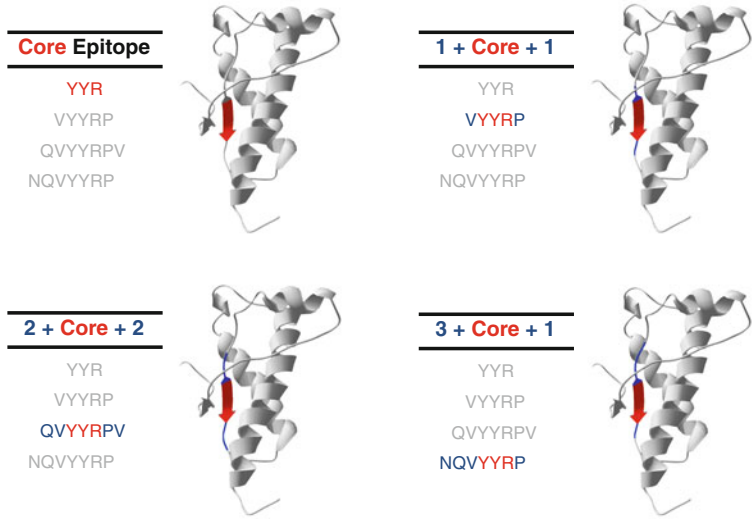

Fig. 3 Consideration of optimized epitopes within the context of natively structured target protein. Amino- and carboxyl-terminal DSE expansions were designed to include amino acids normally found within the hydrophobic core of PrPC. Lack of DSE surface exposure was used to maintain conformational specificity of induced immune responses

Initially this was governed largely around the hypothesis that epitopes of greater length would correlate with more substantial immune responses. The expansions of the core epitope to including flanking regions of the natural target protein sequence were performed with the caveat that the expansions should not compromise the conformational specificity of the ensuing immune response. As such, expansions to the core epitopes were performed with consideration of the crystallographic structure of the native form of PrP^C where the direction and magnitude of the expansions to the YYR core were selected to avoid surface exposure [36] (Fig. 3). A panel of vaccines representing these expansions were expressed as C-terminal fusions to the leukotoxin carrier protein and evaluated for immunogenicity. This approach was successful in identifying expansions with marked improvements to immunogenicity while retaining specificity for the misfolded isomer [36, 37].

While this approach resulted in vaccines of appropriate immunogenicity and specificity, the process was inefficient from the perspectives of time, cost, and animal resources. In an effort to improve on this process, an additional step was introduced to apply an algorithm that predicts the immunogenicity of the expanded epitopes based in the presence of B cell epitopes [24, 38]. This approach provides an in silico, high-throughput mechanism to prioritize epitope expansions. Through this approach novel DSEs were rapidly translated into immunogenic peptide-based vaccines capable of inducing misfolding-specific immune responses [24]. The publically available platform, termed Epitope Immunogenicity

Characterization (EpIC), automatically generates and assesses peptide epitopes that differ by a single amino acid, constructed as a panel of expansions around the core epitope of interest. This program adapts the input/output formats of the original BepiPred program specifically for manipulation of peptide epitopes, and increases the potential for enhanced immunogenicity and vaccine utility (Fig. 4).

A complete overview of the stages and steps involved in the generation and testing of a PrP^{Sc}-specific vaccine is provided in Fig. 5.

Rank	Score	Core Epitope Sequence	Number Before	Number After	Residues	Expanded Epitope Sequence
1	1.165	YYR	4	1	161-168	PNQVYYRP
2	1.147	YYR	4	10	161-177	PNQVYYRPVDQYSNQNN
3	1.106	YYR	4	9	161-176	PNQVYYRPVDQYSNQN
4	1.073	YYR	4	4	161-171	PNQVYYRPVDQ
5	1.061	YYR	4	8	161-175	PNQVYYRPVDQYSNQ
6	1.052	YYR	0	10	165-177	YYRPVDQYSNQNN
7	1.020	YYR	5	10	160-177	YPNQVYYRPVDQYSNQNN
8	1.019	YYR	4	7	161-174	PNQVYYRPVDQYSN
9	1.017	YYR	4	3	161-170	PNQVYYRPVD
10	0.992	YYR	0	9	165-176	YYRPVDQYSNQN

Fig. 4 Output from epitope immunogenicity characterization (EpIC) algorithm. EpIC optimization is performed through sequential addition of single amino acids to the N- and C-terminus of the target core epitope followed by comparative analysis of the expanded epitope immunogenicity using the BepiPRED algorithm. Expansions of the core target epitope are ranked based on average predicted immunogenicity score. For each expansion listed, the number of residues added before and after the core epitope, the residue numbers corresponding to the target protein sequence, and the expanded epitope sequence are indicated

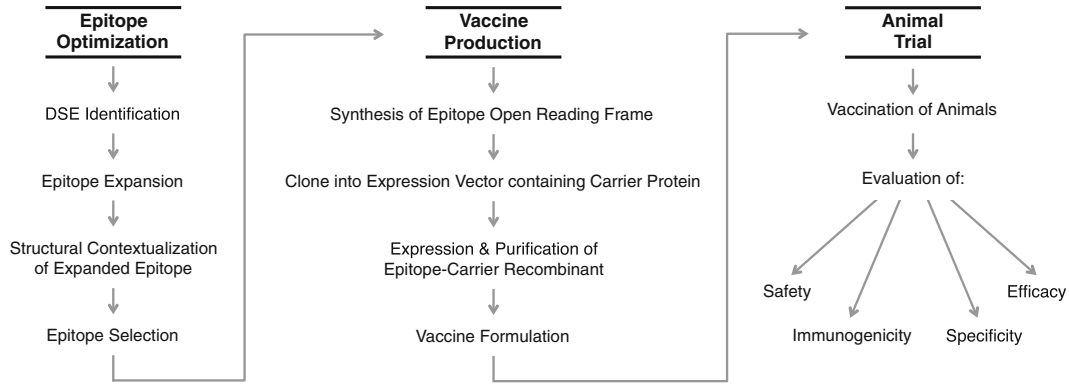

Fig. 5 Epitope-optimized peptide vaccine design and evaluation flowchart

2 Materials

2.1 Epitope Optimization

1. Epitope Immunogenicity Characterization (EpIC) software available at http://saphire.usask.ca/saphire/epic.
2. NCBI protein database (http://www.ncbi.nlm.nih.gov/protein).
3. Core epitope representing the minimal sequence of the target area of interest.
4. NCBI protein database, http://www.ncbi.nlm.nih.gov/protein.
5. A macromolecular structure-viewing program such as CN3D, http://www.ncbi.nlm.nih.gov/Structure/CN3D/cn3d.shtml.

2.2 Formulation and Delivery of the Optimized Epitope

1. Synthetic gene corresponding to the optimized epitope.
2. IPTG-inducible expression plasmid for carrier expression with restriction sites enabling C-terminal fusion of the synthetic gene to the carrier gene.
3. Restriction enzymes and required buffers for sub-cloning.
4. T4 DNA ligase and 10× buffer.
5. *E. coli* DH5α chemically competent cells.
6. Luria Broth agar plates with kanamycin: 10 g tryptone, 5 g yeast extract, 10 g NaCl, 1.5 % agar, 50 μg/mL kanamycin (per L).
7. Agarose gel electrophoresis apparatus.
8. QIAquick gel extraction kit (QIAGEN, Toronto, ON).
9. QIAprep spin miniprep kit (QIAGEN, Toronto, ON).
10. *E. coli* BL21 (DE3) chemically competent cells (Merck Millipore, Billerica, MA).
11. Luria Broth with kanamycin: 10 g Tryptone, 5 g yeast extract, 10 g NaCl, 50 μg/mL kanamycin (per L).
12. Isopropyl-β-d-1-thiogalactopyranoside (IPTG) (Sigma-Aldrich, St. Louis, MO).
13. Lysozyme (Sigma, St. Louis, MO).
14. 50 % Sucrose filter sterilized.
15. 100 mM Tris buffer pH 8.0.
16. RIPA buffer:20 mM Tris pH 7.5, 300 mM NaCl, 2 % (w/v) deoxycholic acid, 2 % (v/v) Igepal.
17. TET buffer: 100 mM Tris pH 8.0, 50 mM EDTA, 2 % (v/v) Triton X-100.
18. 4 M Guanidine or 6 M urea for inclusion body solubilization.
19. Water bath incubator for restriction digest and ligation reactions.
20. Benchtop microcentrifuge.
21. Shaking incubator for growth of liquid cultures.

22. Spectrophotometer for monitoring culture density.
23. Centrifuge.
24. Sonicator.
25. Polyacrylamide gel electrophoresis apparatus and required reagents for denaturing gels.

2.3 Vaccine Immunogenicity

1. Lkt recombinant fusion protein solubilized in 4 M guanidine.
2. 0.1 M Phosphate-buffered saline: 0.044 M NaH_2PO_4, 0.061 M Na_2HPO_4, 0.145 M NaCl, pH 7.2.
3. Emulsigen-D (MVP Technologies, Omaha, NE).
4. 25-Gauge needle 5/8″ long or 22-gauge 1″ needle depending on the viscosity of the injection.

2.3.1 Vaccination of Mice

2.3.2 Vaccination of Large Animals (Sheep, Deer, or Elk)

1. Lkt recombinant fusion protein solubilized in 4 M guanidine-HCl.
2. 0.1 M PBS: 0.044 M NaH_2PO_4, 0.061 M Na_2HPO_4, 0.145 M NaCl, pH 7.2.
3. Emulsigen-D (MVP Technologies, Omaha, NE).
4. 20-gauge, 1.5 in. needles.

2.3.3 Quantification of Antibody Responses through ELISA

1. 96-Well polystyrene microtiter plates (Immulon 2HB, Dynatech, Gaithersburg, MD).
2. Coating buffer: 15 mM Sodium carbonate, 35 mM sodium bicarbonate, pH 9.6.
3. Synthetic lyophilized peptides corresponding to the optimized sequence motif displayed on the recombinant protein.
4. Purified carrier protein in the absence of any added epitopes (*see* **Note 5**).
5. Purified target protein of interest.
6. ELISA blocking solution: 10 mM Tris, 150 mM NaCl, 0.05 % Tween 20, 1 % skim milk powder.
7. Alkaline phosphatase (AP)-conjugated rabbit anti-mouse IgG, AP-conjugated rabbit anti-sheep IgG, or AP-conjugated rabbit anti-deer IgG secondary antibodies (Kirkgaard and Perry Laboratories, Gaithersburg, MD).
8. PNPP substrate buffer: 0.5 mM $MgCl_2$, 1 M diethanolamine, pH 9.8, 1–2 mg/mL *p*-nitrophenyl phosphate.
9. Microplate reader.

2.4 Specificity of the Induced Immune Response

1. Pre-packed protein A IgG purification columns (Thermo-Scientific, Rockford, IL).
2. Bradford reagent.
3. 6D11 anti-PrP antibody (Signet Laboratories, Deadham, MA).

4. M-280 Tosylactivated Dynabeads (Invitrogen, Waltham, MA).
5. PBS.
6. Dynabead coupling wash buffer: 0.1 % Bovine serum albumin, PBS.
7. Dynabead coupling blocking buffer: 0.1 % Bovine serum albumin, 0.2 M Tris–HCl pH 8.5.
8. Normal and scrapie-infected mouse brains.
9. Brain homogenate lysis buffer: 100 mM NaCl, 10 mM EDTA, 0.5 % Nonidet P-40, 0.5 % sodium deoxycholate, 10 mM Tris–HCl, pH 7.5.
10. Dynabeads magnetic stand (Invitrogen, Waltham, MA).
11. IP wash buffer: 2 % Nonidet P-40, 2 % Tween-20, PBS, pH 7.4.
12. SDS-PAGE loading buffer without reducing agents.
13. SDS-PAGE apparatus and required standard buffers.
14. Polyvinylidene difluoride membrane (Thermo-scientific, Rockford, IL).
15. Western blot blocking buffer: 5 % Skim milk powder, 10 mM Tris–HCl pH 7.6, 150 mM NaCl, 0.05 % Tween-20.
16. 6H4 primary antibody (Prionics, Zurich, Switzerland).
17. HRP-conjugated sheep anti-mouse IgG (GE Healthcare Life Sciences, Baie d'Urfe, QC).
18. Amersham ECL Western Blotting Detection Reagent (GE Healthcare Life Sciences, Baie d'Urfe, QC).

2.5 Vaccine Safety (See Note 8)

1. Pre-immune and immune serum from vaccinated animals.

2.5.1 In Vitro Template-Directed Misfolding in Brain Homogenates

2. Materials for generating 10 % brain homogenate as described in Subheading 2.4.
3. Shaking incubator.
4. Benchtop microcentrifuge.
5. Proteinase K (Sigma-Aldrich, St. Louis, MO).
6. PBS.
7. Phenylmethylsufonyl fluoride (PMSF) (Sigma-Aldrich, St. Louis, MO).

2.5.2 In Vitro Template-Directed Misfolding with Recombinant Protein

1. *E. coli*-expressed recombinant PrP^{C} protein.
2. Proteinase K (Sigma-Aldrich, St. Louis, MO).
3. PBS.
4. PMSF (Sigma-Aldrich, St. Louis, MO).
5. Shaking incubator.
6. Benchtop microcentrifuge.
7. SDS-PAGE and western blotting materials as listed in Subheading 2.4.

2.5.3 In Vivo Template-Directed Misfolding

1. Brain homogenate lysis buffer: 100 mM NaCl, 10 mM EDTA, 0.5 % Nonidet P-40, 0.5 % sodium deoxycholate, 10 mM Tris–HCl, pH 7.5.
2. Proteinase K (Sigma-Aldrich, St. Louis, MO).
3. PMSF.
4. Water-bath incubator for digests.
5. SDS-PAGE and western blotting apparatus.
6. Mouse monoclonal PrP antibody 6H4 (Prionics, Zurich, Switzerland).
7. Mouse monoclonal PrP antibody 6D11 (Santa Cruz).
8. AP-conjugated goat anti-mouse IgG (H + L) (Kirkegaard and Perry Laboratories).
9. AP-conjugated CleanBlot IP Detection Reagent (Thermo-Fisher, Hampton, NH).
10. SIGMAFAST BCIP/NBT tablets (Sigma, St. Louis, MO).
11. Document scanner.
12. Scientific image processing software, Image J 1.40 g (http://imagej.nih.gov/ij/).
13. Benchmark staining platform (Ventana Medical Systems, Tuscon, AZ).
14. HRP-labeled multimer detection system: BMK Ultraview DAB Paraffin detection kit (Ventana Medical Systems, Tuscon, AZ).
15. Mouse anti-TSE clone F99/97.6.1 primary antibody (VMRD Inc, Pullman, WA).
16. Homozygous female tga20/tga20 mice (Strain:B6;129S7-Prnptm1CweTg[Prnp]a20CweCnrm).

2.6 Vaccine Efficacy: Challenge of Large Animal Species (Sheep, Deer, or Elk)

1. Appropriate infectious brain.
2. PBS.
3. Mechanical homogenizer.
4. Appropriate size syringe.

2.7 Protein Misfolding Cyclic Amplification

2.7.1 Preparation of Brain Homogenate Substrate

1. Syrian golden hamsters (for ovine protein misfolding cyclic amplification (PMCA)) or appropriate cervidized *PRNP* transgenic mouse (for cervid PMCA).
2. Perfusion buffer (PBS, 5 mM EDTA).
3. 30 mL Syringe.
4. Potter homogenizers.
5. PBS tablets (Bio Basic Inc., Markham, ON).
6. Soto homogenization buffer: 1× Tablet PBS, 0.15 M NaCl, 4 mM EDTA, 1 % Triton X-100, 1× complete protease inhibitor cocktail (Roche, Basel, Switzerland).

7. 10× Heparin solution: 48 USP/mL prepared in 1× tablet PBS. (Polysciences Inc., Warrington, PA).
8. Centrifuge.

2.7.2 Isolation of PBMCs from Challenged Animals

1. EDTA-coated blood tubes (BD, Franklin Lakes, NJ).
2. Centrifuge.
3. PBSA (calcium/magnesium-free PBS).
4. PBSA, 0.1 % EDTA.
5. Double-distilled water (ddH_2O).
6. 10× PBSA.
7. 60 % Percoll (GE Lifesciences, Pittsburgh, PA).
8. 15 mL Centrifuge tubes.

2.7.3 Amplification of Protease-Resistant Material by PMCA

1. Ultracentrifuge.
2. 10 % Noninfectious brain homogenate substrate.
3. Soto conversion buffer.
4. Qsonica q700 Sonicator (Qsonica, Newtown, CT).
5. Incubator (to house sonicator).
6. 0.2 mL Thin-walled PCR tubes.
7. –80 °C Freezer.

2.7.4 Digestion and Detection of Amplified Proteinase K-Resistant Material Generated from PMCA

1. SDS-PAGE apparatus and wet western blotting apparatus (BioRad, Hercules, CA).
2. Block heater.
3. Vortex mixer.
4. Shaker.
5. VersaDoc Molecular Imager (BioRad).
6. Transparent sealable (ziplock) bags.
7. Proteinase K (Sigma, St. Louis, MO).
8. Triton-X.
9. SDS.
10. PVDF membrane.
11. Transfer filter paper.
12. Laemmli sample buffer (2×).
13. 2-Mercaptoethanol.
14. 12 % Precise Protein Gels, 12-well format (Thermo Scientific, Waltham, MA).
15. Tris-Hepes running buffer.
16. Tris/glycine.
17. Methanol (95–100 %).

18. Nonfat skim milk powder or casein.
19. PBS.
20. Primary antibody:
    (a) Ovine Millipore mAB 1562 [3F4] (Millipore, Philadelphia, PA).
    (b) Cervid Prionics mAB 6H4 (Prionics, Zurich, Switzerland).
21. Secondary antibody, ovine goat anti-mouse IgG horseradish peroxidase labeled (BioRad).
22. Precision Plus Protein WesternC Standard (BioRad).
23. Precision Protein StrepTactin-HRP (BioRad).
24. ECL-Prime Chemiluminescent Detection Reagent (GE Healthcare, Amersham, UK).
25. Tween-20.

3 Methods

3.1 Epitope Optimization

3.1.1 Automated In Silico Epitope Optimization

1. Access the software platform Epitope Immunogenicity Characterization (EpiC) (*see* **Note 1**).
2. Input the amino acid sequence of the target protein, such as the prion protein of the species of interest, in FASTA format, obtained from the NCBI protein database.
3. Input core epitopes of interest.
4. Input the amino acid sequence of linker regions between repeat motifs.
5. Input the desired epitope repeat pattern reflecting overall presentation of the expanded core epitope as well as the location of the linker sequences (*see* **Note 2**).
6. Input any epitope length restrictions.
7. The output of EpIC prioritizes candidate peptides based on predicted immunogenicity (*see* **Note 3**).
8. Expansions that are predicted to be immunogenic should then be considered with respect to their positioning within the context of the three-dimensional structure of the target protein (following section).

3.1.2 Epitope Optimization Based on Structural Considerations

1. Search the NCBI protein database for a three-dimensional structure of the native conformation of the target protein.
2. Visualize the structure in CN3D.
3. Consider the epitope expansions predicted by EpIC to be immunogenic within the context of the three-dimensional structure of the target protein and prioritize expansions that remain buried (non-surface exposed) within the native structure.

3.2 Formulation and Delivery of the Optimized Epitope

1. Select a carrier protein (*see* **Note 4**). Our vaccines were generated using a 96 kDa truncated version of the 110 kDa leukotoxin protein derived from *Pasteurella haemolytica* as a carrier protein. The following methods are specific to this carrier platform.
2. Using a commercial service, synthesize genes, optimized for bacterial expression, corresponding to the top candidate epitope expansions from the previous sections, with appropriate 5′ and 3′ restrictions sites enabling excision and insertion into expression vector (*see* **Note 2**).
3. Sub-clone the appropriate fragments into an appropriate expression vector such that the epitopes are generated as recombinant fusions with the carrier protein (*see* **Note 5**).
4. Perform sequence verification of the cloned constructs.
5. Transform the chimeric Lkt expression vectors into BL21(DE3) competent cells, using standard protocols, for growth and IPTG induction as follows. Generate production cultures by inoculating 200–500 mL of LB broth containing 50 μg/mL kanamycin with 1/50 volume of fresh overnight culture. Incubate at 37 °C with shaking until the culture reaches an $O.D._{600}$ of ~0.6. Induce protein expression with 1 mM IPTG and incubate for 3 h at 37 °C with shaking. Harvest cells by centrifugation at $10{,}000 \times g$ for 15 min at 4 °C.
6. In the case of Lkt recombinants, the proteins are isolated as inclusion bodies as follows. Resuspend production culture cell pellets in 25 % sucrose and 50 mM Tris pH 8.0 and freeze at −20 °C. Thaw pellets at room temperature, then add 2.5 mg of lysozyme per mL of resuspended pellet, and incubate on ice for 15 min. Add four volumes of 5 RIPA:4TET detergent mix, invert samples quickly, and vigorously vortex to ensure complete cell lysis. Sonicate samples at 80 % for 20 s three times and then isolate the inclusion body pellet by centrifugation at $16{,}900 \times g$ for 20 min at 4 °C. Resuspend inclusion body pellets in 4 M guanidine or 6 M urea. For other carrier proteins appropriate purification methods to achieve >80 % purity should be investigated.
7. Evaluate the purity of the isolated protein by denaturing polyacrylamide gel electrophoresis. The purity should be greater than 85 %.

3.3 Vaccine Immunogenicity

3.3.1 Vaccination of Mice

1. Formulate 10 μg of the Lkt recombinant fusion in PBS with 30 % Emulsigen-D for a final injection volume of 100 μL per vaccine dose.
2. Vaccinate mice ($n = 8$) through subcutaneous (SC) injection between shoulder blades to mid back (dorsum).

3. Perform three vaccinations at 3-week intervals (days 0, 21, and 42).
4. Obtain serum samples on days 0, 21, 28, 42, 49, and 70 though tail bleeds.
5. After the final bleed, animals are bled out and sacrificed unless there is an interest in defining the duration of response in which case animals should be maintained and bled at monthly intervals.

3.3.2 Vaccination of Large Animals (Sheep, Deer, or Elk)

1. Inject animals SC with 50 μg of Lkt recombinant fusion prepared in PBS and 30 % Emulsigen-D in an injection volume of 1 mL. Injections are to be performed at the lateral cervical area in a triangle bounded by the shoulder, dorsum of the neck, and the lateral processes of the cervical spine using 20-gauge, 1.5 in. needles with needles placed in a tenting manner.
2. Administer vaccines three times at 6-week intervals (days 0, 42, and 84).
3. Collect serum samples at 3-week intervals starting at day 0 for quantification of antibody responses.
4. After the final bleed, animals are sacrificed unless there is an interest in defining the duration of response in which case animals should be maintained and bled at monthly intervals.

3.3.3 Quantification of Antibody Responses through ELISA

1. Through a commercial provider obtain peptides corresponding to the optimized sequence motif displayed on the recombinant protein.
2. Through either a commercial provider or expression and synthesis in the lab, obtain the carrier protein in the absence of any added epitopes (*see* **Note 5**).
3. Through a commercial provider obtain the target protein (PrP^C of species of interest) (*see* **Note 6**).
4. Coat 96-well polystyrene microtiter plates overnight with 0.5 μg per well of the synthetic peptide, 0.1 μg per well of target protein, or 0.1 μg per well of purified carrier protein in a final volume of 100 μL per well in coating buffer.
5. Wash the plates six times with distilled water (dH_2O) and then block with 200 μL per well of ELISA blocking solution.
6. Incubate the plates for 30 min at room temperature and then wash six times with dH_2O.
7. In ELISA blocking solution, dilute serum samples 1:40 and then serially dilute 1:4 with a final volume of 100 μL per well.
8. Incubate plates for 1 h at room temperature and then wash six times with dH_2O.
9. Add 100 μL of alkaline phosphatase (AP)-conjugated rabbit anti-mouse immunoglobulin gamma (IgG), AP-conjugated

goat anti-sheep IgG, or AP-conjugated rabbit anti-deer IgG at a 1:4000, 1:2000, or 1:1000 dilution, in ELISA blocking solution, to each well to detect bound murine, ovine, and cervid IgG, respectively.

10. Incubate for 1 h at room temperature, wash plate six times with dH_2O, and then add 100 μL *p*-nitrophenyl phosphate (PNPP) at 1 mg/mL in PNPP substrate buffer to each well for 1 h (murine) or 2 mg/mL PNPP substrate buffer for 2 h (ovine).
11. Read plates at 405 nm with a 490 reference.
12. ELISA titers are expressed as the reciprocal of the highest serum dilution resulting in which a reading exceeds two standard deviations above the negative control (pre-immune).

3.4 Specificity of the Induced Immune Response

1. Purify total IgG from immune sera and pre-immune sera using protein A columns according to the manufacturer's instructions.
2. Determine the protein concentration of the purified IgG using the Bradford method and adjust to approximately 2 mg/mL.
3. Couple 50 μg purified IgG and 30 μg 6D11 positive control antibodies to 7×10^8 tosyl-activated dynabeads in 1 mL PBS for 20 h at 37 °C according to the manufacturer's instructions. Wash beads twice with wash buffer and then incubate with blocking buffer for 4 h at 37 °C. Wash twice with washing buffer, resuspend antibody-conjugated beads in 1 mL PBS, and store at 4 °C.
4. Prepare 10 % homogenates of normal and scrapie-infected mouse brain in brain homogenate lysis buffer.
5. Immunoprecipitate PrP^C and PrP^{Sc} from the non-infected and scrapie-infected brain homogenates as follows. Incubate 50 μL of antibody-conjugated beads in 945 μL lysis buffer in the presence of 5 μL of 10 % brain homogenate, non-infected and scrapie infected, at room temperature for 3 h. Wash beads three times with IP wash buffer, remove all liquid, and resuspend in 30 μL SDS-PAGE sample buffer without reducing agents. Incubate samples at 95 °C for 5 min, and then centrifuge at $1000 \times g$ for 3 min.
6. Analyze the samples for PrP binding using SDS-PAGE and immunoblotting as follows. Separate proteins using a 12 % denaturing poly-acrylamide gel and then transfer proteins to a PVDF membrane at 125 mA for 2 h. Incubate membrane in blocking buffer for 1 h. Remove block and incubate with 6H4 antibody at 1:5000, wash with TBST, and incubate with HRP-conjugated sheep anti-mouse IgG at 1:3000. Wash the membrane three times in TBST and develop using standard protocols.

3.5 Vaccine Safety (See Note 8)

3.5.1 In Vitro Template-Directed Misfolding in Brain Homogenates

1. Separately pool the pre-bleed and post-vaccination serum samples from all vaccinated animals and apply to brain homogenates.
2. Incubate the brain homogenate and sera mixtures with shaking at 37 °C for 24 h in an attempt to convert PrP^{C} to PrP^{Sc}.
3. Centrifuge briefly to bring down liquid, and then digest 20 μL with 20 μg/mL of Proteinase K (PK) at 37 °C for 30 min with shaking. Undigested controls are incubated the same way with an equivalent volume of PBS.
4. Stop the digests by adding PMSF to a final concentration of 2 mM.
5. Combine the samples with an equal volume of 2× SDS-PAGE loading dye containing 0.5 % v/v β-mercaptoethanol.
6. Analyze by 12 % polyacrylamide SDS-PAGE and western blotting as described in Subheading 3.4.

3.5.2 In Vitro Template-Directed Misfolding with Recombinant Protein

1. Combine 2 μg of *E. coli*-expressed recombinant PrP^{C} protein with an equivalent quantity of monoclonal antibody or polyclonal PrP^{Sc}-specific antibody in a total volume of 40 μL of sterile PBSA.
2. Incubate reactions for 24 h at 37 °C on an orbital shaker at ~200 rpm.
3. After brief centrifugation to bring down liquid, digest 20 μL of the sample with 20 μg/mL of Proteinase K (PK) at 37 °C for 30 min with shaking. Undigested controls are to be incubated the same way with an equivalent volume of PBS.
4. Halt the digests by adding PMSF to a final concentration of 2 mM.
5. Combine the samples with an equal volume of 2× Laemmli SDS-PAGE loading dye containing 0.5 % v/v β-mercaptoethanol.
6. Analyze by 12 % polyacrylamide SDS-PAGE and western blotting as described in Subheading 3.4.

3.5.3 In Vivo Template-Directed Misfolding

1. Vaccinate sheep by the protocol described in Subheading 3.3.2.
2. Monitor the animals daily for clinical signs of scrapie. Ensure that observations occur at standard times (i.e., prior to feeding) throughout the duration of the trial and that observing personnel remain consistent. Score animals for the presence or absence of neurological changes with respect to hypersensitivity to motion, rubbing against objects or structures, general incoordination, changes to gait (particularly "high-stepping"), head or neck tremors, and excessive lip smacking. Animals exhibiting any of the above symptoms should be euthanized and processed to confirm scrapie postmortem.

3. Assay the obex and cerebellum samples for the presence of Proteinase K (PK)-resistant PrP^{Sc} (from Määttänen et al. [39]). Thaw obex or cerebellum samples on ice and homogenize to 10 % in ice-cold brain lysis buffer, as previously described [40]. Digest individual or combined homogenates with Proteinase K at final concentrations of 0, 5, 10, 15, 20, 25, and 50 μg/mL for 1 h at 37 °C. Stop digests by adding PMSF to a final concentration of 2 mM to all samples.
4. Analyze each homogenate sample using SDS-PAGE (50 μg/lane) and western blotting to detect remaining PrP after digests. Primary antibody 6H4 and secondary antibody AP-conjugated goat anti-mouse IgG (H + L) were used to detect brain PrP, while spleen PrP was detected with the primary antibody 6D11 and secondary anti-body AP-conjugated Clean-BlotTM IP Detection Reagent. React AP-conjugated antibodies with SIGMAFAST-BCIP/NBT substrate for 15–60 min, air-dry, and scan. Calculate and compare PrP band intensity percentages for PK digests compared with the undigested control using Image J 1.40 g.
5. Perform IHC examination of obex, cerebellum, and rectal lymphoid follicles coupled with ELISA tests for PK-resistant PrP^{Sc} in obex and cerebellum [24].
   (a) Immunohistochemical staining was conducted at Prairie Diagnostic Services (Saskatoon, SK) using the Benchmark staining platform and an HRP-labeled multimer detection system (BMK Ultraview DAB Paraffin detection kit, Ventana Medical Systems, Tuscon, AZ). Heat-induced epitope retrieval consisted of applying CC1 extended incubation followed by Protease 3 for 2 min (these and other reagents are proprietary and included in proprietary kit from Ventana Medical Systems Inc.). Incubate with mouse anti-TSE primary antibody for 32 min at a dilution of 1:1500.

3.5.4 In Vivo Template-Directed Misfolding in Transgenic Mice

1. Vaccinate homozygous female tga20/tga20 mice according to the protocol described in Subheading 3.3.1. Age vaccinated animals to approximately 1 year (*see* **Note 10**).
2. Age-matched negative control female tga20 mice ($n = 6$) to approximately 1 year without vaccination.
3. Quantify the extent of PrP^{Sc} formation within the brains of vaccinated and age-matched control mice using the methods described in Subheading 3.5.3.

3.6 Vaccine Efficacy

3.6.1 Vaccination and Challenge of Animals

1. Vaccinate the appropriate species of appropriate genotype according to the protocol described in Subheading 3.3.2.
2. Challenge animals with 5 g of appropriate infectious inoculum delivered as a 10 % homogenate to the oropharynx. Ensure ingestion of inoculum.

3. Monitor animals daily for the onset of prion disease symptoms by a standardized and regimented observation protocol.

3.7 Monitoring Disease Progression Using PMCA on Blood Samples

3.7.1 Preparation of Brain Homogenate Substrate

1. Harvest whole brain from euthanized Syrian golden hamster following perfusion with 60 mL PBS containing 5 mM EDTA (note: substitute the appropriate cervidized transgenic mouse for PMCA on deer or elk samples). Immediately freeze brains and store at −80 °C until use.
2. On the day of use, Syrian golden hamster brain was thawed and homogenized in 8 mL Soto conversion buffer and 1 mL heparin solution to create a 10 % w/v mixture (note: 9 mL of Soto conversion buffer and no heparin solution is used when preparing brain material for cervid-specific PMCA). Further incubate brain homogenate at 4 °C for 30 min, centrifuge at 1000 × *g* for 1 min to pellet large cellular debris, and isolate supernatant to serve as substrate for PMCA cycling.

3.7.2 Isolation of PBMCs from Challenged Animals

1. Draw blood from challenged and vaccinated animals in EDTA-coated blood tubes. Purify PBMCs from individual animals using Percoll purification:
2. Centrifuge blood at 1400 × *g* for 20 min at RT with break off. Collect buffy coat and bring to 10 mL with PBSA + 0.1 % EDTA.
3. Layer cell suspension onto 5 mL 60 % isotonic Percoll and centrifuge at 2000 × *g* for 20 min at RT break off.
4. Isolate cell layer, bring to 15 mL volume with PBSA + 0.1 % EDTA, and centrifuge at 300 × *g* for 8 min at 4 °C with the break on. Gently discard the supernatant. (Note: Skip steps "d." and "e." if cell pellet is free of red blood cells.)
5. To remove red blood cells, resuspend cell pellet in 9 mL ddH_2O for 30 s, quench with 1 mL 10× PBSA, and further bring to 15 mL volume with PBSA + 0.1 % EDTA. Centrifuge at 300 × *g* for 8 min at 4 °C with the break on. Gently discard the supernatant.
6. Resuspend cell pellet in 15 mL PBSA + 0.1 % EDTA, and centrifuge at 300 × *g* for 8 min at 4 °C with the break on. Gently discard the supernatant.
7. Resuspend cell pellet in 15 mL PBSA *without EDTA* and centrifuge at 150 × *g* for 8 min at 4 °C with the break on. Gently discard the supernatant.
8. Resuspend cell pellet in 15 mL PBSA *without EDTA* and centrifuge at 300 × *g* for 8 min at 4 °C with the break on. Ensure complete removal of supernatant. Store cell pellet at −80 °C.

3.7.3 Use of Isolated PBMCs as Seed for PMCA

1. Subject PBMCs to three freeze-thaw cycles, and centrifuge lysates at 100,000 × *g* for 1 h at 4 °C.
2. Resuspend the cell pellet 100 μL normal 10 % golden Syrian hamster brain homogenate (or appropriate brain homogenate for cervid PMCA).
3. Serially dilute sample tenfold from 10^{-1} to 10^{-9} in 10 % brain homogenate and transfer dilutions to 0.2 mL thin-walled PCR tubes.
4. Subject all samples to 26-min incubations at 33 °C followed by 40 s pulse sonication at 35 % amplitude within a microsonicator for ovine amplification (note: 45 % amplitude for cervid PMCA) (Qsonica q700).
5. Repeat this PMCA program until 38 rounds of sonication are completed, and immediately freeze at −80 °C for 30 min upon completion.
6. Thaw samples and dilute 1:10 into fresh 10 % brain homogenate for a second round of PMCA.
7. Repeat this procedure until four and seven rounds of PMCA for ovine and cervid samples, respectively.

3.7.4 Digestion and Detection of Amplified Proteinase K-Resistant Material Generated from PMCA

1. Digest 40 μL of ovine PMCA samples with 10 μL 1 mg/mL PK for 20 min at 37 °C. For cervid samples, digest 40 μL of PMCA samples with 10 μL of 250 mg/mL PK solution diluted in Hoover buffer (0.1 % Triton X-100 and 4 % w/v SDS) for 30 min at 45 °C.
2. Substitute PK for 10 μL ddH_2O when assaying negative control PMCA samples. Dilute digests 1:1 with 2× Laemmli solution containing 0.5 % v/v β-mercaptoethanol, and boil at 100 °C for 5 min.
3. Resolve digests by SDS-PAGE for 60 min at 110 V.
4. Transfer resolved digests to PVDF membrane by wet transfer at 20 V overnight.
5. Briefly incubate the blot in methanol and air-dry for 20 min. Briefly transfer the dried blot into methanol and PBS.
6. Block membrane using 5 % nonfat dried milk in PBS + 0.1 % Tween-20 (PBST) for 1 h with gentle and constant rocking. Remove blocking solution. Note that all further incubations and washes are conducted with constant and gentle rocking.
7. Ovine PK-resistant material was probed for using 3F4 monoclonal antibody (Millipore) diluted 1:10,000 in PBST for 1 h at RT (note to use 6H4 monoclonal antibody for detection of cervid material (Prionics)). Remove primary detection solution.

8. Wash the membrane 3× using 10 mL PBST buffer for 10 min.
9. Add goat anti-mouse IgG-HRP diluted 1:10,000 and Precision Protein StrepTactin-HRP diluted 1:10,000 in PBST, and incubate for 1 h at RT.
10. Wash the membrane 3× using 10 mL PBST buffer for 10 min.
11. Further wash the membrane 2× using 10 mL PBS for 5 min. Remove all excess PBS.
12. Bring ECL-Prime Chemiluminescent Detection Reagent (Amersham) to RT and mix reagents A and B 1:1 in 2 mL volume per membrane. Add detection reagent to membrane, cover from light, and incubate for 7 min. Remove all detection reagent and place within a ziplock bag while ensuring to remove air bubbles.
13. Image chemiluminescence within a VersaDoc Molecular Imager (BioRad).

Monitoring Disease Progression Using PMCA on Fecal Samples

1. Isolate feces from challenged and vaccinated animals and store at −80 °C until use.
2. Thaw feces and dilute to 10 % w/v in Soto Conversion Buffer, vortex briefly, and nutate for 2 h at RT.
3. Centrifuge mixture at 1000×*g* for 1 min, and isolate supernatant.
4. Dilute supernatant 1:10 in Syrian golden hamster brain homogenate and subject to PMCA cycling and detection as described above in Subheadings 3.7.3 and 3.7.4 (note: substitute appropriate transgenic mouse for cervid-specific PMCA).

4 Notes

1. Recently our group has automated the process of sequence optimization of DSEs. The publically available platform will automatically generate and assess peptide epitopes that differ by a single amino acid, constructed as a panel of expansions around the core epitope of interest. The panel of expansions is presented as forward-back-back repeat motifs and analyzed with the BepiPred program to identify expansions that incorporate B-cell epitope characteristics. This program adapts the input/output formats of the original BepiPred program specifically for manipulation of peptide epitopes, and increases the potential for enhanced immunogenicity and vaccine utility.
2. In the context of the final recombinant carrier protein epitopes are in a forward-back-back presentation that is repeated four times [36].

3. The output of EpiC ranks the epitope expansions on the basis of average prediction score. For each expanded epitope, the average prediction score, core epitope sequence prior to manipulation, the number of residues added to the N- and C-terminal sides, the residues represented within the target protein sequence, the complete expanded epitope sequence, and the final epitope repeat sequence that underwent analysis are also provided. From this information the user has the ability to select epitope expansions for vaccine development based on predicted immunogenicity and specificity.
4. A number of carrier proteins for peptide epitopes have been described [41]. For our efforts in vaccine development for prion disease Lkt has considerable advantages in terms of cost, demonstrated safety and efficacy in livestock vaccines, and ease of production and licensing for use in veterinary vaccines. Optimization of formulation and delivery involved presentation of these epitopes as fusions to the carrier protein leukotoxin, an RTX toxin derived from Mannheimia haemolytica that targets ruminant leukocytes and antigen-presenting cells. This carrier contains numerous T cell epitopes and is capable of stimulating strong antibody responses [42]. The 105 kDa toxin requires acylation by the lktC gene product for conversion to a toxic form but a non-acylated, truncated version of Lkt has been developed for delivery of self-peptides to a variety of species [43].
5. For the production of the Lkt-epitope fusions the genetic fragments corresponding to the expanded epitopes were subcloned into plasmid pAA352, which contains a gene encoding a 96 kDa version of the Lkt protein such that the antigens are expressed as C-terminal fusions.
6. Monitoring the antibody responses against the carrier protein is of potential value in confirming the delivery as well as setting a benchmark for comparison of epitope specificity for different epitope expansions in different trials.
7. Typically for efforts towards the development of vaccine whose immune responses are not meant to react with the native conformation of a protein we will also perform ELISAs against the properly folded target protein to obtain initial evidence of whether the epitope selection and expansion achieve the desired specificity of response [24].
8. While an absence of reactivity of the immune serum with the natively folded protein in ELISAs provides a measure of confidence of the desired specificity it is also important to ensure both this absence of reactivity with the target protein under more physiological conditions as well as to demonstrate reactivity with the misfolded species. For these objectives immuno-

precipitation experiments against appropriate biological samples are a relatively sensitive and reliable approach.

9. One of the primary concerns that are often raised around the concept of induction of PrP^{Sc} antibodies is the potential for these antibodies to serve as templates to promote the misfolding of PrP^{C} that could initiate or accelerate a prion disease [37].
10. Antibody-induced misfolding of PrP^{C} may only occur at low frequency in wild-type animals. As such, investigation of the ability of PrP^{Sc}-specific antibodies to promote PrP^{C} misfolding is more reliably addressed in sensitized animal models of prion disease. Specifically, homozygous tga20 mice, which carry approximately 60 copies of the *PRNP* gene and express approximately sixfold more PrP than wild-type mice, are highly susceptible to the development of prion disease [39]. tga20/tga20 mice (Strain:B6;129S7-Prnptm1CweTg[Prnp]a20CweCnrm) carry multiple copies of the PRNP gene and express approximately tenfold more PrP than wild-type mice.
11. Under normal circumstances the probability of human exposure to prions is insufficient to justify the use of a prion vaccine for the general population. In situations of specific individuals with genetic predisposition to prion disease (familial prion diseases account for 5–15 % of human TSE occurrences) a prion vaccine that can prevent or delay the onset of symptoms may be a valuable therapeutic tool [44]. The strategy to selectively employ a prion vaccine to genetically at-risk individuals must consider that the same genetic changes that bestow increased risk to prion disease may impact the specificity and outcomes of PrP^{Sc}-specific vaccination. As such, prior to the application of a PrP^{Sc}-specific prion vaccine to genetically predisposed subjects a characterization of the binding proclivities of the induced antibodies within the context of the specific PrP^{C} sequence variation of the patient should be performed [44].

References

1. Silveira JR, Caughey B, Baron GS (2004) Prion protein and the molecular features of transmissible spongiform encephalopathy agents. Curr Top Microbiol Immunol 284:1–50
2. Collinge J (2001) Prion diseases of humans and animals: their causes and molecular basis. Annu Rev Neurosci 24:519–550
3. Geschwind MD (2009) Clinical trials for prion disease: difficult challenges, but hope for the future. Lancet Neurol 8:304–306
4. Collee JG, Bradley R (1997) BSE: a decade on – part I. Lancet 349:636–641
5. Collee JG, Bradley R (1997) BSE: a decade on – part 2. Lancet 349:715–721
6. Palmer CM (1996) A week that shook the meat industry: the effects on the UK beef industry of the BSE crisis. Br Food J 98:17–25
7. Williams ES, Miller MW, Kreeger TJ et al (2002) Chronic wasting disease of deer and elk: a review with recommendations for management. J Wildl Manag 66:551–563
8. Schneider K, Fangerau H, Michaelsen B, Raab WH-M (2008) The early history of the transmissible spongiform encephalopathies exemplified by scrapie. Brain Res Bull 77:343–355
9. Sandberg MK, Al-Doujaily H, Sigurdson CJ et al (2010) Chronic wasting disease prions are

not transmissible to transgenic mice overexpressing human prion protein. J Gen Virol 91:2651–2657

10. Bessen RA, Marsh RF (1994) Distinct PrP properties suggest the molecular basis of strain variation in transmissible mink encephalopathy. J Virol 68:7859–7868
11. Hamir AN, Kunkle RA, Miller JM et al (2006) Experimental second passage of chronic wasting disease (CWDmule deer) agent to cattle. J Comp Pathol 134:63–69
12. Hamir AN, Miller JM, Kunkle RA et al (2007) Susceptibility of cattle to first-passage intracerebral inoculation with chronic wasting disease agent from white-tailed deer. Vet Pathol 44:487–493
13. Hamir AN, Greenlee JJ, Nicholson EM et al (2011) Experimental transmission of chronic wasting disease (CWD) from elk and white-tailed deer to fallow deer by intracerebral route: final report. Can J Vet Res 75:152
14. Almberg ES, Cross PC, Johnson CJ et al (2011) Modeling routes of chronic wasting disease transmission: environmental prion persistence promotes deer population decline and extinction. PLoS One 6:e19896
15. Wasserberg G, Osnas EE, Rolley RE, Samuel MD (2009) Host culling as an adaptive management tool for chronic wasting disease in white-tailed deer: a modelling study. J Appl Ecol 46:457–466
16. Schauber EM, Woolf A (2003) Wildl Soc Bull 31(3):610–616
17. Prusiner SB (1982) Novel proteinaceous infectious particles cause scrapie. Science 216:136–144
18. Aguzzi A, Sigurdson C, Heikenwaelder M (2008) Molecular mechanisms of prion pathogenesis. Annu Rev Pathol 3:11–40
19. Meyer-Luehmann M (2006) Exogenous induction of cerebral-amyloidogenesis is governed by agent and host. Science 313:1781–1784
20. Kfoury N, Holmes BB, Jiang H et al (2012) Trans-cellular propagation of Tau aggregation by fibrillar species. J Biol Chem 287: 19440–19451
21. Hansen C, Angot E, Bergström A-L et al (2011) α-Synuclein propagates from mouse brain to grafted dopaminergic neurons and seeds aggregation in cultured human cells. J Clin Invest 121:715–725
22. Münch C, O'Brien J, Bertolotti A (2011) Prion-like propagation of mutant superoxide dismutase-1 misfolding in neuronal cells. Proc Natl Acad Sci U S A 108:3548–3553
23. Ren P-H, Lauckner JE, Kachirskaia I et al (2009) Cytoplasmic penetration and persistent infection of mammalian cells by polyglutamine aggregates. Nat Cell Biol 11: 219–225
24. Marciniuk K, Määttänen P, Taschuk R et al (2014) Development of a multivalent, PrP(Sc)-specific prion vaccine through rational optimization of three disease-specific epitopes. Vaccine 32:1988–1997
25. Sigurdsson EM, Brown DR, Daniels M et al (2002) Immunization delays the onset of prion disease in mice. Am J Pathol 161:13–17
26. Hanan E, Goren O, Eshkenazy M, Solomon B (2001) Immunomodulation of the human prion peptide 106-126 aggregation. Biochem Biophys Res Commun 280:115–120
27. Koller MF, Grau T, Christen P (2002) Induction of antibodies against murine full-length prion protein in wild-type mice. J Neuroimmunol 132:113–116
28. Rosset MB, Ballerini C, Grégoire S et al (2004) Breaking immune tolerance to the prion protein using prion protein peptides plus oligodeoxynucleotide-CpG in mice. J Immunol 172:5168–5174
29. Polymenidou M, Heppner FL, Pellicioli EC et al (2004) Humoral immune response to native eukaryotic prion protein correlates with anti-prion protection. Proc Natl Acad Sci U S A 101(Suppl 2):14670–14676
30. Schwarz A, Krätke O, Burwinkel M et al (2003) Immunisation with a synthetic prion protein-derived peptide prolongs survival times of mice orally exposed to the scrapie agent. Neurosci Lett 350:187–189
31. Gilch S, Wopfner F, Renner-Müller I et al (2003) Polyclonal anti-PrP auto-antibodies induced with dimeric PrP interfere efficiently with PrPSc propagation in prion-infected cells. J Biol Chem 278:18524–18531
32. Cashman NR, Loertscher R, Nalbantoglu J et al (1990) Cellular isoform of the scrapie agent protein participates in lymphocyte activation. Cell 61:185–192
33. Arsenault RJ, Li Y, Potter A et al (2012) Induction of ligand-specific PrP (C) signaling in human neuronal cells. Prion 6: 477–488
34. Solforosi L, Criado JR, McGavern DB et al (2004) Cross-linking cellular prion protein triggers neuronal apoptosis in vivo. Science 303:1514–1516
35. Paramithiotis E, Pinard M, Lawton T et al (2003) A prion protein epitope selective for the pathologically misfolded conformation. Nat Med 9:893–899
36. Hedlin PD, Cashman NR, Li L et al (2010) Design and delivery of a cryptic PrP(C) epitope

for induction of PrP(Sc)-specific antibody responses. Vaccine 28:981–988

37. Taschuk R, Marciniuk K, Määttänen P et al (2014) Safety, specificity and immunogenicity of a PrP(Sc)-specific prion vaccine based on the YYR disease specific epitope. Prion 8:51–59
38. Roggen EL (2008) B-cell epitope engineering: a matter of recognizing protein features and motives. Drug Discov Today Technol 5:e49–e55
39. Määttänen P, Taschuk R, Ross L et al (2013) PrP(Sc)-specific antibodies do not induce prion disease or misfolding of PrP(C) in highly susceptible Tga20 mice. Prion 7:434–439
40. Li L, Guest W, Huang A et al (2009) Immunological mimicry of PrPC-PrPSc interactions: antibody-induced PrP misfolding. Protein Eng Des Sel 22:523–529
41. Pichichero ME (2013) Protein carriers of conjugate vaccines: characteristics, development, and clinical trials. Hum Vaccin Immunother 9:2505–2523
42. Potter AA, Manns JG (1998) GnRH-leukotoxin chimeras. US Patent 5,723,129
43. Gerdts V, Mutwiri G, Richards J et al (2013) Carrier molecules for use in veterinary vaccines. Vaccine 31:596–602
44. Madampage CA, Määttänen P, Marciniuk K et al (2013) Binding of bovine T194A PrPC by PrPSc-specific antibodies: potential implications for immunotherapy of familial prion diseases. Prion 7:301–311

Part VIII

Vaccines for Substance Abuse and Toxins

Chapter 38

Ricin-Holotoxin-Based Vaccines: Induction of Potent Ricin-Neutralizing Antibodies

Tamar Sabo, Chanoch Kronman, and Ohad Mazor

Abstract

Ricin is one of the most potent and lethal toxins known to which there is no available antidote. Currently, the most promising therapy is based on neutralizing antibodies elicited by active vaccination or given passively. Here, detailed protocols are provided for the production of two ricin holotoxin-based vaccines: monomerized subunit-based vaccine, and a formaldehyde-based ricin toxoid vaccine. Both vaccines were found to be stable with no toxic activity reversion even after long-term storage while eliciting high anti-ricin antibody titers possessing a potent neutralizing activity. The use of these vaccines is highly suitable for both the production of sera that can be used in passive protection experiments and immunization aimed to isolate potent anti-ricin monoclonal antibodies.

Key words Ricin, Holotoxin, Toxoid, Subunit-based vaccine immunization, Neutralizing antibodies, Acetylcholinesterase, HEK293 cells

1 Introduction

Ricin, derived from the plant *Ricinus communis*, consists of two covalently linked subunits: The A-subunit (RTA; Fig. 1) is an *N*-glycosidase that irreversibly inactivates the 28S rRNA of the mammalian 60S ribosome subunit, and the B-subunit (RTB; Fig. 1) is a galactose-specific lectin that mediates the binding of the toxin to the cell membrane [1]. The availability and ease of production and dissemination of the highly toxic ricin render it an attractive tool for bioterrorism and led to the classification of this toxin as a category B select agent by the Center for Disease Control and Prevention (CDC). Currently, there is no available antidote against ricin exposure and to date the most promising anti-ricin therapy is based on neutralizing antibodies elicited by active vaccination or given passively. While RTA-based vaccines can induce the formation of potent ricin-neutralizing antibodies, recent studies have demonstrated that neutralizing epitopes also exist on RTB, suggesting that a holotoxin vaccination should be considered [2–4].

Sunil Thomas (ed.), *Vaccine Design: Methods and Protocols: Volume 1: Vaccines for Human Diseases*, Methods in Molecular Biology, vol. 1403, DOI 10.1007/978-1-4939-3387-7_38,

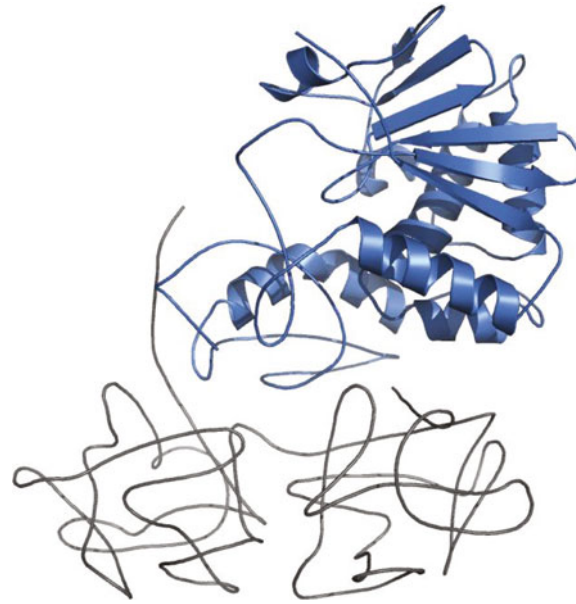

Fig. 1 Crystal structure of ricin holotoxin. Ricin A-subunit (RTA) is colored in *blue* and the B-subunit (RTB) in *gray* (PDB 2AAI)

We and others have found that animals immunized by holotoxin-based vaccines have developed high titers of anti-ricin antibodies that exhibit high affinity and possess excellent neutralization potency [5–9].

In order to inactivate the toxin while retaining its key epitopes needed for efficient immunization, we developed a method by which ricin can be treated with a reducing agent that separates the inter-subunit covalent disulfide bond, thus forming a subunit-based nontoxic vaccine. By adding an alkylation step to this process, we were able to produce a stable and immunogenic preparation that was successfully used for animal immunization.

One of the most direct approaches to inactivate a toxin is to expose it to formaldehyde. Indeed, the resulting ricin-toxoid is a very efficient immunogen that was shown to produce high titers of neutralizing antibodies [5, 10–13]. Use of the ricin-toxoid was limited due to the finding by Griffiths et al. [14] that upon removal of residual formaldehyde from the formulation, the toxic activity returned to the preparation within several days. However, we found that by adopting an earlier version of formaldehyde-based method for inactivation of ricin [15], a very stable vaccine preparation can be made that shows no reversion of ricin toxic activity, even after several months of storage. In addition, we developed a protocol that enables direct vaccination of animals using the native ricin toxin emulsified in adjuvant, a method which was also found to be safe and efficient in the elicitation of high titers of neutralizing antibodies.

Here, we provide detailed protocols for the preparation of ricin-holotoxin-based vaccines by the three different approaches mentioned and the optimal immunization schedules to produce anti-ricin-neutralizing antibodies. We also include a detailed description of our novel sensitive cell-based assay [5], which is used to determine the residual toxicity of ricin in the vaccine preparation and to monitor the production of ricin-neutralizing antibodies throughout the immunization process.

2 Materials

2.1 Equipment

1. Cell culture incubator (37 °C in a humidified 5 % CO_2).
2. 96-Well plate-based colorimeter.
3. General laboratory consumables (1.5 ml micro tubes, 15 and 50 ml centrifuge tubes, cell culture flasks, etc.).
4. Sterile cell culture 96-well plates.
5. ELISA 96-well polystyrene plates with high protein absorption capacity (e.g., Maxisorb, Nunc).
6. Dialysis bags of 10–15 kDa cutoff (alternatively: centrifugal filters with a 10 kDa cutoff).

2.2 Reagents and Buffers

1. Pure ricin in PBS.
2. HEK293-AChE cell line.
3. Dulbecco's modified Eagle medium (DMEM).
4. Tissue culture-grade fetal bovine serum (FBS).
5. Tissue culture-grade 0.05 % trypsin-EDTA.
6. Tissue culture-grade L-glutamine (200 mM).
7. PAT-medium: DMEM supplemented with 10 % AChE-depleted FBS and 2 mM L-glutamine.
8. Dithiothretol (DTT), 1 M.
9. Iodoacetamide 0.5 M (92.5 mg/ml in buffer PBS9): Prepare fresh at the same day and keep covered in aluminum foil at 4 °C.
10. Complete and incomplete Freund's adjuvant.
11. Alkaline-phosphatase-conjugated anti-rabbit antibody.
12. *p*-Nitrophenyl phosphate (PNPP) substrate freshly dissolved in DDW.
13. Benzotonium chloride.
14. ATC/DTNB substrate solution: 0.1 mg/ml BSA, 0.3 mM 5,5′-dithio-bis-(2-nitrobenzoic acid), 50 mM sodium phosphate buffer, pH 8.0, and 0.5 mM acetylthiocholine iodide (ATC).

15. Formaldehyde (37 %).
16. Phosphate-buffer saline (10 mM, pH 7.4. 150 mM NaCl; PBS).
17. Tris–HCl 1 M, pH 8.0.
18. Tris–HCl 1 M, pH 9.0.
19. Buffer PBS9: To 9 ml of PBS add 1 ml of Tris–HCl 1 M pH 9.0. Prepare fresh at the same day and keep at 4 °C.
20. ELISA coating buffer: $NaHCO_3$, 50 mM, pH 9.6.
21. ELISA blocking solution: PBS containing 2 % BSA, 0.05 % Tween-20, and 0.05 % azide.
22. ELISA wash buffer: PBS containing 0.05 % Tween-20.

3 Methods

3.1 Preparation of Ricin Subunit-Based Vaccine

In order to produce a nontoxic vaccine while retaining maximal similarity to the basic structure of ricin, the toxin is treated with a reducing agent in a way that separates the two subunits from each other. To prevent reversion of this process and the reformation of an active toxin, an alkylation step was added to irreversibly modify the free thiols in the vaccine preparation.

1. In a 50 ml tube, prepare 9 ml stock solution of ricin diluted in PBS to a concentration of 1 mg/ml. Pass 100 μl into a 1.5 ml micro tube labeled as "BKG" and keep for further analysis to determine background levels.
2. To the 50 ml tube, slowly add dropwise 1 ml of buffer PBS9 and mix gently.
3. Slowly add dropwise 1.1 ml of DTT 1 M and mix gently.
4. Incubate for 2 h at room temperature. By the end of the incubation period pass 100 μl into a 1.5 ml micro tube, label it as "Ricin-DTT," and keep for further analysis.
5. To the ricin-containing 50 ml tube add slowly 2.75 ml of iodoacetamide 0.5 M and mix gently.
6. Cover the 50 ml tube in aluminum foil and incubate for 2 h at room temperature. At the end of the incubation period pass 100 μl into a 1.5 ml micro tube and label it as "Ricin-IAA."
7. Determine that there are no free non-alkylated thiol residues in the preparation: Prepare three micro tubes, each containing 190 μl of PBS. Add 10 μl from either of the tubes marked as "BKG," "Ricin-DTT," or "Ricin-IAA." To each micro tube add 20 μl of DTNB, mix well, and transfer 100 μl to a 96-well microtiter plate. Measure the optical density in each well at the wavelength of 412 nm while subtracting the reference value read at 650 nm.

Calculate the ratio "Ricin-DTT"/"BKG" (should be >10) and "Ricin-IAA"/"BKG" (should be <2) (*see* **Note 1**).

8. Transfer the mixture into a dialysis bag (10–15 kDa cutoff) and place it in a beaker containing 2 l of PBS. Dialyze for 48 h at 4 °C under constant stirring, changing the PBS reservoir every 12 h.
9. Pass the mixture to a 50 ml tube and centrifuge for 20 min at 17,000 × *g*.
10. Quantify the protein concentration in the supernatant by measuring absorbance at 280 nm. Aliquot in micro tubes and keep at −20 °C.
11. Remove one aliquot to determine residual ricin activity according to the method described under Subheading 3.3 (*see* **Note 2**).

3.2 Preparation of Ricin-Toxoid

Another strategy to produce a safe and effective holotoxin-based vaccine is by inactivating the toxin with formaldehyde. In this protocol, we use a 4.2 % formaldehyde-buffered solution and incubate the mixture at 42–47 °C for extended durations. The resulting preparation was found to be very stable and can be stored for several months without any sign for reversion of ricin toxicity.

1. In a 50 ml tube, prepare 22 ml stock solution of ricin diluted in PBS to a concentration of 2 mg/ml.
2. Freshly dilute the 37 % formaldehyde stock to 8.4 % by mixing 17 ml PBS and 5 ml formaldehyde. Slowly add dropwise 22 ml of the phosphate-buffered formaldehyde to the ricin-containing 50 ml tube (the final concentration of formaldehyde is 4.2 % and that of ricin is 1 mg/ml) (*see* **Note 3**).
3. Incubate the mixture at 47 °C for 18 h.
4. Transfer the mixture to 42 °C and incubate for 30 h.
5. Pour the mixture into a dialysis bag (10–15 kDa cutoff) and place it in a beaker containing 2 l of PBS. Leave for 8 h at 4 °C under constant stirring.
6. Transfer the dialysis bag to a beaker containing 2 l of DDW and continue the dialysis at 4 °C under constant stirring, changing the DDW reservoirevery 12 h.
7. Pass the mixture to a 50 ml tube and centrifuge for 20 min at 17,000 × *g*.
8. Quantify the protein concentration in the supernatant by measuring absorbance at 280 nm.
9. Add benzotonium chloride to a final concentration of 25 μg/ml, aliquot, and store at 4 °C.
10. Determine the residual ricin activity according to the method described under Subheading 3.3 (*see* **Note 2**).

3.3 In Vitro Assessment of Ricin Activity

Residual toxicity in each vaccine preparation should be determined to ascertain that it is safe for immunization. The use of a cell-based assay is advised at this step, since it enables to determine the toxicity of the whole toxin. Here, we provide a detailed protocol for an assay that is based on genetically engineered HEK293-AChE cells that constitutively synthesize and secrete large amounts of acetylcholinesterase (AChE) to the culture medium [16] and any changes in the enzyme level can be sensitively and accurately measured. However, other cell-based assays can be used at this step to determine residual ricin toxicity in the vaccine preparations.

1. HEK293-AChE cells are maintained at 37 °C in a humidified 5 % CO_2 incubator. The cells are cultured in DMEM supplemented with 10 % FBS and 2 mM glutamine and should be subcultured every 3–4 days, upon reaching about 80 % confluence.
2. Detach the cells using trypsin and resuspend in the culture medium to a concentration of 1×10^6 cells/ml in a total volume of 8 ml.
3. Fill six rows of a cell culture 96-well plate by dispensing 100 μl of cell suspension into each well. Rows 1–3 will be used to determine the activity of ricin and rows 4–6 will be used to evaluate the residual activity of the ricin-toxoid preparation.
4. Prepare a 200 μl stock solution of ricin (20 ng/ml) in culture medium in a 1.5 ml micro tube marked 1, and prepare ten micro tubes marked 2–11, each filled with 100 μl of culture medium. Dilute the toxin seriallyby transferring 100 μl from tube #1 to tube #2 and so on to tube #11.
5. Prepare a 200 μl stock solution of 20 μg/ml of detoxified ricin (reduced or toxoid) in culture medium in a 1.5 ml micro tube marked 12, and prepare ten micro tubes marked 13–22, each filled with 100 μl of culture medium. Make serial dilution by transferring 100 μl from tube #12 to the next tube and so on to tube #22 (*see* **Note 4**).
6. Transfer 11 μl from tube #1 to the first three wells in column #1 of the 96-well plate that contains the cell suspension (triplicate points for each tested concentration) and continue accordingly with micro tubes #2 to #11.
7. Repeat the procedure using the samples from tubes 12–22, by transferring the samples into rows 4–6.
8. To column #12, add 11 μl of culture media (this column will be served as the 100 % control).
9. Incubate the 96-well plate at 37 °C in a humidified 5 % CO_2 incubator for 16 h.
10. Replace the culture medium from the three rows of the 96-well plate with fresh 100 μl PAT medium (*see* **Note 5**) and incubate for 2 h.

11. AChE levels are measured in a 96-well microtiter plate. To each well, transfer 11 μl from the 96-well plate and add 100 μl of ATC/DTNB substrate solution. Measure color formation rate in a 96-well plate-based colorimeter that enables kinetic measurements. The optical density in each well should be measured at the wavelength of 412 nm while subtracting the reference value read at 650 nm. The reaction is measured for a period of 5 min, with 30-s intervals, and expressed as V_{max} (mO.D./min) (*see* **Note 6**).
12. Express the AChE levels in each well as percent of control (untreated cells in column 12) and plot the average value of each triplicate as a function of the correspondingricin concentration. Fit the curve using nonlinear regression and determine the concentration needed to reduce levels of secreted AChE to 50 % (IC_{50}).

3.4 Immunization

The following protocol describes the immunization schedules for three ricin-holotoxin-based preparation: native ricin, subunit-based preparation and ricin-toxoid. We found that all three preparations can lead to the elicitation of high anti-ricin titers and to potent neutralizing antibodies. Nevertheless, the epitope profiles recognized by the elicited anti-ricin antibodies (anti-RTA, anti-RTB, and anti-sugar antibodies) in each immunization protocol may vary.

The low toxicity of the subunit-based preparation and of the ricin-toxoid permits an immunization schedule in which a constant and high dose is applied from the start. However, due to the high toxicity of native ricin even when emulsified in Freund's adjuvant, animals are immunized with the native toxin in a stepwise manner with escalating doses of toxin until a minimal level of neutralizing antibodies titer is elicited.

1. Maintain New Zealand white rabbits at 20–22 °C and a relative humidity of 50 ± 10 % on a 12-h light/dark cycle, fed with commercial rodent chow and provided with tap water ad libitum (*see* **Note 7**).
2. To a 15 ml tube, add the desired amount of ricin preparation (either native ricin, subunit preparation, or the ricin-toxoid; *see* **Note 8**) and fill with PBS to a final volume of 2 ml. Add 2 ml of complete Freund's adjuvant and vortex for 2 h at room temperature (*see* **Note 9**).
3. From each rabbit, collect a pre-immune blood sample and then separate and store the serum at −20 °C.
4. Immunize the rabbits by four subcutaneous injections of 250 μl of the ricin-toxoid emulsion given at different sites.
5. Three weeks after the immunization, collect a blood sample and then separate and store the serum at −20 °C.

6. Four weeks after the immunization, boost the animals as described above, except that incomplete Freund's adjuvant is used instead of complete adjuvant.
7. Boost the animals at 1-month intervals (*see* **Note 10**) and collect blood samples 3 weeks after each boost.
8. Coat ELISA 96-well plate with ricin (5 μg/ml in coating buffer) one row for each tested serum sample and one row for backgroundand incubate at room temperature overnight.
9. On the following day, aspirate the ricin-containing buffer, wash the wells three times using wash buffer, add to each well 250 μl of blocking solution, and incubate for 1 h at room temperature.
10. Remove blocking solution and add 90 μl of blocking solution to the first well in each row and 50 μl to the remaining wells.
11. Add 10 μl of the tested serum sample to well #1, mix well, and dilute serially by transferring 50 μl to the next well. Repeat throughout the entire row and discard 50 μl from the wells of column 12. Incubate for 1 h at room temperature.
12. Wash the wells three times using wash buffer and add to each well 50 μl of alkaline-phosphatase-conjugated anti-rabbit antibody. Incubate for 1 h at room temperature.
13. Wash the wells three times, add to each well 50 μl of PNPP substrate, and incubate until color has developed. Read plate at wavelength of 405 nm while subtracting the reference value read at 650 nm (*see* **Note 11**).
14. Plot the optical density as a function of the serum per dilution (Fig. 2a). Fit the curve using nonlinear regression and deter-

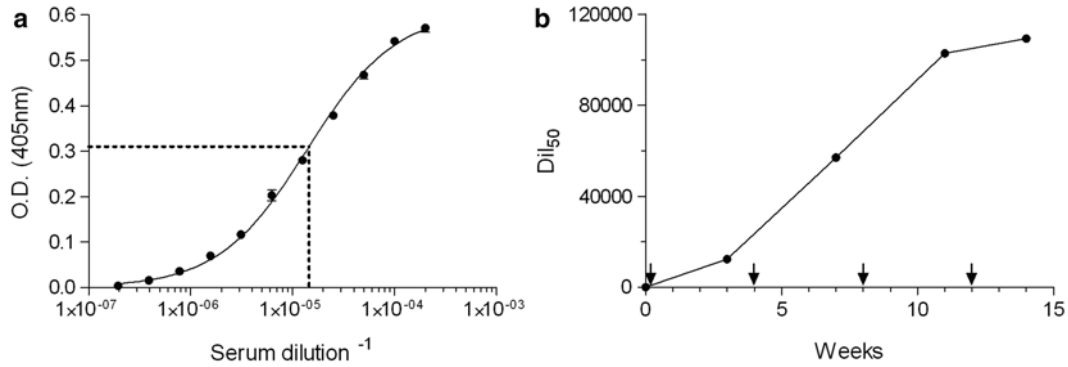

Fig. 2 Serum elicited anti-ricin antibodies following ricin-toxoid immunization. (**a**) Representative ELISA of immunized rabbit anti-ricin serum. *Dashed line* indicates the serum dilution at the 50 % binding point (Dil_{50}). (**b**) Profile of anti-ricin antibody elicitation in rabbit serum following immunization with ricin-toxoid. *Arrows* indicate immunization time points

mine the half dilution value (DIL_{50}) for each serum sample (Fig. 2b) (*see* **Note 12**).

15. Characterize the functional activity of the anti-ricin antibodies using the in vitro neutralization assay (*see* Subheading 3.5) or any other method of choice (*see* **Note 13**).

3.5 In Vitro Neutralization Assay

We utilized the cell-based assay that determines ricin toxicity to determine the formation of ricin-neutralizing antibodies throughout the immunization process. As mentioned above, any cell-based assay that can detect ricin activity can be used at this step. Moreover, in vitro cell-free assays can also be applied in order to determine the specific formation of RTA-neutralizing antibodies.

1. Detach the cells using trypsin and resuspend in the culture medium to a concentration of 1×10^6 cells/ml in a total volume of 4 ml for each tested sample.
2. Dispense 100 μl of cell suspension into the wells of three rows of a 96-well plate.
3. Prepare a 20 ng/ml stock solution of ricin (1.5 ml) in culture medium, and transfer 200 μl to a 1.5 ml micro tube marked 1, and 100 μl to 9 additional micro tubes marked 2–10.
4. To tube #1, add 22 μl of the tested rabbit sera, mix well, and dilute serially by transferring 100 μl from tube #1 to tube #2 and so on.
5. Transfer 11 μl from tube #1 to three wells in column #1 of the 96-well plate that contains the cell suspension (triplicate points for each antibody dilution) and continue accordingly with the other micro tubes.
6. To column #11 add 11 μl from the ricin stock solution (positive control) and to column #12 add 11 μl of culture media (100 % control).
7. Incubate the 96-well plate at 37 °C in a humidified 5 % CO_2 incubator for 16 h.
8. Replace the culture medium from the three rows of the 96-well plate with fresh 100 μl PAT medium and incubate for 2 h.
9. Measure AChE levels in each well (as described under Subheading 3.3), express it as percent of control (untreated cells in column 12), and plot the average value of each triplicate as a function of the serum per dilution (Fig. 3a). Fit the curve using nonlinear regression and determine the effective dilution of serum needed to neutralize 50 % (ED_{50}) of the toxin (*see* **Note 14**).
10. Continue with monthly booster injections until the ED_{50} value reaches plateau (Fig. 3b).

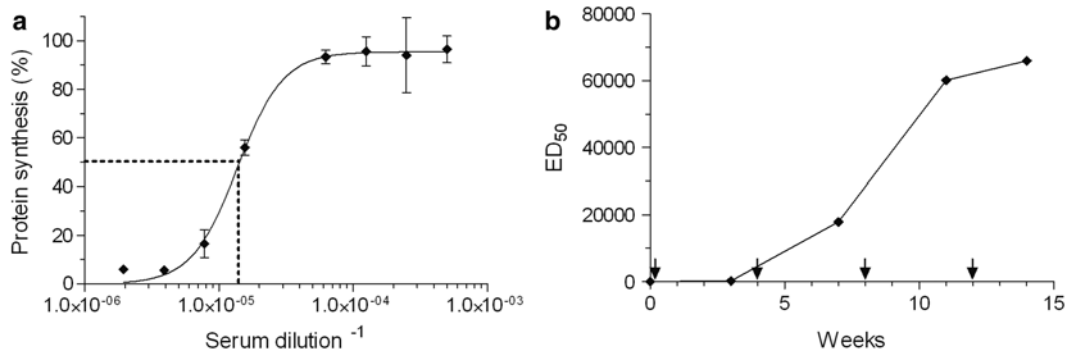

Fig. 3 In vitro neutralization assay. (**a**) Representative profile of ricin neutralization by sera of ricin-toxoid-immunized rabbit. *Dashed line* indicates the serum dilution needed to inhibit 50 % of ricin activity (ED_{50}). (**b**) Profile of ricin-neutralizing antibodies elicited in rabbit serum following immunization with ricin-toxoid. *Arrows* indicate immunization time points

4 Notes

1. Efficient alkylation of free thiols is necessary for irreversible monomerization of the toxin subunits in order to produce a safe and stable vaccine preparation. Therefore, if the ratio of "Ricin-IAA"/"BKG" is >2, either repeat **steps 5** and **6** at a longer incubation period or use a freshly prepared iodoacetamide stock solution.
2. The residual ricin activity in the preparations should be less than 1 %; otherwise it may be toxic to the immunized animals.
3. Extra care should be paid at this point as adding formaldehyde too fast can precipitate the protein. Gentle vortexing can be applied throughout this step.
4. It is expected that the residual ricin activity in the preparations will be less than 1% of that of the original stock and therefore the stock concentration of the ricin-toxoid is 1000 times higher than the ricin stock. If a linear curve is not generated then this step should be repeated using higher or lower stock concentrations, accordingly.
5. To reduce the background signal arising from cholinesterases originated from the supplemented FBS, cholinesterase-depleted FBS is used. However, the culture medium can be replaced with fresh DMEM and the background should be properly subtracted from all reading.
6. Typically, the AChE levels in the control untreated cells are in the range of 200–300 mO.D./min. The enzyme concentration can be measured accurately up to 300 mO.D./min. If a higher

value is reached then a smaller volume of the culture medium should be taken (e.g., 5 μl from the tested wells and 6 μl of fresh medium). A much lower value may imply that improper amount of cells were seeded and the test should be repeated.

7. An approval should be obtained from an ethic committee before the beginning of the immunization, according to local regulations.
8. The doses for primary immunization are native toxin—1 μg; subunit preparation—60 μg; and ricin-toxoid—100 μg.
9. Since a significant amount of the formed homogenous solution cannot be recovered from the tube wall, we double the starting volume.
10. The boost doses for the native toxin are 4, 25, and 100 μg. The subunit preparation and the ricin-toxoid boosts are administered at 60 μg and 100 μg, respectively, throughout the immunization schedule.
11. In order to produce a reliable and accurate curve, the color development should be monitored carefully so that measurement would be performed when the absorbance in the wells containing the lowest serum dilution is in the range of 0.5–0.8 O.D. Above that point the rate of color development is not linear and therefore will affect the interpretations of the results.
12. We found that monitoring the immunization process by determining the DIL_{50} in each time point is much more accurate than the classic endpoint titer. The major drawback of the endpoint titer assay is that duplicates can vary significantly (by a factor of 2–4) and require the use of geometrical mean, etc. Therefore, changes in the antibody titer between consecutive boosts that are less than twofold might be unnoticed and will lead to premature cessation of the immunization process. However, the DIL_{50} value is a continuous number that allows good replicates (with deviations of usually <15 %) and therefore better reflects the immunization status.
13. Other methods to assess the quality of the elicited anti-ricin antibodies that may apply at this stage are among others measuring the apparent affinity toward ricin (using BIAcore, Octet, etc.); determining functional affinity (using a chaotrophic agent such as KSCN); and determining the relative distribution of antibodies that recognize each of the two subunits of ricin or the sugar moieties and performing an *in vivo* protection assay.
14. It is important to make sure that the positive control (ricin without serum) leads to 90–95 % inhibition and that a full curve is obtained; otherwise start from higher sera dilution.

Acknowledgements

We thank Dr. Eytan Elhanany, Dr. Yoav Gal, Ron Alcalay, Nehama Seliger, and Sharon Erlich for contributing to the development of protocols.

References

1. Olsnes S, Kozlov JV (2001) Ricin. Toxicon 39:1723–1728
2. O'Hara JM, Yermakova A, Mantis NJ (2011) Immunity to ricin: fundamental insights into toxin-antibody interactions. Curr Top Microbiol Immunol 357:209–241
3. Vance DJ, Tremblay JM, Mantis NJ, Shoemaker CB (2013) Stepwise engineering of heterodimeric single domain camelid VHH antibodies that passively protect mice from ricin toxin. J Biol Chem 288:36538–36547
4. Yermakova A, Mantis NJ (2011) Protective immunity to ricin toxin conferred by antibodies against the toxin's binding subunit (RTB). Vaccine 29:7925–7935
5. Cohen A, Mechaly A, Sabo T, Alcalay R et al (2014) Characterization and epitope mapping of the polyclonal antibody repertoire elicited by ricin-holotoxin based vaccination. Clin Vaccine Immunol 21:1534–1540
6. Gal Y, Mazor O, Alcalay R, Seliger N et al (2014) Antibody/doxycycline combined therapy for pulmonary ricinosis: attenuation of inflammation improves survival of ricin-intoxicated mice. Toxicol Rep 1:496–504
7. Maddaloni M, Cooke C, Wilkinson R, Stout AV et al (2004) Immunological characteristics associated with the protective efficacy of antibodies to ricin. J Immunol 172:6221–6228
8. Pincus SH, Das A, Song K, Maresh GA et al (2014) Role of Fc in antibody-mediated protection from ricin toxin. Toxins 6:1512–1525
9. Pratt TS, Pincus SH, Hale ML, Moreira AL et al (2007) Oropharyngeal aspiration of ricin as a lung challenge model for evaluation of the therapeutic index of antibodies against ricin A-chain for post-exposure treatment. Exp Lung Res 33:459–481
10. Griffiths GD, Bailey SC, Hambrook JL, Keyte M et al (1997) Liposomally-encapsulated ricin toxoid vaccine delivered intratracheally elicits a good immune response and protects against a lethal pulmonary dose of ricin toxin. Vaccine 15:1933–1939
11. Griffiths GD, Phillips GJ, Bailey SC (1999) Comparison of the quality of protection elicited by toxoid and peptide liposomal vaccine formulations against ricin as assessed by markers of inflammation. Vaccine 17:2562–2568
12. Kende M, Yan C, Hewetson J, Frick MA et al (2002) Oral immunization of mice with ricin toxoid vaccine encapsulated in polymeric microspheres against aerosol challenge. Vaccine 20:1681–1691
13. Yan C, Rill WL, Malli R, Hewetson J et al (1996) Intranasal stimulation of long-lasting immunity against aerosol ricin challenge with ricin toxoid vaccine encapsulated in polymeric microspheres. Vaccine 14:1031–1038
14. Griffiths GD, Phillips GJ, Holley J (2007) Inhalation toxicology of ricin preparations: animal models, prophylactic and therapeutic approaches to protection. Inhal Toxicol 19:873–887
15. Yan C, Rill WL, Malli R, Hewetson J et al (1995) Dependence of ricin toxoid vaccine efficacy on the structure of poly(lactide-co-glycolide) microparticle carriers. Vaccine 13:645–651
16. Kronman C, Velan B, Gozes Y, Leitner M et al (1992) Production and secretion of high levels of recombinant human acetylcholinesterase in cultured cell lines: microheterogeneity of the catalytic subunit. Gene 121:295–304

Chapter 39

Synthesis of Hapten-Protein Conjugate Vaccines with Reproducible Hapten Densities

Oscar B. Torres, Carl R. Alving, and Gary R. Matyas

Abstract

The ability to prepare hapten-carrier conjugates reproducibly with consistent lot-to-lot hapten densities and protein yields is a critical component of hapten vaccine development. This entails the development of appropriate coupling chemistries that do not cause protein precipitation and the development of methods to quantify hapten density. Recently, extensive efforts have been devoted to design vaccines against drugs of abuse. We describe, herein, a method for conjugation of a morphine-like hapten (MorHap) to tetanus toxoid (TT), which involves conjugation of MorHap to the surface lysines of TT through the N-hydroxysuccinimide portion of a heterobifunctional linker and the subsequent attachment of the thiol on MorHap to the maleimide portion of the cross-linker. Methods are described for the analytical quantification of the hapten density of the conjugates using modified Ellman's test, trinitrobenzenesulfonic acid (TNBS) assay, and matrix-assisted laser desorption ionization time-of-flight mass spectrometry (MALDI-TOF MS).

Key words Hapten-protein conjugates, Hapten density, Drugs of abuse, Heroin vaccine, MorHap, Tetanus toxoid, Thiol-maleimide chemistry, Ellman's test, Trinitrobenzenesulfonic acid assay, MALDI-TOF MS

1 Introduction

Vaccines to drugs of abuse function by generating antibodies against the psychoactive drugs [1]. The induced antibodies sequester the drug by capturing it in the blood and preventing it from crossing the blood–brain barrier. This prevents the drug from engaging its receptor, and thereby preventing euphoria and addiction. Drugs of abuse are too small to induce sufficient antibodies to block the effects of the drug. An immunologic approach to this problem is to design a hapten which mimics the drug and has a functional group that can be coupled to a protein carrier [2, 3]. One example of a surrogate heroin/morphine hapten is MorHap, which is covalently attached to the carrier through the sulfhydryl group [4]. The covalent attachment of a hapten to the protein yields a hapten conjugate, which can be mixed with an adjuvant

Sunil Thomas (ed.), *Vaccine Design: Methods and Protocols: Volume 1: Vaccines for Human Diseases*, Methods in Molecular Biology, vol. 1403, DOI 10.1007/978-1-4939-3387-7_39,

and given as a vaccine formulation [5]. Hapten-protein conjugates are crucial for generating high-titer and high-affinity antibodies [6]. The functional efficacy of a vaccine against a drug of abuse depends on the presence of high amounts of circulating antibody that can bind the drug tightly [7]. Immunization of mice with MorHap-TT conjugates mixed with liposomes containing monophosphoryl lipid A as an adjuvant generated high-heroin/morphine-antibody titers [8]. Consequently, immunized mice were protected against heroin challenge using antinociception assays [4, 9].

Hapten density, which is the number of haptens covalently attached to the surface of a protein molecule, affects vaccine efficacy [10, 11]. Haptens are frequently attached to the carrier protein using carbodiimide chemistry, which involves formation of an amide bond from the carboxylic acid of the haptenic surrogate and the surface amines (e.g., lysines) of the protein. Since proteins contain carboxylic acid residues, intramolecular amide formation and intermolecular coupling between protein molecules occur. These unwarranted reactions produced conjugates with variable hapten densities and protein aggregates that are difficult to characterize. Immunization of animals with irreproducible hapten-protein conjugates may either compromise the potency of the vaccine or result in irreproducible responses. Hapten density can be controlled using an optimized coupling procedure that takes into consideration the conjugation chemistry, nature of the protein, and stoichiometric ratios between reacting partners. The maleimide-thiol chemistry was used to circumvent the reproducibility issues of carbodiimide-based coupling [12]. In this approach, the haptenic surrogate contains a thiol and is attached to the protein in a two-step process. The surface amines of the protein are first reacted with a heterobifunctional linker, via the N-hydroxysuccinimide ester (NHS) end of the linker. The linker-protein intermediate is subsequently reacted with the hapten through the other end of the linker that contains maleimide to give the final hapten-protein conjugates. The hapten density is controlled by adjusting the stoichiometric ratios between the linker and the protein [13]. The protein yield of the hapten-protein conjugates is maximized using an optimal stoichiometric ratio between the protein-linker intermediate and the hapten. We used tetanus toxoid (TT) as a carrier because (1) it is highly soluble in physiological buffer, (2) it has ~30–35 surface amines amenable for hapten attachment, and (3) it is the antigen in a licensed tetanus vaccine and is a carrier in polysaccharide conjugate vaccines [10, 14]. The reproducibility of the hapten-protein conjugates can be quantitatively evaluated through analytical characterization of the hapten density and protein yield [13]. Hapten density has been assessed by direct and indirect methods. Matrix-assisted laser desorption ionization time-of-flight mass spectrometry (MALDI-TOF MS) is a direct method of measuring hapten density because

it measures changes in mass before and after conjugation [13, 15, 16]. The 2,4,6-trinitrobenzenesulfonic acid (TNBS) assay and modified Ellman's test are indirect methods of assessing hapten density [13, 17–19]. TNBS accounts for the number of surface amines before and after conjugation, while Ellman's test uses the difference in the maleimide contents before and after hapten addition. In the present strategy, an optimized procedure for the coupling of MorHap to TT is presented. Using the optimized procedure, we demonstrated the synthesis of seven MorHap-TT conjugates with reproducible hapten density and protein yield. The methods described are applicable for the conjugation of haptenic surrogates of drugs of abuse, such as heroin, cocaine, nicotine, and methamphetamine to immunogenic proteins and for vaccine formulations that involve thiol-maleimide chemistry.

2 Materials

Prepare all aqueous solutions using deionized water and analytical grade reagents. Prepare and store all reagents at room temperature (unless indicated otherwise).

2.1 Deprotection and Purification of MorHap

1. MorHap (MW 614.46 g/mol) or thiol-based hapten. Store at −20 °C (*see* **Note 1**).
2. Trifluoroacetic acid (TFA), triisopropylsilane (TIS), dichloromethane (DCM), chloroform, and petroleum ether (Sigma, St. Louis, MO, USA).
3. Teflon-lined screw-cap glass vial (Thermo Fischer Scientific, Waltham, MA, USA) (*see* **Note 2**).
4. Dry-seal glass vacuum desiccator (WHEATON, Millville, NJ, USA).
5. Vacuum pump with controller (BÜCHI, Flawil, Switzerland).
6. Thin-layer chromatography (TLC) Plates-Silica Gel 60 F254 Coated (VWR International, Radnor, PA).
7. TLC chamber and UV lamp.
8. ACQUITY ultraperformance liquid chromatography/tandem quadrupole detector (UPLC/TQD) system (Waters, Cambridge, MA).

2.2 Synthesis and Purification of MorHap-TT Conjugates

1. Tetanus toxoid (MW 152,533.0 g/mol) in saline (Statens Serum Institut, Copenhagen, Denmark). Store at 4 °C (*see* **Note 3**).
2. Dialysis cassettes: Slide-A-Lyzer G2 with 10 K molecular weight cut-off (MWCO) (Thermo Fischer Scientific).
3. Spin desalting column: 10 mL Zeba with 7 K MWCO (Thermo Fischer Scientific). Store at 4 °C.

4. N-hydroxysuccinimide-$(PEG)_2$-maleimide ($SM(PEG)_2$) linker (Thermo Fischer Scientific). Store at –20 °C.
5. 2.0 mL Microcentrifuge tube, ThermoMixer C with SmartBlock™ 2.0 mL accessory (Eppendorf, Hamburg, Germany).
6. Allegra™ 25R Centrifuge (Beckman Coulter, Pasadena, CA, USA).
7. Polysulfone membrane filter with 0.22 μm pore size (Pall Corporation, Port Washington, NY, USA).
8. Phosphate-buffered saline (PBS) conjugation buffer, pH 7.2: Dissolve one pouch content of BupH™ Phosphate Buffered Saline Packs (Thermo Scientific) in a final volume of 500 mL water to make 100 mM sodium phosphate and 150 mM NaCl, pH 7.2 (*see* **Note 4**). Filter the buffer through a 500 mL filter system with 0.22 μm pore size (Corning, Corning, NY, USA). Store at 4 °C.
9. Linker stock solution: Dissolve 100 mg of SM $(PEG)_2$ linker (MW 425.39 g/mol) by directly adding 840 μL DMSO to the entire contents of the vial (*see* **Note 5**). Vortex the vial until all the solids are dissolved. The final concentration of the stock solution is 250 mM. Store the remaining solution at –20 °C (*see* **Note 6**).
10. 1× Dulbecco's phosphate-buffered saline (DPBS), pH 7.4: Mix 100 mL 10× DPBS, without calcium and magnesium (Quality Biological Inc., Gaithersburg, MD, USA), and 900 mL water to make 10 mM Na_2HPO_4, 1.8 mM KH_2PO_4, 2.7 mM KCl, and 137 mM NaCl, pH 7.4. Store at 4 °C.

2.3 Protein Quantification

1. Bicinchoninic acid (BCA) Protein Assay Kit (Thermo Fischer Scientific). Store at 4 °C (*see* **Note 7**).
2. 1× DPBS, pH 7.4. Store at 4 °C.
3. Clear polystyrene 96-well plates (Thermo Fischer Scientific) (*see* **Note 8**).
4. SpectraMax M5 (Molecular Devices, Sunnyvale, CA).

2.4 Ellman's Assay and Modified Ellman's Test

1. $Na_2HPO_4{\cdot}7H_2O$ (sodium phosphate dibasic heptahydrate), sodium 2-mercaptoethanesulfonate (MESNA) (*see* **Note 9**), 5-5′-dithiobis(2-nitrobenzoic acid), or Ellman's reagent (*see* **Note 10**), UV-transparent 96-well plates (Sigma).
2. 0.1 M Sodium phosphate buffer (PB), pH 8: Dissolve 26.81 g Sodium phosphate dibasic heptahydrate (MW 268.07 g/mol) in 950 mL water. Adjust the pH with 1 N or 6 N HCl to pH 8.0. Make up to 1 L with water.
3. 0.1 M Sodium phosphate buffer (PB), pH 7.2: Dissolve 26.81 g sodium phosphate dibasic heptahydrate in 950 mL water.

Adjust the pH with 1 N or 6 N HCl to pH 7.2. Make up to 1 L with water.

4. SpectraMax M5 (Molecular devices).
5. 500 μM MESNA stock solution: Dissolve 8.21 mg MESNA (MW 164.18 g/mol) with 75 mL 0.1 M PB, pH 8.0. Transfer the solution to a 100 mL volumetric flask. Make up to 100 mL with 0.1 M PB, pH 8.0 (*see* **Note 11**).
6. MESNA standards: Prepare 0, 2, 4, 8, 16, 32, 64, and 125 μM solutions of MESNA by appropriate dilution of the stock solution in 0.1 M PB, pH 8.0.
7. 10 mM Ellman's reagent: Dissolve 39.63 mg Ellman's reagent (MW 396.35 g/mol) in 10 mL 0.1 M PB, pH 8.0.

2.5 2,4,6-Trinitrobenzene Sulfonic Acid (TNBS) Assay

1. 1 % TNBS in methanol (G-Biosciences, St. Louis, MO, USA). Store at −20 °C (*see* **Note 12**).
2. $NaHCO_3$ (sodium bicarbonate), L-glutamic acid, UV-transparent 96-well plates (Sigma).
3. SpectraMax M5 (Molecular devices).
4. 0.1 M Sodium bicarbonate, pH 8.0: Dissolve 8.4 g Sodium bicarbonate (MW 84.01 g/mol) in 950 mL water. Adjust the pH with 1 N or 6 N HCl to pH 8.0. Make up to 1 L with water.
5. 0.01 % TNBS assay solution: Add 100 μL 1 % TNBS to 9.9 mL 0.1 M sodium bicarbonate (*see* **Note 13**).
6. 500 μM L-Glutamic acid stock solution: Dissolve 7.36 mg L-glutamic acid (MW 147.13 g/mol) in 100 mL 0.1 M sodium bicarbonate, pH 8.0. Store at 4 °C (*see* **Note 14**).
7. L-Glutamic acid standards: Prepare 0, 7.5, 15, 30, 60, 120, 240, and 360 μM of L-glutamic acid by appropriate dilution of the stock solution in 0.1 M sodium bicarbonate (*see* **Note 15**).

2.6 MALDI-TOF MS

1. IgG (MW 148,500.0 g/mol) from human serum reagent grade, ≥95 % (SDS-PAGE), essentially salt-free, lyophilized powder. Store at 4 °C (*see* **Note 16**).
2. Sinapinic acid (SA) matrix substance for MALDI TOF-MS. Store at 4 °C (Sigma).
3. Mass spectrometry-grade TFA (Sigma).
4. Mass spectrometry-grade acetonitrile (ACN), water, and acetone (VWR International).
5. 10 μL ZipTip C_4 resin (Millipore, Billerica, MA).
6. MALDI-TOF 384-well stainless plate, Axima MegaTOF™ (Shimadzu Scientific Instruments, Columbia, MD). The Axima MegaTOF™ is capable of ultrahigh mass analysis up to the megadalton level.
7. 2 % ACN (in water with 0.1 % TFA).

8. 50 % ACN (in water with 0.1 % TFA).
9. 80 % ACN (in water with 0.1 % TFA).
10. 100 % ACN (with 0.1 % TFA).
11. 10 mg/mL SA in acetone.
12. 10 mg/mL SA in 50 % ACN (in water with 0.1 % TFA).
13. 10 mg/mL IgG in 50 % ACN (in water with 0.1 % TFA).

3 Methods

The goal of this experiment is to synthesize seven MorHap-TT conjugates with varying hapten densities. The synthesis, purification, and characterization of MorHap-TT conjugates is a 3-day process. An effective approach to this rigorous process is to employ the following experimental plan:

Day 1: Deprotection of MorHap and Dialysis of Tetanus Toxoid (Subheadings 3.1 and 3.4)

Day 2: Purification of MorHap and Synthesis of MorHap-TT conjugates (Subheadings 3.2, 3.3, 3.5, 3.6, and 3.7)

Day 3: Analytical characterization of the conjugates (Subheadings 3.8 and 3.9)

3.1 Deprotection of MorHap

The reaction for the deprotection of MorHap is shown in Fig. 1.

1. Weigh 30.0 mg trityl-protected MorHap in Teflon-lined screw-cap glass vial (*see* **Note 17**).
2. Add 3.28 mL chloroform (87.5 %) followed by 375 μL TFA (10 %) to the vial. Vortex the yellow solution and add 95 μL TIS (2.5 %). Shake the mixture for 1 h at room temperature (*see* **Note 18**).
3. Put the glass vial inside a dry-seal glass vacuum desiccator. Start the vacuum at 200 psi and gradually decrease the vacuum by 50 psi every 10 min. Concentrate the reaction mixture under 0–10 psi overnight (*see* **Note 19**).

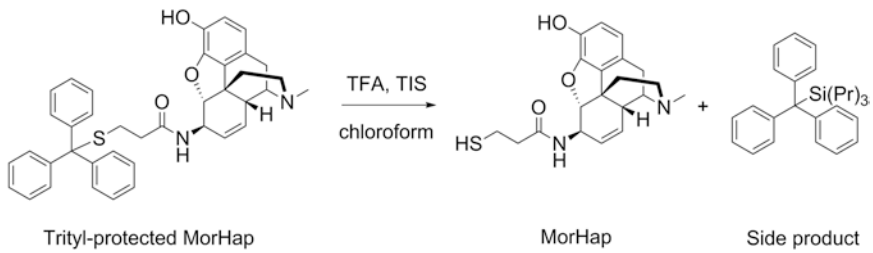

Fig. 1 TFA-induced deprotection of trityl-protected MorHap

3.2 Purification of MorHap

1. Wash the crude residue with 1 mL petroleum ether and monitor the removal of the trityl side product using TLC with DCM as the mobile phase. Wash the residue one or two more times until the trityl side product is not visible under UV (*see* **Note 20**). Remove the residual pet ether under high vacuum for 15 min.
2. Solubilize the white solid in 3.0 mL water by sonication and filter the mixture through a polysulfone membrane filter.
3. Confirm the identification of MorHap using ACQUITY UPLC/TQD system (MorHap + H^+ = 373.15 g/mol). Store the solution at 4 °C.

3.3 Ellman's Assay

The reaction for the determination of [–SH] using Ellman's assay is shown in Fig. 2.

1. Add 4 μL MorHap solution into 796 μL 0.1 M PB, pH 8.0 (dilution factor (DF) = 200) and treat with 160 μL Ellman's reagent (*see* **Note 21**).
2. Similarly, add 160 μL of Ellman's reagent to 800 μL of the MESNA standards.
3. Pipet 200 μL of the yellow solutions in triplicates into a UV-transparent 96-well plate.
4. Using SpectraMax M5, read the absorbance of the MorHap and MESNA standards at 412 nm.
5. Measure the sulfhydryl concentration, [–SH], from the standard calibration curve. Quantify the concentration of MorHap, [MorHap], using [–SH] × DF.

3.4 Dialysis of Tetanus Toxoid

1. Transfer 1.8 L PBS, pH 7.2 in a 2 L beaker equipped with a magnetic stirrer and hydrate four dialysis cassettes in PBS for 2 min (*see* **Note 22**). Fill each dialysis cassettes with 2.5 mL TT. *To ensure sterility of the TT stock, use sterile tips to pipet out TT from the vial.*

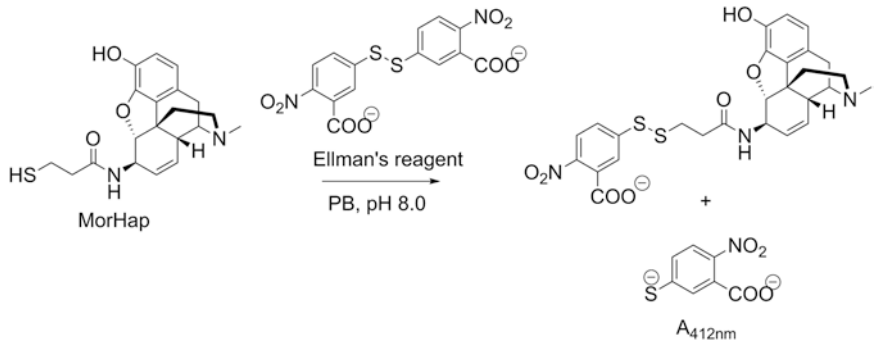

Fig. 2 Determination of sulfhydryl group using Ellman's assay

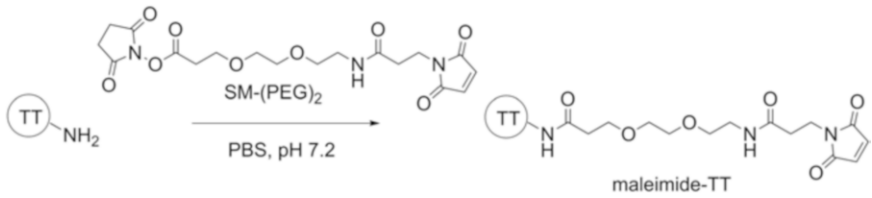

Fig. 3 Synthesis of maleimide-TT conjugates using a heterobifunctional linker, $SM(PEG)_2$

2. Dialyze TT against PBS, pH 7.2 at 4 °C with three buffer replacements after 2 h, 16 h (overnight), and 18 h.
3. Pool the contents of the dialysis cassettes in a 15 mL centrifuge tube and quantify the protein concentration of the dialyzed TT using BCA assay.

3.5 Synthesis and Purification of Maleimide-TT Intermediates

The reaction for the synthesis of maleimide-TT intermediates is shown in Fig. 3.

1. Label seven microcentrifuge tubes with 5, 10, 25, 50, 100, 200, and 400. The numbers correspond to linker:protein molar ratios. The scale of the reaction is 2.5 mg TT.
2. Pipet 1.52 mL dialyzed TT ([TT] = 1645 μg/mL) into each one of the seven microcentrifuge tubes.
3. Add 0.4, 0.7, 1.7, 3.3, 6.6, 13.1, and 26.2 μL 250 mM SM $(PEG)_2$ linker to 5, 10, 25, 50, 100, 200, and 400 labeled microcentrifuge tubes, respectively. Mix the solution gently.
4. Place the microcentrifuge tubes in Thermomixer C (300 rpm, 25 °C) and allow the reaction to proceed for 2 h.
5. Add dropwise the reaction mixtures into pre-equilibrated 10 mL spin desalting columns and centrifuge at 1000 × *g* for 2 min (*see* **Note 23**).
6. Collect the seven maleimide-TT eluates and measure the protein yield using BCA assay.

3.6 Modified Ellman's Test

The reaction for the determination of maleimide content of maleimide-TT intermediates is shown in Fig. 4.

1. Suspend 82.8 μL maleimide-TT ([maleimide-TT] = 1450 μg/mL) into 557.2 μL 0.1 M PB, pH 7.2 (*see* **Note 24**). Depending on the protein concentration of the maleimide-TT conjugates; add appropriate volume of 0.1 M PB, pH 7.2 to make 640 μL.
2. Treat all the maleimide-TT solutions and 640 μL 0.1 M PB, pH 7.2 (without proteins) with 160 μL 500 μM MESNA.
3. Incubate the reaction mixture at room temperature for 5 min. The total volume is 800 μL and final protein concentration is ~1 μM.

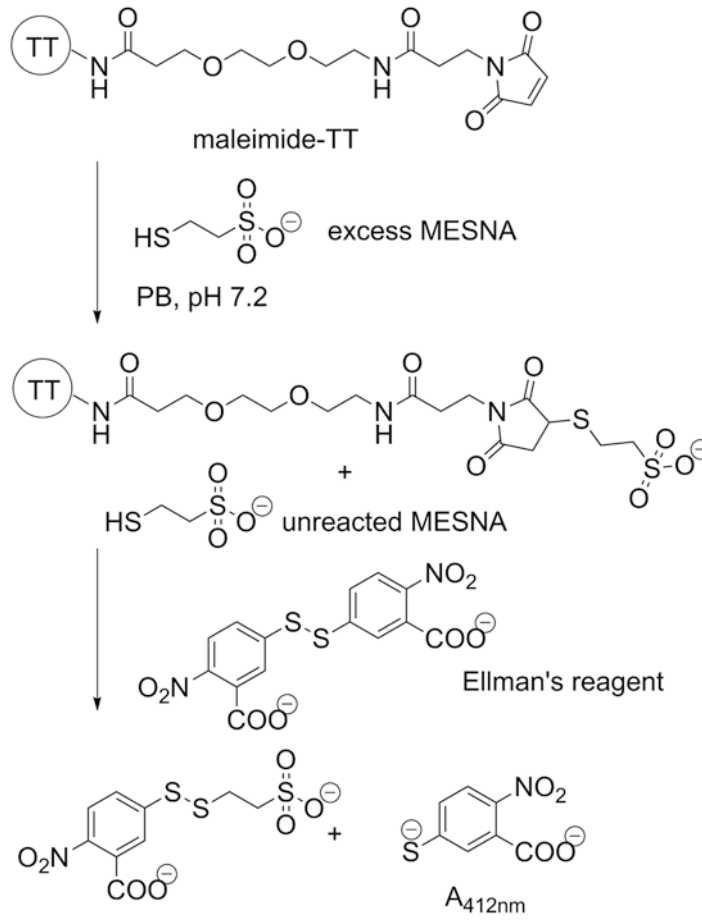

Fig. 4 Indirect method of measuring hapten density of MorHap-TT conjugates using modified Ellman's test

4. Back-titrate the unreacted MESNA by adding 160 μL 10 mM Ellman's reagent. Vortex the reaction mixture.
5. Standard curve is prepared by adding 160 μL 10 mM Ellman's reagent to 800 μL of the MESNA standards.
6. Pipet 200 μL of the reaction mixtures and standards in triplicates into a UV-transparent 96-well plate.
7. Using SpectraMax M5, read the absorbance of the reaction mixtures and MESNA standards at 412 nm.
8. The amount of unreacted MESNA, $[MESNA]_{final}$, is determined from the calibration curve. The initial concentration of MESNA, $[MESNA]_{initial}$, is the solution without proteins that is described in **step 2**.

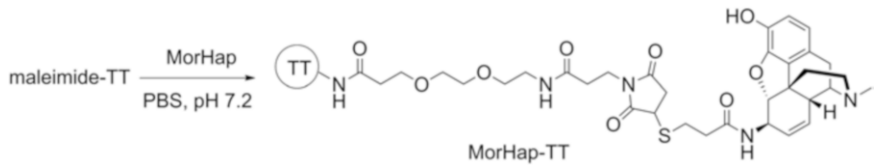

Fig. 5 Synthesis of MorHap-TT conjugates using maleimide-thiol conjugation chemistry

9. The number of maleimides per protein is calculated using the formula

$$\text{Number of maleimides} = \frac{([\text{MESNA}]_{\text{initial}} - [\text{MESNA}]_{\text{final}})}{[\text{maleimide} - \text{TT}]}$$

10. Hapten density is equal to the number of maleimides.

3.7 Synthesis and Purification of MorHap-TT Conjugates

The reaction for the synthesis of MorHap-TT conjugates is shown in Fig. 5.

1. Label seven microcentrifuge tubes with 5, 10, 25, 50, 100, 200, and 400. The scale of the reaction is 1.0 mg maleimide-TT.
2. Pipet 690 μL of maleimide-TT ([maleimide-TT] = 1450 μg/mL) into each one of the corresponding microcentrifuge tubes. The volumes may vary depending on the protein concentration of the maleimide-TT conjugates.
3. Add 45.0 μL MorHap ([MorHap] = 14.6 mM from Ellman's assay) and add 265.0 μL PBS, pH 7.2. Equalize the volume of the reaction mixtures to 1 mL by adding the corresponding volumes of PBS, pH 7.2. The molar ratio of MorHap to protein is ~100.
4. Incubate the reaction mixtures in Thermomixer C (300 rpm, 25 °C) for 2 h.
5. Transfer the reaction mixtures into pre-hydrated dialysis cassettes.
6. Dialyze TT against 1× DPBS, pH 7.4 at 4 °C with three buffer replacements after 2 h, 16 h (overnight), and 18 h.
7. *Sterile* filter the dialysates through a polysulfone membrane into a *sterile vial*.
8. Measure the protein concentration of MorHap-TT conjugates using BCA assay. Store at 4 °C.

3.8 TNBS Assay of MorHap-TT Conjugates

The reaction for the quantification of amines in proteins is shown in Fig. 6.

1. Suspend 84.3 μL MorHap-TT ([MorHap-TT] = 890 μg/mL) into 165.7 μL 0.1 M sodium bicarbonate, pH 8.0. Depending on the protein concentration of the MorHap-TT conjugates;

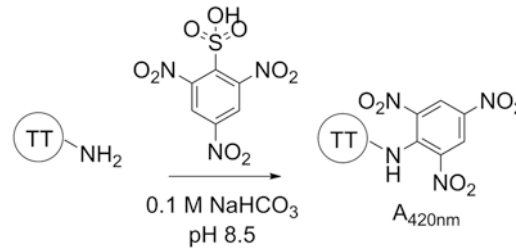

Fig. 6 Indirect method of measuring hapten density of MorHap-TT conjugates using TNBS assay

add appropriate volume of 0.1 M sodium bicarbonate, pH 8.0 to make 250 μL.

2. Treat all the MorHap-TT solutions and TT starting material with 250 μL 0.01 % TNBS. The total volume is 500 μL and final protein concentration is ~1 μM.
3. Standard curve is prepared by mixing 250 μL L-glutamic acid standards and 250 μL 0.01 % TNBS. The final concentration of L-glutamic acid is half the initial concentration.
4. Incubate the reaction mixture for 2 h at 37 °C.
5. Pipet 100 μL of the reaction mixtures and standards in triplicates into a UV-transparent 96-well plate.
6. Using SpectraMax M5, read the absorbance of the reaction mixtures and L-glutamic acid standards at 420 nm.
7. The free amine concentration, [Amine], is determined from the calibration curve. The number of amines per protein is calculated using the expression

$$\text{Number of amines} = \frac{[\text{Amine}]}{[\text{MorHap} - \text{TT}]}$$

8. Hapten density is the difference in the number of free amines before and after conjugation.

3.9 MALDI-TOF MS of MorHap-TT Conjugates

1. Equilibrate the Zip Tip C_4 resin by washing it in sequence with 100 % ACN (one time), 50 % ACN (three times), and 2 % ACN (three times) (*see* **Note 25**).
2. Transfer 100 μL MorHap-TT conjugate into a microcentrifuge tube.
3. Load 10 μL MorHap-TT conjugate into the resin by pipetting the sample up and down ten times. Dump the liquid into a separate container.
4. Repeat **step 3** ten more times or until the 100 μL volume is depleted.

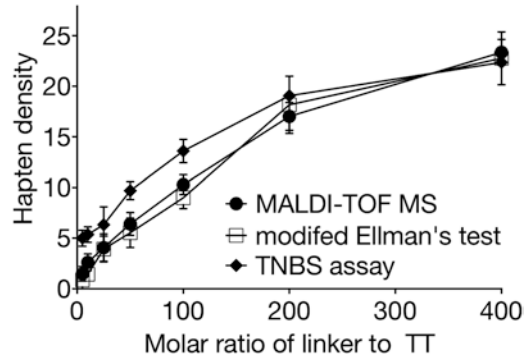

Fig. 7 The effect of linker ratios on the hapten density of MorHap-TT conjugates

5. Desalt the MorHap-TT conjugate by washing the resin with 2 % ACN (three times).
6. Elute the MorHap-TT conjugate by pipetting the sample up and down into 10 μL 80 % ACN.
7. Spot 0.5 μL 10 mg/mL SA in acetone into a MALDI-TOF stainless plate. Allow the spot to air-dry.
8. To the dried spot of SA, layer 0.5 μL of the MorHap-TT conjugate (*see* **Note 26**).
9. Briefly add 0.5 μL 10 mg/mL SA in 50 % ACN on top of the sample. Allow the "matrix-sample-matrix" spot to air-dry.
10. Repeat **steps 1–9** for TT starting material and **steps 7–9** for the IgG sample.
11. Calibrate the Axima MegaTOF™ using IgG. Determine the mass of the MorHap-TT conjugates and TT starting material. Hapten density is calculated using the expression

$$\text{Hapten density} = \frac{\text{Mass}_{\text{MorHap-TT}} - \text{Mass}_{\text{TT}}}{\text{Mass}_{\text{MorHap-linker}}}$$

The net mass addition of MorHap and linker, $\text{Mass}_{\text{MorHap-linker}}$, was 682.27 g/mol.

Reproducible MorHap-TT conjugates were obtained using the optimized as adjudged by modified Ellman's test (*see* **Note 27**), TNBS assay (*see* **Note 28**), and MALDI-TOF MS (Fig. 7). In addition, the yields of the conjugates were very high (94–100 %) as indicated by BCA assay.

4 Notes

1. MorHap is a morphine/heroin-like hapten and is coupled to TT through SM $(PEG)_2$ linker. It is trityl-protected to avoid oxidation of the thiol into disulfide group.

2. Teflon-lined screw cap is recommended because it is resistant to TFA.
3. TT is highly purified tetanus toxin from *Clostridium tetani* and has been detoxified by formaldehyde. The pH of the undialyzed sample is acidic and contains ≤54 mg/L formaldehyde. Maintain the sterility of the vial.
4. The buffer must be free of amine-containing compounds (e.g., Tris) because they react with the NHS moiety of SM $(PEG)_2$. Unwarranted amines in the buffer result in lower hapten densities.
5. SM $(PEG)_2$ is a heterobifunctional linker with NHS group at one end and maleimide group at the other end. It also contains two units of polyethylene glycol (PEG), which render it water soluble. The presence of NHS group makes SM $(PEG)_2$ water sensitive. Opening of the vial without equilibration at room temperature must be avoided as it causes water condensation inside the vial. In addition, DMSO tends to absorb atmospheric water. Hence, DMSO container must be capped and parafilmed after use.
6. The stability of SM $(PEG)_2$ is longer in anhydrous conditions and at low temperatures.
7. Refer to the Thermo Fischer Scientific instruction manual for complete details of performing the assay. The BCA Assay combines the reduction of Cu^{2+} to Cu^{1+} by protein in an alkaline medium with the highly sensitive and selective colorimetric detection of the Cu^{1+} through complex formation with bicinchoninic acid. The assay contains Reagent A (sodium carbonate, sodium bicarbonate, BCA, and sodium tartrate in 0.1 M sodium hydroxide), Reagent B (4 % cupric sulfate), and bovine serum albumin (BSA) albumin standard ampules (2000 μg/mL). Typical calibration standard concentrations are 2000, 1500, 1000, 750, 500, 250, 125, 25, and 0 μg/mL. In a conventional assay 200 μL of Reagent B is mixed with 10 mL Reagent A to obtain the BCA working solution. Standards and unknown samples (25 μL) are prepared in triplicates into a 96-well plate and are subsequently treated with 200 μL of BCA working solution. The reaction mixture is incubated at 37 °C for 30 min. The absorbance of the purple complex is read at 562 nm.
8. Ordinary clear polystyrene can be used since the reading is at 562 nm, which is far from the UV region.
9. MESNA is a water-soluble, sulfhydryl-containing compound. Like other thiols, it is prone to air oxidation. The sample container must be tightly sealed and parafilmed.
10. Ellman's reagent is used for quantitating free sulfhydryl groups in solution. Ellman's reagent reacts with a free sulfhydryl group

to yield a mixed disulfide and 2-nitro-5-thiobenzoic acid, which can be measured at 412 nm.

11. Since MESNA oxidizes readily in basic buffer, the stock solution must be freshly prepared.
12. The reaction of TNBS with primary amines (e.g., ε-amino group of lysine and α-amino group of amino acids) generates a highly chromogenic product that can be measured at 420 nm.
13. The solution must be used immediately after preparation since TNBS can be hydrolyzed by hydroxyl ion to unreactive species.
14. L-Glutamic acid is highly soluble at pH 8.0 and contains a primary amine. Other water-soluble amines can be used also as standards.
15. The concentration of the standards will be reduced after the addition of the TNBS reagent. The final concentrations of 7.5, 15, 30, 60, 120, 240, and 360 standards are 3.25, 7.5, 15, 30, 60, 120, and 180, respectively. The standard curve may not be linear outside this calibration range.
16. The IgG standard must be salt-free for effective calibration of mass. Salt interferes with ionization and consequently results in a mass spectrum with poor signals.
17. Prior to weighing, the sample must be equilibrated at room temperature to avoid condensation of moisture inside the vial.
18. The reaction must be done in the fume hood. Wear eye goggles when transferring TFA as it is highly corrosive. Pipet tips with built-in filter must be used.
19. The amount of vacuum must be decreased gradually. Abrupt vacuum change may cause sample to evaporate vigorously resulting in spillage.
20. The assay must be done inside the fume hood. Avoid exposure to UV light.
21. The Ellman's assay and modified Ellman's test can be run simultaneously in a 96-well plate.
22. Hydration increases membrane flexibility and allows it to adjust more readily to the sample loading and removal of excess air.
23. Refer to the Thermo Fischer Scientific instruction manual for complete details of equilibrating the spin desalting column. The 10 mL column is washed three times with PBS, pH 7.2 prior to use.
24. PB, pH 7.2 must be used and not PB, pH 8.0 as the hydrolysis of maleimide to maleamic acid is relatively faster at higher pH.
25. Prevent the resin from drying by leaving small amount of the solvents on top of the resin.

26. The MorHap-protein can be re-spotted up to three times to the same spot if the protein concentration is low (<100 μg/mL).
27. Active maleimides were not observed in the MorHap-TT conjugates, which suggest complete quenching by the hapten.
28. The overestimation of hapten density by TNBS may be due to conformational changes induced in the protein and/or a masking effect of the nonmodified amines by the neighboring haptens obstructing the reaction between nonmodified amines and TNBS. This resulted in an underestimation of the remaining free surface amines on TT, thereby giving an overestimation of the hapten density.

Acknowledgements

This work was supported through a Cooperative Agreement Award (No. W81XWH-07-2-067) between the Henry M. Jackson Foundation for the Advancement of Military Medicine and the US Army Medical Research and Materiel Command (MRMC). The work was partially supported by an Avant Garde award to Gary R. Matyas from the National Institute on Drug Abuse (NIH Grant No. 1DP1DA034787-01).
Disclaimer: The views expressed in this chapter are those of the authors and do not necessarily reflect the official policy of the Department of the Army, Department of Defense, or the US Government.

References

1. Kosten TR, Domingo CB (2013) Can you vaccinate against substance abuse? Expert Opin Biol Ther 13:1093–1097
2. Landsteiner K, Jacobs J (1935) Studies on the sensitization of animals with simple chemical compounds. J Exp Med 61:643–656
3. Landsteiner K, Jacobs J (1936) Studies on the sensitization of animals with simple chemical compounds. J Exp Med 64:625–639
4. Matyas GR, Rice KC, Cheng K, Li F et al (2014) Facial recognition of heroin vaccine opiates: type 1 cross-reactivities of antibodies induced by hydrolytically stable haptenic surrogates of heroin, 6-acetylmorphine, and morphine. Vaccine 32:1473–1479
5. Alving CR, Matyas GR, Torres O, Jalah R, Beck Z (2014) Adjuvants for vaccines to drugs of abuse and addiction. Vaccine 32:5382–5389
6. Kinsey BM, Jackson DC, Orson FM (2009) Anti-drug vaccines to treat substance abuse. Immunol Cell Biol 87:309–314
7. Orson FM, Kinsey BM, Singh RA, Wu Y, Gardner T, Kosten TR (2007) The future of vaccines in the management of addictive disorders. Curr Psychiatry Rep 9:381–387
8. Matyas GR, Mayorov AV, Rice KC, Jacobson AE et al (2013) Liposomes containing monophosphoryl lipid A: a potent adjuvant system for inducing antibodies to heroin hapten analogs. Vaccine 31:2804–2810
9. Li F, Cheng K, Antoline JF, Iyer MR, Matyas GR, Torres OB, Jalah R, Beck Z, Alving CR, Parrish DA, Deschamps JR, Jacobson AE, Rice KC (2014) Synthesis and immunological effects of heroin vaccines. Org Biomol Chem 12:7211–7232
10. Carroll FI, Blough BE, Pidaparthi RR, Abraham P et al (2011) Synthesis of mercapto-(+)-methamphetamine haptens and their use for obtaining improved epitope density on (+)-methamphetamine conjugate vaccines. J Med Chem 54:5221–5228

11. Pryde DC, Jones LH, Gervais DP, Stead DR, Blakemore DC, Selby MD, Brown AD, Coe JW, Badland M, Beal DM, Glen R, Wharton Y, Miller GJ, White P, Zhang N, Benoit M, Robertson K, Merson JR, Davis HL, McCluskie MJ (2013) Selection of a novel anti-nicotine vaccine: influence of antigen design on antibody function in mice. PLoS One 8, e76557
12. Hermanson GT (2008) Bioconjugation techniques, 2nd edn. Elsevier Inc., San Diego, CA
13. Torres OB, Jalah R, Rice KC, Li F et al (2014) Characterization and optimization of heroin hapten-BSA conjugates: method development for the synthesis of reproducible hapten-based vaccines. Anal Bioanal Chem 406:5927–5937
14. Pichichero ME (2013) Protein carriers of conjugate vaccines: characteristics, development, and clinical trials. Hum Vaccin Immunother 9:2505–2523
15. Adamczyk M, Buko A, Chen YY, Fishpaugh JR, Gebler JC, Johnson DD (1994) Characterization of protein-hapten conjugates. 1. Matrix-assisted laser desorption ionization mass spectrometry of immuno BSA-hapten conjugates and comparison with other characterization methods. Bioconjug Chem 5:631–635
16. Singh KV, Kaur J, Varshney GC, Raje M, Suri CR (2004) Synthesis and characterization of hapten-protein conjugates for antibody production against small molecules. Bioconjug Chem 15:168–173
17. Habeeb AF (1966) Determination of free amino groups in proteins by trinitrobenzenesulfonic acid. Anal Biochem 14:328–336
18. Sashidhar RB, Capoor AK, Ramana D (1994) Quantitation of epsilon-amino group using amino acids as reference standards by trinitrobenzene sulfonic acid. A simple spectrophotometric method for the estimation of hapten to carrier protein ratio. J Immunol Methods 167:121–127
19. Lemus R, Karol MH (2008) Conjugation of haptens. Methods Mol Med 138:167–182

Part IX

Vaccines for Allergy

Chapter 40

Production of Rice Seed-Based Allergy Vaccines

Hidenori Takagi and Fumio Takaiwa

Abstract

Recombinant hypoallergenic derivative is the next generation of tolerogen replacing the natural allergen extract to increase safety and efficacy. Japanese cedar pollinosis is the predominant seasonal allergy disease in Japan. A rice seed-based oral vaccine containing the recombinant hypoallergens derived from these allergens was developed. Efficacy of this rice-based allergy vaccine was evaluated by oral administration in animal models.

Key words Cedar pollen allergen, Transgenic rice, Allergy vaccine

1 Introduction

Allergen-specific immunotherapy (AIT) is the only curative treatment for allergic diseases. The conventional AIT treatment is achieved by subcutaneous or sublingual administration using natural allergen extract over the period of more than 3 years. This treatment is sometimes accompanied by side effects of anaphylaxis shock. To resolve these poor outcomes, safer, effective, and more convenient treatment is desired. Japanese cedar pollinosis is the predominant seasonal allergy disease in Japan. Major allergens are identified to be Cry j 1 and Cry j 2. A rice-seed-based oral vaccine containing the recombinant hypoallergens derived from these major allergens was developed as an alternative to the conventional therapies. The tertiary structures of allergens required for these specific IgE binding were destructed by fragmentation and molecular shuffling in the form of tail-to-head orientation. Low allergenicity for these modified allergens was evaluated by reduced binding activity to the specific IgE and reduced beta-glucosaminidase release from basophils. The destructed Cry j 1 and Cry j 2 were expressed and deposited in ER-derived protein bodies (PB-Is) in endosperm of transgenic rice seed. Efficacy of rice-based allergy vaccines and ability to induce immune tolerance to the allergens were confirmed by oral administration of transgenic rice seeds to mouse models.

Sunil Thomas (ed.), *Vaccine Design: Methods and Protocols: Volume 1: Vaccines for Human Diseases*, Methods in Molecular Biology, vol. 1403, DOI 10.1007/978-1-4939-3387-7_40,

The success of the allergy vaccine is attributed to high dose of accumulation and deposition in protein bodies which exhibit high resistance to harsh conditions and digestive enzymes in gastrointestinal tract, providing an efficient oral allergen delivery system.

2 Materials

2.1 Reagents for Production of Transgenic Rice Lines

1. *Cfr*9I restriction enzyme.
2. Entry clone plasmids designed for Multisite Gateway LR reaction (Fig. 1).
3. A binary vector designed for Multisite Gateway LR reaction (Fig. 1).
4. Gateway LR clonase II plus enzyme mix (Fig. 1).

2.2 Reagents and Antibodies for Allergenicity Tests

1. Nitrocellulose membrane.
2. Blocking solution (Block Ace, DS Pharma Biomedical, Japan).
3. TBS-T solution (25 mM Tris, 138 mM NaCl, 2.7 mM KCl, 0.1 % Tween-20, pH 7.4).
4. Anti-mouse IgE secondary antibodies conjugated to biotin (Southern Biotech, USA).
5. Streptavidin-horseradish peroxidase (HRP) conjugate.
6. Enhanced chemiluminescence (ECL)-HRP substrate solution.
7. Deionized water.
8. Dulbecco's modified Eagle's medium (DMEM).
9. Fetal bovine serum (FBS) (HyClone, USA).
10. Penicillin-streptomycin-glutamine mixed solution.
11. Tyrode's solution (Sigma-Aldrich, USA).
12. Bovine serum albumin (BSA).
13. HEPES.
14. p-Nitrophenyl N-acetyl-beta-d-glucosaminide (Sigma-Aldrich, USA).
15. Sodium citrate.
16. Glycine.

2.3 Instruments, Reagents, Antigens, and Antibodies for Efficacy Tests

1. Multi-beads shocker (Yasui Kikai, Osaka, Japan).
2. Deionized water.
3. Phosphate-buffered saline (PBS) (137 mM NaCl, 2.68 mM KCl, 8.1 mM $Na_2HPO_4 \cdot 12H_2O$, 1.47 mM KH_2PO_4, pH 7.4).
4. Total protein extract of Japanese cedar pollen (LSL, Japan).

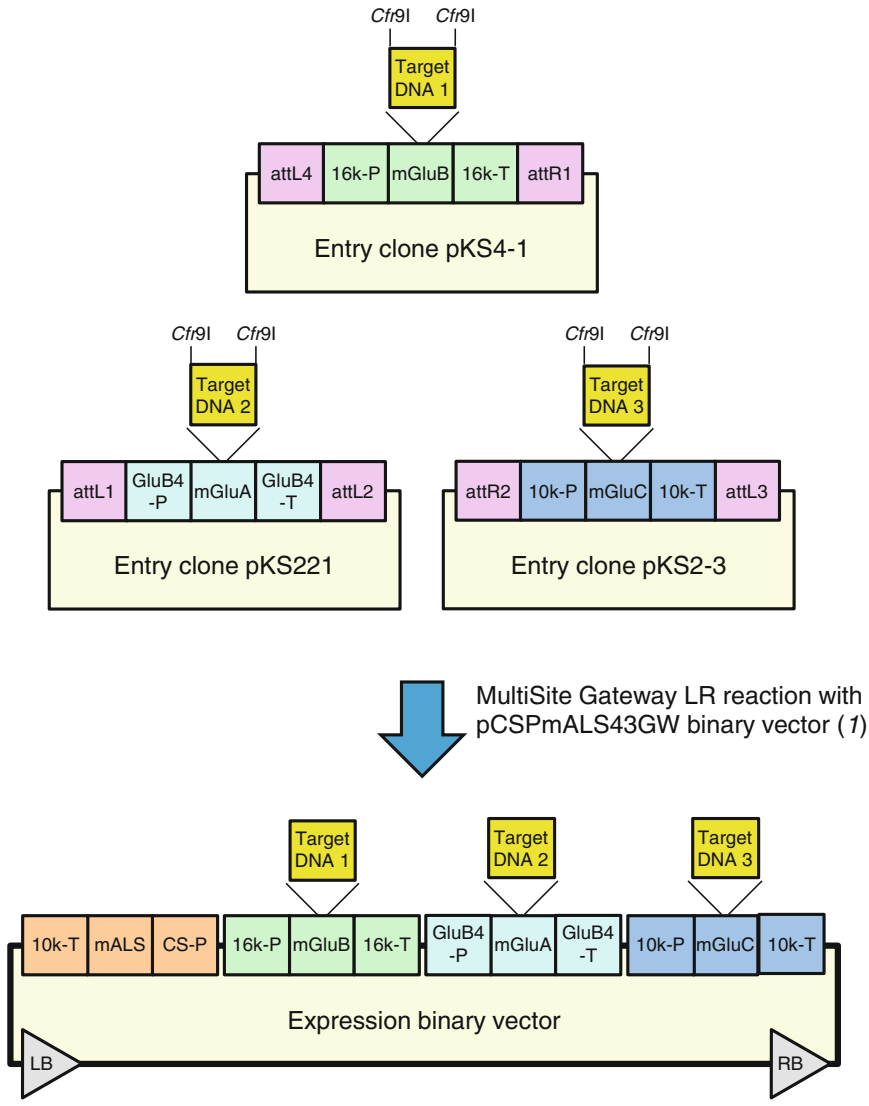

Fig. 1 Schematic drawing of entry clones and expression binary vector. The target gene DNAs are sub-cloned into the *Cfr*9I site of the entry clone plasmids (pKS4-1/pKS221/pKS2-3). For the expression of multiple target gene DNAs, these expression cassettes are integrated into a binary vector (pCSPmALS43GW) by the MultiSite Gateway LR clonase reaction. *att* Gateway attachment region, *16k-P* 16 kDa prolamin promoter, *mGluB* modified glutelin B (GluB)-coding region, *16k-T* 16 kDa prolamin terminator, *GluB4-P* glutelin B4 (GluB4) promoter, *mGluA* modified glutelin A (GluA)-coding region, *GluB4-T* glutelin B4 (GluB4) terminator, *10k-P* 10 kDa prolamin promoter, *mGluC* modified glutelin C (GluC)-coding region, *10k-T* 10 kDa prolamin terminator, *CS-P* callus-specific promoter, *mALS* mutated acetolactate synthase-coding region, *LB* left border, *RB* right border

5. Aluminium hydroxide (Alum).
6. Recombinant mouse IL-4.
7. CD4 (L3T4) MicroBeads (Miltenyi Biotec, Germany).
8. autoMACS Pro Separator (Miltenyi Biotec, Germany).

9. Complete medium (DMEM/F-12 supplemented with 10 % FBS, 1× PBS, 50 μM 2-mercaptoethanol, 10 mM HEPES, and 1× penicillin-streptomycin-glutamine mixed solution).
10. Celltiter 96 aqueous one solution cell proliferation assay (Promega, USA).
11. Anti-mouse IgE capture antibody (Southern Biotech, USA).
12. Anti-mouse IgG capture antibody (Southern Biotech, USA).
13. Carbonate-bicarbonate buffer (Sigma-Aldrich, USA).
14. PBS-T solution (1× PBS containing 0.1 % Tween-20, pH 7.4).
15. Blocking solution (Block Ace, DS Pharma Biomedical, Japan).
16. Streptavidin-HRP conjugate.
17. TMB solution (BD Biosciences, USA).
18. HCl.
19. Histamine ELISA test kit (Neogen, USA).
20. Cytospin3 (Thermo Shandon, USA).
21. Diff-Quik stain kit (Dade Behring, Germany).

3 Methods

3.1 Production of Transgenic Rice Seed-Based Allergy Vaccines

1. Design and PCR-amplify the target gene DNAs (*see* **Note 1**).
2. Sub-clone the target gene DNAs into the *Cfr*9I site of the entry clone plasmids (Fig. 1) (*see* **Note 2**).
3. For the expression of multiple target gene DNAs, integrate the expression cassettes (endosperm-specific promoters/signal peptide/target gene DNAs/terminators) into a binary vector such as pCSPmALS43GW by the MultiSite Gateway LR clonase reaction (Fig. 1) (*see* **Note 3**).
4. Electrotransform *Agrobacterium* cells with the expression binary vector (*see* **Note 4**).
5. Perform *Agrobacterium*-mediated transformation of rice calli to integrate the expression binary vector into the rice genome (*see* **Note 4**).
6. Select and regenerate calli to obtain transgenic rice plants (*see* **Note 4**).

3.2 Evaluation of the Allergenicity of Antigens

3.2.1 Dot-Blot IgE Binding Assay

1. Prepare the target antigen (*see* **Note 5**).
2. Spot 1–2 μl of the antigen sample onto the nitrocellulose membrane.
3. Block the membrane in the blocking solution at room temperature (RT) for 1 h.

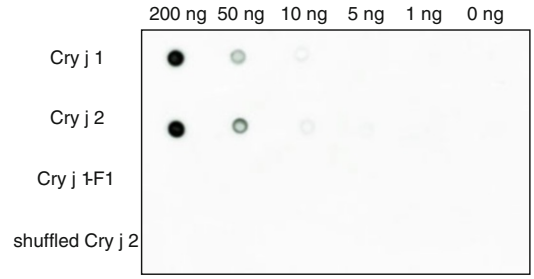

Fig. 2 An experimental example of dot-blot IgE binding assay [1]. Purified native Cry j 1 and Cry j 2 (Asahi Food & Healthcare Co., Japan), recombinant Cry j 1-F1 [1], and shuffled Cry j 2 [1] were dotted onto a nitrocellulose membrane at 200 ng, 50 ng, 10 ng, 5 ng, 1 ng, and 0 ng, and incubated with sera from BALB/c mice immunized with Japanese cedar pollen. IgE bound to Cry j 1/2, Cry j 1-F1, and shuffled Cry j 2 were detected with anti-mouse IgE-biotin and streptavidin-HRP, and then visualized by autoradiography. The result shows that IgE reactivity of Cry j 1-F1 and shuffled Cry j 2 is markedly reduced when compared to that of native Cry j 1/2

4. Incubate the membrane in the sera from mice immunized with Japanese cedar pollen allergen (as described in Subheading 3.3) at RT for 1–2 h or at 4 °C for 16–24 h.
5. Wash the membrane in TBS-T solution 3–5 times.
6. Incubate the membrane in anti-mouse IgE secondary antibodies conjugated to biotin at RT for 1–2 h or at 4 °C for 16–24 h.
7. Wash the membrane as described in **step 5**.
8. Incubate the membrane in the streptavidin-HRP conjugate solution at RT for 30–60 min.
9. Wash the membrane as described in **step 5**.
10. Incubate the membrane in the ECL-HRP substrate solution at RT for 5–10 min to let the signal develop.
11. Rinse the membrane 2–3 times with deionized water and detect the HRP-derived signal. An experimental example is shown in Fig. 2.

3.2.2 RBL-2H3 Basophil Degranulation Test

1. Prepare the target antigen (*see* **Note 5**).
2. Maintain RBL-2H3 cells in DMEM containing 10 % FBS and 1× penicillin-streptomycin-glutamine mixed solution at 37 °C/5 % CO_2.
3. Seed the RBL-2H3 cells at a 1×10^5/well into a 96-well cell culture plate.
4. Sensitize the RBL-2H3 cells with 1/100 volume of sera from mice immunized with Japanese cedar pollen allergen (as described in Subheading 3.3) for 16–24 h at 37 °C/5 % CO_2.

5. Wash the RBL-2H3 cells three times with 100 μl Tyrode's solution containing 0.1 % BSA and 25 mM HEPES (pH 7.4).
6. Add the target antigen in 200 μl Tyrode's solution containing 0.1 % BSA and 25 mM HEPES (pH 7.4).
7. Incubate the RBL-2H3 cells for 1 h at 37 °C/5 % CO_2.
8. Aliquot 50 μl supernatant to a new 96-well plate.
9. Add 50 μl of 3 μM p-nitrophenyl N-acetyl-beta-d-glucosaminide (a substrate for beta-glucosaminidase) in 40 mM sodium citrate (pH 4.5) to the supernatant.
10. Incubate the solution for 1–3 h at 37 °C.
11. Add 10 μl of 2 M glycine (pH 10) to terminate the enzyme reaction.
12. Read the optical density at 405 nm.
13. Calculate the percentage of beta-hexosaminidase released from the RBL-2H3 cells (*see* **Note 6**).

3.3 Oral Feeding of Rice and Sensitization of Mice

1. Prepare transgenic rice seed accumulating antigens and/or non-transgenic control rice seed.
2. Remove the hull of rice seed.
3. Ground unpolished brown rice seed to a fine powder using a mill or multi-beads shocker.
4. Suspend the rice powder in an appropriate volume of deionized water or PBS.
5. Mix well the rice powder solution just before the administration to mice.
6. Administer the rice powder solution to mice using a gastric tube.
7. For *ad libitum* feeding of rice seed, feed the rice powder using a feeding container (*see* **Note 7**).
8. Following the rice feeding period, sensitize the mice by intraperitoneal injection of 0.1 mg total protein extract of Japanese cedar pollen mixed with 5 mg alum and 0.1 μg recombinant mouse IL-4 (*see* **Note 8**).
9. At 7 days after the first sensitization, boost the mice with the intraperitoneal injection of 0.1 mg total protein extract of Japanese cedar pollen mixed with 5 mg alum.
10. At 14 days after the second sensitization, examine the efficacy of rice seed-based allergy vaccines as described in Subheading 3.4.

3.4 Evaluation of the Efficacy of Rice Seed-Based Allergy Vaccines

3.4.1 Splenic $CD4^+$ T Cell Responses and Cytokines

1. At 14 days after the second sensitization as in Subheading 3.3, **step 10**, sacrifice the mouse, remove the spleen, and isolate splenic cells.
2. To isolate $CD4^+$ T cells, stain the splenic cells by CD4 (L3T4) MicroBeads according to the manufacturer's instructions.

3. Magnetically isolate splenic $CD4^+$ T cells using the autoMACS Pro Separator according to the manufacturer's instructions.
4. Seed the cells at 1×10^5/well into a 96-well cell culture plate in 100 μl complete medium.
5. Add 100 μl antigen-presenting cells prepared from spleens of naive BALB/c mice at 3×10^5/well in the complete medium.
6. Add filter-sterilized total protein extract of Japanese cedar pollen dissolved in the complete medium at 10 μg/ml.
7. Incubate the plate for 4–6 days at 37 °C/5 % CO_2.
8. Aliquot 100 μl cell culture supernatant to a new tube for cytokine assay (*see* **Note 9**).
9. Using the celltiter 96 aqueous one solution cell proliferation assay solution, determine the number of viable cells in the proliferation assay according to the manufacturer's instructions.

3.4.2 Allergen-Specific IgE, IgG Antibodies and Histamine

1. Coat the wells of a 96-well microplate with 50–100 μl capture antibody solution at a concentration of 2 μg/ml in 50 mM carbonate-bicarbonate buffer.
2. Incubate the plate at 4 °C for 16–24 h.
3. Wash the plate 3–5 times with 200 μl PBS-T solution.
4. Block the coated wells by adding 200 μl blocking solution.
5. Incubate the plate at RT for 1–2 h.
6. Add 50–100 μl of appropriately diluted serum sample to the plate.
7. Incubate the plate at RT for 1–2 h.
8. Wash the plate as in **step 3**.
9. Add 50 μl biotinylated total protein extract of Japanese cedar pollen (*see* **Note 10**).
10. Incubate the plate at RT for 1–2 h.
11. Wash the plate as in **step 3**.
12. Add 50 μl of 1/5000 diluted streptavidin-HRP conjugate.
13. Incubate the plate at RT for 0.5–1 h.
14. Wash the plate as in **step 3**.
15. Add 50 μl TMB solution.
16. Incubate the plate at RT for 10–30 min to let the signal develop.
17. Add 50 μl of 1 N HCl solution to terminate the HRP-TMB reaction.
18. Read the optical density at 450 nm.
19. Measure the levels of serum histamine by using histamine ELISA test kit according to the manufacturer's instructions.

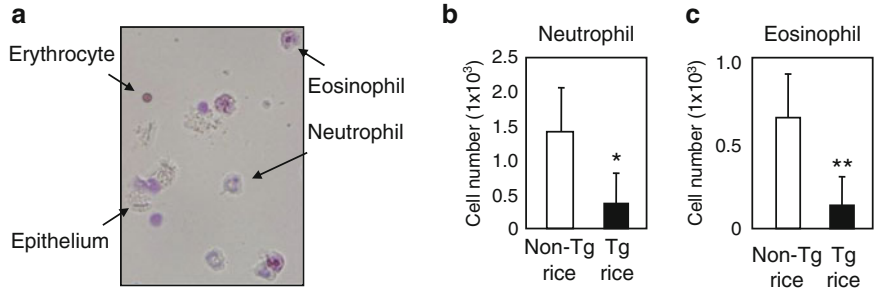

Fig. 3 Inflammatory granulocytes in the nasal lavage fluid of mice [1]. (**a**) A representative staining of nasal lavage fluid. The number of neutrophils (**b**) and eosinophils (**c**) in the nasal lavage was significantly lower in the group of mice fed allergy vaccine rice (Tg rice) when compared to that in the control group of mice fed non-transgenic rice (Non-Tg rice). $^{**}p < 0.01$ and $^{*}p < 0.05$ for the group of mice fed Tg rice in comparison with the group of mice fed Non-Tg rice

3.4.3 Inflammatory Granulocytes in the Nasal Lavage Fluid

1. Fix the mouse in a supine position and perform a tracheotomy.
2. Inject 150 μl PBS from the larynx to the nasal cavity.
3. Collect the nasal passage recovered from the anterior nares.
4. Cytospin the nasal passage onto a glass slide using Cytospin3.
5. Air-dry the glass slide briefly.
6. Stain the glass slide with Diff-Quik stain kit.
7. Count eosinophils and neutrophils with a microscope. An experimental example is shown in Fig. 3.

3.4.4 Sneezing

1. Sensitize mice twice with the total protein extract of Japanese cedar pollen as described in Subheading 3.3, **steps 8** and **9**.
2. Dissolve the total protein extract of Japanese cedar pollen at 1 μg/ml in PBS.
3. At 14 days after the second sensitization, administer 20 μl pollen protein prepared as in **step 2** via the intranasal route (10 μl to each nostril).
4. Repeat the intranasal challenge as in **step 3** once a day for 1 week.
5. After the last intranasal challenge, count the number of sneezing observed in 2–5 min.

4 Notes

1. For optimized translation in rice seed, the target gene DNAs can be designed using codons frequently used in the genes coding for rice seed storage proteins [1].
2. In the entry clone plasmids, the *Cfl*9I site locates at the variable region of the C-terminal of glutelin acidic subunits; there-

fore the target gene DNAs are expressed as a fusion protein with glutelin acidic subunits.

3. The binary plasmid CSP mALS 43 GW contains the mutated rice acetolactate synthase (mALS) marker gene, which is expressed under the control of the rice callus-specific promoter (CSP). Compared to the hygromycin-based selection, CSP:mALS-based callus-specific selection offers higher accumulation levels of the target gene products in transgenic rice seed [2].
4. The details for the management of *Agrobacterium* cells and rice calli for rice transformation are described previously [3].
5. The target antigen should be prepared as a soluble form in non-denaturing buffer conditions, since the allergen-IgE binding is thought to be conformation dependent [4].
6. The total amount of beta-hexosaminidase released from the RBL-2H3 cells is obtained by lysing the RBL-2H3 cells in the presence of 0.2 % Triton-X100, and is used for the calculation of the percentage of beta-hexosaminidase release in each test.
7. Approximately 2.0–2.5 g rice powder is daily consumed by each BALB/c mouse at age of 6–10 weeks when the mouse can access to normal chow and drinking water *ad libitum*.
8. Recombinant mouse IgE can enhance the induction of Japanese cedar allergen-specific IgE responses [5].
9. Cytokines, including IL-4, IL-5, IL-6, IL-10, IL-17, IFN-gamma, and TGF-beta, can be measured using commercially available ELISA kits according to the manufacturer's instructions.
10. Total protein extract of Japanese cedar pollen can be biotinylated by using a biotin protein labeling kit according to the manufacturer's instructions.

References

1. Wakasa Y, Takagi H, Hirose S et al (2013) Oral immunotherapy with transgenic rice seed containing destructed Japanese cedar pollen allergens, Cry J 1 and Cry J 2, against Japanese cedar pollinosis. Plant Biotechnol J 11:66–76
2. Wakasa Y, Ozawa K, Takaiwa F (2009) Higher-level accumulation of foreign gene products in transgenic rice seeds by the callus-specific selection system. J Biosci Bioeng 107:78–83
3. Wakasa Y, Takaiwa F (2012) Use of a callus-specific selection system to develop transgenic rice seed accumulating a high level of recombinant protein. Methods Mol Biol 847:467–479
4. Midoro-Horiuti T, Schein CH, Mathura V et al (2006) Structural basis for epitope sharing between group 1 allergens of cedar pollen. Mol Immunol 43:509–518
5. Takagi H, Hiroi T, Yang L et al (2005) A rice-based edible vaccine expressing multiple T cell epitopes induces oral tolerance for inhibition of Th2-mediated IgE responses. Proc Natl Acad Sci U S A 102:17525–17530

Chapter 41

Allergy Vaccines Using a *Mycobacterium*-Secreted Antigen, Ag85B, and an IL-4 Antagonist

Yusuke Tsujimura and Yasuhiro Yasutomi

Abstract

In recent decades, the prevalence of allergic diseases, including bronchial asthma, airway hypersensitivity, hay fever, and atopic dermatitis, has been increasing in the industrialized world, and effective treatments probably require manipulating the inflammatory response to pathogenic allergens. T helper (Th) 2 cells are thought to play a crucial role in the initiation, progression, and persistence of allergic responses in association with production of interleukin (IL)-4, IL-5, and IL-13. Therefore, a strategy of a shift from Th2- to Th1-type immune response may be valuable in the prophylaxis and management of allergic diseases. It is also necessary to develop prophylactic and therapeutic treatment that induces homeostatic functions in the multifaceted allergic environment, because various factors including innate and adaptive immunity, mucosal immune response, and functional and structural maintenance of local tissue might be involved in the pathogenesis of allergic disorders. We review herein recent findings related to the curative effect for mouse models of asthma and atopic dermatitis using DNA-, virus-, and protein-based vaccines of a *Mycobacterium* secretion antigen, Ag85B, and a plasmid encoding cDNA of antagonistic IL-4 mutant.

Key words Vaccine, Asthma, Atopic dermatitis, Ag85B, Mutant IL-4, DNA, HPIV2, Recombinant protein, Th1, Th2, IFN-γ, IL-4

1 Introduction

Interleukin (IL)-4 has numerous biological activities relevant to the mediation of allergic inflammation [1]. IL-4 is essential for the switching and secretion of IgE and IgG1 by B cells with promotion of the Th2 phenotype and mast cell proliferation. The action of IL-4 is not limited to the initiation of Th2 responses but may also stimulate other cellular responses that contribute to the manifestations of allergic disease [2, 3]. These findings suggest that inhibition of the action of IL-4 may be helpful for suppression of allergic reactions.

There are two possible strategies of immunotherapy for inhibiting the development of allergic inflammation. One strategy is inducing strong Th1-type immune responses in order to suppress

Sunil Thomas (ed.), *Vaccine Design: Methods and Protocols: Volume 1: Vaccines for Human Diseases*, Methods in Molecular Biology, vol. 1403, DOI 10.1007/978-1-4939-3387-7_41,

the induction of Th2 responses. One immunogenic protein that can induce a strong Th1-type immune response in hosts sensitized by Bacillus Calmette-Guerin (BCG) is thought to be Ag85B. Ag85B is a 30-kDa major secretion protein that is well conserved in *Mycobacterium* species. Studies on a tuberculosis vaccine have revealed strong activities of Ag85B for priming naïve T cells for Th1 effector cells under the appropriate conditions and for inducing strong Th1-type immune responses in mice as well as in humans [4]. Recently, we have reported the possibility of using Ag85B DNA as an immunological strategic tool to induce both Th1 and Treg cells in immunotherapy for AD and allergic asthma [5, 6]. In addition, the airway epithelium and innate immune cells are considered to be essential controllers of inflammatory, immune, and regenerative responses to allergens that contribute to asthma pathogenesis [7]. Dysfunction of the epithelium leading to chronic injury was suggested to be a consequence of sustained airway inflammation that is associated with Th2-driven adaptive immunity [8]. Tissue homeostasis at exposed surfaces of the lung is regulated by Th17-related cytokines, especially IL-22, in the innate immune system [9]. Therefore, new therapeutic strategies for allergic asthma might be necessary to induce both innate immunity and adaptive immunity. Our results showed a strong inhibitory effect of recombinant Ag85B protein on the development of allergic airway inflammation with induction of a Th1 response, IL-17 and IL-22 production, and expression of genes associated with tissue homeostasis and wound healing in bronchial tissues [10]. These results indicated the possibility of Ag85B as a novel vaccine for allergic diseases.

Another type of immunotherapy utilizes direct blocking of Th2 responses to inhibit the induction of Th2 responses in allergic diseases. An IL-4 double mutant (IL-4DM, Q116D/Y119D), which forms unproductive complexes with the IL-4Rα chain, acts as an antagonist by inhibiting the formation of heterodimers with other receptors. IL-4-binding inhibitors act not only by inhibiting IL-4 binding to its receptor but also by preventing IL-13 from eliciting its activity, since the IL-4Rα chain also forms a functional signaling component of the IL-13R heterodimer (IL-13Rα1 chain/IL-4Rα chain) [11, 12]. The applicability of plasmid DNA of IL-4DM to gene therapy for allergic inflammation has been assessed by intraperitoneal inoculation of the plasmid DNA in mouse models of asthma and AD [13–15].

Recombinant viral vectors are promising vaccine candidates for eliciting antigen-specific immune responses [16, 17]. The vaccines induce a full spectrum of immune responses including humoral and cellular immune responses. These immune responses such as mucosal immune responses can be initially induced at the viral vector infection site [18]. Moreover, the viral vector itself has adjuvant

activities through the innate immune system [19]. Human parainfluenza type 2 virus (HPIV2) is a member of the genus *Rubulavirus* of the family Paramyxoviridae and possesses a single-stranded, nonsegmented, and negative-stranded RNA genome. This virus does not have a DNA phase during its life cycle and can avoid genetic modifications. Additionally, with technological advances in reverse genetics, this virus has become replication incompetent by elimination of some viral genes [20]. Furthermore, HPIVs efficiently infect the respiratory tract but do not spread far beyond the respiratory tract, which is an important safety factor. HPIV-based vectors have proven the effect in inducing local immunity and systemic immunity against foreign antigens [21]. Thus, HPIVs have several advantages as vaccine vectors.

In this paper, we provide evidence for the potential usefulness of several strategies using DNA-, HPIV2-, and protein-based vaccines of Ag85B and IL-4 antagonistic mutant DNA as a novel approach for inducing an anti-allergic effect.

2 Materials

We examined the prophylactic and curative effect for the allergic disease using protein-based (Subheading 2.1), virus-based (Subheading 2.2), and DNA-based (Subheading 2.3) vaccines of *Mycobacterium* secretion antigen, Ag85B, and DNA vaccine vector encoding IL-4 antagonist (Subheading 2.4).

2.1 Recombinant Protein Ag85B (rAg85B) Production

1. Plasmids containing the Ag85B gene were transformed into *E. coli* TG1.
2. The expressed inclusion body (IB) was harvested from the disrupted cell pellet by a homogenizer with lysis buffer (30 mM sodium phosphate, 100 mM NaCl, 5 mM EDTA, and 0.5 % Triton X-100).
3. This IB of Ag85B was unfolded in 8 M urea and refolded by dilution to 0.4 M urea.
4. The urea in the refolding buffer was removed by anion-exchange chromatography using 20 mM Tris buffer and 20 mM Tris buffer with 1 M NaCl (pH 8.5).
5. The refolded Ag85B was loaded on a cation exchange column, and crude Ag85B was passed through the resin using 50 mM NaOAc buffer and 50 mM NaOAc buffer with 1 M NaCl (pH 6.0).
6. Ag85B was purified by anion-exchange chromatography using 20 mM Tris buffer and 20 mM Tris buffer with 1 M NaCl (pH 7.6).

2.2 Construction of Recombinant Human Parainfluenza Type 2 (rHPIV2)-Ag85B

rHPIV2-Ag85B was constructed according to the method reported previously [20].

1. Two nucleotide changes [ATG to TAG (position of 89aa) and AAG to TAG (259aa)] were introduced into the M frame of the plasmid pPIV2, a full-length cDNA copy of the HPIV2 anti-genome (Fig. 1a).
2. The 6n length cDNA of Ag85B, followed by the transcriptional end sequence of the NP gene (R2), intergenic sequence (IG), and transcriptional start signal of the V/P gene (R1) (which was synthesized by PCR using appropriate primers), was inserted into a *Not* I site of the plasmid DNA encoding the replication-deficient rHPIV2 genome described above.
3. The virus (rHPIV2-Ag85B) was recovered by cotransfection of each anti-genomic plasmid and plasmids expressing NP, P, M, and L into BSRT7/5 cells expressing T7 RNA polymerase.
4. The cells were harvested and then cocultured with fresh Vero cells every 48 h.
5. Approximately 90 % of the cells showed syncytia formation in the tenth coculture.
6. Cos7 cells were transfected with the plasmid expressing M and cocultured with the abovementioned tenth cocultured cells for virus propagation (Fig. 1b).
7. The supernatant was centrifuged at 9000 × *g* for 12 h at 4 °C.
8. The virus pellet was suspended in Opti-MEM (Invitrogen, Carlsbad, CA, USA).
9. Virus titers were determined by the cytopathic effect (CPE) method using Vero cells and were expressed as 50 % tissue culture infectious dose ($TCID_{50}$).

2.3 DNA Vaccine of Ag85B

The Ag85B expression vector pcDNA-Ag85B has been constructed by cloning of a PCR product that possesses an Ag85B open reading frame lacking a single sequence into *Kpn*I-*Apa*I sites of pcDNA3.1 (Invitrogen, CA). This vaccine preparation was performed as previously described [22].

1. *E. coli* expression vector pKK233-2 was digested with both *Eco*RI and *Hind*III.
2. An approximately 300-bp *Eco*RI-*Hind*III fragment including the *trc* promoter, the Shine-Dalgarno sequence, and the *Nco*I cloning site was obtained, and this was recloned into the *Eco*RI-*Hind*III site of pUC18.
3. The unique *Pst*I site of the resulting plasmid (designated pUCK10) was changed to an *Xho*I site by inserting an *Xho*I linker into the *Pst*I site, which was blunted by using a DNA-blunting kit. This plasmid was named pUCK20.

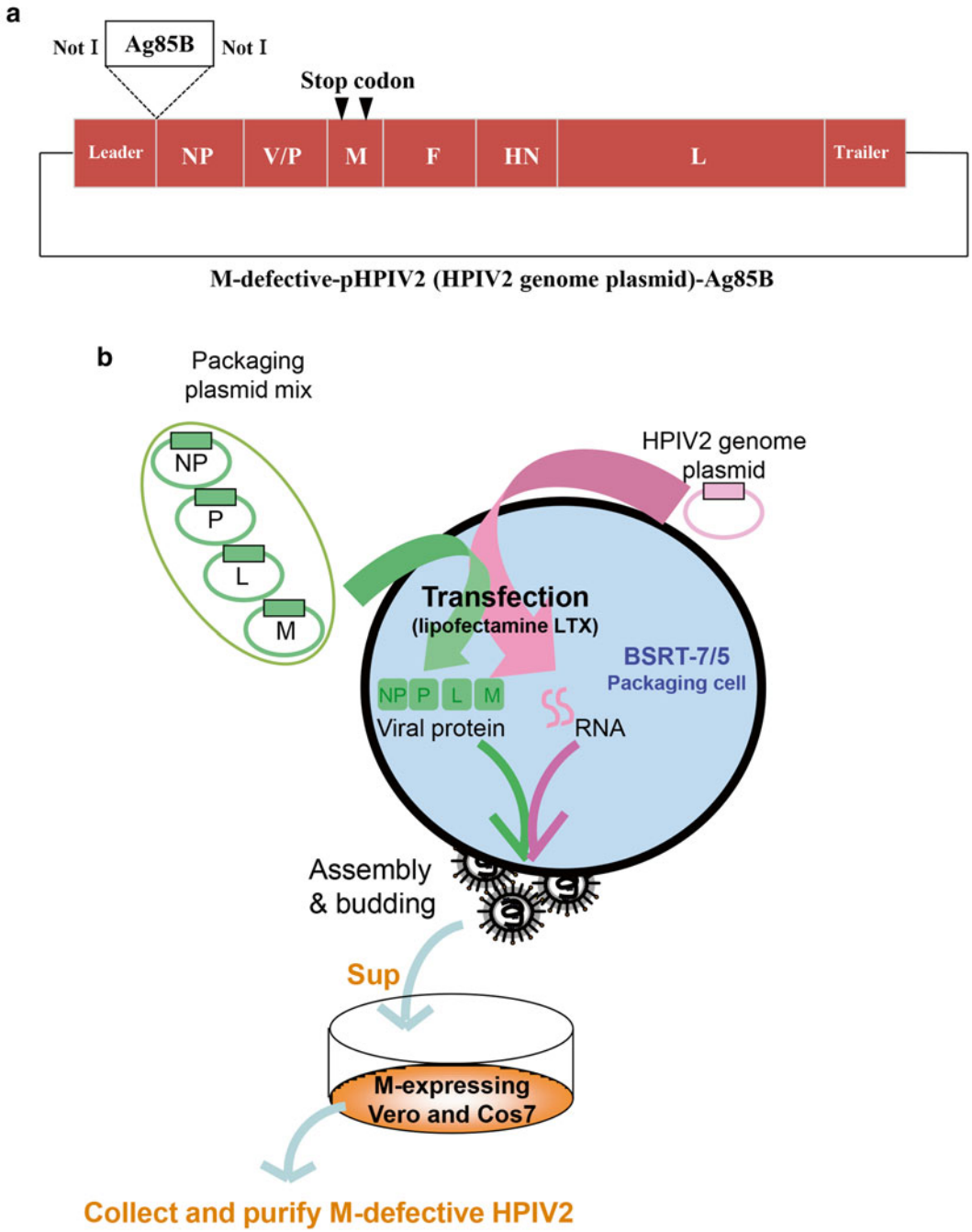

Fig. 1 Schematic illustration of constructs and reverse genetics method. In the construct of recombinant HPIV2-Ag85B for generating a replication-deficient virus, two stop codons (*solid triangles*) were introduced to the M gene (**a**). As the application of reverse genetics to this recombinant virus, the elimination of alternative gene products encoded in the M gene, which is essential for virus particle formation, was carried out (**b**)

4. pKAH20, into which a 2.0-kbp *Hinc*II fragment had been subcloned, was digested with either *Xho*I and *Hind*III or *Ban*I and *Xho*I.
5. Digestion generated a 1.1-kbp *Xho*I-*Hind*III fragment and a 0.5-kbp *Ban*I-*Xho*I fragment.
6. These fragments included the sequence for Ser-183 to the C-terminal Arg-285 and the sequence for Val-13 to Pro-182 of the *M. kansasii* Ag85B gene, respectively, and were similarly isolated by the DE81 paper method.
7. The 1.1-kbp fragment was ligated with *Xho*I-*Hind*III double-digested pUCK20, giving rise to plasmid pUCK100. This plasmid, however, lacked the sequence for Phe-1 to Pro-182.
8. The 0.5-kbp *Ban*I-*Xho*I fragment was inserted into the *Nco*I-*Xho*I site of pUCK100 by using two kinds of synthetic adaptors connected between the *Nco*I and *Ban*I sites.
9. The sequences for adaptor A (wild type) were 5′-CATGTTCTCC CGTCCCGGCCTGCCGGTGGAGTACCACCAG-3′ for the upper strand and5′-GCACCTGGTGGTACTCCACCGGCA GGCCGGGACGGGAGAA-3′ for the lowerstrand, and those for adaptor B (AT-rich type) were 5′-CATGTTCTCTCGTCC TGGTCTGCCGGTTGAATACCACCAG-3′ for the upper strand and 5′-GCACCTGGTGGTATTCAACCGGCAGA CCAGGACGAGAGAA-3′ for the lower strand.
10. The resulting plasmids, named pUCK200 and pUCK201, contained adaptors A and B, respectively.

2.4 DNA Vaccine of IL-4 Double Mutant (IL-4DM, Q116D/Y119D)

The IL-4 expression vector was described previously [23].

1. The cDNA coding region of mouse IL-4 was amplified by polymerase chain reaction (PCR) based on the cDNA sequence of mouse IL-4.
2. The mouse IL-4 fragment was inserted into *Bam*HI and *Eco*RI filled in pcDNA3.1(+) (Invitrogen, CA, USA) under the tissue plasminogen activator (TPA) leader sequence and then digested with *Bam*HI and *Sac*I.
3. A QuickChange™ Site-Directed Mutagenesis Kit (Stratagene, CA, USA) was used for mutagenesis of mouse IL-4.
4. The oligonucleotide primers used to prepare mouse IL-4DM (Q116D/Y119D) were 5′-CTAAAGAGCATCATGGATATGG ATGACTCGTAGTCTAGAG-3′ for the upper strand and 5′-CTCTAGACTACGAGTCATCCATATCCATGATGCT CTTTAG-3′ for the lower strand.
5. The IL-4 mutant fragments were ligated into pcDNA3.1(+).
6. Mouse IL-4DM plasmid DNA was purified using a Plasmid Mega Kit (Qiagen, Chatsworth, CA) and diluted with sterilized physiological saline (Fig. 2).

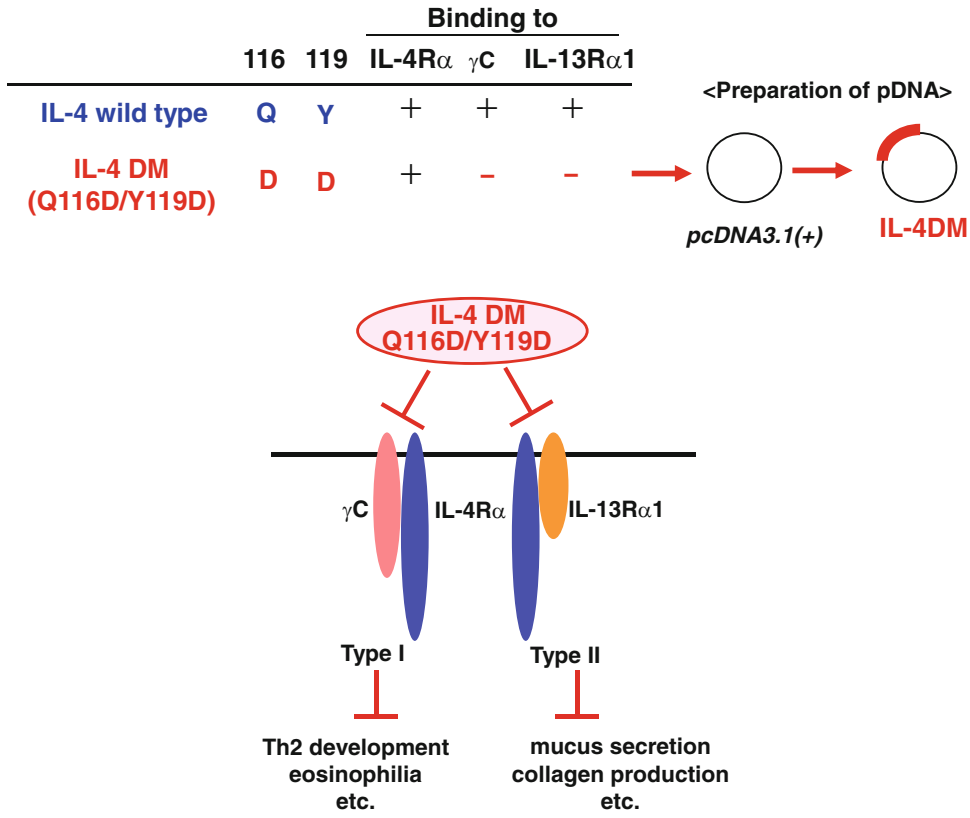

Fig. 2 IL-4DM has no ligand-binding properties to both common gamma chain (γC) and IL-13Rα1. A functional IL-4 receptor is composed of two transmembrane proteins, the IL-4Rα chain binds to IL-4 with high affinity, leading to dimerization with either the common gamma chain (γC), or IL-13Rα1, which results in formation of the type I or type II receptor complex, respectively. The IL-4 mutant Q116D/Y119D acts as an antagonist by forming unproductive complexes with the IL-4Rα chain through prevention of binding to γC or IL-13Rα1

3 Methods

We evaluated the effect of Ag85B in a mouse model of asthma using protein-based (Subheading 3.1) and DNA-based (Subheading 3.3) vaccine. Moreover, the effective anti-allergic responses in a mouse atopic dermatitis by using Ag85B gene vaccine in virus (Subheading 3.2) and plasmid DNA (Subheading 3.4) were confirmed. And, effects of IL-4 antagonistic DNA vaccination in allergic diseases were assessed through the mouse model of asthma (Subheading 3.5) or atopic dermatitis (Subheading 3.6).

3.1 Effect of rAg85B on Allergic Airway Inflammation

1. BALB/c mice (6 weeks old, female) were intraperitoneally (i.p.) immunized with 10 μg ovalbumin (OVA) with 1 mg aluminum hydroxide on days 0 and 14.
2. On days 21–25 after the first immunization, mice were exposed to aerosolized 5 % OVA for 20 min.

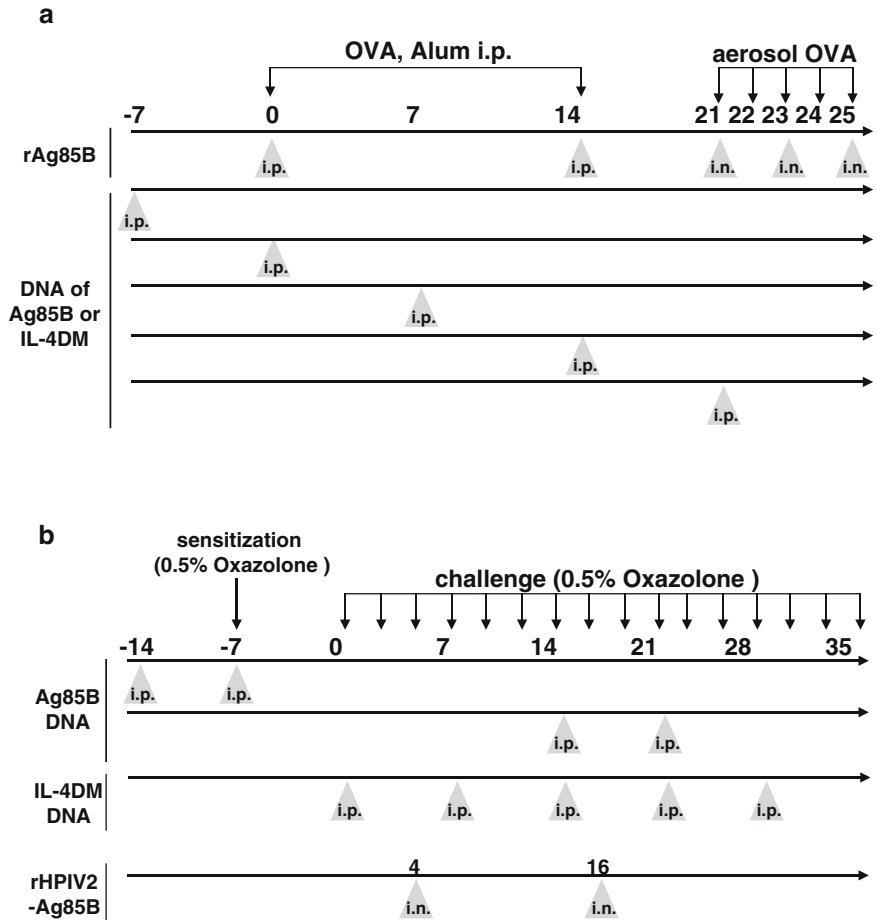

Fig. 3 Schematic diagram of the strategy used in this work. Experimental design used to investigate the effects of recombinant Ag85B protein (rAg85B) and cDNA of Ag85B and mutant IL-4 (IL-4DM) on OVA-induced allergic inflammation (**a**). Schedule for the development of a hapten-induced atopic dermatitis model and vaccination of rHPIV2-Ag85B and the vector expressing DNA of Ag85B and IL-4DM (**b**)

3. Three hours prior to OVA inhalation, the mice were intraperitoneally (i.p.) (100 μg; days 0 and 14) and intranasally (i.n.) (20 μg; days 21, 23, and 25) administered rAg85B (Fig. 3a) (*see* **Note 1**).
4. The purity of rAg85B was evaluated by silver staining of SDS-PAGE gel, the limulus amebocyte lysate (LAL) assay, and the TLR/NLR ligand screening test (*see* **Notes 2–5**).

3.2 Sensitization and Challenge Schedule of rHPIV2-Ag85B for Atopic Dermatitis

A repeated hapten sensitization and challenge system was used in this experiment.

1. Oxazolone (OX) (Sigma, St. Louis, MO) was dissolved in acetone/olive oil (1:1).

2. Mice were initially sensitized by pasting 20 μl of 0.5 % OX solution to their right ear 7 days prior to the first challenge (day −7).
3. OX solution (0.5 %, 20 μl) was repeatedly applied to the right ear three times per week from day 0 until day 21.
4. Repeated application of OX causes delayed-type hypersensitivity followed by immediate-type and late-phase reaction.
5. For vaccination, mice were infected intranasally under general anesthesia with 5×10^6 $TCID_{50}$ of the virus in 20 μl inoculum or PBS on day 4.
6. On day 16, mice were vaccinated again with PBS, rHPIV2-Ag85B, or control rHPIV2 vector intranasally or subcutaneously to the pinna skin.
7. Ear swelling was measured with thickness gauge calipers before and 6 h after the last OX challenge on day 21.
8. Blood and pinna skin were also sampled (Fig. 3b) (*see* **Notes 6** and 7).

3.3 Experimental Protocol of Ag85B DNA Vaccine Administration for Allergic Asthma

Induction of allergic airway inflammation was subjected to the assay with rAg85B as described in Subheading 3.1.

1. Mice were intraperitoneally administered 50 μg of plasmid DNA encoding Ag85B DNA once on day −7, 0, 7, 14, or 21.
2. An empty plasmid (pcDNA 3.1(+)) vector was used as a control (Fig. 3a) (*see* **Notes 8** and **9**).

3.4 Administration of Ag85B DNA Vaccine for Atopic Dermatitis

The procedures for OX sensitization and challenge for induction of mouse atopic dermatitis are described in Subheading 3.2.

1. The Ag85B expression vector pcDNA-Ag85B was diluted with sterilized physiological saline.
2. One hundred micrograms of pcDNA-Ag85B was injected intraperitoneally on days −14 and −7 for evaluation of prophylactic effects or on days 14 and 21 for assessment of therapeutic effects (Fig. 3b) (*see* **Notes 8** and **10**).

3.5 Experimental Protocol of IL-4 Antagonistic Mutant DNA Administration for Allergic Asthma

Induction of allergic airway inflammation was subjected to the assay with rAg85B as described in Subheading 3.1.

1. Mice were intraperitoneally administered 100 μg of plasmid DNA encoding IL-4DM once on day 0, 7, 14, or 21.
2. An empty plasmid (pcDNA 3.1(+)) vector was used as a control (Fig. 3a) (*see* **Notes 11** and **12**).

3.6 IL-4 Antagonist DNA Vaccination for Atopic Dermatitis

The procedures for sensitization and challenge in a mouse model of atopic dermatitis induced by OX are described in Subheading 3.2.

1. Mice were administered 100 μg of IL-4DM DNA intraperitoneally on days 0, 7, 14, 21, and 28.
2. A control plasmid (pcDNA3.1(+)) vector and IL-4 DNA were also injected on the same days (Fig. 3b) (*see* **Notes 11** and **13**).

4 Notes

1. We found that highly purified recombinant Ag85B protein (rAg85B) had a suppressive effect depending on induction of a Th1 immune response in a mouse model of allergic lung inflammation. Remarkably, rAg85B administration also promoted IL-17 and IL-22 production in both Th17 cells in lymph nodes (LNs) and various innate immune cells such as gamma delta T (γδT) cells, NKp46$^+$ cells, lymphoid tissue inducer (LTi)-like cells, and CD11c$^+$ cells in BAL fluid. More interestingly, Th17-related cytokines induced by rAg85B were involved in enhancement of the expression of genes related to maintenance of tissue homeostasis [10].
2. Many studies on a protein overexpression system using *E. coli* have shown contamination of the protein with endotoxins, especially LPS. Therefore, it would be important to show the data which supports the purity of the products. The purity of rAg85B was evaluated by silver staining of SDS-PAGE gel and the LAL assay (less than 0.02 EU (endotoxin units)/ml), and the TLR/NLR ligand screening test indicated that rAg85B is not contaminated with any innate immune receptor-binding stimulants.
3. The endotoxin value of Ag85B was measured by kinetic turbidimetric LAL assays (Lonza). The test was carried out according to the manufacturer's instructions. The endotoxin value was measured kinetically on ELISA after mixing a sample and LAL reagent and was calculated automatically according to the standard curve. Purified Ag85B had a purity of >95 % as analyzed by SDS-PAGE and was contaminated with less than 0.02 EU/mg of endotoxin. Protein quantitation was carried out by UV spectroscopy at 280 nm.
4. The recombinant purified Ag85B was solubilized in sample buffer to the desired concentration and boiled for 5 min. Then 15 μl/well from each sample was separated on 10 % SDS gel using a mini-PROTEAN electrophoresis instrument (Bio-Rad Laboratories). Silver staining of the gel was performed according to the standard protocol of EzStain Silver (ATTO) (Fig. 4a).

5. The presence of TLR and NLR ligands was tested in recombinant human embryonic kidney 293 (HEK293) cell lines that utilize a nuclear factor-kB-inducible SEAP (secreted embryonic alkaline phosphatase) reporter gene as the readout. The HEK293-derived cells functionally express a given TLR or NOD gene from humans or mice. A recombinant HEK293 cell line for the reporter gene was used as a negative control. Positive control ligands were heat-killed *Listeria monocytogenes* (HKLM) for TLR2, Poly(I:C) for TLR3, lipopolysaccharide (LPS) for TLR4, flagellin for TLR5, CL097 for TLR7, CL075 and poly(dT) for TLR8, CpG ODN for TLR9, C12-iEDAP for NOD1, and L18-MDP for NOD2. rAg85B (10 μg/mL) was added to the reaction mixture. TLR/NLR ligand screening was performed by InvivoGen (Fig. 4b).
6. The efficacy of rHPIV2 engineered to express Ag85B (rHPIV2-Ag85B) was evaluated in a mouse model of AD induced by repeated oxazolone (OX) challenge. Ear swelling, dermal cell infiltration, and serum IgE level were significantly suppressed in the rHPIV2-Ag85B-treated mouse group accompanied by elevated IFN-γ and IL-10 mRNA expression and suppressed IL-4, TNF-α, and MIP-2 mRNA expression. The treated mice showed no clinical symptoms of croup or systemic adverse reactions. The respiratory tract epithelium captured rHPIV2 effectively without remarkable cytotoxic effects [24].
7. Human parainfluenza type 2 virus (HPIV2) is one of the human respiratory pathogens and is a member of the genus *Rubulavirus* of the family Paramyxoviridae in the order Mononegavirales. It infects various cell types but has little cytopathic effect. Moreover, the virus replicates exclusively in the cytoplasm of infected cells, does not have a DNA phase during its life cycle, and can thus avoid the possibility of integration of foreign genes into the host DNA genome [25]. HPIV2 possesses a nonsegmented and negative-stranded RNA genome of 15,654 nucleotides [26–28]. The coding proteins are nucleocapsid (NP), V (V), phospho (P), matrix (M), fusion (F), hemagglutinin-neuraminidase (HN), and polymerase (L) proteins. M protein underlies the lipid bilayer to ensure the structural integrity of viral particles and is essential for interactions between the viral envelope and the RNP complex. This association leads to the budding and release of viral particles from the cell surface [29]. Thus, the elimination of M protein from HPIV2 leads to the generation of a replication-deficient virus (Fig. 1). This alteration might allow safer application to animals than that in the case of an original proliferating virus vector.

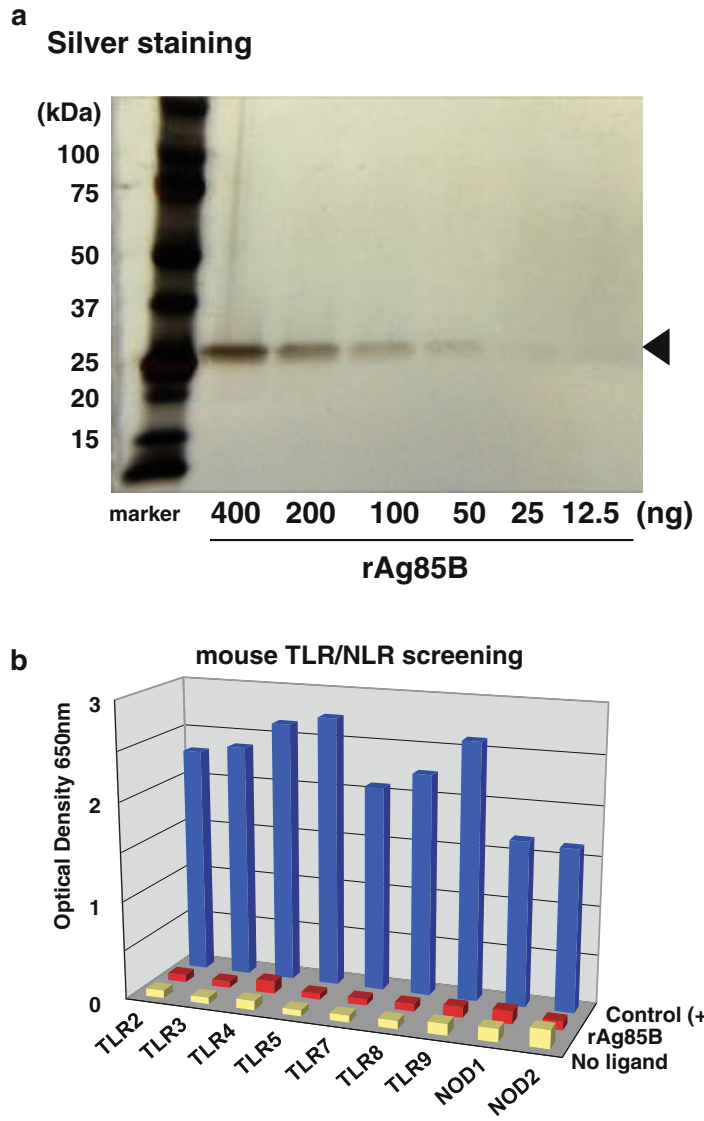

Fig. 4 Purity of rAg85B. The purity of rAg85B was evaluated by SDS-PAGE separation and silver staining of rAg85B (**a**). TLR/NLR ligand screening performed by InvivoGen demonstrated no effect of rAg85B on toll-like and NOD-like receptors (**b**)

Immune responses to vaccine vectors prevent the induction of aimed immune responses against recombinant antigens. Preexisting anti-vector antibodies constitute an obstacle for use in humans [30–32]. A recent study showed that multiple administrations of rHPIV2-Ag85B had greater preventive effects than did immunization two times with rHPIV2-Ag85B [33]. From these findings, intranasal administration of the HPIV2 vector is considered to be effective for human use.

8. There have been considerable developments in genetic vaccine technology over the past two decades. A cost-effective and promising strategy can be applied for curing allergies. The major advantages of DNA vaccination is the induction of both humoral and cellular responses, both MHC I and II presentation, ability to polarize T cell help for type 1 or 2 immune response only to selected antigens, stability during storage and shipping, simplicity of formulation and preparation, efficiency in production and modification, safety without an infective agent, and ease of development and production. However, plasmid DNA immunization does not fully elicit cellular immune responses in some cases. The use of an adjuvant in vaccination is thought to be effective for enhancing immune responses [34]. Previous studies showed the effectiveness of Ag85B as an adjuvant for enhancing cellular immune responses induced by a DNA vaccine [35, 36]. Thus, Ag85B is also a promising adjuvant for enhancing cytotoxic T lymphocyte (CTL) responses in a DNA vaccination strategy.
9. Immunization of BALB/c mice with alum-adsorbed ovalbumin (OVA) followed by aspiration with aerosolized OVA resulted in the development of allergic airway inflammation. Administration of Ag85B DNA before aerosolized OVA challenge protected the mice from subsequent induction of allergic airway inflammation. Serum and bronchoalveolar lavage IgE levels, extent of eosinophil infiltration, and levels of Th2-type cytokines in Ag85B DNA-administered mice were significantly lower than those in control plasmid-immunized mice, and levels of Th1- and regulatory T cell-type cytokines were enhanced by Ag85B administration [5].
10. The effect of plasmid DNA encoding Ag85B on AD skin lesions induced by oxazolone (OX) application was examined. Mice were immunized with Ag85B DNA before OX sensitization or during the repeated elicitation phase. Both therapies resulted in significant suppression of immediate-type response, improved clinical appearance, reduced dermal cell infiltration, reduced IL-4 production, and augmented IFN-γ mRNA expression with an increase of Foxp3+ regulatory T cells in the skin sections [6].
11. IL-4 elicits a wide variety of cellular responses by binding to high-affinity receptor complexes expressed on the surface of cells. The IL-4-specific receptor is composed of an IL-4Rα chain paired with a common γ chain (γC) forming a type I IL-4 receptor complex that is primarily responsible for regulating Th2 development and inflammation. The IL-4Rα chain can also pair with the IL-13Rα1 chain, forming the type II receptor that is responsible for effector activities such as airway hypersensitivity, collagen production, and mucus hypersecretion.

The IL-4 mutant Q116D/Y119D, which forms unproductive complexes with the IL-4Rα chain, acts as an antagonist by inhibiting the formation of heterodimers with other receptors (Fig. 2). However, results of experiments using animal models have shown that IL-4 inhibitors have some disadvantages for clinical use. Although the pharmacokinetic half-lives of the IL-4 mutant and soluble forms of IL-4R protein are very short in vivo, a high concentration of these molecules in plasma must be maintained for a long period in order for them to have suppressive effects on allergic inflammation. Thus, these molecules must be administered in large quantity, many times, and over a long period during the antigen sensitization and challenging periods in order for them to have suppressive effects on allergic inflammation.

12. A single administration of IL-4DM DNA before the aerosolized OVA challenge protected the mice from the subsequent induction of allergic airway inflammation. Serum IgE level and extent of eosinophil infiltration in bronchoalveolar lavage from IL-4DM DNA-administered mice were significantly lower than those in bronchoalveolar lavage from control plasmid-immunized mice [13].
13. Mice treated with the control plasmid developed severe dermatitis with Th2-type-cytokine dominance at 2 weeks after elicitation with oxazolone, and plasma IgE and histamine levels were increased. On the other hand, in IL-4DM-treated mice, the dermatitis was significantly suppressed, and plasma IgE and histamine levels were also decreased along with local overproduction of IFN-γ [14, 15].

Acknowledgements

Works that were supported by Health Science Research Grants from the Ministry of Health, Labor, and Welfare of Japan and the Ministry of Education, Culture, Sports, Science, and Technology of Japan are described in this report.

References

1. Drazen JM, Arm JP, Austen KF (1996) Sorting out the cytokines of asthma. J Exp Med 183:1–5
2. Brown MA, Hural J (1997) Functions of IL-4 and control of its expression. Crit Rev Immunol 17:1–32
3. Noben-Trauth N, Hu-Li J, Paul WE (2000) Conventional, naive CD4+ T cells provide an initial source of IL-4 during Th2 differentiation. J Immunol 165:3620–3625
4. Takatsu K, Kariyone A (2003) The immunogenic peptide for Th1 development. Int Immunopharmacol 3:783–800
5. Karamatsu K et al (2012) Single systemic administration of Ag85B of mycobacteria DNA inhibits allergic airway inflammation in a mouse model of asthma. J Asthma Allergy 5:71–79

6. Mori H et al (2009) Administration of Ag85B showed therapeutic effects to Th2-type cytokine-mediated acute phase atopic dermatitis by inducing regulatory T cells. Arch Dermatol Res 301:151–157
7. Lambrecht BN, Hammad H (2012) The airway epithelium in asthma. Nat Med 18:684–692
8. Holgate ST (2012) Innate and adaptive immune responses in asthma. Nat Med 18:673–683
9. Sonnenberg GF, Fouser LA, Artis D (2011) Border patrol: regulation of immunity, inflammation and tissue homeostasis at barrier surfaces by IL-22. Nat Immunol 12:383–390
10. Tsujimura Y et al (2014) Effects of mycobacteria major secretion protein, Ag85B, on allergic inflammation in the lung. PLoS One 9:e106807
11. Nelms K, Keegan AD, Zamorano J, Ryan JJ, Paul WE (1999) The IL-4 receptor: signaling mechanisms and biologic functions. Annu Rev Immunol 17:701–738
12. Reinemer P, Sebald W, Duschl A (2000) The interleukin-4-receptor: from recognition mechanism to pharmacological target structure. Angew Chem Int Ed Engl 39:2834–2846
13. Nishikubo K et al (2003) A single administration of interleukin-4 antagonistic mutant DNA inhibits allergic airway inflammation in a mouse model of asthma. Gene Ther 10:2119–2125
14. Morioka T et al (2009) IL-4/IL-13 antagonist DNA vaccination successfully suppresses Th2 type chronic dermatitis. Br J Dermatol 160:1172–1179
15. Nakanishi T, Yamanaka K, Kakeda M, Tsuda K, Mizutani H (2013) Mutant interleukin-4/13 signaling blockade successfully suppresses acute phase inflammation. Arch Dermatol Res 305:241–247
16. Draper SJ, Heeney JL (2010) Viruses as vaccine vectors for infectious diseases and cancer. Nat Rev Microbiol 8:62–73
17. Clark KR, Johnson PR (2001) Gene delivery of vaccines for infectious disease. Curr Opin Mol Ther 3:375–384
18. Halle S et al (2009) Induced bronchus-associated lymphoid tissue serves as a general priming site for T cells and is maintained by dendritic cells. J Exp Med 206:2593–2601
19. Okano S et al (2011) Provision of continuous maturation signaling to dendritic cells by RIG-I-stimulating cytosolic RNA synthesis of Sendai virus. J Immunol 186:1828–1839
20. Kawano M et al (2001) Recovery of infectious human parainfluenza type 2 virus from cDNA clones and properties of the defective virus without V-specific cysteine-rich domain. Virology 284:99–112
21. Bukreyev A et al (2004) Mucosal immunisation of African green monkeys (Cercopithecus aethiops) with an attenuated parainfluenza virus expressing the SARS coronavirus spike protein for the prevention of SARS. Lancet 363:2122–2127
22. Matsuo K et al (1990) Cloning and expression of the gene for the cross-reactive alpha antigen of Mycobacterium kansasii. Infect Immun 58:550–556
23. Meng X et al (2002) Keratinocyte gene therapy: cytokine gene expression in local keratinocytes and in circulation by introducing cytokine genes into skin. Exp Dermatol 11:456–461
24. Kitagawa H et al (2013) Intranasally administered antigen 85B gene vaccine in non-replicating human Parainfluenza type 2 virus vector ameliorates mouse atopic dermatitis. PLoS One 8, e66614
25. Tompkins SM et al (2007) Recombinant parainfluenza virus 5 (PIV5) expressing the influenza A virus hemagglutinin provides immunity in mice to influenza A virus challenge. Virology 362:139–150
26. Kawano M et al (1990) Sequence of the fusion protein gene of human parainfluenza type 2 virus and its 3′ intergenic region: lack of small hydrophobic (SH) gene. Virology 178:289–292
27. Kawano M et al (1990) Complete nucleotide sequence of the matrix gene of human parainfluenza type 2 virus and expression of the M protein in bacteria. Virology 179:857–861
28. Ohgimoto S et al (1990) Sequence analysis of P gene of human parainfluenza type 2 virus: P and cysteine-rich proteins are translated by two mRNAs that differ by two nontemplated G residues. Virology 177:116–123
29. Lamb RA, Kolakofsky D (2001) Paramyxoviridae: the viruses and their replication. In: Knipe DM, Howley PM (eds) Fields virology, 4th edn. Lippincott Williams & Wilkins, Philadelphia, pp 1305–1340
30. Sumida SM et al (2005) Neutralizing antibodies to adenovirus serotype 5 vaccine vectors are directed primarily against the adenovirus hexon protein. J Immunol 174:7179–7185
31. Catanzaro AT et al (2006) Phase 1 safety and immunogenicity evaluation of a multiclade HIV-1 candidate vaccine delivered by a replication-defective recombinant adenovirus vector. J Infect Dis 194:1638–1649
32. Priddy FH et al (2008) Safety and immunogenicity of a replication-incompetent adenovirus type 5 HIV-1 clade B gag/pol/nef vaccine in healthy adults. Clin Infect Dis 46:1769–1781
33. Watanabe K et al (2014) Recombinant Ag85B vaccine by taking advantage of characteristics of human parainfluenza type 2 virus vector showed Mycobacteria-specific immune responses by intranasal immunization. Vaccine 32:1727–1735

34. Donnelly JJ, Ulmer JB, Shiver JW, Liu MA (1997) DNA vaccines. Annu Rev Immunol 15:617–648
35. Takamura S, Matsuo K, Takebe Y, Yasutomi Y (2005) Ag85B of mycobacteria elicits effective CTL responses through activation of robust Th1 immunity as a novel adjuvant in DNA vaccine. J Immunol 175:2541–2547
36. Kuromatsu I et al (2001) Induction of effective antitumor immune responses in a mouse bladder tumor model by using DNA of an alpha antigen from mycobacteria. Cancer Gene Ther 8:483–490

Chapter 42

Development of House Dust Mite Vaccine

Qiuxiang Zhang and Chunqing Ai

Abstract

Mucosal vaccine based on lactic acid bacteria is an attractive strategy for prevention and treatment of allergic diseases. Here we describe the development of recombinant *Lactococcus lactis* expressing house dust mite (HDM) allergen as an oral vaccine. The major HDM allergen Der p2 is first codon optimized and synthesized to achieve the maximum expression level in *L. lactis*. After double digested by *Nco*I and *Xba*I, the *derp2* fragment is ligated to the same double-digested pNZ8148 vector. The ligation is transformed to *L. lactis* NZ9000 and correct transformant is verified by sequencing. Western blot analysis is employed to confirm Derp2 expression in *L. lactis* after nisin induction.

Key words Lactic acid bacteria, House dust mite, Allergy, Mucosal vaccine

1 Introduction

Allergic asthma is a common chronic disease that affects the airways, which is becoming a public health problem worldwide [1]. House dust mite (HDM) is an important source of allergens responsible for allergic sensitization, which afflicts 70–80 % of asthmatics [2]. Among more than 30 HDM allergens, Derp2 is one of the most potent and common allergens which can cause allergic response in most HDM allergic patients [3]. Specific immunotherapy is considered to be the only curative treatment [4], but it is limited by the poor quality of natural allergen extracts. Recombinant allergens can be produced in large amounts in *Escherichia coli*, yeasts, or insect cell at low cost [5–7]. However, the complicated purification process may limit its application in clinic treatment.

Lactic acid bacteria (LAB) are gram-positive bacteria with GRAS (generally regarded as safe) status, which have been used in fermentation and preservation of food for decades. They are attractive candidates for delivering biologically active proteins through mucosal routes due to their safety and intrinsic immunomodulation properties [8, 9]. To date, protective effects of genetically engineered *Lactococcus lactis* strains for a wide range of diseases have been demonstrated in some animal experiments and clinical

Sunil Thomas (ed.), *Vaccine Design: Methods and Protocols: Volume 1: Vaccines for Human Diseases*, Methods in Molecular Biology, vol. 1403, DOI 10.1007/978-1-4939-3387-7_42,

trials [10–12]. This novel strategy can effectively avoid adverse side effects, and thus it is suitable as maintenance treatment for chronic diseases.

Here, we develop a kind of HDM vaccine by expressing the Derp2 allergen in *L. lactis* using a nisin-controlled gene expression system (NICE). To achieve maximum expression level, the *derp2* gene is first optimized according to the codon bias in *L. lactis*. Western blot analysis is employed to confirm Derp2 expression in *L. lactis* after nisin induction.

2 Materials

Prepare all media and solutions using ultrapure water (Milli-Q ultrapure water system, Millipore, 18 MΩ cm at 25 °C).

2.1 Media

1. LB (Luria–Bertani) broth: Tryptone 10 g; yeast extract 5 g; NaCl 10 g (1000 mL). Add all the above reagents to a 1 L glass beaker. Add water to a volume of 800 mL. Mix thoroughly and make up to 1000 mL with H_2O. Adjust pH to 7.5 with NaOH and autoclave at 121 °C for 20 min. For LB plates, add 13 g of agar to LB broth before autoclaving.
2. GM17 media: Peptone 5 g, soy peptone 5 g, beef extract 5 g, yeast extract 2.5 g, magnesium sulfate 0.25 g, disodium-β-glycerophosphate 19 g, glucose 5 g. Add all the above reagents to a 1 L glass beaker. Add water to a volume of 800 mL (*see* **Note 1**). Mix thoroughly and make up to 1000 mL with H_2O. Sterilize at 115 °C 15 min and store at 4 °C. For GM17 agar, add 13 g of agar to GM17 media before autoclaving. For GM17 plates with antibiotic, add the appropriate amount of the selective antibiotic to sterile GM17 agar media that has been pre-cooled to 50 °C.
3. SGM17 media: Add 0.5 M sucrose and 1.8 % (w/v) glycine into the GM17 media before autoclaving. Weigh 171 g sucrose and 18 g glycine into the GM17 media before dissolving the reagents (*see* **Note 2**).
4. SGM17MC media: Add 20 mM $MgCl_2$ and 2 mM $CaCl_2$ into the SGM17 medium before autoclaving (*see* **Note 3**). To make the 2 M $MgCl_2$ stock, weigh 19 g anhydrous $MgCl_2$ into 100 mL H_2O and mix. For the 2 M $CaCl_2$ stock, weigh 22 g anhydrous $CaCl_2$ into 100 mL H_2O and mix. Sterilize them at 120 °C for 20 min.

2.2 DNA Electrophoresis Reagents

1. 50× TAE buffer: Tris base 242 g, disodium EDTA 18.61 g, acetate (100 % acetic acid) 57.1 mL. Add the Tris base and EDTA to approximately 700 mL H_2O and stir until completely dissolve. Add the acetic acid and adjust the volume to 1 L. To make 1× TAE buffer from 50× TAE stock (*see* **Note 4**), dilute 20 mL of stock into 980 mL of H_2O.

2. 1 % agarose: Measure 1 g agarose, and pour agarose powder into microwavable flask along with 100 mL 1× TAE buffer.
3. 6× loading buffer: 4 g sucrose, 25 mg bromophenol blue (0.25 %). Add the reagents to a beaker, add 10 mL H_2O, and stir. Store at 4 °C (*see* **Note 5**).

2.3 Competent L. lactis Cell Preparation and Electroporation Solutions

1. Wash buffer: 0.5 M sucrose and 10 % (v/v) glycerol. Measure 10 mL glycerol and 70 mL H_2O, and mix completely. Pour the mixture into a 250 mL beaker with 17.1 g sucrose and adjust the volume to 100 mL (*see* **Note 6**).
2. Chloramphenicol (Cm) (*see* **Note 7**): 5 mg/mL. Dissolve 0.05 g Cm stock in 10 mL 100 % ethanol. Mix vigorously to ensure the antibiotic is fully dissolved. Filter sterilize solution using a 0.2 μm syringe filter. Aliquots (500 μL) can be stored at −20 °C for a year.

2.4 Derp2 Protein Expression

1. Nisin: 10 mg/mL. Dissolve 0.01 g nisin (2.5 %, Sigma) in 1 mL of 0.02 N HCl. Keep the mixture at room temperature for 3–4 h to completely dissolve nisin. Store the aliquots (500 μL) at −20 °C (*see* **Note 8**). To prepare 0.01 N HCl, firstly add 100 mL H_2O into a 1 L beaker, pipette 0.42 mL HCl (37 %) in it, and then adjust the volume to 500 mL.
2. TCA (trichloroacetic acid): 100 %. Add 227 mL of H_2O into a bottle containing 500 g TCA (*see* **Note 9**).
3. NaOH: 50 mM. Add 8 g NaOH into 150 mL H_2O little by little and keep stirring. Then dilute the solution to make 200 mL (*see* **Note 10**).
4. PBS: NaCl 137 mM, KCl 2.7 mM, Na_2HPO_4 10 mM, KH_2PO_4 1.8 mM. Usually prepare 1 L of 10× PBS stock. Dissolve NaCl 80 g, KCl 2 g, $Na_2HPO_4{\cdot}12H_2O$ 35.8 g, KH_2PO_4 2 g in 800 mL H_2O. Adjust the pH to 7.4 with HCl, and then add H_2O to 1 L. Dispense the solution into aliquots, and sterilize them by autoclaving for 20 min at 121 °C or by filter sterilization. Store PBS at room temperature.

2.5 SDS-PAGE Components

1. Resolving gel buffer: 1.5 M Tris–HCl, pH 8.8. Weigh 90.9 g Tris into 400 mL H_2O. Mix and adjust with HCl to pH 8.8. Make up to 500 mL with H_2O. Store at 4 °C.
2. Stacking gel buffer: 1 M Tris–HCl, pH 6.8. Weigh 60.6 g Tris and prepare a 500 mL solution as in previous step. Store at 4 °C.
3. 30 % acrylamide/bis solution (29:1 acrylamide/bis): Add 29 g of acrylamide (*see* **Note 11**) and 1 g bis-acrylamide into a 100 mL graduated cylinder containing about 50 mL H_2O. Heat the solution at 37 °C to dissolve the chemicals. Make up to 100 mL with H_2O and filter the solution through a 0.45 μm membrane

filter. Store the solution in dark bottles at 4 °C for less than 1 month.

4. Ammonium persulfate (AP): 10 % (w/v). Add 0.1 g ammonium persulfate in 1 mL H_2O and store at –20 °C in 50–100 μL aliquots (*see* **Note 12**).
5. N,N,N,N′-tetramethylethylenediamine (TEMED) (Sigma): Store at 4 °C in dark bottle.
6. SDS: 10 % (w/v). Add 10 g SDS (*see* **Note 13**) into 100 mL H_2O. Store at room temperature.
7. SDS running buffer (5×): Tris 15 g, glycine 94 g, SDS 5 g. Add all the chemicals into 900 mL H_2O. Make up to 1 L with H_2O. Store at room temperature.
8. SDS sample loading buffer (6×): 375 mM Tris–Cl (pH 6.8), 12 % SDS, 60 % glycerol, β-mercaptoethanol (2-ME) 0.5 mL, 0.06 % bromophenol blue. Combine 1 M Tris–HCl (pH 6.8) 3.75 mL, glycerol 6 mL, SDS 1.2 g, 2-ME 0.5 mL, bromophenol blue 6 mg. Add H_2O to total volume of 10 mL. Store at –20 °C in 0.5 mL aliquots.

2.6 Western Blot Buffers

1. Transfer buffer: Tris 3.03 g, glycine 14.4 g, methanol 200 mL, SDS 0.37 g. Mix all these reagents and H_2O to a final volume of 1000 mL.
2. PBST: PBS containing 0.05 % Tween-20. Pipette 0.5 mL Tween-20 into 0.95 L PBS and mix completely.
3. Blocking buffer: 5 % milk in PBST. Store at 4 °C.

3 Methods

3.1 Synthesis of derp2 Fragment

1. According to the *derp2* sequence (GenBank: AF276239.1) and codon usage bias of *L. lactis*, apply codon optimizing using online tools (*see* **Note 14**).
2. Chemically synthesize the *derp2* fragment and ligate to the pUC57 vector. This step is accomplished by Sangon, China.

3.2 Augment of derp2 Fragment by PCR

1. Set up a 50 μL reaction with 10× pyrobest buffer 5 μL, dNTP (2.5 mM) 3 μL, pUC57-derp2 (0.1 μg) 1 μL, primer 8 N-F (10 μM) 0.5 μL, primer 8 N-R (10 μM) 0.5 μL, TaqE (pyrobest) 0.5 μL, H_2O (DNA and DNase free) 39.5 μL (*see* **Note 15**) in a PCR tube (*see* **Note 16**).
2. Set the PCR (Bio-Rad) procedure as follows: step 1, 95 °C 5 min; step 2, 95 °C 30 s, step 3, 58 °C 30 s, step 4, 72 °C 45 s. Repeat steps 2–4 for 32 times. Step 5, 72 °C 5 min and keep on 4 °C (*see* **Note 17**).

3.3 Electrophoresis of derp2 Fragment

1. Prepare 1 % agarose and microwave for 1–3 min until the solution becomes clear (*see* **Note 18**). Add 5 μL of gold view dye (or other alternative dye) when the solution cool down to about 50–55 °C. Place a wide comb and pour the melted agarose solution into the gel tank. After a complete solidification (it should appear milky white), put the agarose gel in the electrophoresis tank.
2. Fill the gel tank with 1× TAE (*see* **Note 19**) to submerge the gel to 2–5 mm depth. Load a molecular weight ladder into the first lane of the gel. Mix 5 volume of the sample with 1 volume of 6× loading buffer, and carefully load the samples into the additional wells of the gel.
3. Run the gel at 80–100 V until the dye line is approximately 75–80 % length of the gel. Put the agarose gel in a UV detector (*see* **Note 20**) and visualize the *derp2* bands (*see* **Note 21**). The correct size is indicated by the DNA marker.

3.4 Purification of derp2 Fragment

Purification is done by Omega gel extraction kit (or other commercial gel purification kits) according to the manufacturer's protocol.

1. Excise the correct size derp2 fragment from the gel with a clean, sterile sharp scalpel. Minimize the size of the gel slice by removing extra agarose (*see* **Note 22**). Weigh the gel slice in a labeled clean microcentrifuge tube.
2. Add 3 volumes of binding buffer to 1 volume of gel (300 μL per 100 mg) (*see* **Note 23**).
3. Incubate at 65 °C for almost 10 min until the solution becomes clear. Mix by vortexing the tube every 2–3 min during the incubation.
4. Place a spin column in a provided 2 mL collection tube. Apply the samples to the column and centrifuge at 10,000 × *g* for 60 s.
5. Discard flow-through. Place the column back into the same tube.
6. Add 750 μL wash buffer to the column and centrifuge at 10,000 × *g* for 60 s.
7. Repeat **step 6**.
8. Discard flow-through and place the column back into the same tube. Centrifuge the column at 10,000 × *g* for an additional 2 min. Keep the column at room temperature for 5 min (*see* **Note 24**).
9. Place the column in a clean 1.5 mL microcentrifuge tube. Add 50 μL elution buffer or water (pH 7.0–8.5), which is preheated to 65 °C, to the center of the membrane (*see* **Note 25**), and centrifuge the column at 10,000 × *g* for 60 s.
10. Analyze the purified *derp2* fragment on a gel following instruction of Subheading 3.3.

3.5 Plasmid pNZ8148 Extraction

Plasmid pNZ8148 in *L. lactis* NZ9000 is a gift from Dr. O. P. Kuipers and is chloramphenicol resistant. The extraction is done by Omega plasmid extraction kit (or other commercial gel purification kits) according to the manufacturer's protocol.

1. Inoculate a single colony of *L. lactis* NZ9000 harboring plasmid pNZ8148 into 5 mL of GM17 media containing 5 μg/mL Cm, and incubate overnight at 30 °C.
2. Harvest the cells (1.5 mL) by centrifugation at 6000 × *g* for 5 min at 4 °C, and discard the supernatant (*see* **Note 26**).
3. Resuspend the cells (*see* **Note 27**) with 200 μL solution I, RNase A, and 50 μL lysozyme; mix thoroughly and incubate at 37 °C for 30–60 min.
4. Add 250 μL solution II (*see* **Note 28**) to the lysed cells, cap the tube and mix by gently inverting the tube 3–5 times, and incubate at room temperature for 5 min (*see* **Note 29**). The lysate should appear viscous.
5. Add 350 μL solution III to each tube. Mix immediately and thoroughly by inverting several 4–6 times. A white precipitate will be formed which contains the bacterial proteins, genomic DNA, and cell debris.
6. Incubate the tube on ice for 5 min and then centrifuge at 12,000 × *g* for 10 min.
7. Place a spin column in a provided collection tube. Carefully transfer the supernatant to the column without any precipitate.
8. Centrifuge at 10,000 × *g* for 1 min. Discard flow-through. Place the column back into the same tube.
9. Add 500 μL solution HB to the column. Centrifuge at 10,000 × *g* for 1 min.
10. Add 700 μL wash buffer to the column and centrifuge at 10,000 × *g* for 1 min.
11. Repeat **step 10**.
12. Discard flow-through and place the column back into the same tube. Centrifuge the column at 10,000 × *g* for an additional 2 min. Keep the column at room temperature for 5 min.
13. Place the column in a clean 1.5 mL microcentrifuge tube. Add 50 μL elution buffer or water (pH 7.0-8.5), which is preheated to 65 °C, to the center of the membrane, and centrifuge the column at 10,000 × *g* for 60 s.
14. Analyze the plasmid on a gel following instruction of Subheading 3.3. Store the remaining plasmid at −20 °C for further use.

3.6 Digestion of derp2 and pNZ8148

1. Combine the following reaction components in an Eppendorf tube: H_2O 17 μL, 10× M buffer 5 μL, BSA 5 μL, purified *derp2* or pNZ8148 20 μL (1 μg), *Nco*I 1.5 μL, *Xba*I 1.5 μL.
2. Mix gently and spin down briefly.
3. Incubate at 37 °C for 4–6 h.
4. Electrophoresis of the digested product on gel following the instruction of Subheading 3.3.
5. Recover the double-digested vector and DNA fragment following the steps mentioned in Subheading 3.4.

3.7 Ligation of pNZ8148 and derp2

1. In a 1.5 mL tube, combine the following components: pNZ8148 (double digested) 6 μL (25 ng), *derp2* (double digested) 15 μL (75 ng), 10× ligation buffer 2.5 μL, T4 DNA ligase 1.5 μL (*see* **Note 30**).
2. Incubate at 16 °C overnight or room temperature for 2 h.
3. Heat inactivate at 65 °C for 10 min.
4. Chill on ice and transform 5 μL of the reaction into 45 μL competent *L. lactis* cells as described in Subheading 3.9.

3.8 Preparation of Competent L. lactis Cells

1. Inoculate 5 mL of SGM17 media with *L. lactis* from glycerol stock, and incubate overnight at 30 °C statically. Use this culture to inoculate 50 mL GM17 and incubate overnight.
2. Inoculate 500 mL of SGM17 with the 10 mL overnight culture, and incubate at 30 °C to an OD_{600} of about 0.4–0.6. This needs 3.5 h approximately.
3. Precool the culture on ice and then collect the cells at 4000 × *g* at 4 °C for 15 min.
4. Wash the pellets with 1 volume ice-cold wash buffer and centrifuge at 4000 × *g* at 4 °C for 15 min.
5. Resuspend the pellets in 0.5 volume ice-cold wash buffer, and incubate on ice for 30 min before centrifugation at 4000 × *g* at 4 °C for 15 min.
6. Resuspend the final pellet in 0.01 volume ice-cold wash buffer.
7. Aliquots of 45 μL are flash-frozen in liquid nitrogen and store at −80 °C until use.

3.9 Transformation of pNZ8148- derp2

1. Flame the reusable electrodes with ethanol for sterilization (or a corresponding disposable cuvette), and evaporate ethanol totally before ice cool.
2. Thaw the competent cells on ice. Add 5 μL ligation of pNZ8148-derp2 immediately when the frost thaws (e.g., near zero degrees) and mix them thoroughly.

3. The following must be conducted as fast as possible: Transfer the mixture into the cold electroporation cuvette (2 mm electrode gap) gently, and tap to drive away the bubbles.
4. Before triggering the discharge, draw 900 μL of ice-cold SGM17MC media into an Eppendorf pipette tip. Electroporate at 2 kV, 200 Ω serial resistor, 25 μF, and immediately wash the cells out of the cuvette into a fresh Eppendorf tube on ice with the 900 μL of cold SGM17MC media ready in a pipette (not later than after 1–2 s after the pulse).
5. Incubate the electroporated cells on ice for 10 min before transfer to 30 °C for 2 h to allow for phenotypic expression.
6. Plate 100 mL of the cells (*see* **Note 31**) on SGM17 plates supplemented with 5 μg/mL of Cm, and incubate the plates for 2–3 days at 30 °C until single colony appears.

3.10 Transformant Selection

1. Pick up single colony into 10 μL H_2O in a 200 μL PCR tube. Use 2 μL of the solution as template. Set up a PCR reaction containing following components: 10× Taq buffer 2 μL, dNTP 0.5 μL, template 2 μL, primer 8N-F (10 μM) 0.5 μL, primer 8N-R (10 μM) 0.5 μL, TaqE 0.5 μL, H_2O 14 μL.
2. Set a PCR procedure as mentioned in Subheading 3.2.
3. Detect the size of the amplification band on a gel using a DNA marker as control according to Subheading 3.3.
4. If the size of the amplified band is correct, inoculate the corresponding colony in GM17 medium with 5 μg/mL Cm and incubate overnight.
5. Plasmid recovery from transformant is done according to Subheading 3.5. Sequence the plasmid for further confirmation with the correct transformant.

3.11 Expression of Derp2 Protein

1. Inoculate the correct transformant into 5 mL GM17 medium with 5 μg/mL Cm, and incubate at 30 °C overnight.
2. Inoculate 500 μL of the overnight culture into 5 mL GM17 medium with 5 μg/mL Cm, and incubate at 30 °C to an OD_{600} of 0.5–0.6. This may need 2.5–3 h.
3. Add 5 μL of 10 mg/mL nisin to induce the expression of Derp2. Incubate at 30 °C for another 6 h for protein extraction.

3.12 Extraction of Protein Derp2

The extraction of protein is performed as described by Le Loir [13].

1. After nisin induction, harvest the cells by a 10 min centrifugation at 4 °C and 5000 × *g*. The supernatant and cells are processed separately.

2. For the supernatant part, filter the supernatant with 0.22 μm filters. Then add 100 % (w/v) TCA into the filtrate to a final concentration of 16 % (w/v). Mix the solution and keep it on ice for 20 min.
3. Centrifuge at 12,000 × *g* at 4 °C for 10 min. Wash the pellet twice with ice-cold acetone, and then dissolve in 1/40 volume of 50 mM NaOH.
4. For the cell pellet part, wash the cells with PBS once, and resuspend in 1/20 volume of PBS. Place the sample in an ice bath, and sonicate the suspension with 3 min bursts of 10 s followed by intervals of 30 s for cooling (*see* **Note 32**).
5. Centrifuge at 4 °C at 12,000 × *g* for 20 min, and collect the supernatant for later use.

3.13 SDS-PAGE Electrophoresis of Derp2 Protein

1. Set the casting frames (clamp two glass plates in the casting frames) on the casting stands. Seal the base of the gel cassette using 1 % agarose.
2. Prepare the separating gel solution in a separate small beaker: Mix H_2O 3.3 mL, 1.5 M Tris (pH 8.8) 2.5 mL, 30 % acrylamide/bis 4 mL, 10 % SDS 0.1 mL, 10 % AP 100 μL, and TEMED 10 μL. Swirl the solution gently but thoroughly. Pipette appropriate amount of separating gel solution into the gap between the glass plates. Fill in H_2O into the gap until an overflow. Wait for 20–30 min to let it gelate.
3. Make the stacking gel in another small beaker: Mix H_2O 2.1 mL, 1 M Tris (pH 6.8) 0.38 mL, 30 % acrylamide/bis 0.5 mL, 10 % SDS 0.03 mL, 10 % AP 30 μL, and TEMED 3 μL. Discard the water and use thin strips of Whatman paper to remove any excess. Pour stacking gel and insert comb without trapping air under the teeth. Wait for 20–30 min to polymerize. Make sure the gel is completely polymerized before removing the comb. Place gel in holder and then transfer to a running tank. Fill in the tank with fresh running buffer but keep the inner and outer chambers separated.
4. Prepare the samples: Mix the proteins prepared in Subheading 3.12 with 1× sample loading buffer, and heat them in boiling water for 5 min. Spin tubes at 12,000 × *g* for 1 min in room temperature centrifuge. Load protein marker in the first lane and samples in other lanes and make sure not to overflow. Cover the top and connect the anodes.
5. Run at 150 V through the stacking gel. Run at 200 V until the dye front reaches the bottom of the gel, and turn off the power supply.

3.14 Western Blot of Derp2 Protein

1. Prepare fresh transfer buffer while the SDS-PAGE is running. Chill buffer at 4 °C.
2. At the end of electrophoresis, remove gels from glass plates. Cut off stacking gel and nick top left-hand corner of resolving gel for orientation. Incubate gels in transfer buffer for 20–30 min.
3. Cut a piece of PVDF membrane to the size of the gel, and clip a corner as the top left-hand corner. Immerse the membrane in methanol for 15 s. Rinse twice with distilled H_2O and once with transfer buffer. Cut out six pieces of Whatman filter paper. Immerse the membrane and filter paper in transfer buffer for 10 min before assembling the filter-PVDF-gel-filter sandwich according to the Bio-Rad reference guide.
4. Open a gel holder cassette in a casserole dish with transfer buffer, black side down. Soak a fiber pad with transfer buffer and place in the center of the black side. Place three pieces of filter paper on top of the fiber pad. Place gel on top of filter paper. Place membrane on top of gel, with the gel's top left mark facing the membrane's top left mark. Roll out the bubbles with glass tube. Place another three pieces of filter paper on top of the membrane. Soak a second piece of fiber pad and place on top of the stack. Roll out the bubbles with glass tube and close the gel holder cassette.
5. Place in a transfer tank (orient the white and black sides of the cassette with the white and black panels of the electrode) and fill with transfer buffer (~800 mL). Place the tank in a Styrofoam box containing ice. Run at 0.65 mA/cm^2 gel for 2 h. Make sure that pre-stained protein markers transfer to PVDF membrane.
6. Block membrane in 20 mL blocking buffer overnight at 4 °C or 1 h at room temperature on rocker in a seal-a-meal bag. Dilute mouse anti-Derp2 antibody (Ab) in blocking buffer (1:1000). Incubate blots with Ab for 1 h at room temperature or overnight at 4 °C on rocker in a seal-a-meal bag.
7. Wash blots with 50 mL 1× PBST on orbital shaker three times, 10 min each.
8. Dilute HRP-conjugated Ab 1:8000. Incubate blots with secondary Ab for 1 h at room temperature.
9. Wash blots with 50 mL 1× TBST on orbital shaker three times, 10 min each.
10. Add 5 mL chemiluminescent substrate to each blot, and incubate for 5 min. Place blots in between transparency film. Push out air bubbles. Develop Western blot. Do a 1 min exposure to check signal intensity. Continue with longer or shorter exposures as needed.

4 Notes

1. Use water bath heating to 40 °C to help dissolve beef extract.
2. After sterilizing, the color of the media will be darker than GM17 because of the sucrose. Also, sucrose can be autoclaved and added separately.
3. $MgCl_2$ and $CaCl_2$ need to be prepared and added separately.
4. For convenience, a concentrated stock of TAE buffer (either 10× or 50×) is often made ahead of time and diluted with water to 1× concentration prior to use.
5. Avoid mold growing in the sucrose.
6. Glycerol (100 %) is viscous. Be sure to measure the correct volume.
7. For culture plates, allow media to cool to 55 °C before adding Cm to a final concentration of 5 μg/mL.
8. The additive in nisin cannot dissolve in HCl. Make sure the mixture is completely thawed and shake vigorously before use.
9. Solid TCA has strong hygroscopicity. So it should be kept in a 100 % liquid form after opening the bottle. TCA is highly corrosive. Be sure to wear protections when preparing the solution.
10. Be sure to use borosilicate glass, and consider immersing the container in a bucket of ice to keep the heat down. Wear safety protections since there is a chance the NaOH solution could splash up.
11. This substance is a biohazard. Wear a mask when weighing acrylamide. Carefully dissolve and filter the solution in a fume hood.
12. It is better to prepare this solution fresh each time.
13. Avoid inhalation of SDS powder. It makes bubbles when dissolving in H_2O.
14. Many amino acids are encoded by more than one codon. Different organisms often show particular preferences for one of the several codons that encode the same amino acid. So optimal codons in an expression host help to achieve faster translation rates and high accuracy.
15. Be sure to keep the reagents on ice. Tap tube gently to mix and spin briefly in microcentrifuge to get all contents to the bottom, and then place on ice until ready to load in the thermocycler. If the thermocycler does not have a heated lid, layer thin film of mineral oil over mixture to prevent evaporation during cycling.
16. Positive and negative controls must be used and run every time.

17. The goal of step 2 is denaturation, to separate the DNA double strands. Step 3 is annealing, to make the primers anneal to complementary sequences of the template DNA. Step 4 is elongation, to synthesize a new DNA strand with complementary dNTPs by the polymerase.
18. To avoid eruptive boiling, it is a good idea to microwave for 45–60 s, stop and swirl, and then continue toward a boil.
19. Use fresh 1× TAE every time.
20. When using UV light, be sure to wear proper UV protection—especially for the eyes and skin.
21. As the *derp2* fragment will be purified for later use, use long-wavelength UV and expose for as short a time as possible to minimize damage to the DNA.
22. Try to get as little excess gel around the band as possible. Take the excised band, and trim the top, bottom, and sides with the scalpel.
23. The maximum amount of gel slice per column is 400 mg. For gel slices >400 mg, use more than one column.
24. This step is to completely remove the residual ethanol from washing buffer, as it may impact the elution efficiency of DNA.
25. Be sure that the elution buffer is dispensed directly onto the membrane for complete elution of bound DNA. To achieve maximum elution efficiency, elution buffer or water can be added twice.
26. If you wish to stop the protocol and continue later, freeze the cell pellets at −20 °C.
27. The bacteria should be resuspended completely by vortexing or pipetting up and down until no cell clumps remain.
28. Store solution II at room temperature. Preheat solution II at 37 °C water bath to dissolve the precipitate in winter.
29. Do not vortex, as this will result in shearing of genomic DNA. Do not allow the lysis reaction to proceed for more than 5 min.
30. It's better to make a 3:1 ratio for insert to vector. You can also optimize the amount of insert and vector to improve ligation efficiency in situations where the 3:1 ratio is not working or when doing more complicated cloning.
31. If the transformation efficiency is low, just centrifuge the cells at 4000 × *g* for 5 min, discard 800 μL of the supernatant. Resuspend the cells with the remaining 200 μL supernatant, and plate all the cells on SGM17 plates.
32. Keep the suspension at all times on ice. Avoid foaming. Do not leave while the sonicator is working. It is possible that the beaker breaks or ice melts due to heat generation.

Acknowledgement

This work was supported by the National Natural Science Foundation of China (No. 31200691) and the National Science and Technology Pillar Program (2013BAD18B01).

References

1. Gregory LG, Lloyd CM (2011) Orchestrating house dust mite-associated allergy in the lung. Trends Immunol 32:402–411
2. Nelson RP Jr et al (1996) Allergen-specific IgE levels and mite allergen exposure in children with acute asthma first seen in an emergency department and in nonasthmatic control subjects. J Allergy Clin Immunol 98:258–263
3. Thomas WR et al (2002) Characterization and immunobiology of house dust mite allergens. Int Arch Allergy Immunol 129:1–18
4. Van Hage-Hamsten M, Valenta R (2002) Specific immunotherapy—the induction of new IgE-specificities? Allergy 57:375–378
5. Dhanapala P, Doran T, Tang ML, Suphioglu C (2015) Production and immunological analysis of IgE reactive recombinant egg white allergens expressed in *Escherichia coli*. Mol Immunol 65:104–112
6. Popovic M et al (2014) Yeast surface display is a novel tool for the rapid immunological characterization of plant-derived food allergens. Immunol Res 61:230–239
7. Pahr S et al (2014) Biochemical, biophysical and IgE-epitope characterization of the wheat food allergen, Tri a 37. PLoS One 9:e111483
8. Huibregtse IL et al (2007) Induction of ovalbumin-specific tolerance by oral administration of *Lactococcus lactis* secreting ovalbumin. Gastroenterology 133:517–528
9. Schwarzer M et al (2011) Neonatal colonization of mice with *Lactobacillus plantarum* producing the aeroallergen Bet v 1 biases towards Th1 and T-regulatory responses upon systemic sensitization. Allergy 66:368–375
10. Zhang Q, Zhong J, Huan L (2011) Expression of hepatitis B virus surface antigen determinants in *Lactococcus lactis* for oral vaccination. Microbiol Res 166:111–120
11. Ai C et al (2014) Genetically engineered *Lactococcus lactis* protect against house dust mite allergy in a BALB/c mouse model. PLoS One 9:e109461
12. Braat H et al (2006) A phase I trial with transgenic bacteria expressing interleukin-10 in Crohn's disease. Clin Gastroenterol Hepatol 4:754–759
13. Le Loir Y, Gruss A, Ehrlich SD, Langella P (1998) A nine-residue synthetic propeptide enhances secretion efficiency of heterologous proteins in *Lactococcus lactis*. J Bacteriol 180:1895–1903

Part X

Development of Tumor Vaccines

Chapter 43

Cancer Vaccines: A Brief Overview

Sunil Thomas and George C. Prendergast

Abstract

Vaccine approaches for cancer differ from traditional vaccine approaches for infectious disease in tending to focus on clearing active disease rather than preventing disease. In this review, we provide a brief overview of different types of vaccines and adjuvants that have been investigated for the purpose of controlling cancer burdens in patients, some of which are approved for clinical use or in late-stage clinical trials, such as the personalized dendritic cell vaccine sipuleucel-T (Provenge) and the recombinant viral prostate cancer vaccine PSA-TRICOM (Prostvac-VF). Vaccines against human viruses implicated in the development and progression of certain cancers, such as human papillomavirus in cervical cancer, are not considered here. Cancers express "altered self" antigens that tend to induce weaker responses than the "foreign" antigens expressed by infectious agents. Thus, immune stimulants and adjuvant approaches have been explored widely. Vaccine types considered include autologous patient-derived immune cell vaccines, tumor antigen-expressing recombinant virus vaccines, peptide vaccines, DNA vaccines, and heterologous whole-cell vaccines derived from established human tumor cell lines. Opportunities to develop effective cancer vaccines may benefit from seminal recent advances in understanding how immunosuppressive barricades are erected by tumors to mediate immune escape. In particular, targeted ablation of these barricades with novel agents, such as the immune checkpoint drug ipilimumab (anti-CTLA-4) approved recently for clinical use, may offer significant leverage to vaccinologists seeking to control and prevent malignancy.

Key words Sipuleucel-T, PSA-TRICOM, MAGE-A3, Algenpantucel-L

1 Introduction

Vaccines against cancer have been explored for over a century, but they have offered more hope than impact compared to the huge impact of vaccines against infectious diseases. However, unlike infectious disease vaccines, which focus mainly on disease prevention, cancer vaccines have focused mainly on disease treatment, a much higher bar to address, given the extant power of cancers on the immune system at levels little understood. Moreover, additional challenges for cancer vaccines to address are that the immune system in the patient is generally damaged, suppressed, or senescent, not only because of tumor burden but also the harmful experience of standard-of-care therapies and the advanced age of

Sunil Thomas (ed.), *Vaccine Design: Methods and Protocols: Volume 1: Vaccines for Human Diseases*, Methods in Molecular Biology, vol. 1403, DOI 10.1007/978-1-4939-3387-7_43,

most cancer patients. On a brighter note, the rapid recent increase in knowledge of immune effector mechanisms and molecular signals responsible for immune suppression is stimulating the development of new modalities with greater promise. In particular, new genetic tools and insights into the key inflammatory and immune molecules to manipulate immunity in cancer patients are presenting themselves. Two recent outstanding reviews are recommended for more in-depth consideration of this area [1, 2]. The brief overview offered here introduces some fundamental issues of specific interest to cancer vaccine development, followed by an illustrative consideration of several types of vaccines that incorporate various cellular and molecular principles, vectors, and clinical trial designs.

2 Tumor Antigens, Adjuvants, and T Cell Help

Questions about what constitutes the best tumor antigen and how to target it have attracted long-standing and mainly unresolved study. Unlike microbial antigens, tumor antigens vary enormously in different cancers and cancer patients. Thus, significant effort has been put into searching for antigens that are widely mutated or aberrantly expressed in specific types of cancer and that are also capable of stimulating efficacious immune responses in preclinical model systems. Two general distinctions in the cancer vaccines that have been studied are those that target specific tumor antigens (more often molecular vaccines) and those that do not discriminate (more often cellular vaccines). Cell lineage-specific proteins can be useful to target, particularly in cancers where the normal tissue may be surgically resected as part of the standard of care (e.g., prostate or breast cancer). Since tumor antigens represent "altered self," the induction of autoimmunity in preclinical and clinical studies by a cancer vaccine can be viewed in positive and negative contexts, depending on its severity and manageability. Consensus lists of tumor antigens considered attractive have been suggested although much work and debate continue [3].

Immunity to infectious disease produced by vaccination relies centrally on an effective adjuvant. Accordingly, adjuvant substances have received great attention from cancer vaccinologists but unfortunately without the breakthrough results produced as in the development of microbial vaccines. Pathogens, particulates, saponins, and emulsions such as incomplete Freund's adjuvant (e.g., Montanides) have all been explored extensively, especially in peptide and recombinant virus vaccine preparations. An excellent recent presentation of this area in detail can be found elsewhere [4].

Since most cancer vaccines have sought to recruit T cell immunity, there also has been much effort dedicated to defining mechanisms of T cell help most relevant to antitumor immune responses. CD4+ T cell help is critical to generate CD8+ T effector cells and CD8+ T memory cells that are closely associated with antitumor

immunity in many cancers (e.g., [5, 6]). However, as mentioned above, because of their similarity to normal cell proteins which are tolerated by the host, tumor antigens tend to trigger weak CD4+ T cell help responses. Thus, cancer vaccines that have been explored may integrate efforts to engage more florid CD4+ T cell help either directly or indirectly. For vaccines that target specific molecules, a complex phenomenon of "epitope spreading" involving drift of immune reactions to other nontargeted antigens is clearly associated with antitumor efficacy. However, limited mechanistic insights into this phenomenon remain scant, and strategies to leverage it in vaccines in any ritualized manner have yet to be done.

3 Patient-Derived Immune Cell Vaccines: Sipuleucel-T (Provenge)

Sipuleucel-T is an autologous dendritic cell (DC) vaccine used to treat prostate cancer that is generated by modifying patient-derived DC to express a fusion protein comprised of prostatic acid phosphatase (PAP) and granulocyte-macrophage colony-stimulating factor (GM-CSF). The treatment has three parts. Patient cells are collected and a leukapheresis method is used to extract the antigen-presenting DC. The cell preparation is then sent to a corporate production facility where they are co-incubated with the fusion protein, which is taken up, processed, and presented on the cell surface. The PAP antigen is nearly universally expressed in prostate cancer cells, and the GM-CSF provides a maturation factor for the DC. In this activated antigen-presenting state, the DCs are then returned to the infusion center where they are readministered to the patient. Three courses of treatment are administered over a period of 6 weeks to trigger an immune response against PAP-positive prostate cancer cells.

In three clinical trials in advanced prostate cancer patients, sipuleucel-T treatment did not significantly extend time to progression, but it did safely lengthen overall survival of patients for an average of 4 months [7]. The vaccine was approved by the US FDA in 2010 as the first immunotherapeutic product to treat cancer, in this case asymptomatic or minimally symptomatic metastatic hormone-refractory prostate cancer. While it was assigned "category 1" status (highly recommended treatment), there has been controversy about its use due to high cost and limited benefits to patients. However, there are now 20 active trials (about half of which have completed recruitment) to test whether sipuleucel-T efficacy can be extended when combined with other standard, approved, and experimental therapies (clinicaltrials.gov). Although the impact of this vaccine has been limited in practical terms to date, its development and continued investigation have offered a clinical proof of concept for the safe and at least partially effective application of immunological principles in managing an advanced cancer that is generally intractable.

4 Recombinant Viral Vaccines Expressing Tumor Antigens: PSA-TRICOM (Prostvac-VF)

PSA-TRICOM is a recombinant viral vaccine that has been developed to treat advanced prostate cancer. The viral backbone is based on poxvirus sequences (derived from vaccinia or fowl pox) which enable expression of prostate-specific antigen (PSA) along with three immune-stimulatory T cell receptor co-regulatory molecules (LFA-3, ICAM-1, and B7.1 comprising the TRICOM element). These co-regulatory molecules were chosen to activate host DC and cytotoxic T effector cells that recognize and kill PSA-expressing prostate cancer cells. As a recombinant poxvirus, PSA-TRICOM is an off-the-shelf vaccine that is directly administered as an injection to patients. As employed clinically, the vaccinia-based vaccine is used to prime patients followed by six booster injections with the fowl pox-based vaccine.

In a Phase II clinical trial of 125 patients with minimally symptomatic metastatic prostate cancer, PSA-TRICOM was administered with GM-CSF (to promote DC activation) and compared to a control arm administered with saline. Similar to the sipuleucel-T findings, PSA-TRICOM vaccination did not affect progression-free survival (PFS), but it did extend overall survival by approximately 8 months [8]. Toxicity was low with fever, nausea, fatigue, and injection site reactions, the most common adverse events. Given this encouraging result, several trials of PSA-TRICOM in combinatorial regimens are now under way, including a highly anticipated study with the immune checkpoint inhibitor ipilimumab [9, 10], along with a global Phase III trial (PROSPECT) orchestrated by the US National Cancer Institute to validate the Phase II results.

5 Peptide Vaccines: MAGE-A3 and NY-ESO1

Among a large number of explorations of peptide antigen-based vaccines, the investigation of the widely expressed tumor antigens MAGE-A3 and NY-ESO1 stands out as paradigms. These antigens are both members of a class of "cancer-testis" antigens of obscure function that are normally expressed in testes but also overexpressed in a large number of diverse human cancers, including in lung cancers and melanomas where they have been explored deeply. Numerous preclinical and clinical studies have indicated that MAGE-A3 and MAGE-A3 fusion proteins formulated with classical immune adjuvants can trigger humoral and cellular immune responses in cancer subjects. However, a large Phase III trial of a MAGE-A3 fusion protein with *H. influenzae* protein D formulated with a proprietary adjuvant (MAGRIT) was stopped in 2014

due to a lack of benefit to lung cancer patients who received it. While this was a disappointing result, there remain over a dozen other clinical trials of MAGE-A3 in this and other disease settings to explore therapeutic combinations, adjuvant selection, and patient selection criteria, among other factors. One shortcoming of short peptide vaccines can be a failure to induce memory CD8+ T cell responses [11], although it is not at all clear this factor can explain the outcome of MAGRIT. On the other hand, smaller trials of virally expressed NY-ESO1 have been encouraging and many studies of this peptide-based vaccine continue, with particular interest in combination studies such as with ipilimumab, like PSA-TRICOM.

6 DNA Vaccines

DNA vaccines offer the opportunity to engineer protein and peptide antigen expression with more detailed design and delivery parameters, for example, to selectively express or assure suitable posttranslational modification of an antigen in the desired target cell and to enhance antigenicity and responsiveness. A vast number of preclinical studies involving numerous "gene vaccines" have established the capability to engender efficacious T cell-mediated tumor attacks against any number of target antigens [12]. These vectors may also often incorporate T cell help-inducing genes, including cytokines, chemokines, co-stimulatory molecules, or DC-targeting antibodies [13]. A similarly vast number of adjuvant and carrier formulations have been explored in both preclinical and clinical trials, with variable success. More recently, skin electroporation methods have been developed that can readily administer DNA vaccines in clinical settings. Briefly, an electric current is delivered across the tissue site at the time of vaccine injection, increasing dose levels and creating a local inflammation that helps recruit antigen-presenting cells and amplify immune responses. In general, DNA vaccination is very well tolerated with little or no side effects beyond the vaccination site. Early concerns about genomic integration or anti-DNA responses that might promote autoimmunity in patients have not proven to be issues [13].

7 Whole-Cell Vaccines Derived from Established Human Tumor Cell Lines: Algenpantucel-L (HyperAcute Pancreas)

A variety of whole-cell vaccines have been explored in human studies historically but with generally limited efficacy. One recent variation that has generated interest has incorporated the human hyperacute immune response into an "off-the-shelf" whole-cell vaccine composed of genetically modified human tumor cell lines

[14, 15]. The hyperacute response is a robust mechanism of xenograft transplant rejection mediated by complement-fixing natural antibodies that recognize alpha-1,3-galactosyl (α-Gal) epitopes, a common cell surface structure found throughout evolution except in certain primate species including humans. Notably, α-Gal antibodies represent 1–2 % of all antibodies in the human peripheral blood, such that a powerful pro-inflammatory stimulus is triggered upon ligand recognition on any foreign species or tissue. In essence, the vaccine strategy coats human tumor cell lines that are lethally irradiated before subdermal injection on a traditional prime and boost schedule [16].

Whole-cell vaccines that exploit this unique pro-inflammatory mechanism have been established to be efficacious in promoting long-lasting antitumor immunity and overall survival in preclinical studies and ongoing clinical studies of resected pancreatic cancer [16]. Roving host DC readily opsonize and phagocytose the α-Gal-coated tumor cells, delivering a large number of tumor cell antigens for processing and presentation to T cells in local lymph nodes. In a Phase II study of 70 resected pancreatic cancer patients, algenpantucel-L was administered in the adjuvant setting and compared to a control arm receiving chemoradiation according to the RTOG-9704 standard of care. Disease-free survival was nearly twice the control arm at the primary endpoint despite a larger proportion of patients with node-positive disease in the experimental arm [16]. Prompted by this result, a randomized Phase III trial started in 2010 to enroll a total of 722 patients, representing the largest clinical trial of resected pancreatic cancer patients performed to date. A second Phase III study has also been initiated more recently to explore combination with standard chemotherapy and chemoradiation in 280 patients with borderline resectable or locally advanced PDA (NCT01836432).

References

1. Butterfield LH (2015) Cancer vaccines. BMJ 350:h988
2. Schlom J, Hodge JW, Palena C, Tsang KY et al (2014) Therapeutic cancer vaccines. Adv Cancer Res 121:67–124
3. Cheever MA, Allison JP, Ferris AS, Finn OJ et al (2009) The prioritization of cancer antigens: a national cancer institute pilot project for the acceleration of translational research. Clin Cancer Res 15:5323–5337
4. Hearnden C, Lavelle EC (2013) Adjuvant strategies for vaccines: the use of adjuvants within the cancer vaccine setting. In: Prendergast GC, Jaffee EM (eds) Cancer immunotherapy: immune suppression and tumor growth, 2nd edn. Elsevier, New York, p 655
5. Galon J, Costes A, Sanchez-Cabo F, Kirilovsky A et al (2006) Type, density, and location of immune cells within human colorectal tumors predict clinical outcome. Science 313:1960–1964
6. Angell H, Galon J (2013) From the immune contexture to the Immunoscore: the role of prognostic and predictive immune markers in cancer. Curr Opin Immunol 25:261–267
7. Sobol I, Thompson RH, Dong H, Krco C, Kwon ED (2015) Immunotherapy in prostate cancer. Curr Urol Rep 16:34
8. Kantoff PW, Schuetz TJ, Blumenstein BA, Glode LM et al (2010) Overall survival analysis of a phase II randomized controlled trial of a Poxviral-based PSA-targeted immunotherapy

in metastatic castration-resistant prostate cancer. J Clin Oncol 28:1099–1105
9. Jochems C, Tucker JA, Tsang KY, Madan RA et al (2014) A combination trial of vaccine plus ipilimumab in metastatic castration-resistant prostate cancer patients: immune correlates. Cancer Immunol Immunother 63:407–418
10. Madan RA, Mohebtash M, Arlen PM, Vergati M et al (2012) Ipilimumab and a poxviral vaccine targeting prostate-specific antigen in metastatic castration-resistant prostate cancer: a phase 1 dose-escalation trial. Lancet Oncol 13:501–508
11. Rezvani K, Yong AS, Mielke S, Jafarpour B et al (2011) Repeated PR1 and WT1 peptide vaccination in Montanide-adjuvant fails to induce sustained high-avidity, epitope-specific CD8+ T cells in myeloid malignancies. Haematologica 96:432–440
12. Rice J, Ottensmeier CH, Stevenson FK (2008) DNA vaccines: precision tools for activating effective immunity against cancer. Nat Rev Cancer 8:108–120
13. Stevenson FK, di Genova G, Ottensmeier CH, Savelyeva N (2013) Genetic vaccines against cancer: design, testing and clinical performance. In: Prendergast GC, Jaffee EM (eds) Cancer immunotherapy: immune suppression and tumor growth, 2nd edn. Elsevier, New York, p 655
14. Rossi GR, Mautino MR, Unfer RC, Seregina TM, Vahanian N, Link CJ (2005) Effective treatment of preexisting melanoma with whole cell vaccines expressing alpha(1,3)-galactosyl epitopes. Cancer Res 65:10555–10561
15. Rossi GR, Unfer RC, Seregina T, Link CJ (2005) Complete protection against melanoma in absence of autoimmune depigmentation after rejection of melanoma cells expressing alpha(1,3)galactosyl epitopes. Cancer Immunol Immunother 54:999–1009
16. Springett GM (2014) Novel pancreatic cancer vaccines could unleash the army within. Cancer Control 21:242–246

Chapter 44

Dendritic Cell Vaccines

Rachel Lubong Sabado, Marcia Meseck, and Nina Bhardwaj

Abstract

Exploitation of the patient's own immune system to induce antitumor immune responses using dendritic cell (DC) immunotherapy has been established in early clinical trials as a safe and promising therapeutic approach for cancer. However, their limited success in larger clinical trials highlights the need to optimize DC vaccine preparations. This chapter describes the methodologies utilized for the preparation of the DC vaccine most commonly used in clinical trials. Optional variations at different stages in DC vaccine preparation, based on the nature of antigen, delivery of antigen, maturation stimuli, and mode of administration for DC vaccines, are also presented for consideration as these are often dependent on the disease setting, desired immune response, and/or resources available.

Key words Dendritic cell, Vaccine, Immunotherapy, Immune response, Tumor

1 Introduction

Dendritic cells (DCs) are commonly recognized as the most potent antigen-presenting cells (APCs), capable of activating both naïve and memory immune responses [1]. Myeloid (mDC) and plasmacytoid (pDC) represent the two major types of DCs found in the peripheral blood. mDCs are found in peripheral tissues, lymphoid organs, and blood and secrete large amounts of interleukin-12 (IL-12) upon activation, which drives immune responses that counter pathogenic organisms or suppress neoplastic cell growth [2, 3]. pDCs are primarily found in the blood and lymphoid organs and can produce up to 1000-fold more type 1 IFNs in response to viral infections than other cell types [4] and have also been implicated in antitumor immunity [5]. However, since these DCs represent only 0.1 % of peripheral blood mononuclear cells (PBMCs), it is difficult and expensive to obtain sufficient numbers of DCs for vaccination.

The method described in this chapter is the most commonly used approach for generating large numbers of DCs for vaccina-

Sunil Thomas (ed.), *Vaccine Design: Methods and Protocols: Volume 1: Vaccines for Human Diseases*, Methods in Molecular Biology, vol. 1403, DOI 10.1007/978-1-4939-3387-7_44, © Springer Science+Business Media New York 2016

tion in clinical trials for cancer and HIV [6–8]. DCs are differentiated from monocytes over a 6–7-day culture period. Monocytes are selected from PBMC based on plastic adherence then cultured for 5 days in the presence of IL-4 and GM-CSF to generate immature DCs. These immature DCs are stimulated to mature by culturing for an additional 1–2 days in the presence of a maturation stimulus to induce differentiation [9, 10]. Given the complexity of DC biology and the lack of controlled comparative studies of the different methods for the preparation of DC vaccines, alternative methods are also discussed.

1.1 DC Preparation

Patients undergo an apheresis procedure or multiple large-volume blood draws to collect sufficient numbers of PBMCs for the culture. Monocytes are selected from PBMCs on the basis of plastic adherence. Alternatively, monocytes may be positively selected using immunomagnetic beads. Monocytes are then cultured in the presence of IL-4 and GM-CSF. After 5 days under these conditions, the monocytes will have differentiated into immature DCs. The immature DCs are induced to become mature DCs through the addition of maturation stimuli to the culture medium. DCs derived using this process are called monocyte-derived DC (MDDC).

Alternative methods for generating sufficient numbers of DCs for clinical trials are available. CD34+ precursors mobilized from the bone marrow by treating patients with G-CSF prior to harvesting by apheresis can also be used to generate DCs [11]. One-week in vitro expansion of the harvested cells in the presence of GM-CSF, Flt3L, and TNFα produces a mixture of MDDCs, DCs that are phenotypically similar to epidermal Langerhans cells (LC), and a large proportion of myeloid cells at different stages of differentiation. Administration of Flt3L for 10 days induces the in vivo expansion of circulating DCs, i.e., 48-fold expansion of mDC and 13-fold expansion of pDC [12]. Sipuleucel-T, the first FDA-approved cell-based therapy for the treatment of hormone-refractory prostate cancer [13], consists of DCs, B cells, monocytes, and NK cells that are cultured ex vivo with a recombinant fusion protein containing prostatic acid phosphatase (PAP) and GM-CSF, before being administered back into patients within 48 h of the apheresis collection [14].

Although transcriptional profiling of DCs generated by these various methods demonstrates fundamental functional differences [15] between them, all of these DCs have stimulated antigen-specific T cell responses in both preclinical and clinical studies. However, there has been no direct comparison of DC generated by the different methods in controlled clinical trials.

1.2 Maturation of DC

Maturation of DCs is a terminal differentiation process that transforms DCs from cells specialized in antigen capture into those geared toward stimulation of immune responses. Matured DCs

exhibit increased expression of costimulatory molecules, enhanced migration into the lymph nodes, and produce the cytokines and chemokines necessary for activating effective T cell responses [16]. As different maturation stimuli can produce DCs with significant phenotypic and functional differences, selection of the appropriate maturation stimulus is important in determining the type of responses to be elicited by the DC vaccine.

Thus far, the majority of clinical trials have used a cocktail of proinflammatory cytokines consisting of TNFα, IL-1β, and IL-6 and PGE_2 to mature DCs. This cocktail of cytokines has been demonstrated to induce the upregulation of MHC class I and II, CD40, CD80, CD86, and CCR7 after 2 days in culture but no IL-12p70 [17]. Despite the apparent lack of IL-12p70 production when compared to other DC maturation stimuli (CD40L trimer, poly-I:C, and LPS), the above cytokine cocktail induced the most uniform maturation in terms of upregulation of DC maturation markers, greatest overall yields and recovery, highest levels of allogeneic T cell proliferation and cytokine production, and priming of Th1 responses [17]. However, the inclusion of PGE_2 may induce differentiation of regulatory T cells and Th2 responses [18], IDO expression [19], and deficiency in IL-12p70 production [20].

Toll-like receptor (TLR) agonists induce differential activation of systemic and local innate immune responses in vivo [21]. TLR activation on DCs induces their maturation, upregulation of costimulatory molecules, and production of cytokines and chemokines [22]. As DCs express a full complement of TLRs, the simultaneous triggering of multiple TLRs on DCs may mediate synergistic effects on DC function resulting in the production of supramolecular levels of IL-12 [23, 24]. Thus, TLR agonists have the potential for inducing optimal DCs for stimulating effective immune responses and conditioning the environment in vivo to favor the development of immune responses. The method described here incorporates the use of the TLR 3 agonist poly-ICLC to mature DCs. DCs stimulated with poly-ICLC have been shown to exhibit the highest production of proinflammatory cytokines and greatest activation of tumor-specific CD8+ T cell responses when compared to other TLR agonists, such as the TLR 4 agonist, LPS, and the TLR 7/TLR 8 agonist R848 [25].

An alternative method for maturing DCs that is currently employed for clinical trials incorporates the use of CD40 ligand (CD40L), which is expressed primarily by activated T cells and B cells and is a principal component of CD4 T cell help that binds to CD40 on DCs [7]. The use of a cytokine cocktail consisting of TNFα, IL-1β, poly-ICLC, IFNα, and IFNγ induces the maturation of DCs called alpha type 1-polarized DCs with the capacity to produce high levels of IL-12p70, migrate in response to CCR7 ligands, and induce CTL responses [26, 27].

1.3 Nature and Delivery of Antigens

Given the characterization of tumor-associated antigens (TAAs) from numerous tumors that elicit cytotoxic T cell responses, tumor cells can be specifically targeted with little or no harmful effect on normal cells. Vaccine approaches targeting TAAs such as cancer/testis [28] and melanocytic differentiation antigens have already been evaluated in clinical trials, but with limited success [29]. Newer approaches for identifying unique tumor antigens to be targeted utilize a combination of high-throughput sequencing of individual tumors to identify tumor-specific somatic variations and statistical models to characterize mutated tumor antigens called neoantigens [30]. This technology can identify somatic variations that are specific to the malignant cells within a given subject's tumor. Carreno et al. recently showed that tumor missense mutations can be specifically and successfully targeted by DC vaccination [31].

Proper delivery of antigens to DCs is critical in determining appropriate activation of CD4+ T cells and/or CD8+ T cells. DCs are typically loaded through incubation with peptides, proteins, or irradiated tumor cells [32]. The choice may be dependent on available resources. Short synthetic peptides (8–15 aa) that correspond to defined epitopes within these TAAs have been used in clinical trials. However, the use of short peptides requires knowledge of the patient's MHC and the defined epitopes that would bind these specific MHC molecules. Synthetic long peptides (SLPs) that are 28–35 aa long and therefore unable to bind directly on MHC molecules are also under investigation [33]. SLPs are preferentially taken up, processed, and presented by DCs via cross presentation [34] leading to activation of both CD4+ and CD8+ T cell responses.

DCs loaded with proteins [35] and autologous or allogeneic tumor/tumor cell line lysates [7, 36–39] have also been used in numerous cancers. An ongoing phase III study in glioblastoma multiforme (GBM) uses autologous tumor lysates loaded on DCs (NCT00045968) [40]. The key advantages to using this strategy are the presence of multiple epitopes presented on different haplotypes with the potential to induce immune responses to a wide spectrum of antigens and prolonged antigen presentation due to the requirement for processing [41].

Bacterial and viral vectors encoding genes expressing TAAs have also been used to load DCs [6, 42–47]. These vectors not only have the ability to elicit natural immune responses against the vector of choice thereby enhancing the immunogenicity of TAAs, but some of them also have the ability to simultaneously induce the maturation of DCs thereby bypassing the need for a separate maturation stimulus. However, preexisting immunity against the vector may limit their ability to induce immune responses in vivo.

Transfection of DCs with mRNA-encoding TAA has been demonstrated to induce potent tumor antigen-specific T cell

responses [48–51]. DCs can be transfected using a cationic lipid, i.e., DOTAP, or mRNA alone via electroporation [52]. Electroporation of DCs has been successfully used in preclinical [53–55] and clinical [56] studies for tumor immunotherapy. Autologous DCs electroporated with RNA-encoding CD40L and HIV antigens were demonstrated to be safe and induced HIV-specific immune responses [57].

1.4 Administration of DC Vaccines

Effective migration to lymph nodes is essential in order for DCs to stimulate T cell responses [58]. Although DC vaccines have been administered using various routes (intradermally, subcutaneously, intravenously, or intratumorally), the optimal route of administration for DC vaccines has yet to be established. Intradermally administered indium-111-labeled MDDC loaded with melanoma peptides remained primarily at the injection site, lost viability, and were cleared within 48 h. More importantly, <5 % of the administered DC vaccine reached the draining lymph nodes [59]. Intratumorally administered DCs remained largely at the injection sites, and none were detected in the draining lymph nodes [60, 61]. On the other hand, intranodally administered MDDC loaded with melanoma peptides redistributed to multiple lymph nodes within 30 min of injection. However, despite direct delivery of DCs into the lymph nodes, the immunologic responses elicited were comparable [59] or no better [61] than those observed with intradermally administered DC vaccine. Interestingly, DC vaccines may not be directly responsible for activating T cells. Instead, DC vaccines act as vehicles for transferring antigens to endogenous APCs which are directly responsible for activating T cell responses [62]. In a recently published study, Mitchell et al. [63] demonstrated that preconditioning the DC vaccine site with the tetanus/diphtheria toxoid (Td) vaccine led to superior DC migration and was associated with improved overall survival (OS) in patients with GBM.

1.5 Clinical Trials

Clinical trials of antigen-pulsed DCs conducted in patients have demonstrated that antigen-loaded DC vaccines are safe and a promising therapeutic approach for cancer and HIV [1]. Some recent clinical trials have shown some exciting clinical responses. DC vaccination in HIV was shown to induce immune responses that were associated with control of viral replication [64]. A study in a small cohort of GBM patients reported 2× longer survival in 50 % of vaccinated patients as compared to standard of care [63]. The results of ongoing large phase III trials testing the efficacy of DC vaccines pulsed with autologous tumor preparations in renal cancer (NCT01582672) and GBM (NCT00045968) should provide additional information regarding the efficacy of this treatment modality.

2 Materials

2.1 Biologicals (See Note 1)

1. Autologous peripheral blood mononuclear cells (PBMCs).
2. Autologous plasma.

2.2 Reagents

1. Recombinant human interleukin-4 (IL-4) (GMP IL-4, R&D Systems). Lyophilized product may be stored up to 1 year in −80 °C. Stock solution (400 IU/μL): reconstitute 1 vial of GMP IL-4 in 5 % human albumin at 400 IU/μL based on the specific activity of the lot used [specific activity (IU/μg) = (1 ÷ ED50) × 10^3]. The presence of albumin in the stock solution helps to stabilize proteins in solution. Reconstituted IL-4 stocks may be stored at −80 °C for up to 3 months. Final working concentration (400 IU/mL): add 1 μL IL-4 stock solution per mL culture medium. Culture medium containing IL-4 at the final concentration may be stored at 4 °C for 1–2 weeks.
2. Recombinant human granulocyte-macrophage colony-stimulating factor (GM-CSF) (Leukine, Sanofi-Aventis). Stock solution (100 IU/μL): reconstitute 1 vial of Leukine with 14 mL 5 % human albumin. The use of albumin helps to stabilize proteins in solution. Reconstituted GM-CSF stocks may be stored at 4 °C for no more than 20 days. Final working concentration (100 IU/mL): add 1 μL GM-CSF stock solution per mL culture medium. Culture medium containing GM-CSF at the final concentration may be stored at 4 °C for 1–2 weeks.
3. Heat-inactivated human autologous plasma. Autologous plasma is clarified by centrifugation at 2000 × *g* for 20 min at room temperature to pellet any residual platelets. The plasma is then transferred to new conical tubes and heat-inactivated for 35 min in a 56 °C water bath. After inactivation, the plasma is centrifuged at 2000 × *g* for 20 min to remove any precipitated material. The clarified, heat-inactivated plasma is collected, aliquoted, and stored at −80 °C until used. The plasma will be used in the culture medium for DC generation, as well as the freezing medium for the DC vaccine. Collecting 200 mL of autologous plasma during the apheresis should be sufficient volume for a standard DC vaccine batch.
4. RPMI-1640 with l-glutamine (Lonza).
5. 1 M HEPES buffer (Lonza).
6. Dimethyl sulfoxide (DMSO) (CryoMACS DMSO, Miltenyi Biotec).
7. Poly-ICLC (Hiltonol, Oncovir, Inc.), 2 mg/mL. Poly-ICLC is in a ready-to-use formulation that is stored at 4 °C. Do not allow the poly-ICLC to freeze. Once opened, poly-ICLC must be used within 2 h as any exposure to RNAse may degrade the product.

8. Human albumin, 5 % solution, USP (Grifols).
9. RPMI/1 % plasma: add 5.1 mL 1 M HEPES and 5.1 mL autologous heat-inactivated plasma to 500 mL RPMI-1640 with l-glutamine. Filter using a 500 mL 0.2 μm Stericup.
10. Freezing medium: 90 % autologous heat-inactivated plasma and 10 % DMSO. For optimal effect, this needs to be prepared fresh and must be kept at 4 °C until used.

2.3 Supplies

1. 225 cm^2 tissue culture flasks (Falcon).
2. 6-well tissue culture plates (Falcon).
3. 50 mL conical tubes (Falcon).
4. 1.8 mL cryovials (Nunc).
5. 500 mL 0.2 μm Stericup (Millipore).

2.4 Equipment

1. Biosafety cabinet.
2. Centrifuge.
3. CO_2 incubator.
4. Inverted microscope.
5. Water bath.
6. Cell counter.
7. Controlled rate freezer.
8. Liquid nitrogen storage freezer.

3 Methods

3.1 D0: Initiate Culture

1. Resuspend PBMCs at a concentration of $1.6–2.2 \times 10^8$ cells/mL in RPMI/1 % plasma (*see* **Note 2**).
2. Seed each flask by adding 1 mL of the PBMC suspension per 225 cm^2 flask. Add 39 mL RPMI/1 % plasma to each flask to bring the final volume to 40 mL/flask.
3. Incubate the flasks in a horizontal position for 1–2 h at 37 °C with 5 % CO_2. Do not stack the flasks on top of each other (*see* **Note 3**).
4. During incubation, prepare RPMI/1 % plasma with cytokines (400 IU/mL IL-4 and 100 IU/mL GM-CSF) and warm to room temperature (*see* **Note 4**).
5. Warm additional bottles of plain RPMI-1640 by placing them at 37 °C. Alternatively, these bottles of RPMI-1640 may be left at room temperature during the incubation period. These will be used for washing the flasks.
6. Remove the flasks from the incubator at the end of the incubation period.

7. Gently swirl the flask and carefully aspirate the medium.
8. Wash each flask by adding 25 mL prewarmed plain RPMI-1640 and pipetting up and down to dislodge loosely adherent cells (*see* **Note 5**). The wash steps may be repeated as necessary to remove all loosely adherent cells.
9. After washing, add 40 mL of the RPMI/1 % plasma with cytokines to each flask.
10. Continue incubating the flasks in a horizontal position at 37 °C with 5 % CO_2.

3.2 Day 2/3: Feeding with Cytokines

1. Prepare RPMI/1 % plasma with 40× cytokines (40 μL of each cytokine per mL of culture medium).
2. Remove the flasks from the incubator and examine the cells under the microscope (*see* **Note 6**).
3. Add 1 mL RPMI/1 % plasma with 40× cytokines to each flask. Mix well by gentle swirling.
4. Place the flasks back into the incubator and continue incubating at 37 °C with 5 % CO_2.

3.3 Day 5: Harvest Immature DCs

1. Remove the flasks from the incubator and examine them under the microscope (*see* **Note 7**).
2. Harvest the suspended cells and conditioned medium from the flasks and transfer to 50 mL conical tubes.
3. Carefully and thoroughly wash the flasks with cold RPMI/1 % plasma to remove loosely adherent cells (*as described in* **Note 5**). Wash steps may be repeated as needed. Examine the flasks between washes to maximize collection of loosely adherent cells. The wash solution should also be collected in the 50 mL conical tubes (*see* **Note 8**).
4. Centrifuge the 50 mL conical tubes at $500 \times g$ for 6 min at room temperature.
5. Aspirate the supernatant from all tubes and resuspend the cells in a small volume of RPMI/1 % plasma (*see* **Note 9**).
6. Combine the contents of all tubes into a single tube. Perform a cell count to determine cell concentration and viability (*see* **Note 10**).
7. Resuspend the cells at a concentration of $1.5–2.0 \times 10^6$ cells/mL in RPMI/1 % plasma with 1× cytokines.
8. Add 1 mL of cells per well in 6-well tissue culture plates. Add an additional 2 mL of RPMI/1 % plasma with 1× cytokines to each well (total volume = 3 mL/well).
9. Add the antigen(s) of interest to each well (*see* **Note 11**). Gently swirl the plates to mix.

10. Incubate the plates at 37 °C with 5 % CO_2 for 1 h.
11. At the end of the 1 h incubation, add 15 μg poly-ICLC to each well (final concentration (5 μg/mL)). Gently swirl the plates to mix and continue incubating at 37 °C with 5 % CO_2 (*see* **Note 12**).

3.4 Day 6: Harvest Mature DCs

1. Remove the plates from the incubator and examine them under the microscope (*see* **Note 13**).
2. Harvest the cells from the plate and transfer to 50 mL conical tubes.
3. Centrifuge the tubes at 500 × *g* for 6 min at 4 °C.
4. Resuspend the cells in a small volume of RPMI/1 % plasma.
5. Perform a cell count to determine the cell concentration and viability (*see* **Note 14**).
6. Prepare freezing medium (90 % autologous, heat-inactivated plasma/10 % DMSO). Keep on ice or at 4 °C until needed.
7. Centrifuge tubes at 500 × *g* for 6 min at 4 °C.
8. Resuspend cells in freezing medium at the desired vaccine concentration (no more than 5×10^7 cells/mL) (*see* **Note 15**).
9. Aliquot at 1 mL per 1.8 mL cryovial.
10. Place cryovials in the controlled rate freezer. Run the default program in the controlled rate freezer for 1.8 mL vials (*see* **Note 16**).
11. Once the controlled rate freezer run has completed, transfer the cryovials to the liquid nitrogen storage freezer (*see* **Notes 17** and **18**).

4 Notes

1. PBMCs and plasma used for the differentiation of DCs are typically collected by an apheresis procedure. A standard non-mobilized apheresis procedure yields approximately $5\text{-}15 \times 10^9$ PBMCs. 200 mL of autologous plasma is also collected at the same time. These are then frozen in aliquots and thawed for DC vaccine production. PBMCs and plasma to be used for the culture will need to be tested and meet the specifications for sterility, mycoplasma, and endotoxin prior to the start of production.
2. Plating PBMCs at this cell concentration will ensure proper saturation of monocytes on the surface of the flask. Monocytes typically account for 10–30 % of the total white blood cells in peripheral blood.

3. During the incubation period, adherent cells such as monocytes will attach to the plastic surface of the flask, while other cells will remain in suspension (non-adherent). By not stacking the flasks on top of each other, the individual flasks will be able to equilibrate more quickly to the incubator temperature during the 1–2 h incubation. It is typically not recommended to go over 2 h during this incubation process as the desired cells may begin to die. Alternatively, CD14+ monocytes may be positively selected using CD14 magnetic beads (Miltenyi Biotec). The CD14+ monocytes will then be incubated with GM-CSF and IL-4 to induce differentiation into immature DCs.
4. The addition of GM-CSF and IL-4 will induce the differentiation of monocytes into immature DCs. GM-CSF is required for cell survival and promotes differentiation of monocytes into DCs. IL-4 ensures that the monocytes differentiate into DCs and not macrophages. Varying doses of GM-CSF and IL-4 have been used by others to differentiate DCs. In our experience, 400 IU/mL IL-4 and 100 IU/mL GM-CSF in the culture medium is sufficient to induce monocyte differentiation into DCs. It is important to note that the specific activity of IL-4 will vary by lot and manufacturer; therefore, it is essential that the specific activity of the specific lot used be confirmed prior to reconstitution.
5. Washing the flasks well with prewarmed or room temperature media is important in order to remove non-adherent cells and ensure a high purity of monocytes in the flasks at the start of the culture. When washing the flasks, always tilt the flasks toward one side. Gently pipette the medium up and down over different areas of the flasks to ensure even washing of the entire flask. Carefully aspirate the wash medium by placing the pipette tip to one side. Be careful not to let the tip of the aspirating pipette touch the surface of the flasks where the monocytes have adhered. Wash steps may be repeated as needed. Check efficiency of washing by looking at the flasks under the microscope after each wash. There should be only a small number of floating cells in the flask. The most common contaminants are B cells, T cells, and platelets. Although the growth of these cells is not supported by the addition of GM-CSF and IL-4, a small fraction of these cells may be carried throughout the culture period and be detected as a contaminant in the end product.
6. The process of differentiation from monocytes to DCs is still ongoing. Refreshing the culture with cytokines at either Day 2 or Day 3 ensures continued differentiation.
7. During the 5-day culture period, the monocytes differentiate into immature DCs. The immature DCs will easily detach

from the plastic surface of the flask. Debris from dead or dying cells may also be evident at this time, but it should be reasonable to expect a yield of 10–15 % from the starting PBMC cell number at Day 0. Losses in specific activity for the cytokine(s) may lead to lower than expected yields. An observation that there is a significant degree of cell death may be due to the loss of GM-CSF activity, while the presence of a significant number of firmly adherent cells may be due to the loss of IL-4 activity.

8. After harvesting the cell suspension from the flasks, there may be a small proportion of cells that remain firmly adherent to the surface of the flasks. These firmly adherent cells are likely macrophages and are not DCs. There is no need to scrape the flasks to collect these firmly adherent cells.
9. A small volume of conditioned medium is typically saved and used for "in-process" testing for sterility and the presence of mycoplasma.
10. Harvested cells should have the morphology of immature DCs, which are relatively large round cells with few or no cytoplasmic extensions. Immature DCs are larger than lymphocytes and loosely adherent.
11. DCs can be loaded with antigen in various forms, such as short peptides, long peptides, whole proteins, and tumor lysates. Short peptides do not require long incubation periods as they do not require processing and are directly loaded into MHC molecules on the surface of the DCs. Long peptides, whole proteins, and tumor lysates require processing and therefore require a longer incubation period, but, typically, no longer than overnight incubation is needed.
12. In order to allow for antigen uptake to take place prior to maturation, 5–10 μg/mL poly-ICLC (polyinosinic-polycytidylic acid-poly-l-lysine carboxymethylcellulose; Hiltonol, Oncovir Inc.) will not be added as a maturation stimulus until an hour after addition of the antigens.
13. Mature DCs have characteristic cytoplasmic extensions from which their name is derived. They are large and non-adherent. Some cell death or debris will also be present.
14. Between Day 5 and Day 6, approximately 30–40 % of the cells will die. Therefore, the overall matured DC yield will be 5–10 % based on the starting PBMC cell count at Day 0.
15. The amount of cells frozen in each aliquot is dependent on the desired number of DCs for each dose of vaccination. The number of DCs administered for each dose of vaccination has ranged from a few million to tens of millions of DCs per injection. The major determining factors for this is the yield of DCs from the preparations and also the number of vaccinations required by the protocol.

16. DCs are frozen using a controlled rate freezer, which is a programmable unit for freezing cells. Using a controlled rate freezer provides greater control over the rate and uniformity of cooling, which is important for preserving cell viability. Alternatively, a Mr. Frosty or similar device may be used; however, the rate of cooling using these alternative methods may vary and could compromise the cell viability observed when the DCs are thawed. After completing the freezing program, the vials of cells are typically stored in the vapor phase of a liquid nitrogen storage freezer. Vials stored in the liquid phase will need to be properly sealed in order to prevent penetration by liquid nitrogen, which can lead to pressure buildup within the vials causing the vials to "explode" upon thawing and could also be a potential source of contamination.
17. All DC vaccines undergo lot release testing prior to administration into patients. Lot release testing for DC vaccines typically includes sterility, endotoxin, mycoplasma, identity by flow cytometry, and potency. By flow cytometry, DCs should express CD11c and have low or negative expression of CD14 with high expression of CD40, CD80, CD86, and HLA-DR. Fully mature DCs will express the canonical maturation marker CD83, although expression will vary from donor to donor and with the maturation stimuli used. Typical potency testing includes stimulation via mixed leukocyte reaction or cytokine secretion (Table 1). Only DC vaccines that meet all of the specifications for lot release testing will be administered into patients.
18. DC vaccines are stored in the liquid nitrogen storage. On the day of administration, one vial of DC vaccine is thawed in a 37 °C water bath, drawn up into the syringe, and administered within 30–60 min after thawing.

Table 1
Lot release testing

Test	Method	Criteria
Cell viability	Trypan blue or equivalent	>70 %
Identity	Flow cytometry—% CD11c+	>50 %
	Flow cytometry—% CD11c+CD14+	<30 %
	Flow cytometry—% CD11c+CD83+	>50 %
Sterility	Direct culture	Negative
Mycoplasma	FDA points to consider	Negative
Endotoxin	Kinetic chromogenic LAL assay	<50 EU/mL
Potency	Cytokine production	Report results

Acknowledgements

We would like to thank Andres Salazar for providing the poly-ICLC. We would also like to thank the staff of the Vaccine and Cell Therapy Laboratory—Farah Hasan, Hanqing Dong, Bike Su Oner, and Marina Aziz—for the help in refining the procedure.

References

1. Palucka K, Banchereau J (2013) Dendritic-cell-based therapeutic cancer vaccines. Immunity 39:38–48
2. Trinchieri G (2003) Interleukin-12 and the regulation of innate resistance and adaptive immunity. Nat Rev Immunol 3:133–146
3. Vignali DA, Kuchroo VK (2012) IL-12 family cytokines: immunological playmakers. Nat Immunol 13:722–728
4. McKenna K, Beignon AS, Bhardwaj N (2005) Plasmacytoid dendritic cells: linking innate and adaptive immunity. J Virol 79:17–27
5. Drobits B, Holcmann M, Amberg N, Swiecki M et al (2012) Imiquimod clears tumors in mice independent of adaptive immunity by converting pDCs into tumor-killing effector cells. J Clin Invest 122:575–585
6. Gandhi RT, O'Neill D, Bosch RJ, Chan ES, Bucy RP, Shopis J et al (2009) A randomized therapeutic vaccine trial of canarypox-HIV-pulsed dendritic cells vs. canarypox-HIV alone in HIV-1-infected patients on antiretroviral therapy. Vaccine 27:6088–6094
7. Palucka AK, Ueno H, Connolly J, Kerneis-Norvell F et al (2006) Dendritic cells loaded with killed allogeneic melanoma cells can induce objective clinical responses and MART-1 specific CD8+ T-cell immunity. J Immunother 29:545–557
8. Redman BG, Chang AE, Whitfield J, Esper P et al (2008) Phase Ib trial assessing autologous, tumor-pulsed dendritic cells as a vaccine administered with or without IL-2 in patients with metastatic melanoma. J Immunother 31:591–598
9. Sabado RL, Miller E, Spadaccia M, Vengco I, Hasan F, Bhardwaj N (2013) Preparation of tumor antigen-loaded mature dendritic cells for immunotherapy. J Vis Exp (78)
10. Miller E, Spadaccia M, Sabado R, Chertova E et al (2015) Autologous aldrithiol-2-inactivated HIV-1 combined with polyinosinic-polycytidylic acid-poly-l-lysine carboxymethylcellulose as a vaccine platform for therapeutic dendritic cell immunotherapy. Vaccine 33: 388–395
11. Banchereau J, Palucka AK, Dhodapkar M, Burkeholder S et al (2001) Immune and clinical responses in patients with metastatic melanoma to CD34(+) progenitor-derived dendritic cell vaccine. Cancer Res 61:6451–6458
12. Marroquin CE, Westwood JA, Lapointe R, Mixon A et al (2002) Mobilization of dendritic cell precursors in patients with cancer by flt3 ligand allows the generation of higher yields of cultured dendritic cells. J Immunother 25:278–288
13. Kantoff PW, Higano CS, Shore ND, Berger ER et al (2010) Sipuleucel-T immunotherapy for castration-resistant prostate cancer. N Engl J Med 363:411–422
14. Small EJ, Schellhammer PF, Higano CS, Redfern CH et al (2006) Placebo-controlled phase III trial of immunologic therapy with sipuleucel-T (APC8015) in patients with metastatic, asymptomatic hormone refractory prostate cancer. J Clin Oncol 24:3089–3094
15. Sikora AG, Hailemichael Y, Overwijk WW (2012) Conference scene: immune effector mechanisms in tumor immunity. Immunotherapy 4:141–143
16. Adams S, O'Neill D, Bhardwaj N (2004) Maturation matters: importance of maturation for antitumor immunity of dendritic cell vaccines. J Clin Oncol 22:3834–3835
17. Lee AW, Truong T, Bickham K, Fonteneau JF et al (2002) A clinical grade cocktail of cytokines and PGE2 results in uniform maturation of human monocyte-derived dendritic cells: implications for immunotherapy. Vaccine 20(Suppl 4):A8–A22
18. Jongmans W, Tiemessen DM, van Vlodrop IJ, Mulders PF, Oosterwijk E (2005) Th1-polarizing capacity of clinical-grade dendritic cells is triggered by Ribomunyl but is compromised by PGE2: the importance of maturation cocktails. J Immunother 28:480–487
19. Krause P, Singer E, Darley PI, Klebensberger J et al (2007) Prostaglandin E2 is a key factor for monocyte-derived dendritic cell maturation: enhanced T cell stimulatory capacity despite IDO. J Leukoc Biol 82:1106–1114

20. Morelli AE, Thomson AW (2003) Dendritic cells under the spell of prostaglandins. Trends Immunol 24:108–111
21. Kwissa M, Nakaya HI, Oluoch H, Pulendran B (2012) Distinct TLR adjuvants differentially stimulate systemic and local innate immune responses in nonhuman primates. Blood 119:2044–2055
22. Schnare M, Barton GM, Holt AC, Takeda K, Akira S, Medzhitov R (2001) Toll-like receptors control activation of adaptive immune responses. Nat Immunol 2:947–950
23. Napolitani G, Rinaldi A, Bertoni F, Sallusto F, Lanzavecchia A (2005) Selected Toll-like receptor agonist combinations synergistically trigger a T helper type 1-polarizing program in dendritic cells. Nat Immunol 6:769–776
24. Boullart AC, Aarntzen EH, Verdijk P, Jacobs JF et al (2008) Maturation of monocyte-derived dendritic cells with Toll-like receptor 3 and 7/8 ligands combined with prostaglandin E2 results in high interleukin-12 production and cell migration. Cancer Immunol Immunother 57:1589–1597
25. Bogunovic D, Manches O, Godefroy E, Yewdall A et al (2011) TLR4 engagement during TLR3-induced proinflammatory signaling in dendritic cells promotes IL-10-mediated suppression of antitumor immunity. Cancer Res 71:5467–5476
26. Mailliard RB, Wankowicz-Kalinska A, Cai Q et al (2004) alpha-type-1 polarized dendritic cells: a novel immunization tool with optimized CTL-inducing activity. Cancer Res 64:5934–5937
27. Lee JJ, Foon KA, Mailliard RB, Muthuswamy R, Kalinski P (2008) Type 1-polarized dendritic cells loaded with autologous tumor are a potent immunogen against chronic lymphocytic leukemia. J Leukoc Biol 84:319–325
28. Whitehurst AW (2014) Cause and consequence of cancer/testis antigen activation in cancer. Annu Rev Pharmacol Toxicol 54:251–272
29. Andrews MC, Woods K, Cebon J, Behren A (2014) Evolving role of tumor antigens for future melanoma therapies. Future Oncol 10: 1457–1468
30. Schumacher TN, Schreiber RD (2015) Neoantigens in cancer immunotherapy. Science 348:69–74
31. Carreno BM, Magrini V, Becker-Hapak M et al (2015) A dendritic cell vaccine increases the breadth and diversity of melanoma neoantigen-specific T cells. Science 348:803–808
32. O'Neill D, Bhardwaj N (2005) Generation of autologous peptide- and protein-pulsed dendritic cells for patient-specific immunotherapy. Methods Mol Med 109:97–112
33. Melief CJ, van der Burg SH (2008) Immunotherapy of established (pre)malignant disease by synthetic long peptide vaccines. Nat Rev Cancer 8:351–360
34. Bijker MS, van den Eeden SJ, Franken KL, Melief CJ, van der Burg SH, Offringa R (2008) Superior induction of anti-tumor CTL immunity by extended peptide vaccines involves prolonged, DC-focused antigen presentation. Eur J Immunol 38:1033–1042
35. Barrou B, Benoit G, Ouldkaci M, Cussenot O et al (2004) Vaccination of prostatectomized prostate cancer patients in biochemical relapse, with autologous dendritic cells pulsed with recombinant human PSA. Cancer Immunol Immunother 53:453–460
36. Salcedo M, Bercovici N, Taylor R, Vereecken P et al (2006) Vaccination of melanoma patients using dendritic cells loaded with an allogeneic tumor cell lysate. Cancer Immunol Immunother 55:819–829
37. Mahdian R, Kokhaei P, Najar HM, Derkow K, Choudhury A, Mellstedt H (2006) Dendritic cells, pulsed with lysate of allogeneic tumor cells, are capable of stimulating MHC-restricted antigen-specific antitumor T cells. Med Oncol 23:273–282
38. Schnurr M, Galambos P, Scholz C, Then F, Dauer M, Endres S, Eigler A (2001) Tumor cell lysate-pulsed human dendritic cells induce a T-cell response against pancreatic carcinoma cells: an in vitro model for the assessment of tumor vaccines. Cancer Res 61:6445–6450
39. Thumann P, Moc I, Humrich J, Berger TG, Schultz ES, Schuler G, Jenne L (2003) Antigen loading of dendritic cells with whole tumor cell preparations. J Immunol Methods 277:1–16
40. Wheeler CJ, Black KL (2009) DCVax-Brain and DC vaccines in the treatment of GBM. Expert Opin Investig Drugs 18:509–519
41. Schnurr M, Chen Q, Shin A, Chen W, Toy T, Jenderek C et al (2005) Tumor antigen processing and presentation depend critically on dendritic cell type and the mode of antigen delivery. Blood 105:2465–2472
42. Jenne L, Schuler G, Steinkasserer A (2001) Viral vectors for dendritic cell-based immunotherapy. Trends Immunol 22:102–107
43. Brockstedt DG, Dubensky TW (2008) Promises and challenges for the development of Listeria monocytogenes-based immunotherapies. Expert Rev Vaccines 7:1069–1084
44. Bellone S, El-Sahwi K, Cocco E, Casagrande F et al (2009) Human papillomavirus type 16 (HPV-16) virus-like particle L1-specific CD8+ cytotoxic T lymphocytes (CTLs) are equally effective as E7-specific CD8+ CTLs in killing autologous HPV-16-positive tumor cells in

cervical cancer patients: implications for L1 dendritic cell-based therapeutic vaccines. J Virol 83:6779–6789
45. Carrasco J, Van Pel A, Neyns B, Lethe B, Brasseur F et al (2008) Vaccination of a melanoma patient with mature dendritic cells pulsed with MAGE-3 peptides triggers the activity of nonvaccine anti-tumor cells. J Immunol 180:3585–3593
46. Butterfield LH, Comin-Anduix B, Vujanovic L et al (2008) Adenovirus MART-1-engineered autologous dendritic cell vaccine for metastatic melanoma. J Immunother 31:294–309
47. Veron P, Allo V, Riviere C, Bernard J, Douar AM, Masurier C (2007) Major subsets of human dendritic cells are efficiently transduced by self-complementary adeno-associated virus vectors 1 and 2. J Virol 81:5385–5394
48. Nair SK, Morse M, Boczkowski D, Cumming RI, Vasovic L, Gilboa E, Lyerly HK (2002) Induction of tumor-specific cytotoxic T lymphocytes in cancer patients by autologous tumor RNA-transfected dendritic cells. Ann Surg 235:540–549
49. Muller MR, Tsakou G, Grunebach F, Schmidt SM, Brossart P (2004) Induction of chronic lymphocytic leukemia (CLL)-specific CD4- and CD8-mediated T-cell responses using RNA-transfected dendritic cells. Blood 103: 1763–1769
50. Nencioni A, Muller MR, Grunebach F, Garuti A, Mingari MC, Patrone F, Ballestrero A, Brossart P (2003) Dendritic cells transfected with tumor RNA for the induction of antitumor CTL in colorectal cancer. Cancer Gene Ther 10:209–214
51. Milazzo C, Reichardt VL, Muller MR, Grunebach F, Brossart P (2003) Induction of myeloma-specific cytotoxic T cells using dendritic cells transfected with tumor-derived RNA. Blood 101:977–982
52. Gilboa E, Vieweg J (2004) Cancer immunotherapy with mRNA-transfected dendritic cells. Immunol Rev 199:251–263
53. Heiser A, Maurice MA, Yancey DR, Coleman DM, Dahm P, Vieweg J (2001) Human dendritic cells transfected with renal tumor RNA stimulate polyclonal T-cell responses against antigens expressed by primary and metastatic tumors. Cancer Res 61:3388–3393
54. Strobel I, Berchtold S, Gotze A, Schulze U, Schuler G, Steinkasserer A (2000) Human dendritic cells transfected with either RNA or DNA encoding influenza matrix protein M1 differ in their ability to stimulate cytotoxic T lymphocytes. Gene Ther 7:2028–2035
55. Koido S, Kashiwaba M, Chen D, Gendler S, Kufe D, Gong J (2000) Induction of antitumor immunity by vaccination of dendritic cells transfected with MUC1 RNA. J Immunol 165:5713–5719
56. Heiser A, Coleman D, Dannull J, Yancey D et al (2002) Autologous dendritic cells transfected with prostate-specific antigen RNA stimulate CTL responses against metastatic prostate tumors. J Clin Invest 109:409–417
57. Routy JP, Boulassel MR, Yassine-Diab B, Nicolette C et al (2010) Immunologic activity and safety of autologous HIV RNA-electroporated dendritic cells in HIV-1 infected patients receiving antiretroviral therapy. Clin Immunol 134:140–147
58. Teijeira A, Russo E, Halin C (2014) Taking the lymphatic route: dendritic cell migration to draining lymph nodes. Semin Immunopathol 36:261–274
59. Verdijk P, Aarntzen EH, Lesterhuis WJ, Boullart AC et al (2009) Limited amounts of dendritic cells migrate into the T-cell area of lymph nodes but have high immune activating potential in melanoma patients. Clin Cancer Res 15:2531–2540
60. Fujiwara S, Wada H, Miyata H, Kawada J, Kawabata R et al (2012) Clinical trial of the intratumoral administration of labeled DC combined with systemic chemotherapy for esophageal cancer. J Immunother 35:513–521
61. Lesterhuis WJ, de Vries IJ, Schreibelt G, Lambeck AJ et al (2011) Route of administration modulates the induction of dendritic cell vaccine-induced antigen-specific T cells in advanced melanoma patients. Clin Cancer Res 17:5725–5735
62. Yewdall AW, Drutman SB, Jinwala F, Bahjat KS, Bhardwaj N (2010) CD8+ T cell priming by dendritic cell vaccines requires antigen transfer to endogenous antigen presenting cells. PLoS One 5(6):e11144
63. Mitchell DA, Batich KA, Gunn MD, Huang MN et al (2015) Tetanus toxoid and CCL3 improve dendritic cell vaccines in mice and glioblastoma patients. Nature 519:366–369
64. Garcia F, Climent N, Guardo AC, Gil C, Leon A, Autran B, Lifson JD, Martinez-Picado J, Dalmau J, Clotet B, Gatell JM, Plana M, Gallart T (2013) A dendritic cell-based vaccine elicits t cell responses associated with control of HIV-1 replication. Sci Transl Med 5(166):166ra162

Chapter 45

T-Cell Epitope Discovery for Therapeutic Cancer Vaccines

Sri Krishna and Karen S. Anderson

Abstract

The success of recent immune checkpoint blockade trials in solid tumors has demonstrated the tremendous potential of immune-mediated treatment strategies for cancer therapy. These immune therapies activate preexisting cytotoxic $CD8^+$ T cells (CTL) to selectively target and eradicate malignant cells. In vitro models suggest that these therapies may be more effective in combination with priming of CTL using cancer vaccines. CTL-mediated tumor targeting is achieved by its recognition of tumor antigenic epitopes presented on human leukocyte antigen (HLA) class I molecules by tumor cells. Discovering CTL-antigenic epitopes is therefore central to the design of therapeutic T-cell vaccines and immune monitoring of these complex immunotherapies. However, selecting and monitoring T-cell epitopes remains difficult due to the extensive polymorphism of HLA alleles and the presence of confounding non-immunogenic self-peptides. To overcome these challenges, this chapter presents methodologies for the design of CTL-targeted vaccines using selection of target HLA alleles, novel integrated computational strategies to predict HLA-class I CTL epitopes, and epitope validation methods using short-term ex vivo T-cell stimulation. This strategy results in the improved efficiency for selecting antigenic epitopes for CTL-mediated vaccines and for immune monitoring of tumor antigens.

Key words T-cell epitope, Cytotoxic $CD8^+$ T cells, HLA typing

1 Introduction

Recent clinical trials of vaccines, checkpoint blockade, and immunotherapy have demonstrated the potential efficacy of harnessing cytotoxic T cells for treatment of many cancers [1, 2]. Unlike multimodality therapy with surgery, radiation, and chemotherapy, immune therapies against tumor-specific or tumor-associated antigens hold great promise for targeted tumor eradication with relatively minimal side effects. Prophylactic subunit vaccines, such as the hepatitis B vaccine (HBV) and the human papilloma virus (HPV) vaccines, stimulate protective antibody responses and have been highly successful with >90 % efficacy [3–5]. However, eradicating preexisting pathogenic infections and malignancies is difficult to achieve by antibody-mediated immunity alone. For

Sunil Thomas (ed.), *Vaccine Design: Methods and Protocols: Volume 1: Vaccines for Human Diseases*, Methods in Molecular Biology, vol. 1403, DOI 10.1007/978-1-4939-3387-7_45,

instance, the prophylactic HPV VLP vaccine has limited efficacy for the therapeutic treatment of existing lesions [6]. Solid tumors, in particular, have a limited number of selective cell surface targets, a striking genomic heterogeneity, and rapid evolution of antigenic escape. Therefore, vaccines that induce T-cell-mediated immunity against established malignancies for therapeutic intervention are needed [1, 2, 6].

The primary goal of immune therapies for tumor eradication has been the induction of cytotoxic CD8+ T cells (CTLs). CTLs are activated by their recognition of 8–11 amino acid peptides derived from proteasomal degradation of either pathogen-derived or self-antigens in association with human leukocyte antigen (HLA) class I molecules [7, 8]. The downstream signaling cascade triggered by the binding of T-cell receptors (TCRs) to epitope-specific peptide-HLA complex causes antigen-specific effector CTL proliferation and the cytolysis of target cells presenting the epitope [9]. The αβTCR-peptide-HLA interaction is thus a critical event in CTL-mediated immunity and is fundamental for rational vaccine design. These CTL epitopes can be incorporated as a component of the therapeutic vaccine, or they can be useful for immune monitoring post-therapy [6].

Identifying immunogenic CTL epitopes remains a major challenge in vaccinology. Three major hurdles impede efficient discovery of CTL epitopes: (1) target antigen selection for vaccine design, (2) the codominance and polymorphism of HLA alleles which vary in populations by ethnicity and geographic location, and (3) the identification of the minimal peptidic sequence that can stimulate antigen-specific effector T-cell responses [10]. Identifying antigenic peptides reduces the cost of vaccine manufacture and limits exposure to competing non-immunogenic peptides within the vaccine formulation [10]. Comprehensive T-cell epitope mapping across different HLA alleles is important to identify relevant epitopes that are antigenically processed and presented on the tumor tissue [11].

Antigens for tumor immune therapy may be derived from mutated, splice-variant, or structurally altered antigens (tumor-specific antigens), overexpressed wild-type antigens (tumor-associated antigens), as well as other neo-antigens against which central or peripheral T-cell tolerance has not been established [2, 12]. Ideal antigens are those that are strongly expressed in tumor tissue and required for tumor pathogenesis. Examples of tumor-specific antigens are the HPV16 viral oncogenes E6 and E7 which are integrated into the host genome in cervical carcinomas and have sustained expression during tumor progression. E6 and E7 are excellent candidates for CTL-mediated recognition of malignant cells harboring these "non-self" antigens [6]. Several groups have targeted E6/E7 in therapeutic vaccines [13], but comprehensive CTL epitope and HLA-restriction mapping of the HPV immunome are still limited [11]. With recent advances in tumor exome and RNAseq analysis, target antigens are

increasingly being discovered using bioinformatics analysis of the tumor genome [14], exome [15–18], or post-hoc analysis of patients in response to immune therapies [19, 20]. Advances in proteomic tools such as mass spectrometry (MS) are now more routinely used to identify the tumor peptidome for antigen discovery [11, 16, 21].

The second limitation of CTL epitope discovery is the codominance and polymorphism of HLA alleles [10, 22]. Bioinformatic and sequence analyses have demonstrated that most HLA-class I alleles can be classified into one of the 9–12 common supertypes of HLA alleles, providing a population coverage of over 90 % within the HLA supertypes [22, 23]. HLA alleles and their supertypes can be obtained using bioinformatic analyses from the global HLA database (http://www.ebi.ac.uk/ipd/imgt/hla/). For targeting HLA alleles from each supertype with maximal population coverage for tumor antigen discovery, we have chosen ten common HLA alleles corresponding to a 60 % of the HLA-A locus and a >35 % HLA-B locus-specific population coverage (HLA-A alleles: A*0101, A*0201, A*0301, A*1101, A*2402; HLA-B alleles: B*0702, B*0801, B*2705, B*3501, B*5701). Using these HLA supertypes, the selected alleles represent the most common representatives of HLA supertypes for a CTL vaccine targeting over 90 % of the global population coverage, according to Lund et al. [22].

There are several methods to define antigenic epitopes for T-cell immunotherapy (Fig. 1). Conventional discovery of CTL epitopes has relied on in vitro or in vivo testing of overlapping peptides spanning the entire target antigen length, followed by peptide deconvolution and serial truncation to identify the minimal immunogenic epitope(s). Alternatively, the protein sequence can be scanned for potential HLA-binding motifs based on known amino acid preferences of different HLAs for peptide binding [24]. Potential peptides can be tested for HLA-binding affinity on cell lines with defective antigen processing such as T2 [11, 24]. Recently, computational tools developed over the past decade have become increasingly reliable for predicting HLA-peptide affinity [25–27]. These computational prediction tools leverage large experimentally derived datasets on peptide-HLA binding for training Markov models or neural networks and have now been expanded to additionally include antigen-processing elements such as proteasomal cleavage patterns [25–28]. Additionally, we and others have developed computational models which predict HLA-binding peptide immunogenicity [29, 30]. These immunogenicity models can be used in conjunction with existing prediction algorithms to further improve efficiency of CTL epitope predictions [30]. Additional algorithms for HLA-class II peptide predictions (reviewed in [31]) can be used concurrently with class I predictions to improve T-cell vaccine targets for tumor antigens.

Predicted CTL epitopes are conventionally tested for HLA binding using recombinant HLA proteins or cellular assays, T-cell

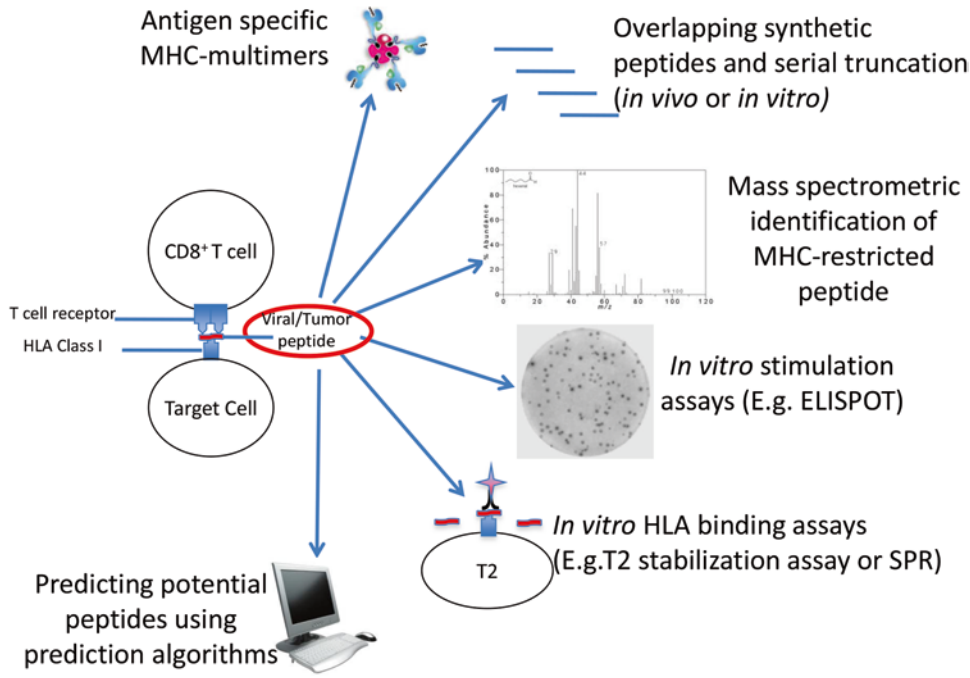

Fig. 1 Techniques to identify CTL epitopes. Note that computationally predicted peptides need validation by one or more experimental techniques

stimulation with ELISPOT assays [11, 24, 32], antigen processing using mass spectrometry[11, 21, 33], or HLA multimers to determine the frequencies of antigen-specific T cells in the peripheral blood (Fig. 1) [34, 35]. Despite these major advances in computational immunology, there is huge variability that exists between the different prediction algorithms [36] and results in a significant number of non-immunogenic false-positive epitopes from a given antigen [34]. Here, we will focus on a reverse immunology CTL epitope discovery strategy that improves the efficiency of epitope prediction and experimental validation by short-term ex vivo T-cell cultures.

1.1 Comparative CTL Epitope Prediction Strategy

CTL epitope identification strategies for tumor and pathogen-derived antigens are predominantly limited to the well-represented HLA-A2 allele. There is a need to define CTL epitopes for other non-A2 major HLA supertypes in order to develop globally relevant immune therapies. A number of open-access prediction algorithms are available for peptide-MHC binding and antigen processing [25–28]. However, a recent study showed that there is huge variability associated with the use of these prediction algorithms depending on the HLA type and antigen chosen [36]. To counter this variation in performance and scores, we employ a strategy that makes use of commonly used algorithms (three HLA-binding tools and two antigen processing). This strategy of pooling multiple epitope

prediction algorithms increases the likelihood of obtaining a true positive epitope. Potential HLA binders for the desired antigen are predicted for the five HLA-A alleles (A*0101, A*0201, A*0301, A*1101, A*2402) and five HLA-B alleles (B*0702, B*0801, B*2705, B*3501, B*5701). Five prediction algorithms are used to predict candidate peptides per antigen per HLA. Three of these algorithms (IEDB-consensus [26], NetMHCpan [28], and Syfpeithi [37]) predict HLA binding, while the other two algorithms (IEDB recommended [27] and SMMPMBEC [27, 38]) predicted candidate peptides based on antigen processing. A common pool of top-ranked peptides from each algorithm is then re-ranked using a normalization score from three binding algorithms, and the top candidate peptides are selected.

1.2 Assessing Peptide Immunogenicity by Short-Term Ex Vivo Cultures (Screen-1)

Of the potential peptidome from a target antigen, only those peptides that can stimulate CD8+ T-cell response in tumor samples will be useful targets for immune therapy. Both epitope targets and HLA restriction of tumor-reactive T cells are largely unknown for both cancers and pathogens. Long overlapping peptides from target antigens have been widely used in T-cell assays, but serial truncation of positive peptides is still required for epitope identification. This is a labor-intensive and expensive process, limited by the number of samples and more difficult for large antigens [10]. The low frequencies of precursor tumor antigen-specific CTLs can be amplified by expansion of antigen-specific CTLs ex vivo in a 10-day stimulation protocol using autologous peripheral blood mononuclear cells (PBMCs) as antigen presenting cells (Fig. 2) [39, 40]. Because of emerging evidence of the role of PD-1/PD-L1 checkpoint blockade to activate a potent antitumor immunity in HPV-associated as well as other tumors [1, 40–42], anti-PD-1 antibody is used on day 1 of our culture protocol to inhibit antigen-specific T-cell suppression. Since candidate peptides are predicted for several HLAs, they are pooled into separate 8–10 peptide pools. Peptide pools are designed to limit intra-pool binding competition by different peptides to the same HLA. Activation of antigen-specific CTLs is identified by standard interferon gamma

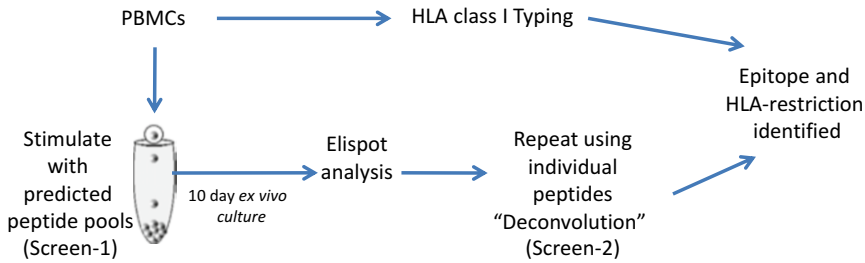

Fig. 2 Assessing peptide pool immunogenicity by short-term ex vivo cultures, epitope deconvolution, and HLA-restriction identification, as described in text

(IFNγ) enzyme-linked immunospot (ELISPOT) assay. The mean spot-forming units (SFUs) from each peptide pool are assessed in triplicate. The mean SFU of any peptide pool greater than twice the mean SFU of negative control (PBS-DMSO or irrelevant peptide pool) with statistical significance ($P < 0.05$ by two-sample T-test) is considered as a positive response.

1.3 HLA-Typing and Positive Peptide Pool Deconvolution (Screen-2)

Once peptide pool(s) that has a positive signal from several patient PBMCs is identified by the primary screen culture protocol, the minimal peptide(s) responsible for CTL stimulation is identified by deconvoluting the peptide pool (Fig. 2). The same ex vivo short-term culture protocol (including anti-PD-1) is repeated now with individual peptides from the positive peptide pool from the initial screen (screen-2). The reactive parent peptide pools from screen-1 are included as a biological replicate. Concurrently, the positive responder's HLA-class I type is identified either by HLA-specific monoclonal antibodies using flow cytometry (low-resolution HLA typing) or by commercial HLA-typing (high-resolution) services such as the type HLA (ProImmune, Oxford, UK). Low-resolution HLA typing by flow cytometry is performed on PBMCs set aside during screen-1 during any of the 2–3 days following day-1 stimulation. High-resolution commercial HLA typing requires genomic DNA (2 μg total) isolated from the PBMCs and sent out to commercial services. Because it requires more material, it is usually done on the last day of the ELISPOT screen. Cells are collected from the ELISPOT plate and washed once, and genomic DNA is isolated.

If there are limitations on sample availability, only those peptides that correspond to the patient's HLA-class I types are tested. In such cases, a small number (~1 million cells) of donor PBMCs is set aside during screen-1, and HLA typing is performed (low and/or high resolution). Once screen-1 is complete, only those candidate peptides from a pool that are predicted to bind the donor's HLA type are tested in the subsequent screen-2. This minimizes the amount of sample and the number of peptides to be tested. However, this approach will not successfully identify cross-reactive promiscuous HLA binders, which can be lost when focusing on donor-HLA-specific candidate peptides.

2 Materials

2.1 Comparative CTL Epitope Prediction Strategy

1. Antigenic protein sequence. Usually obtained from literature or from National Center for Biotechnology (NCBI) RefSeq database [43] and UniProt servers [44].
2. Immune epitope database (IEDB) MHC-peptide binding algorithms: NetMHCpan, IEDB-consensus binding prediction tool, both accessible at http://tools.immuneepitope.org/main/tcell/.

3. SYFPEITHI epitope prediction algorithm (binding) accessible at http://www.syfpeithi.de/bin/MHCServer.dll/EpitopePrediction.htm.
4. IEDB antigen-processing algorithms: IEDB-consensus antigen-processing tool, SMMPMBEC antigen-processing algorithms (http://tools.immuneepitope.org/main/tcell/).
5. Microsoft Excel or database software.
6. R statistical software [45].

2.2 Assessing Peptide Immunogenicity by Short-Term Ex Vivo Cultures (Screen-1)

1. 1× tissue-culture grade phosphate buffered saline (PBS) (Cellgro, Mediatech, Manassas, VA, USA).
2. Dimethyl sulfoxide (DMSO) (Sigma, St. Louis, MO, USA).
3. Acetic acid (Amresco, Solon, OH, USA).
4. T-cell culture media: To RPMI-1640 (ATCC, Manassas, VA, USA), add 100 U(μg)/mL penicillin-streptomycin (Gibco, Grand Island, NY, USA), 10 mM HEPES (Gibco, Grand Island, NY, USA), 2 mM L-glutamine (Gibco, Grand Island, NY, USA), and 10 % human serum (Gemcell, West Sacramento, CA, USA) (Heat Inactivated, 56 °C, Follow Corning Cellgro's Heat inactivation protocol). Filter through 0.22 μm Corning sterile filter. Store at 4 °C. Check for contamination before every use and potential increase in pH (can be buffered through HEPES) (*see* **Notes 1** and **2**).
5. Recombinant human IL-7 (R&D Systems, Minneapolis, MN, USA): Reconstitute at 50 μg/mL in sterile PBS. Keep at −80 °C. Working solution at 1 μg/mL in sterile 1× PBS, stored at 4 °C until use. Final concentration in culture at 10 ng/mL (5 ng/mL also works well) and can be stored at 4 °C.
6. Recombinant human IL-2 (R&D Systems, Minneapolis, MN, USA): Reconstitute at 100 μg/mL (=1,640,000 U/mL) in 100 mM sterile acetic acid. Add 100 μL acetic acid into 16.6 mL water to make 100 mM acetic acid; filter through 0.22 μm Corning sterile filter. Store at -80 °C. Working solution is 2000 U/mL in sterile PBS. Final concentration in culture is 20 U/mL and can be stored at 4 °C.
7. Peptide pools (ProImmune, Oxford, UK, other commercial sources are also available): Peptide purity ordered is >70 %. Reconstitute all stock peptides at 20 mg/mL in DMSO or according to manufacturer specifications (for certain peptides) and store at −20 °C. To create a working peptide pool, add each peptide corresponding to 1 mg/mL final concentration and make up the rest of the volume in sterile 1× PBS to 1 mL. Make smaller 100 μL aliquots and store at −20 °C. Working peptide pool tube can be stored at 4 °C for about 2 months. Final concentration in culture is 10 μg/mL.

8. CEF-peptide pool (ProImmune, Oxford, UK): Reconstitute at 20 mg/mL in DMSO. Follow manufacturer's instructions and make a 1 mg/mL stock using sterile 1× PBS. Store in −20 °C and an aliquot in 4 °C. Final concentration in culture is 1 μg/mL.
9. Phytohemagglutinin M form (PHA-M), for positive stimulation (Gibco, Grand Island, NY, USA).
10. DMSO in 1× sterile PBS can be used as a negative control.
11. Anti-PD-1 antibody (optional): Antihuman CD279 (PD-1) purified, clone eBioJ105 (eBioscience, San Diego, CA, USA). Store at 4 °C. Stock concentration 0.5 mg/mL. Working concentration is 1 μg/mL. Store at 4 °C.
12. Levy counting chamber (Hausser Scientific, Horsham, PA, USA).
13. Centrifuge (Beckman Coulter, Pasadena, CA, USA).
14. Antihuman IFNγ monoclonal antibody, clone 1-D1K (1 mg/mL) (Mabtech, Cincinnati, OH, USA). Store at 4 °C.
15. Biotinylated antihuman IFNγ monoclonal antibody, 7-B6-1 biotin (1 mg/mL) (Mabtech, Cincinnati, OH, USA). Store at 4 °C.
16. BCIP/NBT Color Development Substrate (Promega, Madison, WI, USA). Store at −20 °C.
17. Ethanol (Avantor Performance Materials, Center Valley, PA, USA).
18. Fetal bovine serum (FBS) (Gibco, Grand Island, NY, USA). Store at −20 °C after heat inactivation for 20 min at 56 °C.
19. Tris (Sigma, St. Louis, MO, USA). Store at room temperature.
20. Magnesium chloride ($MgCl_2$) (Sigma, St. Louis, MO, USA). Store at room temperature.
21. Sodium chloride (NaCl) (Sigma, St. Louis, MO, USA). Store at room temperature.
22. MultiScreen filter plate, 2EM004M9 or MSIPS4W10 (Millipore, Billerica, MA, USA).
23. AID or other ELISPOT reader (Autoimmun Diagnostika, Strassberg, Germany).
24. 1× PBS 0.5 % FBS buffer for ELISPOT washes (0.5 % FBS wash solution).

2.3 HLA-Typing and Positive Peptide Pool Deconvolution (Screen-2)

1. Materials 1 through 23 from Subheading 2.2.
2. Individual peptides from the immunogenic peptide pool identified through screen-1. Reconstitute all stock peptides at 20 mg/mL in DMSO or according to manufacturer specifications (for certain peptides) and store at −20 °C. To create a working peptide solution, make a 1 mg/mL final concentration and make up the rest of the volume in sterile 1× PBS to 1 mL. Make smaller 100 μL aliquots and store at 20 °C. Working peptide tubes can be stored at 4 °C for about 2 months. Final concentration in culture is 10 μg/mL.

3. Fluorescently conjugated monoclonal antibodies (mAbs) for the 10 HLA alleles listed in Subheading 1.1. Usually obtained from commercial sources (e.g., HLA-A2 mAb clone BB7.2-PE conjugated; from BD Pharmingen, San Jose, CA, USA) (*see* **Notes 3** and **4**).
4. Fluorescently conjugated isotype controls (e.g., mouse IgG2a-PE for HLA-A2 staining, BD Pharmingen, San Jose, CA, USA).
5. Attune or a similar flow cytometer (Life Technologies, Grand Island, NY, USA).
6. Staining buffer. 1× PBS (Cellgro, Mediatech, Manassas, VA, USA) with 1 % bovine serum albumin (BSA, Sigma, St. Louis, MO, USA).
7. DNAzol Reagent (Life Technologies, Grand Island, NY, USA) for genomic DNA isolation.
8. Sodium hydroxide monobasic (Sigma, St. Louis, MO, USA) used with DNAzol.
9. 100 % ethanol (Avantor Performance Materials, Center Valley, PA).
10. Nuclease-free water (Hyclone, Thermo Fisher Scientific, Waltham, MA, USA).
11. Cold-table top centrifuge (Thermo Fisher Scientific, Waltham, MA, USA).
12. Nanodrop 2000 C (Thermo Fisher Scientific, Waltham, MA, USA).

3 Methods

3.1 Comparative CTL Epitope Prediction Strategy

1. Access the IEDB CTL epitope prediction server: (http://tools.immuneepitope.org/main/tcell/).
2. Select "Peptide binding to MHC class I molecules" link.
3. Enter the antigen protein sequence in FASTA format (*see* **Note 5**).
4. Select "Consensus" or "NetMHCpan" as the prediction method.
5. Select "human" as the MHC source species.
6. Select the desired "HLA allele" (each of the HLA-A's and HLA-B's listed in Subheading 1.3).
7. Select "all lengths" as the predicted peptide length.
8. Choose "Percentile rank" for IEDB-consensus and "Predicted IC50" for NetMHCpan as the output type to sort the peptides.
9. Choose "XHTML table" as the output format.
10. Download the results as an excel file.

11. Select "Proteasomal cleavage/TAP transport/MHC class I combined predictor" from the IEDB CTL epitope prediction server main page.
12. Enter the antigen protein sequence in FASTA format.
13. Select "IEDB recommended" or "SMMPMBEC" as the prediction method.
14. Repeat **steps 5**–**7** for the different HLA alleles (*see* **Note 6**).
15. Sort the peptide list by "Total score" for both the algorithms (should be in a decreasing order).
16. Repeat **steps 9** and **10**.
17. Access the SYFPEITHI epitope prediction server at: http://www.syfpeithi.de/bin/MHCServer.dll/EpitopePrediction.htm.
18. Select the "MHC type" for each of the HLA alleles.
19. Choose "All mers" for peptide length.
20. Paste the antigen protein sequence in non-FASTA format. Click Run.
21. Save the output by copying all the predicted peptides into MS Excel and removing blank spaces between different lengths (*see* **Note 7**).
22. From each prediction algorithm's output per HLA, select the top two-thirds (66 %) of all predicted peptides (i.e., for 100 predicted peptides, select the top 66). Do this for each prediction algorithm's output in MS Excel or database program (*see* **Note 8**).
23. By using a local script on R, create a separate list of peptides common between the five prediction algorithms (*see* **Note 9**).
24. Using the output scores as described above, normalize the common pool of predicted peptides as follows (*see* **Note 10**):
    (a) For algorithms displaying results ranging from a low score to high score (IEDB-consensus binding and NetMHCpan), $\overline{\delta_i} = (\delta_i - \delta_{\min}) / (\delta_{\max} - \delta_{\min})$, where $\overline{\delta_i}$ represents the normalized score of the peptide; δi, the assigned output score by the prediction algorithm; $\delta_{\min}$, the minimum score assigned in prediction output; and $\delta_{\max}$, the maximum score assigned in the entire prediction output.
    (b) For Syfpeithi, which displays results ranging from a high score to low score, $\overline{\delta_i} = (\delta_i - \delta_{\max}) / (\delta_{\min} - \delta_{\max})$ (*see* **Note 7**).
25. Calculate the average binding score S_B from the three normalized binding scores.
26. Using the "sort" function in MS Excel, sort the S_B score list ranging from the lowest to the highest. Lower the S_B score, higher its probability of being a candidate peptide (*see* **Note 10**).

27. Select the top candidate peptides including promiscuous binders (usually up to 5 or 10, depending on feasibility; *see* **Note 11**) and order synthetic peptides for immunogenicity assessment. Greater than 70 % purity is sufficient for T-cell assays.
28. Once synthesized peptides are received, reconstitute the peptides according to manufacturer's instructions.
29. Create the peptide pools by having between 1 and 3 binders per HLA allele within each pool. This limits intra-pool binding competition by different peptides for the same HLA. Store the peptide pools at 4 °C (*see* **Note 12**).

3.2 Predicted Peptide Pool Immunogenicity Assessment by Short-Term Ex Vivo Cultures

1. Obtain a frozen PBMC cryovial from liquid nitrogen and rapidly thaw in 37 °C water bath.
2. Pipette the cells drop by drop into a 15 mL tube with pre-warmed T-cell culture media.
3. Centrifuge at 300 × *g* for 5 min, remove supernatant for wash.
4. Resuspend cells gently in T-cell culture media. Count cells using a hemacytometer. Set aside 500,000 PBMCs for low-resolution HLA typing (Subheading 3.3).
5. Prepare cell suspension at 1×10^6 cells/mL. Seed cells in a round bottom 96-well plate, 200 μL/well (=200,000 cells/well) (*see* **Note 13**).
6. On day 1, stimulate with 20 U/mL IL-2, 10 ng/mL IL-7 (1 μg/mL Anti PD-1 optional), and 10 μg/mL peptide pool or CEF-peptide pool (*see* **Note 14**). Use 1 % PHA-M for positive control stimulation (2 μL/well).
7. On day 5, remove 100 μL media from each well and add 100 μL/well fresh T-cell culture media. Add IL-2 for final concentration at 20 U/mL and peptide pool at concentration 10 μg/well.
8. On day 7, pre-wet an ELISPOT plate with 35 % ethanol for 3–4 min at room temperature under hood, 35 μL/well (*see* **Note 15**).
9. Wash with sterile water for five times, 200 μL/well (*see* **Note 16**).
10. Coat with capture antibody 1-D1K, 100 μL/well. Dilute capture antibody in 1× PBS at final concentration 5 μg/mL.
11. Seal the plate and incubate at 4 °C overnight.
12. On day 8, wash with RPMI1640 (serum free is fine) for five times, 200 μL /well.
13. Add T-cell culture media, 200 μL/well. Keep at room temperature in the hood for 30 min.
14. On day 8, remove 100 μL media from each well and add 100 μL/well fresh T-cell culture media. Add IL-2 for final

concentration at 20 U/mL, and peptide pool at concentration 10 μg/well. Add IL-2 for final concentration at 20 U/mL (*see* **Note 17**).

15. Add cells from each of the wells (200 μL/well) from the culture plate into a corresponding well on the ELISPOT plate, triplicate for assays. Stimulate with antigenic peptide at final concentration 10 μg/mL (2 μg/200 μL). The same quantity of CEF-peptide pool as peptide controls. Use 1 % PHA-M (2 μL/well) for positive control.
16. Cover with plate lid and incubate in CO_2 incubator for 48 h (days 8–10).
17. On day 10, wash with sterile 1× PBS for three times, 200 μL/well. Save the cells for genomic DNA isolation (high-resolution HLA typing, Subheading 3.3).
18. Wash with 0.5 % FBS wash solution for three times, 200 μL/well giving 5-min intervals between washes.
19. Add detection antibody 7-B6-1 Biotin, 100 μL/well. Dilute detection antibody in 0.5 % FBS wash solution at final concentration 1 μg/mL.
20. Seal the plate and incubate at room temperature for 2 h in the dark. (Leave the sealed plate in the hood if preferred.)
21. Wash with 1× PBS for three times, 150 μL/well.
22. Wash with 0.5 % FBS wash solution for three times, 150 μL/well, 5-min interval between washes.
23. Add streptavidin-ALP, 100 μL/well. Dilute streptavidin-ALP in 0.5 % FBS wash solution at final concentration 1:1000.
24. Incubate at room temperature (preferably dark) for 1 h.
25. Wash with 1× PBS for three times, 150 μL/well.
26. Wash with 0.5 % FBS wash solution for three times, 150 μL/well.
27. Add BCIP/NBT mixed solution, 100 μL well.
28. Watch for spot development (*see* **Note 18**).
29. Stop reaction by rinsing with cool tap water.
30. Dry the plate in the dark at room temperature overnight (leave the lid partially open).
31. Read the ELISPOT plate after 24–48 h on the AID ELISPOT reader.
32. Calculate mean SFUs for each peptide pool.

3.3 HLA-Typing and Positive Peptide Pool Deconvolution (Screen-2)

1. Low-resolution HLA typing can be performed using the 500,000 cells set aside on day 1 of screen-1 (*see* **Note 19**).
2. Pool the cells in media into a single tube and wash once with staining buffer (500 × *g*, 3 min, table top centrifuge).

3. Divide the washed PBMCs into appropriate number of HLAs and isotype controls to be tested (*see* **Note 4**), in 100 μL staining buffer per tube (*see* **Note 20**).
4. Add appropriate mAbs and isotype controls to be analyzed according to the manufacturer's instructions (*see* **Note 21**).
5. Incubate on ice in the dark for 30 min.
6. Wash twice with staining buffer. Resuspend in a final volume of 200–300 μL 1× PBS for flow cytometry analysis.
7. Run isotype controls first on the flow cytometer, set the gate on live lymphocyte population, and collect 10,000 events/gate.
8. Run the individual samples stained with HLA-mAbs next, collect 10,000 events/gate, and analyze.
9. Genomic DNA (gDNA) extraction for high-resolution commercial HLA typing is performed on the last day (day 10) of screen-1; when incubating, PBMCs are washed from the ELISPOT plate.
10. Collect cells from the ELISPOT plate (contains media) in a reservoir.
11. Wash the ELISPOT plate with 1× PBS and collect remaining cells in the reservoir.
12. Pool cells from reservoir into a 15 mL conical tube.
13. Centrifuge the cells, 500 × *g*, 3 min. Remove supernatant.
14. Wash the pellet once with 5 mL 1× sterile PBS, centrifuge and remove the supernatant.
15. Add 500 μL DNAzol directly to the pellet (*see* **Note 22**).
16. Follow manufacturer's protocols and isolate gDNA (*see* **Note 23**).
17. Determine the concentration of gDNA using nanodrop. gDNA can be stored in −20 °C, and 2 μg gDNA is shipped to the company for high-resolution HLA typing.
18. Once screen-1 (Subheading 3.2) is completed, perform data analysis to identify the peptide pool with statistically significant higher mean SFUs compared to the negative control using MS Excel.
19. Repeat the *ex vivo* short-term culture protocol (**steps 1** through **32**) using individual peptides from the reactive peptide pool from screen-1 (*see* **Note 24**).
20. At the end of the short-term culture, analyze mean SFU from individual peptides as described before and correlate with donor-HLA type to identify reactive CTL epitope and its HLA restriction.

4 Notes

1. Human serum can be very viscous causing the filter unit to clog during media filtration. Use an extra layer of sterile filter paper (cut to fit the filter unit size) on the 0.22 μm membrane to prevent this.
2. If needed, Anti-Anti (Antibiotic:Antimycotic, Gibco, Grand Island, NY, USA) can be added to T-cell culture media to prevent fungal contamination. However, penicillin-streptomycin should not be added if Anti-Anti is used since it contains both the antibiotics. Stock solution is 100×, stored in 5 mL aliquots at −20 °C.
3. Please note that some HLA-mAbs can cross-react with other HLA supertypes. For instance, we have observed that the HLA-A3 mAb often has some low-level cross-reactivity with HLA-A2 mAb. Manufacturers often indicate this in their product description, and data should therefore be interpreted with appropriate caution.
4. It is preferable to purchase all the HLA-mAbs in one or two fluorescent conjugates. This minimizes the number of isotype controls to be used in each HLA-typing experiment.
5. File can also be chosen and uploaded from local drive in FASTA format.
6. Peptide predictions can be performed based on proteasomal cleavage patterns under normal ("constitutive") or inflammatory conditions ("immuno"). Default proteasome type is "immuno"; it can be changed to "constitutive" if desired.
7. Ensure that the output of the prediction is in the right order; some algorithms rank from a high score to low score (e.g., Syfpeithi), while others rank from low to high score (e.g., NetMHCpan).
8. Since every possible predicted peptide is represented in all the algorithms, top 66 % of predicted peptides ensure that only the common peptides, which are most probable binders and antigenically processed, are selected.
9. The easiest way to ensure that a common pool of predicted peptides are obtained from the different algorithms is to ensure that the common peptide list is shorter than the number of peptides from the top 66 % of list of predicted peptides (since, each algorithm ranks the predicted peptides in different orders).
10. Ensure that the normalized scores range from 0 to 1. A peptide's S_B score is closer to 0 which indicates that it has been predicted as strong binder in all three binding algorithms and is antigenically processed. Note that a score of 0 indicates the top predicted peptide in all the algorithms.

11. Promiscuous HLA binders are defined as peptides binding to multiple HLA-class I alleles are prioritized since they represent CTL targeting of several HLA alleles with fewer antigenic epitopes. Any such promiscuous HLA binder ranked within the top ranks (ranked by their 5 S_B scores) across multiple alleles can be selected for immunogenicity assessment.
12. Limit the total number of peptides per pool to 10 to ensure that peptides do not interfere with each other during the assays.
13. Protect all four sides on the 96-well plate, the last columns and rows with plain media (36 wells). This minimizes contamination and evaporation.
14. If IL-7 and anti-PD-1 are used, they should not be added after the first stimulation, because of increased background.
15. Watch the plate carefully to ensure that the ethanol wets the wells thoroughly. If it doesn't seem to be wetting the well, dump the wells and add the ethanol again. If the wells are not pre-wet with ethanol enough, antibody coating can be hindered.
16. This step and subsequent steps until **step 15** should be performed under the laminar flow hood. This ensures that no contamination happens on the ELISPOT plate.
17. The wells can be pooled into a single tube and resuspended gently to reduce inter-well variability when analyzed. However, if biological replicates are essential, pooling of the wells need not be done, and each well is transferred to its counterpart on the ELISPOT plate.
18. The CEF-peptide pool or PHA wells can be checked for spot development. The wells should not be overexposed, which will increase background, and no spots will be visible. Usually 6–8 min is sufficient.
19. Flow-cytometric analysis of donor HLAs can be done on day 1 of or during subsequent days of the short-term culture, from separate wells containing cells for HLA tying (IL-2 is added to retain cell viability). Once HLA mAb staining is done, it is preferable to run the samples on the same day.
20. From this step, samples are maintained on ice under the dark (to minimize fluorescence fading). Cover the ice bucket with aluminum foil if preferred.
21. HLA-mAbs usually have strong binding. In our experience, 3–4 μL mAb/100 μL sample has been sufficient for HLA typing even if the recommended volume is 10 μL/test.
22. Use wide-bore tips by cutting a little distance away from the edge of the tip to avoid shearing of gDNA.

23. In case of low yield of gDNA during ethanol precipitation, do not spool the gDNA as instructed; rather, precipitate and wash the gDNA by centrifuging at maximum speed in a chilled centrifuge.
24. The original peptide pool (from screen-1) of which the individual peptides are being analyzed can be included as a confirmation step for the assay.

Acknowledgements

We thank Diego Chowell for assistance with the normalization of prediction algorithms and epitope discovery strategy. This chapter describes work supported by institutional funds from Arizona State University to S.K. and K.S.A.

References

1. Kim H-J, Cantor H (2014) The path to reactivation of antitumor immunity and checkpoint immunotherapy. Cancer Immunol Res 2:926–936
2. Mellman I, Coukos G, Dranoff G (2011) Cancer immunotherapy comes of age. Nature 480:480–489
3. Penny ME, Aranda C, Vardas E, Moi H, Jessen H, Hillman R, Chang Y, Ferris D, Rouleau D, Bryan J, Ph D, Marshall JB, Vuocolo S, Barr E, Radley D, Haupt RM, Guris D (2011) Efficacy of quadrivalent HPV vaccine against HPV infection and disease in males. N Engl J Med 364:401–411
4. Chang M-H, Shen C-J, Lai M-S, Hsu H-M, Tzee-Chung W, Kong M-S, Liang D-C, Shau W-Y, Chen D-S (1997) Universal Hepatitis B vaccination in Taiwan and the incidence of hepatocellular carcinoma. N Engl J Med 336: 1855–1859
5. Center for Disease Control and Prevention (2005) A comprehensive immunization strategy to eliminate transmission of Hepatitis B virus infection in the United States recommendations of the advisory committee. CDC MMWR Rep 54:1–32
6. Trimble CL, Frazer IH (2009) Development of therapeutic HPV vaccines. Lancet Oncol 10:975–980
7. Grakoui A, Bromley SK, Sumen C, Davis MM, Shaw AS, Allen PM, Dustin ML (1999) The immunological synapse: a molecular machine controlling T cell activation. Science 285:221–227
8. Blum JS, Wearsch PA, Cresswell P (2013) Pathways of antigen processing. Annu Rev Immunol 31:443–473
9. Hennecke J, Wiley DC (2001) T cell receptor-MHC interactions up close. Cell 104:1–4
10. Purcell AW, McCluskey J, Rossjohn J (2007) More than one reason to rethink the use of peptides in vaccine design. Nat Rev Drug Discov 6:404–414
11. Riemer AB, Keskin DB, Zhang G, Handley M, Anderson KS, Brusic V, Reinhold B, Reinherz EL (2010) A conserved E7-derived cytotoxic T lymphocyte epitope expressed on human papillomavirus 16-transformed HLA-A2+ epithelial cancers. J Biol Chem 285:29608–29622
12. Ernst B, Anderson KS (2015) Immunotherapy for the treatment of breast cancer. Curr Oncol Rep 17(2):5
13. Ma B, Xu Y, Hung C, Wu T (2010) HPV and therapeutic vaccines: where are we in 2010 ? Curr Cancer Ther Rev 6:81–103
14. Rajasagi M, Shukla SA, Fritsch EF, Keskin DB, DeLuca D, Carmona E, Zhang W, Sougnez C, Cibulskis K, Sidney J, Stevenson K, Ritz J, Neuberg D, Brusic V, Gabriel S, Lander ES, Getz G, Hacohen N, Wu CJ (2014) Systematic identification of personal tumor-specific neoantigens in chronic lymphocytic leukemia. Blood 124:453–462
15. Segal NH, Parsons DW, Peggs KS, Velculescu V, Kinzler KW, Vogelstein B, Allison JP (2008) Epitope landscape in breast and colorectal cancer. Cancer Res 68:889–892

16. Yadav M, Jhunjhunwala S, Phung QT, Lupardus P, Tanguay J, Bumbaca S, Franci C, Cheung TK, Fritsche J, Weinschenk T, Modrusan Z, Mellman I, Lill JR (2014) Predicting immunogenic tumour mutations by combining mass spectrometry and exome sequencing. Nature 515:572–576
17. Pulido J, Kottke T, Thompson J, Galivo F, Wongthida P, Diaz RM, Rommelfanger D, Ilett E, Pease L, Pandha H, Harrington K, Selby P, Melcher A, Vile R (2012) Using virally expressed melanoma cDNA libraries to identify tumor-associated antigens that cure melanoma. Nat Biotechnol 30:337–343
18. Rammensee H-G, Singh-Jasuja H (2013) HLA ligandome tumor antigen discovery for personalized vaccine approach. Expert Rev Vaccines 12:1211–127
19. Snyder A, Makarov V, Merghoub T, Yuan J, Zaretsky JM, Desrichard A, Walsh LA, Postow MA, Wong P, Ho TS, Hollmann TJ, Bruggeman C, Kannan K, Li Y, Elipenahli C, Liu C, Harbison CT, Wang L, Ribas A, Wolchok JD, Chan TA (2014) Genetic basis for clinical response to CTLA-4 blockade in melanoma. N Engl J Med 371:2189–2199
20. Rizvi NA, Hellmann MD, Kvistborg P, Makarov V, Jonathan J, Lee W, Yuan J, Wong P, Ho TS, Miller ML, Rekhtman N, Moreira AL, Bruggeman C, Gasmi B, Merghoub T, Wolchok JD, Schumacher TN, Chan TA (2015) Mutational landscape determines sensitivity to PD-1 blockade in non-small cell lung cancer. Science 348:124–128
21. Fortier M-H, Caron E, Hardy M-P, Voisin G, Lemieux S, Perreault C, Thibault P (2008) The MHC class I peptide repertoire is molded by the transcriptome. J Exp Med 205:595–610
22. Lund O, Nielsen M, Kesmir C, Petersen AG, Lundegaard C, Worning P, Sylvester-Hvid C, Lamberth K, Røder G, Justesen S, Buus S, Brunak S (2004) Definition of supertypes for HLA molecules using clustering of specificity matrices. Immunogenetics 55:797–810
23. Sette A, Sidney J (1999) Nine major HLA class I supertypes account for the vast preponderance of HLA-A and -B polymorphism. Immunogenetics 50:201–212
24. Vonderheide RH, Anderson KS, Hahn WC, Butler MO, Schultze JL, Nadler LM (2001) Characterization of HLA-A3-restricted cytotoxic T lymphocytes reactive against the widely expressed tumor antigen telomerase. Clin Cancer Res 7:3343–3348
25. Honeyman MC, Brusic V, Stone NL, Harrison LC (1998) Neural network-based prediction of candidate T-cell epitopes. Nat Biotechnol 16:966–969
26. Moutaftsi M, Peters B, Pasquetto V, Tscharke DC, Sidney J, Bui H-H, Grey H, Sette A (2006) A consensus epitope prediction approach identifies the breadth of murine T(CD8+)-cell responses to vaccinia virus. Nat Biotechnol 24:817–819
27. Tenzer S, Peters B, Bulik S, Schoor O, Lemmel C, Schatz MM, Kloetzel P-M, Rammensee H-G, Schild H, Holzhütter H-G (2005) Modeling the MHC class I pathway by combining predictions of proteasomal cleavage, TAP transport and MHC class I binding. Cell Mol Life Sci 62:1025–1037
28. Nielsen M, Lundegaard C, Blicher T, Lamberth K, Harndahl M, Justesen S, Røder G, Peters B, Sette A, Lund O, Buus S (2007) NetMHCpan, a method for quantitative predictions of peptide binding to any HLA-A and -B locus protein of known sequence. PLoS One 2:1–10
29. Calis JJA, Maybeno M, Greenbaum J, Weiskopf D, De Silva AD, Sette A, Keşmir C, Peters B (2013) Properties of MHC Class I presented peptides that enhance immunogenicity. PLoS Comput Biol 9:1–13
30. Chowell D, Krishna S, Becker PD, Cocita C, Shu J, Tan X, Greenberg PD, Klavinskis LS, Blattman JN, Anderson KS (2015) TCR contact residue hydrophobicity is a hallmark of immunogenic CD8+ T cell epitopes. Proc Natl Acad Sci 112:E1754–E1762
31. Nielsen M, Lund O, Buus S, Lundegaard C (2010) MHC Class II epitope predictive algorithms. Immunology 130:319–328
32. Vonderheide RH, Schultze JL, Anderson KS, Maecker B et al (2001) Equivalent induction of telomerase-specific cytotoxic T lymphocytes from tumor-bearing patients and healthy individuals. Cancer Res 61:8366–8370
33. Hirano N, Butler MO, Xia Z, Berezovskaya A, Murray AP, Ansén S, Nadler LM (2006) Efficient presentation of naturally processed HLA class I peptides by artificial antigen-presenting cells for the generation of effective antitumor responses. Clin Cancer Res 12:2967–29675
34. Newell EW, Sigal N, Nair N, Kidd B, Greenberg HB, Davis MM (2013) Combinatorial tetramer staining and mass cytometry analysis facilitate T-cell epitope mapping and characterization. Nat Biotechnol 31:623–629
35. Newell EW, Davis MM (2014) Beyond model antigens: high-dimensional methods for the analysis of antigen-specific T cells. Nat Biotechnol 32:149–157
36. Lin HH, Ray S, Tongchusak S, Reinherz EL, Brusic V (2008) Evaluation of MHC class I peptide binding prediction servers: applications for vaccine research. BMC Immunol 9:1–13

37. Rammensee H, Bachmann J, Emmerich NPN, Bachor OA, Stevanović S (2000) SYFPEITHI: database for MHC ligands and peptide motifs. Immunogenetics 213–219
38. Kim Y, Sidney J, Pinilla C, Sette A, Peters B (2009) Derivation of an amino acid similarity matrix for peptide: MHC binding and its application as a Bayesian prior. BMC Bioinformatics 10:394
39. Hida N, Maeda Y, Katagiri K, Takasu H, Harada M, Itoh K (2002) A simple culture protocol to detect peptide-specific cytotoxic T lymphocyte precursors in the circulation. Cancer Immunol Immunother 51:219–228
40. Parikh F, Duluc D, Imai N, Clark A, Misiukiewicz K et al (2014) Chemoradiotherapy-induced upregulation of PD-1 antagonizes immunity to HPV-related oropharyngeal cancer. Cancer Res 74:7205–7216
41. Lyford-Pike S, Peng S, Young GD, Taube JM, Westra WH et al (2013) Evidence for a role of the PD-1:PD-L1 pathway in immune resistance of HPV-associated head and neck squamous cell carcinoma. Cancer Res 73: 1733–1741
42. Binder DC, Engels B, Arina A, Yu P, Slauch JM et al (2013) Antigen-specific bacterial vaccine combined with anti-PD-L1 rescues dysfunctional endogenous T cells to reject long-established cancer. Cancer Immunol Res 1:123–133
43. Pruitt KD, Brown GR, Hiatt SM, Thibaud-Nissen F et al (2014) RefSeq: an update on mammalian reference sequences. Nucleic Acids Res 42:756–763
44. Consortium TU (2014) UniProt: a hub for protein information. Nucleic Acids Res 43:D204–D212
45. Development Core Team R (2008) R: a language and environment for statistical computing. R Foundation for Statistical Computing, Vienna, Austria

Chapter 46

Peptide-Based Cancer Vaccine Strategies and Clinical Results

Erika Schneble, G. Travis Clifton, Diane F. Hale, and George E. Peoples

Abstract

Active cancer immunotherapy is an exciting and developing field in oncology research. Peptide vaccines, the use of isolated immunogenic tumor-associated antigen (TAA) epitopes to generate an anticancer immune response, are an attractive option as they are easily produced and administered with minimal toxicity. Multiple TAA-derived peptides have been identified and evaluated with various vaccine strategies currently in clinical testing. Research suggests that utilizing vaccines in patients with minimal-residual disease may be a more effective strategy compared to targeting patients with widely metastatic disease as it avoids the immune suppression and tolerance associated with higher volumes of more established disease. Clinical trials also suggest that vaccines may need to be tailored and administered to specific cancer subtypes to achieve maximum efficacy. Additionally, numerous immunomodulators now in research and development show potential synergy with peptide vaccines. Our group has focused on a simpler, single-peptide strategy largely from the HER2/*neu* protein. We will discuss our experience thus far as well as review other peptide vaccine strategies that have shown clinical efficacy.

Key words Cancer vaccine, Peptide, Immunotherapy, Tumor-associated antigen

1 Introduction

Cancer immunotherapy has evolved with greater understanding of cancer-mediated immunosuppression, tolerance, and immunosurveillance escape. Immunotherapy can be divided into active and passive approaches [1] with active immunization engaging the endogenous immune system to mount an immunologic response. The attraction of active immunotherapy includes the possibility to treat cancer while also providing long-lasting immune protection. A single active immunotherapeutic dendritic cell (DC) cancer vaccine (Provenge®; Sipuleucel-T) is approved by theFood and Drug Administration (FDA) [2]. The newer immune checkpoint blockade agents that stimulate endogenous active immunotherapeutic response [3–6] are also approved by the FDA.

Sunil Thomas (ed.), *Vaccine Design: Methods and Protocols: Volume 1: Vaccines for Human Diseases*, Methods in Molecular Biology, vol. 1403, DOI 10.1007/978-1-4939-3387-7_46,

A variety of different vaccination approaches remain under investigation for the treatment of cancer. Peptide vaccination is an active immunotherapy where an immunogenic peptide is administered, often with the use of an immunoadjuvant, to stimulate T-cell immunity. Peptide vaccinations are are presented on major histocompatibility complexes (MHC), the ultimate target for T cells in cancer recognition, with numerous antigen-specific antitumor immune responses having been documented in humans [7–9].Peptide vaccines are arguably the most promising and practical vaccination approach due to their simplicity, ease of production, and safety.

Highly varied in characterization from the antigenic source used to the concurrent use of adjuvants and/or immune modulators, the shared premise of peptide vaccines is to prime effector cells to seek and destroy cancer cells. With approaches ranging from a simple peptide vaccine to autologous whole tumor methods, each approach has specific advantages and disadvantages. Use of a specific peptide simplifies immunologic and safety monitoring given that the targeting of a specific epitope by a clonal population of T cells can be easily enumerated by flow cytometry [2–4]. However, the specificity of a single peptide potentially narrows the tumor target spectrum making it relevant to fewer patients. More complex vaccine strategies allow for application of a vaccine to a larger patient population; however, these complexities often threaten development and clinical acceptance of a particular vaccine strategy. DC vaccines utilize antigen-presenting cells from a patient primed with TAAs to create an antigen-specific immunologic response and have shown clinical benefit in overall survival [2]. Unfortunately, DC-based vaccines are technically difficult to manufacture and often inherently expensive to produce. Infectious vectors may be capable of producing a more robust immune response, but safety remains a concern with notable toxicity documented to include a death from an adenovirus vector [10, 11].

Various methods exist to enhance peptide immunogenicity. Researchers are exploring the effects of cancer vaccines when administered with cytokines and/or other immune agents [12]. Another approach to magnify immunogenicity is to modify the peptide itself. Examples of this strategy include the AE37 peptide from AE36 (HER2/*neu* derived), the gp100 melanoma antigen, and rindopepimut (PEPvIII) from EGFR. These three strategies are discussed below.

1.1 Ideal Setting for Treatment

An understanding of the biology of cancer tolerance is paramount in the development of new immunotherapies. Immunotherapeutic approaches should enhance vaccine-primed immune cell fitness and allow for a tumor microenvironment that is accessible to immune cell infiltration. Although cancer immunotherapy has focused increasingly on complex genetic manipulations of immune

effector cells and/or complicated vaccination methods, simpler strategies are now showing promise despite past failure to produce clinical benefits. Historically, peptide vaccines provoked an increase in CD8+ cytotoxic T cells within peripheral blood that did not correlate with tumor regression [13]. However, these failed trials occurred largely in the presence of metastatic disease. Current research suggests a minimal disease burden to be a more appropriate environment for vaccine treatment [14]. At completion of adjuvant therapy, cancer volume and immune suppression are minimized, thus lowering the obstacles for the stimulated immune system to overcome [15].

In the setting of more advanced malignancy to include larger tumor size and nodal involvement, patients are functionally immune suppressed compared to earlier stage of disease [16]. In animal models, large tumor volumes are more resistant to immunotherapy secondary to various mechanisms that include an increase in immunosuppressive cytokines, regulatory T cells and myeloid-derived suppressor cells, and downregulation of antigen processing and presentation [15, 17–19]. Human trials have also shown evidence that vaccines are more effective when patients are disease-free [20]. An autologous tumor cell hybridoma vaccine used in follicular lymphoma demonstrated efficacy in patients with complete response to chemotherapy, while advanced patients did not benefit from the vaccination in a separate trial [20–22]. Ultimately, if efficacy is proven, the use of a peptide vaccine strategy may be applied in the preventive setting. Given many patients will remain disease-free without intervention, these trials will require substantial numbers of patients and long-term follow-up to demonstrate efficacy.

1.2 TAA and Peptide Choice

Early debate in vaccine developments centered on selection and delivery of the ideal antigen with options from mutated proteins present exclusively in cancer to overexpressed or inappropriately expressed normal proteins. The ideal antigen should be expressed only in tumor cells while being both tumorigenic and immunogenic. The tumor target in a single epitope vaccine can be exceptionally narrow which may be positive due to greater specificity as well as negative in that the specific peptide may be relevant to fewer patients. Additional drawbacks include HLA restriction, particularly in regard to CD8+ lymphocyte targeting peptides, as general patient populations may not be optimal for clinical trials. Although more complex vaccine strategies can offer more antigens, the vaccine becomes more difficult to produce, administer, and monitor. Examining individual peptides allows for greater understanding for the next generation of peptide and combination therapies. The use of a single peptide allows for evaluation of immunologic and clinical efficacy of that epitope alone, whereas the efficacy and clinical relevance of TAAs when used in a multiple epitope vaccine may be impossible to determine.

Due to space restrictions, it is not possible to review all the peptide vaccines. Clinical trials of gp100, tecemotide (Stimuvax®; Biomara, Alberta, CA), and rindopepimut have provided strong evidence for peptide-based vaccines. We will discuss these therapies, clinical trials using multi-peptide strategies, and our own experience with the HER2/*neu*-derived peptides E75, GP2, and AE37 as well as the folate binding protein-derived peptide, E39.

2 Gp100 Vaccine

The gp100 peptide vaccine has been studied in the treatment of melanoma [23]. The modified HLA-A2*0201 bound gp100:209-217(210M) peptide was found to have greater binding affinity than the unmodified glycoprotein (gp)100 peptide with an increased ability to generate in vitro cytotoxic T-lymphocyte (CTL) response [24–28]. After vaccination with gp100:209–217(210M) peptide, high levels of circulating T cells capable of recognizing and killing melanoma cancer cells occurred in vitro, leading to the hypothesis that treatment with a cytokine such as interleukin-2 (IL-2) could be synergistic. As such, the gp100 vaccine is not only an example of modifying a peptide to enhance immunogenicity but using concurrent immunotherapies to enhance immunogenic response as well. A phase II study in patients with metastatic melanoma immunized with the gp100:209–217(210M) peptide vaccine in Montanide ISA-51 (incomplete Freund's adjuvant), followed by high-dose IL-2, led to objective clinical responses in 13 of 31 patients (42 %) [23], a response rate higher than with IL-2 alone.

After this early report of the gp100 peptide vaccine [23], the Cytokine Working Group initiated a series of three phase II studies to confirm the efficacy of the vaccine [29]. These three studies, involving 39–42 patients in each study, used the same peptide vaccine administered with one of three IL-2 schedules. With response rates ranging from 13 % to 24 %, these phase II studies did not include an IL-2 only control group, thus limiting conclusions regarding efficacy of the vaccine alone. However, the response rates seen were similar to those reported in a large, non-randomized, single-institution study of IL-2 with the vaccine as compared with IL-2 without the vaccine (22 % vs 13 %, $p=0.01$) [30].

A multicenter randomized phase III trial examining high-dose IL-2 with or without gp100 peptide in incomplete Freund's adjuvant for patients with metastatic melanoma enrolled 185 patients. A significant improvement was seen in overall response rate (16 % vs 6 %, $p=0.03$) and progression-free survival (2.2 vs 1.6 months, $p=0.008$) within the vaccine group compared to the control. A trend toward improved median overall survival (OS) in the gp100 group compared to IL-2 alone group also occurred although it was

not statistically significant (17.8 vs 11.1 months, $p=0.06$, respectively) [31].

In another recent randomized trial studying ipilimumab with or without gp100 vaccine, combination therapy was not superior to ipilimumab alone [3]. It is unclear why synergy has been exhibited with IL-2 but not with ipilimumab [3]. Further trials will surely seek to reexamine and validate prior conclusions.

3 Tecemotide Vaccine

Historically, melanoma and renal cell carcinoma have been considered the most immunogenic malignancies as opposed to the low immune reactivity of lung cancer. However, the recent success of nivolumab, a human immunoglobulin G4 programmed death 1 (PD-1) immune checkpoint inhibitor antibody, in non-small cell lung cancer (NSCLC) has challenged this paradigm [32]. The peptide vaccine tecemotide, also known as L-BLP25 (Stimuvax®; Biomara, Alberta, CA), has been tested in a variety of MUC1-expressing malignancies but predominantly in NSCLC. Tecemotide utilizes a portion of the extracellular domain of MUC1 (aa107-131), a glycosylated phosphoprotein frequently overexpressed in malignant tissues [33–36], combined with the immunoadjuvant monophosphoryl lipid A in a liposomal carrier. Antigen-specific T-cell proliferation and interferon-gamma secretion were confirmed in preclinical studies with early phase I and II trials exhibiting low toxicity [37–39].

The first phase III study of tecemotide, START (stimulating targeted antigenic responses to NSCLC), was a randomized, placebo-controlled, double-blind trial of 1513 patients from 33 countries. The trial included patients with inoperable stage III NSCLC after treatment with definitive chemoradiation (CRT). Initial results were disappointing as survival was not significantly increased with tecemotide treatment following CRT as compared to the placebo (25.8 vs 22.4 months, $p=0.11$) [40]. However, a survival benefit was noticed in the prespecified subset analysis of patients who were treated with concomitant CRT compared to those treated with sequential CRT (29.4 vs 20.8 months, $p=0.03$) [41]. Benefit was also shown in the exploratory biomarker analysis of patients with elevated sMUC1 or ANA levels.

Critical response to the design of the initial phase III trial included the view that the ability to achieve therapeutic effects in unresected patients without simultaneous use of checkpoint inhibitors such as anti-CTLA4 or anti-PD1 antibodies is an unrealistic expectation. Also possible is that NSCLC may be resistant to immunotherapy, although this argument, as previously stated, has been challenged by nivolumab's recent success. Another criticism of this trial (and common to peptide vaccination in general) is the

high specificity of the immunogenic target, a single TAA, given malignant cells can generate immunoediting and immunologic escape [42]. The patient population may have been too general; the exclusion of those with low peripheral T lymphocyte and/or high immunosuppressive cell counts from future vaccination trials may be a better strategy [43].

Subsequent trials aimed to employ lessons learned from the initial studies. The START2 trial addressed patients who received concurrent CRT followed by tecemotide maintenance therapy [44]. The INSPIRE trial focused on a Japanese population with stage II NSCLC, whereas the START trial focused largely on a Caucasian population [45]. Unfortunately, both of these studies have been discontinued. However, phase II trials for tecemotide for rectal cancer [46] and in combination with androgen deprivation therapy for prostate cancer [47] are ongoing. The Eastern Cooperative Oncology Group (ECOG) is also investigating combination tecemotide and bevacizumab after CRT for stage IIIA or stage IIIB unresectable NSCLC [48].

4 Rindopepimut Vaccine

An up and coming therapy for treatment of glioblastoma multiforme (GBM) is the epidermal growth factor receptor (EGFR)-derived peptide, rindopepimut or PEPvIII-KLH (Celldex Therapeutics, Phillipsburg, NJ), an EGFRvIII-specific, 14-mer peptide shown to elicit humoral and cellular immune response when coupled with keyhole limpet hemocyanin (KLH). Clinically, overexpression and amplification of the EGFR gene is associated with poor oncologic prognosis [49], and in GBM, EGFR amplification and overexpression occur in 50 % and 90 % of specimens, respectively [50, 51]. EGFR class III variant (EGFRvIII) is an activated mutant of the wild-type tyrosine kinase. Although absent from normal tissues, EGFRvIII is present in a substantial number of human cancers, including malignant gliomas.

The VICTORI study evaluated the efficacy of an EGFRvIII-based DC vaccine [52]. Despite encouraging results, the high cost and difficulty of producing a DC-based vaccine on a large scale led to the phase II multicenter ACTIVATE study where PEPvIII-KLH was directly administered in combination with granulocyte macrophage colony stimulating factor (GM-CSF) [53]. ACTIVATE enrolled 19 adults with EGFRvIII-expressing, newly diagnosed primary GBM (WHO Grade IV). Prior to vaccination, patients underwent >95 % volumetric tumor resection, radiation, and concurrent temozolomide (TMZ). Similar to the prior VICTORI study, significant adverse effects were not present aside from irritation at the injection site. PEPvIII- and EGFRvIII-specific immune response predicted greater median survival. Compared to histori-

cal, matched unvaccinated controls, median time to progression was significantly improved (12 vs 7.1 months, $p = 0.0058$, respectively). If tumors recurred, pathological samples were evaluated for EGFRvIII expression with none found to have positive staining [54]. The ACT II trial followed the same scheme as ACTIVATE although with different TMZ dosing schedule. TMZ-associated lymphopenia was observed although immune response was either sustained or enhanced with TMZ treatments [55].

Ongoing trials include the phase III ACT IV (NCT01480479) in newly diagnosed, surgically resected, EGFRvIII-positive GBM. This two-arm, randomized trial investigates rindopepimut's efficacy when added to the current standard of care, TMZ. Rindopepimut is administered with GM-CSF as immunoadjuvant. KLH, the immunogenic carrier protein within rindopepimut, is not anticipated to have significant therapeutic effect and is thus used as a control [56]. ReACT (NCT01480479) is a phase II study evaluating the efficacy of adding rindopepimut to bevacizumab in recurrent EGFRvIII-positive GBM patients. Patients are divided into two groups, those never treated with bevacizumab and those refractory to bevacizumab. Patients receive either rindopepimut with GM-CSF or KLH as control [57].

5 HER2/*neu*: E75, GP2, AE37 Vaccines

Our group has evaluated three different HER2/*neu*-derived single-peptide vaccines for the treatment of preventing breast cancer recurrence. HER2/*neu* holds potential due to its ability to drive the oncogenic response, and its low-to-absent expression on healthy tissue. The peptide of choice is delivered with GM-CSF as immunoadjuvant with intradermal inoculation after standard-of-care chemotherapy, radiation, and surgery as indicated. The first cancer vaccine evaluated by our group was the nine amino-acid peptide, E75 (HER2/*neu* 369-377, KIFGSLAFL) from the HER2/*neu*'s extracellular domain. NeuVax™ (E75 + GM-CSF) has recently completed enrollment in a phase III clinical trial [58]. The second vaccine evaluated by our group was another 9 amino-acid peptide, GP2 (HER2/*neu* 654-662, IISAVVGIL), from the transmembrane domain of HER2/*neu*. Similar to E75, CD8+ lymphocyte stimulation occurs albeit at a lower binding infinity than E75 [59]. The third peptide, AE37, is CD4+ lymphocyte-eliciting Ii-key (LRMI) hybrid with AE36 from the intracellular domain of HER2/*neu* (776-790; Ac-GVGSPYVSRLLGICL-NH_2) and obviates the need for MHC-class restriction. The addition of the 4 amino-acid Ii-key moiety makes AE37 150-fold more immunogenic than AE36 [60].

6 E75

E75 (or nelipepimut-S) is an MHC-class I-, HLA-A2-, and HLA-A3-restricted epitope and one of the most studied TAAs. Preclinical studies showed E75 to be the immunodominant epitope of the HER2 protein. Other preclinical works revealed that patients with HER2/*neu*-expressing malignancies had some level of preexisting E75 immunity and that dendritic cells stimulated with E75 were capable of achieving E75-specific cytotoxicity in peripheral mononuclear cells [61–67]. Although evaluated within the context of dendritic cell vaccination in breast, ovarian, and gastric cancers [62, 66], E75 has been studied most extensively in peptide-based vaccines. Previously tested in metastatic breast, ovarian, and colorectal cancers with a variety of immunoadjuvants, it was found to be safe and immunogenic as a peptide vaccine although failing to produce a clinical tumor response in metastatic patients [68–70].

A phase I, dose-escalation trial was conducted in prostate cancer patients who had undergone surgical resection and were clinically disease-free. Of the 40 patients enrolled, 21 HLA-A2-positive patients were given 100, 500, or 1000 mcg of E75 along with 250 mcg of GM-CSF in monthly, intradermal inoculations for 4–6 months, while the 19 HLA-A2-negative patients were followed as controls. Vaccinated patients exhibited an immunologic response with minimal toxicity observed. There were, however, no differences in biochemical (prostate-specific antigen) recurrence rate, clinical recurrence rate, or overall survival at a median follow-up of 58 months except when patients who did not complete the vaccination series were excluded [71, 72].

Expanding E75 into breast cancer, two phase I trials were initiated in node-negative and node-positive breast cancer patients, respectively. All patients were clinically disease-free after the completion of standard surgical, chemotherapeutic, and radiation therapy. HLA-A2-positive patients with any level of HER2/*neu* expression were vaccinated while HLA-A2-negative patients were followed as controls. Both trials demonstrated immunologic responses to vaccination with low toxicity [73]. These trials were transitioned to phase II trials enrolling high-risk node-negative and node-positive patients in parallel. Based on modeled predicted binding and preclinical data, E75 was suggested to bind HLA-A3 in addition to HLA-A2. Thus, HLA-A3 patients were enrolled into the vaccine arm, while HLA-A2/A3-negative patients were followed as controls [73]. At the completion of the trial, 108 HLA-A2/A3-positive patients were vaccinated while 79 HLA-A2/A3-negative patients were followed as controls for 60 months. The groups were well matched with the exception of vaccine patients being more likely hormone receptor negative. The vaccine

was well tolerated with only 1.9 % experiencing grade 3 toxicities, and no grade 4 or 5 toxicities are observed.

The study concluded at 5-year follow-up with disease-free survival (DFS) for vaccinated patients at 89.7 % compared to 80.2 % for control patients ($p=0.08$). Prespecified group analysis was performed in respect to HER2/*neu* expression, optimal biologic dosing (OBD), and receipt of booster inoculations. Patients who derived the greatest benefit from the vaccine included those patients who were HER2/*neu* IHC 1+ or 2+ in the vaccine arm with 88.1 % DFS compared to controls at 77.5 % DFS ($p=0.16$). Those who received the OBD of the vaccine (1000 mcg E75, 250 mcg GM-CSF) derived even greater benefit [74]. Of the 37 patients who received the OBD, the 5-year DFS rate was 94.6 % compared to controls at 77.5 % ($p=0.05$). Additionally, the 21 patients who received booster inoculations every 6 months to maintain E75-specific immunity, an addition that was initiated midway through the trial to combat waning immunity, had a 5-year DFS rate of 95.2 % ($p=0.11$) [75, 76]. These results support that a sufficient quantity of immunostimulation (optimal dosing) and duration (booster inoculations) is necessary to attain maximal clinical benefit from this CD8+ eliciting vaccine.

NeuVax™ (nelipepimut-S or E75 + GM-CSF) is currently in a phase III PRESENT trial (Prevention of Recurrence in Early-Stage Node-Positive Breast Cancer with Low to Intermediate HER2 Expression with NeuVax™ Treatment) that enrolled patients with HER2/*neu* IHC 1+, 2+ tumors. The PRESENT trial (NCT01479244) has recently closed enrollment of node-positive, clinically disease-free, HLA-A2/A3-positive patients who have completed standard-of-care therapy. Patients were randomized to vaccination with E75 + GM-CSF given at the OBD with booster inoculations or an identical schedule of GM-CSF alone. Primary endpoint is 3-year DFS [58].

The effect of E75 in HER2/*neu* overexpressing patients is less clear, but preclinical data [77] and past experience in phase II trials suggest synergism with trastuzumab. As past studies were instituted prior to trastuzumab becoming standard of care, subsets of patients who did and did not receive trastuzumab with vaccination are available for comparison. Among patients who did receive trastuzumab and were subsequently vaccinated ($n=21$), there were no recurrences. Given these data, an additional phase II trial (NCT02297698) is examining E75 in conjunction with trastuzumab in HER2/*neu* overexpressing (IHC 3+ or FISH >2.2) patients at high risk for recurrence: node-positive patients after standard-of-care therapies or patients who did not have a pathologic complete response to neoadjuvant chemotherapy [78].

7 GP2

Similar to E75, GP2 stimulates CD8+ lymphocytes although with a lower binding affinity as a subdominant epitope [59] and may be effective in overexpressing patients after or in combination with trastuzumab. Theoretically, the GP2 vaccine may have less inherent tolerance to overcome, particularly in breast cancer patients with tumors expressing higher HER2/*neu* levels. After preclinical testing confirmed CD8+ lymphocyte stimulation [79], phase I clinical testing explored dose and vaccination optimization. The trial enrolled HLA-A2-positive, clinically disease-free, lymph node-negative breast cancer patients. Eighteen patients were enrolled and vaccinated in escalating dosing groups of GP2 + GM-CSF given as six monthly intradermal inoculations. Toxicities were minimal with no grade 3 or higher toxicities observed. In vivo and ex vivo immunologic responses were robust including an increase in E75-specific cytotoxic T lymphocytes suggesting epitope spreading [80].

A prospective, randomized, single-blind phase II trial has enrolled high-risk breast cancer patients who are clinically disease-free after completion of standard-of-care therapy. HLA-A2-positive patients were randomized to receive six monthly inoculations followed by four booster inoculations every 6 months of either 500 mcg of GP2 with 125 mcg of GM-CSF (vaccine group) vs 125 mcg of GM-CSF alone (control group). Of the 180 patients enrolled, the vaccine ($n = 89$) and control ($n = 91$) groups were well matched. Toxicities were minimal and attributed largely to GM-CSF with only one grade 3 toxicity. At a median follow-up of 34 months, there was no difference in the rate of DFS between the vaccine group and the control group by intention-to-treat analysis (85 % vs 81 %, $p = 0.57$, respectively). A prespecified per-treatment analysis, which excluded patients who recurred or developed secondary malignancies during the initial 6-month primary inoculation series, demonstrated a DFS rate of 94 % in the vaccine group compared to 85 % in the control group ($p = 0.17$) [81].

This trial enrolled a higher rate of HER2/*neu* overexpressing patients (IHC 3+ or FISH >2.2) than the previous E75 trial with all patients receiving trastuzumab as part of their standard-of-care therapy. Within this prespecified subgroup, the intention-to-treat DFS rate was 94 % in the vaccine group and 89 % in the control group ($p = 0.86$), whereas the per-treatment DFS was 100 % in the vaccine group and 89 % in the control group ($p = 0.08$). These results serve as further data of the previously discussed synergistic effect between CD8-eliciting, MHC-class I peptide vaccination and trastuzumab therapy [82].

8 AE37

AE37 differs from our other HER2/*neu*-derived peptide vaccines in that it targets CD4+ lymphocytes and is not HLA restricted due to promiscuous binding. AE37 may be most effective in triple-negative breast cancer as a CD4+ lymphocyte targeting vaccine. Preclinical investigations demonstrated effective priming of CD4+ lymphocytes and antitumor activity in animal models [83, 84]. The phase I trial enrolled clinically disease-free, lymph node-negative breast cancer patients with any level of HER2/*neu* expression. Escalating doses were delivered to 15 patients with GM-CSF as six monthly inoculations. Only grade 1 and 2 toxicities were observed with strong local reactions at times so robust that the GM-CSF was removed in subsequent dosing. In vivo and ex vivo immunologic response was demonstrated in the vaccinated population [85]. Regulatory T cells (CD4+ CD25+ FOXP3+ CTLs) were also found to decrease after vaccination [86].

Given these results, a prospective, randomized, single-blinded phase II trial enrolling high-risk breast cancer patients who were clinically disease-free after completing standard-of-care therapy was initiated. Patients, regardless of HLA-type, were randomized to receive six monthly inoculations followed by four booster inoculations every 6 months of either 500 mcg of AE37 with 125 mcg of GM-CSF (vaccine group) vs 125 mcg of GM-CSF alone (control group).

Of the 298 patients enrolled, 153 were in the vaccine group and 145 in the control group. Clinicopathologic characteristics were well matched. The vaccine was again shown to be safe without any grade 3 or higher local toxicity and with only one patient experiencing grade 3 systemic toxicity [81]. The primary intention-to-treat analysis was prespecified to be performed at 39 events, which occurred at 30 months median follow-up and demonstrated 87.6 % DFS in the vaccine group compared to 86.2 % in the control group ($p = 0.70$). In the prespecified subset analyses, patients with low HER2 expression (IHC 1+ or 2+, FISH <2.2) demonstrated 86.8 % DFS in the vaccine group compared to 82 % in the control group ($p = 0.21$). The triple-negative subgroup of patients (ER negative, PR negative, HER2/*neu* IHC 1–2+) showed the greatest benefit with 84 % DFS in vaccinated patients compared to 64 % DFS in the control patients ($p = 0.12$) [81]. The vaccine may work best in the triple-negative subtype given the inherent immunogenicity of this cancer subtype, and AE37 may lead to a more generalized enhancement of the innate immune response to breast cancer. Evidence for the importance of the immune response in the triple-negative breast cancer subtype includes the finding that increased intratumoral CD8+ lymphocytes has been independently associated with a better prognosis in basal-type triple-negative breast cancers but not other breast cancer subtypes. B-cell meta-

gene expression is also associated with a better prognosis in breast cancer [87, 88].

Individualization of care to gain maximum clinical benefit, a common theme in modern cancer treatment and immunotherapy, thus applies to the HER2/*neu*-derived peptide cancer vaccines described above. The E75 vaccine is apparently best suited for HER2/*neu* 1–2+ patients, while GP2 appears to be most effective in HER2/*neu* 3+ patients, and AE37 demonstrated its best effect in patients with triple-negative ($ER^-/PR^-/HER1\text{-}2^+$) breast cancer.

9 Folate-Binding Protein Vaccine

Folate-binding protein (FBP) is another protein utilized by our group in vaccine trials. Overexpressed in the vast majority of ovarian and endometrial cancers, as well as 20–50 % of epithelial cancers to include breast cancer [89–91], FBP has also been shown to be functionally relevant with increased expression and folate uptake in malignancy [92]. FBP overexpression has been associated with higher grade, stage, and percentage of cells in s-phase [92], failure to response to platinum-based chemotherapy, and reduced survival for ovarian cancer patients with residual disease after surgical treatment [93]. Given FBP holds relatively isolated visibility to the immune system, it is an attractive target with passive or active immunotherapeutic techniques. In respect to other epithelial cancers, FBP overexpression is associated with resistance of melanoma cells to methotrexate and colon cancer cells to 5-fluorouracil [94, 95] as well as worse prognosis in breast cancer [96] and uterine adenocarcinoma [96].

E39 is an FBP-derived immunogenic peptide (191–199) [97, 98] capable of enhancing tumor-associated lymphocyte (TAL) proliferation and antitumor function [99]. Again following the same vaccine model used by our group, E39 is administered in combination with GM-CSF adjuvant for six monthly inoculations during the primary vaccine series followed by two booster inoculations administered every 6 months thereafter. The phase I safety trial began as a 3×3, dose-escalation (100, 500, 1000 mcg of E39) study and transitioned to a phase IIa trial comparing expanded dose cohorts. Disease-free endometrial and ovarian cancer patients were enrolled after standard of care with HLA-A2-positive patients vaccinated, and HLA-A2-negative patients followed prospectively as a control group. Preliminary results of our phase IIa trial of the E39 + GM-CSF adjuvant cancer vaccine in ovarian and endometrial cancer patients showed strong immunogenic response and recurrence reduction, particularly among the 1000 mcg dose cohort. Currently there is only one recurrence in the 100 mcg dose cohort compared with 50 % recurrence in the control group ($p = 0.01$) [100].

10 Multi-peptide Vaccines

It is possible that single-agent immunotherapies have reached limitations, and trials combining multiple agents are necessary to advance cancer treatment. Including immune modulators such as checkpoint blockade agents (e.g., CTLA-4 or PD-1/PD-L1 antibodies) in vaccine strategies may improve the overall immune response and thus clinical outcome [101, 102]. Another possibility is to include multiple epitopes in one vaccine.

The majority of peptide-based cancer vaccines incorporate MHC-class I-restricted peptides to activate CD8+ CTLs, but activation of CD4+ helper T cells may also be critical for tumor elimination. Various trials have examined a multi-peptide approach. A phase II trial utilized the cancer-testis antigen LY6K, CDCA1, and IMP3 peptides for immunotherapeutic treatment of head and neck squamous cell cancer. CTL-specific responses were associated with a longer overall survival than those without CTL induction. When CTL induction for multiple peptides was demonstrated, better clinical responses were observed as well [103].

A multicenter randomized trial examined 167 patients with resected stage IIB to IV melanoma who were randomly assigned to four vaccination study arms. Researchers sought to test whether melanoma-associated helper peptides could augment CD8+ T-cell responses as well as the effect of cyclophosphamide pretreatment on CD4+ or CD8+ T-cell response. Subjects were vaccinated with 12 class I MHC-restricted melanoma peptides (12MP) to stimulate CD8+ T cells and were randomly assigned to receive either a tetanus helper peptide or a mixture of six melanoma-associated helper peptides (6MHP) to stimulate CD4+ T cells. Before vaccination, patients were also randomly assigned to receive cyclophosphamide (CY) pretreatment or not. The results were surprising with melanoma-associated helper peptides actually decreasing CD8+ T-cell responses to the melanoma vaccine ($p < 0.001$). CY pretreatment had no immunologic or clinical effect [104].

Another multicenter randomized trial divided 147 patients with stage IV melanoma into four treatment groups: those vaccinated with 12 MHC-class I-restricted melanoma peptides (12MP) only (group A), 12MP plus a tetanus peptide (group B), 12MP plus a mixture of 6 melanoma helper peptides (6MHP, group C), and 6MHP only (group D) in IFA plus GM-CSF. Groups A–D exhibited CTL response rates to 12MP of 43 %, 47 %, 28 %, and 5 % with helper T-lymphocyte response rates to 6MHP of 3 %, 0 %, 40 %, and 41 %, respectively. Partial response in 7/148 (4.7 %) evaluable patients was the best clinical response with no difference among study arms. A significant association between clinical and immune response was found in respect to 6MHP, but MHPs failed to augment CTL response to 12MP. The authors concluded that

helper peptide vaccine certainly merit further investigation, as does combination with other potentially synergistic active therapies to improve antigen expression and CTL infiltration of metastases [105].

The Mel 60 trial (NCT02126579) is a multisite, FDA-approved phase I/II study utilizing the same long peptides with the addition of TLR agonists for resected stage IIB–IV melanoma. The primary objective is to evaluate the safety and immunogenicity of vaccination with a mixture of long peptides for patients with histologically or cytologically proven stage IIB–IV melanoma rendered clinically free of disease by surgery, other therapy, or spontaneous remission [106]. There are no reportable results yet to date [107].

11 Conclusions

Peptide vaccines are an attractive immunotherapeutic option. They are simple to manufacture and administer while boasting a consistent record of safety. Although results are encouraging within the adjuvant setting, inefficacy is shown thus far in metastatic cancer. Despite past trials eliciting immunogenic responses with peptide vaccination, a large breakthrough was the ability to correlate these responses with clinical outcome in the adjuvant setting [108]. Ultimately, the extent to which peptide cancer vaccines will be useful in treating metastatic patients will likely depend on rational combinations with other immunotherapeutic agents that alter the tumor microenvironment.

A variety of peptide-based cancer vaccines to date provide important lessons applicable to future vaccine development. First, several peptide vaccines targeting a single TAA have shown clinical activity suggesting that the induction of a strong endogenous antigen-specific immune response may be sufficient to engage the host immune system in a much broader anticancer response leading to clinical benefit. Second, the consistent efficacy of smaller adjuvant phase II trials supports initiation of large phase III trials examining peptide vaccine therapy in patients with minimal-residual disease. Proving efficacy of cancer vaccines in the adjuvant settings may eventually allow expansion to patients with aggressive and more advanced disease but in combination with other agents. Trials support the use of booster inoculations to maintain immunity especially in the adjuvant setting. The phase II E75 trial showed initial waning immunity corresponding with increase recurrences in the vaccine arm. Booster inoculations were able to maintain immunity, and those who received scheduled booster inoculations were less likely to recur. Third, the results indicate that vaccine formulations should be tailored to the specifics of the tumor and patient population being targeted. As cancer care is

moved to more personalized and targeted therapy, this data suggest that immunotherapy should follow this strategy. With peptide vaccines, it is logical to ensure that the targeted antigen is expressed by the tumor, but the binding affinity may need to be tailored to match antigen expression. This becomes particularly relevant with the use of subdominant epitopes with lower binding affinity against antigens with higher expression levels to avoid or overcome tolerance. Using our peptide vaccines as an example, E75, a dominant epitope of HER2/*neu*, appears most effective in HER2/*neu* low-expressing breast cancer. GP2, a subdominant epitope of HER2/*neu*, has greatest potential in HER2/*neu* overexpressing breast cancers, especially in combination with trastuzumab. AE37, the MHC-class II-targeted vaccine, holds promise in triple-negative ($ER^-/PR^-/HER1\text{-}2^+$) breast cancers.

Finally, growing evidence suggests that peptide vaccines work synergistically with other immunotherapies to include monoclonal antibody therapy [109], cytokines, and immunomodulators. Beneficial immunomodulatory effects may be present in combining cancer vaccination with chemotherapy or radiation, an area being actively investigated [110–112]. Checkpoint blockade is a particularly noteworthy area of interest with promising effectiveness in various cancer types when used alone [113, 114]. Combining checkpoint blockade with cancer vaccines may eventually lead to effective treatments in patients with more advanced disease.

12 Future Directions

Although a simple strategy, peptide vaccination is subject to a complex immunoregulatory milieu. The detailed mechanisms underlying the beneficial effects of various peptide vaccines are still not fully elucidated. Numerous immune-suppressing molecules and immune regulatory checkpoints have implications in the suppression of in vivo T-cell response. Combination of gp100 vaccine with IL-2 and HER2/*neu* peptide vaccines with trastuzumab appears to be two examples of this synergy. Caution regarding cumulative toxicities with multi-agent therapies should be considered given the possibility of inducing additional circulating cytokines. Additional clinical trials should elucidate a more complete understanding.

The challenges that remain include identifying the best and/or combination of TAAs, selecting the most effective adjuvant, and identifying concurrent immunotherapies that maximize synergistic effects. It is likely that vaccines may only be effective for certain subgroups of patients. This will have significant impact on future trial design and development. Regardless, the encouraging results thus far support a future role of peptide vaccination in the treatment of cancer.

References

1. Rosenberg SA (2004) Shedding light on immunotherapy for cancer. N Engl J Med 350:1461–1463
2. Kantoff PW, Higano CS, Shore ND, Berger ER et al (2010) Sipuleucel-T immunotherapy for castration-resistant prostate cancer. N Engl J Med 363:411–422
3. Hodi FS, O'Day SJ, McDermott DF, Weber RW, Sosman JA et al (2010) Improved survival with ipilimumab in patients with metastatic melanoma. N Engl J Med 363:711–723
4. Robert C, Long GV, Brady B, Dutriaux C, Maio M et al (2014) Nivolumab in previously untreated melanoma without BRAF mutation. N Engl J Med 372:320–330
5. Alexander M. Eggermont VC-S, Grob JJ, Dummer R et al (2014) Ipilimumab versus placebo after complete resection of stage III melanoma: Initial efficacy and safety results from the EORTC 18071 phase III trial. J Clin Oncol 32:5s
6. Waqar SN, Morgensztern D (2015) Immunotherapy for non-small cell lung cancer: are we on the cusp of a new era? Expert Rev Clin Immunol 11(8):871–873
7. Townsend AR, Gotch FM, Davey J (1985) Cytotoxic T cells recognize fragments of the influenza nucleoprotein. Cell 42:457–467
8. Townsend AR, Rothbard J, Gotch FM, Bahadur G, Wraith D, McMichael AJ (1986) The epitopes of influenza nucleoprotein recognized by cytotoxic T lymphocytes can be defined with short synthetic peptides. Cell 44:959–968
9. Maryanski JL, Pala P, Corradin G, Jordan BR, Cerottini JC (1986) H-2-restricted cytolytic T cells specific for HLA can recognize a synthetic HLA peptide. Nature 324:578–579
10. Marshall E (1999) Gene therapy death prompts review of adenovirus vector. Science 286:2244–2245
11. Bolhassani A, Zahedifard F (2012) Therapeutic live vaccines as a potential anticancer strategy. Int J Cancer 131:1733–1743
12. Overwijk WW, Theoret MR, Restifo NP (2000) The future of interleukin-2: enhancing therapeutic anticancer vaccines. Cancer J Sci Am 6(Suppl 1):S76–S80
13. Rosenberg SA, Sherry RM, Morton KE, Scharfman WJ et al (2005) Tumor progression can occur despite the induction of very high levels of self/tumor antigen-specific CD8+ T cells in patients with melanoma. J Immunol 175:6169–6176
14. Hale DF, Clifton GT, Sears AK, Vreeland TJ, Shumway N, Peoples GE, Mittendorf EA (2012) Cancer vaccines: should we be targeting patients with less aggressive disease? Expert Rev Vaccines 11:721–731
15. Hsieh CL, Chen DS, Hwang LH (2000) Tumor-induced immunosuppression: a barrier to immunotherapy of large tumors by cytokine-secreting tumor vaccine. Hum Gene Ther 11:681–692
16. Adler A, Stein JA, Ben-Efraim S (1980) Immunocompetence, immunosuppression, and human breast cancer. III. Prognostic significance of initial level of immunocompetence in early and advanced disease. Cancer 45:2074–2083
17. Marigo I, Dolcetti L, Serafini P, Zanovello P, Bronte V (2008) Tumor-induced tolerance and immune suppression by myeloid derived suppressor cells. Immunol Rev 222:162–179
18. Pan PY, Wang GX, Yin B, Ozao J, Ku T, Divino CM, Chen SH (2008) Reversion of immune tolerance in advanced malignancy: modulation of myeloid-derived suppressor cell development by blockade of stem-cell factor function. Blood 111:219–228
19. Melani C, Chiodoni C, Forni G, Colombo MP (2003) Myeloid cell expansion elicited by the progression of spontaneous mammary carcinomas in c-erbB-2 transgenic BALB/c mice suppresses immune reactivity. Blood 102:2138–2145
20. Schuster SJ, Neelapu SS, Gause BL, Janik JE et al (2011) Vaccination with patient-specific tumor-derived antigen in first remission improves disease-free survival in follicular lymphoma. J Clin Oncol 29:2787–2794
21. Freedman A, Neelapu SS, Nichols C, Robertson MJ et al (2009) Placebo-controlled phase III trial of patient-specific immunotherapy with mitumprotimut-T and granulocyte-macrophage colony-stimulating factor after rituximab in patients with follicular lymphoma. J Clin Oncol 27:3036–3043
22. Levy R, Ganjoo KN, Leonard JP, Vose JM, Flinn IW et al (2014) Active idiotypic vaccination versus control immunotherapy for follicular lymphoma. J Clin Oncol 32:1797–1803
23. Rosenberg SA, Yang JC, Schwartzentruber DJ, Hwu P et al (1998) Immunologic and therapeutic evaluation of a synthetic peptide vaccine for the treatment of patients with metastatic melanoma. Nat Med 4:321–327
24. Cormier JN, Salgaller ML, Prevette T, Barracchini KC et al (1997) Enhancement of cellular immunity in melanoma patients immunized with a peptide from MART-1/Melan A. Cancer J Sci Am 3:37–44

25. Marincola FM, Rivoltini L, Salgaller ML, Player M, Rosenberg SA (1996) Differential anti-MART-1/MelanA CTL activity in peripheral blood of HLA-A2 melanoma patients in comparison to healthy donors: evidence of in vivo priming by tumor cells. J Immunother Emphasis Tumor Immunol 19:266–277
26. Parmiani G, Castelli C, Pilla L, Santinami M, Colombo MP, Rivoltini L (2007) Opposite immune functions of GM-CSF administered as vaccine adjuvant in cancer patients. Ann Oncol 18:226–232
27. Rivoltini L, Kawakami Y, Sakaguchi K, Southwood S et al (1995) Induction of tumor-reactive CTL from peripheral blood and tumor-infiltrating lymphocytes of melanoma patients by in vitro stimulation with an immunodominant peptide of the human melanoma antigen MART-1. J Immunol 154:2257–2265
28. Salgaller ML, Afshar A, Marincola FM, Rivoltini L, Kawakami Y, Rosenberg SA (1995) Recognition of multiple epitopes in the human melanoma antigen gp100 by peripheral blood lymphocytes stimulated in vitro with synthetic peptides. Cancer Res 55:4972–4979
29. Sosman JA, Carrillo C, Urba WJ, Flaherty L, Atkins MB et al (2008) Three phase II cytokine working group trials of gp100 (210M) peptide plus high-dose interleukin-2 in patients with HLA-A2-positive advanced melanoma. J Clin Oncol 26:2292–2298
30. Smith FO, Downey SG, Klapper JA, Yang JC, Sherry RM et al (2008) Treatment of metastatic melanoma using interleukin-2 alone or in conjunction with vaccines. Clin Cancer Res 14:5610–5618
31. Schwartzentruber DJ, Lawson DH, Richards JM, Conry RM et al (2011) gp100 peptide vaccine and interleukin-2 in patients with advanced melanoma. N Engl J Med 364:2119–2127
32. Sundar R, Cho BC, Brahmer JR, Soo RA (2015) Nivolumab in NSCLC: latest evidence and clinical potential. Ther Adv Med Oncol 7:85–96
33. Vlad AM, Kettel JC, Alajez NM, Carlos CA, Finn OJ (2004) MUC1 immunobiology: from discovery to clinical applications. Adv Immunol 82:249–293
34. Karsten U, von Mensdorff-Pouilly S, Goletz S (2005) What makes MUC1 a tumor antigen? Tumour Biol 26:217–220
35. Rahn JJ, Chow JW, Horne GJ, Mah BK, Emerman JT, Hoffman P, Hugh JC (2005) MUC1 mediates transendothelial migration in vitro by ligating endothelial cell ICAM-1. Clin Exp Metastasis 22:475–483
36. Yin L, Li Y, Ren J, Kuwahara H, Kufe D (2003) Human MUC1 carcinoma antigen regulates intracellular oxidant levels and the apoptotic response to oxidative stress. J Biol Chem 278:35458–35464
37. Agrawal B, Krantz MJ, Reddish MA, Longenecker BM (1998) Rapid induction of primary human CD4+ and CD8+ T cell responses against cancer-associated MUC1 peptide epitopes. Int Immunol 10:1907–1916
38. Palmer M, Parker J, Modi S, Butts C, Smylie M, Meikle A, Kehoe M, MacLean G, Longenecker M (2001) Phase I study of the BLP25 (MUC1 peptide) liposomal vaccine for active specific immunotherapy in stage IIIB/IV non-small-cell lung cancer. Clin Lung Cancer 3:49–57, discussion 58
39. North S, Butts C (2005) Vaccination with BLP25 liposome vaccine to treat non-small cell lung and prostate cancers. Expert Rev Vaccines 4:249–257
40. Butts C, Socinski MA, Mitchell PL, Thatcher N et al (2014) Tecemotide (L-BLP25) versus placebo after chemoradiotherapy for stage III non-small-cell lung cancer (START): a randomised, double-blind, phase 3 trial. Lancet Oncol 15:59–68
41. Mitchell P, Thatcher N, Socinski MA, Wasilewska-Tesluk E et al (2015) Tecemotide in unresectable stage III non-small-cell lung cancer in the phase III START study: updated overall survival and biomarker analyses. Ann Oncol 26:1134–1142
42. Zitvogel L, Tesniere A, Kroemer G (2006) Cancer despite immunosurveillance: immunoselection and immunosubversion. Nat Rev Immunol 6:715–727
43. Yoshiyama K, Terazaki Y, Matsueda S, Shichijo S et al (2012) Personalized peptide vaccination in patients with refractory non-small cell lung cancer. Int J Oncol 40:1492–1500
44. ClinicalTrials.gov (2014) Tecemotide following concurrent chemo-radiotherapy for non-small cell lung cancer (START2). Accessed 19 May 2015
45. Ohyanagi F, Horai T, Sekine I, Yamamoto N et al (2011) Safety of BLP25 liposome vaccine (L-BLP25) in Japanese patients with unresectable stage III NSCLC after primary chemoradiotherapy: preliminary results from a Phase I/II study. Jpn J Clin Oncol 41:718–722
46. ClinicalTrials.gov (2014) A multi-center, randomized, open-label, mechanism of action trial on the biological effects of the therapeutic

cancer vaccine Stimuvax® (L-BLP25) in rectal cancer subjects undergoing neoadjuvant chemoradiotherapy. Accessed 19 May 2015
47. ClinicalTrials.gov (2015) A randomized phase II study of tecemotide in combination with standard androgen deprivation therapy and radiation therapy for untreated, intermediate and high risk prostate cancer patients. Accessed 19 May 2015
48. ClinicalTrials.gov (2014) A phase II study of L-BLP25 and bevacizumab in unresectable stage IIIA and IIIB non-squamous non-small cell lung cancer after definitive chemoradiation. Accessed 19 May 2015
49. Neal DE, Sharples L, Smith K, Fennelly J, Hall RR, Harris AL (1990) The epidermal growth factor receptor and the prognosis of bladder cancer. Cancer 65:1619–1625
50. Ekstrand AJ, James CD, Cavenee WK, Seliger B, Pettersson RF, Collins VP (1991) Genes for epidermal growth factor receptor, transforming growth factor alpha, and epidermal growth factor and their expression in human gliomas in vivo. Cancer Res 51:2164–2172
51. Jaros E, Perry RH, Adam L, Kelly PJ, Crawford PJ et al (1992) Prognostic implications of p53 protein, epidermal growth factor receptor, and Ki-67 labelling in brain tumours. Br J Cancer 66:373–385
52. Sampson JH, Archer GE, Mitchell DA, Heimberger AB et al (2009) An epidermal growth factor receptor variant III-targeted vaccine is safe and immunogenic in patients with glioblastoma multiforme. Mol Cancer Ther 8:2773–2779
53. Heimberger AB, Hussain SF, Aldape K, Sawaya R et al (2006) Tumor-specific peptide vaccination in newly-diagnosed patients with GBM. J Clin Oncol 24(18S):2529
54. Schmittling RJ, Archer GE, Mitchell DA, Heimberger A et al (2008) Detection of humoral response in patients with glioblastoma receiving EGFRvIII-KLH vaccines. J Immunol Methods 339:74–81
55. Sampson JH, Archer GE, Bigner D, Davis T, Friedman HS, Keler T et al (2008) Effect of EGFRvIII-targeted vaccine (CDX-110) on immune response and TTP when given with simultaneous standard and continuous temozolomide in patients with GBM. J Clin Oncol 26 (abstr)
56. ClinicalTrials.gov (2015) An international, randomized, double-blind, controlled study of rindopepimut/GM-CSF with adjuvant temozolomide in patients with newly diagnosed, surgically resected, EGFRvIII-positive glioblastoma. Accessed 20 May 2015
57. ClinicalTrials.gov (2014) A phase II study of rindopepimut/GM-CSF in patients with relapsed EGFRvIII-positive glioblastoma. Accessed 20 May 2015
58. ClinicalTrials.gov (2011) Efficacy and safety study of NeuVax™ (nelipepimut-S or E75) vaccine to prevent breast cancer recurrence (PRESENT). Accessed 28 April 2014
59. Peoples GE, Goedegebuure PS, Smith R, Linehan DC, Yoshino I, Eberlein TJ (1995) Breast and ovarian cancer-specific cytotoxic T lymphocytes recognize the same HER2/neu-derived peptide. Proc Natl Acad Sci U S A 92:432–436
60. Humphreys RE, Adams S, Koldzic G, Nedelescu B, von Hofe E, Xu M (2000) Increasing the potency of MHC class II-presented epitopes by linkage to Ii-Key peptide. Vaccine 18:2693–2697
61. Fisk B, Anderson BW, Gravitt KR, O'Brian CA et al (1997) Identification of naturally processed human ovarian peptides recognized by tumor-associated CD8+ cytotoxic T lymphocytes. Cancer Res 57:87–93
62. Kono K, Takahashi A, Sugai H, Fujii H, Choudhury AR, Kiessling R, Matsumoto Y (2002) Dendritic cells pulsed with HER-2/neu-derived peptides can induce specific T-cell responses in patients with gastric cancer. Clin Cancer Res 8:3394–3400
63. Kawashima I, Hudson SJ, Tsai V, Southwood S, Takesako K, Appella E, Sette A, Celis E (1998) The multi-epitope approach for immunotherapy for cancer: identification of several CTL epitopes from various tumor-associated antigens expressed on solid epithelial tumors. Hum Immunol 59:1–14
64. Sotiropoulou PA, Perez SA, Iliopoulou EG, Missitzis I et al (2003) Cytotoxic T-cell precursor frequencies to HER-2 (369-377) in patients with HER-2/neu-positive epithelial tumours. Br J Cancer 89:1055–1061
65. Lustgarten J, Theobald M, Labadie C, LaFace D, Peterson P et al (1997) Identification of Her-2/Neu CTL epitopes using double transgenic mice expressing HLA-A2.1 and human CD.8. Hum Immunol 52:109–118
66. Brossart P, Wirths S, Stuhler G, Reichardt VL, Kanz L, Brugger W (2000) Induction of cytotoxic T-lymphocyte responses in vivo after vaccinations with peptide-pulsed dendritic cells. Blood 96:3102–3108
67. Anderson BW, Peoples GE, Murray JL, Gillogly MA, Gershenson DM, Ioannides CG (2000) Peptide priming of cytolytic activity to HER-2 epitope 369-377 in healthy individuals. Clin Cancer Res 6:4192–4200
68. Zaks TZ, Rosenberg SA (1998) Immunization with a peptide epitope (p369-377) from HER-2/neu leads to peptide-specific cytotoxic T lymphocytes that fail to recognize

HER-2/neu+ tumors. Cancer Res 58:4902–4908
69. Knutson KL, Schiffman K, Cheever MA, Disis ML (2002) Immunization of cancer patients with a HER-2/neu, HLA-A2 peptide, p369–377, results in short-lived peptide-specific immunity. Clin Cancer Res 8:1014–1018
70. Murray JL, Gillogly ME, Przepiorka D, Brewer H et al (2002) Toxicity, immunogenicity, and induction of E75-specific tumorlytic CTLs by HER-2 peptide E75 (369-377) combined with granulocyte macrophage colony-stimulating factor in HLA-A2+ patients with metastatic breast and ovarian cancer. Clin Cancer Res 8:3407–3418
71. Hueman MT, Dehqanzada ZA, Novak TE, Gurney JM et al (2005) Phase I clinical trial of a HER-2/neu peptide (E75) vaccine for the prevention of prostate-specific antigen recurrence in high-risk prostate cancer patients. Clin Cancer Res 11:7470–7479
72. Gates JD, Carmichael MG, Benavides LC, Holmes JP et al (2009) Longterm followup assessment of a HER2/neu peptide (E75) vaccine for prevention of recurrence in high-risk prostate cancer patients. J Am Coll Surg 208:193–201
73. Peoples GE, Gurney JM, Hueman MT, Woll MM et al (2005) Clinical trial results of a HER2/neu (E75) vaccine to prevent recurrence in high-risk breast cancer patients. J Clin Oncol 23:7536–7545
74. Holmes JP, Gates JD, Benavides LC, Hueman MT et al (2008) Optimal dose and schedule of an HER-2/neu (E75) peptide vaccine to prevent breast cancer recurrence: from US Military Cancer Institute Clinical Trials Group Study I-01 and I-02. Cancer 113:1666–1675
75. Mittendorf EA, Clifton GT, Holmes JP, Schneble E, van Echo D, Ponniah S, Peoples GE (2014) Final report of the phase I/II clinical trial of the E75 (nelipepimut-S) vaccine with booster inoculations to prevent disease recurrence in high-risk breast cancer patients. Ann Oncol 25:1735–1742
76. Holmes JP, Clifton GT, Patil R, Benavides LC et al (2011) Use of booster inoculations to sustain the clinical effect of an adjuvant breast cancer vaccine: from US Military Cancer Institute Clinical Trials Group Study I-01 and I-02. Cancer 117:463–471
77. Taylor C, Hershman D, Shah N, Suciu-Foca N, Petrylak DP et al (2007) Augmented HER-2 specific immunity during treatment with trastuzumab and chemotherapy. Clin Cancer Res 13:5133–5143
78. Mittendorf EA, Schneble EJ, Ibrahim NK et al (2014) Combination immunotherapy with trastuzumab and the HER2 vaccine E75 (nelipepimut-S) in high-risk HER2+ breast cancer patients to prevent recurrence. San Antonio Breast Cancer Symposium abstr OT3-1-09
79. Mittendorf EA, Storrer CE, Foley RJ, Harris K, Jama Y, Shriver CD, Ponniah S, Peoples GE (2006) Evaluation of the HER2/neu-derived peptide GP2 for use in a peptide-based breast cancer vaccine trial. Cancer 106:2309–2317
80. Carmichael MG, Benavides LC, Holmes JP, Gates JD, Mittendorf EA, Ponniah S, Peoples GE (2010) Results of the first phase 1 clinical trial of the HER-2/neu peptide (GP2) vaccine in disease-free breast cancer patients: United States Military Cancer Institute Clinical Trials Group Study I-04. Cancer 116:292–301
81. Mittendorf EA, Schneble EJ, Ibrahim NK et al (2014) Primary analysis of the prospective, randomized, single-blinded phase II trial of AE37 vaccine versus GM-CSF alone administered in the adjuvant setting to high-risk breast cancer patients. J Clin Oncol 32:5s (abstr 638)
82. Mittendorf EA, Schneble EJ, Perez SA et al (2014) Primary analysis of the prospective, randomized, phase II trial of GP2+GM-CSF vaccine versus GM-CSF alone administered in the adjuvant setting to high-risk breast cancer patients. J Clin Oncol 32:5s (abstr 638)
83. Sotiriadou NN, Kallinteris NL, Gritzapis AD, Voutsas IF et al (2007) Ii-Key/HER-2/neu(776-790) hybrid peptides induce more effective immunological responses over the native peptide in lymphocyte cultures from patients with HER-2/neu+tumors. Cancer Immunol Immunother 56(5):601–613
84. Voutsas IF, Gritzapis AD, Mahaira LG, Salagianni M, von Hofe E, Kallinteris NL, Baxevanis CN (2007) Induction of potent CD4+ T cell-mediated antitumor responses by a helper HER-2/neu peptide linked to the Ii-Key moiety of the invariant chain. Int J Cancer 121:2031–2041
85. Holmes JP, Benavides LC, Gates JD, Carmichael MG et al (2008) Results of the first phase I clinical trial of the novel II-key hybrid preventive HER-2/neu peptide (AE37) vaccine. J Clin Oncol 26:3426–3433
86. Gates JD, Clifton GT, Benavides LC, Sears AK, Carmichael MG et al (2010) Circulating regulatory T cells (CD4+CD25+FOXP3+) decrease in breast cancer patients after vaccination with a modified MHC class II HER2/neu (AE37) peptide. Vaccine 28:7476–7482
87. Rody A, Karn T, Liedtke C, Pusztai L, Ruckhaeberle E, Hanker L et al (2011) A

clinically relevant gene signature in triple negative and basal-like breast cancer. Breast Cancer Res 13(5):R97
88. Liu S, Lachapelle J, Leung S, Gao D, Foulkes WD, Nielsen TO (2012) CD8+ lymphocyte infiltration is an independent favorable prognostic indicator in basal-like breast cancer. Breast Cancer Res 14:R48
89. Garin-Chesa P, Campbell I, Saigo PE, Lewis JL Jr, Old LJ, Rettig WJ (1993) Trophoblast and ovarian cancer antigen LK26. Sensitivity and specificity in immunopathology and molecular identification as a folate-binding protein. Am J Pathol 142:557–567
90. Alberti S, Miotti S, Fornaro M, Mantovani L, Walter S, Canevari S, Menard S, Colnaghi MI (1990) The Ca-MOv18 molecule, a cell-surface marker of human ovarian carcinomas, is anchored to the cell membrane by phosphatidylinositol. Biochem Biophys Res Commun 171:1051–1055
91. Li PY, Del Vecchio S, Fonti R, Carriero MV, Potena MI et al (1996) Local concentration of folate binding protein GP38 in sections of human ovarian carcinoma by in vitro quantitative autoradiography. J Nucl Med 37:665–672
92. Toffoli G, Cernigoi C, Russo A, Gallo A, Bagnoli M, Boiocchi M (1997) Overexpression of folate binding protein in ovarian cancers. Int J Cancer 74:193–198
93. Toffoli G, Russo A, Gallo A, Cernigoi C, Miotti S, Sorio R, Tumolo S, Boiocchi M (1998) Expression of folate binding protein as a prognostic factor for response to platinum-containing chemotherapy and survival in human ovarian cancer. Int J Cancer 79:121–126
94. Sanchez-del-Campo L, Montenegro MF, Cabezas-Herrera J, Rodriguez-Lopez JN (2009) The critical role of alpha-folate receptor in the resistance of melanoma to methotrexate. Pigment Cell Melanoma Res 22:588–600
95. Liu J, Kolar C, Lawson TA, Gmeiner WH (2001) Targeted drug delivery to chemoresistant cells: folic acid derivatization of FdUMP[10] enhances cytotoxicity toward 5-FU-resistant human colorectal tumor cells. J Org Chem 66:5655–5663
96. Hartmann LC, Keeney GL, Lingle WL, Christianson TJ, Varghese B, Hillman D, Oberg AL, Low PS (2007) Folate receptor overexpression is associated with poor outcome in breast cancer. Int J Cancer 121:938–942
97. Peoples GE, Anderson BW, Lee TV, Murray JL, Kudelka AP, Wharton JT, Ioannides CG (1999) Vaccine implications of folate binding protein, a novel cytotoxic T lymphocyte-recognized antigen system in epithelial cancers. Clin Cancer Res 5:4214–4223
98. Kim DK, Lee TV, Castilleja A, Anderson BW, Peoples GE et al (1999) Folate binding protein peptide 191-199 presented on dendritic cells can stimulate CTL from ovarian and breast cancer patients. Anticancer Res 19:2907–2916
99. Peoples GE, Anderson BW, Fisk B, Kudelka AP, Wharton JT, Ioannides CG (1998) Ovarian cancer-associated lymphocyte recognition of folate binding protein peptides. Ann Surg Oncol 5:743–750
100. Greene JM, Schneble EJ, Berry JS, Trappey AF et al (2015) Preliminary results of the phase I/IIa dose finding trial of a folate binding protein vaccine (E39+GM-CSF) in ovarian and endometrial cancer patients to prevent recurrence. J Clin Oncol 33(suppl; abstr e14031)
101. Gao J, Bernatchez C, Sharma P, Radvanyi LG, Hwu P (2013) Advances in the development of cancer immunotherapies. Trends Immunol 34:90–98
102. Cannistra SA (2008) Challenges and pitfalls of combining targeted agents in phase I studies. J Clin Oncol 26:3665–3667
103. Yoshitake Y, Fukuma D, Yuno A, Hirayama M et al (2015) Phase II clinical trial of multiple peptide vaccination for advanced head and neck cancer patients revealed induction of immune responses and improved OS. Clin Cancer Res 21:312–321
104. Slingluff CL Jr, Petroni GR, Chianese-Bullock KA, Smolkin ME et al (2011) Randomized multicenter trial of the effects of melanoma-associated helper peptides and cyclophosphamide on the immunogenicity of a multipeptide melanoma vaccine. J Clin Oncol 29:2924–2932
105. Slingluff CL Jr, Lee S, Zhao F, Chianese-Bullock KA et al (2013) A randomized phase II trial of multiepitope vaccination with melanoma peptides for cytotoxic T cells and helper T cells for patients with metastatic melanoma (E1602). Clin Cancer Res 19:4228–4238
106. Wages NA, Slingluff CL Jr, Petroni GR (2015) A phase I/II adaptive design to determine the optimal treatment regimen from a set of combination immunotherapies in high-risk melanoma. Contemp Clin Trials 41:172–179
107. ClinicalTrials.gov (2015) Phase I/II trial of a long peptide (LPV7) Plus TLR Agonists (MEL60). Accessed 21 June 2015
108. Schneble EJ, Berry JS, Trappey FA, Clifton GT, Ponniah S, Mittendorf E, Peoples GE (2014) The HER2 peptide nelipepimut-S

(E75) vaccine (NeuVax) in breast cancer patients at risk for recurrence: correlation of immunologic data with clinical response. Immunotherapy 6:519–531
109. Mittendorf EA, Storrer CE, Shriver CD, Ponniah S, Peoples GE (2006) Investigating the combination of trastuzumab and HER2/neu peptide vaccines for the treatment of breast cancer. Ann Surg Oncol 13:1085–1098
110. Barker CA, Postow MA (2014) Combinations of radiation therapy and immunotherapy for melanoma: a review of clinical outcomes. Int J Radiat Oncol Biol Phys 88:986–997
111. Middleton G, Silcocks P, Cox T, Valle J, Wadsley J et al (2014) Gemcitabine and capecitabine with or without telomerase peptide vaccine GV1001 in patients with locally advanced or metastatic pancreatic cancer (TeloVac): an open-label, randomised, phase 3 trial. Lancet Oncol 15:829–840
112. Takakura K, Koido S, Kan S, Yoshida K, Mori M, Hirano Y et al (2015) Prognostic markers for patient outcome following vaccination with multiple MHC Class I/II-restricted WT1 peptide-pulsed dendritic cells plus chemotherapy for pancreatic cancer. Anticancer Res 35:555–562
113. Topalian SL, Hodi FS, Brahmer JR, Gettinger SN, Smith DC et al (2012) Safety, activity, and immune correlates of anti-PD-1 antibody in cancer. N Engl J Med 366:2443–2454
114. Wolchok JD, Kluger H, Callahan MK, Postow MA et al (2013) Nivolumab plus ipilimumab in advanced melanoma. N Engl J Med 369:122–133

Chapter 47

Preconditioning Vaccine Sites for mRNA-Transfected Dendritic Cell Therapy and Antitumor Efficacy

Kristen A. Batich, Adam M. Swartz, and John H. Sampson

Abstract

Messenger RNA (mRNA)-transfected dendritic cell (DC) vaccines have been shown to be a powerful modality for eliciting antitumor immune responses in mice and humans; however, their application has not been fully optimized since many of the factors that contribute to their efficacy remain poorly understood. Work stemming from our laboratory has recently demonstrated that preconditioning the vaccine site with a recall antigen prior to the administration of a dendritic cell vaccine creates systemic recall responses and resultantly enhances dendritic cell migration to the lymph nodes with improved antitumor efficacy. This chapter describes the generation of murine mRNA-transfected DC vaccines, as well as a method for vaccine site preconditioning with protein antigen formulations that create potent recall responses.

Key words Dendritic cells, Bone marrow, Transcription, mRNA, Electroporation, Preconditioning, Protein antigen formulation, Intradermal

1 Introduction

Dendritic cells (DCs) are specialized antigen-presenting cells (APCs) that play a pivotal role in the induction of T and B cell immunity [1]. DCs have the exceptional ability to activate and educate naive CD4+ and CD8+ T cells, a critical priming event that occurs predominantly in secondary lymphoid organs such as the spleen and draining lymph nodes. DCs prime cytotoxic T cell responses when they capture antigen, migrate to secondary lymphoid organs, and present antigen complexed with major histocompatibility complex (MHC) class I and II molecules, which is required for T cell receptor activation and antigen-specific T cell responses [2]. Utilizing this defined cascade of events, DCs can be pulsed or electroporated with antigen and will subsequently assemble antigen-derived peptides for presentation to T cells. Antigen thus can be delivered to DCs ex vivo via (1) peptide-pulsed DCs [3, 4], (2) co-incubation with whole tumor homogenate [5, 6], or (3) electroporation with tumor antigen-derived messenger RNA

Sunil Thomas (ed.), *Vaccine Design: Methods and Protocols: Volume 1: Vaccines for Human Diseases*, Methods in Molecular Biology, vol. 1403, DOI 10.1007/978-1-4939-3387-7_47,

(mRNA) [7–9]. Both preclinical and clinical studies have demonstrated that immunization with antigen-specific electroporated DCs can prime a cytotoxic cell response that is tumor specific and provides protective immunity [10, 11]. Thus, DC-based therapy is currently being evaluated in clinical trials for a variety of tumors.

DCs transfected with mRNA offer a powerful and tractable vaccine platform for eliciting immune responses against tumor antigens. A common strategy begins with the in vitro transcription of mRNAs encoding a tumor antigen. DCs transfected with these in vitro-transcribed (IVT) mRNAs generate short tumor antigen-specific peptides, some of which are able to complex with MHC molecules. These MHC-peptide complexes are then presented on the surface of DCs, where they can interact with and activate tumor antigen-cognate T cells.

1.1 Generation of In Vitro-Transcribed mRNA

IVT mRNA is a particularly appealing means of delivering antigen to DCs due to its short half-life, ease of production, and inability to integrate into the genome. Tumor epitopes derived from mRNA can be loaded onto MHC I or MHC II by incorporating molecular tags that traffic antigen to these loading compartments, such as ubiquitin or lysosome-associated membrane protein 1 (LAMP1) [12], respectively. Consequently, mRNA-transfected DCs can be used to engender CD4+ and CD8+ T cell immune responses. An oft-used alternative to delivering tumor epitopes onto surface MHC molecules of DCs is by pulsing with MHC-restricted peptides. These peptides compete with endogenously processed epitopes on the cell surface for binding to MHC molecules. A drawback of pulsing with MHC-restricted peptides is that it generally requires knowledge of the underlying MHC haplotypes expressed in an individual, considering that diverse MHC polymorphisms exhibit varying peptide-binding characteristics. However, because tumor antigen encoded by IVT mRNA is processed by endogenous MHC-peptide-loading mechanisms, mRNA-derived tumor antigen is not MHC haplotype restricted.

1.2 Bone Marrow-Derived DC Vaccine Preparation and Electroporation

DCs of both myeloid and lymphoid lineages are derived from the bone marrow and have been characterized in both mice and humans. As such, DC precursors can be harvested and differentiated in vitro using a series of growth factors and cytokines conducive to the mature DC of interest. Myeloid DCs can be generated in vitro either (1) by harvest of early common progenitor cells in the bone marrow (predominantly murine protocols) [13] or (2) by isolation of monocytes from peripheral blood (human cancer vaccine protocols) [14]. Ultimately, such precursors are differentiated into mature DCs with provision of granulocyte macrophage colony-stimulating factor (GM-CSF) as a key stimulus [15] and interleukin-4 (IL-4) as a potent activator of IL-12 production [16, 17].

1.3 Immunophenotyping of DC Vaccine Prior to Injection

Although there is currently no consensus on the optimal DC vaccine, it is well accepted that DCs used in vaccines must be in a mature state, as immature DCs can lead to immunological tolerance toward an antigen [18]. DC maturation can be defined phenotypically and includes expression of costimulatory molecules (e.g., CD80, CD86) and activation markers (e.g., MHC II) [19]. This phenotype is typically induced by a prolonged incubation period in maturation cocktails that include cytokines and toll-like receptor (TLR) ligands [20]. However, many of these treatments have been shown to inhibit IVT mRNA expression [21], and, in our experience, this step is not required to elicit DC vaccine-mediated antitumor immune responses in mice. This may be explained by the fact that IVT mRNA behaves as a TLR3 agonist [22].

1.4 Vaccine Site Preconditioning and Intradermal DC Vaccination

Aside from the activation status of DCs used in vaccines, there are several other factors that influence their effectiveness, such as their ability to effectively migrate to draining lymph nodes upon antigen encounter in the periphery. Effective homing of dendritic cells to local draining lymph nodes is a key event for the priming of naïve T cells and induction of antigen-specific immune responses. Clinical trials with corroborating preclinical studies have demonstrated that generally less than 5 % of injected DCs actually reach the vaccine site-draining lymph nodes (VDLNs) [23–25]. To address this limitation, preclinical investigations by Martin-Fontecha et al. revealed that preconditioning the vaccine site with inflammatory cytokines or mature, unpulsed DCs could significantly increase the migration of a subsequent DC vaccine to VDLNs [26].

In the preclinical setting, a variety of adjuvants have been employed to induce local inflammation with the goal of enhancing the immunogenicity of administered tumor-specific DCs or tumor-derived peptides [27, 28]. Protein antigens offer the advantage of inducing robust T cell responses with cytokine activation that can subsequently potentiate the magnitude of innate inflammatory responses [29] and control of infection [30]. Preclinical studies have demonstrated that the induction of memory CD4+-dependent inflammatory cytokines and chemokines in mice did not require conserved pathogen recognition pathways and acted independently of interferon-γ (IFN-γ) and tumor necrosis factor-α (TNF-α) [29]. As a result, memory CD4+ T cell activation can be leveraged to enhance non-cognate innate inflammatory responses.

Our previous work has identified a role for CD4+ T cell recall responses to protein antigens in facilitating the migration of DC vaccines to draining lymph nodes. Preconditioning the vaccine site with a potent recall antigen (i.e., an antigen for which the host has prior immunity) such as tetanus-diphtheria (Td) toxoid produced

a local and systemic response that facilitated the lymph node homing of tumor antigen-specific DC vaccines and promoted a significant decrease in growth of established tumors [31]. Although the exact mechanism remains to be elucidated, this outcome appears to require activated CD4+ T cells and host production of the chemokine CCL3.

In this chapter, the development and delivery of mRNA-transfected murine DCs are described. Methods outlined include the differentiation of DCs from murine bone marrow precursors, in vitro transcription of mRNA, antigen loading via electroporation, phenotypic validation by flow cytometry, and a vaccination protocol. Additionally, detailed instructions for recall antigen preconditioning are also presented.

2 Materials

The materials used are listed below. Comparable products from other suppliers should also be effective.

2.1 Generation of In Vitro Transcribed mRNA

1. Modified pGEM-4Z vector (Promega, Madison, WI).
2. SpeI-HF restriction enzyme + CutSmart® buffer (New England Biolabs, Ipswich, MA).
3. DNA Clean and Concentrator-25 (Zymo Research, Irvine, CA).
4. 1.5 mL microcentrifuge tubes (Eppendorf, Hamburg, Germany).
5. DNase/RNase-free ultrapure water (Life Technologies, Carlsbad, CA).
6. Agarose gel electrophoresis system (Thermo Scientific, Waltham, MA).
7. mMESSAGE mMACHINE T7 Transcription Kit (Life Technologies, Carlsbad, CA).
8. RNeasy Mini Kit (Qiagen, Valencia, CA).
9. NanoDrop-1000 spectrophotometer (Thermo Scientific, Waltham, MA).
10. Ethanol (Sigma Aldrich, St. Louis, MO).
11. Agarose (BioExpress, Kaysville, UT).
12. TAE buffer (BioExpress, Kaysville, UT).
13. 1 kb DNA ladder (New England Biolabs, Ipswich, MA).
14. 250 mL Erlenmeyer flask.
15. SYBR® safe DNA gel stain (Life Technologies, Carlsbad, CA).
16. 6× gel loading dye (New England Biolabs, Ipswich, MA).

17. FluorChem FC2 UV transilluminator with camera (Alpha Innotech, San Jose, CA).
18. 37 % formaldehyde solution (Sigma-Aldrich, St. Louis, MO).
19. MOPS (Sigma-Aldrich, St. Louis, MO).
20. 2× RNA loading dye (New England Biolabs, Ipswich, MA).
21. Sodium acetate (Sigma-Aldrich, St. Louis, MO).
22. EDTA (Sigma-Aldrich, St. Louis, MO).
23. Ultrapure DEPC-treated water (Life Technologies, Carlsbad, CA).
24. 0.5–10 kb RNA ladder (Life Technologies, Carlsbad, CA).

2.2 Bone Marrow-Derived DC Vaccine Preparation and Electroporation

2.2.1 Bone Marrow DC Preparation

1. Syngeneic mice of desired number.
2. Sterile scissors, Mayo scissors, sterile chucks, and sterile gauze.
3. Two pairs of sterile forceps.
4. 70 % ethanol.
5. Halothane or isoflurane and gas chamber.
6. 50 mL conical tubes (BD, Franklin Lakes, NJ).
7. RPMI 1640 (Gibco, Grand Island, NY).
8. Penicillin/streptomycin (P/S) (Gibco, Grand Island, NY) (store in 5.5 mL aliquots at −20 °C).
9. Heat-inactivated fetal bovine serum (FBS) (Gemini, West Sacramento, CA).
10. 55 mM β-mercaptoethanol (ME) (Gibco, Grand Island, NY).
11. 100 mM sodium pyruvate (Gibco, Grand Island, NY).
12. 10 mM nonessential amino acids (NEAA) (Gibco, Grand Island, NY).
13. 1 M HEPES buffer (Gibco, Grand Island, NY).
14. 200 mM l-glutamine (Gibco, Grand Island, NY) (store in 4 mL aliquots at −20 °C) (may be refrozen).
15. GM-CSF (Gemini, West Sacramento, CA) (store at −20 °C).
16. IL-4 (Gemini, West Sacramento, CA) (store at −20 °C).
17. Cell lysis buffer (10×; BD Pharm Lyse: BD, Franklin Lakes, NJ) diluted 1:10 in sterile H_2O (DNase, RNase free).
18. 100 mm tissue culture dishes (BD, Franklin Lakes, NJ).
19. 70 μm cell screens (BD, Franklin Lakes, NJ).
20. 25 g needles (BD, Franklin Lakes, NJ) and 10 mL syringes (BD, Franklin Lakes, NJ).
21. Trypan blue and hemocytometer.

22. 6-well tissue culture plates (BD, Franklin Lakes, NJ).
23. Pipet-Aid with 5, 10, and 25 mL pipettes.
24. 250 mL conical tubes (Corning, NY).
25. Complete DC media (CDCM)—To a 500 mL bottle of RPMI 1640, add the following:

27.5 (5 %) FCS, 5.5 mL penicillin/streptomycin (stored frozen), 2 mL l-glutamine (stored frozen), 550 μl β-ME, 5.5 mL sodium pyruvate, 5.5 mL NEAA, 5.5 mL HEPES. Thaw 10 μg GM-CSF (should be stored in frozen aliquots of 200 μL) and 10 μg IL-4 (also stored frozen in aliquots of 200 μL). Pour entire bottle of media over a 0.2 μm, 500 mL sterile vacuum filtration unit (*see* **Note 1**).

2.2.2 mRNA Electroporation of DCs

1. 50 mL conical tubes (BD, Franklin Lakes, NJ).
2. 60 mm tissue culture dishes (BD, Franklin Lakes, NJ).
3. Opti-MEM media (Gibco, Grand Island, NY).
4. 2 mm gene pulser cuvettes with sterile disposable fine-tipped transfer pipette (BTX Harvard Apparatus, Holliston, MA).
5. Electroporator (BTX model ECM 830).
6. Fresh complete DC media (CDCM)—To a 500 mL bottle of RPMI 1640, add the following:

27.5 (5 %) FCS, 5.5 mL penicillin/streptomycin (stored frozen), 2 mL l-glutamine (stored frozen), 550 μl β-ME, 5.5 mL sodium pyruvate, 5.5 mL NEAA, 5.5 mL HEPES. Thaw 10 μg GM-CSF (should be stored in frozen aliquots of 200 μL) and 10 μg IL-4 (also stored frozen in aliquots of 200 μL).

2.3 Immunophenotyping of DC Vaccine Prior to Injection

1. FACSCalibur™ cell analyzer (Becton Dickinson, Franklin Lakes, NJ).
2. 12 × 75 mm polystyrene tubes (VWR, Radnor, PA).
3. Phosphate-buffered saline (Life Technologies, Carlsbad, CA).
4. Fetal bovine serum (Gemini, West Sacramento, CA).
5. PE mouse anti-mouse I-A^b antibody (Becton Dickinson, Franklin Lakes, NJ).
6. PE hamster anti-mouse CD11c antibody (Becton Dickinson, Franklin Lakes, NJ).
7. PE hamster anti-mouse CD80 antibody (Becton Dickinson, Franklin Lakes, NJ).
8. PE rat anti-mouse CD86 antibody (Becton Dickinson, Franklin Lakes, NJ).
9. PE rat anti-mouse Ly-6G antibody (Becton Dickinson, Franklin Lakes, NJ).

2.4 Vaccine Site Preconditioning and Intradermal DC Vaccination

1. FACS tubes with caps (BD, Franklin Lakes, NJ).
2. 0.5 mL monoject insulin syringes (Covidien, Dublin, Ireland).
3. 1.5 mL microcentrifuge tubes (Eppendorf, Hamburg, Germany).
4. 70 % ethanol.
5. Sterile gauze pads, 2 × 2.
6. Td toxoid vaccine in prefilled syringes (or other protein antigen vaccine formulation in alum) (*see* **Note 2**).

3 Methods

The following is a procedure for generating and implementing an mRNA-transfected murine DC vaccine in combination with vaccine site preconditioning with a recall antigen. This process begins with the development of mRNA-transfected murine DCs (*see* Subheadings 3.1 and 3.2). The next steps involve immunophenotyping of the DC vaccine (*see* Subheading 3.3) followed by vaccine site preconditioning and intradermal DC vaccination (*see* Subheading 3.4).

3.1 Generation of In Vitro Transcribed mRNA

3.1.1 Preparation of Plasmid Template for In Vitro Transcription

Several commercial plasmid vectors exist for IVT. At a minimum, IVT templates must include a promoter and the coding sequence for the antigen of interest, which should be derived from cDNA. Poly(A) sequences may be added directly into the template sequence or can be added following IVT using poly(A) tailing kits. The promoters for IVT are generally those that are recognized by phage RNA polymerase (e.g., T7, T3, SP6), which are compatible with numerous commercial IVT kits. Several IVT plasmid templates also incorporate untranslated regions (UTRs) flanking the antigen coding sequence in order to help stabilize IVT mRNA. UTRs from globins are a common choice due to the inherent stability of globin mRNAs [32]. Finally, a unique restriction enzyme cleavage site should be placed at the intended transcriptional termination site to allow for plasmid linearization (*see* **Note 3**).

The IVT templates used in our lab are cloned into the pGEM-4Z backbone under the T7 promoter. The start codon for the antigen coding sequence is preceded by the minimal kozak sequence GCCACC. Constructs also contain a 5′ and 3′ UTR from *Xenopus laevis* β-globin mRNA to enhance mRNA stabilization. The 3′ UTR is followed by poly(A) sequence 62 base pairs in length, which terminates with a SpeI restriction enzyme cleavage site (Fig. 1).

Prior to performing IVT, plasmid templates are linearized via a restriction enzyme cut site immediately following the poly(A) sequence:

1. In a DNase-free 1.5 mL microcentrifuge tube, add 30 µg of plasmid DNA (resuspended in Tris-Cl) and bring volume up to 43 µL using ultrapure water. Add 5 µL 10× CutSmart® buffer and 2 µL (40 U) of restriction enzyme (*see* **Note 4**: restriction enzyme may be at different concentration than 20 U/µL. Adjust accordingly. Keep in mind that RE are in glycerol, and keep glycerol content to <5 %).
2. Gently, pipette up and down several times to mix the reaction, followed by brief pulse centrifugation.
3. Incubate for 3 hr in a 37 °C water bath to ensure complete digestion of plasmid (*see* **Note 5**).
4. To the completed reaction, add 100 µL DNA-binding buffer from Zymo Research DNA Clean and Concentrator-25 kit, and add entire volume to supplied spin column.
5. Centrifuge at ~10,000 × *g* for 30 s at RT. Discard flow through.
6. Wash column two times using 200 µL DNA wash buffer, spinning at ~10,000 × *g* for 30 s at RT. Discard flow through.

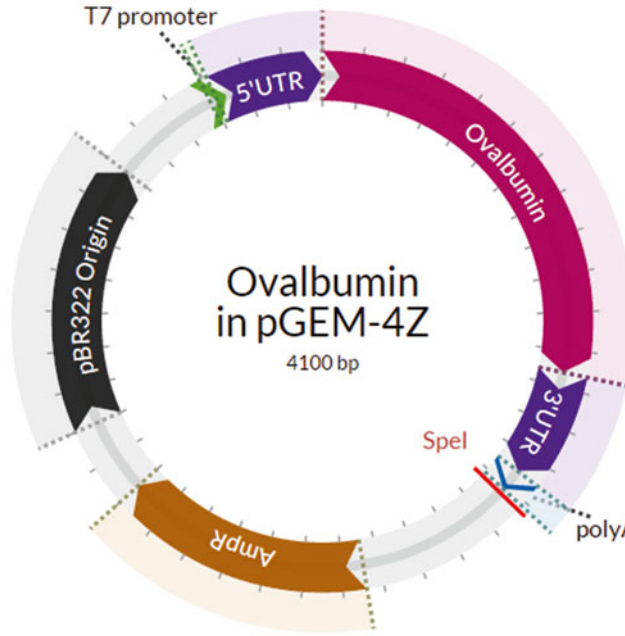

Fig. 1 Plasmid map of sample T7 polymerase-transcribed IVT vector used in our lab. The cDNA-derived sequence for chicken ovalbumin was cloned between UTRs obtained from *Xenopus laevis* β-globin cDNA. The poly(A) tail is encoded by a 62 base pair sequence, which is immediately followed by a SpeI restriction enzyme cleavage site to allow for plasmid linearization

7. Place spin column in new DNase-free microcentrifuge tube and elute in 25 μL elution buffer.
8. Determine DNA concentration using NanoDrop spectrophotometer.
9. Store plasmid sample at −20 °C until further use.

Optional: Confirm plasmid linearization by running 1 μg digested and undigested DNA on a 1 % agarose/TAE gel (Fig. 2a). Combine 100 mL 1× TAE buffer and 1 mg agarose in a 250 mL Erlenmeyer flask; mix by swirling. Microwave for 2 min, swirling mixture every 30 s. Mix 10 μL SYBR® safe stain into molten agarose, pour into agarose gel mold, insert appropriate lane comb, and allow mixture to congeal. Immerse solidified gel in 1× TAE and remove comb. Prepare 1 μg digested and undigested plasmids in water and 1× gel loading dye. Load lanes with 5 μL 1 kb DNA ladder and plasmid samples. Run gel at 4–10 V/cm for approximately 45 min. Visualize/image using UV transilluminator.

3.1.2 In Vitro Transcription

Several commercial in vitro transcription kits are available that produce high-yield, high-purity capped mRNA from phage promoters. Many kits contain a standard $m^7G(5')ppp(5')G$ cap analog that can incorporate onto mRNA in the reverse orientation, leading to translational inefficiencies. Alternatively, some kits contain a modified $m^7(3'\text{-}O\text{-methyl})\text{-}(5')ppp(5')G$ ARCA cap analog that can only be incorporated onto mRNA in the correct orientation, generating 100 % functional mRNA. Our lab uses Life Technologies mMESSAGE mMACHINE T7 Transcription Kit, which yields a 1:20 DNA template input-mRNA output ratio:

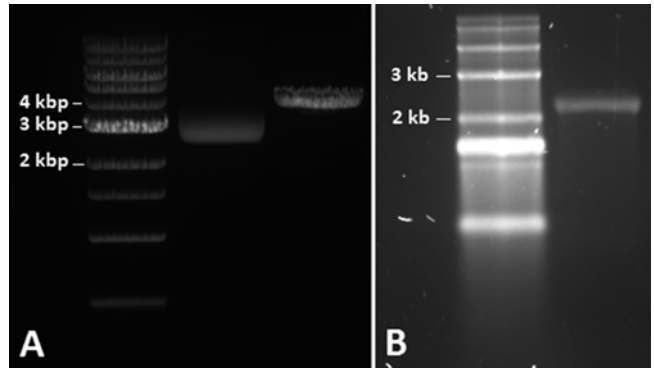

Fig. 2 Confirmation of plasmid linearization and single IVT mRNA product using gel electrophoresis. (**a**) Verification of plasmid linearization using 1 % agarose/TAE gel electrophoresis. From *left* to *right*: NEB 1 kb DNA ladder, 1 μg undigested ovalbumin in pGEM (*see* Fig. 1), and 1 μg Spe1-digested ovalbumin in pGEM (expected MW = 4100 bp). (**b**) Verification of single IVT mRNA product using 1.5 % denaturing agarose gel electrophoresis. From *left* to *right*: Invitrogen 0.5–10 kb RNA ladder and 1 μg IVT ovalbumin mRNA (expected MW = 2054 bases)

1. Thaw frozen IVT reagents, leaving RNA polymerase enzyme mix on ice.
2. In a DNase/RNase-free 1.5 mL microcentrifuge tube, add 5 μg linearized plasmid template and bring volume to 30 μL with nuclease-free water.
3. Assembling reaction at RT, add 50 μL 2× NTP/CAP, 10 μL 10× reaction buffer, and 10 μL enzyme mix.
4. Gently, pipette up and down several times to mix the reaction, followed by brief pulse centrifugation.
5. Incubate in a 37 °C water bath for 2 hr.
6. Add 5 μL TURBO DNase, mix by gently pipetting up and down.
7. Incubate in a 37 °C water bath for 15 min.
8. Add 350 μL RLT buffer from RNeasy kit and 250 μL 100 % ethanol, gently mix by pipetting.
9. Apply entire mixture to RNeasy spin column.
10. Centrifuge at 8000 × *g* for 30 s at RT. Discard flow through.
11. Wash column two times with 500 μL RPE buffer, spinning at 8000 × *g* for 1 min at RT. Discard flow through each time.
12. Place column in new nuclease-free microcentrifuge tube and spin at max speed to remove residual RPE buffer.
13. Place column in new nuclease-free microcentrifuge tube, add 40 μL nuclease-free water to the center of the column membrane, and elute by spinning at 8000 × *g* for 1 min at RT (*see* **Note 6**).
14. Determine mRNA concentration using NanoDrop spectrophotometer.
15. Bring mRNA concentration to 1 μg/μL in RNase-free water, prepare 10 μL aliquots, and freeze at −80 °C until further use.

Optional: Confirm presence of single mRNA product by running 1 μg IVT mRNA on 1.5 % denaturing agarose gel (Fig. 2b). Prepare 10× MOPS running buffer by combining 400 mM MOPS (pH 7.0), 100 mM sodium acetate, and 10 mM EDTA. Combine 72 mL DEPC-treated water and 1.5 mg agarose in 250 mL RNase-free Erlenmeyer flask (*see* **Note 7**). Microwave for 2 min, swirling mixture every 30 s. Let gel cool to ~60 °C then add 10 mL 10× MOPS running buffer, 18 mL 37 % formaldehyde solution, and 10 μL SYBR® gold nucleic acid stain into molten agarose (*see* **Note 8**); mix by swirling. Pour mixture into agarose gel mold, insert appropriate lane comb, and allow mixture to congeal. Prepare RNA samples in RNA loading dye, followed by heat denaturation at 65 °C for 10 min. Load lanes with 5 μL RNA ladder and IVT mRNA sample. Run gel at 4–10 V/cm for approximately 45 min. Visualize/image using UV transilluminator.

3.2 Bone Marrow-Derived DC Vaccine Preparation and Electroporation

Day 0

3.2.1 Bone Marrow DC Preparation

1. Sacrifice mouse in gas chamber. Perform cervical displacement on mice. Wash mouse by submersion in 70 % ethanol.
2. Place mouse on sterile gauze on sterile chuck. Cut the achilles tendon on one hind leg. Then, beginning at this site, use scissors to extend skin opening up the entire rear length of the leg. Peel the skin from the ankle up the entire length of the leg, exposing the musculature. Cut the patellar tendon, found on the anterior surface. Turning the leg over again, bend the leg backward at the knee, exposing the proximal tibia. Continue to push, exposing the tibia to the ankle. Holding the foot and tibia firmly in opposing hands, loosen the joint by gentle twisting until the tibia can be pulled in one swift motion from the foot. Clean the bone with gauze and place on ice in conical containing cold RPMI-P/S. Returning to the same leg, cut the remaining foot and lower leg muscles off at the knee, leaving only the upper leg. Slide the scissors in between the muscle and anterior surface of the femur. Spread the scissors to bluntly dissect the muscle off the bone. Repeat for the posterior surface of the bone. This will leave the distal femur and attached patella exposed. Grasp the exposed end of the femur and pull outwards from the body at a 45° angle to dislocate the hip. At this point, the scissors can be used to feel between the dislocated head of the femur and pelvis and to cut the femur away. Once the bone is removed, the patella may be grasped with the finger and folded back over the femur to remove it. Much of the musculature will come with the patella, and the femur may then be easily cleaned with gauze and placed in RPMI-Penicillin/Streptomycin (P/S) with 10 % FBS. Repeat this procedure for each leg of each mouse.
3. Once both legs have been removed, the sternum may be removed. Make a horizontal incision in the skin, over the area of the xiphoid process. The proximal flap may then be grasped and pulled rostrally, exposing the rib cage and shoulders. Pectoral muscles should be detached from the chest wall. Then, make a horizontal incision in the peritoneum, over the xiphoid process. Sliding the scissors rostrally under the sternum, bluntly dissect the organs away from the sternum. Scissors may then be used to cut along each side of the sternum, toward the head. Cut horizontally proximal to the manubrium to detach the sternum. Place it on ice in the same conical tube containing the long bones in RPMI-P/S. Repeat **steps 1** through **3** for each mouse.

4. Following bone harvest, transport bones to tissue culture hood.
5. Decant off RPMI-P/S + 10 % FBS and pour long bones and sternums separately into 100 mm dishes. Add enough fresh RPMI-P/S + 10 % FBS to submerge bones.
6. For long bones, use scissors or Mayos to cut off the distal (white) ends of the tibias and proximal (head) ends of the femurs. Place bones in fresh dish containing RPMI-P/S + 10 % FBS.
7. Fill a 10 mL syringe with RPMI-P/S + 10 % FBS from dish containing bones, and place a 25 g needle on the end. The needle can be inserted into the proximal (uncut) end of tibia or distal (uncut) end of femur (patella must have been removed) and used to squirt marrow out the cut end. Bones should be white when emptied. Subsequently insert the needle into the opposite (cut) end of the bone to ensure efficient marrow harvest. The marrow will appear as long red strings in dish. If all RPMI mixture is expelled from the syringe, remove the needle, refill from the same dish, and attach a fresh needle.
8. Once all long bones are emptied and discarded, use just the 10 cc syringe to draw the marrow and RPMI mixture up and down in the dish until marrow is dispersed and dissociated.
9. Transfer marrow through a 70 μm cell screen fitted on a 45° angle into a 50 mL conical tube. Let sit until sternum marrow is harvested.
10. For sternums, cut away xiphoid and loose muscle still attached. Transfer to fresh dish containing RMPI-P/S + 10 % FBS.
11. Holding sternums at one end with forceps (keep submerged), crush the sternum from one end to the other with Mayos, squeezing out the marrow (as if from a tube of toothpaste). Repeat until sternum is white. Discard sternums.
12. Repeat **steps 10** and **11** for sternums. If space allows, marrow may be added to same conical and cell screen as long bones.
13. Spin the cell suspension at $500 \times g \times 5$ min $\times 4$ °C.
14. Resuspend pellet (combine pellets if there are more than one) in 5 mL lysis buffer per five mice harvested. Incubate in 37 °C bath for 3–4 min.
15. Stop reaction by adding 25–30 mL cold RPMI + 10 % FBS. Spin as in **step 13**.
16. Resuspend pellet in 10 mL freshly made CDCM. Run cells over another 70 μm cell screen into a new 50 mL conical on ice. This will remove any lysed cell aggregates.

17. Count cell numbers via trypan blue exclusion (using a 1:20 dilution of cell suspension: trypan blue).
18. Adjust cell concentration to 1×10^6/mL and plate in 6-well plates at 3 mL per well. Incubate at 37 °C, 5 % CO_2, humidified (*see* **Note 9**).

Day 3 wash: Removal of nonadherents

1. Harvest media from wells, three at a time, using a Pipet-aid with 10 mL pipette. (Place tip down the side of each well to draw up media—do not scrape the bottom of the well with the pipette.)
2. With the Pipet-Aid on "slow," expel media in circle down inside wall of well and draw back up. Do this once per well for all three wells.
3. Discard media and replace with 3 mL fresh CDCM per well. Repeat these steps for all wells and reincubate in Day 0 **Step 18** conditions.

Day 7: Harvesting of nonadherents prior to electroporation

1. With Pipet-Aid on "fast" and a 10 mL pipette, harvest media from wells three at a time.
2. For each well, expel media in circular fashion down sides of well and draw back up. Perform this wash three times for each well in the three-well set, one after the other.
3. Save the collected media (*see* **Note 10**) and cells by transferring to a 250 mL conical on ice. Discard 6-well plates. Repeat for all wells, and pool cells and media in 250 mL conicals.
4. Spin cells $500 \times g \times 5$ min $\times 4$ °C. Following spin, save the decanted media (will be used later in Subheading 3.2.2).
5. Resuspend pellet in 10 mL cold Opti-MEM media, and count via trypan blue.

3.2.2 mRNA Electroporation of DCs

1. Once total cell count is calculated on Day 7 harvest, wash cell suspension twice in cold, fresh Opti-MEM media at $500 \times g \times 5$ min $\times 4$ °C.
2. Adjust cell concentration to 2.5×10^7/mL in Opti-MEM media (will need 5×10^6/200 μL in Opti-MEM for this electroporation step).
3. Obtain IVT mRNA to be electroporated (*see* Subheading 3.1). Keep on ice when not using.
4. First mix cell suspension thoroughly and transfer 200 μL cell suspension to bottom corner of a 2 mm fresh electroporator cuvette.
5. Mix mRNA (10 μg, 10 μL) with a single aliquot of cells by pipetting up and down 8–10 times (do not allow bubbles to form) using a P-10.

6. Using a P-200, mix the mRNA/cell suspension *immediately* in the gene pulser cuvette up and down 8–10 times (without creating bubbles).
7. Place cuvette in electroporator with plastic notch on cuvette facing outward and pulse at 300 V for 500 μs (ECM 830 electroporator; BTX, San Diego, CA) (*see* **Note 11**).
8. Using sterile disposable dropper from cuvette package, transfer electroporated cells and RNA *immediately* into 5 mL 50 % conditioned media (2.5 mL fresh CDCM + 2.5 mL saved media (*see* Subheading 3.2.1) in a 60 mm tissue culture dish. Repeat **steps 4–8** for each aliquot. Reincubate cells at 37 °C, 5 % CO_2, humidified for 6 to 24 h.

3.3 Immunophenotyping of DC Vaccine Prior to Injection

3.3.1 Immunophenotyping

At this point, 2–3 × 10^6 cells from each group may be set aside on ice for phenotyping (using murine antibodies for CD11c, Ly6G, CD80, and CD86, and MHC II (I-Ab)). Alternatively, cells leftover after vaccination may be brought back for phenotyping (Fig. 3).

3.3.2 Intradermal Vaccination

1. Harvest cells from 60 mm culture dishes 6–24 h after mRNA electroporation using a 10 mL sterile pipette and Pipet-Aid on "fast."

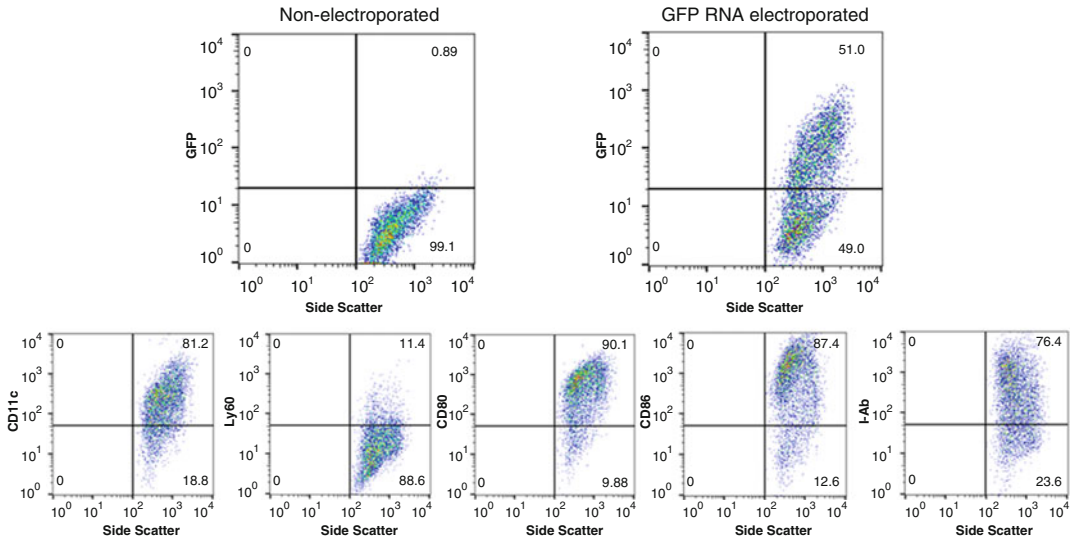

Fig. 3 Representative panel of RNA-transfected DC maturation markers prior to injection. *Top*: DCs electroporated with green fluorescent protein (GFP) RNA (transcribed as above) were analyzed for effective RNA uptake and protein expression by flow cytometry 24 h following electroporation. *Bottom*: DCs were stained for phenotypic and costimulatory markers on Day 7 prior to vaccination. CD11c, integrin with high expression on myeloid or conventional DC; Ly6G, myeloid differentiation antigen that remains highly expressed on bone marrow granulocytes and peripheral; CD80 (B7-1) and CD86 (B7-2), costimulatory molecules expressed on DCs required for T cell activation and survival; I-Ab, MHC class II haplotype in C57BL/6 mouse background

2. Pool cells that were electroporated with the same RNA species in 50 mL conicals on ice. Spin 500 × *g* × 5 min × 4 °C.
3. Resuspend pellet in 5 mL 1× PBS and count. Respin cells, washing two more times in 1× PBS, and resuspend in PBS at desired concentration for vaccination (usually 10×10^6 DC/mL). Transfer to capped FACS tubes and place on ice. Be sure to agitate cells prior to drawing into syringe for vaccination (*see* Subheading 3.4.2).

3.4 Vaccine Site Preconditioning and Intradermal DC Vaccination

3.4.1 Vaccine Site Preconditioning

Primary immunization: To be administered 2 weeks prior to vaccine site preconditioning for adequate induction of immunity to protein antigen (Fig. 4).

1. Expel 500 μL (5 Lf) of the prefilled Tenivac® into a sterile 1.5 mL Eppendorf tube.
2. Take 100 μL (1 Lf) of the Tenivac® vaccine into a 0.5 mL insulin syringe.
3. Holding the mouse supine in one hand, with a firm grasp on the back of the neck/shoulders and tail tucked tightly under the pinky finger, extend one leg straight out and tuck the foot under the pinky, exposing the quadriceps muscle above the femur.
4. Position the insulin needle (bevel facing upwards) completely parallel to the mouse femur and gently guide the needle tip under the skin into the quadriceps muscle. You should feel considerable resistance against the needle tip. This means that the needle is appropriately inserted in dense muscle.
5. Inject 50 μL Tenivac® into the first quadriceps muscle at a slow rate. Let the needle sit in the muscle for 3 s and slowly withdraw the needle out of the leg in 1 s increments. This helps prevent backflow of the vaccine out of the injection path.
6. Uncover the first leg and extend the other leg as described above, tucking the foot again under the pinky.
7. Insert the needle completely parallel as described in Step 4 and inject the remaining 50 μL Tenivac® as in **Step 5**.
8. Two weeks later, repeat 50 μL as a booster immunization in a single quadriceps muscle (**Step 5**).

Recall stimulus with preconditioning: To be administered at a single site intradermally in the groin 2 weeks following booster intramuscular immunization. This step requires the mouse to be anesthetized in an isoflurane chamber with oxygen flow:

1. Ensure the mouse is adequately anesthetized with slowed breathing rate for 30 s. Position the mouse in a supine position.

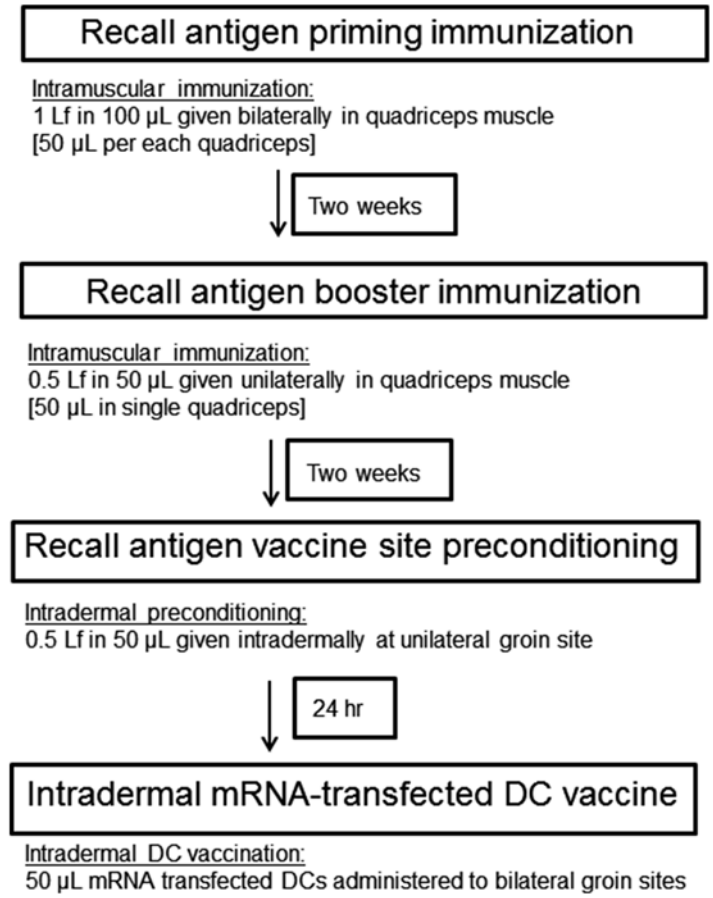

Fig. 4 Immunization schema for preconditioning DC vaccine site with protein antigen vaccine formulations. The following recall antigen preconditioning protocol requires a primary intramuscular immunization and booster immunization separated by two weeks followed by an intradermal single preconditioning 2 weeks thereafter

2. Wet a piece of sterile gauze with 70 % ethanol and fold the gauze. Gently press on a single groin site and wipe the hair and skin to clean the area.
3. Take 50 µL (0.5 Lf) of the protein antigen formulation (i.e., Tenivac®) into a 0.5 mL insulin syringe.
4. Again positioning the needle completely parallel to the groin skin (bevel facing upwards), slowly insert the needle tip under the epidermal skin layer. As this is an intradermal preconditioning administration, one should very clearly see the needle bevel under the skin, almost as if the skin layer were transparent to expose the needle tip.
5. Once the needle can be appreciated in the intradermal compartment, slowly release 50 µL of Tenivac® under the skin.

6. Leave the needle under the skin for at least 3 s after injecting all 50 μL and slowly withdraw the needle tip, in 1 s increments. The slow withdrawal of the needle during this step is absolutely critical, because the high pressures in the intradermal vaccine bleb have a tendency to expel the formulation out of the injection tract.
7. Return the mouse to normal arousal state and wait 24 h for intradermal DC vaccination.

3.4.2 Intradermal DC Vaccination

Intradermal vaccination in bilateral groin sites with mRNA-transfected DCs occurs 24 h following vaccine site preconditioning of a single groin site. This step requires the mouse to be anesthetized in an isoflurane chamber with oxygen flow:

1. Take cell suspension from Subheading 3.3.2 and mix well. Draw up 100 μL per mouse to be vaccinated (50 μL per each groin side).
2. Again ensure the mouse is adequately anesthetized with slowed breathing rate for 30 s. Position the mouse in a supine position.
3. Wet a piece of sterile gauze with 70 % ethanol and fold the gauze. Gently press on both left and right groin sites, wiping the hair and skin to clean the area.
4. For each groin site, position the needle completely parallel to the groin skin (bevel facing upwards), slowly insert the needle tip under the epidermal skin layer. As this is another intradermal administration, one should very clearly see the needle bevel under the skin, almost as if the skin layer were transparent to expose the needle tip.
5. Once the needle can be appreciated in the intradermal compartment, slowly release 50 μL of the DCs in 1× PBS under the skin.
6. Leave the needle under the skin for at least 3 s after injecting all 50 μL and slowly withdraw the needle tip, in 1 s increments. The slow withdrawal of the needle during this step is required to control for high pressures within the intradermal bleb that may to expel the formulation out of the injection tract.
7. Return the mouse to normal arousal state.

4 Notes

1. Complete DC media (CDCM) should be made on Day 0 and used only for that DC prep (i.e., on Days 0–9). It should not be stored for multiple uses. Occasionally, bone marrow culture

yields will be high enough to warrant more than one 500 mL bottle per prep.

2. Alum-containing protein antigen formulations can be used at this step for preconditioning of vaccine sites prior to DC injection. We have previously used the Td toxoid vaccine (Sanofi Aventis, Tenivac®), which produced inflammation at the preconditioning site (erythema and induration) and activated CD4+ T cells. Other protein antigen formulations similar to Td toxoid that activate the CD4+ T cell compartment may show similar efficacy in preconditioning the DC vaccine site.
3. RNA polymerases are very processive enzymes. Therefore, circular plasmids should be linearized prior to in vitro transcription to avoid the production of RNAs that exceed the region of interest, as this may affect downstream applications.
4. SpeI-HF used by our lab is supplied at 20 U/μL. If using a restriction enzyme that is at a different concentration, adjust the volume accordingly to achieve 40 U. Restriction enzymes are typically suspended in glycerol, which can inhibit enzymatic reactions. Maintain final glycerol concentration to <5 %.
5. Shorter incubation times may suffice. Refer to the enzymatic activity specifications for each enzyme. If incubating for longer periods of time (e.g., overnight), use a restriction enzyme with reduced nonspecific activity (e.g., high-fidelity enzymes from NEB).
6. Our lab has experienced increased yields by returning eluate to spin column membrane and re-eluting.
7. To avoid RNase-mediated degradation of samples, all glassware should be baked at >180 °C or soaked in 0.1 % DEPC-treated water for several hours, followed by autoclaving. Plastics can be soaked in 0.1 % DEPC-treated water for several hours then rinsed or sprayed with RNase cleaning product.
8. Formaldehyde is a carcinogen. Therefore, it is strongly recommended that a dedicated chemical fume hood be used for all formaldehyde work.
9. Each DC bone marrow preparation is outlined to use five mice for each harvest and DC vaccination experiment. Therefore, one can expect a generation of 350×10^6 total marrow cells to be extracted from a total of five mice on Day 0. Upon Day 7, the usual number of DCs cultivated should reach 50×10^6 cells total. These numbers are the average numbers generated for Days 0 and 7 for a 5-mouse bone marrow procedure.
10. The difference in the technique for Day 3 and Day 7 washes in the DC bone marrow procedure reflects the morphologic changes in cultured DCs with time. On Day 3, it is absolutely critical that cells are washed with the Pipet-Aid on "slow."

However, on Day 7, the DCs alter their adherent properties and can be found in the supernatant of the wells. This is why on Day 7, the nonadherent cell mixture is saved and replated. For Day 7 washes, the Pipet-Aid should be operated on the "fast" setting.

11. For the RNA electroporation step, the highest number of viable electroporated DCs will be achieved if the operator moves as quickly as possible. The quickest and most effective procedure for electroporation is to first remove the 200 µl aliquot of DCs into the electroporator cuvette with a P-200 pipette. Then, take a P-10 pipette and mix thoroughly (3–5 times) 10 µL of the RNA in its microcentrifuge tube. Pipette 10 µL RNA and inject into the deep corner of the floor of the cuvette with the DCs. Quickly transfer to the P-200 and mix this RNADC suspension (eight times is sufficient) without generating bubbles in the cuvette. This entire process (from the insertion of the cells to the implantation of the cuvette into the electroporator) should not exceed 15 s.

References

1. Steinman RM, Cohn ZA (1973) Identification of a novel cell type in peripheral lymphoid organs of mice. I. Morphology, quantitation, tissue distribution. J Exp Med 137:1142–1162
2. Banchereau J, Steinman RM (1998) Dendritic cells and the control of immunity. Nature 392:245–252
3. Yu JS, Wheeler CJ, Zeltzer PM et al (2001) Vaccination of malignant glioma patients with peptide-pulsed dendritic cells elicits systemic cytotoxicity and intracranial T-cell infiltration. Cancer Res 61:842–847
4. Okada H, Kalinski P, Ueda R et al (2011) Induction of CD8+ T-cell responses against novel glioma-associated antigen peptides and clinical activity by vaccinations with {alpha}-type 1 polarized dendritic cells and polyinosinic-polycytidylic acid stabilized by lysine and carboxymethylcellulose in patients with recurrent malignant glioma. J Clin Oncol 29:330–336
5. Yamanaka R, Abe T, Yajima N et al (2003) Vaccination of recurrent glioma patients with tumour lysate-pulsed dendritic cells elicits immune responses: results of a clinical phase I/II trial. Br J Cancer 89:1172–1179
6. Cho DY, Yang WK, Lee HC et al (2012) Adjuvant immunotherapy with whole-cell lysate dendritic cells vaccine for glioblastoma multiforme: a phase II clinical trial. World Neurosurg 77:736–744
7. Boczkowski D, Nair SK, Nam JH, Lyerly HK, Gilboa E (2000) Induction of tumor immunity and cytotoxic T lymphocyte responses using dendritic cells transfected with messenger RNA amplified from tumor cells. Cancer Res 60:1028–1034
8. Boczkowski D, Nair SK, Snyder D, Gilboa E (1996) Dendritic cells pulsed with RNA are potent antigen-presenting cells in vitro and in vivo. J Exp Med 184:465–472
9. Nair SK, Morse M, Boczkowski D et al (2002) Induction of tumor-specific cytotoxic T lymphocytes in cancer patients by autologous tumor RNA-transfected dendritic cells. Ann Surg 235:540–549
10. Nair SK, De Leon G, Boczkowski D et al (2014) Recognition and killing of autologous, primary glioblastoma tumor cells by human cytomegalovirus pp 65-specific cytotoxic T cells. Clin Cancer Res 20:2684–2694
11. Nair SK, Boczkowski D, Morse M et al (1998) Induction of primary carcinoembryonic antigen (CEA)-specific cytotoxic T lymphocytes in vitro using human dendritic cells transfected with RNA. Nat Biotechnol 16:364–369
12. Bonehill A, Heirman C, Tuyaerts S et al (2004) Messenger RNA-electroporated dendritic cells presenting MAGE-A3 simultaneously in HLA class I and class II molecules. J Immunol 172:6649–6657
13. Inaba K, Inaba M, Romani N et al (1992) Generation of large numbers of dendritic cells

from mouse bone marrow cultures supplemented with granulolcyte/macrophage colony-stimulating factor. J Exp Med 176:1693–1702
14. Nair S, Archer GE, Tedder TF (2012) Isolation and generation of human dendritic cells. Curr Protoc Immunol 7, Unit 7.32:1–23
15. Inaba K, Swiggard WJ, Steinman RM et al (2009) Isolation of dendritic cells. Curr Protoc Immunol 86:I:3.7:3.7.1–3.7.19
16. Lutz MB, Schnare M, Menges M et al (2002) Differential functions of IL-4 receptor types I and II for dendritic cell maturation and IL-12 production and their dependency on GM-CSF. J Immunol 169:3574–3580
17. Hochrein H, O'Keeffe M, Luft T et al (2000) Interleukin (IL)-4 is a major regulatory cytokine governing bioactive IL-12 production by mouse and human dendritic cells. J Exp Med 192:823–833
18. Mahnke K, Schmitt E, Bonifaz L, Enk AH, Jonuleit H (2002) Immature, but not inactive: the tolerogenic function of immature dendritic cells. Immunol Cell Biol 80:477–483
19. Reis e Sousa C (2006) Dendritic cells in a mature age. Nat Rev Immunol 6:476–483
20. Van Brussel I, Berneman ZN, Cools N (2012) Optimizing dendritic cell-based immunotherapy: tackling the complexity of different arms of the immune system. Mediators Inflamm 2012:690643
21. Schuurhuis DH, Lesterhuis WJ, Kramer M et al (2009) Polyinosinic polycytidylic acid prevents efficient antigen expression after mRNA electroporation of clinical grade dendritic cells. Cancer Immunol Immunother 58:1109–1115
22. Karikó K, Ni H, Capodici J, Lamphier M, Weissman D (2004) mRNA is an endogenous ligand for Toll-like receptor 3. J Biol Chem 279:12542–12550
23. De Vries I, Krooshoop D, Scharenborg N et al (2003) Effective migration of antigen-pulsed dendritic cells to lymph nodes in melanoma patients is determined by their maturation state. Cancer Res 63:7–12
24. Eggert A, Schreurs M, Boerman O et al (1999) Biodistribution and vaccine efficiency of murine dendritic cells are dependent on the route of administration. Cancer Res 59:3340–3345
25. Eggert A, van der Voort R, Torensma R et al (2003) Analysis of dendritic cell trafficking using EGFP-transgenic mice. Immunol Lett 89:17–24
26. Martin-Fontecha A, Sebastiani S, Hopken UE et al (2003) Regulation of dendritic cell migration to the draining lymph node: impact on T lymphocyte traffic and priming. J Exp Med 198:615–621
27. Prins RM, Craft N, Bruhn KW et al (2006) The TLR-7 agonist, imiquimod, enhances dendritic cell survival and promotes tumor antigen-specific T cell priming: relation to central nervous system antitumor immunity. J Immunol 176:157–164
28. Chagnon F, Tanguay S, Ozdal OL et al (2005) Potentiation of a dendritic cell vaccine for murine renal cell carcinoma by CpG oligonucleotides. Clin Cancer Res 11:1302–1311
29. Strutt TM, McKinstry KK, Dibble JP et al (2010) Memory CD4+ T cells induce innate responses independently of pathogen. Nat Med 16:558–564
30. Narni-Mancinelli E, Campisi L, Bassand D et al (2007) Memory CD8+ T cells mediate antibacterial immunity via CCL3 activation of TNF/ROI+ phagocytes. J Exp Med 204:2075–2087
31. Mitchell DA, Batich KA, Gunn MD et al (2015) Tetanus toxoid and CCL3 improve dendritic cell vaccines in mice and glioblastoma patients. Nature 519:366–369
32. Russell JE, Liebhaber SA (1996) The stability of human beta-globin mRNA is dependent on structural determinants positioned within its 3′ untranslated region. Blood 87:5314–5323

Chapter 48

Development of Antibody-Based Vaccines Targeting the Tumor Vasculature

Xiaodong Zhuang and Roy Bicknell

Abstract

A functional vasculature is essential for tumor progression and malignant cell metastasis. Endothelial cells lining blood vessels in the tumor are exposed to a unique microenvironment, which in turn induces expression of specific proteins designated as tumor endothelial markers (TEMs). TEMs either localized at the plasma membrane or secreted into the extracellular matrix are accessible for antibody targeting, which can be either infused or generated de novo via vaccination.

Recent studies have demonstrated vaccines against several TEMs can induce a strong antibody response accompanied by a potent antitumor effect in animal models. These findings present an exciting field for novel anticancer therapy development. As most of the TEMs are self-antigens, breaking tolerance is necessary for a successful vaccine. This chapter describes approaches to efficiently induce a robust antibody response against the tumor vasculature.

Key words TEMs, Adjuvant

1 Introduction

The tumor microenvironment is markedly different from that of a healthy tissue. The tumor vasculature is commonly hypoxic and acidic and, because of poor vessel development, shows reduced blood perfusion and shear stress [1]. These differences gives rise to a different expression signature in tumor vessels compared to those in healthy tissue [2]. Targeting TEMs can impede tumor growth in animal models [3]. TEMs localized at either the plasma membrane or secreted into the extracellular matrix are accessible for antibody targeting.

Compared to currently available anti-angiogenic drugs such as small molecule tyrosine kinase inhibitors or monoclonal antibodies, vaccination is a less advanced but promising approach that has many advantages. The main advantage of active vaccination is the possibility of generating antibody production within individual

Sunil Thomas (ed.), *Vaccine Design: Methods and Protocols: Volume 1: Vaccines for Human Diseases*, Methods in Molecular Biology, vol. 1403, DOI 10.1007/978-1-4939-3387-7_48,

patients for long-term protection. Such protection otherwise can only be achieved by repeated administration of anti-angiogenic drugs such as bevacizumab [4]. The specificity of the immune response elicited by a vaccine could potentially be more restricted to the target, which means less toxicity than other anti-angiogenic agents.

The tumor endothelial cell has many advantages over the carcinoma cell as a therapeutic target. Endothelial cells have greater genetic stability than the transformed tumor cells that have mechanisms to avoid immune recognition such as downregulation of MHC I on their surface [5]. Further, endothelial cells which form the vessel lumen are directly in contact with the blood and highly accessible to the immune system, compared to tumor cells located at distance from the vessels. Restriction of one vessel can lead to the death of many tumor cells and the effect is amplified. Finally, targeting tumor vasculature may also be effective in a wider spectrum of cancer patients, because the angiogenic processes are similar in different tumor types.

Recent studies in experimental mouse models have shown reduction in tumor growth after vaccination with endothelial expressed antigens, including the vascular endothelial growth factor receptor 2 (VEGFR2), Delta-like ligand 4 (DLL4), Endoglin/CD105, and the extra domain-B of fibronectin (reviewed in [3, 6–8]). For effective immunotherapy, the choice of tumor endothelial marker is critical. For example, a well-characterized TEM Robo4 has recently been shown to be a superior target to VEGFR2 [9]. Mai et al. demonstrated that while internalizing antibodies targeting VEGFR2 and Robo4 that both inhibit tumor growth, there was significant toxicity associated with those targeting VEGFR2 but not with those targeting Robo4 [9]. This is likely to reflect the expression of VEGFR2 on endothelium in healthy tissue compared with Robo4 that is restricted to the tumor endothelium [10–14]. Another recent study confirmed that vaccination against Robo4 using various immunization approaches retards tumor growth in animal models without toxic side effects [15].

Most TEMs are self-antigens which do not easily raise T-cell help to induce antigen-specific antibodies. Therefore, the selection of adjuvant for the vaccination is critical for a successful vaccine. Although Freund's adjuvant evokes an immune response against self-antigens, due to its mineral oil base and heat-killed *Mycobacterium* tuberculosis, it is toxic to humans and cannot be used in clinical trials [16, 17]. Hence, there is a need for the identification of new adjuvants or vaccination strategies to enhance the immunogenicity against self-antigens. Alum-based adjuvants have been proven safe and are commonly used in human vaccination. It has been shown that alum-based vaccination mainly induces Th2-dependent antibody responses [18].

In this chapter, we describe two alum-based vaccination approaches which have been shown to induce specific antibodies against the tumor vasculature. The two approaches involve: (1)

modified vaccine immunogens by a self-foreign conjugate antigen and (2) a carrier priming strategy to achieve rapid antibody induction without an adjuvant. Finally, we describe the use of a newly validated nontoxic biodegradable adjuvant Montanide ISA 720 to induce a robust antibody response against the tumor vasculature.

2 Materials

2.1 Alum-Based Vaccination

1. HiTrap Protein A HP columns (GE Healthcare Life Sciences, Buckinghamshire, UK).
2. 9 % aluminum potassium sulfate [formula: $Al_2(SO_4)_3$] (Sigma, Gillingham, UK).
3. Papain (Sigma, Gillingham, UK).

2.2 Carrier Priming Vaccination

1. Purified human Fc (Bethyl, Montgomery, USA).
2. Chicken γ-globulin (CGG; Sigma, Gillingham, UK).
3. 25 % glutaraldehyde (Sigma, Gillingham, UK).
4. UltraPure™ 1 M Tris–HCl buffers (Life Technologies, Glasgow, UK).

2.3 Vaccination Using Montanide as an Adjuvant

1. CpG 1826 (Sigma, St. Louis, USA).
2. Montanide ISA 720 (SEPPIC, Paris, France).

2.4 Examination of the Vasculature

1. Polyclonal Meca32 antibody (R&D System, Abingdon, UK).
2. FITC-conjugated secondary antibody (Invitrogen, Paisley, UK).
3. DAPI (Invitrogen, Paisley, UK).
4. Laser scanning confocal microscope (Carl Zeiss, Welwyn Garden City, UK).
5. Polyclonal fibrinogen antisera (Dako, Glostrup, Denmark).
6. Monoclonal anti-Ly6G and Ly-6C antibody (BD Pharmingen™, Oxford, UK).

2.5 Tumor Models

1. Lewis lung carcinoma cell line (ATCC, Manassas, USA).
2. 4T1 breast cancer cell line (ATCC, Manassas, USA).

3 Methods

3.1 Alum-Based Vaccination Using Self-Foreign Fusion Protein as the Antigen

As mentioned above, most TEMs are self-antigens, which commonly results in an immune tolerance. Thus, for a successful vaccine, breaking tolerance is essential. This can be achieved by vaccination with a self-foreign fusion protein. The foreign part of

the fusion protein is highly immunogenic to the host immunity; therefore, it can easily elicit a strong immune response. Here we describe the use of the Fc region of human immunoglobulin as the foreign element. The Fc tag can be fused to the C-terminus of a self-antigen and result in a robust antibody induction to both the foreign and self-part of the fusion antigen using alum adjuvants. Besides being foreign to most model animals, the human Fc tag is also a useful tool for purification of the fusion protein using a protein A column.

3.1.1 Alum-Antigen Preparation

1. Reconstitute 9 % aluminum potassium sulfate in water.
2. Mix an equal volume of the antigen and 9 % aluminum potassium sulfate and adjust pH to 6.5 (*see* **Note 1**).
3. Incubate the mix for 1 h at room temperature in the dark, and then wash the alum-antigen precipitate twice with an appropriate amount of PBS (*see* **Note 2**).
4. The antigen-alum precipitate is finally resuspended in an appropriate volume and is ready for in vivo use.

3.1.2 Immunization Protocol

1. Age-matched adult mice (6–8 weeks) should be used (*see* **Note 3**).
2. Immunize each mouse intraperitoneally with 50 μg of the prepared alum-antigen mix. Recommended injection volume: 200 μl.
3. 14 days later, immunize mice again with the same alum-antigen mix. For certain antigens, for example, the oncofetal antigens Robo4 and CLEC14A, this boosting vaccination is not essential ([15], unpublished data).
4. 28 days post the initial immunization, antigen-specific antibody can be assessed in tail bleeds (*see* **Note 4**).
5. The level of antigen-specific antibody can be determined by ELISA assay. The coating antigens can be generated by papain cleavage of the Fc tag from the fusion antigen [15, 19].

3.2 Carrier Priming Vaccination

Prior vaccination with a carrier protein in an adjuvant ensures a high frequency of carrier-specific memory T cells to provide help to self-antigen-specific B cells (Fig. 1). This strategy can lead to an efficient and rapid onset of antigen-specific antibody production, which develops faster than primary responses in naive animals [18]. The priming antigen can be the foreign part of the self-foreign fusion protein, for example, human Fc or a foreign protein, to which the self-antigen is chemically cross-linked such as the chicken γ-globulin (CGG).

3.2.1 Priming Antigen Preparation

1. Purified human Fc can be used directly for antigen priming for an Fc-tagged self-antigen.
2. CGG can be cross-linked to self-antigens using glutaraldehyde [20].

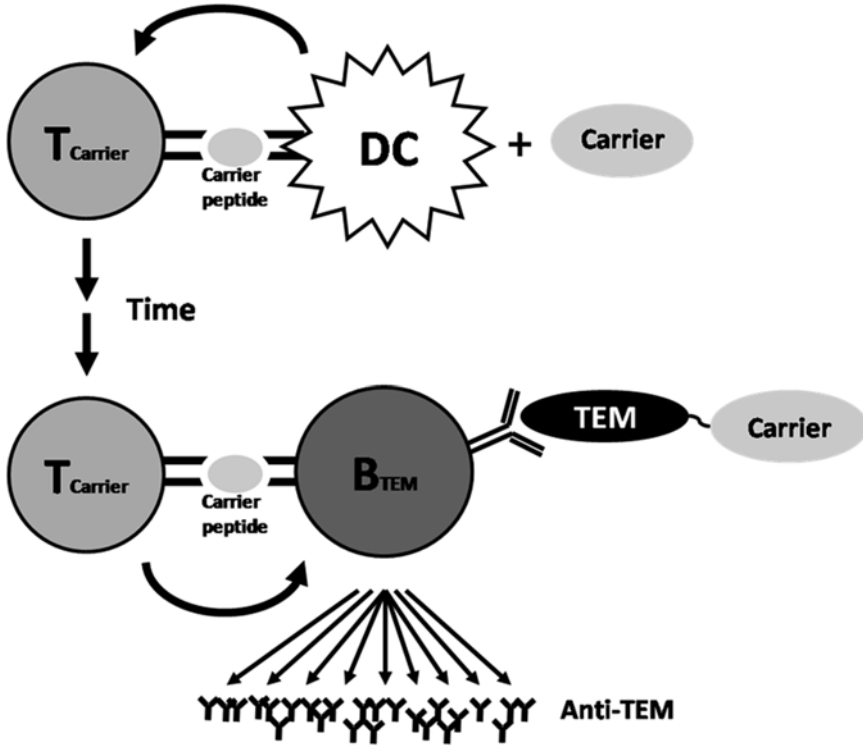

Fig. 1 Carrier priming strategy for rapid production of antibodies. Pre-vaccination of a carrier protein in a strong adjuvant ensures the presence of carrier-specific memory T cells, which allows rapid antibody production to the TEM (self-antigen) upon subsequent exposure to TEM-carrier conjugates

3. Mix 2 μl of 25 % glutaraldehyde with 1 ml of PBS containing 1 mg of antigen and 1 mg of CGG (pH 7.5–8).
4. The reaction mix is incubated at RT for 10 min and quenched by adding 100 μl of 1 M Tris–HCl (pH 8).
5. The mix needs to be dialyzed with PBS overnight to remove glutaraldehyde.
6. Human Fc or the CGG cross-linked antigen can be precipitated with alum as described in Subheading 3.1.1., **item 1**.

3.2.2 Immunization Protocol

1. For antigen priming, intraperitoneally inject 50 μg of human Fc protein or CGG with alum adjuvant per mouse. Recommended injection volume: 200 μl.
2. Five weeks later, intraperitoneally inject 50 μg of human Fc fusion protein or CGG cross-linked antigen per mouse without an adjuvant.
3. A control group immunized with only pure human Fc protein or CGG alone should be included into the experiment.
4. The antibody response is quantitated 21 days later.

3.3 Vaccination Using Montanide as an Adjuvant

Femel et al. have recently shown that immunization of mice against the extra domain-B (ED-B) of fibronectin expressed in the tumor vasculature reduces tumor growth and metastasis [21]. In this study, they used a biodegradable adjuvant Montanide ISA 720 (M720) and a single-stranded CpG DNA (CpG 1826) which can induce high antibody levels against this self-antigen in vaccinated mice. M720/CpG has proven to be as potent as Freund's in terms of the amount of antibody induced [22].

3.3.1 Immunization Protocol

1. Mix 50 μg of CpG 1826 with 50 μg of the antigen protein solution.
2. The CpG/antigen mix is subsequently mixed with an equal volume of Montanide ISA 720.
3. Immunize each mouse in the groin with 100 μg of antigen-Montanide mix.
4. Two weeks later, perform an identical booster vaccination.
5. A robust antibody response should be seen 1 week later.

3.4 Examination of the Vasculature in Vaccinated Animals

It is important to examine the vasculature in the organs and tumors derived from vaccinated mice. To be able to confirm the effect of vascular targeting induced by the vaccination, immunofluorescence (IF) can be used to analyze the vascular density, vascular leakage, and the level of inflammation caused by the vaccination [15].

3.4.1 Visualization of Mouse Vasculature by IF

1. The visualization of mouse vasculature can be achieved by IF of paraffin-embedded mouse organs or tumor tissues.
2. Frozen mouse tissue sections can be stained with the Meca32 polyclonal antibody for 1 h.
3. Following a TBS-0.1 % Tween-20 wash, the sections can be visualized with 10 μg/ml of FITC-conjugated secondary antibody.
4. Permanently mount the slides with ProLong Gold anti-fade reagent including DAPI to counterstain cell nuclei.
5. At this point the stained slides can be stored at −20 °C for at least 3 months.
6. Examine the stained slides using a laser scanning confocal microscope.

3.4.2 Evaluation of Vascular Leakage and Inflammation

1. Fibrinogen and neutrophil staining are proven indicators of vascular leakage and inflammation.
2. Tumor sections can be treated with 1 in 500 diluted polyclonal fibrinogen antisera or 1 in 1000 diluted monoclonal anti-Ly6G and Ly-6C antibody.

3. After overnight incubation at 4 °C, sections are then probed with 15 μg/mL of rhodamine or FITC-conjugated secondary antibody.
4. Slides can be permanently mounted with ProLong Gold antifade reagent including DAPI to counterstain cell nuclei. Sections are then examined using a laser scanning confocal microscope.

3.5 Tumor Models

In vivo tumor models in mice have been used extensively to document the effect of potential therapies. Since human xenograft tumor models carried out in immunodeficient mice are not suitable for vaccine studies, most of the vaccine studies of vascular targeting have used syngeneic tumor models in immunocompetent mice. Tumor cells can be inoculated into their site of natural origin (orthotopic) or at a different site (ectopic). Ectopic subcutaneous tumor models have made an important contribution to the development of cancer treatments. But orthotopic models are considered of more physiological relevance. Studies performed in orthotopic tumor models may be preferred for investigating new treatment strategies since the microenvironment in which the cells reside determines the tumor phenotype. Models that probably better mimic human tumor progression are possibly spontaneously arising tumors in genetically engineered mice [23].

3.5.1 Lewis Lung Carcinoma Model (Subcutaneous Model)

The Lewis lung carcinoma (LLC) tumor model on the background of the C57/BL6 mouse has been widely used to assess the efficacy of vascular disrupting substances. An advantage of LLC model is its reliability of tumor take and uniform growth rate.

Implantation Protocol

1. Lewis lung carcinoma cells can be maintained in 10 % FBS, DMEM (*see* **Note 5**).
2. Lewis lung cells can be injected subcutaneously into the mouse flank. For reliable tumor take, a dose of 1×10^6 cells in 200 μl of PBS per mouse is recommended.
3. Tumor size can be measured twice or three times weekly using a caliper, and tumor volume is calculated following the formula: length × width^2 × 0.4 [24]. ANOVA analysis is performed for the comparison of tumor growth between vaccinated and control mice.
4. LLC tumors tend to reach a substantial size between 18 and 21 days post-tumor cell inoculation (*see* **Note 6**).

3.5.2 T1 Breast Cancer Model (Orthotopic Model)

Most implanted tumors do not metastasize naturally [25]. The 4T1 mouse breast cancer cell line (BALB/c background) was originally isolated by Fred Miller and colleagues at the Karmanos Cancer Institute [26]. When implanted orthotopically, 4T1 tends

to develop highly metastatic tumors that can metastasize to the lung, liver, lymph nodes, and brain without the resection of the primary tumor [25, 27, 28]. More importantly, the metastatic pattern of 4T1 tumor closely mirrors that of human breast cancer. A useful 4T1 cell line stably expressing firefly luciferase has been reported which allows quantitation of primary and the kinetics of metastasis in real time [29]. Therefore, the 4T1 breast cancer model has been used widely in studies for evaluating antitumor and anti-angiogenic effects of many cancer drugs [29, 30].

Implantation Protocol

1. 4T1 cells can be maintained in 10 % FBS, DMEM.
2. 4T1 tumor cells at a dose of 2.5×10^5 cells in 200 μl PBS can be implanted into the mammary fat pad around the fourth right nipple of 6–8-week female immunocompetent BALB/c mice (*see* **Note 7**).
3. Once tumors become visible, which is normally 4–6 days post-implantation, they are measured three times per week until the end of the experiment.
4. Tumor size is measured as previously described in Subheading 3.1.1.
5. 4T1 tumors tend to reach a substantial size after 18 days post-tumor cell implantation.
6. Metastasis of 4T1 tumor cells usually occurs within 2–4 weeks after tumor implantation. The metastasis can only be measured after culling the mice, or if using luciferase-engineered 4T1 cells, metastasis can be detected by injecting luciferin and quantified using an in vivo imaging system (*see* **Note 8**).

3.5.3 RIP-Tag2 Pancreatic Cancer Model

Transgenic mouse models that spontaneously develop tumors are by some thought to be most physiologically relevant to human cancers. A mouse model that is believed to reflect multistep human tumorigenesis is the transgenic RIP-Tag2 model of pancreatic insulinoma. These mice express the *Simian virus 40* (SV40) large tumor antigen (Tag) oncoprotein under the control of the rat insulin promoter (RIP) in the insulin-producing cells of the pancreatic islets of Langerhans [31]. The vasculature of RIP-Tag2 tumor has been shown to express a recently identified tumor vascular target CLEC14A [32].

3.5.4 Tumor Progression Features

1. Around 50 % of the pancreatic islets will turn hyperplastic with the histological characteristics of carcinoma in situ.
2. Before developing into neoplasia, the islets need to vascularize. By 7–8 weeks of age, 10 % of the hyperplastic islets succeed to proceed from hyperplasia to neoplasia.

3. Approximately 3 % of the total 400 islets develop into solid tumors and invasive carcinomas by the age of 12–15 weeks.
4. RIP-Tag2 mouse dies around 16 weeks of age from hypoglycemia due to overproduction of insulin.

4 Notes

1. A white alum-antigen precipitate will be visible at this point.
2. For example, with 1 ml of reaction mix, wash the precipitate in 1 ml of sterile PBS.
3. Mice less than 6 weeks old are still undergoing active angiogenesis and are therefore not suitable for testing vascular targeting drugs.
4. 20 μl of blood from each tail bleed is incubated at 37 °C for 1 h, following 8000 × *g* centrifugation for 10 min. The supernatant is normally sufficient for antibody analysis.
5. Lewis lung carcinoma is a semi-adherent cell line. During cell passaging, simply remove the medium containing the non-adherent cells, treat the remaining cells at the bottom with trypsin, and passage at 1 in 4 dilutions as normal adherent cells.
6. Ulceration of Lewis lung carcinoma tumor occurs at a high frequency from day 21 post-tumor cell inoculation. Remember to take a measurement of the tumor size before culling the ulcerated mice.
7. When injecting 4T1 cells, one should lift the skin surrounding the nipple. The needle should be pointing up toward the nipple to avoid mis-injecting the cells into the peritoneum.
8. Quantification of the luminescence signal from mice should be performed in a consistent manner. For example, the waiting time (normally 10 min) after luciferin injection should be consistent for each batch of mice. This is to minimize variations in the speed of luciferin delivery and the level of substrate activation. The time for anesthetizing animals should be the same because anesthetization slows the heart beat, reducing body fluid circulation and affecting the delivery rate of the luciferin to the tumor site.

Acknowledgements

We thank Kai-Michael Toellner for the advice and help regarding the alum-based vaccination protocol.

References

1. Dachs GU, Chaplin DJ (1998) Micro environmental control of gene expression: implications for tumor angiogenesis, progression, and metastasis. Semin Radiat Oncol 8:208–216
2. Zhuang X, Cross D, Heath VL, Bicknell R (2011) Shear stress, tip cells and regulators of endothelial migration. Biochem Soc Trans 39:1571–1575
3. Matejuk A, Leng Q, Chou ST, Mixson AJ (2011) Vaccines targeting the neovasculature of tumors. Vasc Cell 3:7
4. Los M, Roodhart JM, Voest EE (2007) Target practice: lessons from phase III trials with bevacizumab and vatalanib in the treatment of advanced colorectal cancer. Oncologist 12:443–450
5. Ridolfi L, Petrini M, Fiammenghi L, Riccobon A, Ridolfi R (2009) Human embryo immune escape mechanisms rediscovered by the tumor. Immunobiology 214:61–76
6. Haller BK, Brave A, Wallgard E et al (2010) Therapeutic efficacy of a DNA vaccine targeting the endothelial tip cell antigen delta-like ligand 4 in mammary carcinoma. Oncogene 29:4276–4286
7. Huijbers EJ, Ringvall M, Femel J et al (2010) Vaccination against the extra domain-B of fibronectin as a novel tumor therapy. FASEB J 24:4535–4544
8. Jarosz M, Jazowiecka-Rakus J, Cichon T et al (2013) Therapeutic antitumor potential of endoglin-based DNA vaccine combined with immunomodulatory agents. Gene Ther 20:262–273
9. Yoshikawa M, Mukai Y, Okada Y et al (2013) Robo4 is an effective tumor endothelial marker for antibody-drug conjugates based on the rapid isolation of the anti-Robo4 cell-internalizing antibody. Blood 121:2804–2813
10. Mura M, Swain RK, Zhuang X et al (2012) Identification and angiogenic role of the novel tumor endothelial marker CLEC14A. Oncogene 31:293–305
11. Grone J, Doebler O, Loddenkemper C, Hotz B, Buhr HJ, Bhargava S (2006) Robo1/Robo4: differential expression of angiogenic markers in colorectal cancer. Oncol Rep 15:1437–1443
12. Huminiecki L, Gorn M, Suchting S, Poulsom R, Bicknell R (2002) Magic roundabout is a new member of the roundabout receptor family that is endothelial specific and expressed at sites of active angiogenesis. Genomics 79: 547–552
13. Seth P, Lin Y, Hanai J, Shivalingappa V, Duyao MP, Sukhatme VP (2005) Magic roundabout, a tumor endothelial marker: expression and signaling. Biochem Biophys Res Commun 332:533–541
14. Marlow R, Binnewies M, Sorensen LK et al (2010) Vascular Robo4 restricts proangiogenic VEGF signaling in breast. Proc Natl Acad Sci U S A 107:10520–10525
15. Zhuang X, Ahmed F, Zhang Y et al (2015) Robo4 vaccines induce antibodies that retard tumor growth. Angiogenesis 18:83–95
16. Opie EL, Freund J (1937) An experimental study of protective inoculation with heat killed Tubercle bacilli. J Exp Med 66:761–788
17. Davenport FM (1968) Seventeen years' experience with mineral oil adjuvant influenza virus vaccines. Ann Allergy 26:288–292
18. Toellner KM, Luther SA, Sze DM et al (1998) T helper 1 (Th1) and Th2 characteristics start to develop during T cell priming and are associated with an immediate ability to induce immunoglobulin class switching. J Exp Med 187:1193–1204
19. Dwyer MA, Huang AJ, Pan CQ, Lazarus RA (1999) Expression and characterization of a DNase I-Fc fusion enzyme. J Biol Chem 274: 9738–9743
20. Garside P, Ingulli E, Merica RR, Johnson JG, Noelle RJ, Jenkins MK (1998) Visualization of specific B and T lymphocyte interactions in the lymph node. Science 281:96–99
21. Femel J, Huijbers EJ, Saupe F et al (2014) Therapeutic vaccination against fibronectin ED-A attenuates progression of metastatic breast cancer. Oncotarget 5:12418–12427
22. Huijbers EJ, Femel J, Andersson K, Bjorkelund H, Hellman L, Olsson AK (2012) The non-toxic and biodegradable adjuvant Montanide ISA 720/CpG can replace Freund's in a cancer vaccine targeting ED-B—a prerequisite for clinical development. Vaccine 30:225–230
23. Francia G, Kerbel RS (2010) Raising the bar for cancer therapy models. Nat Biotechnol 28: 561–562
24. Attia MA, Weiss DW (1966) Immunology of spontaneous mammary carcinomas in mice. V. Acquired tumor resistance and enhancement in strain A mice infected with mammary tumor virus. Cancer Res 26: 1787–1800
25. Crnic I, Christofori G (2004) Novel technologies and recent advances in metastasis research. Int J Dev Biol 48:573–581
26. Miller FR, Miller BE, Heppner GH (1983) Characterization of metastatic heterogeneity among subpopulations of a single mouse

mammary tumor: heterogeneity in phenotypic stability. Invasion Metastasis 3:22–31

27. Aslakson CJ, Miller FR (1992) Selective events in the metastatic process defined by analysis of the sequential dissemination of subpopulations of a mouse mammary tumor. Cancer Res 52:1399–1405
28. Pulaski BA, Ostrand-Rosenberg S (1998) Reduction of established spontaneous mammary carcinoma metastases following immunotherapy with major histocompatibility complex class II and B7.1 cell-based tumor vaccines. Cancer Res 58:1486–1493
29. Tao K, Fang M, Alroy J, Sahagian GG (2008) Imagable 4T1 model for the study of late stage breast cancer. BMC Cancer 8:228
30. Huang X, Wong MK, Yi H et al (2002) Combined therapy of local and metastatic 4T1 breast tumor in mice using SU6668, an inhibitor of angiogenic receptor tyrosine kinases, and the immunostimulator B7.2-IgG fusion protein. Cancer Res 62:5727–5735
31. Hanahan D (1985) Heritable formation of pancreatic beta-cell tumours in transgenic mice expressing recombinant insulin/simian virus 40 oncogenes. Nature 315: 115–122
32. Zanivan S, Maione F, Hein MY et al (2013) SILAC-based proteomics of human primary endothelial cell morphogenesis unveils tumor angiogenic markers. Mol Cell Proteomics 12:3599–3611

Part XI

Formulation and Stability of Vaccines

Chapter 49

Practical Approaches to Forced Degradation Studies of Vaccines

Manvi Hasija, Sepideh Aboutorabian, Nausheen Rahman, and Salvador F. Ausar

Key words stability, degradation pathways, stress testing, formulation, photo-degradation, thermal degradation

1 Introduction

Vaccines, like other biological formulations, are sensitive to many environmental stress conditions such as heat, shear, and exposure to light that can produce irreversible physicochemical changes and loss of potency. The formulation development of vaccines encompasses a series of steps designed to develop a safe and efficacious dosage form that can withstand the various stresses that the product may encounter during manufacturing, storage, distribution, and administration. In early stages of vaccine development, forced degradation studies are crucial for providing information about potential degradation pathways, optimal formulation conditions, and potential stabilizer excipients that can prevent or slow down product degradation. Additionally, forced degradation studies are key for developing stability indicating assays. Forced degradation studies aim to accelerate the degradation rate of a vaccine's drug substance or drug product by exposing them to various external stress conditions such as heat, light, shear, and extreme pH [1, 2].

One of the most common stresses used in industry during formulation development is thermal stress. Thermal stress studies can provide information on the thermal stability of a vaccine by monitoring the temperature dependence of a physicochemical or biological property of a product [3]. Thermal stress can be studied alone or in combination with other types of stresses such as pH and ionic strength and it can be performed by exposing the products under isothermal incubation conditions or by temperature ramping

Sunil Thomas (ed.), *Vaccine Design: Methods and Protocols: Volume 1: Vaccines for Human Diseases*, Methods in Molecular Biology, vol. 1403, DOI 10.1007/978-1-4939-3387-7_49,

at a given heating rate. While temperature ramping experiments provide thermodynamic information of the process, isothermal stress experiments provide insight into kinetics of the product degradation. Temperature ramping experiments can be conducted by a number of different techniques, the one most extensively used in formulation development of biologics is differential scanning calorimetry [4, 5]. Vaccine formulations, unlike protein pharmaceuticals, are typically prepared at a relatively low concentration of antigen and may include adjuvants such as aluminum salts. This poses a challenge to most methods used for detecting thermal unfolding because of either poor sensitivity to detect low antigen concentration or interference from the presence of adjuvants in the formulation. A method that has been increasingly employed for thermal unfolding is extrinsic fluorescence, also known as differential scanning fluorimetry [6, 7]. This method possesses many advantages compared to traditional methods especially when dealing with a large number of samples, low antigen concentrations, antigens adsorbed to aluminum salt adjuvants, and attenuated viruses [8, 9]. Extrinsic fluorescence can be easily automated in multi-well formats, allowing for simultaneous testing of multiple formulation conditions and stress combinations [6, 8].

Although temperature ramping studies are quick and convenient, they cannot describe the degradation kinetics of a product, so isothermal stress testing may also be required. Additionally, isothermal stress experiments typically measure chemical degradation properties of the vaccine components by looking at chromatographic or electrophoretic profiles, thus complementing the biophysical data generated from temperature ramping experiments. Determining the appropriate assays, stress temperatures, and durations on a case-by-case basis is extremely important to detect vaccine degradation. Comparison of different conditions can be conducted by analysis of covariance (ANCOVA) for zero order systems or by the use of advanced kinetic analyses in the case of nonlinear degradation profiles [10, 11]. A key parameter in these types of kinetic studies is the rate constant, which provides a measure of the rate of degradation under a given set of conditions.

Mechanical stress is common during manufacturing, storage, shipment, and administration of vaccine products. Mechanical stress can results in physical instability of a product, such as aggregate formation and can be a major cause of loss of protein or viral activity. This type of stress testing is strongly encouraged during the preformulation/formulation development of a vaccine [2], and can include agitation (shaking or stirring), pumping, vortexing, sonication, and shear stress to evaluate stabilizing properties of excipients such as surfactants. These compounds are commonly used as excipients in vaccine formulation to reduce surface induced aggregation. One theory that explains how surfactants are used to protect the vaccine antigen is the adsorption competition between the antigen and surfactant to the air–liquid or glass–liquid interfaces. Surfactants

protect the antigen by limiting the exposure to these interfaces and by reducing potential unfolding and aggregation [1, 2].

Depending on the stage of development and the objective of the mechanical stress study, the experimental design and setup can include stress tests such as agitation (stirring or shaking) and pumping. As mechanical stress studies can be used to evaluate the influence of manufacturing operations such as mixing or filling on antigen stability, study design parameters should be selected to represent the manufacturing process [1]. A typical mechanical stress study used for formulation screening involves shaking samples at 250–350 rpm for several hours at room temperature in the presence of selected stabilizers.

Vaccines are exposed to light (artificial or sunlight) in various situations, such as during production, shipment, storage, and administration to the patient. Most vaccine products on the market are recommended to be "protected from direct light" and have secondary packaging to avoid long term direct sunlight [12, 13]. Vaccine formulation characteristics such as pH, temperature, polarity, and protein structure may influence the photodegradation pathways of amino acids undergoing transfer of electrons to excited energy states [13]. The peptide backbone as well as Cys, Trp, Tyr, and Phe amino acids are known to be light-sensitive and are prone to photodegradation [2]. The conformation of a protein may also influence its photodegradation process. Pigault and Gerard found by assessing proteins with Trp of varying degrees of burial that photodegradation depends on the location of the residue in the protein, exposure to an aqueous interface, and neighboring amino acids in the primary sequence and secondary structure [14]. Additional factors that may also affect protein conformation, such as pH, ligands, or salts, can impact the sites of energy transfer and result in the formation of reactive radical species.

ICH guideline Q1B provides information regarding the specific experimental setup for photostability studies, including the type of light source and the extent of exposure. The guidance recommends using a cool white fluorescent lamp with a near-UV lamp. The UVA light wavelengths range from 320 to 400 nm while the cool white light wavelengths are within the visible range with more light from the violet and blue regions [13]. The ICH guidance differentiates between "forced degradation photostability testing" and "confirmatory photostability testing"; with the former being recommended for early stage development, and the latter for late stage developmental products. In the case of forced degradation studies, while the ICH guidance does not recommend specific conditions during early stage development, light exposure studies are typically conducted at 0.5, 1, and 2 times the conditions recommended by the ICH guidance in order to understand a vaccine's photosensitivity and elucidate its degradation pathways. In addition, proper controls such as light protected samples are essential. For confirmatory photostability testing, the conditions recom-

mended by ICH guidance include exposure to at least 1.2 million lux hours of visible light (400–800 nm) and at least 200 Wh per square meter (Wh/m^2) of UV light (320–400 nm). Any significant changes observed on drug product under these conditions results in a recommendation for the product to be protected from direct light and have adequate primary and secondary packaging [15].

In this chapter we provide the basic protocols for the forced degradation and formulation of vaccine products with respect to thermal, pH, mechanical and light stresses. We also provide relevant examples to illustrate the outcomes of such studies for protein-based vaccines and attenuated viruses-based vaccines.

2 Materials and Instrumentation

2.1 Thermal Degradation

2.1.1 Temperature Ramping Studies Using Extrinsic Fluorescence

1. Vaccine candidate.
2. 1.5 mL polypropylene tubes (Eppendorf, NY, USA).
3. 10 mM sodium acetate buffer at pH 5, 5.5, and 6.
4. 10 mM sodium phosphate buffer at pH 6.5, 7, and 7.5.
5. 10 mM Tris–HCl buffer at pH 8, 8.5, and 9 each in combination with 0, 0.1, 0.15, 0.2, 0.3, 0.4, 0.5, 0.7, and 0.9 M NaCl.
6. 1 mg/mL propidium iodide (Molecular Probes®, Eugene, OR, USA).
7. SYPRO Orange (Molecular Probes®, Eugene, OR, USA).
8. Benchtop centrifuge equipped with 96-well plate adapter (Eppendorf, NY, USA).
9. Stratagene Mx3005p RT-PCR instrument (Stratagene, La Jolla, CA, USA).
10. 96-well polypropylene plates (Stratagene, La Jolla, CA, USA).
11. Optical cap (8× strip) (Stratagene, La Jolla, CA, USA).

2.1.2 Isothermal Incubation and Detection by Microfluidics-Based Capillary Electrophoresis (Caliper LabChip® GXII)

1. Caliper LabChip® GXII (Caliper Life Sciences, Hopkinton, MA, USA).
2. Vaccine candidate.
3. Sterile 3 mL glass vials with rubber stoppers and aluminum caps (West Pharma, USA).
4. Buffers: 10 mM Tris–HCl pH 8.3, 50 mM sodium acetate buffer pH 5.6, 50 mM sodium acetate buffer pH 5.0, 50 mM sodium acetate buffer pH 4.6.
5. Incubator suitable for 55 °C incubation.
6. HT Protein Express Lab Chip (Caliper Life Sciences, Hopkinton, MA, USA).
7. HT Protein Express Reagent Kit (Caliper Life Sciences, Hopkinton, MA, USA).

8. 96-well skirted plates.
9. 1 M DTT (Sigma-Aldrich®, Saint Louis, MO, USA).

2.2 Photo-degradation

1. Vaccine candidate.
2. Sterile 3 mL glass vials with rubber stoppers and aluminum caps (West Pharma, USA).
3. Aluminum foil.
4. 1 cm pathlength quartz cuvettes (Starna®, Atascadero, CA).
5. CARON 6540 Series Model 6540A Photostability Chamber (Caron, Marietta, OH).
6. Chirascan™ CD Spectrometer (Applied Photophysics, Surrey, UK).

2.3 Mechanical Stress

1. Vaccine candidate.
2. Sterile 3 mL glass vials with rubber stoppers and aluminum caps (West Pharma, USA).
3. TBS buffer: 10 mM Tris–HCl pH 7.4, 150 mM NaCl.
4. Tween 80 (Croda International, USA).
5. Pluronic F68 (Sigma-Aldrich, USA).
6. Laboratory shaker (Advanced Digital Shaker Model 3500, VWR, USA).
7. Micro-Flow Imaging (MFI™) system (Brightwell, Ottawa, ON, Canada).

3 Methods of Forced Degradation

3.1 Temperature Ramping Experiments Using Extrinsic Fluorescence Spectroscopy

The method described below uses fluorescent dyes to detect protein unfolding or virus disassembly (capsid instability) in 96-well plates using a real-time PCR (RT-PCR) instrument [8, 9]. Since fluorescence intensity is not significantly affected by sample turbidity, this technique can be used for vaccines containing a diverse range of adjuvants including aluminum salts [8].

For the detection of protein unfolding, polarity sensitive dyes such as ANS or SYPRO Orange are typically used. These dyes increase in the fluorescence intensity when bound to the nonpolar regions of proteins exposed upon thermal unfolding.

To detect virus disassembly, nucleic acid binding dyes are added to the viral suspension prior to temperature ramping. In intact viral particles, the nucleic acid is protected by the capsid and lipid bilayer envelope and does not interact with the dye. An increase in temperature induces capsid disruption, which makes the viral genome accessible to the dye and results in a progressive increase in the fluorescence intensity (Fig. 1).

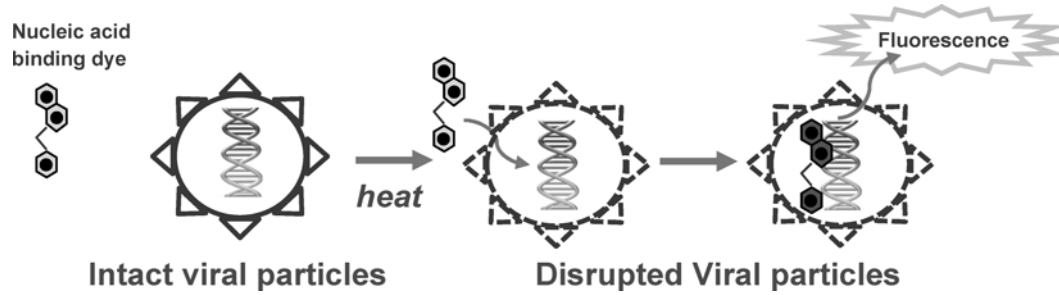

Fig. 1 Diagram representing the intact and disrupted viral particles with extrinsic dye bound to the nucleic acid upon thermal stress

The extrinsic fluorescence method can be performed under different formulation conditions including pH, ionic strength, and pharmaceutical excipients. The protocol below describes the application of extrinsic fluorescence to study the impact of pH and ionic strength on vaccine candidates.

1. Dispense buffers of different pH values in 1.5 mL polypropylene tubes and adjust the ionic strength by adding the appropriate amount of NaCl solutions (*see* **Note 1**).
2. Dilute the vaccine to the desired concentration (*see* **Note 2**).
3. Add the dye just prior to transfer to the 96-well plate. Once filled, seal the plate and centrifuge at 200 rpm for 2 min to eliminate any bubbles and to bring the entire sample volume down from the sides and into the well (*see* **Note 3**).
4. Program the RT-PCR instrument to obtain melting curves and start the temperature ramping. Recommended instrument settings are as follows (*see* **Note 4**):
   (a) Starting temperature: 25 °C
   (b) Final temperature: 98 °C
   (c) Increment: 1 °C
   (d) Equilibration time at each temperature: 3 min
   (e) Heating rate 1 °C/min
   (f) Reading settings: SYPRO Orange (excitation 470 nm, emission 570 nm); propidium iodide (excitation 535 nm, emission 617 nm)
5. Once the run is completed, export the dissociation curve (negative first derivative of the heating traces) as a file to Microsoft Excel software for further analysis.
6. Calculate the midpoint of thermal melting (T_m) from the exported derivative data in Microsoft Excel by finding the local minimum of the first derivative plot (*see* **Note 5**).

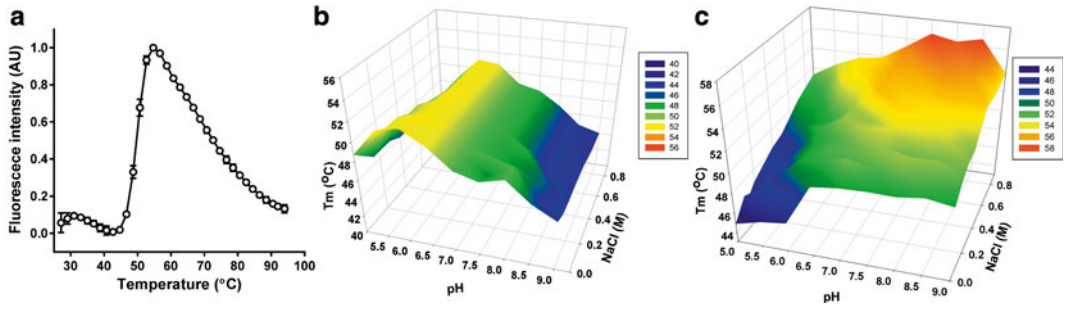

Fig. 2 Representative heating trace for a recombinant protein antigen adsorbed to aluminum hydroxide adjuvant obtained at pH 7, 150 mM NaCl using SYPRO Orange as extrinsic probe (**a**). Surface plot for the effects of pH and ionic strength on the thermal transition (T_m) for recombinant protein antigen adsorbed to aluminum hydroxide adjuvant using SYPRO Orange (**b**) and for an attenuated virus vaccine candidate using propidium iodide as extrinsic probe (**c**)

Figure 2a shows a representative thermal unfolding curve for a recombinant protein antigen adsorbed to aluminum salt adjuvant using SYPRO Orange as the extrinsic probe. The thermal transition event occurred near 50 °C when nonpolar regions of the protein interacted with SYPRO Orange to dramatically increase fluorescence intensity. A decrease in fluorescence intensity was observed after the curve reached maximum signal, and can be attributed to the thermal quenching of the dye's fluorescence at elevated temperatures. A screening of pH and ionic strength conditions for a recombinant protein- and virus-based vaccine can be easily assessed by this method in a short period of time. Figure 2b and c show the thermostability surface plots relative to pH and ionic strength for a recombinant protein vaccine and an attenuated virus-based vaccine respectively. For the recombinant protein-based vaccine, a noticeable impact of pH on thermal stability was observed, with the highest thermal stability (highest T_m values) near pH 6. Ionic strength, however, did not appear to have a significant effect on the thermal stability of the protein (Fig. 2b). For the attenuated virus-based vaccine, thermal stability was clearly enhanced under conditions of pH 7.5–8.5 and relatively high ionic strength (Fig. 2c).

3.2 Isothermal Incubation

Forced degradation studies under isothermal incubation are executed to understand the kinetics of product degradation. Typically the product is exposed to a selected stress temperature for a determined amount of time and the product is evaluated by a defined quality attribute such as potency or purity. The method below describes the isothermal incubation of an adjuvanted recombinant protein to investigate optimal pH for the formulation.

1. To examine the effect of temperature and pH on a recombinant protein-based vaccine adsorbed to an experimental adjuvant, prepare formulations in appropriate buffers adjusted to desired pH levels.

2. Aliquot material into sterile glass vials (or other suitable storage container systems), 1 mL per vial.
3. Store vials at normal and accelerated temperatures (*see* **Note 6**). For this example, the stored conditions were 4 °C and 55 °C with time points of 0, 1, 2, or 3 weeks.
4. At the end of the incubation period, pull samples and store at 4 °C or ≤−60 °C until tested.
5. Analyze protein samples using a suitable critical quality attribute such as purity (*see* **Note 7**). In this example, a microfluidics-based capillary electrophoresis technique was performed according to the manufacturer's instructions.
6. Plot % purity as a function of incubation time and compare formulations using appropriate statistical methods (*see* **Note 8**).

In Fig. 3, incubation of the adjuvanted vaccine under accelerated temperature (55 °C for 3 weeks) was used to investigate the impact of pH on the kinetics of degradation using a microfluidic capillary electrophoresis assay. By fitting the data with a general linear model, the rates of degradation at pH 7.5 and 8.0 were found to be significantly higher than those obtained at pH 6.5 and 7.0 ($p = 0.0013$, ANCOVA). On the basis of these results it can be concluded that product stability is significantly improved at pH 6.5–7.0.

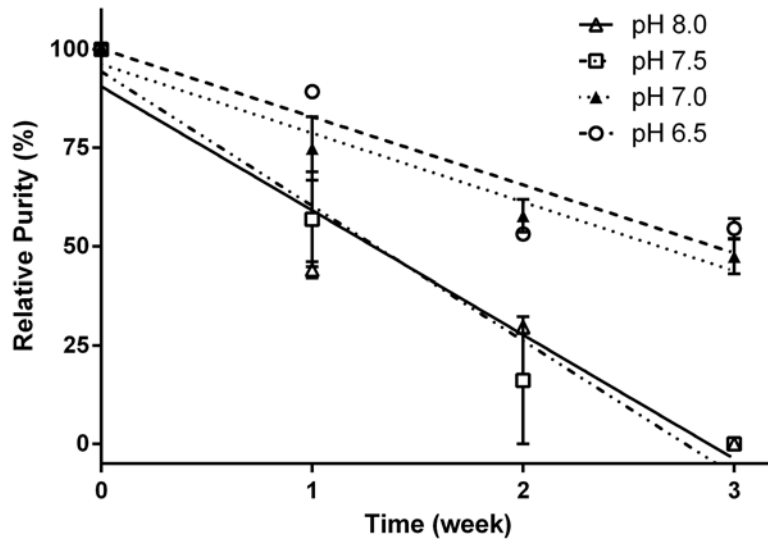

Fig. 3 Forced degradation of an adjuvanted recombinant protein under isothermal incubation at 55 °C. The vaccine was formulated under different pH, stressed at 55 °C for 3 weeks and characterized by microfluidic capillary electrophoresis (Caliper Labchip) by measuring relative purity

3.3 Photo-degradation

To understand vaccine photosensitivity and elucidate degradation pathways, light exposure using a photostability chamber with both visible and UVA radiation is recommended by ICH Q1B Guideline. The guideline recommends a condition of at least 1.2 million lux hours of visible light (400–800 nm) and at least 200 Wh/m^2 of UV light (320–400 nm) [15]. In the protocol below, 0.5, 1, and 2 times the exposure levels recommended by the ICH guidelines were tested at room temperature. Non-exposed samples were prepared by wrapping vials in aluminum foil and incubated alongside the exposed samples.

1. Aliquot materials to be evaluated into clear glass vials (1 mL per vial). Use water and alcohol resistant marker to label. Labels on each vial should be placed on the cap of the vial (*see* **Note 9**). Refer to Table 1 for exposure conditions and labeling.
2. For non-exposed control—label "D" and immediately wrap in aluminum foil. Control condition D is exposed to the same maximum light setting as condition C.
3. Store the vials at 4 °C until ready for photodegradation testing (*see* **Note 10**).
4. Place experimental vials (condition A) in the photostability chamber. All glass vials should be placed horizontally and in the center of the shelf to get maximal light exposure (*see* **Note 11**).
5. Start the photodegradation chamber and expose vials with long wave UltraViolet A (UVA) radiation first (upper chamber). Set exposure to 100 Wh/m^2 and start the experiment (*see* **Note 12**). In this example the temperature was set to 25 °C throughout the study.
6. Once UVA experiment is completed, transfer all vials to the bottom chamber for Visible (VIS) radiation test. Set VIS light exposure to 600 klux and start the study.
7. Once experiment is completed, wrap vials with aluminum foil for condition A and store at 4 °C until ready for testing.
8. Repeat **steps 4–8** for conditions (B, C, and D) according to settings in Table 1.

Table 1
Photo exposure conditions for experimental and control samples subjected to photodegradation studies

Letter identifier	A	B	C	D
Condition	0.5× ICH	1× ICH	2× ICH	Wrapped control (2× ICH)
VIS illuminance (Klux h)	600	1200	2400	2400
UVA irradiance (Wh/m^2)	100	200	400	400

3.3.1 Characterization of Photodegraded Protein Vaccine

Several physicochemical characterization methods can be used to detect photodegradation of protein vaccines. Below we describe the intrinsic fluorescence method to investigate damage to Trp residues upon increasing photo exposure. Intrinsic fluorescence is particularly useful for protein adsorbed to adjuvants since the turbidity conferred by the adjuvant suspension does not interfere with the fluorescence detection. To evaluate protein fragmentation, a generic SDS-PAGE method can be used.

1. To perform a fluorescence experiment using a fluorometer, set excitation wavelength to 295 nm (excitation bandwidth = 1 nm, time per point = 0.5 s) and emission wavelengths for spectra collection from 307 to 400 nm (spectra resolution = 1 nm).
2. Prior to spectra collection, mix sample by inversion to ensure homogeneity.
3. Load quartz cuvette with 1.2 mL of sample. Place cuvette in the instrument and record spectrum for each condition (A, B, C, and D).
4. Export and analyze data by plotting the maximum excitation as a function of exposure.

In Fig. 4, intrinsic fluorescence was used to investigate damage of Trp upon photo exposure. With increasing exposure to light, a progressive decrease in the intensity of the fluorescence spectrum of Trp was observed for the adjuvanted protein formulation (Fig. 4a). A significant downward trend was detected by analyzing the intensity of the peak maximum (340 nm) as a function of exposure condition (Fig. 4b). This suggests that the Trp residues of the antigen were damaged by increasing light exposure.

To investigate the impact of photo exposure on the protein integrity a generic SDS-PAGE test was performed. As shown in Fig. 4c, protein purity analysis revealed a progressive degradation with increasing photo exposure for the adjuvanted protein, indicating high susceptibility to light stress.

3.4 Mechanical Stress

With the purpose of mimicking real-life mechanical stresses which vaccine formulations experience during manufacturing, storage, and shipping; horizontal/vertical shakers, stirred reactors, and pumps are utilized as stress testing methods [1]. The experimental design depends on the phase of development and the aim of the study. In the protocol below, a shaking experiment is described for the evaluation of the effects of surfactants on vaccine aggregation.

1. Dispense formulations in glass vials or a different container system appropriate for the formulation under study. For each formulation, prepare vials for testing at time zero (T0), and additional time points such as 1 and 24 h of agitation (*see* **Note 13**).
2. Collect T0 samples and store at 4 °C until testing.

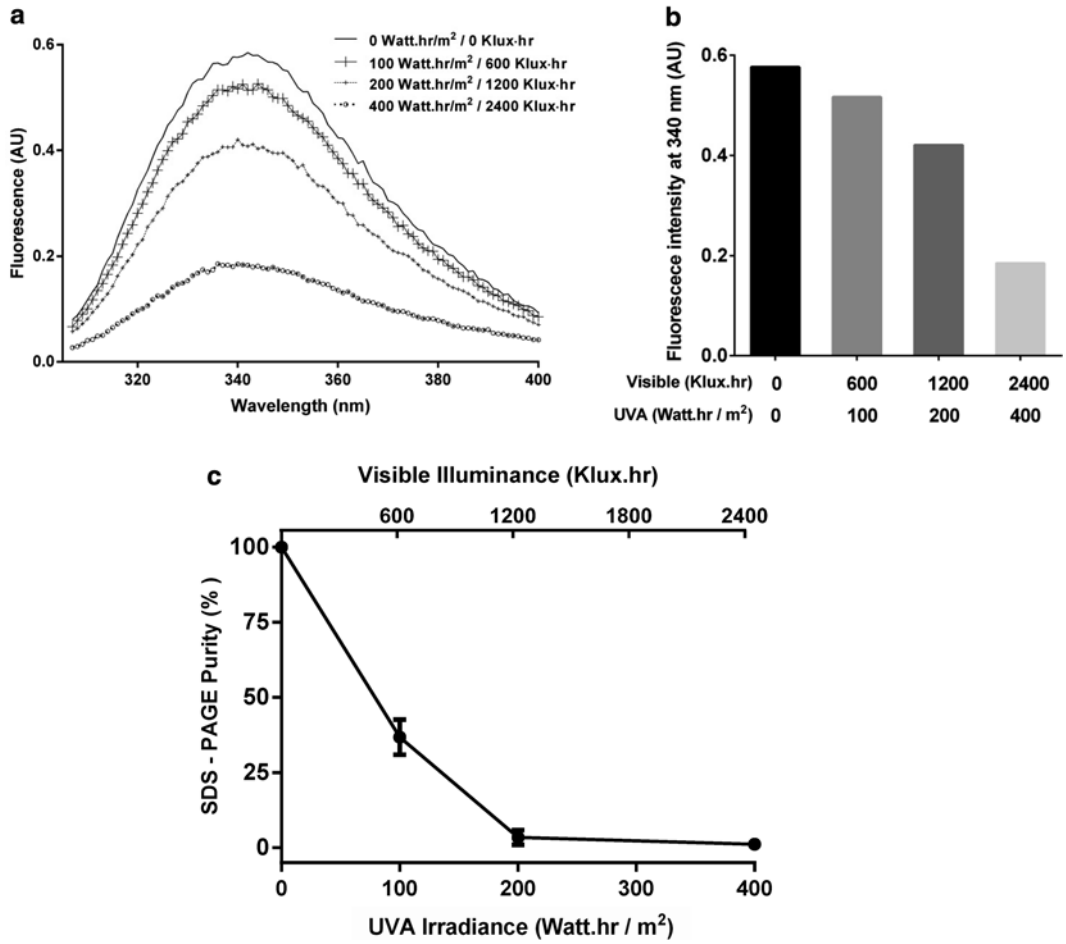

Fig. 4 Effects of photo exposure on intrinsic fluorescence of Trp and protein integrity. Intrinsic fluorescence spectra of an adjuvanted protein antigen were obtained for samples exposed to increasing irradiance (**a**). Fluorescence intensity at the peak maximum (340 nm) monitored as a function of increasing photo exposure to UVA and Vis light (**b**). Effect of photo exposure on protein integrity as monitored by SDS-PAGE purity (**c**)

3. Place the rest of the vials in horizontal position on a shaker at the appropriate speed under room temperature. For the example in the Fig. 5, a speed of 250 rpm for up to 24 h was sufficient (*see* **Note 14**).
4. At the end of each time point, remove samples from shaker and place them in storage at 4 °C.
5. Perform testing for samples collected at the various time points.
6. In order to test for protein solubility, centrifuge samples for 15 min at 20,800 × *g* and determine the amount of total protein in the supernatant by the method of reverse-phase high performance liquid chromatography (RP-HPLC).

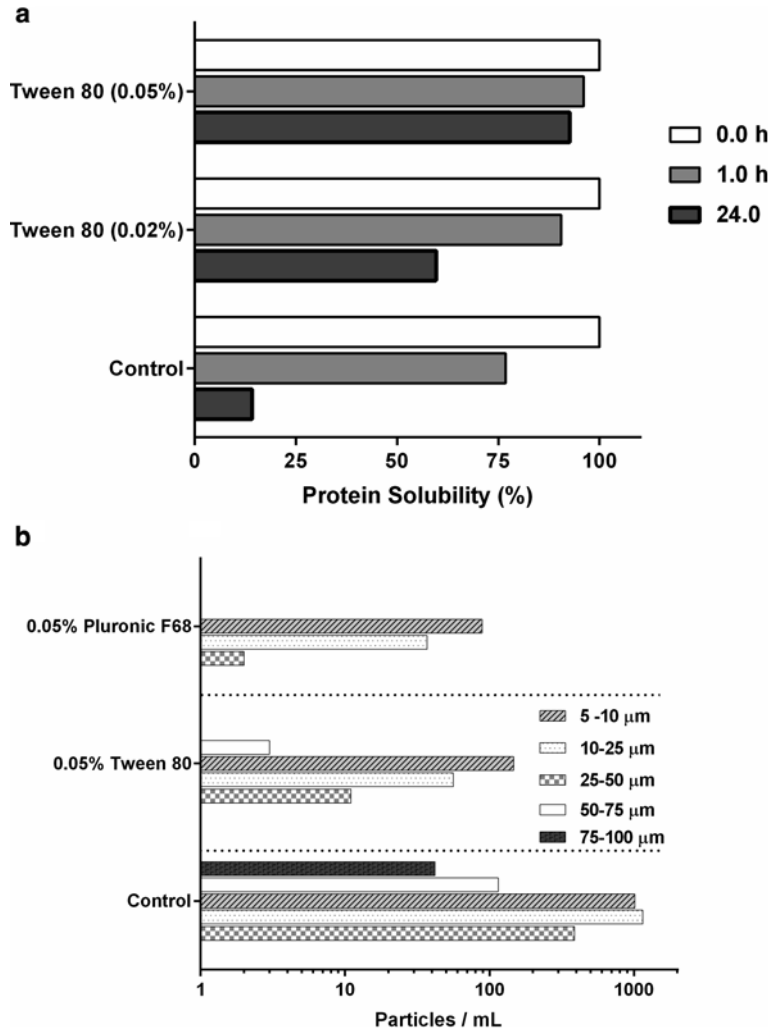

Fig. 5 Effect of shaking at 250 rpm for up to 24 h on the solubility of a recombinant protein antigen in the presence of Tween 80 (**a**). The effects of two different surfactants on the formation of subvisible particles after 6 h of continuous agitation at 250 rpm is illustrated in (**b**)

In Fig. 5a, we show an example where we evaluate the effect of a non-ionic surfactant (Tween 80) on a protein antigen. Final formulations contained 50 µg/mL of protein antigen with 0.02 % or 0.05 % Tween 80. Samples were analyzed for protein solubility by RP-HPLC (*see* **Note 15**). Data revealed that the presence of surfactants in the formulation reduced protein aggregation and precipitation caused by mechanical stress. Figure 5b shows another example where agitation was used to study the effect of two different surfactants, Tween 80 and Pluronic F68, on the aggregation of a protein antigen. By means of Micro-Flow Imaging (MFI™), the particle count of formulations within different size range intervals was analyzed in samples collected at T0 or agitated for more than

6 h. A noticeable decrease in both size of particles and number was observed for formulation containing surfactants (Fig. 5b).

4 Notes

1. For a complete pH and salt screening as a function of temperature, a pH range of 4–9 and a NaCl concentration range between 0 and 1 M are recommended.
2. For protein antigens, as a rule of thumb a concentration between 50 and 300 μg/mL is desired. For viral antigens, a dilution study is required to select the optimal concentrations.
3. Several dyes available on the market to study extrinsic fluorescence. We obtained optimal results with propidium iodide dye and for viral vaccine formulations, and with SYPRO Orange dye for protein-based formulations. Final dye concentration needs to be optimized on a case-by-case base.
4. Based on these settings, total running time for 96 samples is approximately 2 h.
5. Local minimum can be found by using the Min, Index, and Match functions in Excel. Care should be taken to confirm the determined value by visually evaluating the derivative and normalized data.
6. An appropriate temperature for thermal stress testing needs to be selected on a case-by-case approach. As a rough guidance, stress temperature of at least 2 to 10 °C below the melting temperature (T_m) is recommended.
7. In early vaccine development stages, critical quality attribute tests are not readily defined. Electrophoretic methods such as SDS-PAGE and microfluidics capillary electrophoresis can be easily used with minimal development time.
8. Analysis of covariance (ANCOVA) method is generally used as a statistical test to compare the equality of degradation slopes. The analysis can be performed by any statistical software package able to conduct analysis of covariance. ANCOVA includes regression and analysis of variance (ANOVA) terms, as well as terms for an interaction effect. The interaction indicates a comparison of slopes between formulations [10, 11].
9. Placing a label on the wall of the vial will block the light beams in reaching the product. In order to ensure maximum light exposure throughout the sample, the label should be placed on the cap of the vial.
10. In order to minimize exposure to light prior to the experiment it is important to keep all samples protected from any light exposure.
11. To understand the product photosensitivity, an incremental light exposure is recommend as depicted in Table 1.

12. The CARON 6540 Series Photodegradation Chamber allows the user to set the overall exposure level for a sample and the unit will automatically turn off the lights when the level of exposure is completed. The chamber temperature should remain constant throughout the study.
13. The duration of agitation should be sufficient to cause aggregation and may vary based on the stability of the formulation under study.
14. As a starting point 250 rpm for up to 24 h is sufficient; however, the speed and time may be optimized for each case.
15. Samples can also be analyzed using other methods such as turbidity (i.e., OD at 360 nm), as well as imaging and particle sizing techniques.

Acknowledgements

We thank Frederick To and Gladys Wong for technical assistance.

References

1. Hawe A, Wiggenhorn M, van de Weert M, Garbe JH, Mahler HC et al (2012) Forced degradation of therapeutic proteins. J Pharm Sci 101:895–913
2. Hasija M, Li L, Rahman N, Ausar SF (2013) Forced degradation studies: an essential tool for the formulation development of vaccines. Vaccine 3:11–33
3. Brandau DT, Jones LS, Wiethoff CM, Rexroad J, Middaugh CR (2003) Thermal stability of vaccines. J Pharm Sci 92:218–231
4. Johnson CM (2013) Differential scanning calorimetry as a tool for protein folding and stability. Arch Biochem Biophys 531:100–109
5. Mueller M, Loh MQT, Tee DHY, Yang Y, Jungbauer A (2013) Liquid formulations for long-term storage of monoclonal IgGs. Appl Biochem Biotechnol 169:1431–1448
6. Niesen FH, Berglund H, Vedadi M (2007) The use of differential scanning fluorimetry to detect ligand interactions that promote protein stability. Nat Protoc 2:2212–2221
7. He F, Hogan S, Latypov RF, Narhi LO, Razinkov VI (2010) High throughput thermostability screening of monoclonal antibody formulations. J Pharm Sci 99:1707–1720
8. Ausar SF, Chan J, Hoque W, James O, Jayasundara K, Harper K (2011) Application of extrinsic fluorescence spectroscopy for the high throughput formulation screening of aluminum-adjuvanted vaccines. J Pharm Sci 100:431–440
9. Walter TS, Ren J, Tuthill TJ, Rowlands DJ, Stuart DI, Fry EE (2012) A plate-based high throughput assay for virus stability and vaccine formulation. J Virol Methods 185:166–170
10. Schofield TL (2009) Vaccine stability study design and analysis to support licensure. Biologicals 37:387–396
11. Clénet D, Imbert F, Probeck P, Rahman N, Ausar SF (2014) Advanced kinetic analysis as a tool for formulation development and prediction of vaccine stability. J Pharm Sci 103:3055–3064
12. Rathore N, Rajan RS (2008) Current perspectives on stability of protein drug products during formulation, fill and finish operations. Biotechnol Prog 24:504–514
13. Kerwin BA, Remmele RL Jr (2007) Protect from light: photodegradation and protein biologics. J Pharm Sci 96:1468–1479
14. Pigault C, Gerard D (1984) Influence of the location of tryptophanyl residues in proteins on their photosensitivity. Photochem Photobiol 40:291–296
15. ICH Q1B (1997) Guidelines for photostability testing of new drug substances and products. Fed Reg 62:27115–27122

ERRATUM

Vaccine Design

Methods and Protocols: Volume 1: Vaccines for Human Diseases

Sunil Thomas

Sunil Thomas (ed.), *Vaccine Design: Methods and Protocols: Volume 1: Vaccines for Human Diseases*, Methods in Molecular Biology, vol. 1403, DOI 10.1007/978-1-4939-3387-7, © Springer Science+Business Media New York 2016

DOI 10.1007/978-1-4939-3387-7_50

The city name for Lankenau Institute for Medical Research was wrongly included as Philadelphia in the editor's affiliation and Preface. The correct city name is Wynnewood. This has been updated in this volume.

The online version of the original book can be found at
http://dx.doi.org/10.1007/978-1-4939-3387-7

INDEX

A

B

Sunil Thomas (ed.), *Vaccine Design: Methods and Protocols: Volume 1: Vaccines for Human Diseases*, Methods in Molecular Biology, vol. 1403, DOI 10.1007/978-1-4939-3387-7, © Springer Science+Business Media New York 2016

C

D

E

F

G

H

I

J

K

L

M

N

O

P

R

S

T

U

V

W

Y

Z